

AD 636 392

FLIGHT TEST ENGINEERING HANDBOOK AFTR NO. 6273

United States Air Force
Edwards Air Force Base, CA

Jan 66

AD836392

FLIGHT TEST ENGINEERING HANDBOOK

RUSSEL M. HERRINGTON
Major, USAF

PAUL E. SHOEMACHER
Captain, USAF

EUGENE P. BARTLETT
1st Lieutenant, USAF

EVERETT W. DUNLAP

REPRODUCED BY
NATIONAL TECHNICAL
INFORMATION SERVICE
U.S. DEPARTMENT OF COMMERCE
SPRINGFIELD, VA 22161

UNITED STATES AIR FORCE
AIR FORCE SYSTEMS COMMAND
AIR FORCE FLIGHT TEST CENTER
EDWARDS AIR FORCE BASE, CALIFORNIA

UNCLASSIFIED

Security Classification

DOCUMENT CONTROL DATA - R&D

(Security classification of title, body of abstract and indexing annotation must be entered when the overall report is classified)

1 ORIGINATING ACTIVITY (Corporate author) United States Air Force, Air Force Systems Command, Air Force Flight Test Center, Edwards AFB, Calif	2a REPORT SECURITY CLASSIFICATION <u>Unclassified</u> 2b GROUP N/A
--	---

3 REPORT TITLE
Flight Test Engineering Handbook AFTR No. 6273

4 DESCRIPTIVE NOTES (Type of report and inclusive dates)
Corrected and revised January 1966

5 AUTHOR(S) (Last name, first name, initial)
Herrington, Russel M., Major, USAF Dunlap, Everett W.
Shoemaker, Paul E., Capt, USAF
Bartlett, Eugene P., 1st Lt, USAF

5 REPORT DATE May 1951	7a TOTAL NO. OF PAGES 687	7b NO. OF REFS 30
---------------------------	------------------------------	----------------------

6a CONTRACT OR GRANT NO. N/A 7 PROJECT NO. N/A 8 N/A 9 N/A	9a ORIGINATOR'S REPORT NUMBER(S) AFTR No. 6273 9b OTHER REPORT NO(S) (Any other numbers that may be assigned this report) N/A
---	---

10 AVAILABILITY/LIMITATION NOTICES
Distribution of this document is unlimited.

11 SUPPLEMENTARY NOTES N/A	12 SPONSORING MILITARY ACTIVITY Air Force Flight Test Center Edwards AFB, California 93523
-------------------------------	--

13 ABSTRACT
Methods of obtaining flight test data for reciprocating engine aircraft (including helicopters) and turbojet aircraft are presented together with various methods of data analysis and data presentation. Correction of aircraft performance to standard conditions is included, as are detailed derivations of correction factors and performance parameters. Numerous graphs and charts containing information required by and useful to the flight test engineer are presented, together with sample data reduction forms and sample flight test programs.

Reproduced from best available copy.

BEST

AVAILABLE

COPY

KEY WORDS	LINK A		LINK B		LINK C	
	ROLE	WT	ROLE	WT	ROLE	WT
ght Test, Aircraft Performance, Reciprocating, bojet, Level Flight Performance, Climb Performance, Descent Performance, Takeoff, Landing, icopter Performance						

INSTRUCTIONS

ORIGINATING ACTIVITY: Enter the name and address of contractor, subcontractor, grantee, Department of Defense activity or other organization (*corporate author*) issuing report.

REPORT SECURITY CLASSIFICATION: Enter the overall security classification of the report. Indicate whether "Restricted Data" is included. Marking is to be in accordance with appropriate security regulations.

GROUP: Automatic downgrading is specified in DoD Directive 5200.10 and Armed Forces Industrial Manual. Enter group number. Also, when applicable, show that optional markings have been used for Group 3 and Group 4 as authorized.

REPORT TITLE: Enter the complete report title in all letters. Titles in all cases should be unclassified. Significant title cannot be selected without classification. Show title classification in all capitals in parentheses immediately following the title.

DESCRIPTIVE NOTES: If appropriate, enter the type of report, e.g., interim, progress, summary, annual, or final. Indicate inclusive dates when a specific reporting period is involved.

AUTHOR(S): Enter the name(s) of author(s) as shown on the report. Enter last name, first name, middle initial. Military, show rank and branch of service. The name of principal author is an absolute minimum requirement.

REPORT DATE: Enter the date of the report as day, month, year, or month, year. If more than one date appears on the report, use date of publication.

TOTAL NUMBER OF PAGES: The total page count shall follow normal pagination procedures, i.e., enter the number of pages containing information.

NUMBER OF REFERENCES: Enter the total number of references cited in the report.

CONTRACT OR GRANT NUMBER: If appropriate, enter applicable number of the contract or grant under which report was written.

PROJECT NUMBER: Enter the appropriate military department identification, such as project number, project number, system numbers, task number, etc.

ORIGINATOR'S REPORT NUMBER(S): Enter the office report number by which the document will be identified and controlled by the originating activity. This number must be unique to this report.

OTHER REPORT NUMBER(S): If the report has been assigned any other report numbers (either by the originator or the sponsor), also enter this number(s).

AVAILABILITY/LIMITATION NOTICES: Enter any limitations on further dissemination of the report, other than those

imposed by security classification, using standard statements such as:

- (1) "Qualified requesters may obtain copies of this report from DDC."
- (2) "Foreign announcement and dissemination of this report by DDC is not authorized."
- (3) "U. S. Government agencies may obtain copies of this report directly from DDC. Other qualified DDC users shall request through _____."
- (4) "U. S. military agencies may obtain copies of this report directly from DDC. Other qualified users shall request through _____."
- (5) "All distribution of this report is controlled. Qualified DDC users shall request through _____."

If the report has been furnished to the Office of Technical Services, Department of Commerce, for sale to the public, indicate this fact and enter the price, if known.

11. SUPPLEMENTARY NOTES: Use for additional explanatory notes.

12. SPONSORING MILITARY ACTIVITY: Enter the name of the departmental project office or laboratory sponsoring (paying for) the research and development. Include address.

13. ABSTRACT: Enter an abstract giving a brief and factual summary of the document indicative of the report, even though it may also appear elsewhere in the body of the technical report. If additional space is required, a continuation sheet shall be attached.

It is highly desirable that the abstract of classified reports be unclassified. Each paragraph of the abstract shall end with an indication of the military security classification of the information in the paragraph, represented as (TS), (S), (C), or (U).

There is no limitation on the length of the abstract. However, the suggested length is from 150 to 225 words.

14. KEY WORDS: Key words are technically meaningful terms or short phrases that characterize a report and may be used as index entries for cataloging the report. Key words must be selected so that no security classification is required. Identifiers, such as equipment model designation, trade name, military project code name, geographic location, may be used as key words but will be followed by an indication of technical context. The assignment of links, rules, and weights is optional.

Reproduced from best available copy.

NOTICE

**THIS DOCUMENT HAS BEEN REPRODUCED
FROM THE BEST COPY FURNISHED US BY
THE SPONSORING AGENCY. ALTHOUGH IT
IS RECOGNIZED THAT CERTAIN PORTIONS
ARE ILLEGIBLE, IT IS BEING RELEASED
IN THE INTEREST OF MAKING AVAILABLE
AS MUCH INFORMATION AS POSSIBLE.**

FOREWORD

The publication of a series of handbooks on the performance testing and evaluation of all types of Air Force aircraft is planned by the Flight Research Division, Air Force Flight Test Center. This handbook has been issued as an interim measure to provide assistance to flight test personnel pending publication of the new series of handbooks. Chapters I and III of the original Technical Report Number 6273 have been replaced by AFFTC Technical Notes 59-22 and 59-47. These technical notes are on airspeed, altitude and temperature measurement, and turbojet engine performance. They represent updated and improved versions of the original contents of TR Number 6273.

As a matter of expediency, the numbering of charts, figures, and equations in the technical notes has been retained. This has led to inconsistency in the numbering system, but, since appropriate references in the text have been changed, it is felt that no confusion will result.

The United States Standard Atmosphere used as the basis for charts and tables in Chapter 1 is equivalent to the International Civil Aviation Organization (ICAO) Standard Atmosphere adopted by NACA on November 20, 1952 and contained in NACA Report 1235 "Standard Atmosphere - Tables and Data for Altitudes to 65,800 Feet", 1955 (Reference 6). The equations of this report were used to extend the tables to 80,000 feet. The properties tabulated in Chapter 1 are identical with those in the ARDC Model Atmosphere, 1956, the U. S. Extension to the ICAO Standard Atmosphere, 1958 (Reference 7) and the ARDC Model Atmosphere, 1959 (Reference 8). One exception should be noted: the sea-level speed of sound is taken as $1116.45 \text{ ft sec}^{-1}$ in Chapter 1, whereas it was $1116.89 \text{ ft sec}^{-1}$ in NACA Report 1235, since the ratio of specific heats, γ , was taken as 1.4 exactly for Chapter 1 and implied as 1.4011 in NACA Report 1235, on the basis of experimental values of sound speed.

The constants and conversion factors used in Chapters 2 through 7 and Appendixes I and II are based on the earlier "Standard Atmosphere Tables and Data", NACA Report 218, 1948. The gas constant, R used in Chapter I, e. g. in the perfect gas law $P_a = \rho R T_a$, has the dimensions $\text{ft}^2/\text{sec}^2\text{K}$. It is equal to the product of the gas constant used in the remaining chapters and the acceleration due to gravity. The dimensions of the latter are ft/K .

While this handbook continues to provide, in general, adequate instruction for conducting performance tests on turbojet and reciprocating engine powered conventional aircraft, Chapter VII, "Helicopter Flight Test Performance and Analysis", is in need of updating. Also, analysis is lacking in regard to high performance aircraft. Caution should be exercised in applying correction procedures to flight data

obtained with this type of aircraft. For example, significant errors may be incurred in making corrections to climb data for wind gradients and for weight because of the simplifying assumptions which have been made.

The addition of a list of references has been made (reference TABLE OF CONTENTS). Contained in these references is considerable supplementary information including data on standard atmospheres ^{6, 7, 8}, a review of aerodynamics prepared by the USAF Experimental Test Pilot School ², and a comprehensive NATO flight test manual prepared under the auspices of the Advisory Group for Aeronautical Research and Development ³.

REPRODUCED FROM
THE NATIONAL ARCHIVES
SERIALS ACQUISITION DIVISION

ABSTRACT

Methods of obtaining flight test data for reciprocating engine aircraft (including helicopters) and turbojet aircraft are presented together with various methods of data analysis and data presentation. Correction of aircraft performance to standard conditions is included, as are detailed derivations of correction factors and performance parameters. Numerous graphs and charts containing information required by and useful to the flight test engineer are presented, together with sample data reduction forms and sample flight test programs.

DISTRIBUTION
OF THIS DOCUMENT
IS UNLIMITED

PUBLICATION REVIEW

Manuscript copy of this report has been reviewed and found satisfactory for publication.

FOR THE COMMANDING GENERAL:


FRANKLIN K. PAUL
Colonel, USAF

Chief, Flight Test Division

TABLE OF CONTENTS

LIST OF REFERENCE AND COMPUTATIONAL CHARTS	ix
INTRODUCTION	xiii
CHAPTER ONE Speed, Altitude, and Temperature Instruments - and Calibration	
Symbols Used in Chapter One	xv
Section 1 The Standard Atmosphere	1
Section 2 Theory of Altitude, Air-Speed, Mach Number and Air Temperature Measurement	7
Section 3 Instrument Error - Theory and Calibration	24
Section 4 Pressure Lag Error - Theory and Calibration	28
Section 5 Position Error - Theory and Calibration	48
Section 6 Calibration of the Free Air Temperature Instrumentation	93
Section 7 Data Reduction Outlines	100
Section 8 Charts	118
Section 9 U. S. Standard Atmosphere Tables	265
CHAPTER TWO Reciprocating Engine Performance	2-1
Section 2.1 Horsepower Determination for Test Conditions	2-1
Section 2.2 Power Correction for Temperature Variation at Constant Manifold Pressure	2-5
Section 2.3 Power Correction for Manifold Pressure Variation Resulting from Temperature Variation and Flight Mach Number Variation	2-6
Section 2.4 Power Correction for Turbosupercharger RPM and Back Pressure Variation at Constant Manifold Pressure	2-13
Section 2.5 Critical Altitude	2-17
Section 2.6 Engine Data Plotting, Prop Load, BMEP Data, Supercharger Operation	2-18
Section 2.7 Fuel Consumption	2-23
Section 2.8 Engine Cooling	2-25

Preceding page blank

CHAPTER THREE Turbojet Engine Performance

	Symbols Used in Chapter Three	3-i
Section 1	Introduction to Thrust Measurement	3-1
Section 2	Turbojet Engine Performance Parameters	3-8
Section 3	Air Induction System Performance	3-15
Section 4	Standardization of Test Data with Engine Parameters	3-29
Section 5	Air Flow Measurement	3-33
Section 6	In-Flight Thrust Measurement	3-40
Section 7	Water Injection	3-62
Section 8	Data Reduction Outlines	3-66
Section 9	Charts	3-68

CHAPTER FOUR Level Flight Performance 4-1

Section 4.1	Density Altitude and Pressure Altitude Flight Test Methods	4-1
Section 4.2	Aerodynamic Forces and Their Relation to Engine Power and Propulsive Thrust	4-2
Section 4.3	Speed-Power Curves - Reciprocating Engine Aircraft	4-6
Section 4.4	Weight Corrections for Speed Power Data - Reciprocating Engine Aircraft	4-9
Section 4.5	Configuration Change Corrections for Speed Power Data	4-11
Section 4.6	The Generalized Power Parameter (PIW) and Speed Parameter (VIW) - Reciprocating Engine Aircraft	4-13
Section 4.7	Fuel Consumption - Range and Endurance - Reciprocating Engine Aircraft	4-16
Section 4.8	Speed Power Curves - Turbojet Aircraft	4-21
Section 4.9	Weight Change Corrections for Speed Power data - Turbojet Aircraft	4-28
Section 4.10	Fuel Consumption - Endurance and Range - Turbojet Aircraft	4-33
Section 4.11	Flight Thrust Measurement Applications to Drag and Lift Coefficient and Aircraft Efficiency Determination	4-42

CHAPTER FIVE	Climb and Descent Performance	5-1
Section 5.1	Rate of Climb Parameters - Derivation	5-1
Section 5.2	Temperature Variation Correction to Rate of Climb Data	5-6
Section 5.3	Weight Variation Correction to Rate of Climb Data	5-9
Section 5.4	Vertical Wind Gradient Correction to Rate of Climb Data	5-11
Section 5.5	Climb Path Acceleration Correction to Rate of Climb Data	5-13
Section 5.6	Temperature Effects on Fuel Consumption and Weight During Climb	5-16
Section 5.7	Determination of Best Rate of Climb and Best Climbing Speed	5-18
Section 5.8	Dimensionless Rate of Climb Plotting	5-22
Section 5.9	General Climb Test Information	5-27
Section 5.10	Rate of Descent Data	5-35
CHAPTER SIX	Take-off and Landing Performance	6-1
Section 6.1	Techniques and Configurations for Take-off Tests - JATO Operation	6-1
Section 6.2	Distance and Height Measurements and Equipment	6-2
Section 6.3	Take-off Data Corrections for Wind, Weight, and Density	6-6
Section 6.4	Landing Performance Tests and Corrections	6-15
Section 6.5	Dimensionless Parameters for Take-off and Landing Performance Data	6-18
CHAPTER SEVEN	Helicopter Flight Test Performance and Analysis	7-1
Section 7.1	Introduction	7-1
Section 7.2	Level Flight Performance	7-3
Section 7.3	Rotor Thrust, Power, and Efficiency in Hovering Flight	7-11

Section 7.4	Climbs and Descents (Autorotation)	7-19
Section 7.5	Fuel Consumption, Endurance and Range	7-26
Section 7.6	Airspeed, Altimeter, and Temperature System Calibrations	7-31
REFERENCES		8-1
APPENDIX I		
	Density Altitude Charts	8-5
	Differential -Static Pressure Ratio versus Mach Number (Supersonic-Normal Shock Condition)	8-17
	Reynolds Number-Mach Number Ratio versus Pressure Altitude and Temperature	8-18
	Supersonic Mach Number Functions	8-20
	Psychrometric Chart	8-33
APPENDIX II		
	Nomenclature	8-35
	Physical Information and Systems of Units	8-46
	Conversion Tables	8-47

LIST OF REFERENCE AND COMPUTATIONAL CHARTS

CHAPTER ONE	Page
CHART 8.1 $H(G/g_{SL})$ versus $h - H(G/g_{SL})$	118
CHART 8.2 M versus T_a for constant t_{ic} and constant Temperature Probe Recovery Factor, K .	120
CHART 8.21 Compressibility Correction to Calibrated Airspeed	126
CHART 8.3 H_c versus V_e/M	128
CHART 8.4 V_{tt} versus t_{ca} for constant M	130
CHART 8.5 M versus V_c for constant H_c and M versus V_c for constant V_{ts} also M_{ic} versus V_{ic} for constant H_{ic}	139
CHART 8.61 $\lambda_{H_{ic}}/\lambda_{SL}$ versus H_{ic} for constant V_{ic}	203
CHART 8.62 $\lambda/\lambda_{H_{ic}}$ versus H_{ic} for constant t_{at}	204
CHART 8.63 $F_1(H_{ic}, V_{ic})$ versus V_{ic} for constant H_{ic}	205
CHART 8.7 H_{ic} versus $\Delta P_p/\Delta H_{pc}$ for constant ΔH_{pc}	207
CHART 8.8 H_{ic} versus $\Delta P_p/\Delta H_{pc}$ for constant ΔP_p	211
CHART 8.9 V_{ic} versus $\Delta P_p/\Delta V_{pc}$ for constant ΔV_{pc}	214
CHART 8.10 V_{ic} versus $\Delta P_p/\Delta V_{pc}$ for constant ΔP_p	216
CHART 8.11 ΔV_{pc} versus V_{ic} for constant $\Delta P_p/q_{cic}$	218
CHART 8.12 $\Delta H_{pc}/\Delta V_{pc}$ versus V_{ic} for constant H_{ic}	222
CHART 8.13 ΔV_{pc} versus ΔP_p for constant V_{ic} and ΔH_{pc} versus ΔP_p for constant H_{ic} also ΔV_{pc} versus ΔH_{pc} for constant V_{ic} and H_{ic}	228
CHART 8.14 M_{ic} versus $\Delta M_{pc}/\Delta H_{pc}$ for constant H_{ic}	235
CHART 8.15 ΔM_{pc} versus $\Delta P_p/P_s$ for constant M_{ic} and ΔH_{pc} versus $\Delta P_p/P_s$ for constant H_{ic} also ΔM_{pc} versus ΔH_{pc} for constant M_{ic} and H_{ic}	240
CHART 8.16 $\Delta M_{pc}/\Delta V_{pc}$ versus M_{ic} for constant H_{ic}	251
CHART 8.17 M_{ic} versus $\Delta M_{pc}/(\Delta P_p/q_{cic})$	256
CHART 8.18 $\Delta P_p/q_{cic}$ versus ΔM_{pc} for constant M_{ic}	260
TABLE 9.2 and 9.3 United States Standard Atmosphere	265
TABLE 9.4 Mach Number for various values of q_c/P_a $q_c/P_a \leq 0.893$ ($M \leq 1.0$)	309
TABLE 9.5 Mach Number for various values of q_c/P_a for $M \geq 1.0$	313
TABLE 9.6 Differential Pressure, q_c for various values of V_c	321
TABLE 9.7 Centigrade - Fahrenheit Conversion Table	337

CHAPTER TWO		Page
CHART 2.31	Manifold Pressure Correction. (For change in Supercharger Inlet Air Temperature) P_2/P_1 , CAT	2-31
CHART 2.32	Manifold Pressure Correction (For change in Carburetor Inlet Air Temperature) P_2/P_1 , CAT	2-32
CHART 2.33	Ram Pressure Ratio - Ram Efficiency - Mach Number M , P_{t2}/P_a , η_R	2-33
CHAPTER THREE		
CHART 9.1	Relation between Total Pressure Recovery and Ram Efficiency	3-68
CHART 9.2	Total Pressure Recovery for Inlets with Sharp Lips	3-69
CHART 9.3	Turbulent Boundary Layer Thickness for Flat-Plates at Zero Angle of Attack as a Function of Flight Speed and Altitude	3-70
CHART 9.4	Pressure Recovery of Boundary Layer Air Admitted into Side-Inlet Installation - Turbulent Flow	3-71
CHART 9.5	Total Momentum Ratio for Various Scoop Height to Boundary Layer Ratios	3-73
CHART 9.6	Total Pressure Recovery for Straight Subsonic Diffusers	3-74
CHART 9.7	Total Pressure Loss in Compound Subsonic Diffuser Bends	3-76
CHART 9.8	M_0 versus P_{t1}/P_{t0} - Normal Shock Conditions	3-77
CHART 9.9	Total Pressure Ratios for 2-Dimensional 2-Shock Compression	3-78
CHART 9.10	Total Pressure Ratios for 2-Dimensional 3-Shock Compression	3-79
CHART 9.11	Total Pressure Ratios for Conical 2-Shock Compression	3-80
CHART 9.12	Mach Number Change Through an Oblique Shock for a Two-Dimensional Wedge	3-81
CHART 9.13	Total Pressure Ratio Across an Oblique Shock for a Two-Dimensional Wedge	3-82
CHART 9.14	Theoretical Additive-Drag Coefficients for Open-Nosed Inlets	3-83
CHART 9.15	Theoretical Additive-Drag Coefficients for Annular Nose Inlets with Conical Flow at the Inlet	3-84
CHART 9.16	Change in Cowl Drag Coefficient with a Change in Mass Flow Ratio as a Function of Mach Number	3-85
CHART 9.17	Idealized Gas Flow with Subcritical Operation	3-86
CHART 9.18	Idealized Gas Flow with Supercritical Operation - Converging Nozzle	3-87
CHART 9.19	Gross Thrust Parameter versus Nozzle Pressure Ratio with Subcritical Operation	3-90
CHART 9.20	Gross Thrust Parameter versus Nozzle Pressure Ratio with Supercritical Operation - Converging Nozzle.	3-91

CHART 9.21	Gross Thrust Parameter versus Nozzle Pressure Ratio with Supercritical Operation - Converging - Diverging Nozzle	3-94
CHART 9.22	P_t'/P_t^s versus Mach Number (Rayleigh Supersonic Pitot Formula)	3-97

CHAPTER FOUR

CHART 4.41	Power Correction for Weight Change $W_t, \Delta W, b, M, H_c$	4-49
CHART 4.71	Natural Log of Initial to Final Gross Weight Ratio for Range and Endurance Computations $W_1/W_2, \log_e W_1/W_2$	4-55
CHART 4.72	Gross Weight Factor for Range and Endurance Computations $W, 2/\sqrt{W}$	4-56

CHAPTER FIVE

CHART 5.21	Rate of Climb Power Correction for Temperature Variation $MP_t/P_a, \sqrt{T_{at}/T_{as}}, W_t$	5-35
CHART 5.22	Turbojet Rate of Climb Power Correction Factor H_c, M, W_t	5-36
CHART 5.23	Turbojet Rate of Climb Power Correction Factor $W/\delta_a, H_c$	5-38
CHART 5.31	Rate of Climb Induced Drag Correction Factor H_c, M, b	5-40
CHART 5.41	Rate of Climb Vertical Wind Gradient Correction Factor $H_c, V_c, dV_w/dh$	5-42
CHART 5.51	Rate of Climb Acceleration Correction Factor H_c, V_c	5-43
CHART 5.52	Rate of Climb Acceleration Correction Factor $H_c, V_c, dV_c/dH_c$	5-44

APPENDIX I

CHART I-1	Density Altitude Charts	8-5
CHART I-2	Differential-Static Pressure Ratio versus Mach Number (Supersonic-Normal Shock Condition)	8-17
CHART I-3	Reynolds Number-Mach Number Ratio versus Pressure Altitude	8-18
CHART I-4	Supersonic (Isentropic) Mach Number Functions	
	M versus P_t/P_s	8-20
	M versus q/P_s	8-21
	M versus q/P_t	8-22
	M versus ρ_t/ρ_s	8-23
	M versus T_t/T_s	8-24
CHART I-5	Supersonic (Normal Shock Conditions) Mach Number Functions	
	M versus P_t'/P_s	8-25
	M versus P_s'/P_s	8-26
	M versus P_t'/P_t	8-27
	M versus ρ_s'/ρ_s	8-28
	M versus T_s'/T_s	8-29
	M versus M'	8-30
	M versus V'/V	8-31
	M versus a'/a	8-32
CHART I-6	Psychrometric Chart	8-33

APPENDIX II

CHART II-1	Nomenclature	8-35
CHART II-2	Physical Information and Systems of Units	8-46
CHART II-3	Conversion Tables	8-47

INTRODUCTION

No single or rigid method of data analysis and presentation has been set down in this report. Rather, an attempt has been made to show various methods of data standardization and plotting. The flight testing agency can best determine the procedures most suited to the particular test, type of aircraft, or type of report desired.

Considerable detail concerning the derivation of correction factors and performance parameters has been included. The function of these derivations is not to prove the results, but to show the methods. When performance analysis problems result from new type of aircraft, engines, or flight conditions, these methods of deriving corrections and parameters may be useful as a starting point.

Aircraft stability and control tests and methods are not included, but will be the subject of a separate report.

Although extreme care was taken in the preparation of this report, there is a possibility that errors are present. Please address correspondence to,

COMMANDER
AIR FORCE FLIGHT TEST CENTER
EDWARDS AIR FORCE BASE
EDWARDS, CALIFORNIA
ATTN: Flight Research Division, FTTER

SYMBOLS USED IN CHAPTER ONE

<u>Term</u>	<u>Definition</u>	<u>Units</u>
a	Speed of sound, $38.967 \sqrt{T_a(^{\circ}K)}$	knots
a _s	Standard day speed of sound, $38.967 \sqrt{T_{as}(^{\circ}K)}$	knots
a _t	Test day speed of sound, $38.967 \sqrt{T_{at}(^{\circ}K)}$	knots
a _{SL}	Speed of sound at standard sea level; 661.48	knots
°C	Degrees centigrade	
C _L	Airplane lift coefficient, $nW/(\rho V_t^2 S/2)$	
C _{Lic}	"Indicated" lift coefficient, $nW/\rho P_s M_{ic}^2 S/2)$	
d	Differential Example: dH _{ic} = differential indicated pressure altitude corrected for instrument error	
d/dt	Time rate of change Example: dH _{ic} /dt = time rate of change of indicated pressure altitude corrected for instrument error	
f _n	Function of () Example: P _s = f ₂ (H _{ic}). This means that P _s is a function of H _{ic} . In other words, P _s may be determined if H _{ic} is known.	
g	Acceleration due to gravity at a point	feet/second ²
g _{SL}	Acceleration due to gravity at standard sea level	32.17405 feet/second ²
G	Gravitational constant	32.17405 feet ² /second ² - geopotential feet
h	Tapeline altitude	feet
H	Geopotential at a point (this is a measure of the gravitational potential energy of a unit mass at this point relative to mean sea level)	geopotential feet
H _c	Pressure altitude, $H_i + \Delta H_{ic} + \Delta H_{icf} + \Delta H_{pc}$	feet
"Hg	Inches of mercury	
H _i	Indicated pressure altitude	feet
H _{ic}	Indicated pressure altitude corrected for instrument error, $H_i + \Delta H_{ic}$	feet

ΔH_{ic}	Altimeter instrument correction	feet
H_{icl}	Indicated pressure altitude corrected for instrument and lag errors, $H_i + \Delta H_{ic} + \Delta H_{icl}$	feet
ΔH_{icl}	Altimeter lag correction	feet
ΔH_p	Altimeter position error corresponding to ΔP_p	feet
ΔH_{pc}	Altimeter position error correction	feet
K_n	A constant Example: $K_5 = 52.86784$	
K	Temperature probe recovery factor	
$^{\circ}K$	Degrees Kelvin	
m	The slope of a line at a point	
M	Flight or free stream Mach number	
M_i	Indicated Mach number	
M_{ic}	Indicated Mach number corrected for instrument error, $M_i + \Delta M_{ic}$	
ΔM_{ic}	Machmeter instrument correction	
ΔM_p	Machmeter position error corresponding to ΔP_p	
ΔM_{pc}	Machmeter position error correction	
n	Load factor	
N_{Pr}	Prandtl number, $\mu/\rho d$ where d is the thermal diffusivity	
N_R	Reynolds number, $\rho L V/\mu$ where L is a characteristic length and V is axial velocity	
P	The applied pressure at time t	"Hg
P_a	Atmospheric pressure corresponding to H_c	"Hg
P_{aSL}	Atmospheric pressure at standard sea level	29.92126"Hg
P_i	The indicated pressure at time t	"Hg
ΔP_p	Static pressure error (or position error)	"Hg
P_s	Pressure corresponding to H_{ic}	"Hg
P_t	Free stream total pressure	"Hg

P_t'	Total pressure at total pressure source (for subsonic speeds, P_t' is equal to the free stream total pressure, P_t . For supersonic speeds, P_t' is equal to the total pressure behind the shock which forms in front of the probe and is therefore not equal to P_t).	"Hg
q	Dynamic pressure, $q = \rho V_t^2 / 2 = 0.7 P_a M^2$	"Hg
q_c	Differential pressure, $P_t' - P_a$ (q_c is also called impact pressure or compressible dynamic pressure)	"Hg
q_{cic}	Differential pressure corresponding to V_{ic} , $P_t' - P_s$	"Hg
r	Radius of the earth	feet
R	Gas constant for dry air	3089.67 feet ² / °K second ²
S	Total wing area	feet ²
t	Time	seconds
t_a	Atmospheric temperature	°C
t_{as}	Standard day atmospheric temperature corresponding to H_c	°C
t_{aSL}	Standard sea level atmospheric temperature	15°C
t_{at}	Test day atmospheric temperature	°C
t_i	Indicated temperature	°C
t_{ic}	Indicated temperature corrected for instrument error, $t_i + \Delta t_{ic}$	°C
Δt_{ic}	Air temperature instrument correction	°C
T_a	Atmospheric temperature	°K
T_{as}	Standard day atmospheric temperature corresponding to H_c	°K
T_{aSL}	Standard sea level atmospheric temperature	288.16°K
T_{at}	Test day atmospheric temperature	°K
T_i	Indicated Temperature	°K
T_{ic}	Indicated temperature corrected for instrument error, $T_i + \Delta T_{ic}$	°K

ΔT_{ic}	Air temperature instrument correction	$^{\circ}\text{K}$
T_t	Total temperature	$^{\circ}\text{K}$
V_c	Calibrated airspeed, $V_i + \Delta V_{ic} + \Delta V_{ic\ell} + \Delta V_{pc}$	knots
V_e	Equivalent airspeed, $V_c + \Delta V_c$ or $V_t \sqrt{\sigma}$	knots
V_i	Indicated airspeed	knots
V_{ic}	Indicated airspeed corrected for instrument error, $V_i + \Delta V_{ic}$	knots
ΔV_{ic}	Airspeed indicator instrument correction	knots
$V_{ic\ell}$	Indicated airspeed corrected for instrument and lag errors, $V_i + \Delta V_{ic} + \Delta V_{ic\ell}$	knots
$\Delta V_{ic\ell}$	Airspeed indicator lag correction	knots
ΔV_p	Airspeed indicator position error corresponding to ΔP_p	knots
ΔV_{pc}	Airspeed indicator position error correction	knots
V_t	True airspeed	knots
V_{ts}	Standard day true airspeed	knots
V_{tt}	Test day true airspeed	knots
W	Aircraft gross weight	pounds
α	Angle of attack	
β	Angle of sideslip	
r	Ratio of specific heats, 1.40 for air	
δ	P_a/P_{aSL}	
δ_{ic}	P_s/P_{aSL}	
θ	T_a/T_{aSL}	
θ_s	T_{as}/T_{aSL}	
θ_t	T_{at}/T_{aSL}	
λ	Lag constant	seconds
λ_{Hic}	Lag constant corresponding to H_{ic}	seconds
λ_s	Static pressure lag constant	seconds
λ_{SL}	Lag constant at standard sea level	seconds
λ_{sSL}	Static pressure lag constant at standard sea level	seconds

λ_t	Total pressure lag constant	seconds
λ_{tSL}	Total pressure lag constant at standard sea level	seconds
μ	Viscosity at temperature T_a	pounds - second/feet ²
$\mu_{H_{ic}}$	Viscosity corresponding to H_{ic}	pounds - second/feet ²
μ_{SL}	Viscosity at standard sea level	3.7452×10^{-7} pounds - second/feet ²
ρ	Air density	slugs/feet ³
ρ_s	Standard day air density corresponding to H_c	slugs/feet ³
ρ_{SL}	Air density at standard sea level	0.0023769 slugs/feet ³
ρ_t	Test day air density	slugs/feet ³
σ	ρ/ρ_{SL}	
σ_s	ρ_s/ρ_{SL}	
σ_t	ρ_t/ρ_{SL}	
τ	Acoustic lag	seconds

CHAPTER ONE

SECTION 1

THE STANDARD ATMOSPHERE

The performance of an aircraft is influenced by the pressure and temperature of the air through which the aircraft is flying. Studies of the earth's atmosphere have shown that these quantities depend primarily on altitude, and vary relatively little from day to day. Consequently, a "standard" atmosphere can be usefully established by definition of a pressure and temperature for each altitude. This standard will approximate the atmospheric conditions for any day fairly closely. By applying small corrections to data acquired on a non-standard day, the data may be reduced to the standard day. This makes possible comparison of results obtained on other days with the same aircraft and with other aircraft.

1.1 THE UNITED STATES STANDARD ATMOSPHERE

For many years a standard atmosphere based on NACA Report No. 218, "Standard Atmosphere - Tables and Data," has been used in the United States. Recently many organizations including the Air Research and Development Command of the United States Air Force have adopted a new standard, the United States Standard Atmosphere, which is consistent with that of the International Civil Aviation Organization. This new standard atmosphere is discussed in NACA Report No. 1235, "Standard Atmosphere - Tables and Data for Altitudes to 65,800 Feet." All charts and tables in this manual are based on the US Standard Atmosphere.

1.1.1 Basic Assumptions:

The United States Standard Atmosphere is derived from the following assumptions which closely approximate true atmospheric conditions:

- (1) The air is dry
- (2) The atmosphere is a perfect diatomic gas:

$$P_a = \rho RT_a \quad 1.1$$

In specific units

$$\rho = 0.022891 \frac{P_a}{T_a} \quad 1.2$$

$$\sigma = 9.6306 \frac{P_a}{T_a} \quad 1.3$$

where

- P_a = atmospheric pressure, "Hg
- T_a = atmospheric temperature, °K
- ρ = atmospheric density, slugs/ft³
- R = the gas constant for dry air, 3089.7 ft²/sec² °K
- σ = density ratio, ρ/ρ_{SL}

(3) Hydrostatic equilibrium exists:

$$dP_a = -\rho g dh \quad 1.4$$

This equation is derived from a consideration of the forces acting in the vertical direction on a small column of air of unit area. (See Figure 1.1)

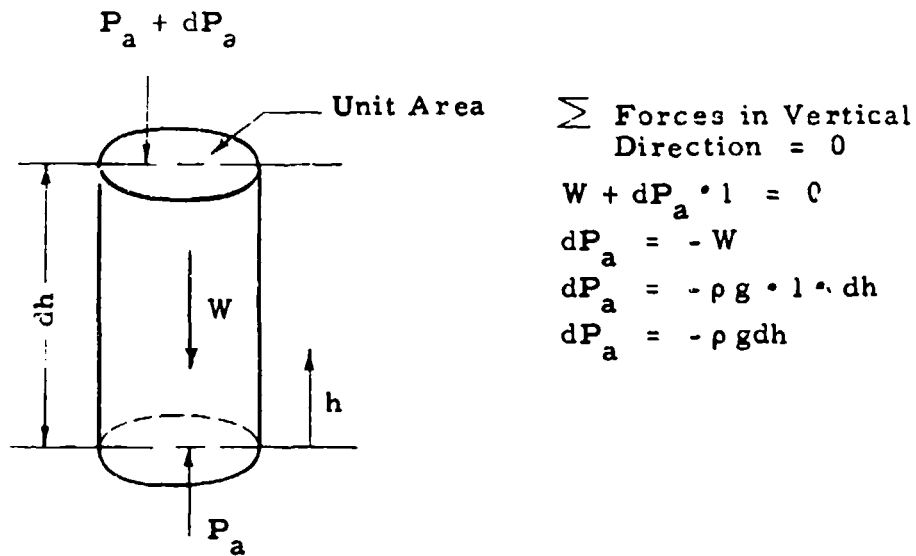


Figure 1.1

Forces Acting on a Small Column of Air of Unit Area

(4) The measure of vertical displacement is geopotential. Geopotential is a measure of the gravitational potential energy of a unit mass at a point relative to mean sea level. It is defined in differential form by the equation

$$G dH = g dh \quad 1.5$$

where

- h = tapeline altitude; i. e., the actual distance from mean sea level to a point in the atmosphere, feet
- g = acceleration due to gravity at the same point, feet/sec²
- H = geopotential at the point, geopotential feet
- G = a dimensional constant, 32.17405 ft²/sec² - geopotential feet) for the above system of units

Each point in the atmosphere has a definite geopotential as "g" is a function of latitude and altitude.

(5) Sea level pressure is 760 mm Hg or 29.92126 inches Hg

(6) Sea level temperature is 15°C or 288.16°K

(7) Temperature variation with geopotential is expressed as a series of straight line segments:

- (a) The temperature lapse rate in the troposphere (sea level to 36,089 geopotential feet) is 0.00198120°C/geopotential feet.
- (b) The temperature above 36,089 geopotential feet and below 82,021 geopotential feet is constant -56.50°C. (The latest issue of "The ARDC Model Atmosphere" should be consulted for data above 82,021 geopotential feet.)

1.1.2 Relationship Between Variables:

From the basic assumptions listed above it is possible to express the atmospheric pressure, temperature, and density as functions of geopotential.

Introducing the definition of geopotential (Equation 1.5) into the equilibrium equation 1.4,

$$dP_a = -\rho G dH \quad 1.6$$

Eliminating ρ by means of the perfect gas equation 1.1,

$$\frac{dP_a}{P_a} = -\frac{G}{R} \frac{dH}{T_a} \quad 1.7$$

Assumption(7) above expresses

$$T_a = f_1(H) \text{ only.}$$

Hence, integration of equation 1.7 is possible with the result

$$P_a = f_2(H) \text{ only.}$$

Finally, from the perfect gas equation,

$$\rho = f_3(H) \text{ only.}$$

For geopotentials below 36,089 geopotential feet

$$\theta = \frac{T_a}{T_{aSL}} = (1 - K_1 H) \quad 1.8$$

$$\delta = \frac{P_a}{P_{aSL}} = (1 - K_1 H)^{5.2561} \quad 1.9$$

$$\sigma = \frac{\rho}{\rho_{SL}} = (1 - K_1 H)^{4.2561} \quad 1.10$$

where

$$K_1 = 6.87535 \times 10^{-6} / \text{geopotential feet}$$

For geopotentials above 36,089 geopotential feet and below 82,021 geopotential feet

$$T_a = -56.50^\circ\text{C} = 216.66^\circ\text{K} \quad 1.11$$

$$\delta = \frac{P_a}{P_{aSL}} = 0.223358 e^{-K_2(H - K_3)} \quad 1.12$$

$$\sigma = \frac{\rho}{\rho_{SL}} = 0.29707 e^{-K_2(H - K_3)} \quad 1.13$$

where

$$K_2 = 4.80634 \times 10^{-5} / \text{geopotential feet}$$

$$K_3 = 36,089.24 \text{ geopotential feet}$$

From the above equations, pressure, temperature, and density, plus several other parameters useful in flight test are tabulated in Table 9.2 for incremental geopotentials of 100 geopotential feet. In addition, P_a in inches Hg and δ are tabulated in Table 9.3 for every 10 geopotential feet. A summary of basic data is given in Table 9.1.

1.1.3 Determination of Tapeline Altitude:

In flight testing, the exact position in space is usually not important; altitude is important only as a means of describing the properties of the air through which the test aircraft is flying. Hence, it

is seldom necessary to determine tapeline altitude. It is sufficient to express the atmospheric properties in terms of geopotential.

If one finds it necessary to determine the tapeline altitude, the acceleration of gravity as a function of tapeline altitude must be defined to allow integration of equation 1.5. An approximate expression is obtained by assuming that the altitude variation of the acceleration of gravity from its sea level value is given by the Newtonian inverse square law*

$$g = g_{SL} \left(\frac{r}{r+h} \right)^2 \quad 1.14$$

where

g_{SL} = the sea level value of the acceleration of gravity, 32.17405 ft/sec²

r = radius of the earth, 20,930,000 feet

h = tapeline altitude, feet.

Introducing this expression into equation 1.5 and integrating yields

$$H = \frac{g_{SL}}{G} \left(\frac{rh}{r+h} \right) \quad 1.15$$

where

$G = 32.17405 \text{ ft}^2/\text{sec}^2$ - geopotential feet

Solving for $h - H(G/g_{SL})$

$$h - H \left(\frac{G}{g_{SL}} \right) = \frac{H^2 \left(\frac{G}{g_{SL}} \right)^2}{\left(r - H \frac{G}{g_{SL}} \right)} \quad 1.16$$

where

$G/g_{SL} = 1 \text{ ft/geopotential feet}$

A plot of altitude correction factor, $h - H(G/g_{SL})$, versus $H(G/g_{SL})$ is given in Chart 8.1. This factor, when added to the geopotential,

*Use of the Newtonian inverse square law is based on the assumption that the earth is a nonrotating sphere composed of spherical shells of equal density. This assumption is very good at altitudes attained in routine flight test work ($H < 100,000$ geopotential feet). For higher altitudes, a more sophisticated analysis may be necessary. A method which is good to several million feet is given in AFCRC TN-56-204, "The ARDC Model Atmosphere, 1956," by R. A. Minzner and W. S. Ripley.

$H(G/g_{SL})$, will give the corresponding tapeline altitude.

1.2 THE NON-STANDARD ATMOSPHERE

Flight test data is always reduced to a standard day so that comparison may be made among data obtained on different days. The usual technique is to present the data in terms of pressure altitude. (Pressure altitude is defined as the geopotential at which a given pressure is found in the standard atmosphere.) Whether found in a standard atmosphere or non-standard atmosphere, any given pressure indicates one and only one corresponding pressure altitude. Therefore, reduction to a standard day consists of making corrections for temperature to the value given in the standard atmosphere corresponding to the test day pressure altitude (or pressure).

The pressure altitude and geopotential are not simply related on a non-standard day. If the geopotential is desired, it is necessary to make a survey of the atmosphere to determine T_a as a function of P_a to allow integration of equation 1.7. Fortunately, this operation is seldom required. However, the computation is outlined in NACA Report No. 538, "Altitude - Pressure Tables Based on the United States Standard Atmosphere".

SECTION 2
THEORY OF ALTITUDE, AIRSPEED, MACH NUMBER AND AIR
TEMPERATURE MEASUREMENT

Pressure altitude, airspeed, Mach number and free air temperature are basic parameters in the performance of aircraft. The instruments used to measure these quantities are the altimeter, the airspeed indicator, the machmeter, and the free air temperature probe. The basic theory of the construction and calibration of these instruments is given in this section. The actual methods employed in their calibration will be given in subsequent sections.

2.1 THE ALTIMETER

Most altitude measurements are made with a sensitive absolute pressure gage, called an altimeter, scaled so that a pressure decrease indicates an altitude increase in accordance with the U.S. Standard Atmosphere. If the altimeter setting* is 29.92, the altimeter will read pressure altitude whether in a standard or non-standard atmosphere.

$$\frac{P_a}{P_{aSL}} = (1 - 6.87535 \times 10^{-6} H_c)^{5.2561}$$

for $H_c < 36,089$ ft 2.1

$$\frac{P_a}{P_{aSL}} = 0.223358 e^{-4.80634 \times 10^{-5} (H_c - 36,089.24)}$$

for $36,089 < H_c < 82,021$ ft 2.2

where

P_a = atmospheric pressure, inches Hg

H_c = pressure altitude, feet

P_{aSL} = 29.92126 inches Hg

*The altimeter setting is an adjustment that allows the scale to be moved so that the altimeter can be made to read field elevation when the aircraft touches the ground. In flight testing, the altimeter setting should be 29.92 in order that the altimeter reading will be pressure altitude.

The altimeter is constructed and calibrated according to this relationship.

The heart of the altimeter is an evacuated metal bellows which expands or contracts with changes in outside pressure. The bellows is connected to a series of gears and levers which cause a pointer to move as the bellows expands or contracts. The whole mechanism is placed in an airtight case which is vented to a static pressure source; the indicator then reads the pressure supplied to the case. The dial is calibrated to indicate pressure altitude. The altimeter construction is shown in Figure 2.1

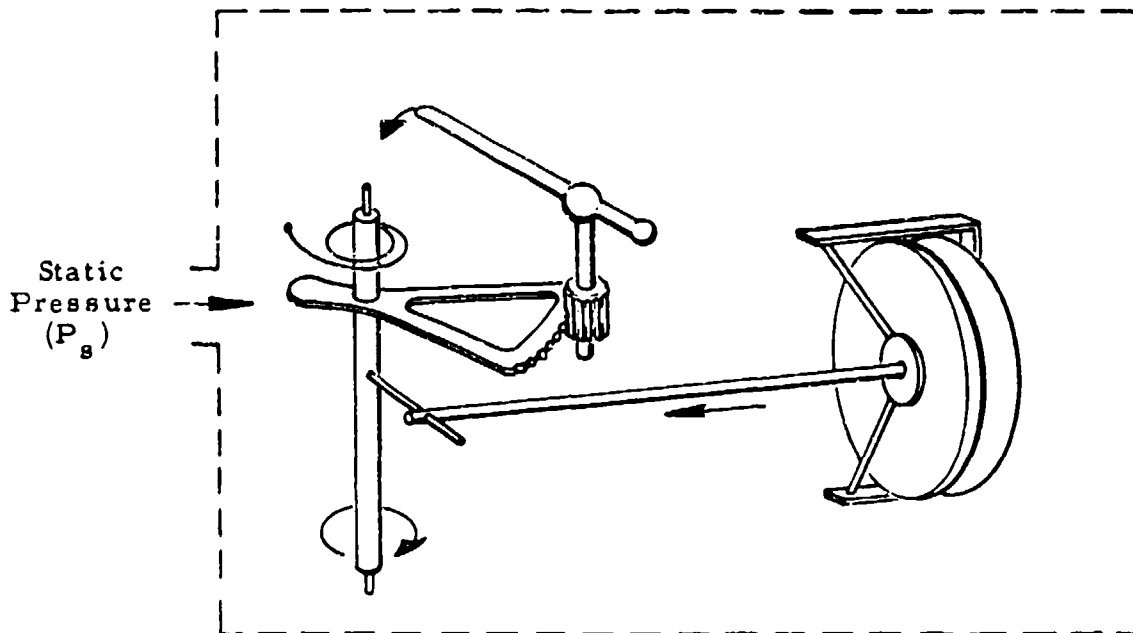


Figure 2.1
Altimeter Schematic

The static pressure measured at the static source of the altimeter (P_s) may differ slightly from the atmospheric pressure (P_a). For any

P_s , the altimeter, when corrected for instrument error,* will indicate the corresponding indicated pressure altitude corrected for instrument error (H_{ic}).

$$\frac{P_s}{P_{aSL}} = (1 - 6.87535 \times 10^{-6} H_{ic})^{5.2561}$$

for $H_{ic} < 36,089$ ft 2.3

$$\frac{P_s}{P_{aSL}} = 0.223358 e^{-4.80634 \times 10^{-5} (H_{ic} - 36,089.24)}$$

for $36,089 < H_{ic} < 82,021$ 2.4

The quantity $P_s - P_a$ is called the static pressure error or position error. The value which is added to H_{ic} to determine H_c is termed the altimeter position error correction. The position error corrections for the altimeter and the other instruments will be considered in later sections.

The altimeters available and their expected characteristics are:

<u>Type</u>	<u>Range - ft</u>	<u>Readability - ft</u>	<u>Repeatability</u>
C-12	0 to 50,000	5	Determined by calibration
C-19	0 to 80,000	5	

2.2 THE AIRSPEED INDICATOR

True airspeed (V_t) is the velocity of an aircraft with respect to the air through which it is flying. It is difficult to measure V_t directly. Instead, it is usually determined from calibrated airspeed (V_c), atmospheric pressure (P_a), and atmospheric temperature (T_a). V_c is obtained from a conventional airspeed indicator, P_a is measured with an altimeter, and T_a is measured with a free air temperature probe.

*The instrument error is an error built into the instrument consisting of such things as scale error and hysteresis. This error is discussed in Section 3.

The airspeed indicator operates on the principle of Bernoulli's compressible equation for frictionless adiabatic (isentropic) flow in which airspeed is expressed as the difference between **total** and static pressures. Therefore, the airspeed indicator consists of a pitot-static pressure system which is used to measure the difference between total and static pressures.

At subsonic speeds Bernoulli's equation expressed as follows is applicable

$$\frac{q_c}{P_a} = \left[1 + \frac{\gamma - 1}{2} \left(\frac{V_t}{a} \right)^2 \right]^{\frac{\gamma}{\gamma - 1}} - 1 \quad 2.5$$

where:

$q_c = P_t - P_a =$ differential pressure. (This is equal to the free stream impact pressure or compressible dynamic pressure ($P_t - P_a$) for subsonic flow)

$P_t =$ free stream total pressure

$P_a =$ free stream static pressure (or atmospheric pressure)

$\gamma =$ ratio of specific heats

$V_t =$ true airspeed

$a =$ local atmospheric speed of sound

For air, $\gamma = 1.40$. Equation 2.5 becomes

$$\frac{q_c}{P_a} = \left[1 + 0.2 \left(\frac{V_t}{a} \right)^2 \right]^{3.5} - 1 \quad 2.6$$

For supersonic flight, a shock wave will form in front of the total pressure probe. Therefore equation (2.5, 2.6) is no longer valid. The solution for supersonic flight is derived by considering a normal shock compression in front of the total pressure tube and an isentropic compression in the subsonic region aft of the shock. The normal shock assumption is good as the pitot tube has a small frontal area so that the radius of the shock in front of the hole may be considered infinite. The resulting equation, known as the Rayleigh supersonic pitot equation, relates the total pressure behind the shock to the free stream ambient

pressure.

$$\frac{q_c}{P_a} = \left[\frac{\gamma + 1}{2} \left(\frac{V_t}{a} \right)^2 \right]^{\frac{\gamma}{\gamma - 1}} \left[\frac{\gamma + 1}{1 - \gamma + 2\gamma \left(\frac{V_t}{a} \right)^2} \right]^{\frac{1}{\gamma - 1}} - 1 \quad 2.7$$

where

$q_c = P_t' - P_a =$ differential pressure. (This is not equal to the free stream impact pressure or compressible dynamic pressure, $P_t - P_a$, for supersonic flow as $P_t' \neq P_t$.)

$P_t' =$ total pressure at total pressure pickup behind the shock. (This is not equal to the free stream total pressure (P_t) for supersonic flight.)

For air, $\gamma = 1.40$. Equation 2.7 becomes

$$\frac{q_c}{P_a} = \frac{7 \left(\frac{V_t}{a} \right)^2 - 1}{6} \left\{ \frac{36 \left(\frac{V_t}{a} \right)^2}{5 \left[7 \left(\frac{V_t}{a} \right)^2 - 1 \right]} \right\}^{3.5} - 1 \quad 2.8$$

This may be written more conveniently in the form

$$\frac{q_c}{P_a} = \frac{K_3 \left(\frac{V_t}{a} \right)^7}{\left[7 \left(\frac{V_t}{a} \right)^2 - 1 \right]^{2.5}} - 1 \quad 2.9$$

where

$$K_3 = \frac{(7.2)^{3.5}}{6} = 166.921$$

Examination of equations (2.5, 2.6) and (2.7, 2.8, 2.9) shows that the true velocity (V_t) is dependent on the local atmospheric properties, speed of sound (a), and static pressure (P_a), as well as the differential pressure (q_c). Therefore, an airspeed indicator measuring differential pressure can be made to read true airspeed at one and only one atmospheric condition. Standard sea level is taken for this condition. Therefore, the dial of the airspeed indicator is scaled so that a given differential pressure will indicate a speed in accordance with equations 2.6 and (2.8, 2.9) in which sea level standard a and P_a are inserted. This sea level standard value of V_t is defined as calibrated airspeed (V_c).

$$\frac{q_c}{P_{aSL}} = \left[1 + 0.2 \left(\frac{V_c}{a_{SL}} \right)^2 \right]^{3.5} - 1 \quad 2.10$$

for $V_c \leq a_{SL}$, and

$$\frac{q_c}{P_{aSL}} = \frac{166.921 \left(\frac{V_c}{a_{SL}} \right)^7}{\left[7 \left(\frac{V_c}{a_{SL}} \right)^2 - 1 \right]^{2.5}} - 1 \quad 2.11$$

for $V_c \geq a_{SL}$.

where

q_c = differential pressure, inches Hg

V_c = calibrated airspeed, knots

a_{SL} = 661.48 knots

P_{aSL} = 29.92126 inches Hg

Airspeed indicators are constructed and calibrated according to these equations.

In operation, the airspeed indicator is similar to the altimeter, but, instead of being evacuated, the inside of the capsule is connected to a total pressure source and the case to the static pressure source. The instrument then senses total pressure (P_t') within the capsule and static pressure (P_s) outside it as shown in Figure 2.2.

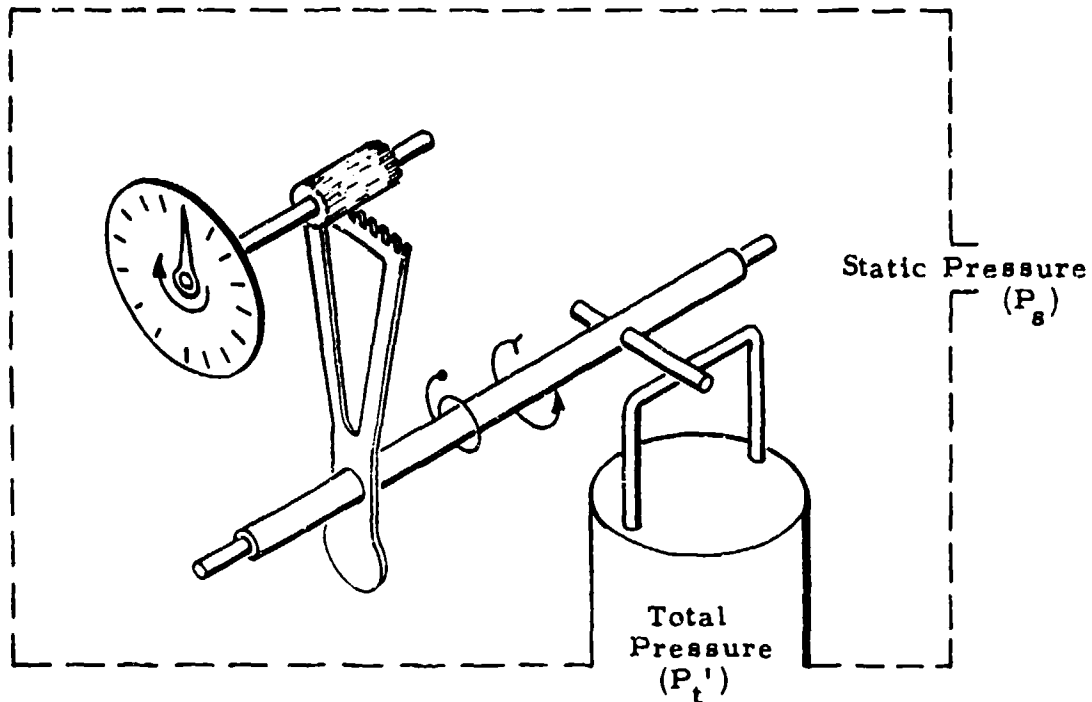


Figure 2.2
Airspeed Indicator Schematic

For any indicated differential pressure (q_{cic}) felt by the instrument, the airspeed indicator, when corrected for instrument error, will indicate the corresponding indicated airspeed corrected for instrument error (V_{ic}), or

$$\frac{q_{cic}}{\rho a_{SL}^2} = \left[1 + 0.2 \left(\frac{V_{ic}}{a_{SL}} \right)^2 \right]^{3.5} - 1 \quad 2.12$$

for $V_{ic} \leq a_{SL}$ and

$$\frac{q_{cic}}{\rho a_{SL}^2} = \frac{166.921 \left(\frac{V_{ic}}{a_{SL}} \right)^7}{\left[7 \left(\frac{V_{ic}}{a_{SL}} \right)^2 - 1 \right]^{2.5}} - 1 \quad 2.13$$

for $V_{ic} \geq a_{SL}$.

In the general case, q_{cic} will differ from q_c as a result of static pressure error. As a result, an airspeed position error correction must be added to V_{ic} to obtain V_c , the desired result. This correction will be discussed in later sections.

q_{cic} in inches Hg is given for various values of V_{ic} in knots in Table 9.5. This table is also good as q_c in inches Hg versus V_c in knots.

At the present time, the following airspeed indicators are commonly used in flight test work.

<u>Type</u>	<u>Range</u>	<u>Readability</u>	<u>Repeatability</u>
F-1	50 to 650 knots	0.5 knots	Determined by calibration
059	50 to 850 knots	0.5 knots	
0153	10 to 150 miles per hour	0.5 miles per hour	

Calibrated airspeed (V_c) represents the true velocity of the aircraft (V_t) at standard sea level conditions only. V_t may be determined at altitude by a knowledge of atmospheric pressure and density (or temperature).

The equivalent airspeed (V_e) is defined as

$$V_e = V_t \sqrt{\sigma} \quad 2.14$$

where σ is the density ratio, ρ/ρ_{SL} .

Solving the subsonic equation 2.6 for V_t^2 .

$$V_t^2 = 5a^2 \left[\left(\frac{q_c}{P_a} + 1 \right)^{2/7} - 1 \right] \quad 2.15$$

The speed of sound in a perfect gas may be expressed as

$$a = \sqrt{\frac{\gamma P_a}{\rho}} \quad 2.16$$

Introducing V_e^2/σ for V_t^2 and replacing $a^2\sigma$ by $\gamma P_a/\rho_{SL}$:

$$V_e = \sqrt{\frac{\gamma P_a}{\rho_{SL}} \left[\left(\frac{q_c}{P_a} + 1 \right)^{2/7} - 1 \right]} \quad 2.17$$

Introducing equation 2.10, the following result is obtained:

$$\frac{V_e}{V_c} = \left\{ \frac{\left[\left(\frac{q_c}{P_a} + 1 \right)^{2/7} - 1 \right]}{\left[\left(\frac{q_c}{P_{aSL}} + 1 \right)^{2/7} - 1 \right]} \frac{P_a}{P_{aSL}} \right\}^{1/2} \quad 2.18$$

From equation 2.14, V_t is simply V_e corrected for the difference between sea level standard density and actual ambient density. This has been shown for subsonic flight only. It could similarly be shown to be true for supersonic flight as well.

This relationship between V_c and V_t is presented for explanation only; a shorter method of obtaining V_t from the same required variables is given later in Section 2.5.

2.3 MACH NUMBER AND THE MACHMETER

2.3.1 Mach Number:

Mach number (M) is defined as the ratio of the true airspeed to the local atmospheric speed of sound

$$M = \frac{V_t}{a} \quad 2.19$$

With the advent of high speed aircraft, Mach number has become a very important parameter in flight testing.

For isentropic flow of a perfect gas, Bernoulli's equation states

$$\frac{P_t}{P_a} = \left(1 + \frac{\gamma - 1}{2} M^2 \right)^{\frac{\gamma}{\gamma - 1}} \quad 2.20$$

where

P_t = free stream total pressure

P_a = free stream static pressure

γ = ratio of specific heats

For air, $\gamma = 1.40$. Equation 2.20 becomes

$$\frac{P_t}{P_a} = (1 + 0.2M^2)^{3.5} \quad 2.21$$

This equation which relates Mach number to the free stream total and static pressures is good for supersonic as well as subsonic flight. It

must be remembered however, that P_t' rather than P_t is measured in supersonic flight.

2.3.2 The Machmeter:

The Machmeter equation for subsonic flight is formed by inserting the definition for M into equation 2.6.

$$\frac{q_c}{P_a} = (1 + 0.2M^2)^{3.5} - 1 \quad 2.22$$

Solving for M

$$M = \sqrt{5 \left[\left(\frac{q_c}{P_a} + 1 \right)^{2/7} - 1 \right]} \quad 2.23$$

For supersonic flight, from equation 2.9

$$\frac{q_c}{P_a} = \frac{166.921M^7}{(7M^2 - 1)^{2.5}} - 1 \quad 2.24$$

Equation 2.24 cannot be solved explicitly for M . It can, however, be put in the following form which is convenient for rapid iteration:

$$M = \sqrt{\left(\frac{q_c}{P_a} + 1 \right) \frac{1}{K_4} \left(1 - \frac{1}{7M^2} \right)^{5/2}} \quad 2.25$$

where

$$K_4 = 1.287560$$

The machmeter is essentially a combination altimeter and airspeed indicator designed to solve these equations for Mach number. An altimeter capsule and an airspeed capsule simultaneously supply signals to a series of gears and levers to produce the Mach number indication. A machmeter schematic is given in Figure 2.3.

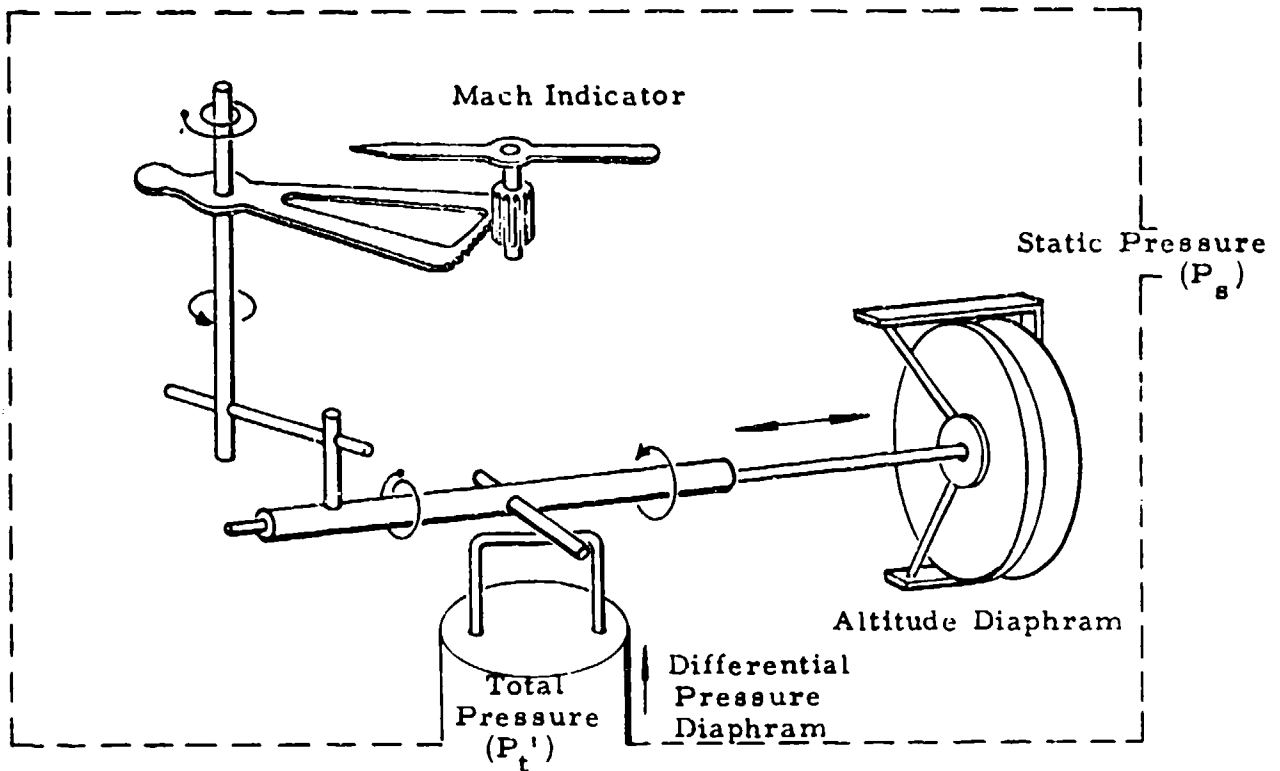


Figure 2.3
Machmeter Schematic

For any static pressure (P_s) and differential pressure ($q_{cic} = P_t' - P_s$) felt by the instrument, the Mach meter, when corrected for instrument error, will indicate the corresponding indicated Mach number corrected for instrument error (M_{ic}), or

$$\frac{q_{cic}}{P_s} = (1 + 0.2M_{ic}^2)^{3.5} - 1 \quad 2.26$$

for $M_{ic} \leq 1.00$, and

$$\frac{q_{cic}}{P_s} = \frac{166.921 M_{ic}^7}{(7M_{ic}^2 - 1)^{2.5}} - 1 \quad 2.27$$

for $M_{ic} \geq 1.00$.

The true Mach number (M) is determined from M_{ic} and the Mach meter position error correction which is a result of the static pressure error, $P_s - P_a$.

These equations relating M to q_c/P_a and M_{ic} to q_{cic}/P_s are useful not only as machmeter equations, but as a means for relating calibrated airspeed and pressure altitude to Mach number. M_{ic} is given for values of q_{cic}/P_s for $M_{ic} \leq 1.00$ in Table 9.4. q_{cic}/P_s is given for values of M_{ic} from 1.00 to 3.00 in Table 9.5. These tables can also be used to find M as a function of q_c/P_a .

At present the accuracy of these meters is **poor** so that they are not suitable for precision work, but as flight-safety indicators only. The machmeters in general use are:

<u>Type</u>	<u>Range</u>	<u>Readability</u>	<u>Repeatability</u>
A1	0.3 to 1.0; 0 to 50,000 feet	0.01	Determined by calibration
A2	0.5 to 1.5; 0 to 50,000 feet	0.01	
G09501	0.7 to 2.5; 0 to 60,000 feet	0.01	

2.4 FREE AIR TEMPERATURE PROBE

The atmospheric temperature is a measurement of the internal thermal energy of the air. Therefore, it is a very important parameter in aircraft and engine performance. Unfortunately, it is difficult to measure accurately in flight. If the air surrounding the probe is brought to a complete stop adiabatically and the probe correctly senses the resulting temperature then

$$\frac{T_{ic}}{T_a} = \frac{T_t}{T_a} = 1 + \frac{\gamma - 1}{2} M^2 \quad 2.28$$

where

T_{ic} = indicated temperature corrected for instrument error, °K

T_t = total temperature, °K

T_a = free stream static temperature, °K

M = free stream Mach number

For various reasons, such as radiation or heat leakage, most probes

do not register the full adiabatic temperature rise. It is, however, acceptable to write

$$\frac{T_{ic}}{T_a} = 1 + K \frac{\gamma - 1}{2} M^2 \quad 2.29$$

For air with $\gamma = 1.40$, this becomes

$$\frac{T_{ic}}{T_a} = 1 + K \frac{M^2}{5} \quad 2.30$$

The value of K represents the percentage of the adiabatic temperature rise detected by the probe and is called the probe recovery factor. For many installations it may be considered a constant, but it may vary with altitude and Mach number, particularly at supersonic speeds. K seldom is less than 0.90 for test installations and is usually between 0.95 and 1.00. Methods for determining K for a given installation are discussed in Section 6.2.

Equation 2.30 is plotted in Chart 8.2 as T_{ic}/T_a versus M for constant K and as T_a versus M for constant t_{ic} and K.

The free air thermometers now in use are all of the electrical resistance type. Their operation is based on the fact that the resistances of the sensing elements change with temperature. To obtain a signal from such a temperature sensing unit the element is placed in a bridge circuit. The circuit is designed so that the indicator registers the ratio of the current flow in two legs which makes the indication independent of the source voltage supply. (See Figure 2.4.)

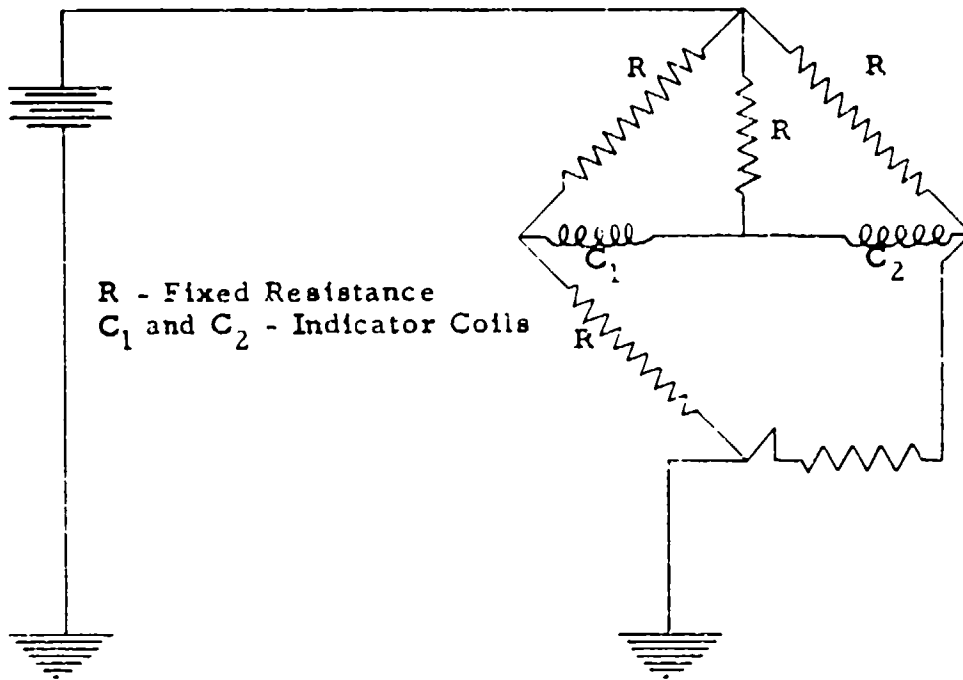


Figure 2.4

Resistance Temperature Bulb Bridge Circuit

The indicator consists of an ammeter whose armature contains both indicator coils wound so that the indication is proportional to the two currents. (See Figure 2.5)

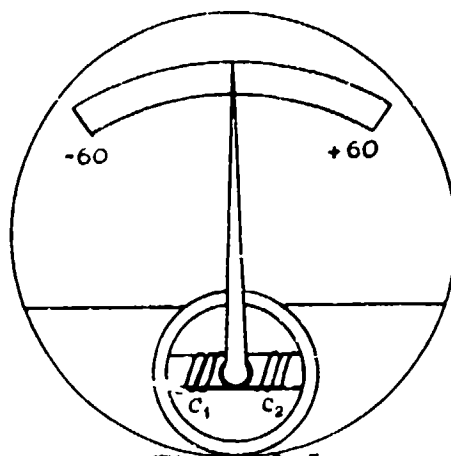


Figure 2.5
Construction of Resistance Temperature Bulb Indicator

The following instrument is in general use:

Type	Range	Readability	Accuracy
C-10	-60 to +60 degrees C (or other range as desired)	0.5 degrees C	± 0.5 degrees C

2.5 THE CALCULATION OF EQUIVALENT AIRSPEED, MACH NUMBER, AND STANDARD DAY TRUE AIRSPEED

2.5.1 Equivalent Airspeed:

The equivalent airspeed (V_e) is frequently used as a basis for reducing flight test data for piston-engined airplanes as it is a direct measure of the free stream dynamic pressure (q),

$$q = \frac{1}{2} \rho V_t^2 = \frac{1}{2} \rho_{SL} V_e^2 = K V_e^2 \quad 2.31$$

V_e may be expressed in terms of pressure altitude (H_c) and Mach number (M) as

$$\frac{V_e}{M} = a \sqrt{\sigma} \quad 2.32$$

This equation is plotted in Chart 8.3 as V_e/M versus H_c .

2.5.2 Mach Number:

The machmeter in its present form should not be used in precision flight test work as it is not sufficiently accurate. Therefore, Mach number must be determined by other means

If the true airspeed and ambient temperature are known, Mach number is defined by the relation

$$M = \frac{V_{tt}}{a_t} \quad 2.33$$

where

V_{tt} = test day true airspeed

a_t = test day speed of sound

The velocity of sound in a perfect gas is proportional to the square root of the temperature, or

$$\frac{a_t}{a_{SL}} = \sqrt{\frac{T_{at}}{T_{aSL}}} \quad 2.34$$

where

T_{at} = test day ambient temperature, °K

a_{SL} = 661.48 knots

T_{aSL} = 288.16°K

Hence

$$a_t = 38.967 \sqrt{T_{at}} \quad \text{knots} \quad 2.35$$

and

$$M = \frac{V_{tt} \text{ (knots)}}{38.967 \sqrt{T_{at} \text{ (°K)}}} \quad 2.36$$

This equation is plotted in Chart 8.4 as V_t versus T_a for constant Mach number lines.

Inasmuch as the true velocity is seldom available directly, Mach number is more conveniently obtained through the compressible flow equation (2.23, 2.25). M is given as a function of q_c/P_a in Tables 9.4 and 9.5. P_a is obtained from pressure altitude (H_c) in the standard atmosphere, Table 9.2 or Table 9.3, and q_c is found from V_c and Table 9.6.

This information is plotted in Chart 8.5 as Mach number (M) versus calibrated airspeed (V_C) for constant pressure altitude (H_C). Given any two of these variables the third may be found directly from this chart. Chart 8.5 is also applicable for indicated quantities corrected for instrument error. In this case, the chart may be interpreted as M_{iC} versus V_{iC} for constant H_{iC} .

2.5.3 Standard Day True Airspeed:

In the previous section, Mach number is expressed as a function of pressure altitude and calibrated airspeed; therefore, at a given H_C and V_C , the test day Mach number is equal to the standard day Mach number.

$$M_{\text{test}} = \frac{V_{tt}}{a_t} = M_{\text{std}} = \frac{V_{ts}}{a_s} = M \quad 2.37$$

where

$$\begin{aligned} V_{ts} &= \text{standard day true airspeed} \\ a_s &= \text{standard day speed of sound} \end{aligned}$$

The verity of this statement is evidenced by the fact that Mach number is a function of P_a and P_t (equation 2.20, 2.21) and therefore can be expressed independent of the ambient temperature. The standard day speed of sound can be expressed as:

$$a_s = 38.967 \sqrt{T_{as}}, \text{ knots} \quad 2.38$$

where

$$T_{as} = \text{standard day ambient temperature} \\ \text{(corresponding to } H_C \text{ in the standard} \\ \text{atmosphere), } ^\circ\text{K}$$

Hence,

$$V_{ts} = 38.967 M \sqrt{T_{as}}, \text{ knots} \quad 2.39$$

where T_{as} is in $^\circ\text{K}$. This equation is plotted in Chart 8.5. This chart can be used to find V_{ts} from M and H_C , M and V_C , or H_C and V_C .

SECTION 3 INSTRUMENT ERROR - THEORY AND CALIBRATION

Several corrections must be applied to the indicated altimeter and airspeed indicator readings before pressure altitude and calibrated airspeed can be determined. The indicated readings must be corrected for instrument error, pressure lag error and position error, in that order. In level unaccelerated flight there will be no pressure lag, in which case the position error correction can be applied directly following the instrument correction. The instrument error is the subject of this section. The pressure lag error and position error are discussed in sections 4 and 5.

3.1 INSTRUMENT ERROR

The altimeter and airspeed indicator are sensitive to pressure and pressure differential respectively, but the dials are calibrated to read altitude and calibrated airspeed according to equations (2.3, 2.4) and (2.12, 2.13). It is not possible to perfect an instrument which can represent such nonlinear equations exactly under all flight conditions. As a result an error exists called instrument error. Instrument error is the result of several things:

- (1) Scale error and manufacturing discrepancies
- (2) Hysteresis
- (3) Temperature changes
- (4) Coulomb and viscous friction
- (5) Inertia of moving parts

The calibration of an altimeter or airspeed indicator for instrument error is usually conducted in an instrument laboratory. A known pressure or pressure differential is applied to the instrument to be tested. The instrument error is determined as the difference between this known pressure and the instrument indicated reading. Such things as friction and temperature errors are considered as tolerances since they are not dependent on the instrument readings.

An instrument with excessive friction or temperature errors should be rejected.

Data should be taken in both directions so that the hysteresis can be determined. Hysteresis is then the difference between the "up" and "down" corrections. An instrument with large hysteresis must be rejected as it is difficult to account for this effect in flight.

As an instrument wears, its calibration changes. Therefore, each instrument should be recalibrated periodically. The repeatability of the instrument is determined from the instrument calibration history. The repeatability of the instrument must be good for the instrument calibration to be meaningful.

3 2 THE ALTIMETER

The altimeter is calibrated by placing it in a vacuum chamber where pressure is measured by a mercury barometer. The chamber pressure is varied up and down throughout the range for which the altimeter is intended to be used. Simultaneous readings of the barometer and altimeter are taken. The instrument correction (ΔH_{ic}) is determined as the difference between the instrument corrected and indicated altitudes.

$$\Delta H_{ic} = H_{ic} - H_i \quad 3.1$$

where H_{ic} corresponds to the applied pressure according to equations 2.3 and 2.4. The results are usually plotted as shown in Figure 3.1.

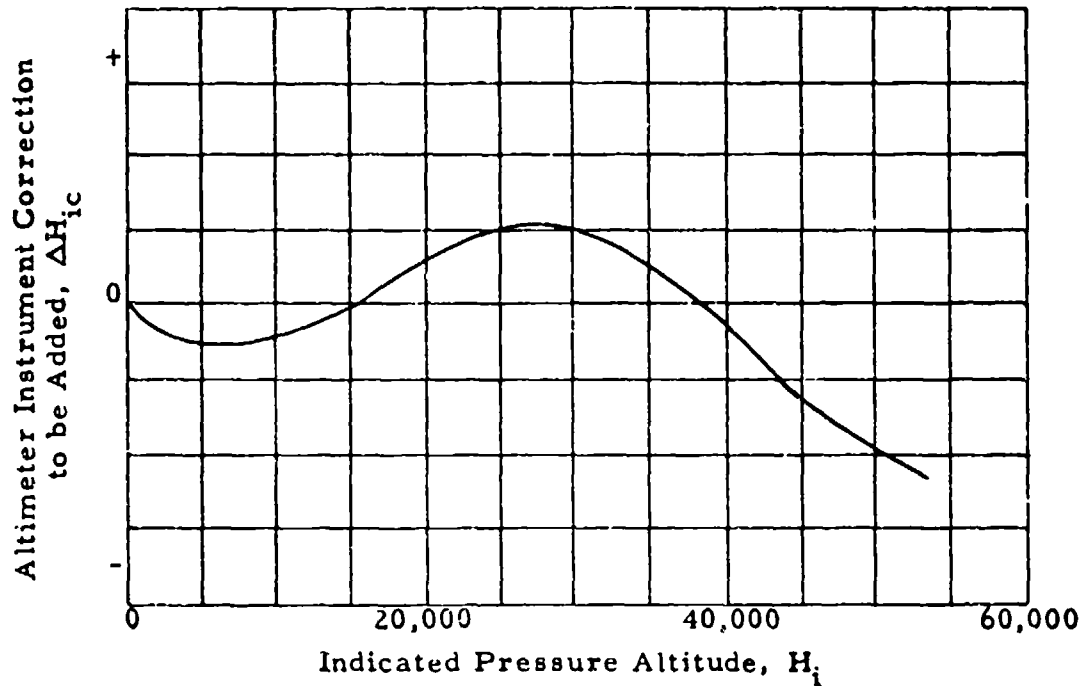


Figure 3.1
Altimeter Instrument Calibration

To use this instrument correction chart, the instrument correction (ΔH_{ic}) is added to the indicated altitude (H_i) to obtain the indicated altitude corrected for instrument error (H_{ic})

$$H_{ic} = H_i + \Delta H_{ic} \quad 3.2$$

In general, at the Air Force Flight Test Center, the altimeter is calibrated every 1,000 feet to 20,000 feet and every 2,000 feet for higher altitudes.

3.3 THE AIRSPEED INDICATOR

The airspeed indicator is calibrated by applying a known differential pressure to the instrument to be calibrated. The pressure is varied up and down throughout the range for which the

instrument is intended to be used. The instrument correction (ΔV_{ic}) is determined as the difference between the instrument corrected and indicated airspeeds.

$$\Delta V_{ic} = V_{ic} - V_i \quad 3.3$$

where V_{ic} corresponds to the applied differential pressure according to equations 2.12 and 2.13. The results are plotted in the same general form as the altimeter instrument correction; the correction is plotted versus the indicated airspeed. To use this instrument correction chart, the instrument correction (ΔV_{ic}) is added to the indicated airspeed (V_i) to obtain the indicated airspeed corrected for instrument error (V_{ic}).

$$V_{ic} = V_i + \Delta V_{ic} \quad 3.4$$

At the AFFTC, the airspeed indicator is calibrated every 10 knots throughout the intended speed range.

SECTION 4

PRESSURE LAG ERROR - THEORY AND CALIBRATION

4.1 PRESSURE LAG ERROR AND THE LAG CONSTANT

The altimeter and airspeed indicator are subject to an error called pressure lag error. This error exists only when the aircraft in which the instruments are installed is changing airspeed or altitude, as during an acceleration or climb. In this case, there is a time lag between such time as the pressure change occurs and when it is indicated on the instrument dial. The effect on the altimeter is obvious; as the aircraft climbs, the instrument will indicate an altitude less than the actual altitude. In the airspeed indicator, the lag may cause a reading too large or too small depending on the proportion of the lag in the total and static pressure systems. Converted to "feet" or "knots", this error is often insignificant. However, it may be significant and should be considered in certain maneuvers such as high speed dives and zoom climbs in which the instrument diaphragms must undergo large pressure rates. Pressure lag is discussed in detail in NACA Report No. 919, "Accuracy of Airspeed Measurements and Flight Calibration Procedures," by Wilbur B. Huston.

Pressure lag is basically a result of:

- (1) Pressure drop in the tubing due to viscous friction.
- (2) Inertia of the air mass in the tubing.
- (3) Instrument inertia and viscous and kinetic friction.
- (4) The finite speed of pressure propagation; i. e., acoustic lag

A detailed mathematical treatment of the response of such a system would be difficult. Fortunately, a very simple approach is possible which will supply adequate lag corrections over a large range of flight conditions encompassing those presently encountered in the performance testing of aircraft. In this approach, it is assumed that the pressure system can be adequately represented by a linear first order equation:

$$-\frac{dP_1(t)}{dt} + \frac{1}{\lambda} P_1(t) = \frac{1}{\lambda} P(t) \quad 4.1$$

where

$P(t)$: the applied pressure at time (t). This is P_S in the case of the altimeter and either P_S or P_1' in the case of the airspeed indicator.

$P_1(t)$: the indicated pressure at time (t).

λ = lag constant

This equation is derived by means of dimensional analysis.

The lag constant for laminar flow of air in tubing can be expressed as:

$$\lambda = \frac{32\mu L^2}{D^2 \delta P} \left(1 + \frac{Q}{LA}\right) \quad 4.2$$

where

μ : coefficient of viscosity of air, slugs/ft-sec

L : length of tubing, feet

D : diameter of tubing, feet

δ : ratio of specific heats, 1.4 for air

P : applied pressure, lbs/feet²

Q : instrument volume, feet³

A : cross-sectional area of tubing, feet²

Many assumptions are made in the formulation of the differential equation and in its solution. The most important of these are:

(1) The rate of change of the applied pressure is nearly constant.

$$P(t) = Kt \quad 4.3$$

where $K = \frac{dP}{dt}$ = a constant. This is a good assumption.

(2) Laminar flow exists. For this to be true, it is necessary that the Reynolds number (N_R) be less than 2000, where

$$N_R \propto \frac{\rho}{\mu} \frac{1}{P} \frac{dP}{dt} \quad 4.4$$

for a given installation. In typical altimeter and airspeed systems, a N_R of 500 is seldom exceeded in flight. Therefore, in laboratory calibrations, pressure rates greater than those encountered in flight should not be applied or erroneous results may be obtained.

(3) The pressure lag is small compared with the applied pressure.

This is generally the case; however, at very high altitudes this assumption becomes critical.

(4) The air and instrument inertias are negligible.

(5) The acoustic lag (τ) is negligible. τ is defined as the time for a pressure disturbance to travel the length of the tubing.

$$\tau = \frac{L}{c} \quad 4.5$$

where

L = length of tubing, feet

c = speed of pressure propagation in the tubing,
1000 feet per second for small diameter tubing.

In flight test application, the acoustic lag contribution is usually small. However, if τ is not small compared to λ , this assumption is not valid and a more detailed analysis such as that outlined in NACA Report No. 919 is necessary.

(6) The pressure drop across orifices and restrictions is negligible. This is true only if a minimum of such restrictions exist so that the tubing is nearly a smooth, straight "pipe" of uniform diameter.

(7) The lag constant (λ) is a constant. This is not strictly true as

$$\lambda \propto \frac{\mu}{\bar{p}} \quad 4.6$$

for a given installation. However, over a small pressure range, λ is nearly constant so that it may be treated as such in the solution of equation 4.1.

The particular solution to the differential equation with these assumptions is:

$$P_i = \frac{dP}{dt} (t - \lambda) \quad 4.7$$

From equation 4.3 and 4.7.

$$P_i = P - \lambda \frac{dP}{dt} \quad 4.8$$

Solving for λ , the definition of the lag constant is

$$\lambda = \frac{P - P_i}{dP/dt} \quad 4.9$$

The lag constant for a given static or total pressure system can be determined experimentally by comparing the indicated and applied pressures for a given pressure rate. This can be done in flight or in the laboratory. In either case, the test should be conducted over a small range of pressures so that the assumption that λ is a constant is not violated.

When the lag constant at one value of μ/P is obtained, it may be extrapolated to other conditions by the expression

$$\frac{\lambda_1}{\lambda_2} = \frac{\mu_1 P_2}{\mu_2 P_1} \quad 4.10$$

which is obtained from equation 4.6. Usually, the test results are reduced to sea level standard static conditions. Then the lag constant at any value of μ and P can be obtained from the expression

$$\lambda = \lambda_{SL} \frac{\mu}{\mu_{SL}} \frac{P_{SL}}{P} \quad 4.11$$

With the lag constants for the static and total pressure systems known, the error in altimeter and airspeed indicator readings due to pressure lag can be calculated for any test point from the basic indicator readings.

Due to the nature of the approximations made in this analysis, is generally not possible to assume that the overall lag error correction can be made with a precision of more than 80 percent. Reduction of instrument and line volumes, however, can usually reduce the system lag errors under any set of conditions to a small percentage of the quantity being measured; in which case, more precise corrections are not required for practical work.

4.2 CORRECTION OF FLIGHT TEST DATA FOR LAG

4.2.1 The Altimeter:

The indicated pressure altitude corrected for instrument error (H_{ic}) is related to the static pressure (P_s) by the differential

equation:

$$dP_s = -G\rho_s dH_{1c} \quad 4.12$$

where ρ_s = the standard day air density.

For small increments, the differentials of equation 4.12 may be assumed to be finite differences.

$$\Delta P_{s\ell} = -G\rho_s \Delta H_{1c\ell} \quad 4.13$$

where

$\Delta P_{s\ell}$ = the static pressure lag:

$$\Delta P_{s\ell} = (P_{s\ell} - P_s) \quad 4.14$$

where

P_s = static pressure corresponding to H_{1c}

$P_{s\ell}$ = static pressure at static pressure source

and

$\Delta H_{1c\ell}$ = altimeter lag error correction:

$$\Delta H_{1c\ell} = (H_{1c\ell} - H_{1c}) \quad 4.15$$

where

H_{1c} = indicated pressure altitude corrected for instrument error

$H_{1c\ell}$ = indicated pressure altitude corrected for instrument and lag error

The lag constant for the static pressure system (λ_s) can be defined from equation 4.9 as:

$$\lambda_s = \frac{P_{s\ell} - P_s}{dP_{s\ell}/dt} = \frac{\Delta P_{s\ell}}{dP_{s\ell}/dt} \quad 4.16$$

With the approximation that

$$\frac{dP_{s\ell}}{dt} = \frac{dP_s}{dt} \quad 4.17$$

equation 4.16 can be written as

$$\lambda_s = \frac{\Delta P_{s\ell}}{dP_s/dt} \quad 4.18$$

Substituting for $\Delta P_{s/l}$ and dP_s/dt

$$\Delta H_{ic} l = \lambda_s \frac{dH_{ic}}{dt} \quad 4.19$$

From equation 4.11

$$\lambda_s = \lambda_{sSL} \frac{\mu}{\mu_{SL}} \frac{P_{aSL}}{P_s} \quad 4.20$$

where λ_{sSL} is the lag constant for the static pressure system at standard sea level conditions.

For convenience in plotting, equation 4.20 is rewritten as

$$\lambda_s = \lambda_{sSL} \frac{\lambda_s H_{ic}}{\lambda_{sSL}} \frac{\lambda_s}{\lambda_s H_{ic}} \quad 4.21$$

where

$$\frac{\lambda_s H_{ic}}{\lambda_{sSL}} = \frac{\mu_{H_{ic}}}{\mu_{SL}} \frac{P_{aSL}}{P_s} \quad 4.22$$

$$\frac{\lambda_s}{\lambda_s H_{ic}} = \frac{\mu}{\mu_{H_{ic}}} \approx \frac{T_{at}}{T_{as}} \quad 4.23$$

The approximation of equation 4.23 is very good for the usual case where the difference between the test and standard day temperatures is small.

Equation 4.22 is plotted as the STATIC LINE of Chart 8.61 in the form

$$\frac{\lambda_{H_{ic}}}{\lambda_{SL}} \text{ versus } H_{ic} \text{ for } V_{ic} = 0 \text{ (STATIC)}$$

(The parameter V_{ic} included on this chart is used in the determination of the total pressure lag constant.)

Equation 4.23 is plotted in Chart 8.62 as

$$\frac{\lambda}{\lambda_{H_{ic}}} \text{ versus } H_{ic} \text{ for } t_{at} (^{\circ}\text{C})$$

In summary, the calculation for altimeter lag error correction ($\Delta H_{ic} l$) at any test point (H_{ic} , t_{at} , dH_{ic}/dt) is then:

$$\Delta H_{ic} l = \frac{\lambda_s}{60} \frac{dH_{ic}}{dt} \quad 4.24$$

where

$$\lambda_s = \lambda_{sSL} \frac{\lambda_{sH_{ic}}}{\lambda_{sSL}} \frac{\lambda_s}{\lambda_{sH_{ic}}} \quad 4.21$$

with dH_{ic}/dt = indicated rate-of-climb corrected for instrument error, feet/minute

λ_{sSL} = sea level static pressure lag constant, from previous calibration, sec

$\frac{\lambda_{sH_{ic}}}{\lambda_{sSL}}$ from Chart 8.61 for H_{ic} , V_{ic} = STATIC

$\frac{\lambda_s}{\lambda_{sH_{ic}}}$ from Chart 8.62 for H_{ic} , t_{at} ($^{\circ}C$)

The indicated altitude corrected for instrument and lag error is then

$$H_{ic\ell} = H_{ic} + \Delta H_{ic\ell} \quad 4.25$$

An example of the calculation of $H_{ic\ell}$ is given with Chart 8.6.

4.2.2 The Airspeed Indicator:

The differential pressure corresponding to the indicated airspeed corrected for instrument error may be given as,

$$q_{cic} = P_t' - P_s \quad 4.26$$

where

P_t' = total pressure felt by the total pressure diaphragm of the airspeed indicator

P_s = static pressure felt by the static pressure diaphragm of the airspeed indicator

With any lag in the total and static pressure systems accounted for,

$$q_{cic\ell} = P_t'\ell - P_s\ell \quad 4.27$$

where

$P_t'\ell$ = total pressure applied to total pressure source of pitot static system

$P_s\ell$ = static pressure applied to static pressure source of pitot static system

Defining the differential pressure error due to lag (Δq_{cicl}) as

$$\Delta q_{cicl} = q_{cicl} - q_{cic} \quad 4.28$$

it follows from equation 4.9 that

$$\begin{aligned} \Delta q_{cicl} &= (P'_{t\ell} - P'_t) - (P_{s\ell} - P_s) \\ &= \lambda_t \frac{dP'_{t\ell}}{dt} - \lambda_s \frac{dP_{s\ell}}{dt} \end{aligned} \quad 4.29$$

Differentiating 4.27 and dividing by dt,

$$\frac{dq_{cicl}}{dt} = \frac{dP'_{t\ell}}{dt} - \frac{dP_{s\ell}}{dt} \quad 4.30$$

Therefore,

$$\Delta q_{cicl} = \lambda_t \frac{dq_{cicl}}{dt} - (\lambda_s - \lambda_t) \frac{dP_{s\ell}}{dt} \quad 4.31$$

With the approximations that:

$$\frac{\Delta q_{cicl}}{dt} = \frac{dq_{cic}}{dt}, \quad \frac{dP_{s\ell}}{dt} = \frac{dP_s}{dt} \quad 4.32$$

equation 4.32 becomes

$$\Delta q_{cicl} = \lambda_t \frac{dq_{cic}}{dt} - (\lambda_s - \lambda_t) \frac{dP_s}{dt} \quad 4.33$$

With the use of the altimeter equation 4.12 which relates dP_s to dH_{ic} , and the airspeed indicator equation (2.12, 2.13) which may be differentiated to give dq_{cic} as a function of dV_{ic} and V_{ic} , equation 4.33 may be modified to give the airspeed indicator lag correction factor ($\Delta V_{ic\ell}$) in terms of dV_{ic}/dt in knots/sec and dH_{ic}/dt in feet/min as

$$\Delta V_{ic\ell} = \lambda_t \frac{dV_{ic}}{dt} + \frac{(\lambda_s - \lambda_t) G \sigma_s \frac{dH_{ic}}{dt}}{170.921 V_{ic} \left[1 + 0.2 \left(\frac{V_{ic}}{a_{SL}} \right)^2 \right]^{2.5}} \quad 4.34$$

for $V_{ic} = a_{SL}$, and

$$\Delta V_{ic\ell} = \lambda_t \frac{dV_{ic}}{dt} + \frac{(\lambda_s - \lambda_t) G \rho_s \frac{dH_{ic}}{dt}}{224,287 \left(\frac{V_{ic}}{a_{SL}} \right)^6 \frac{\left[2 \left(\frac{V_{ic}}{a_{SL}} \right)^2 - 1 \right]}{\left[7 \left(\frac{V_{ic}}{a_{SL}} \right)^2 - 1 \right]^{3.5}}} \quad 4.35$$

for $V_{ic} = a_{SL}$, where

$$\Delta V_{ic\ell} = V_{ic\ell} - V_{ic} \quad 4.36$$

and V_{ic} = indicated airspeed corrected for instrument error

$V_{ic\ell}$ = indicated airspeed corrected for instrument and lag error

This may be written as:

$$\Delta V_{ic\ell} = \lambda_t \frac{dV_{ic}}{dt} + \frac{(\lambda_s - \lambda_t)}{60} \frac{dH_{ic}}{dt} \times F_1(H_{ic}, V_{ic}) \quad 4.37$$

where

$$F_1(H_{ic}, V_{ic}) = \frac{G \sigma_s}{2.84869 V_{ic} \left[1 + 0.2 \left(\frac{V_{ic}}{a_{SL}} \right)^2 \right]^{2.5}} \quad 4.38$$

for $V_{ic} \leq a_{SL}$, and

$$F_1(H_{ic}, V_{ic}) = \frac{G \rho_s}{3738.11} \frac{\left[7 \left(\frac{V_{ic}}{a_{SL}} \right)^2 - 1 \right]^{3.5}}{\left(\frac{V_{ic}}{a_{SL}} \right)^6 \left[2 \left(\frac{V_{ic}}{a_{SL}} \right)^2 - 1 \right]} \quad 4.39$$

for $V_{ic} \geq a_{SL}$, where σ_s and ρ_s are measured at H_{ic} . $F_1(H_{ic}, V_{ic})$ has been plotted versus V_{ic} with H_{ic} as the parameter in Chart 8.63.

As in the case of the altimeter,

$$\lambda_s = \lambda_{sSL} \frac{\lambda_{sH_{ic}}}{\lambda_{sSL}} \frac{\lambda_s}{\lambda_{sH_{ic}}} \quad 4.21$$

Similarly,

$$\lambda_t = \lambda_{tSL} \frac{\lambda_{tH_{ic}}}{\lambda_{tSL}} \frac{\lambda_t}{\lambda_{tH_{ic}}} \quad 4.40$$

where

$$\frac{\lambda_{tH_{ic}}}{\lambda_{tSL}} = \frac{\mu_{H_{ic}}}{\mu_{SL}} \frac{P_{aSL}}{P_s + q_{cic}} \quad 4.41$$

$$\frac{\lambda_t}{\lambda_{tH_{ic}}} = \frac{\mu}{\mu_{H_{ic}}} \approx \frac{T_{at}}{T_{as}} \quad 4.42$$

Equation 4.41 has been plotted in Chart 8.61 as

$\frac{\lambda_{H_{ic}}}{\lambda_{SL}}$ versus H_{ic} for V_{ic}

Equation 4.42 has been plotted in Chart 8.62 as

$$\frac{\lambda}{\lambda_{H_{ic}}} \quad \text{versus } H_{ic} \text{ for } t_{at}(\text{°C})$$

In summary, the calculation for airspeed indicator lag error correction ($\Delta V_{ic\ell}$) at any test point (H_{ic} , t_{at} , V_{ic} , dV_{ic}/dt , dH_{ic}/dt) is then:

$$\Delta V_{ic\ell} = \lambda_t \frac{dV_{ic}}{dt} + \frac{(\lambda_s - \lambda_t)}{60} \frac{dH_{ic}}{dt} \times F_1(H_{ic}, V_{ic}) \quad 4.43$$

where

$$\lambda_s = \lambda_{sSL} \frac{\lambda_{sH_{ic}}}{\lambda_{sSL}} \frac{\lambda_a}{\lambda_{sH_{ic}}} \quad 4.21$$

$$\lambda_t = \lambda_{tSL} \frac{\lambda_{tH_{ic}}}{\lambda_{tSL}} \frac{\lambda_t}{\lambda_{tH_{ic}}} \quad 4.40$$

with

dV_{ic}/dt = indicated acceleration corrected for instrument error, knots/second

dH_{ic}/dt = indicated rate-of-climb corrected for instrument error, feet/minute

λ_{sSL} = sea level static pressure lag constant, from previous calibration, seconds

λ_{tSL} = sea level total pressure lag constant, from previous calibration, seconds

$\frac{\lambda_{sH_{ic}}}{\lambda_{sSL}}$ from Chart 8.61 for H_{ic} , $V_{ic} = \text{STATIC}$

$\frac{\lambda_t}{\lambda_{H_{ic}}} = \frac{\lambda_s}{\lambda_{sH_{ic}}}$ from Chart 8.62 for H_{ic} , $t_a(\text{°C})$

$\frac{\lambda_{tH_{ic}}}{\lambda_{tSL}}$ from Chart 8.61 for H_{ic} , V_{ic}

$F_1(H_{ic}, V_{ic})$ from Chart 8.63 for H_{ic} , V_{ic}

Then the indicated airspeed corrected for instrument and lag error is

$$V_{ic\ell} = V_{ic} + \Delta V_{ic\ell} \quad 4.44$$

Data reduction outline 7.1 is included in Section 7 as a guide in performing this calculation. A numerical example is given with Chart 8.6.

4.3 DETERMINATION OF THE LAG CONSTANT

With the aid of equation 4.2 it is possible to compute theoretically the lag constants for an aircraft pitot-static system. The lag constants used for flight corrections, however, should not be computed, but should be determined experimentally, either in flight or in the laboratory. The computed lag constant is useful only as a rough check of the approximate magnitude of the lag error that may be expected under certain flight conditions.

4.3.1 Laboratory Calibration:

The lag constant (λ) has been defined in a previous section as

$$\lambda = \frac{P - P_i}{dP/dt} \quad 4.9$$

where

P = the applied pressure at time t

P_i = the indicated pressure at time t

This equation suggests the use of a laboratory procedure to determine λ in which a steady rate of change of pressure is applied to the aircraft pitot-static system with P , P_i and dP/dt all determined as a function of time.

4.3.1.1 The Static Pressure Lag Constant

The static pressure lag constant can be determined by the use of an experimental apparatus similar to that shown in Figure 4.1

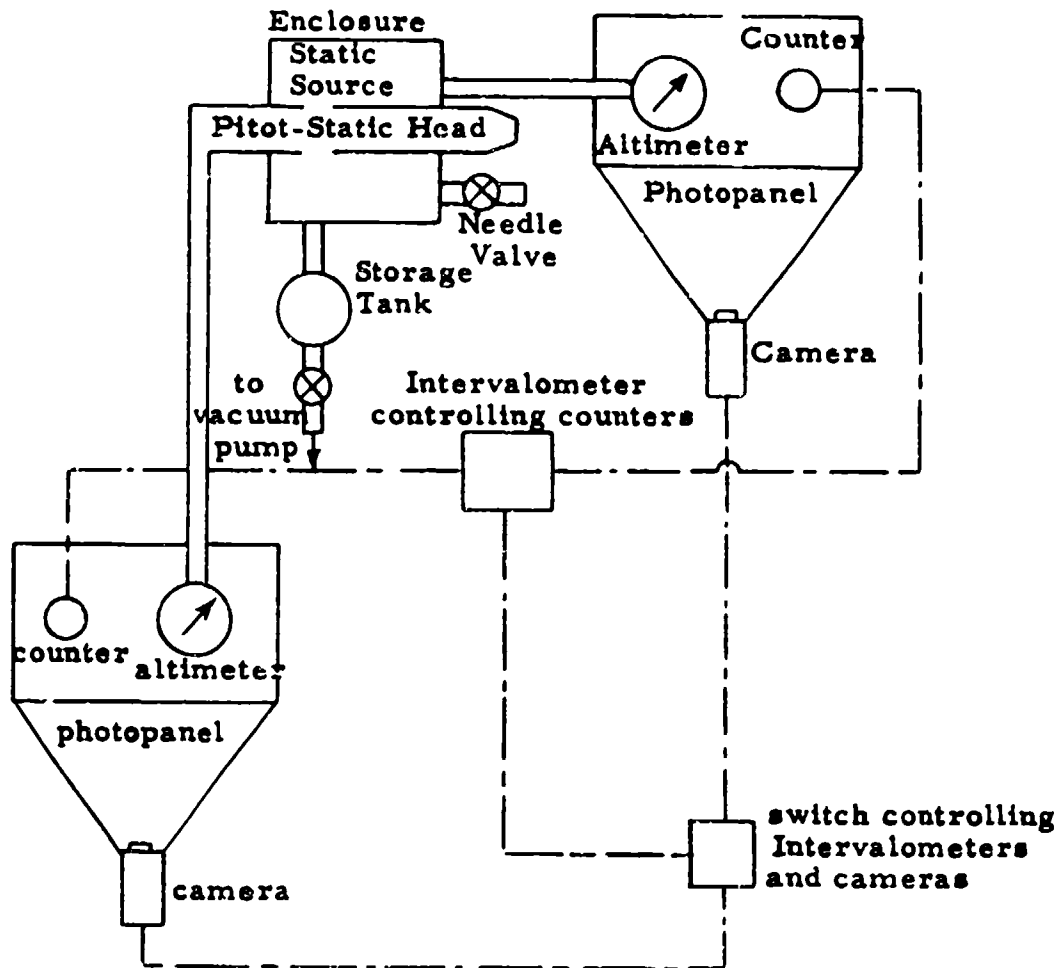


Figure 4.1

Schematic of Equipment for Determination
of Altimeter Lag Constant

The static pressure vent on the probe is sealed in a close fitting enclosure. An altimeter (or pressure gage) is mounted on a photo-panel as close as possible to the enclosure. Another altimeter (or pressure gage) is connected to the static pressure system. Timing counters operating at a one-per-second rate from an intervalometer are installed as shown in the figure. The pressure in the enclosure is lowered to the

limit of the adjacent altimeter by means of a vacuum pump. The cameras and intervalometer are started and the needle valve is opened gradually to maintain a dh/dt of about 5000 feet per minute.

If pressure gages are used, the data from the two camera films is most conveniently plotted in accordance with equation 4.16 as shown in Figure 4.2.

$$\lambda_s = \frac{P_{s\ell} - P_s}{dP_{s\ell}/dt}$$

Here, $P_{s\ell}$ is the pressure in the enclosure and P_s is the pressure indicated by the aircraft static pressure system. At a given P_s , λ_s is equal to the time increment between P_s and $P_{s\ell}$.

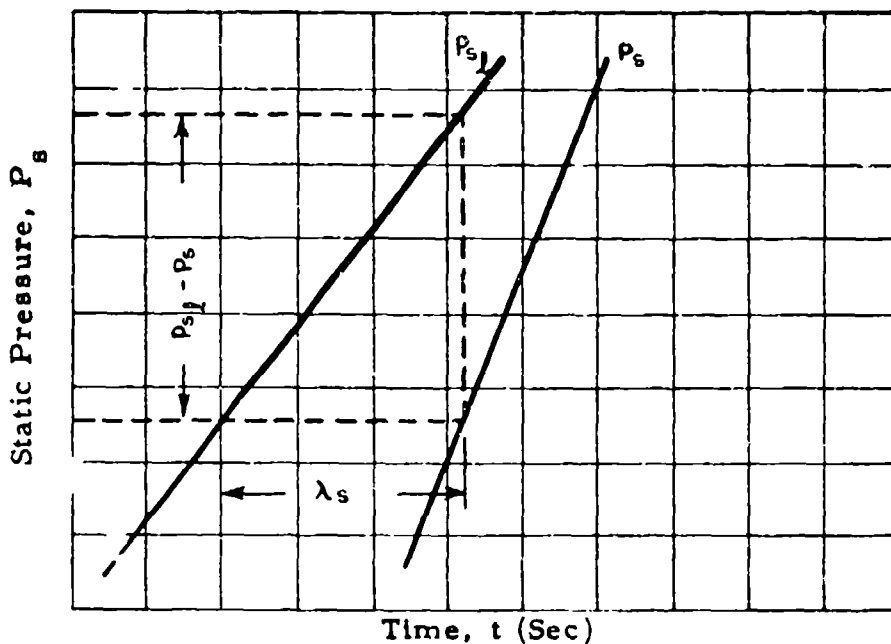


Figure 4.2

Plot Used to Determine Altimeter Lag Constant, λ_s

If altimeters are used rather than pressure gages, it is convenient to plot the data in accordance with equation 4.19 (see Figure 4.3).

$$\lambda_s = \frac{H_{ic\ell} - H_{ic}}{dH_{ic}/dt} \quad 4.45$$

Again, the lag constant for a given H_{ic} is given by the interval between the two lines representing the indicated and actual simulated altitudes.

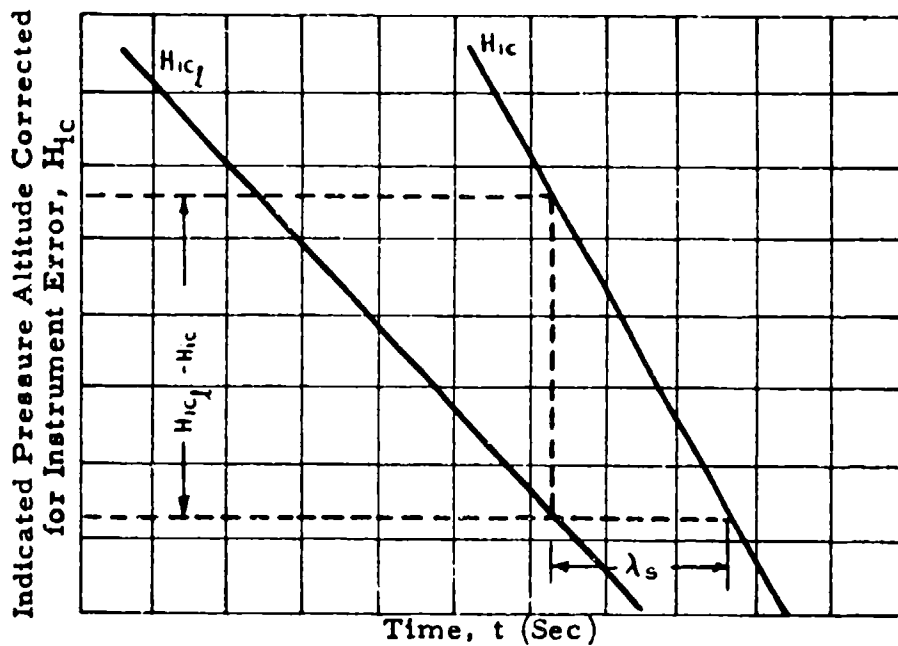


Figure 4.3

Plot Used to Determine Altimeter Lag Constant, λ_s

The value for λ_s obtained at any altitude, is the lag constant for the static pressure corresponding to that altitude and the temperature of the room in which the test was conducted. The sea level static pressure lag constant (λ_{sSL}) can be determined from the relation

$$\lambda_{sSL} = \lambda_s \frac{T_{aSL}}{T_a} \frac{P_s}{P_{aSL}}$$

where

T_a = room temperature

P_s = pressure in the enclosure

This equation is applied to a number of pressures of Figure 4.2 or altitudes of Figure 4.3. From this information, a final value for λ_{SSL} is selected. In general, the values obtained for high altitudes will be the most reliable, as λ_s , the quantity with the most uncertainty, is larger. A sample format for the determination of λ_{SSL} is included as data reduction outline 7.2.

4.3.1.2 The Total Pressure Lag Constant

The total pressure lag constant can be determined by the use of a somewhat modified apparatus. In this case, a pressure is applied to the total pressure source and the static pressure source is left open to pick up atmospheric pressure. Either pressure gages or airspeed indicators may be used. (If airspeed indicators are used the pressure applied to the total pressure source should not exceed ambient pressure by an amount greater than the q_{CIC} corresponding to the maximum V_{ic} for which the airspeed indicator was designed.) The applied pressure is bled off slowly to give the change in pressure (or airspeed) as a function of time.

If pressure gages are used, the data may be plotted in accordance with the definition of the total pressure lag constant (λ_t). From equation 4.9

$$\lambda_t = \frac{P_{t\ell} - P_t'}{dP_{t\ell}'/dt} \quad 4.47$$

where $P_{t\ell}$ is the pressure in the enclosure and P_t' is the pressure indicated by the aircraft total pressure system. Such a plot is shown in Figure 4.4.

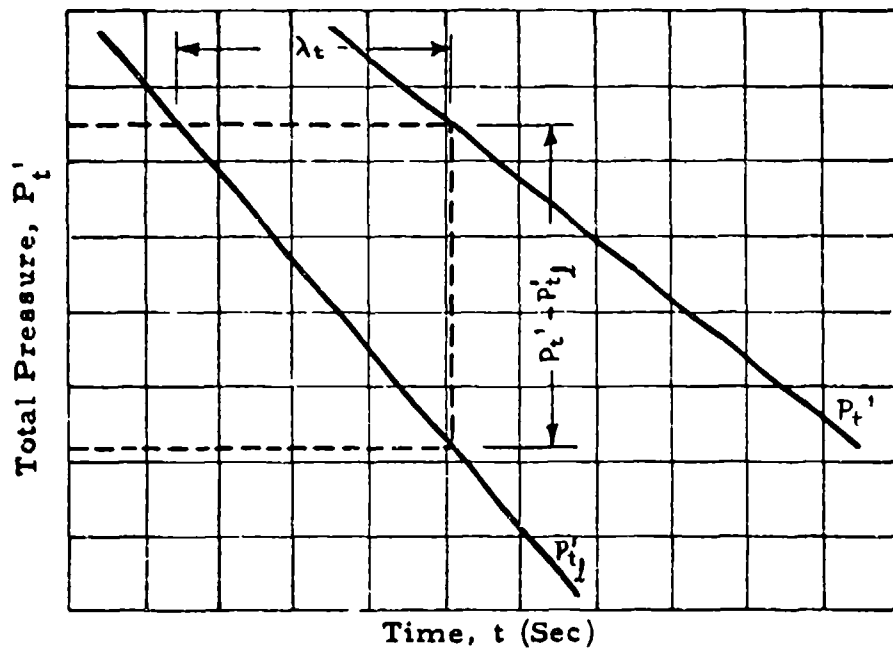


Figure 4.4
Plot Used to Determine Total Pressure
Lag Constant, λ_t

Here, as before, the total pressure lag constant at a given P_t' is equal to the time increment between P_t' and $P_{t'l}$.

It is usually more convenient to use airspeed indicators. With the applied static pressure held constant, $dH_{ic}/dt = 0$; therefore, from equations (4.34, 4.35)

$$\lambda_t = \frac{\Delta V_{ic}l}{dV_{ic}/dt} = \frac{V_{ic}l - V_{ic}}{dV_{ic}/dt} \quad 4.48$$

Hence, the data can be plotted as in Figure 4.5. Then, the total pressure lag constant at a given V_{ic} is equal to the time increment between V_{ic} and $V_{ic}l$.

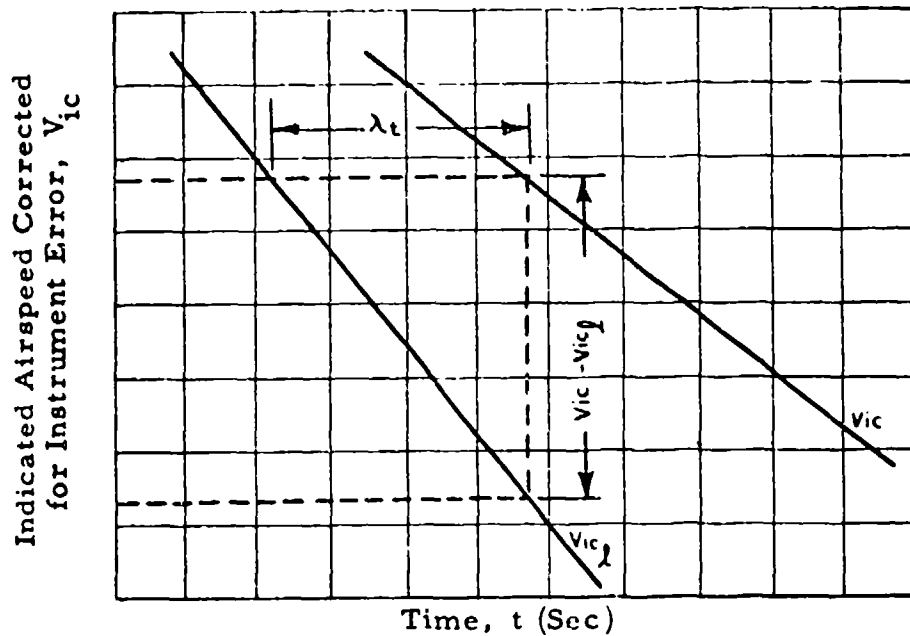


Figure 4.5
Plot Used to Determine Total Pressure
Lag Constant, λ_t

The value for λ_t obtained at any airspeed is the lag constant for the total pressure corresponding to that airspeed and the temperature of the room in which the test was conducted. The sea level total pressure lag constant is then obtained from the relation

$$\begin{aligned} \lambda_{tSL} &= \lambda_t \frac{T_{aSL}}{T_a} \frac{P_t'}{P_{aSL}} \\ &= \lambda_t \frac{T_{aSL}}{T_a} \frac{(q_{cic} + P_s)}{P_{aSL}} \end{aligned} \quad 4.49$$

where $q_{cic} = f(V_{ic})$ and is given in Table 9.6. A sample format for the determination of the sea level lag constant is included as data reduction outline 7.3.

4.3.2 In-Flight Calibration:

Little experience has been obtained with in-flight methods for determining lag constants. However, since ground calibrations must be extrapolated to altitude where lag constants are much greater,

in-flight calibrations do have an obvious advantage in that they can be determined more accurately provided suitable measurements can be made. Special equipment which is not generally available is necessary, however. Using in-flight methods, tapeline altitude is measured while the aircraft is changing flight conditions rapidly, as during a maximum power climb. (These measurements are perhaps best made with Askania cameras.) Tapeline altitudes are then converted to pressure altitudes by means of radiosonde data. A special installation must be made in the aircraft to provide correlation of altitudes recorded on the ground to those recorded in the aircraft.

4.3.2.1 The Static Pressure Lag Constant

The static pressure lag constant can be determined in flight as the aircraft climbs or dives. The indicated altitude (H_i) is compared to the pressure altitude (H_c) where

$$H_c = H_i + \Delta H_{ic} + \Delta H_{ic\ell} + \Delta H_{pc} \quad 4.50$$

where

ΔH_{ic} = altimeter instrument error correction corresponding to H_i

$\Delta H_{ic\ell}$ = altimeter lag error correction corresponding to H_{ic}

ΔH_{pc} = altimeter position error correction corresponding to $H_{ic\ell}$

The altimeter lag error correction is determined as

$$\Delta H_{ic\ell} = H_c - H_i - \Delta H_{pc} \quad 4.51$$

With $\Delta H_{ic\ell}$ known, the static pressure lag constant can be determined from

$$\lambda_s = \frac{\Delta H_{ic\ell}}{dH_{ic}/dt} \quad 4.45$$

dH_{ic}/dt can be determined from a time history of the test aircraft altimeter. The rate-of-climb indicator can be used but it may introduce considerable error as it is subject to lag error. The

pressure altitude at which the test aircraft is operating (H_c) can be determined either by the use of a pacer aircraft or by radar tracking. These methods are discussed in Section 5.6. The altimeter position error correction (ΔH_{pc}) must be known from a previous calibration.

The use of this method is limited by the accuracy with which $\Delta H_{ic\ell}$ can be determined. This requires that the position error correction and the pressure altitude must be known with considerable accuracy, for it is quite possible that the error due to pressure lag can be completely hidden by errors in these quantities. Therefore, lag constants determined by this method should not be accepted without some reservation.

4.3.2.2 The Total Pressure Lag Constant

Inflight methods for determining the total pressure lag constant are not presently used due to difficulty encountered in the measurement of the calibrated airspeed with sufficient accuracy. The airspeed indicator lag error correction has been expressed as

$$\Delta V_{ic\ell} = \lambda_t \frac{dV_{ic}}{dt} + (\lambda_s - \lambda_t) \frac{dH_{ic}}{dt} \times F_1(H_{ic}, V_{ic}) \quad 4.37$$

Several flight procedures are theoretically possible by which λ_t can be determined

- (1) Level acceleration ($dH_{ic}/dt = 0$)

$$\lambda_t = \frac{\Delta V_{ic\ell}}{dV_{ic}/dt} \quad 4.52$$

- (2) Climb or dive at constant V_{ic} ($dV_{ic}/dt = 0$)

$$\lambda_t = \lambda_s - \frac{\Delta V_{ic\ell}}{dH_{ic}/dt \times F_1(H_{ic}, V_{ic})} \quad 4.53$$

- (3) Climb or dive at a constant acceleration or deceleration

$$\lambda_t = \frac{\Delta V_{ic\ell} - \lambda_s \frac{dH_{ic}}{dt} \times F_1(H_{ic}, V_{ic})}{\frac{dV_{ic}}{dt} - \frac{dH_{ic}}{dt} F_1(H_{ic}, V_{ic})} \quad 4.54$$

In all of these procedures, it is necessary to determine $\Delta V_{ic\ell}$
where

$$\Delta V_{ic\ell} = V_c - V_{ic} - \Delta V_{pc} \quad 4.55$$

Tracking methods are not reliable to give velocities accurately and the pacers are not calibrated for lag; therefore, it is not possible to obtain V_c with sufficient accuracy to give a reliable $\Delta V_{ic\ell}$ and hence λ_t .

SECTION 5
POSITION ERROR - THEORY AND CALIBRATION

In addition to instrument error and pressure lag error, the altimeter and airspeed indicator are subject to another error called position error. Once corrections for instrument and pressure lag error have been made, position error may be accounted for and suitable corrections made. Under steady level flight conditions there is no lag error, in which case position error corrections can be made directly following the instrument error correction.

5.1 ORIGIN OF POSITION ERROR

Determination of the pressure altitude and airspeed at which an aircraft is operating is dependent on the measurement of free stream impact pressure and free stream static pressure by the aircraft pitot-static system as evidenced by equations (2.1, 2.2) and (2.10, 2.11). Generally, the pressures registered by the pitot-static system differ from free stream pressures as a result of:

- (1) The existence of other than free stream pressures at the pressure source.
- (2) Error in the local pressure at the source caused by the pressure sensors.

The resulting error is called position error. In the general case, position error may result from error at both the static and total pressure sources. For most flight test work it may be presumed that all of the position error originates at the static pressure source. The possibility of a total pressure error must, however, always be considered.

5.1.1 Total Pressure Error:

As an aircraft moves through the air, a static pressure disturbance is generated in the air producing a static pressure field around the aircraft. At subsonic speeds, the flow perturbations due to the aircraft static pressure field are very nearly isentropic in nature and hence do not affect the total pressure. Therefore, as long as the total pressure source is not located behind a propeller, in the

wing wake, in a boundary layer, or in a region of localized supersonic flow, the total pressure error due to the position of the total pressure head in the aircraft pressure field will usually be negligible. Normally, it is possible to locate the total pressure pickup properly and thus avoid any difficulty. This is most desirable as such things as localized supersonic flow regions produce rather erratic readings.

An aircraft capable of supersonic speeds should be supplied with a nose boom pitot-static system so that the total pressure pickup will be located ahead of any shock waves formed by the aircraft. This condition is essential for it is difficult to correct for total pressure errors which result when oblique shock waves exist ahead of the pickup. The shock wave due to the pickup itself is considered in the calibration equation (2.10, 2.11) discussed in Section 2.2.

Failure of the total pressure sensor to register the local pressure may result from the shape of the pitot-static head, inclination to flow, or a combination of both. Pitot-static tubes have been designed in many varied shapes. These tubes are tested in wind tunnels before installation to assure good design. Some are suitable only for relatively low speeds while others are designed to operate in supersonic flight as well. Therefore, if a proper design is selected and the pitot lips are not burred or dirty, there should be no error in total pressure due to the shape of the probe. Errors in total pressure caused by the angle of incidence of a probe to the relative wind are negligible for most flight conditions. Commonly used probes produce no significant errors at angles of attack or sideslip up to approximately 20 degrees. This range of insensitivity can be increased by using either a shielded or a swivel head probe.

5.1.2 Static Pressure Error:

The static pressure field surrounding an aircraft in flight is a function of speed and altitude as well as the secondary parameters, angle of attack, Mach number, and Reynolds number. Hence, it is seldom

possible to find a location for the static pressure source where the free stream pressure will be sensed under all flight conditions. Therefore, an error in the measurement of the static pressure due to the position of the static pressure orifice in the aircraft pressure field will generally exist.

At subsonic speeds, it is often possible to find some position on the aircraft fuselage where the static pressure error is small under all flight conditions. Therefore, aircraft limited to subsonic flight are best instrumented by the use of a flush static pressure port in such a position. The problem of the selection of an optimum static pressure orifice location is discussed in NACA Report 919, "Accuracy of Airspeed Measurements and Flight Calibration Procedures".

Aircraft capable of supersonic flight should be provided with a nose boom installation to minimize the possibility of total pressure error. This position is also advantageous for the measurement of static pressure as the effects of the aircraft pressure field will not be felt ahead of the aircraft bow wave. Therefore, at supersonic speeds when the bow wave is located downstream of the static pressure orifices, there will be no error due to the aircraft pressure field (See Figure 5.1).

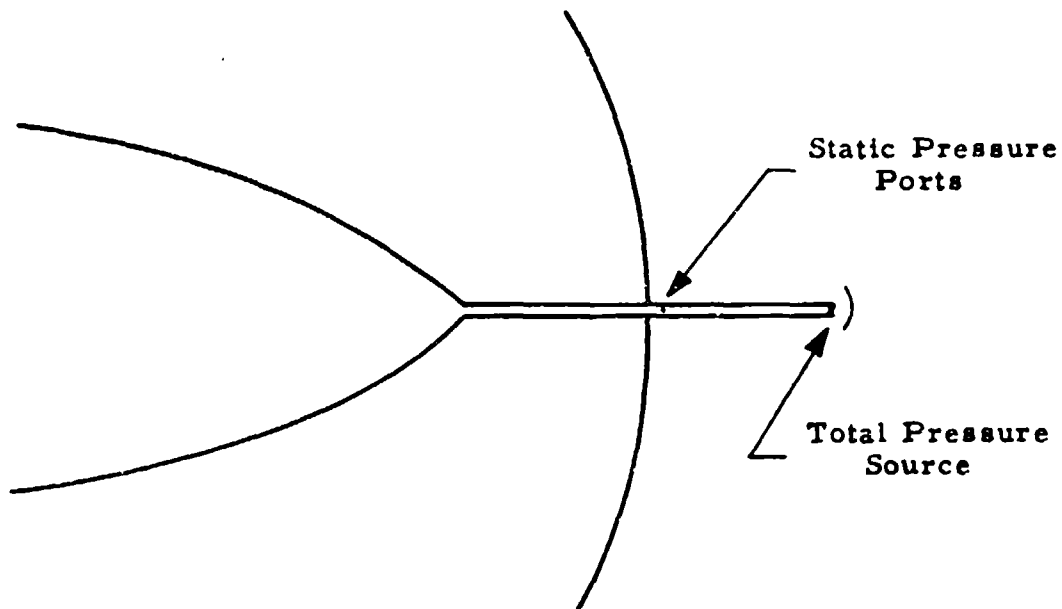


Figure 5.1
Bow Wave of Supersonic Aircraft That Has
Passed Behind Static Pressure Ports

Any error which will exist is a result of the probe itself. Hence, the calibration at supersonic speeds may be derived from wind tunnel tests on the probe, or flight tests of the probe on another aircraft. Assuming the head registers the local static pressure without error, any error which exists is a result of interference from shoulder on the boom installation, or of influence on the static pressure from the shock wave in front of the boom. Available evidence suggests that free stream static pressure will exist if the static ports are located more than 8-10 tube diameters behind the nose of the pitot-static tube and 4-6 diameters in front of the shoulder. (See Figure 5.2).

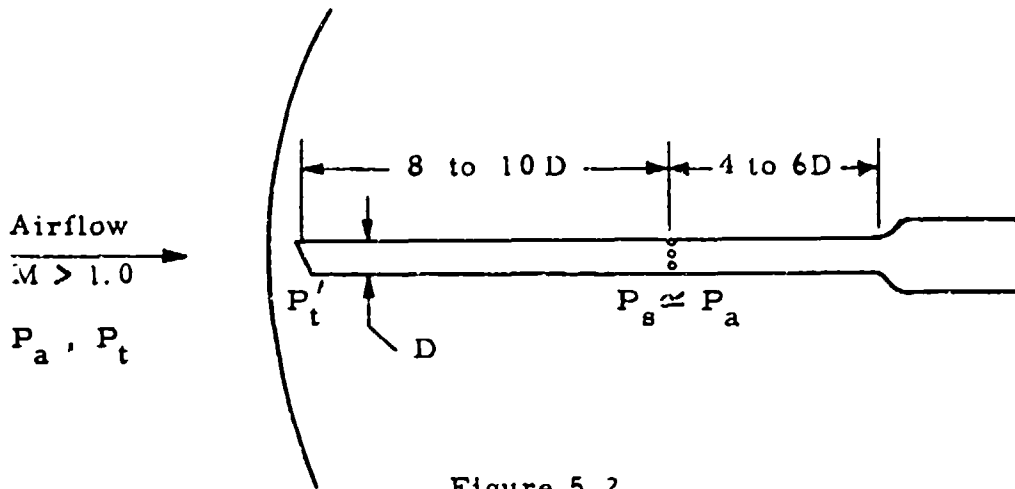


Figure 5.2
Detached Shock Wave in Front of
Pitot-Static Probe

In addition to the static pressure error introduced by the position of the static pressure orifices in the pressure field of the aircraft, there may be error in the registration of the local static pressure due primarily to inclination of flow. Error due to sideslip is often minimized in the case of flush static ports by the location of holes on opposite sides of the fuselage manifolded together. In the case of boom installations, circumferential location of the static pressure ports will reduce the adverse effect of sideslip and angle of attack. The use of a swivel head also reduces this form of error.

5.2 DEFINITION OF POSITION ERROR

From the previous discussion it is seen that position error is created at the static pressure source by the pressure field around the aircraft. It should be borne in mind that position error in the total source may exist, resulting, for instance, from imperfections in the pitot tube. Sufficient airspeed calibrations should always be made on test aircraft to determine the possible existence of position error in the total pressure. Since in nearly all installations this does not occur

the following derivations consider pressure error in the static source only.

The relation of static pressure at any point within the pressure field of an aircraft to the free stream static pressure depends on Mach number (M), angle of attack (α), sideslip angle (β), Reynolds number (N_R) and Prandtl number (N_{Pr}).

$$\frac{P_s}{P_a} = f_1 (M, \alpha, \beta, N_R, N_{Pr}) \quad 5.1$$

(The symbol f denotes a functional relationship which is usually different each time it appears). Defining the position error, ΔP_p , as

$$\Delta P_p = P_s - P_a \quad 5.2$$

equation 5.1 can be written as

$$\frac{\Delta P_p}{P_a} = f_2 (M, \alpha, \beta, N_R, N_{Pr}) \quad 5.3$$

Sideslip angles can be kept small; N_{Pr} is approximately constant; and N_R effects are negligible as long as the static pressure source is not located in a thick boundary layer. Hence, equation 5.3 can be simplified to

$$\frac{\Delta P_p}{P_a} = f_3 (M, \alpha) \quad 5.4$$

With no loss in generality, this equation can be changed to read:

$$\frac{\Delta P_p}{q_{cic}} = f_4 (M_{ic}, CL_{ic}) \quad 5.5$$

with

$$M_{ic} = f_5 \left(\frac{q_{cic}}{P_s} \right) \quad 2.26, 2.27$$

$$CL_{ic} = \frac{nW}{\rho P_s M_{ic}^2 S/2} = \frac{nW}{\rho_{ic}} \frac{1}{M_{ic}^2} \frac{2}{\rho_{ic} S P_{aSL}} \quad 5.6$$

where

q_{cic} = indicated differential pressure, $P_t' - P_s$

n = load factor

W = airplane gross weight

γ = ratio of specific heats, 1.4 for air

S = wing area, constant for a given airplane

δ_{ic} = pressure ratio corresponding to H_{ic} , P_g/P_{aSL}

The term $\Delta P_p/q_{cic}$ is termed the position error pressure coefficient, and is very useful in the reduction of position error data. From the definition of C_{Lic}

$$\frac{\Delta P_p}{q_{cic}} = f_6 \left(\frac{nW}{\delta_{ic}}, M_{ic} \right) \quad 5.7$$

Frequently weight and load factor effects may be neglected when presenting position error data; however, for aircraft carrying large fuel loads and whose weight accordingly may change markedly during the course of a flight or for aircraft in windup turns, the "nW" effects should be taken into account.

Consequently, when the relationship between the variables in equation 5.7 has been determined by means of a calibration, the following chart can be prepared for all weights and all load factors for the given aircraft in a given configuration.

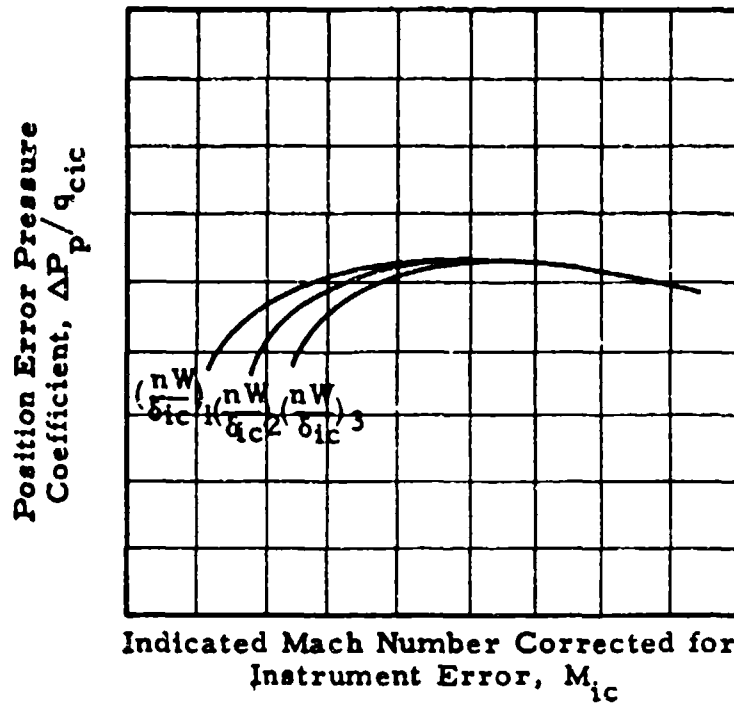


Figure 5.3
 Non-Dimensional Plot of Position Error Data
 to Include Weight and Load Factor Variation

5.3 RELATIONSHIP BETWEEN VARIOUS FORMS OF THE POSITION ERROR

The static pressure position error (ΔP_p) causes error in the altimeter and airspeed indicator readings and in the Mach number calculated from these quantities. The resulting errors are designated ΔH_p , ΔV_p and ΔM_p respectively:

$$\Delta H_p = H_{ic} - H_c \tag{5.8}$$

where

H_c = pressure altitude

H_{ic} = indicated pressure altitude corrected for instrument error

$$\Delta V_p = V_{ic} - V_c \tag{5.9}$$

where

V_c = calibrated airspeed

V_{ic} = indicated airspeed corrected for instrument error

$$\Delta M_p = M_{ic} - M \quad 5.10$$

where

M = Mach number

M_{ic} = indicated Mach number corrected for instrument error

(In these definitions it is assumed that there is no lag error.) In general, it is more convenient to work with position error corrections rather than with the error itself, or

$$\Delta H_{pc} = H_c - H_{ic} = -\Delta H_p \quad 5.11$$

$$\Delta V_{pc} = V_c - V_{ic} = -\Delta V_p \quad 5.12$$

$$\Delta M_{pc} = M - M_{ic} = -\Delta M_p \quad 5.13$$

It can be seen that the corrections are added to the indicated quantities to obtain the actual quantities.

When the position error is produced entirely by pressure coefficient variation at the static source, it is possible to relate altimeter position error directly to airspeed and machmeter position errors (since in most installations the altimeter and airspeed indicator utilize the same static source). It is possible to develop equations relating ΔP_p , ΔH_{pc} , ΔV_{pc} , ΔM_{pc} , and $\Delta P_p/q_{cic}$. This is the subject of the following section.

5.3.1 ΔP_p and ΔH_{pc} :

The differential pressure equation for the altimeter can be written as

$$dP_s = -G_{\rho_s} dH_{ic} \quad 5.14$$

$$\frac{dP_s}{dH_{ic}} = -0.0010813\sigma_s \quad 5.15$$

where

dP_s = differential static pressure, "Hg

dH_{ic} = differential indicated pressure altitude corrected for instrument error, feet

ρ_s = standard day air density at H_{ic}, slugs/feet³

G = gravitational constant, 32.17405 feet/second²

σ_s = standard day air density ratio at H_{ic} , ρ_s/ρ_{SL}

In the case of small errors, these differential quantities may be treated as finite differences. In this case,

$$dP_s = P_s - P_a = \Delta P_p, \text{ "Hg} \quad 5.16$$

$$dH_{ic} = H_{ic} - H_c = \Delta H_p = -\Delta H_{pc} \quad 5.17$$

With this approximation

$$\frac{\Delta P_p}{\Delta H_{pc}} = 0.0010813 \sigma_s, \frac{\text{"Hg}}{\text{feet}} \quad 5.18$$

where σ_c is the standard day air density ratio at H_{ic} . Then

$$\Delta P_p = \left(\frac{\Delta P_p}{\Delta H_{pc}} \right) \Delta H_{pc} \quad 5.19$$

This approximation is good for small errors, say $\Delta H_{pc} < 1000$ feet, but cannot be used for large errors without introducing some error.

The exact relationship between ΔP_p and ΔH_{pc} can be obtained by insertion of $\sigma_s = f(H)$, equation 1.10, 1.13 into the altimeter equation 1.6 and integrating.

$$\int_1^2 dP_a = P_2 - P_1 = -0.0010813 \int_1^2 \sigma dH \quad 5.20$$

where 1 represents the actual quantity and 2 represents the indicated quantity. With this nomenclature

$$P_2 - P_1 = P_s - P_a = \Delta P_p \quad 5.21$$

Hence

$$\Delta P_p = -0.0010813 \int_{H_c}^{H_{ic}} \sigma dH \quad 5.22$$

where

$$\sigma = (1 - 6.87535 \times 10^{-6} H)^{4.2561} \quad 1.10$$

for $H \leq 36,089$ feet, and

$$\sigma = 0.29707 e^{-4.80634 \times 10^{-5} (H - 36,089.24)} \quad 1.13$$

for $H \geq 36,089$ feet. Performing this integration and expanding in terms of ΔH_{pc} by use of the Binomial theorem, an infinite series is obtained. Fortunately, only the first two terms are significant. With this simplification, the result can be expressed as

$$\frac{\Delta P_p}{\Delta H_{pc}} = 0.0010813 \sigma_s, \frac{\text{"Hg}}{\text{feet}} \quad 5.23$$

where σ_s is measured at $(H_{ic} + \frac{\Delta H_{pc}}{2})$.

$$\sigma_s = 1 - 6.87535 \times 10^{-6} (H_{ic} + \frac{\Delta H_{pc}}{2})^{4.2561} \quad 5.24$$

for $(H_{ic} + \frac{\Delta H_{pc}}{2}) \leq 36,089$ feet, and

$$\sigma_s = 0.29707e^{-4.80634 \times 10^{-5} [(H_{ic} + \frac{\Delta H_{pc}}{2}) - 36,089.24]} \quad 5.25$$

for $(H_{ic} + \frac{\Delta H_{pc}}{2}) \geq 36,089$ feet. Equation 5.23 is plotted in several forms:

$$\frac{\Delta P_p}{\Delta H_{pc}} \text{ versus } H_{ic} \text{ for } \Delta H_{pc} \quad 8.7$$

$$\frac{\Delta P_p}{\Delta H_{pc}} \text{ versus } H_{ic} \text{ for } \Delta P_p \quad 8.8$$

$$\Delta H_{pc} \text{ versus } \Delta P_p \text{ for } H_{ic} \quad 8.13$$

Another way to determine ΔP_p from ΔH_{pc} is to find the values for P_s and P_a in the Standard Atmosphere, Table 9.2 or 9.3, corresponding to H_{ic} and H_c and subtract.

Example:

Given: $H_{ic} = 17,140$ feet $\Delta H_{pc} = 550$ feet

Required: ΔP_p in "Hg

Solution:

$$H_c = H_{ic} + \Delta H_{pc} = 17,690 \text{ feet}$$

From Table 9.3:

$$P_s = 15.480 \text{ "Hg}; P_a = 15.134 \text{ "Hg}$$

$$\Delta P_p = P_s - P_a = 0.346 \text{ "Hg}$$

5.3.2 ΔP_p and ΔV_{pc} :

An approximate expression for the relationship between ΔP_p and ΔV_{pc} can be obtained by taking the first derivative of the standard airspeed indicator equation, and considering the derivative to be a finite difference. The resulting equation is good for small errors, say $\Delta V_{pc} < 10$ knots. The standard airspeed indicator equation is given in Section 2 as

$$\frac{q_{cic}}{P_{aSL}} = \left[1 + 0.2 \left(\frac{V_{ic}}{a_{SL}} \right)^2 \right]^{3.5} - 1 \quad 2.12$$

for $V_{ic} \leq a_{SL}$, and

$$\frac{q_{cic}}{P_{aSL}} = \frac{166,921 \left(\frac{V_{ic}}{a_{SL}} \right)^7}{\left[7 \left(\frac{V_{ic}}{a_{SL}} \right)^2 - 1 \right]^{2.5}} - 1 \quad 2.13$$

for $V_{ic} \geq a_{SL}$. The definition of q_{cic} is

$$q_{cic} = P_t' - P_s \quad 5.26$$

With no error in the total pressure, equation 5.26 can be differentiated to give

$$d(q_{cic}) = -d(P_s) \quad 5.27$$

Differentiating equation 2.12 and replacing dq_{cic} by its equivalent, $-dP_s$, gives the result:

$$\frac{dP_s}{dV_{ic}} = - \frac{1.4 P_{aSL}}{a_{SL}} \frac{V_{ic}}{a_{SL}} \left[1 + 0.2 \left(\frac{V_{ic}}{a_{SL}} \right)^2 \right]^{2.5} \quad 5.28$$

for $V_{ic} \leq a_{SL}$

where

dP_s = differential static pressure

dV_{ic} = differential airspeed

Assuming the derivatives to be finite differences

$$dP_s = P_s - P_a \quad 5.29$$

$$dV_{ic} = V_{ic} - V_c = \Delta V_p = -\Delta V_{pc} \quad 5.30$$

With this approximation

$$\frac{\Delta P_p}{\Delta V_{pc}} = \frac{1.4 P_a a_{SL}}{a_{SL}} \frac{V_{ic}}{a_{SL}} \left[1 + 0.2 \left(\frac{V_{ic}}{a_{SL}} \right)^2 \right]^{2.5} \quad 5.31$$

for $V_{ic} \leq a_{SL}$. Similarly, for the case that $V_{ic} \geq a_{SL}$

$$\frac{\Delta P_p}{\Delta V_{pc}} = 52.854 \left(\frac{V_{ic}}{a_{SL}} \right)^6 \frac{\left[2 \left(\frac{V_{ic}}{a_{SL}} \right)^2 - 1 \right]}{\left[7 \left(\frac{V_{ic}}{a_{SL}} \right)^2 - 1 \right]^{3.5}} \quad 5.32$$

Then

$$\Delta P_p = \left(\frac{\Delta P_p}{\Delta V_{pc}} \right) \Delta V_{pc} \quad 5.33$$

The exact expression relating ΔP_p and ΔV_{pc} is derived in the following manner for the case when no error in the total pressure source exists.

$$q_{cic} = P_t' - P_s = f(V_{ic}) \quad 2.12, 2.13$$

For the case of no position error

$$q_c = P_t' - P_a = f(V_c) \quad 2.10, 2.11$$

as $q_{cic} = q_c$ and $V_{ic} = V_c$ with no position error. Now

$$\Delta P_p = P_s - P_a = (P_t' - P_a) - (P_t' - P_s) = q_c - q_{cic}$$

Therefore,

$$\Delta P_p = q_c - q_{cic} = f(V_c) - f(V_{ic}) \quad 5.34$$

Since $V_c = V_{ic} + \Delta V_{pc}$, it is possible to expand the right hand side of this equation into a series for ΔV_{pc} by use of the Binomial Theorem. The resulting series may be discontinued after the second term with no loss in accuracy for $\Delta V_{pc} \leq 50$ knots. The resulting equation takes the form

$$\begin{aligned} \frac{\Delta P_p}{\Delta V_{pc}} = & \frac{1.4 P_a a_{SL}}{a_{SL}} \frac{V_{ic}}{a_{SL}} \left[1 + 0.2 \left(\frac{V_{ic}}{a_{SL}} \right)^2 \right]^{2.5} \\ & + \frac{0.7 P_a a_{SL}}{a_{SL}} \left[1 + 0.2 \left(\frac{V_{ic}}{a_{SL}} \right)^2 \right]^{1.5} \left[1 + 1.2 \left(\frac{V_{ic}}{a_{SL}} \right)^2 \right] \frac{\Delta V_{pc}}{a_{SL}} \end{aligned} \quad 5.35$$

for $V_{ic} \leq a_{SL}$, and

$$\begin{aligned} \frac{\Delta P_p}{\Delta V_{pc}} = & 52.854 \left(\frac{V_{ic}}{a_{SL}} \right)^6 \frac{\left[2 \left(\frac{V_{ic}}{a_{SL}} \right)^2 - 1 \right]}{\left[7 \left(\frac{V_{ic}}{a_{SL}} \right)^2 - 1 \right]^{3.5}} & 5.36 \\ & + 52.854 \left(\frac{V_{ic}}{a_{SL}} \right)^5 \frac{\left[7 \left(\frac{V_{ic}}{a_{SL}} \right)^4 - 4.5 \left(\frac{V_{ic}}{a_{SL}} \right)^2 + 3 \right]}{\left[7 \left(\frac{V_{ic}}{a_{SL}} \right)^2 - 1 \right]^{4.5}} \frac{\Delta V_{pc}}{a_{SL}} \end{aligned}$$

for $V_{ic} \geq a_{SL}$. Note that the first term is identical with that obtained by the approximate method. The second term may be considered as a correction to the first term that must be applied for large ΔV_{pc} .

Equation (5.35, 5.36) has been plotted in several forms for the convenience of the reader

$\frac{\Delta P_p}{\Delta V_{pc}}$ versus V_{ic} for ΔV_{pc}	Chart	8.9
$\frac{\Delta P_p}{\Delta V_{pc}}$ versus V_{ic} for ΔP_p	Chart	8.10
ΔV_{pc} versus ΔP_p for V_{ic}	Chart	8.13

5.3.3 ΔV_{pc} and $\Delta P_p/q_{cic}$:

The position error pressure coefficient is very useful as a parameter in high speed flight ($M_{ic} > 0.6$). To facilitate obtaining $\Delta P_p/q_{cic}$ from ΔV_{pc} , a graph of ΔV_{pc} versus V_{ic} for $\Delta P_p/q_{cic}$ is plotted as Chart 8.11. This chart is determined from the following considerations.

$$\frac{\Delta P_p}{q_{cic}} = \frac{(\Delta P_p/P_{aSL})}{(q_{cic}/P_{aSL})} \quad 5.37$$

From equations (5.35, 5.36, 2.12, 2.13, and 5.37)

$$\frac{\Delta P_p}{q_{ic}} = \frac{\left\{ 1.4 \frac{V_{ic}}{a_{SL}} \left[1 + 0.2 \left(\frac{V_{ic}}{a_{SL}} \right)^2 \right]^{2.5} \frac{\Delta V_{pc}}{a_{SL}} \right\} + \left\{ 0.7 \left[1 + 0.2 \left(\frac{V_{ic}}{a_{SL}} \right)^2 \right]^{1.5} \left[1 + 1.2 \left(\frac{V_{ic}}{a_{SL}} \right)^2 \right] \left(\frac{\Delta V_{pc}}{a_{SL}} \right)^2 \right\}}{\left[1 + 0.2 \left(\frac{V_{ic}}{a_{SL}} \right)^2 \right]^{3.5} - 1} \quad 5.38$$

for $V_{ic} \leq a_{SL}$, and

$$\frac{\Delta P_p}{q_{ic}} = \frac{\frac{7 \frac{V_{ic}}{a_{SL}} \left[2 \left(\frac{V_{ic}}{a_{SL}} \right)^2 - 1 \right] \frac{\Delta V_{pc}}{a_{SL}}}{7 \left(\frac{V_{ic}}{a_{SL}} \right)^2 - 1} + \frac{7 \left[7 \left(\frac{V_{ic}}{a_{SL}} \right)^4 - 4.5 \left(\frac{V_{ic}}{a_{SL}} \right)^2 + 3 \right] \left(\frac{\Delta V_{pc}}{a_{SL}} \right)^2}{\left[7 \left(\frac{V_{ic}}{a_{SL}} \right)^2 - 1 \right]^2}}{\left(\frac{V_{ic}}{a_{SL}} \right)^2 \left[1 - \frac{\left[7 \left(\frac{V_{ic}}{a_{SL}} \right)^2 - 1 \right]^{2.5}}{166.921 \left(\frac{V_{ic}}{a_{SL}} \right)^7} \right]} \quad 5.39$$

for $V_{ic} \geq a_{SL}$.

5.3.4 ΔH_{pc} and ΔV_{pc} :

When working with small errors, say ΔH_{pc} 1000 feet or ΔV_{pc} knots, the value of ΔH_{pc} can be determined from ΔV_{pc} , or vice versa, by the following relation which is obtained by dividing the approximate equations (5.35 and 5.36) by 5.22.

$$\frac{\Delta H_{pc}}{\Delta V_{pc}} = \frac{58.566}{\sigma_s} \left(\frac{V_{ic}}{a_{SL}} \right) \left[1 + 0.2 \left(\frac{V_{ic}}{a_{SL}} \right)^2 \right]^{2.5} \quad 5.40$$

for $V_{ic} \leq a_{SL}$, and

$$\frac{\Delta H_{pc}}{\Delta V_{pc}} = \frac{48,880}{\sigma_s} \left(\frac{V_{ic}}{a_{SL}} \right)^6 \frac{2 \left(\frac{V_{ic}}{a_{SL}} \right)^2 - 1}{\left[7 \left(\frac{V_{ic}}{a_{SL}} \right)^2 - 1 \right]^{3.5}} \quad 5.41$$

for $V_{ic} \geq a_{SL}$, where σ_s is measured at H_{ic} . This equation has been plotted in Chart 8.12 as $\Delta H_{pc}/\Delta V_{pc}$ versus V_{ic} for H_{ic} .

For the case of larger errors where equations 5.18 and 5.31, 5.32 are not valid, the resulting equation 5.40, 5.41 and Chart 8.12 are of course not valid. In this case, one should use Chart 8.13 which is developed from the following relation which in turn is obtained by consideration of equations 5.35, 5.36 and 5.23.

$$\Delta P_p = 0.0010813 \sigma_s \Delta H_{pc} \quad 5.42$$

$$= 1.4 P_{aSL} \frac{V_{ic}}{a_{SL}} \left[1 + 0.2 \left(\frac{V_{ic}}{a_{SL}} \right)^2 \right]^{2.5} \frac{\Delta V_{pc}}{a_{SL}} \\ + 0.7 P_{aSL} \left[1 + 0.2 \left(\frac{V_{ic}}{a_{SL}} \right)^2 \right]^{1.5} \\ \left[1 + 1.2 \left(\frac{V_{ic}}{a_{SL}} \right)^2 \right] \left(\frac{\Delta V_{pc}}{a_{SL}} \right)^2$$

for $V_{ic} \leq a_{SL}$, and

$$= 1168.45 P_{aSL} \left(\frac{V_{ic}}{a_{SL}} \right)^6 \frac{\left[2 \left(\frac{V_{ic}}{a_{SL}} \right)^2 - 1 \right] \frac{\Delta V_{pc}}{a_{SL}}}{\left[7 \left(\frac{V_{ic}}{a_{SL}} \right)^2 - 1 \right]^{3.5}} \quad 5.43$$

$$+ 1168.45 P_{aSL} \left(\frac{V_{ic}}{a_{SL}} \right)^5 \frac{\left[7 \left(\frac{V_{ic}}{a_{SL}} \right)^4 - 4.5 \left(\frac{V_{ic}}{a_{SL}} \right)^2 + 3 \right] \left(\frac{\Delta V_{pc}}{a_{SL}} \right)^2}{\left[7 \left(\frac{V_{ic}}{a_{SL}} \right)^2 - 1 \right]^{4.5}}$$

for $V_{ic} \geq a_{SL}$

where σ_s is measured at $(H_{ic} + \frac{\Delta H_{pc}}{2})$. Chart 8.13 is in the form of ΔV_{pc} versus ΔP_p for V_{ic} and ΔP_p versus ΔH_{pc} for H_{ic} , or simply ΔV_{pc} versus ΔH_{pc} for V_{ic} and H_{ic} .

5.3.5 ΔM_{pc} and ΔH_{pc} :

The Mach number equation may be written as

$$\frac{P_t'}{P_s} = (1 + 0.2M_{ic}^2)^{3.5} \quad 5.44$$

for $M_{ic} \leq 1.00$. Differentiating, with P_t' constant,

$$\frac{dP_s}{dM_{ic}} = -\frac{1.4P_s M_{ic}}{(1 + 0.2M_{ic}^2)} \quad 5.45$$

Making the approximations

$$dP_s = P_s - P_a = \Delta P_p \quad 5.46$$

$$dM_{ic} = M_{ic} - M = \Delta M_p = -\Delta M_{pc} \quad 5.47$$

the relation between the static pressure error and the Mach number position correction is obtained.

$$\frac{\Delta P_p}{\Delta M_{pc}} = \frac{1.4P_s M_{ic}}{(1 + 0.2M_{ic}^2)} \quad 5.48$$

This approximate equation is valid for small errors. The Mach number position correction can be related to the altimeter position correction by dividing equation 5.22 by equation 5.52 and introducing the perfect gas equation 1.3.

$$\frac{\Delta M_{pc}}{\Delta H_{pc}} = 0.007438 \frac{(1 + 0.2M_{ic}^2)}{T_{as} M_{ic}} \quad 5.49$$

for $M_{ic} \leq 1.00$, where T_{as} is the standard day temperature corresponding to H_{ic} .

In the supersonic case, $M_{ic} \geq 1.00$

$$\frac{P_t'}{P_s} = \frac{166.921M_{ic}^7}{(7M_{ic}^2 - 1)^{2.5}} \quad 5.50$$

Proceeding as in the subsonic case

$$\frac{\Delta P_p}{\Delta M_{pc}} = \frac{7P_s(2M_{ic}^2 - 1)}{M_{ic}(7M_{ic}^2 - 1)} \quad 5.51$$

and

$$\frac{\Delta M_{pc}}{\Delta H_{pc}} = 0.001488 \frac{M_{ic} (7M_{ic}^2 - 1)}{T_{as}(2M_{ic}^2 - 1)} \quad 5.52$$

for $M_{ic} \geq 1.00$, where T_{as} corresponds to H_{ic} .

Equation 5.49, 5.52 has been plotted in Chart 8.14 in the form:

$$\Delta M_{pc}/\Delta H_{pc} \text{ versus } M_{ic} \text{ for } H_{ic} \quad \text{Chart} \quad 8.14$$

Chart 8.14 and the above equations on which it is based are valid only for small errors, say $\Delta M_{pc} < 0.04$ or $\Delta H_{pc} < 1000$ feet.

For larger errors, a better approximation is necessary. The exact result can be obtained from the following analysis. In general, for $M_{ic} \leq 1.00$.

$$\frac{P_t'}{P_s} = (1 + 0.2M_{ic}^2)^{3.5} \quad 5.53$$

For the case of no position error,

$$\frac{P_t'}{P_a} = (1 + 0.2M^2)^{3.5} \quad 5.54$$

With

$$\Delta P_p = P_s - P_a \quad 5.2$$

and

$$\Delta M_{pc} = M - M_{ic} \quad 5.17$$

it is possible to express the exact relationship

$$\frac{\Delta P_p}{P_s} = f(M_{ic}, \Delta M_{pc}) \quad 5.55$$

Expanding by the Binomial Theorem and retaining the first two terms yields the result

$$\frac{\Delta P_p}{P_s} = \frac{1.4M_{ic}\Delta M_{pc}}{(1 + 0.2M_{ic}^2)} + \frac{0.7(1 - 1.6M_{ic}^2)\Delta M_{pc}^2}{(1 + 0.2M_{ic}^2)^2} \quad 5.56$$

for $M_{ic} \leq 1.00$. Similarly for the supersonic case ($M_{ic} \geq 1.00$)

$$\frac{\Delta P_p}{P_s} = \frac{7(2M_{ic}^2 - 1)\Delta M_{pc}}{M_{ic}(7M_{ic}^2 - 1)} - \frac{7(21M_{ic}^4 - 23.5M_{ic}^2 + 4)\Delta M_{pc}^2}{M_{ic}^2(7M_{ic}^2 - 1)^2} \quad 5.57$$

The final result is obtained by dividing equation 5.27 by equations 5.60, 5.61

$$\begin{aligned} \frac{\Delta P_p}{P_s} &= 0.0010813 \frac{\sigma_s}{P_s} \Delta H_{pc} & 5.58 \\ &= \frac{1.4 M_{ic} \Delta M_{pc}}{(1 + 0.2 M_{ic}^2)} + \frac{0.7(1 - 1.6 M_{ic}^2) \Delta M_{pc}^2}{(1 + 0.2 M_{ic}^2)^2} \end{aligned}$$

for $M_{ic} \leq 1.00$, and

$$\begin{aligned} \frac{\Delta P_p}{P_s} &= 0.0010813 \frac{\sigma_s}{P_s} \Delta H_{pc} & 5.59 \\ &= \frac{7(2 M_{ic}^2 - 1)}{M_{ic}(7 M_{ic}^2 - 1)} \Delta M_{pc} - \frac{7(21 M_{ic}^4 - 23.5 M_{ic}^2 + 4) \Delta M_{pc}^2}{M_{ic}^2 (7 M_{ic}^2 - 1)^2} \end{aligned}$$

for $M_{ic} \geq 1.00$, where P_s is measured at H_{ic} and σ_s is measured at $(H_{ic} + \frac{\Delta H_{pc}}{2})$. This equation is plotted in Chart 8.15 in the form of ΔH_{pc} versus $\Delta P_p/P_s$ for H_{ic} , and ΔM_{pc} versus $\Delta P_p/P_s$ for M_{ic} , or simply ΔM_{pc} versus ΔH_{pc} for M_{ic} and H_{ic} .

5.3.6 ΔM_{pc} and ΔV_{pc} :

For small errors, say $\Delta M_{pc} < 0.04$ or $\Delta V_{pc} < 10$ knots, the ratio $\Delta M_{pc}/\Delta V_{pc}$ can be obtained by multiplying equations 5.49, 5.52, 5.40, 5.41 with the result

$$\frac{\Delta M_{pc}}{\Delta V_{pc}} = \frac{P_{aSL}}{a_{SL}} \frac{1}{P_s} \frac{V_{ic}}{a_{SL}} \left[1 + 0.2 \left(\frac{V_{ic}}{a_{SL}} \right)^2 \right]^{2.5} \frac{(1 + 0.2 M_{ic}^2)}{M_{ic}} \quad 5.60$$

for $V_{ic} \leq a_{SL}$, $M_{ic} \leq 1.00$;

$$\frac{\Delta M_{pc}}{\Delta V_{pc}} = \frac{P_{aSL}}{5 a_{SL}} \frac{1}{P_s} \frac{V_{ic}}{a_{SL}} \left[1 + 0.2 \left(\frac{V_{ic}}{a_{SL}} \right)^2 \right]^{2.5} \frac{M_{ic}(7 M_{ic}^2 - 1)}{(2 M_{ic}^2 - 1)} \quad 5.61$$

for $V_{ic} \leq a_{SL}$, $M_{ic} \geq 1.00$; and

$$\frac{\Delta M_{pc}}{\Delta V_{pc}} = \frac{166.921 P_{aSL}}{a_{SL}} \frac{1}{P_s} \frac{\left(\frac{V_{ic}}{a_{SL}} \right)^6 \left[2 \left(\frac{V_{ic}}{a_{SL}} \right)^2 - 1 \right]}{\left[7 \left(\frac{V_{ic}}{a_{SL}} \right)^2 - 1 \right]^{3.5}} \frac{M_{ic}(7 M_{ic}^2 - 1)}{(2 M_{ic}^2 - 1)} \quad 5.62$$

for $V_{ic} \geq a_{SL}$, Equations (5.60, 5.61, 5.62) are plotted in Chart 8.16 in the form

$$\frac{\Delta M_{pc}}{\Delta V_{pc}} \text{ versus } M_{ic} \text{ for } H_{ic} \quad \text{Chart 8.16}$$

No chart has been prepared in which one can directly relate ΔM_{pc} to ΔV_{pc} for the case of very large position error where Chart 8.16 is not valid. In the case of large error, it is possible to determine ΔM_{pc} from ΔV_{pc} , or vice versa, by the following indirect method:

- (1) Given ΔV_{pc} and V_{ic} , determine $\Delta P_p/q_{cic}$ from Chart 8.11
- (2) Determine M_{ic} from V_{ic} and H_{ic} and Chart 8.5
- (3) Determine ΔM_{pc} from M_{ic} and $\Delta P_p/q_{cic}$ and Chart 8.18

5.3.7 ΔM_{pc} and $\Delta P_p/q_{cic}$:

For small errors, say $\Delta M_{pc} < 0.04$, the ratio $\Delta M_{pc}/(\Delta P_p/q_{cic})$ may be formed by dividing equation (2.26, 2.27) by equation (5.48, 5.51) with the result

$$\frac{\Delta M_{pc}}{(\Delta P_p/q_{cic})} = \frac{(1 + 0.2M_{ic}^2)}{1.4M_{ic}} \left[(1 + 0.2M_{ic}^2)^{3.5} - 1 \right] \quad 5.63$$

for $M_{ic} \leq 1.00$ and

$$\frac{\Delta M_{pc}}{(\Delta P_p/q_{cic})} = \frac{M_{ic} \left[166.921M_{ic}^7 - (7M_{ic}^2 - 1)^{2.5} \right]}{7(7M_{ic}^2 - 1)^{1.5}(2M_{ic}^2 - 1)} \quad 5.64$$

for $M_{ic} \geq 1.00$. This equation is plotted in Chart 8.17 in the form

$$\frac{\Delta M_{pc}}{(\Delta P_p/q_{cic})} \text{ versus } M_{ic} \quad \text{Chart 8.17}$$

The expression for large errors is obtained by dividing equations (5.56 and 5.57) by equations (2.26 and 2.27).

$$\frac{\Delta P_p}{q_{cic}} = \frac{1.4M_{ic} \Delta M_{pc}}{(1 + 0.2M_{ic}^2)} + \frac{0.7(1 - 1.6M_{ic}^2)\Delta M_{pc}^2}{(1 + 0.2M_{ic}^2)^2} \quad 5.65$$

$$\left[(1 + 0.2M_{ic}^2)^{3.5} - 1 \right]$$

for $M_{ic} \leq 1.00$, and

$$\frac{\Delta P_p}{q_{cic}} = \frac{7(2M_{ic}^2 - 1)\Delta M_{pc}}{M_{ic}(7M_{ic}^2 - 1)} - \frac{7(21M_{ic}^4 - 23.5M_{ic}^2 + 4)\Delta M_{pc}^2}{M_{ic}^2(7M_{ic}^2 - 1)^2}$$

$$\left[\frac{166.921 M_{ic}^7}{(7M_{ic}^2 - 1)^{2.5}} - 1 \right] \quad 5.66$$

for $M_{ic} \geq 1.00$. Equations (5.65 and 5.66) is plotted in Chart 8.18 in the form

$\frac{\Delta P_p}{q_{cic}}$ versus ΔM_{pc} for M_{ic}

Chart 8.18

5.4 EXTRAPOLATION OF RESULTS

In general, the position error corrections must be established by a flight calibration made under all flight conditions. In some cases, however, it is possible to extrapolate over a wide range of conditions from a calibration over the speed range at one altitude. It has been shown that

$$\frac{\Delta P_p}{q_{cic}} = f_1 (M_{ic}, C_{Lic}) \quad 5.5$$

$$= f_2 (M_{ic}, \frac{nW}{\delta_{ic}}) \quad 5.6$$

To derive this relation experimentally for direct application to any flight condition would thus require calibrations at several weights and load factors over the full altitude and speed range of the aircraft. The appropriate assumptions on which predictions to other conditions can be made from tests at one altitude depend on the Mach number and are considered in this section for several ranges of that parameter.

5.4.1 Low Mach Number Range ($M_{ic} < 0.6$):

For low Mach numbers, the effects of compressibility on pressure error may be considered negligible. Without introducing serious error, it may be said that the pressure coefficient is a function only of lift coefficient (C_L) as shown in Figure 5.4.

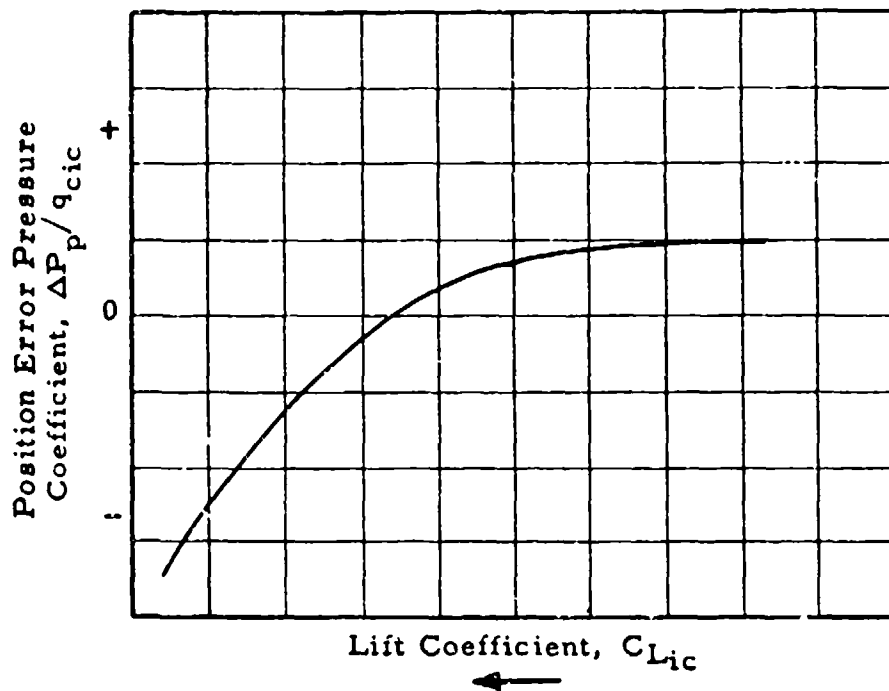


Figure 5.4

$\Delta P_p/q_{cic}$ versus C_L for Typical
Wing Tip Probe (Good for Low Speed Only)

This plot will represent the flow field around the probe for all flight conditions in the low Mach number range.

The position error calibrations for a low speed aircraft are often presented in another manner.

$$\frac{\Delta P}{q_{cic}} = f_3(C_{L_{ic}}) \quad 5.67$$

Since $C_L = nW / (\rho_{sl} V_e^2 S/2)$ and in the low Mach number range $V_c \approx V_e$, it can be assumed that

$$C_L = \frac{nW}{\rho_{sl} V_c^2 S/2} \quad 5.68$$

or

$$C_{L_{ic}} = \frac{nW}{\rho_{sl_{ic}} V_{ic}^2 S/2} \quad 5.69$$

Substituting equation 5.69 in equation 5.67

$$\frac{\Delta P_p}{q_{cic}} = f_4\left(\frac{nW}{V_{ic}^2}\right) = f_5\left(\frac{nW}{V_{ic}}\right) \quad 5.70$$

It is possible to obtain a curve of $\Delta P_p/q_{cic}$ versus $\sqrt{nW/V_{ic}}$ from the results of a position error calibration over the C_L range at one altitude. From this plot, the position error pressure coefficient at any relevant altitude, weight and normal acceleration can be obtained.

A typical plot of $\Delta P_p/q_{cic}$ versus V_{ic} showing nW variation and Mach number effects at the higher speeds is given in Figure 5.5. It may be seen from this figure that a change in nW at low speed can cause a substantial change in position error.

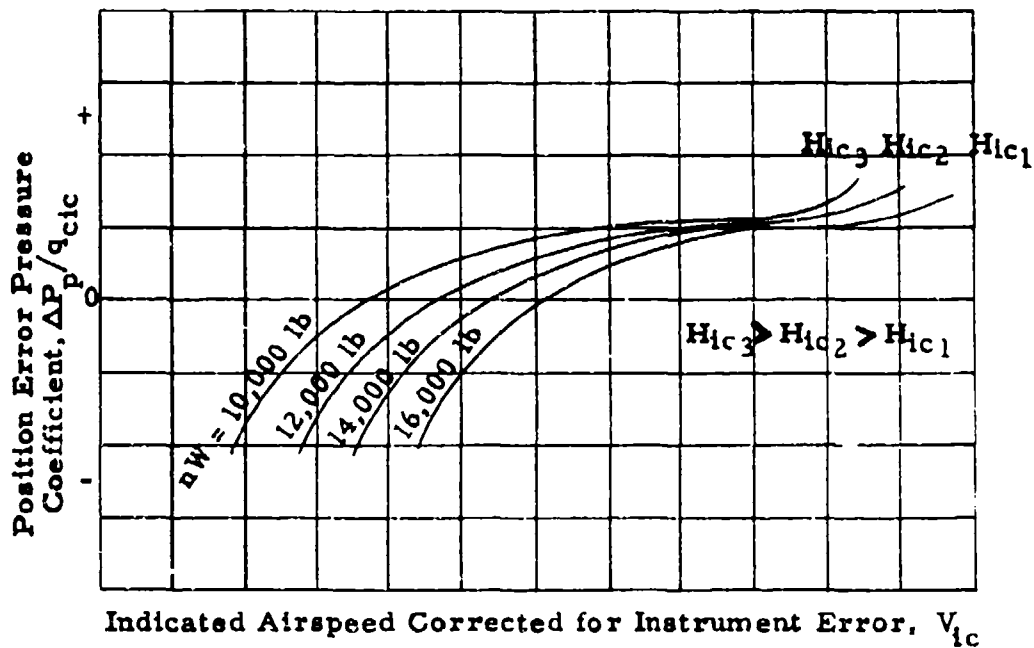


Figure 5.5

Plot of $\Delta P_p/q_{cic}$ versus V_{1c} for Low Speed Aircraft

The altimeter position error correction for low speed aircraft can be extrapolated from one altitude to another altitude at the same indicated airspeed corrected for instrument error (V_{ic}) as long as there are no appreciable changes in weight or load factor. It has been shown for low speed aircraft in which there are no Mach effects that

$$\frac{\Delta P_p}{q_{cic}} = f(V_{ic}) \text{ only} \quad 5.71$$

for constant nW . Therefore, at a given V_{ic} , and hence q_{cic} , and constant weight and load factor, the static pressure error (ΔP_p) is constant during altitude changes. Hence, for a given V_{ic} and constant nW

$$\Delta H_{pc2} = \Delta H_{pc1} \frac{\left(\frac{\Delta P_p}{\Delta H_{pc}}\right)_1}{\left(\frac{\Delta P_p}{\Delta H_{pc}}\right)_2} \quad 5.72$$

In the case of small errors, equation 5.22 yields the result,

$$\Delta H_{pc2} = \Delta H_{pc1} \left(\frac{\sigma_{s1}}{\sigma_{s2}}\right) \quad 5.73$$

where σ_{s1} is the density ratio at H_{ic1} , and σ_{s2} is the density ratio at H_{ic2} . In that the position error in the low speed range is always small, the problem of large error does not need to be considered here. Equation 5.77 states that the altimeter position error correction can be extrapolated to another altitude at the same V_{ic} by multiplication of ΔH_{pc} by the ratio of the standard day air densities. This procedure is good only in the low speed range when there are no Mach number effects and when the variation in nW is not of significance.

5.4.2 Medium Subsonic and Transonic Mach Number Range (0.6 < M_{ic} < 1.0):

In this Mach number range, the position error pressure coefficient will in general depend on both M_{ic} and C_{Lic} so the

general equation must be considered.

$$\frac{\Delta P_p}{q_{cic}} = f_1 (M_{ic}, C_{L_{ic}}) \quad 5.5$$

$$= f_2 (M_{ic}, \frac{nW}{\delta_{ic}}) \quad 5.6$$

Therefore, in the general case a position error calibration must be conducted at several altitude and weight combinations. In many installations however, the effect of the $C_{L_{ic}}$ parameter is negligible in this Mach number range. In this case, a calibration at one altitude can be extrapolated to other altitudes. The existence of any $C_{L_{ic}}$ effect should be investigated by performing tests at two widely different altitudes and plotting curves of $\Delta P_p/q_{cic}$ versus M_{ic} for the values of nW/δ_{ic} . The result for a typical nose boom installation is shown in Figure 5.6. This curve shows that nW/δ_{ic} effects exist in the system tested. This curve would be a single line if there were no $C_{L_{ic}}$ effects.

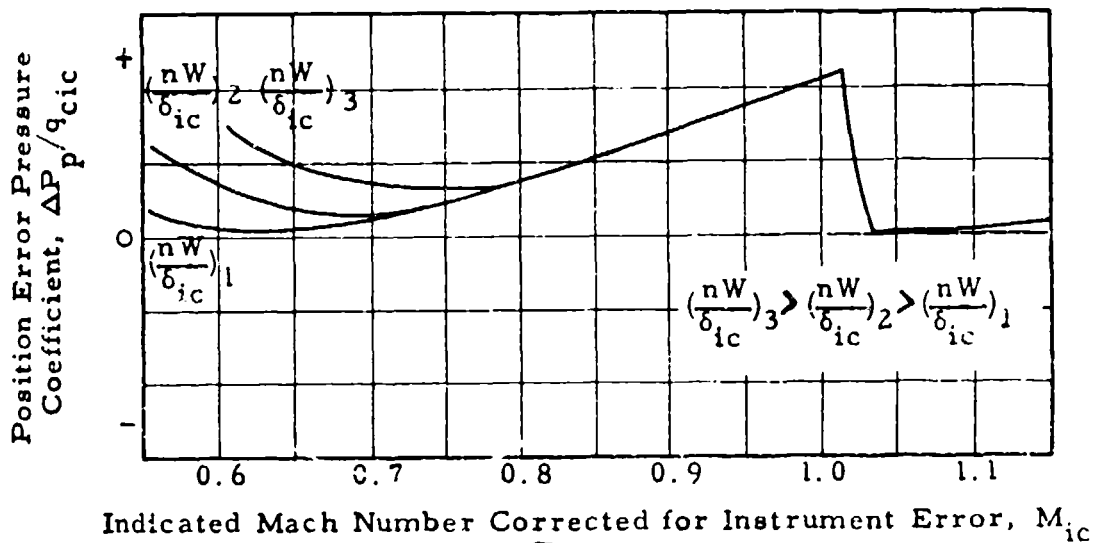


Figure 5.6

Plot of $\Delta P_p/q_{cic}$ versus M_{ic} for a Typical Nose Boom Installation
Showing nW/q_{ic} Effects at Low Speed End

When there are no appreciable $C_{L_{ic}}$ effects as indicated by a single curve of $\Delta P_p/q_{cic}$ (versus M_{ic} for all nW/δ_{ic}) the altimeter position error correction at one altitude can be extrapolated to any other altitude at the same M_{ic} . With no $C_{L_{ic}}$ effect.

$$\frac{\Delta P_p}{q_{cic}} = f(M_{ic}) \text{ only} \quad 5.74$$

Equations 5.63, 5.64 and 5.65 state

$$\Delta M_{pc} = f(M_{ic}, \frac{\Delta P_p}{q_{cic}}) \quad 5.63, 5.64, 5.65$$

From these equations, it follows that ΔM_{pc} is a function of M_{ic} only and hence independent of altitude when there are no $C_{L_{ic}}$ effects.

$$\Delta M_{pc} = f(M_{ic}) \text{ only} \quad 5.75$$

Therefore, one may write

$$\Delta H_{pc2} = \Delta H_{pc1} \frac{\left(\frac{\Delta M_{pc}}{\Delta H_{pc}}\right)}{\left(\frac{\Delta M_{pc}}{\Delta H_{pc}}\right)_2} \quad 5.76$$

for $M_{ic1} = M_{ic2}$. In the case of small errors, equation 5.49, 5.52 yields the result

$$\Delta H_{pc2} = \Delta H_{pc1} \left(\frac{T_{as2}}{T_{as1}}\right) \quad 5.77$$

for $M_{ic1} = M_{ic2}$, where T_{as1} and T_{as2} are the standard day air temperatures corresponding to H_{ic1} and H_{ic2} respectively. In the case of large errors, it would appear that the above method of extrapolation would no longer be valid as equations (5.53 and 5.56) from which it is derived are no longer valid. Fortunately this is not the case and equation 5.81 can be used for very large errors, say $\Delta H_{pc} < 3000$ feet, with no appreciable loss of accuracy.

5.4.3 Supersonic Mach Number Range ($M_{ic} > 1.0$):

An aircraft capable of supersonic flight should be equipped with a nose boom installation. In this case, the aircraft bow wave will pass behind the static pressure holes at a M_{ic} of 1.03 or so. At higher

Mach numbers, the effect of the lift coefficient on the position error pressure coefficient will be zero as the pressure field of the aircraft will not be felt in front of the bow wave. Therefore, any pressure error that does exist will be a function of Mach number only so that a plot of $\Delta P_p/q_{cic}$ versus M_{ic} will be valid for all altitudes. In the usual case, this error is quite small and may be zero.

5.5 CORRELATION OF RESULTS OF POSITION ERROR CALIBRATIONS

In the position error calibration methods discussed in the next section, data is usually obtained in the form of ΔH_{pc} or ΔV_{pc} for the altitude at which the test was conducted. In this section, methods by which data from different calibrations can best be correlated is given. The final report presentation is usually given as ΔH_{pc} and ΔV_{pc} versus V_{ic} with H_{ic} as the parameter. This can be done for both light weight and heavy weight configurations if weight is an important parameter.

For low speeds in which there are no Mach number effects, the position error obtained from several calibrations is best correlated by the use of a plot of ΔV_{pc} versus V_{ic} . Such a plot will be a single line which is good for all altitudes for a constant nW with the absence of M_{ic} effects.

It has been shown that in the low Mach number range

$$\frac{\Delta P_p}{q_{cic}} = f_1(V_{ic}) \text{ only} \quad 5.70$$

for constant nW . From Section 5.3.3

$$\Delta V_{pc} = f_2\left(\frac{\Delta P_p}{q_{cic}}, V_{ic}\right) \quad 5.38, 5.39$$

Therefore, in the absence of Mach number effects

$$\Delta V_{pc} = f_3(V_{ic}) \text{ only} \quad 5.78$$

for constant nW

At higher speeds, when there is the possibility of both M_{ic} and C_{Lic} effects, the results of calibrations are best correlated by a plot of $\Delta P_p/q_{cic}$ or ΔM_{pc} versus M_{ic} . It has been shown in the previous section that this will usually be a single line for $M_{ic} > 0.6$ except for possible low speed nW/δ_{ic} breakoffs.

5.6 CALIBRATION METHODS

The static pressure error can be determined by any method in which the indicated static pressure and the free stream static pressure are obtained at the same time. The indicated pressure is obtained by installing a sensitive aneroid such as an altimeter in the static pressure system to be calibrated. The free stream static pressure can be obtained directly from a measurement of the atmospheric pressure or indirectly from a measurement of airspeed, in which case the total pressure error must be known or assumed to be zero. The direct method is called an altimeter calibration. Some of the more common methods are: the tower fly-by, the pacer and aircraft fly-by, the altitude pressure comparison methods, and the trailing bomb method. The indirect method is called an airspeed calibration. Airspeed calibrations can be obtained by the speed course method and the pacer and radar methods when airspeeds are compared. In general, the accuracy of the altimeter calibration is far superior to the airspeed calibration as the altimeter is a relatively accurate instrument compared to the airspeed indicator concerning such things as hysteresis and repeatability. It will be shown, however, that at very low speeds an airspeed calibration may be superior.

The choice of a method will, in general, depend on the instrumentation available, the degree of accuracy required, and the speed and altitude range for which a calibration is desired. The most desirable method or combination of methods is one which requires a minimum of time, equipment and manpower to arrive at an accurate calibration over the entire speed and altitude range of the aircraft; it must be quick and inexpensive, yet reliable and complete. Several methods are discussed in this section with this in mind. Each method is described in detail. Then the advantages and disadvantages of each are discussed so that the reader may choose the method or combination of methods which best fulfills his need.

5.6.1 The Tower Fly-By Method(See Data Reduction Outline 7.5):

The tower fly-by is a low altitude method in which the altitude indicated by the aircraft pitot-static system is compared to the actual pressure altitude to determine the static pressure error. A theodolite is set up in a control tower or a tall building at a known distance from a line marked on a runway. The aircraft to be calibrated is flown at constant speed over this course as close to theodolite level as possible but at least one full wing span off the ground to be out of ground effect. As the aircraft passes the theodolite position, the pilot records altitude (H_i) and airspeed (V_i); the theodolite operator measures the vertical angle to the aircraft. The atmospheric pressure at the theodolite station is measured with an absolute pressure gage or altimeter, or static pressure and temperature are measured at the ground and reference level static pressure is computed on the basis of the standard temperature lapse rate. The true pressure altitude of the aircraft is determined by adding the physical difference in height between the theodolite and the aircraft to the pressure altitude at theodolite level.

$$H_c = H_c \text{ at theodolite level} + \Delta h \quad 5.79$$

where Δh is determined from the theodolite reading. This operation is valid, even during extreme atmospheric conditions, as the pressure gradient will not vary from standard enough to cause appreciable error in the small height difference between the aircraft and the theodolite. This method is illustrated in the following figure.

Pilot Records:
Indicated Airspeed, V_i
Indicated Altitude, H_i

Theodolite Operator Records:
Pressure Altitude of Tower
Vertical Angle to Aircraft, α

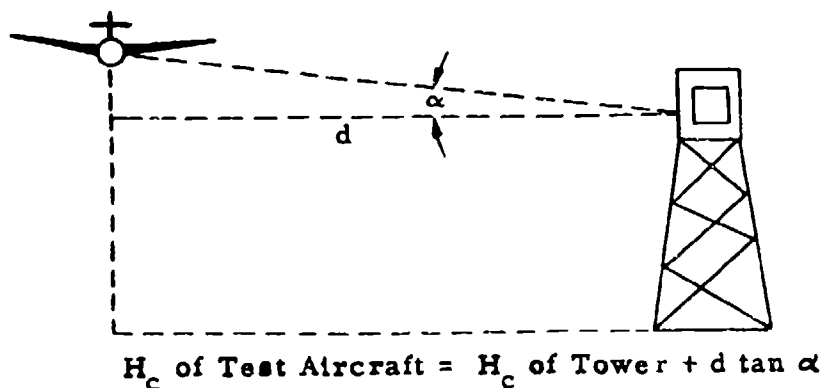


Figure 5.7
Tower Fly-by Method

The tower fly-by method is limited to level flight speeds above stalling speed by a safe margin. The upper speed limit may be set by local restrictions prohibiting supersonic flight at or near ground level in a congested area.

The static pressure error can be determined with very good accuracy by the use of this method. At low speeds, however, any error in the measurement of the static pressure error becomes very important when converted to airspeed position error (ΔV_p) as evidenced by equation (5.35, 5.36). This effect is illustrated in Figure 5.8.

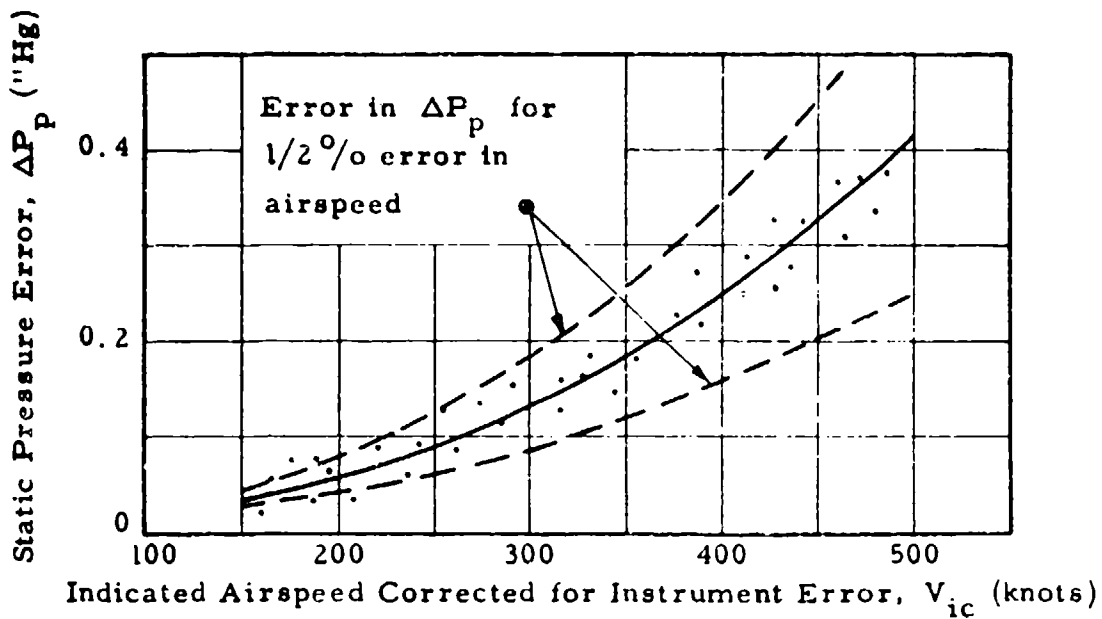


Figure 5.8
 Plot of ΔP_p vs V_{ic} Determined from Tower
 Fly-By Calibrations

At the Air Force Flight Test Center, with the use of conventional aircraft instrumentation and a "visual theodolite", this method is not used for speeds below 200 knots or so for this reason.

The tower fly-by method is very quick, requiring only a few minutes per point for the flight and manual data reduction. It is relatively inexpensive as 1 hour of flight time will cover adequately the speed range of the aircraft and no extensive equipment is necessary.

In an improvement of this technique, two ground stations may be used, one on each side of the lined course. This allows the aircraft to deviate from the runway without introducing error.

One disadvantage of the tower fly-by method, as discussed above, is the hazard of flying at high speed near the ground. This hazard can be eliminated by the use of a modified system. In this method, a photograph is taken as the aircraft passes over a camera which is directed vertically upward from a position on the marked course. The tapeline altitude of the aircraft is then determined from the focal

length of the camera and the proportion of the size of the image on film to the true dimensions of the object. The static pressure at this altitude can be computed or determined by flying the test aircraft at a speed for which the pressure error is known. Good results have been obtained with the use of a conventional 35mm camera up to altitudes of 1000 feet. This method is discussed in the report, "Position Error Determination by Stadiametric Ranging with a 35mm Movie Camera," Technical Report No. 2-55, Test Pilot Training Division, U.S. Naval Air Test Center (Patuxent River, Maryland), June 24, 1955 by W. J. Hesse.

5.6.2 The Ground Speed Course Method (See Data Reduction Outline 7.6):

The ground speed course is another low altitude method which is especially good at low speeds. It is best used in conjunction with the tower fly-by method to obtain a low altitude position error calibration over the entire speed range. This is an "airspeed calibration" in that the error in airspeed is measured directly from which the static pressure error may be determined - providing the error in total pressure is known or can be assumed to be zero.

The aircraft to be calibrated is flown over a course of known length at a uniform speed and at constant altitude. True airspeed is obtained from time and distance data. Calibrated airspeed, calculated from true airspeed, is compared to the airspeed indicated by the aircraft pitot-static system to obtain the error in airspeed due to static pressure error. The conversion of V_t to V_c requires that both pressure altitude and free air temperature be known. The pressure altitude can be obtained by adding the pressure altitude corresponding to the ground atmospheric pressure to the estimated height of the aircraft above the ground. Instead of estimating the height of the aircraft above the ground, an iterative process can be used where the instrument corrected altimeter reading is first used to find position error. This position error can then be used to correct the altimeter reading and the process repeated. Ambient temperature is

determined from indicated readings recorded in the aircraft. This method is described in Figure 5.9.

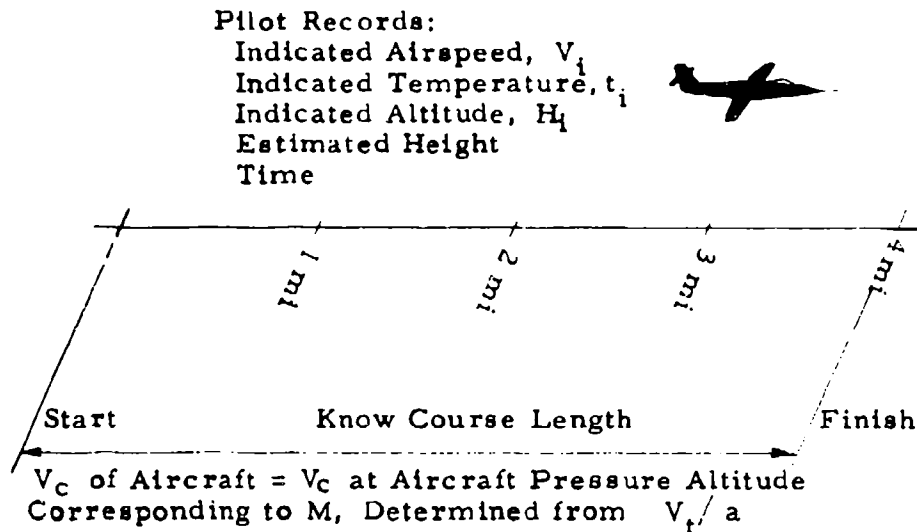


Figure 5.9
 Ground Speed Course Method

The aircraft should be flown on reciprocal headings at each speed so that the effect of head and tail wind can be averaged out. The averaged ground speed is assumed to be true speed. The aircraft should be allowed to drift with the wind so that the adverse effect of cross wind can be eliminated. The test should not be conducted on a windy day for any shifting winds introduce error in true speed. The aircraft should be fairly well stabilized as the timing gives average speed. However, the holding of an exact speed is not critical. The speed course should be flown at least one wing span above the ground to be out of ground effect. This distance should be kept to a safe minimum, however, because of the need for an estimation of the aircraft height.

Theoretically, this method is good for all level flight speeds above the stalling speed of the aircraft. The accuracy obtained, however, is a function of the timing method and the length of the course and diminishes as speed increases. At high speeds, errors in time

measurement may cause the error in airspeed to be obscured by errors in the measurement of true speed. Therefore, this method gives best results at low speeds and can be used at high speeds only if adequate timing equipment is used and the course is relatively long. The Air Force Flight Test Center maintains a ground speed course approximately 4 miles long. Time is kept with a stop watch operated by the pilot or by an aircraft observer. This course is not used for speeds above 250 knots.

The accuracy of the ground speed course is poor even in the low speed range. There is always a scatter of points due to timing errors, shifting winds and the estimate of temperature at aircraft height which is needed for calculation of true speed. However, the results obtained at low speeds are in general better than those obtained by the tower fly-by method.

The ground speed course is inexpensive and very simple to maintain and operate. Each double point takes approximately 10 minutes for the flight and 10 minutes for manual data reduction.

A variation of the ground speed course is the photogrid method. The test is conducted in the same manner except that true speed is determined by means of a camera, a timer, and a calibrated grid installed in a control tower or other vantage point by a runway. As the aircraft passes the camera station, photographs are taken through the grid. The film record gives accurate speed and altitude of the aircraft. (See Figure 5.10.) This method can be used only when a low wind condition exists or when the wind direction is approximately parallel to the runway or the same errors will be introduced as when crabbing on a speed course.

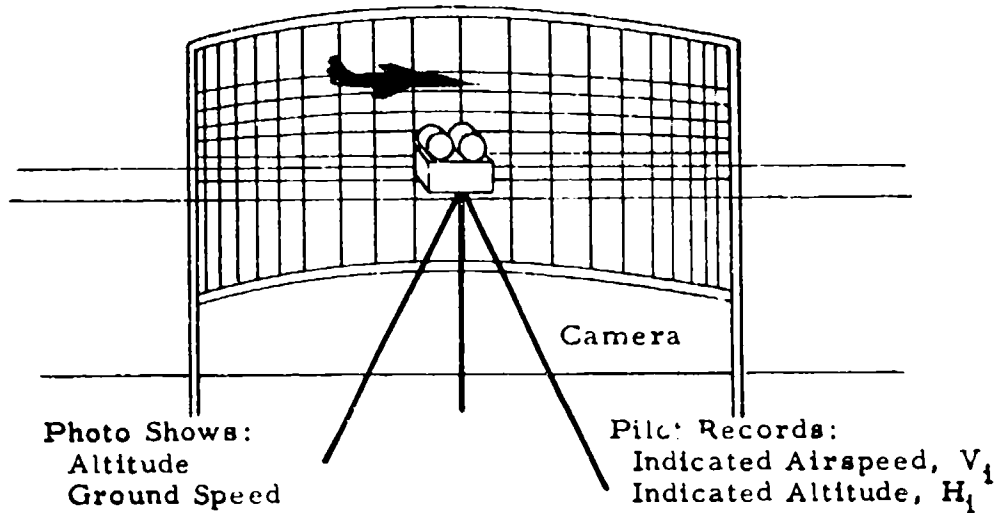


Figure 5.10
Photogrid Method.

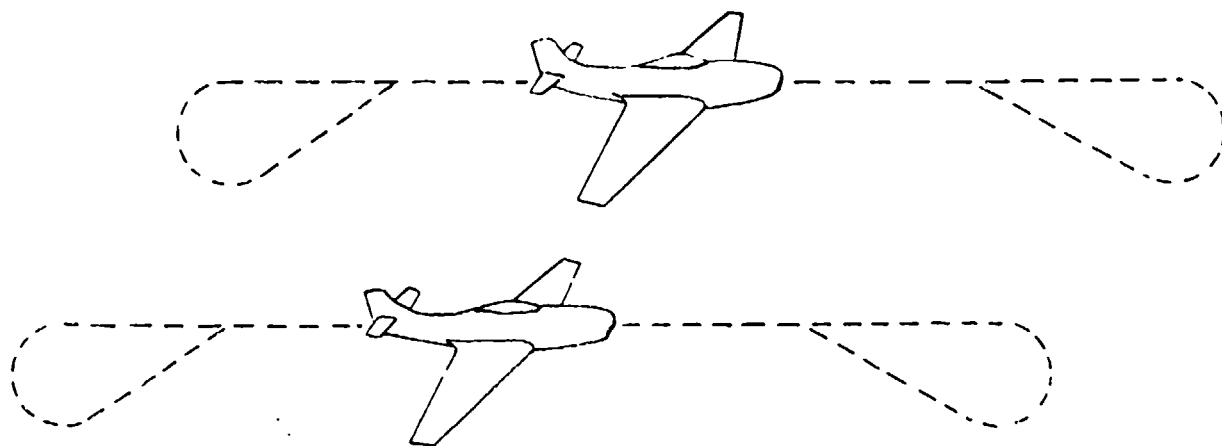
5.6.3 The Pacer Method (See Data Reduction Outline 7.7):

The tower fly-by and ground speed course methods which have been discussed are good for low altitude calibrations. These calibrations may be extrapolated to higher altitudes as discussed in Section 5.4. However, such extrapolations are not always possible. Furthermore, any extrapolations that are made should be checked at altitude. Therefore, calibration methods are necessary by which an aircraft can be calibrated at altitude. One such method is the pacer method in which the test aircraft is calibrated against another previously calibrated aircraft called a pacer. This method is very useful when frequent routine calibrations of aircraft are required.

In the basic form of this method the test aircraft and pacer are flown side by side approximately one wing span apart to prevent aircraft pressure field interaction. When the aircraft are stabilized at the desired speed and altitude, the pilots read the airspeed and altitude simultaneously, or record the data on a photopanel. (See Figure 5.11) A static pressure calibration can be obtained directly from a comparison

of the altitudes or indirectly from a comparison of airspeeds. By comparing both altitude and airspeed readings a check can be made for error in the total pressure system. (An error in total pressure should be suspected if ΔV_{pc} determined by a comparison of airspeeds is consistently greater than ΔV_{pc} determined by a comparison of altimeter readings.) This procedure is followed for a series of speeds at a given altitude to determine the static pressure error as a function of airspeed for that altitude. In this form, the pacer method is limited to the altitude and speed capabilities of the reference aircraft.

Calibrated Aircraft Pilot Records:
 Indicated Airspeed, V_i
 Indicated Altitude, H_i



Test Aircraft Pilot Records:
 Indicated Airspeed, V_t
 Indicated Altitude, H_t

Pressure Altitude of Both Aircraft, H_c
 = Calibrated Aircraft's $H_i + \Delta H_{ic} + H_{pc}$

Figure 5.11

The Pacer Method

It is possible to make calibrations at speeds greater than the speed capabilities of the reference aircraft by the use of a variation called the aircraft fly-by method. Here, the test aircraft flies past the pacer aircraft at the same altitude. With the pressure altitude known from the pacer calibration, the static pressure error may be obtained at any

speed for that altitude. It has the advantage over the basic method in that it is faster as it is not necessary to stabilize the airspeed. In the aircraft fly-by method, it is necessary that both aircraft be at the same altitude. Any deviation may be estimated or the test aircraft may be photographed as it passes by. It is helpful if the pacer aircraft can lay a trail, for example a contrail, as a reference. This allows the test aircraft to accelerate up the reference trail with data being taken as it closes on the pacer aircraft and then either pass the pacer or decelerate back down the reference trail. The acceleration-deceleration technique has the advantage that with data taken both ways the effect of lag can be averaged out or shown to be negligible. This technique is very useful for obtaining data in the transonic region. It is possible to get data up to Mach 1.2 or so with a subsonic pacer. Use of a contrail provides very accurate data since the altitude of a contrail does not usually vary more than 20 or 30 feet within 2 miles of the source. One disadvantage is that persistent contrails are sometimes difficult to obtain. In this case the pacer should be equipped with a smoke generator capable of leaving a well defined trail. Use of a smoke generator is presently limited to non-afterburning operation, however, since the smoke from existing smoke generators is nearly dissipated by the jet exhaust in afterburning.

The calibration of the test aircraft is, of course, only as good as the pacer calibration. For this reason aircraft must be kept exclusively as pacers. They should be calibrated in flight and have their instruments recalibrated at least once a month to insure the accuracy of their calibrations.

The primary advantages of the pacer method over other altitude methods are the simplicity of scheduling, testing and data reduction, the speed and accuracy with which results can be obtained and the fact that the pacer is not restricted to one geographical area. In short, the pacer method is more convenient.

The practicality of the pacer method as compared to other methods depends on how often calibrations are required. Unless calibrations are required relatively frequently the cost of maintaining aircraft solely as pacers is prohibitive. However, when frequent calibrations are required, the pacer method becomes very practical. In general, the cost of keeping the pacer in the air is offset by the reduction in flying time necessary to establish a calibration.

5.6.4 Altitude Pressure Comparison Methods Requiring Pressure Survey (See Data Reduction Outline 7.8):

In this method the position of the aircraft in flight is fixed in space by the use of a radar-theodolite system or a phototheodolite complex such as an Askania range. The static pressure error is determined by comparing the aircraft indicated altitude to the pressure altitude which is determined from the tapeline altitude by means of a pressure survey.

The pressure survey can be conducted in one of several ways:

1. The test aircraft can be tracked by the radar or phototheodolite equipment as it climbs through the required altitude range at a low speed for which the static pressure error is known. It is then flown through the surveyed region at higher speeds for which a calibration is desired. It is possible to use another aircraft which has previously been calibrated to make this pressure survey. In either case, it should be noted that a survey made using this technique can be no better than the original calibration.
2. A radiosonde ballon transmitting pressure measurements can be tracked to determine pressure as a function of tapeline altitude.

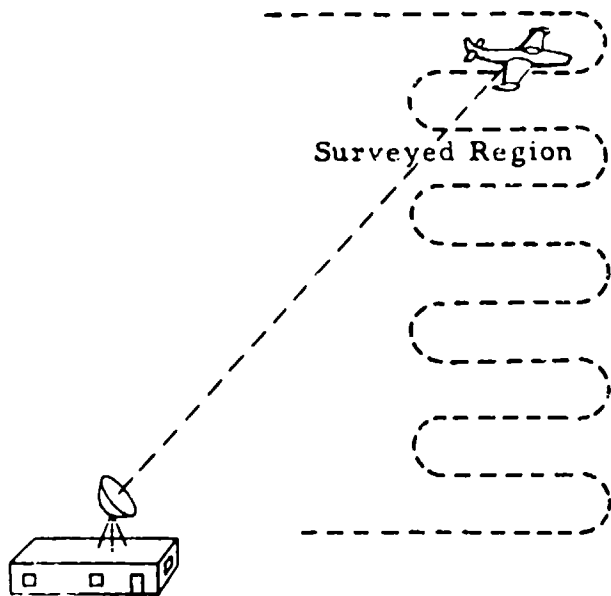
Better accuracy can be obtained by the use of a modified pressure capsule which is more accurate.

3. Data from a radiosonde balloon transmitting temperature and pressure can be used to find temperature as a function of pressure and the relation between altitude and pressure deduced by integration.

$$H = -\frac{R}{G} \sum_{P_{aSL}}^{P_a} \left(\frac{T_a}{P_a} \right) (\Delta P_a) \quad 1.17$$

This integration is discussed in "Mach Number Measurements and Calibrations During Flight at High Speeds and at High Altitudes Including Data for the D-558-II Research Airplane," NACA RM H55J18, 1956 (Confidential) by Brunn and Stillwell. With the use of the same equipment, this method gives much better results than does technique 2.

The results of the pressure survey are plotted as pressure or pressure altitude versus tapeline altitude. The test aircraft is then flown in the surveyed region, recording airspeed and altitude as the radar or phototheodolite records height. The true pressure altitude for each test point is determined from the radar height and pressure survey curve. (See Figure 5.12).



SURVEY

Radar Records:

Height

Calibrated Aircraft Pilot Records:

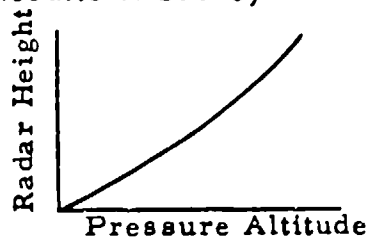
Indicated Airspeed, V_i

Indicated Altitude, H_i

Then:

$$H_c = H_i + \Delta H_{ic} + \Delta H_{pc}$$

Results of Survey Plotted As



CALIBRATION

Radar Records:

Height

Test Aircraft Pilot Records:

Indicated Airspeed, V_i

Indicated Altitude, H_i

Then:

$$H_c = \text{Pressure Altitude at Radar Height on Survey Plot.}$$

Figure 5.12

Altitude Pressure Comparison Method Using Radar

When a phototheodolite system is used the aircraft is tracked from a series of stations with cameras to determine the position in space. The tapeline altitude is determined by triangulation. A minimum of two stations is required for a fix. It is desirable to obtain data from more stations to give additional fixes, which reduces the uncertainty of the measurement. The accuracy with which tapeline altitude can be obtained is very good. However, the overall accuracy of the pressure error determination is limited by that of the pressure survey. Because of the complexity of the tracking system, the data must be processed on a digital computer. Hence,

the data reduction time is apt to be quite large. In addition, the process is quite expensive as it requires costly equipment, large crews to maintain and operate the equipment, and machine data reduction.

The tapeline altitude can be calculated from the elevation and slant range given by a radar-theodolite assembly. The data reduction for this type of installation is much less time consuming than that required by the above installation as one station gives all the necessary information. The radar unit will not give quite as accurate results as those which can be obtained with the photo-theodolite range but its accuracy can be at least as good as that of the pressure survey.

At the Air Force Flight Test Center, radar tracking has been found to be very satisfactory, reliable and relatively economical. Provided that the target carries a beacon, it can be tracked out to a slant range of nearly 100 miles. More refined information, obtained by using a bore-sight camera to correct for radar hunt in azimuth and elevation, can be obtained out to about 20 miles, depending on contrast and so on. The accuracy of the height data is comparable to that with which the associated pressure can be measured or computed, but good velocity data cannot be obtained unless the target is flying in a steady manner. This is illustrated in Figure 5.13 in which a time history from a typical radar calibration is given. A relatively low frequency hunt is apparent which prevents use of the data to deduce velocity unless quite a long record can be averaged. However, when the aim is to calibrate the static pressure source, the radar method is used because of its simplicity and economy. When a more precise trajectory is required, capable of yielding ground speeds directly, the Askania range is used. This gives substantial improvement in precision but cost and complication are much greater than those of a radar calibration. A minimum of four cameras is considered essential and six or more are used if the target is to be tracked over a distance of the order of that covered by the bore-sight radar.

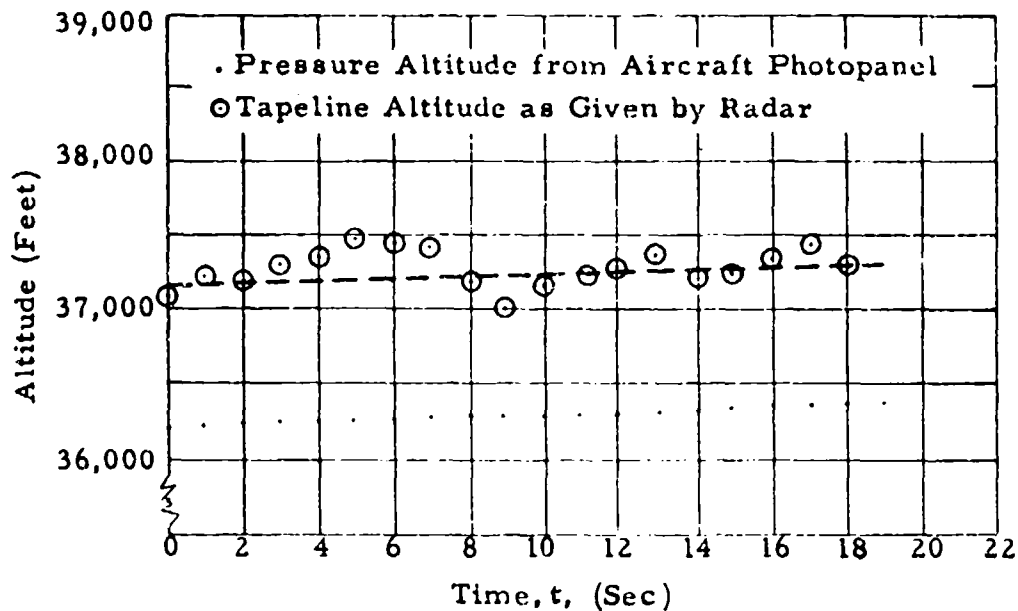


Figure 5.13
Results of a Radar Calibration Showing
Typical Low Frequency Hunt

These techniques are costly and tedious but they can be used in many situations where some of the less complicated methods fail. They permit calibrations in high speed dives and maneuvers, as well as in level flight, and allow calibration of rocket powered aircraft and missiles as long as they stay within the range of the tracking equipment.

5.6.5 The All-Altitude Speed Course:

The principle of the ground speed course can be used at altitude to determine the error in airspeed measurement in the aircraft pitot-static system. However, the establishment of an altitude speed course which will give comparable accuracy is difficult. It is necessary to use an elaborate timing device and electronic or optical means to establish the course length. The accurate measurement of temperature at altitude presents a problem. One must rely either on a previously calibrated free air temperature probe or the weather service and a pressure survey. Also the higher winds which usually exist at altitude cause considerable scatter of data. Therefore, the speed course is not recommended for

altitude calibrations.

A certified speed course has been established at the AFFTC for the purpose of obtaining internationally accepted speed records. It is possible to use this course as a speed course to obtain position error. It is an optical course approximately 10 miles long at 35,000 feet. The overall accuracy of the speeds obtained are to the order of 0.15 percent. Therefore, there is little error in the measurement of ground speed by this method. However, the problems of conversion to true speed and calibrated airspeed and the determination of pressure altitude make the use of the course for this purpose quite impractical.

5.6.6 The Trailing Bomb Method:

In this method a static pressure source is built into a "bomb" which is suspended on a long cable and allowed to trail well below and aft of the aircraft so as to be out of the aircraft pressure field and thus to record free stream static pressure. This is compared to the indicated static pressure (or altitude) to give the static pressure error. The pressures from the two sources may be connected by means of a sensitive differential pressure gage to give the pressure error directly. Hence the accuracy can be very good as long as the trailing bomb is out of the aircraft pressure field.

At low speeds the weight of the bomb is enough to keep it below the test aircraft. At higher speeds, say above 200 knots indicated, the bomb must be fitted with small wings set at a negative angle of attack to keep it out of the slipstream of the aircraft. This, however, introduces the instability problems of a towed glider.

This method is good at stalling speed as long as the downwash at high angles of attack does not cause instability. The upper limit in speed is the speed at which the system encounters high speed instability. It is believed that this high speed instability is due to cable oscillations which originate near the aircraft and are amplified by aerodynamic forces as they travel down the cable.

Years ago when aircraft were not capable of high speeds this was a very popular method. In the case of modern aircraft, this method has lost its popularity because of the high speed instability problem. It is still sometimes used, however, for the calibration of low speed aircraft such as transports.

SECTION 6

CALIBRATION OF THE FREE AIR TEMPERATURE INSTRUMENTATION

6.1 INSTRUMENT ERROR

The major errors in the temperature indicating system are a result of variation of the resistance temperature coefficient in the sensing element and electrical defects in the bridge circuit and ammeter. Errors caused by the sensing elements are minimized by the selection of good quality elements from the manufacturer's lots. The standard tolerance is ± 2 degrees C; however, units having a maximum error of ± 0.5 degrees C are selected for flight test work. A laboratory calibration is conducted to determine errors in the bridge circuit and indicator. The instrument is calibrated every 2 degrees C over the temperature range of anticipated use. A typical calibration plot is shown in Figure 6.1.

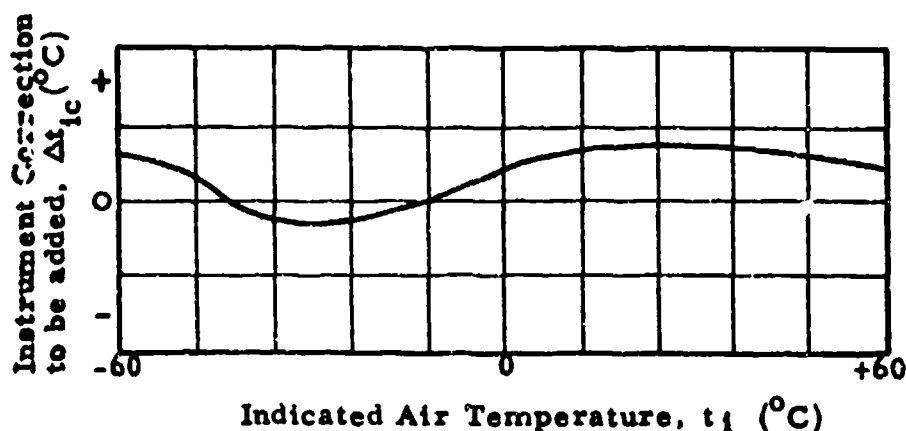


Figure 6.1

Free Air Temperature Instrument Calibration Plot

The indicated temperature corrected for instrument error (T_{ic}) is obtained from this curve, as

$$T_{ic} = T_i + \Delta T_{ic} \quad 6.1$$

where

T_i = indicated temperature

ΔT_{ic} = free air temperature instrument correction corresponding to T_i

6.2 DETERMINATION OF THE TEMPERATURE PROBE RECOVERY FACTOR

The equation for the free air temperature probe was derived in Section 2.4 as

$$\frac{T_{ic}}{T_a} = 1 + \frac{KM^2}{5} \quad 2.30$$

where

- T_a = free air temperature, °K
- T_{ic} = indicated temperature corrected for instrument error, °K
- M = free stream Mach number
- K = temperature probe recovery factor

Values of K should be determined in flight as they depend on the installation. Usually at subsonic speeds variation in K with Mach number and altitude is not significant. At supersonic speeds, however, where temperature rises are much larger, variations in K may exist which must be well established in order that ambient temperatures may be calculated accurately. It is considered advisable to determine values of K throughout the speed range at a high and a low altitude to investigate possible variations in K . This is quite frequently done in conjunction with one or more of the airspeed calibration methods described in Section 5. Several techniques are discussed in the following paragraphs by which temperature probe recovery factors can be determined. The use of radiosonde temperatures in lieu of data derived from free air temperature instruments is also considered.

1. The aircraft is flown at a series of Mach numbers and the data is plotted as K versus M where

$$K = \left(\frac{T_{ic}}{T_a} - 1 \right) \frac{5}{M^2} \quad 6.2$$

This data is readily obtained in conjunction with airspeed calibrations when a pacer aircraft is used, since ambient temperatures can be obtained with a calibrated probe. The results of a typical calibration are given in Figure 6.2.

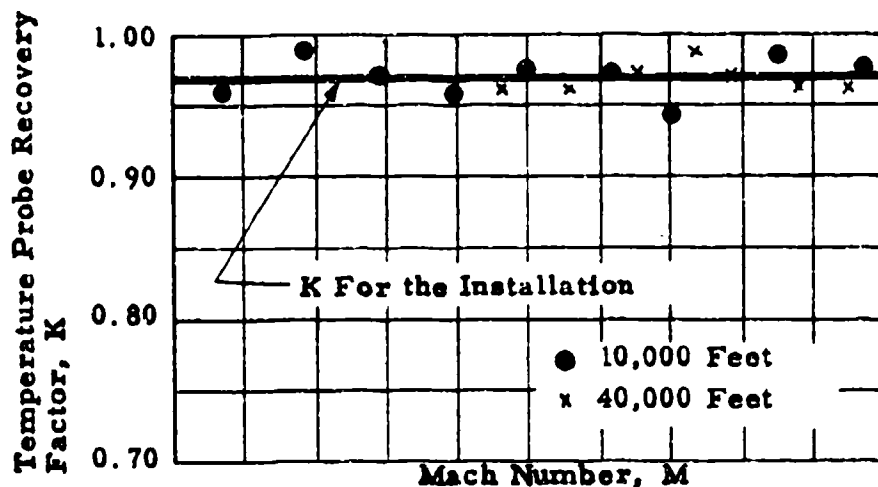


Figure 6.2
Plot of K versus M Used to Determine
The Temperature Probe Recovery Factor, K

Indicated temperatures, recorded while conducting speed-power tests, together with radiosonde temperatures may be used conveniently to make a similar presentation. Care must be taken in this case to avoid systematic errors in ambient temperature measurements.

2. The aircraft is flown at a series of speeds at a constant pressure altitude. It is therefore necessary to prepare tables in advance showing altimeter reading (H_1) at which the aircraft is to be flown for each airspeed.

$$H_1 = H_c - \Delta H_{ic} - \Delta H_{pc} \quad 6.3$$

where

H_c = pressure altitude at which test is to be made

ΔH_{ic} = altimeter instrument correction corresponding to H_i

ΔH_{pc} = altimeter position error correction corresponding to H_{ic}

The results are plotted as $1/T_{ic}$ versus M^2/T_{ic} . When this is done, the slope of a line faired through the data is equal to $(-K/5)$ as

$$\frac{1}{T_{ic}} = \frac{1}{T_a} - \frac{K}{5} \frac{M^2}{T_{ic}} \quad 6.4$$

The intercept on the $1/T_{ic}$ axis is $1/T_a$. Repeat tests made at different air temperatures will give a series of parallel straight lines if K is a constant for the installation. Figure 6.3 shows a plot where runs have been made at two altitudes.

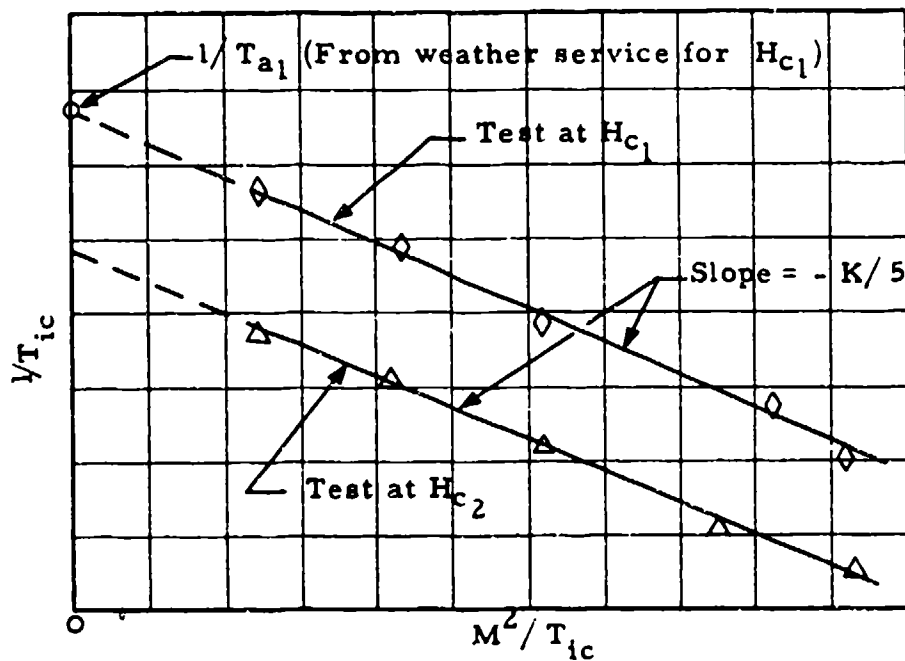


Figure 6.3

Plot of $1/T_{ic}$ versus M^2/T_{ic} Used to Determine the Temperature Probe Recovery Factor, K

This method has the advantage that K can be determined independently of T_a , although it is essential that it remains constant. If T_a is known, say from radiosonde data, it can be used to help establish the slope of the line.

3. Recovery factors can also be determined in conjunction with airspeed calibrations made with the tower fly-by method. In this case a very nearly constant pressure altitude is maintained during each pass by the tower. By recording temperature in the tower and in the aircraft for each pass, the value of K can be established using either of the presentations described in the preceding paragraphs. This method assumes that temperatures recorded in the tower are the same as the ambient temperatures at the probe located on the aircraft. Errors may be incurred if the aircraft is flown higher than the tower, which it usually is, and a pronounced temperature gradient exists. Tower fly-bys are best made during the early morning, however, when the air is most stable near the ground and temperature gradients are small.

4. The speed course method of obtaining airspeed calibrations also yields data from which values of K can be computed. From Section 2.52

$$M = \frac{V_{tt}}{38.967 \sqrt{T_{at}}} \quad 2.36$$

Substituting this expression into equation 2.30

$$T_{ic} = T_a + \frac{KV_t^2}{7592} \quad 6.5$$

where V_t is in knots and T_{ic} and T_a are in °K. The results are plotted as T_{ic} versus V_t . Then, the slope of a line faired through the data is equal to $(+K/7592)$. The intercept on the T_{ic} axis is T_a . (See Figure 6.4)

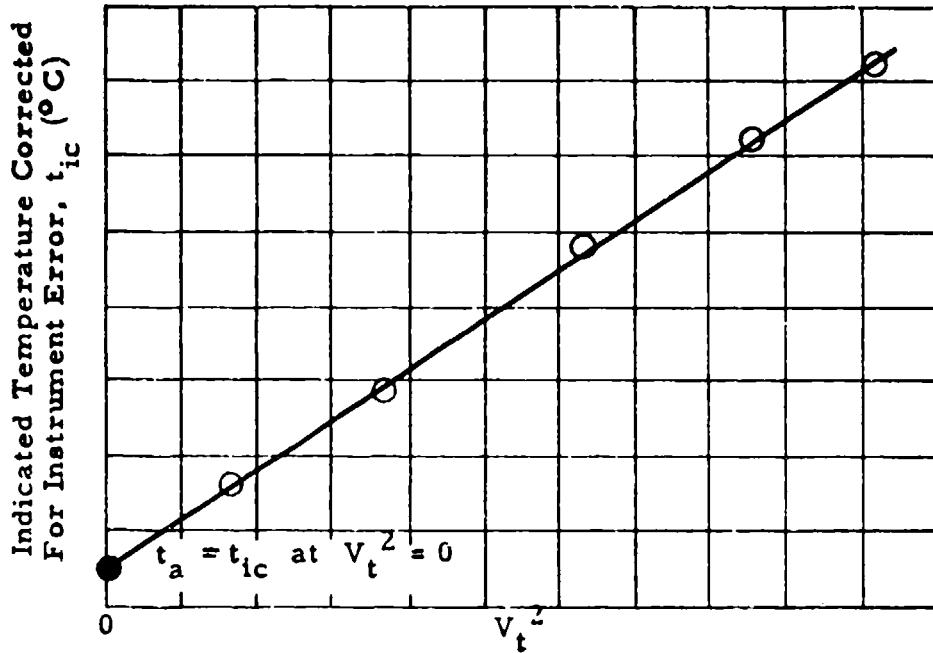


Figure 6.4
 Plot of t_{ic} vs V_t^2 Used to Determine the
 Temperature Probe Recovery Factor, K

T_a can be used with this method also as an aid in establishing the slope of the line through the test points. It is necessary, however, to have low wind conditions or a considerable error in V_t^2 and hence K may result.

When the value of K is established, free air temperature is most easily determined from equation 2.30. Chart 8.2 has been included in Section 8 to facilitate this operation.

Temperature probe recovery factors for supersonic flight may be determined from the methods described in paragraphs 1 and 2 above. Supersonic pacer aircraft with well established probe calibrations for the flight conditions obtained with high speed test aircraft are not generally

available, however, the method described in paragraph 2, where the test aircraft is flown at constant pressure altitude, may be used but additional flight time will probably be required to define K values satisfactorily. Consequently, the use of radiosonde data is likely to be best at supersonic speeds. Recommended temperature accuracies of radiosondes listed in Air Weather Service TR105-133 are

- $\pm 1.5^{\circ}\text{C}$ from $+40^{\circ}\text{C}$ to -50°C
- $\pm 2.0^{\circ}\text{C}$ from -50°C to -70°C
- $\pm 3.0^{\circ}\text{C}$ from -70°C to -90°C

These values were recommended as representing reasonable accuracies to be expected of the temperature data obtained from radiosondes used by the various United States meteorological services. For most accurate results, ambient temperatures from radiosonde data should be based on three or more soundings obtained from stations surrounding the area in which the test aircraft is flown. These soundings should be made within 2 or 3 hours of the time test data is taken. Also, it is best to examine the most recent weather charts prior to flight so that possible frontal passages with significant temperature differences may be avoided.

SECTION 7
DATA REDUCTION OUTLINES

7.1 CORRECTION OF AIRSPEED INDICATOR AND ALTIMETER FOR PRESSURE LAG DURING CONSTANT CLIMB, CONSTANT DESCENT, AND/OR ACCELERATION (See Section 4. 2)

1	λ_{sSL}	sec	Altimeter Lag Constant at Standard Sea Level, from previous calibration
2	λ_{tSL}	sec	Total Pressure Lag Constant at Standard Sea Level, from previous calibration
3	V_{ic}	knots	Indicated Airspeed Corrected for Instrument Error
4	H_{ic}	feet	Indicated Altitude Corrected for Instrument Error
5	dH_{ic}/dt	ft/min	Apparent Rate of Climb (+) or Descent(-), from time history of (4) or from R/C indicator
6	dV_{ic}/dt	kt/sec	Apparent Acceleration (+) or Deceleration (-), from time history of (3)
7	t_a	°C	True Atmospheric Temperature, from t_{ic} and K and M and Chart 8. 2 or from weather service.
8	$\lambda/\lambda H_{ic}$		Lag Constant Temperature Correction, from (4) and (7) and Chart 8. 62
9	$\lambda_{sH_{ic}}/\lambda_{sSL}$		Static Pressure Lag Constant Ratio, from (4) and Chart 8. 61 for $V_{ic} = \text{STATIC}$
10	$\lambda_{tH_{ic}}/\lambda_{tSL}$		Total Pressure Lag Constant Ratio, from (4) and (3) and Chart 8. 61
11	λ_s	sec	Altimeter Lag Constant, (1) x (8) x (9)
12	λ_t	sec	Total Pressure Lag Constant, (2) x (8) x (10)
13	ΔH_{icl}	feet	Altimeter Lag Correction, (11) x (5) \div 60

14	$F_l(H_{ic}, V_{ic})$		Airspeed Indicator Lag Factor, from (3) and (4) and Chart 8.63
15	ΔV_{icl}	knots	Airspeed Indicator Lag Correction, $(12) \times (6) + [(11) - (12)] \times (14) \times (5) \div 60$
16	H_{icl}	feet	Indicated Pressure Altitude Corrected for Instrument and Lag Error, $(4) + (13)$
17	V_{icl}	knots	Indicated Airspeed Corrected for Instrument and Lag Error, $(3) + (15)$

7.2 LABORATORY CALIBRATION FOR THE STATIC PRESSURE LAG CONSTANT (See Section 4.3)

Case a: When pressure gages are used

1			Counter Number
2	t	sec	Time
3	T_a	$^{\circ}K$	Room Temperature, $^{\circ}C + 273.16$
4	P_{sl}	"Hg	Probe Enclosure Static Pressure Gage Reading
5	P_s	"Hg	Aircraft Static Pressure Gage Reading
6	Plot (4) and (5) versus (2) on one graph. (At any pressure coordinate, the time difference between (4) and (5) is the static pressure lag constant for that pressure. This lag will decrease as pressure increases.)		
7	λ_s	sec	Static Pressure Lag Constant for any Pressure, from (6)
8	P_s/P_{aSL}		Pressure Ratio at the Pressure used to Determine (7)
9	λ_{sSL}	sec	Sea Level Static Pressure Lag Constant, $(7) \times (8) \times \frac{288.16}{(3)}$

Case b: When altimeters are used

1			Counter Number
2	t	sec	Time
3	T _a	°K	Room Temperature, °C + 273.16
4	H _{i1}	feet	Probe Enclosure Altimeter Reading
5	ΔH _{ic}	feet	Probe Enclosure Altimeter Instrument Correction Corresponding to (4)
6	H _{ic1}	feet	Probe Enclosure Simulated Pressure Altitude, Corrected for Instrument Error, (4) + (5)
7	H _i	feet	Aircraft Altimeter Reading
8	ΔH _{ic}	feet	Aircraft Altimeter Instrument Correction Corresponding to (7)
9	H _{ic}	feet	Aircraft Indicated Pressure Altitude Corrected for Instrument Error, (7) + (8)
10	Plot (6) and (9) versus (2) on one graph. (At any altitude coordinate, the time difference between (6) and (9) is the static pressure lag constant for that altitude. This lag will increase as altitude increases.)		
11	λ _s	sec	Static Pressure Lag Constant for any Altitude, from (10)
12	P _s /P _{aSL}		Pressure Ratio at the Pressure used to Determine (11)
13	λ _{sSL}	sec	Sea Level Static Pressure Lag Constant, (12) x (11) x $\frac{288.16}{(3)}$

7.3 LABORATORY CALIBRATION FOR THE TOTAL PRESSURE LAG CONSTANT (See Section 4.3)

Case a: When pressure gages are used

1			Counter Number
2	t	sec	Time
3	T _a	°K	Room Temperature, °C + 273.16
4	P _{t'} 1	"Hg	Probe Enclosure Total Pressure Gage Reading
5	P _{t'}	"Hg	Aircraft Total Pressure Gage Reading
6	Plot (4) and (5) versus (2) on one graph. (At any pressure coordinate, the time difference between (4) and (5) is the total pressure lag constant for that pressure. This lag will decrease as pressure increases.)		
7	λ _t	sec	Total Pressure Lag Constant for any Pressure, from (6)
8	P _{t'} /P _a SL		Pressure Ratio at the Pressure Used to Determine (7), (5)/29.92
9	λ _t SL	sec	Sea Level Total Pressure Lag Constant, (7) x (8) $\frac{288.16}{(3)}$

Case b: When airspeed indicators are used

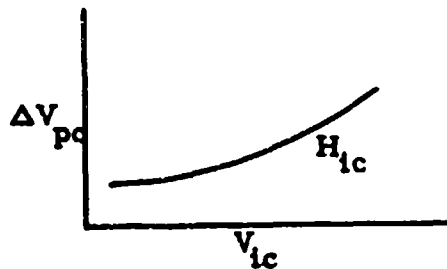
1			Counter Number
2	t	sec	Time
3	T _a	°K	Room Temperature, °C + 273.16
4	P _a	"Hg	Room Ambient Pressure
5	V _{il}	knots	Probe Enclosure Airspeed Indicator Reading
6	ΔV _{ic}	knots	Probe Enclosure Airspeed Indicator Instrument Correction Corresponding to (5)
7	V _{icl}	knots	Probe Enclosure Indicated Airspeed Corrected for Instrument Error, (5) + (6)

8	V_i	knots	Aircraft Airspeed Indicator Reading
9	ΔV_{ic}	knots	Aircraft Airspeed Indicator Instrument Correction Corresponding to (5)
10	V_{ic}	knots	Aircraft Indicated Airspeed Corrected for Instrument Error, (8) + (9)
11	Plot (7) and (10) versus (2) on one graph. (At any airspeed coordinate, the time difference between (7) and (10) is the total pressure lag constant for that airspeed. This lag will decrease as airspeed increases.)		
12	λ_t	sec	Total Pressure Lag Constant for any Airspeed, from (11)
13	q_{cic}	"Hg	Differential Pressure Corresponding to the Airspeed Used to Determine (12), from Table 9.6
14	P_t'	"Hg	Total Pressure Corresponding to the Airspeed Used to Determine (12), (4) + (13)
15	P_t'/P_{aSL}		Pressure Ratio at the Airspeed Used to Determine (12), (14)/29.92
16	λ_{tSL}	sec	Sea Level Total Pressure Lag Constant, (12) x (15) x $\frac{288.16}{(3)}$

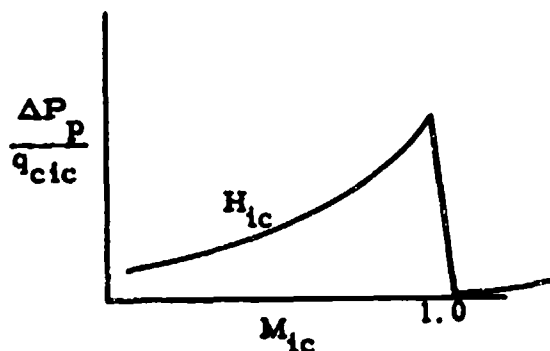
7.4 PRESENTATION OF RESULTS OF POSITION ERROR CALIBRATIONS AND EXTRAPOLATION PROCEDURES (See Section 5.4)

A position error calibration is usually conducted at a series of speeds for a given altitude. From this data it is possible to determine ΔV_{pc} (and/or $\Delta P_p/q_{cic}$) for a series of V_{ic} (or M_{ic}) at a given H_{ic} as shown in Data Reduction Outlines 7.5, 7.6, 7.7 and 7.8. This information should be plotted in accordance with the following outline:

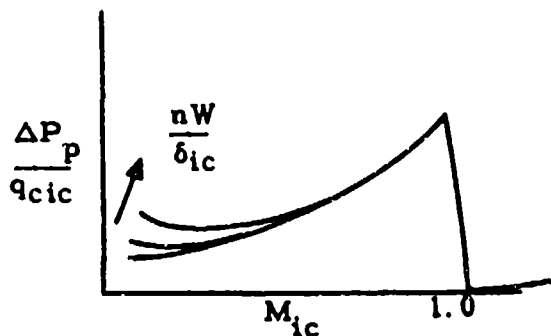
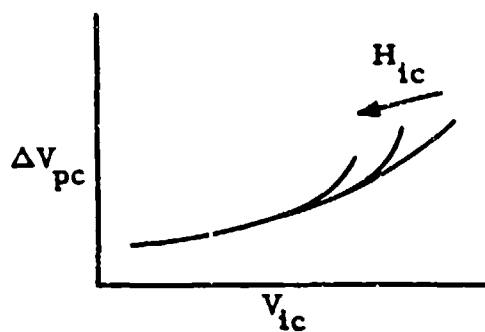
For $M_{ic} < 0.6$, plot ΔV_{pc} versus



For $M_{ic} > 0.6$, plot $\Delta P_p / q_{cic}$ versus M_{ic} for H_{ic}



The plot of ΔV_{pc} versus V_{ic} is good for all altitudes for which there are no Mach number effects. (Mach number effects will appear as altitude breakoffs at the high speed end of the curve.) The plot of $\Delta P_p / q_{cic}$ versus M_{ic} is good for all altitudes for which there are no CL_{ic} (nW / δ_{ic}) effects. (Such effects will appear as nW / δ_{ic} breakoffs, usually at the low speed end of the curve.) A check at a second altitude should be made to see if there are any such altitude breakoffs: The following typical result may be obtained.



In the final report, the position error is usually plotted as ΔH_{pc} and ΔV_{pc} versus V_{ic} for constant H_{ic} . For each H_{ic} for which such plots are desired:

1	H_{ic}	feet	Indicated Altitude Corrected for Instrument Error for which plot is desired.
2	V_{ic}	knots	Arbitrary Indicated Airspeed Corrected for Instrument Error.
3	M_{ic}		Indicated Mach Number Corrected for Instrument Error, from (1) and (2) and Chart 8.5.
4	$\frac{\Delta P_p}{q_{cic}}$		Position Error Pressure Coefficient, from plot of $\Delta P_p/q_{cic}$ versus M_{ic} for (3) and (1).
5	ΔV_{pc}	knots	Airspeed Indicator Position Error Correction, from (2) and (4) and Chart 8.11 or from plot of ΔV_{pc} versus V_{ic} for (1) and (2).
6	ΔH_{pc}	feet	Altimeter Position Error Correction, from (5) and (2) and (1) and Chart 8.13. (For small errors, say $\Delta V_{pc} < 10$ knots, the approximate Chart 8.12 may be used.)
7	Plot ΔV_{pc} and ΔH_{pc} versus V_{ic} for H_{ic} . Repeat for other H_{ic} .*		

* In the case of low speed aircraft in which there are no M_{ic} effects or high speed aircraft in which there are no nW/δ_{ic} effects, the curve of ΔH_{pc} versus V_{ic} for one altitude can be extrapolated to other altitudes by the following procedure:

Case a: Low Speed Aircraft (No M_{ic} effect)

1	H_{ic1}	feet	Indicated Altitude Corrected for Instrument Error Corresponding to an Arbitrary V_{ic}
2	ΔH_{pc1}	feet	Altimeter Position Error Correction Corresponding to (1)
3	σ_1		Density Ratio Corresponding to (1), from Table 9.2
4	H_{ic2}	feet	Arbitrary Indicated Altitude Corrected for Instrument Error
5	σ_2		Density Ratio Corresponding to (4), from Table 9.2
6	ΔH_{pc2}	feet	Altimeter Position Error Correction Corresponding to (4) for same V_{ic} as (1), $(2) \times (3) \div (5)$

Case b: High Speed Aircraft (No nW/δ_{ic} effect)

1	H_{ic1}	feet	Indicated Altitude Corrected for Instrument Error Corresponding to an Arbitrary V_{ic} .
2	ΔH_{pc1}	feet	Altimeter Position Error Correction Corresponding to (1)
3	T_{as1}	$^{\circ}K$	Air Temperature Corresponding to (1), from Table 9.2
4	H_{ic2}	feet	Arbitrary Indicated Altitude Corrected for Instrument Error
5	T_{as2}	$^{\circ}K$	Air Temperature Corresponding to (4), from Table 9.2
6	ΔH_{pc2}	feet	Altimeter Position Error Correction Corresponding to (4) for same V_{ic} as (1), $(2) \times (5) \div (3)$

7.5 THE TOWER FLY-BY METHOD (See Section 5.6.1)

1			Pass Number
2			Time of Day
3			Theodolite Reading
4	Δh	feet	Aircraft Height Above (+) or Below (-) Theodolite Reference Altitude, from (3)
5	P_a	"Hg	Pressure at Reference Altitude, from weather service or theodolite altimeter set at 29.92 and Corrected for Instrument Error. (If altimeter is used (6) below is obtained directly.)
6		feet	Theodolite Reference Pressure Altitude, from (5) and standard atmosphere (Table 9.2)
7	H_c	feet	Pressure Altitude of Aircraft, (6) + (4)
8	H_i	feet	Aircraft Indicated Altitude
9	ΔH_{ic}	feet	Aircraft Altimeter Instrument Correction Corresponding to (8)
10	H_{ic}	feet	Indicated Pressure Altitude Corrected for Instrument Error, (8) + (9)
11	ΔH_{pc}	feet	Aircraft Altimeter Position Error Correction (7) - (10)
12	V_i	knots	Aircraft Indicated Airspeed
13	ΔV_{ic}	knots	Airspeed Indicator Instrument Correction Corresponding to (12)
14	V_{ic}	knots	Indicated Airspeed Corrected for Instrument Error, (12) + (13)
15	M_{ic}		Indicated Mach Number Corrected for Instrument Error, from (10) and (14) and Chart 8.5

16	ΔV_{pc}	knots	Airspeed Indicator Position Error Correction, from (10) and (11) and (14) and Chart 8.13. (For small errors, say $\Delta H_{pc} < 1000$ feet, the approximate Chart 8.12 can be used)
17	$\frac{\Delta P_p}{\rho_{cic}}$		Position Error Pressure Coefficient, from (14) and (16) and Chart 8.11. (This must be determined only for $M_{ic} > 0.6$ or so.)

Note: For presentation of results and extrapolation, see Data Reduction Outline 7.4.

7.6 THE GROUND SPEED COURSE METHOD (See Section 5.6.2)

1			Pass Number
2		feet	Course Length
3	Δt_1	sec	Time Across
4	Δt_2	sec	Time Back
5	V_{g1}	ft/sec	Ground Speed Across, (2) \div (3)
6	V_{g2}	ft/sec	Ground Speed Back, (2) \div (4)
7	V_t	ft/sec	True Speed or Average Ground Speed, (5) + (6) \div 2
8	V_t	knots	True Speed, 0.5921 x (7)
9	Δh	feet	Estimated Height of the Aircraft Above the Ground
10	t_a	$^{\circ}C$	Atmospheric Temperature at Aircraft Height, Ground Temperature - 0.00198 (9)
11	M		Mach Number, from (8) and (10) and Chart 8.4
12	V_i	knots	Indicated Airspeed

13	ΔV_{ic}	knots	Airspeed Indicator Instrument Correction Corresponding to (12)
14	V_{ic}	knots	Indicated Airspeed Corrected for Instrument Error, (12) + (13)
15	H_i	feet	Indicated Altitude
16	ΔH_{ic}	feet	Altimeter Instrument Correction Corresponding to (15)
17	H_{ic}	feet	Indicated Altitude Corrected for Instrument Error, (15) + (16)
18	M_{ic}		Indicated Mach Number Corrected for Instrument Error, from (14) and (17) and Chart 8.5
19	ΔM_{pc}		Machmeter Position Error Correction, (11) - (18)
20	$\frac{\Delta P_p}{\rho_{cic}}$		Position Error Pressure Coefficient, from (19) and (18) and Chart 8.18. (For small errors, say $\Delta M_{pc} < 0.04$, the approximate Chart 8.17 may be used.)
21	ΔV_{pc}	knots	Airspeed Indicator Position Error Correction, from (14) and (20) and Chart 8.11

Note: For presentation of results and extrapolation, see Data Reduction Outline 7.4

7.7 THE PACER METHOD (See Section 5.6.3)

Case a: The Stabilized Flight Method

1			Pass Number
2	H_c	feet	Pressure Altitude, pacer $H_i + \Delta H_{ic} + \Delta H_{pc}$
3	V_c	knots	Calibrated Airspeed, pacer $V_i + \Delta V_{ic} + \Delta V_{pc}$

4	H_i	feet	Test Aircraft Indicated Altitude
5	ΔH_{ic}	feet	Test Aircraft Altimeter Instrument Correction Corresponding to (4)
6	H_{ic}	feet	Test Aircraft Indicated Altitude Corrected for Instrument Error, (4) + (5)
7	ΔH_{pc}	feet	Test Aircraft Altimeter Position Error Correction (2) - (6)
8	V_i	knots	Test Aircraft Indicated Airspeed
9	ΔV_{ic}	knots	Test Aircraft Airspeed Indicator Instrument Correction Corresponding to (8)
10	V_{ic}	knots	Test Aircraft Indicated Airspeed Corrected for Instrument Error, (8) + (9)
11	ΔV_{pc}	knots	Test Aircraft Airspeed Indicator Position Error Correction, (3) - (10) or from (7) and (6) and (10) and Chart 8.13. (For small errors, say $\Delta H_{pc} < 1000$ feet, the approximate Chart 8.12 may be used.)

Note: With the altimeter and airspeed indicator systems both using the same static source, ΔH_{pc} and ΔV_{pc} are related according to Chart 8.12 or 8.13. In the pacer calibration ΔH_{pc} and ΔV_{pc} are both determined independently; hence one of the values is redundant. The altimeter is a much more reliable instrument than the airspeed indicator regarding such things as repeatability and hysteresis so, in general, it is best to rely on the calibrated ΔH_{pc} and calculate ΔV_{pc} . It is possible, however, for low airspeeds and low altitudes that ΔV_{pc} may give better results.

12	M_{ic}		Indicated Mach Number Corrected for Instrument Error, from (6) and (10) and Chart 8.5
13	$\frac{\Delta P_p}{\rho_{ic}}$		Position Error Pressure, Coefficient, from (10) and (11) and Chart 8.11. (This step is necessary only for $M_{ic} > 0.6$ or so.)

Note: For presentation of results and extrapolation, see Data Reduction Outline 7.4

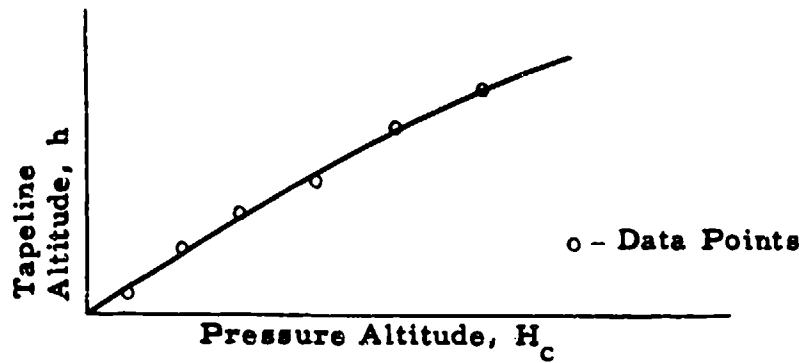
Case b: The Aircraft Fly-By Method

1			Pass Number
2	H_c	feet	Pressure Altitude, pacer $H_i + \Delta H_{ic} + \Delta H_{pc}$
3	H_i	feet	Test Aircraft Indicated Altitude
4	ΔH_{ic}	feet	Test Aircraft Altimeter Instrument Correction Corresponding to (3)
5	H_{ic}	feet	Test Aircraft Indicated Altitude Corrected for Instrument Error, (3) + (4)
6	ΔH_{pc}	feet	Test Aircraft Altimeter Position Error Correction, (2) - (5)
7	V_i	knots	Test Aircraft Indicated Airspeed
8	ΔV_{ic}	knots	Test Aircraft Airspeed Indicator Instrument Correction Corresponding to (7)
9	V_{ic}	knots	Test Aircraft Indicated Airspeed Corrected for Instrument Error, (7) + (8)
10	ΔV_{pc}	knots	Test Aircraft Airspeed Indicator Position Error Correction, from (6) and (5) and (9) and Chart 8.13. (For small errors, say $\Delta H_{pc} < 1000$ feet, the approximate Chart 8.12 may be used.)
11	M_{ic}		Indicated Mach Number Corrected for Instrument Error, from (5) and (9) and Chart 8.5
12	$\frac{\Delta P_p}{\rho_{ic}}$		Position Error Pressure Coefficient, from (9) and (10) and Chart 8.11. (This step is necessary only for $M_{ic} > 0.6$ or so.)

Note: For presentation of results and extrapolation see Data Reduction Outline 7.4

7.8 ALTITUDE PRESSURE COMPARISON METHODS REQUIRING PRESSURE SURVEY (See Section 5.6.4)

- 1 Determine a survey plot of tapeline altitude versus pressure altitude by one of the methods discussed in Section 5.6.4



2	h	feet	Tapeline Altitude, from radar or Askania data.
3	H_c	feet	Aircraft Pressure Altitude, from (1) and (2)
4	H_i	feet	Indicated Altitude
5	ΔH_{ic}	feet	Altimeter Instrument Correction Corresponding to (4)
6	H_{ic}	feet	Indicated Altitude Corrected for Instrument Error, (4) + (5)
7	ΔH_{pc}	feet	Altimeter Position Error Correction, (3) - (6)
8	V_i	knots	Indicated Airspeed
9	ΔV_{ic}	knots	Airspeed Indicator Instrument Correction Corresponding to (8)
10	V_{ic}	knots	Indicated Airspeed Corrected for Instrument Error, (8) + (9)
11	M_{ic}		Indicated Mach Number Corrected for Instrument Error, from (6) and (10) and Chart 8.5

12	ΔV_{pc}	knots	Airspeed Indicator Position Error Correction, from (7) and (6) and (10) and Chart 8.13. (For small errors, say $\Delta H_{pc} < 1000$ feet, the approximate Chart 8.12 may be used.)
13	$\frac{\Delta P_p}{\rho_{cic}}$		Position Error Pressure Coefficient, from (10) and (12) and Chart 8.11. (This step is necessary only for $M_{ic} > 0.6$ or so.)

Note: For presentation of results and extrapolation see Data Reduction Outline 7.4.

7.9 CALIBRATION FOR TEMPERATURE PROBE RECOVERY FACTOR (See Section 6.2)

Case a: K determined from plot of K versus M

1			Pass Number
2	H_i	feet	Altimeter Reading
3	ΔH_{ic}	feet	Altimeter Instrument Correction Corresponding to (2)
4	H_{ic}	feet	Indicated Pressure Altitude Corrected for Instrument Error, (2) + (3)
5	ΔH_{pc}	feet	Altimeter Position Error Correction Corresponding to (4)
6	H_c	feet	True Pressure Altitude, (4) + (5)
7	V_i	knots	Airspeed Indicator Reading
8	ΔV_{ic}	knots	Airspeed Indicator Instrument Correction Corresponding to (7)
9	V_{ic}	knots	Indicated Airspeed Corrected for Instrument Error, (7) + (8)
10	ΔV_{pc}	knots	Airspeed Indicator Position Error Correction Corresponding to (9)

11	V_c	knots	Calibrated Airspeed, (9) + (10)
12	M		Free Stream Mach Number, from (6) and (11) and Chart 8.5
13	t_i	°C	Temperature Probe Reading
14	Δt_{ic}	°C	Temperature Probe Instrument Correction Corresponding to (13)
15	t_{ic}	°C	Indicated Temperature Corrected for Instrument Error, (13) + (14)
16	T_{ic}	°K	Indicated Temperature Corrected for Instrument Error, (15) + 273.16
17	T_a	°K	Ambient Temperature, from previously calibrated probe or from weather service
18	T_{ic}/T_a		(16) ÷ (17)
19	K		Temperature Probe Recovery Factor, $5 \left[\frac{(18) - 1}{(12)^2} \right]$
20	Plot (19) versus (12) and fair a line through the points giving an average value for K. See Figure 6.2		
21	K		Temperature Probe Recovery Factor, from plot of (20)

Case b: K determined from plot of $1/T_{ic}$ versus M^2/T_{ic}

1 to 16 as in case "a" above

17	$1/T_{ic}$	$1/°K$	$1/(16)$
18	M^2		$(12)^2$
19	M^2/T_{ic}	$1/°K$	$(18) \times (17)$
20	Plot (17) versus (19) and fair a straight line through the points. (If T_a is known it may be plotted as $1/T_a = 1/T_{ic}$ at $M^2 = 0$ and be used to fair in the line.) See Figure 6.3		

21	m		<p>Slope of the straight line of (20). For any two points on the line, 1 and 2, the slope is equal to:</p> $m = \frac{\left(\frac{1}{T_{ic}}\right)_2 - \left(\frac{1}{T_{ic}}\right)_1}{\left(\frac{M^2}{T_{ic}}\right)_2 - \left(\frac{M^2}{T_{ic}}\right)_1}$
----	---	--	--

22	K		Temperature Probe Recovery Factor, - 5 x (21)
----	---	--	---

Case c: K determined from plot of T_{ic} versus V_t^2 (Speed Course Method)

1			Pass Number
2		feet	Course Length
3	Δt_1	sec	Time Across
4	Δt_2	sec	Time Back
5	V_{t_1}	ft/sec	Ground Speed Across, (2) ÷ (3)
6	V_{t_2}	ft/sec	Ground Speed Back, (2) ÷ (4)
7	V_t	ft/sec	True Airspeed, (assumed to be Average Ground Speed,) [(5) + (6)] ÷ 2
8	V_{t_2}	knots	True Airspeed, 0.5921 x (7)
9	V_t	knots ²	(8) ²
10	t_i	°C	Temperature Probe Reading
11	Δt_{ic}	°C	Temperature Probe Instrument Correction Corresponding to (10)
12	t_{ic}	°C	Indicated Temperature Corrected for Instrument Error, (10) + (11)
13	T_{ic}	°K	Indicated Temperature Corrected for Instrument Error (12) + 273.16

14 | Plot (13) versus (9) and fair a straight line through the data. (If T_a is known it may be plotted as $T_a = T_{ic}$ at $V_t^2 = 0$ and be used to fair in the line.) See Figure 6.4.

15 | m | | Slope of the straight line of (14). For any two points on the line, 1 and 2, the slope is equal to:

$$m = \frac{(T_{ic})_2 - (T_{ic})_1}{(V_t^2)_2 - (V_t^2)_1}$$

16 | K | | Temperature Probe Recovery Factor, 7592 x (15)

SECTION 8: CHARTS

CHART 8.1

(See paragraph 1.1.3)

**GEOPOTENTIAL ALTITUDE, $H (G/g_{SL})$, (Thousands of Feet) versus
ALTITUDE CORRECTION FACTOR, $h - H (G/g_{SL})$, (Feet)**

$$h - H\left(\frac{G}{g_{SL}}\right) = \frac{H^2 \left(\frac{G}{g_{SL}}\right)^2}{r - H\left(\frac{G}{g_{SL}}\right)}$$

where: H = geopotential altitude, geopotential feet
 h = tapeline altitude, feet
 r = 20,930,000 feet
 G/g_{SL} = 1 foot/geopotential foot

Example:

Given: H = 76,500 geopotential feet

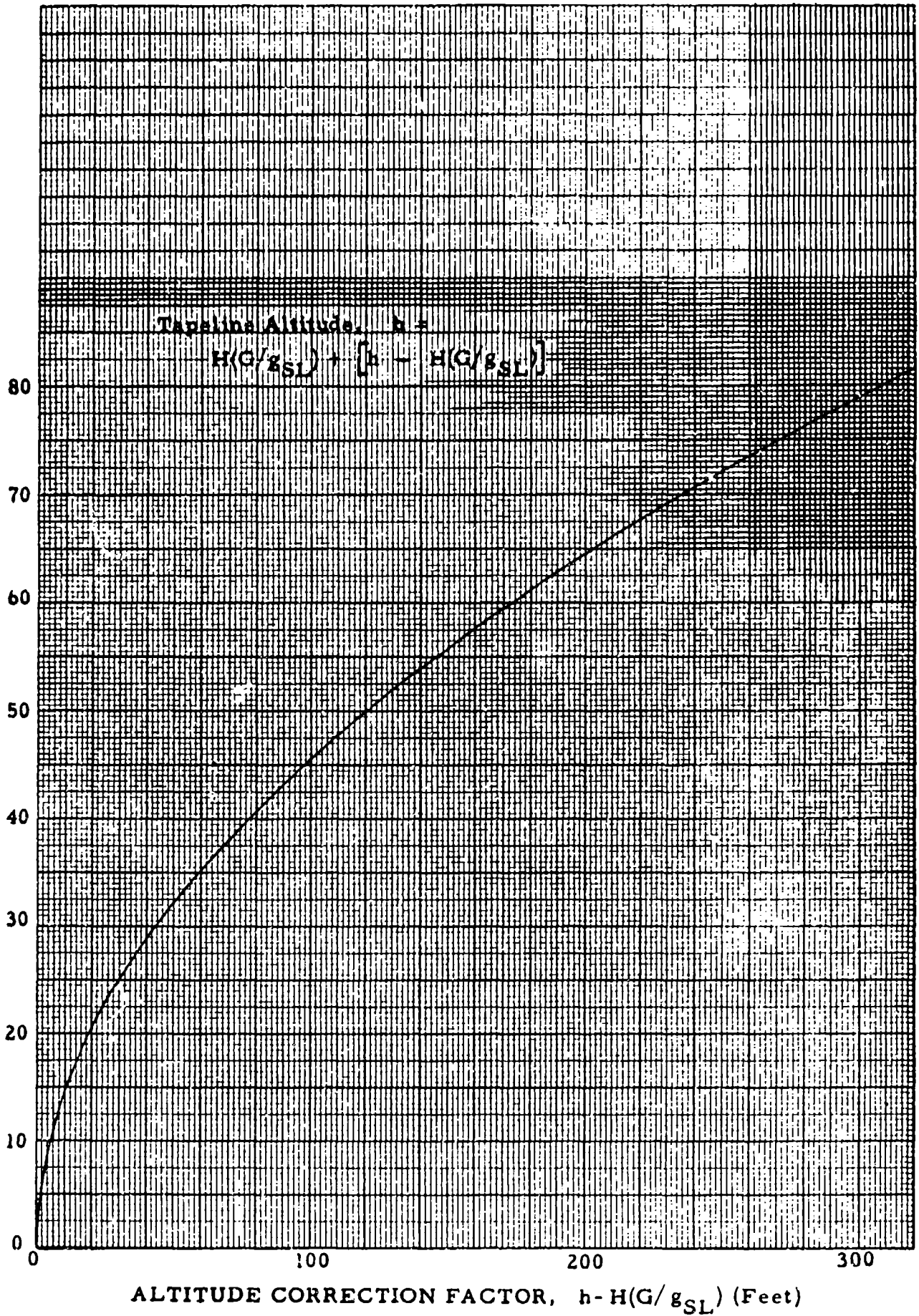
Required: Tapeline altitude, h in feet

Solution: $H(G/g_{SL}) = 76,500$ feet

From Chart 8.1, $h - H(G/g_{SL}) = 283$ feet

$$h = \left[H(G/g_{SL}) \right] + \left[h - H(G/g_{SL}) \right] = 76,783 \text{ feet}$$

GEOPOTENTIAL, $H(G/g_{SL})$ (Thousands of Feet)



ALTITUDE CORRECTION FACTOR, $h - H(G/g_{SL})$ (Feet)

CHART 8.2

(See paragraph 2.4)

MACH NUMBER, M vs ATMOSPHERE TEMPERATURE, T_a ($^{\circ}\text{K}$) or t_a ($^{\circ}\text{C}$) for INDICATED TEMPERATURE, t_{ic} ($^{\circ}\text{C}$) = CONSTANT and TEMPERATURE PROBE RECOVERY FACTOR, K = CONSTANT

ALSO

MACH NUMBER, M vs RATIO OF INDICATED TO ATMOSPHERIC TEMPERATURE, T_{ic}/T_a ($^{\circ}\text{K}/^{\circ}\text{K}$) for TEMPERATURE PROBE RECOVERY FACTOR, K = CONSTANT

$$\frac{T_{ic}}{T_a} = 1 + K \frac{M^2}{5}$$

Example:

Given: $M = 0.785$; $K = 0.80$; $t_{ic} = 15^{\circ}\text{C}$

Required: $\frac{T_{ic}}{T_a}$ and t_a ($^{\circ}\text{C}$)

Solution: Use Page 1 of Chart 8.2. For the given conditions,

$$\frac{T_{ic}}{T_a} = 1.0985; \quad t_a = -11.0^{\circ}\text{C}$$

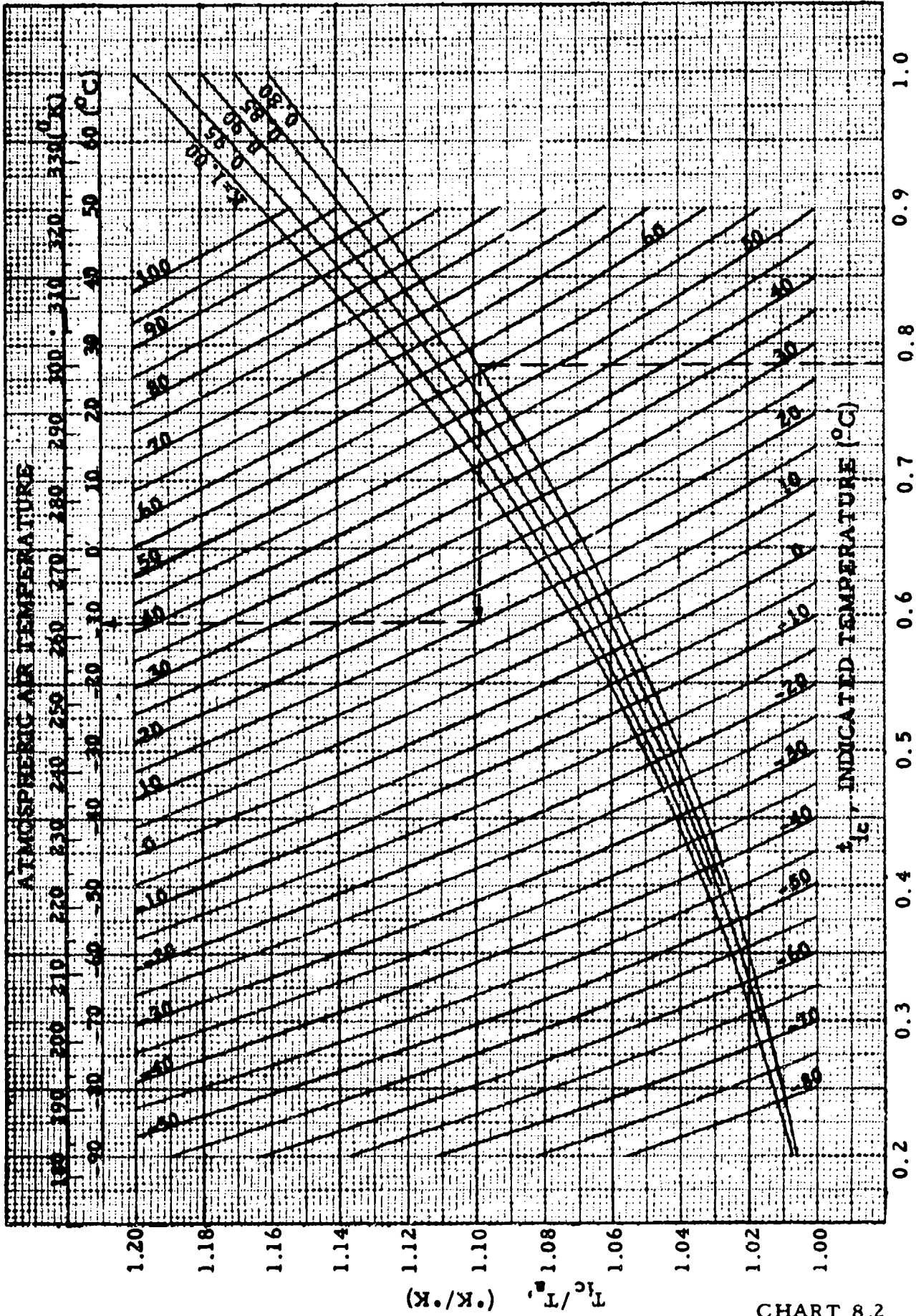
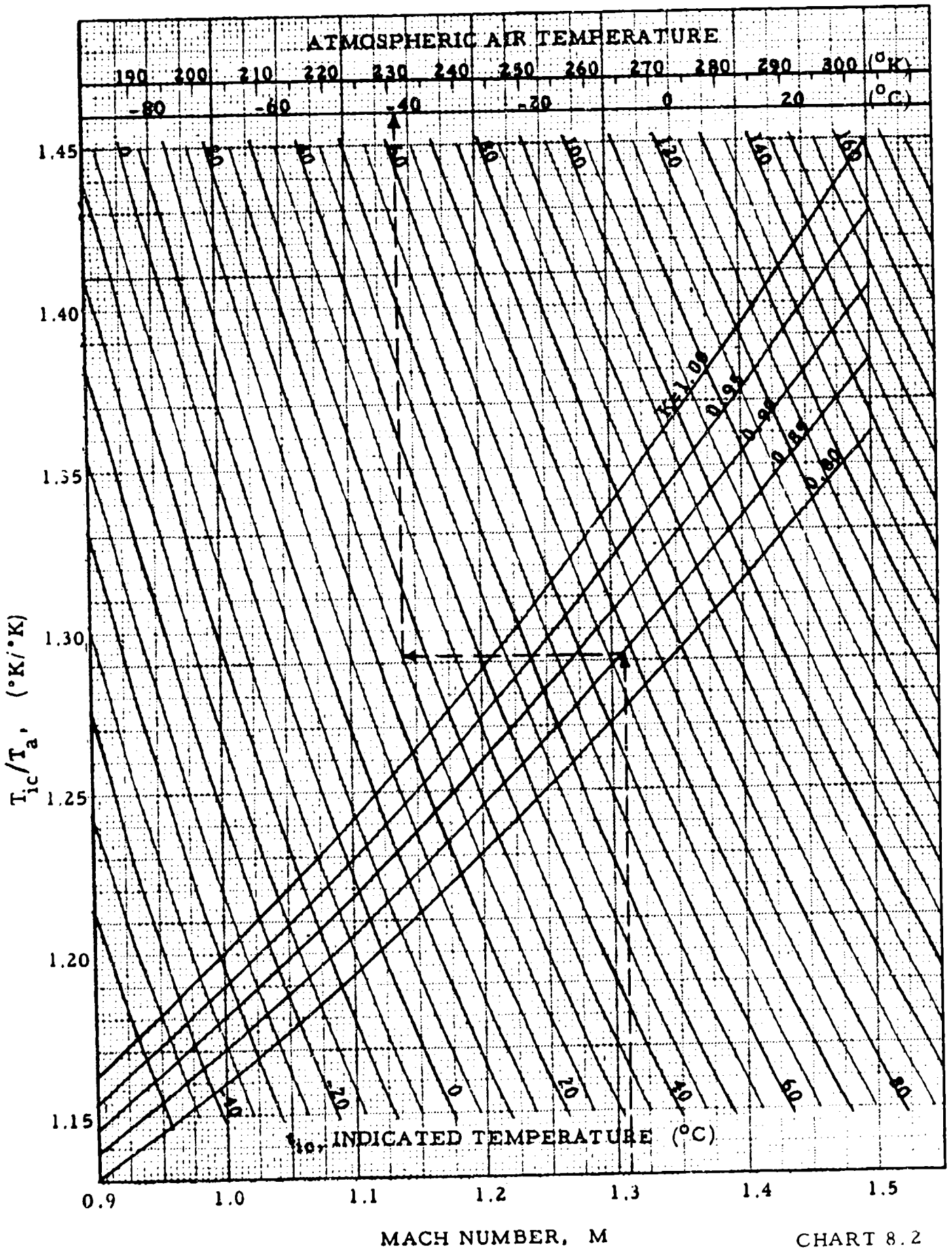


CHART 8.2



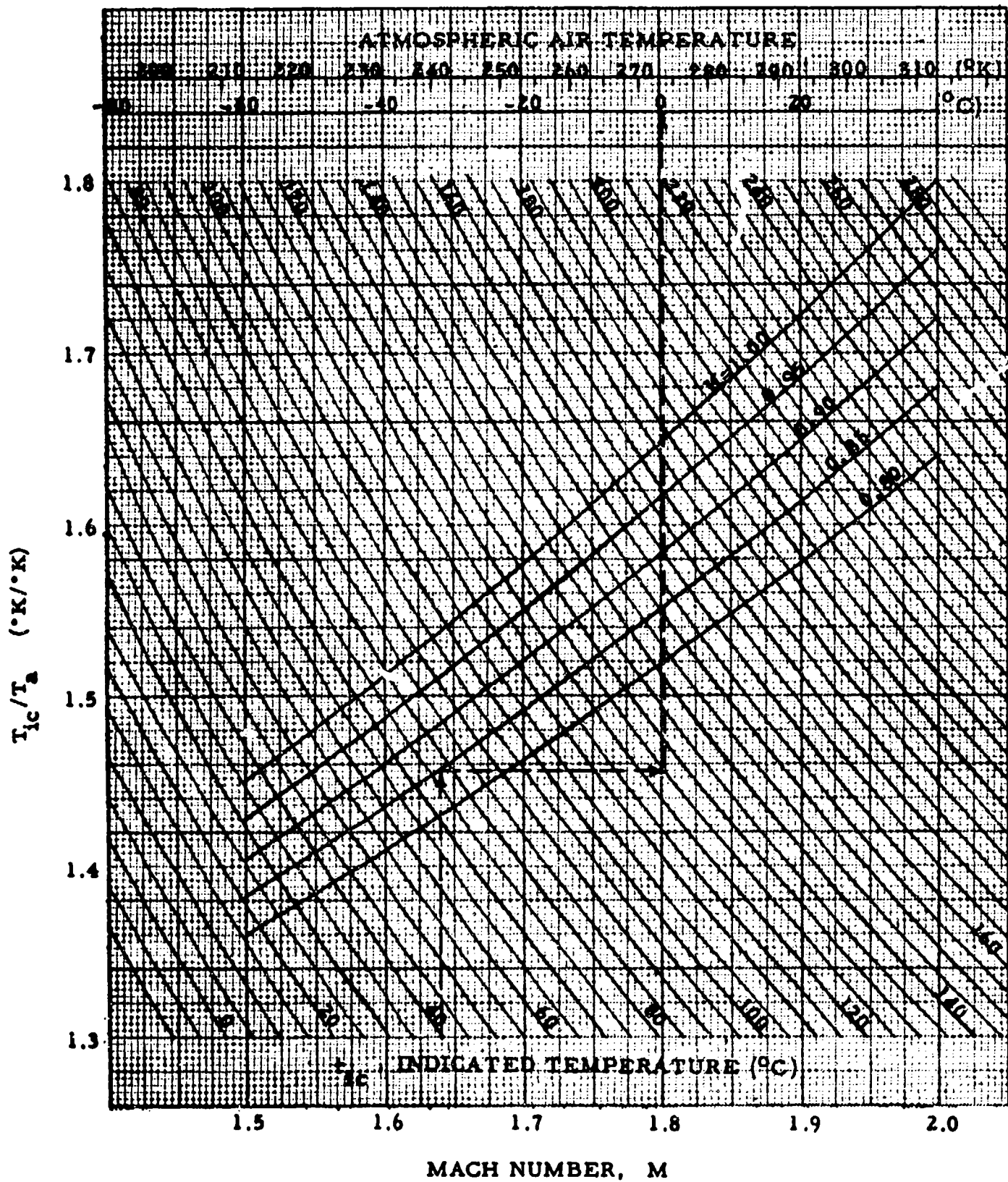
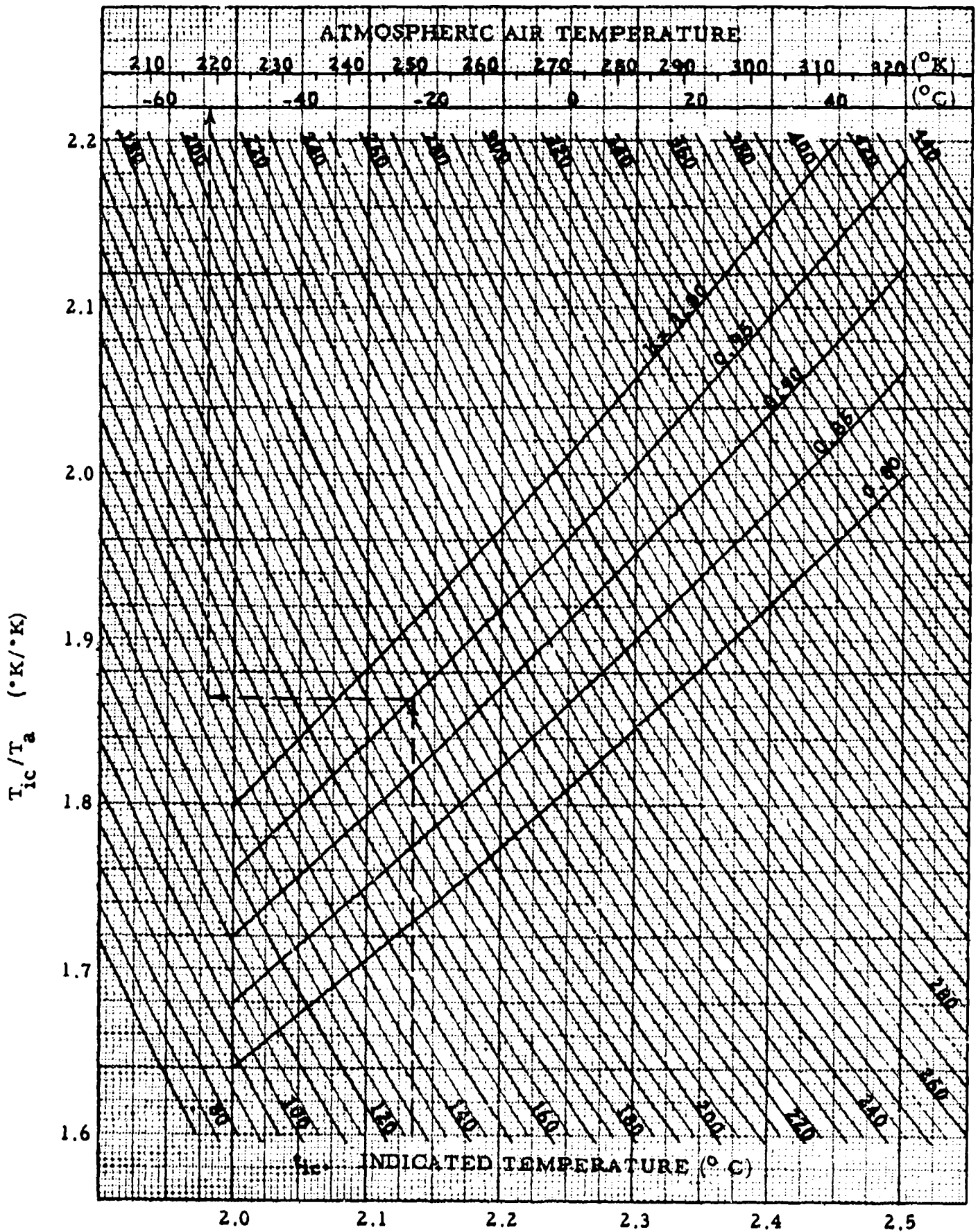


CHART 8.2

ATMOSPHERIC AIR TEMPERATURE



MACH NUMBER, M

CHART 8.2

ATMOSPHERIC AIR TEMPERATURE

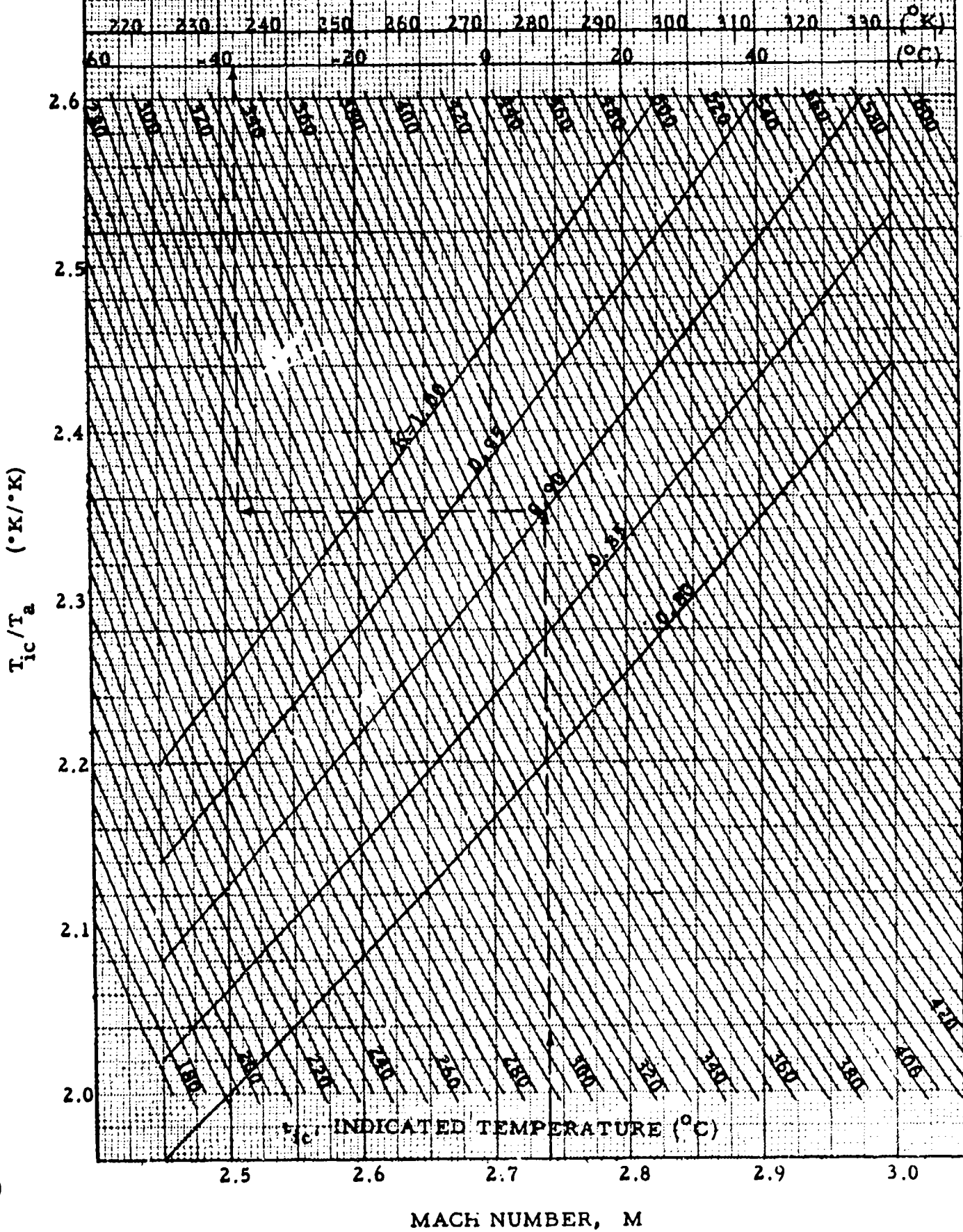
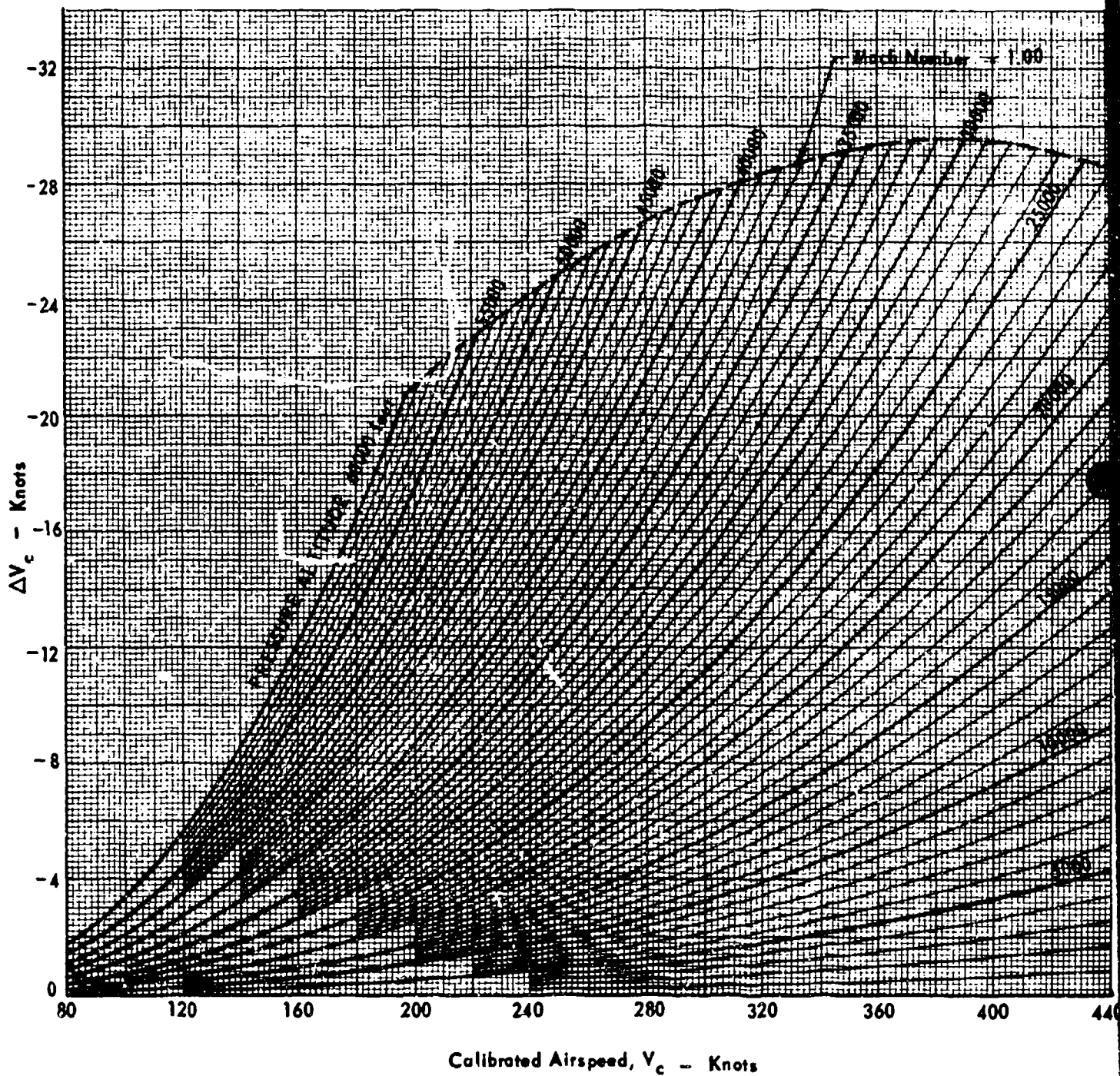


CHART 8.2

COMPRESSIBILITY CORRECTION TO CALIBRATED AIRSPEED

$$V_i \sqrt{\sigma} = V_e = V_c + \Delta V_c$$



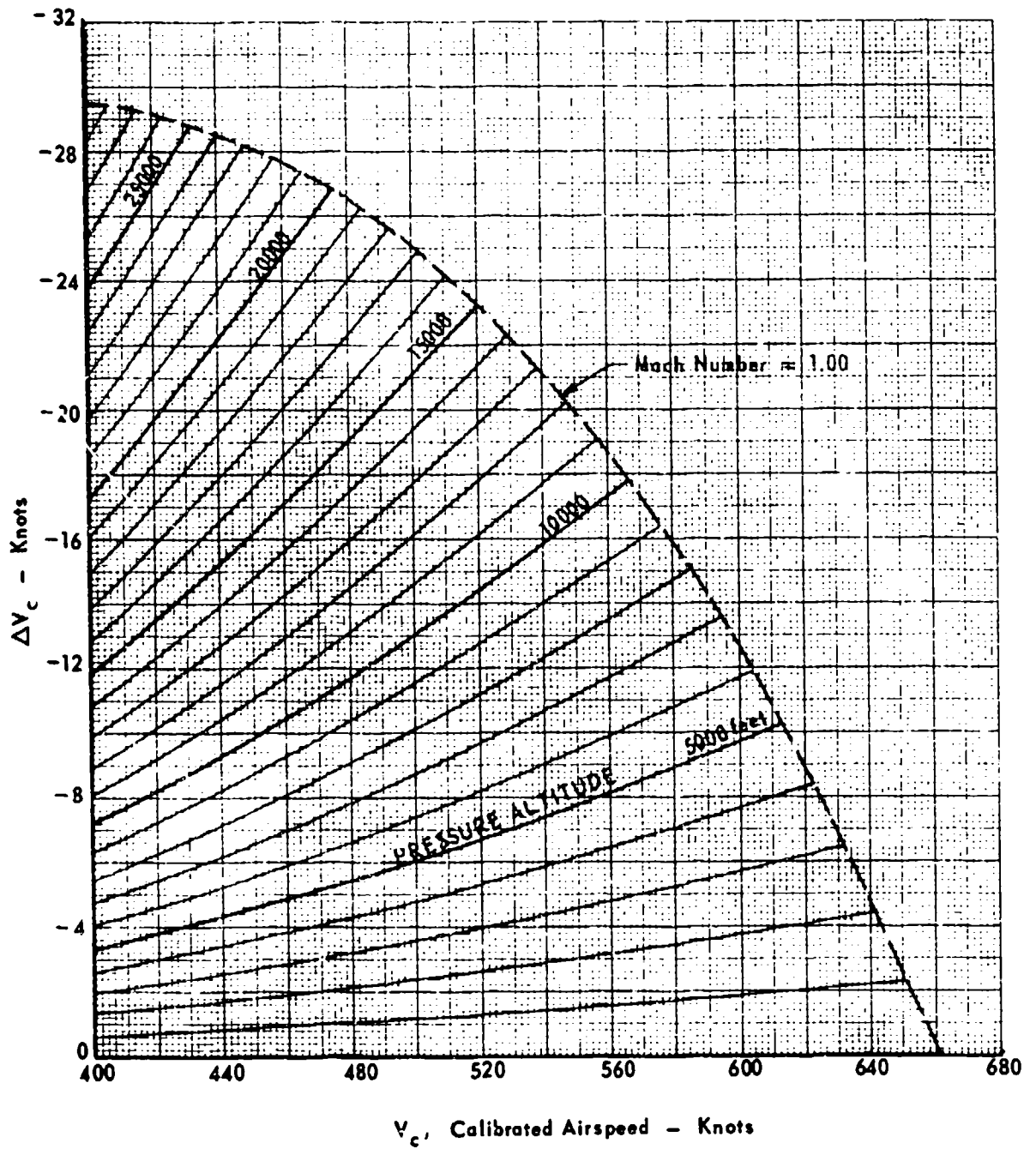


CHART 8.3

(See paragraph 2.5.1)

**PRESSURE ALTITUDE, H_c (Thousands of Feet) versus EQUIVALENT
SPEED - MACH NUMBER RATIO, V_e/M (Knots)**

$$\frac{V_e}{M} = a \sqrt{\sigma}$$

where a and σ correspond to H_c

Example:

Given: $M = 0.39$; $H_c = 18,000$ Feet

Required: V_e in Knots

Solution: $\frac{V_e}{M} = 466$ Knots

$$V_e = \left(\frac{V_e}{M}\right) M = 139.8 \text{ Knots}$$

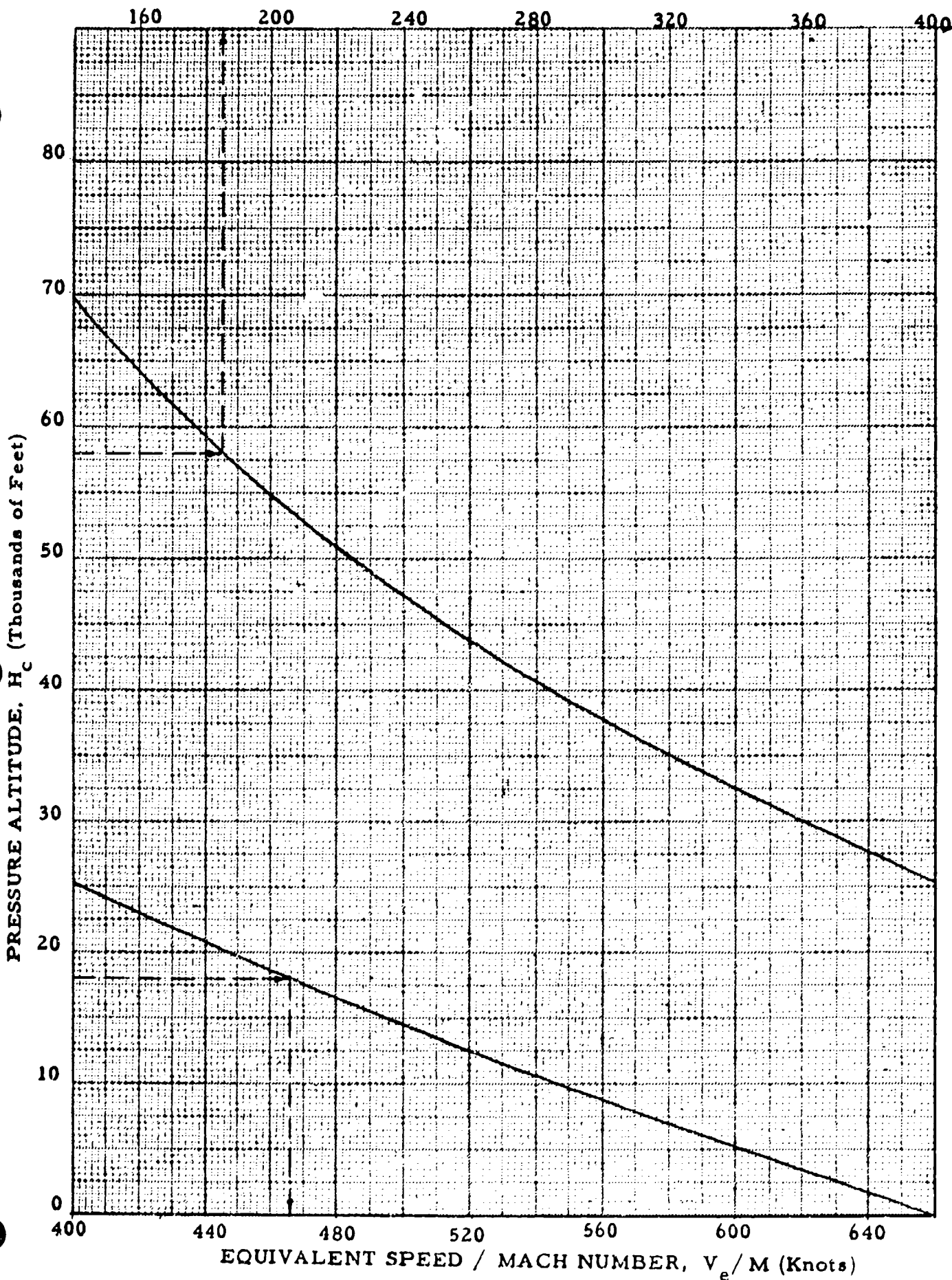


CHART 8.4

(See paragraph 2.5.2)

TEST DAY TRUE SPEED, V_{tt} versus TEST DAY ATMOSPHERIC TEMPERATURE, t_{at} ($^{\circ}\text{C}$) for MACH NUMBER, $M = \text{CONSTANT}$

$$V_{tt} = 38.967M \sqrt{t_{at} (^{\circ}\text{C}) + 273.16}, \text{ knots}$$

ALSO

TRUE SPEED FOR STANDARD DAY, V_{ts} versus STANDARD DAY ATMOSPHERIC TEMPERATURE, t_{as} ($^{\circ}\text{C}$) for MACH NUMBER, $M = \text{CONSTANT}$

$$V_{ts} = 38.967M \sqrt{t_{as} (^{\circ}\text{C}) + 273.16}, \text{ knots}$$

where t_{as} corresponds to H_c .

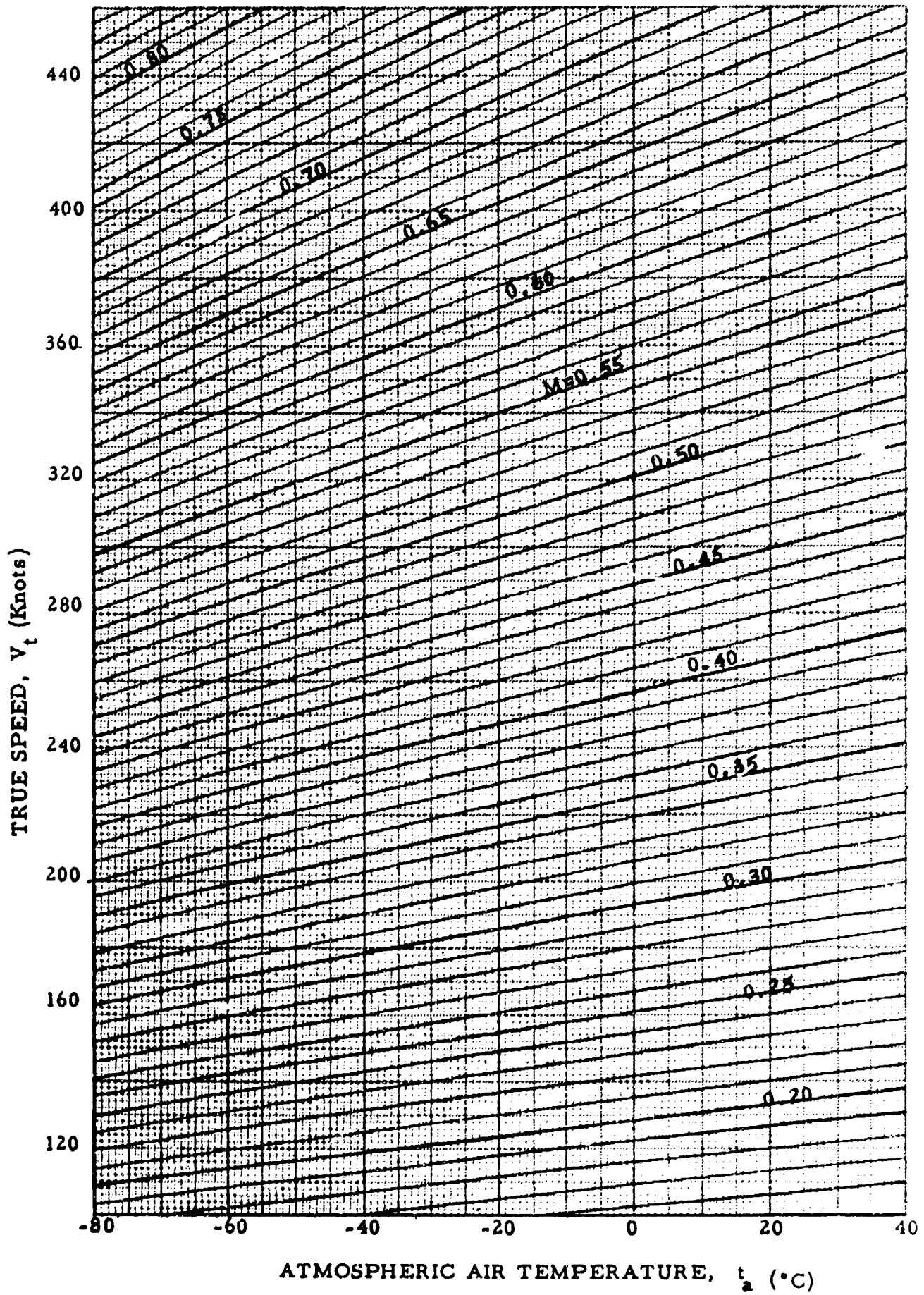
Example:

Given: $M = 2.15$; $t_{at} = -60^{\circ}\text{C}$

Required: V_{tt} in knots

Solution: Use Page 4 of Chart 8.4. For the given conditions

$V_{tt} = 1223$, knots



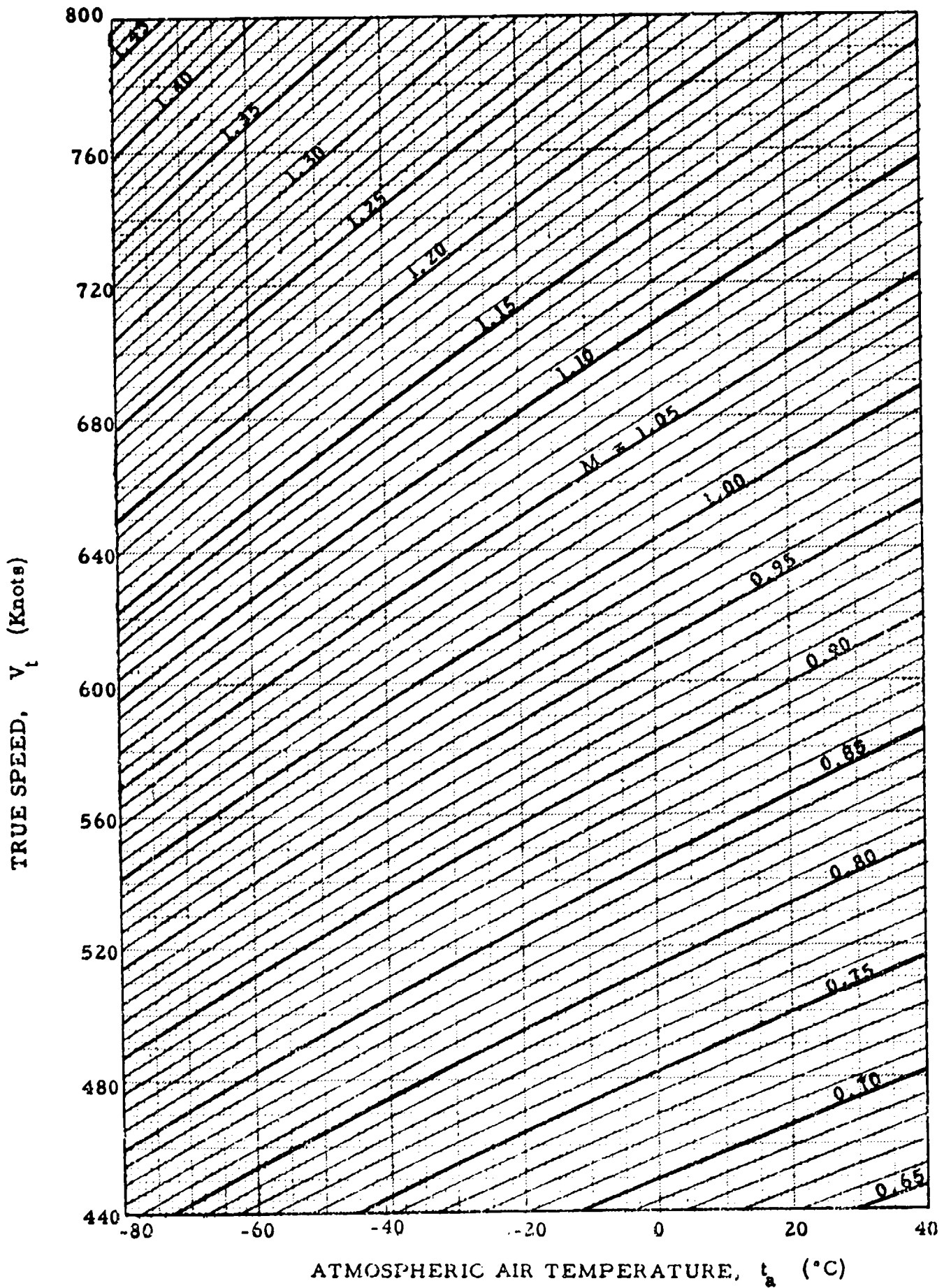


CHART 8.4

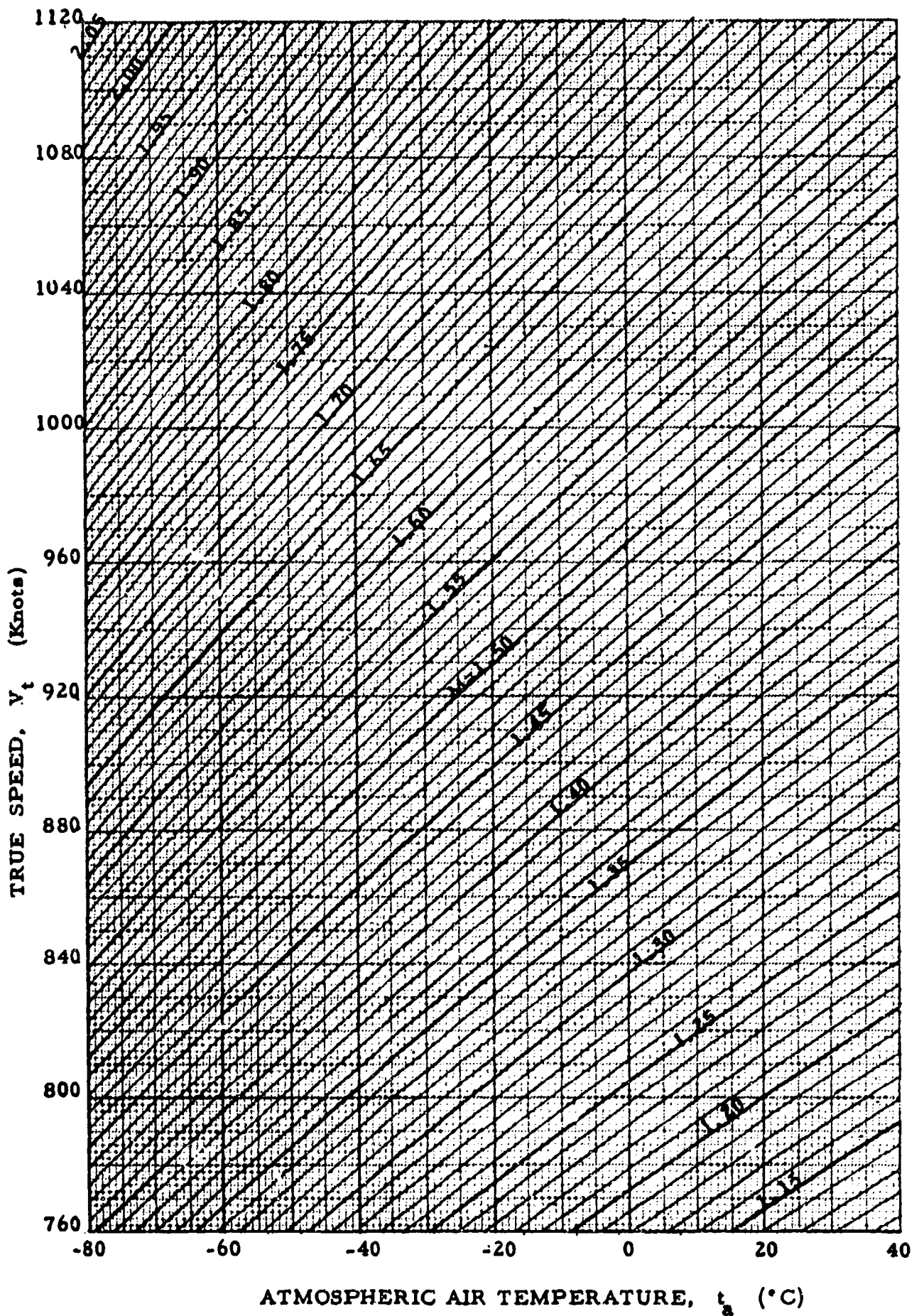


CHART 8.4

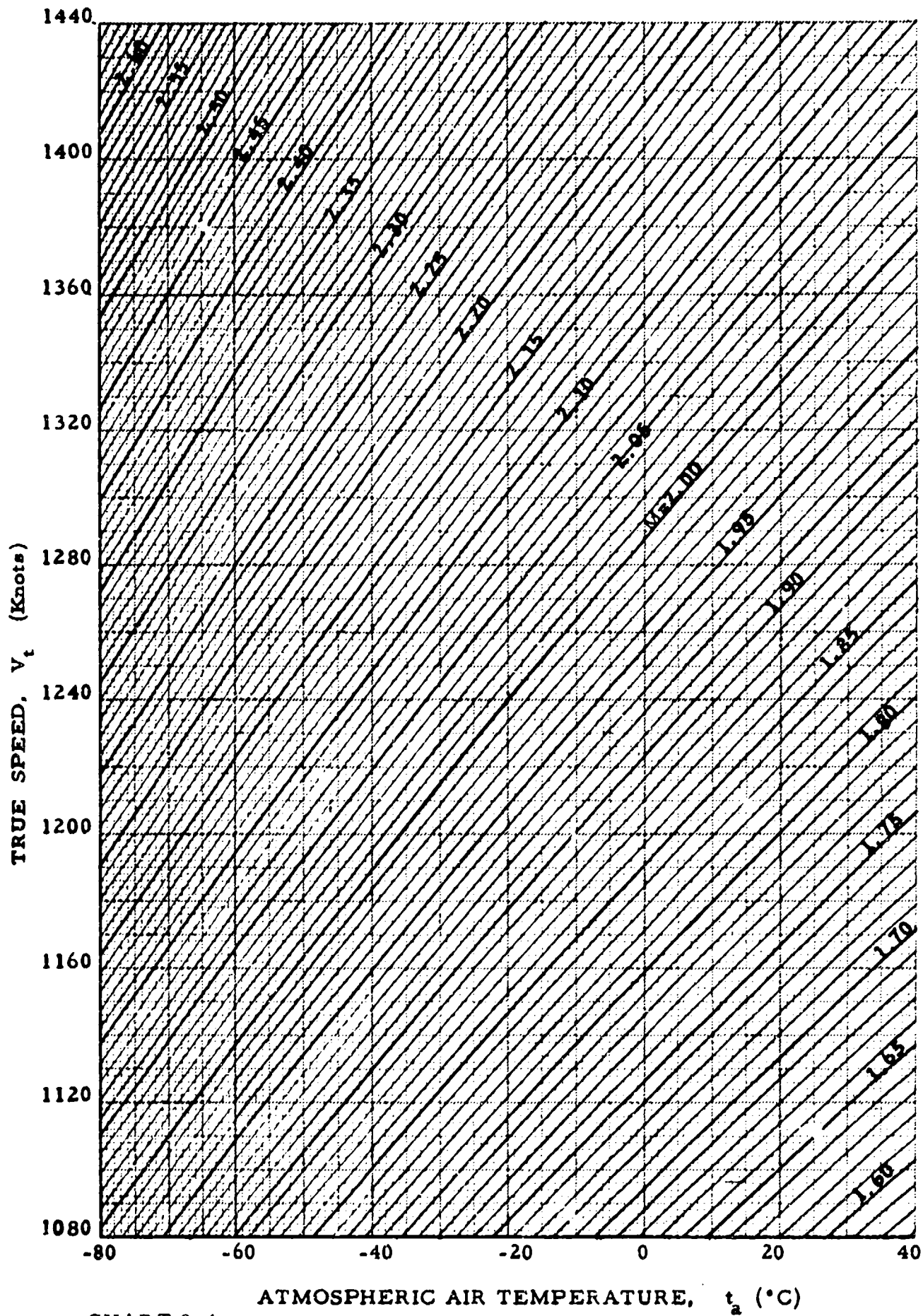


CHART 8.4

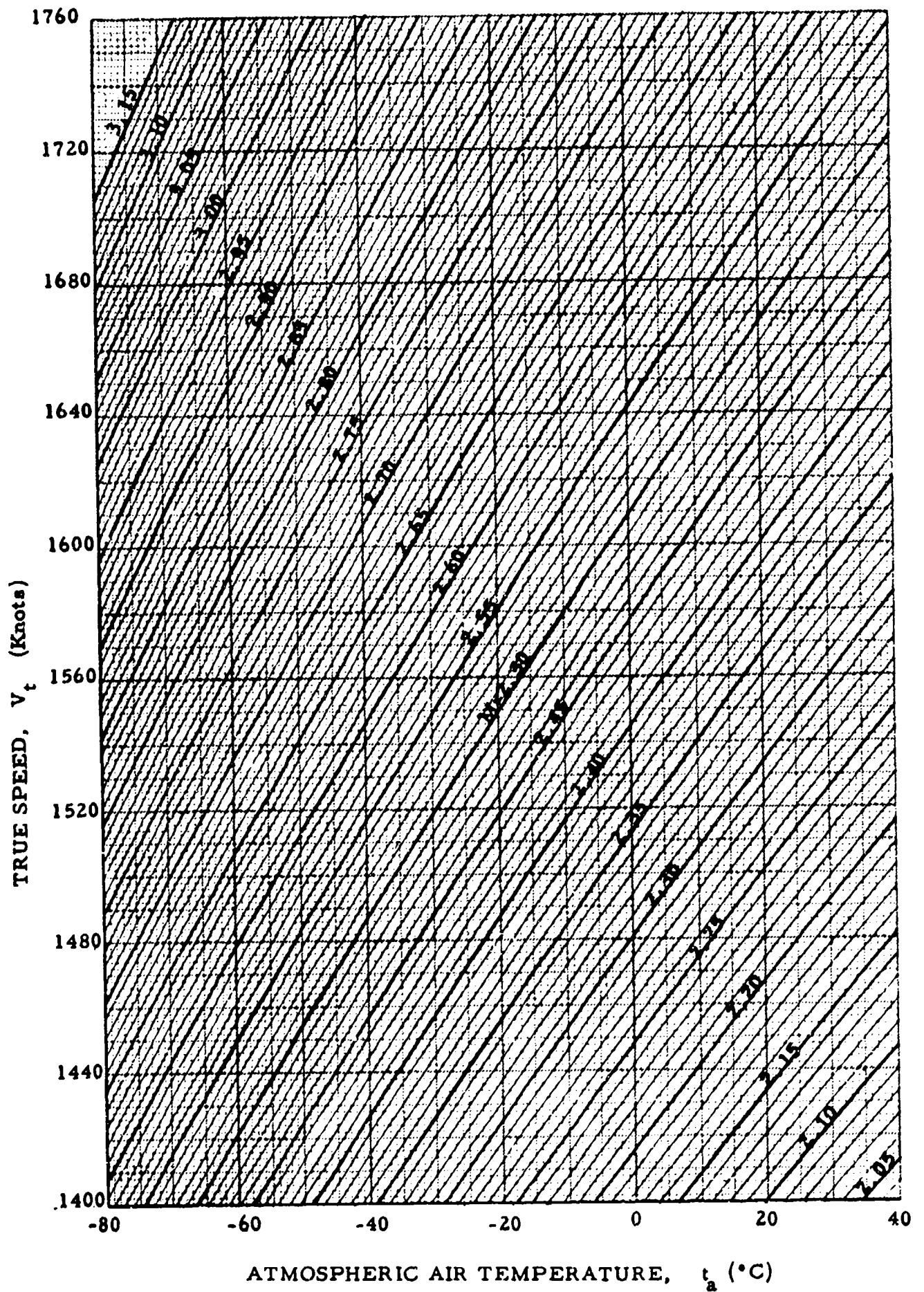


CHART 8.4

CHART 8.5

(See paragraph 2.5.2)

MACH NUMBER, M versus CALIBRATED AIRSPEED, V_c for
PRESSURE ALTITUDE, $H_c = \text{CONSTANT}$

and

MACH NUMBER, M versus CALIBRATED AIRSPEED, V_c for
STANDARD DAY TRUE SPEED, $V_{ts} = \text{CONSTANT}$

ALSO

INDICATED MACH NUMBER CORRECTED FOR INSTRUMENT ERROR,
 M_{ic} versus INDICATED AIRSPEED CORRECTED FOR INSTRUMENT
ERROR, V_{ic} for INDICATED PRESSURE ALTITUDE CORRECTED FOR
INSTRUMENT ERROR, $H_{ic} = \text{CONSTANT}$

Given: H_c and V_{ts}

$$1 \quad (a) \quad \frac{T_{as}}{T_{aSL}} = 1 - 6.87535 \times 10^{-6} H_c \quad H_c \leq 36,089.24 \text{ feet}$$

$$(b) \quad \frac{T_{as}}{T_{aSL}} = 0.751874 \quad H_c \geq 36,089.24 \text{ feet}$$

$$2 \quad \frac{a_s}{a_{SL}} = \left(\frac{T_{as}}{T_{aSL}} \right)^{1/2}$$

$$3 \quad M = \frac{V_{ts}}{a_s} = \frac{V_{ts}}{a_{SL}} \frac{a_s}{a_{SL}}$$

$$4 \quad (a) \quad \frac{q_c}{P_a} = \left[(1 + 0.2M^2)^{3.5} - 1 \right] \quad M \leq 1.00$$

$$(b) \quad \frac{q_c}{P_a} = \left[\frac{(166.921 M^7)}{(7M^2 - 1)^{2.5}} - 1 \right] \quad M \geq 1.00$$

$$5 \quad \frac{q_c}{P_{aSL}} = \frac{q_c}{P_a} \frac{P_a}{P_{aSL}}$$

$$6 \quad (a) \quad \frac{P_a}{P_{aSL}} = \left(\frac{T_{as}}{T_{aSL}} \right)^{5.2561} \quad H_c \leq 36,089.24 \text{ feet}$$

$$(b) \quad \frac{P_a}{P_{aSL}} = 0.223358e^{-4.80634 \times 10^{-5}(H_c - 36,089.24)} \quad H_c \geq 36,089.24 \text{ feet}$$

$$7 \quad (a) \quad \frac{V_c}{a_{SL}} = 2.23607 \sqrt{\left(\frac{q_c}{P_{aSL}} + 1 \right)^{2/7} - 1} \quad \frac{q_c}{P_{aSL}} \leq 0.89293$$

$$(b) \quad \frac{V_c}{a_{SL}} = 0.881284 \sqrt{\left(\frac{q_c}{P_{aSL}} + 1 \right) \left[1 - \frac{1}{7 \left(\frac{V_c}{a_{SL}} \right)^2} \right]^{5/2}} \quad \frac{q_c}{P_{aSL}} \geq 0.89293$$

$$8 \quad V_c = \left(\frac{V_c}{a_{SL}} \right) a_{SL}$$

where $a_{SL} = 661.48$ knots

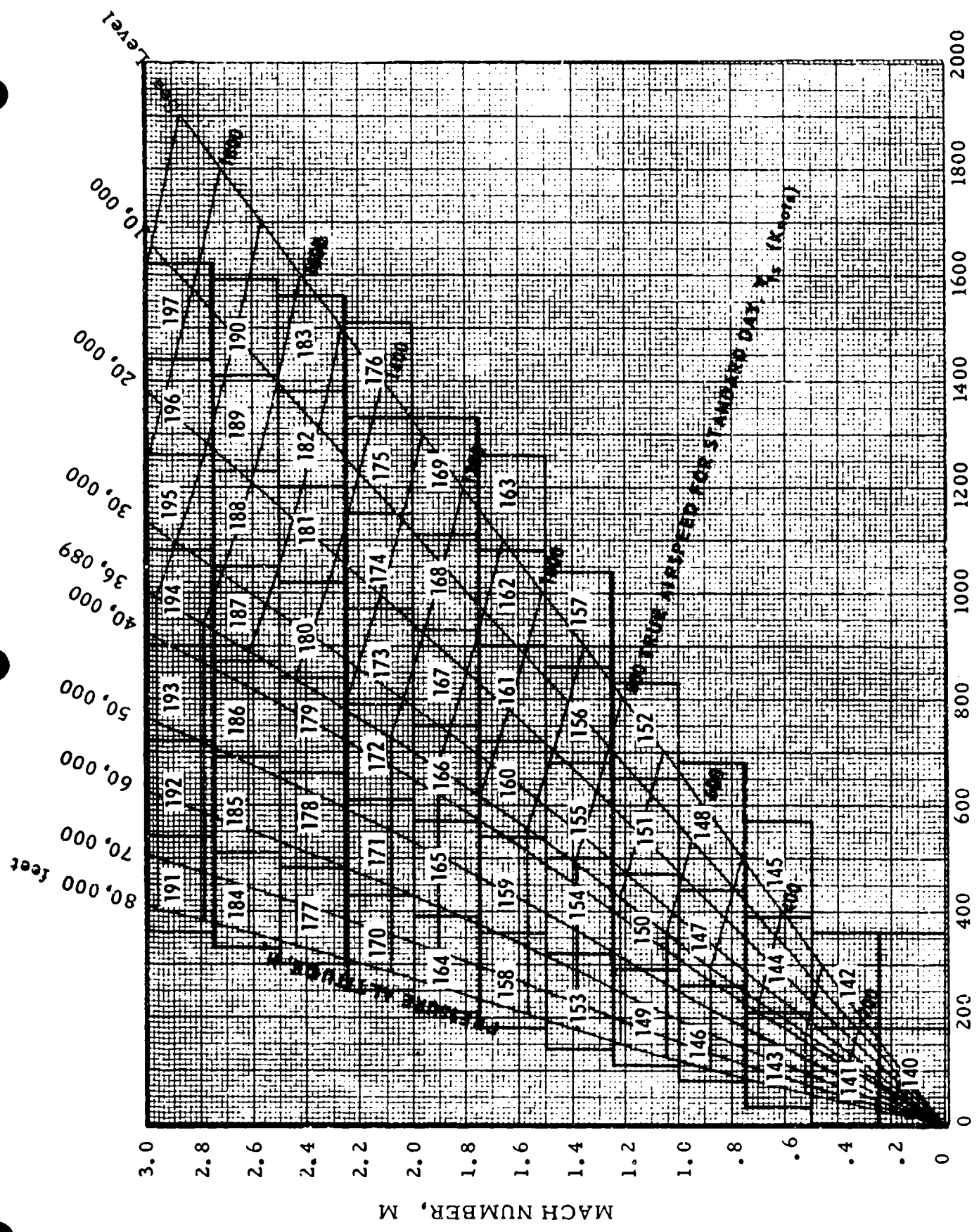
Example:

1. Given: $M = 1.60$; $V_c = 400$ knots

Required: H_c and V_{ts}

Solution: Use Page 21 of Chart 8.5. $H_c = 52,850$ feet; $V_{ts} = 917.2$ knots

2. Given: $M = 1.20$; $H_c = 50,000$
 Required: V_c and V_{ts}
 Solution: Use Page 12 of Chart 8.5. $V_c = 308.7$ knots;
 $V_{ts} = 688.1$ knots
3. Given: $H_c = 35,000$ feet; $V_c = 200$ knots
 Required: M and V_{ts}
 Solution: Use Page 5 of Chart 8.5. $M = 0.6023$; $V_{ts} = 347.1$ knots
4. Given: $M_{ic} = 1.60$; $V_{ic} = 400$ knots
 Required: H_{ic}
 Solution: Use Page 21 of Chart 8.5. $H_{ic} = 52,850$ feet
5. Given: $M_{ic} = 1.20$; $H_{ic} = 50,000$ feet
 Required: V_{ic}
 Solution: Use Page 12 of Chart 8.5. $V_{ic} = 308.7$ knots
6. Given: $H_{ic} = 35,000$ feet, $V_{ic} = 200$ knots
 Required: M_{ic}
 Solution: Use Page 5 of Chart 8.5. $M_{ic} = 0.6023$



CALIBRATED AIRSPEED, V_c (Knots)

CHART 8.5

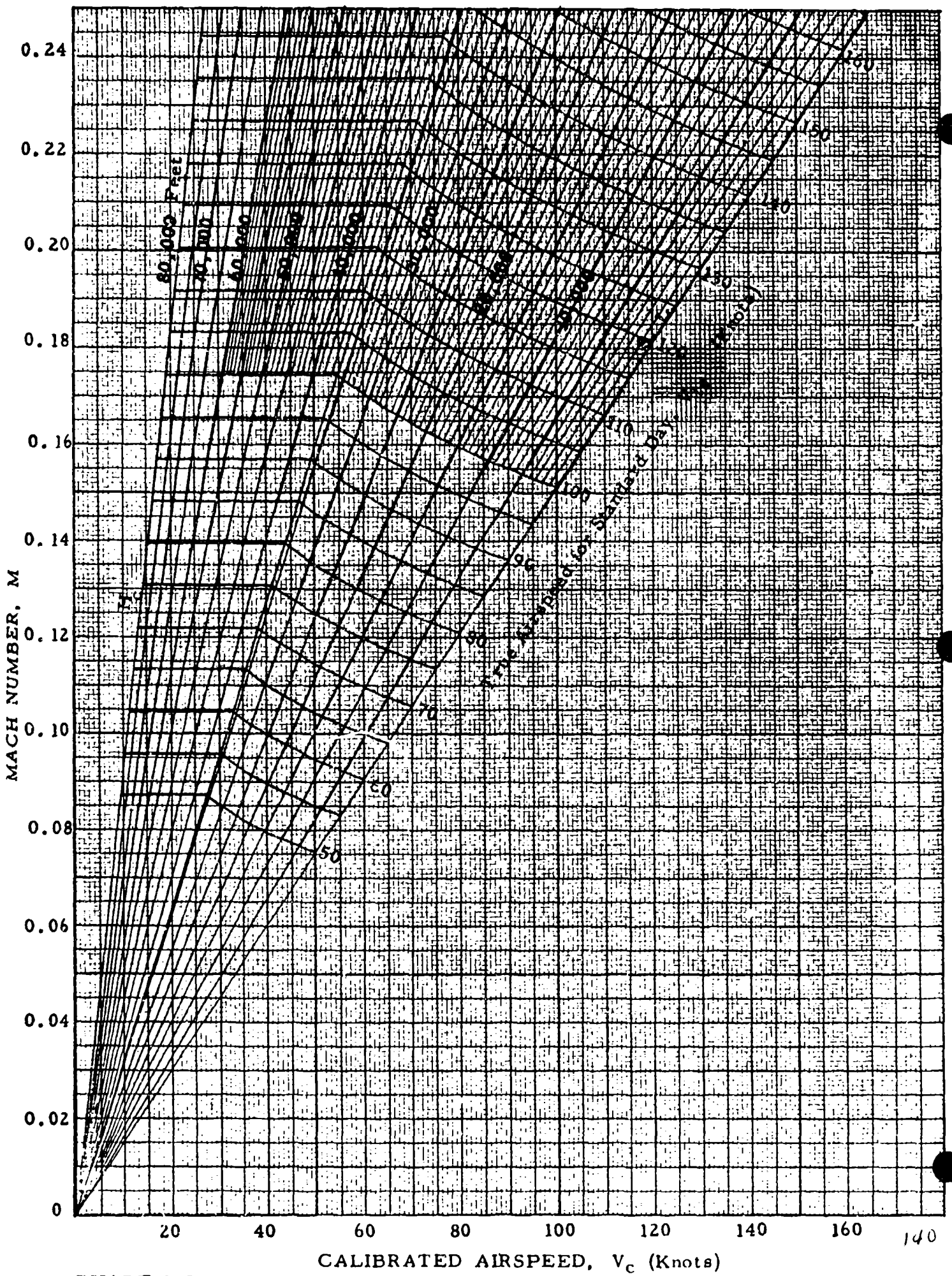
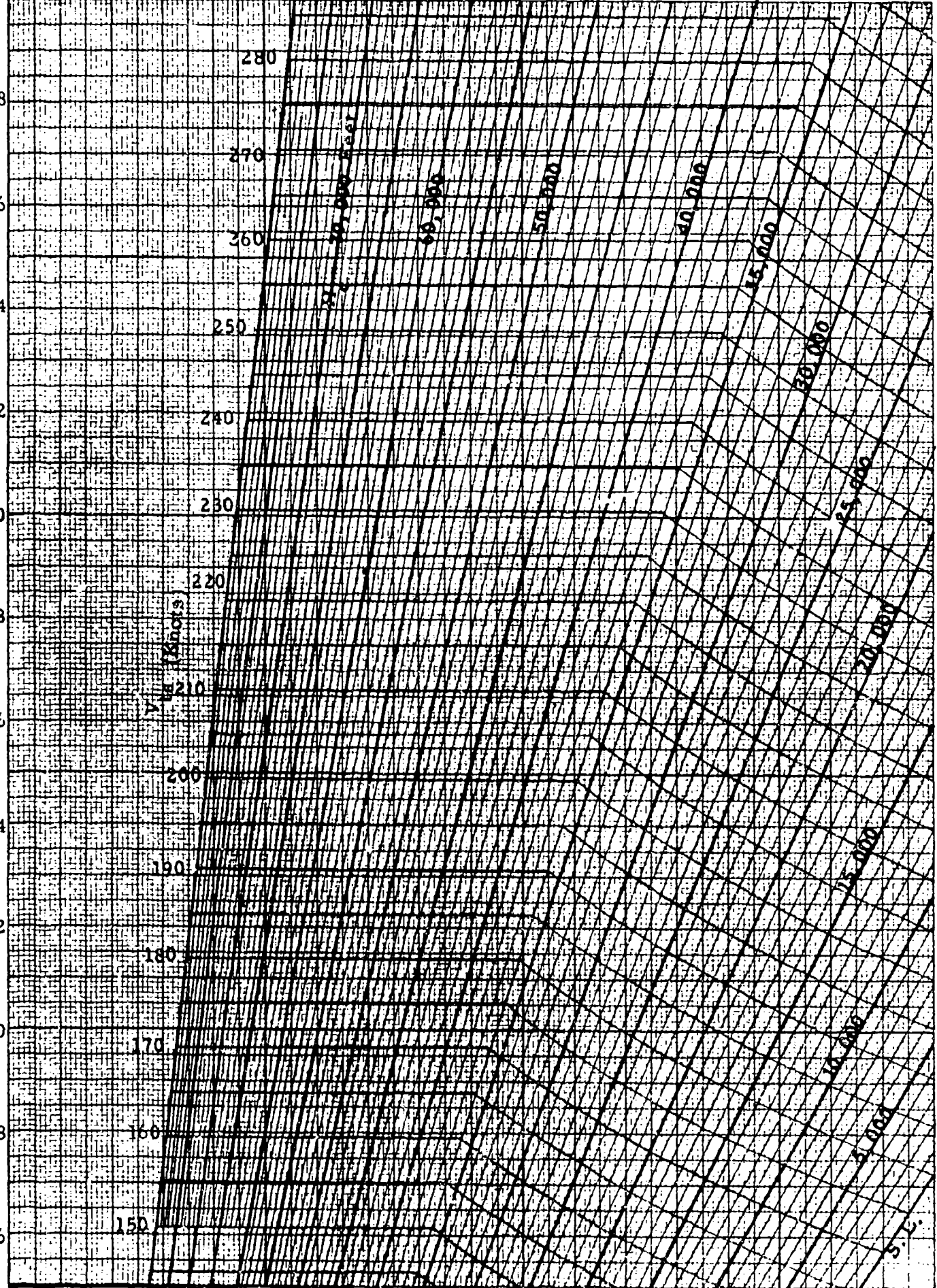


CHART 8.5

MACH NUMBER, M

0.48
0.46
0.44
0.42
0.40
0.38
0.36
0.34
0.32
0.30
0.28
0.26



0 20 40 60 80 100 120 140 160 180
CALIBRATED AIRSPEED, V_c (Knots)

141

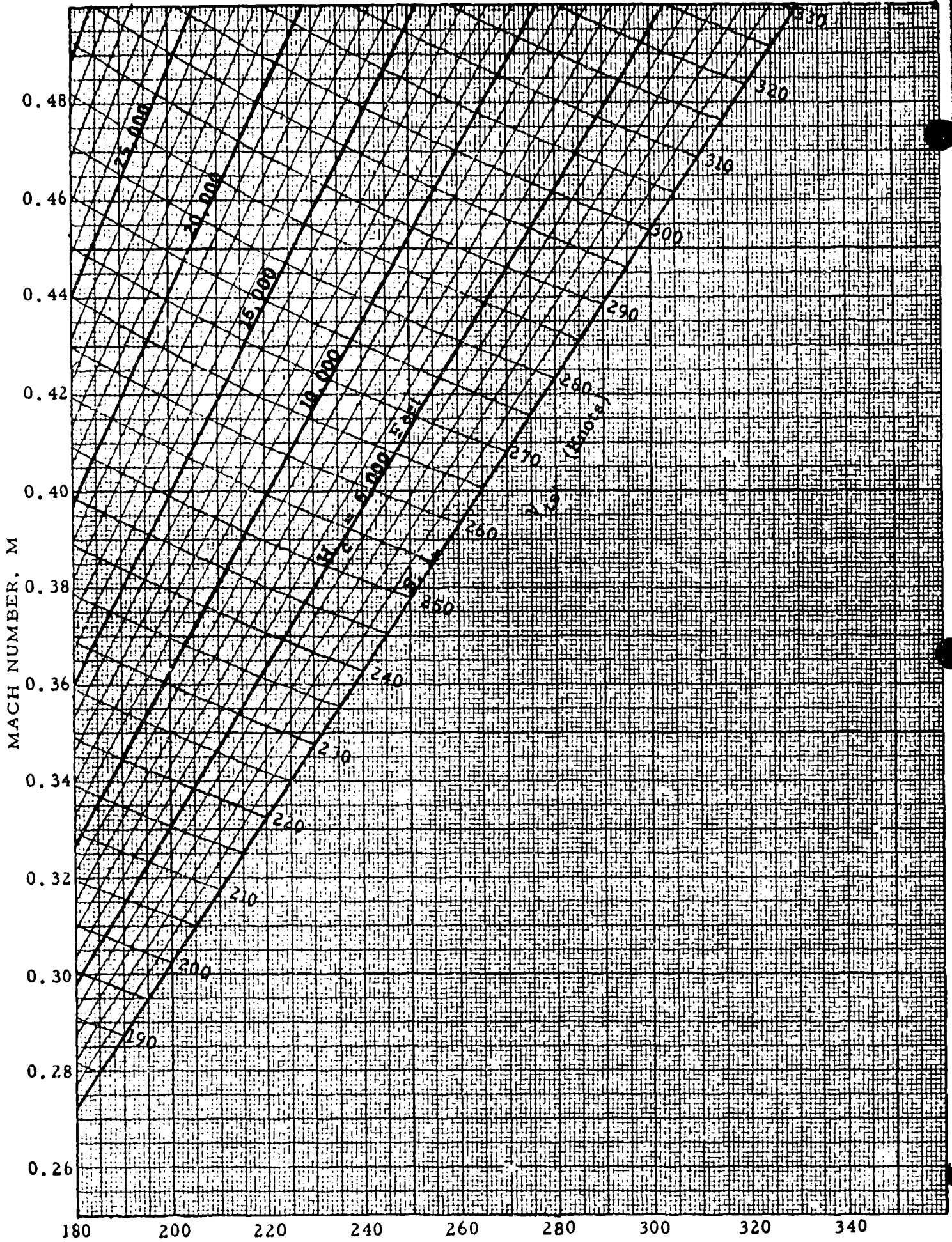
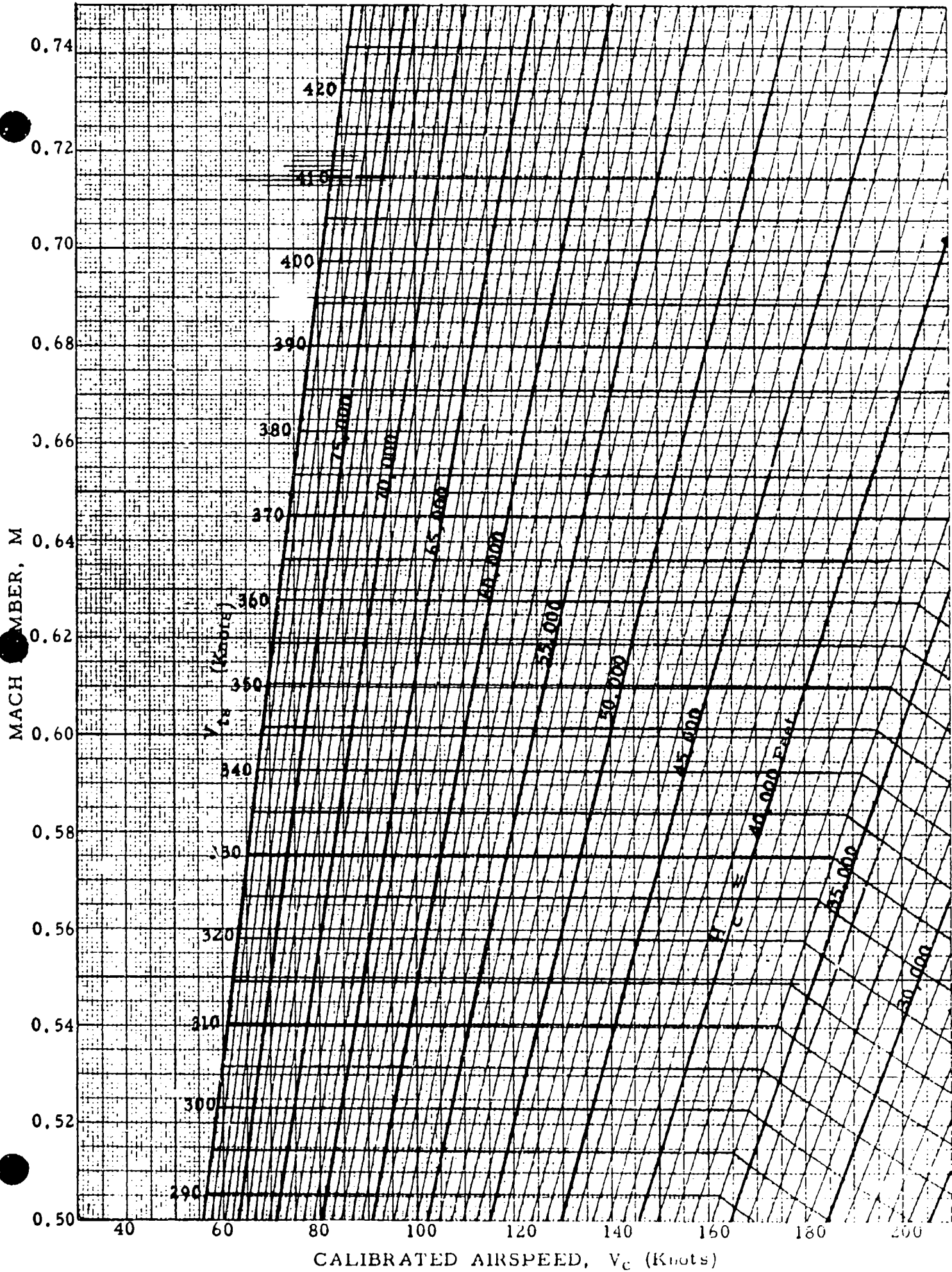


CHART 8.5

CALIBRATED AIRSPEED, V_c (Knots)



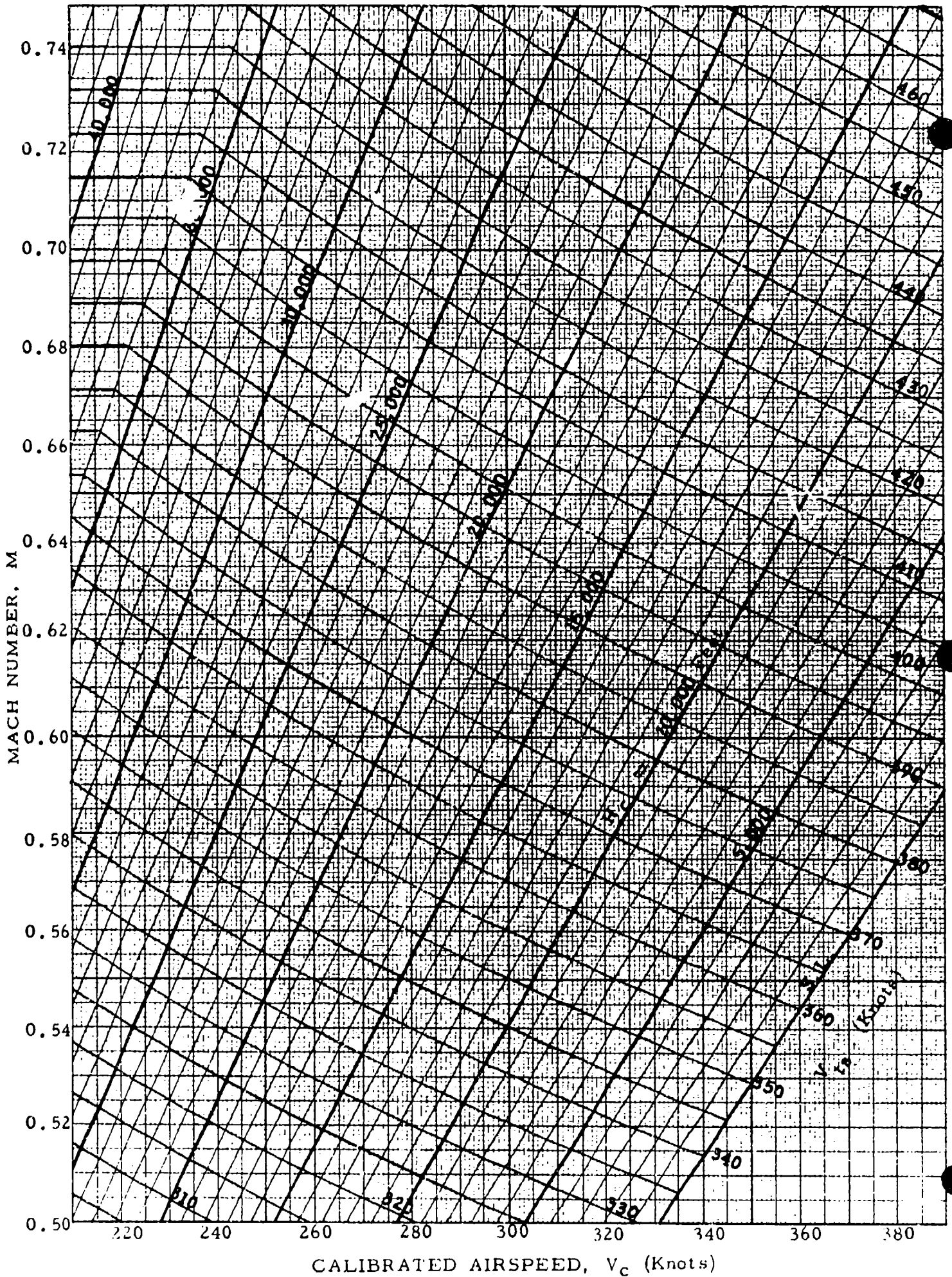
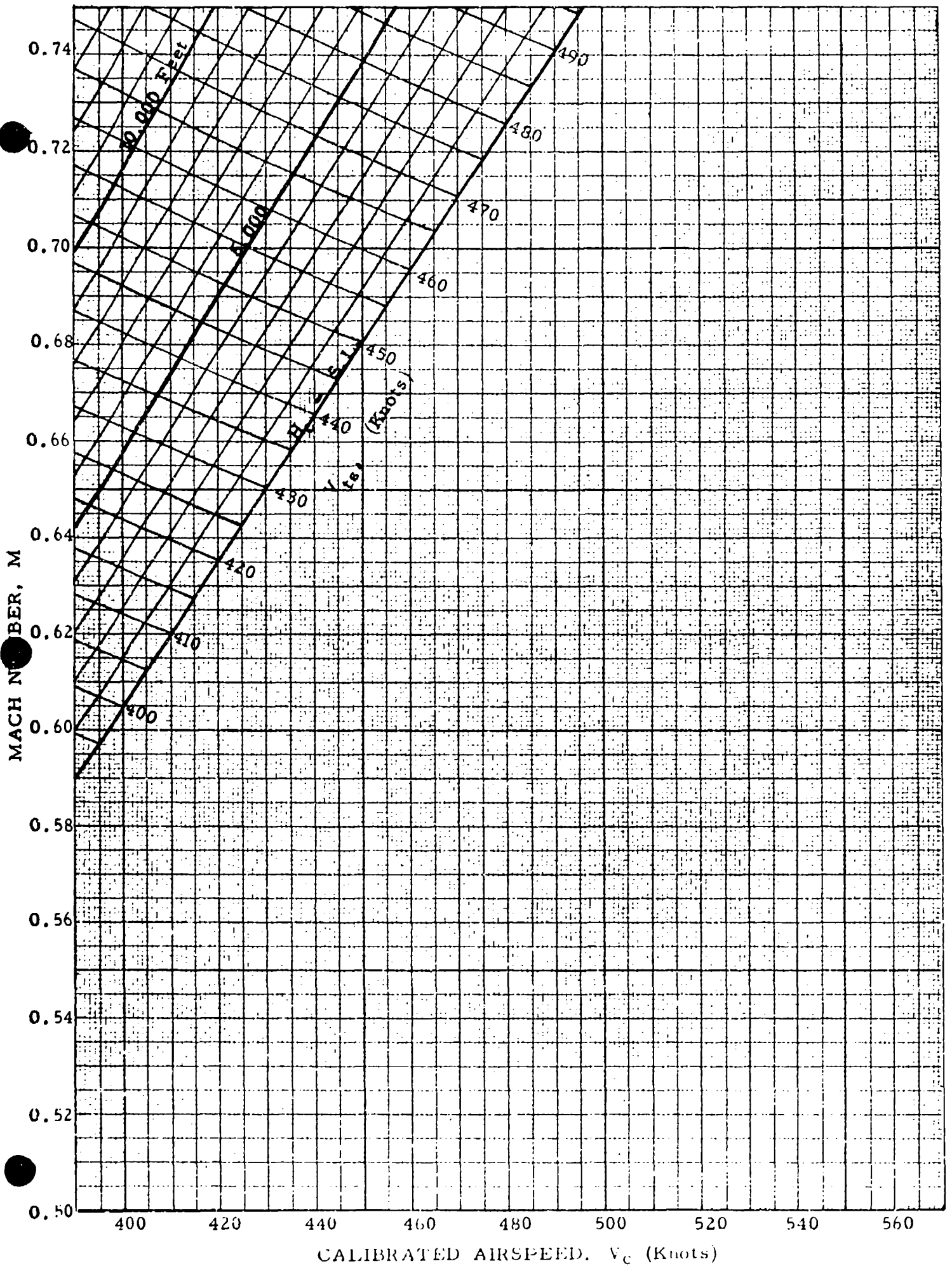


CHART 8.5



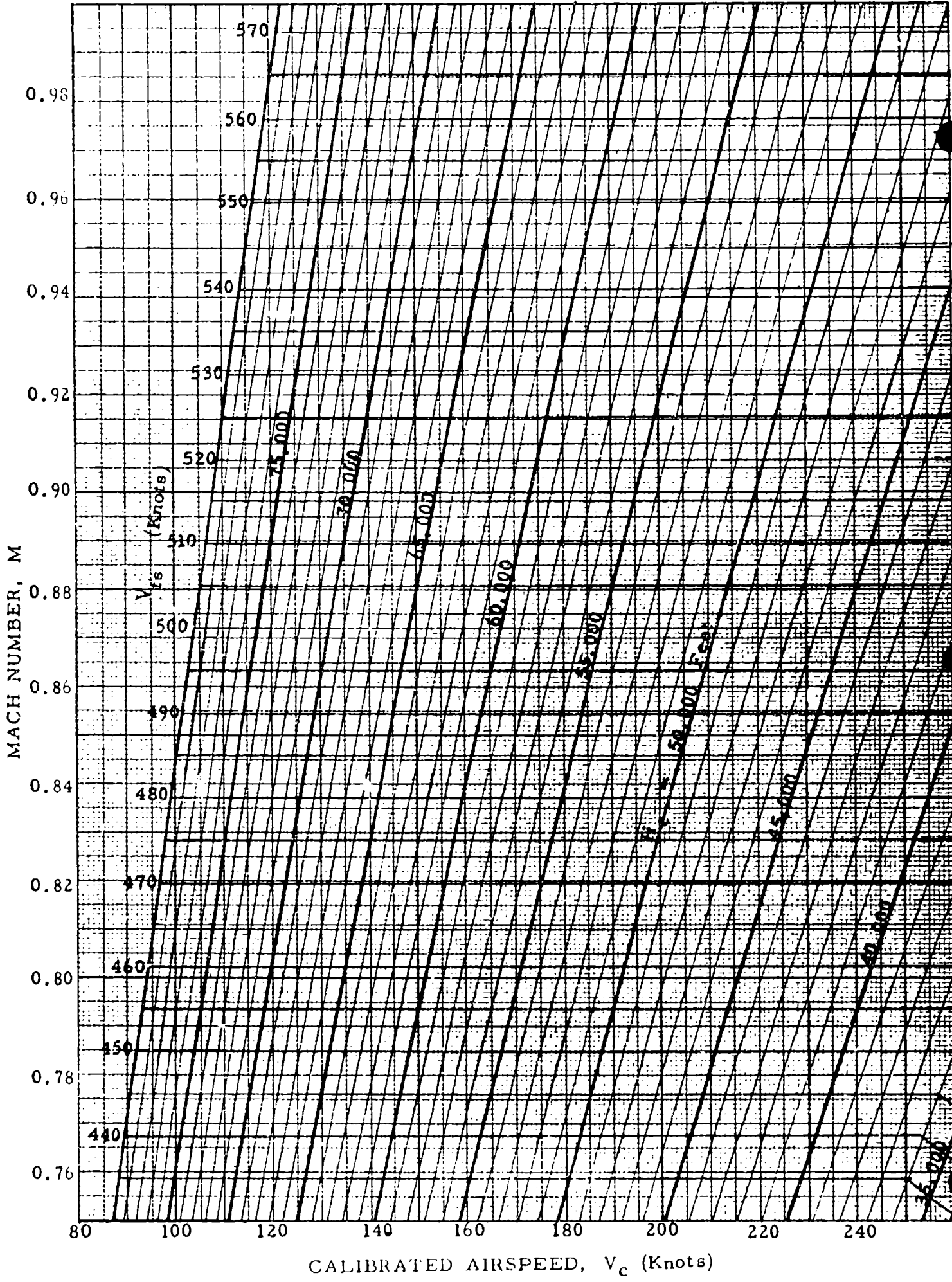
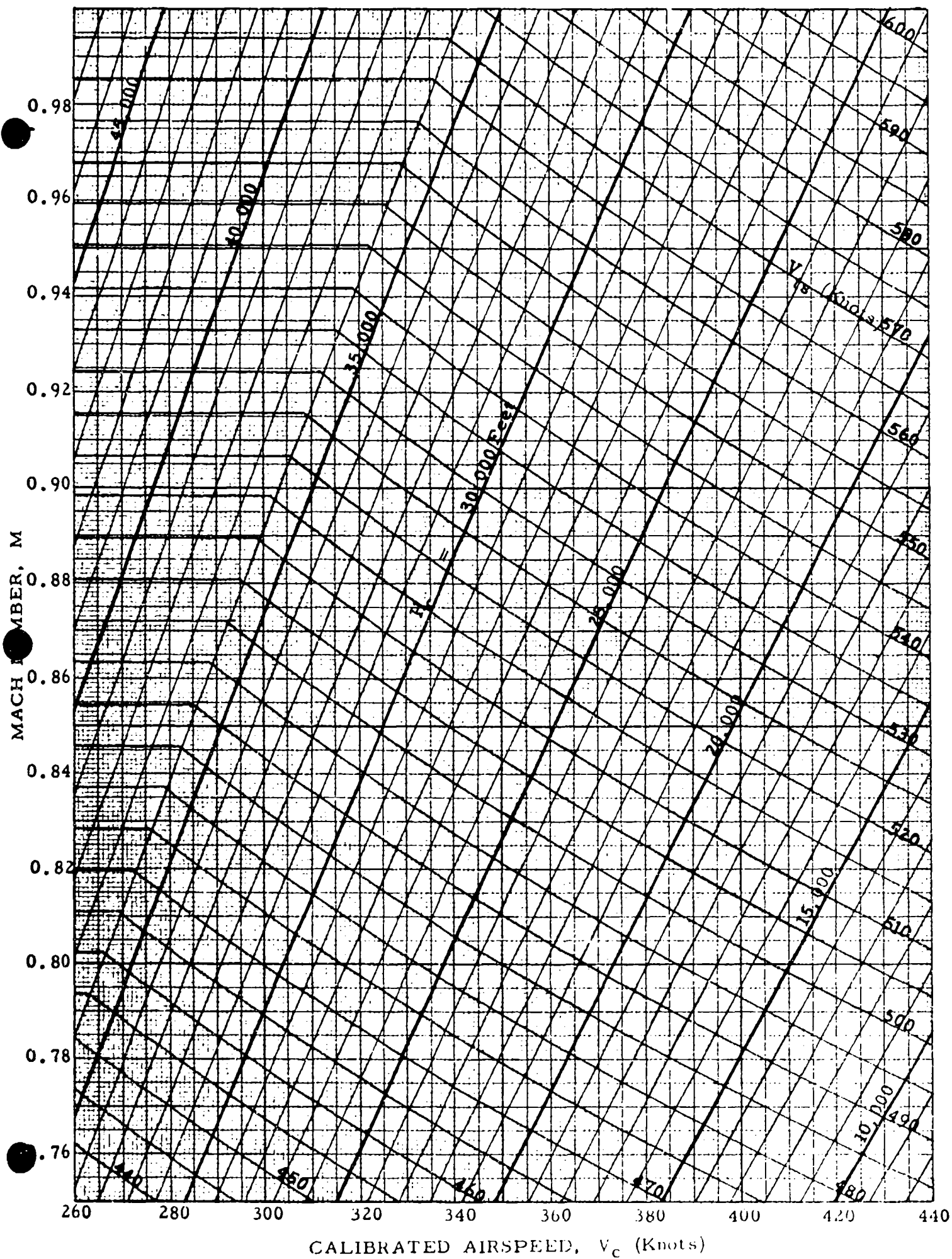


CHART 8.5



CALIBRATED AIRSPEED, V_c (Knots)

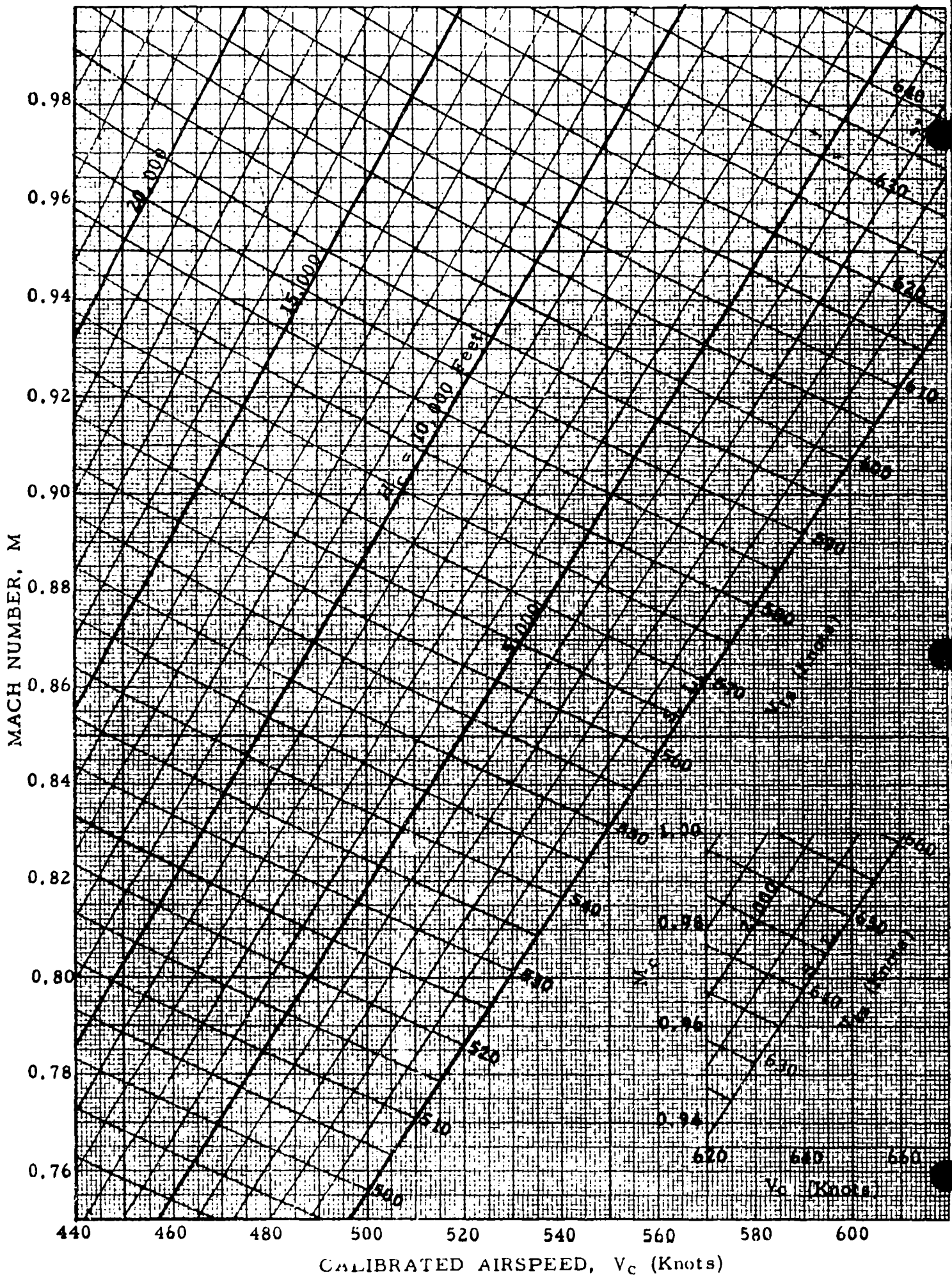
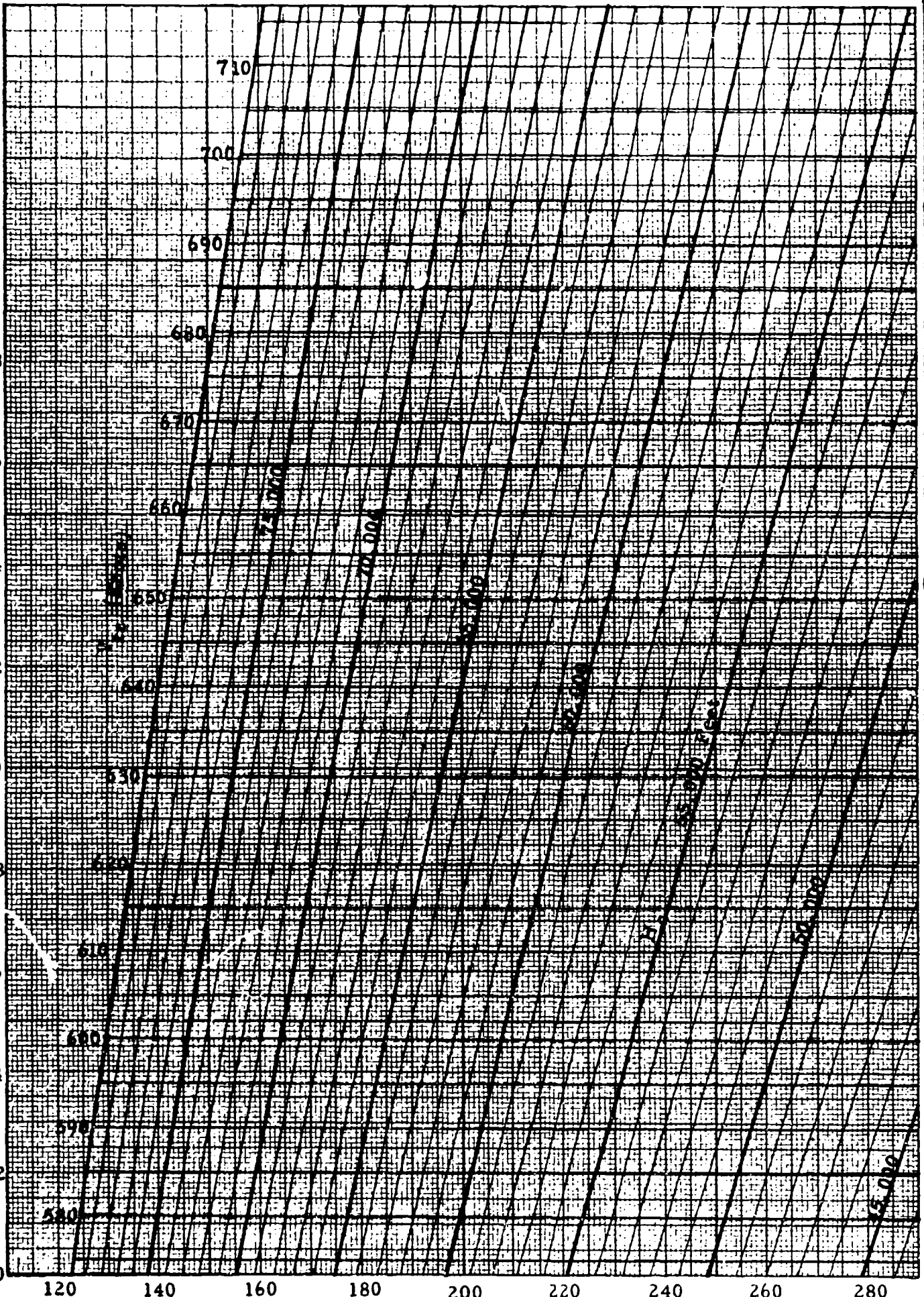


CHART 8.5

CALIBRATED AIRSPEED, V_c (Knots)

MACH NUMBER, M

1.24
1.22
1.20
1.18
1.16
1.14
1.12
1.10
1.08
1.06
1.04
1.02
1.00



CALIBRATED AIRSPEED, V_c (Knots)

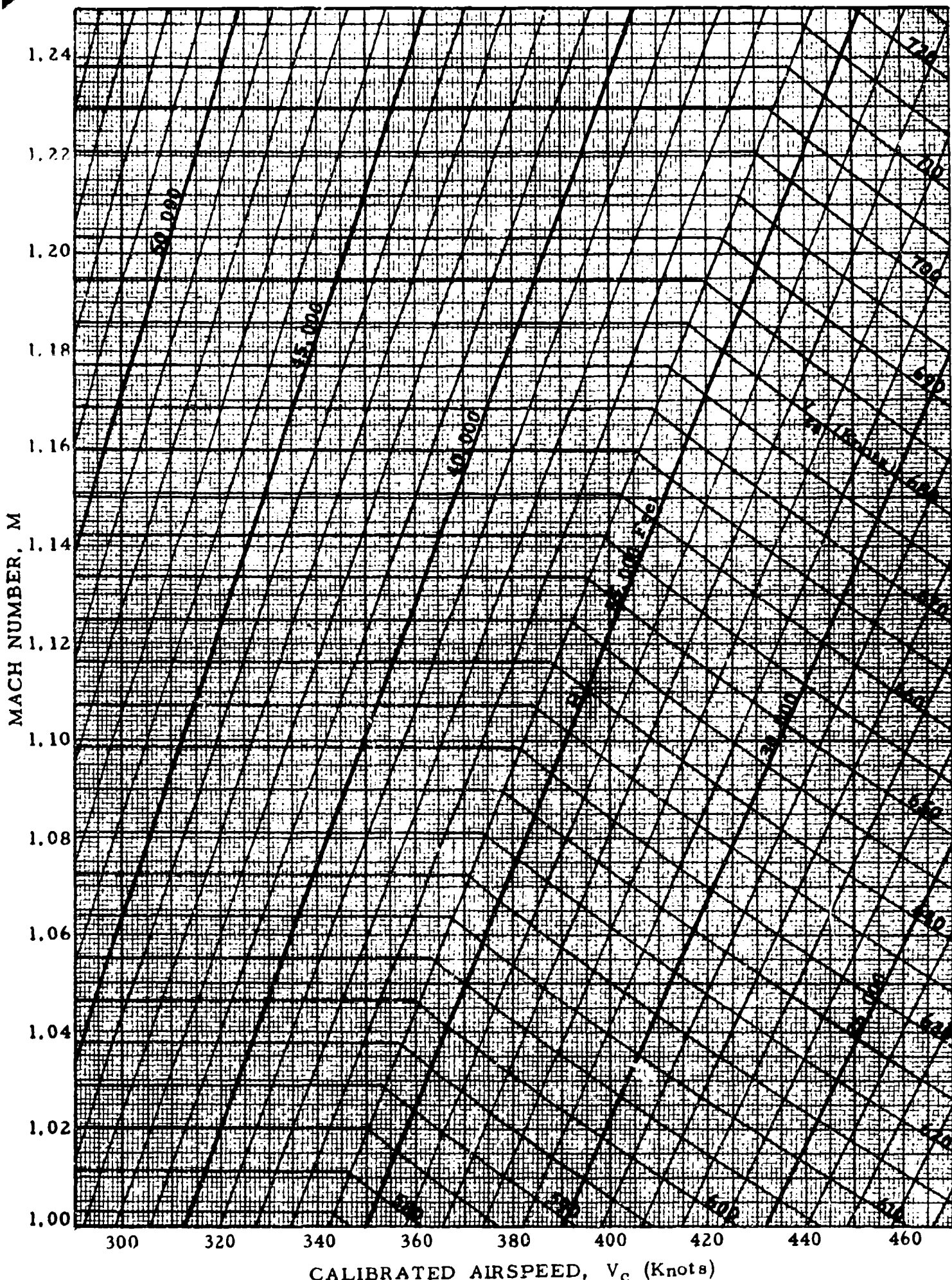
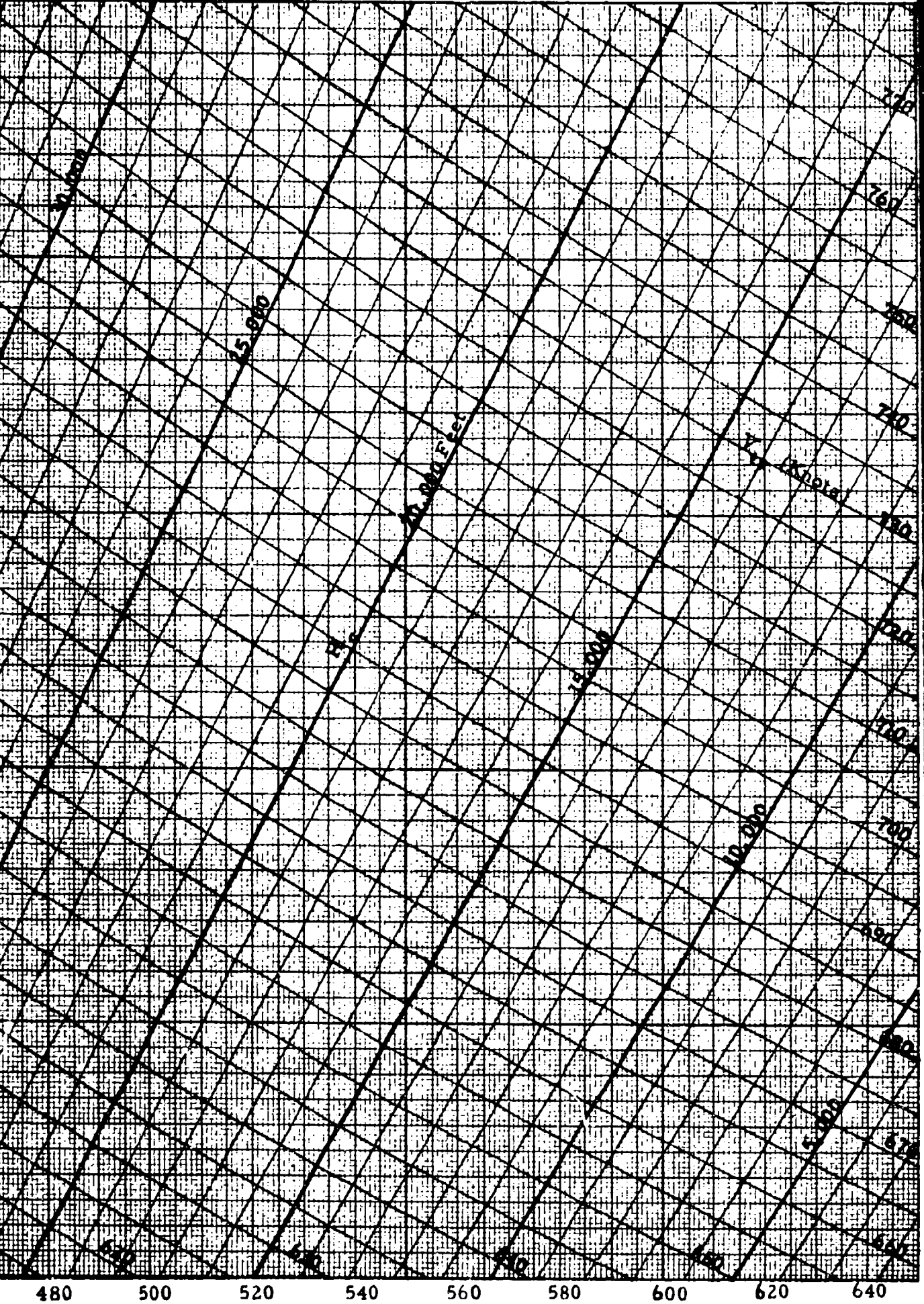


CHART 8.5

MACH NUMBER, M

1.24
1.22
1.20
1.18
1.16
1.14
1.12
1.10
1.08
1.06
1.04
1.02
1.00



CALIBRATED AIRSPEED, V_c (Knots)

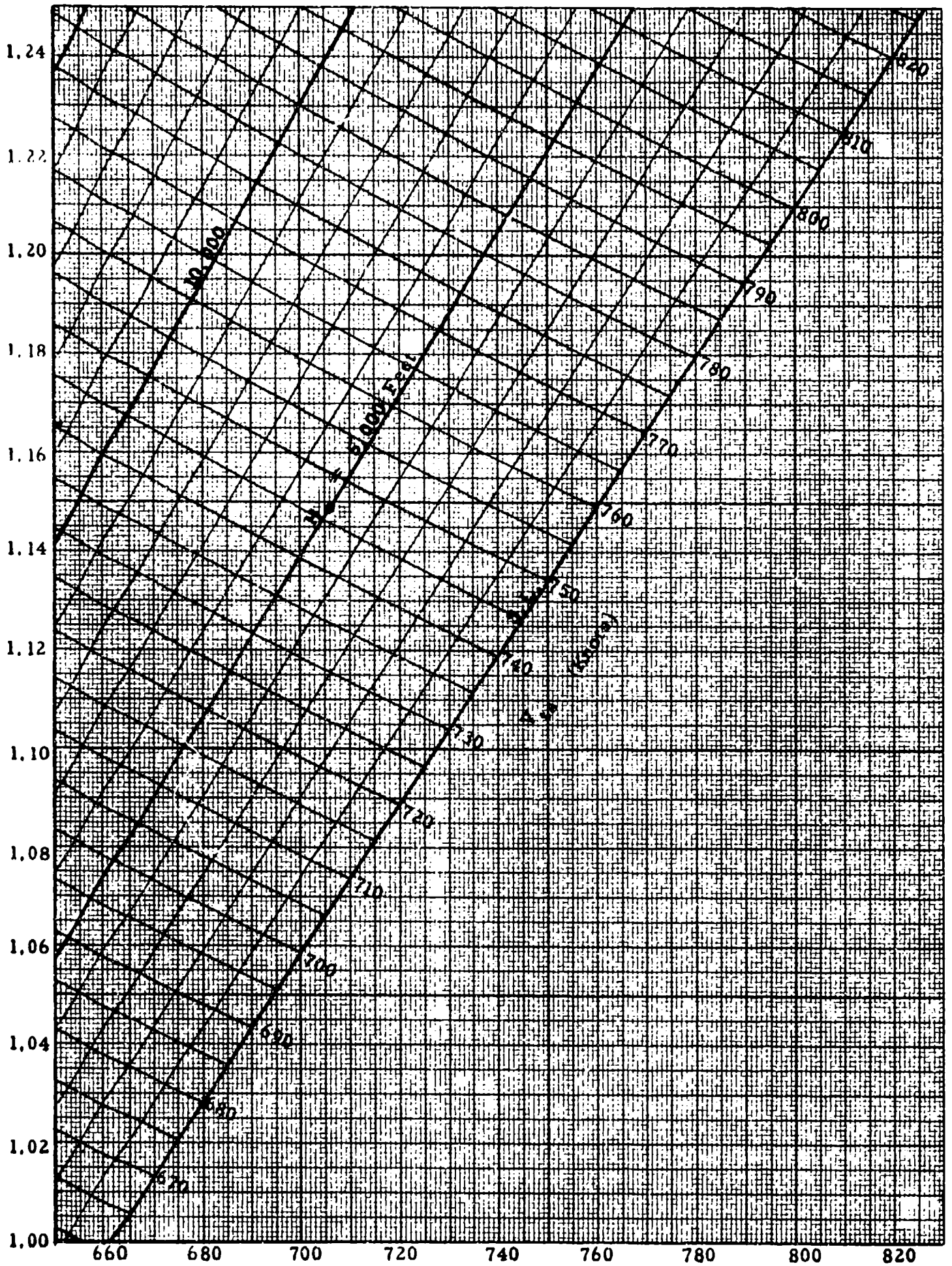
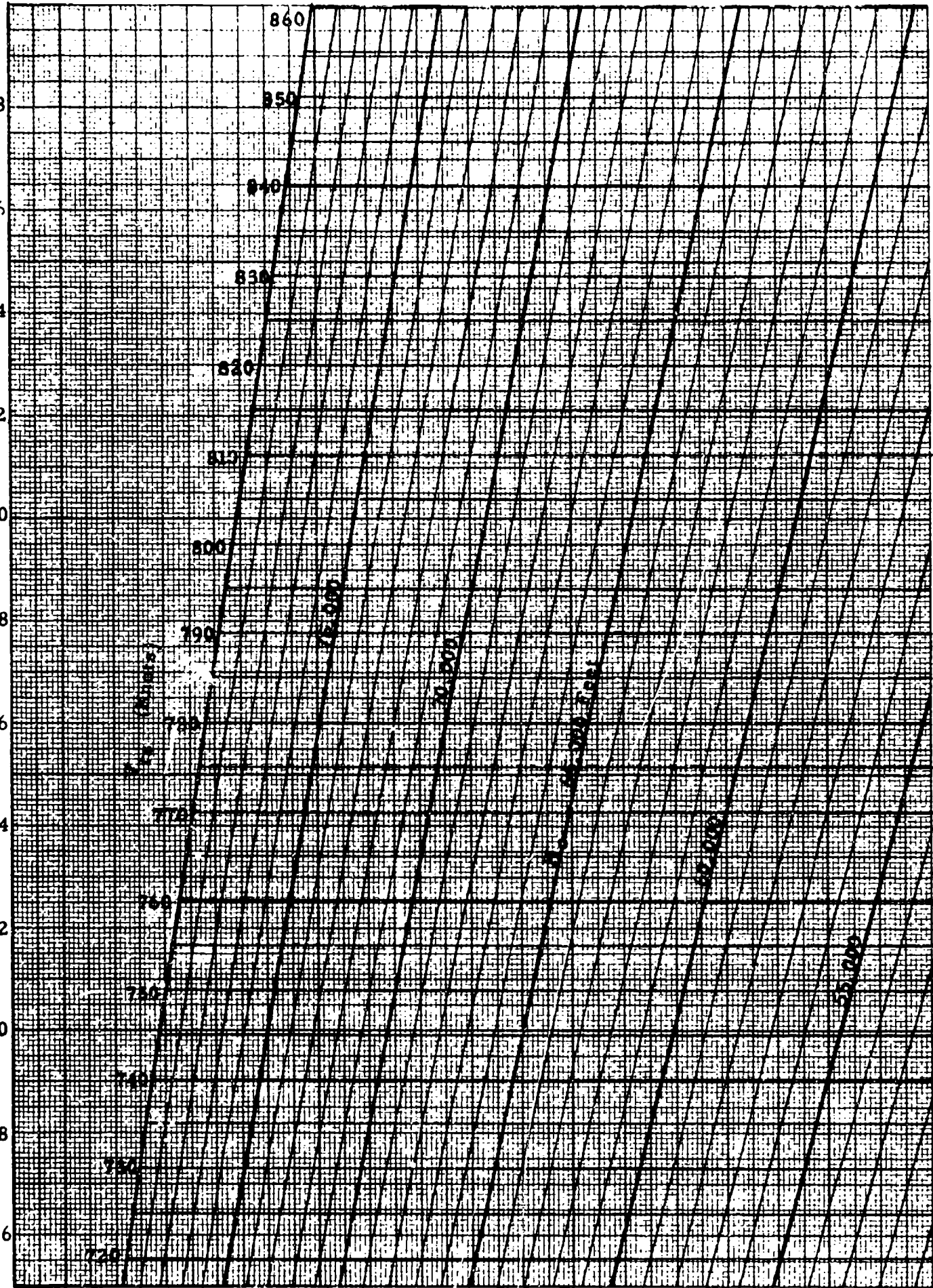


CHART 8.5

CALIBRATED AIRSPEED, V_c (Knots)
152

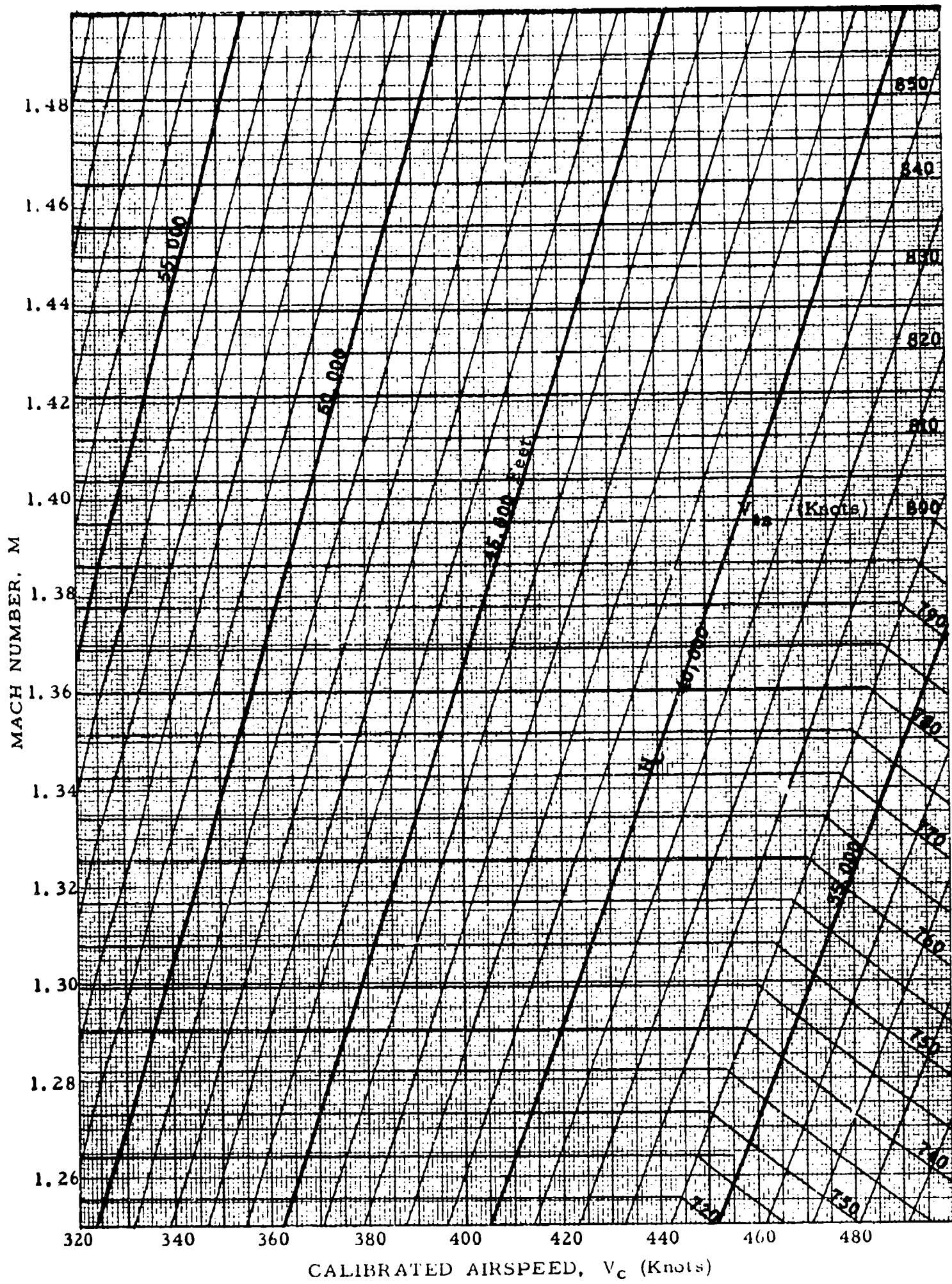
MACH NUMBER, M

1.48
1.46
1.44
1.42
1.40
1.38
1.36
1.34
1.32
1.30
1.28
1.26



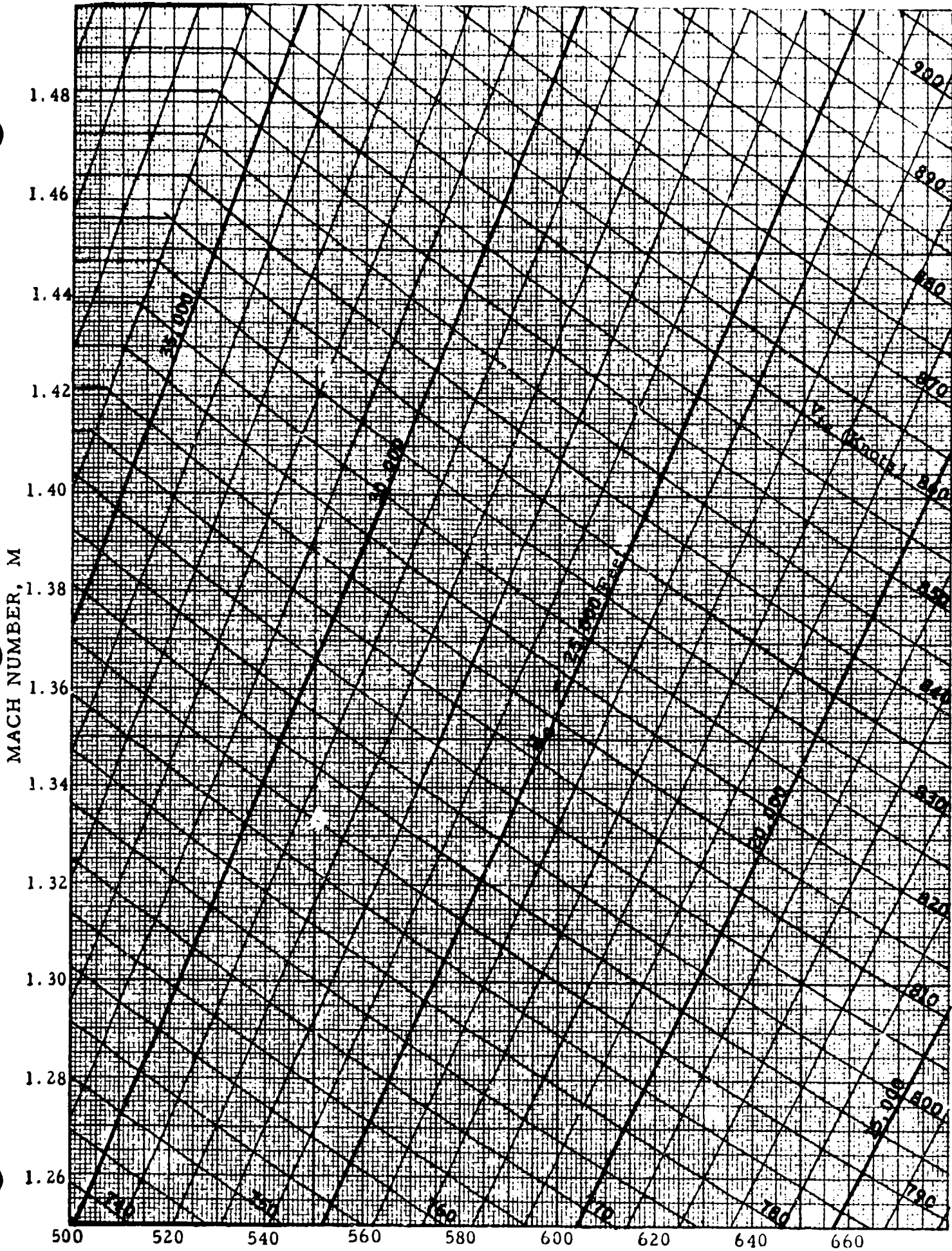
140 160 180 200 220 240 260 280 300

CALIBRATED AIRSPEED, V_c (Knots)



CALIBRATED AIRSPEED, V_c (Knots)

CHART 8.5



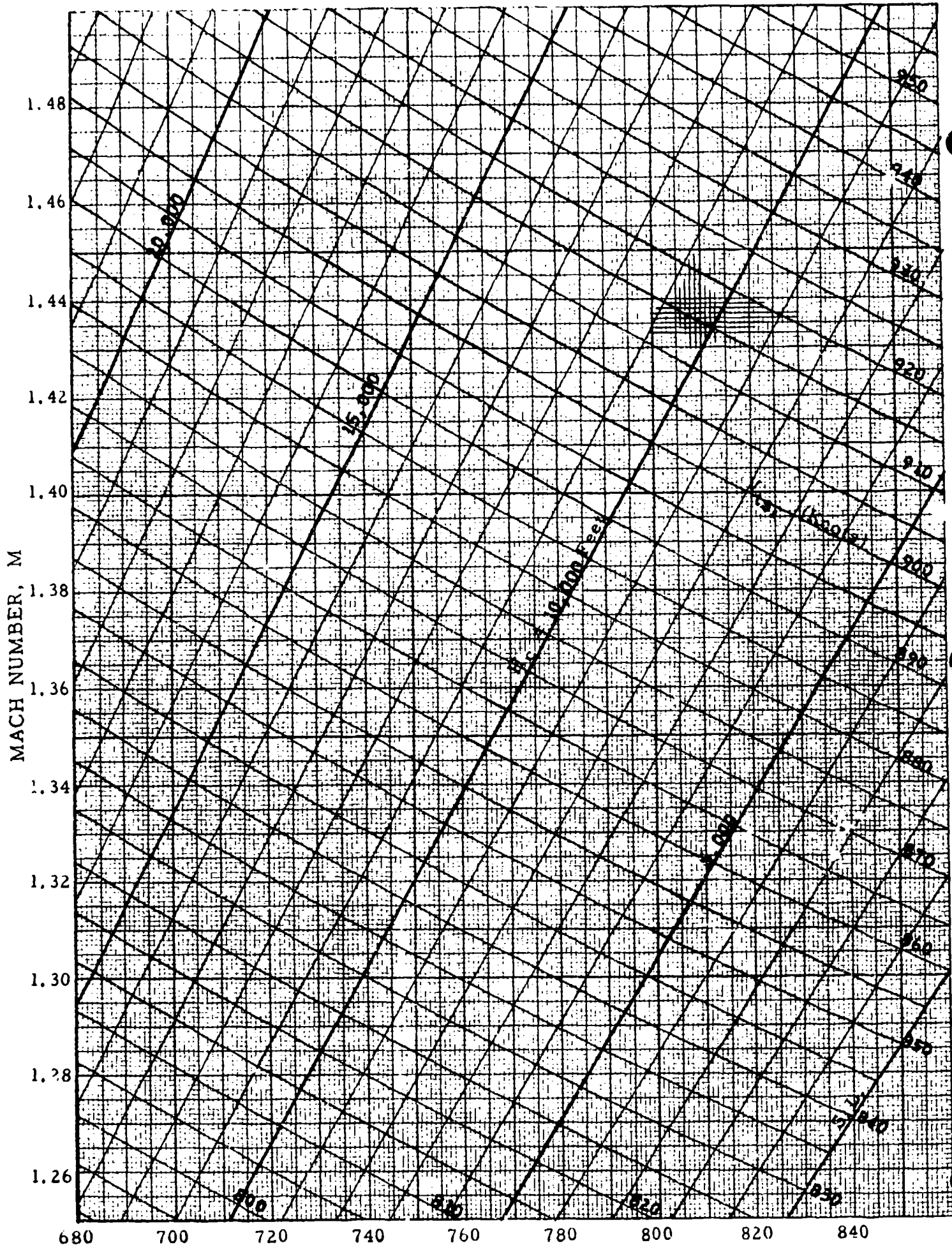
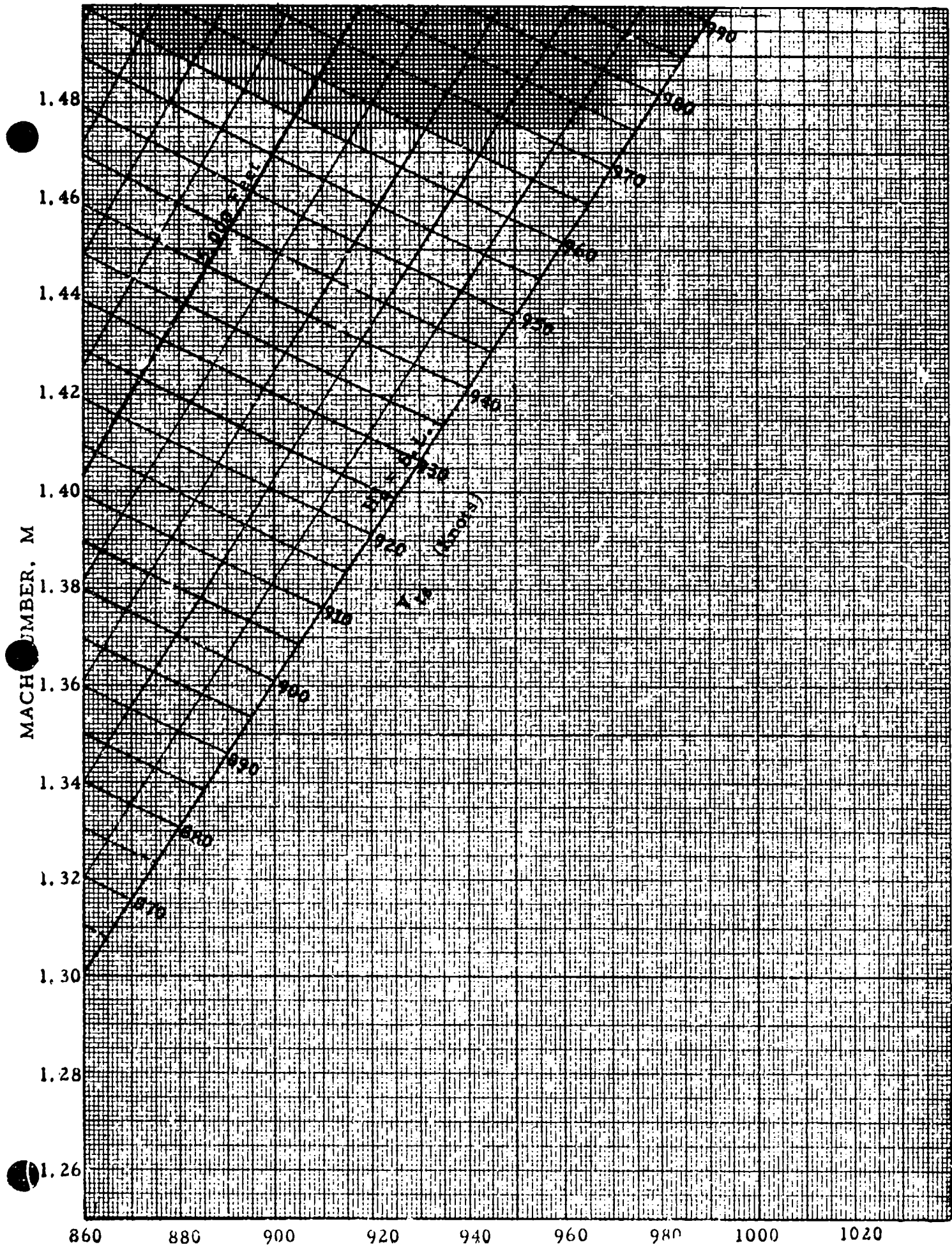


CHART 8.5

CALIBRATED AIRSPEED, V_c (Knots)



MACH NUMBER, M

860 880 900 920 940 960 980 1000 1020

CALIBRATED AIRSPEED, V_c (Knots)

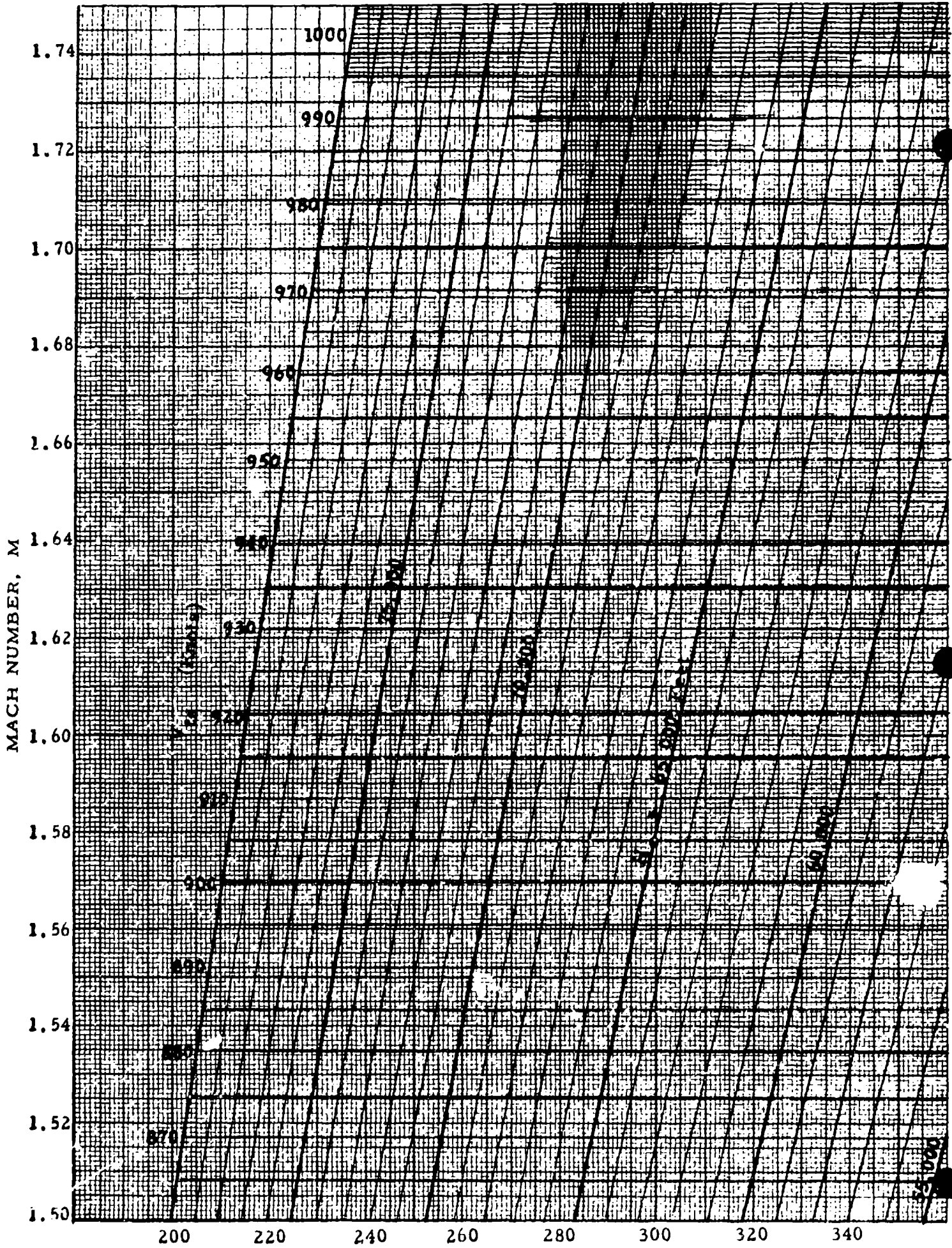
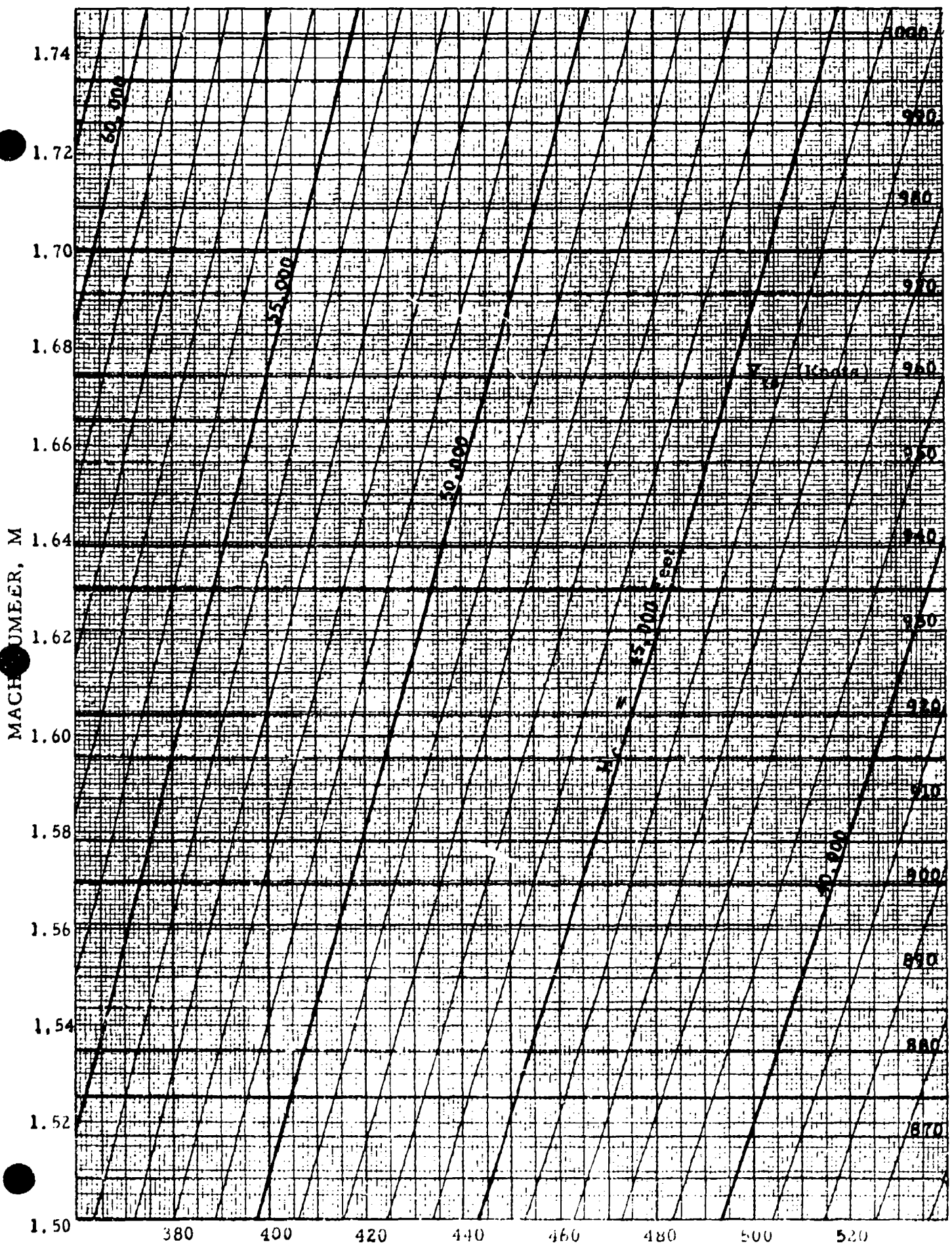


CHART 8.5

CALIBRATED AIRSPEED, V_c (Knots)



CALIBRATED AIRSPEED, V_c (KNOTS)

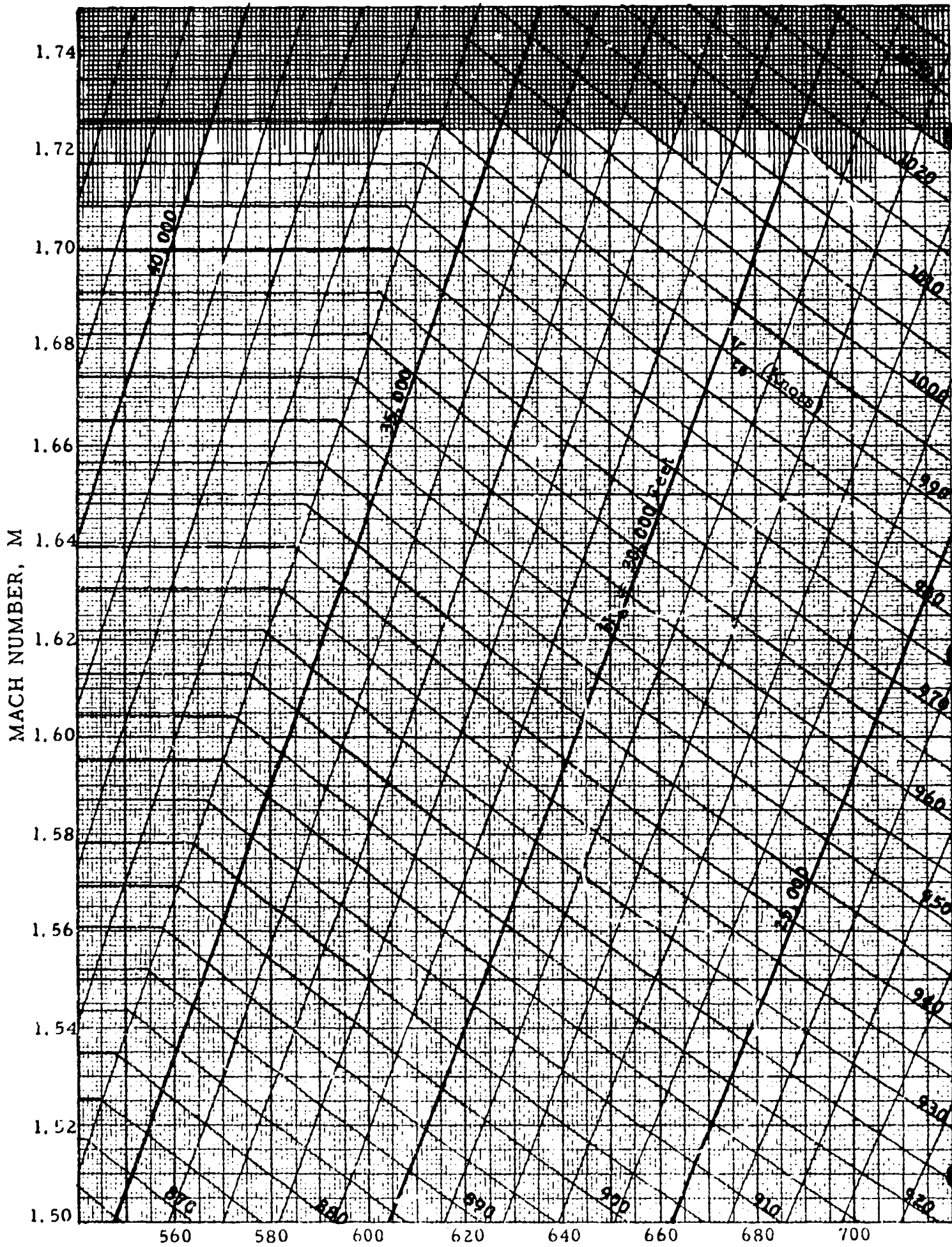
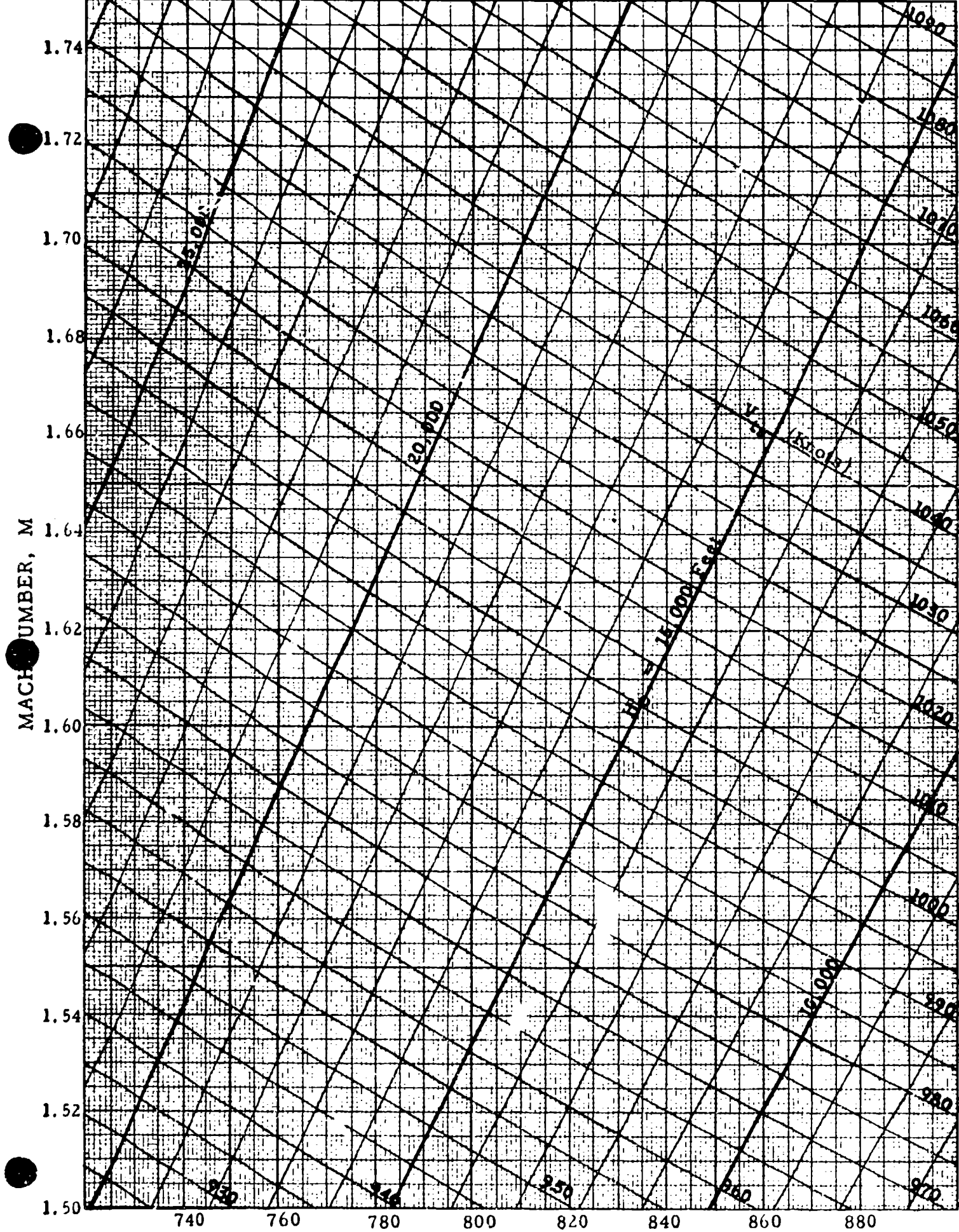


CHART 8.5

CALIBRATED AIRSPEED, V_c (Knots)



CALIBRATED AIRSPEED, V_c (Knots)

CHART 8.5

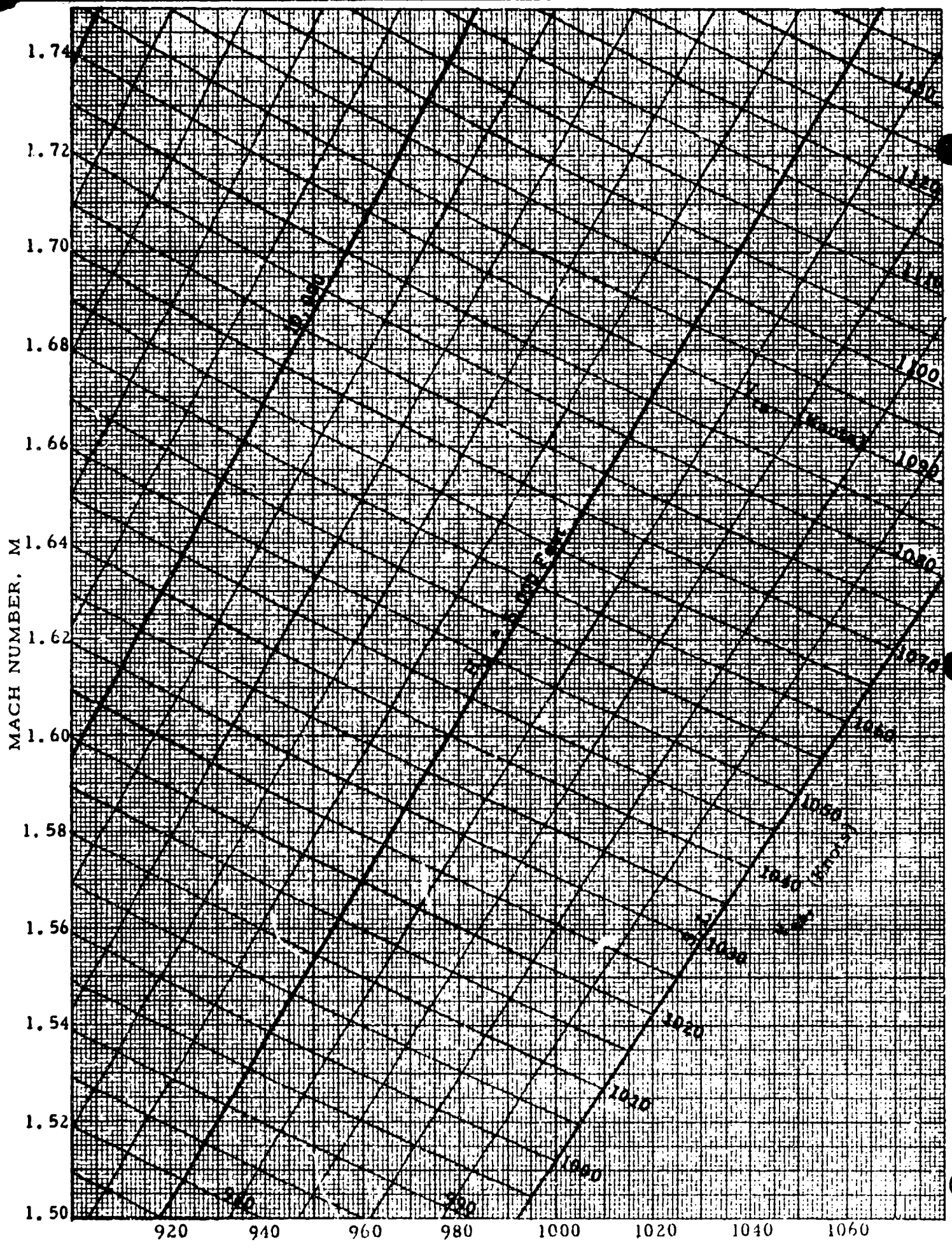
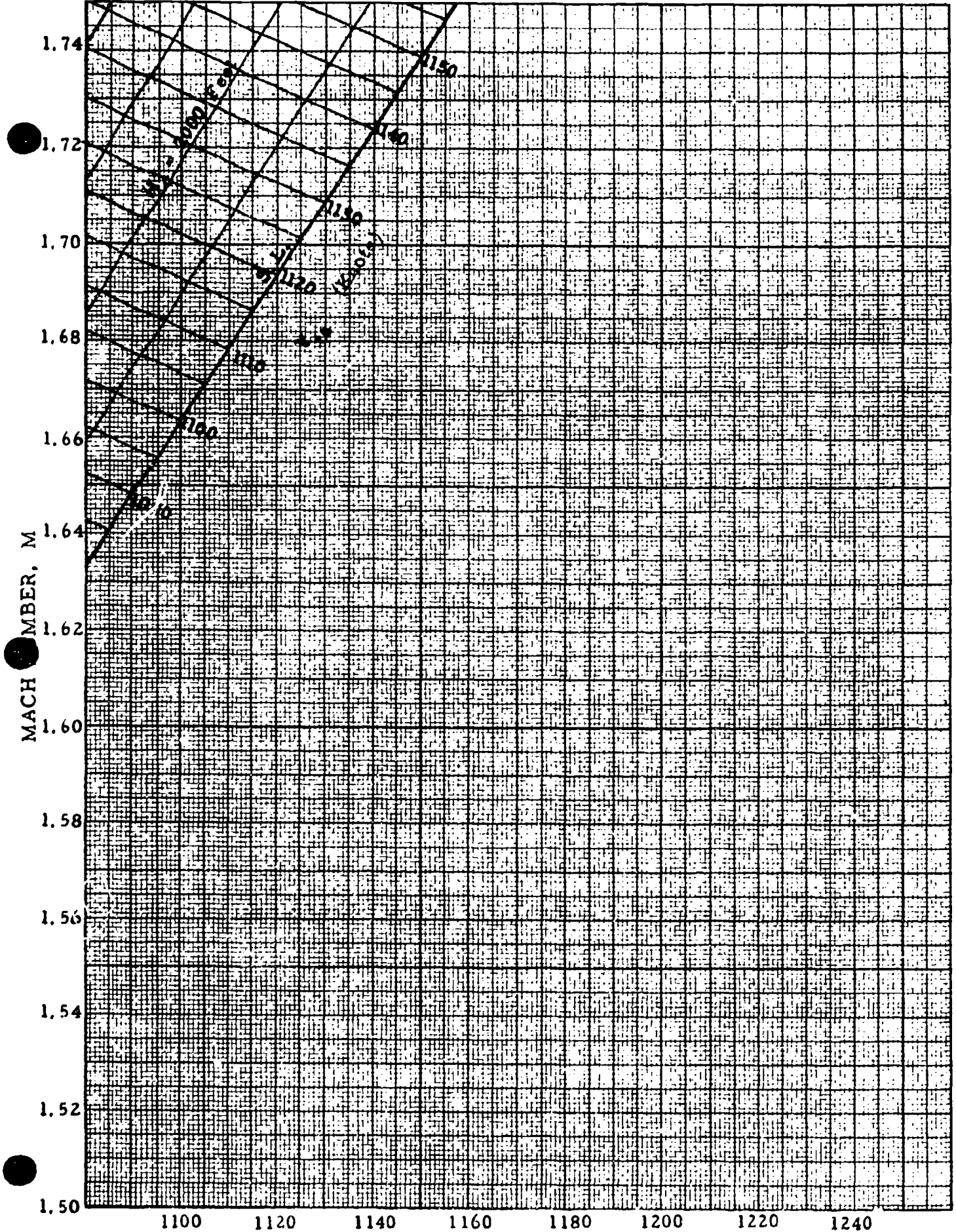


CHART 8.5

CALIBRATED AIRSPEED, V_c (Knots)



MACH NUMBER, M

1100 1120 1140 1160 1180 1200 1220 1240

CALIBRATED AIRS. EED, V_c (Knots)

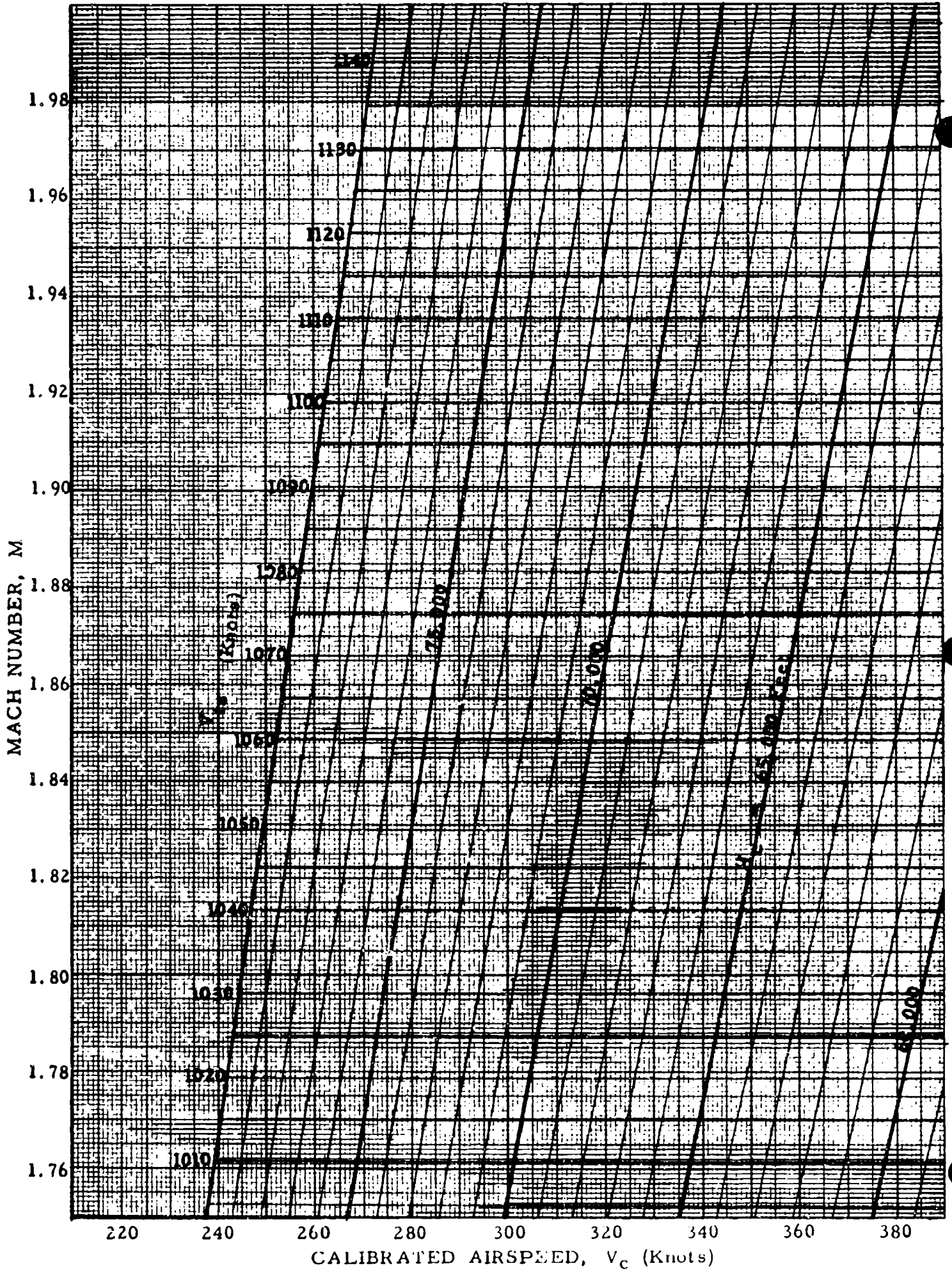


CHART 8.5

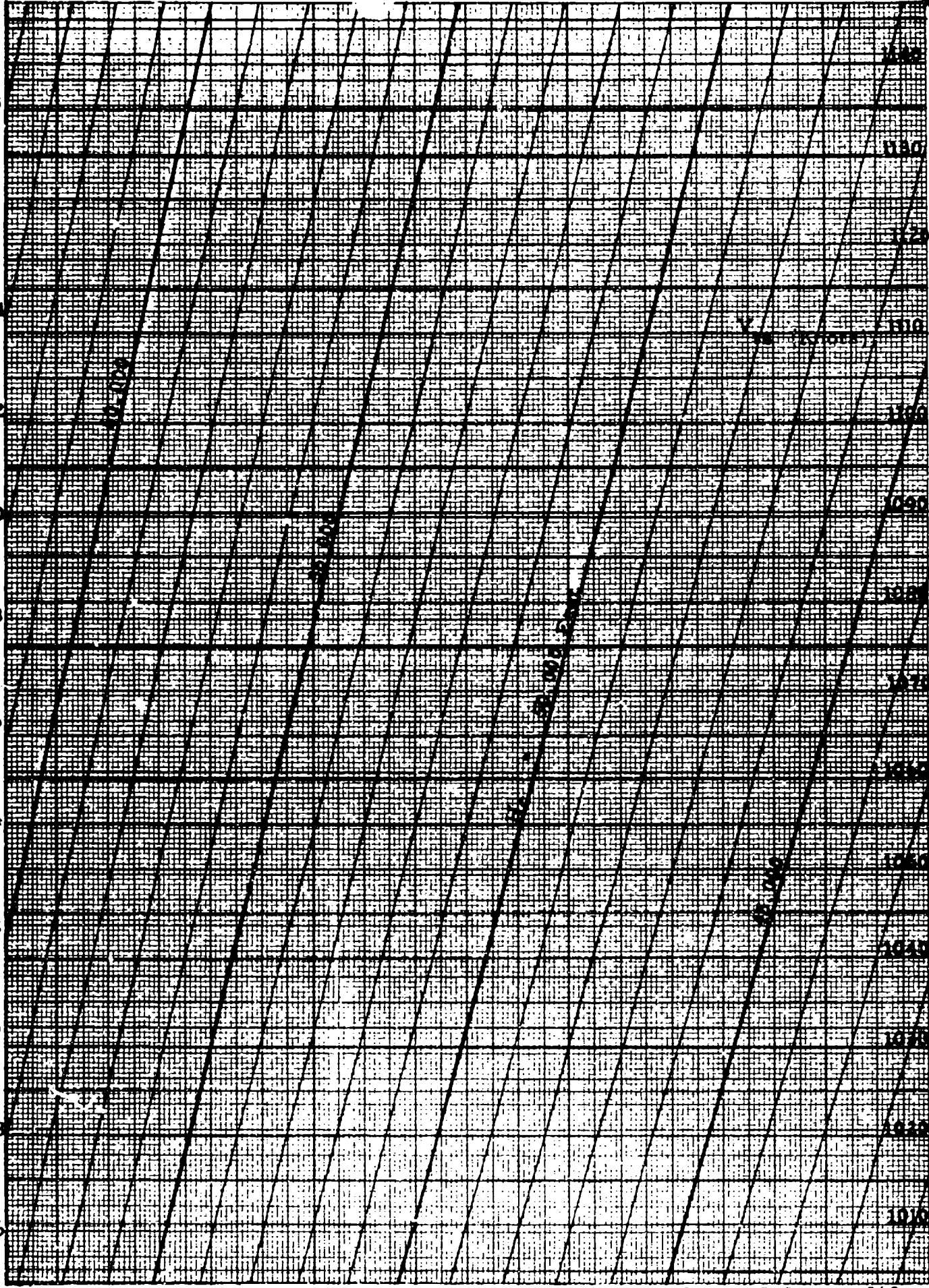
MACH NUMBER, M

1.98
1.96
1.94
1.92
1.90
1.88
1.86
1.84
1.82
1.80
1.78
1.76

400 420 440 460 480 500 520 540 560

CALIBRATED AIRSPEED, V_c (Knots)

CHART 8.5



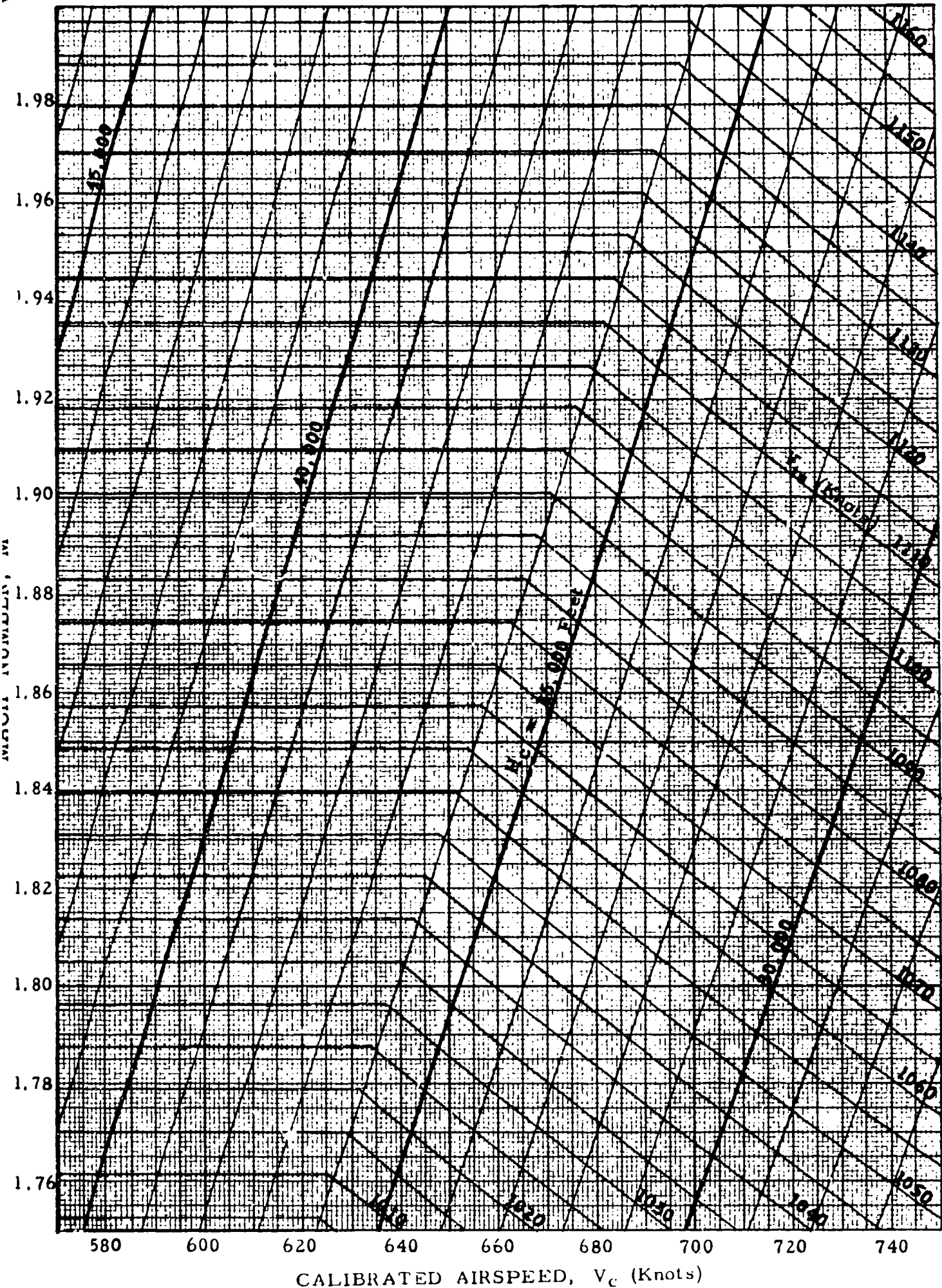
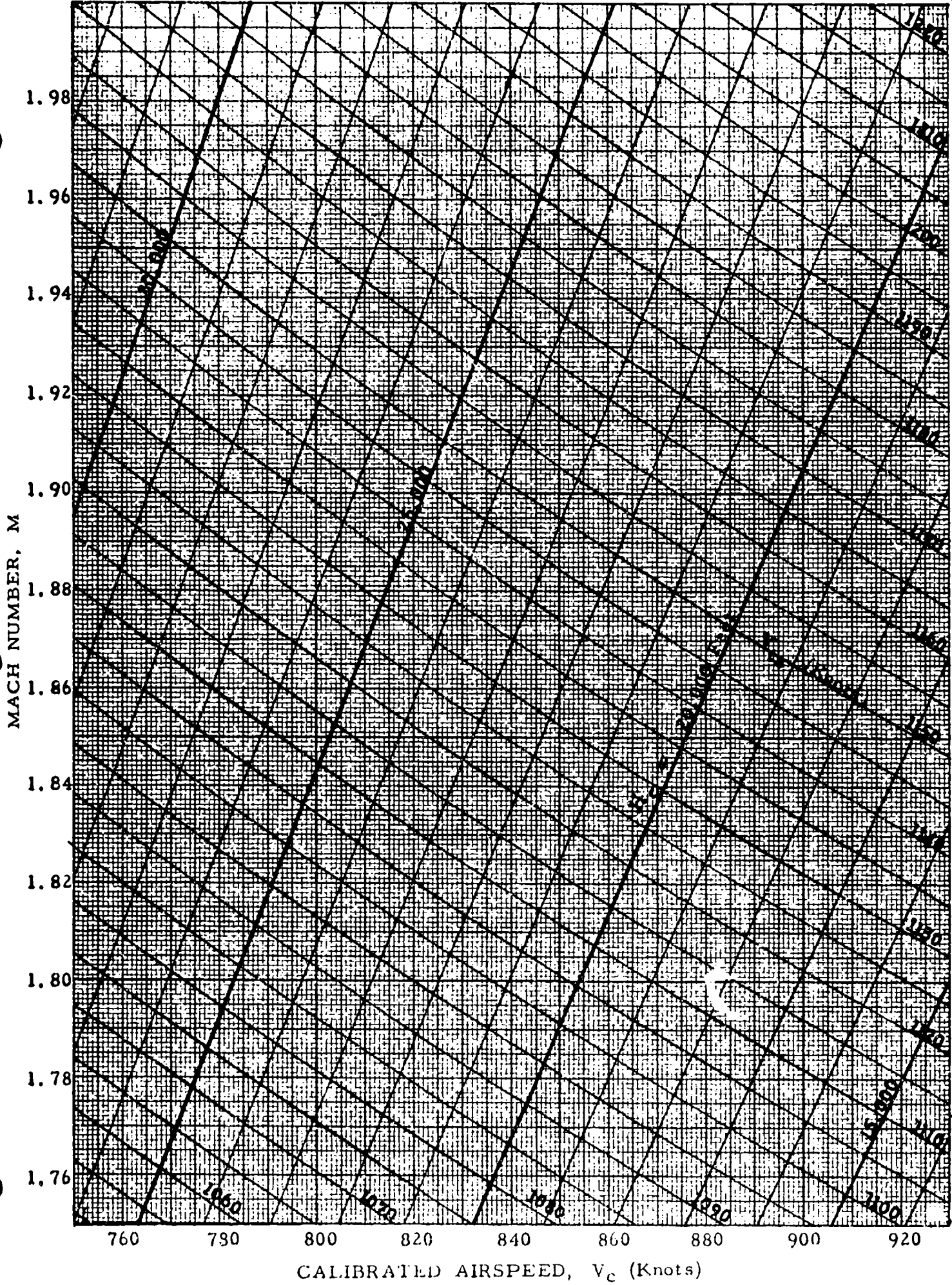
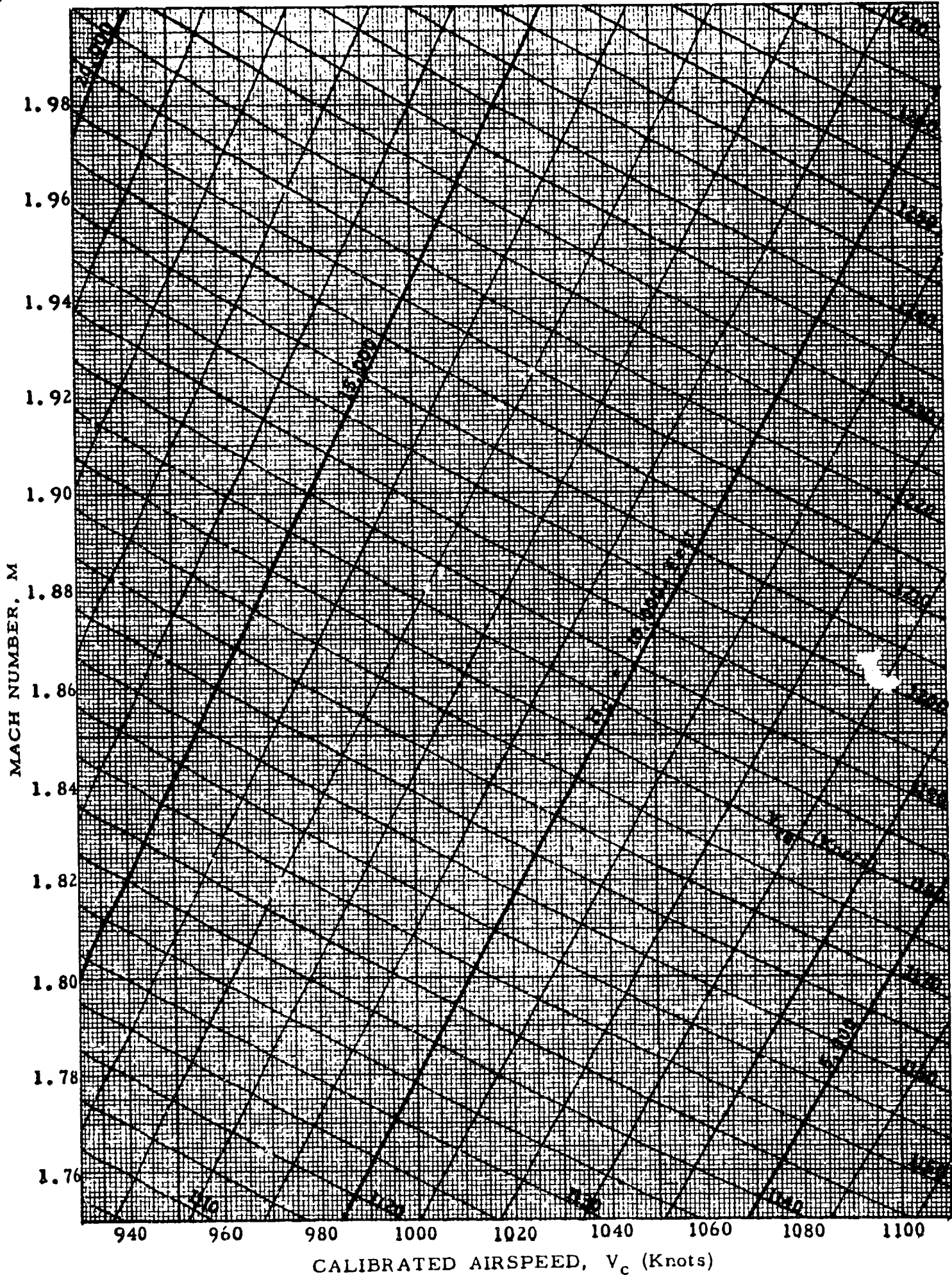
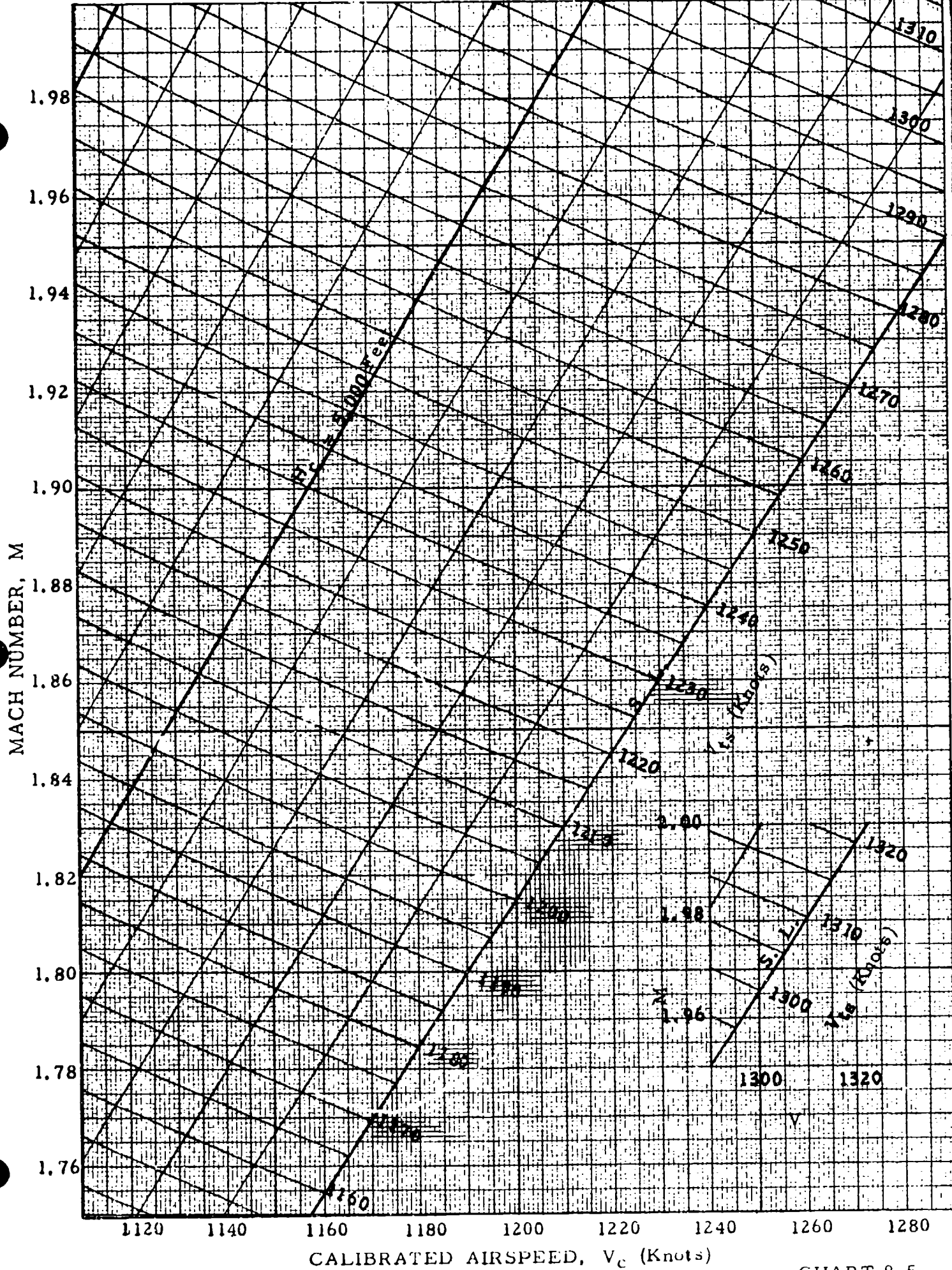


CHART 8.5



CALIBRATED AIRSPEED, V_c (Knots)





CALIBRATED AIRSPEED, V_c (Knots)

CHART 8.5

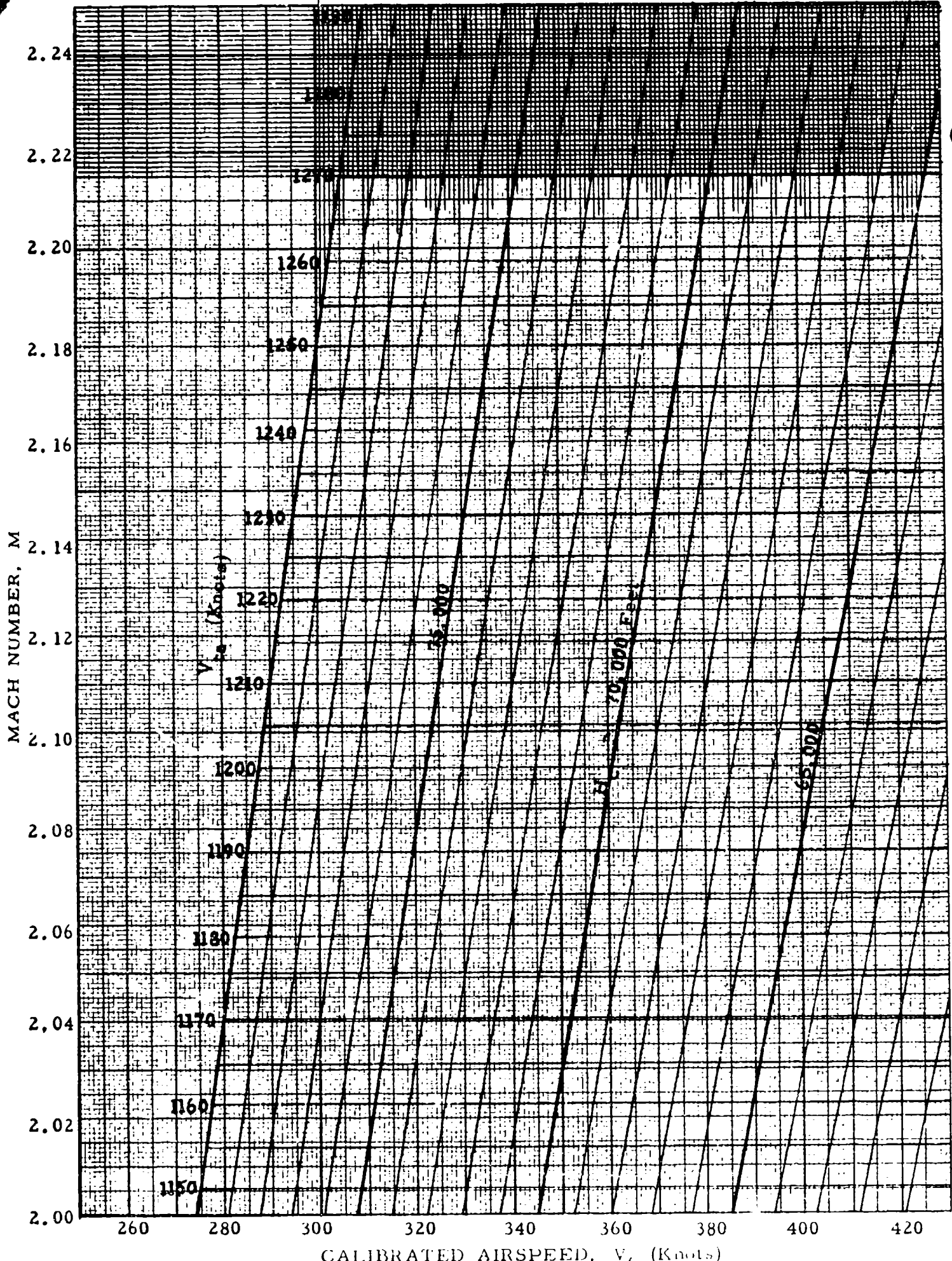


CHART 8.5

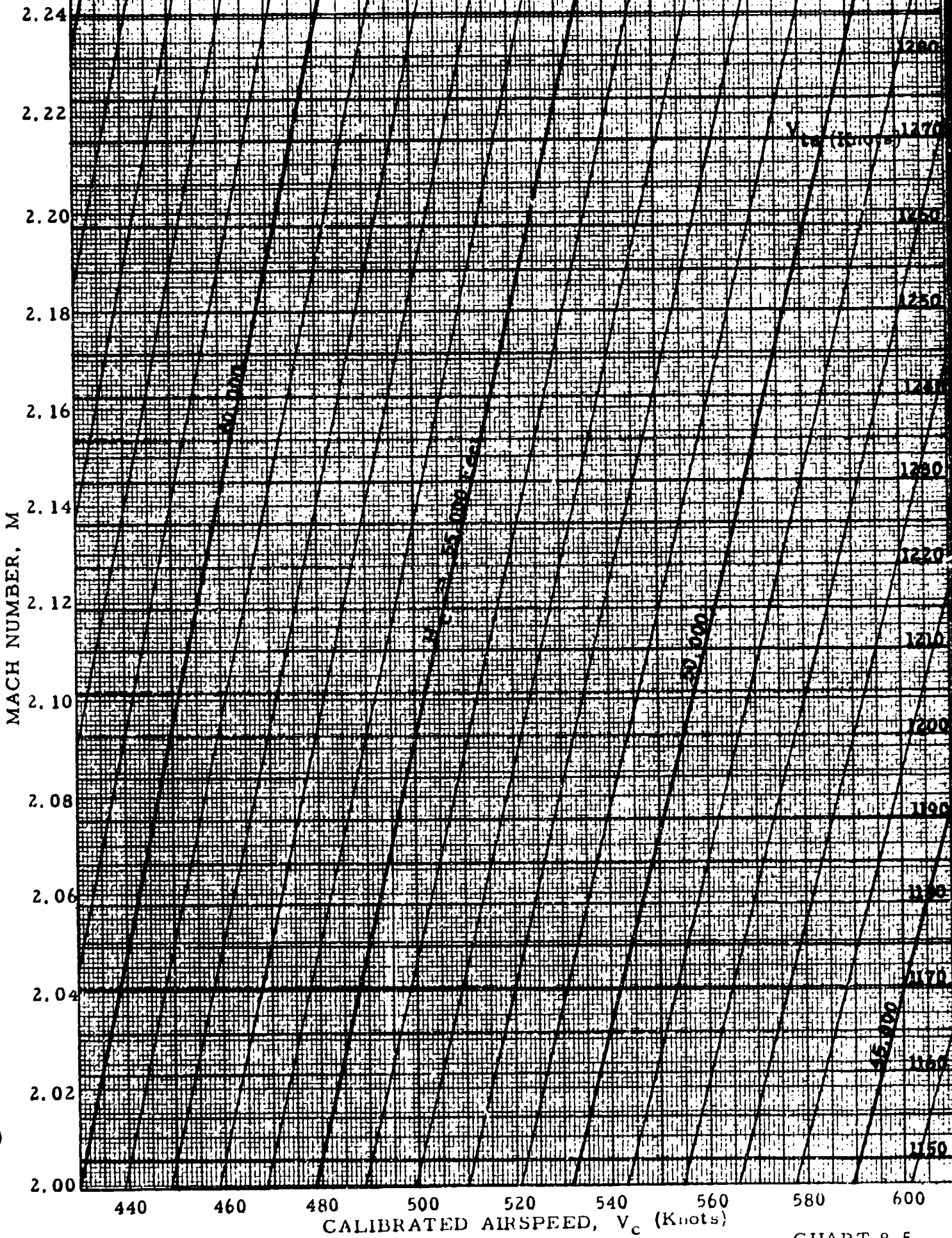


CHART 8.5

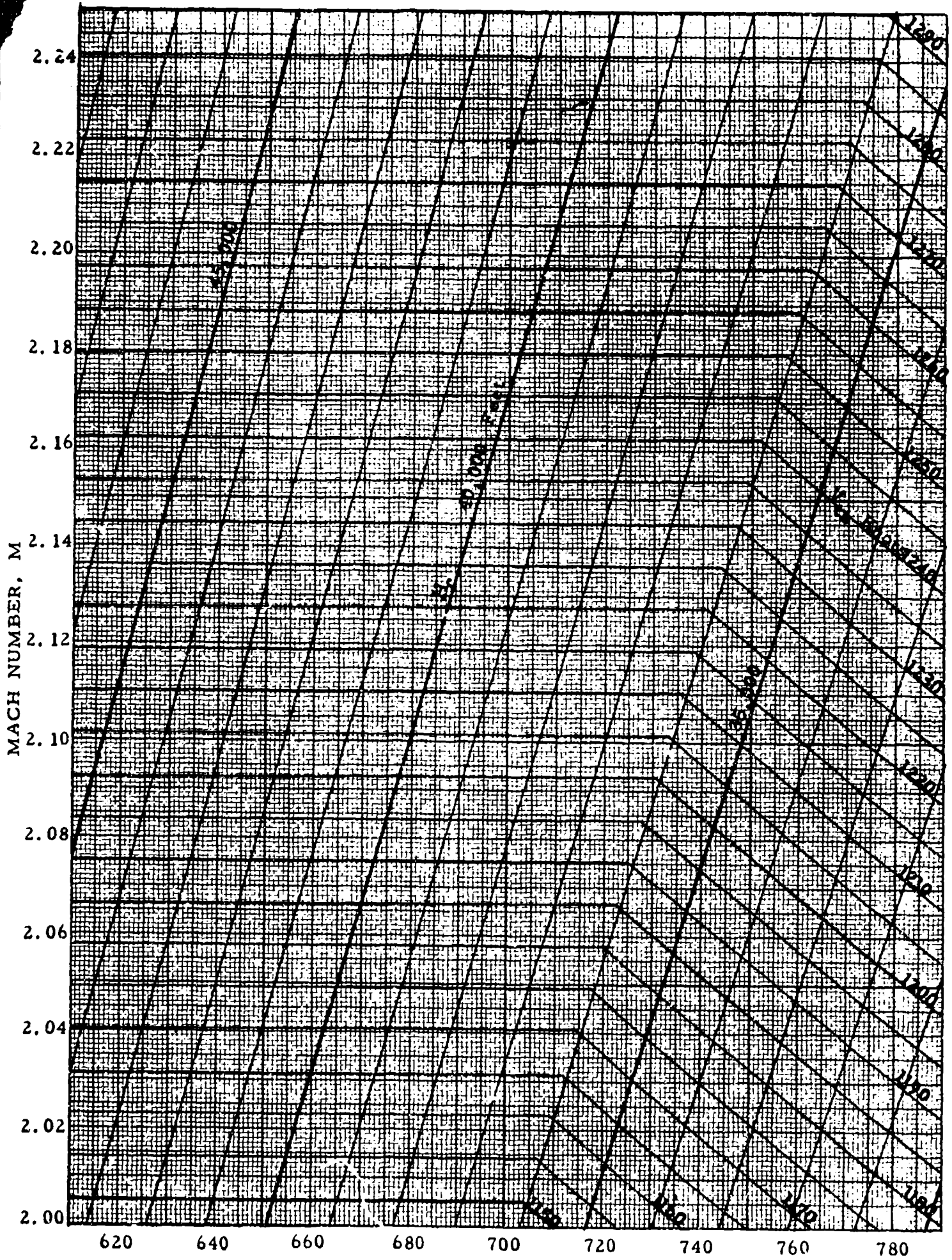
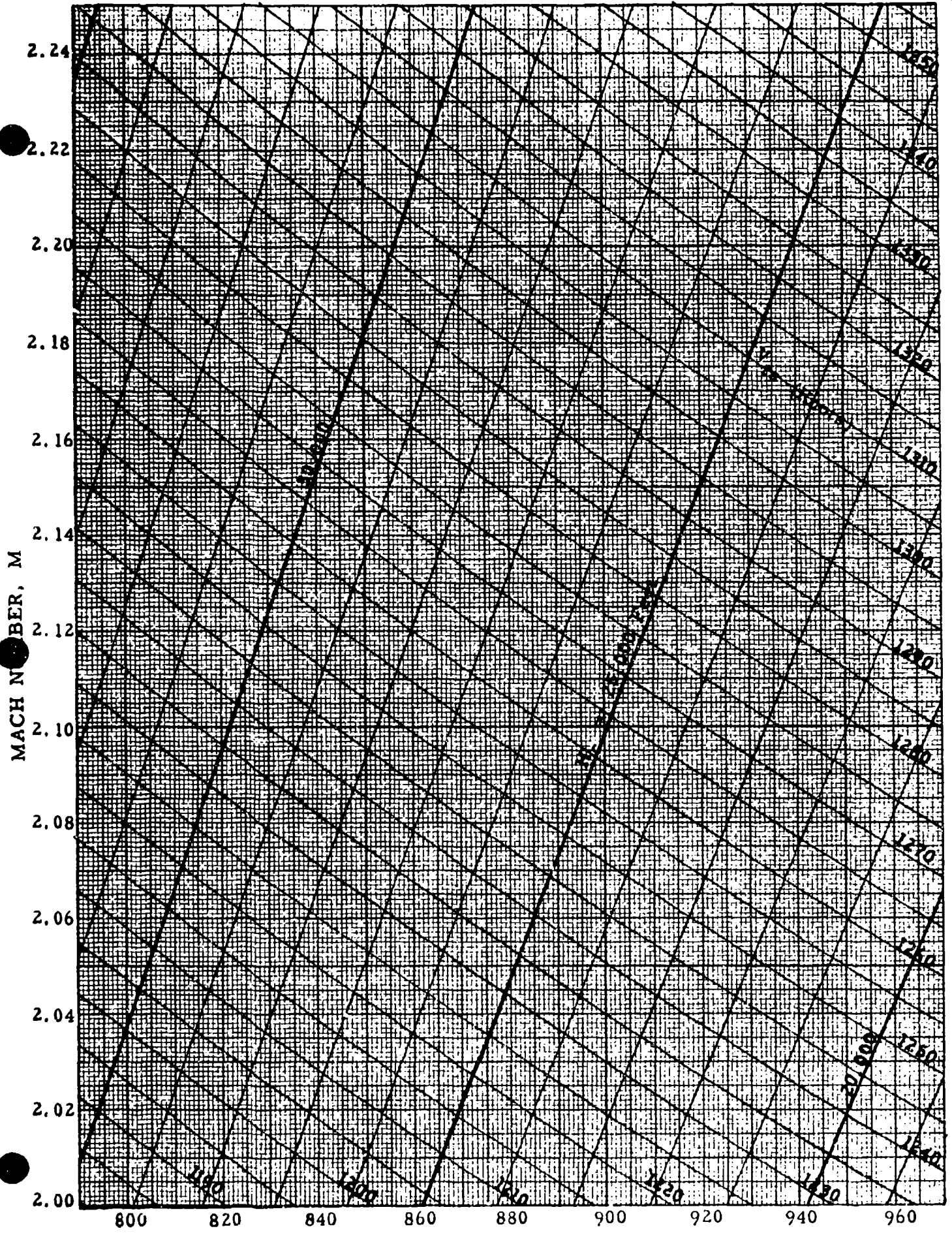


CHART 8.5

CALIBRATED AIRSPEED, V_c (Knots)



MACH NUMBER, M

CALIBRATED AIRSPEED, V_c (Knots)

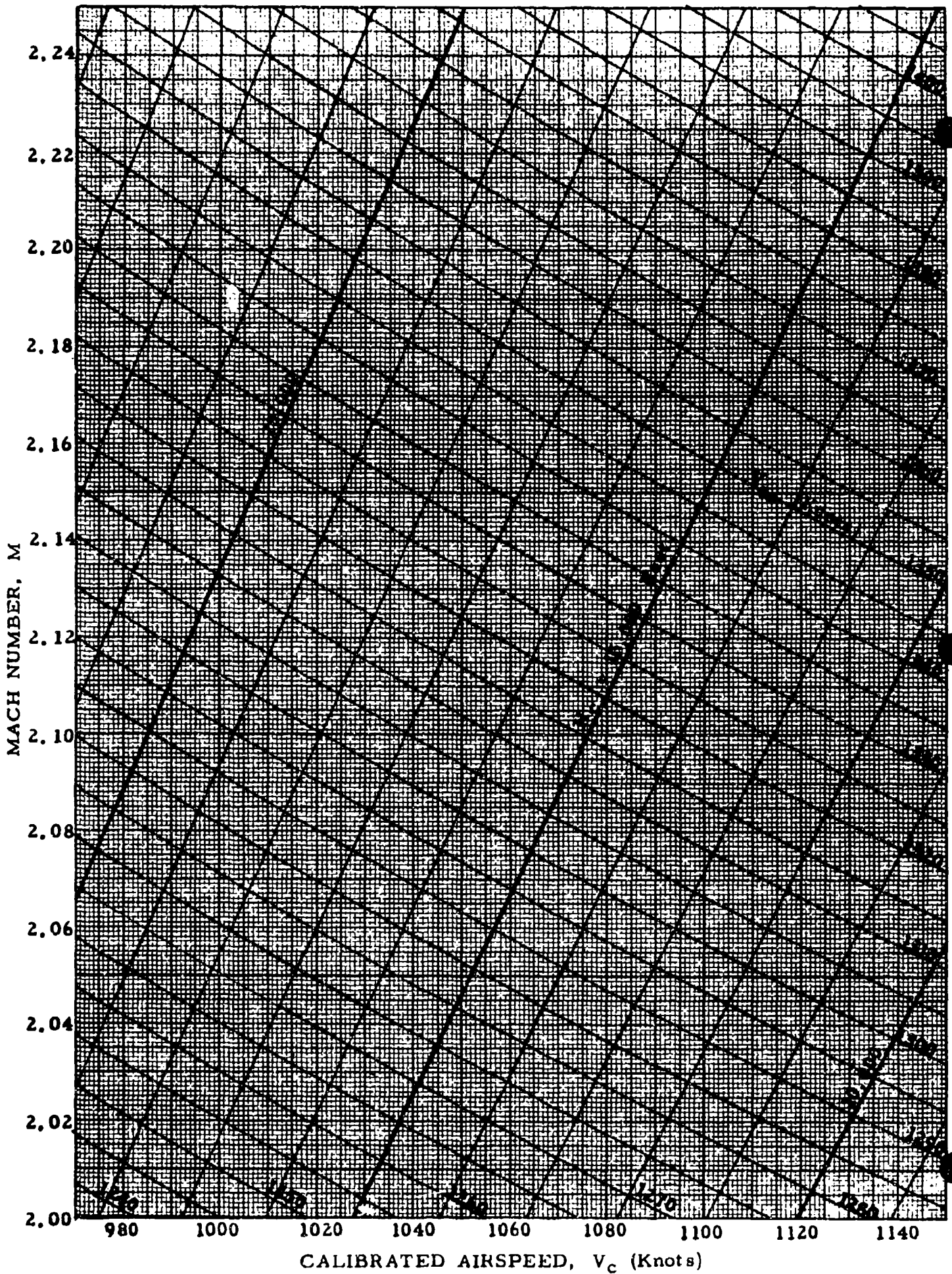
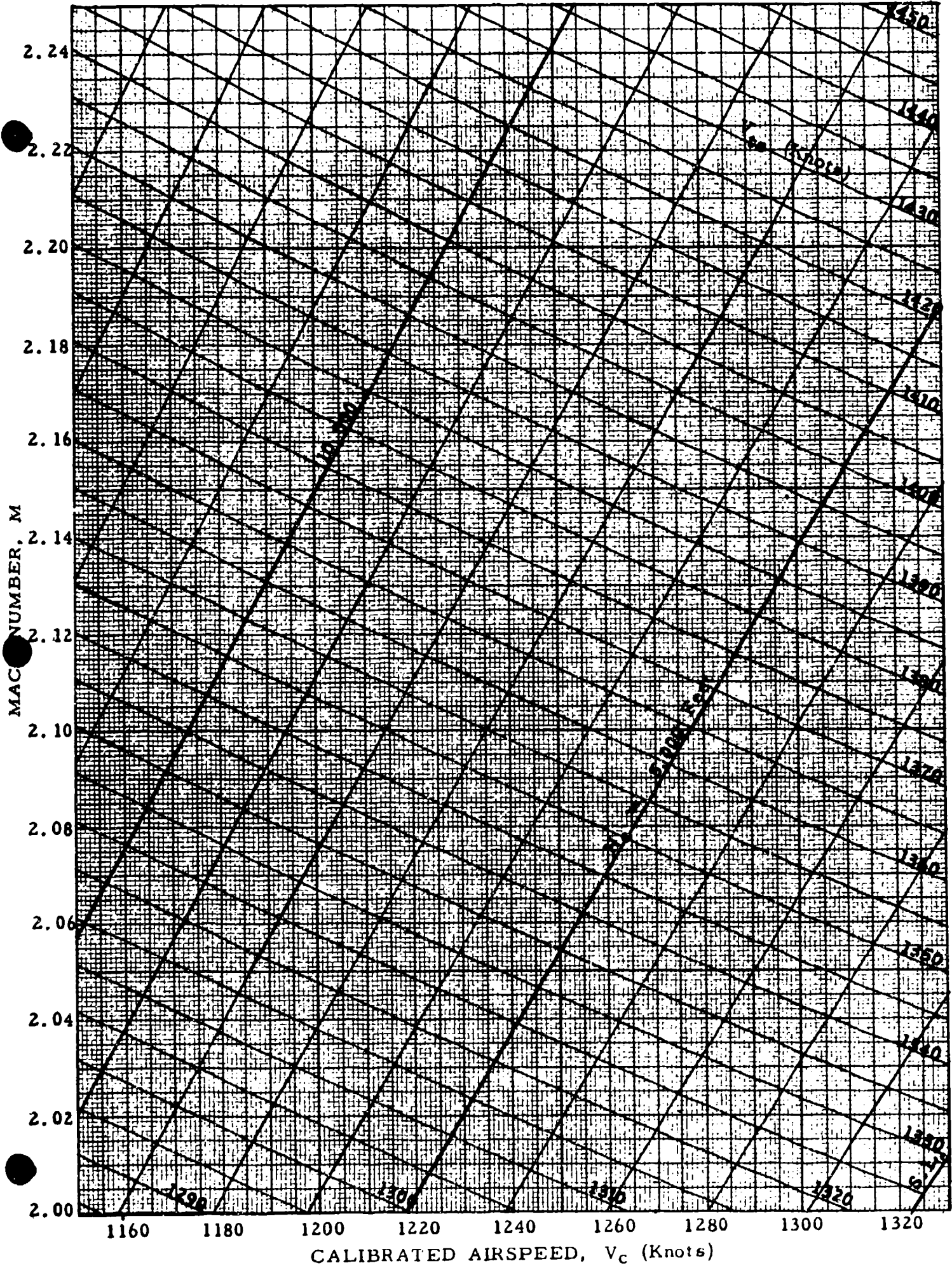


CHART 8.5



CALIBRATED AIRSPEED, V_C (Knots)

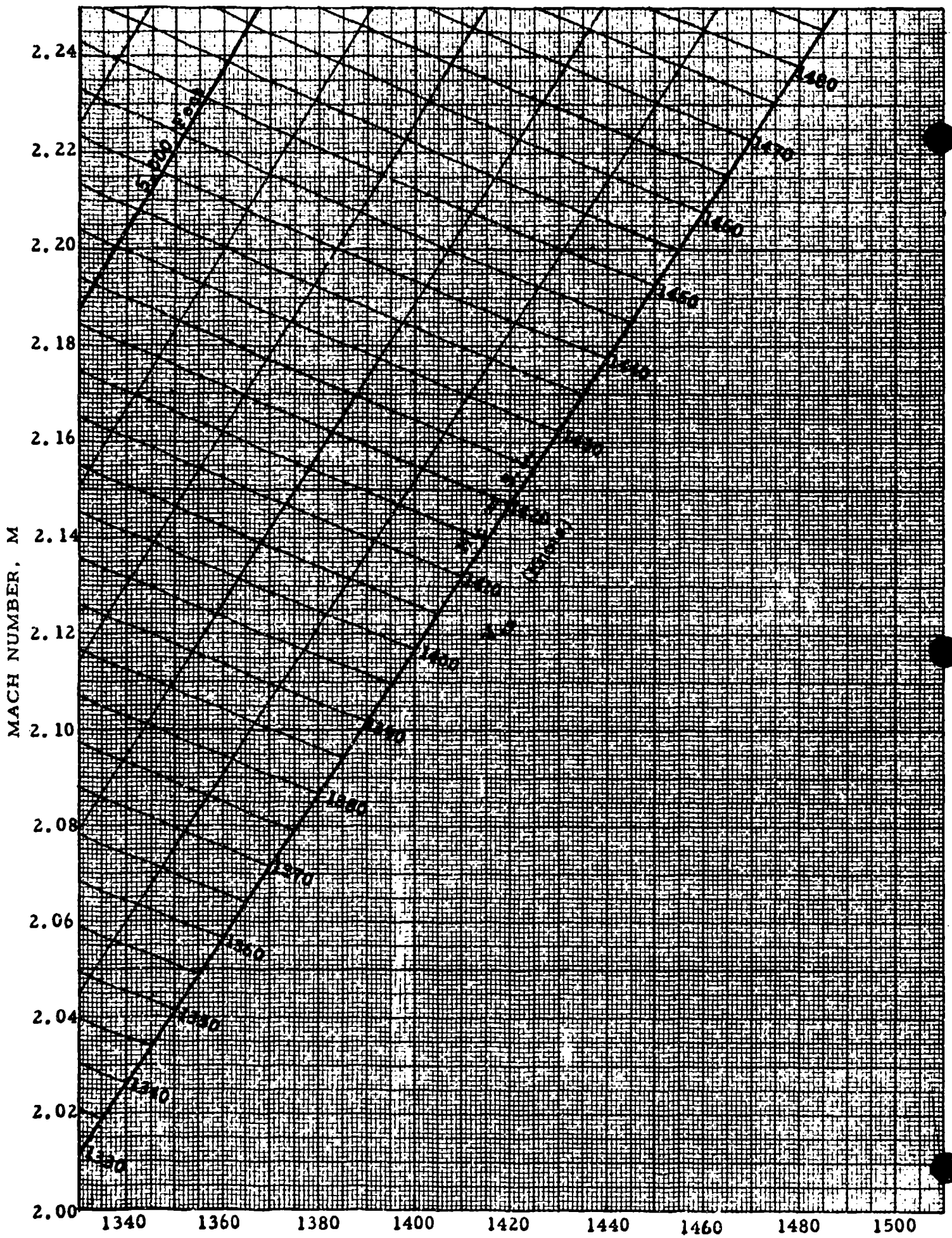
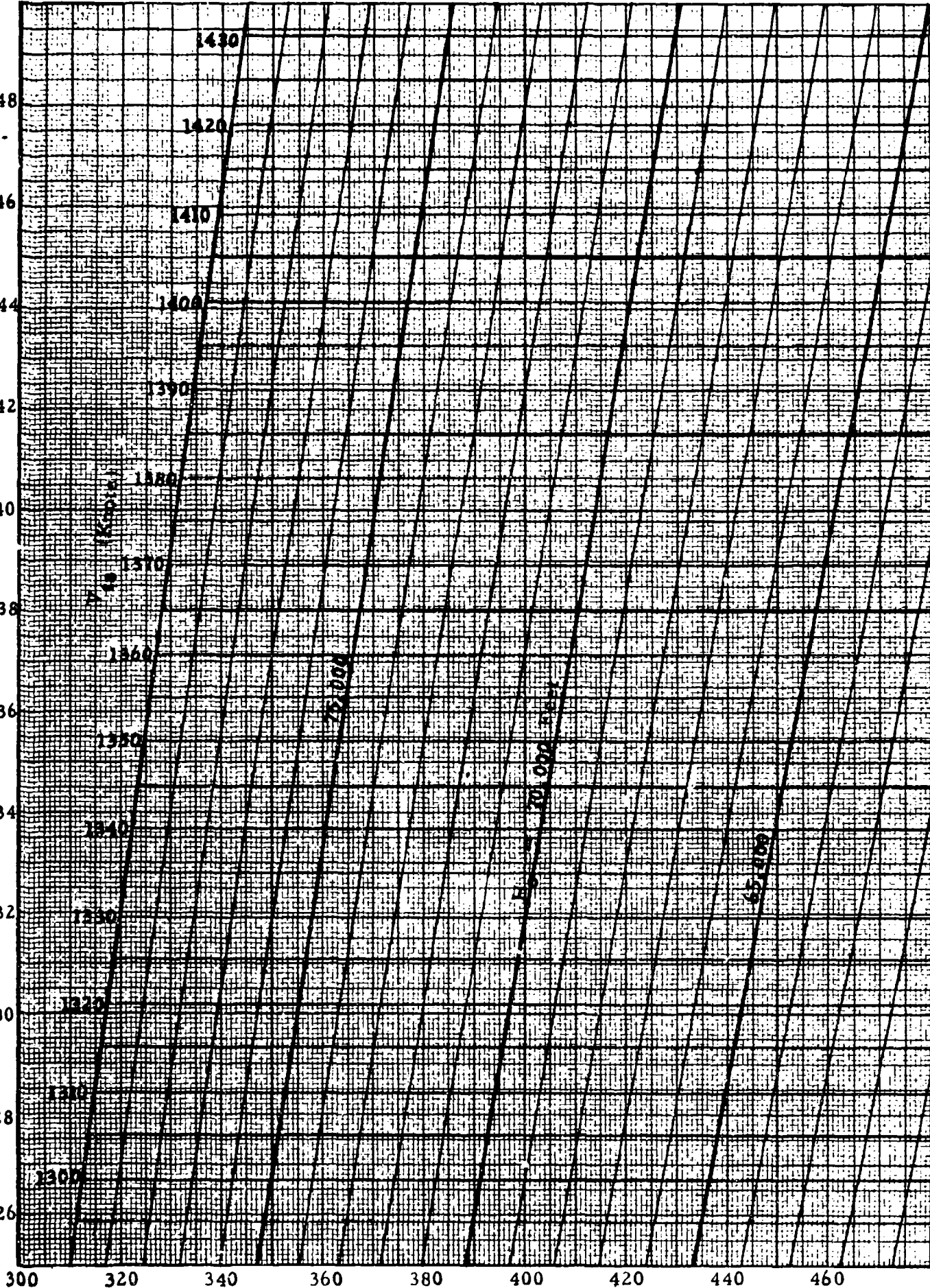


CHART 8.5

MACH NUMBER, M

2.48
2.46
2.44
2.42
2.40
2.38
2.36
2.34
2.32
2.30
2.28
2.26



CALIBRATED AIRSPEED, V_c (Knots)

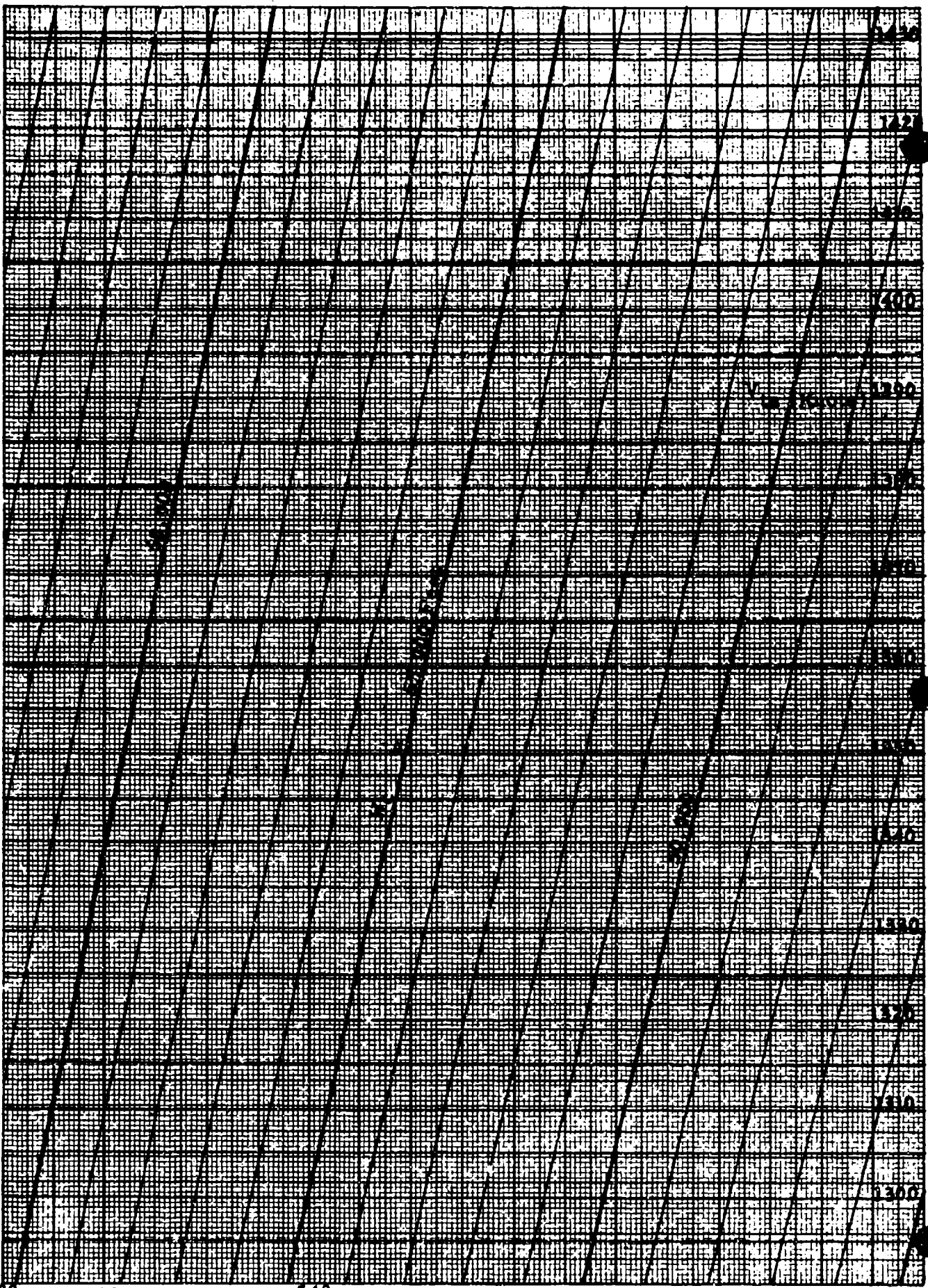
MACH NUMBER, M

2.48
2.46
2.44
2.42
2.40
2.38
2.36
2.34
2.32
2.30
2.28
2.26

480 500 520 540 560 580 600 620 640

CALIBRATED AIRSPEED, V_c (Knots)

CHART 8.5



MACH NUMBER, M

2.48
2.46
2.44
2.42
2.40
2.38
2.36
2.34
2.32
2.30
2.28
2.26

660 680 700 720 740 760 780 800 820

CALIBRATED AIRSPEED, V_c (Knots)

1430
1420
1410
1400

V_c (Knots) 1500

1500

1520

1550

1600

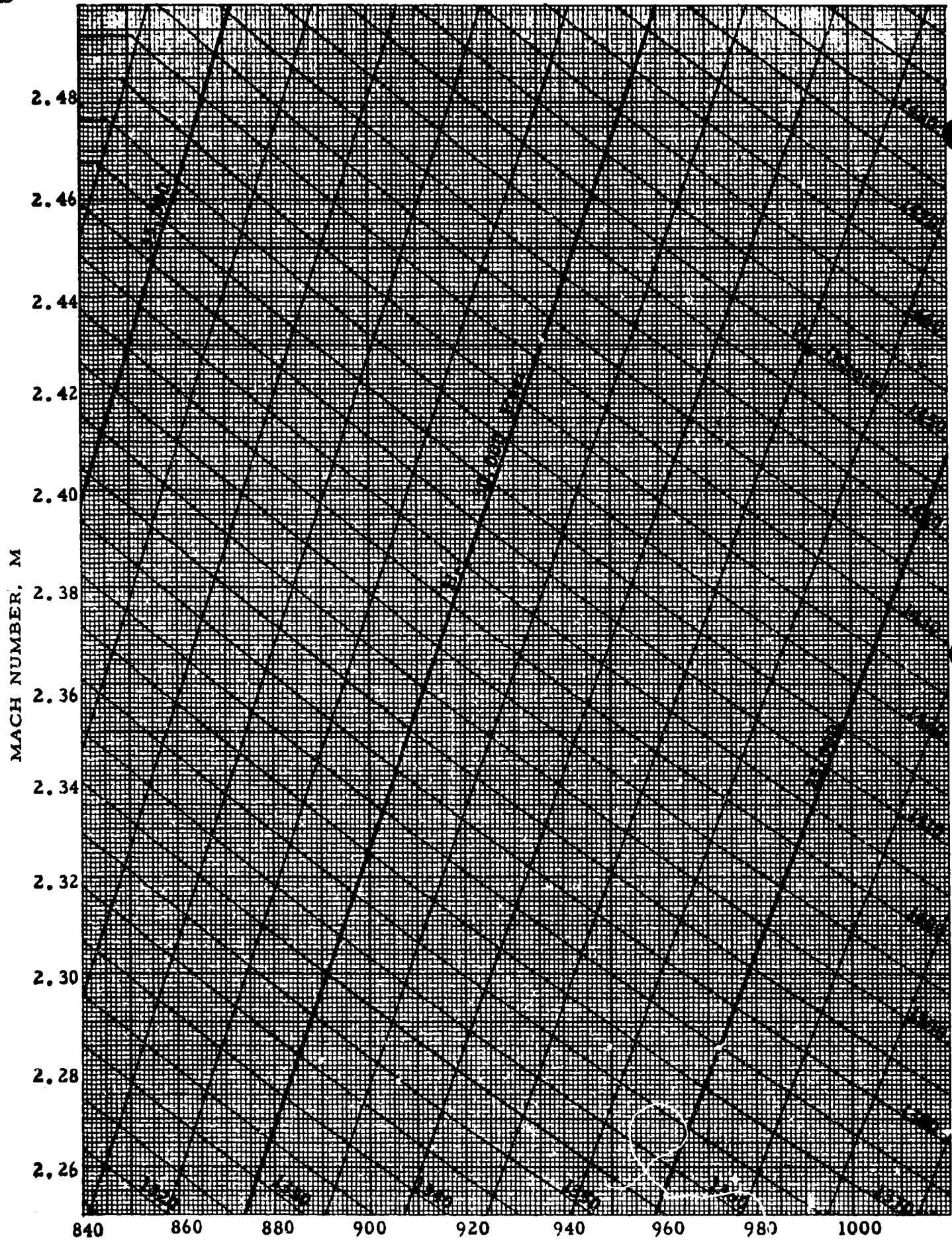
1650

1700

1800

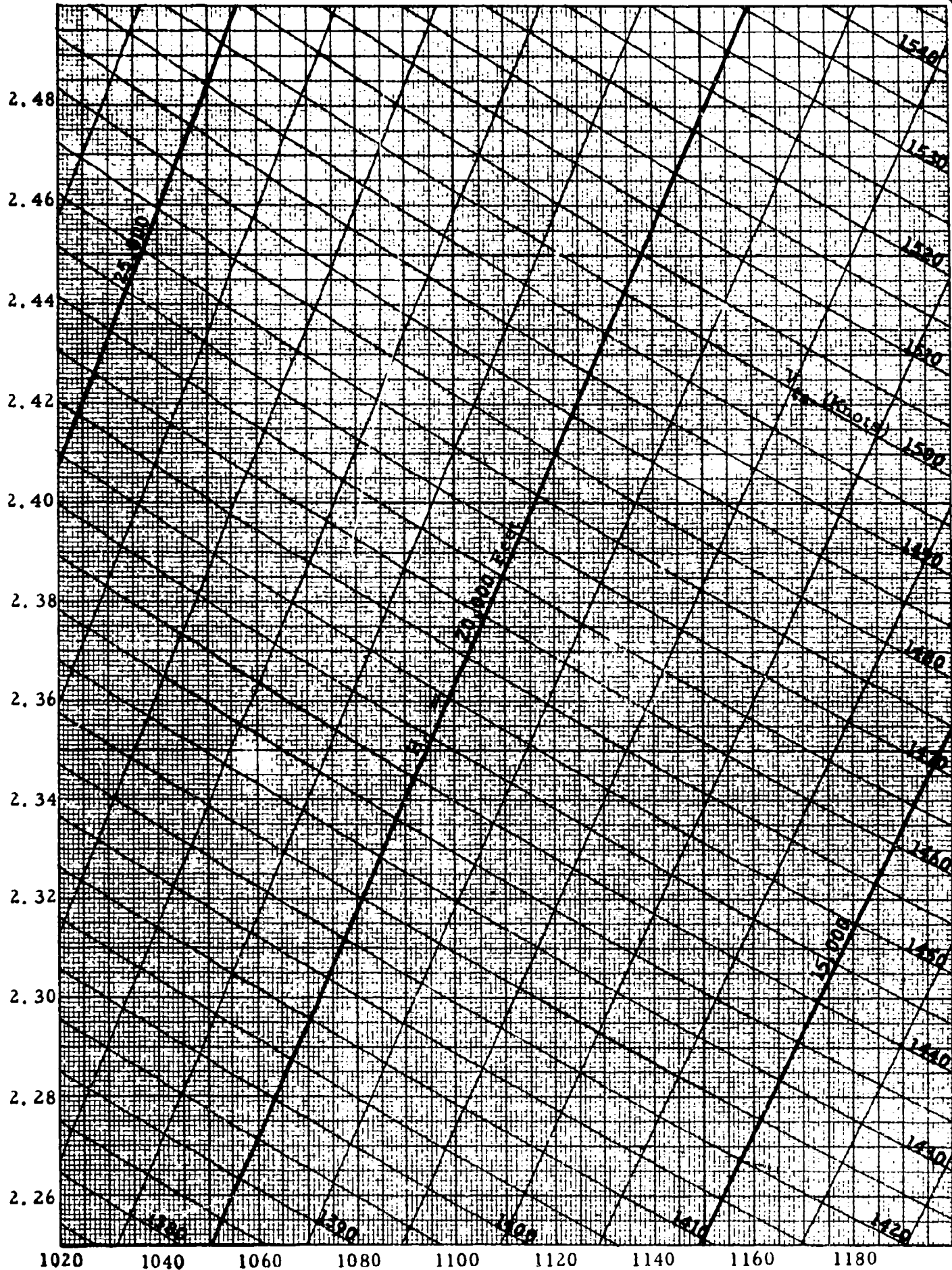
1900

2000



CALIBRATED AIRSPEED, V_c (Knots)

MACH NUMBER, M



CALIBRATED AIRSPEED, V_c (Knots)

CHART 8.5

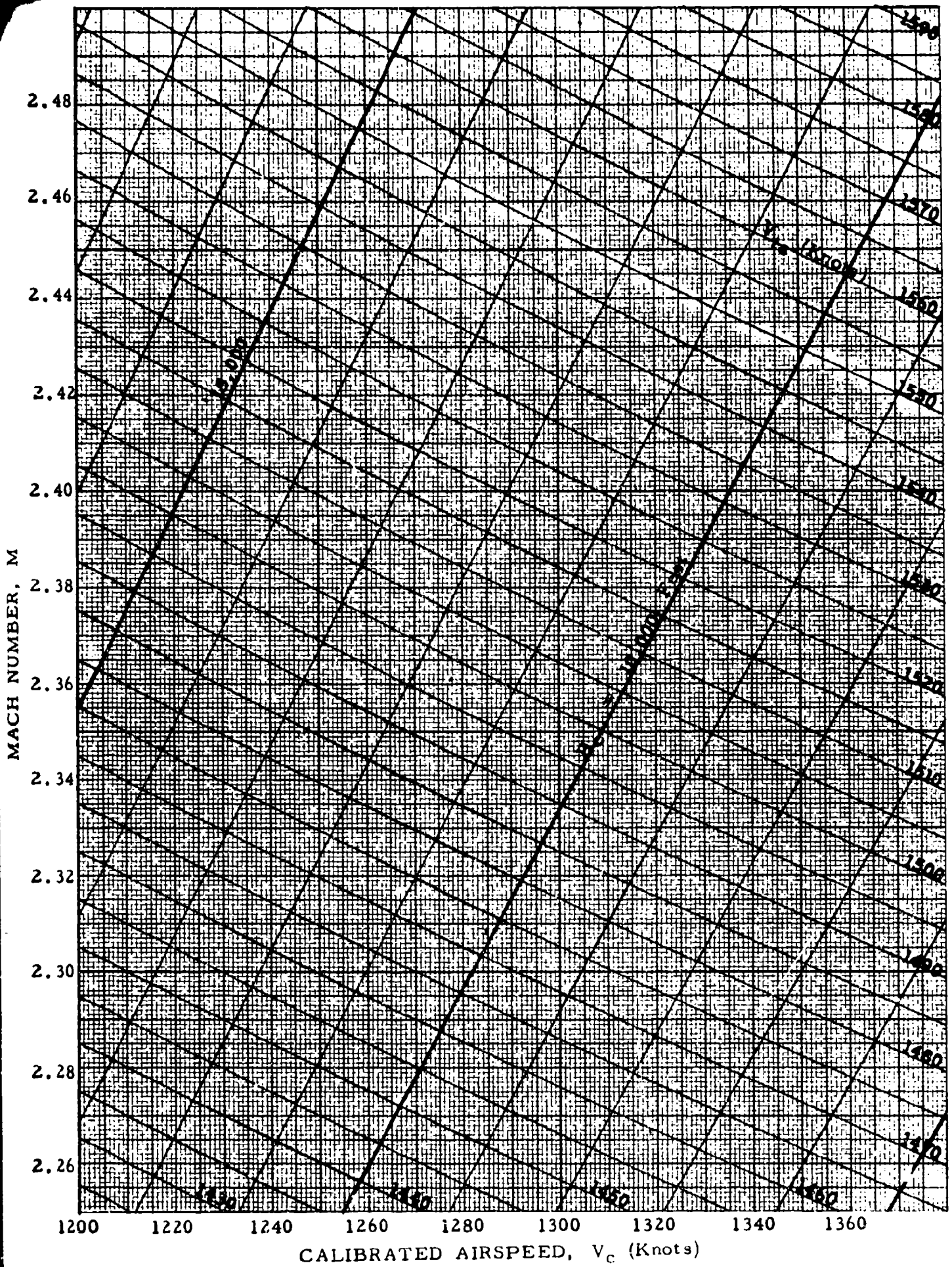
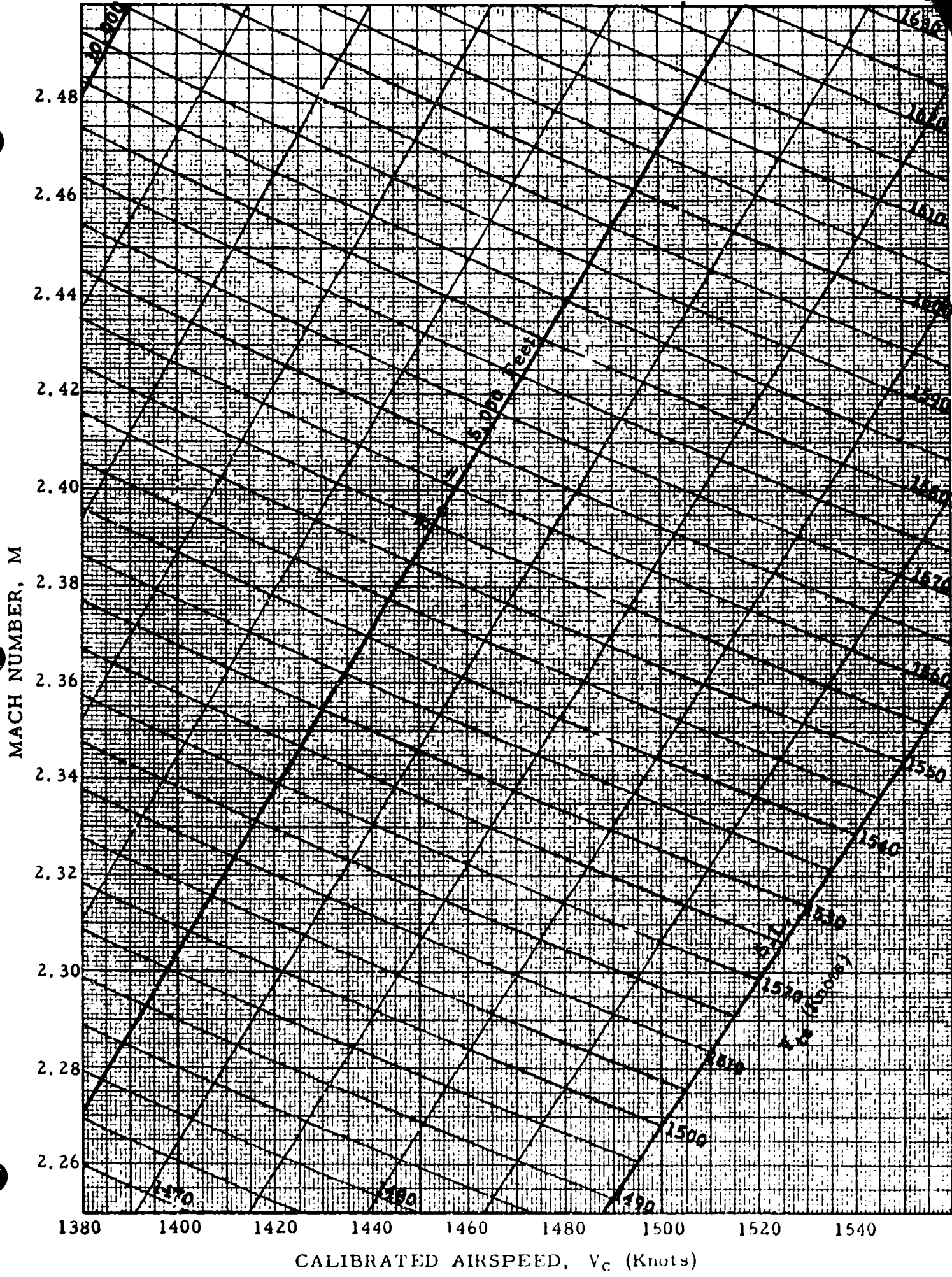


CHART 8.5



CALIBRATED AIRSPEED, V_c (Knots)

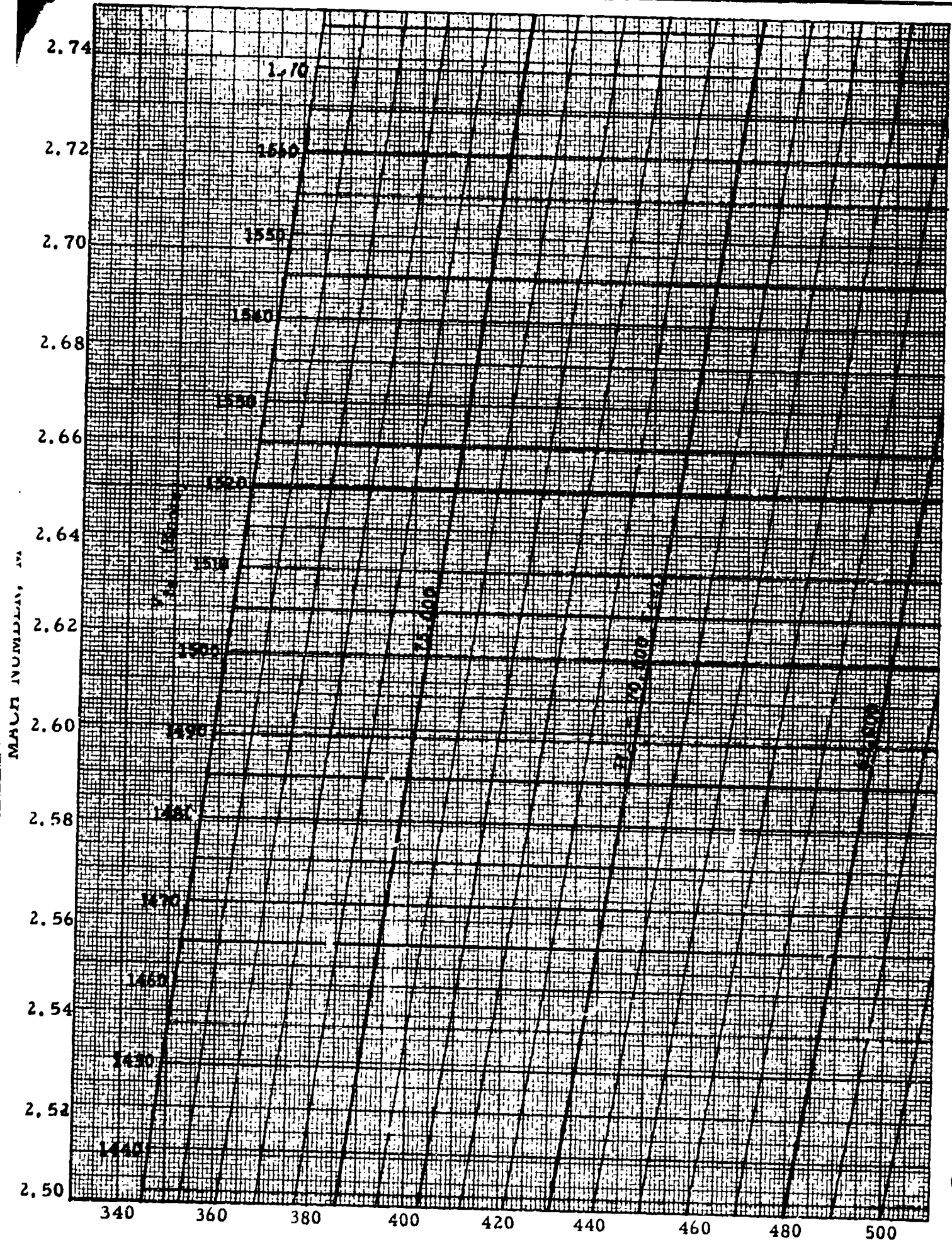


CHART 8.5

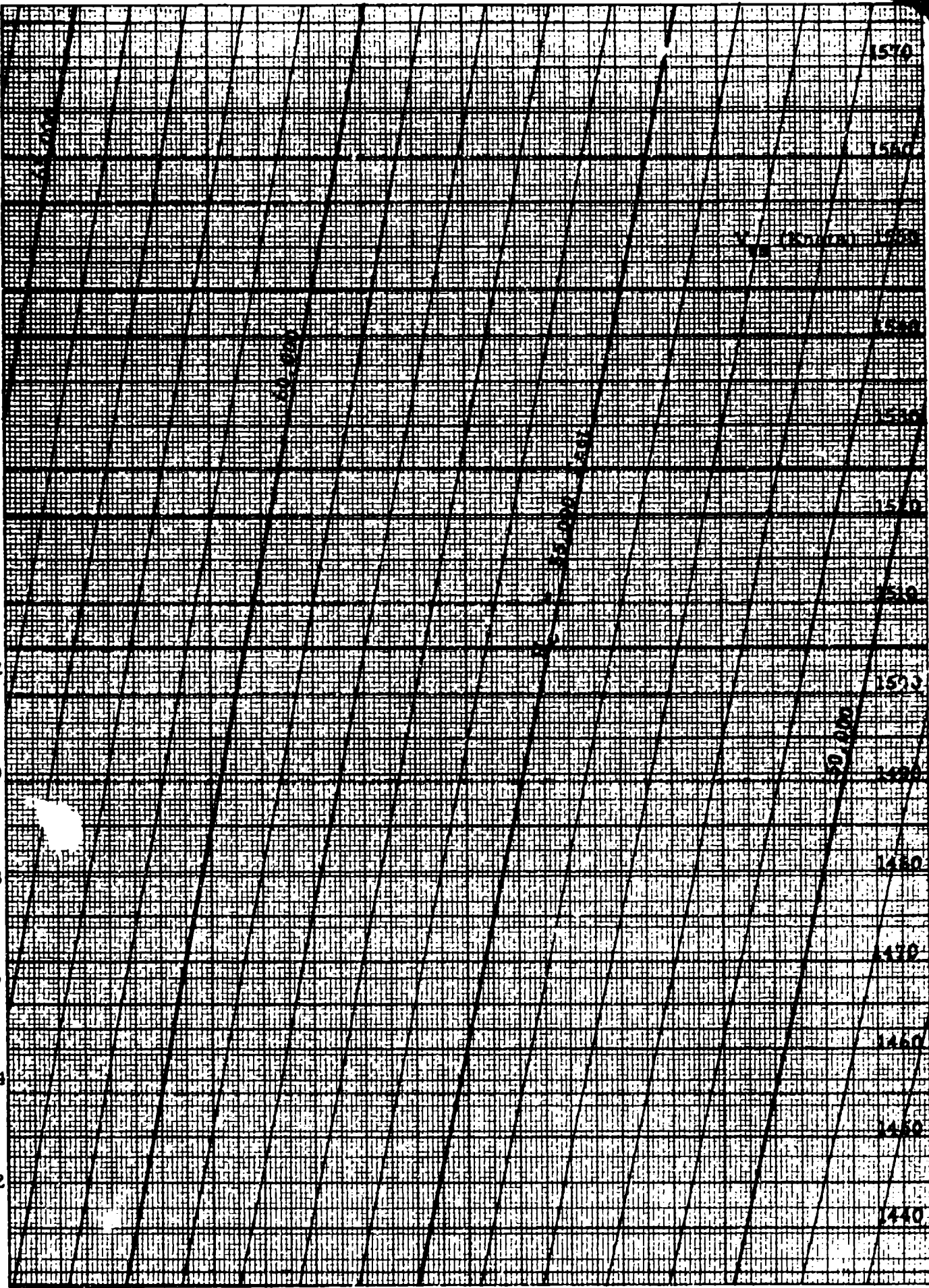
CALIBRATED AIRSPEED, V_c (Knots)

MACH NUMBER, M

2.74
2.72
2.70
2.68
2.66
2.64
2.62
2.60
2.58
2.56
2.54
2.52
2.50

520 540 560 580 600 620 640 660 680

CALIBRATED AIRSPEED, V_C (Knots)



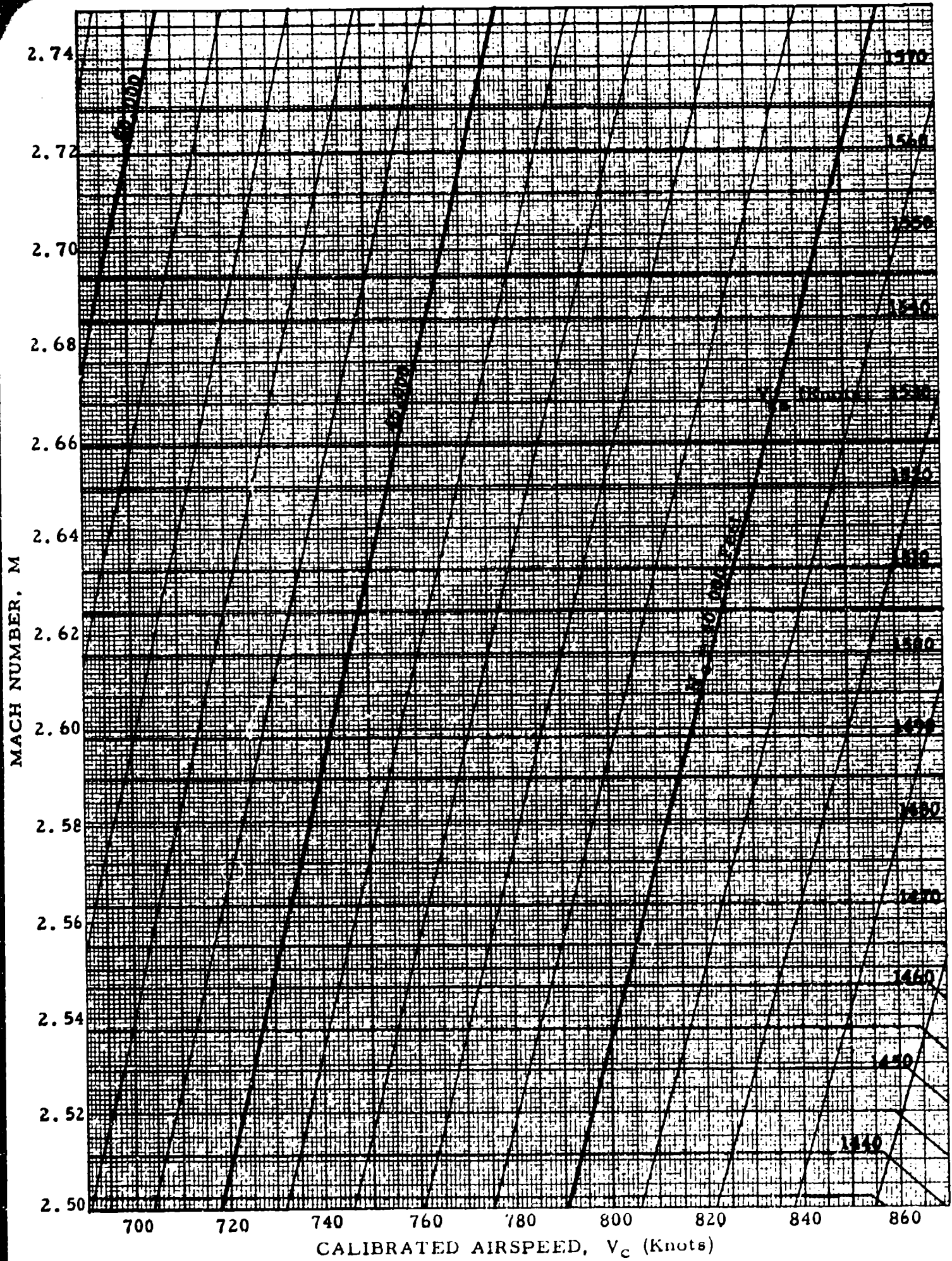
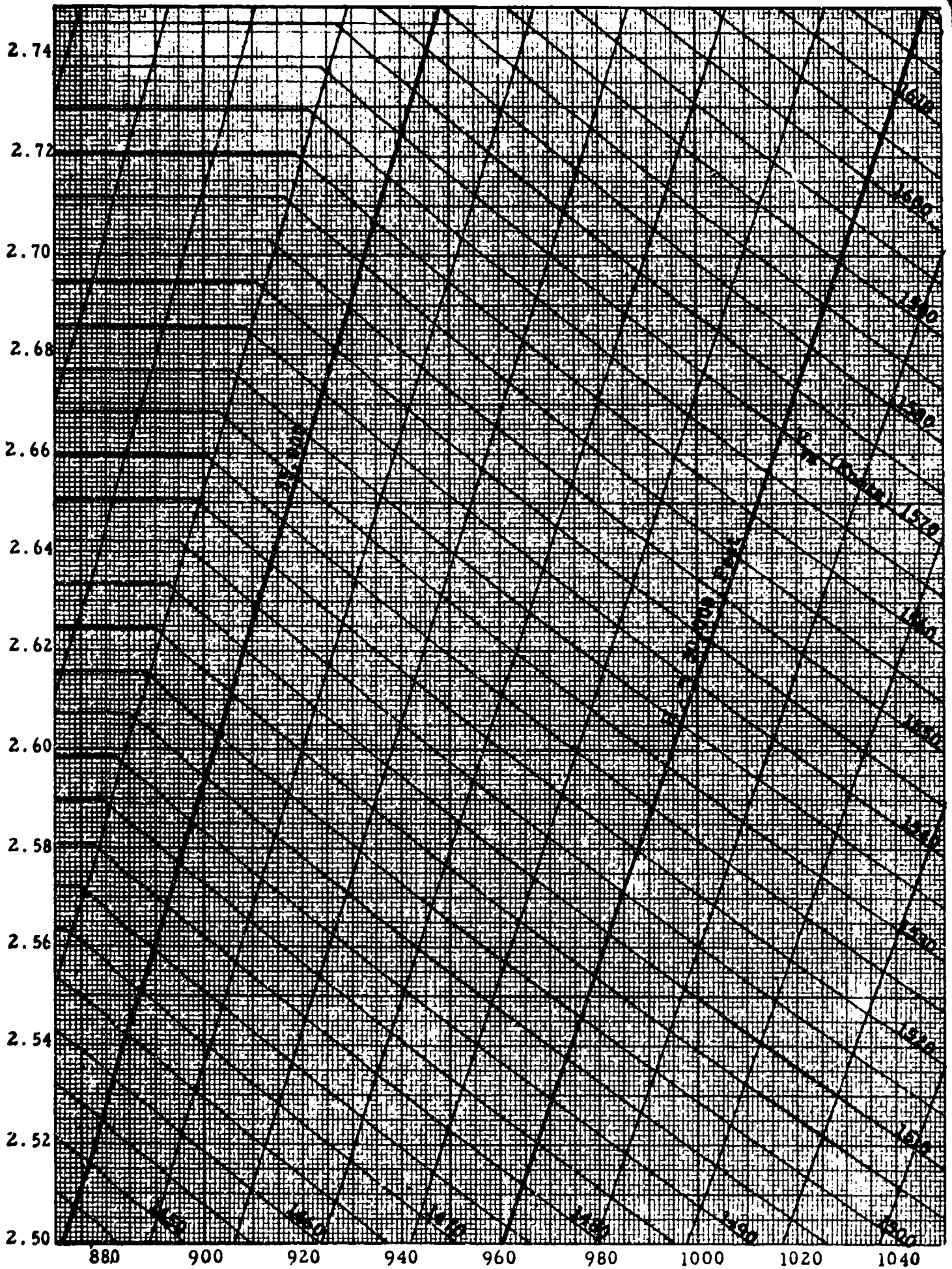


CHART 8.5



CALIBRATED AIRSPEED, V_c (Knots)

CHART 8.5

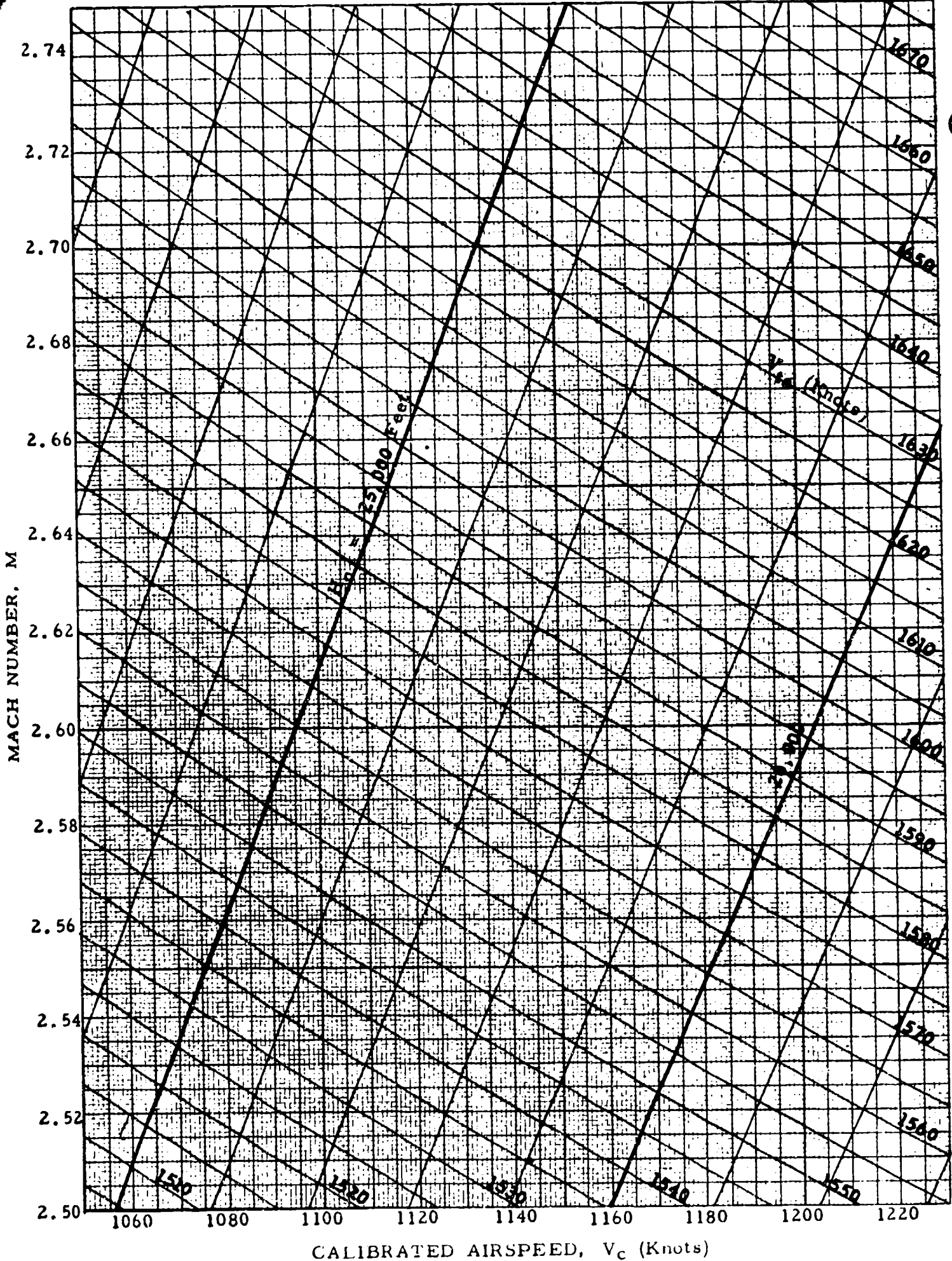
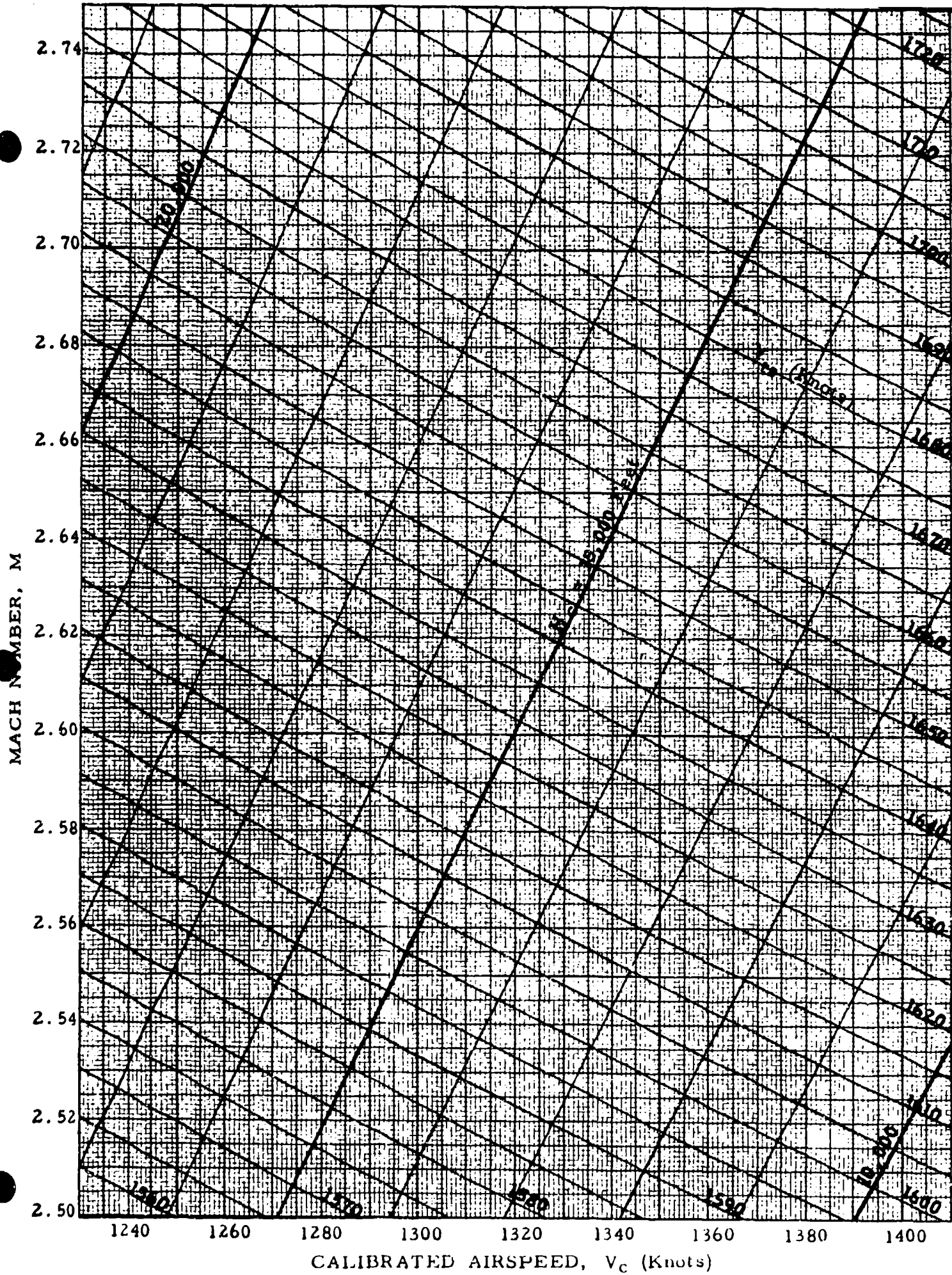


CHART 8.5



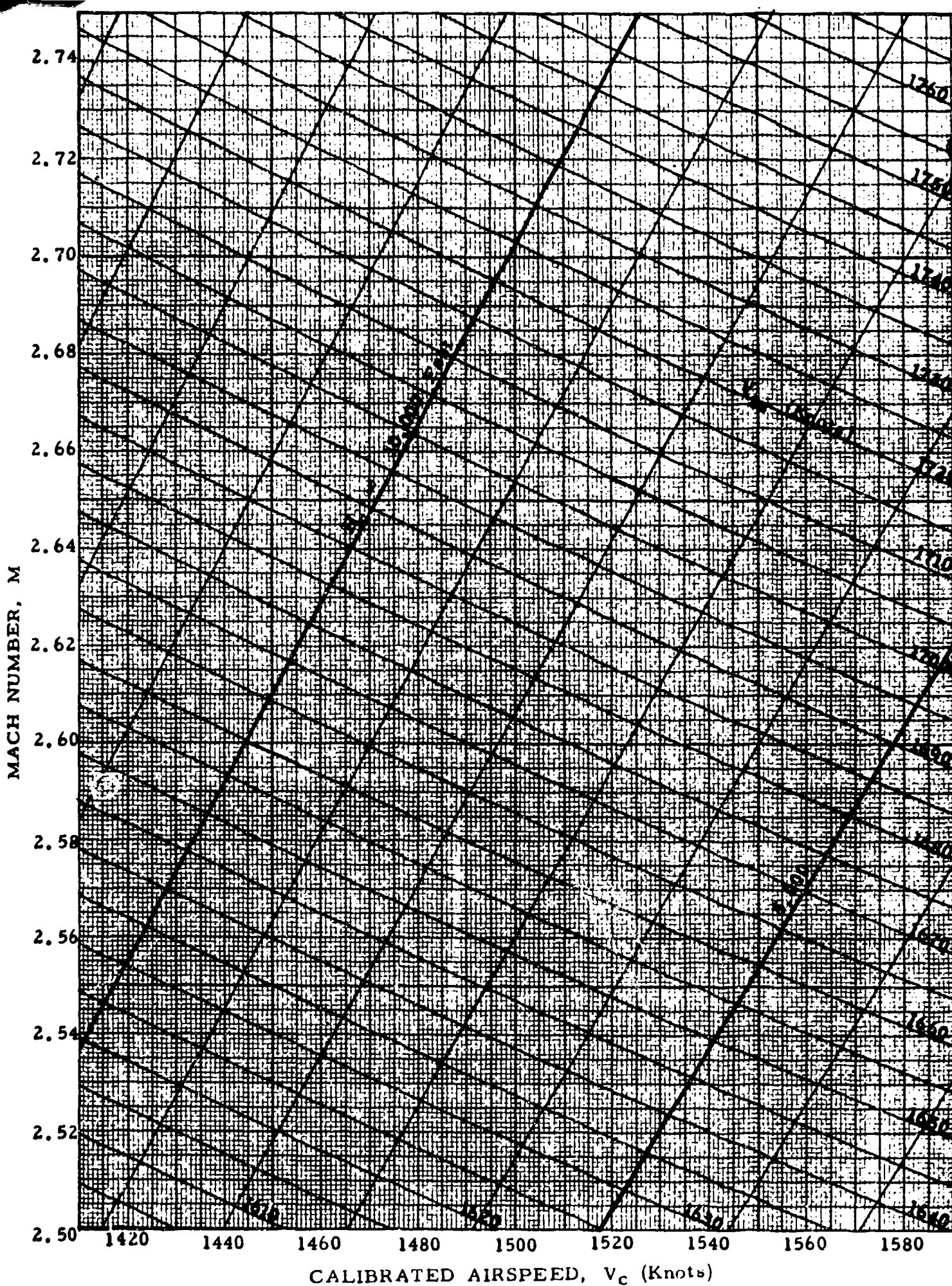
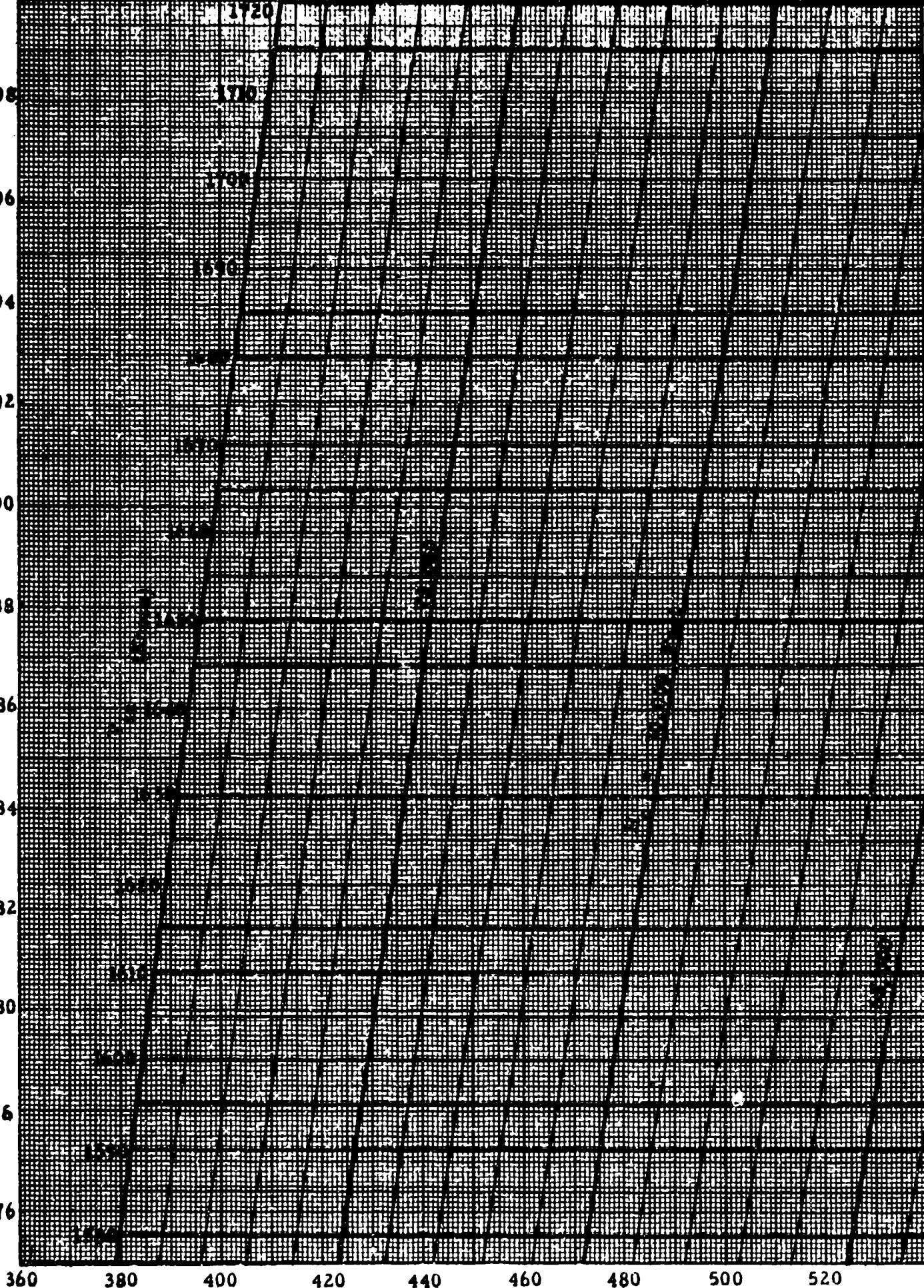


CHART 8.5

MACH NUMBER, M

2.98
2.96
2.94
2.92
2.90
2.88
2.86
2.84
2.82
2.80
2.76
2.76

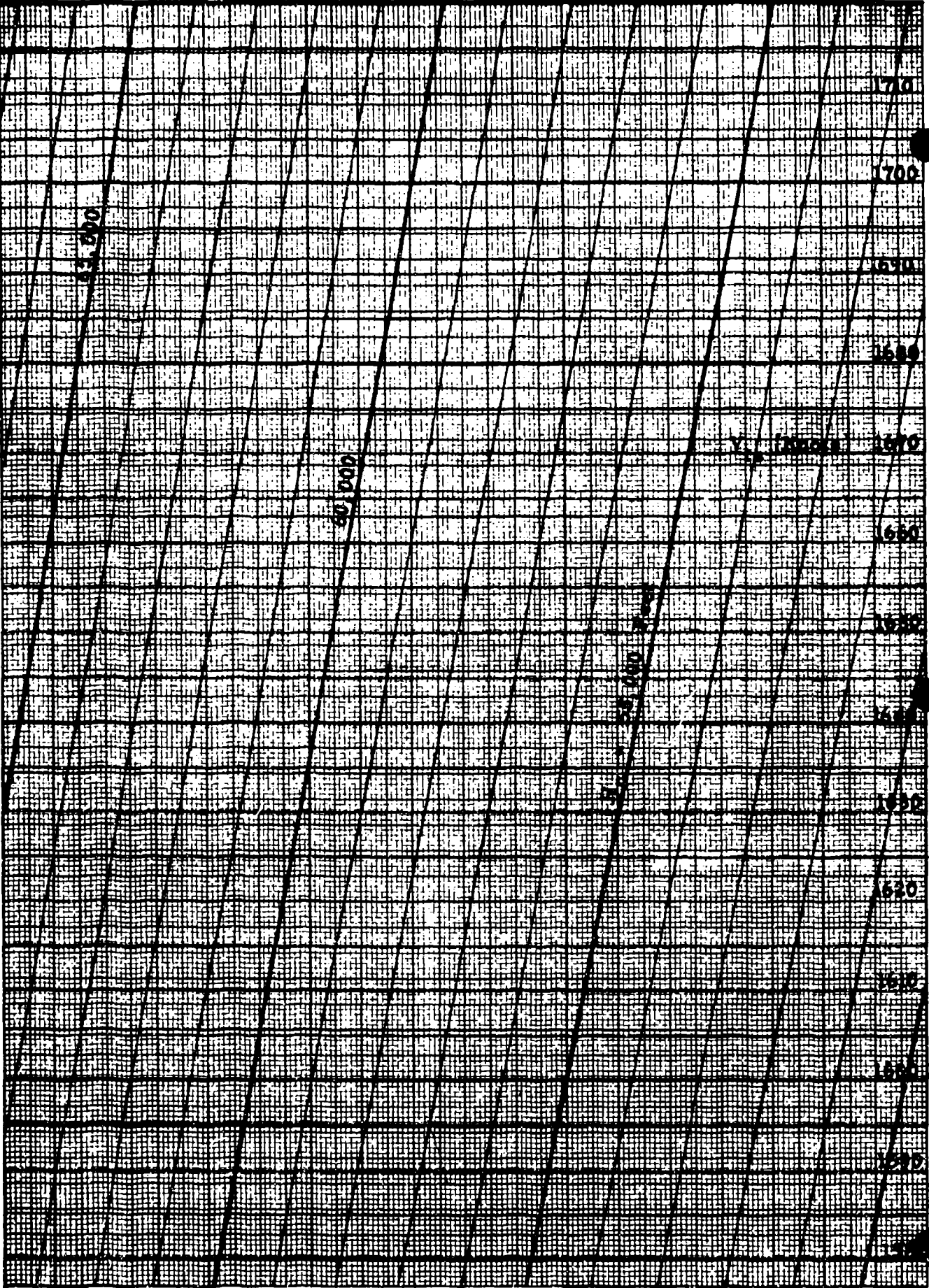


CALIBRATED AIRSPEED, V_c (Knots)

CHART 8.5

MACH NUMBER, M

2.98
2.96
2.94
2.92
2.90
2.88
2.86
2.84
2.82
2.80
2.78
2.76



540 560 580 600 620 640 660 680 700

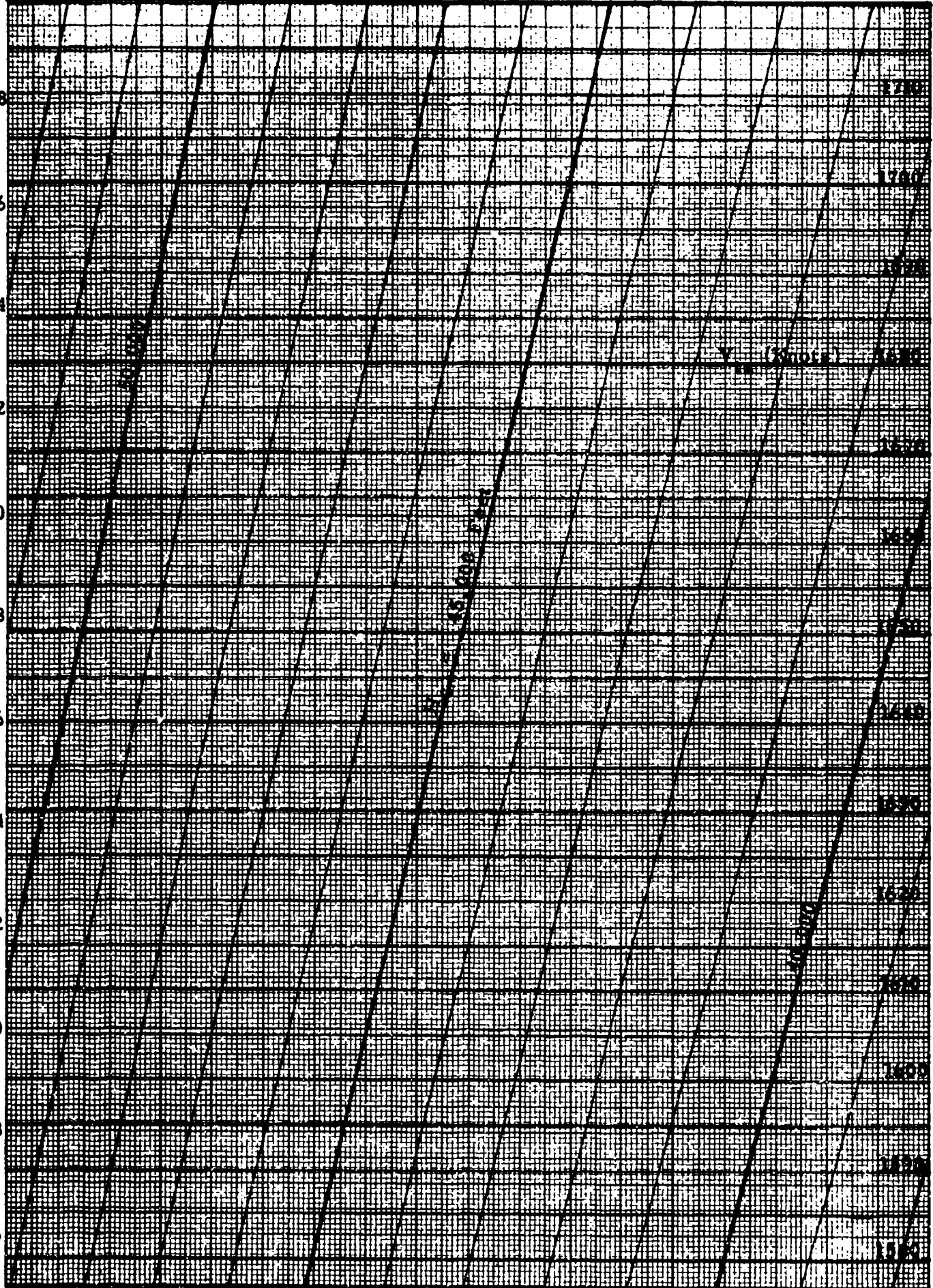
CALIBRATED AIRSPEED, V_c (Knots)

MACH NUMBER, M

2.98
2.96
2.94
2.92
2.90
2.88
2.86
2.84
2.82
2.80
2.78
2.76

720 740 760 780 800 820 840 860 880

CALIBRATED AIRSPEED, V_C (Knots)



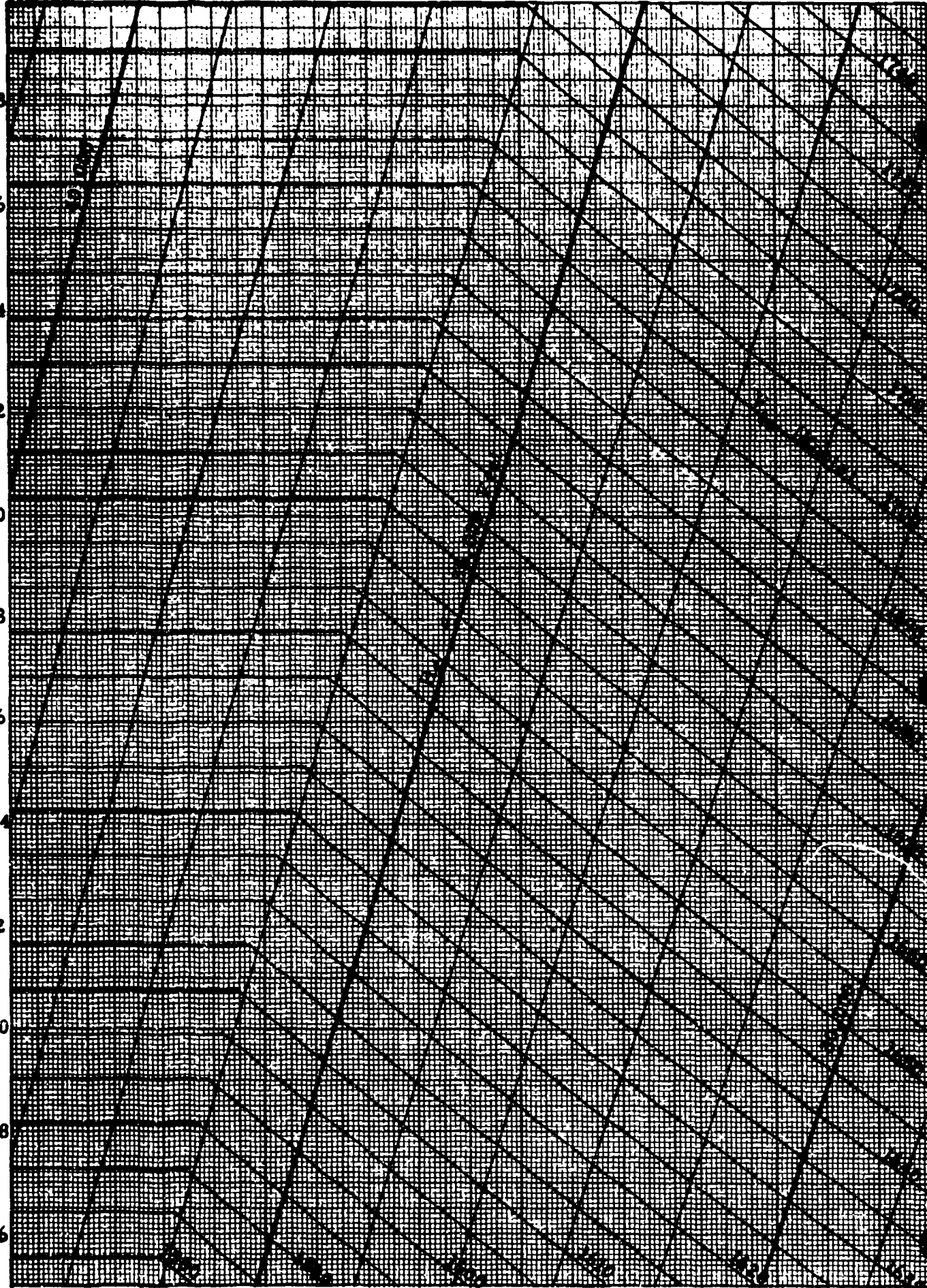
MACH NUMBER, M

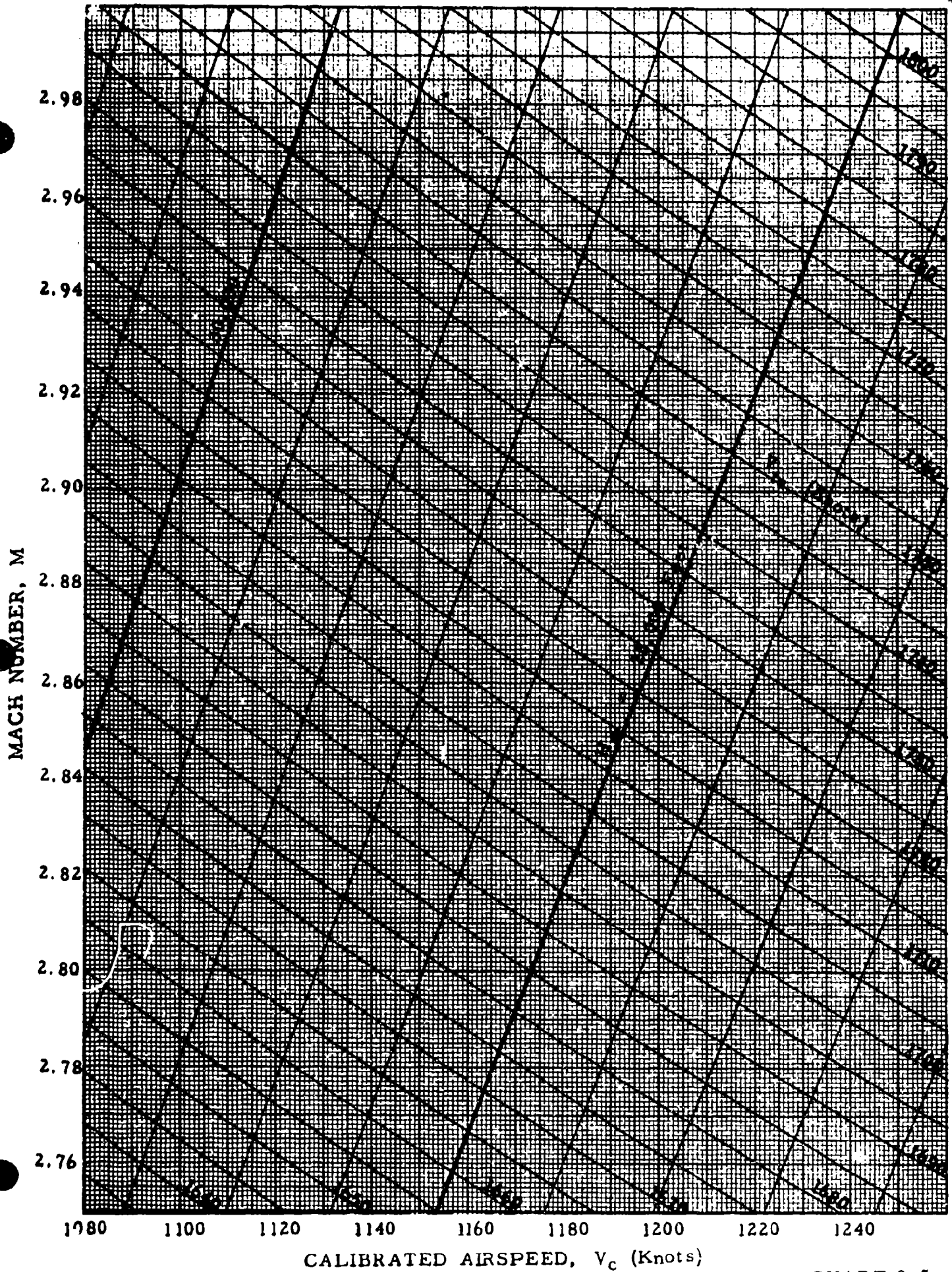
2.98
2.96
2.94
2.92
2.90
2.88
2.86
2.84
2.82
2.80
2.78
2.76

900 920 940 960 980 1000 1020 1040 1060

CALIBRATED AIRSPEED, V_C (Knots)

CHART 8.5





CALIBRATED AIRSPEED, V_c (Knots)

CHART 8.5

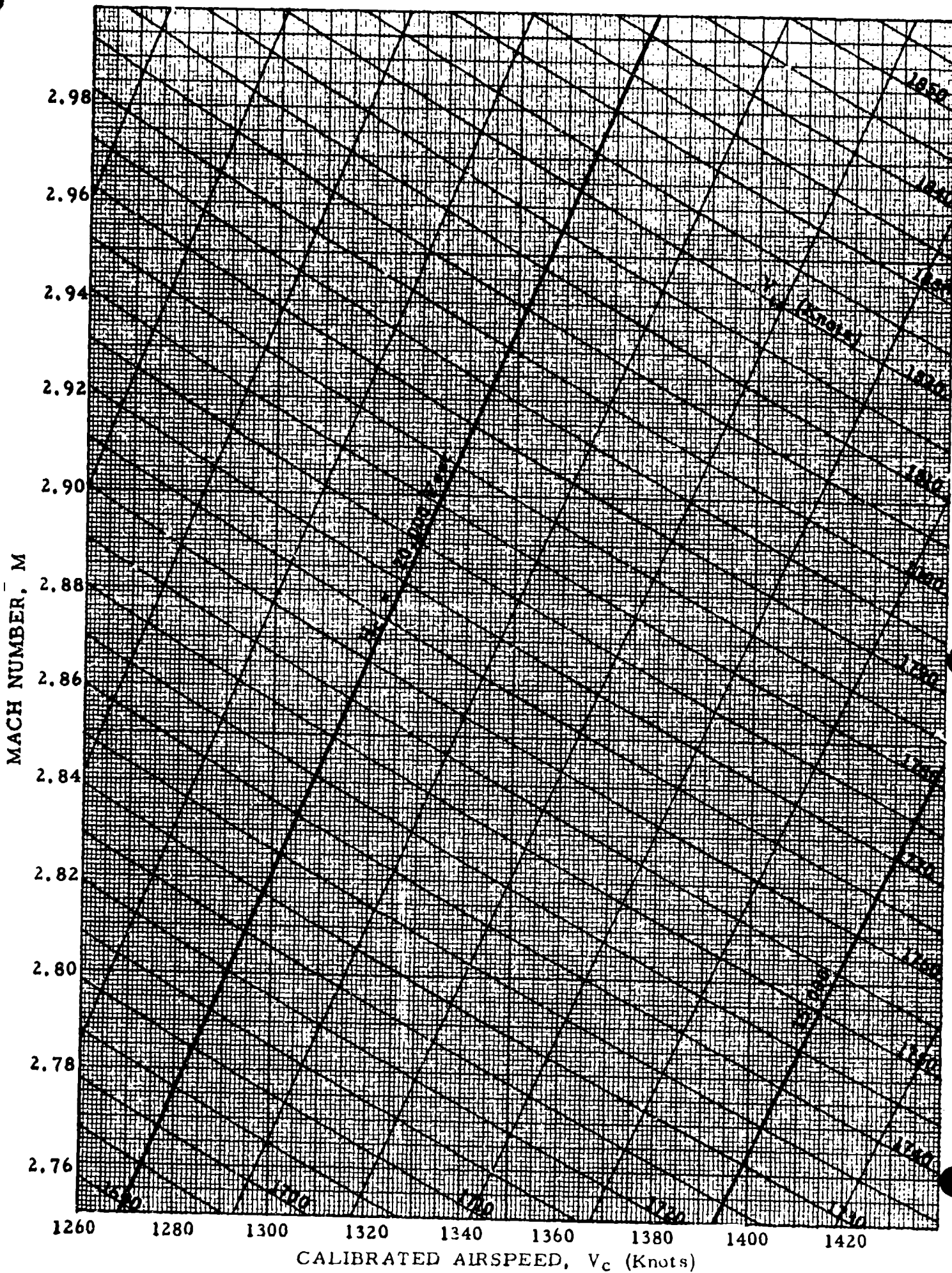
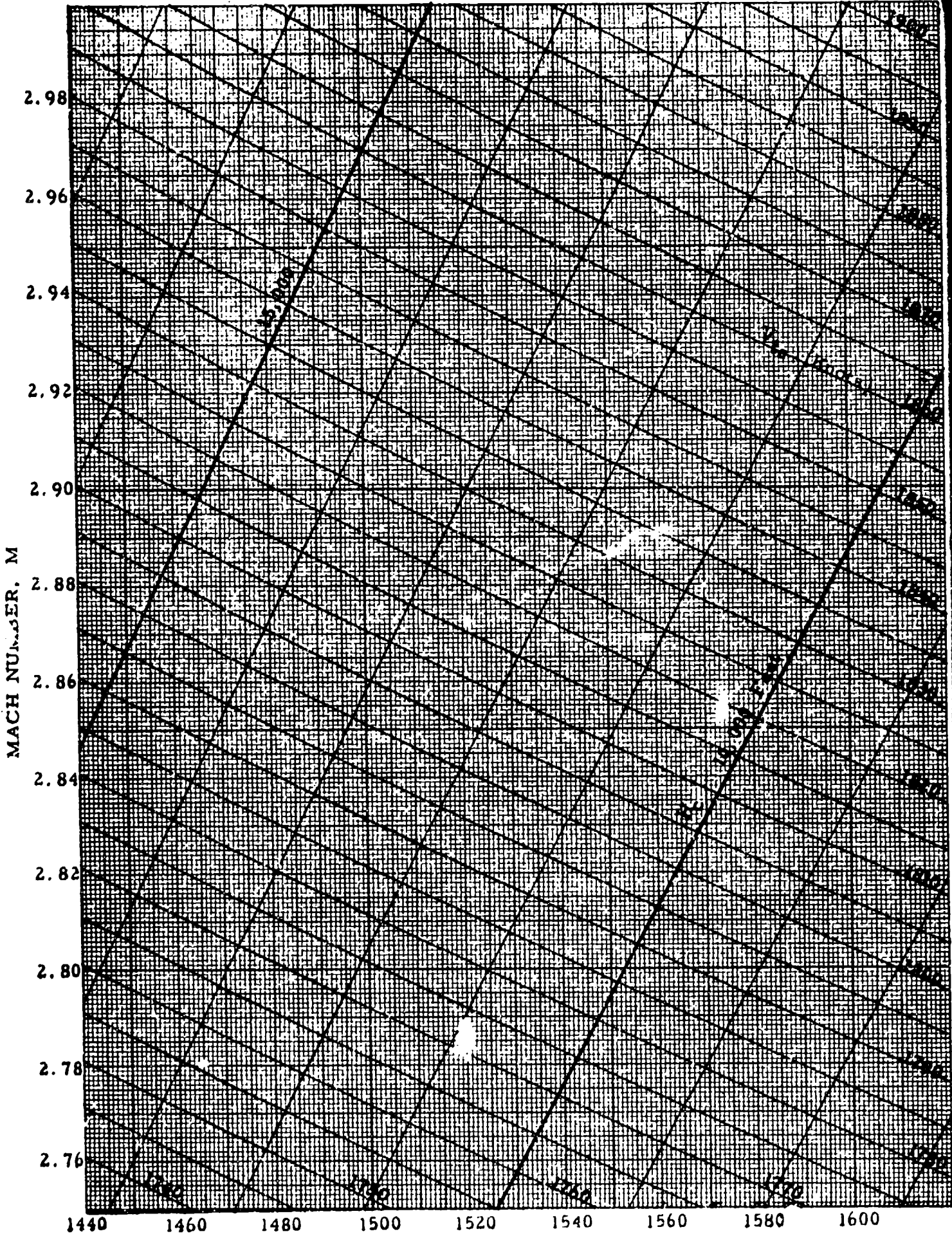


CHART 8.5



CALIBRATED AIRSPEED, V_c (Knots)

8.6 THE CORRECTION OF ALTIMETER AND/OR AIRSPEED INDICATOR READINGS FOR PRESSURE LAG ERROR

CHART 8.61

(See paragraph 4.2.1)

LAG CONSTANT RATIO, $\lambda_{H_{ic}} / \lambda_{SL}$ versus INDICATED PRESSURE ALTITUDE CORRECTED FOR INSTRUMENT ERROR, H_{ic} (Thousands of Feet) for INDICATED AIRSPEED CORRECTED FOR INSTRUMENT ERROR, V_{ic} (Knots) = CONSTANT

$$\frac{\lambda_{H_{ic}}}{\lambda_{SL}} = \frac{\mu_{H_{ic}}}{\mu_{SL}} \frac{P_{aSL}}{P_s + q_{cic}}$$

CHART 8.62

(See paragraph 4.2.1)

LAG CONSTANT TEMPERATURE CORRECTION FACTOR, $\lambda / \lambda_{H_{ic}}$ versus INDICATED PRESSURE ALTITUDE CORRECTED FOR INSTRUMENT ERROR, H_{ic} (Thousands of Feet) for TEST DAY ATMOSPHERIC TEMPERATURE, t_{at} ($^{\circ}C$) = CONSTANT

$$\frac{\lambda}{\lambda_{H_{ic}}} = \frac{T_{at}}{T_{as}}$$

where T_{as} corresponds to H_{ic} .

CHART 8.63

(See paragraph 4.2.2)

AIRSPED INDICATOR LAG FACTOR, $F_1(H_{ic}, V_{ic})$ versus INDICATED AIRSPED CORRECTED FOR INSTRUMENT ERROR, V_{ic} (Knots) for INDICATED PRESSURE ALTITUDE CORRECTED FOR INSTRUMENT ERROR, H_{ic} (Feet) = CONSTANT, and dH_{ic}/dt in feet per minute.

$$F_1(H_{ic}, V_{ic}) = \frac{G \sigma_s}{2.84869 V_{ic} \left[1 + 0.2 \left(\frac{V_{ic}}{a_{SL}} \right)^2 \right]^{2.5}} \quad V_{ic} \leq a_{SL}$$

$$F_1(H_{ic}, V_{ic}) = G \rho_s \frac{\left[7 \left(\frac{V_{ic}}{a_{SL}} \right)^2 - 1 \right]^{3.5}}{3738.11 \left(\frac{V_{ic}}{a_{SL}} \right)^6 \left[2 \left(\frac{V_{ic}}{a_{SL}} \right)^2 - 1 \right]} \quad V_{ic} \geq a_{SL}$$

where σ_s and ρ_s correspond to H_{ic}

ALTIMETER

$$\Delta H_{icl} = \frac{\lambda_s}{60} \frac{dH_{ic}}{dt} \quad 4.24$$

where

$$\lambda_s = \lambda_{sSL} \frac{\lambda_{sH_{ic}}}{\lambda_{sSL}} \frac{\lambda_s}{\lambda_{sH_{ic}}} \quad 4.21$$

and dH_{ic}/dt = feet/minute

λ_{sSL} = seconds

$\lambda_{sH_{ic}}/\lambda_{sSL}$ from Chart 8.61 for H_{ic}, V_{ic} = STATIC

$\lambda_s/\lambda_{sH_{ic}}$ from Chart 8.62 for H_{ic} , t_{at} ($^{\circ}C$)

AIRSPEED INDICATOR

$$\Delta V_{icl} = \lambda_t \frac{dV_{ic}}{dt} + \frac{(\lambda_s - \lambda_t)}{60} F_1(H_{ic}, V_{ic}) \frac{dH_{ic}}{dt} \quad 4.43$$

where

$$\lambda_s = \lambda_{sSL} \frac{\lambda_s H_{ic}}{\lambda_{sSL}} \frac{\lambda_s}{\lambda_s H_{ic}} \quad 4.21$$

$$\lambda_t = \lambda_{tSL} \frac{\lambda_t H_{ic}}{\lambda_{tSL}} \frac{\lambda_t}{\lambda_t H_{ic}} \quad 4.40$$

and $dV_{ic}/dt = \text{knots/second}$

$dH_{ic}/dt = \text{feet/minute}$

λ_{tSL} and $\lambda_{sSL} = \text{seconds}$

$\lambda_{sH_{ic}}/\lambda_{sSL}$ from Chart 8.61 for H_{ic} , $V_{ic} = \text{STATIC}$

$\lambda_{tH_{ic}}/\lambda_{tSL}$ from Chart 8.61 for H_{ic} , V_{ic}

$\lambda/\lambda_{H_{ic}}$ from Chart 8.62 for H_{ic} , t_{at} ($^{\circ}C$)

$F_1(H_{ic}, V_{ic})$ from Chart 8.63 for H_{ic} , V_{ic}

Example:

Given: $\lambda_{sSL} = 0.60$; $\lambda_{tSL} = 0.10$

$V_{ic} = 800 \text{ knots}$; $H_{ic} = 30,000 \text{ feet}$; $t_{at} = -30^{\circ}C$

$\frac{dV_{ic}}{dt} = 3 \text{ knots/second}$; $\frac{dH_{ic}}{dt} = 10,000 \text{ feet/minute}$

Required: ΔH_{icl} and ΔV_{icl}

Solution: From Chart 8.61 for $H_{ic} = 30,000$ feet, $V_{ic} = \text{STATIC}$

$$\frac{\lambda_s H_{ic}}{\lambda_s SL} = 2.80$$

From Chart 8.61 for $H_{ic} = 30,000$ feet, $V_{ic} = 800$ knots

$$\frac{\lambda_t H_{ic}}{\lambda_t SL} = 0.50$$

From Chart 8.62 for $H_{ic} = 30,000$ feet; $t_{at} = -30^\circ\text{C}$

$$\frac{\lambda}{\lambda_{H_{ic}}} = 1.063$$

From equation 4.21

$$\lambda_s = 0.60 (2.80) (1.063) = 1.786$$

From equation 4.40

$$\lambda_t = 0.10 (0.50) (1.063) = 0.053$$

From equation 4.24 for $dH_{ic}/dt = 10,000$ feet/minute

$$\Delta H_{icl} = \frac{1.786}{60} (10,000) = 298 \text{ feet}$$

From Chart 8.63 for $H_{ic} = 30,000$ feet, $V_{ic} = 800$ knots

$$F_1 (H_{ic}, V_{ic}) = 0.0030$$

From equation 4.43 for $dV_{ic}/dt = 3$ knots/second,

$$dH_{ic}/dt = 10,000 \text{ feet/minute}$$

$$\Delta V_{icl} = 0.053 (3) + \frac{(1.786 - 0.053)}{60} (.0030) 10,000$$

$$= 0.159 + 0.866 = 1.025 \text{ knots}$$

$\lambda_{H_{ic}} / \lambda_{SL}$

22
20
18
16
14
12
10
8
6
4
2
0

SL 10 20 30 40 50 60 70 80

INDICATED PRESSURE ALTITUDE, H_{ic} (Thousands of Feet)

$\gamma_{ic} = 0$ (Static)

100 Knots

150

200

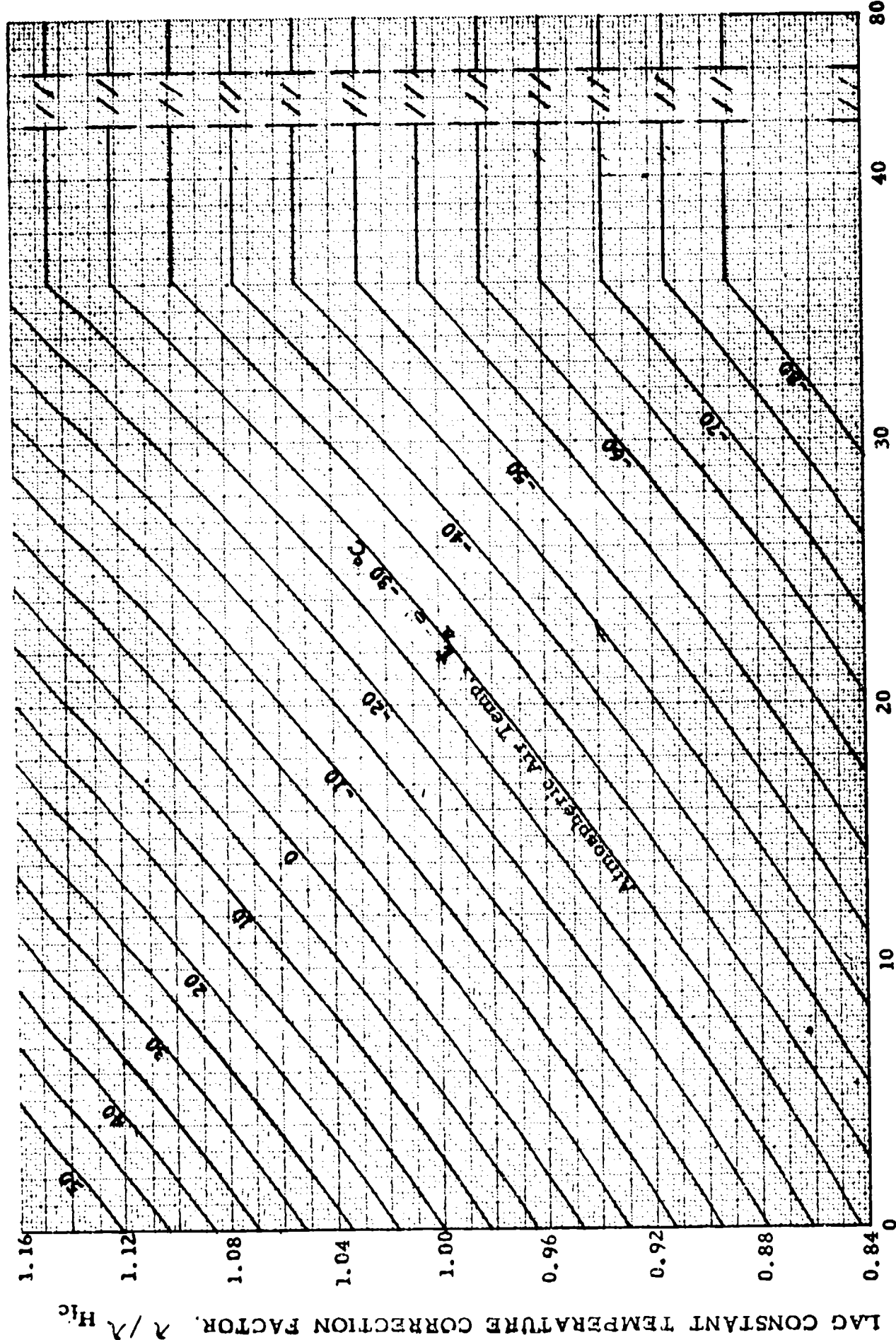
250

300

400

500

600



INDICATED PRESSURE ALTITUDE, H_{ic} (Thousands of Feet)

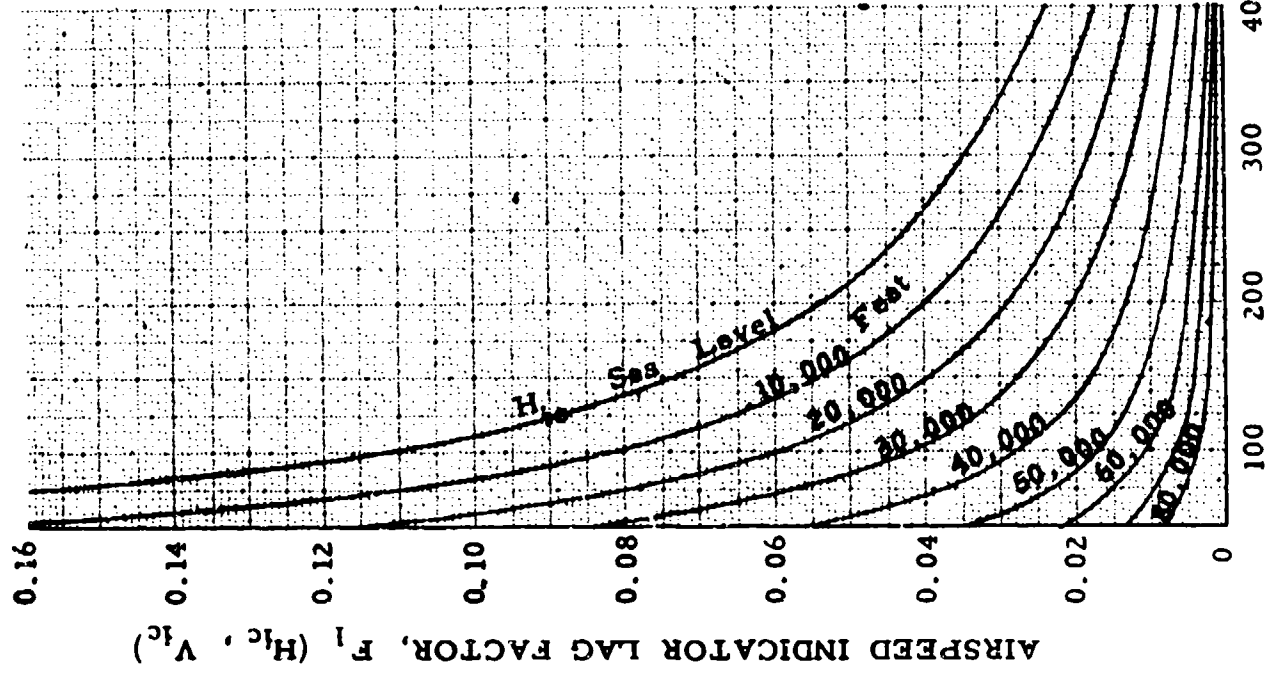
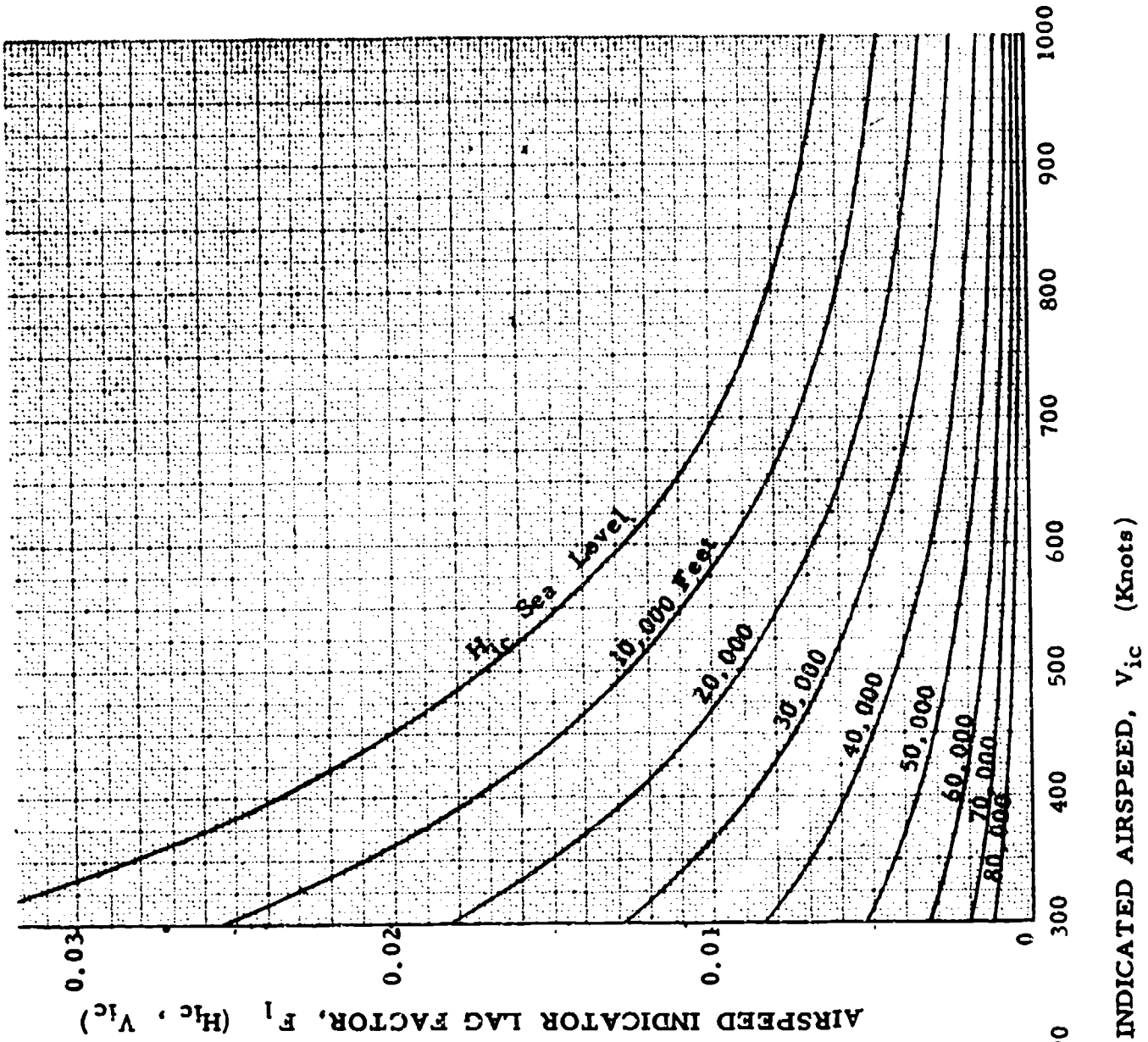


CHART 8.63

CHART 8.7

(See paragraph 5.3.1)

INDICATED PRESSURE ALTITUDE CORRECTED for INSTRUMENT ERROR, H_{ic} (Thousands of Feet) versus $\Delta P_p / \Delta H_{pc}$, ("Hg/Feet) for ΔH_{pc} (Feet) = CONSTANT

$$\frac{\Delta P_p}{\Delta H_{pc}} = 0.0010813 \sigma_3, \text{ "Hg/feet}$$

where σ_3 is measured at $(H_{ic} + \frac{\Delta H_{pc}}{2})$

Example:

Given: $H_{ic} = 35,000$ feet; $\Delta H_{pc} = +2000$ feet

Required: ΔP_p in "Hg

Solution: Use Page 2 of Chart 8.7. For the given conditions,

$$\frac{\Delta P_p}{\Delta H_{pc}} = 0.000322 \text{ "Hg/feet}$$

$$\Delta P_p = \frac{\Delta P_p}{\Delta H_{pc}} \Delta H_{pc} = +0.644 \text{ "Hg}$$

INDICATED PRESSURE ALTITUDE, H_{ic} (Thousands of Feet)

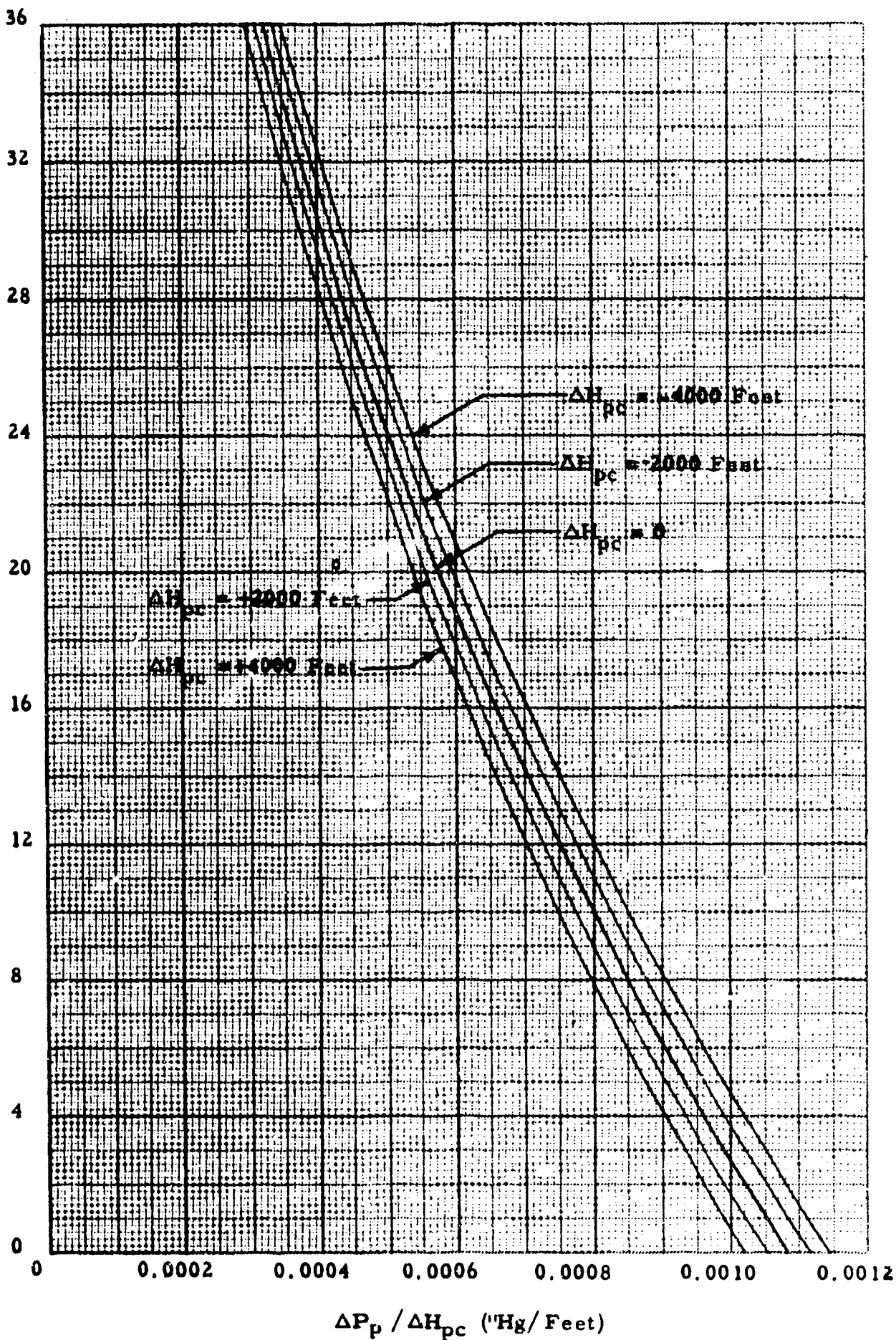


CHART 8.7

INDICATED PRESSURE ALTITUDE. H_{ic} (Thousands of Feet)

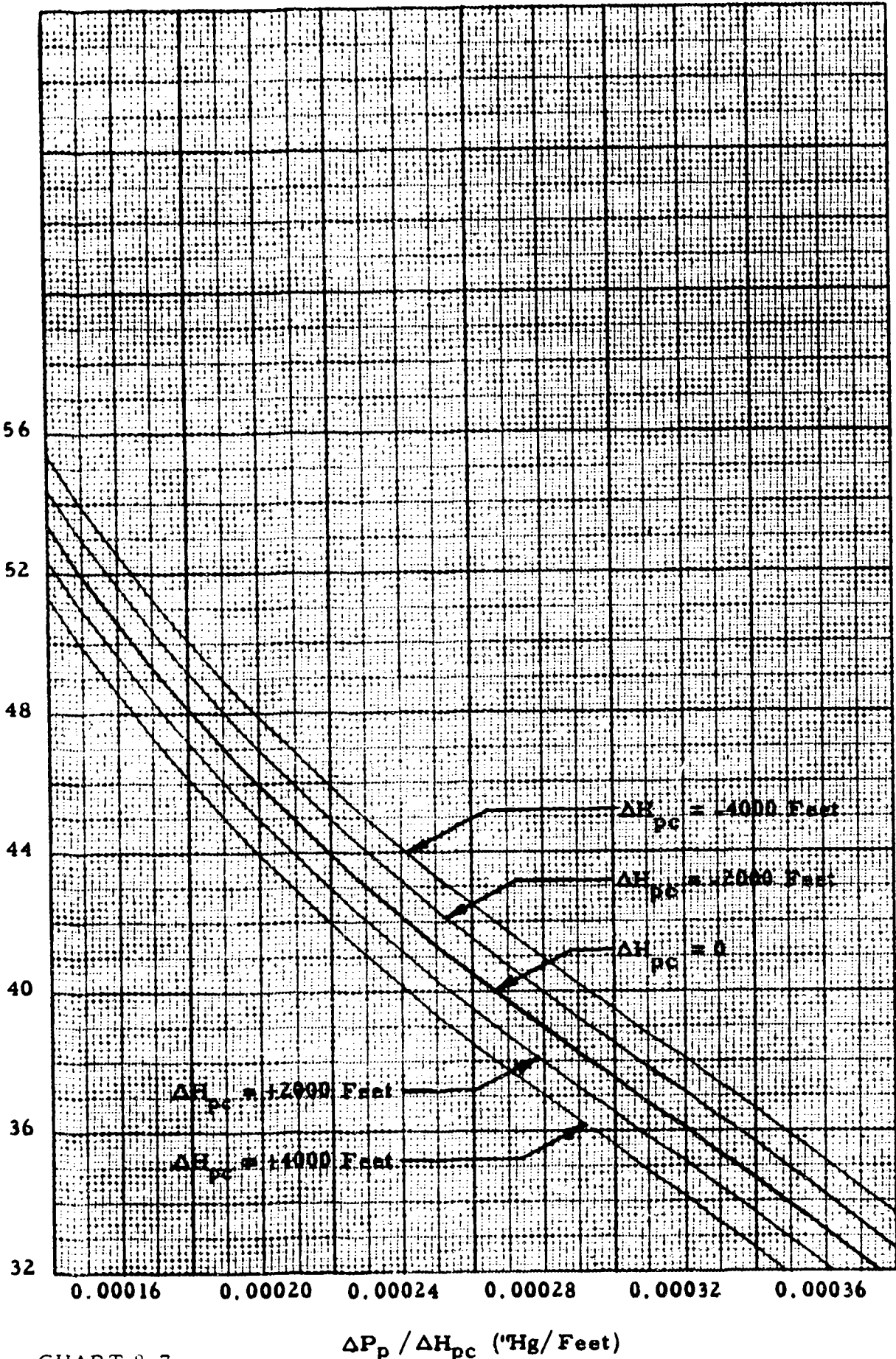


CHART 8.7

$\Delta P_p / \Delta H_{pc}$ ("Hg/ Feet)

INDICATED PRESSURE ALTITUDE, H_{ic} (Thousands of Feet)

80
76
72
68
64
60
56
52

0.00002 0.00004 0.00006 0.00008 0.00010 0.00012 0.00014

$\Delta P_p / \Delta H_{pc}$ ('Hg/ Feet)

$\Delta H_{pc} = -4000$ Feet

$\Delta H_{pc} = -2000$ Feet

$\Delta H_{pc} = 0$

$\Delta H_{pc} = +2000$ Feet

$\Delta H_{pc} = +4000$ Feet

CHART 8.7

CHART 8.8
(See paragraph 5.3.1)

INDICATED PRESSURE ALTITUDE CORRECTED for INSTRUMENT ERROR, H_{ic} (Thousands of Feet) versus $\Delta P_p / \Delta H_{pc}$, ("Hg/Feet) for ΔP_p , ("Hg) = CONSTANT

$$\frac{\Delta P_p}{\Delta H_{pc}} = 0.0010813 \sigma_z, \text{ "Hg/feet}$$

where σ_z is measured at $(H_{ic} + \frac{\Delta H_{pc}}{2})$

Example:

Given: $H_{ic} = 52,000$ feet; $\Delta P_p = -0.50$ "Hg

Required: ΔH_{pc} in feet

Solution: Use Page 2 of Chart 8.8. For the given conditions,

$$\begin{aligned} \frac{\Delta P_p}{\Delta H_{pc}} &= 0.000162 \\ \Delta H_{pc} &= \frac{\Delta P_p}{\left(\frac{\Delta P_p}{\Delta H_{pc}} \right)} = 3090 \text{ feet} \end{aligned}$$

INDICATED PRESSURE ALTITUDE, H_{ic} (Thousands of Feet)

36
32
28
24
20
16
12
8
4
0

0.0003 0.0004 0.0005 0.0006 0.0007 0.0008 0.0009 0.0010 0.0011

$\Delta P_p / \Delta H_{pc}$ ("Hg/Feet)

$\Delta P_p = +2.0$ "Hg

$\Delta P_p = +4.0$ "Hg

$\Delta P_p = -4.0$ "Hg

$\Delta P_p = -2.0$ "Hg

$\Delta P_p = 0$

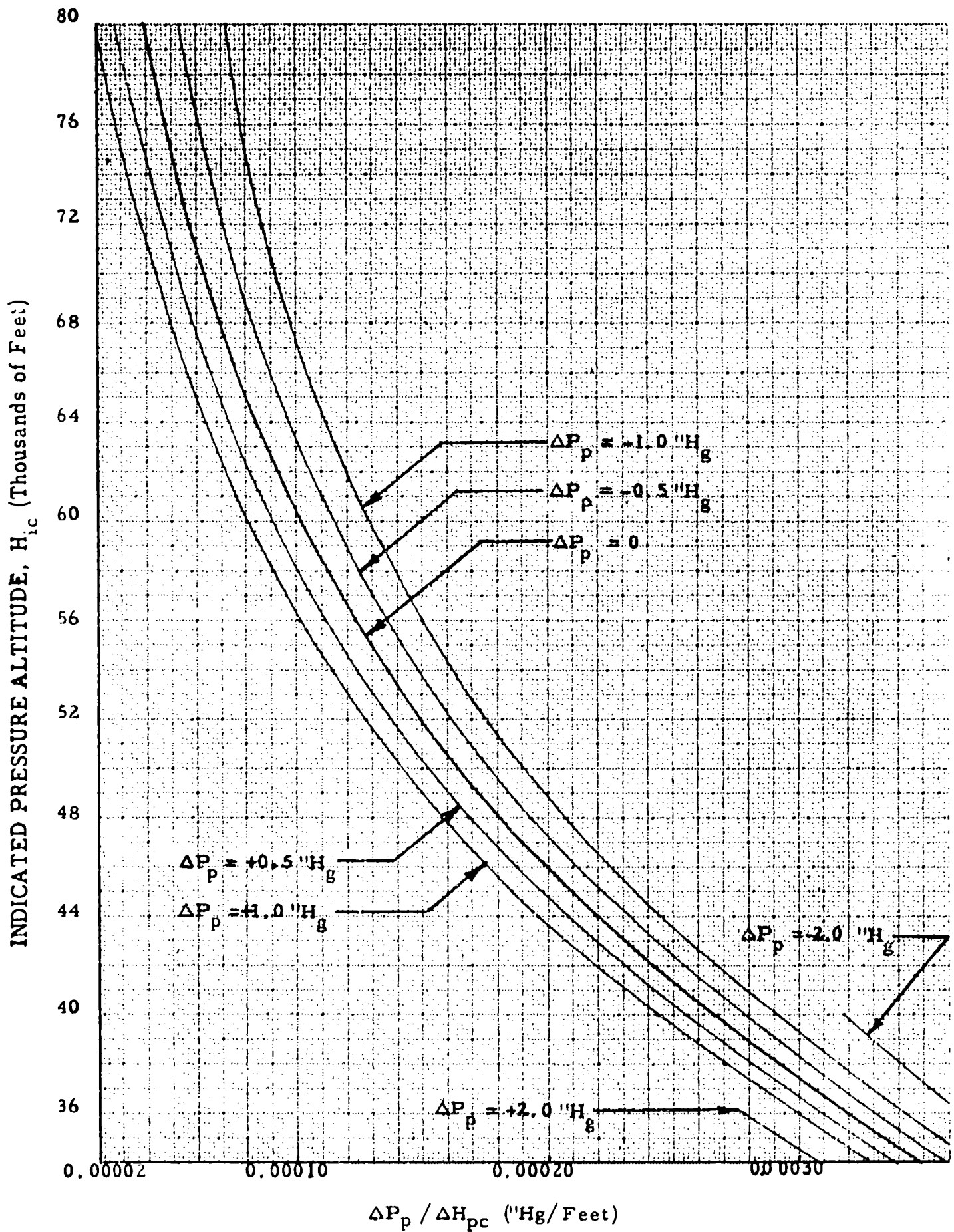


CHART 8.8

CHART 8.9

(See paragraph 5.3.2)

INDICATED AIRSPEED CORRECTED for INSTRUMENT ERROR,

V_{ic} (Knots) versus $\Delta P_p / \Delta V_{pc}$ ("Hg/Knot) for ΔV_{pc} (Knots) = CONSTANT

$$\frac{\Delta P_p}{\Delta V_{pc}} = \frac{1.4 P_{aSL}}{a_{SL}} \left(\frac{V_{ic}}{a_{SL}} \right) \left[1 + 0.2 \left(\frac{V_{ic}}{a_{SL}} \right)^2 \right]^{2.5} \quad V_{ic} \leq a_{SL}$$

$$+ \frac{0.7 P_{aSL}}{a_{SL}} \left[1 + 0.2 \left(\frac{V_{ic}}{a_{SL}} \right)^2 \right]^{1.5} \left[1 + 1.2 \left(\frac{V_{ic}}{a_{SL}} \right)^2 \right] \frac{\Delta V_{pc}}{a_{SL}}$$

$$\frac{\Delta P_p}{\Delta V_{pc}} = 52,854 \left(\frac{V_{ic}}{a_{SL}} \right)^6 \frac{\left[2 \left(\frac{V_{ic}}{a_{SL}} \right)^2 - 1 \right]}{\left[7 \left(\frac{V_{ic}}{a_{SL}} \right)^2 - 1 \right]^{3.5}} \quad V_{ic} \geq a_{SL}$$

$$+ 52,854 \left(\frac{V_{ic}}{a_{SL}} \right)^5 \frac{\left[7 \left(\frac{V_{ic}}{a_{SL}} \right)^4 - 4.5 \left(\frac{V_{ic}}{a_{SL}} \right)^2 + 3 \right]}{\left[7 \left(\frac{V_{ic}}{a_{SL}} \right)^2 - 1 \right]^{4.5}} \frac{\Delta V_{pc}}{a_{SL}}$$

where $P_{aSL} = 29.92126$ "Hg, $a_{SL} = 661.48$ knots

Example:

Given: $V_{ic} = 300$ knots; $\Delta V_{pc} = -20$ knots

Required: ΔP_p in "Hg

Solution: For the given conditions,

$$\frac{\Delta P_p}{\Delta V_{pc}} = 0.0305 \text{ "Hg/knot}$$

$$\Delta P_p = \frac{\Delta P_p}{\Delta V_{pc}} \Delta V_{pc} = -0.610 \text{ "Hg}$$

INDICATED AIRSPEED, V_{ic} (Knots)

1000
900
800
700
600
500
400
300
200
100
0

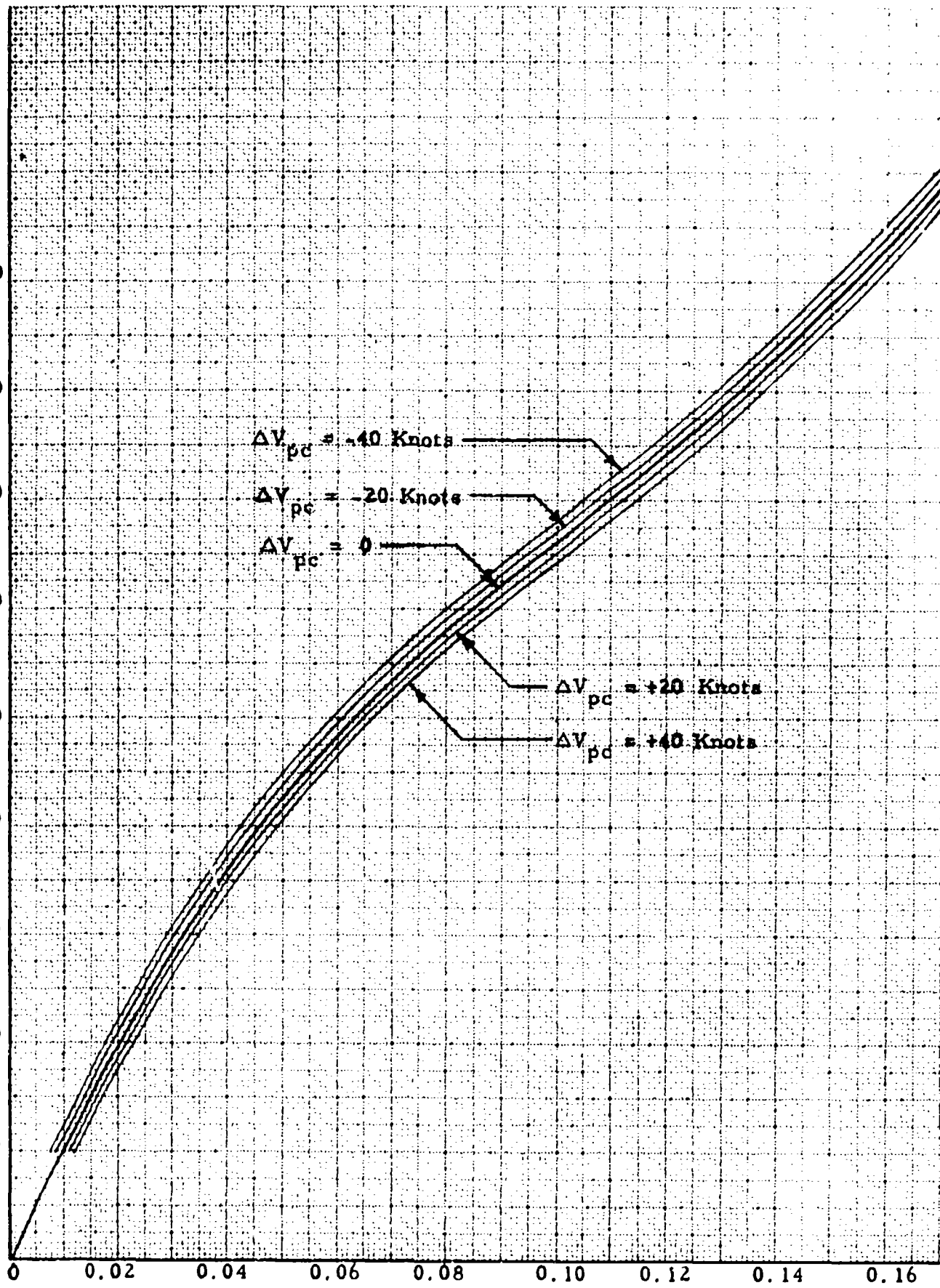


CHART 8.9

$\Delta P_p / \Delta V_{pc}$ ('Hg/ Knot)

CHART 8.10
(See paragraph 5.3.2)

INDICATED AIRSPEED CORRECTED FOR INSTRUMENT ERROR,
 V_{ic} (Knots) versus $\Delta P_p / \Delta V_{pc}$ ("Hg/Knot) for ΔP_p ("Hg) = CONSTANT

$$\frac{\Delta P_p}{\Delta V_{pc}} = \frac{1.4 P_{aSL}}{a_{SL}} \left(\frac{V_{ic}}{a_{SL}} \right) \left[1 + 0.2 \left(\frac{V_{ic}}{a_{SL}} \right)^2 \right]^{2.5} \quad V_{ic} \leq a_{SL}$$

$$+ \frac{0.7 P_{aSL}}{a_{SL}} \left[1 + 0.2 \left(\frac{V_{ic}}{a_{SL}} \right)^2 \right]^{1.5} \left[1 + 1.2 \left(\frac{V_{ic}}{a_{SL}} \right)^2 \right] \frac{\Delta V_{pc}}{a_{SL}}$$

$$\frac{\Delta P_p}{\Delta V_{pc}} = 52.854 \left(\frac{V_{ic}}{a_{SL}} \right)^6 \frac{\left[2 \left(\frac{V_{ic}}{a_{SL}} \right)^2 - 1 \right]}{\left[7 \left(\frac{V_{ic}}{a_{SL}} \right)^2 - 1 \right]^{3.5}} \quad V_{ic} \geq a_{SL}$$

$$+ 52.854 \left(\frac{V_{ic}}{a_{SL}} \right)^5 \frac{\left[7 \left(\frac{V_{ic}}{a_{SL}} \right)^4 - 4.5 \left(\frac{V_{ic}}{a_{SL}} \right)^2 + 3 \right]}{\left[7 \left(\frac{V_{ic}}{a_{SL}} \right)^2 - 1 \right]^{4.5}} \frac{\Delta V_{pc}}{a_{SL}}$$

where $P_{aSL} = 29.92126$ "Hg; $a_{SL} = 661.48$ knots

Example:

Given: $V_{ic} = 550$ knots; $\Delta P_p = +2.0$ "Hg

Required: ΔV_{pc} in knots

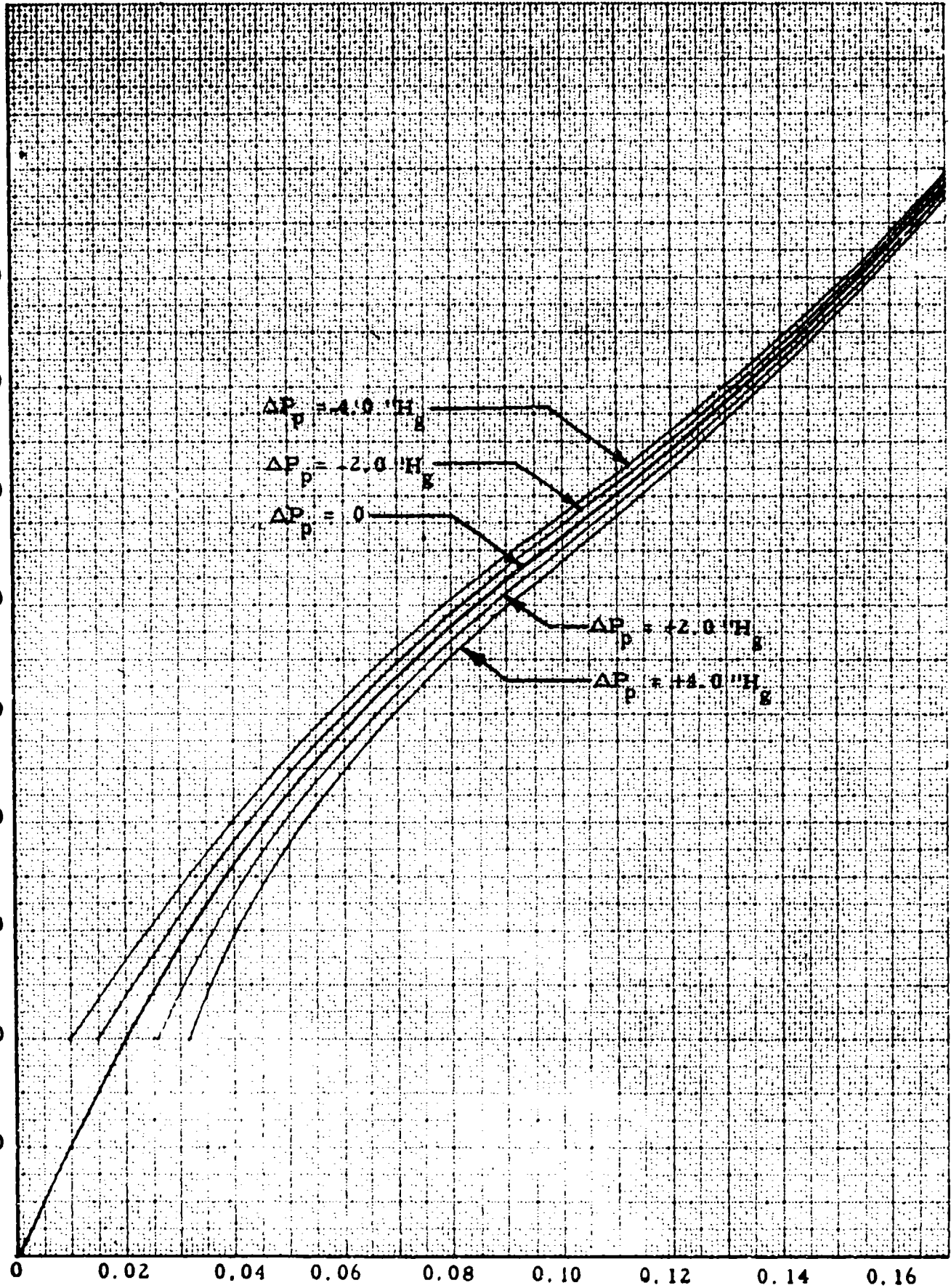
Solution: For the given conditions,

$$\frac{\Delta P_p}{\Delta V_{pc}} = 0.0763$$

$$\Delta V_{pc} = \left(\frac{\Delta P_p / \Delta P_p}{\Delta V_{pc}} \right) = 26.2 \text{ knots}$$

INDICATED AIRSPEED, V_{ic} (Knots)

1000
900
800
700
600
500
400
300
200
100
0



$\Delta P_p / \Delta V_{pc}$ ("Hg/Knot)

CHART 8.10

CHART 8.11

(See paragraph 5.3.3)

AIRSPED POSITION ERROR CORRECTION, ΔV_{pc} (Knots) versus
INDICATED AIRSPEED CORRECTED FOR INSTRUMENT ERROR,
 V_{ic} (Knots) for POSITION ERROR PRESSURE COEFFICIENT, $\Delta P_p/q_{cic}$

For $V_{ic} \leq a_{SL}$,

$$\frac{\Delta P_p}{q_{cic}} = \frac{\left\{ 1.4 \left(\frac{V_{ic}}{a_{SL}} \right) \left[1 + 0.2 \left(\frac{V_{ic}}{a_{SL}} \right)^2 \right]^{2.5} \frac{\Delta V_{pc}}{a_{SL}} \right\} + \left\{ 0.7 \left[1 + 0.2 \left(\frac{V_{ic}}{a_{SL}} \right)^2 \right]^{1.5} \left[1 + 1.2 \left(\frac{V_{ic}}{a_{SL}} \right)^2 \right] \left(\frac{\Delta V_{pc}}{a_{SL}} \right)^2 \right\}}{\left[1 + 0.2 \left(\frac{V_{ic}}{a_{SL}} \right)^2 \right]^{3.5} - 1}$$

For $V_{ic} \geq a_{SL}$,

$$\frac{\Delta P_p}{q_{cic}} = \frac{7 \left(\frac{V_{ic}}{a_{SL}} \right) \frac{\left[2 \left(\frac{V_{ic}}{a_{SL}} \right)^2 - 1 \right]}{\left[7 \left(\frac{V_{ic}}{a_{SL}} \right)^2 - 1 \right]} \frac{\Delta V_{pc}}{a_{SL}} + 7 \frac{\left[7 \left(\frac{V_{ic}}{a_{SL}} \right)^4 - 4.5 \left(\frac{V_{ic}}{a_{SL}} \right)^2 + 3 \right]}{\left[7 \left(\frac{V_{ic}}{a_{SL}} \right)^2 - 1 \right]^2} \left(\frac{\Delta V_{pc}}{a_{SL}} \right)^2}{\left(\frac{V_{ic}}{a_{SL}} \right)^2 \left[1 - \frac{\left[7 \left(\frac{V_{ic}}{a_{SL}} \right)^2 - 1 \right]^{2.5}}{166.921 \left(\frac{V_{ic}}{a_{SL}} \right)^7} \right]}$$

where $a_{SL} = 661.48$ knots

Example:

Given: $V_{ic} = 700$ knots; $\Delta V_{pc} = -20$ knots

Required: $\Delta P_p/q_{cic}$

Solution: Use Page 2 of Chart 8.11. For the given conditions,

$\Delta P_p/q_{cic} = -0.070$

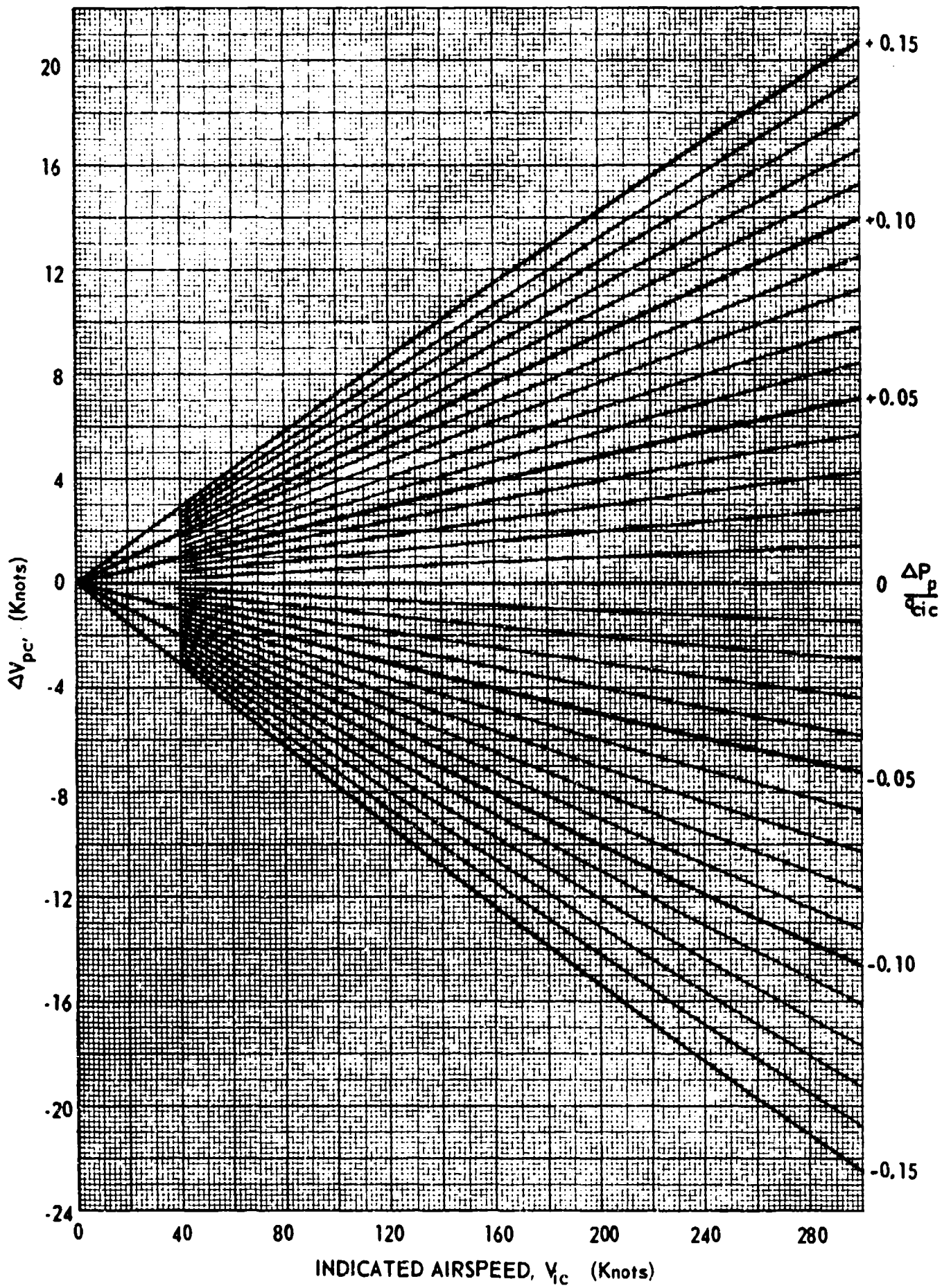
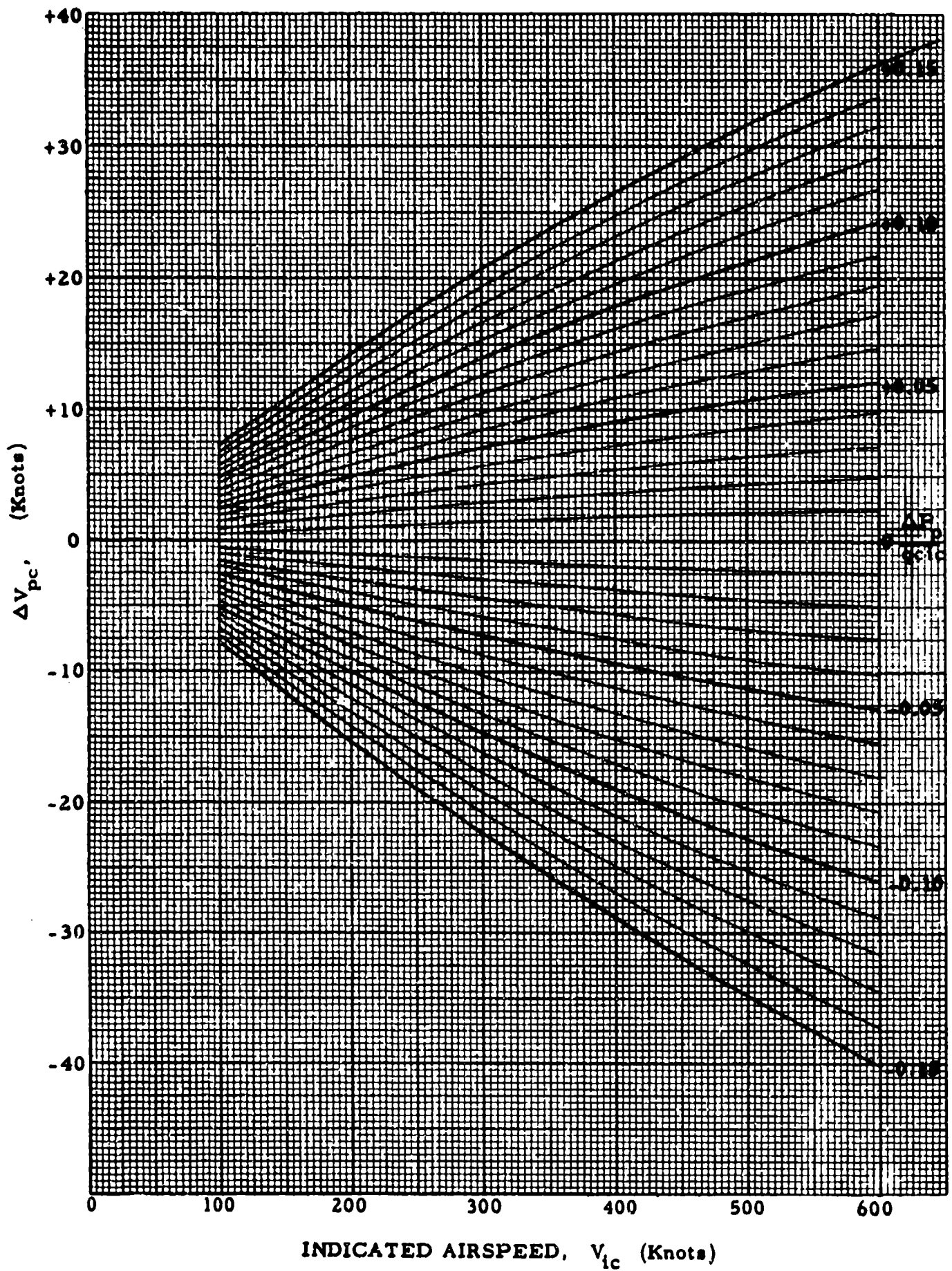


CHART 8.11



INDICATED AIRSPEED, V_{ic} (Knots)

CHART 8.11

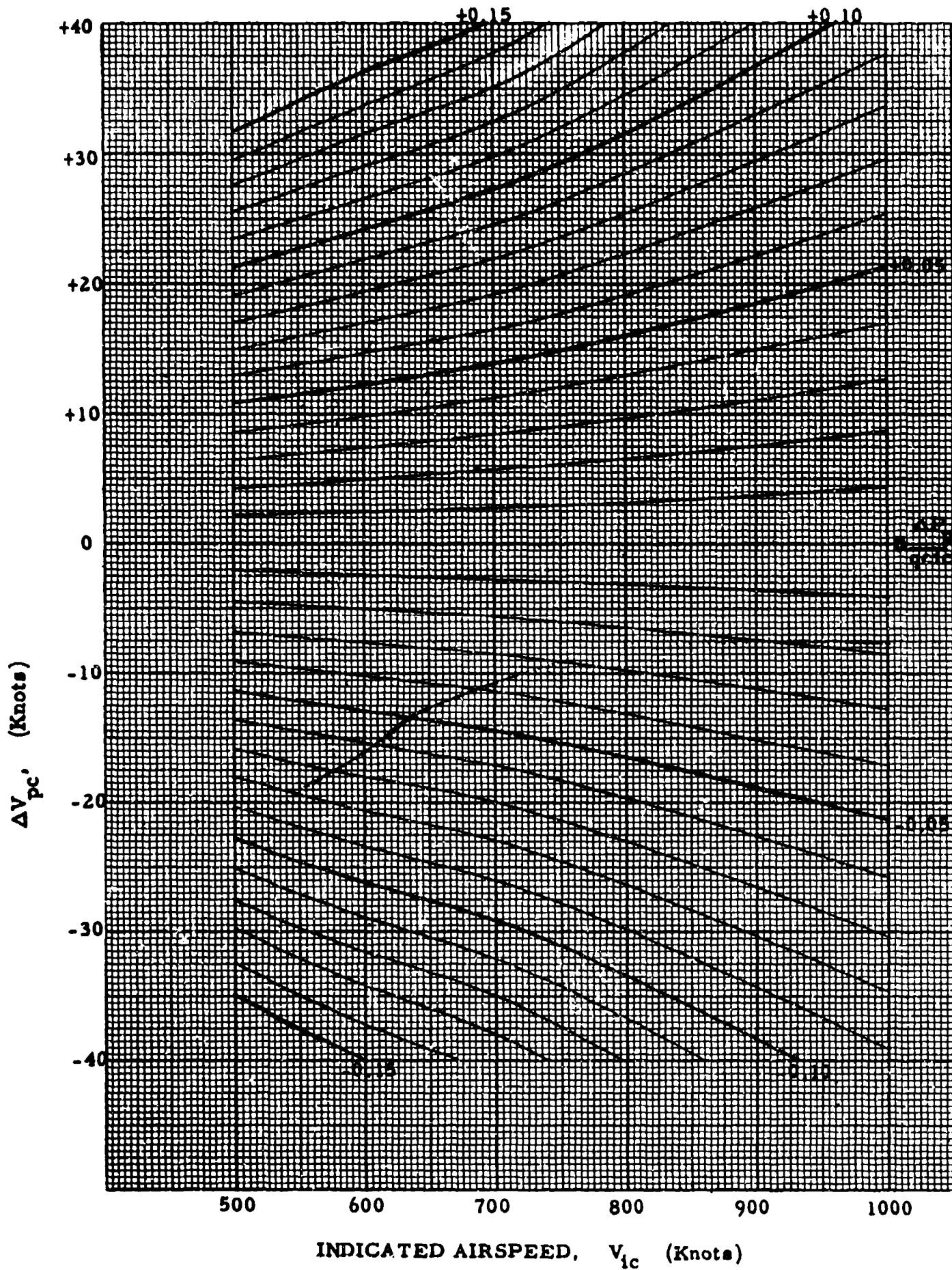


CHART 8.11

CHART 8.12

(See paragraph 5.3.4)

RATIO OF ALTIMETER TO AIRSPEED INDICATOR POSITION ERROR CORRECTIONS, $\Delta H_{pc} / \Delta V_{pc}$ (Feet/Knots) versus INDICATED AIRSPEED CORRECTED FOR INSTRUMENT ERROR, V_{ic} (Knots) for INDICATED PRESSURE ALTITUDE CORRECTED FOR INSTRUMENT ERROR, H_{ic} (Feet) = CONSTANT

$$\frac{\Delta H_{pc}}{\Delta V_{pc}} = \frac{58,566}{\sigma_3} \left(\frac{V_{ic}}{a_{SL}} \right) \left[1 + 0.4 \left(\frac{V_{ic}}{a_{SL}} \right)^2 \right]^{2.5} \quad V_{ic} \leq a_{SL}$$

$$\frac{\Delta H_{pc}}{\Delta V_{pc}} = \frac{48,880}{\sigma_3} \left(\frac{V_{ic}}{a_{SL}} \right)^6 \frac{\left[2 \left(\frac{V_{ic}}{a_{SL}} \right)^2 - 1 \right]}{\left[7 \left(\frac{V_{ic}}{a_{SL}} \right)^2 - 1 \right]}^{3.5} \quad V_{ic} \geq a_{SL}$$

where σ_3 is measured at H_{ic} and $a_{SL} = 661.48$ knots

Note: This curve is valid for small errors only, (say $\Delta H_{pc} < 1000$ feet or $\Delta V_{pc} < 10$ knots). Chart 8.13 should be used for larger errors.

Example:

Given: $H_{ic} = 20,000$ feet; $V_{ic} = 600$ knots; $\Delta H_{pc} = 2000$ feet

Required: ΔV_{pc} in knots

Solution: Use Page 1 of Chart 8.12. For the given conditions,

$$\Delta H_{pc} / \Delta V_{pc} = 147 \text{ feet/knots}$$

$$\Delta V_{pc} = \frac{\Delta H_{pc}}{\Delta H_{pc} / \Delta V_{pc}} = 13.6 \text{ knots}$$

Note: The exact solution is found from Chart 8.13 to be 13.0 knots.

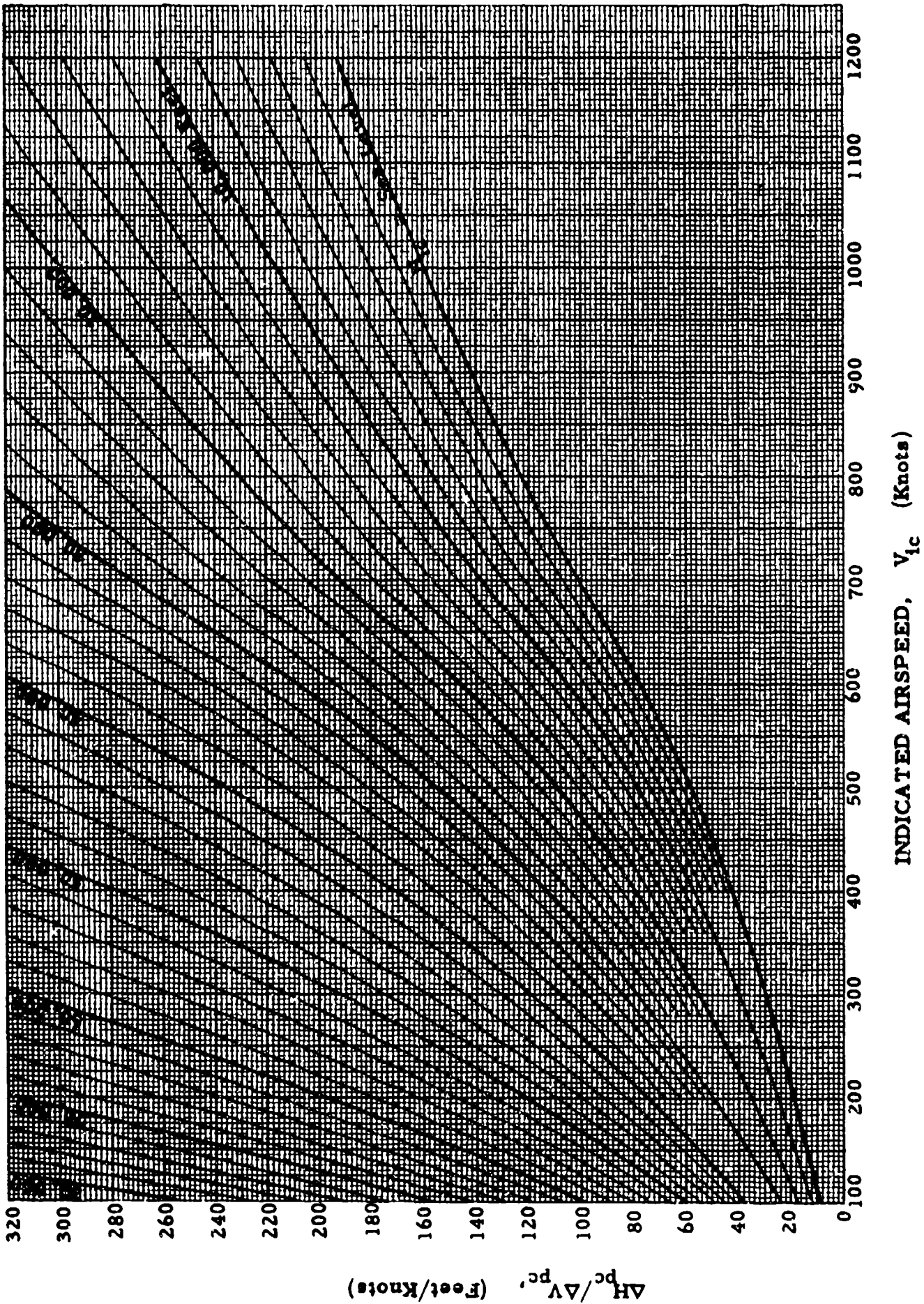
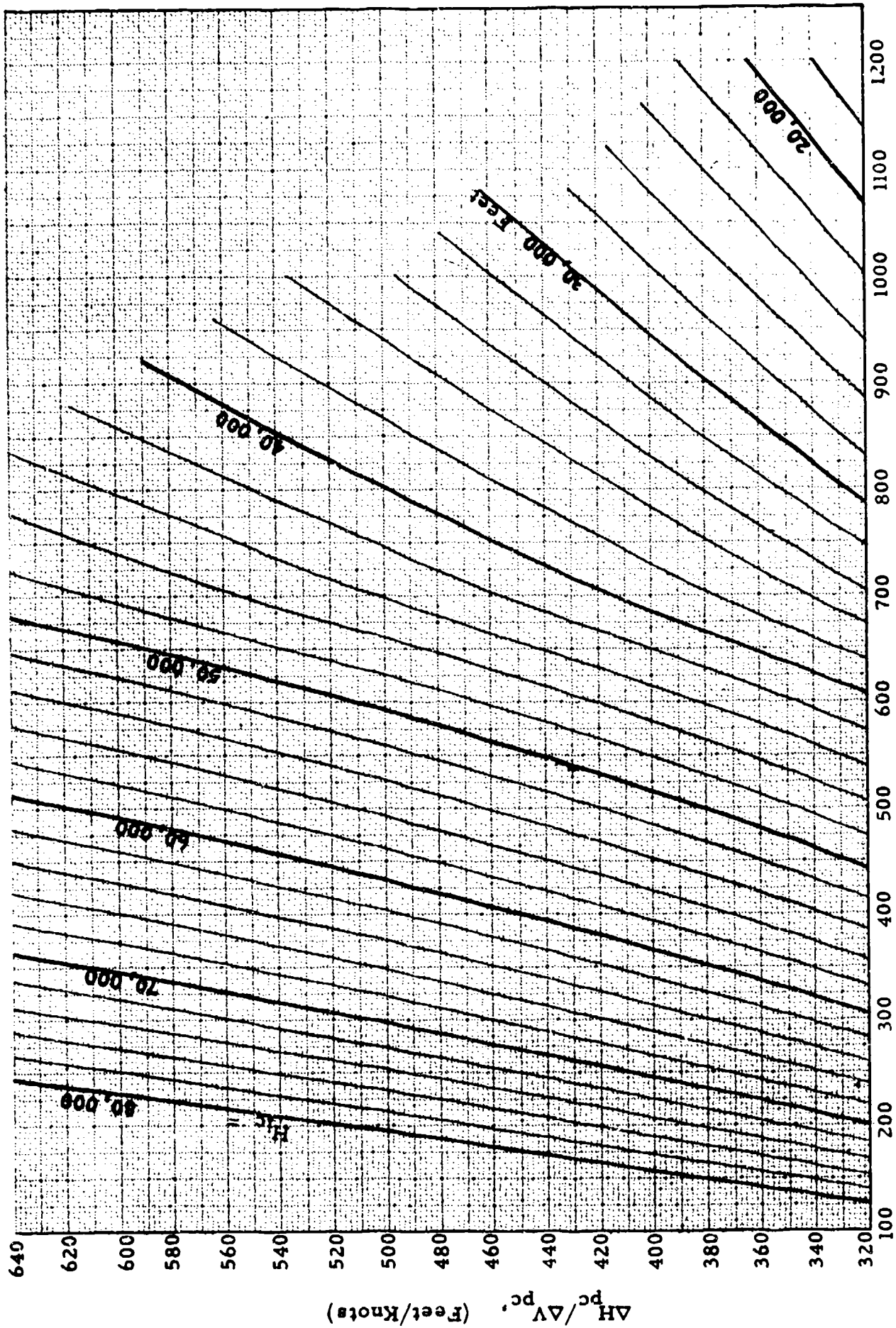


CHART 8.12



INDICATED AIRSPEED, V_{1c} (Knots)

CHART 8.12

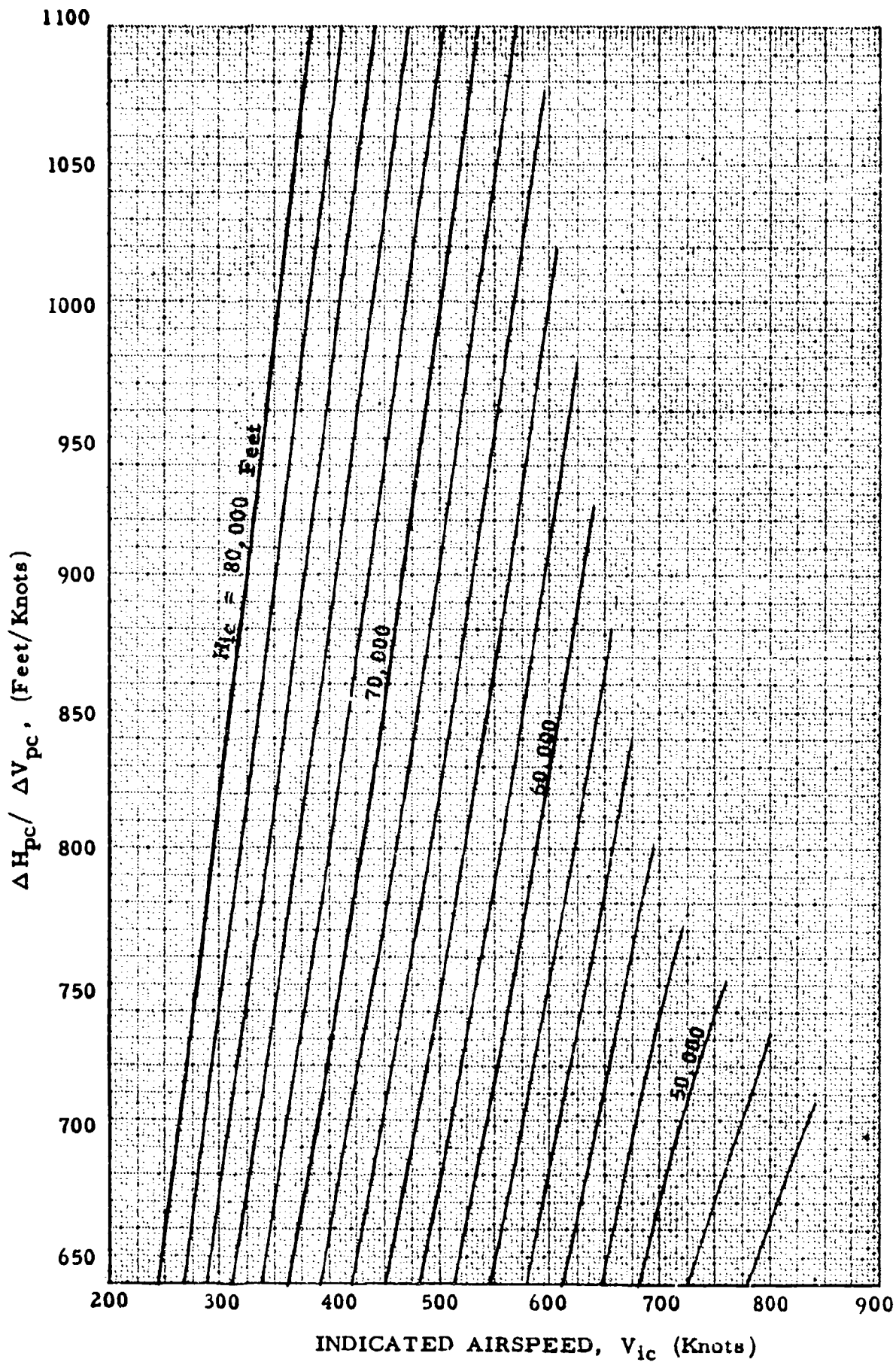


CHART 8.12

CHART 8.13

(See paragraph 5, 3. 4)

AIRSPED POSITION ERROR CORRECTION, ΔV_{pc} (Knots) versus STATIC PRESSURE ERROR, ΔP_p ("Hg) for INDICATED AIRSPEED CORRECTED FOR INSTRUMENT ERROR, V_{ic} (Knots) = CONSTANT

and

ALTIMETER POSITION ERROR CORRECTION, ΔH_{pc} (Feet) versus STATIC PRESSURE ERROR, ΔP_p ("Hg) for INDICATED PRESSURE ALTITUDE CORRECTED FOR INSTRUMENT ERROR, H_{ic} (Feet) = CONSTANT

ALSO

AIRSPED POSITION ERROR CORRECTION, ΔV_{pc} (Knots) versus ALTIMETER POSITION ERROR CORRECTION, ΔH_{pc} (Feet) for INDICATED AIRSPEED CORRECTED FOR INSTRUMENT ERROR, V_{ic} (Knots) = CONSTANT and INDICATED PRESSURE ALTITUDE CORRECTED FOR INSTRUMENT ERROR, H_{ic} (Feet) = CONSTANT

$$\Delta P_p = 0.0010813 \sigma_s \Delta H_{pc}$$

for $V_{ic} \leq a_{SL}$

$$= 1.4 P_{aSL} \left(\frac{V_{ic}}{a_{SL}} \right) \left[1 + 0.2 \left(\frac{V_{ic}}{a_{SL}} \right)^2 \right]^{2.5} \frac{\Delta V_{pc}}{a_{SL}}$$

$$+ 0.7 P_{aSL} \left[1 + 0.2 \left(\frac{V_{ic}}{a_{SL}} \right)^2 \right]^{1.5} \left[1 + 1.2 \left(\frac{V_{ic}}{a_{SL}} \right)^2 \right] \left(\frac{\Delta V_{pc}}{a_{SL}} \right)^2$$

for $V_{ic} \geq a_{SL}$

$$= 7K P_{aSL} \left(\frac{V_{ic}}{a_{SL}} \right)^6 \frac{\left[2 \left(\frac{V_{ic}}{a_{SL}} \right)^2 - 1 \right]}{\left[7 \left(\frac{V_{ic}}{a_{SL}} \right)^2 - 1 \right]^{3.5}} \frac{\Delta V_{pc}}{a_{SL}}$$

$$+ 7K P_{aSL} \left(\frac{V_{ic}}{a_{SL}} \right)^5 \frac{\left[7 \left(\frac{V_{ic}}{a_{SL}} \right)^4 - 4.5 \left(\frac{V_{ic}}{a_{SL}} \right)^2 + 3 \right] \left(\frac{\Delta V_{pc}}{a_{SL}} \right)^2}{\left[7 \left(\frac{V_{ic}}{a_{SL}} \right)^2 - 1 \right]^{4.5}}$$

where $K = 166.921$; $P_{aSL} = 29.92126$ "Hg; $a_{SL} = 661.48$ knots

and σ_s is measured at $H_{ic} + \frac{\Delta H_{pc}}{2}$

Example:

Given: $H_{ic} = 35,000$ feet; $\Delta H_{pc} = +2000$ feet

Required: ΔP_p in "Hg

Solution: Use Page 3 of Chart 8.13 for positive errors.

For the given conditions,

$$\Delta P_p = 0.645 \text{ "Hg}$$

Example 2:

Given: $V_{ic} = 300$ knots; $\Delta V_{pc} = -20$ knots

Required: ΔP_p in "Hg

Solution: Use Page 4 of Chart 8.13 for negative errors

For the given conditions

$$\Delta P_p = -0.610 \text{ "Hg}$$

Example 3:

Given: $V_{ic} = 400$ knots; $H_{ic} = 30,000$ feet; $\Delta V_{pc} = +20$ knots

Required: ΔH_{pc} in feet

Solution: Use Page 3 of Chart 8.13 for positive errors.

For the given conditions,

$$\Delta H_{pc} = +2440 \text{ feet}$$

Note: The approximate solution is found from Chart 8.12 to be

$$\Delta H_{pc} = 2260 \text{ feet.}$$

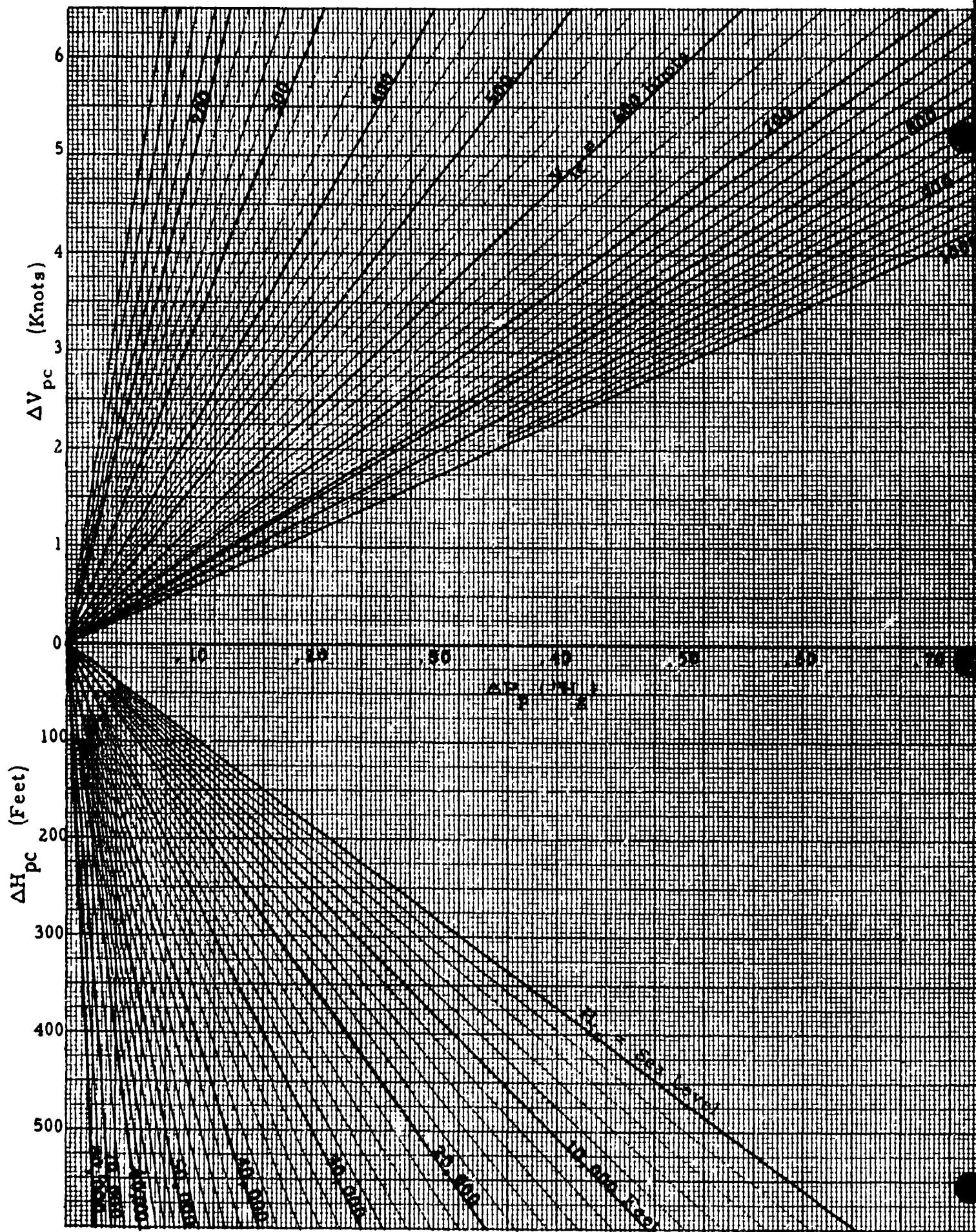
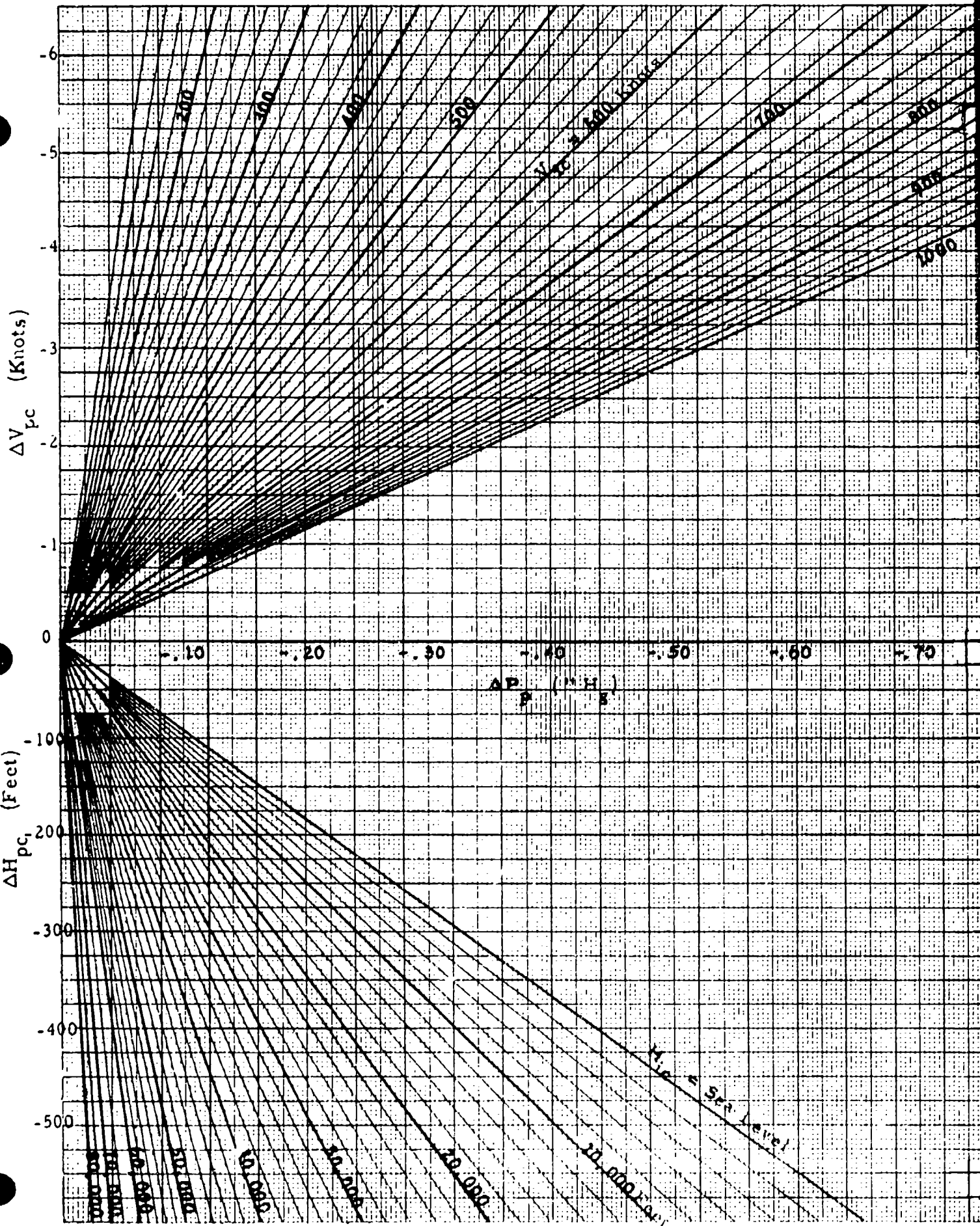


CHART 8.13



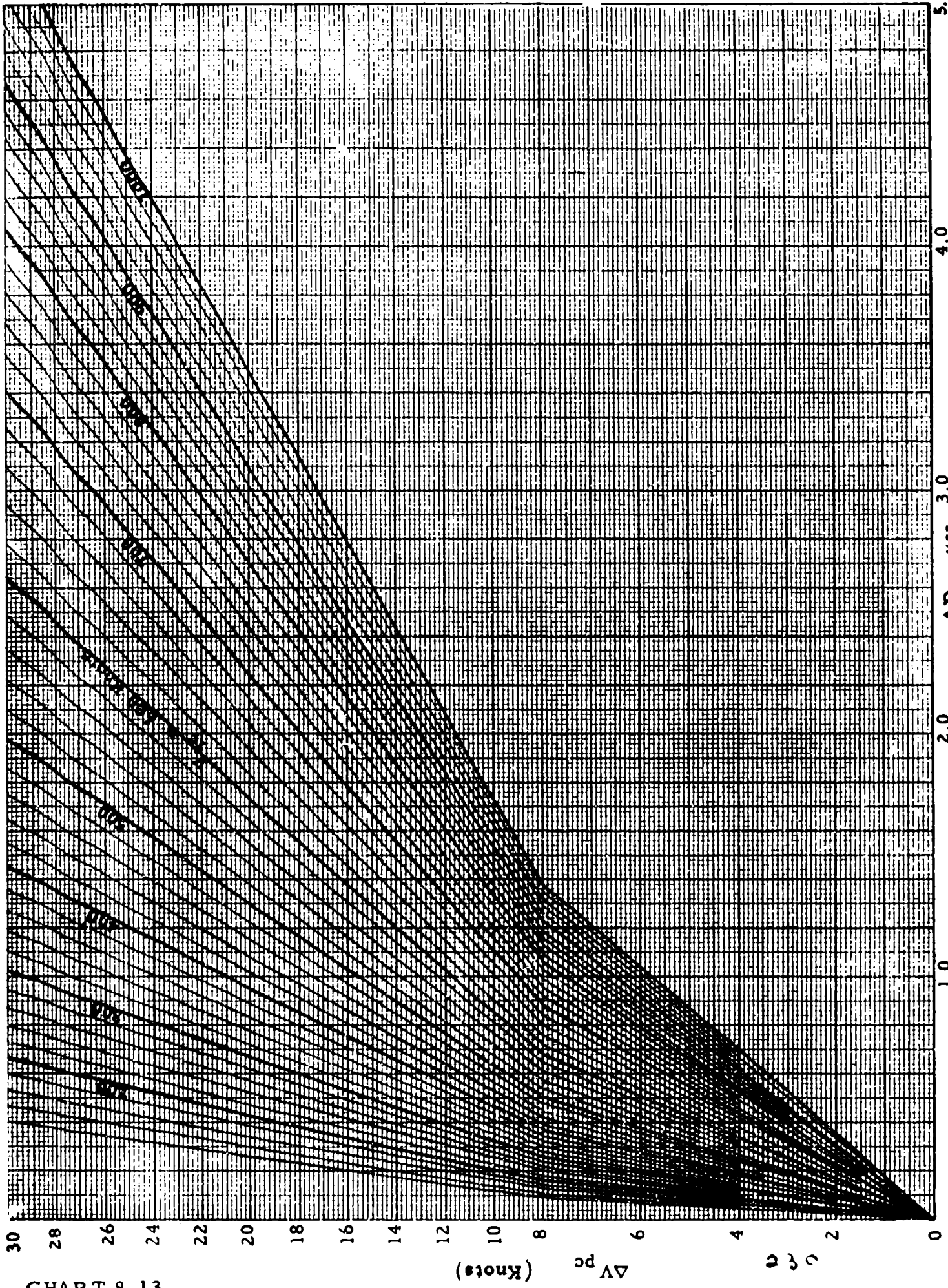


CHART 8.13

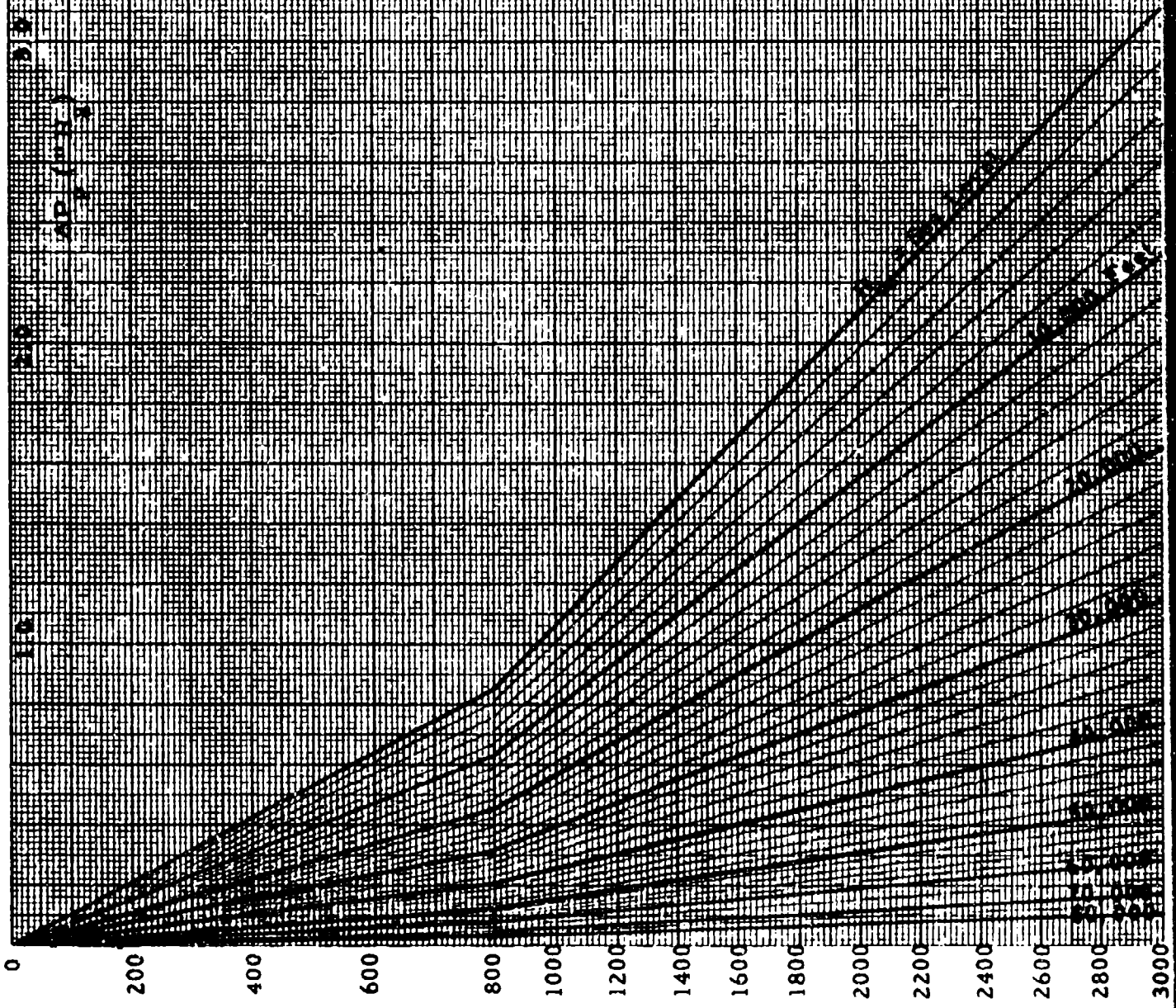
0 200 400 600 800 1000 1200 1400 1600 1800 2000 2200 2400 2600 2800 3000

100

ΔH_{pc} (Feet)

231

CHART 8.13



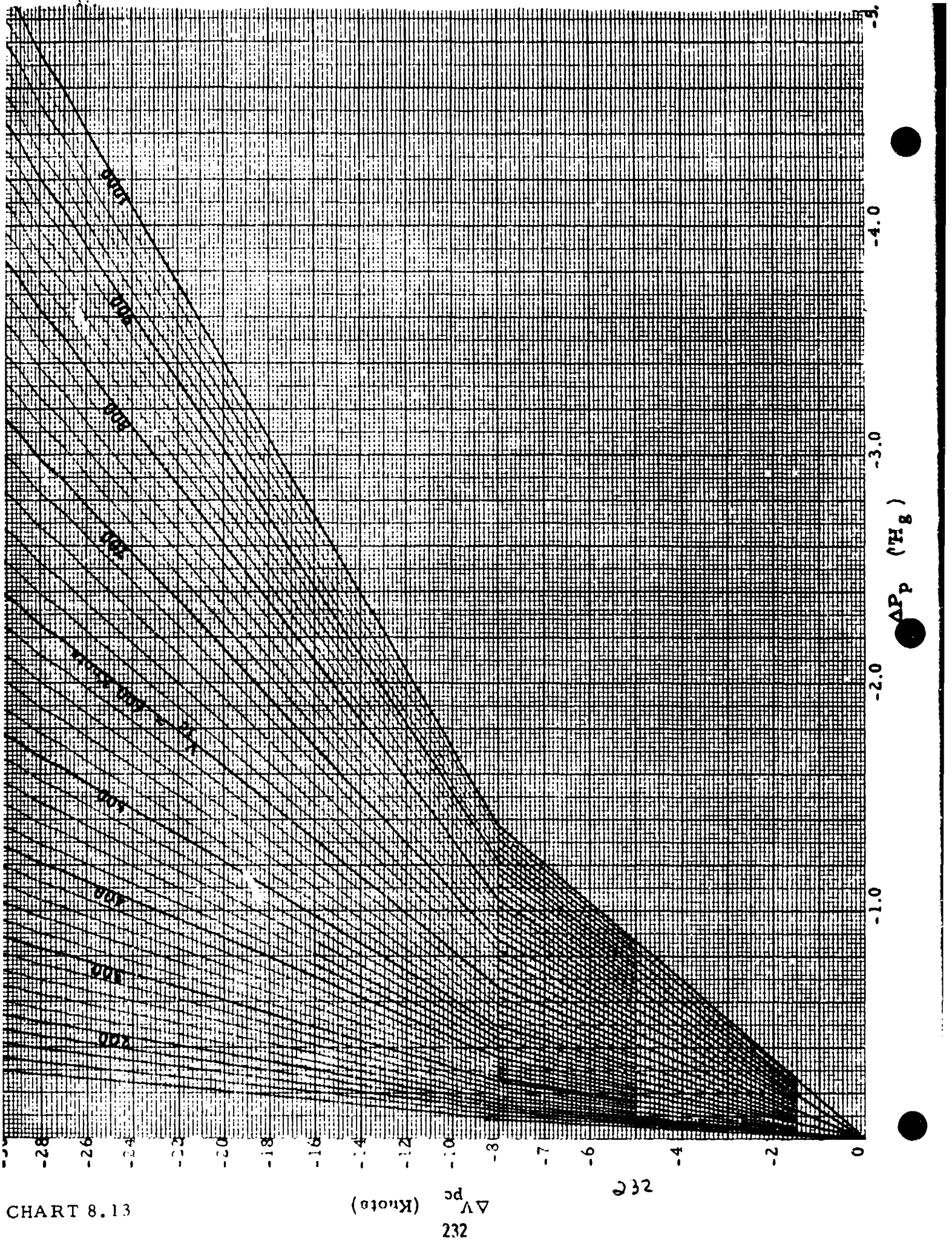


CHART 8.13

232

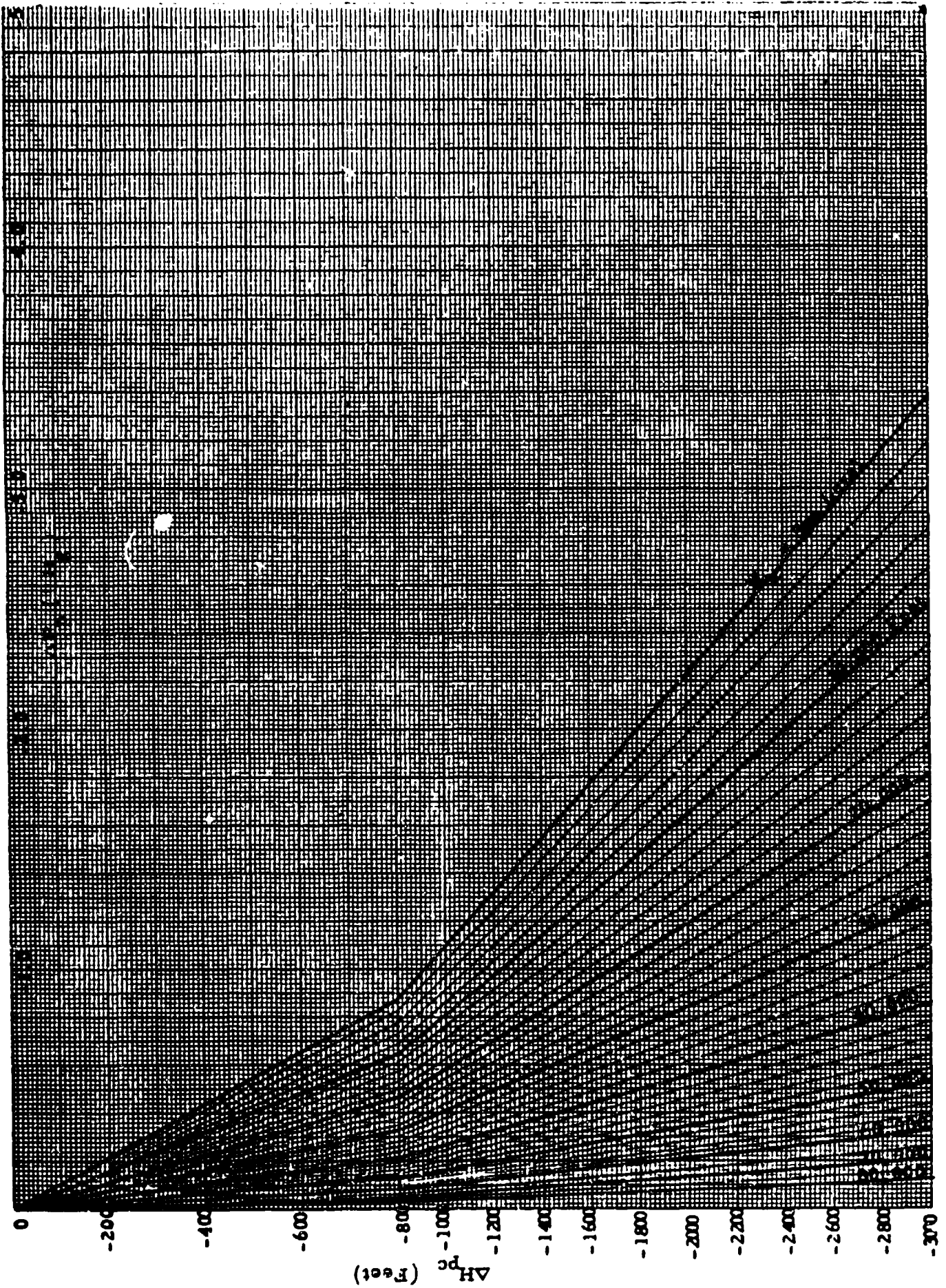


CHART 8.14
(See paragraph 5.3.5)

INDICATED MACH NUMBER CORRECTED FOR INSTRUMENT ERROR, M_{ic} versus RATIO OF MACH METER TO ALTIMETER POSITION ERROR CORRECTIONS, $\Delta M_{pc} / \Delta H_{pc}$ (1/Feet) for INDICATED PRESSURE ALTITUDE CORRECTED FOR INSTRUMENT ERROR, H_{ic} (Feet) = CONSTANT

$$\frac{\Delta M_{pc}}{\Delta H_{pc}} = 0.007438 \frac{(1 + 0.2 M_{ic}^2)}{T_{as} M_{ic}} \quad M_{ic} \leq 1.00$$

$$\frac{\Delta M_{pc}}{\Delta H_{pc}} = 0.001488 \frac{M_{ic}}{T_{as}} \frac{(7 M_{ic}^2 - 1)}{(2 M_{ic}^2 - 1)} \quad M_{ic} \geq 1.00$$

where T_{as} is measured at H_{ic} .

Note: This curve is valid for small errors only, (say $\Delta H_{pc} < 1000$ feet or $\Delta M_{pc} < 0.04$). Chart 8.15 should be used for larger errors.

Example:

Given: $M_{ic} = 2.30$; $H_{ic} = 46,000$ feet; $\Delta H_{pc} = -800$ feet

Required: ΔM_{pc}

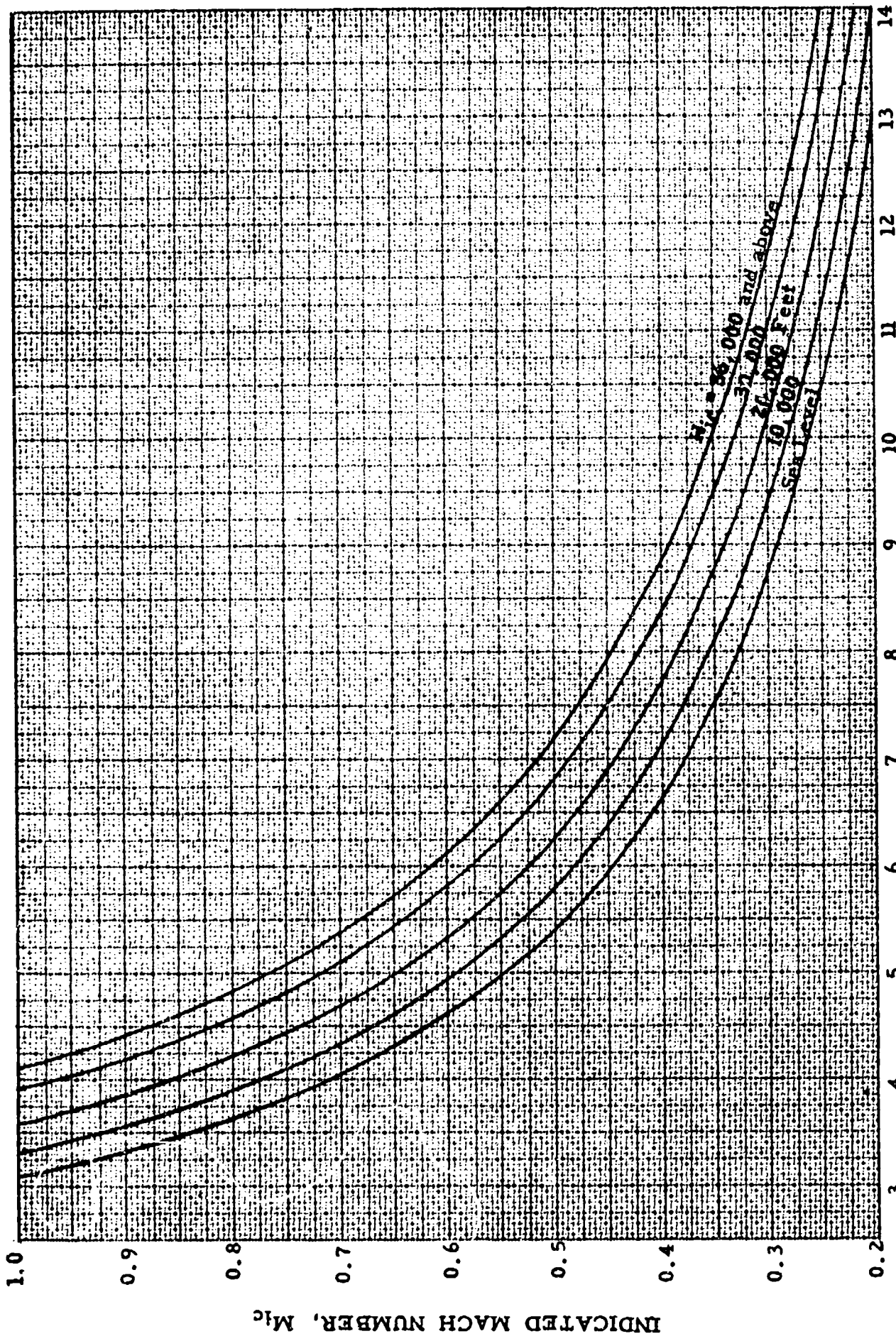
Solution: Use Page 3 of Chart 8.14. For the given conditions,

$$\frac{\Delta M_{pc}}{\Delta H_{pc}} = 5.94 \times 10^{-5} \frac{1}{\text{Feet}}$$

$$\Delta M_{pc} = \frac{\Delta M_{pc}}{\Delta H_{pc}} \Delta H_{pc} = 0.0475$$

Note: The exact solution is found from Chart 8.15 to be

$$\Delta M_{pc} = -0.0470$$



INDICATED MACH NUMBER, M_{ic}

$(\Delta M_{pc} / \Delta H_{pc}) \times 10^5 \sim (10^5 / \text{Feet})$

CHART 8.14

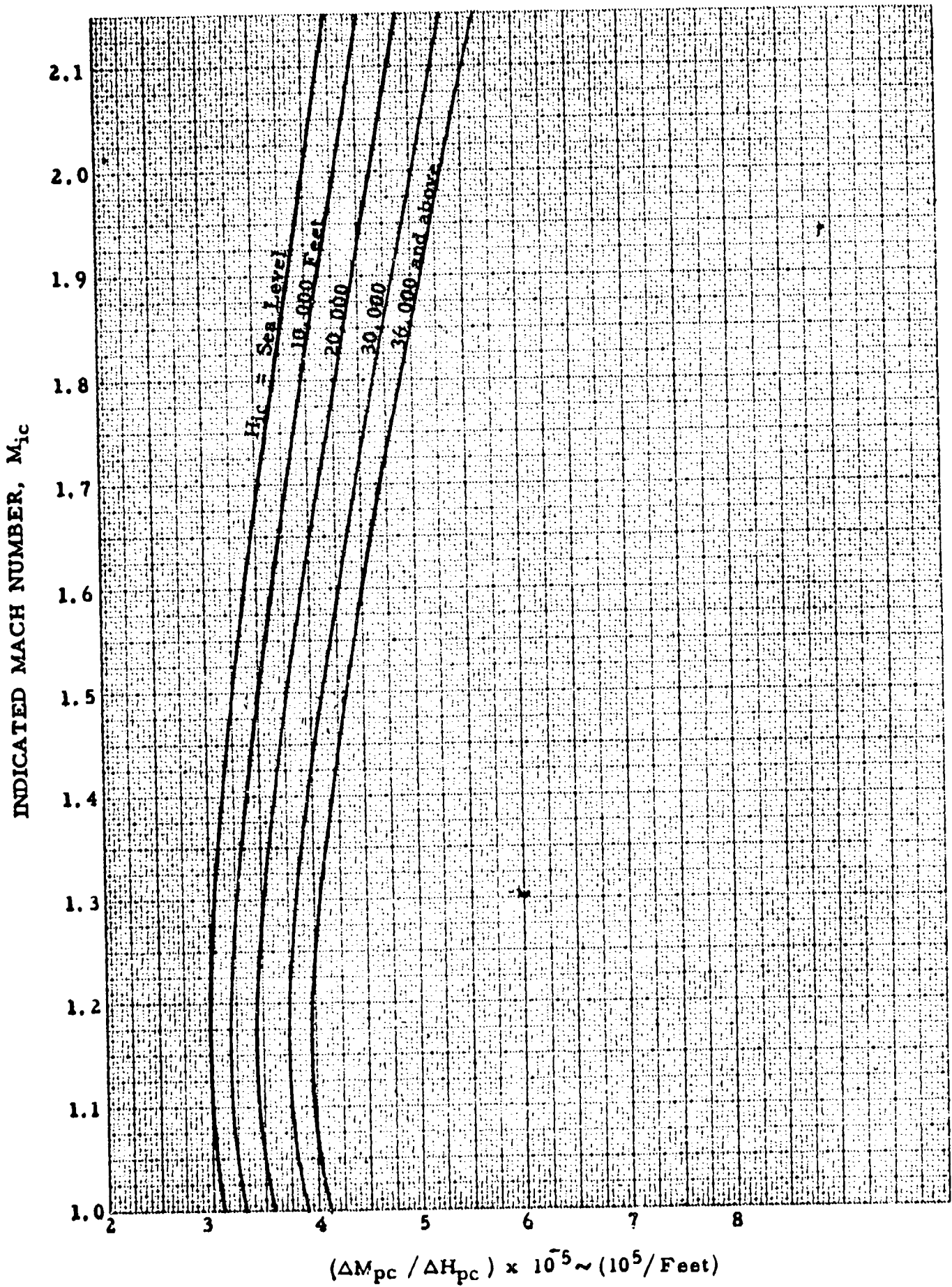
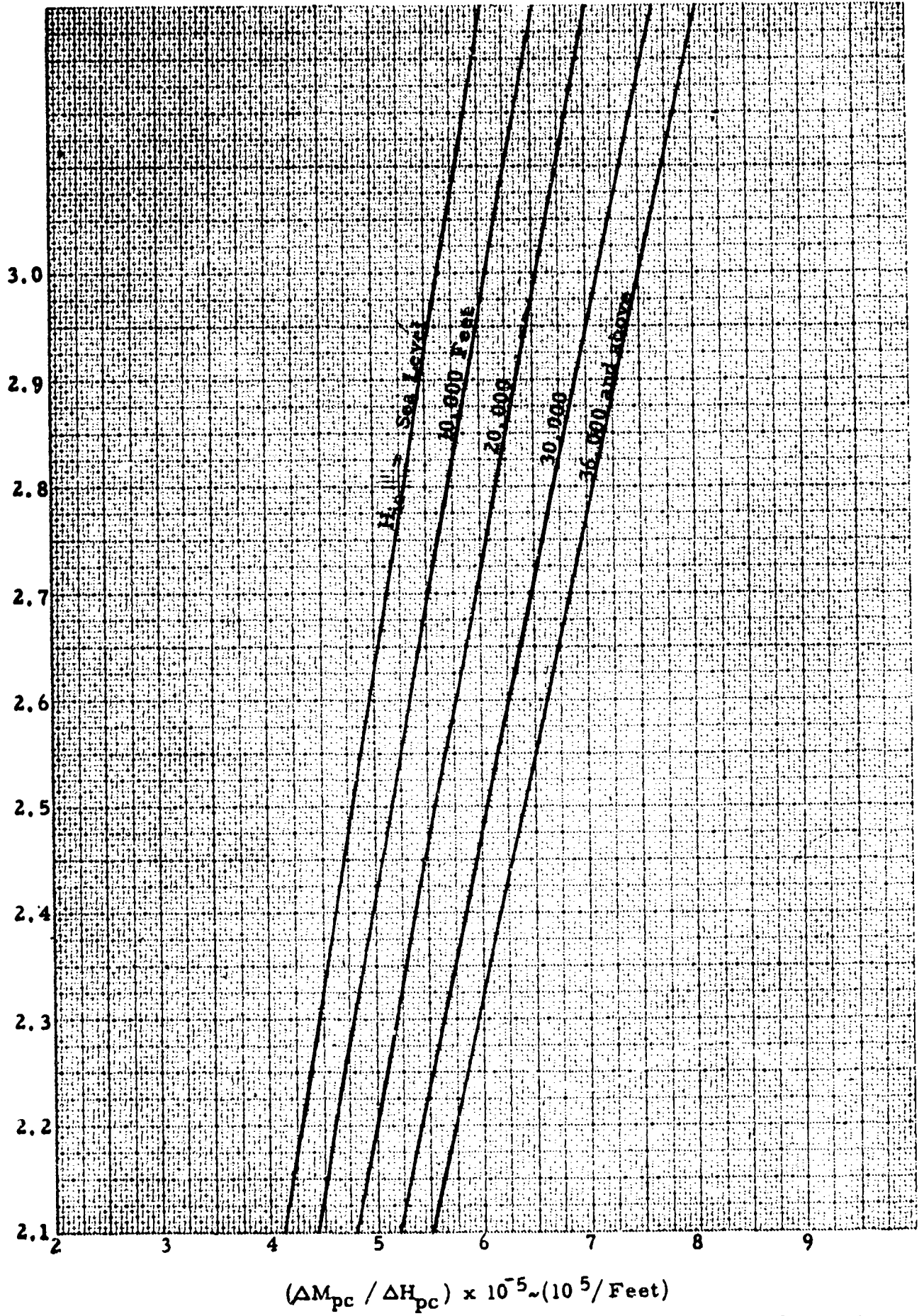


CHART 8.14

INDICATED MACH NUMBER, M_{ic}



$(\Delta M_{pc} / \Delta H_{pc}) \times 10^{-5} (10^5 / \text{Feet})$

CHART 8.15

(See paragraph 5.3.5)

MACH METER POSITION ERROR CORRECTION, ΔM_{pc} versus RATIO OF STATIC PRESSURE ERROR TO INDICATED STATIC PRESSURE, $\Delta P_p / P_s$ for INDICATED MACH NUMBER CORRECTED FOR INSTRUMENT ERROR, $M_{ic} = \text{CONSTANT}$

and

ALTIMETER POSITION ERROR CORRECTION, ΔH_{pc} (Feet) versus RATIO OF STATIC PRESSURE ERROR TO INDICATED STATIC PRESSURE, $\Delta P_p / P_s$ for INDICATED PRESSURE ALTITUDE CORRECTED FOR INSTRUMENT ERROR, $H_{ic} = \text{CONSTANT}$

ALSO

MACH METER POSITION ERROR CORRECTION, ΔM_{pc} versus ALTIMETER POSITION ERROR CORRECTION, ΔH_{pc} (Feet) for INDICATED MACH NUMBER CORRECTED FOR INSTRUMENT ERROR, $M_{ic} = \text{CONSTANT}$ and INDICATED PRESSURE ALTITUDE CORRECTED FOR INSTRUMENT ERROR, H_{ic} (Feet) = CONSTANT

$$\begin{aligned} \frac{\Delta P_p}{P_s} &= 0.0010813 \frac{\sigma_s}{P_s} \Delta H_{pc} \\ &= \frac{1.4 M_{ic} \Delta M_{pc}}{(1 + 0.2 M_{ic}^2)} + \frac{0.7(1 - 1.6 M_{ic}^2) \Delta M_{pc}^2}{(1 + 0.2 M_{ic}^2)^2} \quad M_{ic} \leq 1.00 \\ &= \frac{7(2 M_{ic}^2 - 1) \Delta M_{pc}}{M_{ic} (7 M_{ic}^2 - 1)} - \frac{7(21 M_{ic}^4 - 23.5 M_{ic}^2 + 4) \Delta M_{pc}^2}{M_{ic}^2 (7 M_{ic}^2 - 1)^2} \quad M_{ic} \geq 1.00 \end{aligned}$$

where P_s is measured at H_{ic} and σ_s is measured at $H_{ic} + \frac{\Delta H_{pc}}{2}$

Example:

Given: $M_{ic} = 1.00$, $H_{ic} = 72,000$ feet; $\Delta H_{pc} = 2400$ feet

Required: ΔM_{pc}

Solution: Use Page 5 of Chart 8.15 for positive errors,

$$\Delta M_{pc} = 0.0968$$

Note: The approximate solution is found from Chart 8.14 to be

$$\Delta M_{pc} = 0.0986$$

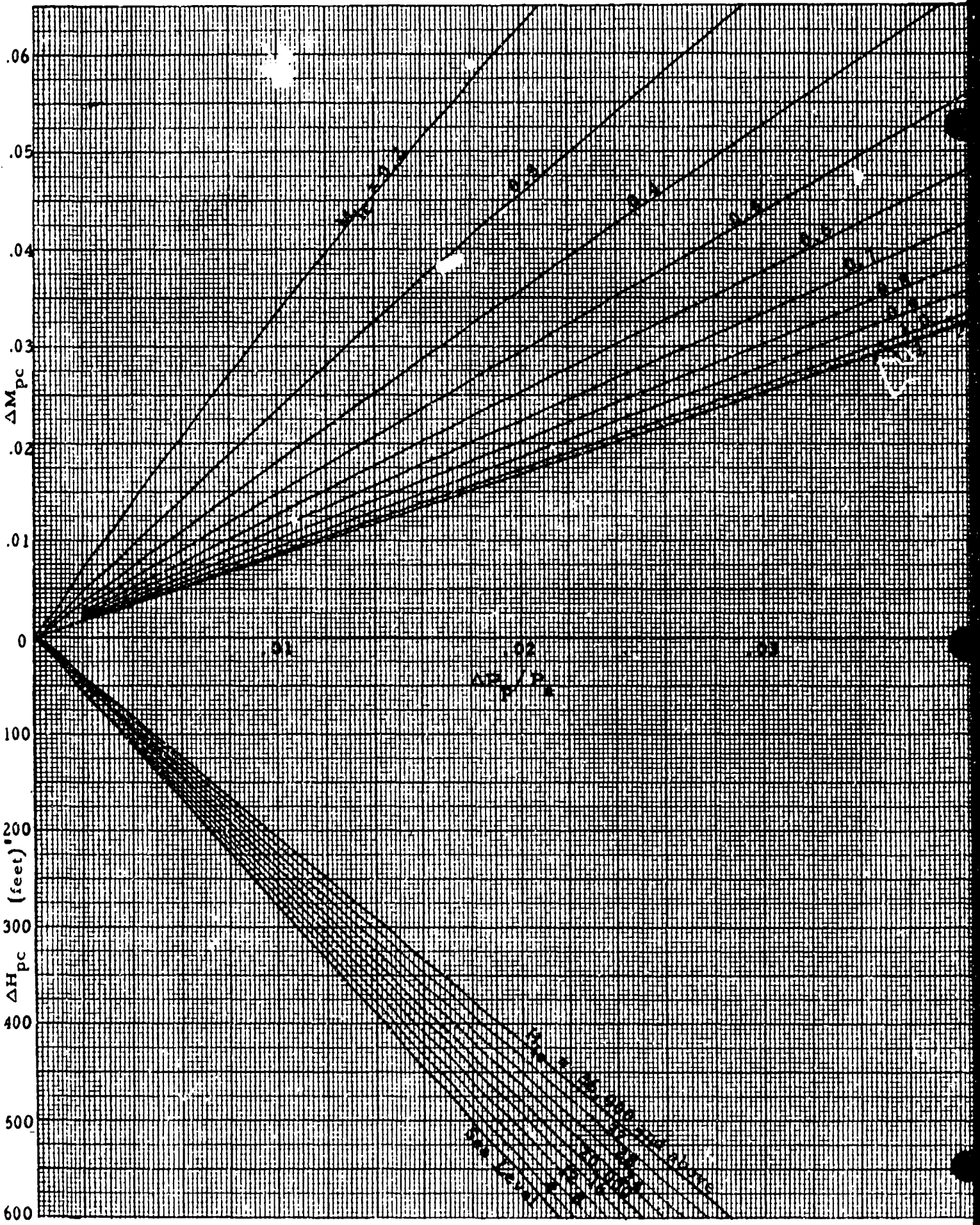
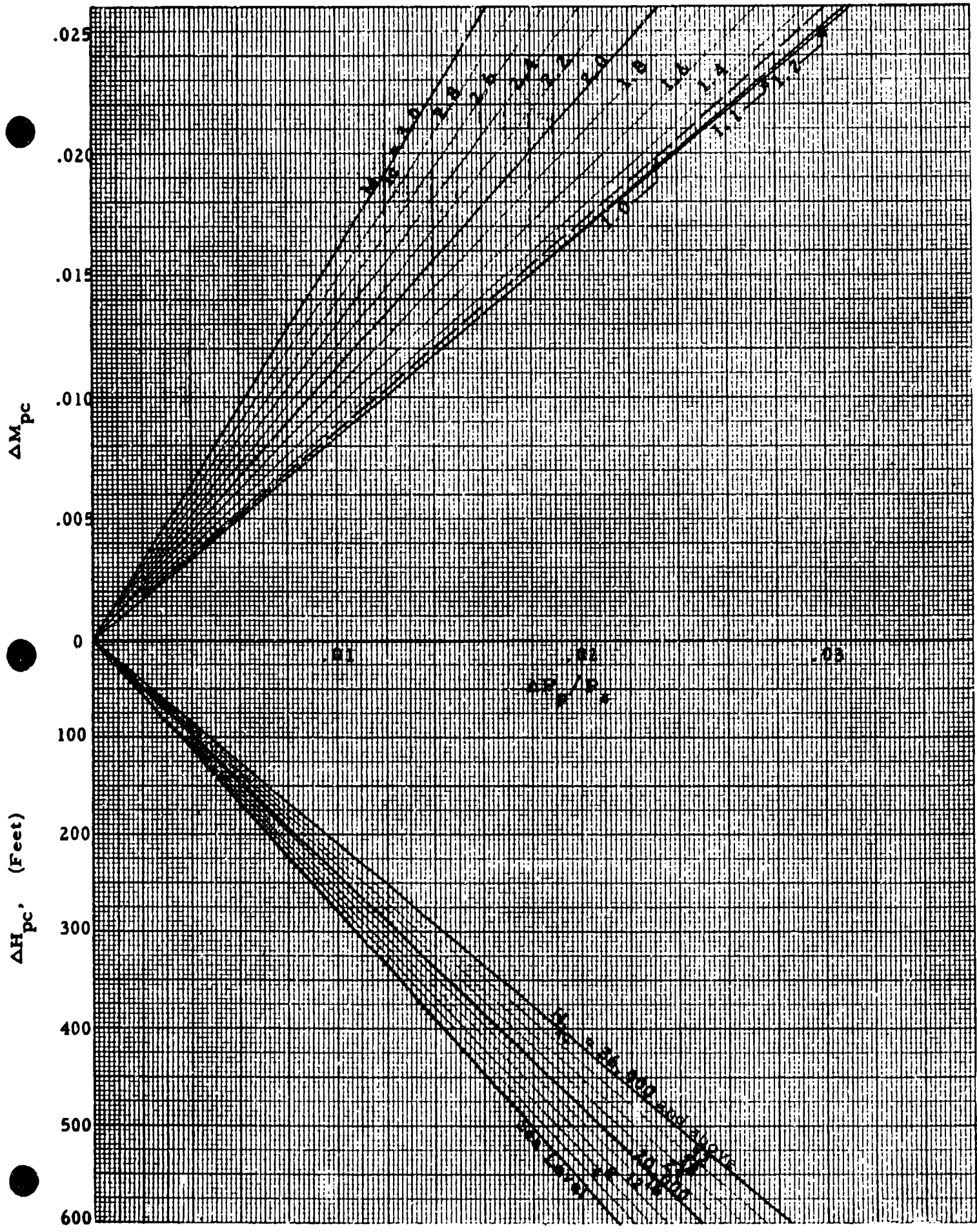


CHART 8.15



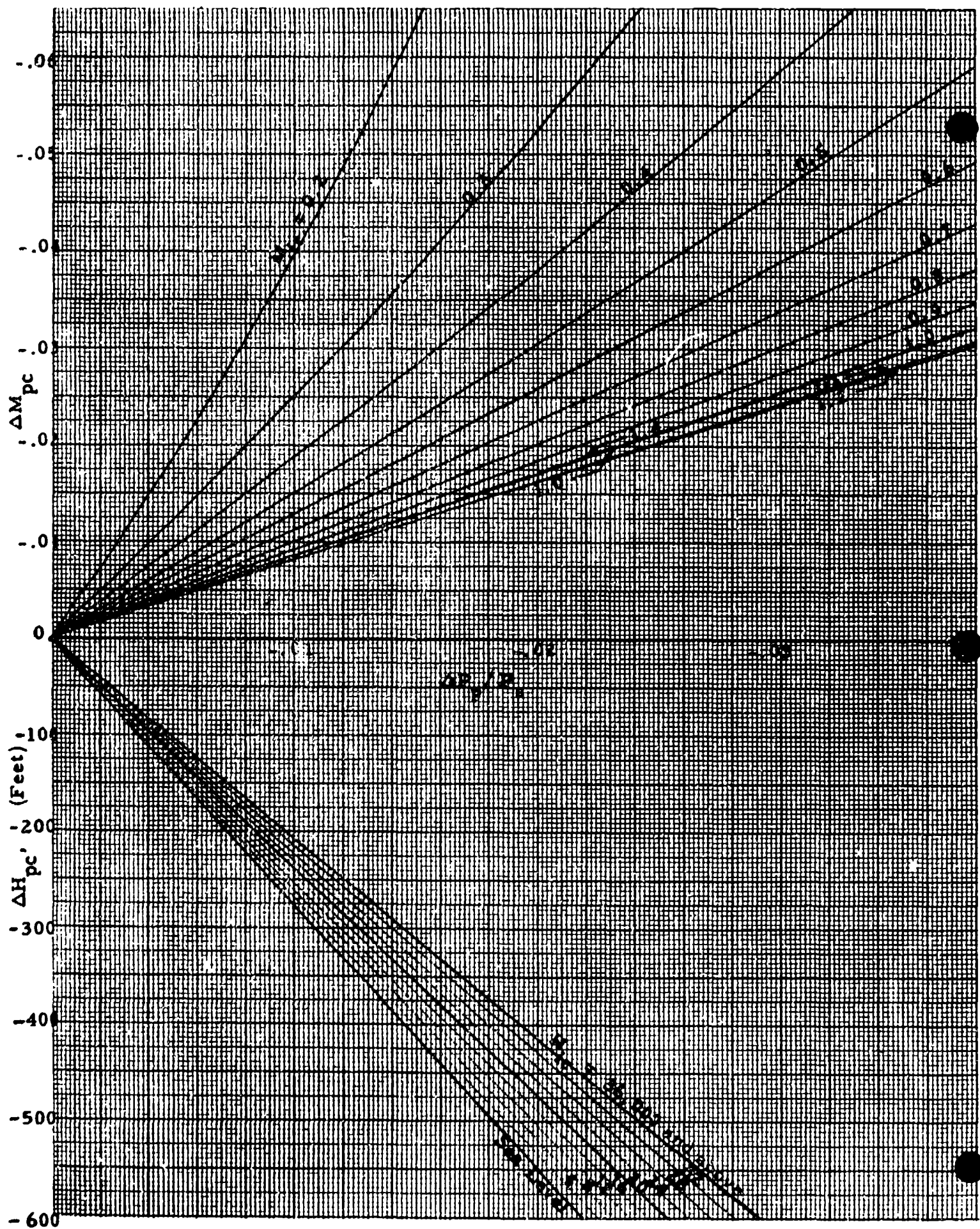
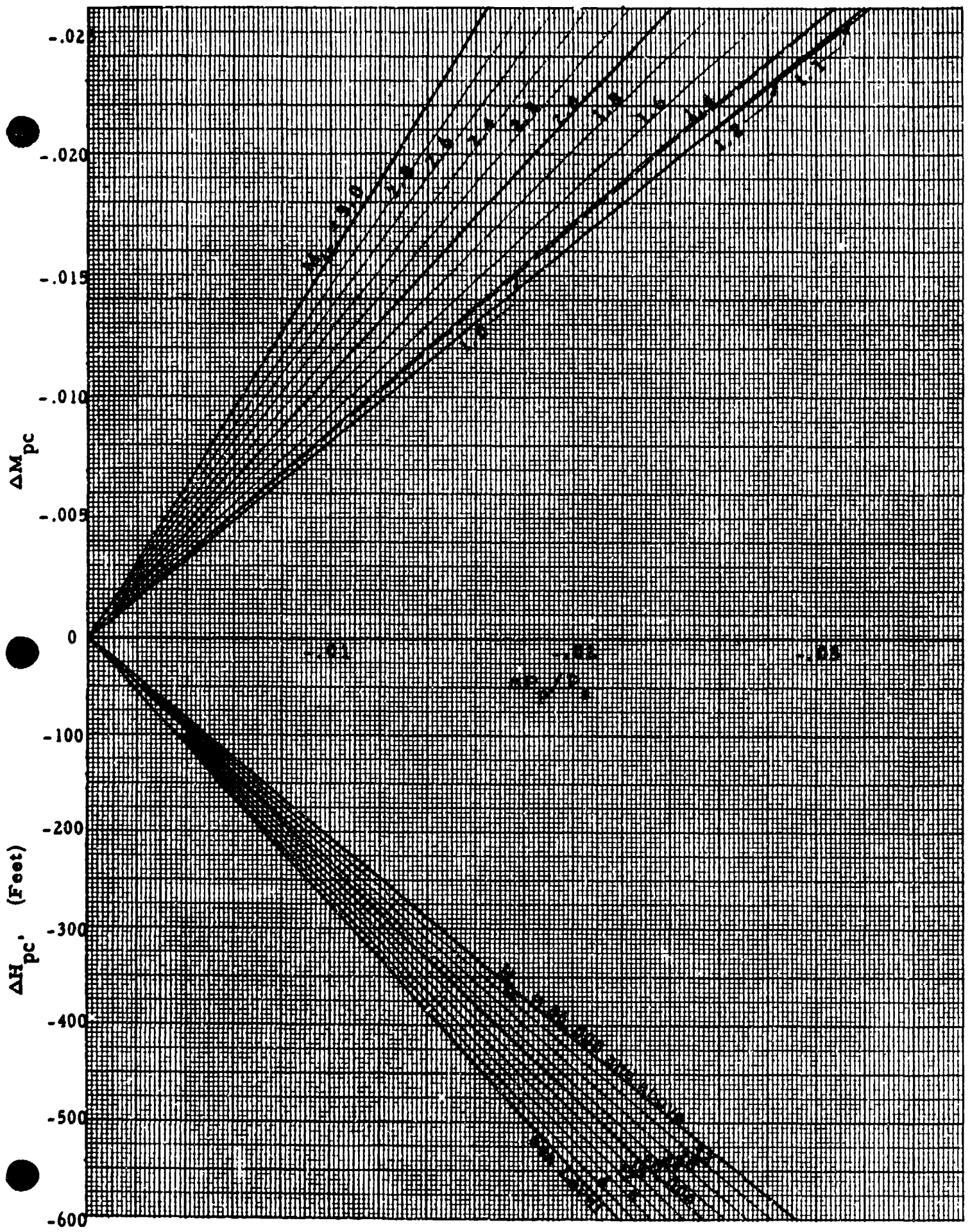


CHART 8.15



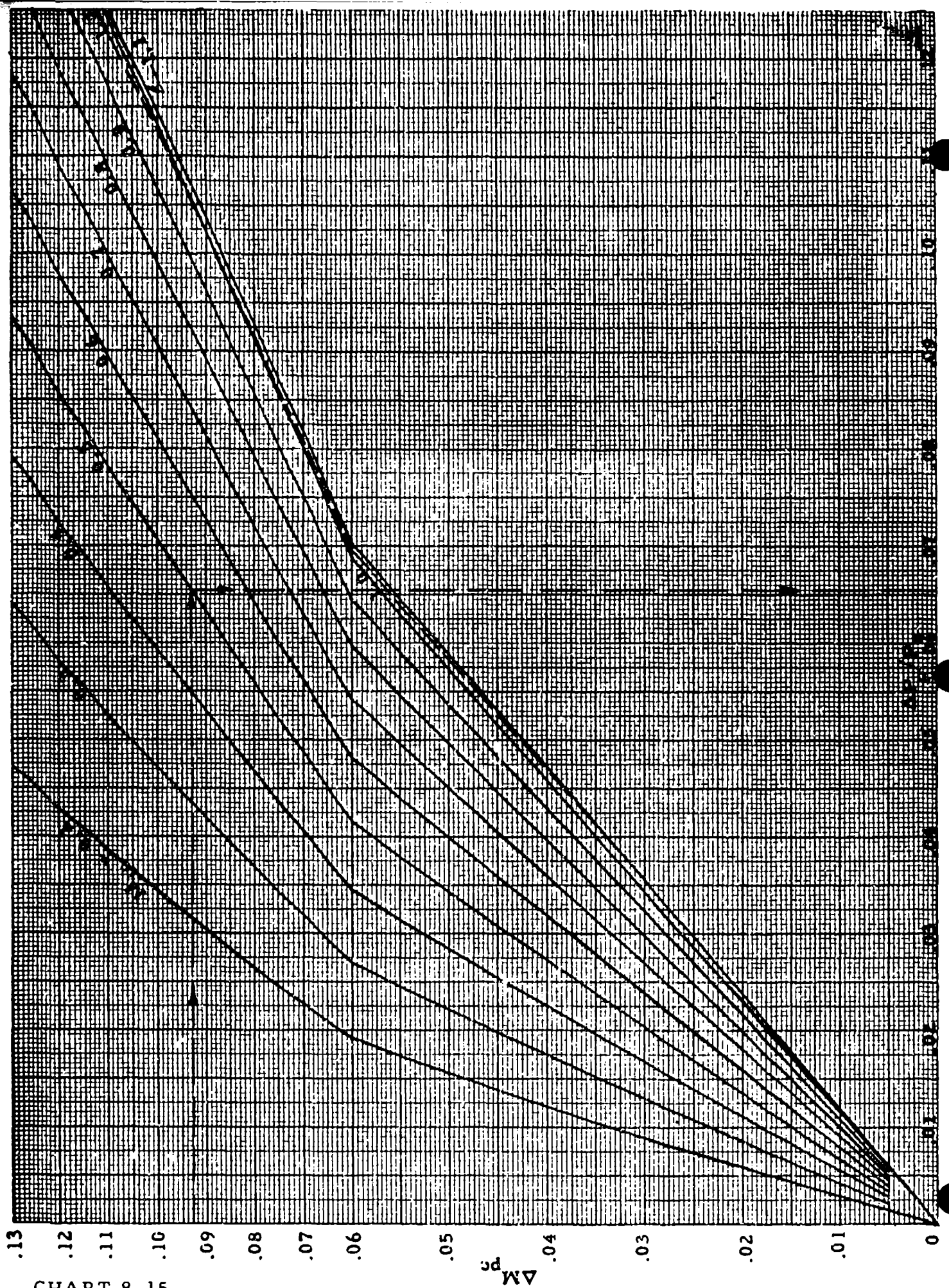


CHART 8.15

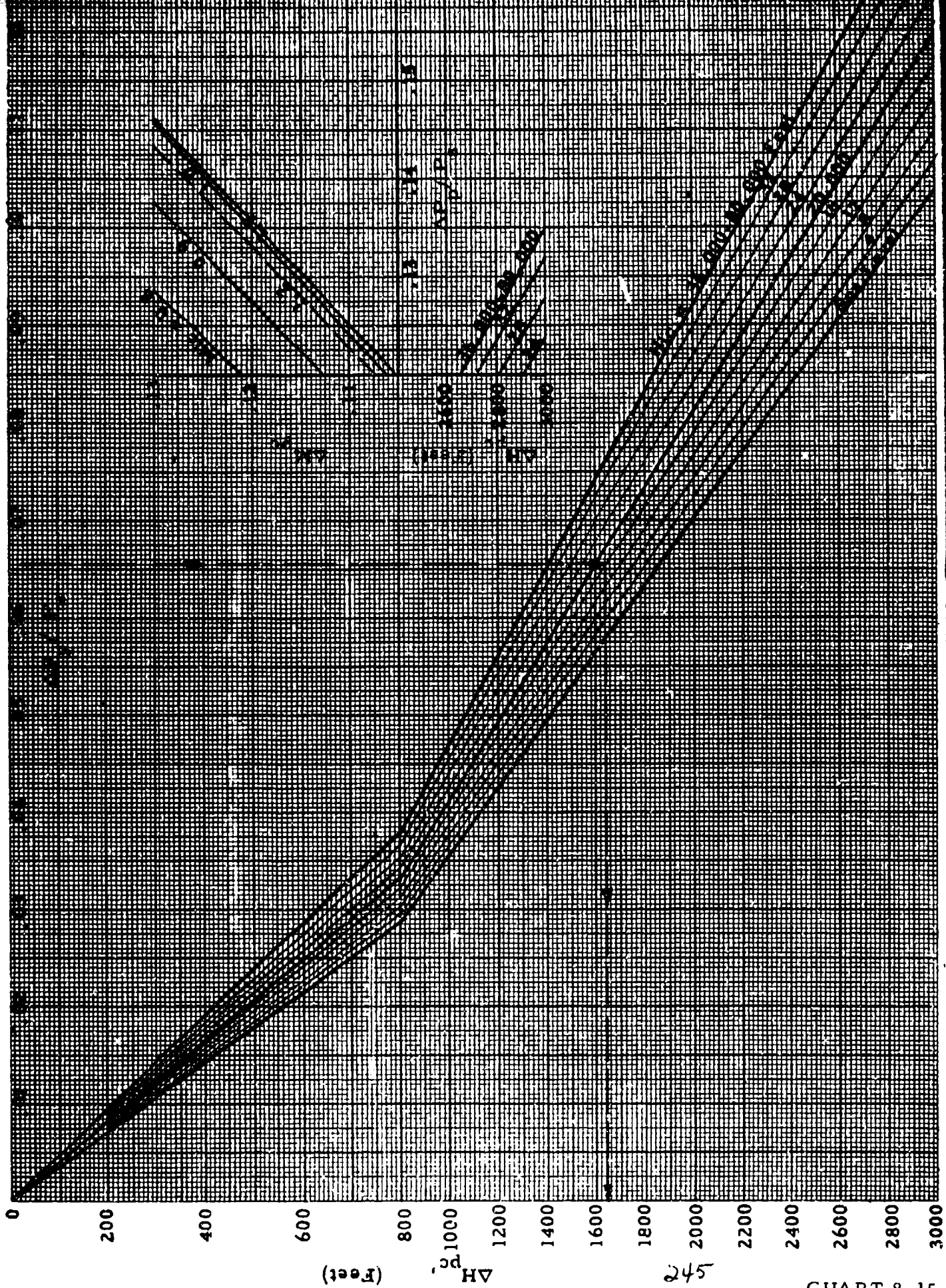
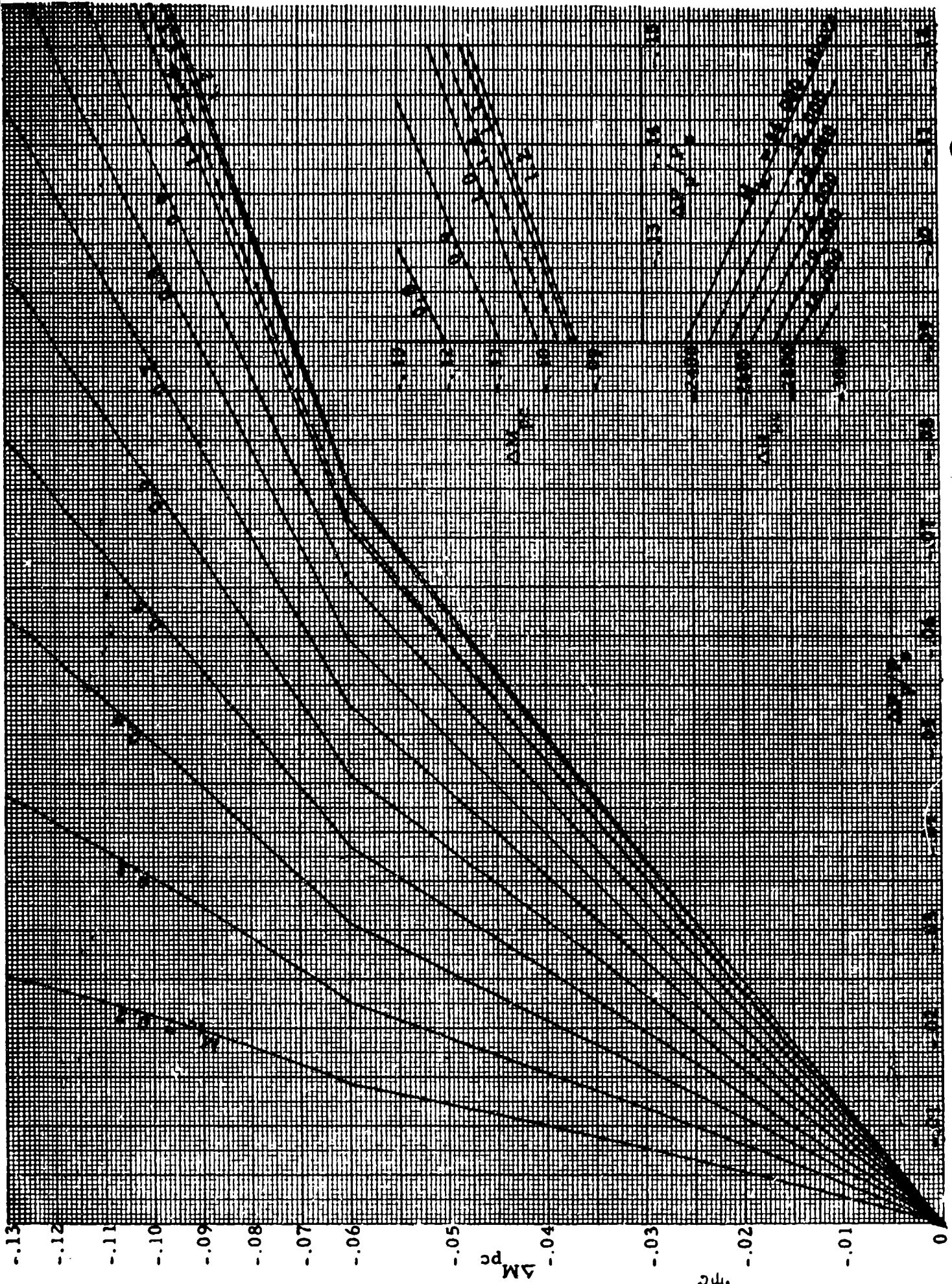
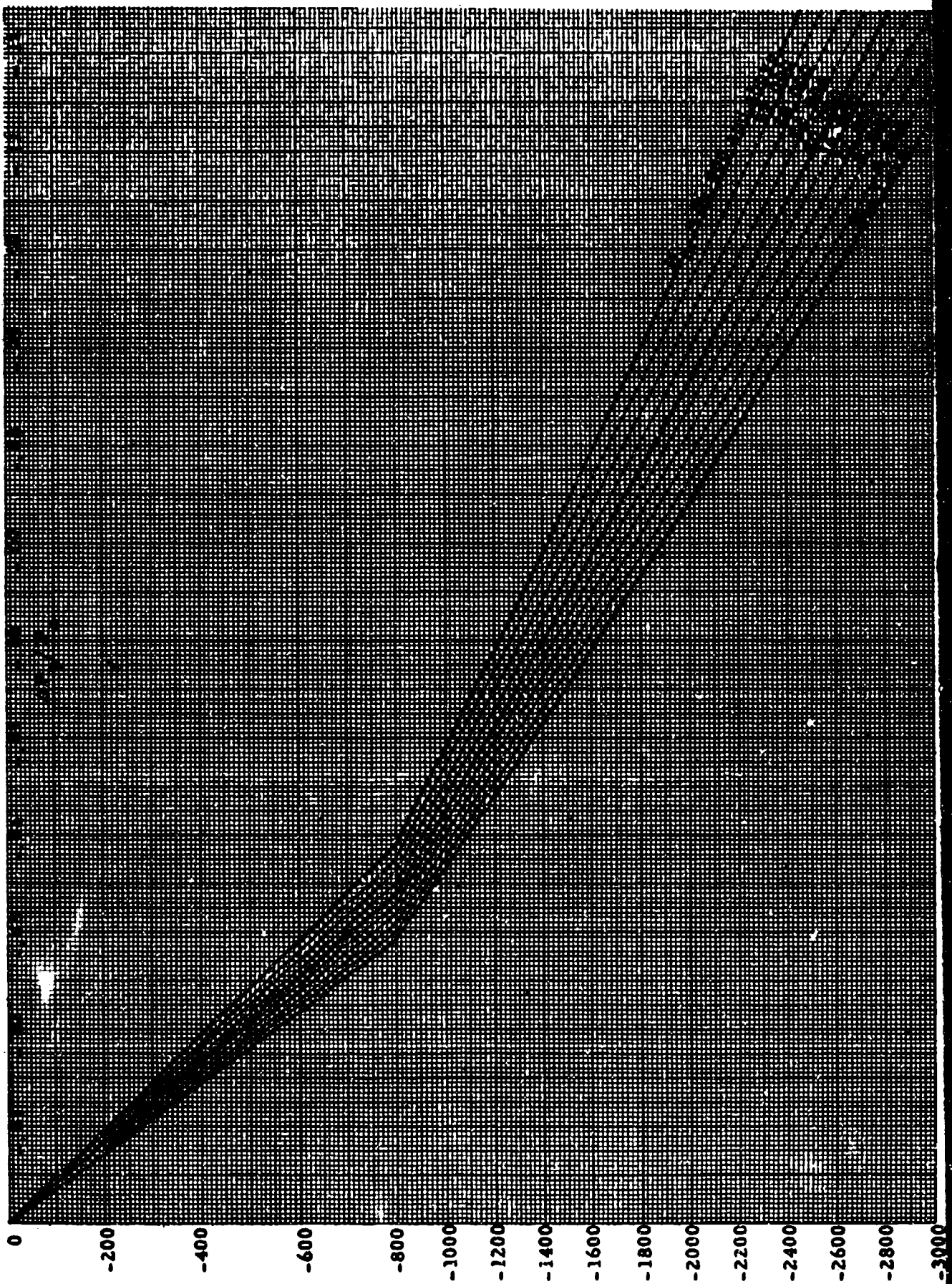


CHART 8.15

245

572





247 ΔH_{pc} (Feet)

CHART 8-15

CHART 8.16

(See paragraph 5.3.6)

RATIO OF MACH METER TO AIRSPEED INDICATOR POSITION ERROR
CORRECTIONS, $\Delta M_{pc} / \Delta V_{pc}$ (1/Knots) versus INDICATED MACH NUMBER
CORRECTED FOR INSTRUMENT ERROR, M_{ic} for INDICATED PRESSURE
ALTITUDE CORRECTED FOR INSTRUMENT ERROR, H_{ic} (Feet) = CONSTANT

$$\frac{\Delta M_{pc}}{\Delta V_{pc}} = \frac{P_{aSL}}{a_{SL}} \frac{1}{P_s} \frac{V_{ic}}{a_{SL}} \left[1 + 0.2 \left(\frac{V_{ic}}{a_{SL}} \right)^2 \right]^{2.5} \frac{(1 + 0.2 M_{ic}^2)}{M_{ic}} \quad \begin{array}{l} V_{ic} \leq a_{SL} \\ M_{ic} \leq 1.00 \end{array}$$

$$\frac{\Delta M_{pc}}{\Delta V_{pc}} = \frac{P_{aSL}}{5 a_{SL}} \frac{1}{P_s} \frac{V_{ic}}{a_{SL}} \left[1 + 0.2 \left(\frac{V_{ic}}{a_{SL}} \right)^2 \right]^{2.5} \frac{M_{ic} (7 M_{ic}^2 - 1)}{(2 M_{ic}^2 - 1)} \quad \begin{array}{l} V_{ic} \leq a_{SL} \\ M_{ic} \geq 1.00 \end{array}$$

$$\frac{\Delta M_{pc}}{\Delta V_{pc}} = \frac{166.921 P_{aSL}}{a_{SL}} \frac{1}{P_s} \frac{\left(\frac{V_{ic}}{a_{SL}} \right)^6 \left[2 \left(\frac{V_{ic}}{a_{SL}} \right)^2 - 1 \right]}{\left[7 \left(\frac{V_{ic}}{a_{SL}} \right)^2 - 1 \right]^{3.5}} \frac{M_{ic} (7 M_{ic}^2 - 1)}{(2 M_{ic}^2 - 1)} \quad \begin{array}{l} V_{ic} \geq a_{SL} \\ M_{ic} \geq a_{SL} \end{array}$$

where $P_{aSL} = 29.92126$ "Hg; $a_{SL} = 661.48$ knots and P_s is measured at H_{ic} .

Note: This curve is valid for small errors only, (say $\Delta V_{pc} < 10$ knots or $\Delta M_{pc} < 0.04$) and should not be used when the position error is larger.

Example:

Given: $M_{ic} = 2.40$; $H_{ic} = 60,000$ feet; $\Delta V_{pc} = 2.0$ knots

Required: ΔM_{pc}

Solution: Use Page 3 of Chart 8.16. For the given conditions,

$$\frac{\Delta M_{pc}}{\Delta V_{pc}} = 0.03945 \frac{1}{\text{Knots}}$$

$$\Delta M_{pc} = \left(\frac{\Delta M_{pc}}{\Delta V_{pc}} \right) \Delta V_{pc} = 0.0789$$

Preceding page blank

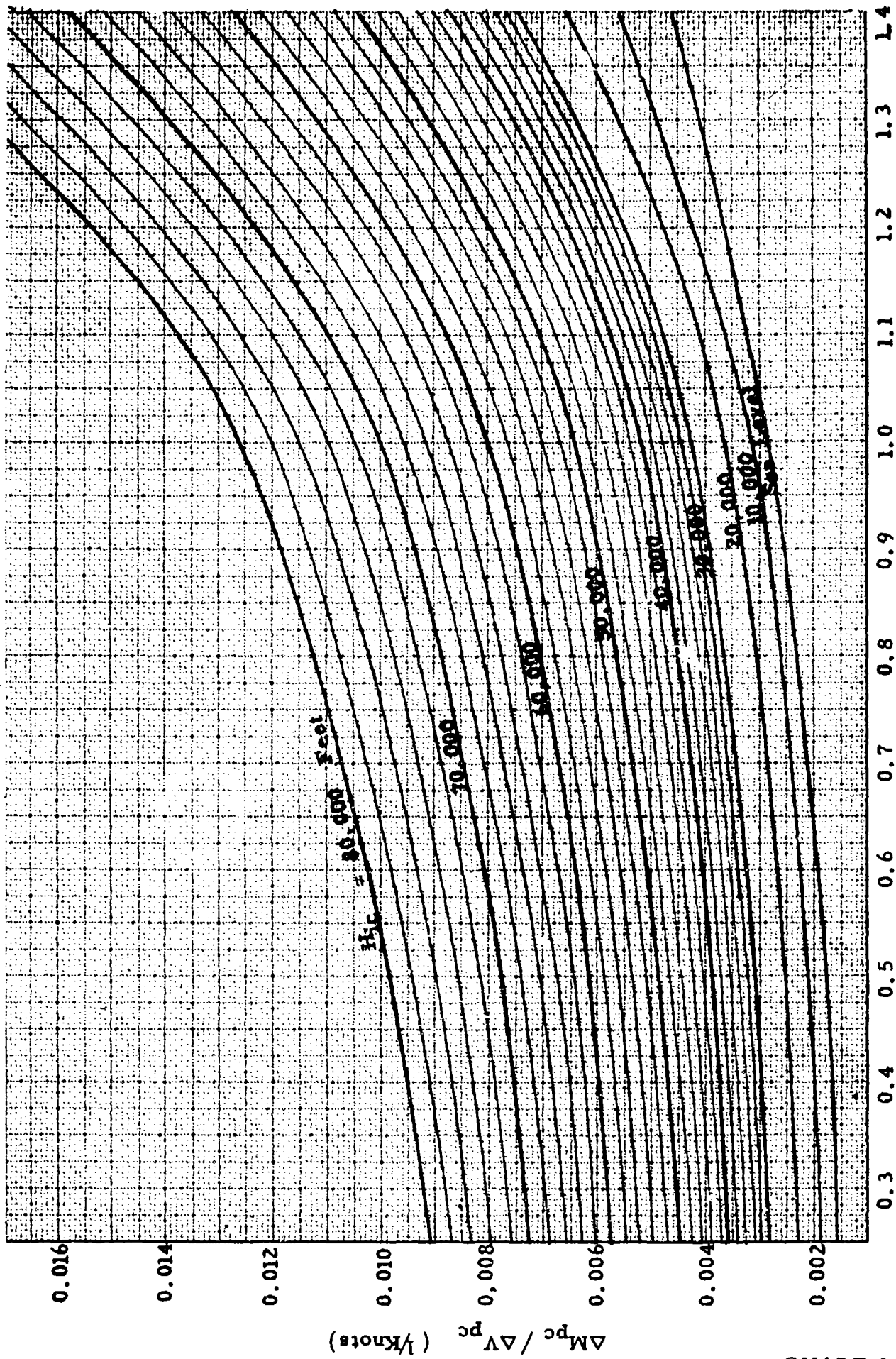
The method to be used in case of larger errors is illustrated by the following example.

Given: $M_{ic} = 1.00$; $H_{ic} = 35,000$ feet; $\Delta V_{pc} = +20$ knots

Required: ΔM_{pc}

- Solution:
1. $V_{ic} = 350$ knots for M_{ic} , H_{ic} and Chart 8.5
 $\Delta P_p/q_{cic} = +0.127$ for V_{ic} , ΔV_{pc} and Chart 8.11
 $\Delta M_{pc} = +0.1000$ for M_{ic} , $\Delta P_p/q_{cic}$ and Chart 8.18
 2. $V_{ic} = 350$ knots for M_{ic} , H_{ic} and Chart 8.5
 $\Delta H_{pc} = +2510$ feet for ΔV_{pc} , V_{ic} , H_{ic} and Chart 8.13
 $\Delta M_{pc} = +0.1000$ for ΔH_{pc} , H_{ic} , M_{ic} and Chart 8.15

Note: Use of the approximate Chart 8.16 gives $\Delta M_{pc} = +0.094$



INDICATED MACH NUMBER, $M_{i,c}$

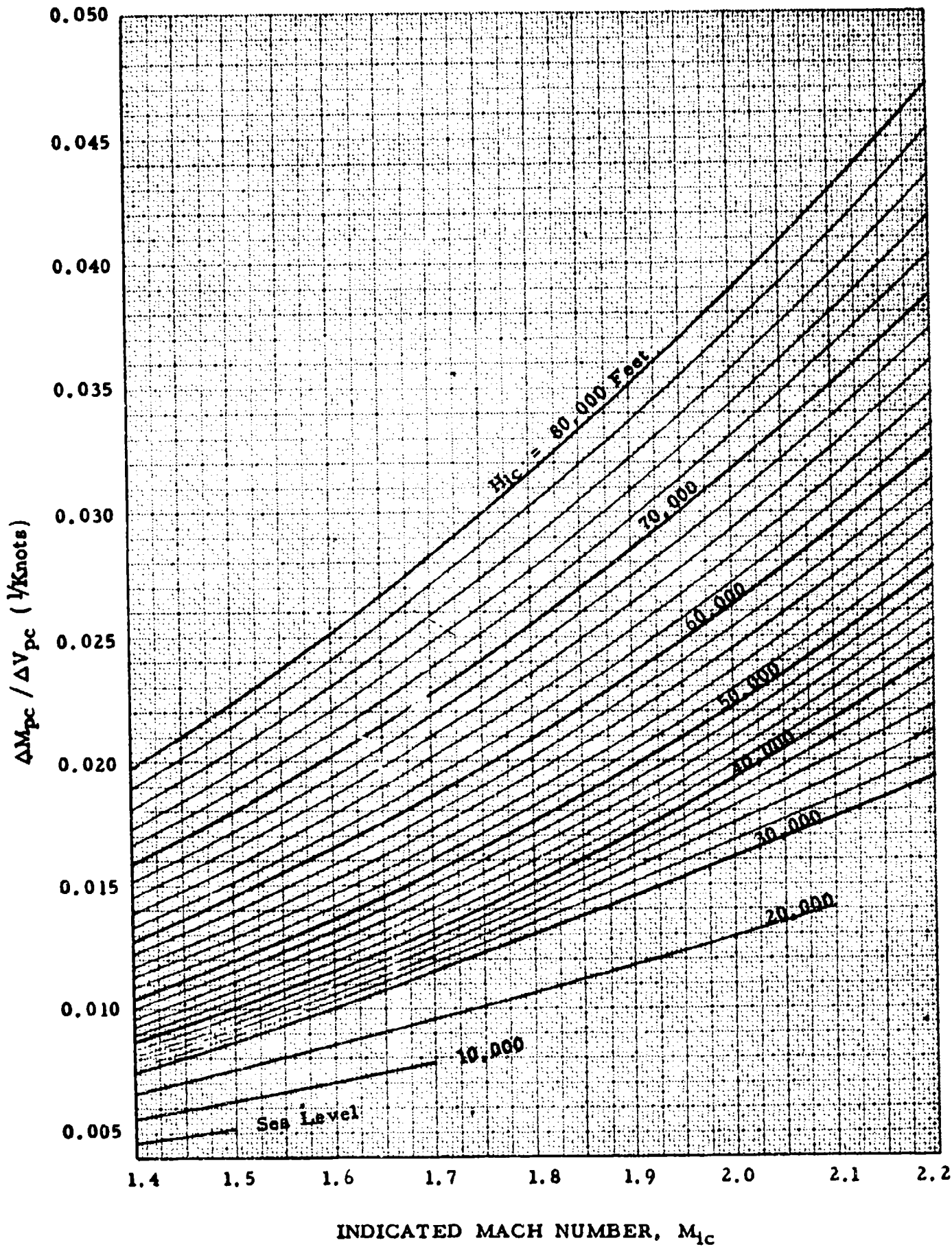
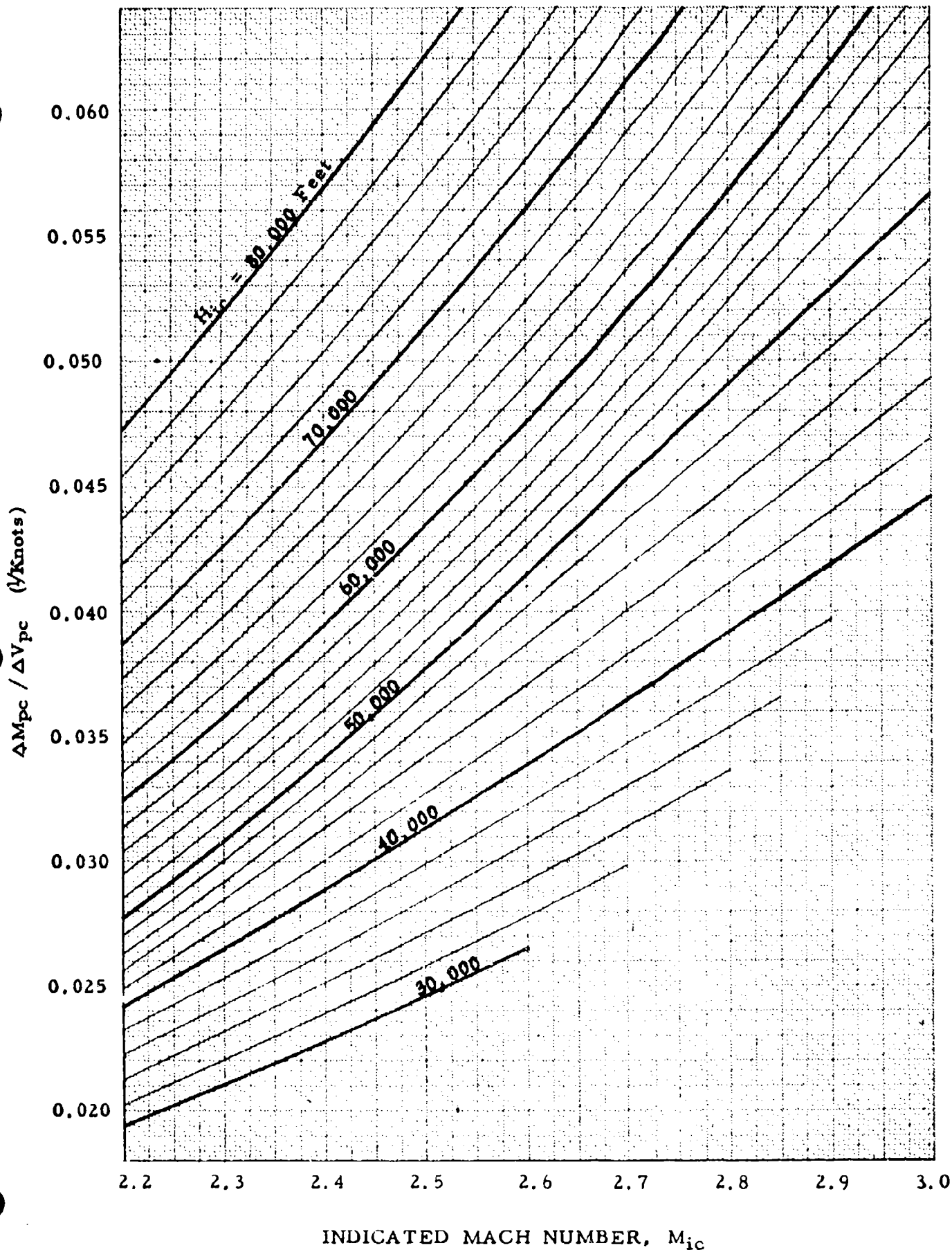


CHART 8.16



INDICATED MACH NUMBER, M_{ic}

CHART 8.16

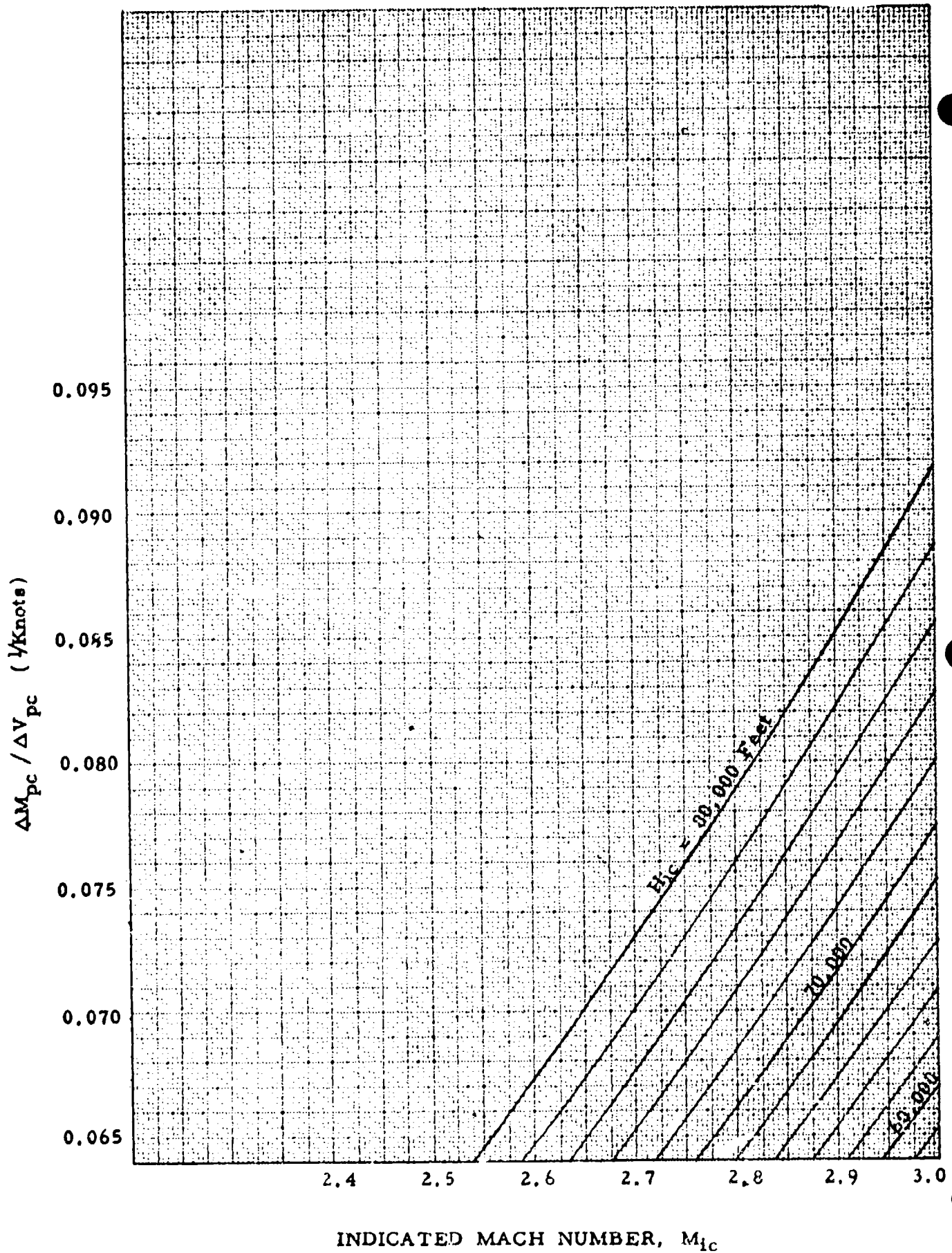


CHART 8.16

CHART 8.17

(See paragraph 5.3.7)

INDICATED MACH NUMBER CORRECTED FOR INSTRUMENT ERROR;
 M_{ic} versus RATIO OF MACH METER POSITION ERROR CORRECTION TO
 POSITION ERROR PRESSURE COEFFICIENT, $\Delta M_{pc} / (\Delta P_p / q_{cic})$

$$\frac{\Delta M_{pc}}{(\Delta P_p / q_{cic})} = \frac{(1 + 0.2 M_{ic}^2)}{1.4 M_{ic}} \left[(1 + 0.2 M_{ic}^2)^{3.5} - 1 \right] \quad M_{ic} \leq 1.00$$

$$\frac{\Delta M_{pc}}{(\Delta P_p / q_{cic})} = \frac{M_{ic} \left[166.921 M_{ic}^7 - (7 M_{ic}^2 - 1)^{2.5} \right]}{7(7 M_{ic}^2 - 1)^{1.5} (2 M_{ic}^2 - 1)} \quad M_{ic} \geq 1.00$$

Note: This curve is valid for small errors only, (say $\Delta M_{pc} < 0.04$ or $\Delta P_p / q_{cic} < 0.04$). Chart 8.18 should be used for larger errors.

Example:

Given: $M_{ic} = 0.85$; $\Delta P_p / q_{cic} = +0.10$

Required: ΔM_{pc}

Solution: Use Page 1 of Chart 8.17. For the given conditions,

$$\Delta M_{pc} / (\Delta P_p / q_{cic}) = 0.58$$

$$\Delta M_{pc} = \frac{\Delta M_{pc}}{(\Delta P_p / q_{cic})} (\Delta P_p / q_{cic}) = +0.058$$

Note: The exact solution is found from Chart 8.18 to be

$$\Delta M_{pc} = +0.0588$$

INDICATED MACH NUMBER, Mic

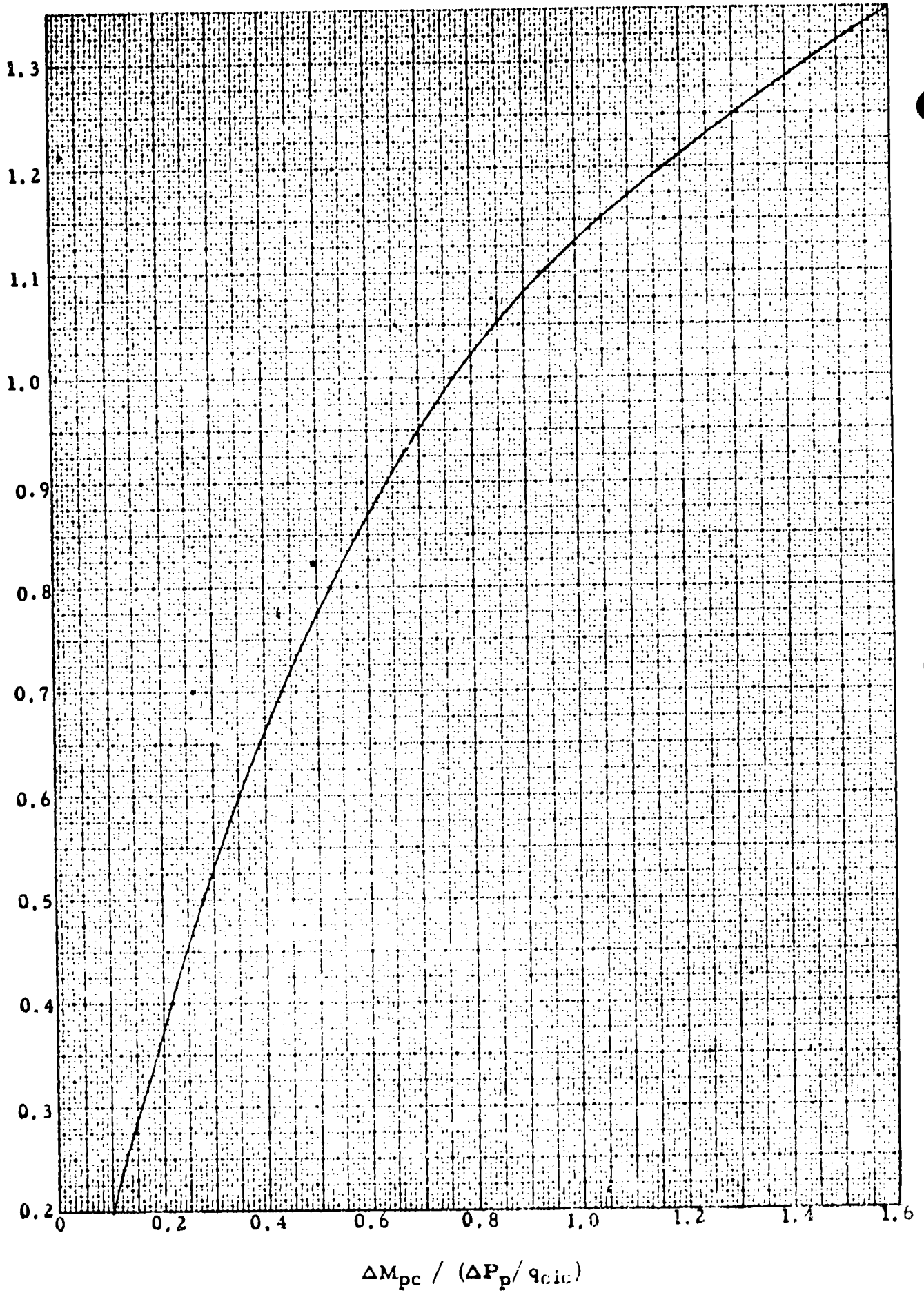
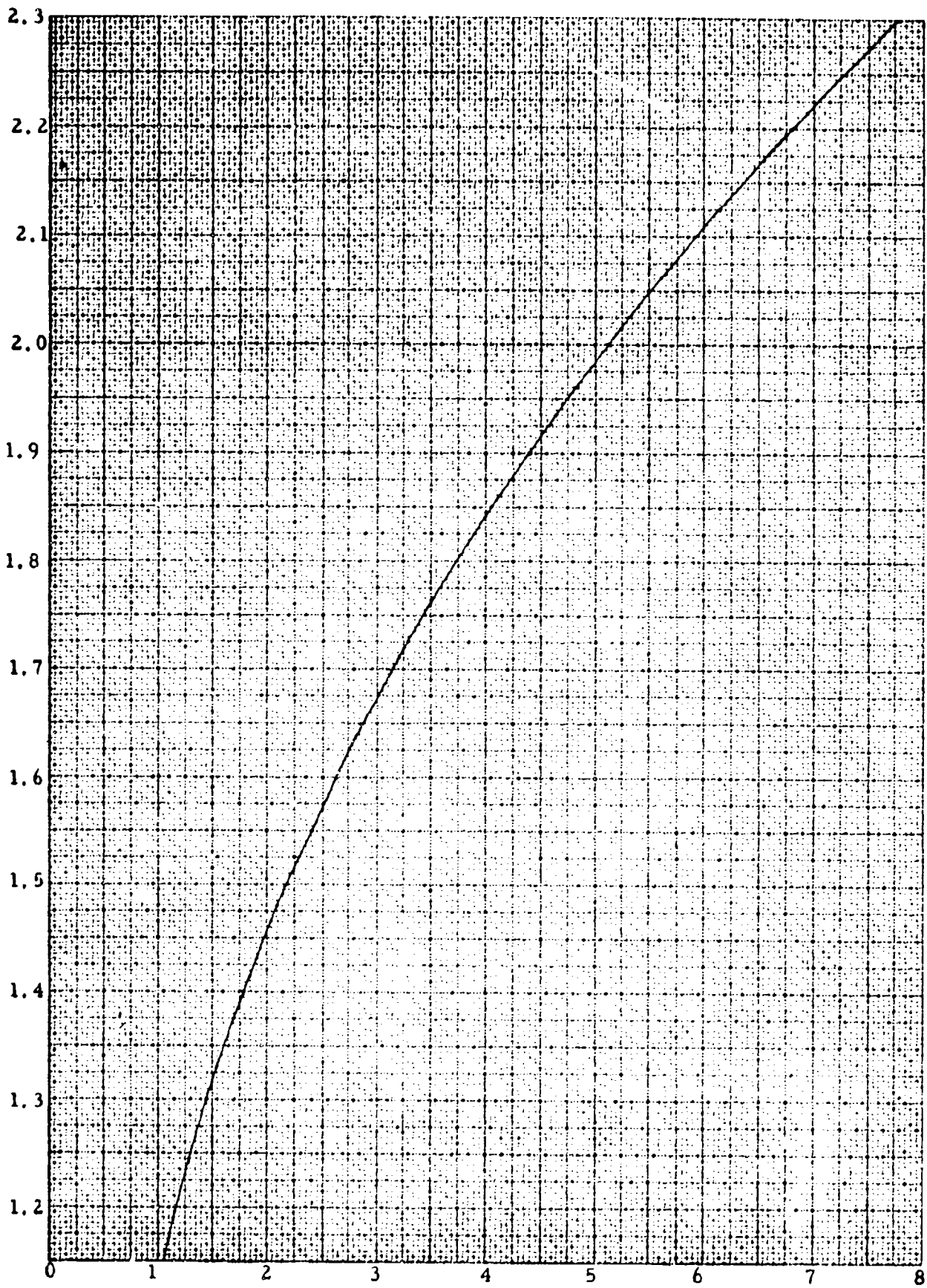


CHART 8.17

INDICATED MACH NUMBER, M_{ic}



$\Delta M_{pc} / (\Delta P_p / \rho_{cic})$

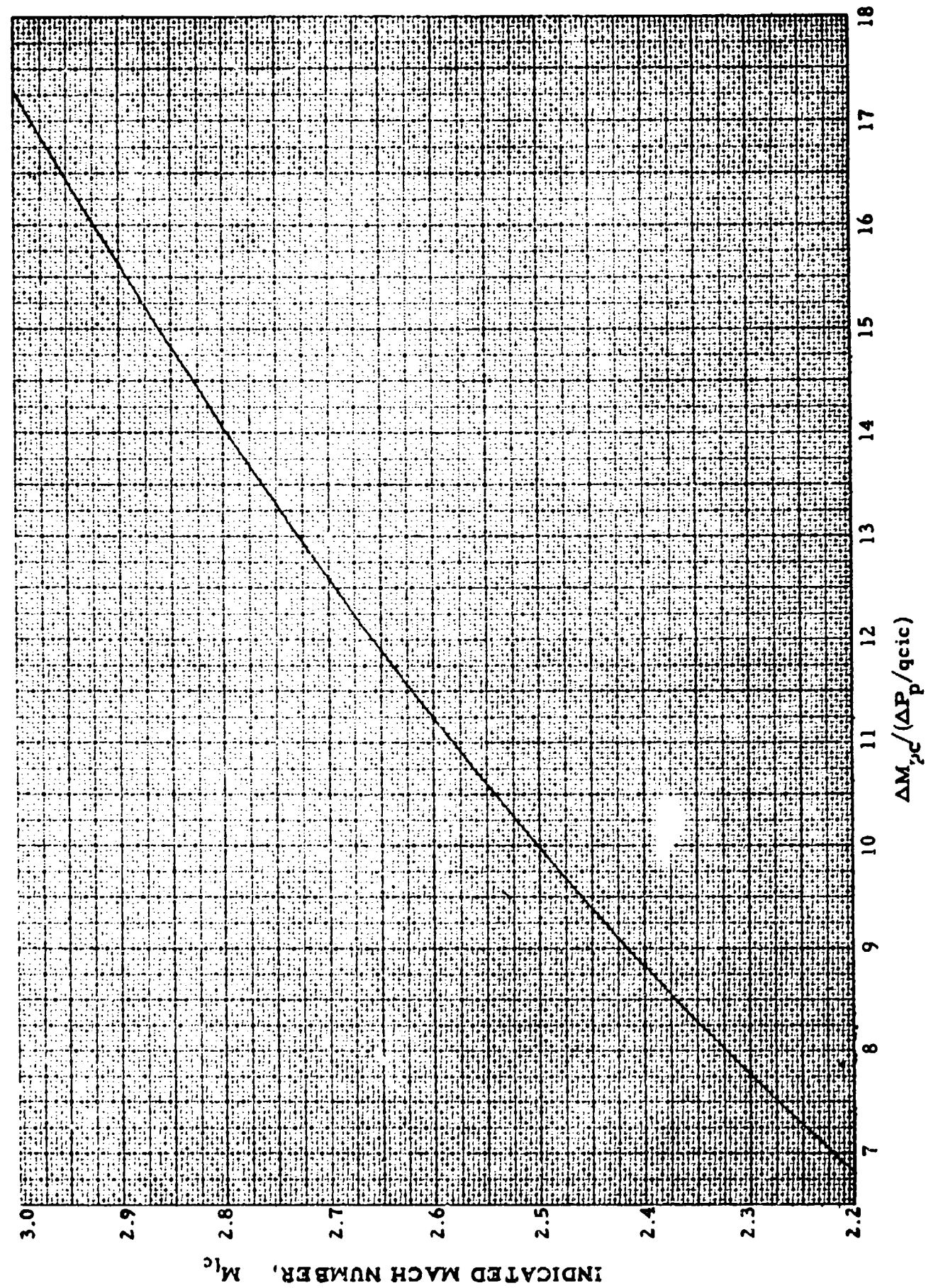


CHART 8.17

CHART 8.18

(See paragraph 5.3.7)

POSITION ERROR PRESSURE COEFFICIENT, $\Delta P_p/q_{cic}$ versus MACH METER POSITION ERROR CORRECTION, ΔM_{pc} for INDICATED MACH NUMBER CORRECTED FOR INSTRUMENT ERROR, $M_{ic} = \text{CONSTANT}$

$$\frac{\Delta P_p}{q_{cic}} = \frac{\frac{1.4 M_{ic} \Delta M_{pc}}{(1 + 0.2 M_{ic}^2)} + \frac{0.7 (1 - 1.6 M_{ic}^2) \Delta M_{pc}^2}{(1 + 0.2 M_{ic}^2)^2}}{(1 + 0.2 M_{ic}^2)^{3.5} - 1} \quad M_{ic} \leq 1.00$$

$$\frac{\Delta P_p}{q_{cic}} = \frac{\frac{7 (2 M_{ic}^2 - 1)}{M_{ic} (7 M_{ic}^2 - 1)} \Delta M_{pc} - \frac{7 (21 M_{ic}^4 - 23.5 M_{ic}^2 + 4) \Delta M_{pc}^2}{M_{ic}^2 (7 M_{ic}^2 - 1)^2}}{\left[\frac{166.921 M_{ic}^7}{(7 M_{ic}^2 - 1)^{2.5}} - 1 \right]} \quad M_{ic} \geq 1.00$$

Example:

Given: $M_{ic} = 1.00$; $\Delta P_p/q_{cic} = +0.14$

Required: ΔM_{pc}

Solution: Use Page 1 of Chart 8.18 for positive errors. For the given conditions,

$$\Delta M_{pc} = +0.111$$

Note: The approximate solution is found from Chart 8.17 to be

$$\Delta M_{pc} = +0.107$$

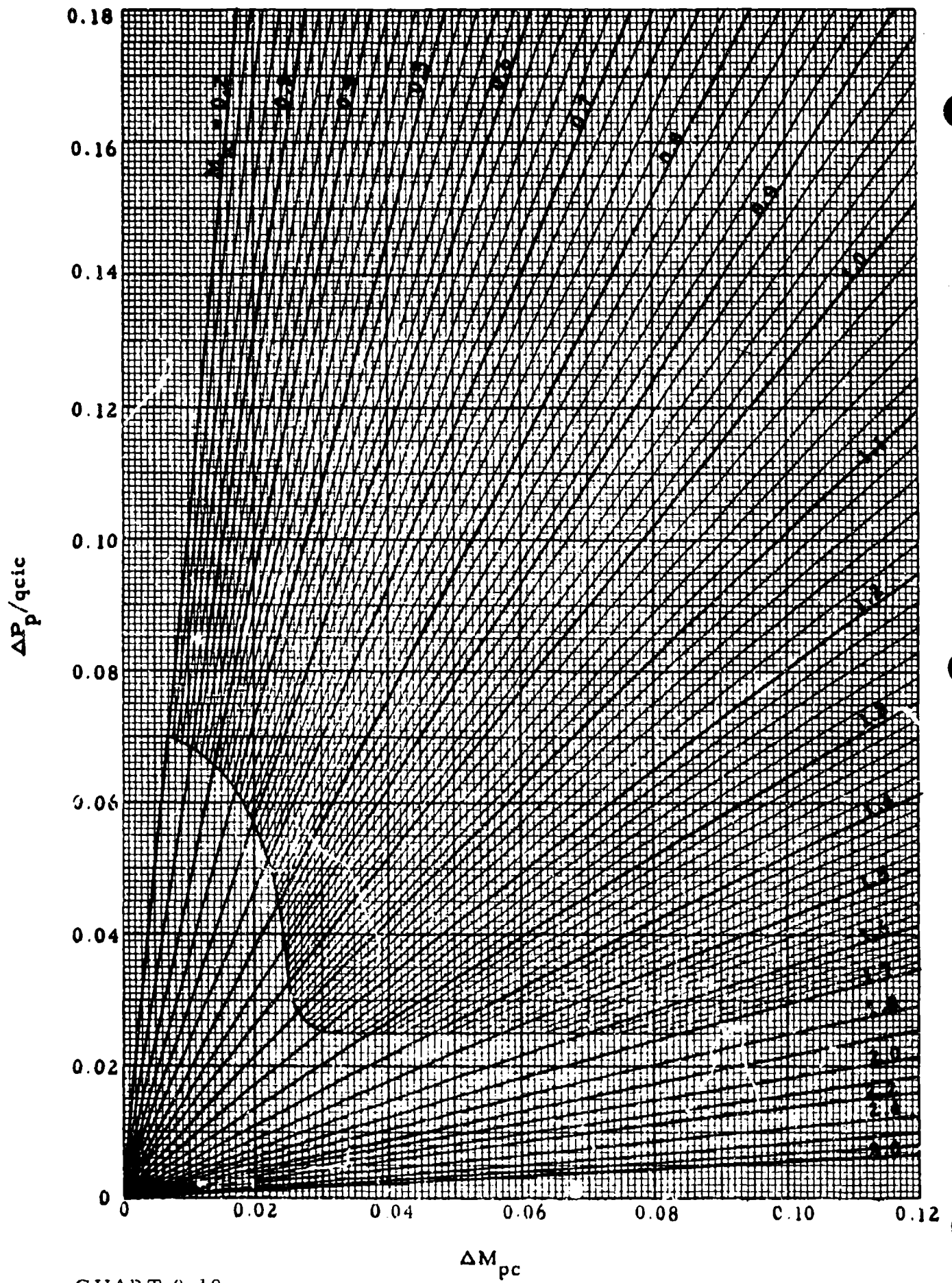
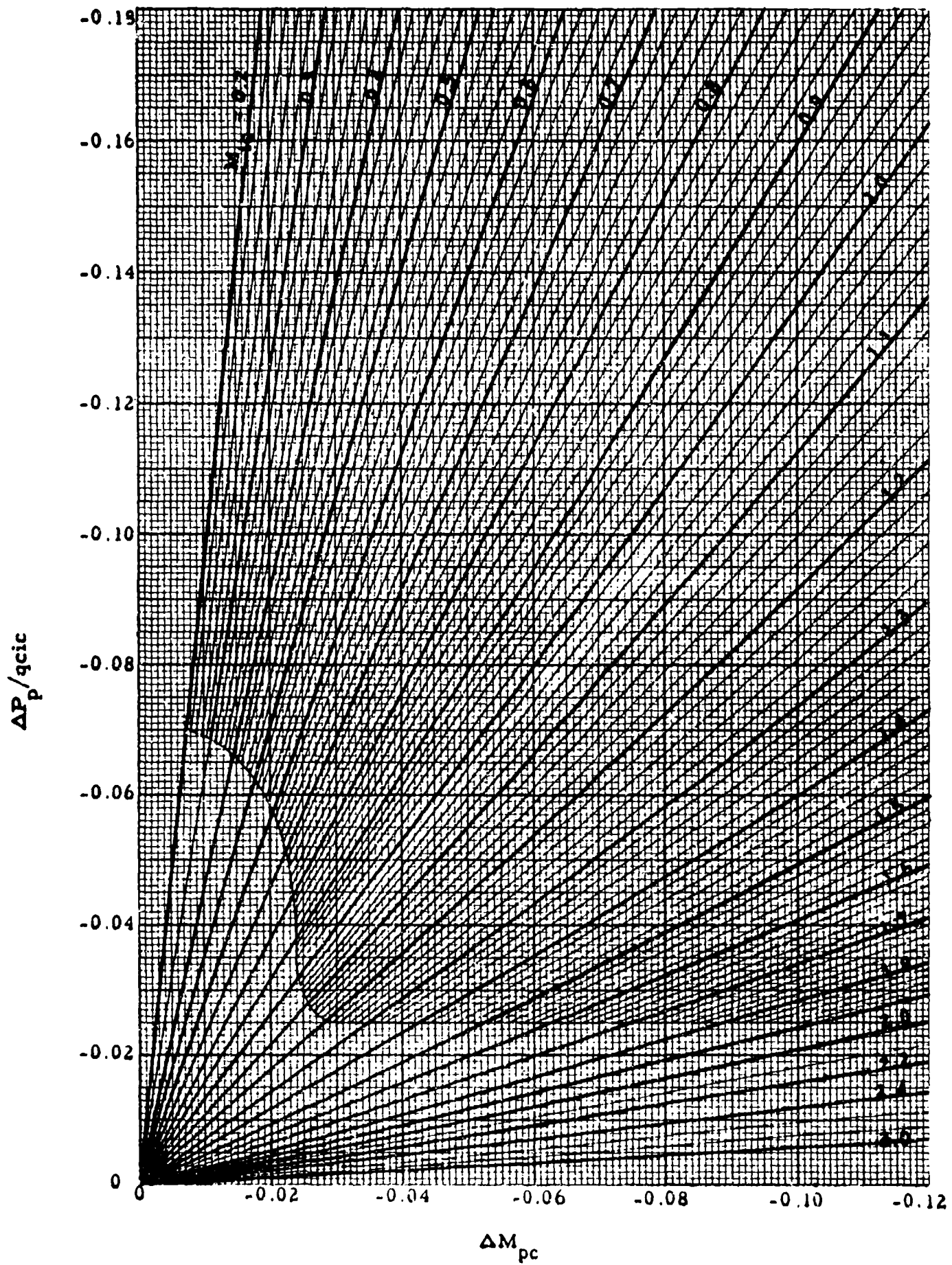


CHART 8.18

ΔM_{pc}



$\Delta P_p / q_{cic}$

ΔM_{pc}

CHART 8.18

TABLE 9.1

UNITED STATES STANDARD ATMOSPHERE - SUMMARY OF BASIC DATA

From NACA Report 1235

Element	Symbol	Values		
		In c.g.s. System	In m.k.s. System	In English System
Standard Sea Level Temperature	t _{SL}	15°C	15°C	59°F
Standard Sea Level Temperature	T _{SL}	288.16°K	288.16°K	518.688°R
Standard Sea Level Pressure	P _{SL}	1.013250 x 10 ⁶ dynes cm ⁻²	1013.250mb	1013.250mb
		76cmHg(std)	760mmHg (std)	29.92126 in.Hg(std)
Standard Sea Level Density	ρ _{SL}	1.2250 x 10 ⁻³ gm cm ⁻³	10332.27 kg m ⁻³	2116.216 lb ft ⁻³
			0.12492 kg sec ² m ⁻⁴	0.0023769 lb sec ² ft ⁻⁴
Geopotential of Tropopause	H*	1.0787315 x 10 ⁹ cm ² sec ⁻²	1.2250 kg (mass)m ⁻³	0.076475 lb (mass) ft ⁻³
Standard Temperature at the Tropopause	t*	-56.50°C	11,000 m'	36,089.24 ft'
Standard Temperature at the Tropopause	T*	-56.50°C	-56.50°C	-69.7°F
Pressure at the Tropopause	P*	216.66°K	216.66°K	389.988°R
		2.2632 x 10 ⁵ dynes cm ⁻²	226.32 mb	226.32 mb
		16.975 cmHg(std)	169.75 mmHg (std)	6.683 in.Hg (std)
Density at Geopotential H*	ρ*	3.6392 x 10 ⁻⁴ gm cm ⁻³	2307.8 kg m ⁻³	472.68 lb ft ⁻³
			0.037109 kg sec ² m ⁻⁴	0.00070612 lb sec ² ft ⁻⁴
Temperature Lapse Rate in Troposphere		6.628155 x 10 ⁻⁸ °C cm ⁻² sec ²	0.0065°C m ⁻¹	0.00356616°F ft ⁻¹
Standard Sea Level Speed of Sound	a _{SL}	34030 cm sec ⁻¹	340.30 m sec ⁻¹	1116.45 sec ⁻¹ ft 661.48 knots
Standard Sea Level Gravitational Acceleration	g _{SL}	980.665 cm sec ⁻²	9.80665 m sec ⁻²	32.17405 ft sec ⁻²

Values

Element	Symbol	In c.g.s. System	In m. k. s. System	In English System
Coefficient of Viscosity of Air at Temperature TSL	μ_{SL}	$1.7932 \times 10^{-4} \text{ gm cm}^{-1} \text{ sec}^{-1}$	$1.8286 \times 10^{-6} \text{ kg sec m}^{-2}$ $1.7932 \times 10^{-5} \text{ kg mass m}^{-1} \text{ sec}^{-1}$	$3.7452 \times 10^{-7} \text{ lb sec ft}^{-2}$ $1.2050 \times 10^{-5} \text{ lb mass ft}^{-1} \text{ sec}^{-1}$
Standard Sea Level Specific Weight	ρ_{SL}	$1.20131 \text{ gm cm}^{-2} \text{ sec}^{-2}$	1.2250 kg m^{-3} $12.013 \text{ kg mass m}^{-2} \text{ sec}^{-2}$	$0.076475 \text{ lb ft}^{-3}$ $2.46051 \text{ lb mass ft}^{-2} \text{ sec}^{-2}$
Dimensional constant, the amount of which determines the magnitude of the unit of H in terms of fundamental units of length and time	G	1	$9.80665 \text{ m}^2 \text{ sec}^{-2} \text{ m}^{-1}$	$32.17405 \text{ ft}^2 \text{ sec}^{-2} \text{ ft}^{-1}$
Gas Constant for Dry Air	R	$2.8704 \times 10^6 \text{ cm}^2 \text{ sec}^{-2} \text{ K}^{-1}$	$2.8704 \times 10^2 \text{ m}^2 \text{ sec}^{-2} \text{ K}^{-1}$	$17.165 \times 10^2 \text{ ft}^2 \text{ sec}^{-2} \text{ R}^{-1}$
Apparent Molecular Weight of Dry Air	M	28.966 gm mol ⁻¹	-----	-----

Note: Prime quantities represent geopotential units

Example: 1m' = 1 geopotential meter

Conversion Factors

- 1 foot = 0.3048 meter
- 1 pound = 0.4535923 kilogram
- 1 nautical mile = 6076.1033 feet
- °K = 273.16 + °C

TABLES 9.2 AND 9.3
THE UNITED STATES STANDARD ATMOSPHERE

For pressure altitude, $H_c < 36,089.24$ feet:

$$P_a = P_{aSL} (1 - 6.87535 \times 10^{-6} H_c)^{5.2561}$$

$$T_a = T_{aSL} (1 - 6.87535 \times 10^{-6} H_c)$$

$$\rho = \rho_{SL} (1 - 6.87535 \times 10^{-6} H_c)^{4.2561}$$

$$a = a_{SL} \left(\frac{T_a}{T_{aSL}} \right)^{0.5}$$

For pressure altitude, $H_c > 36,089.24$ feet:

$$P_a = 6.6832 e^{-4.80634 \times 10^{-5} (H_c - 36,089.24)}$$

$$T_a = 216.66 \text{ } ^\circ\text{K}$$

$$\rho = 0.00070612 e^{-4.80634 \times 10^{-5} (H_c - 36,089.24)}$$

$$a = 573.58 \text{ knots}$$

Preceding page blank

TABLE 9.2

THE UNITED STATES STANDARD ATMOSPHERE

Hc (Feet)	P _a ("Hg)	δ P _a /P _{aSL}	1/ δ	T _a (°K)	$\sqrt{T_a}$	θ T _a /T _{aSL}	$\sqrt{\theta}$
-1000	31.018	1.0366	.9646	290.15	17.034	1.0069	1.0034
-900	30.907	1.0329	.9680	289.95	17.028	1.0062	1.0031
-800	30.796	1.0292	.9715	289.74	17.022	1.0055	1.0027
-700	30.686	1.0255	.9750	289.54	17.016	1.0048	1.0024
-600	30.575	1.0218	.9785	289.34	17.010	1.0041	1.0021
-500	30.465	1.0182	.9821	289.14	17.004	1.0034	1.0017
-400	30.356	1.0145	.9856	288.97	16.999	1.0028	1.0014
-300	30.247	1.0108	.9892	288.77	16.993	1.0021	1.0010
-200	30.138	1.0072	.9928	288.56	16.987	1.0014	1.0007
-100	30.029	1.0036	.9963	288.36	16.981	1.0007	1.0003
0	29.921	1.0000	1.0000	288.16	16.975	1.0000	1.0000
100	29.813	.9963	1.0036	287.96	16.969	.9993	.9997
200	29.705	.9927	1.0072	287.76	16.963	.9986	.9993
300	29.598	.9892	1.0109	287.55	16.957	.9979	.9990
400	29.491	.9856	1.0145	287.35	16.951	.9972	.9986
500	29.384	.9820	1.0182	287.18	16.946	.9966	.9983
600	29.278	.9785	1.0219	286.98	16.940	.9959	.9979
700	29.172	.9749	1.0255	286.78	16.934	.9952	.9976
800	29.066	.9714	1.0294	286.58	16.929	.9945	.9972
900	28.960	.9679	1.0331	286.37	16.923	.9938	.9969
1000	28.855	.9643	1.0369	286.17	16.917	.9931	.9966
1100	28.750	.9608	1.0407	285.97	16.911	.9924	.9962
1200	28.646	.9573	1.0445	285.77	16.905	.9917	.9959
1300	28.542	.9539	1.0483	285.60	16.900	.9911	.9955
1400	28.438	.9504	1.0521	285.39	16.894	.9904	.9952
1500	28.334	.9469	1.0559	285.19	16.888	.9897	.9948
1600	28.231	.9435	1.0598	284.99	16.882	.9890	.9945
1700	28.128	.9400	1.0637	284.79	16.876	.9883	.9941
1800	28.025	.9366	1.0676	284.59	16.870	.9876	.9938
1900	27.923	.9332	1.0715	284.39	16.864	.9869	.9934
2000	27.821	.9298	1.0754	284.18	16.858	.9862	.9931
2100	27.719	.9264	1.0794	284.01	16.853	.9856	.9928
2200	27.617	.9230	1.0834	283.81	16.847	.9849	.9924
2300	27.516	.9196	1.0873	283.61	16.841	.9842	.9921
2400	27.415	.9162	1.0913	283.41	16.835	.9835	.9917
2500	27.315	.9129	1.0954	283.20	16.829	.9828	.9914
2600	27.214	.9095	1.0994	283.00	16.823	.9821	.9910
2700	27.114	.9062	1.1034	282.80	16.817	.9814	.9907
2800	27.015	.9028	1.1075	282.60	16.811	.9807	.9903
2900	26.915	.8995	1.1116	282.43	16.806	.9801	.9900

TABLE 9.3

THE UNITED STATES STANDARD ATMOSPHERE

H_c (Feet)	σ ρ/ρ_{SL}	$\sqrt{\sigma}$	$1/\sqrt{\sigma}$	$\sqrt{\theta/\theta_0}$	$1/\delta\sqrt{\theta}$	a (Knots)
-1000	1.0296	1.0147	.9855	.9679	.9613	663.73
-900	1.0266	1.0132	.9870	.9711	.9652	663.52
-800	1.0236	1.0117	.9884	.9742	.9689	663.27
-700	1.0206	1.0103	.9898	.9774	.9727	663.07
-600	1.0176	1.0088	.9913	.9807	.9767	662.97
-500	1.0147	1.0073	.9928	.9838	.9805	662.60
-400	1.0117	1.0059	.9941	.9870	.9843	662.41
-300	1.0088	1.0044	.9956	.9902	.9882	662.14
-200	1.0058	1.0029	.9971	.9935	.9922	661.94
-100	1.0029	1.0015	.9985	.9967	.9961	661.68
0	1.0000	1.0000	1.0000	1.0000	1.0000	661.48
100	.9970	.9985	1.0015	1.0033	1.0040	661.28
200	.9941	.9971	1.0029	1.0066	1.0080	661.02
300	.9912	.9956	1.0044	1.0099	1.0121	660.82
400	.9883	.9942	1.0058	1.0132	1.0161	660.55
500	.9854	.9927	1.0074	1.0165	1.0200	660.36
600	.9825	.9912	1.0089	1.0198	1.0241	660.09
700	.9796	.9898	1.0103	1.0232	1.0282	659.89
800	.9768	.9883	1.0116	1.0265	1.0323	659.63
900	.9739	.9869	1.0133	1.0300	1.0364	659.43
1000	.9710	.9854	1.0148	1.0334	1.0406	659.23
1100	.9682	.9840	1.0163	1.0368	1.0448	658.97
1200	.9653	.9825	1.0178	1.0402	1.0490	658.77
1300	.9625	.9811	1.0193	1.0436	1.0530	658.50
1400	.9596	.9796	1.0208	1.0471	1.0573	658.31
1500	.9568	.9782	1.0223	1.0505	1.0615	658.04
1600	.9540	.9767	1.0239	1.0540	1.0658	657.84
1700	.9511	.9753	1.0253	1.0575	1.0700	657.58
1800	.9483	.9739	1.0268	1.0610	1.0743	657.38
1900	.9455	.9724	1.0284	1.0645	1.0787	657.12
2000	.9427	.9710	1.0299	1.0681	1.0831	656.92
2100	.9399	.9695	1.0315	1.0717	1.0874	656.72
2200	.9371	.9681	1.0330	1.0752	1.0918	656.45
2300	.9344	.9666	1.0346	1.0788	1.0962	656.26
2400	.9316	.9652	1.0361	1.0823	1.1006	655.99
2500	.9288	.9638	1.0376	1.0860	1.1050	655.79
2600	.9261	.9623	1.0392	1.0895	1.1094	655.53
2700	.9233	.9609	1.0407	1.0932	1.1140	655.33
2800	.9205	.9595	1.0422	1.0968	1.1184	655.07
2900	.9178	.9581	1.0437	1.1006	1.1230	654.87

H_c (Feet)	P_a ("Hg)	δ P_a/P_{aSL}	$1/\epsilon$	T_a (°K)	$\sqrt{T_a}$	θ T_a/T_{aSL}	$\sqrt{\theta}$
3000	26.816	.8962	1.1157	282.22	16.800	.9794	.9896
3100	26.717	.8929	1.1198	282.02	16.794	.9787	.9893
3200	26.619	.8896	1.1240	281.82	16.788	.9780	.9889
3300	26.521	.8863	1.1282	281.62	16.782	.9773	.9886
3400	26.423	.8830	1.1323	281.42	16.775	.9766	.9882
3500	26.325	.8798	1.1365	281.22	16.769	.9759	.9879
3600	26.228	.8765	1.1407	281.01	16.763	.9752	.9875
3700	26.131	.8733	1.1450	280.84	16.758	.9746	.9872
3800	25.034	.8701	1.1492	280.64	16.752	.9739	.9869
3900	25.938	.8668	1.1535	280.44	16.746	.9732	.9865
4000	25.841	.8636	1.1578	280.24	16.740	.9725	.9862
4100	25.746	.8604	1.1621	280.03	16.734	.9718	.9858
4200	25.650	.8572	1.1665	279.83	16.728	.9711	.9855
4300	25.555	.8540	1.1708	279.63	16.722	.9704	.9851
4400	25.460	.8509	1.1752	279.43	16.716	.9697	.9848
4500	25.365	.8477	1.1796	279.26	16.711	.9691	.9844
4600	25.270	.8445	1.1840	279.05	16.705	.9684	.9841
4700	25.176	.8414	1.1884	278.85	16.699	.9677	.9837
4800	25.082	.8382	1.1929	278.65	16.693	.9670	.9834
4900	24.989	.8351	1.1973	278.45	16.687	.9663	.9830
5000	24.895	.8320	1.2018	278.25	16.681	.9656	.9827
5100	24.802	.8289	1.2063	278.05	16.675	.9649	.9823
5200	24.710	.8258	1.2108	277.84	16.669	.9642	.9820
5300	24.617	.8227	1.2154	277.67	16.663	.9636	.9816
5400	24.525	.8196	1.2200	277.47	16.657	.9629	.9813
5500	24.433	.8166	1.2245	277.27	16.651	.9622	.9809
5600	24.342	.8135	1.2292	277.07	16.645	.9615	.9806
5700	24.250	.8104	1.2338	276.86	16.639	.9608	.9802
5800	24.159	.8074	1.2384	276.66	16.633	.9601	.9799
5900	24.068	.8044	1.2431	276.46	16.627	.9594	.9795
6000	23.978	.8013	1.2478	276.26	16.621	.9587	.9792
6100	23.888	.7983	1.2525	276.09	16.616	.9581	.9788
6200	23.798	.7953	1.2572	275.88	16.610	.9574	.9785
6300	23.708	.7923	1.2620	275.68	16.604	.9567	.9781
6400	23.618	.7893	1.2668	275.48	16.598	.9560	.9778
6500	23.529	.7863	1.2716	275.28	16.592	.9553	.9774
6600	23.440	.7834	1.2764	275.08	16.585	.9546	.9770
6700	23.352	.7804	1.2812	274.88	16.579	.9539	.9767
6800	23.264	.7775	1.2861	274.67	16.573	.9532	.9763
6900	23.175	.7745	1.2910	274.50	16.568	.9526	.9760

H_c (Feet)	$\frac{\sigma}{\rho/PSL}$	$\sqrt{\sigma}$	$1/\sqrt{\sigma}$	$\sqrt{\theta/\delta}$	$1/\delta\sqrt{\theta}$	a (Knots)
3000	.9151	.9566	1.0454	1.1042	1.1275	654.59
3100	.9123	.9552	1.0469	1.1079	1.1321	654.39
3200	.9096	.9538	1.0484	1.1116	1.1367	654.13
3300	.9069	.9523	1.0501	1.1153	1.1412	653.93
3400	.9042	.9509	1.0516	1.1190	1.1458	653.67
3500	.9015	.9495	1.0532	1.1228	1.1506	653.47
3600	.8988	.9481	1.0547	1.1265	1.1552	653.20
3700	.8961	.9466	1.0564	1.1304	1.1599	653.01
3800	.8934	.9452	1.0580	1.1342	1.1647	652.81
3900	.8907	.9438	1.0595	1.1380	1.1694	652.54
4000	.8880	.9424	1.0611	1.1419	1.1743	652.34
4100	.8854	.9410	1.0627	1.1457	1.1789	652.08
4200	.8827	.9395	1.0644	1.1496	1.1838	651.88
4300	.8801	.9381	1.0660	1.1534	1.1886	651.62
4400	.8774	.9367	1.0676	1.1574	1.1936	651.42
4500	.8748	.9353	1.0692	1.1612	1.1983	651.15
4600	.8721	.9339	1.0708	1.1652	1.2033	650.96
4700	.8695	.9325	1.0724	1.1691	1.2082	650.69
4800	.8669	.9311	1.0740	1.1731	1.2132	650.49
4900	.8643	.9297	1.0756	1.1770	1.2180	650.23
5000	.8616	.9283	1.0772	1.1811	1.2232	650.03
5100	.8590	.9269	1.0789	1.1850	1.2281	649.76
5200	.8564	.9255	1.0805	1.1891	1.2333	649.57
5300	.8538	.9241	1.0821	1.1931	1.2382	649.30
5400	.8512	.9226	1.0839	1.1972	1.2434	649.10
5500	.8487	.9212	1.0855	1.2012	1.2485	648.84
5600	.8461	.9198	1.0872	1.2054	1.2538	648.64
5700	.8435	.9184	1.0889	1.2094	1.2587	648.38
5800	.8409	.9171	1.0904	1.2136	1.2640	648.18
5900	.8384	.9156	1.0922	1.2177	1.2692	647.91
6000	.8358	.9143	1.0937	1.2219	1.2746	647.71
6100	.8333	.9129	1.0954	1.2260	1.2797	647.45
6200	.8307	.9115	1.0971	1.2303	1.2851	647.25
6300	.8282	.9101	1.0988	1.2344	1.2904	646.99
6400	.8257	.9087	1.1005	1.2387	1.2958	646.79
6500	.8231	.9073	1.1022	1.2429	1.3010	646.52
6600	.8206	.9059	1.1039	1.2471	1.3064	646.26
6700	.8181	.9045	1.1056	1.2514	1.3119	646.06
6800	.8156	.9031	1.1073	1.2557	1.3174	645.80
6900	.8131	.9017	1.1090	1.2601	1.3229	645.60

H_c (Feet)	P_a ("Hg)	δ P_a/P_{aSL}	$1/\delta$	T_a (°K)	$\sqrt{T_a}$	θ T_a/T_{aSL}	$\sqrt{\theta}$
7000	23.088	.7716	1.2959	274.30	16.562	.9519	.9756
7100	23.000	.7687	1.3008	274.10	16.556	.9512	.9753
7200	22.913	.7657	1.3058	273.90	16.550	.9505	.9749
7300	22.826	.7628	1.3108	273.69	16.544	.9498	.9746
7400	22.739	.7599	1.3158	273.49	16.538	.9491	.9742
7500	22.653	.7570	1.3208	273.29	16.532	.9484	.9739
7600	22.567	.7542	1.3258	273.09	16.525	.9477	.9735
7700	22.481	.7513	1.3309	272.92	16.520	.9471	.9732
7800	22.395	.7484	1.3360	272.71	16.514	.9464	.9728
7900	22.310	.7456	1.3411	272.51	16.508	.9457	.9725
8000	22.225	.7427	1.3462	272.31	16.502	.9450	.9721
8100	22.140	.7399	1.3514	272.11	16.496	.9443	.9718
8200	22.055	.7371	1.3566	271.91	16.490	.9436	.9714
8300	21.971	.7343	1.3618	271.71	16.484	.9429	.9710
8400	21.887	.7314	1.3670	271.50	16.477	.9422	.9707
8500	21.803	.7286	1.3723	271.33	16.472	.9416	.9703
8600	21.719	.7259	1.3776	271.13	16.466	.9409	.9700
8700	21.636	.7231	1.3829	270.93	16.460	.9402	.9696
8800	21.553	.7203	1.3882	270.73	16.454	.9395	.9693
8900	21.470	.7175	1.3935	270.52	16.448	.9388	.9689
9000	21.388	.7148	1.3989	270.32	16.441	.9381	.9686
9100	21.305	.7120	1.4043	270.12	16.435	.9374	.9682
9200	21.223	.7093	1.4098	269.92	16.429	.9367	.9679
9300	21.142	.7065	1.4152	269.75	16.424	.9361	.9675
9400	21.060	.7038	1.4207	269.54	16.418	.9354	.9671
9500	20.979	.7011	1.4262	269.34	16.412	.9347	.9668
9600	20.898	.6984	1.4317	269.14	16.406	.9340	.9664
9700	20.817	.6957	1.4372	268.94	16.399	.9333	.9661
9800	20.737	.6930	1.4428	268.74	16.393	.9326	.9657
9900	20.656	.6903	1.4484	268.54	16.387	.9319	.9654
10000	20.577	.6877	1.4541	268.33	16.381	.9312	.9650
10100	20.497	.6850	1.4597	268.16	16.376	.9306	.9647
10200	20.417	.6823	1.4654	267.96	16.369	.9299	.9643
10300	20.338	.6797	1.4711	267.76	16.363	.9292	.9639
10400	20.259	.6771	1.4768	267.56	16.357	.9285	.9636
10500	20.180	.6744	1.4826	267.35	16.351	.9278	.9632
10600	20.102	.6718	1.4884	267.15	16.345	.9271	.9629
10700	20.024	.6692	1.4942	266.95	16.339	.9264	.9625
10800	19.946	.6666	1.5001	266.75	16.332	.9257	.9622
10900	19.868	.6640	1.5059	266.58	16.327	.9251	.9618

TABLE 9.2

H_c (Feet)	σ ρ/ρ_{SL}	$\sqrt{\sigma}$	$1/\sqrt{\sigma}$	$\sqrt{\theta/\delta}$	$1/\delta\sqrt{\theta}$	a (Knots)
7000	.8106	.9004	1.1106	1.2643	1.3283	645.34
7100	.8081	.8990	1.1123	1.2688	1.3340	645.15
7200	.8056	.8976	1.1141	1.2731	1.3395	644.88
7300	.8032	.8962	1.1158	1.2775	1.3451	644.68
7400	.8007	.8948	1.1176	1.2819	1.3506	644.42
7500	.7982	.8935	1.1192	1.2864	1.3564	644.22
7600	.7958	.8921	1.1210	1.2908	1.3621	643.96
7700	.7933	.8907	1.1227	1.2953	1.3678	643.76
7800	.7909	.8893	1.1245	1.2997	1.3734	643.59
7900	.7884	.8880	1.1261	1.3043	1.3793	643.29
8000	.7860	.8866	1.1279	1.3087	1.3850	643.03
8100	.7836	.8852	1.1297	1.3133	1.3909	642.85
8200	.7811	.8838	1.1315	1.3178	1.3966	642.57
8300	.7787	.8825	1.1331	1.3223	1.402	642.30
8400	.7763	.8811	1.1349	1.3270	1.408	642.10
8500	.7739	.8797	1.1368	1.3316	1.414	641.84
8600	.7715	.8784	1.1384	1.3363	1.420	641.64
8700	.7691	.8770	1.1403	1.3409	1.426	641.38
8800	.7667	.8756	1.1421	1.3456	1.432	641.18
8900	.7643	.8743	1.1438	1.3503	1.438	640.91
9000	.7619	.8729	1.1456	1.3550	1.444	640.72
9100	.7595	.8715	1.1474	1.3597	1.450	640.45
9200	.7572	.8702	1.1492	1.3645	1.456	640.25
9300	.7548	.8688	1.1510	1.3693	1.462	639.99
9400	.7525	.8675	1.1527	1.3740	1.469	639.72
9500	.7501	.8661	1.1546	1.3789	1.475	639.52
9600	.7478	.8648	1.1563	1.3836	1.481	639.26
9700	.7454	.8634	1.1582	1.3886	1.487	639.06
9800	.7431	.8621	1.1600	1.3934	1.494	638.79
9900	.7408	.8607	1.1618	1.3984	1.500	638.59
10000	.7384	.8593	1.1637	1.4032	1.506	638.31
10100	.7361	.8580	1.1655	1.4082	1.513	638.13
10200	.7338	.8566	1.1674	1.4131	1.519	637.86
10300	.7315	.8553	1.1692	1.4180	1.526	637.60
10400	.7292	.8540	1.1710	1.4231	1.532	637.40
10500	.7269	.8526	1.1729	1.4281	1.539	637.13
10600	.7246	.8513	1.1747	1.4332	1.545	636.94
10700	.7223	.8499	1.1766	1.4382	1.552	636.67
10800	.7200	.8486	1.1784	1.4434	1.559	636.47
10900	.7178	.8472	1.1804	1.4485	1.566	636.21

H_c (Feet)	P_a ("Hg)	δ P_a/P_{aSL}	$1/\delta$	T_a (°K)	$\sqrt{T_a}$	θ T_a/T_{aSL}	$\sqrt{\theta}$
11000	19.790	.6614	1.5118	266.38	16.321	.9244	.9614
11100	19.713	.6588	1.5177	266.17	16.315	.9237	.9611
11200	19.636	.6562	1.5237	265.97	16.309	.9230	.9607
11300	19.559	.6537	1.5297	265.77	16.302	.9223	.9604
11400	19.483	.6511	1.5357	265.57	16.296	.9216	.9600
11500	19.407	.6486	1.5417	265.37	16.290	.9209	.9597
11600	19.331	.6460	1.5478	265.16	16.284	.9202	.9593
11700	19.255	.6435	1.5539	264.99	16.279	.9196	.9589
11800	19.179	.6410	1.5600	264.79	16.272	.9189	.9586
11900	19.104	.6384	1.5661	264.59	16.266	.9182	.9582
12000	19.029	.6359	1.5723	264.39	16.260	.9175	.9579
12100	18.954	.6334	1.5785	264.19	16.254	.9168	.9575
12200	18.879	.6309	1.5848	263.98	16.248	.9161	.9571
12300	18.805	.6285	1.5910	263.78	16.241	.9154	.9568
12400	18.731	.6260	1.5973	263.58	16.235	.9147	.9564
12500	18.657	.6235	1.6036	263.41	16.230	.9141	.9561
12600	18.583	.6210	1.6100	263.21	16.224	.9134	.9557
12700	18.510	.6186	1.6164	263.00	16.217	.9127	.9553
12800	18.437	.6161	1.6228	262.80	16.211	.9120	.9550
12900	18.364	.6137	1.6293	262.60	16.205	.9113	.9546
13000	18.291	.6113	1.6357	262.40	16.199	.9106	.9543
13100	18.219	.6089	1.6422	262.20	16.192	.9099	.9539
13200	18.147	.6064	1.6488	262.00	16.186	.9092	.9535
13300	18.075	.6040	1.6554	261.82	16.181	.9086	.9532
13400	18.003	.6016	1.6619	261.62	16.175	.9079	.9528
13500	17.931	.5992	1.6686	261.42	16.168	.9072	.9525
13600	17.860	.5969	1.6752	261.22	16.162	.9065	.9521
13700	17.789	.5945	1.6820	261.02	16.156	.9058	.9517
13800	17.718	.5921	1.6887	260.81	16.150	.9051	.9514
13900	17.647	.5898	1.6954	260.61	16.143	.9044	.9510
14000	17.577	.5874	1.7022	260.41	16.137	.9037	.9507
14100	17.507	.5851	1.7090	260.24	16.132	.9031	.9503
14200	17.437	.5827	1.7159	260.04	16.126	.9024	.9499
14300	17.367	.5804	1.7228	259.83	16.119	.9017	.9496
14400	17.298	.5781	1.7297	259.63	16.113	.9010	.9492
14500	17.228	.5758	1.7367	259.43	16.107	.9003	.9488
14600	17.159	.5735	1.7436	259.23	16.101	.8996	.9485
14700	17.090	.5712	1.7507	259.03	16.094	.8989	.9481
14800	17.022	.5689	1.7577	258.83	16.088	.8982	.9478
14900	16.953	.5666	1.7648	258.65	16.083	.8976	.9474

TABLE 9.2

H_c (Feet)	σ ρ/ρ_{SL}	$\sqrt{\sigma}$	$1/\sqrt{\sigma}$	$\sqrt{\theta/\delta}$	$1/\delta\sqrt{\theta}$	a (Knots)
11000	.7155	.8459	1.1822	1.4535	1.572	635.94
11100	.7132	.8446	1.1840	1.4588	1.579	635.75
11200	.7110	.8432	1.1860	1.4639	1.586	635.48
11300	.7087	.8419	1.1878	1.4692	1.593	635.28
11400	.7065	.8406	1.1896	1.4743	1.599	635.03
11500	.7043	.8392	1.1916	1.4796	1.6067	634.82
11600	.7020	.8379	1.1935	1.4848	1.6136	634.56
11700	.6998	.8366	1.1953	1.4901	1.6206	634.29
11800	.6976	.8352	1.1973	1.4955	1.6276	634.09
11900	.6953	.8339	1.1992	1.5007	1.6345	633.83
12000	.6931	.8326	1.2011	1.5062	1.6417	633.63
12100	.6909	.8312	1.2031	1.5115	1.6488	633.36
12200	.6887	.8299	1.2050	1.5168	1.6557	633.10
12300	.6865	.8286	1.2069	1.5224	1.6631	632.90
12400	.6843	.8273	1.2088	1.5277	1.6702	632.64
12500	.6821	.8259	1.2108	1.5333	1.6776	632.44
12600	.6800	.8246	1.2127	1.5387	1.6846	632.17
12700	.6778	.8233	1.2146	1.5442	1.6920	631.91
12800	.6756	.8220	1.2165	1.5498	1.6994	631.71
12900	.6735	.8207	1.2185	1.5553	1.7068	631.45
13000	.6713	.8194	1.2204	1.5610	1.7142	631.25
13100	.6691	.8180	1.2225	1.5666	1.7217	630.98
13200	.6670	.8167	1.2244	1.5722	1.7292	630.72
13300	.6648	.8154	1.2264	1.5779	1.7368	630.52
13400	.6627	.8141	1.2284	1.5835	1.7442	630.26
13500	.6606	.8128	1.2303	1.5894	1.7521	630.06
13600	.6584	.8115	1.2323	1.5950	1.7596	629.79
13700	.6563	.8102	1.2343	1.6008	1.7674	629.53
13800	.6542	.8089	1.2362	1.6066	1.7750	629.33
13900	.6521	.8076	1.2382	1.6124	1.7828	629.07
14000	.6500	.8062	1.2404	1.6184	1.7908	628.87
14100	.6479	.8049	1.2424	1.6241	1.7985	628.60
14200	.6458	.8036	1.2444	1.6300	1.8064	628.34
14300	.6437	.8023	1.2464	1.6360	1.8144	628.14
14400	.6416	.8010	1.2484	1.6419	1.8224	627.88
14500	.6395	.7997	1.2505	1.6478	1.8304	627.61
14600	.6375	.7984	1.2525	1.6539	1.8386	627.41
14700	.6354	.7971	1.2545	1.6598	1.8464	627.15
14800	.6333	.7958	1.2566	1.6660	1.8548	626.95
14900	.6313	.7945	1.2587	1.6720	1.8629	626.69

H_c (Feet)	P_a ("Hg)	δ P_a/P_{aSL}	$1/\delta$	T_a (°K)	$\sqrt{T_a}$	θ T_a/T_{aSL}	$\sqrt{\theta}$
15000	16.885	.5643	1.7719	258.45	16.076	.8969	.9470
15100	16.817	.5620	1.7791	258.25	16.070	.8962	.9467
15200	16.750	.5598	1.7863	258.05	16.064	.8955	.9463
15300	16.682	.5575	1.7935	257.85	16.058	.8948	.9459
15400	16.615	.5553	1.8008	257.64	16.051	.8941	.9456
15500	16.548	.5530	1.8081	257.44	16.045	.8934	.9452
15600	16.481	.5508	1.8154	257.24	16.039	.8927	.9449
15700	16.414	.5486	1.8228	257.07	16.033	.8921	.9445
15800	16.348	.5463	1.8302	256.87	16.027	.8914	.9441
15900	16.282	.5441	1.8376	256.66	16.021	.8907	.9438
16000	16.216	.5419	1.8451	256.46	16.014	.8900	.9434
16100	16.150	.5397	1.8526	256.26	16.008	.8893	.9430
16200	16.085	.5375	1.8601	256.06	16.002	.8886	.9427
16300	16.019	.5354	1.8677	255.86	15.996	.8879	.9423
16400	15.954	.5332	1.8753	255.66	15.989	.8872	.9419
16500	15.889	.5310	1.8830	255.48	15.984	.8866	.9416
16600	15.825	.5288	1.8907	255.28	15.978	.8859	.9412
16700	15.760	.5267	1.8984	255.08	15.971	.8852	.9408
16800	15.696	.5245	1.9062	254.88	15.965	.8845	.9405
16900	15.632	.5224	1.9140	254.68	15.959	.8838	.9401
17000	15.568	.5203	1.9218	254.47	15.952	.8831	.9397
17100	15.505	.5182	1.9297	254.27	15.946	.8824	.9394
17200	15.441	.5160	1.9376	254.07	15.940	.8817	.9390
17300	15.378	.5139	1.9456	253.90	15.934	.8811	.9386
17400	15.315	.5118	1.9536	253.70	15.928	.8804	.9383
17500	15.252	.5097	1.9617	253.49	15.922	.8797	.9379
17600	15.190	.5076	1.9697	253.29	15.915	.8790	.9375
17700	15.127	.5055	1.9778	253.09	15.909	.8783	.9372
17800	15.065	.5035	1.9860	252.89	15.902	.8776	.9368
17900	15.003	.5014	1.9942	252.69	15.896	.8769	.9364
18000	14.942	.4993	2.0024	252.49	15.890	.8762	.9361
18100	14.880	.4973	2.0107	252.31	15.884	.8756	.9357
18200	14.819	.4952	2.0191	252.11	15.878	.8749	.9353
18300	14.758	.4932	2.0274	251.91	15.872	.8742	.9350
18400	14.697	.4912	2.0358	251.71	15.865	.8735	.9346
18500	14.636	.4891	2.0442	251.51	15.859	.8728	.9342
18600	14.576	.4871	2.0527	251.30	15.853	.8721	.9339
18700	14.515	.4851	2.0613	251.10	15.846	.8714	.9335
18800	14.455	.4831	2.0698	250.90	15.840	.8707	.9331
18900	14.395	.4811	2.0784	250.73	15.834	.8701	.9328

TABLE 9.2

H_c (Feet)	σ ρ/PSL	$\sqrt{\sigma}$	$1/\sqrt{\sigma}$	$\sqrt{\theta/\delta}$	$1/\delta\theta$	a (Knots)
15000	.6292	.7932	1.2607	1.6781	1.8712	626.42
15100	.6271	.7920	1.2626	1.6843	1.8794	626.22
15200	.6251	.7907	1.2647	1.6904	1.8877	625.96
15300	.6231	.7894	1.2668	1.6965	1.8960	625.69
15400	.6210	.7881	1.2689	1.7029	1.9047	625.50
15500	.6190	.7868	1.2710	1.7090	1.9129	625.23
15600	.6170	.7855	1.2731	1.7154	1.9216	625.03
15700	.6149	.7842	1.2752	1.7217	1.9301	624.77
15800	.6129	.7829	1.2773	1.7279	1.9386	624.50
15900	.6109	.7816	1.2794	1.7344	1.9473	624.30
16000	.6089	.7804	1.2814	1.7407	1.9559	624.04
16100	.6069	.7791	1.2835	1.7470	1.9645	623.78
16200	.6049	.7778	1.2857	1.7536	1.9735	623.58
16300	.6029	.7765	1.2878	1.7600	1.9822	623.30
16400	.6009	.7752	1.2900	1.7664	1.9909	623.04
16500	.5990	.7740	1.2920	1.7731	2.0001	622.84
16600	.5970	.7727	1.2942	1.7796	2.0090	622.58
16700	.5950	.7714	1.2963	1.7861	2.0178	622.31
16800	.5931	.7701	1.2985	1.7928	2.0270	622.11
16900	.5911	.7689	1.3006	1.7994	2.0361	621.85
17000	.5891	.7676	1.3028	1.8060	2.0451	621.58
17100	.5872	.7663	1.3050	1.8128	2.0543	621.39
17200	.5853	.7651	1.3070	1.8195	2.0636	621.12
17300	.5833	.7638	1.3092	1.8262	2.0728	620.86
17400	.5814	.7625	1.3115	1.8331	2.0823	620.66
17500	.5794	.7612	1.3137	1.8399	2.0916	620.39
17600	.5775	.7600	1.3158	1.8467	2.1010	620.13
17700	.5756	.7587	1.3180	1.8537	2.1106	619.93
17800	.5737	.7575	1.3201	1.8605	2.1201	619.67
17900	.5718	.7562	1.3224	1.8674	2.1295	619.40
18000	.5699	.7549	1.3247	1.8745	2.1393	619.21
18100	.5680	.7537	1.3268	1.8815	2.1490	618.95
18200	.5661	.7524	1.3291	1.8885	2.1587	618.68
18300	.5642	.7511	1.3314	1.8957	2.1686	618.49
18400	.5623	.7499	1.3335	1.9027	2.1783	618.22
18500	.5604	.7486	1.3358	1.9098	2.1882	617.96
18600	.5585	.7474	1.3380	1.9171	2.1983	617.76
18700	.5567	.7461	1.3403	1.9242	2.2081	617.49
18800	.5548	.7449	1.3425	1.9314	2.2182	617.23
18900	.5529	.7436	1.3448	1.9388	2.2284	617.03

H _c (Feet)	P _a ("Hg)	δ P _a /P _{aSL}	1/ δ	T _a (°K)	$\sqrt{T_a}$	θ T _a /T _{aSL}	$\sqrt{\theta}$
19000	14.336	.4791	2.0871	250.53	15.828	.8694	.9324
19100	14.276	.4771	2.0958	250.32	15.822	.8687	.9320
19200	14.217	.4751	2.1045	250.12	15.815	.8680	.9317
19300	14.158	.4731	2.1133	249.92	15.809	.8673	.9313
19400	14.099	.4712	2.1221	249.72	15.803	.8666	.9309
19500	14.040	.4692	2.1310	249.52	15.796	.8659	.9306
19600	13.982	.4673	2.1399	249.32	15.790	.8652	.9302
19700	13.923	.4653	2.1489	249.14	15.784	.8646	.9298
19800	13.865	.4634	2.1579	248.94	15.778	.8639	.9294
19900	13.807	.4614	2.1669	248.74	15.771	.8632	.9291
20000	13.750	.4595	2.1760	248.54	15.765	.8625	.9287
20100	13.692	.4576	2.1852	248.34	15.759	.8618	.9283
20200	13.635	.4557	2.1944	248.13	15.752	.8611	.9280
20300	13.578	.4537	2.2036	247.93	15.746	.8604	.9276
20400	13.521	.4518	2.2129	247.73	15.739	.8597	.9272
20500	13.464	.4500	2.2222	247.56	15.734	.8591	.9269
20600	13.407	.4481	2.2315	247.36	15.728	.8584	.9265
20700	13.351	.4462	2.2410	247.15	15.721	.8577	.9261
20800	13.295	.4443	2.2504	246.95	15.715	.8570	.9257
20900	13.239	.4424	2.2600	246.75	15.708	.8563	.9254
21000	13.183	.4406	2.2695	246.55	15.702	.8556	.9250
21100	13.128	.4387	2.2792	246.35	15.695	.8549	.9246
21200	13.072	.4369	2.2888	246.15	15.689	.8542	.9243
21300	13.017	.4350	2.2985	245.97	15.684	.8536	.9239
21400	12.962	.4332	2.3082	245.77	15.677	.8529	.9235
21500	12.907	.4313	2.3180	245.57	15.671	.8522	.9231
21600	12.852	.4295	2.3279	245.37	15.664	.8515	.9228
21700	12.798	.4277	2.3378	245.17	15.658	.8508	.9224
21800	12.744	.4259	2.3478	244.96	15.651	.8501	.9220
21900	12.690	.4241	2.3578	244.76	15.645	.8494	.9216
22000	12.636	.4223	2.3678	244.56	15.638	.8487	.9213
22100	12.582	.4205	2.378	244.39	15.633	.8481	.9209
22200	12.529	.4187	2.388	244.19	15.626	.8474	.9205
22300	12.475	.4169	2.398	243.99	15.620	.8467	.9202
22400	12.422	.4151	2.408	243.78	15.614	.8460	.9198
22500	12.369	.4134	2.418	243.58	15.607	.8453	.9194
22600	12.316	.4116	2.429	243.38	15.601	.8446	.9190
22700	12.264	.4098	2.439	243.18	15.594	.8439	.9187
22800	12.211	.4081	2.450	242.98	15.588	.8432	.9183
22900	12.159	.4063	2.460	242.80	15.582	.8426	.9179

TABLE 9.2

H_c (Feet)	σ ρ/PSL	$\sqrt{\sigma}$	$1/\sqrt{\sigma}$	$\sqrt{\theta/\delta}$	$1/\delta\theta$	a (Knots)
19000	.5511	.7424	1.3470	1.9460	2.2385	616.77
19100	.5492	.7411	1.3493	1.9533	2.2486	616.50
19200	.5474	.7399	1.3515	1.9608	2.259	616.30
19300	.5455	.7386	1.3539	1.9682	2.269	616.04
19400	.5437	.7374	1.3561	1.9756	2.279	615.77
19500	.5419	.7361	1.3585	1.9832	2.290	615.58
19600	.5400	.7349	1.3607	1.9906	2.300	615.31
19700	.5382	.7337	1.3630	1.9981	2.311	615.05
19800	.5364	.7324	1.3654	2.0056	2.321	614.78
19900	.5346	.7312	1.3676	2.0133	2.332	614.58
20000	.5328	.7299	1.3701	2.0209	2.343	614.32
20100	.5310	.7287	1.3723	2.0285	2.353	614.05
20200	.5292	.7275	1.3746	2.0364	2.364	613.86
20300	.5274	.7262	1.3770	2.0441	2.375	613.59
20400	.5256	.7250	1.3793	2.0518	2.386	613.33
20500	.5238	.7238	1.3816	2.0598	2.397	613.13
20600	.5220	.7225	1.3841	2.0676	2.408	612.86
20700	.5202	.7213	1.3864	2.0754	2.419	612.60
20800	.5185	.7201	1.3887	2.0833	2.431	612.34
20900	.5167	.7188	1.3912	2.0914	2.442	612.14
21000	.5149	.7176	1.3935	2.0994	2.453	611.87
21100	.5132	.7164	1.3959	2.1074	2.465	611.61
21200	.5114	.7152	1.3982	2.1156	2.476	611.41
21300	.5097	.7139	1.4008	2.1236	2.488	611.15
21400	.5079	.7127	1.4031	2.1317	2.499	610.88
21500	.5062	.7115	1.4055	2.1398	2.511	610.62
21600	.5044	.7103	1.4079	2.1482	2.522	610.42
21700	.5027	.7090	1.4104	2.1565	2.534	610.15
21800	.5010	.7078	1.4128	2.1647	2.546	609.89
21900	.4993	.7066	1.4152	2.1730	2.558	609.62
22000	.4975	.7054	1.4176	2.1815	2.570	609.43
22100	.4958	.7042	1.4201	2.1899	2.582	609.16
22200	.4941	.7030	1.4225	2.1983	2.594	608.90
22300	.4924	.7017	1.4251	2.2070	2.606	608.70
22400	.4907	.7005	1.4276	2.2155	2.618	608.43
22500	.4890	.6993	1.4300	2.2240	2.631	608.17
22600	.4873	.6981	1.4325	2.2325	2.643	607.90
22700	.4856	.6969	1.4349	2.2414	2.656	607.71
22800	.4840	.6957	1.4374	2.2500	2.668	607.43
22900	.4823	.6945	1.4399	2.2587	2.680	607.17

H_c (Feet)	P_a ("Hg)	δ P_a/P_{aSL}	$1/\delta$	T_a (°K)	$\sqrt{T_a}$	θ T_a/T_{aSL}	$\sqrt{\theta}$
23000	12.107	.4046	2.471	242.60	15.576	.8419	.9175
23100	12.055	.4029	2.481	242.40	15.569	.8412	.9172
23200	12.003	.4011	2.492	242.20	15.563	.8405	.9168
23300	11.952	.3994	2.503	242.00	15.556	.8398	.9164
23400	11.901	.3977	2.514	241.80	15.550	.8391	.9160
23500	11.849	.3960	2.525	241.59	15.543	.8384	.9157
23600	11.798	.3943	2.535	241.39	15.537	.8377	.9153
23700	11.748	.3926	2.546	241.22	15.531	.8371	.9149
23800	11.697	.3909	2.557	241.02	15.525	.8364	.9145
23900	11.646	.3892	2.569	240.82	15.518	.8357	.9142
24000	11.596	.3875	2.580	240.61	15.512	.8350	.9138
24100	11.546	.3859	2.591	240.41	15.505	.8343	.9134
24200	11.496	.3842	2.602	240.21	15.499	.8336	.9130
24300	11.446	.3825	2.613	240.01	15.492	.8329	.9126
24400	11.397	.3809	2.625	239.81	15.486	.8322	.9123
24500	11.347	.3792	2.636	239.63	15.480	.8316	.9119
24600	11.298	.3776	2.648	239.43	15.474	.8309	.9115
24700	11.249	.3759	2.659	239.23	15.467	.8302	.9111
24800	11.200	.3743	2.671	239.03	15.461	.8295	.9108
24900	11.152	.3727	2.683	238.83	15.454	.8288	.9104
25000	11.103	.3710	2.694	238.63	15.448	.8281	.9100
25100	11.055	.3694	2.706	238.42	15.441	.8274	.9096
25200	11.006	.3678	2.718	238.22	15.434	.8267	.9093
25300	10.958	.3662	2.730	238.05	15.429	.8261	.9089
25400	10.911	.3646	2.742	237.85	15.422	.8254	.9085
25500	10.863	.3630	2.754	237.65	15.416	.8247	.9081
25600	10.815	.3614	2.766	237.44	15.409	.8240	.9077
25700	10.768	.3598	2.778	237.24	15.403	.8233	.9074
25800	10.721	.3583	2.790	237.04	15.396	.8226	.9070
25900	10.674	.3567	2.803	236.84	15.390	.8219	.9066
26000	10.627	.3551	2.815	236.64	15.383	.8212	.9062
26100	10.580	.3536	2.827	236.46	15.377	.8206	.9058
26200	10.534	.3520	2.840	236.26	15.371	.8199	.9055
26300	10.487	.3505	2.852	236.06	15.364	.8192	.9051
26400	10.441	.3489	2.865	235.86	15.358	.8185	.9047
26500	10.395	.3474	2.878	235.66	15.351	.8178	.9043
26600	10.349	.3459	2.891	235.46	15.345	.8171	.9039
26700	10.304	.3443	2.903	235.25	15.338	.8164	.9036
26800	10.258	.3428	2.916	235.05	15.331	.8157	.9032
26900	10.213	.3413	2.929	234.88	15.326	.8151	.9028

H_c (Feet)	σ ρ/PSL	$\sqrt{\sigma}$	$1/\sqrt{\sigma}$	$\sqrt{\theta/\delta}$	$1/\delta\sqrt{\theta}$	a (Knots)
23000	.4806	.6933	1.4424	2.2674	2.693	606.90
23100	.4789	.6921	1.4449	2.2764	2.706	606.70
23200	.4773	.6909	1.4474	2.2853	2.719	606.44
23300	.4756	.6897	1.4499	2.2941	2.731	606.18
23400	.4740	.6885	1.4524	2.3030	2.744	605.91
23500	.4723	.6873	1.4550	2.3122	2.757	605.71
23600	.4707	.6861	1.4575	2.3212	2.770	605.45
23700	.4690	.6849	1.4601	2.3302	2.783	605.18
23800	.4674	.6837	1.4626	2.3392	2.797	604.92
23900	.4657	.6825	1.4652	2.3486	2.810	604.72
24000	.4641	.6813	1.4678	2.3578	2.823	604.46
24100	.4625	.6801	1.4704	2.3669	2.837	604.19
24200	.4609	.6789	1.4730	2.3762	2.850	603.93
24300	.4593	.6777	1.4756	2.3854	2.864	603.66
24400	.4577	.6765	1.4782	2.3951	2.877	603.46
24500	.4560	.6753	1.4808	2.404	2.891	603.20
24600	.4544	.6742	1.4832	2.413	2.905	602.93
24700	.4528	.6730	1.4859	2.423	2.919	602.67
24800	.4512	.6718	1.4885	2.433	2.933	602.47
24900	.4497	.6706	1.4912	2.442	2.947	602.21
25000	.4481	.6694	1.4939	2.452	2.961	601.94
25100	.4465	.6682	1.4966	2.461	2.975	601.68
25200	.4449	.6671	1.4990	2.471	2.990	601.48
25300	.4433	.6659	1.5017	2.481	3.004	601.22
25400	.4418	.6647	1.5044	2.491	3.018	600.95
25500	.4402	.6635	1.5072	2.501	3.033	600.69
25600	.4387	.6623	1.5099	2.511	3.047	600.42
25700	.4371	.6612	1.5124	2.521	3.062	600.22
25800	.4355	.6600	1.5152	2.531	3.077	599.96
25900	.4340	.6588	1.5179	2.541	3.092	599.69
26000	.4324	.6576	1.5207	2.551	3.106	599.43
26100	.4309	.6565	1.5232	2.561	3.121	599.17
26200	.4294	.6553	1.5260	2.572	3.137	598.97
26300	.4278	.6541	1.5288	2.582	3.152	598.70
26400	.4263	.6530	1.5314	2.592	3.167	598.44
26500	.4248	.6518	1.5342	2.602	3.182	598.17
26600	.4233	.6506	1.5370	2.613	3.198	597.91
26700	.4218	.6495	1.5396	2.623	3.214	597.71
26800	.4203	.6483	1.5425	2.634	3.229	597.45
26900	.4188	.6472	1.5451	2.644	3.245	597.18

H_c (Feet)	P_a ($"Hg$)	δ P_a/P_{aSL}	$1/\delta$	T_a ($^{\circ}K$)	$\sqrt{T_a}$	θ T_a/T_{aSL}	$\sqrt{\theta}$
27000	10.166	.3398	2.942	234.68	15.319	.8144	.9024
27100	10.123	.3383	2.955	234.48	15.313	.8137	.9020
27200	10.078	.3368	2.968	234.27	15.306	.8130	.9017
27300	10.033	.3353	2.982	234.07	15.299	.8123	.9013
27400	9.988	.3338	2.995	233.87	15.293	.8116	.9009
27500	9.944	.3323	3.008	233.67	15.286	.8109	.9005
27600	9.900	.3308	3.022	233.47	15.280	.8102	.9001
27700	9.856	.3294	3.035	233.29	15.274	.8096	.8998
27800	9.812	.3279	3.049	233.09	15.267	.8089	.8994
27900	9.768	.3264	3.063	232.89	15.261	.8082	.8990
28000	9.724	.3250	3.076	232.69	15.254	.8075	.8986
28100	9.681	.3235	3.090	232.49	15.248	.8068	.8982
28200	9.638	.3221	3.104	232.29	15.241	.8061	.8978
28300	9.595	.3206	3.118	232.08	15.234	.8054	.8975
28400	9.552	.3192	3.132	231.88	15.228	.8047	.8971
28500	9.509	.3178	3.146	231.71	15.222	.8041	.8967
28600	9.466	.3163	3.160	231.51	15.215	.8034	.8963
28700	9.424	.3149	3.175	231.31	15.209	.8027	.8959
28800	9.381	.3135	3.189	231.10	15.202	.8020	.8955
28900	9.339	.3121	3.203	230.90	15.195	.8013	.8952
29000	9.297	.3107	3.218	230.70	15.189	.8006	.8948
29100	9.255	.3093	3.232	230.50	15.182	.7999	.8944
29200	9.213	.3079	3.247	230.30	15.176	.7992	.8940
29300	9.172	.3065	3.262	230.12	15.170	.7986	.8936
29400	9.130	.3051	3.276	229.92	15.163	.7979	.8932
29500	9.089	.3037	3.291	229.72	15.157	.7972	.8928
29600	9.048	.3024	3.306	229.52	15.150	.7965	.8925
29700	9.007	.3010	3.321	229.32	15.143	.7958	.8921
29800	8.966	.2996	3.337	229.12	15.137	.7951	.8917
29900	8.925	.2983	3.352	228.91	15.130	.7944	.8913
30000	8.885	.2969	3.367	228.71	15.123	.7937	.8909
30100	8.845	.2956	3.382	228.54	15.118	.7931	.8905
30200	8.804	.2942	3.398	228.34	15.111	.7924	.8901
30300	8.764	.2929	3.413	228.14	15.104	.7917	.8898
30400	8.724	.2915	3.429	227.93	15.098	.7910	.8894
30500	8.685	.2902	3.445	227.73	15.091	.7903	.8890
30600	8.645	.2889	3.460	227.53	15.084	.7896	.8886
30700	8.605	.2876	3.476	227.33	15.077	.7889	.8882
30800	8.566	.2863	3.492	227.13	15.071	.7882	.8878
30900	8.527	.2849	3.508	226.95	15.065	.7876	.8874

TABLE 9.2

H_c (Feet)	σ ρ/PSL	$\sqrt{\sigma}$	$1/\sqrt{\sigma}$	$\sqrt{\theta/\delta}$	$1/\delta\sqrt{\theta}$	a (Knts)
27000	.4173	.6460	1.5480	2.655	3.260	596.92
27100	.4157	.6448	1.5509	2.666	3.276	596.65
27200	.4143	.6437	1.5535	2.677	3.292	596.45
27300	.4128	.6425	1.5564	2.637	3.308	596.19
27400	.4113	.6413	1.5593	2.698	3.325	595.93
27500	.4098	.6402	1.5620	2.709	3.341	595.66
27600	.4083	.6390	1.5649	2.720	3.357	595.40
27700	.4068	.6379	1.5676	2.731	3.374	595.20
27800	.4054	.6367	1.5706	2.742	3.390	594.93
27900	.4039	.6356	1.5733	2.753	3.407	594.67
28000	.4025	.6344	1.5763	2.764	3.423	594.40
28100	.4010	.6333	1.5790	2.776	3.440	594.14
28200	.3996	.6321	1.5820	2.787	3.457	593.88
28300	.3981	.6310	1.5848	2.798	3.474	593.68
28400	.3967	.6298	1.5878	2.810	3.491	593.41
28500	.3952	.6287	1.5906	2.821	3.509	593.15
28600	.3938	.6276	1.5934	2.833	3.526	592.88
28700	.3923	.6264	1.5964	2.844	3.543	592.62
28800	.3909	.6253	1.5992	2.856	3.561	592.35
28900	.3895	.6241	1.6023	2.867	3.579	592.16
29000	.3881	.6230	1.6051	2.879	3.596	591.89
29100	.3867	.6219	1.6080	2.891	3.614	591.62
29200	.3853	.6207	1.6111	2.903	3.632	591.35
29300	.3838	.6196	1.6139	2.915	3.650	591.09
29400	.3824	.6184	1.6171	2.927	3.668	590.82
29500	.3810	.6173	1.6200	2.939	3.686	590.56
29600	.3796	.6162	1.6228	2.951	3.705	590.36
29700	.3782	.6150	1.6260	2.963	3.723	590.10
29800	.3769	.6139	1.6289	2.975	3.742	589.83
29900	.3755	.6128	1.6319	2.987	3.761	589.57
30000	.3741	.6117	1.6348	3.000	3.779	589.30
30100	.3727	.6105	1.6380	3.012	3.798	589.05
30200	.3713	.6094	1.6410	3.024	3.817	588.78
30300	.3700	.6083	1.6439	3.037	3.837	588.58
30400	.3686	.6072	1.6469	3.050	3.856	588.32
30500	.3672	.6060	1.6502	3.062	3.875	588.06
30600	.3659	.6049	1.6532	3.075	3.894	587.79
30700	.3645	.6038	1.6562	3.088	3.914	587.53
30800	.3632	.6027	1.6592	3.100	3.934	587.26
30900	.3618	.6016	1.6622	3.113	3.953	587.00

H_c (Feet)	P_a ("Hg)	δ P_a/P_{aSL}	$1/\delta$	T_a (°K)	$\sqrt{T_a}$	θ T_a/T_{aSL}	$\sqrt{\theta}$
31000	8.488	.2836	3.524	226.75	15.058	.7869	.8871
31100	8.449	.2823	3.541	226.55	15.052	.7862	.8867
31200	8.410	.2810	3.557	226.35	15.045	.7855	.8863
31300	8.371	.2798	3.573	226.15	15.038	.7848	.8859
31400	8.333	.2785	3.590	225.95	15.032	.7841	.8855
31500	8.295	.2772	3.607	225.74	15.025	.7834	.8851
31600	8.256	.2759	3.623	225.54	15.018	.7827	.8847
31700	8.218	.2746	3.640	225.37	15.012	.7821	.8843
31800	8.181	.2734	3.657	225.17	15.006	.7814	.8839
31900	8.143	.2721	3.674	224.97	14.999	.7807	.8836
32000	8.105	.2709	3.691	224.76	14.992	.7800	.8832
32100	8.068	.2696	3.708	224.56	14.985	.7793	.8828
32200	8.030	.2684	3.725	224.36	14.979	.7786	.8824
32300	7.993	.2671	3.743	224.16	14.972	.7779	.8820
32400	7.956	.2659	3.760	223.96	14.965	.7772	.8816
32500	7.919	.2646	3.778	223.79	14.959	.7766	.8812
32600	7.882	.2634	3.795	223.58	14.953	.7759	.8808
32700	7.846	.2622	3.813	223.38	14.946	.7752	.8804
32800	7.809	.2610	3.831	223.18	14.939	.7745	.8801
32900	7.773	.2597	3.849	222.98	14.932	.7738	.8797
33000	7.737	.2585	3.867	222.78	14.926	.7731	.8793
33100	7.700	.2573	3.885	222.57	14.919	.7724	.8789
33200	7.665	.2561	3.903	222.37	14.912	.7717	.8785
33300	7.629	.2549	3.922	222.20	14.906	.7711	.8781
33400	7.593	.2537	3.940	222.00	14.900	.7704	.8777
33500	7.557	.2525	3.958	221.80	14.893	.7697	.8773
33600	7.522	.2514	3.977	221.60	14.886	.7690	.8769
33700	7.487	.2502	3.996	221.39	14.879	.7683	.8765
33800	7.452	.2490	4.015	221.19	14.873	.7676	.8761
33900	7.417	.2478	4.034	220.99	14.866	.7669	.8757
34000	7.382	.2467	4.053	220.79	14.859	.7662	.8754
34100	7.347	.2455	4.072	220.62	14.853	.7656	.8750
34200	7.312	.2444	4.091	220.41	14.846	.7649	.8746
34300	7.278	.2432	4.110	220.21	14.840	.7642	.8742
34400	7.244	.2421	4.130	220.01	14.833	.7635	.8738
34500	7.209	.2409	4.150	219.81	14.826	.7628	.8734
34600	7.175	.2398	4.169	219.61	14.819	.7621	.8730
34700	7.141	.2386	4.189	219.41	14.812	.7614	.8726
34800	7.107	.2375	4.209	219.20	14.806	.7607	.8722
34900	7.074	.2364	4.229	219.03	14.800	.7601	.8718

TABLE 9.2

H_c (Feet)	σ ρ/ρ_{SL}	$\sqrt{\sigma}$	$1/\sqrt{\sigma}$	$\sqrt{\theta/\delta}$	$1/\delta\sqrt{\theta}$	a (Knots)
31000	.3605	.6004	1.6656	3.127	3.974	586.80
31100	.3592	.5993	1.6686	3.140	3.994	586.53
31200	.3578	.5982	1.6717	3.153	4.014	586.27
31300	.3565	.5971	1.6748	3.166	4.034	586.01
31400	.3551	.5960	1.6779	3.179	4.054	585.74
31500	.3538	.5949	1.6810	3.192	4.075	585.48
31600	.3525	.5938	1.6841	3.205	4.095	585.21
31700	.3512	.5926	1.6875	3.219	4.116	584.95
31800	.3499	.5916	1.6903	3.232	4.137	584.68
31900	.3486	.5904	1.6938	3.246	4.158	584.48
32000	.3473	.5893	1.6969	3.260	4.180	584.22
32100	.3460	.5882	1.7001	3.274	4.201	583.96
32200	.3447	.5871	1.7033	3.287	4.222	583.69
32300	.3434	.5860	1.7065	3.301	4.244	583.43
32400	.3421	.5849	1.7097	3.315	4.265	583.16
32500	.3408	.5838	1.7129	3.329	4.287	582.90
32600	.3395	.5827	1.7161	3.343	4.309	582.63
32700	.3382	.5816	1.7194	3.357	4.331	582.37
32800	.3370	.5805	1.7227	3.371	4.353	582.17
32900	.3357	.5794	1.7259	3.386	4.376	581.91
33000	.3344	.5783	1.7292	3.400	4.398	581.64
33100	.3332	.5772	1.7325	3.414	4.421	581.38
33200	.3319	.5762	1.7355	3.429	4.443	581.11
33300	.3306	.5751	1.7388	3.443	4.466	580.85
33400	.3294	.5740	1.7422	3.458	4.489	580.58
33500	.3281	.5729	1.7455	3.473	4.512	580.32
33600	.3269	.5718	1.7489	3.487	4.535	580.05
33700	.3256	.5707	1.7522	3.502	4.559	579.79
33800	.3244	.5696	1.7556	3.517	4.582	579.52
33900	.3232	.5685	1.7590	3.532	4.606	579.26
34000	.3219	.5674	1.7624	3.548	4.630	579.06
34100	.3207	.5664	1.7655	3.563	4.654	578.80
34200	.3195	.5653	1.7690	3.578	4.678	578.53
34300	.3183	.5642	1.7724	3.593	4.703	578.27
34400	.3171	.5631	1.7759	3.609	4.727	578.00
34500	.3158	.5620	1.7794	3.624	4.751	577.74
34600	.3146	.5610	1.7825	3.640	4.776	577.47
34700	.3134	.5599	1.7860	3.655	4.801	577.21
34800	.3122	.5588	1.7895	3.671	4.826	576.95
34900	.3110	.5577	1.7931	3.687	4.851	576.68

H _c (Feet)	P _a ("Hg)	δ P _a /P _{aSL}	1/δ	T _a (°K)	√T _a	θ T _a /T _{aSL}	√θ
35000	7.040	.2353	4.249	218.83	14.793	.7594	.8714
35100	7.007	.2341	4.270	218.63	14.786	.7587	.8710
35200	6.973	.2330	4.290	218.43	14.779	.7580	.8706
35300	6.940	.2319	4.311	218.22	14.772	.7573	.8702
35400	6.907	.2308	4.331	218.02	14.766	.7566	.8698
35500	6.874	.2297	4.352	217.82	14.759	.7559	.8694
35600	6.841	.2286	4.373	217.62	14.752	.7552	.8690
35700	6.809	.2275	4.394	217.45	14.746	.7546	.8686
35800	6.776	.2264	4.415	217.24	14.739	.7539	.8683
35900	6.744	.2254	4.436	217.04	14.732	.7532	.8679
36000	6.711	.2243	4.457	216.84	14.726	.7525	.8675
36100	6.679	.2232	4.479	216.66	14.719	.7519	.8671
36200	6.647	.2221	4.501	216.66	14.719	.7519	.8671
36300	6.615	.2211	4.522	216.66	14.719	.7519	.8671
36400	6.584	.2200	4.544	216.66	14.719	.7519	.8671
36500	6.552	.2189	4.566	216.66	14.719	.7519	.8671
36600	6.521	.2179	4.588	216.66	14.719	.7519	.8671
36700	6.489	.2168	4.610	216.66	14.719	.7519	.8671
36800	6.458	.2158	4.632	216.66	14.719	.7519	.8671
36900	6.427	.2148	4.655	216.66	14.719	.7519	.8671
37000	6.396	.2137	4.677	216.66	14.719	.7519	.8671
37100	6.366	.2127	4.700	216.66	14.719	.7519	.8671
37200	6.335	.2117	4.722	216.66	14.719	.7519	.8671
37300	6.305	.2107	4.745	216.66	14.719	.7519	.8671
37400	6.274	.2097	4.768	216.66	14.719	.7519	.8671
37500	6.244	.2087	4.791	216.66	14.719	.7519	.8671
37600	6.215	.2077	4.814	216.66	14.719	.7519	.8671
37700	6.185	.2067	4.837	216.66	14.719	.7519	.8671
37800	6.155	.2057	4.861	216.66	14.719	.7519	.8671
37900	6.125	.2047	4.884	216.66	14.719	.7519	.8671
38000	6.096	.2037	4.908	216.66	14.719	.7519	.8671
38100	6.067	.2027	4.931	216.66	14.719	.7519	.8671
38200	6.038	.20180	4.955	216.66	14.719	.7519	.8671
38300	6.009	.20083	4.979	216.66	14.719	.7519	.8671
38400	5.980	.19987	5.003	216.66	14.719	.7519	.8671
38500	5.951	.19892	5.027	216.66	14.719	.7519	.8671
38600	5.923	.19797	5.051	216.66	14.719	.7519	.8671
38700	5.894	.19701	5.075	216.66	14.719	.7519	.8671
38800	5.866	.19607	5.100	216.66	14.719	.7519	.8671
38900	5.838	.19513	5.124	216.66	14.719	.7519	.8671

TABLE 9.2

H_c (Feet)	σ ρ/PSL	$\sqrt{\sigma}$	$1/\sqrt{\sigma}$	$\sqrt{\theta/\delta}$	$1/\delta\sqrt{\theta}$	a (Knots)
35000	.3098	.5567	1.7963	3.703	4.877	576.42
35100	.3086	.5556	1.7999	3.719	4.902	576.15
35200	.3075	.5545	1.8034	3.735	4.928	575.89
35300	.3063	.5534	1.8070	3.751	4.953	575.62
35400	.3051	.5524	1.8103	3.767	4.979	575.36
35500	.3039	.5513	1.8139	3.783	5.005	575.09
35600	.3027	.5502	1.8175	3.800	5.032	574.83
35700	.3016	.5492	1.8208	3.816	5.058	574.57
35800	.3004	.5481	1.8245	3.833	5.085	574.37
35900	.2992	.5471	1.8278	3.850	5.112	574.10
36000	.2981	.5460	1.8315	3.867	5.139	573.84
36100	.2969	.5449	1.8352	3.884	5.166	573.58
36200	.2954	.5436	1.8396	3.902	5.190	573.58
36300	.2940	.5423	1.8441	3.921	5.215	573.58
36400	.2926	.5410	1.8485	3.940	5.240	573.58
36500	.2912	.5397	1.8530	3.959	5.266	573.58
36600	.2898	.5384	1.8574	3.978	5.291	573.58
36700	.2884	.5371	1.8619	3.997	5.317	573.58
36800	.2870	.5358	1.8664	4.017	5.342	573.58
36900	.2857	.5345	1.8709	4.036	5.368	573.58
37000	.2843	.5332	1.8753	4.055	5.394	573.58
37100	.2829	.5319	1.8799	4.075	5.420	573.58
37200	.2816	.5307	1.8844	4.095	5.446	573.58
37300	.2802	.5294	1.8889	4.114	5.472	573.58
37400	.2789	.5281	1.8935	4.134	5.499	573.58
37500	.2775	.5269	1.8980	4.154	5.525	573.58
37600	.2762	.5256	1.9026	4.174	5.552	573.58
37700	.2749	.5243	1.9072	4.194	5.579	573.58
37800	.2736	.5231	1.9117	4.215	5.605	573.58
37900	.2723	.5218	1.9164	4.235	5.632	573.58
38000	.2709	.5206	1.9210	4.255	5.660	573.58
38100	.2697	.5193	1.9256	4.276	5.687	573.58
38200	.2684	.5181	1.9302	4.296	5.714	573.58
38300	.2671	.5168	1.9349	4.317	5.742	573.58
38400	.2658	.5156	1.9395	4.338	5.770	573.58
38500	.2645	.5144	1.9442	4.359	5.797	573.58
38600	.2633	.5131	1.9488	4.380	5.825	573.58
38700	.2620	.5119	1.9535	4.401	5.853	573.58
38800	.2607	.5107	1.9583	4.422	5.881	573.58
38900	.2595	.5094	1.9630	4.443	5.910	573.58

H_c (Feet)	P_a ("Hg)	δ P_a/P_{aSL}	$1/\delta$	T_a (°K)	$\sqrt{T_a}$	θ T_a/T_{aSL}	$\sqrt{\theta}$
39000	5.810	.19419	5.149	216.66	14.719	.7519	.8671
39100	5.782	.19326	5.174	216.66	14.719	.7519	.8671
39200	5.754	.19233	5.199	216.66	14.719	.7519	.8671
39300	5.727	.19142	5.224	216.66	14.719	.7519	.8671
39400	5.699	.19049	5.249	216.66	14.719	.7519	.8671
39500	5.672	.18958	5.274	216.66	14.719	.7519	.8671
39600	5.645	.18868	5.300	216.66	14.719	.7519	.8671
39700	5.618	.18776	5.325	216.66	14.719	.7519	.8671
39800	5.591	.18687	5.351	216.66	14.719	.7519	.8671
39900	5.564	.18597	5.377	216.66	14.719	.7519	.8671
40000	5.537	.18508	5.403	216.66	14.719	.7519	.8671
40100	5.511	.18419	5.429	216.66	14.719	.7519	.8671
40200	5.484	.18331	5.455	216.66	14.719	.7519	.8671
40300	5.458	.18243	5.481	216.66	14.719	.7519	.8671
40400	5.432	.18155	5.508	216.66	14.719	.7519	.8671
40500	5.406	.18068	5.534	216.66	14.719	.7519	.8671
40600	5.380	.17982	5.561	216.66	14.719	.7519	.8671
40700	5.354	.17896	5.587	216.66	14.719	.7519	.8671
40800	5.328	.17810	5.614	216.66	14.719	.7519	.8671
40900	5.303	.17724	5.642	216.66	14.719	.7519	.8671
41000	5.278	.17640	5.668	216.66	14.719	.7519	.8671
41100	5.252	.17555	5.696	216.66	14.719	.7519	.8671
41200	5.227	.17471	5.723	216.66	14.719	.7519	.8671
41300	5.202	.17387	5.751	216.66	14.719	.7519	.8671
41400	5.177	.17303	5.779	216.66	14.719	.7519	.8671
41500	5.152	.17221	5.806	216.66	14.719	.7519	.8671
41600	5.127	.17138	5.835	216.66	14.719	.7519	.8671
41700	5.103	.17056	5.863	216.66	14.719	.7519	.8671
41800	5.079	.16974	5.891	216.66	14.719	.7519	.8671
41900	5.054	.16893	5.919	216.66	14.719	.7519	.8671
42000	5.030	.16812	5.948	216.66	14.719	.7519	.8671
42100	5.006	.16731	5.976	216.66	14.719	.7519	.8671
42200	4.982	.16651	6.005	216.66	14.719	.7519	.8671
42300	4.958	.16571	6.034	216.66	14.719	.7519	.8671
42400	4.934	.16492	6.063	216.66	14.719	.7519	.8671
42500	4.910	.16412	6.093	216.66	14.719	.7519	.8671
42600	4.887	.16334	6.122	216.66	14.719	.7519	.8671
42700	4.863	.16255	6.152	216.66	14.719	.7519	.8671
42800	4.840	.16178	6.181	216.66	14.719	.7519	.8671
42900	4.817	.16100	6.211	216.66	14.719	.7519	.8671

TABLE 9.2

H_c (Feet)	σ ρ/ρ_{SL}	$\sqrt{\sigma}$	$1/\sqrt{\sigma}$	$\sqrt{\theta/\delta}$	$1/\delta/\theta$	a (Knots)
39000	.2582	.5082	1.9677	4.465	5.938	573.58
39100	.2570	.5070	1.9724	4.486	5.967	573.58
39200	.2558	.5058	1.9772	4.508	5.996	573.58
39300	.2545	.5046	1.9819	4.529	6.024	573.58
39400	.2533	.5033	1.9867	4.551	6.054	573.58
39500	.2521	.5021	1.9915	4.573	6.083	573.58
39600	.2509	.5009	1.9962	4.595	6.112	573.58
39700	.2497	.4997	2.0011	4.618	6.142	573.58
39800	.2485	.4985	2.0059	4.640	6.171	573.58
39900	.2473	.4973	2.0107	4.662	6.201	573.58
40000	.2461	.4961	2.0155	4.685	6.231	573.58
40100	.2449	.4949	2.0204	4.707	6.261	573.58
40200	.2438	.4938	2.0253	4.730	6.291	573.58
40300	.2426	.4926	2.0301	4.753	6.321	573.58
40400	.2414	.4914	2.0350	4.776	6.352	573.58
40500	.2403	.4902	2.0399	4.799	6.382	573.58
40600	.2391	.4890	2.0448	4.822	6.413	573.58
40700	.2380	.4879	2.0497	4.845	6.444	573.58
40800	.2368	.4867	2.0547	4.868	6.475	573.58
40900	.2357	.4855	2.0596	4.892	6.506	573.58
41000	.2346	.4844	2.0646	4.915	6.537	573.58
41100	.2334	.4832	2.0695	4.939	6.569	573.58
41200	.2323	.4820	2.0745	4.963	6.600	573.58
41300	.2312	.4809	2.0795	4.987	6.632	573.58
41400	.2301	.4797	2.0845	5.011	6.664	573.58
41500	.2290	.4786	2.0895	5.035	6.696	573.58
41600	.2279	.4774	2.0946	5.059	6.729	573.58
41700	.2268	.4763	2.0996	5.083	6.761	573.58
41800	.2257	.4751	2.1046	5.108	6.794	573.58
41900	.2246	.4740	2.1097	5.132	6.826	573.58
42000	.2236	.4729	2.1148	5.157	6.859	573.58
42100	.2225	.4717	2.1199	5.182	6.892	573.58
42200	.2214	.4706	2.1250	5.207	6.926	573.58
42300	.2204	.4695	2.1301	5.232	6.959	573.58
42400	.2193	.4683	2.1352	5.257	6.992	573.58
42500	.2182	.4672	2.1404	5.283	7.026	573.58
42600	.2172	.4661	2.1455	5.308	7.060	573.58
42700	.2162	.4650	2.1507	5.334	7.094	573.58
42800	.2151	.4639	2.1558	5.359	7.128	573.58
42900	.2141	.4627	2.1610	5.385	7.163	573.58

H_c (Feet)	P_a ("Hg)	δ P_a/P_{aSL}	$1/\delta$	T_a (°K)	$\sqrt{T_a}$	θ T_a/T_{aSL}	$\sqrt{\theta}$
43000	4.794	.16023	6.241	216.66	14.719	.7519	.8671
43100	4.771	.15946	6.271	216.66	14.719	.7519	.8671
43200	4.748	.15870	6.301	216.66	14.719	.7519	.8671
43300	4.725	.15794	6.331	216.66	14.719	.7519	.8671
43400	4.702	.15718	6.362	216.66	14.719	.7519	.8671
43500	4.680	.15642	6.393	216.66	14.719	.7519	.8671
43600	4.657	.15567	6.423	216.66	14.719	.7519	.8671
43700	4.635	.15492	6.454	216.66	14.719	.7519	.8671
43800	4.613	.15418	6.485	216.66	14.719	.7519	.8671
43900	4.591	.15345	6.516	216.66	14.719	.7519	.8671
44000	4.569	.15271	6.548	216.66	14.719	.7519	.8671
44100	4.547	.15198	6.579	216.66	14.719	.7519	.8671
44200	4.525	.15125	6.611	216.66	14.719	.7519	.8671
44300	4.503	.15053	6.643	216.66	14.719	.7519	.8671
44400	4.482	.14980	6.675	216.66	14.719	.7519	.8671
44500	4.460	.14908	6.707	216.66	14.719	.7519	.8671
44600	4.439	.14837	6.739	216.66	14.719	.7519	.8671
44700	4.418	.14766	6.772	216.66	14.719	.7519	.8671
44800	4.397	.14695	6.805	216.66	14.719	.7519	.8671
44900	4.375	.14624	6.838	216.66	14.719	.7519	.8671
45000	4.354	.14554	6.871	216.66	14.719	.7519	.8671
45100	4.334	.14485	6.903	216.66	14.719	.7519	.8671
45200	4.313	.14415	6.937	216.66	14.719	.7519	.8671
45300	4.292	.14346	6.970	216.66	14.719	.7519	.8671
45400	4.271	.14277	7.004	216.66	14.719	.7519	.8671
45500	4.251	.14208	7.038	216.66	14.719	.7519	.8671
45600	4.231	.14141	7.071	216.66	14.719	.7519	.8671
45700	4.210	.14073	7.105	216.66	14.719	.7519	.8671
45800	4.190	.14005	7.140	216.66	14.719	.7519	.8671
45900	4.170	.13938	7.174	216.66	14.719	.7519	.8671
46000	4.150	.13871	7.209	216.66	14.719	.7519	.8671
46100	4.130	.13805	7.243	216.66	14.719	.7519	.8671
46200	4.110	.13739	7.278	216.66	14.719	.7519	.8671
46300	4.091	.13672	7.314	216.66	14.719	.7519	.8671
46400	4.071	.13607	7.349	216.66	14.719	.7519	.8671
46500	4.051	.13542	7.384	216.66	14.719	.7519	.8671
46600	4.032	.13477	7.420	216.66	14.719	.7519	.8671
46700	4.013	.13412	7.456	216.66	14.719	.7519	.8671
46800	3.993	.13348	7.491	216.66	14.719	.7519	.8671
46900	3.974	.13284	7.527	216.66	14.719	.7519	.8671

TABLE 9.2

H_c (Feet)	σ ρ/PSL	$\sqrt{\sigma}$	$1/\sqrt{\sigma}$	$\sqrt{\theta/\delta}$	$1/\delta\theta$	a (Knots)
43000	.2131	.4616	2.1662	5.411	7.197	573.58
43100	.2120	.4605	2.1715	5.437	7.232	573.58
43200	.2110	.4594	2.1767	5.463	7.266	573.58
43300	.2100	.4583	2.1819	5.490	7.301	573.58
43400	.2090	.4572	2.1872	5.516	7.337	573.58
43500	.2080	.4561	2.1924	5.543	7.372	573.58
43600	.2070	.4550	2.1977	5.570	7.408	573.58
43700	.2060	.4539	2.2030	5.597	7.444	573.58
43800	.2050	.4528	2.2083	5.623	7.479	573.58
43900	.2040	.4518	2.2136	5.650	7.515	573.58
44000	.20310	.4507	2.2189	5.678	7.551	573.58
44100	.20213	.4496	2.2242	5.705	7.588	573.58
44200	.20117	.4485	2.2296	5.732	7.624	573.58
44300	.20020	.4474	2.2349	5.760	7.661	573.58
44400	.19924	.4464	2.2403	5.788	7.698	573.58
44500	.19828	.4453	2.2457	5.816	7.735	573.58
44600	.19733	.4442	2.2511	5.844	7.772	573.58
44700	.19639	.4432	2.2566	5.872	7.810	573.58
44800	.19545	.4421	2.2620	5.900	7.847	573.58
44900	.19451	.4410	2.2674	5.929	7.886	573.58
45000	.19358	.4400	2.2729	5.957	7.923	573.58
45100	.19265	.4389	2.2783	5.986	7.961	573.58
45200	.19173	.4379	2.2838	6.015	8.000	573.58
45300	.19080	.4368	2.2893	6.044	8.038	573.58
45400	.18989	.4358	2.2948	6.073	8.077	573.58
45500	.18897	.4347	2.3004	6.102	8.116	573.58
45600	.18807	.4337	2.3059	6.131	8.155	573.58
45700	.18717	.4326	2.3114	6.161	8.194	573.58
45800	.18627	.4316	2.3170	6.191	8.234	573.58
45900	.18538	.4306	2.3226	6.221	8.274	573.58
46000	.18449	.4295	2.3282	6.251	8.314	573.58
46100	.18360	.4285	2.3338	6.281	8.353	573.58
46200	.18273	.4275	2.3394	6.311	8.394	573.58
46300	.18184	.4264	2.3450	6.342	8.435	573.58
46400	.18098	.4254	2.3507	6.372	8.475	573.58
46500	.18011	.4244	2.3563	6.403	8.516	573.58
46600	.17924	.4234	2.3620	6.433	8.557	573.58
46700	.17839	.4224	2.3677	6.465	8.598	573.58
46800	.17753	.4213	2.3734	6.496	8.639	573.58
46900	.17668	.4203	2.3791	6.527	8.681	573.58

H_c (Feet)	P_a ("Hg)	δ P_a/P_{aSL}	$1/\delta$	T_a (°K)	$\sqrt{T_a}$	θ T_a/T_{aSL}	$\sqrt{\theta}$
47000	3.955	.13221	7.563	216.66	14.719	.7519	.8671
47100	3.936	.13157	7.600	216.66	14.719	.7519	.8671
47200	3.917	.13094	7.637	216.66	14.719	.7519	.8671
47300	3.899	.13031	7.674	216.66	14.719	.7519	.8671
47400	3.880	.12969	7.710	216.66	14.719	.7519	.8671
47500	3.861	.12907	7.747	216.66	14.719	.7519	.8671
47600	3.843	.12845	7.785	216.66	14.719	.7519	.8671
47700	3.824	.12783	7.822	216.66	14.719	.7519	.8671
47800	3.806	.12722	7.860	216.66	14.719	.7519	.8671
47900	3.783	.12660	7.898	216.66	14.719	.7519	.8671
48000	3.770	.12600	7.936	216.66	14.719	.7519	.8671
48100	3.752	.12540	7.974	216.66	14.719	.7519	.8671
48200	3.734	.12480	8.012	216.66	14.719	.7519	.8671
48300	3.716	.12419	8.052	216.66	14.719	.7519	.8671
48400	3.698	.12360	8.090	216.66	14.719	.7519	.8671
48500	3.680	.12301	8.129	216.66	14.719	.7519	.8671
48600	3.662	.12242	8.168	216.66	14.719	.7519	.8671
48700	3.645	.12183	8.208	216.66	14.719	.7519	.8671
48800	3.627	.12125	8.247	216.66	14.719	.7519	.8671
48900	3.610	.12067	8.287	216.66	14.719	.7519	.8671
49000	3.593	.12009	8.327	216.66	14.719	.7519	.8671
49100	3.576	.11951	8.367	216.66	14.719	.7519	.8671
49200	3.558	.11894	8.407	216.66	14.719	.7519	.8671
49300	3.541	.11837	8.448	216.66	14.719	.7519	.8671
49400	3.524	.11780	8.489	216.66	14.719	.7519	.8671
49500	3.507	.11724	8.529	216.66	14.719	.7519	.8671
49600	3.491	.11668	8.570	216.66	14.719	.7519	.8671
49700	3.474	.11611	8.612	216.66	14.719	.7519	.8671
49800	3.457	.11556	8.653	216.66	14.719	.7519	.8671
49900	3.441	.11500	8.695	216.66	14.719	.7519	.8671
50000	3.424	.11445	8.737	216.66	14.719	.7519	.8671
50100	3.408	.11390	8.779	216.66	14.719	.7519	.8671
50200	3.391	.11336	8.821	216.66	14.719	.7519	.8671
50300	3.375	.11281	8.864	216.66	14.719	.7519	.8671
50400	3.359	.11227	8.907	216.66	14.719	.7519	.8671
50500	3.343	.11173	8.950	216.66	14.719	.7519	.8671
50600	3.327	.11120	8.992	216.66	14.719	.7519	.8671
50700	3.311	.11067	9.035	216.66	14.719	.7519	.8671
50800	3.295	.11014	9.079	216.66	14.719	.7519	.8671
50900	3.279	.10961	9.123	216.66	14.719	.7519	.8671

TABLE 9.2

(Feet)	σ p/PSL	$\sqrt{\sigma}$	$1/\sqrt{\sigma}$	$\sqrt{\theta/\delta}$	$1/\delta\sqrt{\theta}$	a (Knots)
47000	.17584	.4193	2.3848	6.558	8.722	573.58
47100	.17499	.4183	2.3905	6.590	8.765	573.58
47200	.17415	.4173	2.3963	6.622	8.807	573.58
47300	.17331	.4163	2.4021	6.654	8.850	573.58
47400	.17249	.4153	2.4078	6.685	8.892	573.58
47500	.17166	.4143	2.4136	6.718	8.935	573.58
47600	.17084	.4133	2.4194	6.750	8.978	573.58
47700	.17002	.4123	2.4252	6.783	9.021	573.58
47800	.16920	.4113	2.4311	6.815	9.065	573.58
47900	.16839	.4103	2.4370	6.849	9.109	573.58
48000	.16758	.4094	2.4428	6.881	9.152	573.58
48100	.16678	.4084	2.4487	6.914	9.196	573.58
48200	.16598	.4074	2.4546	6.947	9.240	573.58
48300	.16518	.4064	2.4605	6.982	9.286	573.58
48400	.16439	.4054	2.4664	7.015	9.330	573.58
48500	.16360	.4045	2.4723	7.049	9.375	573.58
48600	.16282	.4035	2.4783	7.083	9.420	573.58
48700	.16204	.4025	2.4842	7.117	9.466	573.58
48800	.16126	.4016	2.4902	7.151	9.511	573.58
48900	.16049	.4006	2.4962	7.185	9.557	573.58
49000	.15972	.3996	2.5022	7.220	9.603	573.58
49100	.15895	.3987	2.5082	7.255	9.649	573.58
49200	.15819	.3977	2.5143	7.290	9.696	573.58
49300	.15743	.3968	2.5203	7.325	9.742	573.58
49400	.15668	.3958	2.5264	7.360	9.789	573.58
49500	.15593	.3949	2.5325	7.395	9.836	573.58
49600	.15518	.3939	2.5385	7.431	9.883	573.58
49700	.15443	.3930	2.5447	7.467	9.932	573.58
49800	.15369	.3920	2.5508	7.503	9.979	573.58
49900	.15295	.3911	2.5570	7.540	10.028	573.58
50000	.15222	.3902	2.5631	7.576	10.076	573.58
50100	.15149	.3892	2.5692	7.612	10.125	573.58
50200	.15077	.3883	2.5754	7.649	10.173	573.58
50300	.15004	.3874	2.5816	7.686	10.222	573.58
50400	.14932	.3864	2.5879	7.723	10.272	573.58
50500	.14861	.3855	2.5941	7.760	10.321	573.58
50600	.14789	.3846	2.6003	7.797	10.371	573.58
50700	.14719	.3837	2.6065	7.835	10.420	573.58
50800	.14648	.3827	2.6128	7.872	10.470	573.58
50900	.14578	.3818	2.6191	7.910	10.521	573.58

H_c (Feet)	P_a ("Hg)	δ P_a/P_{aSL}	$1/\delta$	T_a (°K)	$\sqrt{T_a}$	θ T_a/T_{aSL}	$\sqrt{\theta}$
51000	3.263	.10908	9.167	216.66	14.719	.7519	.8671
51100	3.248	.10856	9.211	216.66	14.719	.7519	.8671
51200	3.232	.10804	9.255	216.66	14.719	.7519	.8671
51300	3.217	.10752	9.300	216.66	14.719	.7519	.8671
51400	3.201	.10700	9.345	216.66	14.719	.7519	.8671
51500	3.186	.10649	9.390	216.66	14.719	.7519	.8671
51600	3.171	.10598	9.435	216.66	14.719	.7519	.8671
51700	3.155	.10547	9.481	216.66	14.719	.7519	.8671
51800	3.140	.10497	9.526	216.66	14.719	.7519	.8671
51900	3.125	.10446	9.573	216.66	14.719	.7519	.8671
52000	3.110	.10396	9.619	216.66	14.719	.7519	.8671
52100	3.095	.10347	9.664	216.66	14.719	.7519	.8671
52200	3.080	.10297	9.711	216.66	14.719	.7519	.8671
52300	3.066	.10247	9.759	216.66	14.719	.7519	.8671
52400	3.051	.10198	9.805	216.66	14.719	.7519	.8671
52500	3.036	.10149	9.853	216.66	14.719	.7519	.8671
52600	3.022	.10101	9.900	216.66	14.719	.7519	.8671
52700	3.007	.10052	9.948	216.66	14.719	.7519	.8671
52800	2.993	.10004	9.996	216.66	14.719	.7519	.8671
52900	2.979	.09956	10.044	216.66	14.719	.7519	.8671
53000	2.964	.09908	10.092	216.66	14.719	.7519	.8671
53100	2.950	.09861	10.141	216.66	14.719	.7519	.8671
53200	2.936	.09813	10.190	216.66	14.719	.7519	.8671
53300	2.922	.09766	10.239	216.66	14.719	.7519	.8671
53400	2.908	.09719	10.289	216.66	14.719	.7519	.8671
53500	2.894	.09673	10.338	216.66	14.719	.7519	.8671
53600	2.880	.09627	10.387	216.66	14.719	.7519	.8671
53700	2.866	.09581	10.437	216.66	14.719	.7519	.8671
53800	2.852	.09535	10.487	216.66	14.719	.7519	.8671
53900	2.839	.09489	10.538	216.66	14.719	.7519	.8671
54000	2.825	.09443	10.589	216.66	14.719	.7519	.8671
54100	2.812	.09398	10.640	216.66	14.719	.7519	.8671
54200	2.798	.09353	10.691	216.66	14.719	.7519	.8671
54300	2.785	.09308	10.743	216.66	14.719	.7519	.8671
54400	2.771	.09264	10.794	216.66	14.719	.7519	.8671
54500	2.758	.09219	10.847	216.66	14.719	.7519	.8671
54600	2.745	.09175	10.899	216.66	14.719	.7519	.8671
54700	2.732	.09131	10.951	216.66	14.719	.7519	.8671
54800	2.719	.09087	11.004	216.66	14.719	.7519	.8671
54900	2.706	.09044	11.057	216.66	14.719	.7519	.8671

TABLE 9.2

H_c (Feet)	σ ρ/PSL	$\sqrt{\sigma}$	$1/\sqrt{\sigma}$	$\sqrt{\sigma}/\delta$	$1/\delta\sqrt{\sigma}$	a (Knots)
51000	.14508	.3809	2.6254	7.949	10.572	573.58
51100	.14439	.3800	2.6317	7.987	10.623	573.58
51200	.14369	.3791	2.6381	8.025	10.674	573.58
51300	.14300	.3782	2.6444	8.064	10.725	573.58
51400	.14231	.3772	2.6508	8.103	10.773	573.58
51500	.14164	.3763	2.6571	8.142	10.829	573.58
51600	.14096	.3754	2.6635	8.181	10.881	573.58
51700	.14028	.3745	2.6700	8.221	10.934	573.58
51800	.13961	.3735	2.6764	8.260	10.986	573.58
51900	.13894	.3727	2.6828	8.300	11.040	573.58
52000	.13827	.3719	2.6893	8.340	11.093	573.58
52100	.13761	.3710	2.6957	8.380	11.145	573.58
52200	.13695	.3701	2.7022	8.420	11.199	573.58
52300	.13629	.3692	2.7088	8.462	11.254	573.58
52400	.13564	.3683	2.7152	8.502	11.308	573.58
52500	.13499	.3674	2.7218	8.543	11.363	573.58
52600	.13434	.3665	2.7283	8.584	11.417	573.58
52700	.13370	.3656	2.7349	8.626	11.472	573.58
52800	.13306	.3648	2.7415	8.667	11.527	573.58
52900	.13242	.3639	2.7481	8.709	11.583	573.58
53000	.13178	.3630	2.7547	8.751	11.639	573.58
53100	.13115	.3621	2.7613	8.793	11.695	573.58
53200	.13052	.3613	2.7680	8.836	11.752	573.58
53300	.12989	.3604	2.7746	8.878	11.808	573.58
53400	.12927	.3595	2.7813	8.921	11.865	573.58
53500	.12865	.3587	2.7880	8.964	11.922	573.58
53600	.12803	.3578	2.7947	9.007	11.979	573.58
53700	.12743	.3570	2.8014	9.050	12.036	573.58
53800	.12681	.3561	2.8082	9.093	12.094	573.58
53900	.12620	.3552	2.8149	9.137	12.153	573.58
54000	.12560	.3544	2.8217	9.182	12.212	573.58
54100	.12500	.3536	2.8285	9.226	12.271	573.58
54200	.12440	.3527	2.8353	9.270	12.330	573.58
54300	.12380	.3518	2.8421	9.315	12.389	573.58
54400	.12321	.3510	2.8489	9.359	12.448	573.58
54500	.12261	.3502	2.8558	9.405	12.509	573.58
54600	.12203	.3493	2.8627	9.450	12.569	573.58
54700	.12144	.3485	2.8695	9.496	12.630	573.58
54800	.12086	.3477	2.8765	9.542	12.691	573.58
54900	.12028	.3468	2.8834	9.587	12.751	573.58

H _c (Feet)	P _a ("Hg)	δ P _a /P _{aSL}	1/δ	T _a (°K)	$\sqrt{T_a}$	θ T _a /T _{aSL}	$\sqrt{\theta}$
55000	2.693	.09000	11.111	216.66	14.719	.7519	.8671
55100	2.680	.08957	11.164	216.66	14.719	.7519	.8671
55200	2.667	.08914	11.218	216.66	14.719	.7519	.8671
55300	2.654	.08871	11.272	216.66	14.719	.7519	.8671
55400	2.641	.08829	11.326	216.66	14.719	.7519	.8671
55500	2.629	.08787	11.380	216.66	14.719	.7519	.8671
55600	2.616	.08745	11.435	216.66	14.719	.7519	.8671
55700	2.603	.08702	11.491	216.66	14.719	.7519	.8671
55800	2.591	.08661	11.546	216.66	14.719	.7519	.8671
55900	2.578	.08619	11.602	216.66	14.719	.7519	.8671
56000	2.566	.08578	11.657	216.66	14.719	.7519	.8671
56100	2.554	.08537	11.713	216.66	14.719	.7519	.8671
56200	2.542	.08496	11.770	216.66	14.719	.7519	.8671
56300	2.529	.08455	11.827	216.66	14.719	.7519	.8671
56400	2.517	.08415	11.883	216.66	14.719	.7519	.8671
56500	2.505	.08374	11.941	216.66	14.719	.7519	.8671
56600	2.493	.08334	11.999	216.66	14.719	.7519	.8671
56700	2.481	.08294	12.056	216.66	14.719	.7519	.8671
56800	2.469	.08254	12.115	216.66	14.719	.7519	.8671
56900	2.458	.08215	12.172	216.66	14.719	.7519	.8671
57000	2.446	.08175	12.232	216.66	14.719	.7519	.8671
57100	2.434	.08136	12.291	216.66	14.719	.7519	.8671
57200	2.422	.08097	12.350	216.66	14.719	.7519	.8671
57300	2.411	.08058	12.410	216.66	14.719	.7519	.8671
57400	2.399	.08020	12.468	216.66	14.719	.7519	.8671
57500	2.388	.07981	12.529	216.66	14.719	.7519	.8671
57600	2.376	.07943	12.589	216.66	14.719	.7519	.8671
57700	2.365	.07905	12.650	216.66	14.719	.7519	.8671
57800	2.353	.07867	12.711	216.66	14.719	.7519	.8671
57900	2.342	.07829	12.773	216.66	14.719	.7519	.8671
58000	2.331	.07792	12.833	216.66	14.719	.7519	.8671
58100	2.320	.07754	12.896	216.66	14.719	.7519	.8671
58200	2.309	.07717	12.958	216.66	14.719	.7519	.8671
58300	2.298	.07680	13.020	216.66	14.719	.7519	.8671
58400	2.287	.07643	13.083	216.66	14.719	.7519	.8671
58500	2.276	.07607	13.145	216.66	14.719	.7519	.8671
58600	2.265	.07570	13.210	216.66	14.719	.7519	.8671
58700	2.254	.07534	13.273	216.66	14.719	.7519	.8671
58800	2.243	.07498	13.336	216.66	14.719	.7519	.8671
58900	2.232	.07462	13.401	216.66	14.719	.7519	.8671

TABLE 9.2

H_c (Feet)	σ ρ/PSL	$\sqrt{\sigma}$	$1/\sqrt{\sigma}$	$\sqrt{\theta/\delta}$	$1/\delta\sqrt{\theta}$	a (Knots)
55000	.11971	.3460	2.8903	9.634	12.813	573.58
55100	.11913	.3452	2.8973	9.680	12.875	573.58
55200	.11856	.3443	2.9042	9.727	12.937	573.58
55300	.11799	.3435	2.9112	9.774	13.000	573.58
55400	.11743	.3427	2.9182	9.821	13.062	573.58
55500	.11686	.3419	2.9252	9.867	13.124	573.58
55600	.11630	.3410	2.9323	9.915	13.187	573.58
55700	.11574	.3402	2.9394	9.964	13.252	573.58
55800	.11519	.3394	2.9464	10.011	13.315	573.58
55900	.11463	.3386	2.9535	10.060	13.380	573.58
56000	.11409	.3378	2.9606	10.108	13.444	573.58
56100	.11354	.3370	2.9678	10.156	13.508	573.58
56200	.11299	.3361	2.9749	10.205	13.573	573.58
56300	.11245	.3353	2.9820	10.255	13.639	573.58
56400	.11192	.3345	2.9892	10.304	13.704	573.58
56500	.11138	.3337	2.9964	10.354	13.771	573.58
56600	.11085	.3329	3.0036	10.404	13.837	573.58
56700	.11031	.3321	3.0108	10.454	13.904	573.58
56800	.10978	.3313	3.0181	10.505	13.972	573.58
56900	.10926	.3305	3.0253	10.555	14.038	573.58
57000	.10873	.3297	3.0327	10.606	14.107	573.58
57100	.10821	.3290	3.0399	10.657	14.174	573.58
57200	.10769	.3282	3.0472	10.708	14.242	573.58
57300	.10718	.3274	3.0546	10.760	14.311	573.58
57400	.10666	.3266	3.0619	10.811	14.379	573.58
57500	.10615	.3258	3.0693	10.864	14.450	573.58
57600	.10564	.3250	3.0767	10.916	14.519	573.58
57700	.10514	.3242	3.0841	10.969	14.588	573.58
57800	.10463	.3235	3.0915	11.022	14.659	573.58
57900	.10413	.3227	3.0989	11.075	14.730	573.58
58000	.10363	.3219	3.1064	11.128	14.800	573.58
58100	.10313	.3211	3.1139	11.182	14.872	573.58
58200	.10264	.3204	3.1214	11.236	14.944	573.58
58300	.10215	.3196	3.1289	11.290	15.016	573.58
58400	.10166	.3188	3.1364	11.345	15.088	573.58
58500	.10117	.3181	3.1440	11.398	15.160	573.58
58600	.10068	.3173	3.1515	11.454	15.234	573.58
58700	.10020	.3165	3.1591	11.509	15.307	573.58
58800	.09972	.3158	3.1667	11.564	15.380	573.58
58900	.09924	.3150	3.1743	11.620	15.454	573.58

H _c (Feet)	P _a ("Hg)	δ P _a /P _{aSL}	1/ δ	T _a (°K)	$\sqrt{T_a}$	θ T _a /T _{aSL}	$\sqrt{\theta}$
59000	2.221	.07426	13.466	216.66	14.719	.7519	.8671
59100	2.211	.07390	13.531	216.66	14.719	.7519	.8671
59200	2.200	.07355	13.596	216.66	14.719	.7519	.8671
59300	2.190	.07320	13.661	216.66	14.719	.7519	.8671
59400	2.179	.07285	13.726	216.66	14.719	.7519	.8671
59500	2.169	.07250	13.793	216.66	14.719	.7519	.8671
59600	2.158	.07215	13.860	216.66	14.719	.7519	.8671
59700	2.148	.07180	13.927	216.66	14.719	.7519	.8671
59800	2.133	.07146	13.993	216.66	14.719	.7519	.8671
59900	2.127	.07112	14.060	216.66	14.719	.7519	.8671
60000	2.117	.07077	14.130	216.66	14.719	.7519	.8671
60100	2.107	.07044	14.196	216.66	14.719	.7519	.8671
60200	2.097	.07010	14.265	216.66	14.719	.7519	.8671
60300	2.087	.06976	14.334	216.66	14.719	.7519	.8671
60400	2.077	.06943	14.403	216.66	14.719	.7519	.8671
60500	2.067	.06910	14.471	216.66	14.719	.7519	.8671
60600	2.057	.06876	14.543	216.66	14.719	.7519	.8671
60700	2.047	.06843	14.613	216.66	14.719	.7519	.8671
60800	2.037	.06810	14.684	216.66	14.719	.7519	.8671
60900	2.0281	.06778	14.753	216.66	14.719	.7519	.8671
61000	2.0183	.06745	14.825	216.66	14.719	.7519	.8671
61100	2.0087	.06713	14.896	216.66	14.719	.7519	.8671
61200	1.9990	.06681	14.967	216.66	14.719	.7519	.8671
61300	1.9894	.06649	15.039	216.66	14.719	.7519	.8671
61400	1.9799	.06617	15.112	216.66	14.719	.7519	.8671
61500	1.9704	.06585	15.186	216.66	14.719	.7519	.8671
61600	1.9610	.06554	15.257	216.66	14.719	.7519	.8671
61700	1.9515	.06522	15.332	216.66	14.719	.7519	.8671
61800	1.9422	.06491	15.405	216.66	14.719	.7519	.8671
61900	1.9329	.06460	15.479	216.66	14.719	.7519	.8671
62000	1.9236	.06429	15.554	216.66	14.719	.7519	.8671
62100	1.9144	.06398	15.629	216.66	14.719	.7519	.8671
62200	1.9052	.06367	15.706	216.66	14.719	.7519	.8671
62300	1.8961	.06337	15.780	216.66	14.719	.7519	.8671
62400	1.8870	.06306	15.857	216.66	14.719	.7519	.8671
62500	1.8779	.06276	15.933	216.66	14.719	.7519	.8671
62600	1.8689	.06246	16.010	216.66	14.719	.7519	.8671
62700	1.8600	.06216	16.087	216.66	14.719	.7519	.8671
62800	1.8510	.06186	16.165	216.66	14.719	.7519	.8671
62900	1.8421	.06157	16.241	216.66	14.719	.7519	.8671

TABLE 9.2

H _c (Feet)	$\frac{\sigma}{\rho/PSL}$	$\sqrt{\sigma}$	$1/\sqrt{\sigma}$	$\sqrt{\theta/\delta}$	$1/\delta\sqrt{\theta}$	a (Knots)
59000	.09877	.3143	3.1820	11.676	15.529	573.58
59100	.09829	.3135	3.1896	11.733	15.605	573.58
59200	.09782	.3128	3.1973	11.789	15.679	573.58
59300	.09735	.3120	3.2050	11.845	15.754	573.58
59400	.09689	.3113	3.2127	11.902	15.830	573.58
59500	.09642	.3105	3.2204	11.960	15.906	573.58
59600	.09596	.3098	3.2281	12.018	15.984	573.58
59700	.09550	.3090	3.2359	12.076	16.061	573.58
59800	.09504	.3083	3.2438	12.134	16.138	573.58
59900	.09459	.3075	3.2515	12.192	16.215	573.58
60000	.09413	.3068	3.2594	12.252	16.295	573.58
60100	.09368	.3061	3.2672	12.309	16.372	573.58
60200	.09323	.3053	3.2750	12.369	16.451	573.58
60300	.09279	.3046	3.2829	12.429	16.531	573.58
60400	.09234	.3039	3.2908	12.488	16.610	573.58
60500	.09190	.3031	3.2987	12.548	16.689	573.58
60600	.09146	.3024	3.3067	12.610	16.772	573.58
60700	.09102	.3017	3.3147	12.671	16.853	573.58
60800	.09058	.3010	3.3226	12.732	16.934	573.58
60900	.09015	.3002	3.3306	12.792	17.014	573.58
61000	.08972	.2995	3.3386	12.855	17.097	573.58
61100	.08929	.2988	3.3466	12.916	17.179	573.58
61200	.08886	.2981	3.3547	12.978	17.261	573.58
61300	.08843	.2974	3.3628	13.041	17.344	573.58
61400	.08801	.2967	3.3709	13.104	17.428	573.58
61500	.08758	.2959	3.3790	13.167	17.513	573.58
61600	.08717	.2952	3.3871	13.230	17.596	573.58
61700	.08675	.2945	3.3953	13.295	17.682	573.58
61800	.08633	.2938	3.4035	13.358	17.766	573.58
61900	.08592	.2931	3.4116	13.422	17.852	573.58
62000	.08550	.2924	3.4199	13.487	17.938	573.58
62100	.08510	.2917	3.4280	13.552	18.025	573.58
62200	.08469	.2910	3.4363	13.618	18.113	573.58
62300	.08428	.2903	3.4445	13.683	18.198	573.58
62400	.08388	.2896	3.4529	13.750	18.288	573.58
62500	.08347	.2889	3.4612	13.816	18.375	573.58
62600	.08307	.2882	3.4695	13.882	18.463	573.58
62700	.08268	.2875	3.4778	13.949	18.552	573.58
62800	.08228	.2868	3.4862	14.017	18.642	573.58
62900	.08188	.2862	3.4946	14.083	18.730	573.58

Hc (Feet)	P _a ("Hg)	δ P _a /P _{aSL}	1/ δ	T _a (°K)	$\sqrt{T_a}$	θ T _a /T _{aSL}	$\sqrt{\theta}$
63000	1.8333	.06127	16.321	216.66	14.719	.7519	.8671
63100	1.8246	.06098	16.398	216.66	14.719	.7519	.8671
63200	1.8158	.06069	16.477	216.66	14.719	.7519	.8671
63300	1.8071	.06039	16.559	216.66	14.719	.7519	.8671
63400	1.7984	.06010	16.638	216.66	14.719	.7519	.8671
63500	1.7898	.05982	16.716	216.66	14.719	.7519	.8671
63600	1.7812	.05953	16.798	216.66	14.719	.7519	.8671
63700	1.7727	.05924	16.880	216.66	14.719	.7519	.8671
63800	1.7642	.05896	16.960	216.66	14.719	.7519	.8671
63900	1.7558	.05868	17.041	216.66	14.719	.7519	.8671
64000	1.7473	.05840	17.123	216.66	14.719	.7519	.8671
64100	1.7389	.05812	17.205	216.66	14.719	.7519	.8671
64200	1.7306	.05784	17.289	216.66	14.719	.7519	.8671
64300	1.7223	.05756	17.373	216.66	14.719	.7519	.8671
64400	1.7140	.05728	17.458	216.66	14.719	.7519	.8671
64500	1.7058	.05701	17.540	216.66	14.719	.7519	.8671
64600	1.6977	.05674	17.624	216.66	14.719	.7519	.8671
64700	1.6895	.05647	17.708	216.66	14.719	.7519	.8671
64800	1.6814	.05620	17.793	216.66	14.719	.7519	.8671
64900	1.6733	.05592	17.882	216.66	14.719	.7519	.8671
65000	1.6653	.05566	17.966	216.66	14.719	.7519	.8671
65100	1.6573	.05539	18.053	216.66	14.719	.7519	.8671
65200	1.6494	.05513	18.138	216.66	14.719	.7519	.8671
65300	1.6415	.05486	18.228	216.66	14.719	.7519	.8671
65400	1.6336	.05460	18.315	216.66	14.719	.7519	.8671
65500	1.6258	.05433	18.406	216.66	14.719	.7519	.8671
65600	1.6179	.05407	18.494	216.66	14.719	.7519	.8671
65700	1.6102	.05382	18.580	216.66	14.719	.7519	.8671
65800	1.6025	.05356	18.670	216.66	14.719	.7519	.8671
65900	1.5948	.05330	18.761	216.66	14.719	.7519	.8671
66000	1.5872	.05305	18.850	216.66	14.719	.7519	.8671
66100	1.5795	.05279	18.943	216.66	14.719	.7519	.8671
66200	1.5720	.05254	19.033	216.66	14.719	.7519	.8671
66300	1.5644	.05229	19.124	216.66	14.719	.7519	.8671
66400	1.5569	.05203	19.219	216.66	14.719	.7519	.8671
66500	1.5495	.05179	19.308	216.66	14.719	.7519	.8671
66600	1.5421	.05154	19.402	216.66	14.719	.7519	.8671
66700	1.5347	.05129	19.497	216.66	14.719	.7519	.8671
66800	1.5273	.05104	19.592	216.66	14.719	.7519	.8671
66900	1.5200	.05080	19.685	216.66	14.719	.7519	.8671

TABLE 9.2

H_c (Feet)	σ ρ/PSL	$\sqrt{\sigma}$	$1/\sqrt{\sigma}$	$\sqrt{\theta/\delta}$	$1/\delta\theta$	a (Knots)
63000	.08149	.2855	3.5030	14.152	18.822	573.58
63100	.08110	.2848	3.5114	14.219	18.911	573.58
63200	.08071	.2841	3.5199	14.287	19.002	573.58
63300	.08032	.2834	3.5284	14.358	19.096	573.58
63400	.07994	.2827	3.5369	14.427	19.188	573.58
63500	.07956	.2821	3.5453	14.495	19.278	573.58
63600	.07918	.2814	3.5539	14.565	19.372	573.58
63700	.07880	.2807	3.5624	14.637	19.467	573.58
63800	.07842	.2800	3.5710	14.706	19.559	573.58
63900	.07804	.2794	3.5796	14.776	19.653	573.58
64000	.07767	.2787	3.5882	14.847	19.747	573.58
64100	.07730	.2780	3.5968	14.919	19.842	573.58
64200	.07693	.2774	3.6055	14.991	19.938	573.58
64300	.07656	.2767	3.6141	15.064	20.035	573.58
64400	.07619	.2760	3.6229	15.137	20.133	573.58
64500	.07582	.2754	3.6316	15.209	20.228	573.58
64600	.07546	.2747	3.6403	15.282	20.325	573.58
64700	.07510	.2740	3.6490	15.355	20.422	573.58
64800	.07474	.2734	3.6578	15.428	20.520	573.58
64900	.07438	.2727	3.6667	15.506	20.623	573.58
65000	.07402	.2721	3.6755	15.578	20.719	573.58
65100	.07367	.2714	3.6843	15.654	20.820	573.58
65200	.07332	.2708	3.6932	15.728	20.918	573.58
65300	.07296	.2701	3.7021	15.805	21.02	573.58
65400	.07261	.2695	3.7110	15.880	21.12	573.58
65500	.07227	.2688	3.7199	15.959	21.22	573.58
65600	.07192	.2682	3.7289	16.036	21.32	573.58
65700	.07158	.2675	3.7378	16.111	21.42	573.58
65800	.07123	.2669	3.7468	16.189	21.53	573.58
65900	.07089	.2663	3.7558	16.268	21.63	573.58
66000	.07055	.2656	3.7648	16.344	21.73	573.58
66100	.07021	.2650	3.7740	16.425	21.84	573.58
66200	.06987	.2643	3.7830	16.503	21.94	573.58
66300	.06954	.2637	3.7921	16.582	22.05	573.58
66400	.06921	.2631	3.8013	16.665	22.16	573.58
66500	.06888	.2624	3.8104	16.742	22.26	573.58
66600	.06855	.2618	3.8195	16.823	22.37	573.58
66700	.06822	.2612	3.8287	16.905	22.48	573.58
66800	.06789	.2606	3.8380	16.988	22.59	573.58
66900	.06756	.2599	3.8472	17.068	22.70	573.58

H_c (Feet)	P_a ("Hg)	δ P_a/P_{aSL}	$1/\delta$	T_a (°K)	\bar{T}_a	θ T_a/T_{aSL}	$\sqrt{\theta}$
67000	1.5127	.05056	19.778	216.66	14.719	.7519	.8671
67100	1.5054	.05031	19.876	216.66	14.719	.7519	.8671
67200	1.4982	.05007	19.972	216.66	14.719	.7519	.8671
67300	1.4911	.04983	20.068	216.66	14.719	.7519	.8671
67400	1.4839	.04959	20.165	216.66	14.719	.7519	.8671
67500	1.4768	.04936	20.259	216.66	14.719	.7519	.8671
67600	1.4697	.04912	20.358	216.66	14.719	.7519	.8671
67700	1.4626	.04888	20.458	216.66	14.719	.7519	.8671
67800	1.4556	.04865	20.555	216.66	14.719	.7519	.8671
67900	1.4487	.04842	20.65	216.66	14.719	.7519	.8671
68000	1.4417	.04818	20.75	216.66	14.719	.7519	.8671
68100	1.4348	.04795	20.85	216.66	14.719	.7519	.8671
68200	1.4279	.04772	20.95	216.66	14.719	.7519	.8671
68300	1.4210	.04749	21.05	216.66	14.719	.7519	.8671
68400	1.4143	.04727	21.15	216.66	14.719	.7519	.8671
68500	1.4075	.04704	21.25	216.66	14.719	.7519	.8671
68600	1.4007	.04681	21.36	216.66	14.719	.7519	.8671
68700	1.3940	.04659	21.46	216.66	14.719	.7519	.8671
68800	1.3873	.04637	21.56	216.66	14.719	.7519	.8671
68900	1.3807	.04614	21.67	216.66	14.719	.7519	.8671
69000	1.3741	.04592	21.77	216.66	14.719	.7519	.8671
69100	1.3675	.04570	21.88	216.66	14.719	.7519	.8671
69200	1.3609	.04548	21.98	216.66	14.719	.7519	.8671
69300	1.3544	.04527	22.08	216.66	14.719	.7519	.8671
69400	1.3479	.04505	22.19	216.66	14.719	.7519	.8671
69500	1.3414	.04483	22.30	216.66	14.719	.7519	.8671
69600	1.3350	.04462	22.41	216.66	14.719	.7519	.8671
69700	1.3286	.04440	22.52	216.66	14.719	.7519	.8671
69800	1.3222	.04419	22.62	216.66	14.719	.7519	.8671
69900	1.3159	.04398	22.73	216.66	14.719	.7519	.8671
70000	1.3096	.04377	22.84	216.66	14.719	.7519	.8671
70100	1.3033	.04356	22.95	216.66	14.719	.7519	.8671
70200	1.2971	.04335	23.06	216.66	14.719	.7519	.8671
70300	1.2908	.04314	23.18	216.66	14.719	.7519	.8671
70400	1.2846	.04293	23.29	216.66	14.719	.7519	.8671
70500	1.2785	.04273	23.40	216.66	14.719	.7519	.8671
70600	1.2723	.04252	23.51	216.66	14.719	.7519	.8671
70700	1.2662	.04232	23.62	216.66	14.719	.7519	.8671
70800	1.2602	.04212	23.74	216.66	14.719	.7519	.8671
70900	1.2541	.04191	23.86	216.66	14.719	.7519	.8671

TABLE 9.2

Hc (Feet)	$\frac{\sigma}{\rho/PSL}$	$\sqrt{\sigma}$	$1/\sqrt{\sigma}$	$\sqrt{\theta/\delta}$	$1/\delta\sqrt{\theta}$	a (Knots)
67000	.06724	.2593	3.8564	17.149	22.80	573.58
67100	.06692	.2587	3.8657	17.235	22.92	573.58
67200	.06660	.2581	3.8751	17.317	23.03	573.58
67300	.06628	.2574	3.8843	17.401	23.14	573.58
67400	.06596	.2568	3.8937	17.485	23.25	573.58
67500	.06564	.2562	3.9031	17.566	23.36	573.58
67600	.06533	.2556	3.9124	17.652	23.47	573.58
67700	.06501	.2550	3.9219	17.739	23.59	573.58
67800	.06470	.2544	3.9313	17.823	23.70	573.58
67900	.06439	.2538	3.9408	17.907	23.81	573.58
68000	.06408	.2531	3.9503	17.997	23.93	573.58
68100	.06378	.2525	3.9597	18.083	24.05	573.58
68200	.06347	.2519	3.9693	18.170	24.16	573.58
68300	.06317	.2513	3.9789	18.258	24.28	573.58
68400	.06286	.2507	3.9884	18.343	24.39	573.58
68500	.06256	.2501	3.9980	18.433	24.51	573.58
68600	.06226	.2495	4.0076	18.523	24.63	573.58
68700	.06196	.2489	4.0173	18.611	24.75	573.58
68800	.06167	.2483	4.0269	18.699	24.87	573.58
68900	.06137	.2477	4.0366	18.792	24.99	573.58
69000	.06108	.2471	4.0463	18.882	25.11	573.58
69100	.06079	.2465	4.0560	18.973	25.23	573.58
69200	.06049	.2460	4.0658	19.065	25.35	573.58
69300	.06020	.2454	4.0756	19.154	25.47	573.58
69400	.05992	.2448	4.0854	19.247	25.59	573.58
69500	.05963	.2442	4.0953	19.342	25.72	573.58
69600	.05934	.2436	4.1051	19.433	25.84	573.58
69700	.05906	.2430	4.1150	19.529	25.97	573.58
69800	.05877	.2424	4.1249	19.622	26.09	573.58
69900	.05849	.2418	4.1348	19.715	26.22	573.58
70000	.05821	.2413	4.1447	19.810	26.34	573.58
70100	.05793	.2407	4.1547	19.905	26.47	573.58
70200	.05765	.2401	4.1647	20.002	26.60	573.58
70300	.05738	.2395	4.1747	20.099	26.73	573.58
70400	.05710	.2390	4.1848	20.198	26.86	573.58
70500	.05683	.2384	4.1948	20.292	26.98	573.58
70600	.05656	.2378	4.205	20.392	27.12	573.58
70700	.05628	.2372	4.215	20.489	27.25	573.58
70800	.05602	.2367	4.225	20.586	27.38	573.58
70900	.05575	.2361	4.235	20.689	27.51	573.58

H_c (Feet)	P_a ("Hg)	δ P_a/P_{aSL}	$1/\delta$	T_a (°K)	$\sqrt{T_a}$	θ T_a/T_{aSL}	$\sqrt{\theta}$
71000	1.2481	.04171	23.97	216.66	14.719	.7519	.8671
71100	1.2422	.04151	24.09	216.66	14.719	.7519	.8671
71200	1.2362	.04131	24.20	216.66	14.719	.7519	.8671
71300	1.2303	.04112	24.31	216.66	14.719	.7519	.8671
71400	1.2243	.04092	24.43	216.66	14.719	.7519	.8671
71500	1.2185	.04072	24.55	216.66	14.719	.7519	.8671
71600	1.2127	.04053	24.67	216.66	14.719	.7519	.8671
71700	1.2068	.04033	24.79	216.66	14.719	.7519	.8671
71800	1.2010	.04014	24.91	216.66	14.719	.7519	.8671
71900	1.1953	.03995	25.03	216.66	14.719	.7519	.8671
72000	1.1896	.03976	25.15	216.66	14.719	.7519	.8671
72100	1.1838	.03957	25.27	216.66	14.719	.7519	.8671
72200	1.1782	.03938	25.39	216.66	14.719	.7519	.8671
72300	1.1725	.03919	25.51	216.66	14.719	.7519	.8671
72400	1.1669	.03900	25.64	216.66	14.719	.7519	.8671
72500	1.1613	.03881	25.76	216.66	14.719	.7519	.8671
72600	1.1557	.03863	25.88	216.66	14.719	.7519	.8671
72700	1.1502	.03844	26.01	216.66	14.719	.7519	.8671
72800	1.1447	.03826	26.13	216.66	14.719	.7519	.8671
72900	1.1392	.03807	26.26	216.66	14.719	.7519	.8671
73000	1.1337	.03789	26.39	216.66	14.719	.7519	.8671
73100	1.1283	.03771	26.51	216.66	14.719	.7519	.8671
73200	1.1229	.03753	26.64	216.66	14.719	.7519	.8671
73300	1.1175	.03735	26.77	216.66	14.719	.7519	.8671
73400	1.1121	.03717	26.90	216.66	14.719	.7519	.8671
73500	1.1068	.03699	27.03	216.66	14.719	.7519	.8671
73600	1.1015	.03681	27.16	216.66	14.719	.7519	.8671
73700	1.0962	.03664	27.29	216.66	14.719	.7519	.8671
73800	1.0910	.03646	27.42	216.66	14.719	.7519	.8671
73900	1.0857	.03629	27.55	216.66	14.719	.7519	.8671
74000	1.0805	.03611	27.69	216.66	14.719	.7519	.8671
74100	1.0753	.03594	27.82	216.66	14.719	.7519	.8671
74200	1.0702	.03577	27.95	216.66	14.719	.7519	.8671
74300	1.0650	.03559	28.09	216.66	14.719	.7519	.8671
74400	1.0600	.03542	28.23	216.66	14.719	.7519	.8671
74500	1.0549	.03526	28.36	216.66	14.719	.7519	.8671
74600	1.0498	.03509	28.49	216.66	14.719	.7519	.8671
74700	1.0448	.03492	28.63	216.66	14.719	.7519	.8671
74800	1.0398	.03475	28.77	216.66	14.719	.7519	.8671
74900	1.0348	.03458	28.91	216.66	14.719	.7519	.8671

TABLE 9.2

H_c (Feet)	σ ρ/ρ_{SL}	$\sqrt{\sigma}$	$1/\sqrt{\sigma}$	$\sqrt{\theta/\delta}$	$1/\delta\sqrt{\theta}$	a (Knots)
71000	.05548	.2355	4.245	20.788	27.64	573.58
71100	.05521	.2350	4.255	20.889	27.78	573.58
71200	.05495	.2344	4.266	20.990	27.91	573.58
71300	.05469	.2338	4.276	21.087	28.04	573.58
71400	.05442	.2333	4.286	21.190	28.18	573.58
71500	.05416	.2327	4.296	21.294	28.32	573.58
71600	.05390	.2322	4.307	21.394	28.45	573.58
71700	.05364	.2316	4.317	21.500	28.59	573.58
71800	.05339	.2311	4.328	21.601	28.73	573.58
71900	.05313	.2305	4.338	21.704	28.86	573.58
72000	.05288	.2299	4.348	21.808	29.00	573.58
72100	.05262	.2294	4.359	21.913	29.14	573.58
72200	.05237	.2288	4.369	22.018	29.28	573.58
72300	.05212	.2283	4.380	22.125	29.42	573.58
72400	.05187	.2277	4.390	22.233	29.57	573.58
72500	.05162	.2272	4.401	22.342	29.71	573.58
72600	.05137	.2267	4.412	22.446	29.85	573.58
72700	.05113	.2261	4.422	22.55	30.00	573.58
72800	.05088	.2256	4.433	22.66	30.14	573.58
72900	.05064	.2250	4.443	22.77	30.29	573.58
73000	.05039	.2245	4.454	22.88	30.43	573.58
73100	.05015	.2239	4.465	22.99	30.58	573.58
73200	.04991	.2234	4.476	23.10	30.72	573.58
73300	.04967	.2229	4.486	23.21	30.87	573.58
73400	.04943	.2223	4.497	23.32	31.02	573.58
73500	.04920	.2218	4.508	23.44	31.17	573.58
73600	.04896	.2213	4.519	23.55	31.32	573.58
73700	.04873	.2207	4.530	23.66	31.47	573.58
73800	.04849	.2202	4.541	23.78	31.63	573.58
73900	.04826	.2197	4.552	23.89	31.77	573.58
74000	.04803	.2192	4.562	24.01	31.93	573.58
74100	.04780	.2186	4.573	24.12	32.08	573.58
74200	.04757	.2181	4.584	24.24	32.24	573.58
74300	.04734	.2176	4.596	24.36	32.40	573.58
74400	.04712	.2171	4.607	24.48	32.55	573.58
74500	.04689	.2165	4.618	24.59	32.70	573.58
74600	.04666	.2160	4.629	24.71	32.86	573.58
74700	.04644	.2155	4.640	24.83	33.02	573.58
74800	.04622	.2150	4.651	24.95	33.18	573.58
74900	.04600	.2145	4.662	25.07	33.35	573.58

H_c (Feet)	P_a ($^{\circ}$ Hg)	δ P_a/P_{aSL}	$1/\delta$	T_a ($^{\circ}$ K)	$\sqrt{T_a}$	θ T_a/T_{aSL}	$\sqrt{\theta}$
75000	1.0298	.03442	29.05	216.66	14.719	.7519	.8671
75100	1.0249	.03425	29.19	216.66	14.719	.7519	.8671
75200	1.0199	.03409	29.33	216.66	14.719	.7519	.8671
75300	1.0151	.03393	29.47	216.66	14.719	.7519	.8671
75400	1.0102	.03376	29.62	216.66	14.719	.7519	.8671
75500	1.0054	.03360	29.76	216.66	14.719	.7519	.8671
75600	1.0006	.03344	29.90	216.66	14.719	.7519	.8671
75700	.9957	.03328	30.04	216.66	14.719	.7519	.8671
75800	.9910	.03312	30.19	216.66	14.719	.7519	.8671
75900	.9862	.03296	30.33	216.66	14.719	.7519	.8671
76000	.9815	.03280	30.48	216.66	14.719	.7519	.8671
76100	.9768	.03265	30.62	216.66	14.719	.7519	.8671
76200	.9721	.03249	30.77	216.66	14.719	.7519	.8671
76300	.9674	.03233	30.93	216.66	14.719	.7519	.8671
76400	.9628	.03218	31.07	216.66	14.719	.7519	.8671
76500	.9582	.03202	31.23	216.66	14.719	.7519	.8671
76600	.9536	.03187	31.37	216.66	14.719	.7519	.8671
76700	.9490	.03172	31.52	216.66	14.719	.7519	.8671
76800	.9445	.03156	31.68	216.66	14.719	.7519	.8671
76900	.9400	.03141	31.83	216.66	14.719	.7519	.8671
77000	.9354	.03126	31.98	216.66	14.719	.7519	.8671
77100	.9309	.03111	32.14	216.66	14.719	.7519	.8671
77200	.9265	.03096	32.29	216.66	14.719	.7519	.8671
77300	.9221	.03082	32.44	216.66	14.719	.7519	.8671
77400	.9176	.03067	32.60	216.66	14.719	.7519	.8671
77500	.9132	.03052	32.76	216.66	14.719	.7519	.8671
77600	.9088	.03037	32.92	216.66	14.719	.7519	.8671
77700	.9045	.03023	33.07	216.66	14.719	.7519	.8671
77800	.9002	.03008	33.24	216.66	14.719	.7519	.8671
77900	.8958	.02994	33.40	216.66	14.719	.7519	.8671
78000	.8915	.02980	33.55	216.66	14.719	.7519	.8671
78100	.8873	.02965	33.72	216.66	14.719	.7519	.8671
78200	.8830	.02951	33.88	216.66	14.719	.7519	.8671
78300	.8788	.02937	34.04	216.66	14.719	.7519	.8671
78400	.8745	.02923	34.21	216.66	14.719	.7519	.8671
78500	.8704	.02909	34.37	216.66	14.719	.7519	.8671
78600	.8662	.02895	34.54	216.66	14.719	.7519	.8671
78700	.8620	.02881	34.71	216.66	14.719	.7519	.8671
78800	.8579	.02867	34.87	216.66	14.719	.7519	.8671
78900	.8538	.02853	35.05	216.66	14.719	.7519	.8671

TABLE 9.2

H_c (Feet)	σ p/PSL	$\sqrt{\sigma}$	$1/\sqrt{\sigma}$	$\sqrt{\sigma}/\delta$	$1/\delta\sqrt{\sigma}$	a (Knots)
75000	.04578	.2140	4.673	25.19	33.50	573.58
75100	.04556	.2134	4.685	25.31	33.67	573.58
75200	.04534	.2129	4.696	25.43	33.82	573.58
75300	.04512	.2124	4.707	25.55	33.98	573.58
75400	.04490	.2119	4.719	25.68	34.16	573.58
75500	.04469	.2114	4.730	25.80	34.32	573.58
75600	.04448	.2109	4.741	25.93	34.48	573.58
75700	.04426	.2104	4.753	26.05	34.65	573.58
75800	.04405	.2099	4.764	26.18	34.82	573.58
75900	.04384	.2094	4.776	26.30	34.98	573.58
76000	.04363	.2089	4.787	26.43	35.16	573.58
76100	.04342	.2084	4.799	26.55	35.32	573.58
76200	.04321	.2079	4.810	26.68	35.49	573.58
76300	.04300	.2074	4.822	26.82	35.67	573.58
76400	.04280	.2069	4.833	26.94	35.83	573.58
76500	.04259	.2064	4.845	27.08	36.01	573.58
76600	.04239	.2059	4.857	27.20	36.18	573.58
76700	.04218	.2054	4.868	27.33	36.35	573.58
76800	.04198	.2049	4.880	27.47	36.54	573.58
76900	.04178	.2044	4.892	27.60	36.71	573.58
77000	.04158	.2039	4.904	27.73	36.89	573.58
77100	.04138	.2034	4.915	27.87	37.07	573.58
77200	.04118	.2029	4.927	28.00	37.24	573.58
77300	.04099	.2024	4.939	28.13	37.41	573.58
77400	.04079	.2020	4.951	28.27	37.60	573.58
77500	.04059	.2015	4.963	28.41	37.78	573.58
77600	.04040	.2010	4.975	28.55	37.97	573.58
77700	.04020	.2005	4.987	28.68	38.14	573.58
77800	.04001	.2000	4.999	28.82	38.33	573.58
77900	.03982	.1996	5.011	28.96	38.51	573.58
78000	.03963	.1991	5.023	29.09	38.69	573.58
78100	.03944	.1986	5.035	29.24	38.89	573.58
78200	.03925	.1981	5.047	29.38	39.07	573.58
78300	.03906	.1976	5.059	29.52	39.26	573.58
78400	.03887	.1972	5.071	29.66	39.45	573.58
78500	.03869	.1967	5.084	29.80	39.64	573.58
78600	.03850	.1962	5.096	29.95	39.83	573.58
78700	.03832	.1958	5.108	30.09	40.02	573.58
78800	.03813	.1953	5.120	30.24	40.22	573.58
78900	.03795	.1948	5.133	30.39	40.42	573.58

H_c (Feet)	P_a ("Hg)	δ P_a/P_{aSL}	$1/\delta$	T_a (°K)	$\sqrt{T_a}$	θ T_a/T_{aSL}	$\sqrt{\theta}$
79000	.8497	.02840	35.21	216.66	14.719	.7519	.8671
79100	.8456	.02826	35.38	216.66	14.719	.7519	.8671
79200	.8416	.02813	35.54	216.66	14.719	.7519	.8671
79300	.8375	.02799	35.72	216.66	14.719	.7519	.8671
79400	.8335	.02786	35.89	216.66	14.719	.7519	.8671
79500	.8295	.02772	36.07	216.66	14.719	.7519	.8671
79600	.8256	.02759	36.24	216.66	14.719	.7519	.8671
79700	.8216	.02746	36.41	216.66	14.719	.7519	.8671
79800	.8176	.02733	36.58	216.66	14.719	.7519	.8671
79900	.8137	.02720	36.76	216.66	14.719	.7519	.8671
80000	.8098	.02706	36.95	216.66	14.719	.7519	.8671

TABLE 9.2

H_c (Feet)	σ p/PSI	$\sqrt{\sigma}$	$1/\sqrt{\sigma}$	$\sqrt{\theta/\delta}$	$1/\delta\sqrt{\theta}$	a (Knots)
79000	.03777	.1943	5.145	30.53	40.60	573.58
79100	.03759	.1939	5.157	30.68	40.80	573.58
79200	.03741	.1934	5.170	30.82	40.99	573.58
79300	.03723	.1929	5.182	30.97	41.20	573.58
79400	.03705	.1925	5.195	31.12	41.39	573.58
79500	.03687	.1920	5.207	31.28	41.60	573.58
79600	.03670	.1916	5.220	31.42	41.79	573.58
79700	.03652	.1911	5.232	31.57	41.99	573.58
79800	.03634	.1906	5.245	31.72	42.19	573.58
79900	.03617	.1902	5.258	31.87	42.39	573.58
80000	.03600	.1897	5.270	32.04	42.61	573.58

TABLE 9.4
MACH NUMBER, M FOR VARIOUS VALUES OF q_c/P_a

For $q_c/P_a \leq 0.893$ ($M \leq 1.00$)

$$\frac{q_c}{P_a} = (1 + 0.2M^2)^{3.5} - 1$$

Note:

$$q_c = P_t' - P_a$$

Where P_t' = free stream total pressure (P_t) for subsonic flight.

ALSO

INDICATED MACH NUMBER CORRECTED FOR INSTRUMENT
ERROR, M_{ic} FOR VARIOUS VALUES OF q_{cic}/P_s

For $q_{cic}/P_s \leq 0.893$ ($M_{ic} \leq 1.00$)

$$\frac{q_{cic}}{P_s} = (1 + 0.2 M_{ic}^2)^{3.5} - 1$$

Note:

$$q_{cic} = P_t' - P_s$$

Where P_t' = free stream total pressure (P_t) for subsonic flight.

Preceding page blank

TABLE 9.4

MACH NUMBER, M FOR VARIOUS VALUES OF q_c/P_a
 $M < 1.00$ (Subsonic)

q_c/P_a	0	1	2	3	4	5	6	7	8	9
0.00	0.0000	0.0377	0.0536	0.0656	0.0757	0.0846	0.0927	0.1001	0.1069	0.1133
.01	.1194	.1252	.1307	.1360	.1411	.1460	.1508	.1554	.1599	.1642
.02	.1684	.1725	.1765	.1804	.1843	.1881	.1918	.1954	.1990	.2025
.03	.2059	.2093	.2126	.2159	.2191	.2223	.2254	.2285	.2315	.2345
.04	.2374	.2403	.2432	.2460	.2488	.2516	.2543	.2570	.2597	.2623
.05	.2647	.2675	.2701	.2726	.2751	.2776	.2801	.2825	.2849	.2873
.06	.2897	.2921	.2944	.2967	.2990	.3013	.3036	.3058	.3080	.3102
.07	.3124	.3146	.3167	.3189	.3210	.3231	.3252	.3273	.3293	.3314
.08	.3334	.3354	.3374	.3394	.3414	.3434	.3453	.3473	.3492	.3511
.09	.3530	.3549	.3568	.3587	.3606	.3624	.3643	.3661	.3679	.3697
.10	.3715	.3733	.3751	.3769	.3786	.3804	.3821	.3839	.3856	.3873
.11	.3890	.3907	.3924	.3941	.3958	.3974	.3991	.4007	.4024	.4040
.12	.4056	.4072	.4089	.4105	.4121	.4137	.4153	.4168	.4184	.4199
.13	.4215	.4231	.4246	.4261	.4277	.4292	.4307	.4322	.4338	.4353
.14	.4367	.4382	.4397	.4412	.4427	.4441	.4456	.4470	.4484	.4499
.15	.4513	.4527	.4542	.4556	.4570	.4584	.4598	.4612	.4626	.4640
.16	.4654	.4668	.4682	.4695	.4709	.4723	.4736	.4750	.4763	.4777
.17	.4790	.4803	.4817	.4830	.4843	.4856	.4869	.4882	.4895	.4908
.18	.4921	.4934	.4947	.4960	.4972	.4985	.4998	.5010	.5023	.5035
.19	.5048	.5060	.5073	.5085	.5098	.5110	.5122	.5135	.5147	.5159
.20	.5171	.5183	.5195	.5207	.5219	.5231	.5243	.5255	.5266	.5278
.21	.5290	.5302	.5313	.5325	.5337	.5348	.5360	.5372	.5383	.5393
.22	.5406	.5417	.5429	.5440	.5452	.5463	.5474	.5485	.5497	.5508
.23	.5519	.5530	.5541	.5552	.5563	.5574	.5585	.5596	.5607	.5618
.24	.5629	.5640	.5651	.5662	.5673	.5683	.5694	.5705	.5716	.5726
.25	.5737	.5748	.5758	.5769	.5779	.5790	.5800	.5811	.5821	.5832
.26	.5842	.5852	.5863	.5873	.5884	.5894	.5904	.5914	.5925	.5935
.27	.5945	.5955	.5965	.5975	.5985	.5995	.6005	.6015	.6025	.6035
.28	.6045	.6055	.6065	.6075	.6084	.6094	.6104	.6114	.6124	.6133
.29	.6143	.6153	.6162	.6172	.6182	.6191	.6201	.6210	.6220	.6229

q_c/P_a	0	1	2	3	4	5	6	7	8	9
.30	.6239	.6248	.6258	.6267	.6277	.6286	.6296	.6305	.6314	.6324
.31	.6333	.6342	.6352	.6361	.6370	.6379	.6388	.6398	.6407	.6416
.32	.6425	.6434	.6443	.6452	.6461	.6470	.6479	.6488	.6497	.6506
.33	.6515	.6524	.6533	.6542	.6551	.6560	.6569	.6578	.6586	.6595
.34	.6604	.6613	.6622	.6630	.6639	.6648	.6656	.6665	.6674	.6682
.35	.6691	.6700	.6708	.6717	.6725	.6734	.6742	.6751	.6759	.6768
.36	.6776	.6784	.6793	.6801	.6810	.6818	.6827	.6835	.6843	.6852
.37	.6860	.6868	.6876	.6885	.6893	.6901	.6909	.6918	.6926	.6934
.38	.6942	.6950	.6958	.6966	.6975	.6983	.6991	.6999	.7007	.7015
.39	.7023	.7031	.7039	.7047	.7055	.7063	.7071	.7079	.7087	.7095
.40	.7103	.7111	.7119	.7127	.7135	.7143	.7151	.7159	.7166	.7174
.41	.7182	.7190	.7197	.7205	.7213	.7221	.7228	.7236	.7244	.7251
.42	.7259	.7267	.7274	.7282	.7290	.7297	.7305	.7312	.7320	.7327
.43	.7335	.7343	.7350	.7358	.7365	.7373	.7380	.7388	.7395	.7403
.44	.7410	.7417	.7425	.7432	.7439	.7446	.7454	.7461	.7468	.7476
.45	.7483	.7490	.7498	.7505	.7512	.7520	.7527	.7534	.7541	.7549
.46	.7556	.7563	.7571	.7578	.7585	.7592	.7599	.7607	.7614	.7621
.47	.7628	.7635	.7642	.7649	.7656	.7663	.7670	.7677	.7684	.7691
.48	.7698	.7705	.7712	.7719	.7726	.7733	.7740	.7747	.7754	.7761
.49	.7768	.7775	.7782	.7788	.7795	.7802	.7809	.7816	.7822	.7829
.50	.7836	.7843	.7850	.7857	.7863	.7870	.7877	.7884	.7890	.7897
.51	.7904	.7911	.7917	.7924	.7931	.7938	.7944	.7951	.7958	.7964
.52	.7971	.7978	.7984	.7991	.7998	.8004	.8011	.8017	.8024	.8030
.53	.8037	.8044	.8050	.8056	.8063	.8070	.8076	.8082	.8089	.8096
.54	.8102	.8109	.8115	.8122	.8128	.8135	.8141	.8148	.8154	.8161
.55	.8167	.8173	.8180	.8186	.8192	.8199	.8205	.8211	.8217	.8224
.56	.8230	.8236	.8243	.8249	.8255	.8262	.8268	.8274	.8280	.8287
.57	.8293	.8299	.8305	.8312	.8318	.8324	.8330	.8336	.8343	.8349
.58	.8355	.8361	.8368	.8374	.8380	.8386	.8392	.8399	.8405	.8411
.59	.8417	.8423	.8429	.8435	.8441	.8447	.8453	.8459	.8465	.8471

TABLE 9.4

q_c/P_a	0	2	3	4	5	6	7	8	9
.60	.8477	.8489	.8495	.8501	.8507	.8513	.8519	.8525	.8531
.61	.8537	.8549	.8555	.8561	.8566	.8572	.8578	.8584	.8590
.62	.8596	.8608	.8614	.8620	.8626	.8632	.8637	.8643	.8649
.63	.8655	.8667	.8673	.8678	.8684	.8690	.8696	.8701	.8707
.64	.8713	.8724	.8730	.8736	.8742	.8747	.8753	.8759	.8764
.65	.8770	.8781	.8787	.8793	.8799	.8804	.8810	.8816	.8821
.66	.8827	.8838	.8844	.8850	.8855	.8861	.8866	.8872	.8877
.67	.8883	.8894	.8900	.8905	.8910	.8916	.8922	.8927	.8932
.68	.8938	.8949	.8955	.8960	.8966	.8971	.8977	.8982	.8988
.69	.8993	.9004	.9009	.9015	.9020	.9025	.9031	.9036	.9042
.70	.9047	.9058	.9063	.9069	.9074	.9080	.9085	.9090	.9096
.71	.9101	.9112	.9117	.9122	.9128	.9133	.9138	.9143	.9149
.72	.9154	.9165	.9170	.9175	.9181	.9186	.9191	.9196	.9202
.73	.9207	.9217	.9223	.9228	.9233	.9238	.9243	.9249	.9254
.74	.9259	.9269	.9275	.9280	.9285	.9290	.9296	.9301	.9306
.75	.9311	.9321	.9326	.9331	.9336	.9342	.9347	.9352	.9357
.76	.9362	.9372	.9377	.9383	.9388	.9393	.9398	.9403	.9408
.77	.9413	.9423	.9428	.9433	.9438	.9443	.9448	.9453	.9458
.78	.9463	.9473	.9478	.9483	.9488	.9493	.9498	.9503	.9508
.79	.9513	.9523	.9528	.9533	.9538	.9542	.9547	.9552	.9557
.80	.9562	.9572	.9577	.9582	.9587	.9592	.9596	.9601	.9606
.81	.9611	.9621	.9625	.9630	.9635	.9640	.9645	.9649	.9654
.82	.9659	.9669	.9673	.9678	.9683	.9688	.9693	.9697	.9702
.83	.9707	.9717	.9722	.9726	.9731	.9736	.9741	.9745	.9750
.84	.9755	.9764	.9769	.9774	.9778	.9783	.9788	.9793	.9797
.85	.9802	.9811	.9816	.9821	.9826	.9830	.9835	.9840	.9844
.86	.9849	.9858	.9863	.9867	.9872	.9877	.9881	.9886	.9890
.87	.9895	.9904	.9909	.9913	.9918	.9923	.9927	.9932	.9936
.88	.9941	.9950	.9955	.9960	.9964	.9969	.9973	.9979	.9982
.89	.9987	.9996	1.0000						

TABLE 9.4

TABLE 9.5
MACH NUMBER, M FOR VARIOUS VALUES OF q_c/P_a
FOR $M \geq 1.00$ (Supersonic)

$$\frac{q_c}{P_a} = \frac{166.921 M^7}{(7 M^2 - 1)^{2.5}}^{-1}$$

Note:

$$q_c = P_t' - P_a$$

Where P_t' = total pressure behind the shock for supersonic flight.

ALSO

q_{cic}/P_s FOR VARIOUS VALUES OF INDICATED MACH NUMBER
CORRECTED FOR INSTRUMENT ERROR, M_{ic} FOR $M_{ic} \geq 1.00$
(Supersonic)

$$\frac{q_{cic}}{P_s} = \frac{166.921 M_{ic}^7}{(7 M_{ic}^2 - 1)^{2.5}}^{-1}$$

Note:

$$q_{cic} = P_t' - P_s$$

Where P_t' = total pressure behind the shock for supersonic flight.

TABLE 9.5

MACH NUMBER, M FOR VARIOUS VALUES OF q_c/P_a $M \geq 1.00$ (Supersonic) $(q_c \text{ Takes Account of Loss Through Normal Shock})$

M	0	1	2	3	4	5	6	7	8	9
1.00	0.893	0.895	0.897	0.900	0.902	0.904	0.906	0.909	0.911	0.913
1.01	.915	.918	.920	.922	.924	.927	.929	.931	.934	.936
1.02	.938	.940	.943	.945	.947	.949	.952	.954	.956	.959
1.03	.961	.963	.966	.968	.970	.973	.975	.977	.980	.982
1.04	.985	.987	.989	.992	.994	.997	.999	1.001	1.004	1.006
1.05	1.008	1.011	1.013	1.016	1.018	1.020	1.023	1.025	1.028	1.030
1.06	1.032	1.035	1.037	1.040	1.042	1.045	1.047	1.050	1.052	1.055
1.07	1.057	1.060	1.062	1.065	1.067	1.070	1.072	1.075	1.077	1.080
1.08	1.082	1.085	1.087	1.090	1.092	1.095	1.097	1.100	1.102	1.105
1.09	1.107	1.110	1.112	1.115	1.117	1.120	1.123	1.125	1.128	1.130
1.10	1.133	1.136	1.138	1.141	1.143	1.146	1.149	1.151	1.154	1.156
1.11	1.159	1.162	1.164	1.167	1.169	1.172	1.175	1.177	1.180	1.182
1.12	1.185	1.188	1.190	1.193	1.196	1.198	1.201	1.204	1.207	1.209
1.13	1.212	1.215	1.217	1.220	1.223	1.226	1.228	1.231	1.234	1.236
1.14	1.239	1.242	1.244	1.247	1.250	1.252	1.255	1.258	1.261	1.263
1.15	1.266	1.269	1.272	1.274	1.277	1.280	1.283	1.286	1.288	1.291
1.16	1.294	1.297	1.300	1.302	1.305	1.308	1.311	1.314	1.316	1.319
1.17	1.322	1.325	1.328	1.330	1.333	1.336	1.339	1.342	1.344	1.347
1.18	1.350	1.353	1.356	1.359	1.361	1.364	1.367	1.370	1.373	1.376
1.19	1.379	1.382	1.385	1.388	1.390	1.393	1.396	1.399	1.402	1.405
1.20	1.408	1.411	1.414	1.416	1.419	1.422	1.425	1.428	1.431	1.434
1.21	1.437	1.440	1.443	1.446	1.449	1.452	1.455	1.458	1.461	1.464
1.22	1.467	1.470	1.472	1.475	1.478	1.481	1.484	1.487	1.490	1.493
1.23	1.496	1.499	1.502	1.505	1.508	1.511	1.514	1.517	1.520	1.523
1.24	1.526	1.529	1.532	1.535	1.539	1.542	1.545	1.548	1.551	1.554
1.25	1.557	1.560	1.563	1.566	1.569	1.572	1.575	1.579	1.582	1.585
1.26	1.588	1.591	1.594	1.597	1.600	1.603	1.606	1.609	1.612	1.615
1.27	1.618	1.622	1.625	1.628	1.631	1.634	1.637	1.641	1.644	1.647
1.28	1.650	1.653	1.656	1.660	1.663	1.666	1.669	1.672	1.675	1.679
1.29	1.682	1.685	1.688	1.691	1.694	1.698	1.701	1.704	1.707	1.710

TABLE 9.5

M	0	1	2	3	4	5	6	7	8	9
1.30	1.714	1.717	1.720	1.723	1.727	1.730	1.733	1.736	1.740	1.743
1.31	1.746	1.749	1.753	1.756	1.759	1.762	1.766	1.769	1.772	1.775
1.32	1.779	1.782	1.785	1.788	1.792	1.795	1.798	1.801	1.805	1.808
1.33	1.811	1.815	1.818	1.821	1.825	1.828	1.831	1.835	1.838	1.841
1.34	1.845	1.848	1.851	1.855	1.858	1.861	1.865	1.868	1.871	1.875
1.35	1.878	1.881	1.885	1.888	1.891	1.895	1.898	1.901	1.905	1.908
1.36	1.912	1.915	1.918	1.922	1.925	1.929	1.932	1.936	1.939	1.942
1.37	1.946	1.949	1.953	1.956	1.960	1.963	1.966	1.970	1.973	1.977
1.38	1.980	1.984	1.987	1.990	1.994	1.997	2.001	2.004	2.008	2.011
1.39	2.014	2.018	2.021	2.025	2.028	2.032	2.035	2.039	2.043	2.046
1.40	2.050	2.053	2.057	2.060	2.064	2.067	2.071	2.074	2.078	2.081
1.41	2.085	2.088	2.092	2.095	2.099	2.102	2.106	2.109	2.113	2.116
1.42	2.120	2.123	2.127	2.131	2.134	2.138	2.141	2.145	2.149	2.152
1.43	2.156	2.159	2.163	2.167	2.170	2.174	2.177	2.181	2.185	2.188
1.44	2.192	2.195	2.199	2.203	2.206	2.210	2.213	2.217	2.221	2.224
1.45	2.228	2.231	2.235	2.239	2.242	2.246	2.250	2.253	2.257	2.261
1.46	2.265	2.268	2.272	2.276	2.279	2.283	2.287	2.290	2.294	2.298
1.47	2.301	2.305	2.309	2.312	2.316	2.320	2.323	2.327	2.331	2.335
1.48	2.338	2.342	2.346	2.349	2.353	2.357	2.361	2.365	2.368	2.372
1.49	2.376	2.380	2.383	2.387	2.391	2.395	2.398	2.402	2.406	2.410
1.50	2.414	2.417	2.421	2.425	2.429	2.432	2.436	2.440	2.444	2.447
1.51	2.451	2.455	2.459	2.463	2.467	2.470	2.474	2.478	2.482	2.486
1.52	2.490	2.494	2.497	2.501	2.505	2.509	2.513	2.517	2.520	2.524
1.53	2.528	2.532	2.536	2.540	2.544	2.547	2.551	2.555	2.559	2.563
1.54	2.567	2.571	2.574	2.578	2.582	2.586	2.590	2.594	2.598	2.602
1.55	2.606	2.610	2.614	2.618	2.622	2.626	2.630	2.634	2.638	2.642
1.56	2.646	2.649	2.653	2.657	2.661	2.665	2.669	2.673	2.677	2.681
1.57	2.685	2.689	2.693	2.697	2.701	2.705	2.709	2.713	2.717	2.720
1.58	2.724	2.728	2.733	2.737	2.741	2.745	2.749	2.753	2.757	2.761
1.59	2.765	2.769	2.773	2.777	2.781	2.785	2.789	2.793	2.797	2.801

TABLE 9.5

M	0	1	2	3	4	5	6	7	8	9
1.60	2.805	2.810	2.814	2.818	2.822	2.826	2.830	2.834	2.836	2.842
1.61	2.846	2.850	2.854	2.858	2.862	2.866	2.870	2.874	2.878	2.882
1.62	2.886	2.891	2.895	2.899	2.903	2.907	2.911	2.916	2.920	2.924
1.63	2.928	2.932	2.936	2.941	2.945	2.949	2.953	2.957	2.961	2.966
1.64	2.970	2.974	2.978	2.982	2.986	2.991	2.995	2.999	3.003	3.007
1.65	3.011	3.016	3.020	3.024	3.028	3.032	3.036	3.041	3.045	3.049
1.66	3.053	3.057	3.062	3.066	3.070	3.074	3.079	3.085	3.087	3.091
1.67	3.096	3.100	3.104	3.109	3.113	3.117	3.121	3.126	3.130	3.134
1.68	3.138	3.143	3.147	3.151	3.156	3.160	3.164	3.168	3.173	3.177
1.69	3.181	3.185	3.190	3.194	3.198	3.203	3.207	3.211	3.215	3.220
1.70	3.224	3.228	3.233	3.237	3.241	3.246	3.250	3.255	3.259	3.263
1.71	3.268	3.272	3.276	3.281	3.285	3.289	3.294	3.298	3.303	3.307
1.72	3.311	3.316	3.320	3.324	3.329	3.333	3.338	3.342	3.346	3.351
1.73	3.355	3.359	3.364	3.368	3.373	3.377	3.381	3.386	3.390	3.394
1.74	3.399	3.403	3.408	3.412	3.417	3.421	3.426	3.430	3.435	3.439
1.75	3.444	3.448	3.453	3.457	3.462	3.466	3.471	3.475	3.480	3.484
1.76	3.488	3.493	3.497	3.502	3.506	3.511	3.515	3.520	3.524	3.529
1.77	3.533	3.538	3.542	3.547	3.551	3.556	3.560	3.565	3.569	3.574
1.78	3.578	3.583	3.587	3.592	3.597	3.601	3.606	3.610	3.615	3.620
1.79	3.624	3.629	3.633	3.638	3.642	3.647	3.652	3.656	3.661	3.665
1.80	3.670	3.675	3.679	3.684	3.688	3.693	3.698	3.702	3.707	3.711
1.81	3.716	3.720	3.725	3.730	3.734	3.739	3.743	3.748	3.753	3.757
1.82	3.762	3.766	3.771	3.776	3.781	3.785	3.790	3.795	3.799	3.804
1.83	3.809	3.813	3.818	3.823	3.828	3.832	3.837	3.842	3.846	3.851
1.84	3.856	3.860	3.865	3.870	3.875	3.879	3.884	3.889	3.893	3.898
1.85	3.903	3.907	3.912	3.917	3.922	3.926	3.931	3.936	3.940	3.945
1.86	3.950	3.955	3.959	3.964	3.969	3.974	3.979	3.983	3.988	3.993
1.87	3.998	4.003	4.007	4.012	4.017	4.022	4.027	4.031	4.036	4.041
1.88	4.046	4.051	4.055	4.060	4.065	4.070	4.075	4.079	4.084	4.089
1.89	4.094	4.099	4.103	4.108	4.113	4.118	4.123	4.127	4.132	4.137

M	0	1	2	3	4	5	6	7	8	9
1.90	4.142	4.147	4.152	4.157	4.161	4.166	4.171	4.176	4.181	4.186
1.91	4.191	4.196	4.201	4.206	4.211	4.215	4.220	4.225	4.230	4.235
1.92	4.240	4.245	4.250	4.255	4.260	4.264	4.269	4.274	4.279	4.284
1.93	4.289	4.294	4.299	4.304	4.309	4.314	4.318	4.323	4.328	4.333
1.94	4.338	4.343	4.348	4.353	4.358	4.363	4.368	4.373	4.378	4.383
1.95	4.388	4.393	4.398	4.403	4.408	4.413	4.418	4.423	4.428	4.433
1.96	4.438	4.443	4.448	4.453	4.458	4.463	4.468	4.473	4.478	4.483
1.97	4.488	4.493	4.498	4.504	4.509	4.514	4.519	4.524	4.529	4.534
1.98	4.539	4.544	4.549	4.554	4.559	4.564	4.569	4.574	4.580	4.585
1.99	4.590	4.595	4.600	4.605	4.610	4.615	4.620	4.626	4.631	4.636
2.00	4.641	4.646	4.651	4.656	4.661	4.666	4.672	4.677	4.682	4.687
2.01	4.692	4.697	4.702	4.707	4.713	4.718	4.723	4.729	4.733	4.738
2.02	4.743	4.748	4.754	4.759	4.764	4.769	4.775	4.780	4.785	4.790
2.03	4.795	4.801	4.806	4.811	4.816	4.822	4.827	4.832	4.837	4.842
2.04	4.848	4.853	4.858	4.863	4.869	4.874	4.879	4.884	4.889	4.895
2.05	4.900	4.905	4.910	4.916	4.921	4.926	4.931	4.936	4.942	4.947
2.06	4.952	4.957	4.963	4.968	4.973	4.979	4.984	4.989	4.995	5.000
2.07	5.005	5.011	5.016	5.021	5.027	5.032	5.037	5.043	5.048	5.053
2.08	5.059	5.064	5.069	5.075	5.080	5.085	5.091	5.096	5.101	5.107
2.09	5.112	5.117	5.123	5.128	5.133	5.139	5.144	5.149	5.155	5.160
2.10	5.165	5.171	5.176	5.182	5.187	5.193	5.198	5.203	5.209	5.214
2.11	5.220	5.225	5.231	5.236	5.241	5.247	5.252	5.258	5.263	5.269
2.12	5.274	5.279	5.285	5.290	5.296	5.301	5.307	5.312	5.317	5.323
2.13	5.328	5.334	5.339	5.345	5.350	5.355	5.361	5.366	5.372	5.377
2.14	5.383	5.388	5.394	5.399	5.405	5.410	5.416	5.421	5.427	5.432
2.15	5.438	5.444	5.449	5.455	5.460	5.466	5.471	5.477	5.482	5.488
2.16	5.493	5.499	5.504	5.510	5.516	5.521	5.527	5.532	5.538	5.543
2.17	5.549	5.554	5.560	5.565	5.571	5.576	5.582	5.588	5.593	5.599
2.18	5.604	5.610	5.615	5.621	5.627	5.632	5.638	5.644	5.649	5.655
2.19	5.661	5.666	5.672	5.678	5.683	5.689	5.694	5.700	5.706	5.711

TABLE 9.5

M	0	1	2	3	4	5	6	7	8	9
2.20	5.717	5.723	5.728	5.734	5.740	5.745	5.751	5.756	5.762	5.768
2.21	5.773	5.779	5.785	5.790	5.796	5.802	5.807	5.813	5.819	5.824
2.22	5.830	5.836	5.841	5.847	5.853	5.859	5.864	5.870	5.876	5.882
2.23	5.887	5.893	5.899	5.904	5.910	5.916	5.922	5.927	5.933	5.939
2.24	5.945	5.950	5.956	5.962	5.968	5.973	5.979	5.985	5.991	5.996
2.25	6.002	6.008	6.014	6.019	6.025	6.031	6.037	6.042	6.048	6.054
2.26	6.060	6.065	6.071	6.077	6.083	6.089	6.095	6.101	6.106	6.112
2.27	6.118	6.124	6.130	6.136	6.142	6.147	6.153	6.159	6.165	6.171
2.28	6.177	6.182	6.188	6.194	6.200	6.206	6.212	6.218	6.223	6.229
2.29	6.235	6.241	6.247	6.253	6.258	6.264	6.270	6.276	6.282	6.288
2.30	6.294	6.300	6.306	6.311	6.317	6.323	6.329	6.335	6.341	6.347
2.31	6.353	6.359	6.365	6.371	6.377	6.383	6.389	6.395	6.401	6.407
2.32	6.413	6.419	6.425	6.431	6.437	6.443	6.448	6.454	6.460	6.466
2.33	6.472	6.478	6.484	6.490	6.496	6.502	6.508	6.514	6.520	6.526
2.34	6.532	6.538	6.544	6.550	6.556	6.562	6.568	6.574	6.580	6.586
2.35	6.592	6.599	6.605	6.611	6.617	6.623	6.629	6.635	6.641	6.647
2.36	6.653	6.659	6.665	6.671	6.677	6.683	6.689	6.695	6.702	6.708
2.37	6.714	6.720	6.726	6.732	6.738	6.744	6.750	6.756	6.762	6.768
2.38	6.774	6.780	6.787	6.793	6.799	6.805	6.811	6.817	6.823	6.830
2.39	6.836	6.842	6.848	6.854	6.860	6.867	6.873	6.879	6.885	6.891
2.40	6.897	6.904	6.910	6.916	6.922	6.928	6.934	6.941	6.947	6.953
2.41	6.959	6.965	6.971	6.977	6.984	6.990	6.996	7.002	7.008	7.014
2.42	7.021	7.027	7.033	7.039	7.046	7.052	7.058	7.064	7.071	7.077
2.43	7.083	7.090	7.096	7.102	7.108	7.115	7.121	7.127	7.133	7.140
2.44	7.146	7.152	7.158	7.165	7.171	7.177	7.183	7.190	7.196	7.202
2.45	7.209	7.215	7.221	7.227	7.234	7.240	7.246	7.252	7.259	7.265
2.46	7.271	7.278	7.284	7.290	7.297	7.303	7.309	7.316	7.322	7.329
2.47	7.335	7.341	7.348	7.354	7.360	7.367	7.373	7.380	7.386	7.392
2.48	7.399	7.405	7.411	7.418	7.424	7.431	7.437	7.443	7.450	7.456
2.49	7.462	7.469	7.475	7.481	7.488	7.494	7.501	7.507	7.513	7.520

TABLE 9.5

M	0	1	2	3	4	5	6	7	8	9
2.50	7.526	7.533	7.539	7.546	7.552	7.558	7.565	7.571	7.578	7.584
2.51	7.591	7.597	7.604	7.610	7.617	7.623	7.630	7.636	7.643	7.649
2.52	7.656	7.662	7.669	7.675	7.682	7.688	7.694	7.701	7.707	7.714
2.53	7.720	7.727	7.733	7.740	7.746	7.753	7.759	7.766	7.772	7.779
2.54	7.785	7.792	7.798	7.805	7.811	7.818	7.825	7.831	7.838	7.844
2.55	7.851	7.857	7.864	7.871	7.877	7.884	7.890	7.897	7.903	7.910
2.56	7.917	7.923	7.930	7.936	7.943	7.949	7.956	7.963	7.969	7.976
2.57	7.982	7.989	7.996	8.002	8.009	8.015	8.022	8.028	8.035	8.042
2.58	8.048	8.055	8.061	8.068	8.075	8.082	8.088	8.095	8.102	8.108
2.59	8.115	8.122	8.128	8.135	8.142	8.148	8.155	8.162	8.168	8.175
2.60	8.182	8.188	8.195	8.202	8.208	8.215	8.222	8.228	8.235	8.242
2.61	8.248	8.255	8.262	8.269	8.275	8.282	8.289	8.295	8.302	8.309
2.62	8.315	8.322	8.329	8.336	8.342	8.349	8.356	8.363	8.370	8.376
2.63	8.383	8.390	8.397	8.404	8.410	8.417	8.424	8.431	8.437	8.444
2.64	8.451	8.458	8.465	8.471	8.478	8.485	8.492	8.498	8.505	8.512
2.65	8.519	8.526	8.532	8.539	8.546	8.553	8.560	8.566	8.573	8.580
2.66	8.587	8.594	8.600	8.607	8.614	8.621	8.628	8.635	8.642	8.649
2.67	8.656	8.662	8.669	8.676	8.683	8.690	8.697	8.704	8.711	8.718
2.68	8.724	8.731	8.738	8.745	8.752	8.759	8.766	8.773	8.780	8.787
2.69	8.793	8.800	8.807	8.814	8.821	8.828	8.835	8.842	8.849	8.855
2.70	8.862	8.869	8.876	8.883	8.890	8.897	8.904	8.911	8.918	8.925
2.71	8.932	8.939	8.946	8.953	8.960	8.967	8.974	8.981	8.988	8.995
2.72	9.002	9.009	9.016	9.023	9.030	9.037	9.044	9.051	9.058	9.065
2.73	9.072	9.079	9.086	9.093	9.100	9.107	9.114	9.121	9.128	9.135
2.74	9.142	9.149	9.156	9.163	9.170	9.177	9.185	9.192	9.199	9.206
2.75	9.213	9.220	9.227	9.234	9.241	9.248	9.256	9.263	9.270	9.277
2.76	9.284	9.291	9.298	9.305	9.312	9.319	9.327	9.334	9.341	9.348
2.77	9.355	9.362	9.369	9.376	9.383	9.390	9.398	9.405	9.412	9.419
2.78	9.426	9.433	9.440	9.448	9.455	9.462	9.469	9.476	9.484	9.491
2.79	9.498	9.505	9.512	9.520	9.527	9.534	9.541	9.548	9.556	9.563

TABLE 9.5

M	0	1	2	3	4	5	6	7	8	9
2.80	9.570	9.577	9.584	9.592	9.599	9.606	9.613	9.620	9.628	9.635
2.81	9.642	9.649	9.656	9.664	9.671	9.678	9.685	9.692	9.700	9.707
2.82	9.714	9.721	9.728	9.736	9.743	9.750	9.758	9.765	9.772	9.780
2.83	9.787	9.794	9.801	9.809	9.816	9.823	9.831	9.838	9.845	9.853
2.84	9.860	9.867	9.874	9.882	9.889	9.896	9.904	9.911	9.918	9.926
2.85	9.933	9.940	9.947	9.955	9.962	9.969	9.977	9.984	9.991	9.999
2.86	10.006	10.013	10.021	10.028	10.035	10.043	10.050	10.058	10.065	10.072
2.87	10.080	10.087	10.095	10.102	10.110	10.117	10.124	10.132	10.139	10.147
2.88	10.154	10.161	10.169	10.176	10.184	10.191	10.198	10.206	10.213	10.221
2.89	10.228	10.235	10.243	10.250	10.258	10.265	10.272	10.280	10.287	10.295
2.90	10.302	10.310	10.317	10.325	10.332	10.340	10.347	10.355	10.362	10.370
2.91	10.377	10.385	10.392	10.400	10.407	10.415	10.422	10.430	10.437	10.445
2.92	10.452	10.460	10.467	10.475	10.482	10.490	10.497	10.505	10.512	10.520
2.93	10.527	10.535	10.542	10.550	10.557	10.565	10.572	10.580	10.587	10.595
2.94	10.602	10.610	10.618	10.625	10.633	10.641	10.648	10.656	10.663	10.671
2.95	10.679	10.686	10.694	10.702	10.709	10.717	10.724	10.732	10.740	10.747
2.96	10.755	10.762	10.770	10.778	10.785	10.793	10.801	10.808	10.816	10.823
2.97	10.831	10.839	10.846	10.854	10.861	10.869	10.877	10.884	10.892	10.900
2.98	10.907	10.915	10.923	10.930	10.938	10.946	10.953	10.961	10.969	10.977
2.99	10.984	10.992	11.000	11.007	11.015	11.023	11.031	11.038	11.046	11.054
3.00	11.061									

TABLE 9.6

DIFFERENTIAL PRESSURE, q_c (" Hg) FOR VARIOUS VALUES
OF CALIBRATED AIRSPEED, V_c (Knots)

$$\frac{q_c}{P_{aSL}} = \left[1 + 0.2 (V_c/a_{SL})^2 \right]^{3.5} - 1 \quad V_c \leq a_{SL}$$

$$\frac{q_c}{P_{aSL}} = \frac{166.921 (V_c/a_{SL})^7}{\left[7 (V_c/a_{SL})^2 - 1 \right]^{2.5}} - 1 \quad V_c \geq a_{SL}$$

where $P_{aSL} = 29,92126$ "Hg

$a_{SL} = 661.48$ Knots

Note:

$$q_c = P_t' - P_a$$

where P_t' = free stream total pressure (P_t) for subsonic flight

P_t' = total pressure behind the shock in supersonic flight

ALSO

INDICATED DIFFERENTIAL PRESSURE, q_{cic} (" Hg) FOR VARIOUS
VALUES OF INDICATED AIRSPEED CORRECTED FOR INSTRUMENT
ERROR, V_{ic} (Knots)

$$\frac{q_{cic}}{P_{aSL}} = \left[1 + 0.2 (V_{ic}/a_{SL})^2 \right]^{3.5} - 1 \quad V_{ic} \leq a_{SL}$$

$$\frac{q_{cic}}{P_{aSL}} = \frac{166.921 (V_{ic}/a_{SL})^7}{\left[7 (V_{ic}/a_{SL})^2 - 1 \right]^{2.5}} - 1 \quad V_{ic} \geq a_{SL}$$

where $P_{aSL} = 29,92126$ " Hg

$a_{SL} = 661.48$ Knots

Note:

$$q_{cic} = P_t' - P_s$$

where P_t' = free stream total pressure (P_t) for subsonic flight

P_t' = total pressure behind the shock for supersonic flight

TABLE 9.6

DIFFERENTIAL PRESSURE, q_c (" Hg) FOR VARIOUS VALUES
OF CALIBRATED AIRSPEED, V_c (Knots)

V_c (Knots)	q_c (" Hg)	V_c (Knots)	q_c (" Hg)	V_c (Knots)	q_c (" Hg)	V_c (Knots)	q_c (" Hg)
0.0	0.0000	20.0	0.0192	40.0	0.0767	60.0	0.1727
0.5	0.0000	20.5	0.0201	40.5	0.0786	60.5	0.1756
1.0	0.0001	21.0	0.0211	41.0	0.0805	61.0	0.1785
1.5	0.0001	21.5	0.0221	41.5	0.0825	61.5	0.1814
2.0	0.0002	22.0	0.0232	42.0	0.0845	62.0	0.1844
2.5	0.0003	22.5	0.0242	42.5	0.0866	62.5	0.1874
3.0	0.0004	23.0	0.0253	43.0	0.0886	63.0	0.1904
3.5	0.0006	23.5	0.0264	43.5	0.0907	63.5	0.1935
4.0	0.0008	24.0	0.0276	44.0	0.0928	64.0	0.1965
4.5	0.0010	24.5	0.0287	44.5	0.0949	64.5	0.1996
5.0	0.0012	25.0	0.0299	45.0	0.0970	65.0	0.2027
5.5	0.0014	25.5	0.0311	45.5	0.0992	65.5	0.2059
6.0	0.0017	26.0	0.0324	46.0	0.1014	66.0	0.2090
6.5	0.0020	26.5	0.0336	46.5	0.1036	66.5	0.2122
7.0	0.0023	27.0	0.0349	47.0	0.1059	67.0	0.2154
7.5	0.0027	27.5	0.0362	47.5	0.1081	67.5	0.2187
8.0	0.0031	28.0	0.0375	48.0	0.1104	68.0	0.2219
8.5	0.0035	28.5	0.0389	48.5	0.1127	68.5	0.2252
9.0	0.0039	29.0	0.0403	49.0	0.1151	69.0	0.2285
9.5	0.0043	29.5	0.0417	49.5	0.1175	69.5	0.2319
10.0	0.0048	30.0	0.0431	50.0	0.1198	70.0	0.2352
10.5	0.0053	30.5	0.0446	50.5	0.1223	70.5	0.2386
11.0	0.0058	31.0	0.0460	51.0	0.1247	71.0	0.2420
11.5	0.0063	31.5	0.0475	51.5	0.1272	71.5	0.2454
12.0	0.0069	32.0	0.0490	52.0	0.1296	72.0	0.2489
12.5	0.0075	32.5	0.0506	52.5	0.1321	72.5	0.2524
13.0	0.0081	33.0	0.0522	53.0	0.1347	73.0	0.2559
13.5	0.0087	33.5	0.0538	53.5	0.1372	73.5	0.2594
14.0	0.0094	34.0	0.0554	54.0	0.1398	74.0	0.2629
14.5	0.0101	34.5	0.0570	54.5	0.1424	74.5	0.2665
15.0	0.0108	35.0	0.0587	55.0	0.1451	75.0	0.2701
15.5	0.0115	35.5	0.0604	55.5	0.1477	75.5	0.2737
16.0	0.0123	36.0	0.0621	56.0	0.1504	76.0	0.2774
16.5	0.0130	36.5	0.0638	56.5	0.1531	76.5	0.2811
17.0	0.0138	37.0	0.0656	57.0	0.1558	77.0	0.2848
17.5	0.0147	37.5	0.0674	57.5	0.1586	77.5	0.2885
18.0	0.0155	38.0	0.0692	58.0	0.1613	78.0	0.2922
18.5	0.0164	38.5	0.0710	58.5	0.1641	78.5	0.2960
19.0	0.0173	39.0	0.0729	59.0	0.1670	79.0	0.2998
19.5	0.0182	39.5	0.0748	59.5	0.1698	79.5	0.3036

V _c (Knots)	q _c (^o Hg)
80.0	0.3075
80.5	0.3113
81.0	0.3152
81.5	0.3192
82.0	0.3231
82.5	0.3271
83.0	0.3311
83.5	0.3351
84.0	0.3391
84.5	0.3432
85.0	0.3473
85.5	0.3514
86.0	0.3555
86.5	0.3597
87.0	0.3639
87.5	0.3681
88.0	0.3723
88.5	0.3766
89.0	0.3809
89.5	0.3852
90.0	0.3895
90.5	0.3939
91.0	0.3983
91.5	0.4027
92.0	0.4071
92.5	0.4116
93.0	0.4161
93.5	0.4206
94.0	0.4251
94.5	0.4297
95.0	0.4342
95.5	0.4388
96.0	0.4435
96.5	0.4481
97.0	0.4528
97.5	0.4575
98.0	0.4623
98.5	0.4670
99.0	0.4718
99.5	0.4766

V _c (Knots)	q _c (^o Hg)
100.0	0.4814
100.5	0.4863
101.0	0.4912
101.5	0.4961
102.0	0.5010
102.5	0.5059
103.0	0.5109
103.5	0.5159
104.0	0.5209
104.5	0.5260
105.0	0.5311
105.5	0.5362
106.0	0.5413
106.5	0.5465
107.0	0.5516
107.5	0.5568
108.0	0.5621
108.5	0.5673
109.0	0.5726
109.5	0.5779
110.0	0.5832
110.5	0.5886
111.0	0.5939
111.5	0.5993
112.0	0.6048
112.5	0.6102
113.0	0.6157
113.5	0.6212
114.0	0.6267
114.5	0.6323
115.0	0.6379
115.5	0.6435
116.0	0.6491
116.5	0.6547
117.0	0.6604
117.5	0.6661
118.0	0.6718
118.5	0.6776
119.0	0.6834
119.5	0.6892

V _c (Knots)	q _c (^o Hg)
120.0	0.6950
120.5	0.7008
121.0	0.7067
121.5	0.7126
122.0	0.7185
122.5	0.7245
123.0	0.7305
123.5	0.7365
124.0	0.7425
124.5	0.7486
125.0	0.7546
125.5	0.7607
126.0	0.7669
126.5	0.7730
127.0	0.7792
127.5	0.7854
128.0	0.7916
128.5	0.7979
129.0	0.8042
129.5	0.8105
130.0	0.8168
130.5	0.8232
131.0	0.8295
131.5	0.8360
132.0	0.8424
132.5	0.8488
133.0	0.8553
133.5	0.8618
134.0	0.8684
134.5	0.8749
135.0	0.8815
135.5	0.8881
136.0	0.8948
136.5	0.9014
137.0	0.9081
137.5	0.9148
138.0	0.9216
138.5	0.9283
139.0	0.9351
139.5	0.9419

V _c (Knots)	q _c (^o Hg)
140.0	0.9488
140.5	0.9556
141.0	0.9625
141.5	0.9694
142.0	0.9764
142.5	0.9833
143.0	0.9903
143.5	0.9974
144.0	1.004
144.5	1.011
145.0	1.019
145.5	1.026
146.0	1.033
146.5	1.040
147.0	1.047
147.5	1.054
148.0	1.062
148.5	1.069
149.0	1.076
149.5	1.084
150.0	1.090
150.5	1.098
151.0	1.106
151.5	1.113
152.0	1.120
152.5	1.128
153.0	1.136
153.5	1.143
154.0	1.151
154.5	1.158
155.0	1.166
155.5	1.173
156.0	1.181
156.5	1.189
157.0	1.197
157.5	1.204
158.0	1.212
158.5	1.220
159.0	1.228
159.5	1.236

TABLE 9.6

V _c (Knots)	q _c (ⁿ Hg)
160.0	1.243
160.5	1.251
161.0	1.259
161.5	1.267
162.0	1.275
162.5	1.283
163.0	1.291
163.5	1.299
164.0	1.307
164.5	1.315
165.0	1.324
165.5	1.332
166.0	1.340
166.5	1.348
167.0	1.356
167.5	1.365
168.0	1.373
168.5	1.381
169.0	1.390
169.5	1.398
170.0	1.406
170.5	1.415
171.0	1.423
171.5	1.432
172.0	1.440
172.5	1.449
173.0	1.457
173.5	1.466
174.0	1.474
174.5	1.483
175.0	1.492
175.5	1.500
176.0	1.510
176.5	1.518
177.0	1.527
177.5	1.536
178.0	1.544
178.5	1.553
179.0	1.562
179.5	1.571

V _c (Knots)	q _c (ⁿ Hg)
180.0	1.580
180.5	1.589
181.0	1.598
181.5	1.607
182.0	1.616
182.5	1.625
183.0	1.634
183.5	1.643
184.0	1.652
184.5	1.661
185.0	1.671
185.5	1.680
186.0	1.689
186.5	1.698
187.0	1.708
187.5	1.717
188.0	1.726
188.5	1.736
189.0	1.745
189.5	1.754
190.0	1.764
190.5	1.773
191.0	1.783
191.5	1.792
192.0	1.802
192.5	1.812
193.0	1.821
193.5	1.831
194.0	1.841
194.5	1.850
195.0	1.860
195.5	1.870
196.0	1.880
196.5	1.889
197.0	1.899
197.5	1.909
198.0	1.919
198.5	1.929
199.0	1.939
199.5	1.949

V _c (Knots)	q _c (ⁿ Hg)
200.0	1.959
200.5	1.969
201.0	1.979
201.5	1.989
202.0	1.999
202.5	2.009
203.0	2.019
203.5	2.030
204.0	2.040
204.5	2.050
205.0	2.060
205.5	2.070
206.0	2.081
206.5	2.091
207.0	2.102
207.5	2.112
208.0	2.123
208.5	2.133
209.0	2.144
209.5	2.154
210.0	2.165
210.5	2.175
211.0	2.186
211.5	2.196
212.0	2.207
212.5	2.218
213.0	2.229
213.5	2.239
214.0	2.250
214.5	2.261
215.0	2.272
215.5	2.283
216.0	2.293
216.5	2.304
217.0	2.315
217.5	2.326
218.0	2.337
218.5	2.348
219.0	2.359
219.5	2.370

V _c (Knots)	q _c (ⁿ Hg)
220.0	2.382
220.5	2.393
221.0	2.404
221.5	2.415
222.0	2.426
222.5	2.439
223.0	2.449
223.5	2.460
224.0	2.471
224.5	2.483
225.0	2.494
225.5	2.506
226.0	2.517
226.5	2.529
227.0	2.540
227.5	2.552
228.0	2.563
228.5	2.575
229.0	2.586
229.5	2.598
230.0	2.610
230.5	2.621
231.0	2.633
231.5	2.645
232.0	2.657
232.5	2.668
233.0	2.680
233.5	2.692
234.0	2.704
234.5	2.716
235.0	2.728
235.5	2.740
236.0	2.752
236.5	2.764
237.0	2.776
237.5	2.788
238.0	2.800
238.5	2.812
239.0	2.825
239.5	2.837

V _c (Knots)	q _c (ⁿ Hg)
240.0	2.849
240.5	2.861
241.0	2.874
241.5	2.886
242.0	2.898
242.5	2.911
243.0	2.923
243.5	2.936
244.0	2.948
244.5	2.961
245.0	2.973
245.5	2.986
246.0	2.998
246.5	3.011
247.0	3.024
247.5	3.036
248.0	3.049
248.5	3.062
249.0	3.074
249.5	3.087
250.0	3.100
250.5	3.113
251.0	3.126
251.5	3.139
252.0	3.152
252.5	3.165
253.0	3.178
253.5	3.191
254.0	3.204
254.5	3.217
255.0	3.230
255.5	3.243
256.0	3.256
256.5	3.269
257.0	3.283
257.5	3.296
258.0	3.309
258.5	3.323
259.0	3.336
259.5	3.349

V _c (Knots)	q _c (ⁿ Hg)
260.0	3.363
260.5	3.376
261.0	3.390
261.5	3.403
262.0	3.417
262.5	3.430
263.0	3.444
263.5	3.458
264.0	3.471
264.5	3.485
265.0	3.499
265.5	3.512
266.0	3.526
266.5	3.540
267.0	3.554
267.5	3.568
268.0	3.581
268.5	3.595
269.0	3.609
269.5	3.623
270.0	3.637
270.5	3.651
271.0	3.665
271.5	3.680
272.0	3.694
272.5	3.708
273.0	3.722
273.5	3.736
274.0	3.750
274.5	3.765
275.0	3.779
275.5	3.793
276.0	3.808
276.5	3.822
277.0	3.837
277.5	3.851
278.0	3.866
278.5	3.880
279.0	3.895
279.5	3.909

V _c (Knots)	q _c (ⁿ Hg)
280.0	3.924
280.5	3.939
281.0	3.953
281.5	3.968
282.0	3.983
282.5	3.997
283.0	4.012
283.5	4.027
284.0	4.042
284.5	4.057
285.0	4.072
285.5	4.087
286.0	4.102
286.5	4.117
287.0	4.132
287.5	4.147
288.0	4.162
288.5	4.177
289.0	4.192
289.5	4.208
290.0	4.223
290.5	4.238
291.0	4.253
291.5	4.269
292.0	4.284
292.5	4.299
293.0	4.315
293.5	4.330
294.0	4.346
294.5	4.361
295.0	4.377
295.5	4.393
296.0	4.408
296.5	4.424
297.0	4.439
297.5	4.455
298.0	4.471
298.5	4.487
299.0	4.502
299.5	4.518

V _c (Knots)	q _c (ⁿ Hg)
300.0	4.534
300.5	4.550
301.0	4.566
301.5	4.582
302.0	4.598
302.5	4.614
303.0	4.630
303.5	4.646
304.0	4.662
304.5	4.678
305.0	4.695
305.5	4.711
306.0	4.727
306.5	4.743
307.0	4.760
307.5	4.776
308.0	4.792
308.5	4.809
309.0	4.825
309.5	4.842
310.0	4.858
310.5	4.875
311.0	4.891
311.5	4.908
312.0	4.925
312.5	4.941
313.0	4.958
313.5	4.975
314.0	4.991
314.5	5.008
315.0	5.025
315.5	5.042
316.0	5.059
316.5	5.076
317.0	5.093
317.5	5.110
318.0	5.127
318.5	5.144
319.0	5.161
319.5	5.178

TABLE 9.6

V _c (Knots)	q _c (" Hg)
320.0	5.195
320.5	5.212
321.0	5.230
321.5	5.247
322.0	5.264
322.5	5.281
323.0	5.299
323.5	5.316
324.0	5.334
324.5	5.351
325.0	5.369
325.5	5.386
326.0	5.404
326.5	5.421
327.0	5.439
327.5	5.456
328.0	5.474
328.5	5.492
329.0	5.510
329.5	5.527
330.0	5.545
330.5	5.563
331.0	5.581
331.5	5.599
332.0	5.617
332.5	5.635
333.0	5.653
333.5	5.671
334.0	5.689
334.5	5.707
335.0	5.725
335.5	5.743
336.0	5.762
336.5	5.780
337.0	5.798
337.5	5.817
338.0	5.835
338.5	5.853
339.0	5.872
339.5	5.890

V _c (Knots)	q _c (" Hg)
340.0	5.909
340.5	5.927
341.0	5.946
341.5	5.964
342.0	5.983
342.5	6.002
343.0	6.020
343.5	6.039
344.0	6.058
344.5	6.077
345.0	6.095
345.5	6.114
346.0	6.133
346.5	6.152
347.0	6.171
347.5	6.190
348.0	6.209
348.5	6.228
349.0	6.247
349.5	6.267
350.0	6.286
350.5	6.305
351.0	6.324
351.5	6.344
352.0	6.363
352.5	6.382
353.0	6.402
353.5	6.421
354.0	6.440
354.5	6.460
355.0	6.479
355.5	6.499
356.0	6.519
356.5	6.538
357.0	6.558
357.5	6.578
358.0	6.597
358.5	6.617
359.0	6.637
359.5	6.657

V _c (Knots)	q _c (" Hg)
360.0	6.677
360.5	6.697
361.0	6.717
361.5	6.737
362.0	6.757
362.5	6.777
363.0	6.797
363.5	6.817
364.0	6.837
364.5	6.857
365.0	6.877
365.5	6.898
366.0	6.918
366.5	6.938
367.0	6.959
367.5	6.979
368.0	7.000
368.5	7.020
369.0	7.041
369.5	7.061
370.0	7.082
370.5	7.102
371.0	7.123
371.5	7.144
372.0	7.165
372.5	7.185
373.0	7.206
373.5	7.227
374.0	7.248
374.5	7.269
375.0	7.290
375.5	7.311
376.0	7.332
376.5	7.353
377.0	7.374
377.5	7.395
378.0	7.416
378.5	7.437
379.0	7.459
379.5	7.480

V _c (Knots)	q _c (" Hg)
380.0	7.501
380.5	7.523
381.0	7.544
381.5	7.566
382.0	7.587
382.5	7.608
383.0	7.630
383.5	7.652
384.0	7.673
384.5	7.695
385.0	7.717
385.5	7.739
386.0	7.760
386.5	7.782
387.0	7.804
387.5	7.826
388.0	7.848
388.5	7.869
389.0	7.891
389.5	7.913
390.0	7.936
390.5	7.958
391.0	7.980
391.5	8.002
392.0	8.024
392.5	8.046
393.0	8.069
393.5	8.091
394.0	8.113
394.5	8.136
395.0	8.158
395.5	8.181
396.0	8.203
396.5	8.226
397.0	8.248
397.5	8.271
398.0	8.294
398.5	8.316
399.0	8.339
399.5	8.362

V _c (Knots)	q _c (ⁿ Hg)
400.0	8.385
400.5	8.408
401.0	8.431
401.5	8.453
402.0	8.476
402.5	8.499
403.0	8.523
403.5	8.546
404.0	8.569
404.5	8.592
405.0	8.615
405.5	8.638
406.0	8.662
406.5	8.685
407.0	8.708
407.5	8.732
408.0	8.755
408.5	8.779
409.0	8.802
409.5	8.826
410.0	8.849
410.5	8.873
411.0	8.897
411.5	8.920
412.0	8.944
412.5	8.968
413.0	8.992
413.5	9.016
414.0	9.040
414.5	9.063
415.0	9.087
415.5	9.112
416.0	9.136
416.5	9.160
417.0	9.184
417.5	9.208
418.0	9.232
418.5	9.257
419.0	9.281
419.5	9.305

V _c (Knots)	q _c (ⁿ Hg)
420.0	9.330
420.5	9.354
421.0	9.378
421.5	9.403
422.0	9.427
422.5	9.452
423.0	9.477
423.5	9.501
424.0	9.526
424.5	9.551
425.0	9.576
425.5	9.600
426.0	9.625
426.5	9.650
427.0	9.675
427.5	9.700
428.0	9.725
428.5	9.750
429.0	9.775
429.5	9.800
430.0	9.826
430.5	9.851
431.0	9.876
431.5	9.901
432.0	9.927
432.5	9.952
433.0	9.978
433.5	10.00
434.0	10.03
434.5	10.05
435.0	10.08
435.5	10.11
436.0	10.13
436.5	10.16
437.0	10.18
437.5	10.21
438.0	10.23
438.5	10.26
439.0	10.29
439.5	10.31

V _c (Knots)	q _c (ⁿ Hg)
440.0	10.34
440.5	10.36
441.0	10.39
441.5	10.42
442.0	10.44
442.5	10.47
443.0	10.50
443.5	10.52
444.0	10.55
444.5	10.57
445.0	10.60
445.5	10.63
446.0	10.65
446.5	10.68
447.0	10.71
447.5	10.73
448.0	10.76
448.5	10.79
449.0	10.81
449.5	10.84
450.0	10.87
450.5	10.90
451.0	10.92
451.5	10.95
452.0	10.98
452.5	11.00
453.0	11.03
453.5	11.06
454.0	11.08
454.5	11.11
455.0	11.14
455.5	11.17
456.0	11.19
456.5	11.22
457.0	11.25
457.5	11.28
458.0	11.30
458.5	11.33
459.0	11.36
459.5	11.39

V _c (Knots)	q _c (ⁿ Hg)
460.0	11.41
460.5	11.44
461.0	11.47
461.5	11.50
462.0	11.52
462.5	11.55
463.0	11.58
463.5	11.61
464.0	11.64
464.5	11.66
465.0	11.69
465.5	11.72
466.0	11.75
466.5	11.78
467.0	11.81
467.5	11.83
468.0	11.86
468.5	11.89
469.0	11.92
469.5	11.95
470.0	11.98
470.5	12.01
471.0	12.03
471.5	12.07
472.0	12.09
472.5	12.12
473.0	12.15
473.5	12.18
474.0	12.21
474.5	12.24
475.0	12.27
475.5	12.29
476.0	12.32
476.5	12.35
477.0	12.38
477.5	12.41
478.0	12.44
478.5	12.47
479.0	12.50
479.5	12.53

TABLE 9.6

V _c (Knots)	q _c (" Hg)
480.0	12.56
480.5	12.59
481.0	12.62
481.5	12.65
482.0	12.68
482.5	12.71
483.0	12.74
483.5	12.77
484.0	12.80
484.5	12.83
485.0	12.86
485.5	12.89
486.0	12.92
486.5	12.95
487.0	12.98
487.5	13.01
488.0	13.04
488.5	13.07
489.0	13.10
489.5	13.13
490.0	13.16
490.5	13.19
491.0	13.22
491.5	13.25
492.0	13.28
492.5	13.31
493.0	13.34
493.5	13.37
494.0	13.40
494.5	13.43
495.0	13.46
495.5	13.49
496.0	13.53
496.5	13.56
497.0	13.59
497.5	13.62
498.0	13.65
498.5	13.68
499.0	13.71
499.5	13.74

V _c (Knots)	q _c (" Hg)
500.0	13.78
500.5	13.81
501.0	13.84
501.5	13.87
502.0	13.90
502.5	13.93
503.0	13.96
503.5	14.00
504.0	14.03
504.5	14.06
505.0	14.10
505.5	14.12
506.0	14.16
506.5	14.19
507.0	14.22
507.5	14.25
508.0	14.28
508.5	14.32
509.0	14.35
509.5	14.38
510.0	14.41
510.5	14.44
511.0	14.48
511.5	14.51
512.0	14.54
512.5	14.57
513.0	14.61
513.5	14.64
514.0	14.67
514.5	14.70
515.0	14.74
515.5	14.77
516.0	14.80
516.5	14.84
517.0	14.87
517.5	14.90
518.0	14.94
518.5	14.97
519.0	15.00
519.5	15.04

V _c (Knots)	q _c (" Hg)
520.0	15.07
520.5	15.10
521.0	15.14
521.5	15.17
522.0	15.20
522.5	15.24
523.0	15.27
523.5	15.30
524.0	15.34
524.5	15.37
525.0	15.40
525.5	15.44
526.0	15.47
526.5	15.51
527.0	15.54
527.5	15.57
528.0	15.61
528.5	15.64
529.0	15.68
529.5	15.71
530.0	15.74
530.5	15.78
531.0	15.81
531.5	15.85
532.0	15.88
532.5	15.92
533.0	15.95
533.5	15.99
534.0	16.02
534.5	16.06
535.0	16.09
535.5	16.13
536.0	16.16
536.5	16.19
537.0	16.23
537.5	16.26
538.0	16.30
538.5	16.33
539.0	16.37
539.5	16.41

V _c (Knots)	q _c (" Hg)
540.0	16.44
540.5	16.48
541.0	16.51
541.5	16.55
542.0	16.58
542.5	16.62
543.0	16.65
543.5	16.69
544.0	16.73
544.5	16.76
545.0	16.80
545.5	16.83
546.0	16.87
546.5	16.90
547.0	16.94
547.5	16.98
548.0	17.01
548.5	17.05
549.0	17.09
549.5	17.12
550.0	17.16
550.5	17.19
551.0	17.23
551.5	17.27
552.0	17.30
552.5	17.34
553.0	17.38
553.5	17.41
554.0	17.45
554.5	17.49
555.0	17.52
555.5	17.56
556.0	17.60
556.5	17.64
557.0	17.67
557.5	17.71
558.0	17.75
558.5	17.78
559.0	17.82
559.5	17.86

V _c (Knots)	q _c (ⁿ Hg)
560.0	17.90
560.5	17.93
561.0	17.97
561.5	18.01
562.0	18.05
562.5	18.09
563.0	18.12
563.5	18.16
564.0	18.20
564.5	18.24
565.0	18.27
565.5	18.31
566.0	18.35
566.5	18.39
567.0	18.43
567.5	18.46
568.0	18.50
568.5	18.54
569.0	18.58
569.5	18.62
570.0	18.66
570.5	18.70
571.0	18.73
571.5	18.77
572.0	18.81
572.5	18.85
573.0	18.89
573.5	18.93
574.0	18.97
574.5	19.01
575.0	19.05
575.5	19.09
576.0	19.12
576.5	19.16
577.0	19.20
577.5	19.24
578.0	19.28
578.5	19.32
579.0	19.36
579.5	19.40

V _c (Knots)	q _c (ⁿ Hg)
580.0	19.44
580.5	19.48
581.0	19.52
581.5	19.56
582.0	19.60
582.5	19.64
583.0	19.68
583.5	19.72
584.0	19.76
584.5	19.80
585.0	19.84
585.5	19.88
586.0	19.92
586.5	19.96
587.0	20.00
587.5	20.04
588.0	20.08
588.5	20.12
589.0	20.16
589.5	20.20
590.0	20.25
590.5	20.29
591.0	20.33
591.5	20.37
592.0	20.41
592.5	20.45
593.0	20.49
593.5	20.53
594.0	20.57
594.5	20.62
595.0	20.66
595.5	20.70
596.0	20.74
596.5	20.78
597.0	20.82
597.5	20.86
598.0	20.91
598.5	20.95
599.0	20.99
599.5	21.03

V _c (Knots)	q _c (ⁿ Hg)
600.0	21.07
600.5	21.12
601.0	21.16
601.5	21.20
602.0	21.24
602.5	21.29
603.0	21.33
603.5	21.37
604.0	21.41
604.5	21.45
605.0	21.50
605.5	21.54
606.0	21.58
606.5	21.63
607.0	21.67
607.5	21.71
608.0	21.75
608.5	21.80
609.0	21.84
609.5	21.88
610.0	21.93
610.5	21.97
611.0	22.01
611.5	22.06
612.0	22.10
612.5	22.14
613.0	22.19
613.5	22.23
614.0	22.27
614.5	22.32
615.0	22.36
615.5	22.41
616.0	22.45
616.5	22.49
617.0	22.54
617.5	22.58
618.0	22.63
618.5	22.67
619.0	22.71
619.5	22.76

V _c (Knots)	q _c (ⁿ Hg)
620.0	22.80
620.5	22.85
621.0	22.89
621.5	22.94
622.0	22.98
622.5	23.03
623.0	23.07
623.5	23.12
624.0	23.16
624.5	23.21
625.0	23.25
625.5	23.30
626.0	23.34
626.5	23.39
627.0	23.43
627.5	23.48
628.0	23.52
628.5	23.57
629.0	23.61
629.5	23.66
630.0	23.71
630.5	23.75
631.0	23.80
631.5	23.84
632.0	23.89
632.5	23.94
633.0	23.98
633.5	24.03
634.0	24.07
634.5	24.12
635.0	24.17
635.5	24.21
636.0	24.26
636.5	24.31
637.0	24.35
637.5	24.40
638.0	24.45
638.5	24.49
639.0	24.54
639.5	24.59

TABLE 9.6

V _c (Knots)	q _c (ⁿ Hg)
640.0	24.63
640.5	24.68
641.0	24.73
641.5	24.78
642.0	24.82
642.5	24.87
643.0	24.92
643.5	24.97
644.0	25.01
644.5	25.06
645.0	25.11
645.5	25.16
646.0	25.20
646.5	25.25
647.0	25.30
647.5	25.35
648.0	25.40
648.5	25.44
649.0	25.49
649.5	25.54
650.0	25.59
650.5	25.64
651.0	25.69
651.5	25.73
652.0	25.78
652.5	25.83
653.0	25.88
653.5	25.93
654.0	25.98
654.5	26.03
655.0	26.08
655.5	26.12
656.0	26.17
656.5	26.22
657.0	26.27
657.5	26.32
658.0	26.37
658.5	26.42
659.0	26.47
659.5	26.52

V _c (Knots)	q _c (ⁿ Hg)
660.0	26.57
660.5	26.62
661.0	26.67
661.5	26.72
662.0	26.77
662.5	26.82
663.0	26.87
663.5	26.92
664.0	26.97
664.5	27.02
665.0	27.07
665.5	27.12
666.0	27.17
666.5	27.22
667.0	27.27
667.5	27.32
668.0	27.37
668.5	27.43
669.0	27.48
669.5	27.53
670.0	27.58
670.5	27.63
671.0	27.68
671.5	27.73
672.0	27.78
672.5	27.83
673.0	27.89
673.5	27.94
674.0	27.99
674.5	28.04
675.0	28.09
675.5	28.14
676.0	28.20
676.5	28.25
677.0	28.30
677.5	28.35
678.0	28.40
678.5	28.46
679.0	28.51
679.5	28.56

V _c (Knots)	q _c (ⁿ Hg)
680.0	28.61
680.5	28.67
681.0	28.72
681.5	28.77
682.0	28.82
682.5	28.88
683.0	28.93
683.5	28.98
684.0	29.04
684.5	29.09
685.0	29.14
685.5	29.19
686.0	29.25
686.5	29.30
687.0	29.35
687.5	29.41
688.0	29.46
688.5	29.51
689.0	29.57
689.5	29.62
690.0	29.68
690.5	29.73
691.0	29.78
691.5	29.84
692.0	29.89
692.5	29.95
693.0	30.00
693.5	30.05
694.0	30.11
694.5	30.16
695.0	30.22
695.5	30.27
696.0	30.33
696.5	30.38
697.0	30.43
697.5	30.49
698.0	30.54
698.5	30.60
699.0	30.65
699.5	30.71

V _c (Knots)	q _c (ⁿ Hg)
700.0	30.76
700.5	30.82
701.0	30.87
701.5	30.93
702.0	30.98
702.5	31.04
703.0	31.09
703.5	31.15
704.0	31.20
704.5	31.26
705.0	31.32
705.5	31.37
706.0	31.43
706.5	31.48
707.0	31.54
707.5	31.59
708.0	31.65
708.5	31.71
709.0	31.76
709.5	31.82
710.0	31.88
710.5	31.93
711.0	31.99
711.5	32.04
712.0	32.10
712.5	32.16
713.0	32.21
713.5	32.27
714.0	32.33
714.5	32.38
715.0	32.44
715.5	32.50
716.0	32.55
716.5	32.61
717.0	32.67
717.5	32.73
718.0	32.78
718.5	32.84
719.0	32.90
719.5	32.95

V _c (Knots)	q _c (^w Hg)
720.0	33.01
720.5	33.07
721.0	33.13
721.5	33.19
722.0	33.24
722.5	33.30
723.0	33.36
723.5	33.42
724.0	33.47
724.5	33.53
725.0	33.59
725.5	33.65
726.0	33.71
726.5	33.76
727.0	33.82
727.5	33.88
728.0	33.94
728.5	34.00
729.0	34.06
729.5	34.11
730.0	34.17
730.5	34.23
731.0	34.29
731.5	34.35
732.0	34.41
732.5	34.47
733.0	34.53
733.5	34.59
734.0	34.64
734.5	34.70
735.0	34.76
735.5	34.82
736.0	34.88
736.5	34.94
737.0	35.00
737.5	35.06
738.0	35.12
738.5	35.18
739.0	35.24
739.5	35.30

V _c (Knots)	q _c (^w Hg)
740.0	35.36
740.5	35.42
741.0	35.48
741.5	35.54
742.0	35.60
742.5	35.66
743.0	35.72
743.5	35.78
744.0	35.84
744.5	35.90
745.0	35.96
745.5	36.02
746.0	36.08
746.5	36.14
747.0	36.20
747.5	36.26
748.0	36.32
748.5	36.38
749.0	36.44
749.5	36.50
750.0	36.56
750.5	36.63
751.0	36.69
751.5	36.75
752.0	36.81
752.5	36.87
753.0	36.93
753.5	36.99
754.0	37.05
754.5	37.12
755.0	37.18
755.5	37.24
756.0	37.30
756.5	37.36
757.0	37.42
757.5	37.49
758.0	37.55
758.5	37.61
759.0	37.67
759.5	37.73

V _c (Knots)	q _c (^w Hg)
760.0	37.80
760.5	37.86
761.0	37.92
761.5	37.98
762.0	38.04
762.5	38.11
763.0	38.17
763.5	38.23
764.0	38.29
764.5	38.36
765.0	38.42
765.5	38.48
766.0	38.54
766.5	38.61
767.0	38.67
767.5	38.73
768.0	38.80
768.5	38.86
769.0	38.92
769.5	38.98
770.0	39.05
770.5	39.11
771.0	39.17
771.5	39.24
772.0	39.30
772.5	39.36
773.0	39.43
773.5	39.49
774.0	39.55
774.5	39.62
775.0	39.68
775.5	39.75
776.0	39.81
776.5	39.87
777.0	39.94
777.5	40.00
778.0	40.07
778.5	40.13
779.0	40.19
779.5	40.26

V _c (Knots)	q _c (^w Hg)
780.0	40.32
780.5	40.39
781.0	40.45
781.5	40.52
782.0	40.58
782.5	40.64
783.0	40.71
783.5	40.77
784.0	40.84
784.5	40.90
785.0	40.97
785.5	41.03
786.0	41.10
786.5	41.16
787.0	41.23
787.5	41.29
788.0	41.36
788.5	41.42
789.0	41.49
789.5	41.55
790.0	41.62
790.5	41.68
791.0	41.75
791.5	41.81
792.0	41.88
792.5	41.95
793.0	42.01
793.5	42.08
794.0	42.14
794.5	42.21
795.0	42.27
795.5	42.34
796.0	42.41
796.5	42.47
797.0	42.54
797.5	42.60
798.0	42.67
798.5	42.74
799.0	42.80
799.5	42.87

TABLE 9.6

V _c (Knots)	q _c (° Hg)
800.0	42.94
800.5	43.00
801.0	43.07
801.5	43.14
802.0	43.20
802.5	43.27
803.0	43.34
803.5	43.40
804.0	43.47
804.5	43.54
805.0	43.60
805.5	43.67
806.0	43.74
806.5	43.80
807.0	43.87
807.5	43.94
808.0	44.01
808.5	44.07
809.0	44.14
809.5	44.21
810.0	44.28
810.5	44.34
811.0	44.41
811.5	44.48
812.0	44.55
812.5	44.61
813.0	44.68
813.5	44.75
814.0	44.82
814.5	44.89
815.0	44.95
815.5	45.02
816.0	45.09
816.5	45.16
817.0	45.23
817.5	45.29
818.0	45.36
818.5	45.43
819.0	45.50
819.5	45.57

V _c (Knots)	q _c (° Hg)
820.0	45.64
820.5	45.70
821.0	45.77
821.5	45.84
822.0	45.91
822.5	45.98
823.0	46.05
823.5	46.12
824.0	46.19
824.5	46.25
825.0	46.32
825.5	46.39
826.0	46.46
826.5	46.53
827.0	46.60
827.5	46.67
828.0	46.74
828.5	46.81
829.0	46.88
829.5	46.95
830.0	47.02
830.5	47.09
831.0	47.16
831.5	47.23
832.0	47.30
832.5	47.37
833.0	47.44
833.5	47.51
834.0	47.58
834.5	47.65
835.0	47.72
835.5	47.79
836.0	47.86
836.5	47.93
837.0	48.00
837.5	48.07
838.0	48.14
838.5	48.21
839.0	48.28
839.5	48.35

V _c (Knots)	q _c (° Hg)
840.0	48.42
840.5	48.49
841.0	48.56
841.5	48.63
842.0	48.70
842.5	48.77
843.0	48.84
843.5	48.91
844.0	48.99
844.5	49.06
845.0	49.13
845.5	49.20
846.0	49.27
846.5	49.34
847.0	49.41
847.5	49.48
848.0	49.55
848.5	49.63
849.0	49.70
849.5	49.77
850.0	49.84
850.5	49.91
851.0	49.98
851.5	50.06
852.0	50.13
852.5	50.20
853.0	50.27
853.5	50.34
854.0	50.42
854.5	50.49
855.0	50.56
855.5	50.63
856.0	50.70
856.5	50.78
857.0	50.85
857.5	50.92
858.0	50.99
858.5	51.07
859.0	51.14
859.5	51.21

V _c (Knots)	q _c (° Hg)
860.0	51.28
860.5	51.36
861.0	51.43
861.5	51.50
862.0	51.57
862.5	51.65
863.0	51.72
863.5	51.79
864.0	51.87
864.5	51.94
865.0	52.01
865.5	52.09
866.0	52.16
866.5	52.23
867.0	52.30
867.5	52.38
868.0	52.45
868.5	52.53
869.0	52.60
869.5	52.67
870.0	52.75
870.5	52.82
871.0	52.89
871.5	52.97
872.0	53.04
872.5	53.11
873.0	53.19
873.5	53.26
874.0	53.34
874.5	53.41
875.0	53.48
875.5	53.56
876.0	53.63
876.5	53.71
877.0	53.78
877.5	53.86
878.0	53.93
878.5	54.01
879.0	54.08
879.5	54.15

V _c (Knots)	q _c (" Hg)	V _c (Knots)	q _c (" Hg)	V _c (Knots)	q _c (" Hg)	V _c (Knots)	q _c (" Hg)
880.0	54.23	900.0	57.25	920.0	60.36	940.0	63.54
880.5	54.30	900.5	57.33	920.5	60.44	940.5	63.62
881.0	54.38	901.0	57.41	921.0	60.51	941.0	63.70
881.5	54.45	901.5	57.48	921.5	60.59	941.5	63.78
882.0	54.53	902.0	57.56	922.0	60.67	942.0	63.86
882.5	54.60	902.5	57.64	922.5	60.75	942.5	63.94
883.0	54.68	903.0	57.71	923.0	60.83	943.0	64.02
883.5	54.75	903.5	57.79	923.5	60.91	943.5	64.10
884.0	54.83	904.0	57.87	924.0	60.99	944.0	64.18
884.5	54.90	904.5	57.95	924.5	61.07	944.5	64.27
885.0	54.98	905.0	58.02	925.0	61.15	945.0	64.35
885.5	55.05	905.5	58.10	925.5	61.22	945.5	64.43
886.0	55.13	906.0	58.18	926.0	61.30	946.0	64.51
886.5	55.20	906.5	58.25	926.5	61.38	946.5	64.59
887.0	55.28	907.0	58.33	927.0	61.46	947.0	64.67
887.5	55.35	907.5	58.41	927.5	61.54	947.5	64.75
888.0	55.43	908.0	58.49	928.0	61.62	948.0	64.83
888.5	55.50	908.5	58.56	928.5	61.70	948.5	64.91
889.0	55.58	909.0	58.64	929.0	61.78	949.0	65.00
889.5	55.66	909.5	58.72	929.5	61.86	949.5	65.08
890.0	55.73	910.0	58.80	930.0	61.94	950.0	65.16
890.5	55.81	910.5	58.87	930.5	62.02	950.5	65.24
891.0	55.88	911.0	58.95	931.0	62.10	951.0	65.32
891.5	55.96	911.5	59.03	931.5	62.18	951.5	65.40
892.0	56.03	912.0	59.11	932.0	62.26	952.0	65.48
892.5	56.11	912.5	59.18	932.5	62.34	952.5	65.57
893.0	56.19	913.0	59.26	933.0	62.42	953.0	65.65
893.5	56.26	913.5	59.34	933.5	62.50	953.5	65.73
894.0	56.34	914.0	59.42	934.0	62.58	954.0	65.81
894.5	56.41	914.5	59.50	934.5	62.66	954.5	65.89
895.0	56.49	915.0	59.57	935.0	62.74	955.0	65.98
895.5	56.57	915.5	59.65	935.5	62.82	955.5	66.06
896.0	56.64	916.0	59.73	936.0	62.90	956.0	66.14
896.5	56.72	916.5	59.81	936.5	62.98	956.5	66.22
897.0	56.79	917.0	59.89	937.0	63.06	957.0	66.30
897.5	56.87	917.5	59.97	937.5	63.14	957.5	66.39
898.0	56.95	918.0	60.04	938.0	63.22	958.0	66.47
898.5	57.02	918.5	60.12	938.5	63.30	958.5	66.55
899.0	57.10	919.0	60.20	939.0	63.38	959.0	66.63
899.5	57.18	919.5	60.28	939.5	63.46	959.5	66.72

TABLE 9.6

V_c (Knots)	q_c ($^{\circ}$ Hg)
960.0	66.80
960.5	66.88
961.0	66.96
961.5	67.04
962.0	67.13
962.5	67.21
963.0	67.30
963.5	67.38
964.0	67.46
964.5	67.54
965.0	67.62
965.5	67.71
966.0	67.79
966.3	67.87
967.0	67.96
967.5	68.04
968.0	68.12
968.5	68.21
969.0	68.29
969.5	68.37

V_c (Knots)	q_c ($^{\circ}$ Hg)
970.0	68.46
970.5	68.54
971.0	68.62
971.5	68.71
972.0	68.79
972.5	68.87
973.0	68.96
973.5	69.04
974.0	69.12
974.5	69.21
975.0	69.29
975.5	69.38
976.0	69.46
976.5	69.54
977.0	69.63
977.5	69.71
978.0	69.80
978.5	69.88
979.0	69.96
979.5	70.05

V_c (Knots)	q_c ($^{\circ}$ Hg)
980.0	70.13
980.5	70.22
981.0	70.30
981.5	70.39
982.0	70.47
982.5	70.55
983.0	70.64
983.5	70.72
984.0	70.81
984.5	70.89
985.0	70.98
985.5	71.06
986.0	71.15
986.5	71.23
987.0	71.32
987.5	71.40
988.0	71.49
988.5	71.57
989.0	71.66
989.5	71.74

V_c (Knots)	q_c ($^{\circ}$ Hg)
990.0	71.83
990.5	71.91
991.0	72.00
991.5	72.08
992.0	72.17
992.5	72.26
993.0	72.34
993.5	72.43
994.0	72.51
994.5	72.60
995.0	72.68
995.5	72.77
996.0	72.86
996.5	72.94
997.0	73.03
997.5	73.11
998.0	73.20
998.5	73.29
999.0	73.37
999.5	73.46
1000.0	73.54

TABLE 9.6

TABLE 9.7

Conversion Formulae - Fahrenheit, Centigrade and Rankine

Fahrenheit to Centigrade

$$C = \frac{5}{9} (F-32)$$

Fahrenheit to Rankine

$$R = F + 459.7$$

Centigrade to Fahrenheit

$$F = \frac{9}{5} C + 32$$

Centigrade to Rankine

$$R = \frac{9}{5} C + 491.7$$

Rankine to Fahrenheit

$$F = R - 459.7$$

Rankine to Centigrade

$$C = \frac{5}{9} (R-491.7)$$

CENTIGRADE - FAHRENHEIT

CONVERSION TABLE

°C		°F	°C		°F	°C		°F
-169.4	-273	-459.4	-138.9	-218	-360.4	-108.3	-163	-261.4
-168.9	-272	-457.6	-138.3	-217	-358.6	-107.8	-162	-259.6
-168.3	-271	-455.8	-137.8	-216	-356.8	-107.2	-161	-257.8
-167.8	-270	-454.0	-137.2	-215	-355.0	-106.7	-160	-256.0
-167.2	-269	-452.2	-136.7	-214	-353.2	-106.1	-159	-254.2
-166.7	-268	-450.4	-136.1	-213	-351.4	-105.6	-158	-252.4
-166.1	-267	-448.6	-135.6	-212	-349.6	-105.0	-157	-250.6
-165.6	-266	-446.8	-135.0	-211	-347.8	-104.4	-156	-248.8
-165.0	-265	-445.0	-134.4	-210	-346.0	-103.9	-155	-247.0
-164.4	-264	-443.2	-133.9	-209	-344.2	-103.3	-154	-245.2
-163.9	-263	-441.4	-133.3	-208	-342.4	-102.8	-153	-243.4
-163.3	-262	-439.6	-132.8	-207	-340.6	-102.2	-152	-241.6
-162.8	-261	-437.8	-132.2	-206	-338.8	-101.7	-151	-239.8
-162.2	-260	-436.0	-131.7	-205	-337.0	-101.1	-150	-238.0
-161.7	-259	-434.2	-131.1	-204	-335.2	-100.6	-149	-236.2
-161.1	-258	-432.4	-130.6	-203	-333.4	-100.0	-148	-234.4
-160.6	-257	-430.6	-130.0	-202	-331.6	-99.4	-147	-232.6
-160.0	-256	-428.8	-129.4	-201	-329.8	-98.9	-146	-230.8
-159.4	-255	-427.0	-128.9	-200	-328.0	-98.3	-145	-229.0
-158.9	-254	-425.2	-128.3	-199	-326.2	-97.8	-144	-227.2
-158.3	-253	-423.4	-127.8	-198	-324.4	-97.2	-143	-225.4
-157.8	-252	-421.6	-127.2	-197	-322.6	-96.7	-142	-223.6
-157.2	-251	-419.8	-126.7	-196	-320.8	-96.1	-141	-221.8
-156.7	-250	-418.0	-126.1	-195	-319.0	-95.6	-140	-220.0
-156.1	-249	-416.2	-125.6	-194	-317.2	-95.0	-139	-218.2
-155.6	-248	-414.4	-125.0	-193	-315.4	-94.4	-138	-216.4
-155.0	-247	-412.6	-124.4	-192	-313.6	-93.9	-137	-214.6
-154.4	-246	-410.8	-123.9	-191	-311.8	-93.3	-136	-212.8
-153.9	-245	-409.0	-123.3	-190	-310.0	-92.8	-135	-211.0
-153.3	-244	-407.2	-122.8	-189	-308.2	-92.2	-134	-209.2
-152.8	-243	-405.4	-122.2	-188	-306.4	-91.7	-133	-207.4
-152.2	-242	-403.6	-121.7	-187	-304.6	-91.1	-132	-205.6
-151.7	-241	-401.8	-121.1	-186	-302.8	-90.6	-131	-203.8
-151.1	-240	-400.0	-120.6	-185	-301.0	-90.0	-130	-202.0
-150.6	-239	-398.2	-120.0	-184	-299.2	-89.4	-129	-200.2
-150.0	-238	-396.4	-119.4	-183	-297.4	-88.9	-128	-198.4
-149.4	-237	-394.6	-118.9	-182	-295.6	-88.3	-127	-196.6
-148.9	-236	-392.8	-118.3	-181	-293.8	-87.8	-126	-194.8
-148.3	-235	-391.0	-117.8	-180	-292.0	-87.2	-125	-193.0
-147.8	-234	-389.2	-117.2	-179	-290.2	-86.7	-124	-191.2
-147.2	-233	-387.4	-116.7	-178	-288.4	-86.1	-123	-189.4
-146.7	-232	-385.6	-116.1	-177	-286.6	-85.6	-122	-187.6
-146.1	-231	-383.8	-115.6	-176	-284.8	-85.0	-121	-185.8
-145.6	-230	-382.0	-115.0	-175	-283.0	-84.4		-184.0
-145.0	-229	-380.2	-114.4	-174	-281.2	-83.9		-182.2
-144.4	-228	-378.4	-113.9	-173	-279.4	-83.3		-180.4
-143.9	-227	-376.6	-113.3	-172	-277.6	-82.8		-178.6
-143.3	-226	-374.8	-112.8	-171	-275.8	-82.2		-176.8
-142.8	-225	-373.0	-112.2	-170	-274.0	-81.7		-175.0
-142.2	-224	-371.2	-111.7	-169	-272.2	-81.1		-173.2
-141.7	-223	-369.4	-111.1	-168	-270.4	-80.6		-171.4
-141.1	-222	-367.6	-110.6	-167	-268.6	-80.0		-169.6
-140.6	-221	-365.8	-110.0	-166	-266.8	-79.4		-167.8
-140.0	-220	-364.0	-109.4	-165	-265.0	-78.9		-166.0
-139.4	-219	-362.2	-108.9	-164	-263.2	-78.3		-164.2

CENTIGRADE - FAHRENHEIT

CONVERSION TABLE

°C		°F	°C		°F	°C		°F
-77.8	-108	-162.4	-47.2	-53	-63.4	-16.7	2	35.6
-77.2	-107	-160.6	-46.7	-52	-61.6	-16.1	3	37.4
-76.7	-106	-158.8	-46.1	-51	-59.8	-15.6	4	39.2
-76.1	-105	-157.0	-45.6	-50	-58.0	-15.0	5	41.0
-75.6	-104	-155.2	-45.0	-49	-56.2	-14.4	6	42.8
-75.0	-103	-153.4	-44.4	-48	-54.4	-13.9	7	44.6
-74.4	-102	-151.6	-43.9	-47	-52.6	-13.3	8	46.4
-73.9	-101	-149.8	-43.3	-46	-50.8	-12.8	9	48.2
-73.3	-100	-148.0	-42.8	-45	-49.0	-12.2	10	50.0
-72.8	-99	-146.2	-42.2	-44	-47.2	-11.7	11	51.8
-72.2	-98	-144.4	-41.7	-43	-45.4	-11.1	12	53.6
-71.7	-97	-142.6	-41.1	-42	-43.6	-10.6	13	55.4
-71.1	-96	-140.8	-40.6	-41	-41.8	-10.0	14	57.2
-70.6	-95	-139.0	-40.0	-40	-40.0	-9.4	15	59.0
-70.0	-94	-137.2	-39.4	-39	-38.2	-8.9	16	60.8
-69.4	-93	-135.4	-38.9	-38	-36.4	-8.3	17	62.6
-68.9	-92	-133.6	-38.3	-37	-34.6	-7.8	18	64.4
-68.3	-91	-131.8	-37.8	-36	-32.8	-7.2	19	66.2
-67.8	-90	-130.0	-37.2	-35	-31.0	-6.7	20	68.0
-67.2	-89	-128.2	-36.7	-34	-29.2	-6.1	21	69.8
-66.7	-88	-126.4	-36.1	-33	-27.4	-5.6	22	71.6
-66.1	-87	-124.6	-35.6	-32	-25.6	-5.0	23	73.4
-65.6	-86	-122.8	-35.0	-31	-23.8	-4.4	24	75.2
-65.0	-85	-121.0	-34.4	-30	-22.0	-3.9	25	77.0
-64.4	-84	-119.2	-33.9	-29	-20.2	-3.3	26	78.8
-63.9	-83	-117.4	-33.3	-28	-18.4	-2.8	27	80.6
-63.3	-82	-115.6	-32.8	-27	-16.6	-2.2	28	82.4
-62.8	-81	-113.8	-32.2	-26	-14.8	-1.7	29	84.2
-62.2	-80	-112.0	-31.7	-25	-13.0	-1.1	30	86.0
-61.7	-79	-110.2	-31.1	-24	-11.2	-0.6	31	87.8
-61.1	-78	-108.4	-30.6	-23	-9.4	0	32	89.6
-60.6	-77	-106.6	-30.0	-22	-7.6	0.6	33	91.4
-60.0	-76	-104.8	-29.4	-21	-5.8	1.1	34	93.2
-59.4	-75	-103.0	-28.9	-20	-4.0	1.7	35	95.0
-58.9	-74	-101.2	-28.3	-19	-2.2	2.2	36	96.8
-58.3	-73	-99.4	-27.8	-18	-0.4	2.8	37	98.6
-57.8	-72	-97.6	-27.2	-17	1.4	3.3	38	100.4
-57.2	-71	-95.8	-26.7	-16	3.2	3.9	39	102.2
-56.7	-70	-94.0	-26.1	-15	5.0	4.4	40	104.0
-56.1	-69	-92.2	-25.6	-14	6.8	5.0	41	105.8
-55.6	-68	-90.4	-25.0	-13	8.6	5.6	42	107.6
-55.0	-67	-88.6	-24.4	-12	10.4	6.1	43	109.4
-54.4	-66	-86.8	-23.9	-11	12.2	6.7	44	111.2
-53.9	-65	-85.0	-23.3	-10	14.0	7.2	45	113.0
-53.3	-64	-83.2	-22.8	-9	15.8	7.8	46	114.8
-52.8	-63	-81.4	-22.2	-8	17.6	8.3	47	116.6
-52.2	-62	-79.6	-21.7	-7	19.4	8.9	48	118.4
-51.7	-61	-77.8	-21.1	-6	21.2	9.4	49	120.2
-51.1	-60	-76.0	-20.6	-5	23.0	10.0	50	122.0
-50.6	-59	-74.2	-20.0	-4	24.8	10.6	51	123.8
-50.0	-58	-72.4	-19.4	-3	26.6	11.1	52	125.6
-49.4	-57	-70.6	-18.9	-2	28.4	11.7	53	127.4
-48.9	-56	-68.8	-18.3	-1	30.2	12.2	54	129.2
-48.3	-55	-67.0	-17.8	0	32.0	12.8	55	131.0
-47.8	-54	-65.2	-17.2	1	33.8	13.3	56	132.8

CENTIGRADE - FAHRENHEIT

CONVERSION TABLE

°C		°F	°C		°F	°C		°F
13.9	57	134.6	43.9	111	231.8	73.9	165	329.0
14.4	58	136.4	44.4	112	233.6	74.4	166	330.8
15.0	59	138.2	45.0	113	235.4	75.0	167	332.6
15.6	60	140.0	45.6	114	237.2	75.6	168	334.4
16.1	61	141.8	46.1	115	239.0	76.1	169	336.2
16.7	62	143.6	46.7	116	240.8	76.7	170	338.0
17.2	63	145.4	47.2	117	242.6	77.2	171	339.8
17.8	64	147.2	47.8	118	244.4	77.8	172	341.6
18.3	65	149.0	48.3	119	246.2	78.3	173	343.4
18.9	66	150.8	48.9	120	248.0	78.9	174	345.2
19.4	67	152.6	49.4	121	249.8	79.4	175	347.0
20.0	68	154.4	50.0	122	251.6	80.0	176	348.8
20.6	69	156.2	50.6	123	253.4	80.6	177	350.6
21.1	70	158.0	51.1	124	255.2	81.1	178	352.4
21.6	71	159.8	51.7	125	257.0	81.7	179	354.2
22.2	72	161.6	52.2	126	258.8	82.2	180	356.0
22.8	73	163.4	52.8	127	260.6	82.8	181	357.8
23.3	74	165.2	53.3	128	262.4	83.3	182	359.6
23.9	75	167.0	53.9	129	264.2	83.9	183	361.4
24.4	76	168.8	54.4	130	266.0	84.4	184	363.2
25.0	77	170.6	55.0	131	267.8	85.0	185	365.0
25.6	78	172.4	55.6	132	269.6	85.6	186	366.8
26.1	79	174.2	56.1	133	271.4	86.1	187	368.6
26.7	80	176.0	56.7	134	273.2	86.7	188	370.4
27.2	81	177.8	57.2	135	275.0	87.2	189	372.2
27.8	82	179.6	57.8	136	276.8	87.8	190	374.0
28.3	83	181.4	58.3	137	278.6	88.3	191	375.8
28.9	84	183.2	58.9	138	280.4	88.9	192	377.6
29.4	85	185.0	59.4	139	282.2	89.4	193	379.4
30.0	86	186.8	60.0	140	284.0	90.0	194	381.2
30.6	87	188.6	60.6	141	285.8	90.6	195	383.0
31.1	88	190.4	61.1	142	287.6	91.1	196	384.8
31.7	89	192.2	61.7	143	289.4	91.7	197	386.6
32.2	90	194.0	62.2	144	291.2	92.2	198	388.4
32.8	91	195.8	62.8	145	293.0	92.8	199	390.2
33.3	92	197.6	63.3	146	294.8	93.3	200	392.0
33.9	93	199.4	63.9	147	296.6	93.9	201	393.8
34.4	94	201.2	64.4	148	298.4	94.4	202	395.6
35.0	95	203.0	65.0	149	300.2	95.0	203	397.4
35.6	96	204.8	65.6	150	302.0	95.6	204	399.2
36.1	97	206.6	66.1	151	303.8	96.1	205	401.0
36.7	98	208.4	66.7	152	305.6	96.7	206	402.8
37.2	99	210.2	67.2	153	307.4	97.2	207	404.6
37.8	100	212.0	67.8	154	309.2	97.8	208	406.4
38.3	101	213.8	68.3	155	311.0	98.3	209	408.2
38.9	102	215.6	68.9	156	312.8	98.9	210	410.0
39.4	103	217.4	69.4	157	314.6	99.4	211	411.8
40.0	104	219.2	70.0	158	316.4	100.0	212	413.6
40.6	105	221.0	70.6	159	318.2	100.6	213	415.4
41.1	106	222.8	71.1	160	320.0	101.1	214	417.2
41.7	107	224.6	71.7	161	321.8	101.7	215	419.0
42.2	108	226.4	72.2	162	323.6	102.2	216	420.8
42.8	109	228.2	72.8	163	325.4	102.8	217	422.6
43.3	110	230.0	73.3	164	327.2	103.3	218	424.4

CENTIGRADE - FAHRENHEIT

CONVERSION TABLE

°C		°F	°C		°F	°C		°F
103.9	219	426.2	133.9	273	523.4	163.9	327	620.6
104.4	220	428.0	134.4	274	525.2	164.4	328	622.4
105.0	221	429.8	135.0	275	527.0	165.0	329	624.2
105.6	222	431.6	135.6	276	528.8	165.6	330	626.0
106.1	223	433.4	136.1	277	530.6	166.1	331	627.8
106.7	224	435.2	136.7	278	532.4	166.7	332	629.6
107.2	225	437.0	137.2	279	534.2	167.2	333	631.4
107.8	226	438.8	137.8	280	536.0	167.8	334	633.2
108.3	227	440.6	138.3	281	537.8	168.3	335	635.0
108.9	228	442.4	138.9	282	539.6	168.9	336	636.8
109.4	229	444.2	139.4	283	541.4	169.4	337	638.6
110.0	230	446.0	140.0	284	543.2	170.0	338	640.4
110.6	231	447.8	140.6	285	545.0	170.6	339	642.2
111.1	232	449.6	141.1	286	546.8	171.1	340	644.0
111.7	233	451.4	141.7	287	548.6	171.7	341	645.8
112.2	234	453.2	142.2	288	550.4	172.2	342	647.6
112.8	235	455.0	142.8	289	552.2	172.8	343	649.4
113.3	236	456.8	143.3	290	554.0	173.3	344	651.2
113.9	237	458.6	143.9	291	555.8	173.9	345	653.0
114.4	238	460.4	144.4	292	557.6	174.4	346	654.8
115.0	239	462.2	145.0	293	559.4	175.0	347	656.6
115.6	240	464.0	145.6	294	561.2	175.6	348	658.4
116.1	241	465.8	146.1	295	563.0	176.1	349	660.2
116.7	242	467.6	146.7	296	564.8	176.7	350	662.0
117.2	243	469.4	147.2	297	566.6	177.2	351	663.8
117.8	244	471.2	147.8	298	568.4	177.8	352	665.6
118.3	245	473.0	148.3	299	570.2	178.3	353	667.4
118.9	246	474.8	148.9	300	572.0	178.9	354	669.2
119.4	247	476.6	149.4	301	573.8	179.4	355	671.0
120.0	248	478.4	150.0	302	575.6	180.0	356	672.8
120.6	249	480.2	150.6	303	577.4	180.6	357	674.6
121.1	250	482.0	151.1	304	579.2	181.1	358	676.4
121.7	251	483.8	151.7	305	581.0	181.7	359	678.2
122.2	252	485.6	152.2	306	582.8	182.2	360	680.0
122.8	253	487.4	152.8	307	584.6	182.8	361	681.8
123.3	254	489.2	153.3	308	586.4	183.3	362	683.6
123.9	255	491.0	153.9	309	588.2	183.9	363	685.4
124.4	256	492.8	154.4	310	590.0	184.4	364	687.2
125.0	257	494.6	155.0	311	591.8	185.0	365	689.0
125.6	258	496.4	155.6	312	593.6	185.6	366	690.8
126.1	259	498.2	156.1	313	595.4	186.1	367	692.6
126.7	260	500.0	156.7	314	597.2	186.7	368	694.4
127.2	261	501.8	157.2	315	599.0	187.2	369	696.2
127.8	262	503.6	157.8	316	600.8	187.8	370	698.0
128.3	263	505.4	158.3	317	602.6	188.3	371	699.8
128.9	264	507.2	158.9	318	604.4	188.9	372	701.6
129.4	265	509.0	159.4	319	606.2	189.4	373	703.4
130.0	266	510.8	160.0	320	608.0	190.0	374	705.2
130.6	267	512.6	160.6	321	609.8	190.6	375	707.0
131.1	268	514.4	161.1	322	611.6	191.1	376	708.8
131.7	269	516.2	161.7	323	613.4	191.7	377	710.6
132.2	270	518.0	162.2	324	615.2	192.2	378	712.4
132.8	271	519.8	162.8	325	617.0	192.8	379	714.2
133.3	272	521.6	163.3	326	618.8	193.3	380	716.0

TABLE 9.7

CENTIGRADE - FAHRENHEIT

CONVERSION TABLE

°C	°F	°C	°F	°C	°F			
193.9	381	717.8	223.9	435	815.0	253.9	489	912.2
194.4	382	719.6	224.4	436	816.8	254.4	490	914.0
195.0	383	721.4	225.0	437	818.6	255.0	491	915.8
195.6	384	723.2	225.6	438	820.4	255.6	492	917.6
196.1	385	725.0	226.1	439	822.2	256.1	493	919.4
196.7	386	726.8	226.7	440	824.0	256.7	494	921.2
197.2	387	728.6	227.2	441	825.8	257.2	495	923.0
197.8	388	730.4	227.8	442	827.6	257.8	496	924.8
198.3	389	732.2	228.3	443	829.4	258.3	497	926.6
198.9	390	734.0	228.9	444	831.2	258.9	498	928.4
199.4	391	735.8	229.4	445	833.0	259.4	499	930.2
200.0	392	737.6	230.0	446	834.8	260.0	500	932.0
200.6	393	739.4	230.6	447	836.6	260.6	501	933.8
201.1	394	741.2	231.1	448	838.4	261.1	502	935.6
201.7	395	743.0	231.7	449	840.2	261.7	503	937.4
202.2	396	744.8	232.2	450	842.0	262.2	504	939.2
202.8	397	746.6	232.8	451	843.8	262.8	505	941.0
203.3	398	748.4	233.3	452	845.6	263.3	506	942.8
203.9	399	750.2	233.9	453	847.4	263.9	507	944.6
204.4	400	752.0	234.4	454	849.2	264.4	508	946.4
205.0	401	753.8	235.0	455	851.0	265.0	509	948.2
205.6	402	755.6	235.6	456	852.8	265.6	510	950.0
206.1	403	757.4	236.1	457	854.6	266.1	511	951.8
206.7	404	759.2	236.7	458	856.4	266.7	512	953.6
207.2	405	761.0	237.2	459	858.2	267.2	513	955.4
207.8	406	762.8	237.8	460	860.0	267.8	514	957.2
208.3	407	764.6	238.3	461	861.8	268.3	515	959.0
208.9	408	766.4	238.9	462	863.6	268.9	516	960.8
209.4	409	768.2	239.4	463	865.4	269.4	517	962.6
210.0	410	770.0	240.0	464	867.2	270.0	518	964.4
210.6	411	771.8	240.6	465	869.0	270.6	519	966.2
211.1	412	773.6	241.1	466	870.8	271.1	520	968.0
211.7	413	775.4	241.7	467	872.6	271.7	521	969.8
212.2	414	777.2	242.2	468	874.4	272.2	522	971.6
212.8	415	779.0	242.8	469	876.2	272.8	523	973.4
213.3	416	780.8	243.3	470	878.0	273.3	524	975.2
213.9	417	782.6	243.9	471	879.8	273.9	525	977.0
214.4	418	784.4	244.4	472	881.6	274.4	526	978.8
215.0	419	786.2	245.0	473	883.4	275.0	527	980.6
215.6	420	788.0	245.6	474	885.2	275.6	528	982.4
216.1	421	789.8	246.1	475	887.0	276.1	529	984.2
216.7	422	791.6	246.7	476	888.8	276.7	530	986.0
217.2	423	793.4	247.2	477	890.6	277.2	531	987.8
217.8	424	795.2	247.8	478	892.4	277.8	532	989.6
218.3	425	797.0	248.3	479	894.2	278.3	533	991.4
218.9	426	798.8	248.9	480	896.0	278.9	534	993.2
219.4	427	800.6	249.4	481	897.8	279.4	535	995.0
220.0	428	802.4	250.0	482	899.6	280.0	536	996.8
220.6	429	804.2	250.6	483	901.4	280.6	537	998.6
221.1	430	806.0	251.1	484	903.2	281.1	538	1000.4
221.7	431	807.8	251.7	485	905.0	281.7	539	1002.2
222.2	432	809.6	252.2	486	906.8	282.2	540	1004.0
222.8	433	811.4	252.8	487	908.6	282.8	541	1005.8
223.3	434	813.2	253.3	488	910.4	283.3	542	1007.6

CENTIGRADE - FAHRENHEIT

CONVERSION TABLE

°C		°F	°C		°F	°C		°F
283.9	543	1009.4	313.9	597	1106.6	343.9	651	1203.8
284.4	544	1011.2	314.4	598	1108.4	344.4	652	1205.6
285.0	545	1013.0	315.0	599	1110.2	345.0	653	1207.4
285.6	546	1014.8	315.6	600	1112.0	345.6	654	1209.2
286.1	547	1016.6	316.1	601	1113.8	346.1	655	1211.0
286.7	548	1018.4	316.7	602	1115.6	346.7	656	1212.8
287.2	549	1020.2	317.2	603	1117.4	347.2	657	1214.6
287.8	550	1022.0	317.8	604	1119.2	347.8	658	1216.4
288.3	551	1023.8	318.3	605	1121.0	348.3	659	1218.2
288.9	552	1025.6	318.9	606	1122.8	348.9	660	1220.0
289.4	553	1027.4	319.4	607	1124.6	349.4	661	1221.8
290.0	554	1029.2	320.0	608	1126.4	350.0	662	1223.6
290.6	555	1031.0	320.6	609	1128.2	350.6	663	1225.4
291.1	556	1032.8	321.1	610	1130.0	351.1	664	1227.2
291.7	557	1034.6	321.7	611	1131.8	351.7	665	1229.0
292.2	558	1036.4	322.2	612	1133.6	352.2	666	1230.8
292.8	559	1038.2	322.8	613	1135.4	352.8	667	1232.6
293.3	560	1040.0	323.3	614	1137.2	353.3	668	1234.4
293.9	561	1041.8	323.9	615	1139.0	353.9	669	1236.2
294.4	562	1043.6	324.4	616	1140.8	354.4	670	1238.0
295.0	563	1045.4	325.0	617	1142.6	355.0	671	1239.8
295.6	564	1047.2	325.6	618	1144.4	355.6	672	1241.6
296.1	565	1049.0	326.1	619	1146.2	356.1	673	1243.4
296.7	566	1050.8	326.7	620	1148.0	356.7	674	1245.2
297.2	567	1052.6	327.2	621	1149.8	357.2	675	1247.0
297.8	568	1054.4	327.8	622	1151.6	357.8	676	1248.8
298.3	569	1056.2	328.3	623	1153.4	358.3	677	1250.6
298.9	570	1058.0	328.9	624	1155.2	358.9	678	1252.4
299.4	571	1059.8	329.4	625	1157.0	359.4	679	1254.2
300.0	572	1061.6	330.0	626	1158.8	360.0	680	1256.0
300.6	573	1063.4	330.6	627	1160.6	360.6	681	1257.8
301.1	574	1065.2	331.1	628	1162.4	361.1	682	1259.6
301.7	575	1067.0	331.7	629	1164.2	361.7	683	1261.4
302.2	576	1068.8	332.2	630	1166.0	362.2	684	1263.2
302.8	577	1070.6	332.8	631	1167.8	362.8	685	1265.0
303.3	578	1072.4	333.3	632	1169.6	363.3	686	1266.8
303.9	579	1074.2	333.9	633	1171.4	363.9	687	1268.6
304.4	580	1076.0	334.4	634	1173.2	364.4	688	1270.4
305.0	581	1077.8	335.0	635	1175.0	365.0	689	1272.2
305.6	582	1079.6	335.6	636	1176.8	365.6	690	1274.0
306.1	583	1081.4	336.1	637	1178.6	366.1	691	1275.8
306.7	584	1083.2	336.7	638	1180.4	366.7	692	1277.6
307.2	585	1085.0	337.2	639	1182.2	378.2	693	1279.4
307.8	586	1086.8	337.8	640	1184.0	367.8	694	1281.2
308.3	587	1088.6	338.3	641	1185.8	368.3	695	1283.0
308.9	588	1090.4	338.9	642	1187.6	368.9	696	1284.8
309.4	589	1092.2	339.4	643	1189.4	369.4	697	1286.6
310.0	590	1094.0	340.0	644	1191.2	370.0	698	1288.4
310.6	591	1095.8	340.6	645	1193.0	370.6	699	1290.2
311.1	592	1097.6	341.1	646	1194.8	371.1	700	1292.0
311.7	593	1099.4	341.7	647	1196.6	371.7	701	1293.8
312.2	594	1101.2	342.2	648	1198.4	372.2	702	1295.6
312.8	595	1103.0	342.8	649	1200.2	372.8	703	1297.4
313.3	596	1104.8	343.3	650	1202.0	373.3	704	1299.2

TABLE 9.7

CENTIGRADE - FAHRENHEIT

CONVERSION TABLE

°C		°F
373.9	705	1301.0
374.4	706	1302.8
375.0	707	1304.6
375.6	708	1306.4
376.1	709	1308.2
376.7	710	1310.0
377.2	711	1311.8
377.8	712	1313.6
378.3	713	1315.4
378.9	714	1317.2
379.4	715	1319.0
380.0	716	1320.8
380.6	717	1322.6
381.1	718	1324.4
381.7	719	1326.2
382.2	720	1328.0
382.8	721	1329.8
383.3	722	1331.6
383.9	723	1333.4
384.4	724	1335.2
385.0	725	1337.0
385.6	726	1338.8
386.1	727	1340.6
386.7	728	1342.4
387.2	729	1344.2
387.8	730	1346.0
388.3	731	1347.8
388.9	732	1349.6
389.4	733	1351.4
390.0	734	1353.2
390.6	735	1355.0
391.1	736	1356.8
391.7	737	1358.6
392.2	738	1360.4
392.8	739	1362.2
393.3	740	1364.0
393.9	741	1365.8
394.4	742	1367.6
395.0	743	1369.4
395.6	744	1371.2
396.1	745	1373.0
396.7	746	1374.8
397.2	747	1376.6
397.8	748	1378.4
398.3	749	1380.2
398.9	750	1382.0
399.4	751	1383.8
400.0	752	1385.6
400.6	753	1387.4
401.1	754	1389.2
401.7	755	1391.0
402.2	756	1392.8
402.8	757	1394.6

°C		°F
403.3	758	1396.4
403.9	759	1398.2
404.4	760	1400.0
405.0	761	1401.8
405.6	762	1403.6
406.1	763	1405.4
406.7	764	1407.2
407.2	765	1409.0
407.8	766	1410.8
408.3	767	1412.6
408.9	768	1414.4
409.4	769	1416.2
410.0	770	1418.0
410.6	771	1419.8
411.1	772	1421.6
411.7	773	1423.4
412.2	774	1425.2
412.8	775	1427.0
413.3	776	1428.8
413.9	777	1430.6
414.4	778	1432.4
415.0	779	1434.2
415.6	780	1436.0
416.1	781	1437.8
416.7	782	1439.6
417.2	783	1441.4
417.8	784	1443.2
418.3	785	1445.0
418.9	786	1446.8
419.4	787	1448.6
420.0	788	1450.4
420.6	789	1452.2
421.1	790	1454.0
421.7	791	1455.8
422.2	792	1457.6
422.8	793	1459.4
423.3	794	1461.2
423.9	795	1463.0
424.4	796	1464.8
425.0	797	1466.6
425.6	798	1468.4
426.1	799	1470.2
426.7	800	1472.0
427.2	801	1473.8
427.8	802	1475.6
428.3	803	1477.4
428.9	804	1479.2
429.4	805	1481.0
430.0	806	1482.8
430.6	807	1484.6
431.1	808	1486.4
431.7	809	1488.2
432.2	810	1490.0

°C		°F
432.8	811	1491.8
433.3	812	1493.6
433.9	813	1495.4
434.4	814	1497.2
435.0	815	1499.0
435.6	816	1500.8
436.1	817	1502.6
436.7	818	1504.4
437.2	819	1506.2
437.8	820	1508.0
438.3	821	1509.8
438.9	822	1511.6
439.4	823	1513.4
440.0	824	1515.2
440.6	825	1517.0
441.1	826	1518.8
441.7	827	1520.6
442.2	828	1522.4
442.8	829	1524.2
443.3	830	1526.0
443.9	831	1527.8
444.4	832	1529.6
445.0	833	1531.4
445.6	834	1533.2
446.1	835	1535.0
446.7	836	1536.8
447.2	837	1538.6
447.8	838	1540.4
448.3	839	1542.2
448.9	840	1544.0
449.4	841	1545.8
450.0	842	1547.6
450.6	843	1549.4
451.1	844	1551.2
451.7	845	1553.0
452.2	846	1554.8
452.8	847	1556.6
453.3	848	1558.4
453.9	849	1560.2
454.4	850	1562.0
455.0	851	1563.8
455.6	852	1565.6
456.1	853	1567.4
456.7	854	1569.2
457.2	855	1571.0
457.8	856	1572.8
458.3	857	1574.6
458.9	858	1576.4
459.4	859	1578.2
460.0	860	1580.0
460.6	861	1581.8
461.1	862	1583.6
461.7	863	1585.4

CENTIGRADE - FAHRENHEIT

CONVERSION TABLE

°C		°F	°C		°F	°C		°F
462.2	864	1587.2	491.7	917	1682.6	521.1	970	1778.0
462.8	865	1589.0	492.2	918	1684.4	521.7	971	1779.8
463.3	866	1590.8	492.8	919	1686.2	522.2	972	1781.6
463.9	867	1592.6	493.3	920	1688.0	522.8	973	1783.4
464.4	868	1594.4	493.9	921	1689.8	523.3	974	1785.2
465.0	869	1596.2	494.4	922	1691.6	523.9	975	1787.0
465.6	870	1598.0	495.0	923	1693.4	524.4	976	1788.8
466.1	871	1599.8	495.6	924	1695.2	525.0	977	1790.6
466.7	872	1601.6	496.1	925	1697.0	525.6	978	1792.4
467.2	873	1603.4	496.7	926	1698.8	526.1	979	1794.2
467.8	874	1605.2	497.2	927	1700.6	526.7	980	1796.0
468.3	875	1607.0	497.8	928	1702.4	527.2	981	1797.8
468.9	876	1608.8	498.3	929	1704.2	527.8	982	1799.6
469.4	877	1610.6	498.9	930	1706.0	528.3	983	1801.4
470.0	878	1612.4	499.4	931	1707.8	528.9	984	1803.2
470.6	879	1614.2	500.0	932	1709.6	529.4	985	1805.0
471.1	880	1616.0	500.6	933	1711.4	530.0	986	1806.8
471.7	881	1617.8	501.1	934	1713.2	530.6	987	1808.6
472.2	882	1619.6	501.7	935	1715.0	531.1	988	1810.4
472.8	883	1621.4	502.2	936	1716.8	531.7	989	1812.2
473.3	884	1623.2	502.8	937	1718.6	532.2	990	1814.0
473.9	885	1625.0	503.3	938	1720.4	532.8	991	1815.8
474.4	886	1626.8	503.9	939	1722.2	533.3	992	1817.6
475.0	887	1628.6	504.4	940	1724.0	533.9	993	1819.4
475.6	888	1630.4	505.0	941	1725.8	534.4	994	1821.2
476.1	889	1632.2	505.6	942	1727.6	535.0	995	1823.0
476.7	890	1634.0	506.1	943	1729.4	535.6	996	1824.8
477.2	891	1635.8	506.7	944	1731.2	536.1	997	1826.6
477.8	892	1637.6	507.2	945	1733.0	536.7	998	1828.4
478.3	893	1639.4	507.8	946	1734.8	537.2	999	1830.2
478.9	894	1641.2	508.3	947	1736.6	537.8	1000	1832.0
479.4	895	1643.0	508.9	948	1738.4	538.4	1001	1833.8
480.0	896	1644.8	509.4	949	1740.2	538.9	1002	1835.6
480.6	897	1646.6	510.0	950	1742.0	539.5	1003	1837.4
481.1	898	1648.4	510.6	951	1743.8	540.0	1004	1839.2
481.7	899	1650.2	511.1	952	1745.6	540.6	1005	1841.0
482.2	900	1652.0	511.7	953	1747.4	541.2	1006	1842.8
482.8	901	1653.8	512.2	954	1749.2	541.7	1007	1844.6
483.3	902	1655.6	512.8	955	1751.0	542.3	1008	1846.4
483.9	903	1657.4	513.3	956	1752.8	542.8	1009	1848.2
484.4	904	1659.2	513.9	957	1754.6	543.4	1010	1850.0
485.0	905	1661.0	514.4	958	1756.4	543.9	1011	1851.8
485.6	906	1662.8	515.0	959	1758.2	544.5	1012	1853.6
486.1	907	1664.6	515.6	960	1760.0	545.0	1013	1855.4
486.7	908	1666.4	516.1	961	1761.8	545.6	1014	1857.2
487.2	909	1668.2	516.7	962	1763.6	546.2	1015	1859.0
487.8	910	1670.0	517.2	963	1765.4	546.7	1016	1860.8
488.3	911	1671.8	517.8	964	1767.2	547.3	1017	1862.6
488.9	912	1673.6	518.3	965	1769.0	547.8	1018	1864.4
489.4	913	1675.4	518.9	966	1770.8	548.4	1019	1866.2
490.0	914	1677.2	519.4	967	1772.6	548.9	1020	1868.0
490.6	915	1679.0	520.0	968	1774.4	549.5	1021	1869.8
491.1	916	1680.8	520.6	969	1776.2	550.0	1022	1871.6

TABLE 9.7

CENTIGRADE - FAHRENHEIT

CONVERSION TABLE

°C		°F	°C		°F
550.6	1023	1873.4	572.3	1062	1943.6
551.2	1024	1875.2	572.8	1063	1945.4
551.7	1025	1877.0	573.4	1064	1947.2
552.3	1026	1878.8	573.9	1065	1949.0
552.8	1027	1880.6	574.5	1066	1950.8
553.4	1028	1882.4	575.0	1067	1952.6
553.9	1029	1884.2	575.6	1068	1954.4
554.5	1030	1886.0	576.2	1069	1956.2
555.0	1031	1887.8	576.7	1070	1958.0
555.6	1032	1889.6	577.3	1071	1959.8
556.2	1033	1891.4	577.8	1072	1961.6
556.7	1034	1893.2	578.4	1073	1963.4
557.3	1035	1895.0	578.9	1074	1965.2
557.8	1036	1896.8	579.5	1075	1967.0
558.4	1037	1898.6	580.0	1076	1968.8
558.9	1038	1900.4	580.6	1077	1970.6
559.5	1039	1902.2	581.2	1078	1972.4
560.0	1040	1904.0	581.7	1079	1974.2
560.6	1041	1905.8	582.3	1080	1976.0
561.2	1042	1907.6	582.8	1081	1977.8
561.7	1043	1909.4	583.4	1082	1979.6
562.3	1044	1911.2	583.9	1082	1981.4
562.8	1045	1913.0	584.5	1084	1983.2
563.4	1046	1914.8	585.0	1084	1985.0
563.9	1047	1916.6	585.6	1086	1986.8
564.5	1048	1918.4	586.2	1087	1988.6
565.0	1049	1920.2	586.7	1088	1990.4
565.6	1050	1922.0	587.3	1089	1992.2
566.2	1051	1923.8	587.8	1090	1994.0
566.7	1052	1925.6	588.4	1091	1995.8
567.3	1053	1927.4	588.9	1092	1997.6
567.8	1054	1929.2	589.5	1093	1999.4
568.4	1055	1931.0	590.0	1094	2001.2
568.9	1056	1932.8	590.6	1095	2003.0
569.5	1057	1934.6	591.2	1096	2004.8
570.0	1058	1936.4	591.7	1097	2006.6
570.6	1059	1938.2	592.3	1098	2008.4
571.2	1060	1940.0	592.8	1099	2010.2
571.7	1061	1941.8	593.4	1100	2012.0

CHAPTER TWO

RECIPROCATING ENGINE PERFORMANCE

SECTION 2.1

Horsepower Determination for Test Conditions

In aircraft performance testing, engine performance is the evaluation of the engine as installed in the aircraft. Since aircraft induction and exhaust systems affect operation, engine manufacturers tests will not indicate the exact installed performance. Tests must be run to determine power available, critical altitude, fuel consumption, and cooling data at standard day operating temperatures. These values not only determine overall airplane performance when applied to the aerodynamic characteristics of the airframe, but also show the quality of the engine installation when compared to the performance of the isolated engine.

Considering the propeller driven aircraft, power is the first characteristic to be studied. The total useful power produced is of primary interest. This is the power with which the aircraft manufacturer can work. It may all be used to drive the propeller or part may be extracted to drive auxiliary equipment. In making guarantees, the total useful power is specified, and the assumption is made that the manufacturer may use it as he wishes. If it is used to run cooling fans, less power will be delivered to the propeller, but less cooling drag may be achieved; if it is used for cabin pressurization or electric generators, weight is saved by the elimination of auxiliary motors. As a result, in performance testing, total power available is considered to be a more useful criteria than the thrust power commonly used by aerodynamicists.

In all propeller engine combinations power is best determined by use of a torquemeter attached to the shaft to measure useful torque output. The horsepower is given by the equation:

$$BHT_t = \text{Torquemeter reading} \times K \times N_{ic}$$

where:

K = a constant determined by dynamometer tests

N_{ic} = engine rpm corrected for instrument error

BHP_t = brake horsepower on the test day

When torquemeters are not available power charts are used. These charts solve for brake horsepower when manifold pressure, rpm, carburetor air temperature, and pressure altitude are known. They are made partly from dynamometer tests and partly from theory. They presume that all additional factors effecting power, such as oil pressure, oil temperature, and cylinder head temperature, remain constant or vary in a predetermined manner. They also assume that the fuel-air mixture is exactly as specified and ignition is perfect. These assumptions are not valid in all installations or operations; so the charts are not exact. They do, however, represent a reasonable approximation in the absence of a better measuring system.

A typical chart consists of three parts, a sea level power graph, an altitude correction graph, and a chart carburetor air temperature graph. To determine the horsepower delivered at any given manifold pressure, rpm, altitude, and carburetor air temperature the following procedure is used on a typical power chart as shown on Figure 2.11.

- (a) Find the point corresponding to the given manifold pressure and rpm on the altitude correction graph, (Point A).
- (b) Find the power which would be delivered if the engine were operating at sea level with the given rpm and M.P., (Point B).
- (c) Transpose Point B to the zero altitude axis of the altitude correction graph, (Point C).
- (d) Connect Point A and Point C by a straight line. This line will represent the variation in power with altitude at the given manifold pressure, rpm, and chart carburetor air temperature.
- (e) Find the horsepower (Point D) at the intersection of the given pressure altitude axis and the line AC. This horsepower is called chart horsepower; it is the horsepower which would be delivered at the given manifold pressure, rpm, pressure altitude, and chart carburetor air temperature.
- (f) Correct chart horsepower to test horsepower by the empirical equation:

$$BHP_t = BHP_c \left(\frac{T_{sc}}{T_{ct}} \right)^n \quad (2.102)$$

where:

- BHP_t = test brake horsepower
- BHP_c = chart brake horsepower
- T_{sc} = chart carburetor air temperature for the pressure altitude. This is generally the standard temperature for the specified altitude, as the manufacturer tests the engine with no cowl or ducting.
- T_{ct} = test carburetor air temperature
- n = exponent specified by power curve, usually (0.5)

If the exponent is (0.5), the chart horsepower correction may be given as a 1% decrease for each 6°C the test carburetor temperature exceeds the chart carburetor air temperature when the temperatures are near 300°K. Manifold mixture temperature is often used in place of carburetor air temperature, as it also is a measure of the temperature of the charge entering the cylinder. If this temperature is used instead of carburetor air temperature, the exponent may change but will still be specified by the power curve. For example, using Figure 2.11, find the test power of an R 2000-11 engine at 30" manifold pressure 2000 rpm, at 18,000 feet, carburetor air temperature -10°C.

Chart Horsepower = 728
Carb air chart = 253°K
Carb air test = 263°K
Test horsepower = 728 x $\sqrt{\frac{253}{263}}$ = 716

In addition to determining power delivered under test conditions, power delivered on a standard day at certain arbitrary settings such as cruise power, maximum continuous power, and military power are required. To determine these powers, the aircraft is flown as near as possible to the desired setting on a test day, and the power obtained is corrected to the power which would be obtained on a standard day at the same pressure altitude. Most power corrections may be resolved into three cases: if the required setting, manifold pressure and rpm does not require full throttle; if the setting does require full throttle; if the setting requires full throttle but manifold pressure may be increased or decreased by a turbosupercharger.

Pratt & Whitney R-2000-11
 Maximum Power,
 High Impeller Gear Ratio,
 Auto Rich Operation.

Prop. Gear Ratio..... 0.500
 Compression Ratio..... 6.5:1
 Sup'ch'ger Gear Ratio.....
 High... 9.52:1
 Impeller Dia. in. 11.3
 Fuel Metering..... FDL2F7-19
 Fuel Grade..... 100/130

Correct HP in accordance with Free Air
 Temp. by applying the following:-
 (A) Add 1% for each 6°C decrease from T_0
 (B) Subtract 1% for each 6°C increase
 from T_0 . (T_0 = std. alt. temp.)

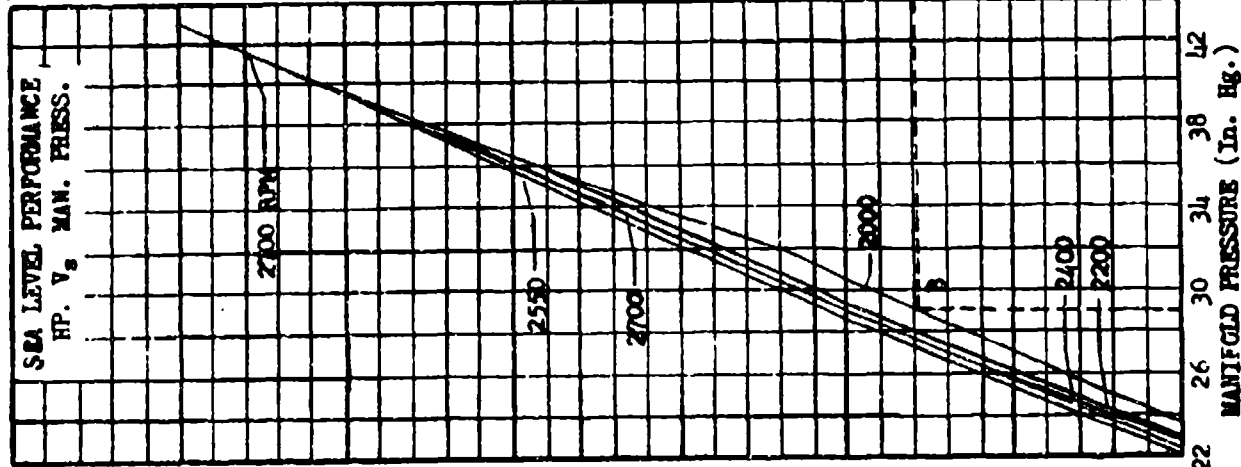
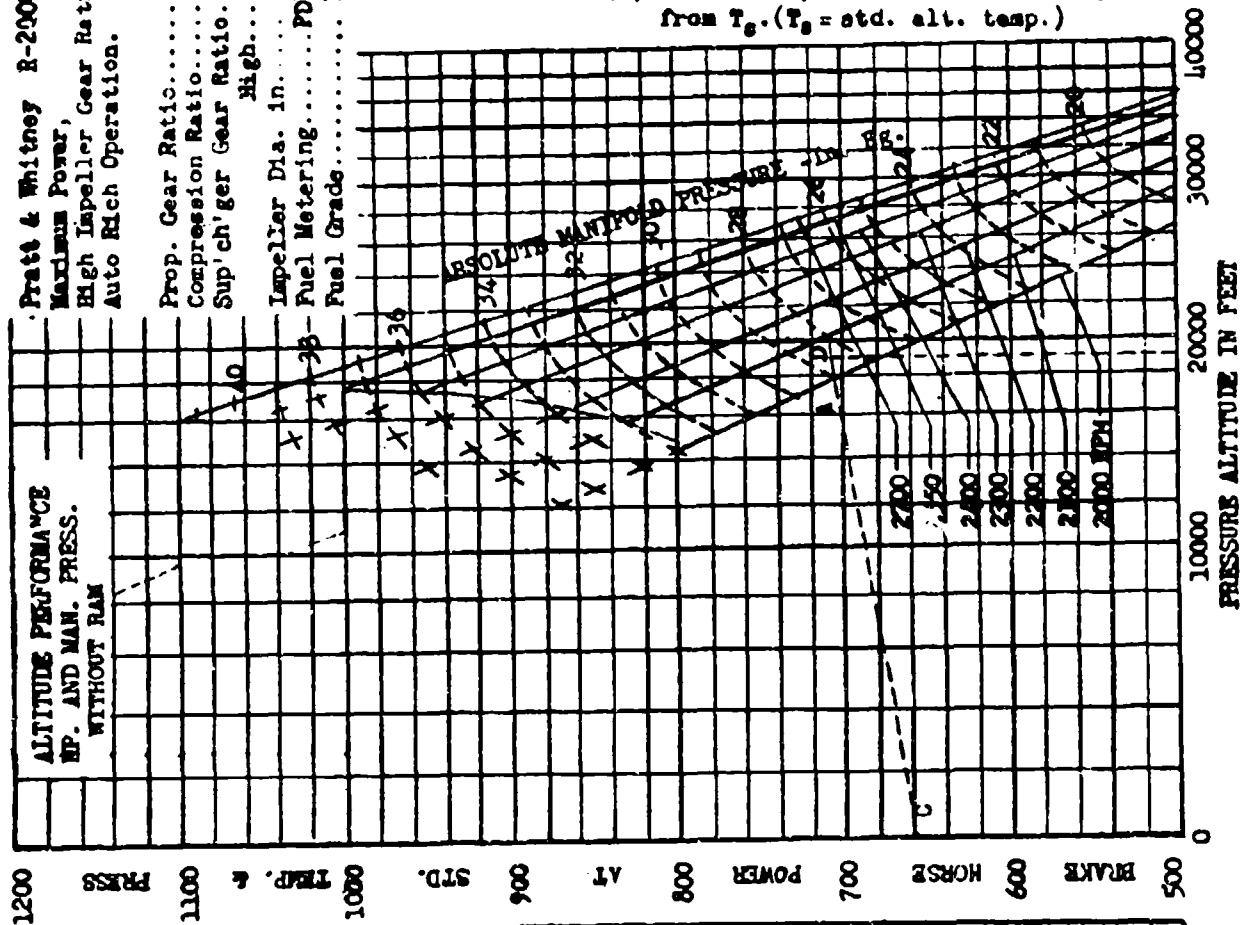


Figure 2.11
 Typical Reciprocating Engine Power Chart

SECTION 2.2

Power Correction for Temperature Variation at Constant Manifold Pressure

This case is used for such problems as determining the cruising power of any engine or the military power of a supercharged engine at altitudes where wide open throttle would exceed the manufacturer's operating limits. In this case the assumption is made that, if the airplane were flown on a standard day, the throttle position would be slightly different from its position on a test day but manifold pressure would be constant.

With manifold pressure and pressure altitude the same on the test day and the standard day, the change in carburetor air temperature will be the only variable effecting power, and the correction can be made by the same relation used in obtaining test horsepower from chart horsepower. Tests have shown that carburetor air temperature will change from test day to standard day by exactly the same amount as free air temperature changes from test day to standard day. Equation 2.201 is used in this case.

$$BHP_s = BHP_t \left(\frac{T_{ct}}{T_{cs}} \right)^n \quad (2.201)$$

where:

- BHP_s = standard day brake horsepower
- T_{cs} = (T_{as} - T_{at} + T_{ct}) standard day carburetor air temperature
- T_{as} = standard ambient temperature
- T_{at} = test ambient temperature
- n = exponent from power chart, usually (0.5)

The following table is an example of test and standard day conditions.

TEST DAY	STANDARD DAY
Pressure Alt 18,000'	Pressure Alt 18,000'
T _a -10°C	T _a -20°C
MP 30"Hg	MP 30"Hg
rpm 2000	rpm 2000
CAT 0°C	CAT -10°C
BHP _t 703	BHP _s 716
Throttle partly open	Throttle slightly retarded from test day position

Another form of equation 2.201 is sometimes used.

$$\Delta BHP \text{ (for } \Delta CAT) = BHP_t \left[\left(\frac{T_{ct}}{T_{cs}} \right)^n - 1 \right] \quad (2.202)$$

where:

- ΔBHP (for ΔCAT) = (BHP_s - BHP_t), brake horsepower correction for carburetor air temperature change

SECTION 2.3

Power Correction for Manifold Pressure Variation Resulting from Temperature Variation and Flight Mach Number Variation

This case is used for problems such as maximum power or cruising power above the critical altitude for the desired power setting. In this case the throttle will be full open in an effort to obtain the desired manifold pressure and rpm; therefore, if the airplane were flown on a standard day the throttle would remain open and manifold pressure as well as carburetor air temperature would change due to the change in free air temperature. The correction for the two effects may be stated in this form:

$$BHP_g = BHP_t + \Delta BHP \text{ (for } \Delta CAT) + \Delta BHP \text{ (for } \Delta MP) \quad (2.301)$$

The first correction term is obtained from the carburetor temperature relation as used in equation 2.202. The manifold pressure correction requires consideration of two effects: the change in pressure ratio of the supercharger due to change in inlet temperature and the change in air inlet ram pressure ratio because of any change in Mach number of the aircraft caused by power changes.

The following table is an example of test and standard day conditions for the case where a turbosupercharger is not involved and manifold pressure and Mach number vary from test to standard day.

TEST DAY		STANDARD DAY	
Test power setting	30" MP	Pressure altitude	20,000
Pressure altitude	20,000	rpm	2000
rpm	2000	T _a	-24°C
T _a	-14°C	MP	27.7 "Hg
MP	27 "Hg	CAT	-14°C
CAT	-4°C	BHP _g	646
BHP _t	630	Throttle wide open	
Throttle wide open			

TEMPERATURE EFFECTS ON MANIFOLD PRESSURE

The exact correction of manifold pressure for change in free air temperature would result in work and instrumentation beyond the scope of flight test, because of the varied thermodynamic processes involved in induction and carburetion. An approximate method has been devised and is presented in Flight Test Section Memorandum Report TSCEP5E-2T, 6/29/45, "A Simplified Manifold Pressure Correction." The basic equation used in this method is:

$$MP_g = (MP_t) (1 + CAT) \quad (2.302)$$

where:

- MP_s = manifold pressure standard "Hg
- (MP_t) = manifold pressure test "Hg
- Δt = $(T_{at} - T_{as})$ different between test day carburetor air temperature and standard day carburetor air temperature $(T_{ct} - T_{cs})$
- C = a constant depending upon the type process employed

The correction constant C is dependent on the pressure ratio of the process, the initial temperature of the process, and whether fuel is vaporized during the process. CHARTS 2.31 and 2.32 at the end of this chapter have been made from equation 2.302 for the value of C in the normal working range. It should be noted that, if the ratio of test manifold pressure to ambient pressure is less than 1.5, this correction is negligible for temperature variations of 5°C or less.

By use of the two graphs, any combination of induction processes for air only or a fuel air mixture may be evaluated. Manifold pressure data reduction methods for typical induction systems are included at the end of this section. It should be noticed that, once the manifold pressure corrections have been established for a typical engine installation, they can be used for all other duplicate installations by use of a small chart showing the corrections at various altitudes for various manifold pressure-rpm combinations.

MACH NUMBER EFFECTS ON MANIFOLD PRESSURE

The determination of the standard day manifold pressure can be obtained by multiplying the temperature corrected manifold pressure by the ratio of the standard and test day ram pressure ratios. The average carburetor inlet has a ram efficiency of about (0.70 to 0.75). Using CHART 2.33 at the end of this chapter, with flight Mach number and ram efficiency, the ratio P_t/P_a may be determined. Obtaining this ratio for both test and standard Mach number, and assuming the test day pressure altitude is held,

$$\frac{P_{ts}/P_a}{P_{tt}/P_a} = \frac{P_{ts}}{P_{tt}} = \frac{MP_s}{MP_{\Delta t}}$$

and

$$MP_s = MP_{\Delta t} \times \frac{P_{ts}}{P_{tt}} \quad (2.303)$$

where:

- MP_s = standard manifold pressure
- $MP_{\Delta t}$ = manifold pressure corrected for temperature variation
- P_{ts} = standard total inlet pressure at standard flight Mach number
- P_{tt} = test total inlet pressure at test Mach number

This correction must be made by successive approximations because standard speed cannot be exactly determined from the polar until power is known. The correction is not normally made unless the airplane Mach number is above .6 and an overall change in speed because of change in power is over 3 knots.

POWER CORRECTION FOR MANIFOLD PRESSURE VARIATION

Having determined standard day manifold pressure, its effect on power must be evaluated. For rough work the change in power is directly proportional to the change in manifold pressure.

$$BHP_s = BHP_t \frac{MP_s}{MP_t} \quad (2.304)$$

or

$$\Delta BHP \text{ (for } \Delta MP) = BHP_t \left(\frac{MP_s}{MP_t} - 1 \right) \quad (2.305)$$

where:

MP_s = temperature and Mach number corrected manifold pressure
 MP_t = test manifold pressure

Better accuracy can be obtained by making plots of BHP_t vs MP_t at various altitudes and rpm's in order to find the rate of change of power with MP as shown in Figure 2.31. With the slopes from such a plot ΔBHP may be calculated. (In the pressure altitude method of data reduction this correction is not required — see Section 4.4 — since only test BHP is plotted; in this case equation 2.304 may be used to approximate standard day MP for the standard day BHP determined from the pressure altitude plot.)

$$\Delta BHP \text{ (for } \Delta MP) = \Delta MP_t \times \frac{d(BHP)}{d(MP)} \quad (2.306)$$

With the temperature corrections of Section 2.2 and the standard manifold pressure an equation for standard day power may be written:

$$BHP_s = BHP_t \left[\left(\frac{T_{tot}}{T_{os}} \right)^n + \frac{MP_s}{MP_t} - 1 \right] \quad (2.307)$$

or

$$BHP_s = BHP_t \left(\frac{T_{tot}}{T_{os}} \right)^n + \Delta MP \frac{d(BHP)}{d(MP)} \quad (2.308)$$

The final standard day power curves are presented in a form similar to that shown in Figure 2.32.

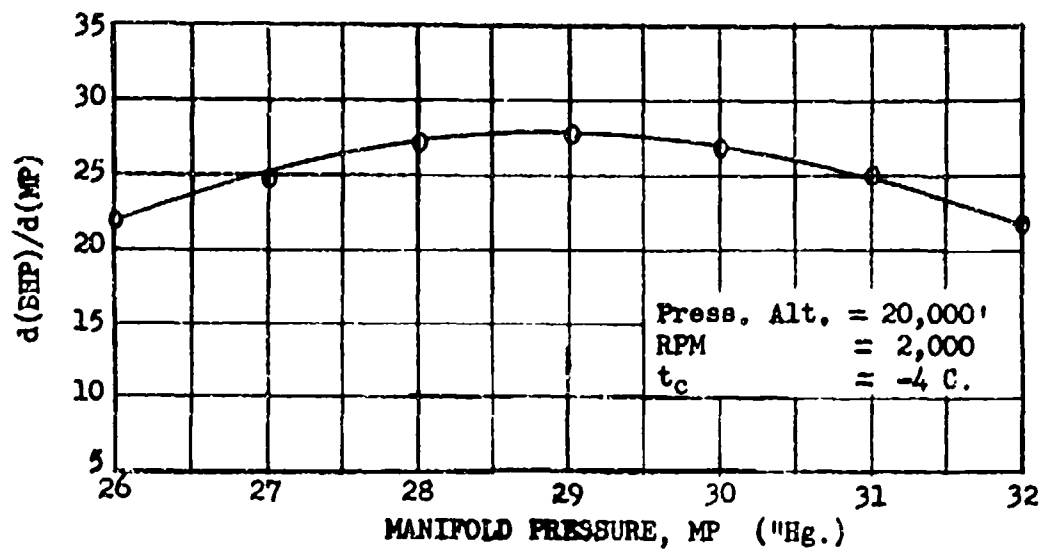
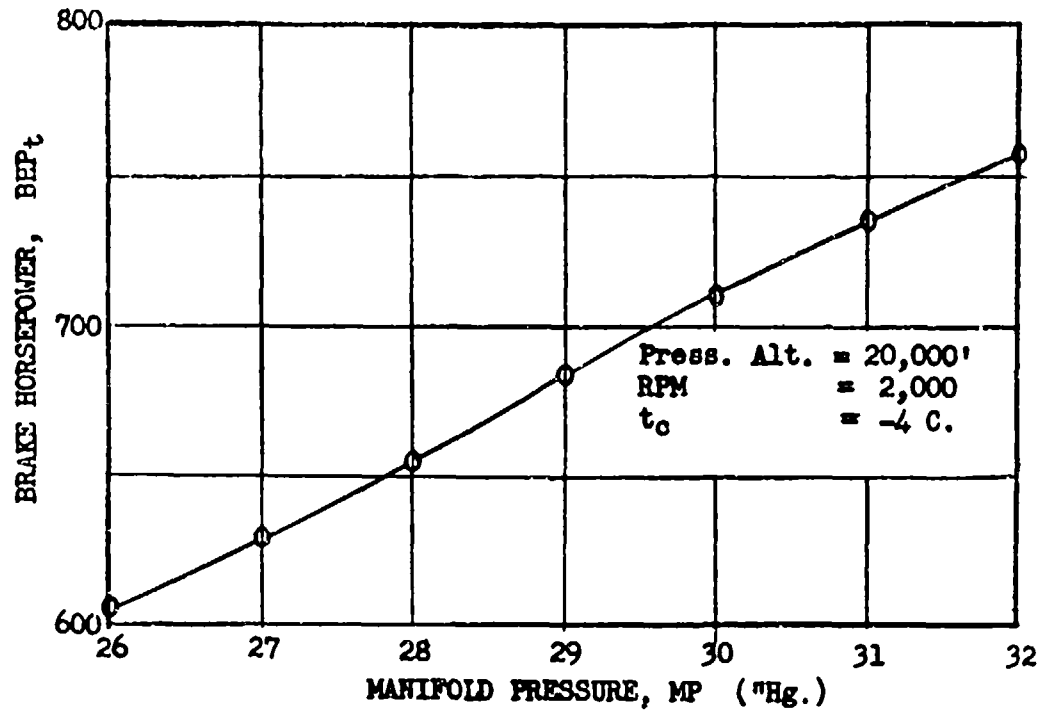


Figure 2.31
 Power Variation for Manifold Pressure Variation
 at Constant RPM and Altitude (Test Data)

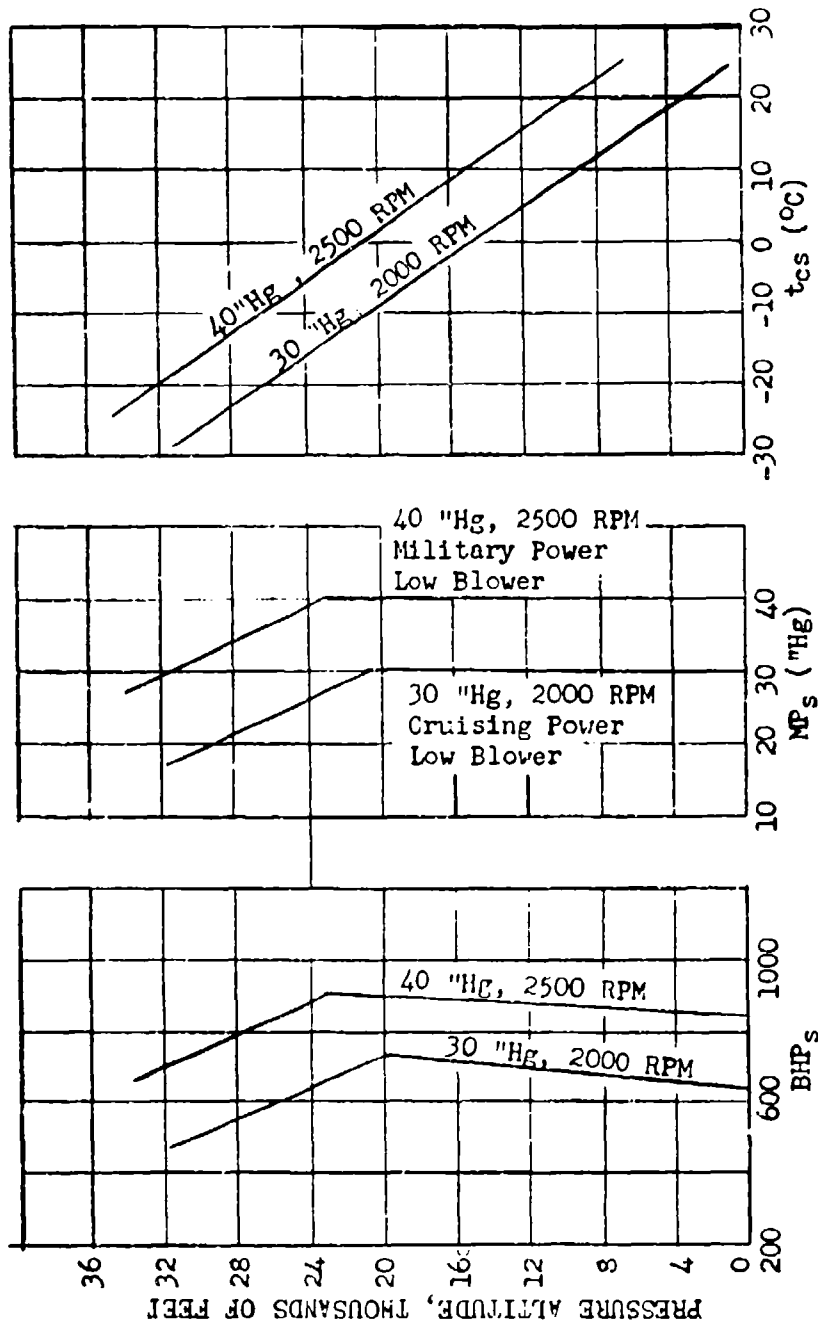


Figure 2.32
Standard Day Engine Data (Internal
Gear Drive Supercharger)

DATA REDUCTION OUTLINE (2.31)

For Correcting Manifold Pressure for Temperature Variation (Wide Open Throttle)

Example 1

Normal installations where the inlet temperature is measured before the fuel is added at the carburetor and before the charge is compressed.

- (1) Test point number
- (2) H_c , pressure altitude
- (3) P_a , inlet (atmospheric) pressure corresponding to (2)
- (4) t_{at} , test atmospheric temperature
- (5) t_{as} , standard atmospheric temperature
- (6) Δt , (4) - (5)
- (7) t_{ot} , test carburetor inlet temperature
- (8) MP_t , test, instrument-corrected manifold pressure
- (9) P_2/P_1 , manifold pressure ratio, (8) \div (3)
- (10) C , from CHART 2.32 and (7) and (9)
- (11) ΔMP , manifold pressure correction (10) \times (8) \times (6)
- (12) MP_s , standard manifold pressure, (8) + (11)

Example II

Fuel injection engine or any supercharger where air only is compressed; also for fuel air mixtures when the inlet temperature is measured after the fuel is vaporized.

NOTE: For this case the data reduction is identical to that for Example 1, except that (4) is substituted for (7) and CHART 2.31 is used to determine C .

Example III

For installations where part of the induction pressure rise is with air only, and the remaining part is with a fuel air mixture. (Turbocharger installations and auxiliary blower installations when operating at constant RPM.)

- (1) Test point number
- (2) H_o , true pressure altitude
- (3) P_a , atmospheric pressure corresponding to (2)
- (4) t_{at} , test atmospheric temperature
- (5) t_{as} , standard atmospheric temperature corresponding to (2)
- (6) Δt , (4) - (5)
- (7) t_{ot} , carburetor air temperature before fuel is added
- (8) P_o , test carburetor deck pressure
- (9) MP_t , test, instrument-corrected manifold pressure, air only stage
- (10) $(P_2/P_1)_a$, carburetor-deck-ambient pressure ratio, (8) \div (3)

- (11) C , from CHART 2.31 and (10) and (4)
(12) ΔMP_a , manifold pressure correction for air only stage (11) x (9) x (6)

Fuel Air Stage

- (13) $(P_2/P_1)_f$, manifold pressure - deck pressure ratio (9) + (8)
(14) C , from CHART 2.32 and (13) and (7)
(15) ΔMP_f , manifold pressure correction for fuel air mixture [(9) + (12)] x (14) x (6)
(16) MP_s , standard manifold pressure (9) + (12) + (15)

SECTION 2.4

Power Correction for Turbosupercharger RPM and Back Pressure Variation at Constant Manifold Pressure

This power correction is used when the throttle is wide open but manifold pressure can be varied by changing turbosupercharger speed. This means that, in going from a test day to a standard day, manifold pressure and rpm will be constant while carburetor air temperature and turbo rpm will change giving a change in power. An example of test and standard day readings for such conditions is presented in the following table:

TEST DAY		STANDARD DAY	
Pressure Altitude	20,000	Pressure Altitude	20,000
T_{at}	-14°C	T_{as}	-24°C
MP_t	42 "Hg	MP_s	42 "Hg
rpm	2250	rpm	2250
t_{at}	27°C	t_{as}	15°C
test turbo rpm	7200	std turbo rpm	7000
BHP	2100	BHP	2150
EBP_t	28	EBP_s	27

The factors affecting power in this case are three: the change in carburetor temperature because of change of free air temperature; the change of carburetor air temperature because of change in turbo speed; and the change in exhaust back pressure. The equation for standard horsepower under these conditions is:

$$BHP_s = BHP_t + \Delta BHP \text{ (for } \Delta CAT) + \Delta BHP \text{ (for } \Delta EBP) \quad (2.401)$$

where:

$$\Delta EBP = \text{change in exhaust back pressure } (EBP_t - EBP_s)$$

The corrections in this equation are usually made empirically. First the assumptions are made that the turbo does not change speed and that a change in manifold pressure would result from inlet temperature variation in going from a test day to a standard day. On this basis a standard day manifold pressure is computed as described in Section 2.3. This manifold pressure correction is defined as,

$$\Delta MP = (MP_t - MP_s) \text{ at test turbo rpm}$$

This ΔMP represents the change in manifold pressure which must be made by a change in turbo rpm. To establish this change in turbo rpm and the other related factors, plots of performance data are made as shown in Figure 2.41. These curves, although not corrected, will show closely the interrelated effect of changing any one of the variables. By entering such a graph at the test turbo rpm and moving an amount equal to ΔMP , a Δ turbo rpm ($RPM_2 - RPM_1$), a ΔEBP ($EBP_2 - EBP_1$) and a ΔCAT ($T_{a2} - T_{a1}$) are established. Standard day values for turbo rpm and exhaust back pressure can then be fixed by direct reading on the graph or by applying the increments for the ΔMP values to the test values.

The total change in carburetor air temperature is the sum of the change because of change in free air temperature and change in turbo rpm.

$$\Delta CAT = T_{as} - T_{at} + \Delta T \text{ (for } \Delta \text{ turbo rpm)}$$

The power change because of carburetor air temperature variation is the same as that discussed in Section 2.2. The change in power because of change in exhaust back pressure has been empirically established as 1% increase in power for each 2 "Hg decrease. With this the standard day power equation is,

$$BHP_s = BHP_t \left[\left(\frac{T_{ot}}{T_{os}} \right)^n + .005 (EBP_t - EBP_s) \right] \quad (2.402)$$

POWER SETTING ERRORS IN FLIGHT

In addition to the correction of power for temperature change it must sometimes be corrected for errors caused by test day manifold pressure or rpm not being set according to schedule. This results from instrument error or human error of the pilot. Rpm errors must be minimized by careful adjustments and anticipation of instrument error, because correction for its variation is not practical. Manifold pressure errors are more easily corrected. Usually the correction is made at the same time that power is corrected for temperature. For a case in which throttle is wide open no correction is required. For a gear supercharged or unsupercharged engine at part throttle, correction is made by manifold pressure-power relationships as described in Section 2.3. For a turbo supercharged engine, correction is made as part of the temperature correction. For example:

Desired MP	60"
Actual flown MP	59"
Rise in MP to standard day computed with assumed constant turbo speed	2"
MP obtained from test MP and assumed rise	61"
Reduction in MP to be accomplished by reducing turbo	-1"

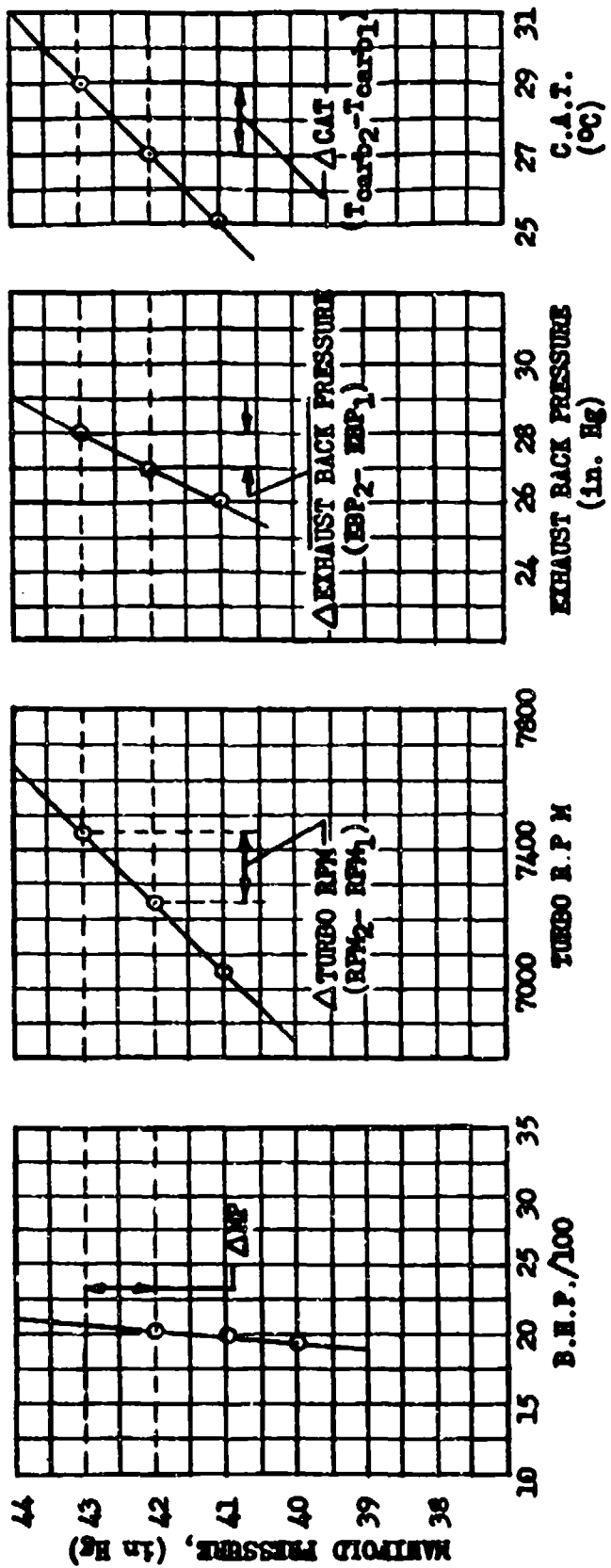


Figure 2.41
 Plot for Determining Effect of Manifold Pressure on
 Turbo RPM, Exhaust Back Pressure, and Carburetor Temperature.

DATA REDUCTION OUTLINE (2.41)

For Determining Standard Turbo RPM and Back Pressure
and CAT for Correcting BHP for Change in
Turbo RPM and Back Pressure

NOTE: Assumed ΔMP for Δt_a , ($t_{at} - t_{ag}$), inlet is first determined with steps of Example III Data Reduction Outline 2.31.

- (17) ΔMP assumed for Δt_a
- (18) Indicated turbo rpm
- (19) Test turbo rpm, (18) + instrument correction
- (20) EBP_i , indicated exhaust back pressure
- (21) EBP_t , test exhaust back pressure (20) + instrument correction
- (22) BHP_{tot} , test BHP at test carburetor temperature
- (23) Δt_{ot} , carburetor temperature increment for assumed ΔMP and a data plot similar to that of Figure 2.41.
- (24) Δ turbo RPM, for assumed ΔMP
- (25) ΔEBP , for assumed ΔMP
- (26) Turbo RPM (standard day) (19) + (24)
- (27) EBP (standard day) (21) + (25)
- (28) t_{og} , standard day carburetor temperature, (7) - (6) + (23)
- (20) BHP_s , standard day BHP, (22) x $\sqrt{(7) \div (28) + (22) \times (25) \times (.005)}$

SECTION 2.5

Critical Altitude

Critical altitude is that altitude where engine performance begins to drop because of the lowered atmospheric pressure. It is defined in two different ways: (1) the altitude at which a specific manifold pressure can no longer be maintained; (2) the altitude at which a specific horsepower can no longer be maintained. In flight test the first definition is generally used, because when an engine is installed in an aircraft, the operating limits such as cruising power, maximum continuous power, and military power are given in terms of manifold pressure and rpm rather than horsepower.

When a complete power available survey is made, critical altitude can be selected from the graph of manifold pressure vs altitude. When only critical altitude is desired, it can be estimated by the pilot; then several full throttle points are flown definitely above critical altitude and are corrected to standard day manifold pressure. Since the drop in manifold pressure is directly proportional to altitude, the point where the line of standard day full throttle manifold pressure intersects the desired manifold pressure ordinate is the critical altitude, as shown in Figure 2.51.

Notice should be taken that the critical altitude of an airplane is dependent on speed because of the ram pressure effect. Critical altitude is usually taken in level stabilized flight, but it is sometimes needed at climbing speeds.

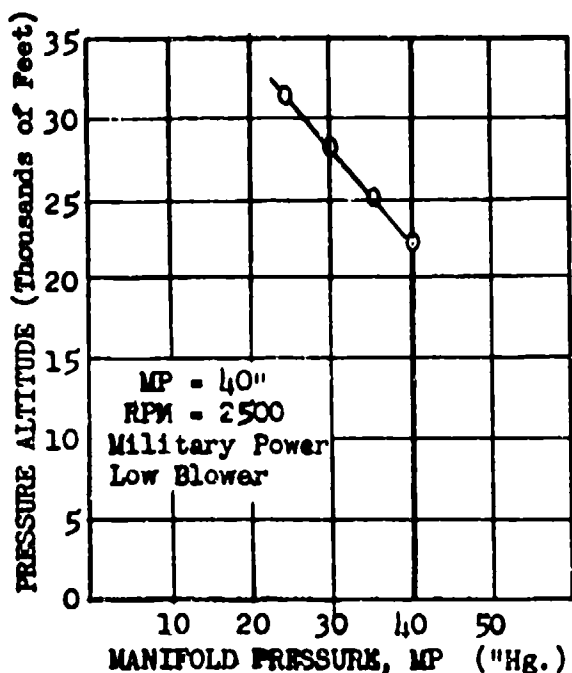


Figure 2.51
Determination of Critical Altitude

SECTION 2.6

Engine Data Plotting, Prop Load, BMEP Data, Supercharger Operation

Sufficient power required data must be obtained so that power required curves covering the full speed range of the airplane may be plotted for at least two altitudes which are considered the most typical cruising altitudes for the test airplane. Each power required curve includes one point at each of the rated power settings of the engines such as war emergency, military, normal rated and maximum cruising powers. The throttles are wide open if the desired manifold pressure cannot be obtained. Sufficient points in the cruising power range are obtained (with the mixture in automatic lean) to complete the speed range with the lowest point at approximately the best climbing speed of the airplane. Cruising power points are obtained at rpm and manifold pressure combinations selected so that the engines are operating between a propeller load curve and the maximum allowable bmeP. At some point near the power required for maximum range cruising, three points are run at the same power with one point at the rpm which lies on the propeller load curve, another point at the maximum allowable bmeP and the third at some intermediate rpm.

Additional power required data is obtained so that power required curves may be drawn at various altitudes; the lowest is obtained at sea level or the minimum practical altitude at the time of the test and the highest is obtained at the highest altitude reached in the check climbs. One high speed part of a power required curve is obtained at approximately each critical altitude. Other high power points are taken so that the maximum altitude increment between the high speed power required curves will not be more than a few thousand feet for all tests above the critical altitude of the airplane. The high speed power required curves consist of at least one point at each of the rated power settings such as war emergency, military, and normal rated for the high and low altitude power required curve and for the power curve near the critical altitude. Other power required curves may be drawn through single points using the more complete curves on either side of it as a guide in determining the proper slope of the curve drawn through the point.

At the critical altitude of the airplane, at least four points are run at the rated rpm of the engines with the first point at the rated manifold pressure and with each succeeding point at about two inches of mercury less manifold pressure. If the slope of the curve through these points does not fit in with the other curves, it is an indication of power curve inaccuracy or rapid change in propeller efficiency. In either case it is necessary to run at least three points at each rpm for all of the power calibrations. From these additional points, the proper slope of the power required curve may be obtained.

A plot of all speed power data run at or corrected to the same take-off gross weight less the weight of fuel used to climb to the test altitude is plotted on one Power vs Speed chart as shown in Figure 2.61. Each power required or partial power required curve is clearly labeled to show the corresponding density altitude and gross weight.

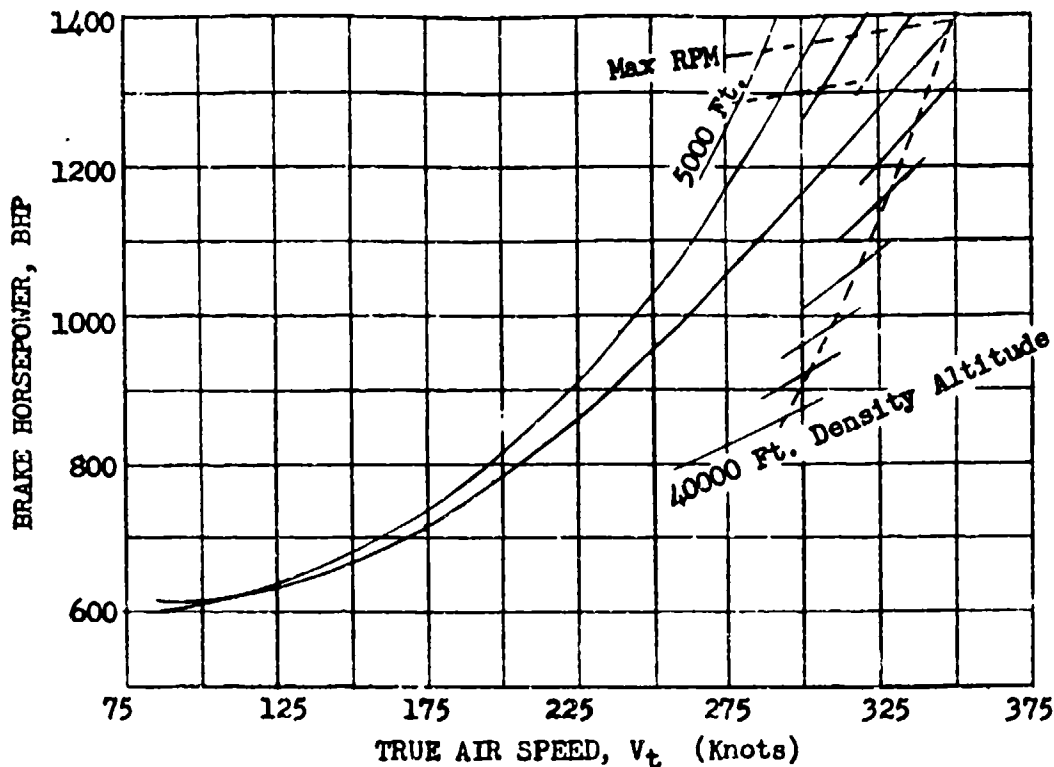


Figure 2.61
Power Required Curves

All power required data at rated manifold pressure or at wide open throttle is corrected to give the power available on a standard day at the rated manifold pressure or at wide open throttle so that curves of BHP available and the corresponding manifold pressure may be plotted against altitude as shown in Figure 2.62. Curves of Speed vs Altitude for the desired power ratings are drawn as shown using points obtained from the power required curves in Figure 2.61. These points are read at the speeds corresponding to the power available at the altitude of the power required curve. The speeds for best climb and the ceiling of the airplane will be of aid in determining the shape of the upper part of the speed curve.

For each gross weight and altitude condition, a power required curve is obtained with the first point at rated power (auto-rich), the second at maximum cruising (auto rich and auto lean), with the rest of the points part of a complete survey of the cruising power range made between the propeller load curve and the curve for limiting bmp as shown in Figure 2.63. The higher cruising

powers are run for both automatic rich and automatic lean mixture settings but only automatic lean mixture setting need be used for the lower powers. Select four or five rpm values covering the cruising range. At each rpm, select manifold pressure values varying from the maximum for limiting bmep to the minimum corresponding to the power from a propeller load curve or to the minimum manifold pressure at which level flight can be maintained for the given rpm. At least three manifold pressure increments should be used for each rpm and the increments should not be greater than three inches of mercury.

The propeller load curve is drawn through the rated power and rated rpm point and determined by the following expression:

$$\left(\frac{N}{N_R}\right)^3 = \frac{bhp}{bhpr} \quad (2.501)$$

where:

N_R = rated rpm (normal)
 $bhpr$ = rated horsepower (normal)

The limiting cruising bmep is specified by the engine manufacturer and is usually about 140 bmep for larger engines. The bmep is determined from the following expression for any given engine rpm and bhp:

$$bmep = \frac{bhp \times 792000}{rpm \times \text{piston displacement}} \quad (2.502)$$

The minimum recommended cruising rpm is determined by speed limitations of the engine or accessories and is specified by the engine manufacturer; it will usually be between 1200 and 1500 rpm. The minimum power for level flight is determined in flight.

In all cruising operation the use of any but the lowest amount of supercharging should be avoided if possible. Airplanes equipped with turbosuperchargers should always be flown with the throttle butterfly wide open when using any turbo (except for what throttle is required for formation flying). Airplanes with gear driven supercharger should always be flown with the superchargers in low speed ratio up to the altitude at which the optimum indicated air speed may be obtained without exceeding the allowable rpm and manifold pressure for automatic lean mixture.

LEVEL FLIGHT DATA

Intercooler Flaps 2 ● Approximately 10,000'
 Intercooler Flaps 5 ● Approximately 20,000'
 Intercooler Flaps 5 ● Approximately 30,000'
 Military Power 2700 RPM 60 °Hg
 M R P 2550 RPM 50.5 °Hg

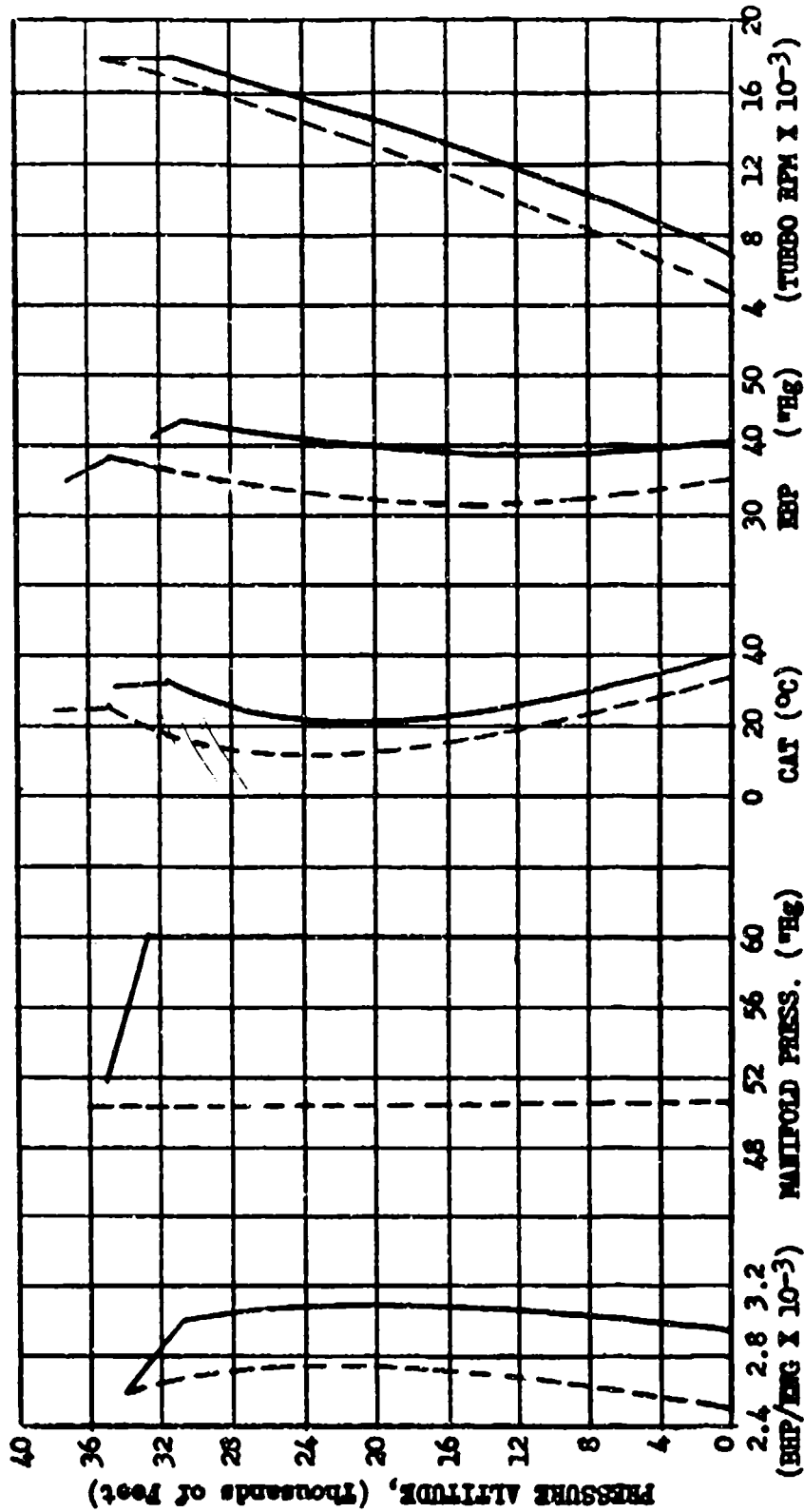


Figure 2.62
 Level Flight Power Data

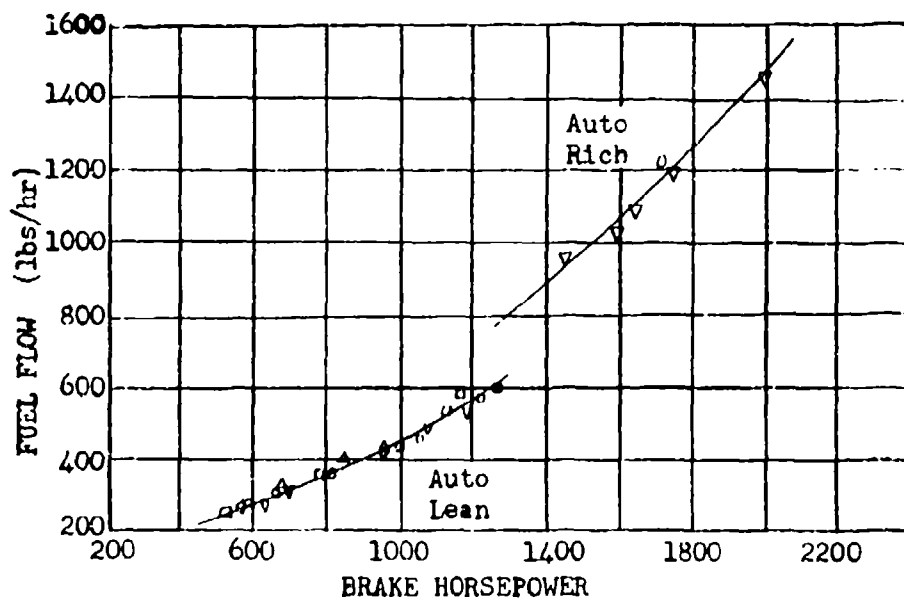
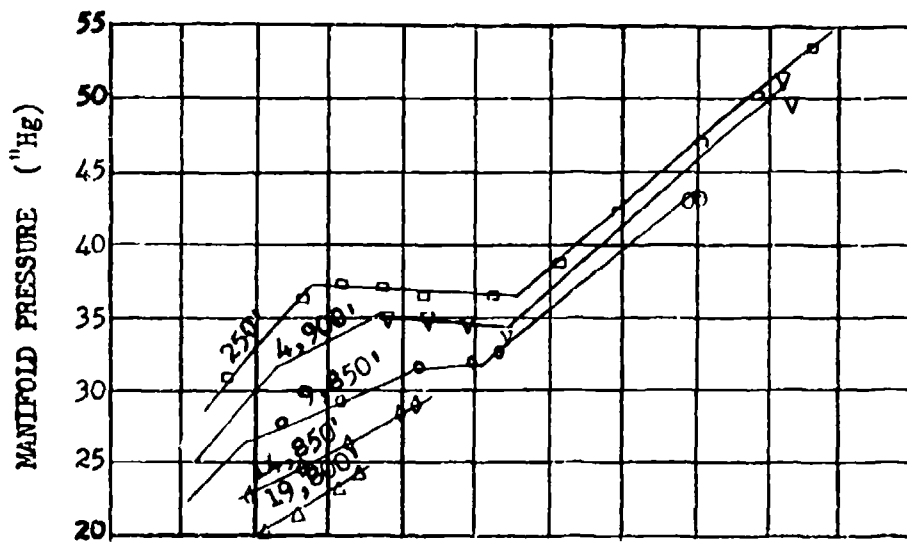
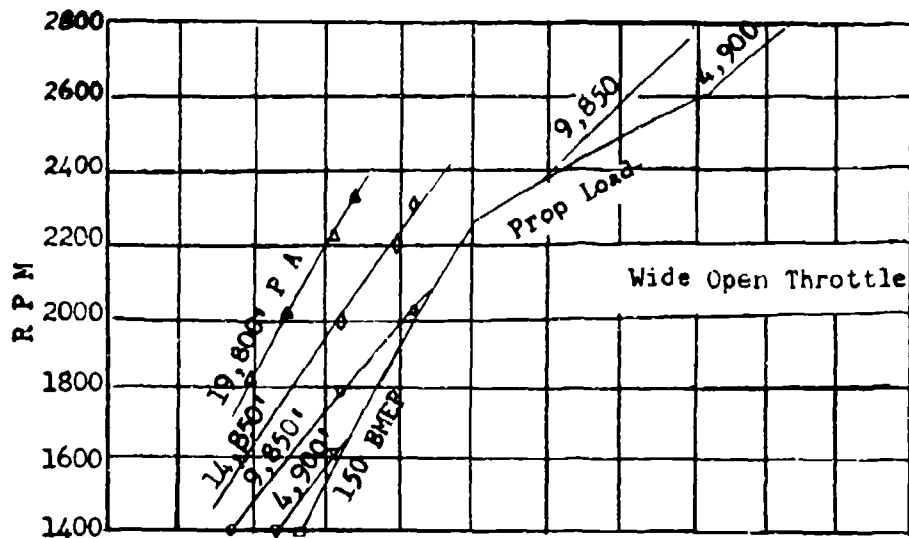


Figure 2.63
Engine Power Data (Low Blower)

SECTION 2.7

Fuel Consumption

Fuel consumption is best measured as pounds per brake horsepower hour, specific fuel flow. From engine theory this is dependent upon mean effective pressure in the cylinder. For a simple engine, with all conditions ideal, power is a function of mean effective pressure, volume of the cylinder, and rpm so that for a given engine specific fuel consumption could be plotted against brake horsepower and rpm, as shown in Figure 2.71.

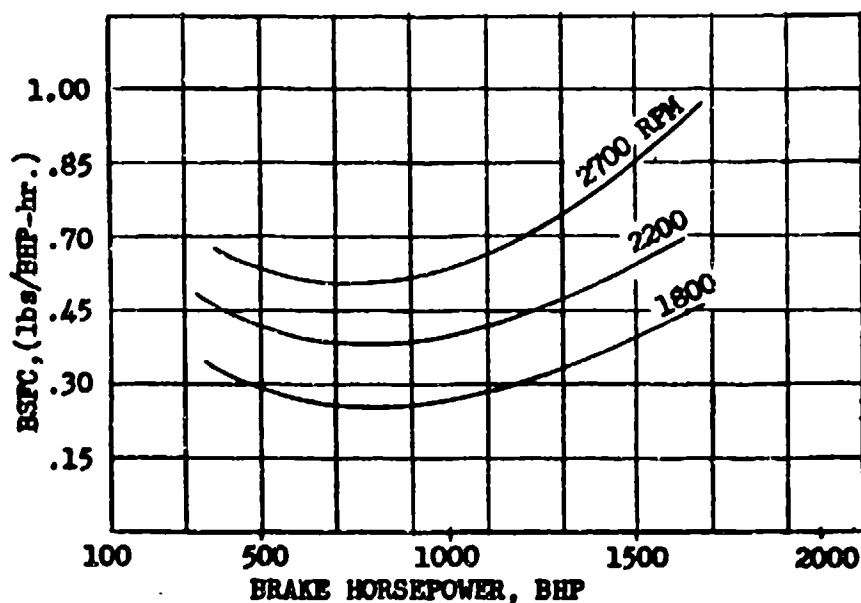


Figure 2.71
Typical Specific Fuel Consumption Curves
for RPM and Horsepower

In practice the specific fuel consumption may also vary with altitude because of carburetion, superchargers, ignition, and accessories. To run tests and make plots as in Figure 2.71 for many altitudes would be tedious and is not required for flight test. The engine manufacturers and government agencies will run such extensive tests and determine a power schedule of mixtures, manifold pressures, rpm, and supercharger ratios for best engine operations. For flight test the only fuel consumption data generally required is that for powers obtained by operation on the normal schedules as shown in Figure 2.72. These points are run at the same time as speed power points so that later air miles per gallon and range can be computed.

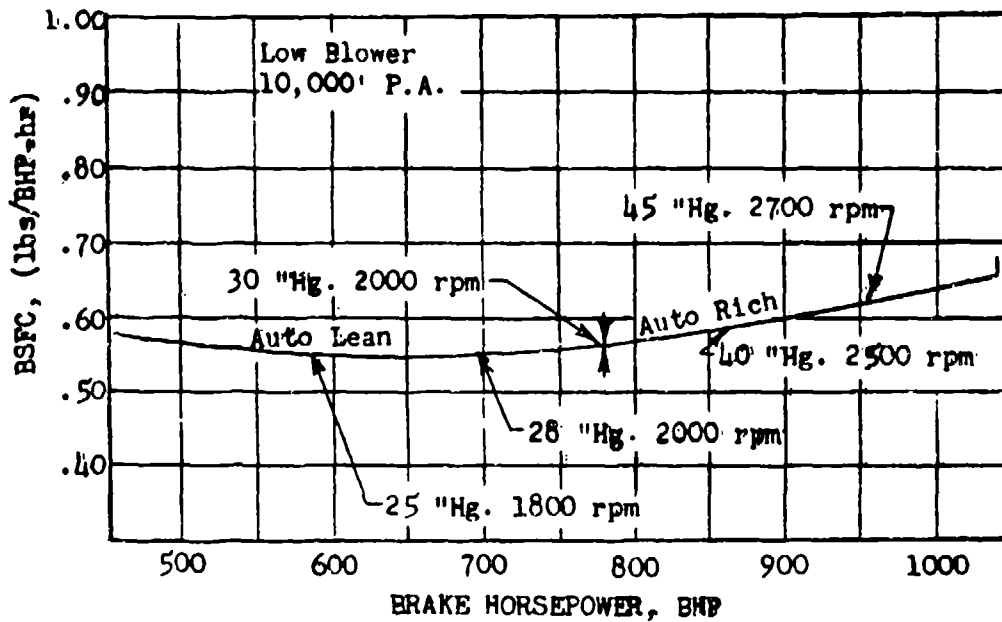


Figure 2.72
Specific Fuel Consumption Data
at Two Mixture Settings

As part of the general engine performance presentation a graph of standard gallons per hour at corresponding settings vs altitude is sometimes required from the specific fuel flow information and is presented as shown in Figure 2.73.

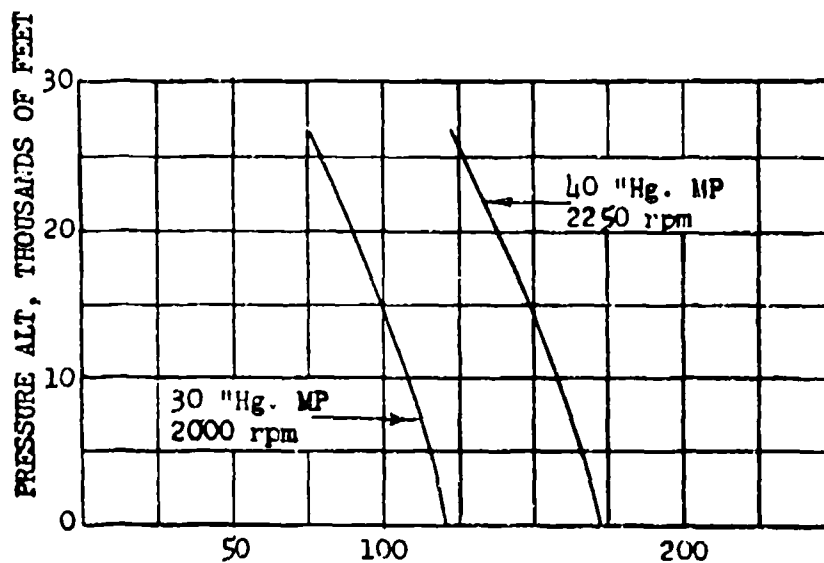


Figure 2.73
Fuel Consumption at Various Altitudes
For Two Engine Conditions

SECTION 2.8

Engine Cooling

The hot strength of metals, and the temperature limits imposed by lubricants and detonation make it necessary to limit the operating temperature of engines and accessories. Army and Navy Aeronautical Specification, "Test Procedures for Aircraft Power Plant Installation (AN-T-62)," has set up a standardized instrumentation and test procedure. This specification should be studied when planning cooling tests.

There are two primary concerns in the cooling problem. These are whether the temperature limits can be maintained for all specified engine operating conditions and the effect on range of the various engine cooling configurations required to operate the engines within prescribed limits.

For determining the cooling requirements of a four-engine aircraft one engine is completely instrumented as specified in (AN-T-62). The remainder have less extensive instrumentation which is used as a cross check to correlate their operation with that of the completely instrumented engine. All temperatures except free air temperature and carburetor air temperature will be corrected to Army summer day conditions which are 23°C higher than NACA standard temperatures. The correction to summer day conditions is made to the indicated ambient temperature corrected for instrument error. This is done by adding the product of the correction factor, given in (AN-T-62), and the difference between the ambient temperature and the Army summer day standard temperature. In recording airflow pressure data each pressure difference may be determined in two ways; by direct measurement, or by subtracting the two values which were measured with reference to the air speed static pressure.

Temperatures and pressures thus determined allow computation of the engine cooling air flow which in turn makes possible a quantitative analysis of the cooling data for use in eliminating engine hot spots.

Figures 2.81, 2.82, and 2.83 are typical examples of how the basic data is presented graphically for the three cases usually considered; ground operation, climb and level flight.

Cooling data may be corrected to standard temperatures by solving equation 2.801

$$\Delta T = K (\text{BHP})^x (\Delta P)^a (\sigma)^b (\text{BSFC})^c \quad (2.801)$$

where:

- ΔT = engine temperature - ambient temperature
- K = constant to be determined
- BHP = brake horsepower
- ΔP = pressure drop through baffles
- σ = density ratio
- BSFC = brake specific fuel consumption
- x, a, b, c = exponents to be determined

In solving for the exponent "c", level flight runs are made at about 10,000 feet pressure altitude in normal and rich mixture settings to determine the effect of mixture on cylinder head temperature. The rpm, bhp, air speed, cowl flap settings, oil cooler flap-settings, and altitude are held constant for both mixture settings. The data obtained at various rpms (1800, 2000, 2200, 2400, and 2550 rpm) from the 10,000 feet speed-power tests in normal and rich mixture are then used to determine the "c" exponent. A complete cylinder head temperature pattern is obtained on the Brown recorder on each run after the temperatures have become stabilized. The exponent "c" is the slope of the plot of $\log \Delta T$ versus \log BSFC. The sign of "c" may change abruptly between manual lean and higher mixture settings.

A pressure survey is made at about 10,000 feet pressure altitude in normal mixture to determine the exponent "a" for the change in baffle pressure. This is accomplished by varying the cowl flap openings on the engine instrumented for cooling and holding the horsepower, rpm, air speed, oil cooler flaps, and altitude constant. Runs are made with the cowl flaps set in increments of 1-inch from full open to the setting resulting in the limit engine temperatures being obtained. On the runs at each 1-inch increments of cowl flap travel, the engine temperatures are stabilized and recorded on the Brown recorder. The power on the engines not being tested is varied to hold a constant air speed for all cowl flap positions at each power setting on the test engine. The exponent "a" is the slope of the plot of $\log \Delta T$ versus $\log \Delta P$.

An altitude survey is obtained in conjunction with the speed-power data at approximately 5000, 10,000 and 15,000 foot altitudes to determine the effect of altitude on engine cooling. The stabilized temperatures obtained during the speed-power test in normal mixture at various rpm are then used to determine the exponent "b". The cowl flaps and oil cooler flaps are held constant at a setting that will give adequate cooling for all altitudes. The exponent "b" is obtained from the slope of the plot of $\log \Delta T$ versus $\log \sigma$. For determining "b" the same BHP's are used at each altitude.

In determining the exponent "x", the level flight data from other stabilized runs are used. Holding ΔP , σ , and BSFC constant, the slope of a plot of $\log \Delta T$ versus \log BHP gives the value of the exponent "x". Test values of ΔP , σ , BSFC, ΔT , and BHP are substituted in the basic equation and K determined. With this equation the engine cooling data can be corrected to a standard day temperature or to a hot day temperature; also, the amount of cowl flaps necessary for any engine power can be determined.

A more simplified method of cooling analysis for rough work can be made by plotting ΔT for various engine components vs cowl flap setting. A ΔV_1 is also plotted on the same graph for a cowl flap drag increase reference. A typical plot of this type is shown in Figure 2.84. Plots of this type made at two speeds and altitudes are useful in determining the ΔT ranges for various cowl flap or oil cooler control positions.

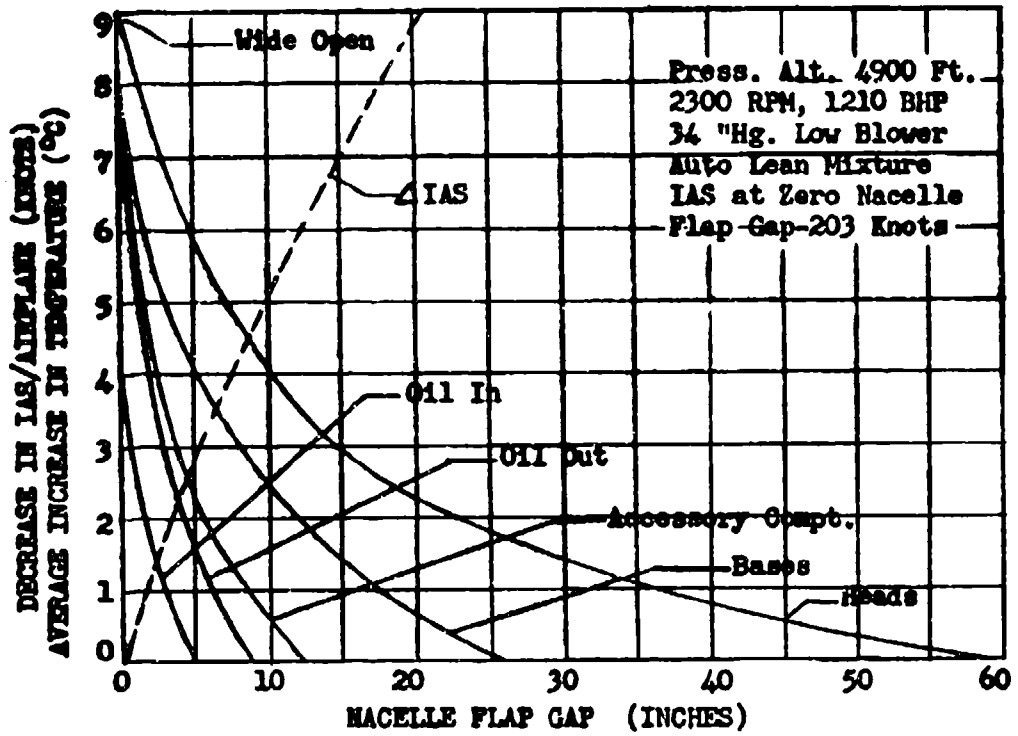


Figure 2.84
Cooling and Speed Loss Data for
Various Nacelle Flap Settings

B-000 USAF No. 0000 GROUND COOLING CHECK
 MIXTURE AIR COWL FLAMES 8" GAP INTERCOOLER 0" GAP OIL COOLER 13.6" GAP

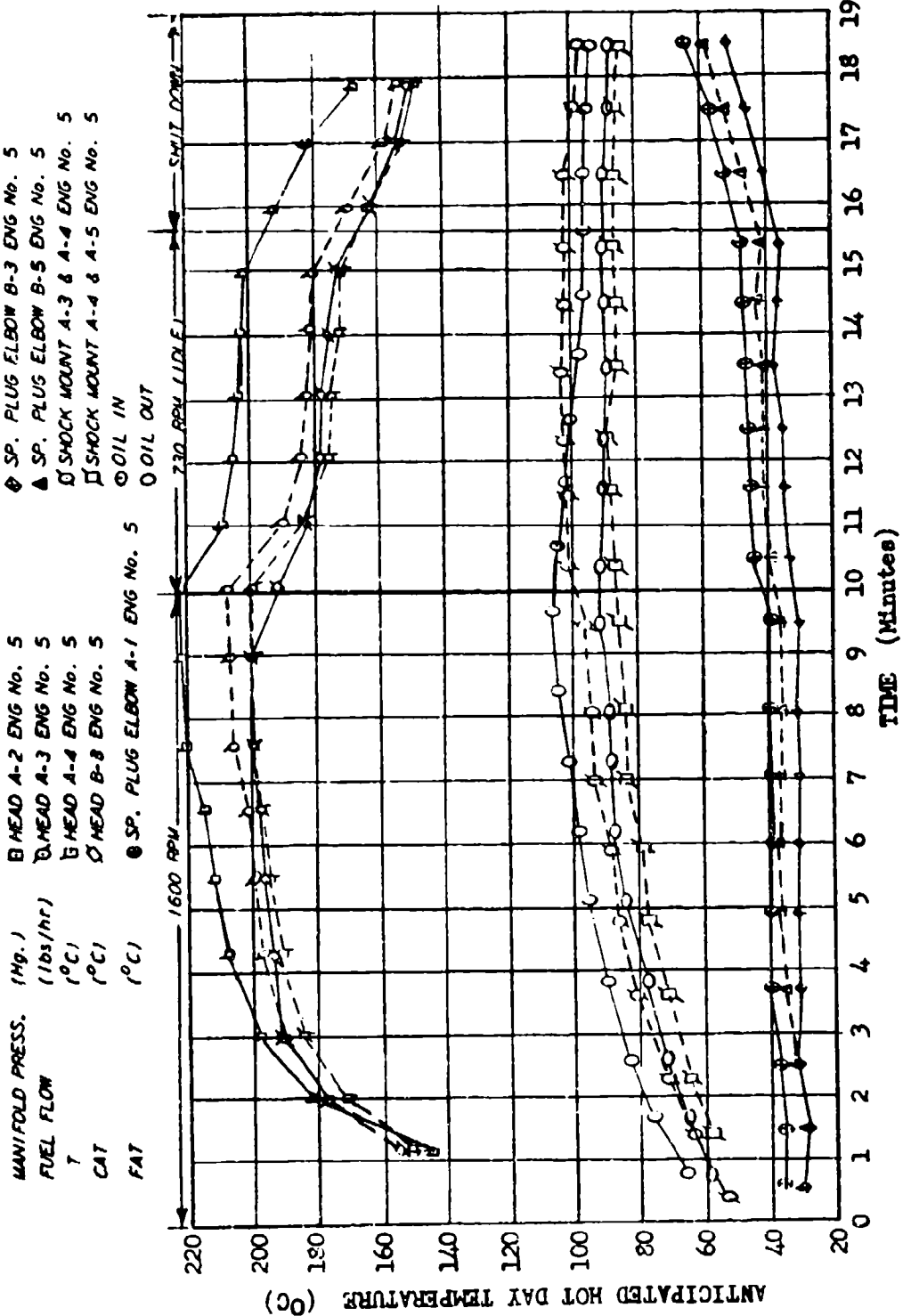
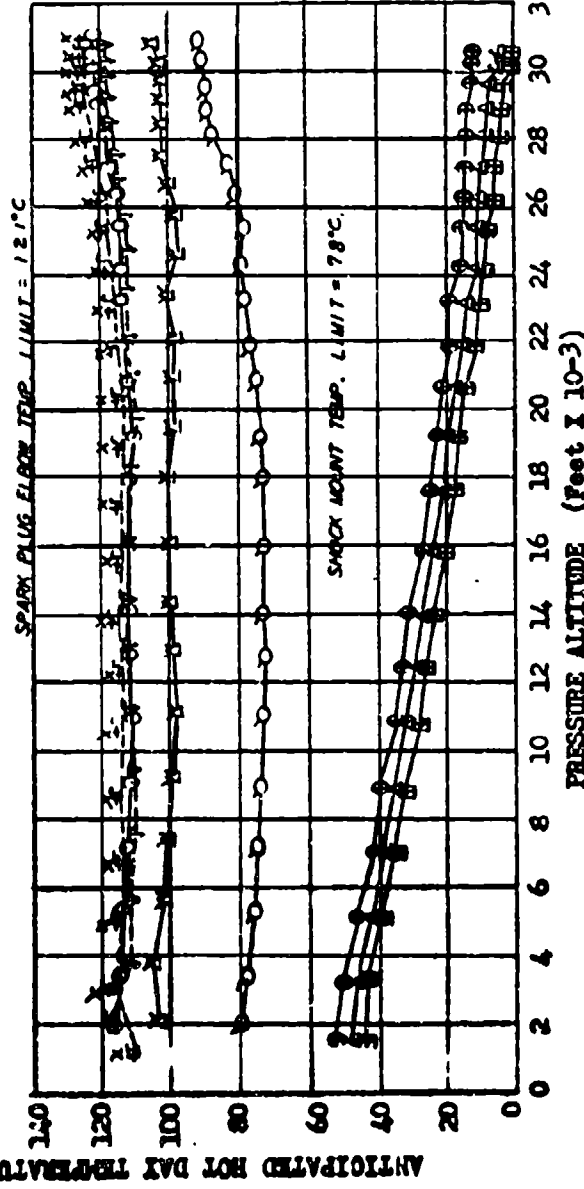
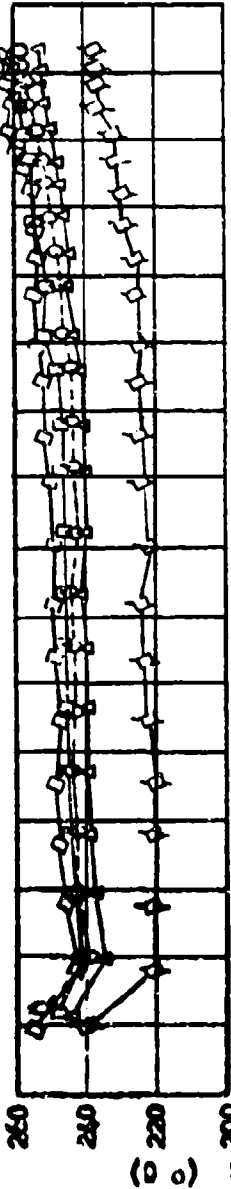


Figure 2.81
 Ground Cooling Check

B-000 USAF No. 00000 FLIGHT No. 000
 POWER-MRP NRP CLIMB TO 30,940 FEET GROSS WEIGHT @ T. O. -145,000 lbs
 MIXTURE-AIR COWL FLAPS-3.2" GAP INTERCOOLER FLAPS-3.5" GAP OIL COOLER FLAPS-4.3" GAP

ENGINE NO.	1	3	4	1	3	4	1	3	4	1	3	4
MANIFOLD PRESSURE	50.9	50.8	51.4	50.8	56.7	57.5	50.8	50.8	50.8	51.4	50.6	50.9
B S F C	2645	2605	2613	2608	2650	2616	2685	2590	2590	2555	2647	2562
C A S (INCHES)	774	746	783	781	743	792	749	756	756	817	750	821
T (°C)	172	172	172	172	172	172	172	172	172	172	172	172
C A T	23.0	22.0	23.5	22.0	22.0	22.5	24.0	26.0	26.0	22.5	25.5	24.0



HEAD TEMP. LIMIT = 292°C.

- ◇ HEAD A-1 ENG NO. 3
- HEAD B-1 ENG NO. 3
- △ HEAD C-1 ENG NO. 3
- ▽ HEAD A-1 ENG NO. 1
- ◇ HEAD A-1 ENG NO. 4
- + BASE B-1 ENG NO. 3
- X BASE B-2 ENG NO. 3
- J BASE B-3 ENG NO. 3
- Y BASE D-4 ENG NO. 1
- V BASE A-1 ENGINO. 4
- ⊙ S.P. ELBOW A-1 ENG NO. 3
- ⊙ S.P. ELBOW B-1 ENG NO. 3
- △ S.P. ELBOW B-5 ENG NO. 3
- ⊙ SHOCK MT. A-1 & A-2 ENG NO. 3
- ⊙ SHOCK MT. A-7 & A-1 ENG NO. 3
- OIL IN ENG NO. 3
- OIL OUT ENG NO. 3

Figure 2.82
 Cooling Data During Climb
 to Altitude

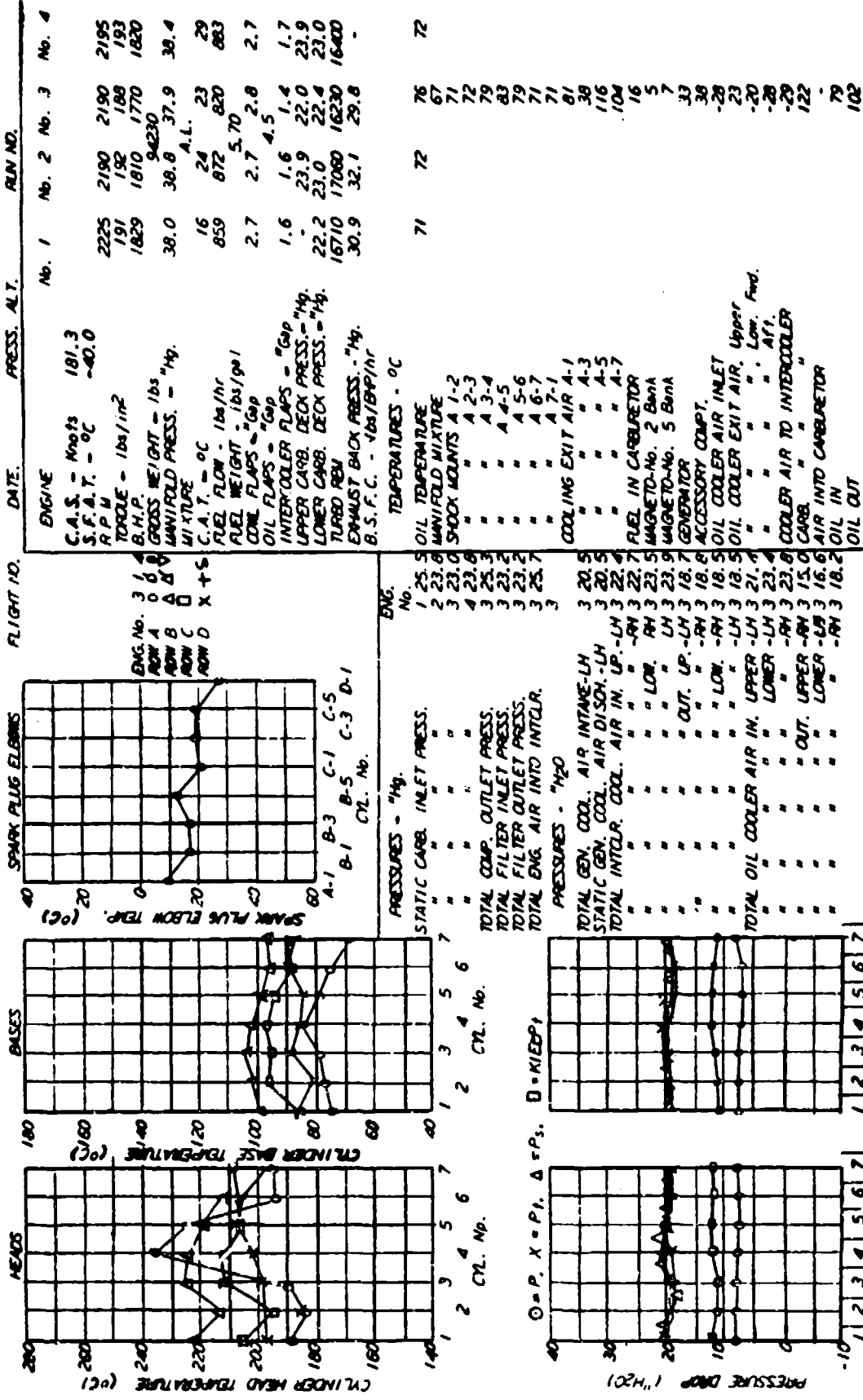
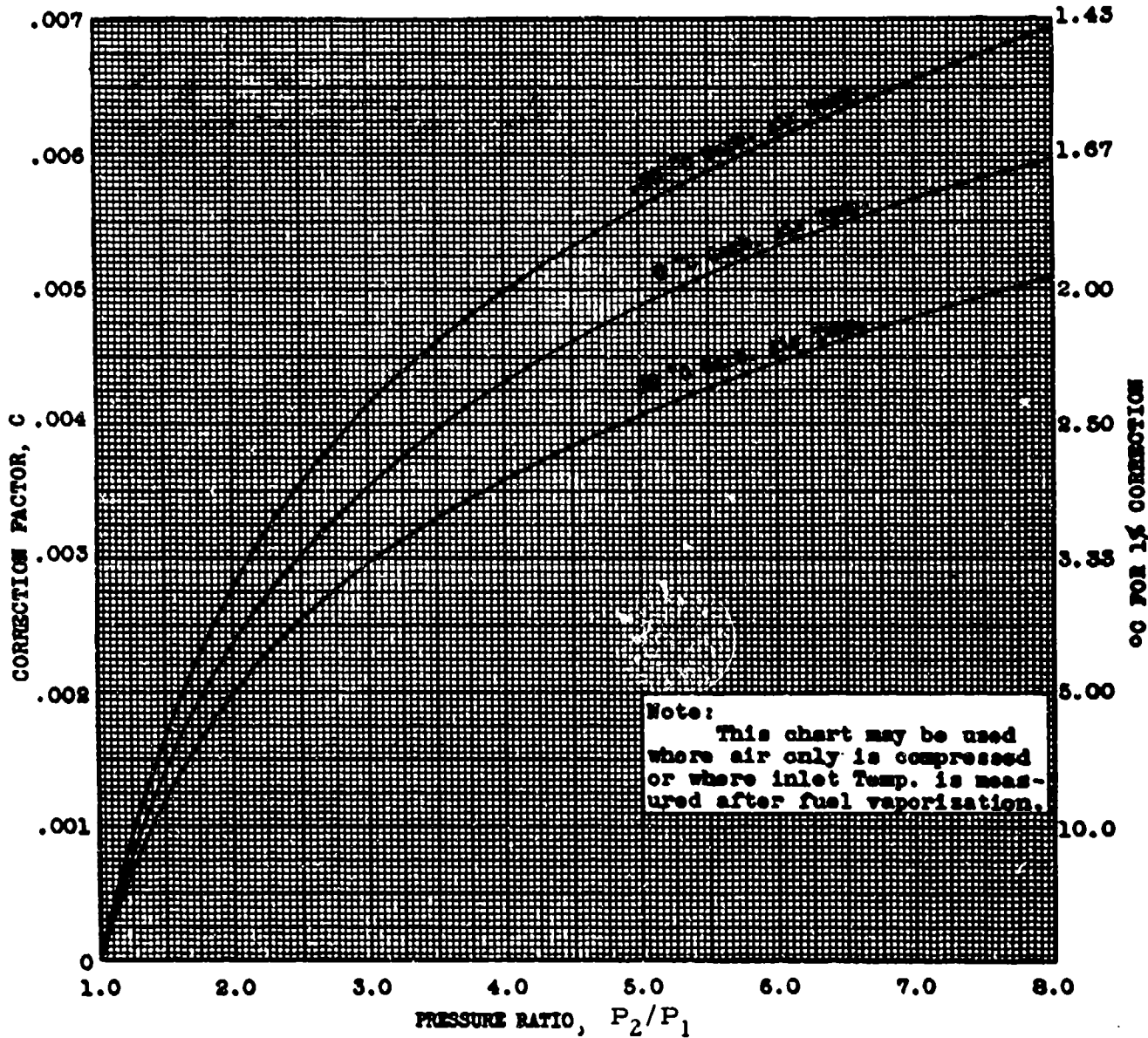


Figure 2.83
Power Calibration and Cooling Run

MANIFOLD PRESS. CORR. (FOR CHANGE IN SUPERCHARGER INLET AIR TEMP.)

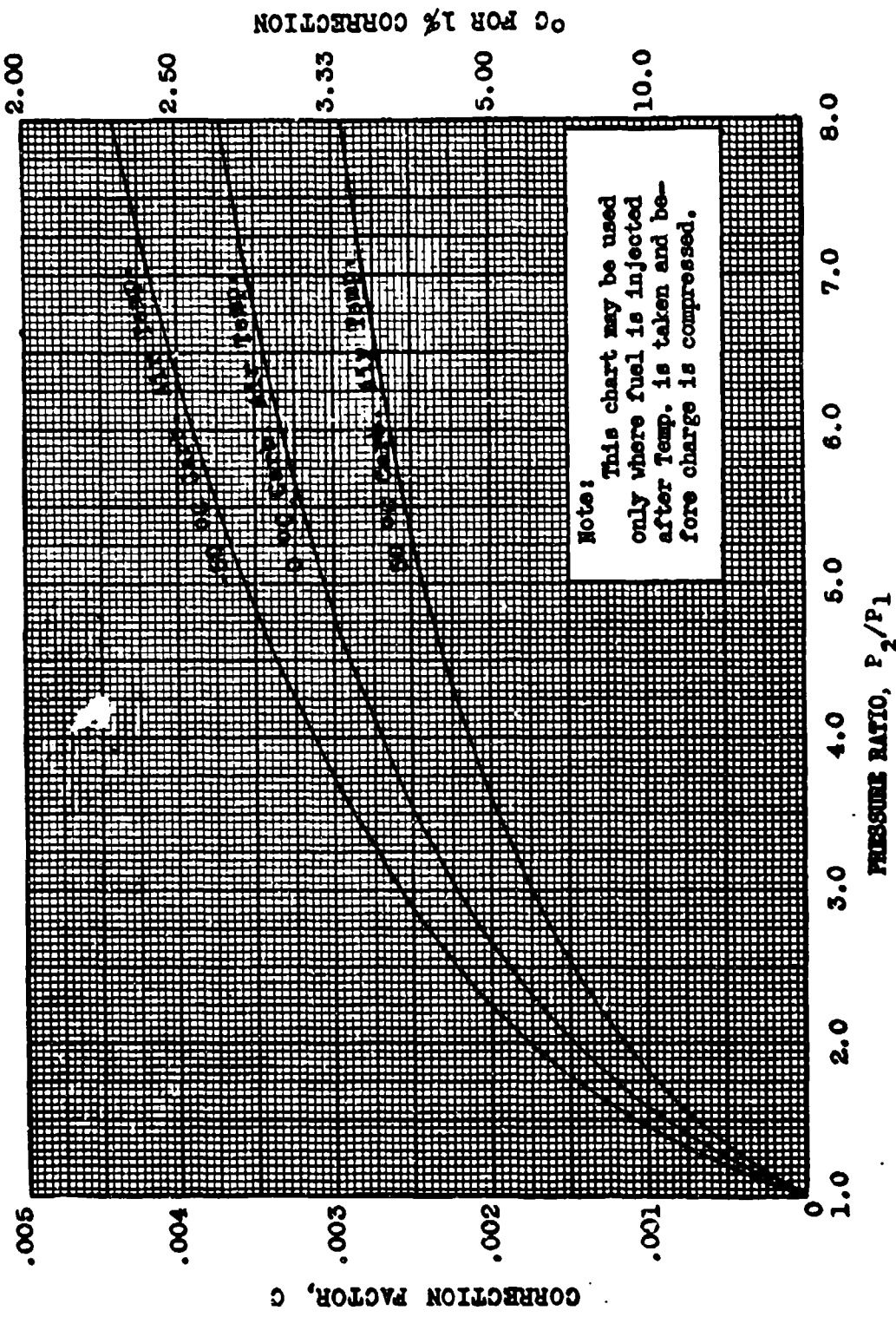
CHART 2.31



AFTR-6273

CHART 2.31

MANIFOLD PRESS. CORR. (FOR CHANGE IN CARB. INLET AIR TEMP.) CHART 2.32

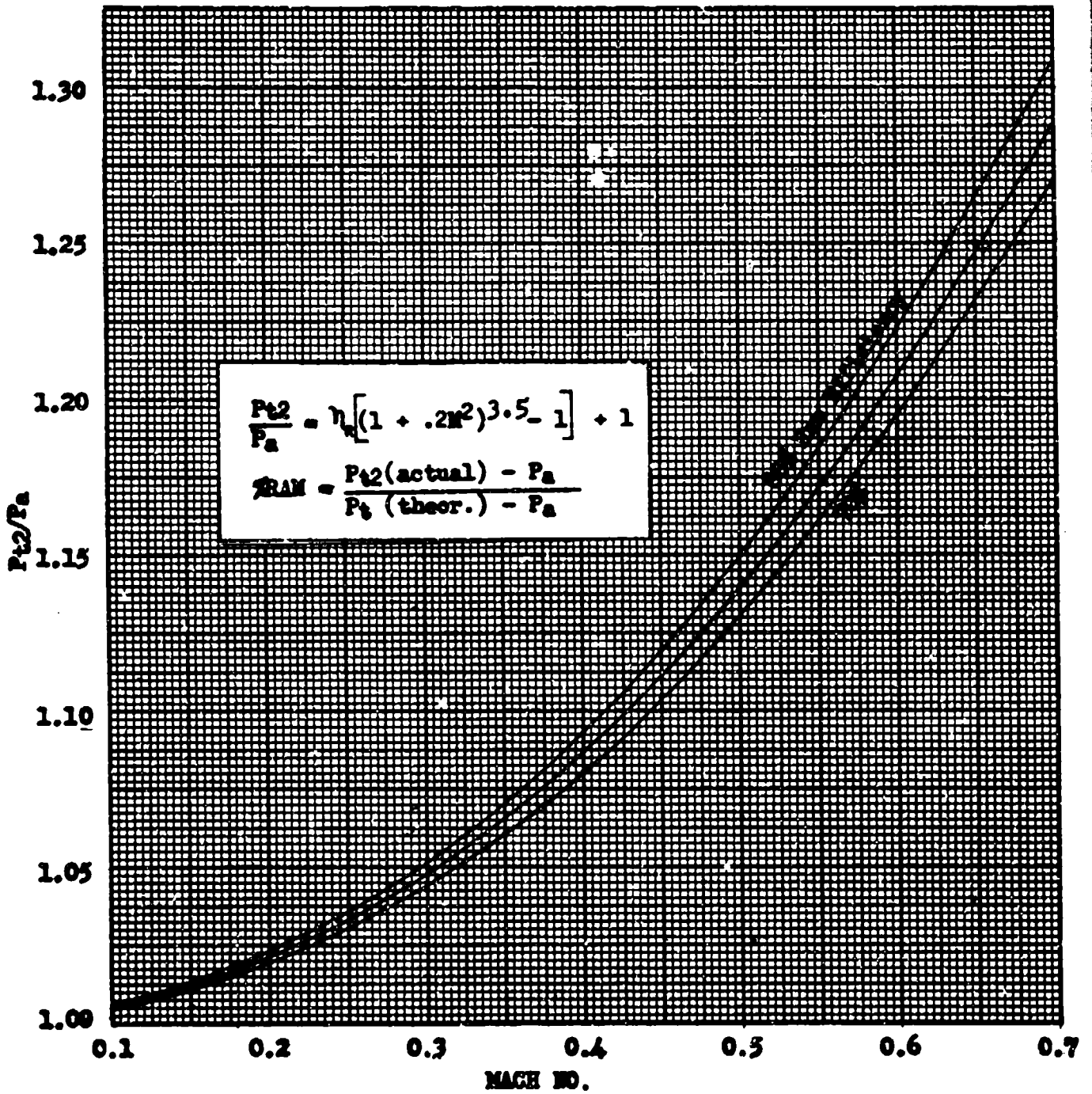


APTR-6273

CHART 2.32

RAM PRESSURE RATIO—RAM EFFICIENCY—MACH NO.

CHART 2.33



AFTR-6273

CHART 2.33

SYMBOLS USED IN CHAPTER THREE

<u>Symbol</u>	<u>Meaning</u>
A	Area
A_c	Inlet capture area
A_r	Ramp or compression surface area
A_s	Area of ejector at primary nozzle exit
A_w	Projected ejector area
B	Mach number parameter, $1 + \frac{\gamma - 1}{2} M^2$
C_{da}	Additive drag coefficient
C_{dp}	Cowl pressure drag coefficient
C_f	Skin friction coefficient, or nozzle thrust coefficient
d	Boundary layer diverter height, or duct diameter
\bar{d}	Hydraulic diameter
D_a	Additive drag
F_o	Ram drag
F_g	Gross thrust
F_{int}	Intrinsic thrust
F_n	Net thrust
F_{post}	Post-exit thrust
F_{pre}	Pre-entry thrust
g	Acceleration of gravity
K_B	Loss coefficient in duct bend
l	Subsonic diffuser length
m	Mass flow
m_1/m_0	Inlet mass flow ratio = A_0/A_c
M	Mach number
N	Engine rotational speed
P_a	Atmospheric pressure
P_s	Static pressure
P_t	Total pressure

P_w	Ejector wall static pressure
q	Dynamic pressure, $\frac{1}{2} \rho V^2$
r	Average radius of curvature for duct bend
R	Universal gas constant (96.031 feet/°K)
R_o	Reynold's number
T_a	Atmospheric temperature
T_s	Static temperature
T_t	Total temperature
V	Velocity
V_s	Secondary flow speed
V_t	Airplane true speed
w_a	Engine airflow
w_{BL}	Airflow through boundary layer bleed system
w_g	Gas flow
w_s	Secondary airflow
X	Nozzle pressure ratio parameter $\left[\frac{P_{t8}}{P_a} \right]^{\frac{\gamma-1}{\gamma}} - 1$
α	Angle of attack
β, β'	Exponents used in dimensional analysis
γ	Ratio of specific heats
δ	Boundary layer thickness or corrected pressure, P_a/P_{SL}
η	Ram efficiency
θ	Corrected temperature
λ	Flow angle relative to free stream direction
π	Non-dimensional parameter
ρ	Air density
σ_l	Cowl position parameter
ϕ	Momentum in boundary layer removal system, $\gamma P_a M_{ABL}$

Subscripts:

0, 1, 2, etc.

BL

e

SL

th

Engine station designations

Boundary layer

Exit

Sea level

Throat

Superscripts:

*

'

Sonic flow conditions

Conditions downstream of normal shock wave

CHAPTER THREE

SECTION 1

INTRODUCTION TO THRUST MEASUREMENT

1.1 PRELIMINARY COMMENTS

The turbojet engine performs a function similar to that of the reciprocating engine with a propeller. With either system thrust is produced in the same manner; that is, by accelerating a mass of air. The difference in the operation of the two systems lies in the volume and velocity of the air or gases affected. The propeller moves a comparatively large volume of air rearward at a relatively low velocity, while the turbojet engine takes in a smaller volume of air, expands it with burning fuel, and expels it to the rear at a high velocity.

The static thrust of a turbojet engine can be determined readily by direct mechanical measurement on the ground. This measurement may be made with strain gages, spring balance, etc., either with the engine installed in an airplane mounted on a thrust stand or with the bare engine located in a test cell. It has been found that even with seemingly identical production turbojet engines, there is an appreciable difference in thrust output. Also, there is a gradual loss of thrust as operating hours are accumulated on an engine. For this reason the static thrust of engines in aircraft undergoing performance testing should be measured periodically.

Thrust measurement in flight becomes considerably more difficult than under static conditions. No satisfactory means of determining thrust by mechanical means, such as strain gages installed at the engine mounts, has been found. Approximate thrust data can be obtained from the engine manufacturer's estimated performance curves. This method is not satisfactory for flight test purposes, however. These curves are based on estimates, or an average engine and do not yield sufficiently accurate thrust data because of variations in output between engines. A useful application of these curves is in making corrections to standard conditions as described in Section 4. In this

case a high degree of accuracy is not required since the amount of the corrections is usually small compared to the total values.

1.2 GENERAL ANALYSIS OF IN-FLIGHT THRUST MEASUREMENT

It is convenient to consider first a simple ducted body in order to define the thrust developed by a turbojet engine. For simplification, the axis of the body is made parallel to the flight path and no mixing of internal and external flow downstream of the nozzle exit is considered (reference Figure 1.1). It is indicated from the momentum theorem that the thrust developed is equal to the rate of change of total momentum (pressure plus momentum flux) of the internal fluid contained within the stream tubes ahead of and behind the body as well as that within the body.

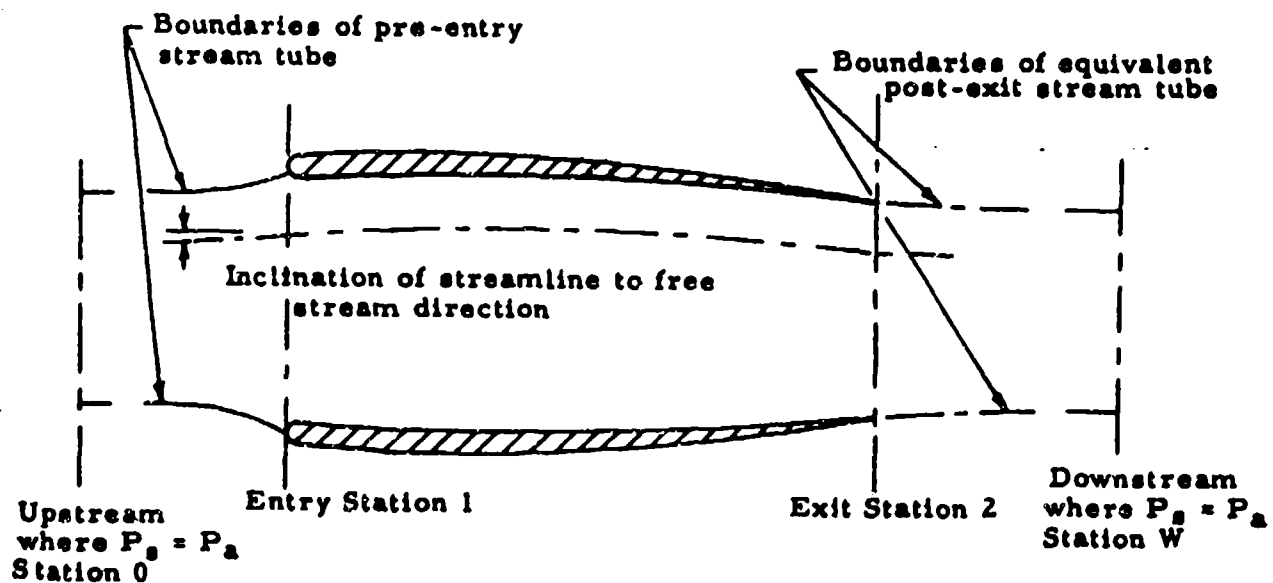


Figure 1.1
Flow Through a Simple Ducted Body

Assuming a uniform velocity distribution, the thrust at any arbitrary plane (P) perpendicular to the flight path can be expressed as

$$\int V \cos \lambda \, dm + \int (P_{sp} - P_a) \, dA_p \quad 1.1$$

where

- V = fluid velocity
- λ = inclination of streamline to free-stream direction
- m = mass flow
- P_{sp} = static pressure at arbitrary plane (P)
- P_a = ambient pressure
- A_p = area containing the internal flow at arbitrary plane (P)

1.3 DEVELOPMENT OF THRUST DEFINITIONS

1.3.1 Net Thrust:

The fundamental definition of the net thrust of a turbojet engine is considered equal to the change of total momentum of the internal fluid between station 0 upstream and station W downstream. Station 0 is sufficiently far upstream that the boundaries of the pre-entry stream tube are parallel to the direction of undisturbed flow and the static pressure in the stream tube is the same as ambient pressure. Similarly, station W is located downstream where pressure disturbances resulting from the passage of the body through the air have disappeared and the static pressure is again ambient. From continuity, $m = \rho VA$ and equation 1.1 may be re-stated as

$$F_N = \int \rho_w V_w^2 \, dA_w - \int \rho_o V_o^2 \, dA_o \quad 1.2$$

F_n is the net thrust in the upstream direction created by the internal flow within the stream tubes extending both upstream and downstream of the body.

1.3.2 Intrinsic Thrust:

To define the thrust produced within the body, reference stations are taken at the entry (station 1) and the exit (station 2). Consideration of the momentum theorem permits equating the rate of change of momentum to the sum of the pressure and friction forces acting on the fluid at the boundaries. Referencing pressures to ambient,

$$\int [(P_{s_{int}} - P_a) \sin \lambda - F \cos \lambda] ds = \int \rho_2 V_2^2 \cos^2 \lambda_2 dA_2 + \int (P_{s_2} - P_a) dA_2 - \int \rho_1 V_1^2 \cos^2 \lambda_1 dA_1 - \int (P_{s_1} - P_a) dA_1 \quad 1.3$$

where

- $P_{s_{int}}$ = internal static pressure
- F = local friction force per unit area
- ds = element of area of internal surface

The left-hand side of the equation represents the force in the free-stream direction exerted on the fluid by the internal surface of the duct. This force is equal to the rate of change of total momentum appearing on the right-hand side of the equation which is equivalent to a force in the free-stream direction exerted by the fluid on the internal surface of the duct. This latter quantity is defined as the intrinsic thrust.

$$F_{int} = \int (\rho_2 V_2^2 \cos^2 \lambda_2 + P_{s_2} - P_a) dA_2 - \int (\rho_1 V_1^2 \cos^2 \lambda_1 + P_{s_1} - P_a) dA_1 \quad 1.4$$

1.3.3 Pre-Entry Thrust and Ram Drag:

A similar analysis can be made of the pre-entry stream tube. To add physical meaning, the diverging portion of the stream tube can be considered as replaced by a thin frictionless membrane. Since the flow field is unchanged, the thrust will not be affected. With reference stations 0 and 1, the force exerted by the fluid due to pressure acting on the interior of the stream tube becomes

$$\int (P_{s_{ext}} - P_a) \sin \lambda \, ds \quad 1.5$$

which is commonly known as additive drag.

where

$$P_{s_{ext}} = \text{external static pressure}$$

As before this force may be set equal to

$$\int (\rho_1 V_1^2 \cos^2 \lambda_1 + P_{s_1} - P_a) \, dA_1 - \int \rho_0 V_0^2 \, dA_0 \quad 1.6$$

which is defined as pre-entry thrust. Since V_0 is uniform, $m_1 = \rho_0 V_0 A_0$ and $\cos \lambda_0 = 1$, the pre-entry thrust is

$$F_{pre} = (\rho_1 V_1^2 \cos^2 \lambda_1 + P_{s_1} - P_a) dA_1 - m_1 V_0 \quad 1.7$$

The term $m_1 V_0$ in the preceding equation is the ram drag, (F_e).

$$F_e = m_1 V_0 \quad 1.8$$

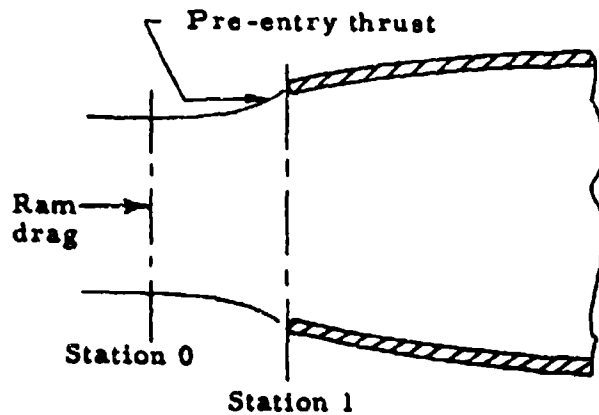


Figure 1.2
Schematic Representation of Inlet Forces on a Normal Shock Inlet

1.3.4 Post-Exit Thrust:

Similarly, reference stations 2 and W may be chosen, and a thrust derived which is defined as the post-exit thrust.

$$F_{\text{post}} = \int \rho_w V_w^2 dA_w - \int (\rho_2 V_2^2 \cos^2 \lambda_2 + P_{s2} - P_a) dA_2 \quad 1.9$$

1.3.5 Standard Net Thrust:

Since net thrust is defined considering flow between stations 0 and W, the net thrust is equal to the sum of the pre-entry thrust, intrinsic thrust and post-exit thrust.

$$F_n = F_{\text{pre}} + F_{\text{int}} + F_{\text{post}} \quad 1.10$$

While the fundamental definition of thrust has been based on the flow between stations 0 and W, the calculation of post-exit thrust cannot be made precisely because of mixing of internal and external flows downstream of the exit. If the pressure surrounding the post-exit stream tube is assumed equal to ambient, the post-exit contribution to thrust becomes zero. This assumption is made to define standard net thrust which is presented in engine specifications by the engine manufacturers.

$$F_{\text{net'd}} = F_{\text{pre}} + F_{\text{int}} = \int (\rho_2 v_2^2 \cos^2 \lambda_2 + P_{s2} - P_a) dA_2 - m_1 V_0 \quad 1.11$$

Practical application of the definitions which have been derived in this section is treated in detail in Section 6.

SECTION 2

TURBOJET ENGINE PERFORMANCE PARAMETERS

2.1 INTRODUCTION

The number of variables which affect the performance of a turbojet engine is quite large. Fortunately its operation is such that the turbojet engine may be submitted to an extensive analytical treatment. Performance characteristics are put in a conveniently usable form by grouping these many dimensional variables into non-dimensional similarity parameters. Advantages of using these non-dimensional parameters are:

1. Better control of these parameters is achieved than can be obtained with the original variables.
2. There are fewer parameters than there were variables so that they can be presented and understood more readily.
3. Fewer test points are required to present the complete performance capabilities of an engine throughout its operating range.

Dimensionless parameters can be determined by the dimensional analysis methods outlined in the following paragraphs. It is emphasized that there are many sets of independent dimensionless parameters which can be formed from a given set of independent variables, and judgment must be exercised in selecting parameters which have the proper significance.

2.2 APPLICATION OF DIMENSIONAL ANALYSIS

The traditional method of applying dimensional analysis is by means of the Buckingham π Theorem. From this theorem it is learned that if in a given problem there are n independent variables (dimensional) and k basic dimensions, (e. g., length, time and mass), then there only $(n - k)$ truly independent non-dimensional (similarity) parameters associated with the problem. Buckingham gives these non-dimensional parameters the symbolic notation $\pi_1, \pi_2, \dots, \pi_{n-k}$.

A method for determining the form of these parameters is described below.

Each of the parameters determined by dimensional analysis will be composed of the product of variables raised to some power. The determination of these exponents is the central problem of dimensional analysis. One variable in each parameter can be chosen arbitrarily to be raised to the first power. As a matter of convenience these first power terms are made those of primary interest (e.g., drag, lift, fuel flow, etc.). Symbolically, the pi-parameters are written

$$\pi_1 = (V_1^{a_1}, V_2^{a_2}, \dots V_k^{a_k}) V_{k+1}$$

$$\pi_2 = (V_1^{\beta_1}, V_2^{\beta_2}, \dots V_k^{\beta_k}) V_{k+2}$$

$$\pi_n = (V_1^{\xi_1}, V_2^{\xi_2}, \dots V_k^{\xi_k}) V_{k+n}$$

where

$\pi_1 \dots \pi_n$ are the dimensionless parameters

$V_{k+1} \dots V_{k+n}$ are the variables of primary interest

$a_i, \beta_i, \dots, \xi_i$ are the exponents to be determined

The exponents are obtained by replacing the variables with their fundamental dimensions of mass, M, length, L, and time, T.

$$[\pi_1] = [M^{a_1} L^{b_1} T^{c_1}]^{a_1} [M^{a_2} L^{b_2} T^{c_2}]^{a_2} [M^{a_3} L^{b_3} T^{c_3}]^{a_3} [M^{a_4} L^{b_4} T^{c_4}]$$

a_i, b_i, c_i are known numbers, for example,

$$[\text{Velocity}] = [M^0 L^1 T^{-1}]$$

The variables are combined into terms having the dimensions

$[M^0 L^0 T^0]$ so we may write

$$[\pi] = M^0 L^0 T^0 = 1 = M^{a_1} L^{b_1} T^{c_1} + M^{a_2} L^{b_2} T^{c_2} + M^{a_3} L^{b_3} T^{c_3} + M^{a_4} L^{b_4} T^{c_4}$$

Now equating exponents of like terms

$$\text{for } M \quad a_1 + a_2 + a_3 + a_4 = 0$$

$$\text{for } L \quad b_1 + b_2 + b_3 + b_4 = 0$$

$$\text{for } T \quad c_1 + c_2 + c_3 + c_4 = 0$$

These are three simultaneous equations which can be used to determine the three unknowns, a_1 , a_2 , and a_3 .

If the factors affecting the performance of a turbojet engine are divided into dependent and independent variables, we may list them as in the following table:

<u>Dependent Variable</u>	<u>Units</u>	<u>Dimensions</u>
airflow, w_a	lb(mass)/sec	$M T^{-1}$
fuel flow, w_f	ft lb/sec	$ML^2 T^{-3}$
exhaust gas temperature, T_{t5}	$^{\circ}K$	$L^2 T^{-2}$
thrust, F_g or F_n	lb	MLT^{-2}
<u>Independent Variable</u>	<u>Units</u>	<u>Dimensions</u>
inlet total pressure, P_{t2}	lb/ft ²	$ML^{-1} T^{-2}$
inlet total temperature, T_{t2}	$^{\circ}K$	$L^2 T^{-2}$
engine speed, N	rad/sec	T^{-1}
free-stream static pressure, P_a	lb/ft ²	$ML^{-1} T^{-2}$
nozzle area, A_g	ft ²	L^2
flight speed, V	ft/sec	LT^{-1}

NOTE: Units are those most convenient for dimensional analysis and do not necessarily conform to those in other sections. Temperatures are considered a measure of enthalpy and fuel flow as energy input. Temperatures, pressures and area were selected at stations, (Reference Figure 2.1), to give the most useful results. Values at other stations might be used without invalidating the results.

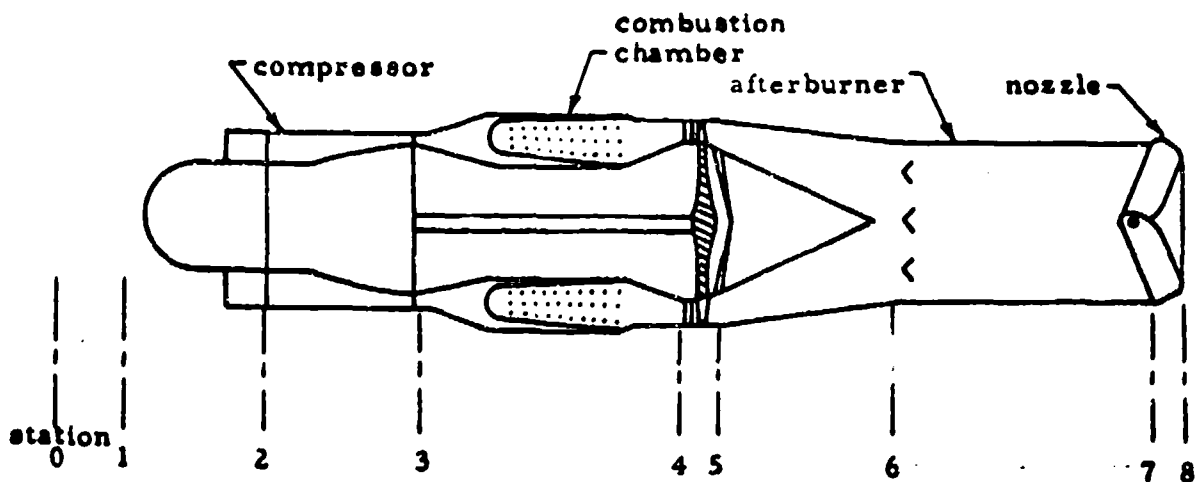


Figure 2.1

Turbojet Engine Station Designations

The above station designations are generally used as subscripts:

- | | |
|---|-------------------|
| 0 | free stream |
| 1 | inlet duct |
| 2 | compressor inlet |
| 3 | compressor outlet |
| 4 | turbine inlet |
| 5 | turbine outlet |

- 6 tailpipe inlet
- 7 tailpipe outlet
- 8 jet nozzle outlet

As an example of the application of dimensional analysis, consider thrust as a function of the independent variables taken from the preceding table.

$$F_g = f(P_{t2}, T_{t2}, N, P_a, A_8)$$

Since there are six variables and three fundamental units, we can determine three pi-parameters, which can be expressed in an equation made up of three dimensionless numbers.

$$\pi_1 = P_{t2}, T_{t2}, A_8, F_g$$

$$\pi_2 = P_{t2}, T_{t2}, A_8, N$$

$$\pi_3 = P_{t2}, T_{t2}, A_8, P_a$$

Substituting their dimensions in place of the variables,

$$[\pi_1] = [ML^{-1}T^{-2}]^{a_1} [L^2T^{-2}]^{a_2} [L^2]^{a_3} [MLT^{-2}]$$

$$[\pi_2] = [ML^{-1}T^{-2}]^{a_1} [L^2T^{-2}]^{a_2} [L^2]^{a_3} [T^{-1}]$$

$$[\pi_3] = [ML^{-1}T^{-2}]^{a_1} [L^2T^{-2}]^{a_2} [L^2]^{a_3} [ML^{-1}T^{-2}]$$

After solving for exponents we have,

$$\pi_1 = \frac{F_g}{A_8 P_{t2}}$$

$$\pi_2 = \frac{N \sqrt{A_0}}{T_{t2}}$$

$$\pi_3 = \frac{P_a}{P_{t2}}$$

Therefore,

$$\frac{F_a}{A_0 P_{t2}} = f \left(\frac{N \sqrt{A_0}}{\sqrt{T_{t2}}}, \frac{P_a}{P_{t2}} \right)$$

Eliminating the area (A_0) for an engine of constant size and inverting π_3 to form ram pressure ratio,

$$\frac{F_a}{P_{t2}} = f \left(\frac{N}{\sqrt{T_{t2}}}, \frac{P_{t2}}{P_a} \right)$$

It is conventional to refer temperatures and pressures to standard sea level conditions by making the following substitutions,

$$\delta_{t2} \left(\frac{P_{t2}}{P_{aSL}} \right) \text{ for } P_{t2}$$

and

$$\theta_{t2} \left(\frac{T_{t2}}{T_{aSL}} \right) \text{ for } T_{t2}$$

we have,

$$\frac{F_a}{\delta_{t2}} = f \left(\frac{N}{\sqrt{\theta_{t2}}}, \frac{P_{t2}}{P_a} \right)$$

By similar analysis the following relationships can be developed.

$$\frac{w_a \sqrt{\theta_{t2}}}{\delta_{t2}} = f \left(\frac{N}{\sqrt{\theta_{t2}}}, \frac{P_{t2}}{P_a} \right)$$

$$\frac{w_f}{\delta_{t2} \sqrt{\theta_{t2}}} = f \left(\frac{N}{\sqrt{\theta_{t2}}}, \frac{P_{t2}}{P_a} \right)$$

$$\frac{T_{t5}}{\theta_{t2}} = f \left(\frac{N}{\sqrt{\theta_{t2}}}, \frac{P_{t2}}{P_a} \right)$$

These equations remain valid with the addition or deletion of constants although the parameters are no longer dimensionless.

Thus far, we have considered only the independent variables which have a primary effect on performance. Other factors, such as viscous effects, combustion efficiency, and the ratio of specific heats have secondary effects on performance particularly at high altitudes and high Mach numbers. It is pointed out that engine manufacturers frequently publish correction curves to be used in conjunction with non-dimensional performance plots which account for these secondary effects.

SECTION 3
AIR INDUCTION SYSTEM PERFORMANCE

3.1 GENERAL COMMENTS

Performance curves for an engine installed in an aircraft are usually presented in terms of conditions existing at the compressor face, i. e., T_{t2}/T_{t0} and P_{t2}/P_{t0} . Adiabatic flow is assumed so that $T_{t2} = T_{t0}$ which can be calculated from the free-stream Mach number and ambient temperatures. In order to determine P_{t2} it is necessary to evaluate the total pressure losses between the free-stream, station "0", and the compressor face, station "2". When these losses are evaluated, the engine performance curves may be obtained in terms of aircraft speed, altitude and free-air temperature.

Air-inlet efficiency is generally expressed in terms of the pressure recovery, P_{t2}/P_{t0} , because it can be shown by a simplified analysis of the turbojet engine that this parameter is directly related to both the net thrust and fuel consumption. For example,

$$\frac{F_{n1} - F_{n2}}{F_{n1}} = L \left(1 - \frac{P_{t2}}{P_{t0}} \right) \quad 3.1$$

where

- F_{n1} = ideal net thrust, ($P_{t2}/P_{t0} = 1.0$)
- F_{n2} = actual net thrust
- P_{t0} = free-stream total pressure
- P_{t2} = total pressure at compressor face
- L = a function of jet efficiency, nozzle exit conditions

L is always greater than 1.0 and is determined by engine design and flight conditions. If the thrust loss is determined for an engine, values of the parameter $(\Delta F_n/F_{n1})/(\Delta P_{t2}/P_{t0})$ are usually between 1.2 and 1.8. Hence, a 1 percent loss in pressure recovery may result in a 1.8 percent loss in net thrust.

The parameter ram efficiency, η , is sometimes used to indicate duct losses.

$$\eta = \frac{P_{t2} - P_a}{P_{t0} - P_a} \quad 3.2$$

where P_a is free-stream static pressure.

Experience has proven that η is a useful parameter for expressing the inlet losses in subsonic flow. A conversion between ram efficiency, η , and total pressure recovery, P_{t2}/P_{t0} , can be expressed as

$$\frac{P_{t2}}{P_{t0}} = \frac{1 + \eta \left[\left(1 + \frac{\gamma - 1}{2} M_0^2 \right)^{\frac{\gamma}{\gamma - 1}} - 1 \right]}{\left(1 + \frac{\gamma - 1}{2} M_0^2 \right)^{\frac{\gamma}{\gamma - 1}}} \quad 3.3$$

If $\gamma = 1.4$ and $B = 1 + \frac{\gamma - 1}{2} M^2$ this becomes

$$\frac{P_{t2}}{P_{t0}} = \frac{1 + \eta (B_0^{3.5} - 1)}{B_0^{3.5}} \quad 3.4$$

This expression is plotted in Chart 9.1.

In the discussion which follows, some of the factors which affect inlet efficiency and approximate methods for estimating the inlet total pressure losses (providing experimental data are not available) are discussed.

3.2 SUBSONIC FLIGHT

Inlet total pressure losses which occur during take-off (or static run-up) and at subsonic flight speeds may be conveniently considered as (a) inlet-entry losses and (b) subsonic-diffuser losses.

3.2.1 Inlet Entry Losses:

Entry losses occur mainly from flow separation at the inlet lips or from the ingestion of boundary-layer flow in the inlet. Inlet total-pressure losses caused by flow interference from aircraft components other than the air induction system are small at subsonic speeds and are usually neglected. Lip losses are important for those conditions where the local stagnation-point streamline occurs outside of the inlet lip (i. e., angle of attack operation with sharp lipped inlets, or for mass flow ratios greater than 1.0 as illustrated in Figure 3.1c).

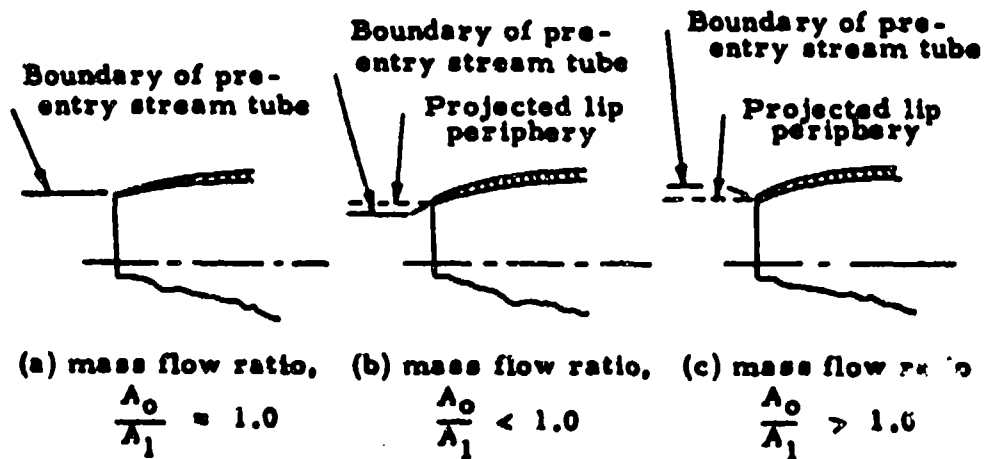


Figure 3.1

Schematic Representation of Mass Flow Ratio

For low speeds and large mass flow ratios, lip separation occurs and a vena contracta is formed within the inlet giving rise to relatively high total pressure losses. Since aircraft designed for supersonic flight generally have sharp inlet lips, the separation condition is aggravated and these aircraft suffer large total pressure losses during static run-up and take-off. The curves in Chart 9.2 give the average pressure recovery, $(P_{t1}/P_{t0})_{LIP}$, for a number of model and full scale inlets at zero and low forward speeds. In order to increase these poor low-speed pressure recoveries and provide an adequate air supply for the engine, some aircraft designed for high-speed flight have auxiliary inlets or "blow in" doors. These auxiliary inlets reduce the operating mass flow of the main inlet and improve the overall pressure recovery.

Boundary-layer flow may enter the inlet for a side inlet installation and give rise to a loss in pressure recovery over a portion of the inlet area because of the local velocity profile. If experimental data is not available on losses due to the boundary-layer effects, an estimate of these losses may be made from the following considerations.

For most installations the entering boundary layer is considered to be turbulent. Boundary-layer thickness, δ , may be estimated for $\alpha = 0$ degrees by use of Chart 9.3*. Angle of attack effects on boundary-layer thickness may be estimated from the following equation for small angles of attack:

$$\delta_{\alpha} = \delta_0 \left(\frac{\delta_{\alpha} - \delta_0}{\delta_0} \right) + \delta_0 \quad 3.5$$

where δ_0 = boundary-layer thickness at $\alpha = 0$

and δ_{α} = boundary-layer thickness at angle of attack of α

*If the inlet is located on the nose portion of the fuselage (i. e., in a flow field more conical in nature than two-dimensional) these boundary-layer thicknesses should be modified by the Mangler transformation factor $1/\sqrt{3}$. For example,

$$\delta_{\text{conical}} = \frac{1}{\sqrt{3}} \delta_{\text{flat plate}}$$

It should be noted that equation 3.5 is applicable only for underlung inlet locations and should be used with caution for other circumferential locations because considerable error may result. (This is especially true at supersonic speeds as will be pointed out later.)

Most side-inlet installations have a boundary-layer diverter, or scoop, such as that schematically shown below.

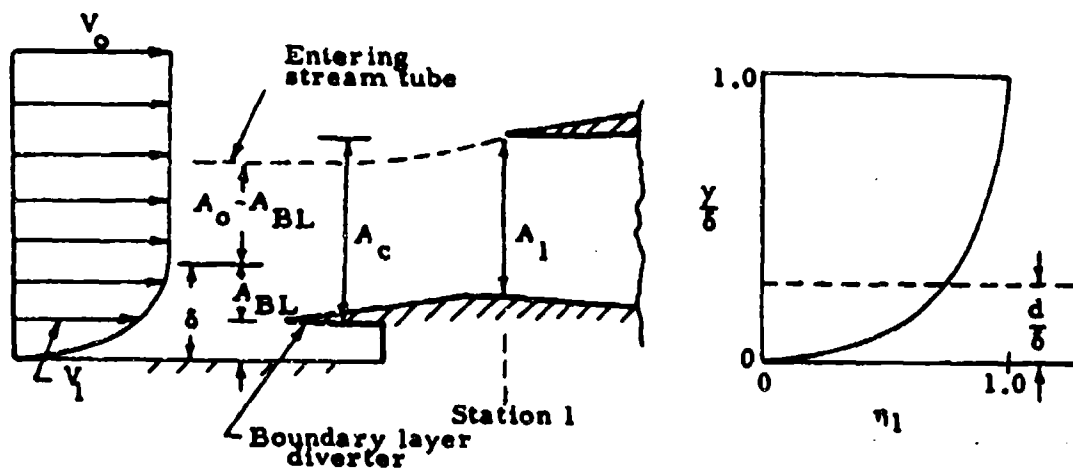


Figure 3.2

Boundary Layer in Side-inlet Installation

The effects of boundary-layer profile on the inlet losses may be calculated in the absence of shock wave boundary-layer interaction for this type of installation with the aid of Chart 9.4* and the following equation for the average value of pressure recovery.

*Note that for most cases a turbulent boundary layer is assumed and it is sufficiently accurate to use a $1/7$ power velocity profile approximation.

$$\left(\frac{P_t}{P_{t_0}} \right)_{\text{avg}} = \frac{P_{t1}}{P_{t_0}} \left]_{d/\delta}^{1.0} \frac{A_{BL}}{A_0} + \frac{P_{t1}}{P_{t_0}} \frac{A_0 - A_{BL}}{A_0} \quad 3.6$$

where $\frac{P_{t1}}{P_{t_0}} \left]_{d/\delta}^{1.0}$ denotes the average pressure recovery of that

part of the boundary layer which is ingested into the duct. (Note that if $d/\delta \geq 1.0$ no correction is required and $A_{BL} = 0$.) In many cases P_{t1}/P_{t_0} is approximately 1.0; however, this term must be evaluated at the same station at which the reference area A_0 is taken. (Reference Figure 3.2.)

3.2.2 Internal Boundary-Layer Removal Systems:

An aircraft inlet designed for high-speed flight may have an internal boundary-layer removal system. Losses are incurred in the use of such a system, whether a ram scoop or suction through slots or perforations. The boundary-layer removal system losses are usually so large that a complete loss in free-stream momentum is usually assumed for the mass flow through the removal system. For example,

$$D_{BL} = m_{BL} V_0 \quad 3.7$$

where

D_{BL} = boundary-layer removal system drag

m_{BL} = boundary-layer removal system mass flow

If the manufacturer does not specify the mass flow, the loss with a ram scoop may be estimated as follows with the aid of Chart 9.5. (Note that a $1/7$ power velocity profile assumption is adequate for this estimate.) Since the drag, D_{BL} , is the change in momentum of the airflow in the direction of flow then,

$$\begin{aligned}
 \text{DBL} &= \phi_0 - \phi_1 \\
 &= \left(1 - \frac{\phi_1}{\phi_0}\right)
 \end{aligned}
 \tag{3.8}$$

where the momentum ratio, ϕ_1/ϕ_0 , may be obtained from Chart 9.5 and ϕ_0 from the following relation.

$$\phi_0 = \gamma P_2 M_0^2 A_{BL}
 \tag{3.9}$$

3.2.3 Subsonic Diffuser Losses:

Subsonic diffuser losses are concerned with those losses within the inlet between stations 1 and 2. Factors which contribute to these losses are skin friction, duct expansion and duct bends or offsets. Total pressure losses resulting from friction and duct expansion can be calculated if one-dimensional compressible flow and no change in skin friction coefficient with length are assumed. The results of such a calculation are shown in Chart 9.6 where the skin friction coefficient C_f is usually estimated with sufficient accuracy from Von Karman's approximate formula for turbulent flow.

$$C_f = \frac{.074}{(R_e)^{1/5}}
 \tag{3.10}$$

R_e = Reynolds number based on average flow properties in the duct and the duct length.

Values of the parameter $\left(\frac{1}{d_2} \times \frac{C_f}{.003}\right)$ between those given in Chart 9.6 can be obtained with sufficient accuracy by linear interpolation. Here d_2 is the hydraulic diameter of the duct at the compressor-face station. Total pressure losses due to compound duct bends may be estimated with sufficient accuracy by use of Chart 9.7. In this figure the loss coefficient, K_B , is related to the duct total

pressure loss through the following relation.

$$\frac{P_{t2}}{P_{t1}} = 1 - K_B \left(1 - \frac{1}{B_1^{3.5}} \right) \quad 3.11$$

where

$$B_1 = 1 + \frac{\gamma - 1}{2} M_1^2$$

Even though Chart 9.7 is plotted for 90-degree bends the loss coefficients for bends other than 90 degrees may be obtained by simple interpolation, (e. g., for 45-degree bends the loss coefficient is reduced by about $\sqrt{2}$). All bends must be generously radiused, however, so that boundary-layer separation does not occur.

The total pressure losses for the entire inlet in subsonic flow may now be expressed as follows:

$$\frac{P_{t2}}{P_{t0}} = \frac{P_{t1}}{P_{t0}} \times \frac{P_{t2}}{P_{t1}} \quad 3.12$$

where

$$\frac{P_{t1}}{P_{t0}} = 1 - \left[\left(1 - \frac{P_{t1}}{P_{t0}} \right)_{BL} + \left(1 - \frac{P_{t1}}{P_{t0}} \right)_{LIP} \right] \quad 3.13$$

$$\frac{P_{t2}}{P_{t1}} = 1 - \left[\left(1 - \frac{P_{t2}}{P_{t1}} \right)_{friction} + \left(1 - \frac{P_{t2}}{P_{t1}} \right)_{bends} \right] \quad 3.14$$

3.3 SUPERSONIC FLIGHT

Inlet total pressure losses which occur during supersonic flight may be calculated from a consideration of the pressure losses associated with the following:

1. Supersonic compression.
2. Entering stream-tube flow non-uniformities (i. e., boundary-layer flow, aircraft attitude effects, interferences effects, etc)

and unsteadiness.

3. Subsonic diffuser design.

The overall performance of the inlet may then be calculated in exactly the same manner as that given in equations 3.12 through 3.14 provided that all total pressure loss factors are included.

3.3.1 Supersonic Compression:

Total pressure losses due to supersonic compression may be calculated from the geometry of the inlet and free-stream Mach number. Theoretical pressure recoveries of normal shock, two-shock and three-shock external compression inlets are illustrated in Figure 3.3.

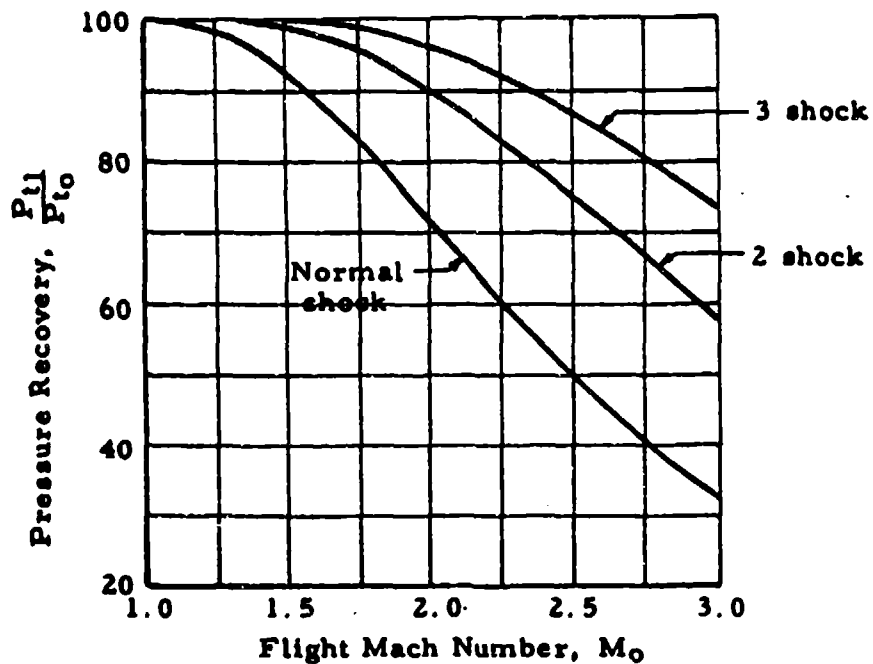


Figure 3.3
Maximum Pressure Recovery, All External Compression

From this figure it may be seen that even the relatively simple two-shock external compression inlet exhibits considerable pressure advantage over the normal shock inlet at Mach numbers over about 1.5. At Mach 2.0, for example, the two-shock inlet operates with a 20 percent improvement in pressure recovery. This may result in approximately 40 percent more thrust for a two-shock inlet than for one using a normal shock inlet. At Mach numbers much above 2.0 even the two-shock inlet yields excessive pressure losses and the more complicated flow geometries appear advantageous. For open nose inlets the total pressure ratio, P_{t1}/P_{t0} , may be obtained directly from the free-stream Mach number and the normal shock pressure ratio given on Chart 9.8. Pressure ratios obtained with other types of inlets are shown in Charts 9.9 through 9.11.

An additional loss arises from the momentum change in the inlet stream-tube between the free-stream and the inlet face when no aircraft components other than those of the air induction system interfere with the stream-tube. This momentum loss occurs at mass flow ratios less than one and is commonly called "pre-entry thrust" or "additive drag". As defined in Section 1, pre-entry thrust is the axial component of the pressure force on the diverging portion of the entering stream-tube between station 0 and station 1.

Expressions for the calculations of additive drag have been developed in coefficient form, ($C_{da} = D_a/q_0A_c$). For open nose inlets,

$$C_{da} = \frac{2}{M_0^2} \left[\frac{B_0^{3.5}}{B_1^{3.5}} \frac{P_{t1}}{P_{t0}} (\gamma M_1^2 + 1) - 1 - \frac{A_0}{A_1} \gamma M_0^2 \right] \quad 3.15$$

For external compression inlets,

$$C_{da} = \frac{2}{\gamma M_0^2} \left[\frac{A_1}{A_c} \frac{B_0^{3.5}}{B_1^{3.5}} \frac{P_{t1}}{P_{t0}} (\gamma M_1^2 + 1) \cos \lambda \right. \\ \left. + \frac{A_r}{A_c} \frac{P_r}{P_{s0}} - 1 - \frac{A_0}{A_c} \gamma M_0^2 \right] + C_f \frac{A_r}{A_c} \quad 3.16$$

where

- C_{da} = additive drag coefficient
- q_0 = free-stream dynamic pressure
- A_c = inlet capture area
- A_r = ramp or other compression surface area
- P_r = effective static pressure on compression surface forward of station 1

The results obtained from these equations are plotted in Charts 9.14 and 9.15. Also shown in Chart 9.15 is the variation of cowl position parameter (angle between axis of inlet and straight line connecting tip of center body with lip of cowl), σ_2 , with mass flow. This parameter is useful for the determination of the maximum mass-flow ratio obtainable through a given conical inlet for a particular test condition.

Variations in inlet drag resulting from changes in mass flow through the inlet will cause changes in the cowl-lip suction force as well as additive drag. At subsonic speeds these two forces cancel each other and no calculation for either is necessary. However, at speeds just above sonic both forces must be calculated for an accurate determination of inlet net drag. At Mach numbers over about 2.0 additive drag becomes the dominating factor and lip suction forces are small (usually negligible) for slender, sharp-lipped inlets*. For

*Slender sharp-lipped inlets are defined as inlets with cowl angles less than 5 degrees and by thickness with the ratio lip thickness/inlet radius less than about 0.07.

nose inlet installations Chart 9.16 may be used for estimating lip suction effects at mass ratios greater than about 0.8. Included in this figure is the corresponding increase in additive drag coefficient to illustrate the relative magnitude of the two forces. For blunt-lipped installations and large cowl angles, experimental results are required to determine lip suction effects.

3.3.2 Flow Non-Uniformities and Unsteadiness Effects:

The major total pressure losses resulting from flow non-uniformity of the inlet face are caused by an entering boundary layer. These total pressure losses may be treated in the same manner discussed previously for subsonic flight; however, the correction for angle of attack effects on boundary-layer thickness must be obtained from experimental data for inlet locations other than the underslung type. This is necessary because experimental results have shown as much as 15 to 20 percent loss in P_{t2}/P_{t0} with variations in circumferential position of the inlet and angles of attack as low as 4 to 6 degrees.

Excessive airflow distortion at the compressor face may result from operation at "off-design" conditions. Inlet performance may be degraded from Mach number and altitude effects as well as from subcritical or supercritical operation. If shock wave boundary-layer separation occurs this condition may be considerably aggravated. With supercritical operation as shown in Figure 3.4C the pressure drop across the normal shock is increased and a lower pressure recovery results. Subcritical flow as in Figure 3.4A is accompanied by a reduction in mass-flow ratio with a consequent increase in additive drag. If the reduction in mass flow ratio is too great, "inlet buzz", discussed in the following paragraph, will occur.

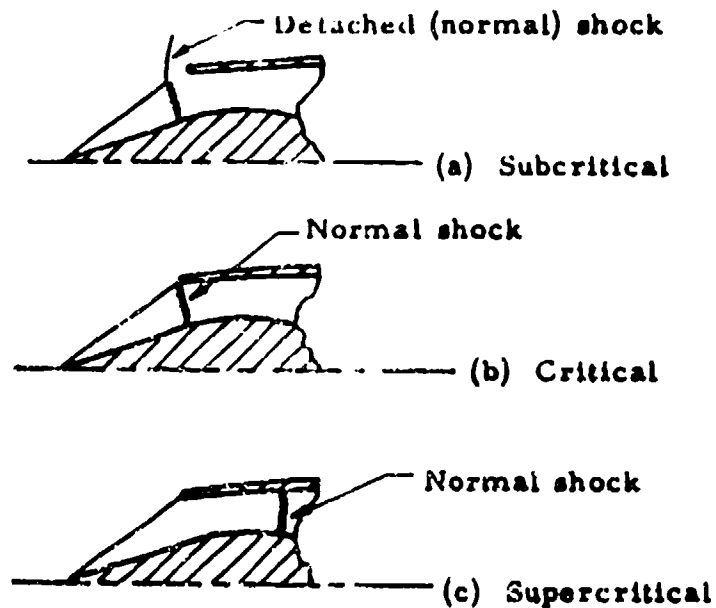


Figure 3.4
Operational Modes of Supersonic External Compression Inlets

Large variations in flow uniformity will give rise to thrust loss, excessive fuel consumption, loss of acceleration margin, hot spots, local blade stalling (rotating compressor stall) and engine vibration with possible structural failure.

Inlet operation at subcritical mass-flow ratios may result in an unsteady flow condition commonly called "inlet buzz". This operation is characterized by rapid changes in the inlet flow pattern which results in rapid fluctuations in in drag as well as total pressure

ratio. Severely reduced engine performance results and for some buzz conditions compressor stall, flame-out, or structural failure may occur.

Flow non-uniformity may also arise from interference effects of other aircraft components on the inlet stream-tube and these effects must be determined from experimental data because no simple means for estimating the magnitudes of these effects exists for all the diverse combinations of flight attitudes and aircraft geometries.

3.3.3 Subsonic Diffuser Losses:

Subsonic diffuser total pressure losses are calculated in a manner similar to that described in paragraph 3.2.3. The entering flow conditions are taken as those just down-stream of the terminal shock and the length of the subsonic diffuser measured from this point.

SECTION 4

STANDARDIZATION OF TEST DATA WITH ENGINE PARAMETERS

4.1 INTRODUCTION

In the process of standardizing test data obtained under off-standard conditions, it is necessary that corrections be made based on the engine parameters developed in Section 2. For example, rate of climb determined during climb tests may be corrected to standard engine speed and standard temperature through the use of correction curves plotted as F_n/δ_{t_2} versus $N/\sqrt{\theta_a}$. These curves are computed from the engine manufacturer's estimated minimum performance curves, as described in Data Reduction Outline 8.1. (Typical estimated minimum performance curves for an engine with a fixed nozzle are illustrated in Figure 4.1.) This correction and others using non-dimensional parameters are made quite readily for aircraft with simple jet engines but are not generally applicable to more advanced engines. Use of the fuel flow parameter and the exhaust gas temperature parameter for establishing corrections for simple jet engines is described in paragraphs 4.2 and 4.3. Similar corrections for more advanced engines are discussed in paragraph 4.4.

4.2 FUEL FLOW PARAMETER

The engine manufacturer's estimated fuel flow curves are seldom used in flight testing, since flow rates are measured with test instrumentation. The same parameters are used, ($w_f/\sqrt{\theta_{t_2}} \delta_{t_2}$ versus $N/\sqrt{\theta_{t_2}}$), in plotting test fuel flow data, however, as are found in estimated curves furnished by the engine manufacturers. Test fuel flows are corrected to standard conditions using test data plotted in this form.

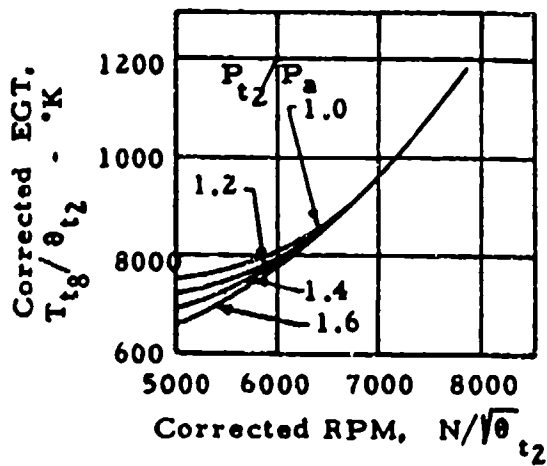
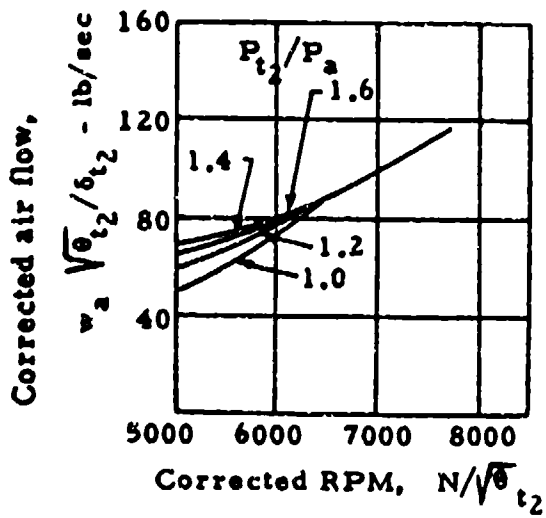
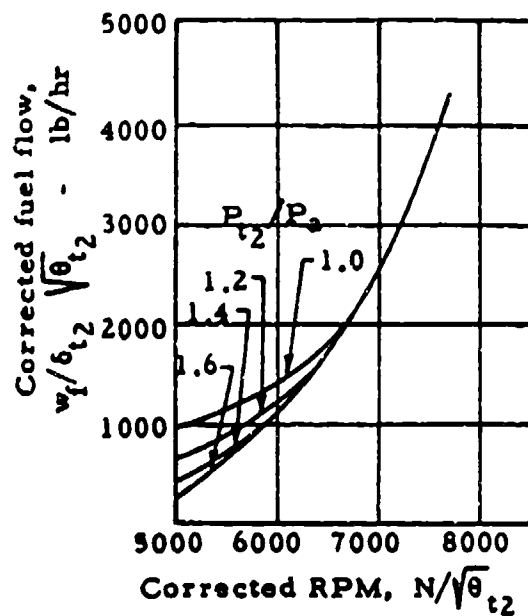
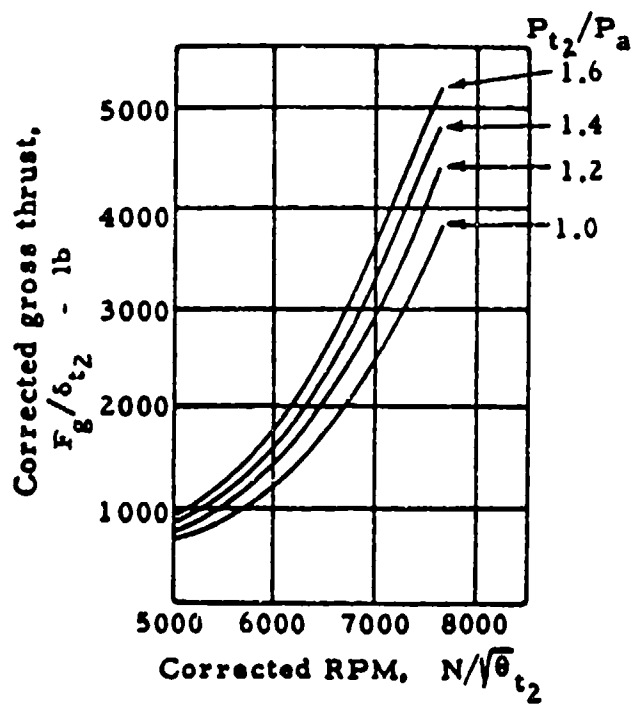


Figure 4.1

Typical Turbojet Engine Characteristics

The effects of changes in specific heat ratio, combustion efficiency, Reynolds number, etc., were neglected, (Reference Section 2), when the dimensionless parameters were developed. Consequently, an exact correlation of test data obtained over a wide range of flight speeds and altitudes cannot be expected. At altitudes up to about 35,000 feet, (depending on the engine design), quite good correlation can be expected. At higher altitudes, however, the neglect of the change in Reynolds number, in particular, becomes increasingly important, and separation from the basic polar occurs as illustrated in Figure 4.2.

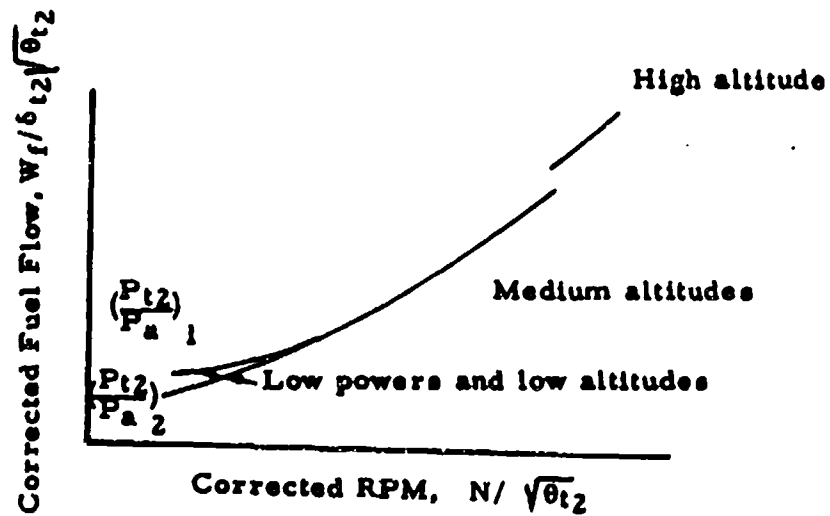


Figure 4.2
Typical Fuel Flow Characteristics

At normal in-flight operating conditions there is no apparent effect from changes in P_{t2}/P_a . At low altitudes with low power settings when flow at the nozzle exit is subcritical, lines of constant P_{t2}/P_a diverge from the basic polar as shown in Figure 4.2.

4.3 EXHAUST GAS TEMPERATURE PARAMETER

Plots of corrected exhaust gas temperature versus corrected rpm from flight test data can be used to apply corrections to exhaust gas temperature and other performance variables. The corrections are necessary when an engine is operated at other than standard exhaust gas temperature. For example, corrections to exhaust gas temperature, thrust and rpm may be made as described in Data Reduction Outline 8.2.

4.4 ADVANCED ENGINES

Many different configurations in nozzles, ejectors, control systems, etc., are in use or will be installed in future aircraft. Because of the variety of configurations which exist and are planned, it is not practical nor possible to describe methods for correcting engine data to standard conditions which are suitable for each type. It frequently is not immediately evident as to when non-dimensional methods are applicable. The characteristics of each of the more complex engines should be studied so that methods may be modified as required for the individual case, and the best means chosen for making corrections to standard conditions.

SECTION 5 AIRFLOW MEASUREMENT

5.1 INTRODUCTION

As was seen in Section 3.1, the thrust of a turbojet engine is dependent on ram drag which requires a knowledge of mass flow through the engine. Three methods of measuring engine airflow in flight have been generally used and are discussed in this Section.

5.2 ENGINE COMPRESSOR AIRFLOW CURVES

Of the three methods for determining airflow, use of engine compressor airflow curves furnished by the engine manufacturers is most common. These curves are generally plotted as

$$\frac{w_a \sqrt{\theta_{t2}}}{\delta_{t2}} \quad \text{vs} \quad \frac{N}{\sqrt{\theta_{t2}}}$$

where $\theta_{t2} = T_{t2}/T_{SL}$ and $\delta_{t2} = P_{t2}/P_{SL}$

Compressor inlet total temperature, T_{t2} , is computed from ambient temperature and free stream Mach number assuming adiabatic flow. Compressor inlet pressure, P_{t2} , is obtained preferably by measurement, but if inlet instrumentation is not installed it can be computed from total free stream pressure and estimated total pressure recovery.

5.3 INLET DUCT METHOD

Airflow can be measured from total temperature and surveys of total and static pressure forward of the compressor face.

From continuity

$$m = \frac{w_a}{g} = \rho VA \quad 5.1$$

where

- m = mass flow, slugs/second
- w_a = weight flow, lb/second
- ρ = density, slugs/ft³
- V = velocity, ft/second
- A = annular area, ft²

ρ , V and A represent values at the station where pressure measurements are taken.

Assuming a perfect gas

$$\rho = \frac{P_s}{gRT_s} \quad 5.2$$

where

- P_s = static pressure, lb/ft²
- R = gas constant, ft-lb/lb °K
- T_s = static temperature, °K

$$V = M \sqrt{g \gamma RT_s} \quad 5.3$$

where

- M = Mach number
- γ = ratio of specific heats

Substituting equations 5.2 and 5.3 in equation 5.1

$$w_a = \frac{P_s A}{RT_s} M \sqrt{g \gamma RT_s}$$

or

$$w_a = P_s A M \sqrt{\frac{\gamma g}{RT_s}} \quad 5.4$$

From the isentropic relation

$$M = \sqrt{\frac{2}{\gamma - 1} \left[\left(\frac{P_t}{P_s} \right)^{\frac{\gamma - 1}{\gamma}} - 1 \right]} \quad 5.5$$

and

$$T_t = T_s \left(1 + \frac{\gamma - 1}{2} M^2\right) \quad 5.6$$

Substituting equations 5.5 and 5.6 in equation 5.4

$$w_a = P_s A \sqrt{\frac{2\gamma}{\gamma - 1} \frac{g}{RT_t} \left[\left(\frac{P_t}{P_s}\right)^{\frac{\gamma - 1}{\gamma}} - 1 \right] \left(\frac{P_t}{P_s}\right)^{\frac{\gamma - 1}{\gamma}}} \quad 5.7$$

Total pressure surveys are commonly made by dividing the duct into equal annular areas with pressure probes located to measure the pressure in each of these areas. Probes should also be located near the wall of the duct to account for boundary-layer effects. Care should be taken to locate the total pressure probes in a straight portion of the duct, and that no struts or other obstructions which would cause pressure gradients are immediately upstream of the probes. Static pressures are measured from either pick-ups located on the total pressure rakes or from wall static taps or a combination of both.

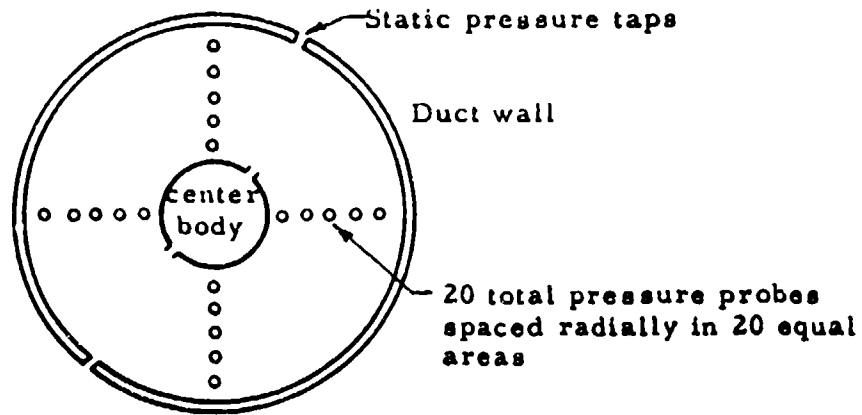


Figure 5.1
Typical Inlet Duct Pressure Instrumentation

5.4 TAILPIPE TEMPERATURE METHOD

Gas flow at the nozzle (which includes both air and fuel) can be calculated using the same basic equations that were used to compute airflow from inlet pressure measurements. Gas flow is frequently expressed as:

$$\frac{w_{g8} \sqrt{T_{t8}}}{P_{s8} A_8} = M_8 \sqrt{\frac{\gamma_8}{R} \left(1 + \frac{\gamma_8 - 1}{2} M_8^2 \right)} \quad 5.8$$

In an ideal converging nozzle the static discharge pressure (P_{s8}) remains constant and equal to the ambient pressure (P_a) until, as the total discharge pressure (P_{t8}) is increased, the maximum obtainable Mach number of one is reached. As P_{t8} is increased further the Mach number remains at one and P_{s8} rises above P_a but the ratio of P_{t8}/P_{s8} remains constant. An exit Mach number less than one is called subcritical and a Mach number of one is called supercritical.

Subcritical

$$P_{t8}/P_{s8} < 1.85$$

$$P_{s8} = P_a$$

$$M_8 < 1.0$$

Supercritical

$$P_{t8}/P_{s8} = 1.85$$

$$P_{s8} > P_a$$

$$M_8 = 1.0$$

Mach number at the exit is:

$$M_8 = \sqrt{\frac{2}{\gamma-1} \left[\left(\frac{P_{t8}}{P_{s8}} \right)^{\frac{\gamma-1}{\gamma}} - 1 \right]} \quad 5.9$$

Substituting equation 5.9 in equation 5.8 and applying standard units, the subcritical flow equation becomes:

$$\frac{w_{g8} \sqrt{T_{t8}}}{P_a A_8} = 116.23 \sqrt{X(1+X)} \quad 5.10$$

where

$$g = 32.174 \text{ ft/sec}^2$$

$$\gamma = 1.33 \text{ (non-afterburning)}$$

$$R = 96.031 \text{ ft/}^\circ\text{K}$$

$$A_8 = \text{ft}^2$$

$$w_{g8} = \text{lb/sec}$$

$$P_{t8}, P_{s8}, P_a = \text{"Hg}$$

$$X = \left(\frac{P_{t8}}{P_{s8}} \right)^{\frac{\gamma-1}{\gamma}} - 1$$

For supercritical flow with $M_8 = 1.0$, equations 5.9 may be written:

$$P_{s8} = P_{t8} \left(\frac{2}{\gamma+1} \right)^{\frac{\gamma}{\gamma-1}} \quad 5.11$$

Substituting equation 5.11 in equation 5.8 with $M = 1.0$,

$$\frac{w_{g8} \sqrt{T_{t8}}}{P_a A_8} = \left(\frac{2}{\gamma+1} \right)^{\frac{\gamma}{\gamma+1}} \sqrt{\frac{2\gamma}{R} \left(1 + \frac{\gamma-1}{2} \right)} \frac{P_{t8}}{P_a} \quad 5.12$$

Assuming $\gamma = 1.33$ for engine operation,

$$\frac{w_{g8} \sqrt{T_{t8}}}{P_a A_8} = 27.54 \frac{P_{t8}}{P_a} \quad 5.13$$

Assuming $\gamma = 1.28$ for afterburner operation,

$$\frac{w_{g8} \sqrt{T_{t8}}}{P_a A_8} = 27.15 \frac{P_{t8}}{P_a} \quad 5.14$$

The ideal gas flow parameter, $w_{g8} \sqrt{T_{t8}}/P_a A_8$, is plotted as a function of P_{t8}/P_a in Charts 9.17 and 9.18.

With a converging-diverging nozzle the gas flow near the nozzle exit where the tailpipe instrumentation is located (as with a swinging rake) becomes supersonic. Since in this case a detached shock stands ahead of the total pressure probe it is necessary to compute Mach number from the Rayleigh supersonic pitot formula.

$$\frac{P_t'}{P_s} = \frac{\left(\frac{\gamma+1}{2} M^2 \right)}{\left(\frac{2\gamma}{\gamma+1} M^2 - \frac{\gamma-1}{\gamma+1} \right)^{\frac{1}{\gamma-1}}} \quad 5.15$$

Use of this equation demands the measurement of static pressure which is quite sensitive to flow alignment. Yaw angles encountered at the nozzle exit are not large enough to cause significant errors in total pressures, but may produce sizeable errors in static pressure measurement (refer to paragraph 6.6.1).

Determination of airflow from tailpipe instrumentation is further complicated by difficulties in measuring exhaust gas temperatures, particularly in afterburning, and is probably the least accurate of the three methods described.

SECTION 6
IN FLIGHT THRUST MEASUREMENT

6.1 INTRODUCTION

Practical applications of measuring the momentum change of the internal flow to obtain in flight thrust of turbojet engines in aircraft will be presented in this section. The thrust produced by a simple jet engine with fixed exhaust nozzle is considered in detail in the following paragraph. More advanced engines with afterburners, ejectors and variable area exhaust nozzles are then considered in succeeding paragraphs.

6.2 FIXED EXHAUST NOZZLE

With subcritical flow it is assumed that the static pressure at the nozzle expands to ambient pressure and gross thrust is defined by the equation.

$$F_g = F_v = \frac{w_{g8}}{g} V_8 \quad 6.1$$

where

w_{g8} = weight flow, lb/sec

V_8 = exit velocity, ft/sec

F_v = velocity thrust, lb

Substituting equations 5.1, 5.2, and 5.3 in equation 6.1 we have,

$$F_g = P_{s8} A_8 \gamma M_8^2 \quad 6.2$$

Substituting equation 5.5

$$F_g = P_{s8} A_8 \frac{2\gamma}{\gamma-1} \left[\left(\frac{P_{t8}}{P_{s8}} \right)^{\frac{\gamma-1}{\gamma}} - 1 \right] \quad 6.3$$

Setting $\left(\frac{P_{t8}}{P_a}\right)^{\frac{\gamma-1}{\gamma}} - 1 = X$ and $P_{s8} = P_a$, we have

$$\frac{F_v}{P_a A_8} = 570.15X \quad 6.4$$

where

P_a = ambient pressure, "Hg

A_8 = nozzle area, ft²

γ = 1.33

Subcritical flow can only be achieved at low power settings at low altitudes. The flow is supercritical for nearly all in-flight conditions where thrust measurement is desired. (i.e., the flow in an ideal converging nozzle is choked and the Mach number at the nozzle exit is unity). In this case P_{s8} rises above P_a and the gross thrust is made up of velocity thrust (F_v) and pressure thrust, (F_p).

$$F_p = A_8 (P_{s8} - P_a) \quad 6.5$$

or

$$F_p = A_8 \left[P_{t8} \left(\frac{2}{\gamma+1}\right)^{\frac{\gamma}{\gamma-1}} - P_a \right] \quad 6.6$$

Adding velocity thrust and pressure thrust the following equation may be written

$$\frac{F_g}{P_a A_8} = \frac{P_{t8}}{P_a} \left(\frac{2}{\gamma+1}\right)^{\frac{\gamma}{\gamma-1}} (\gamma+1) - 1 \quad 6.7$$

substituting constants,

$$\frac{F_g}{P_a A_8} = 70.727 \left(1.259 \frac{P_{t8}}{P_a} - 1\right) \quad 6.8$$

The assumption that $\gamma = 1.33$ is made with a suitable degree of accuracy since the variation in γ with exhaust gas temperature may range from about 1.32 to 1.36, but this variation causes a change in $(2/\gamma+1)^{\gamma/\gamma-1}(\gamma+1)$ of less than 0.5 percent.

The ideal gross thrust parameter, $F_g/P_a A_g$, from equations 6.4 and 6.8 has been plotted as a function of P_{t8}/P_a in Charts 9.19 and 9.20.

The preceding derivations are based on an ideal nozzle assuming isentropic one dimensional flow. This condition is not completely realized, however. A correction factor must be applied to account for deviations from an ideal nozzle as well as losses from wall friction and errors in pressure measurement.

The correction factor for computing thrust (nozzle thrust coefficient) is defined as:

$$C_f = \frac{\left(\frac{F_g}{A_g P_a} \right)_{\text{actual}}}{\left(\frac{F_g}{A_g P_a} \right)_{\text{theoretical}}}$$

where

$F_{g\text{actual}}$ is the mechanically measured thrust

$F_g/A_g P_a$ is the theoretical gross thrust parameter

A is nozzle area, ft^2

P_a is atmospheric pressure, "Hg

Differences in thrust coefficient exist between engine-tailpipe combinations of the same model. Consequently, for most accurate in-flight thrust measurements, a ground static calibration of each installation should be made and repeated if the engine or tailpipe or both are changed. When this is done the nozzle total pressure ratio may be measured satisfactorily with a single probe. Static thrust calibrations may be obtained with the aircraft mounted on a thrust stand or with a

bare engine to which a bellmouth inlet is attached. When installed thrust is determined on a thrust stand, pressure gradients are set up from air entering the inlet duct which may result in pressure forces and give erroneous gross thrust readings. This effect is likely to be most pronounced on high speed aircraft whose inlet total pressure recoveries are quite low at zero forward speed. In a bellmouth inlet pressure drops and consequently pressure forces are minimized.

The maximum pressure ratios obtained during static thrust calibrations are less than those encountered in flight, except with low power settings at low altitudes. Pressure ratios of 2 to 2.5, depending on ambient temperature, are generally found statically while values of 3 to 3.5 are typical for cruise conditions and may be as high as 10 or more at high speeds and altitudes. Consequently, thrust coefficient data obtained during static conditions must be extrapolated to higher nozzle pressure ratios in order to compute thrust in flight. For a simple conical nozzle the value of thrust coefficient is constant at about 0.98 for nozzle pressure ratios greater than about 1.9 as shown in Figure 6.1.

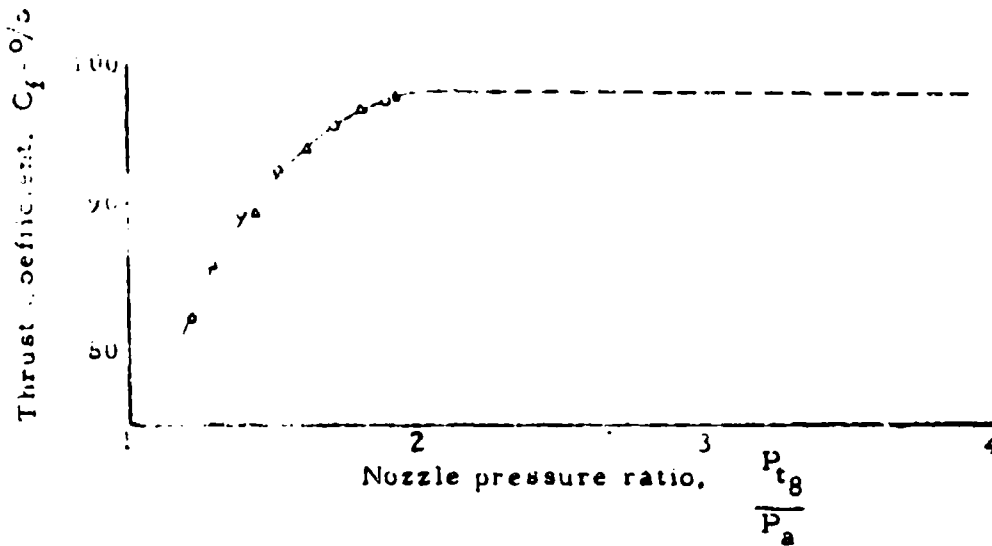


Figure 6.1

Thrust Coefficient for Simple Conical Nozzle

Gross thrust can then be calculated for in-flight values of P_{t8}/P_a using the following equations.

Subcritical

$$F_g = 570.13 P_a A_8 C_f X \quad 6.9$$

Supercritical

$$F_g = 70.727 P_a A_8 C_f \left(1.259 \frac{P_{t8}}{P_a} - 1 \right) \quad 6.10$$

Ram drag has been previously defined as

$$m_1 V_0 = \frac{w_a}{g} V_{\text{aircraft}}$$

where

w_a = inlet airflow, lb/sec

Substituting units the following equation may be written

$$F_e = .0525 w_a V_{tt} \quad 6.11$$

where

V_{tt} = airplane test day true speed, knots

Engine airflow is determined by one of the three methods described in Section 5.

If tailpipe instrumentation is used, the calculated gas flow is generally assumed equal to the inlet airflow. This assumption is normally satisfactory since the fuel added makes up only about 2 percent of the airflow and is approximately the compressor leakage. Also, a gas flow coefficient must be applied to the calculated theoretical gas flow to account for the same deviations from ideal nozzle flow as the nozzle thrust coefficient.

6.3 THRUST AUGMENTATION

Methods of obtaining thrust augmentation which are in general use are afterburning and, to a lesser extent, water injection. Afterburning is considered in this section and water injection in Section 7.

The turbojet engine may have its thrust increased by a substantial amount by burning additional fuel in the turbine exhaust ahead of the exit nozzle. This is possible since the quantity of air passing through the engine is about four times that required for combustion, and the remaining 75 percent is capable of supporting additional combustion if more fuel is added. An afterburner is made up of only four fundamental parts; the afterburner duct, fuel nozzles or spraybars, flame holders, and two-position or variable area exhaust nozzle.

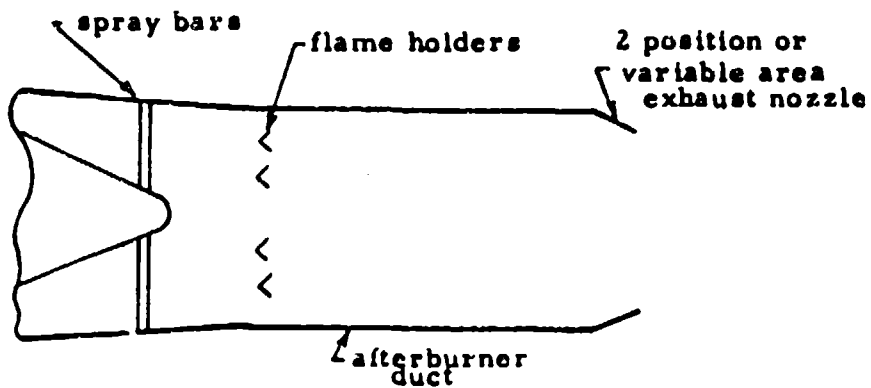


Figure 6.2
Afterburner Components

The thrust of an engine with afterburner may be computed as for a simple jet engine. Thrust coefficient data should be obtained during static thrust calibrations with the afterburner both on and off (reference Figure 6.3).

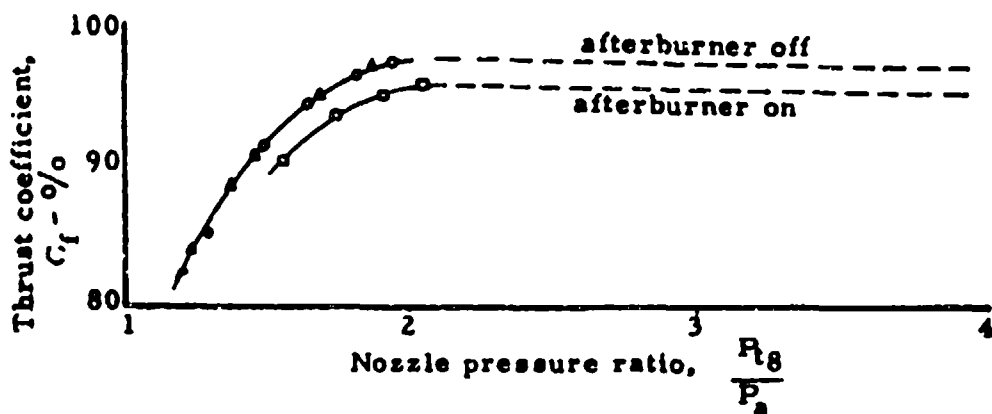


Figure 6.3
Thrust Coefficient for Engine with Afterburner and
Two Position Nozzle

Measurement of nozzle total pressure becomes more difficult with an afterburner-equipped engine because of much higher temperatures at the nozzle. A rake may be mounted across the diameter of the nozzle but since the rake is located in the extremely hot gas stream some method of cooling (such as with compressor bleed air) is essential. Also, such a rake is subject to deterioration from the extreme heat and will probably be rather short lived. When testing bare engines in test chambers, water-cooled rakes mounted at the exhaust nozzle are generally used but have not been found suitable for installation in aircraft.

Another means of determining jet thrust is from turbine outlet pressure, (usually from probes installed by the engine manufacturer). The relationship shown in Figure 6.4 to determine nozzle total pressure, P_{t8} , from turbine outlet total pressure, P_{t5} , may be obtained from engine calibrations in a test chamber. For this relationship to be valid flow at the exhaust nozzle must be choked. P_{t8} is measured with a water-cooled rake. (Losses in total pressure between stations 5 and 8 are incurred largely by friction losses across the flameholder).

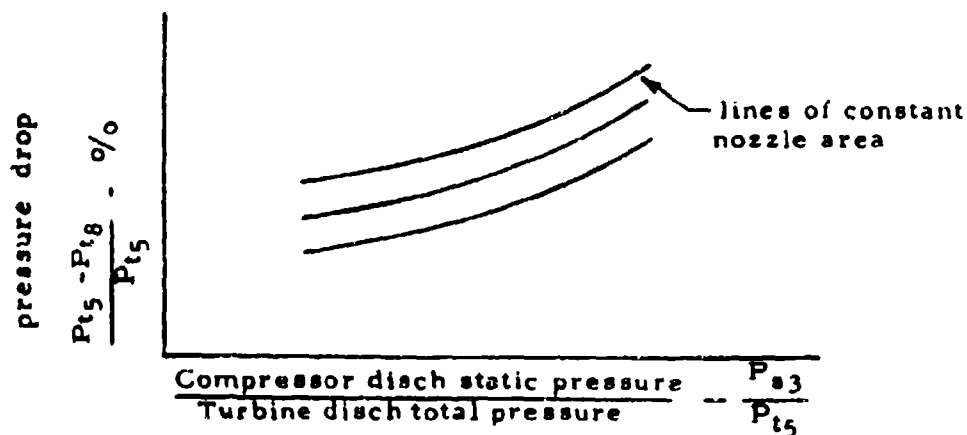


Figure 6.4
Afterburner Pressure Drop

To determine gross thrust from turbine outlet total pressure and curves similar to those in Figure 6.4, equation 6.10 may be modified to:

$$F_g = 70.727A_8C_f \left[1.259P_{t5} \left(1 - \frac{P_{t5} - P_{t8}}{P_{t5}} \right) - P_a \right] \quad 6.11$$

6.4 EJECTOR

An exhaust ejector as illustrated in Figure 6.5 may be used to pump tailpipe cooling air. A properly designed ejector provides adequate cooling with the afterburner operating but does not severely penalize performance at cruise power settings.

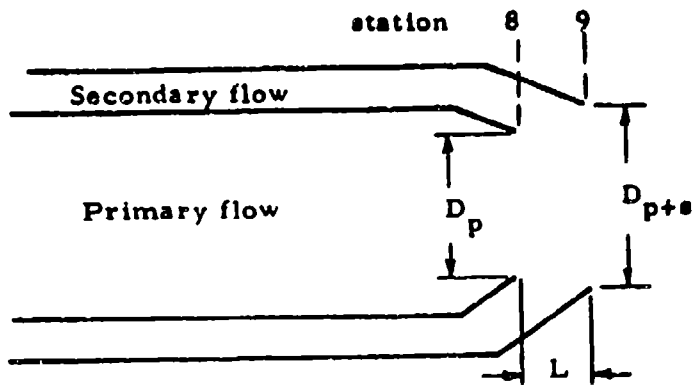


Figure 6.5

Typical Convergent Ejector Installation

Secondary flow originates at an intake in the vicinity of the engine air induction system inlet, or may stem from bleed passages located in the induction system subsonic diffuser. The secondary air then passes through the engine compartment, where it serves as a cooling medium, and is subsequently exhausted through the ejector outlet. In addition to the converging ejector shown in Figure 6.5, either cylindrical or converging-diverging ejectors may be employed. With a properly designed ejector, flow may be made to approach idealized flow through a converging-diverging nozzle, as described in paragraph 6.5.

The geometry of an ejector is critical for obtaining satisfactory ejector performance. The parameters diameter ratio, D_{p+s}/D_p , and spacing ratio, L/D_p , are used to describe ejector geometry. The spacing ratio should not be so large that expansion of the primary flow within the ejector results in impingement on the inner surface of the ejector. Also, the diameter ratio should not be large enough to cause circulation of external air over the shroud trailing edge, with a resulting reduction in secondary flow rate and an increase in base drag. Typical fixed ejector configurations are generally defined by spacing ratios of approximately 0.40 and diameter ratios of approximately 1.20.

The addition of an ejector to an engine installation further complicates the measurement of net thrust. In addition to the measurement of primary thrust, the ram drag and gross thrust of the secondary flow must also be considered.

This thrust contribution may be stated as:

$$F_{nej} = \frac{w_s}{g} V_s + (P_{s8} - P_a) A_s - \int_{sta 9}^{sta 8} (P_w - P_a) dA_w - \frac{w_s}{g} V_t \quad 6.12$$

where

- F_{nej} = ejector net thrust
- w_s = secondary weight flow
- V_s = secondary flow speed

- P_{s8} = static pressure of secondary flow at station 8
 P_a = ambient pressure
 A_s = area of ejector at primary nozzle exit
 P_w = ejector wall static pressure
 A_w = projected ejector area between stations 8 and 9
 V_t = airplane true speed

The velocity thrust (first term on right side of equation 6.12) may be modified using methods similar to those in Section 6, resulting in equation 6.13:

$$F_{nej} = P_{s8} A_s \left(\frac{2\gamma_s}{\gamma_s - 1} \right) \left[\left(\frac{P_{t8}}{P_{s8}} \right)^{\frac{\gamma_s - 1}{\gamma_s}} - 1 \right] + (P_{s8} - P_a) A_s - \int_{sta 9}^{sta 8} (P_w - P_a) dA_w - \frac{w_s}{g} V_t \quad 6.13$$

The secondary passage usually contains nozzle actuators and other equipment so that a uniform velocity profile is not obtained and accurate measurement of secondary total and static pressure is difficult. A high degree of accuracy in total pressure measurement is not required, however, since the secondary velocity thrust is small relative to the primary thrust. A detailed survey of static pressures at station 8 and axially along the ejector shroud is required in some installations. Such installations include those in which over-expansion of the primary jet occurs with a resulting shock wave system within the ejector, and those in which large ejector included angles are encountered. In these instances pressure forces become quite significant. When ejector included angles are small, the projected area A_w may be small enough so that the third term in equation 6.13 may be omitted. With cylindrical ejectors A_w is, of course, zero.

The general equation for determining net thrust for an installation with an ejector is

$$F_n = F_{gp} + P_s A_8 \left(\frac{2 \gamma_s}{\gamma_s - 1} \right) \left[\left(\frac{P_{t8}}{P_{s8}} \right)^{\frac{\gamma_s - 1}{\gamma_s}} - 1 \right] + (P_{s8} - P_a) A_s - \int_{\text{sta 9}}^{\text{sta 8}} (P_w - P_a) dA_w - \frac{W}{g} V_o$$

6.14

The primary gross thrust, F_{gp} , is calculated as described in the preceding paragraph, and the ratio of specific heats in the secondary stream, γ_s , is assumed equal to 1.4.

Instead of the above procedures entailing internal pressure measurements, it may be more desirable to gather data with a swinging rake which samples pressures along a cross section of both the primary and secondary jets. Application of the swinging rake to thrust measurement is treated separately in paragraph 6.6.

6.5 CONVERGING-DIVERGING NOZZLE

A gain in thrust may be realized by replacing the more conventional conical nozzle with a converging-diverging nozzle. The increased engine performance is partially offset, however, by increased weight and is obtained at the expense of added controls and mechanical complication. The diverging portion of the nozzle in operational turbojet engines is formed aerodynamically rather than by physical structure (reference Figure 6.6).

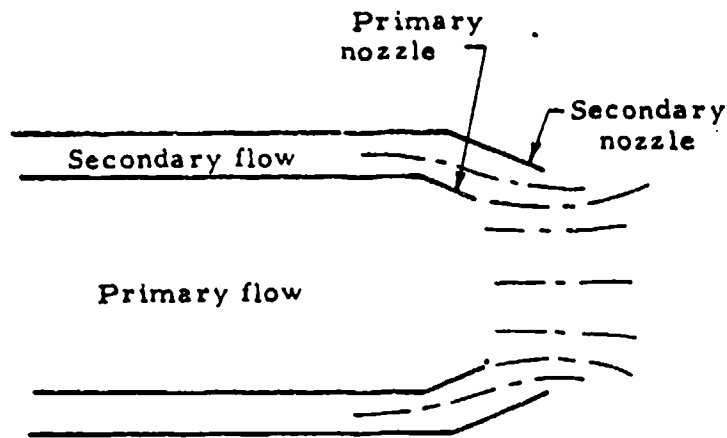


Figure 6.6

Schematic Diagram of Aerodynamic
Converging-Diverging Nozzle

For optimum performance throughout the operating range it is necessary to modulate both the primary and secondary nozzle areas and the spacing ratio, L/D_p .

In a converging-diverging nozzle, idealized flow is supersonic and fully expanded at the nozzle exit, and the gross thrust is

$$F_g = \frac{w_g}{g} \cdot V_e \quad 6.15$$

Restating equation 5.4 with the Mach number equal to unity at the throat

$$w_{gth} = P_{sth} A_{th} \sqrt{\frac{\gamma g}{RT_{sth}}} \quad 6.16$$

From the relations

$$P_{sth} = P_{tth} \left(\frac{2}{\gamma+1} \right)^{\frac{\gamma}{\gamma-1}} \quad 6.17$$

and

$$\frac{T_{tth}}{T_{sth}} = 1 + \frac{\gamma-1}{2} M^2 \quad 6.18$$

$$w_g = P_{tth} \left(\frac{2}{\gamma+1} \right)^{\frac{\gamma}{\gamma-1}} A_{th} \sqrt{\frac{g}{RT_{tth}} \frac{(\gamma+1)}{2}} \quad 6.19$$

Velocity at the nozzle exit may be expressed as

$$V_e = M_e \sqrt{gYRT_{se}} \quad 6.20$$

From equation 6.18

$$V_e = \frac{M_e \sqrt{gYRT_{te}}}{1 + \frac{\gamma-1}{2} M_e^2} \quad 6.21$$

Since the flow is fully expanded at the nozzle exit

$$M_e = \sqrt{\frac{2}{\gamma-1} \left[\left(\frac{P_{te}}{P_a} \right)^{\frac{\gamma-1}{\gamma}} - 1 \right]} \quad 6.22$$

and

$$V_e = \sqrt{\frac{\frac{2}{\gamma-1} \left[\left(\frac{P_{te}}{P_a} \right)^{\frac{\gamma-1}{\gamma}} - 1 \right] \gamma R T_{te}}{1 + \left[\left(\frac{P_{te}}{P_a} \right)^{\frac{\gamma-1}{\gamma}} - 1 \right]}} \quad 6.23$$

$$= \sqrt{\frac{2\gamma}{\gamma-1} g R T_{te} \left[1 - \left(\frac{P_a}{P_{te}} \right)^{\frac{\gamma-1}{\gamma}} \right]}$$

Substituting equations 6.19 and 6.23 in equation 6.15 to find gross thrust,

$$F_g = \frac{P_{tth} \left(\frac{2}{\gamma+1} \right)^{\frac{\gamma}{\gamma-1}}}{g} A_{th} \sqrt{\frac{\gamma g}{R T_{tth}} (\gamma+1) \frac{\gamma}{\gamma-1} g R T_{te} \left[1 - \left(\frac{P_a}{P_{te}} \right)^{\frac{\gamma-1}{\gamma}} \right]} \quad 6.24$$

Since P_t and T_t are constant in adiabatic flow, $P_{tth} = P_{te}$ and $T_{tth} = T_{te}$.

$$F_g = P_{tth} \left(\frac{2}{\gamma+1} \right)^{\frac{\gamma}{\gamma-1}} A_{th} \sqrt{\frac{\gamma+1}{\gamma-1} \left[1 - \left(\frac{P_a}{P_{tth}} \right)^{\frac{\gamma-1}{\gamma}} \right]} \quad 6.25$$

Forming the ideal gross thrust parameter

$$\frac{F_g}{P_a A_{th}} = \frac{P_{tth}}{P_a} \left(\frac{2}{\gamma+1} \right)^{\frac{\gamma}{\gamma-1}} \sqrt{\frac{\gamma+1}{\gamma-1} \left[1 - \left(\frac{P_a}{P_{tth}} \right)^{\frac{\gamma-1}{\gamma}} \right]} \quad 6.26$$

Equation 6.26 is presented in graphical form in Chart 9.21.

It has been pointed out previously that in a converging nozzle the flow is subcritical at nozzle pressure ratios less than approximately 1.85. At higher pressure ratios the convergent exhaust nozzle is choked and operates with a supercritical pressure ratio. In this case the static pressure at the exit is larger than atmospheric pressure; that is, the gases are underexpanded. In a converging-diverging nozzle complete expansion occurs with idealized flow, resulting in a somewhat higher thrust when the flow is supercritical. This difference in thrust is shown in Figure 6.7. It can be seen from this figure that in subsonic flight (maximum pressure ratios of the order of 4) the gain in thrust is too slight to warrant installation of a converging-diverging nozzle. In supersonic flight, however, where the pressure ratios become much higher, a substantial increase in thrust is possible.

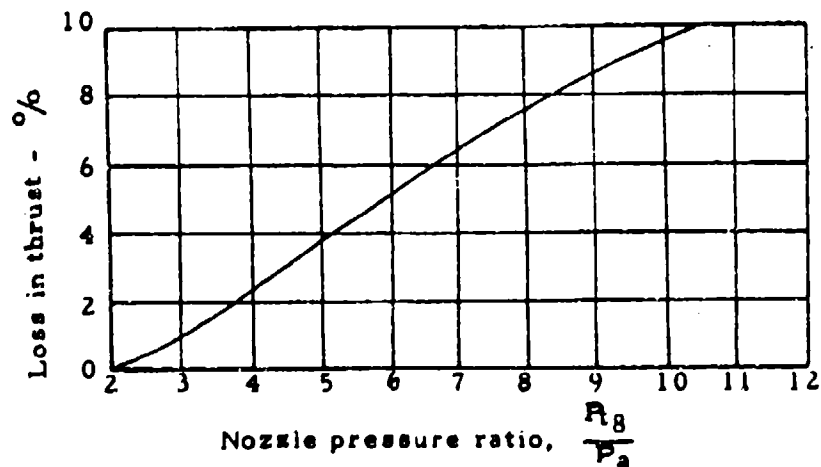


Figure 6.7

Theoretical Loss in Thrust Due to Underexpansion

6.6 SWINGING RAKE

Stationary air-cooled probes located in the nozzle exit have been employed with adequate results. Probes of this sort are subject to damage from high temperatures, however. Swinging rakes may provide the best means for measuring the jet thrust of more advanced engines, such as those with afterburners and ejectors. Rakes of this design are normally stowed outside the jet exhaust where they are cooled by freestream air. They are driven across the tailpipe when data is being recorded in about 4 or 5 seconds, so that prolonged exposure to the hot jet is avoided and a cooling system is not required. The thrust contribution of an ejector together with the thrust created by the basic engine may be computed from data obtained with a swinging rake. Also, better mean values of pressure are obtained with a swinging rake than with a fixed probe, although pressures are still measured along only one cross section.

The jet of high performance engines expands rapidly, particularly at high power settings, resulting in Mach numbers which are well supersonic downstream of the nozzle. Hence, it is desirable to measure both total and static pressures at a common point in a plane as near the nozzle exit as possible. Several different designs have been utilized, although none of them satisfy this condition exactly. These designs include installations which sense both total and static pressures on the same probe, and those which sense pressures on different probes but in the same plane (reference Figure 6.8).

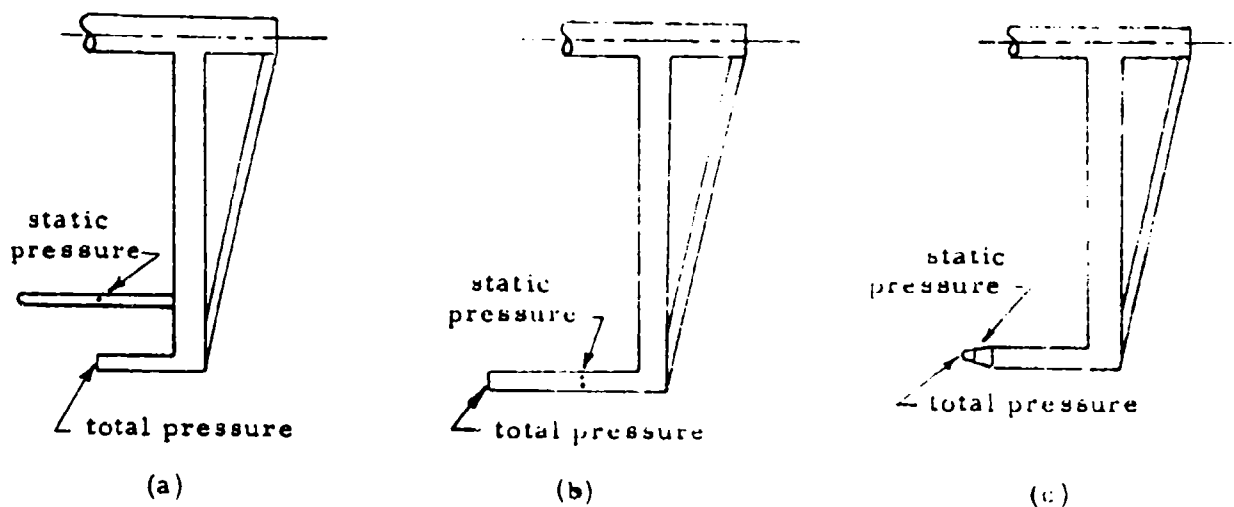
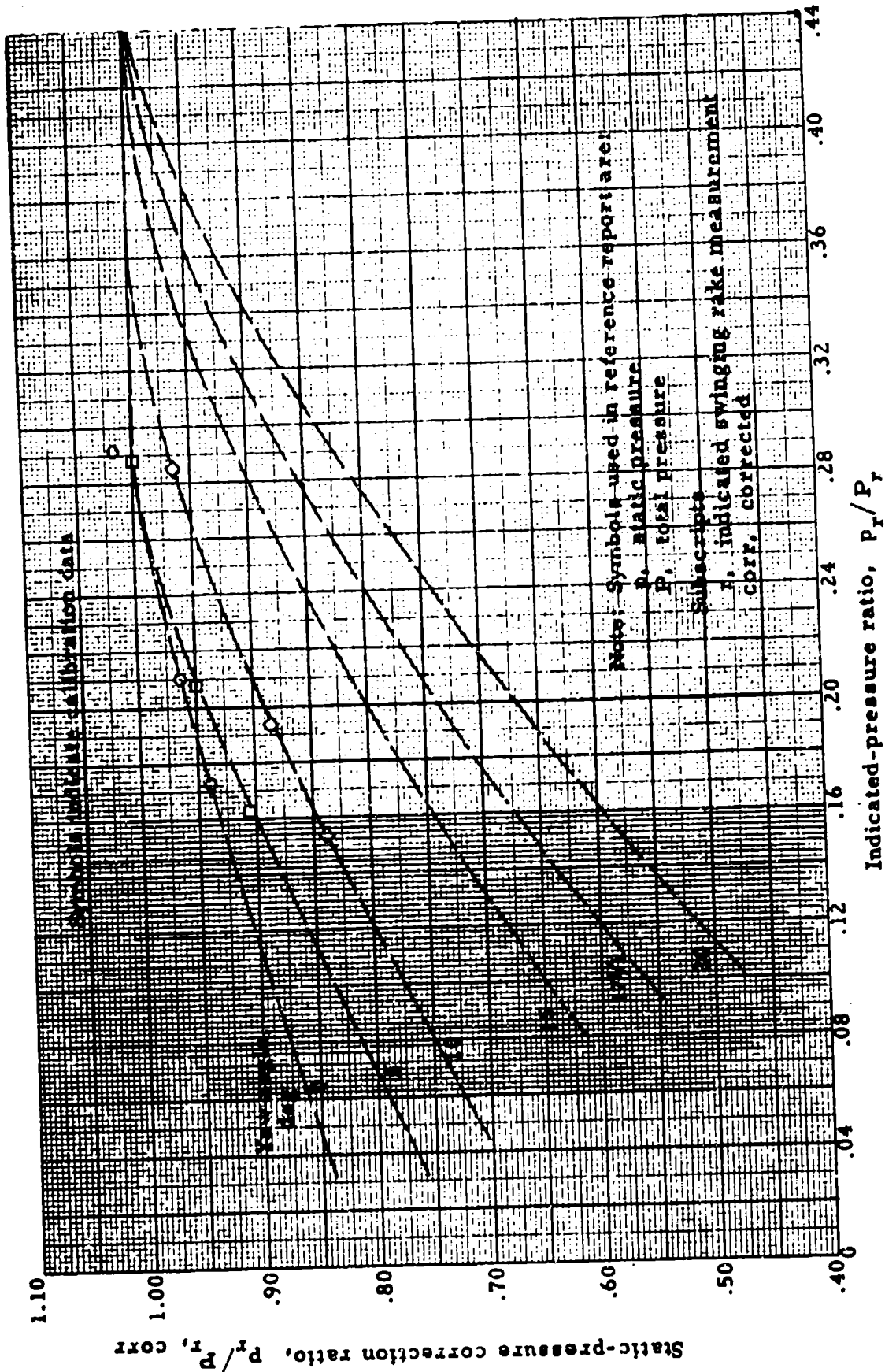


Figure 6.8
Various Designs of Swinging Rakes

In designs similar to that shown in Figure 6.8 (a), the probes should be as close as possible without creating excessive aerodynamic interference. Another type of installation which is perhaps the best compromise for obtaining both total and static pressures at the same point makes use of a pitot-static probe with static pressure measured on a conical surface.

6.6.1 Sources of Error:

Little information is available on the flow angularities which exist at the nozzle exit. Flow angularities of approximately 15 to 20 degrees due to swirl of the primary jet should be expected based on NACA Research Memorandum E57H28, "Experimental Results of an Investigation of Two Methods of In-Flight Thrust Measurement Applicable to Afterburning Turbojet Engines with Ejectors", by Harry E. Bloomer. No significant effect on total pressure results from flow angles of this magnitude with an adequately designed pitot tube. Static pressures are subject to quite substantial errors, however, as shown by Figure 6.9 extracted from RM E57H28.



(a) Static-pressure correction ratio; static-pressure orifice 5.5 diameters behind probe nose and 7.75 diameters ahead of rake body.

Figure 6.9

As is pointed out in this memorandum, it would seem that large errors in thrust measurement might result with supersonic flow since the static pressure is used to correct the total pressure for bow shock. Errors in static pressure are not as serious as might be anticipated, as demonstrated in Figure 6.10 which shows variations in gross thrust from errors in static pressure.

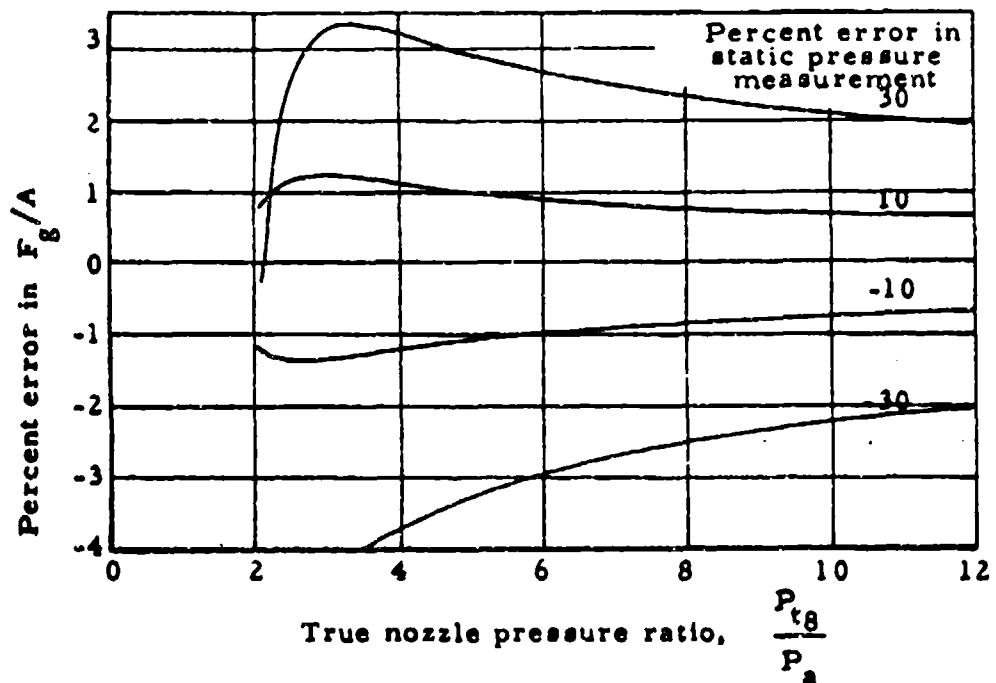


Figure 6.10

Error in F_g/A vs Nozzle Pressure Ratio for Assumed Errors in Static Pressure

Exact information on yaw angles cannot be expected for flight test installations. Approximate corrections can be made, however, to bring static pressures to within say ± 10 percent of their true values and keep the error in gross thrust caused by inaccuracies

in static pressure to within ± 1 percent.

Constant values of γ , (1.33 for non-afterburning and 1.28 for afterburning), may be used for the entire swing without introducing significant errors. Errors in total pressure may be introduced by lag, particularly during the portion of the traverse where pressure gradients are large. Lag errors may be minimized by averaging pressures taken during traverses in opposite directions. The accurate determination of probe position, from which nozzle area is found, is necessary for achieving satisfactory accuracies in thrust computation. Measurement of probe position is made more difficult by possible bending of the rake body from aerodynamic forces and thermal stresses.

6.6.2 Calculation of Gross Thrust:

The following equation may be used to compute thrust with a swinging rake:

$$F_g = \int \left\{ P_{s9} \left[\frac{2\gamma}{\gamma-1} \left(\frac{P_{t9}}{P_{s9}} \right)^{\frac{\gamma}{\gamma-1}} - \frac{\gamma+1}{\gamma-1} \right] - P_a \right\} dA_9 \quad 6.27$$

Static pressures are first corrected for yaw angle. Indicated total pressures are used directly when the flow is subsonic. With supersonic flow the total pressure behind a detached shock is sensed. In this case Mach number may be computed from the Rayleigh supersonic pitot formula (reference Chart 9.22).

$$\frac{P_t}{P_s} = \frac{\left(\frac{\gamma+1}{2} M^2 \right)^{\frac{\gamma}{\gamma-1}}}{\left(\frac{2\gamma}{\gamma+1} M^2 - \frac{\gamma-1}{\gamma+1} \right)^{\frac{\gamma}{\gamma-1}}} \quad 5.15$$

The isentropic relation,

$$\frac{P_{t9}}{P_{s9}} = \left(1 + \frac{\gamma-1}{2} M^2 \right)^{\frac{\gamma}{\gamma-1}}$$

may be used to determine P_{t9}/P_{s9} .

The area included by the probe traverse is computed from a calibration of the angular displacement of the probe from the vertical centerline versus distance from the center of the nozzle. Pressures may then be plotted as illustrated in Figure 6.11.

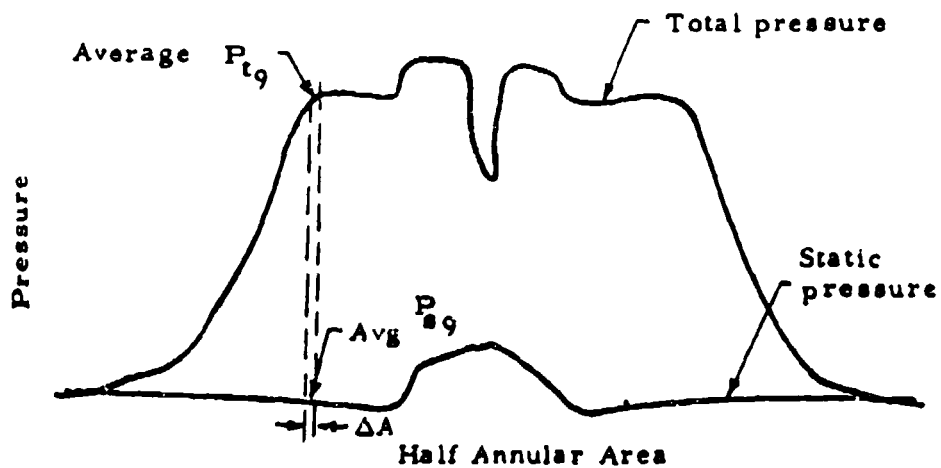


Figure 6.11
Typical Total and Static Pressure Distributions
from Swinging Rake

Gross thrust may be computed from equation 6.27 using a mechanical integration procedure, by summing values of ΔF_g calculated from average P_{t9} and average P_{s9} over ΔA (reference Figure 6.11). This procedure involves rather lengthy calculations and is not adaptable to test programs where large quantities of data are processed. Here, a machine solution which makes use of curve fits of total and static pressure distributions is virtually essential.

SECTION 7 WATER INJECTION

7.1 INTRODUCTION

Thrust augmentation may be obtained by injecting water or other liquids into the airstream anywhere from the compressor inlet to the rear of the burner. A mixture of water and methyl alcohol is frequently used. The alcohol prevents freezing and also provides additional heating which compensates for the heat lost through evaporation of the water-alcohol mixture. The additional heat is supplied when the alcohol burns. Water-alcohol is usually injected in the compressor inlet, in the combustion chamber or at both locations simultaneously. An increase in thrust from about 10 to 25 percent can be obtained, depending on the type of installation, amount of water injected and the flight conditions. This increase in thrust is achieved at very high total liquid flow rates and can be employed for only short periods of time. Consequently, the use of water injection is generally limited to improving take-off performance.

Compared to afterburning, water injection is less efficient and more limited in the augmentation ratios which can be obtained. Water injection does have the advantage of simplicity of installation and operation and does not entail as large an installation weight penalty as afterburning. Also, a performance penalty is not incurred during cruise as is the case with an afterburner installation. For relatively small short duration thrust increases, water injection may, therefore, be the more suitable of the two systems.

7.2 INJECTION IN THE COMPRESSOR INLET

Water injection in the compressor inlet has the advantage that a greater amount of thrust augmentation is produced per pound of liquid injected. Increases in thrust are produced from the three following effects:

1. The mass flow is increased. Some of this increase is due to the mass of the injected liquid, and some from a reduction in compressor inlet temperature. It is theoretically possible to cool the inlet air to the saturation temperature before it enters the compressor. The air is not cooled to that extent in practice, however, since the rate of evaporation is limited principally by spray droplet size and air turbulence. As the spray passes into the compressor, further cooling is obtained by additional evaporation during the mechanical compression process.

2. The power required to operate the compressor at a constant pressure ratio is decreased. This is also caused by the lowered inlet temperature which decreases the required change in enthalpy necessary to perform a given amount of compression.

3. A higher pressure ratio from the compressor is obtained. This increased pressure ratio is attributed to the increased density of the gases flowing through the compressor.

Further, the decrease in compressor discharge temperature tends to be reflected in a lower exhaust gas temperature. Although the lowered compressor power input requirement tends to increase exhaust gas temperature, the net effect is generally to produce a lower temperature. Hence, more fuel, with higher mass flows, is added to the combustion chamber in order to retain the same exhaust gas temperature. These effects combine to increase the thrust output.

7.3 COMBUSTION CHAMBER INJECTION

Thrust may be increased by injecting water or a water-alcohol mixture into the combustion chamber. The turbine inlet pressure is increased thereby, and a higher total mass flow results. The total mass flow tends to be reduced, however, due to changing the equilibrium running conditions of the compressor with the addition of

water injection. The compressor pressure ratio is increased while the compressor rotative speed remains constant, so that the airflow is reduced. Hence, the amount of augmentation is dependent on the operating characteristics of the compressor. (See Figure 7.1).

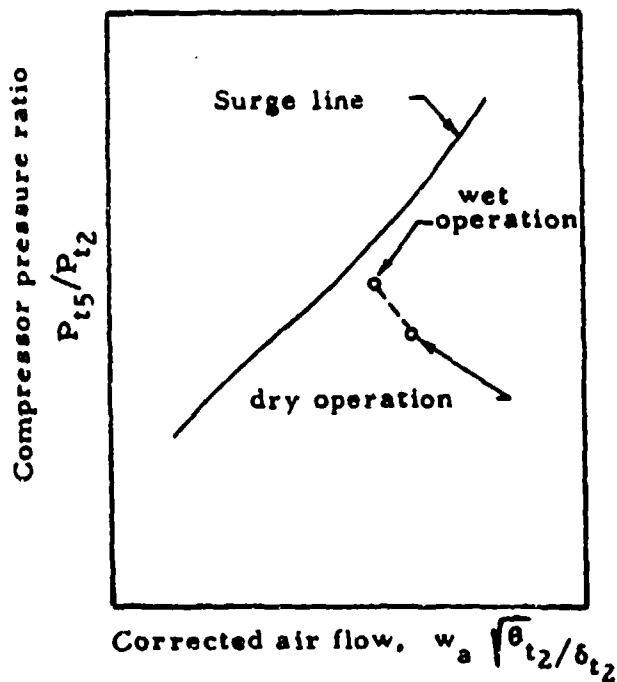


Figure 7.1
Simplified Compressor Performance Chart

At equilibrium, the compressor flow is lower, but the turbine and nozzle exit flow is higher as is the nozzle pressure ratio and consequently thrust. Compressor surge will limit the amount of liquid which can be injected into the combustion chamber. Practical increases in thrust are limited for this reason to about 15 to 20 percent.

SECTION 8
DATA REDUCTION

8.1 CONVERSION OF ESTIMATED PERFORMANCE CURVES TO CORRECTION PLOT ($F_n/\delta t_2$ versus $N/\sqrt{\theta_a}$)

1. Mach number desired
2. P_{t2}/P_{t0} from plot of P_{t2}/P_0 versus M
3. $P_{t0}/P_a = (1 + .2M^2)^{3.5}$
4. P_{t2}/P_a , (2) x (3)
5. $N/\sqrt{\theta_a}$, select values to cover the flight range
6. $(T_{t2}/T_a)^{1/2} = (1 + .2M^2)^{1/2}$
7. $N/\sqrt{\theta_{t2}}$, (5)/(6)
8. $F_g/\delta t_2$ from engine manufacturer's estimated gross thrust curves at (4) and (7)
9. $w_a\sqrt{\theta_{t2}}/\delta t_2$ from engine manufacturer's estimated airflow curves at (4) and (7)
10. $F_e/\delta t_2$, (9) x (1) x 34.73/(6)
11. $F_n/\delta t_2$, (8) - (10)
12. Plot (11) versus (5) for Mach numbers selected in (1)

8.2 DETERMINATION OF EXHAUST GAS TEMPERATURE, RPM AND NET THRUST CORRECTIONS FOR OFF-STANDARD EXHAUST GAS TEMPERATURE

1. T_{t5_t} , test exhaust gas temperature
2. N_t , test engine speed
3. N_s , standard engine speed
4. θ_{at} , T_{at}/T_{asL}
5. θ_{as} , T_{as}/T_{asL}
6. T_{t5_t}/θ_{at} , (1)/(4)
7. $N_t/\sqrt{\theta_{at}}$, (2)/ $\sqrt{(4)}$
8. $N_s/\sqrt{\theta_{as}}$, (3)/ $\sqrt{(5)}$

9. $T_{t5_{max}}$, maximum allowable exhaust gas temperature
10. $T_{t5_{max}}/\theta_{as}$, corrected maximum allowable exhaust gas temperature, (9)/(5)
11. T_{t5_g}/θ_{as} , standard corrected exhaust gas temperature corresponding to (8) from plot of (6) and (7) at (8)

Case I: (11) less than (10)

12. T_{t5_g} , (11) x (5)
13. $\Delta F_n/\delta t_2$ from plot of $F_n/\delta t_2$ versus $N/\sqrt{\theta_a}$ at (7) and (8)

Case II: (11) greater than (10)

14. $(N/\sqrt{\theta_{as}})_{max}$, corrected rpm corresponding to (10) from plot of (6) and (7) at (10)
15. N_{max} , standard maximum engine speed, (14) x (5)
16. $\Delta F_n/\delta t_2$ from plot of $F_n/\delta t_2$ versus $N/\sqrt{\theta_a}$ at (14) and (7)

8.3 DETERMINATION OF NOZZLE THRUST COEFFICIENT

1. $F_{g_{actual}}$ from the mechanical thrust measuring equipment
2. A_g from measurements of the exhaust nozzle
3. P_a , static pressure to which the nozzle is discharging, from barometer or altimeter
4. P_{tg} , instrument corrected total pressure from probe(s) located in exhaust nozzle
5. P_{tg}/P_a , nozzle pressure ratio, (4)/(3)
6. $(F_g/A_g P_a)_{theo}$, theoretical gross thrust parameter from Chart 9.17 or 9.18 and (5)
7. $(F_g/A_g P_a)_{actual}$ (1)/(2) (3)
8. C_f , nozzle thrust coefficient, (7)/(6)
9. Plot (8) versus (5)

Chart 9.1 RELATION BETWEEN TOTAL PRESSURE RECOVERY AND RAM EFFICIENCY

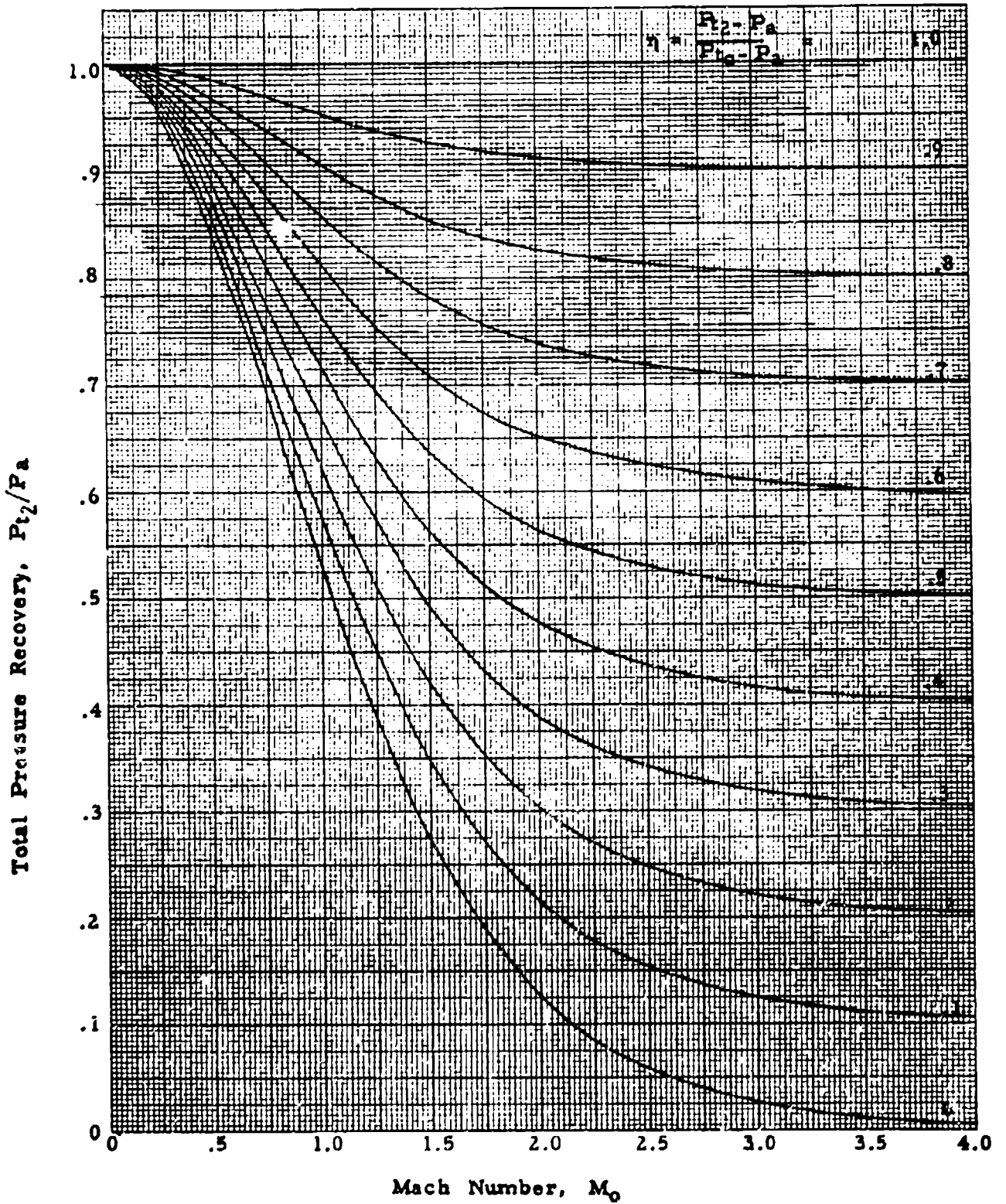


Chart 9.2 TOTAL PRESSURE RECOVERY FOR INLETS WITH SHARP LIPS

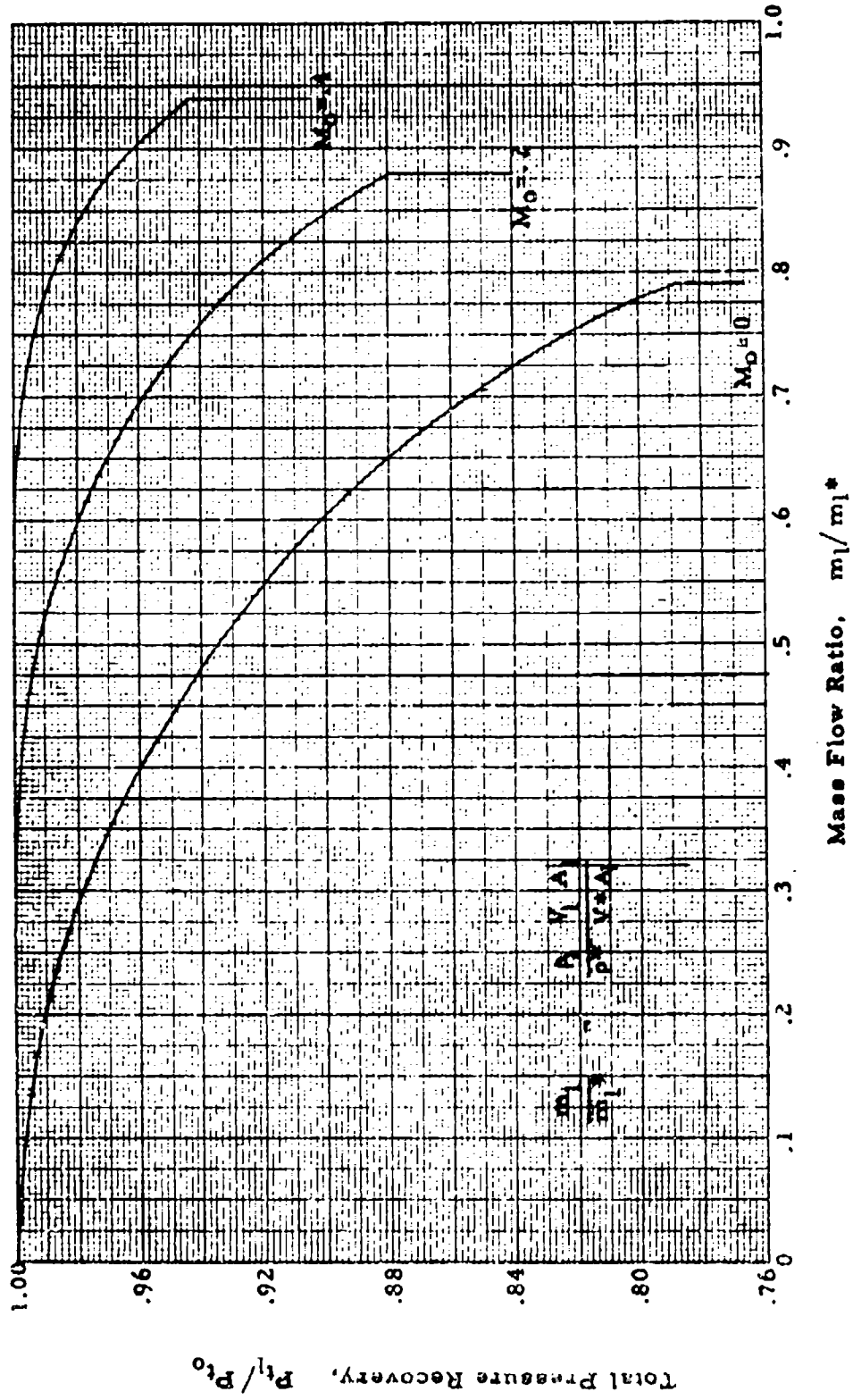
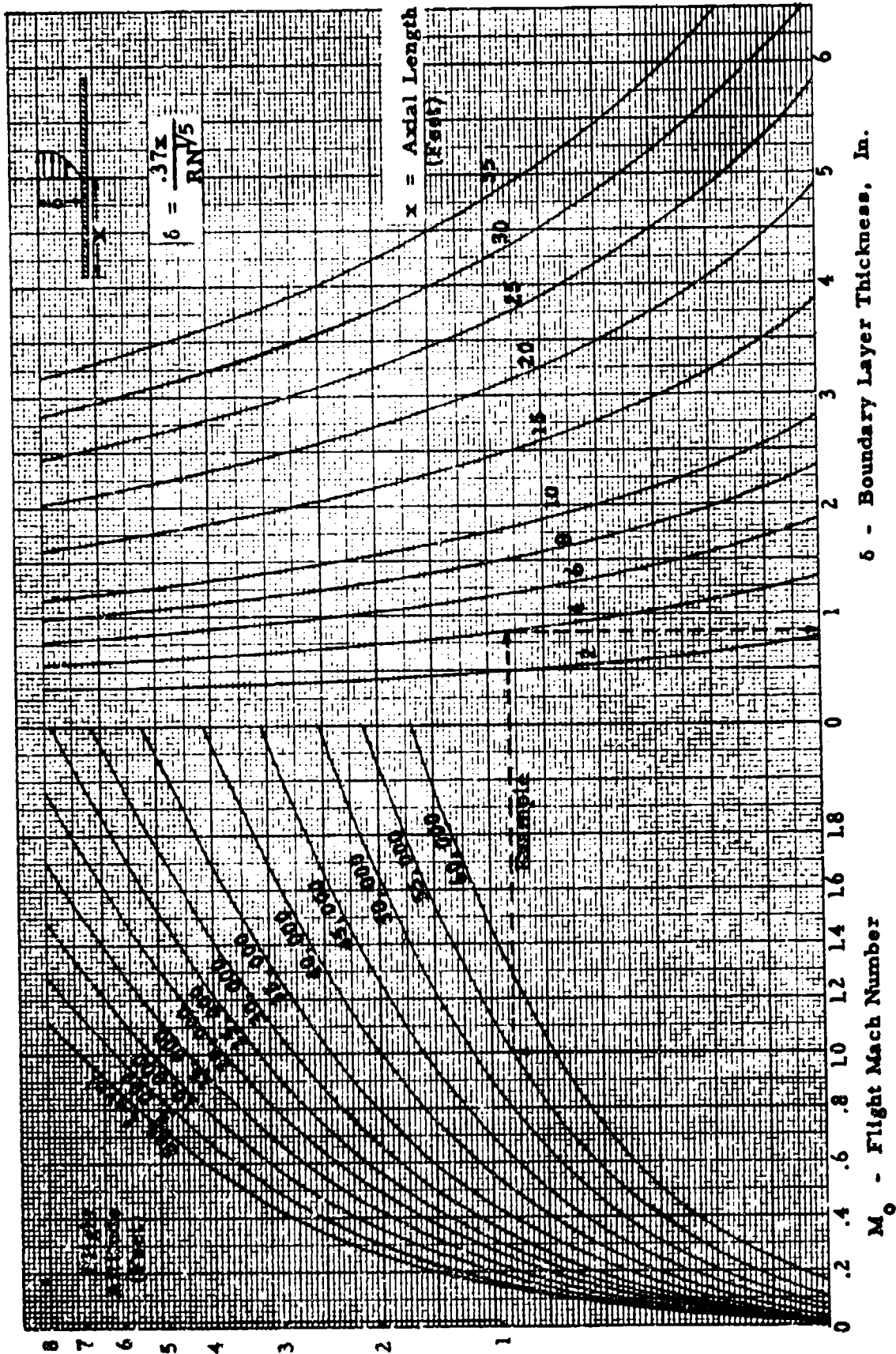


Chart 9.3 TURBULENT BOUNDARY LAYER THICKNESS FOR FLAT - PLATES AT ZERO ANGLE OF ATTACK AS A FUNCTION OF FLIGHT SPEED AND ALTITUDE



3-70
 $Re \times 10^{-6}$ Per Foot - 1/ft

Chart 9.4 (a) PRESSURE RECOVERY OF BOUNDARY LAYER AIR ADMITTED INTO SIDE - INLET INSTALLATION - TURBULENT FLOW

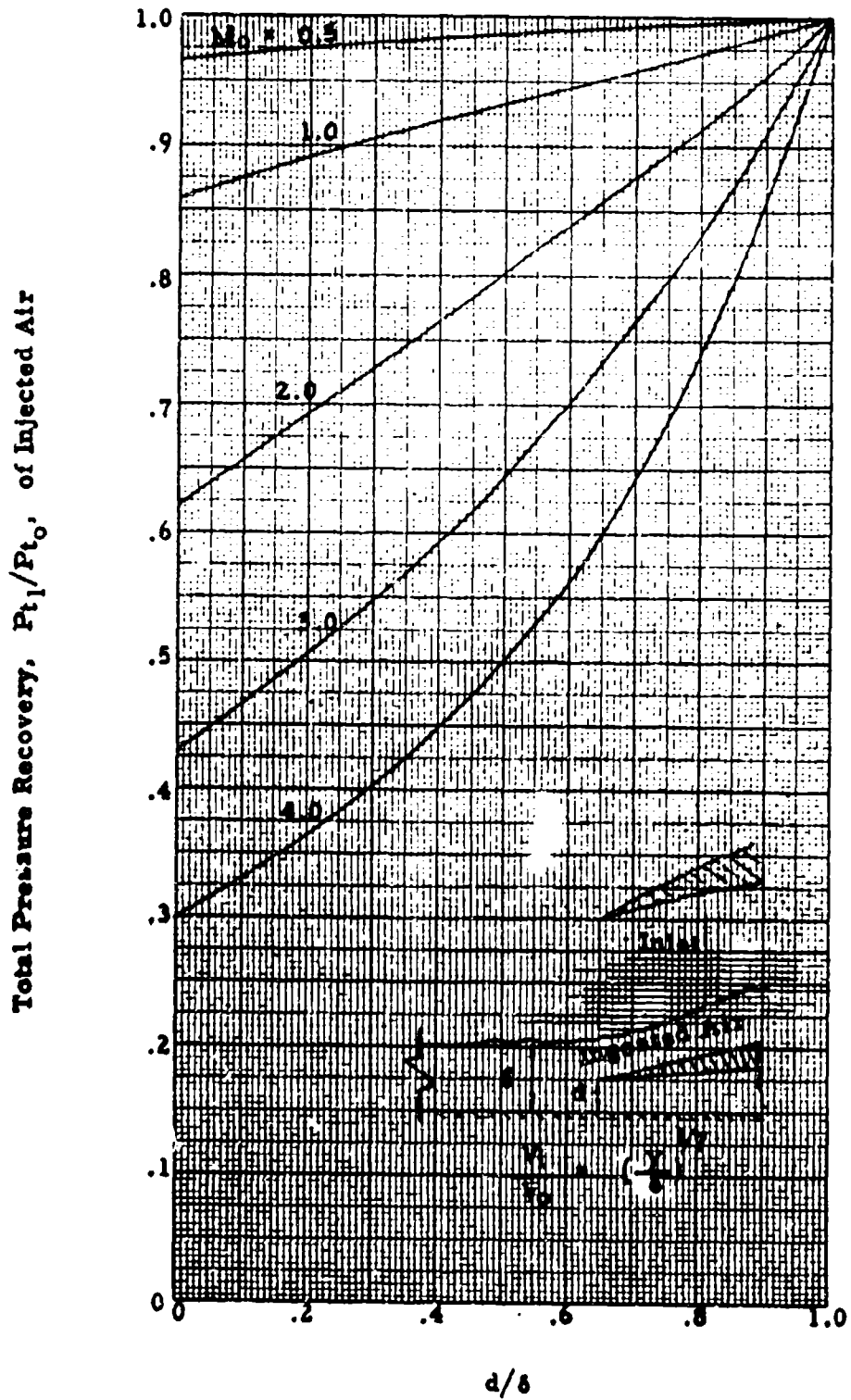


Chart 9.4(b) PRESSURE RECOVERY OF BOUNDARY LAYER
 AIR ADMITTED INTO SIDE-INLET INSTALLATION
 - LAMINAR FLOW

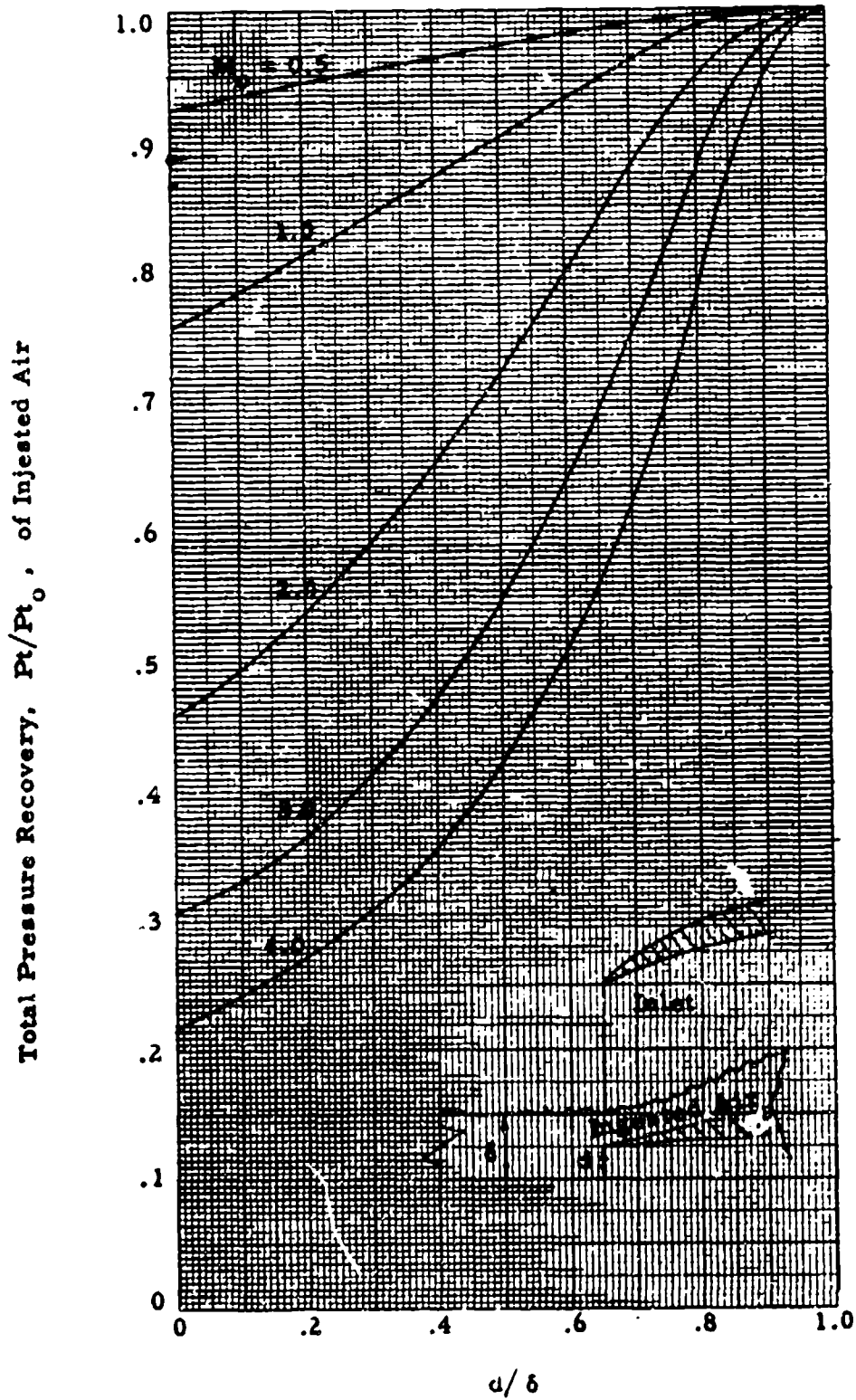


Chart 9.5 TOTAL MOMENTUM RATIO FOR VARIOUS SCOOP HEIGHT TO BOUNDARY LAYER RATIOS

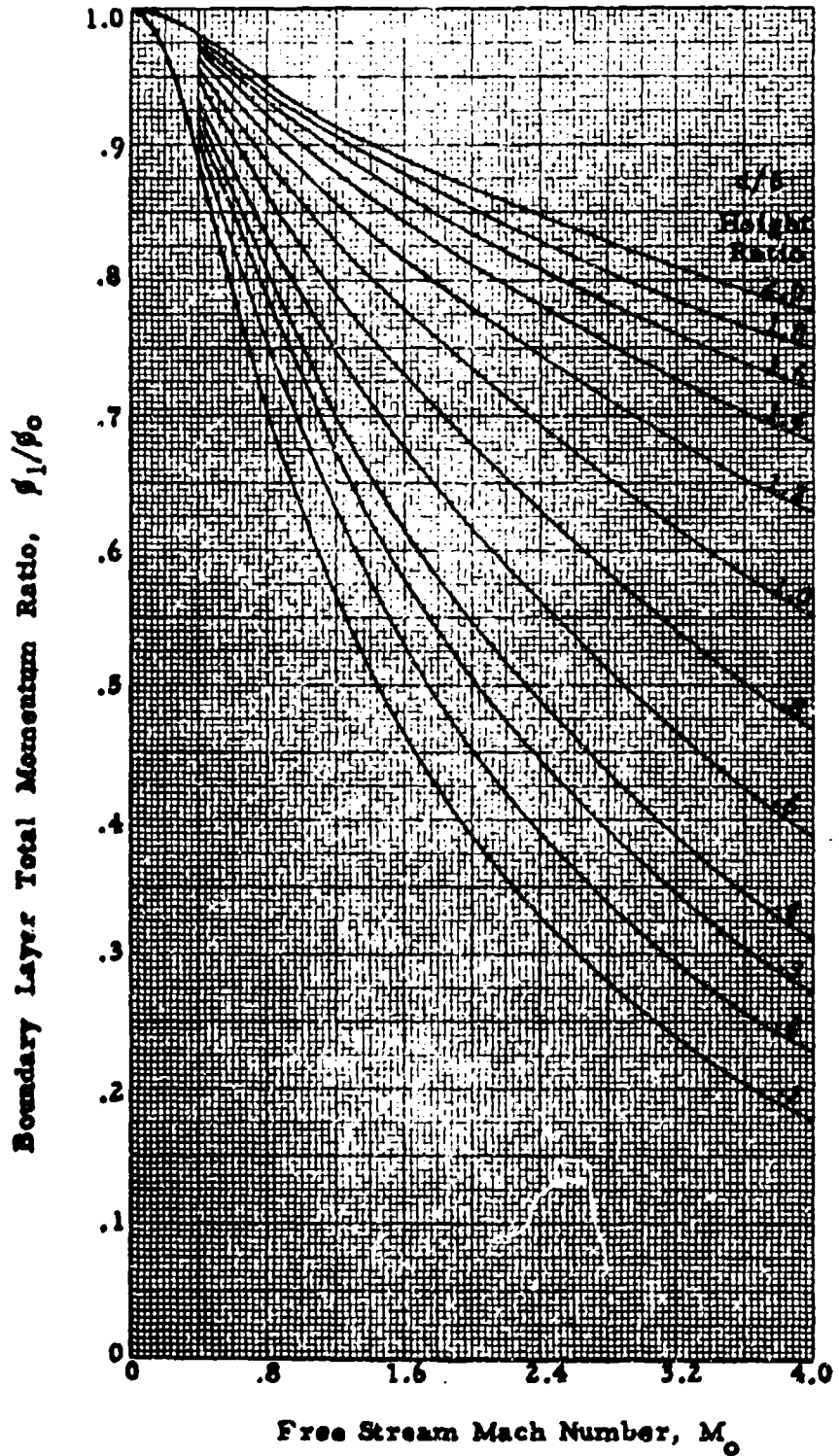
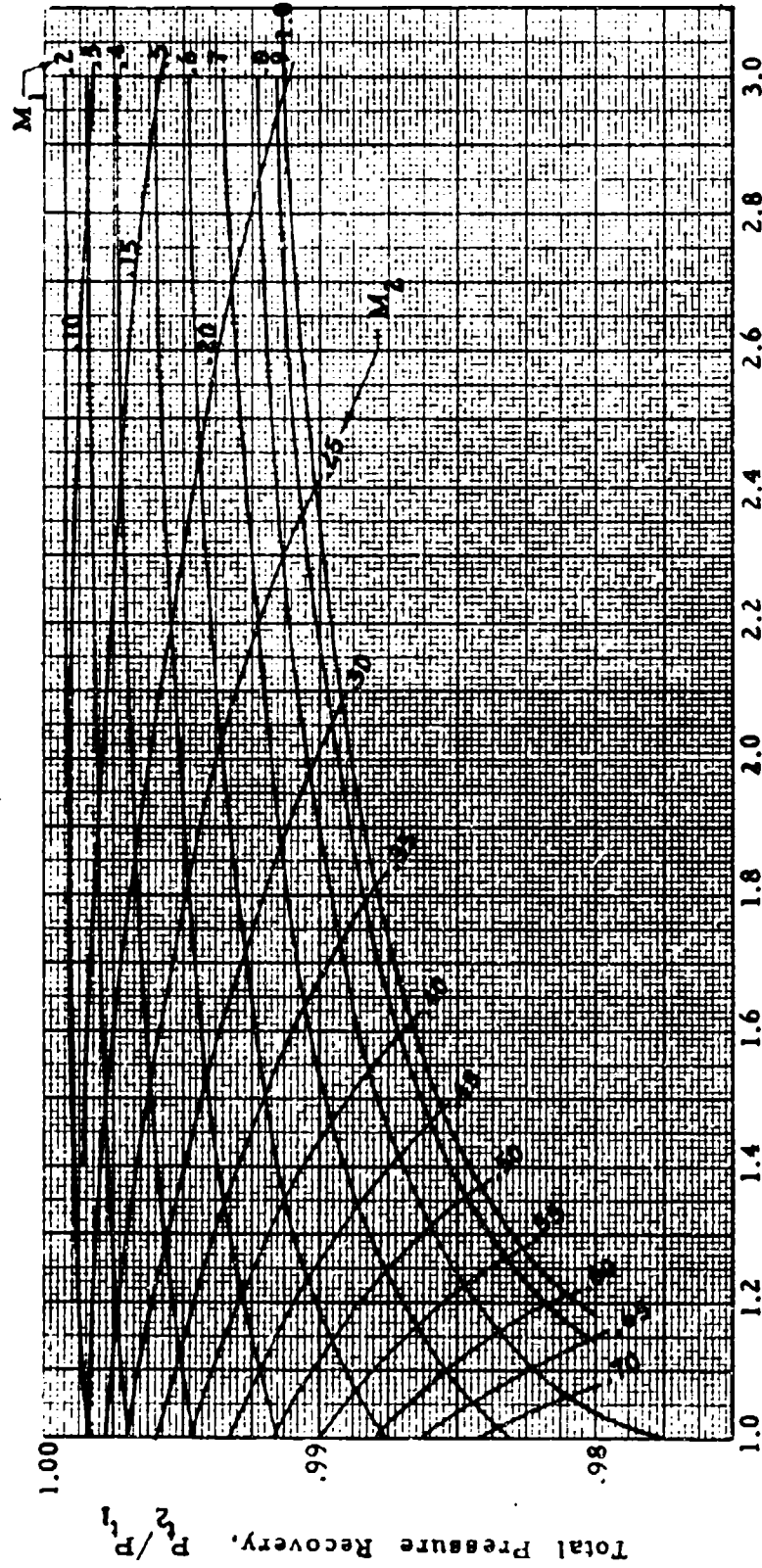


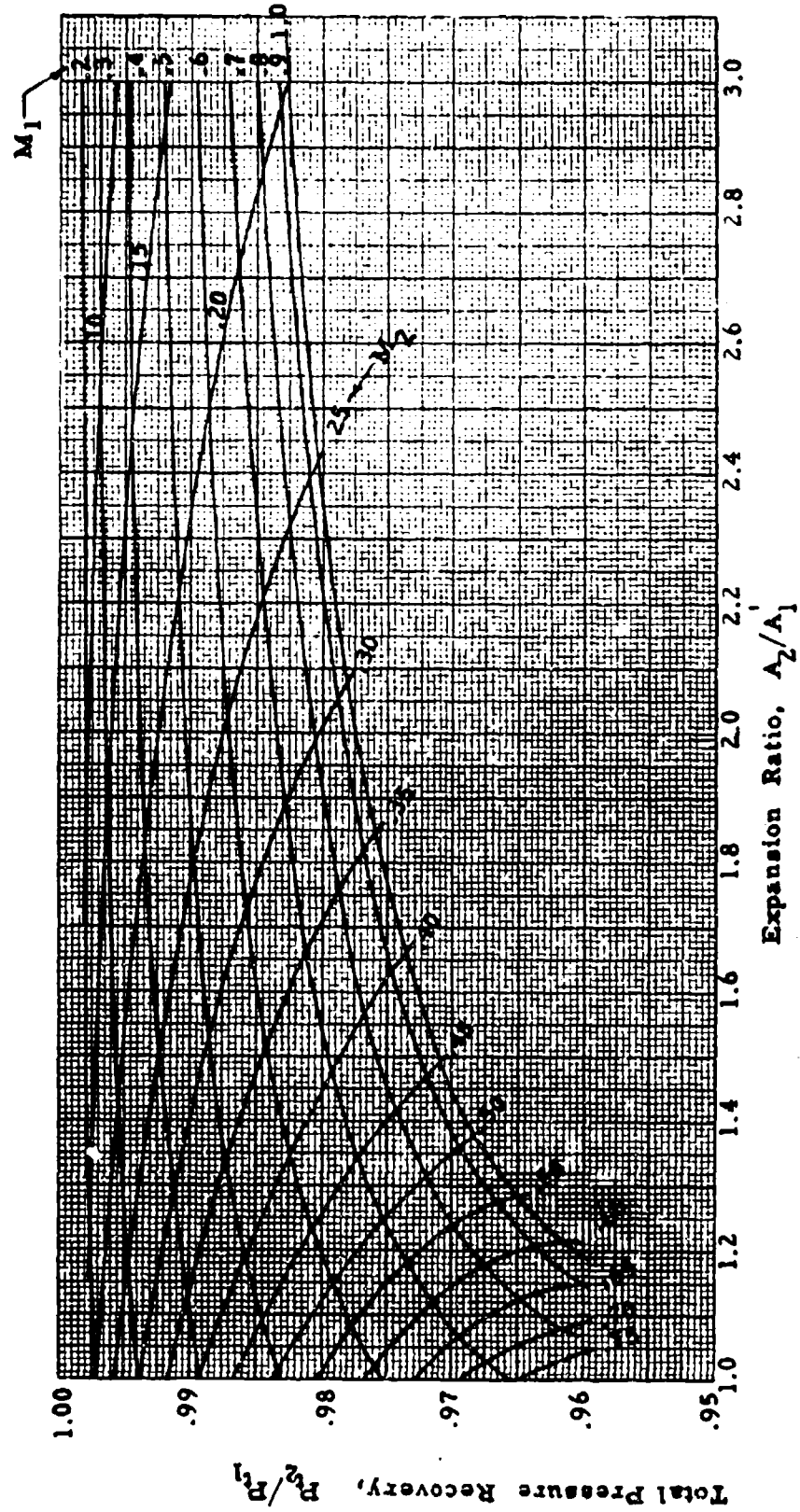
Chart 9.6 (a) TOTAL PRESSURE RECOVERY FOR STRAIGHT SUBSONIC DIFFUSERS



Expansion Ratio, A_2/A_1

$$\left(\frac{1}{\alpha_2} \times \frac{C_1}{.003} \right) = 4.0$$

Chart 9.6 (b) TOTAL PRESSURE RECOVERY FOR STRAIGHT SUBSONIC DIFFUSERS



$$\text{Expansion Ratio, } A_2/A_1 = \left(\frac{1}{M_1^2} \times \frac{C_f}{.003} \right) = 8.0$$

Chart 9.7 TOTAL PRESSURE LOSS IN COMPOUND SUBSONIC DIFFUSEE BENDS

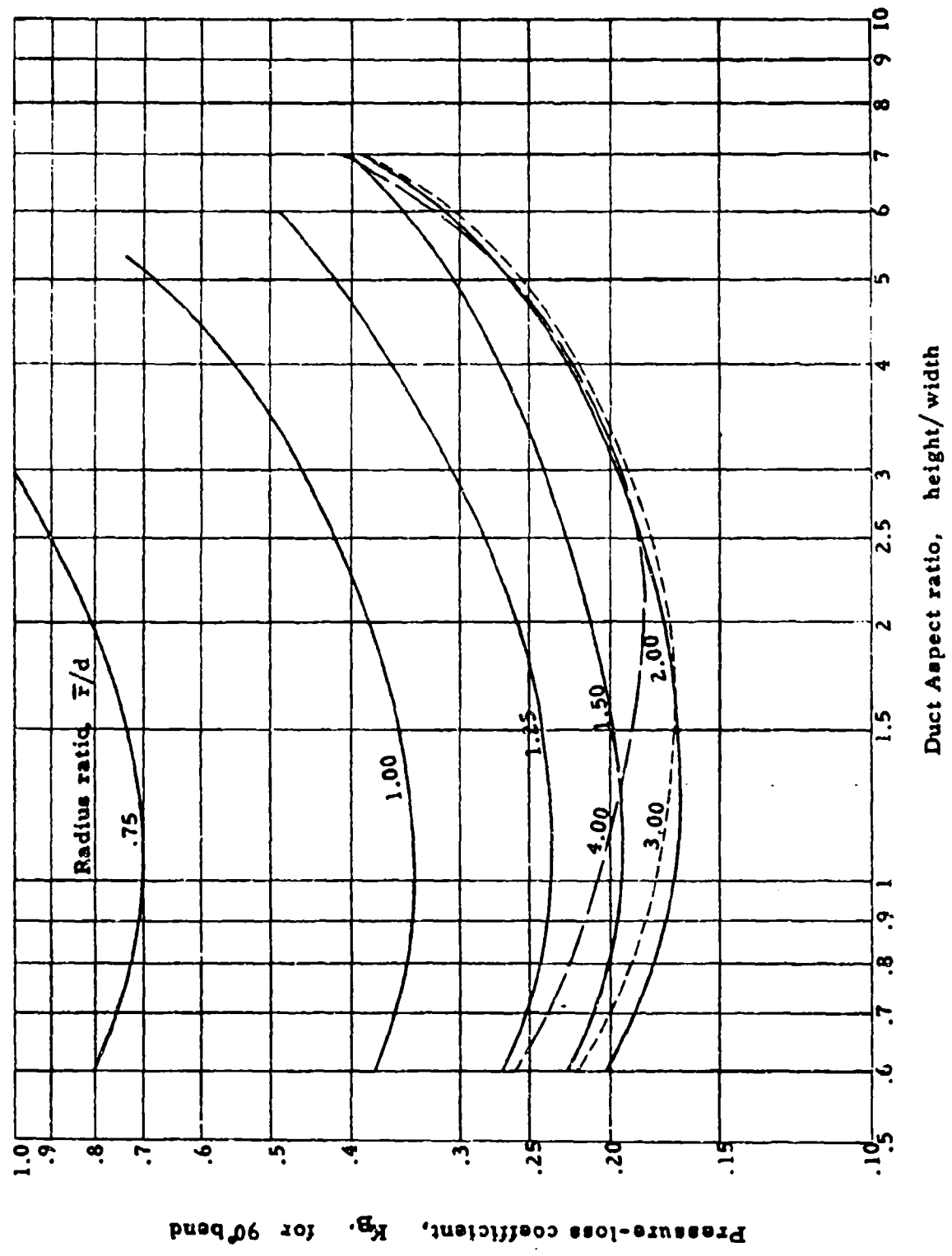


Chart 9.8 M_0 vs P_{t1}'/P_{t0} - NORMAL SHOCK CONDITIONS, $\gamma = 1.4$

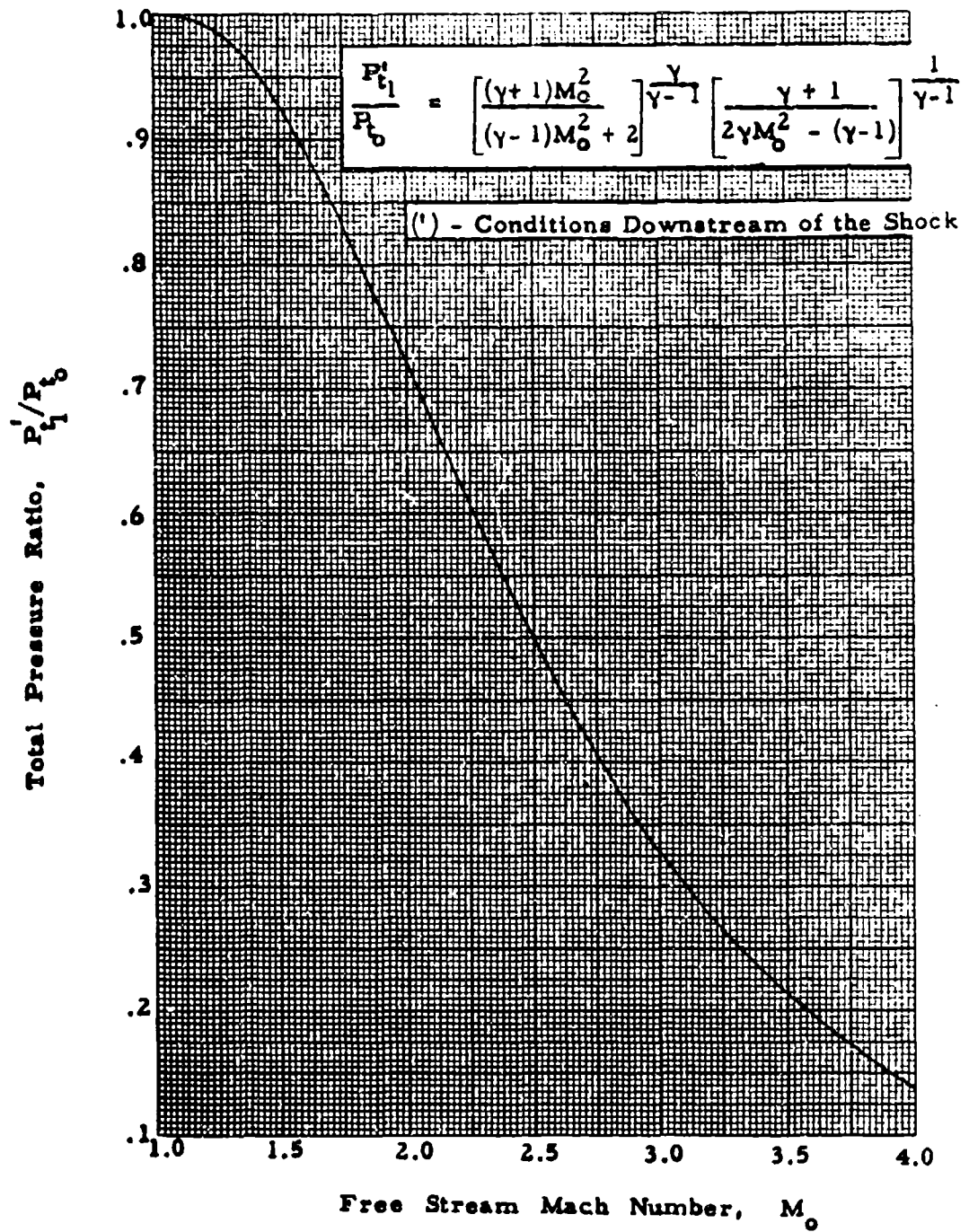


Chart 9.9 TOTAL PRESSURE RATIOS FOR 2 - DIMENSIONAL
2 - SHOCK COMPRESSION

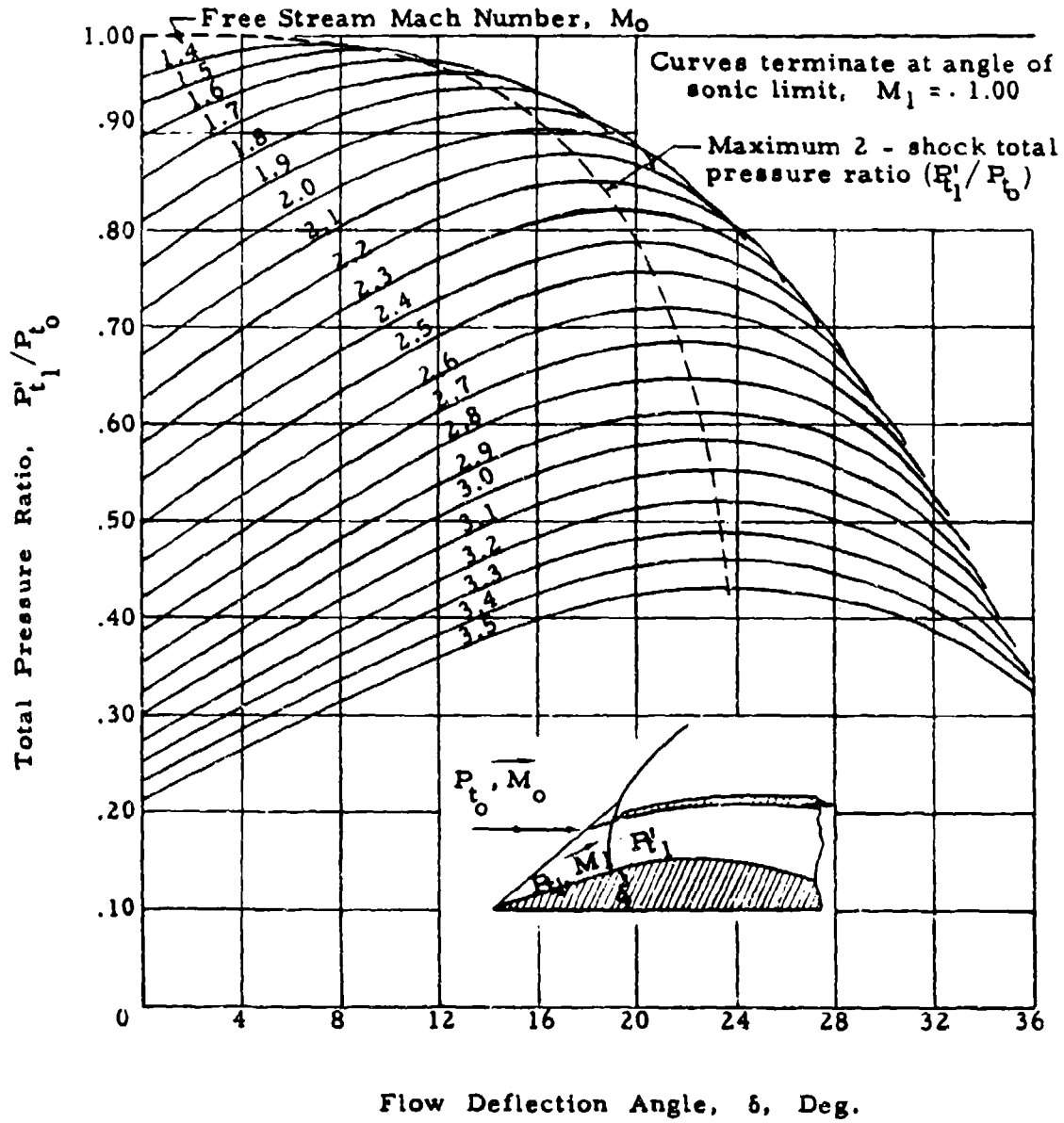


Chart 9.10 TOTAL - PRESSURE RATIOS FOR 2 DIMENSIONAL
3 - SHOCK COMPRESSION

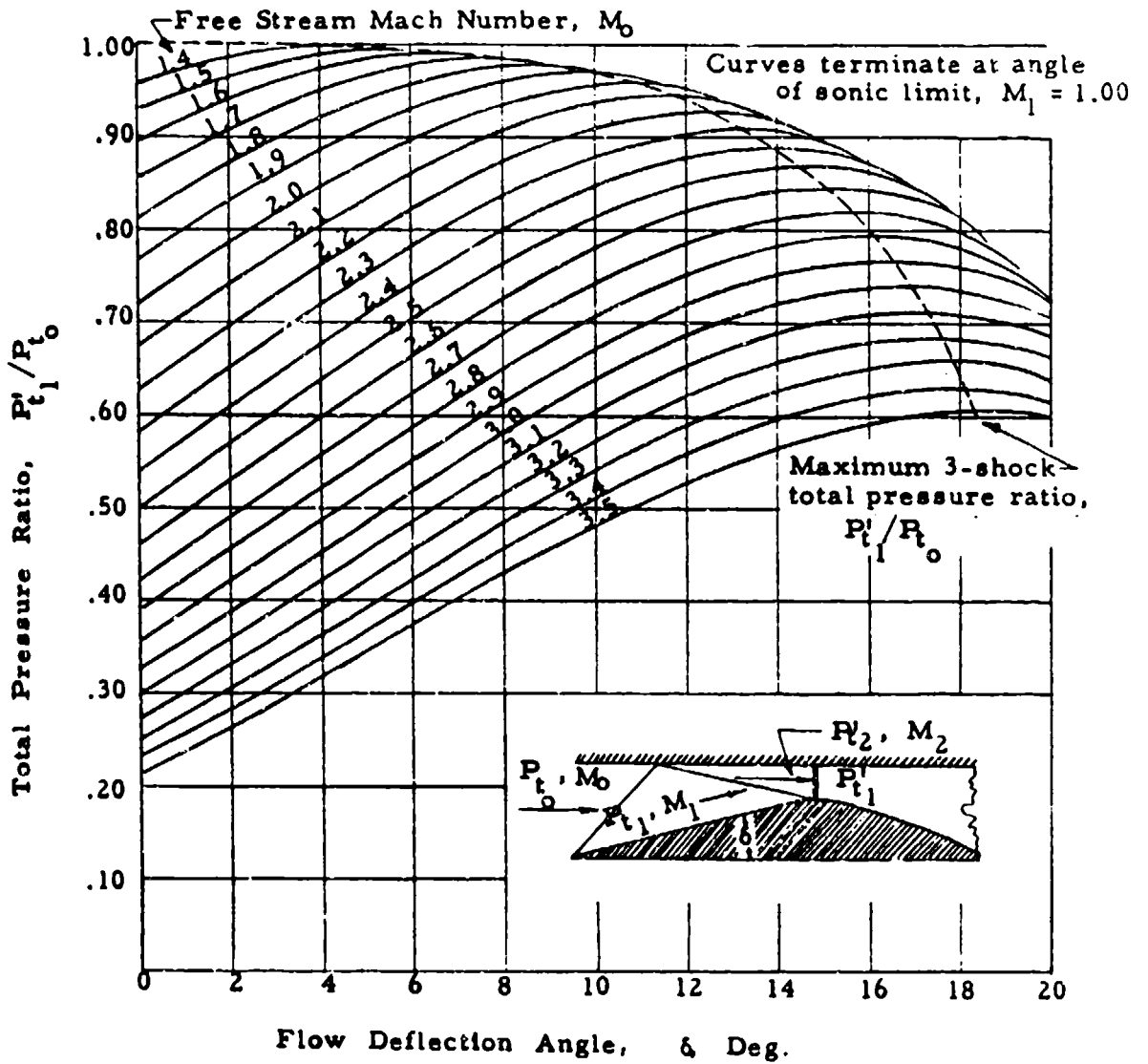


Chart 9.11 TOTAL PRESSURE RATIOS FOR CONICAL 2-SHOCK
COMPRESSION

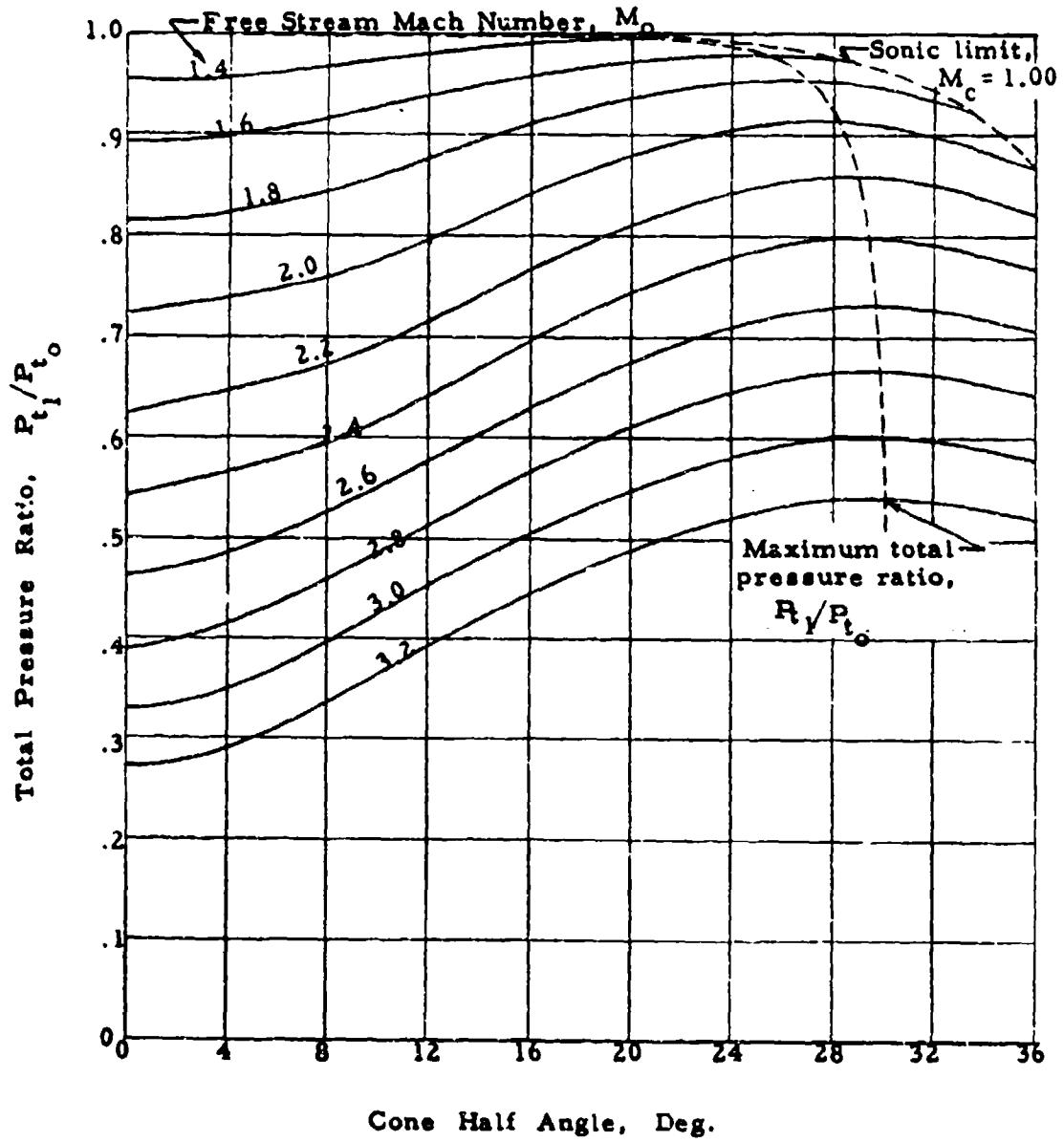


Chart 9.12 MACH NUMBER CHANGE THROUGH AN OBLIQUE SHOCK
FOR A TWO DIMENSIONAL WEDGE

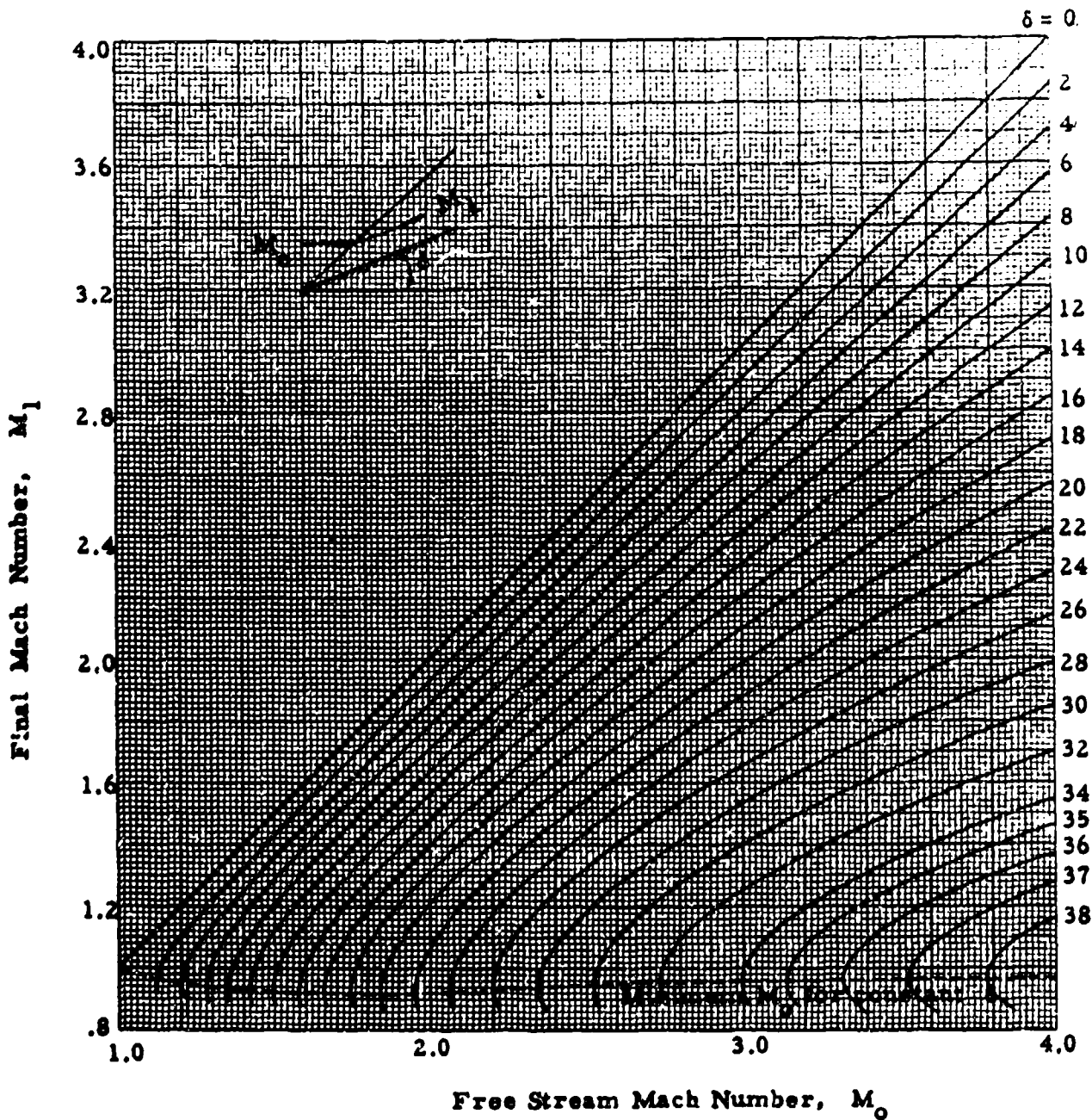


Chart 9.13 TOTAL PRESSURE RATIO ACROSS AN OBLIQUE SHOCK FOR A TWO DIMENSIONAL WEDGE

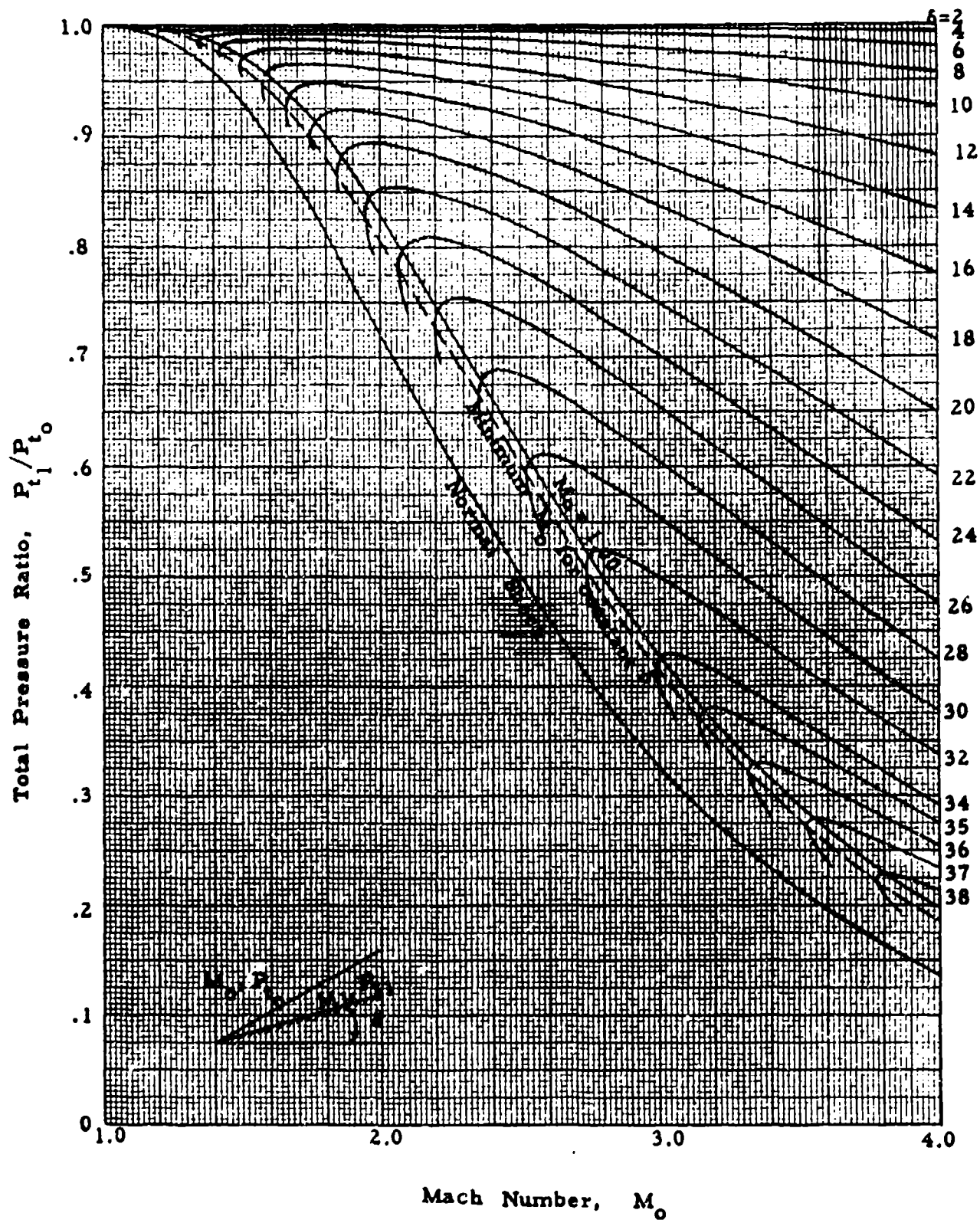
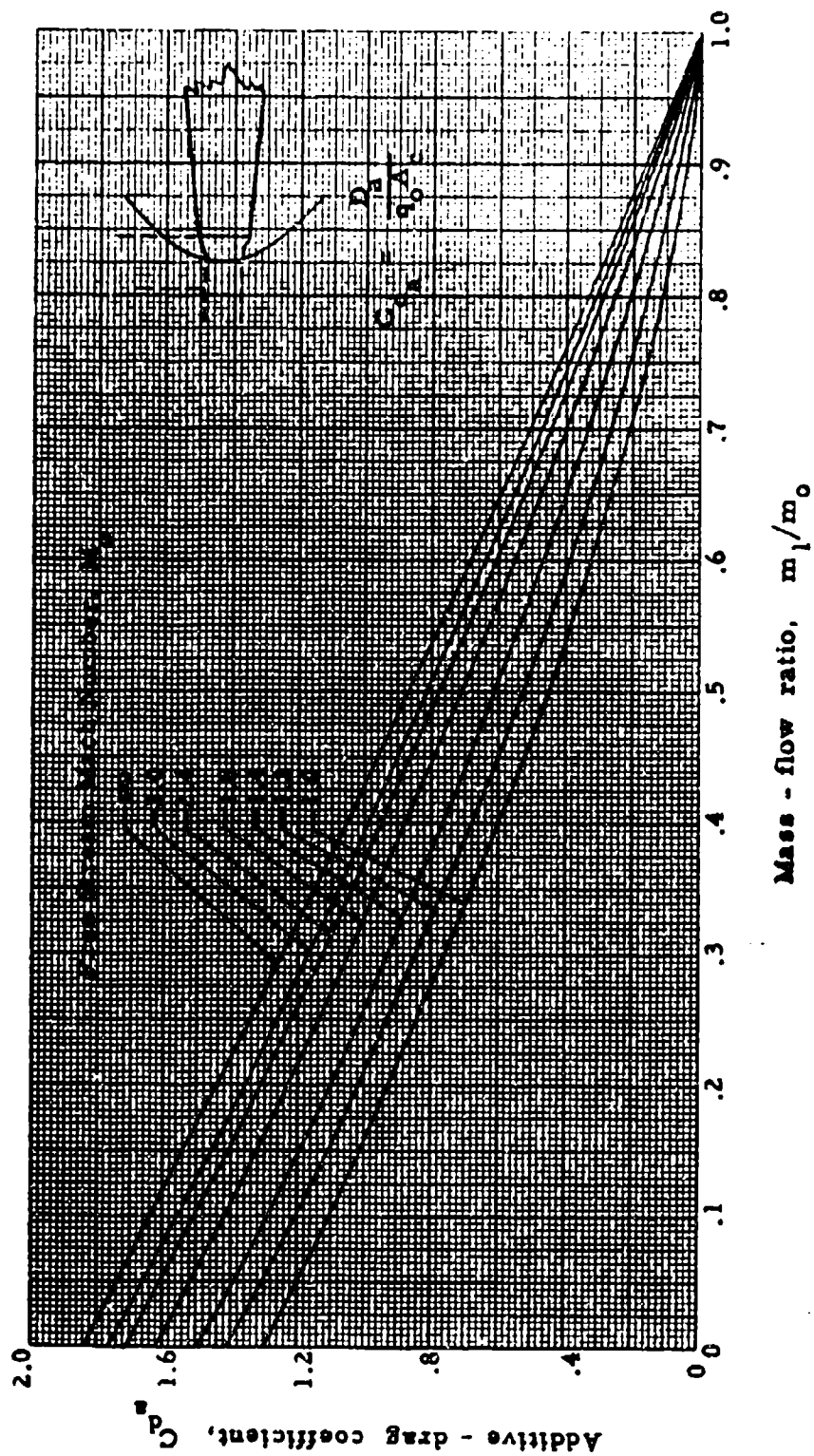
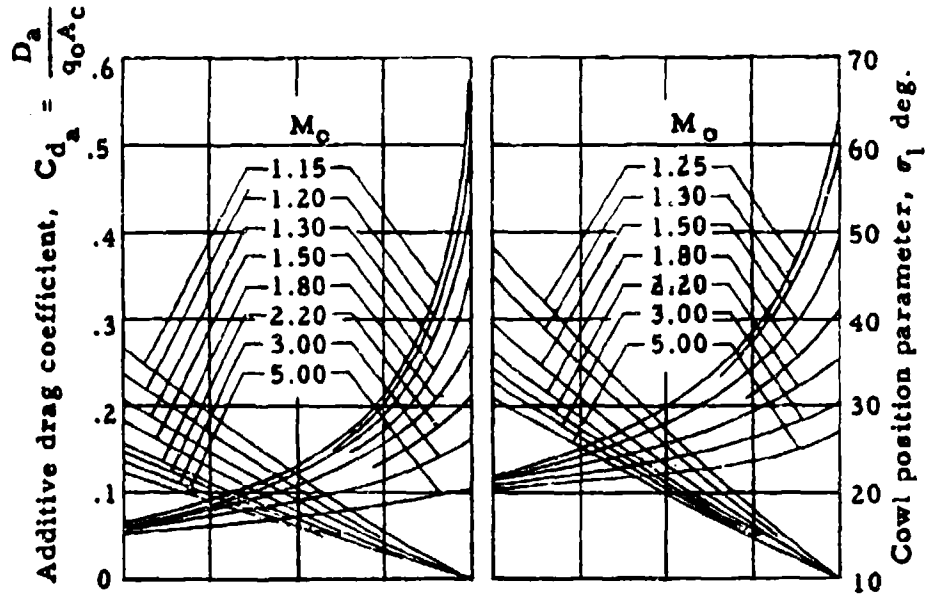


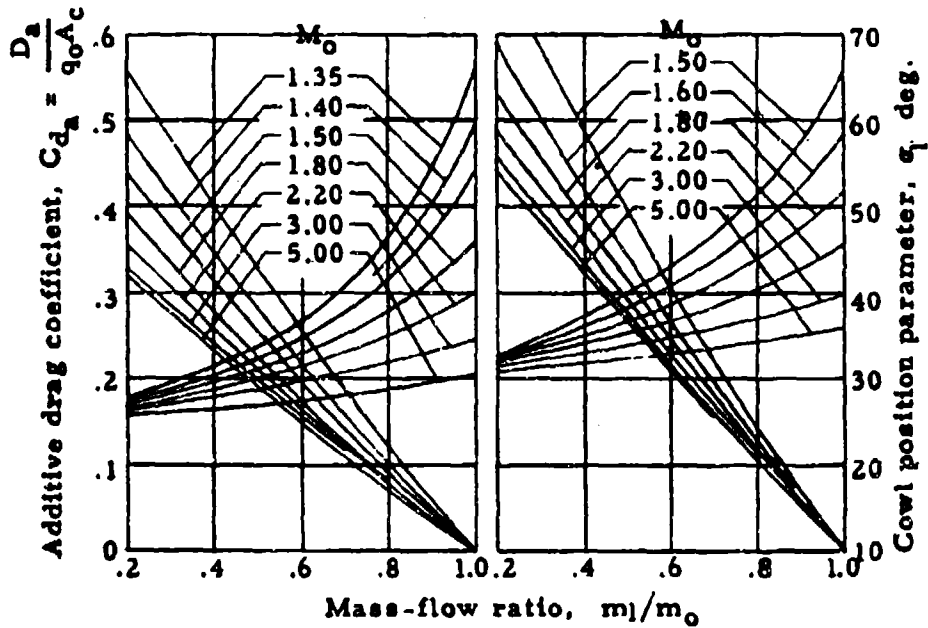
Chart 9.14 THEORETICAL ADDITIVE - DRAG COEFFICIENTS FOR OPEN - NOSED INLETS



**Chart 9.15 THEORETICAL ADDITIVE-DRAG COEFFICIENTS
FOR ANNULAR NOSE INLETS WITH CONICAL FLOW
AT THE INLET**



(a) Cone half-angle 15° (b) Cone half-angle 20°



(c) Cone half-angle 25° (d) Cone half-angle 30°

Chart 9.16 CHANGE IN COWL DRAG COEFFICIENT WITH A CHANGE IN MASS FLOW RATIO AS A FUNCTION OF MACH NUMBER

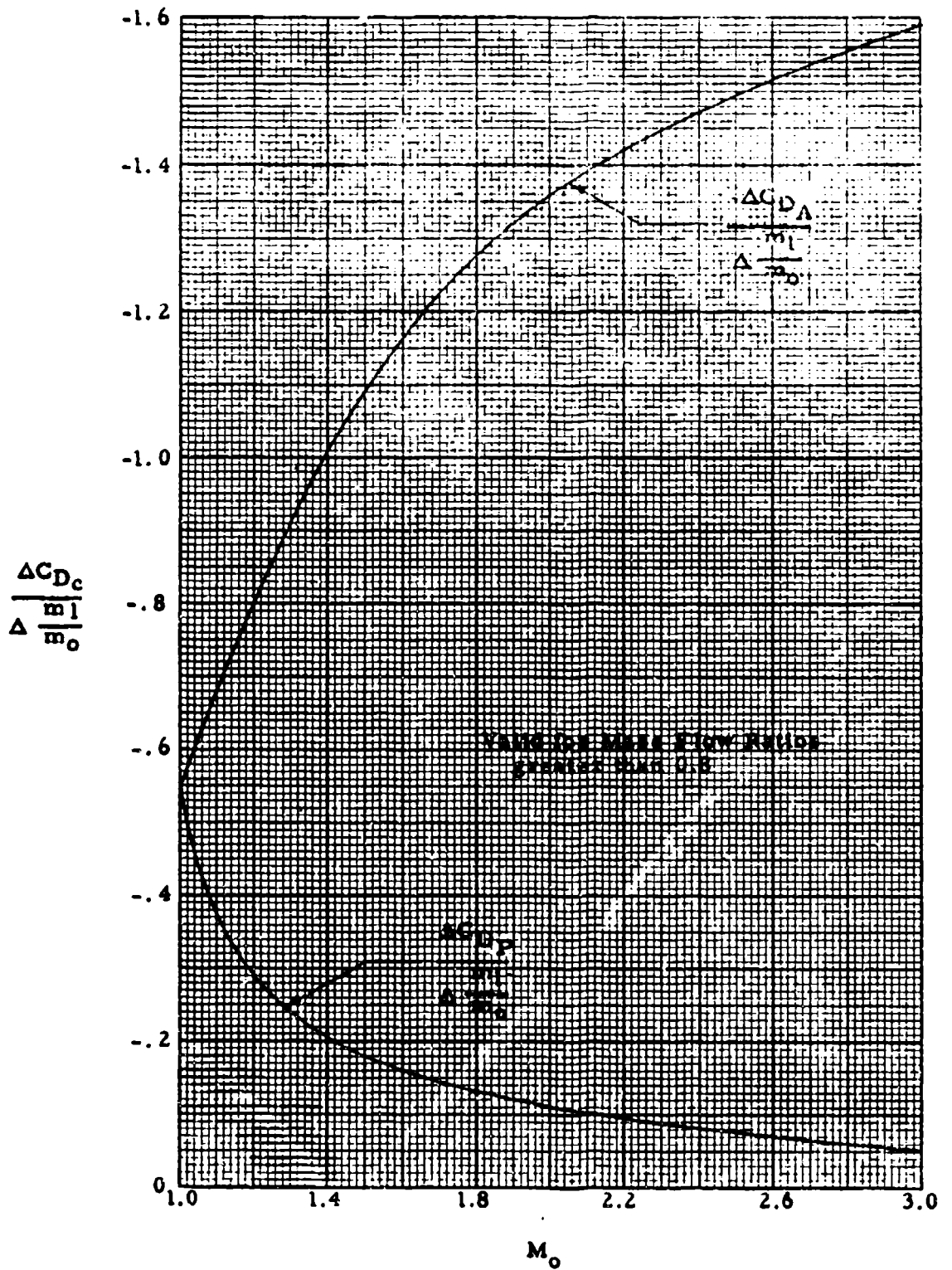


Chart 9.17 IDEALIZED GAS FLOW WITH SUBCRITICAL OPERATION

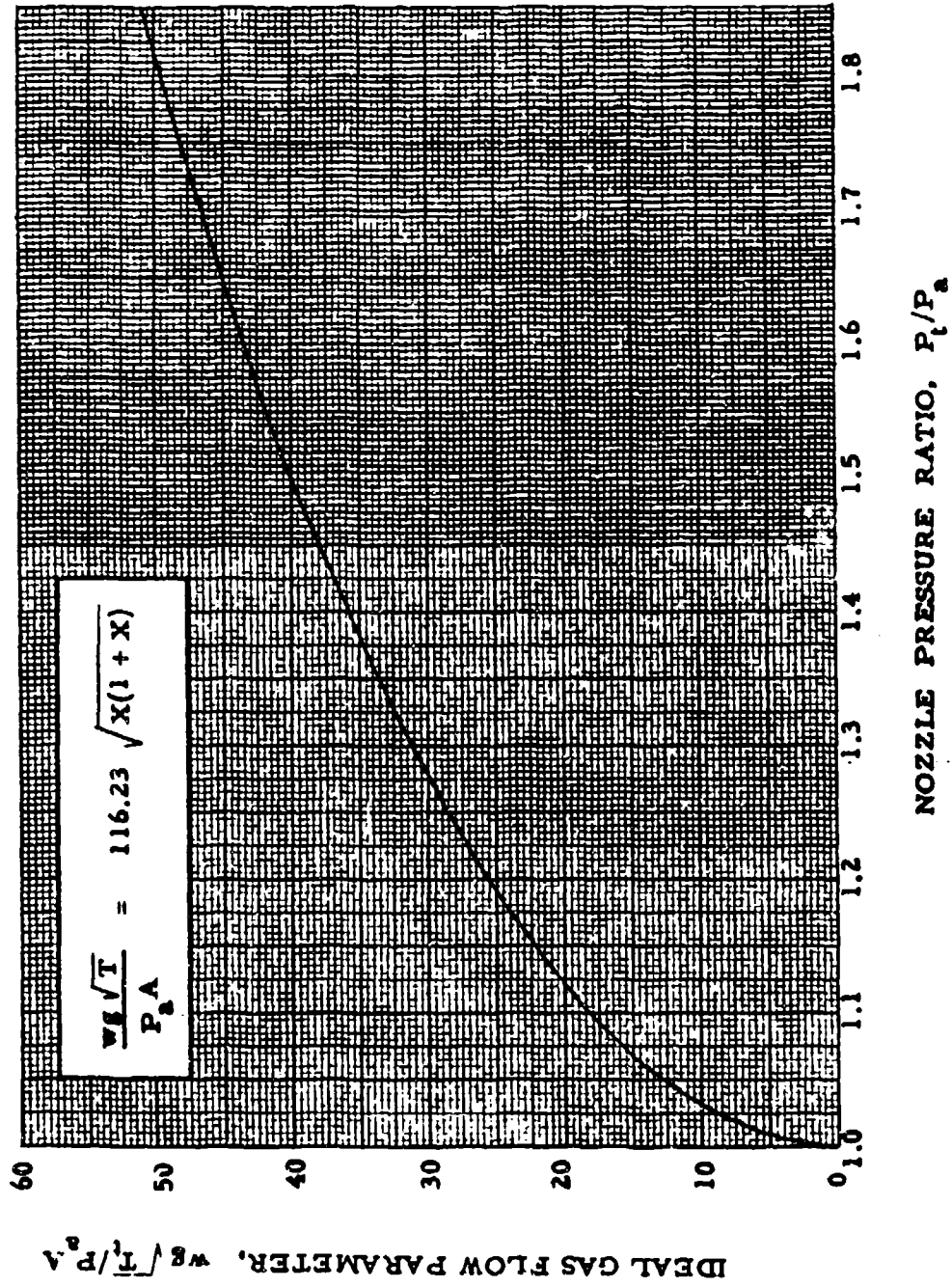


Chart 9.28 IDEALIZED GAS FLOW WITH SUPERCRITICAL OPERATION- CONVERGING NOZZLE

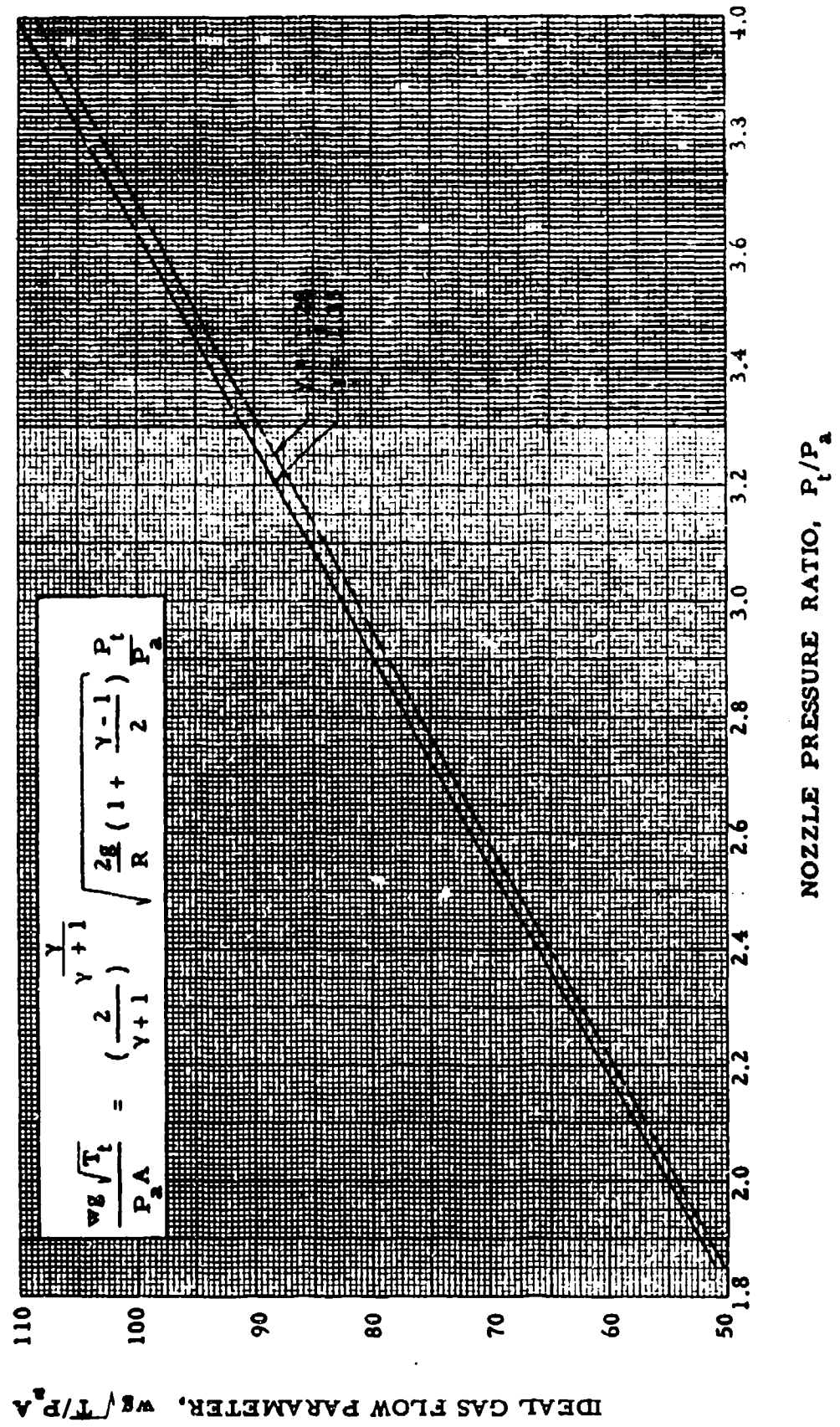
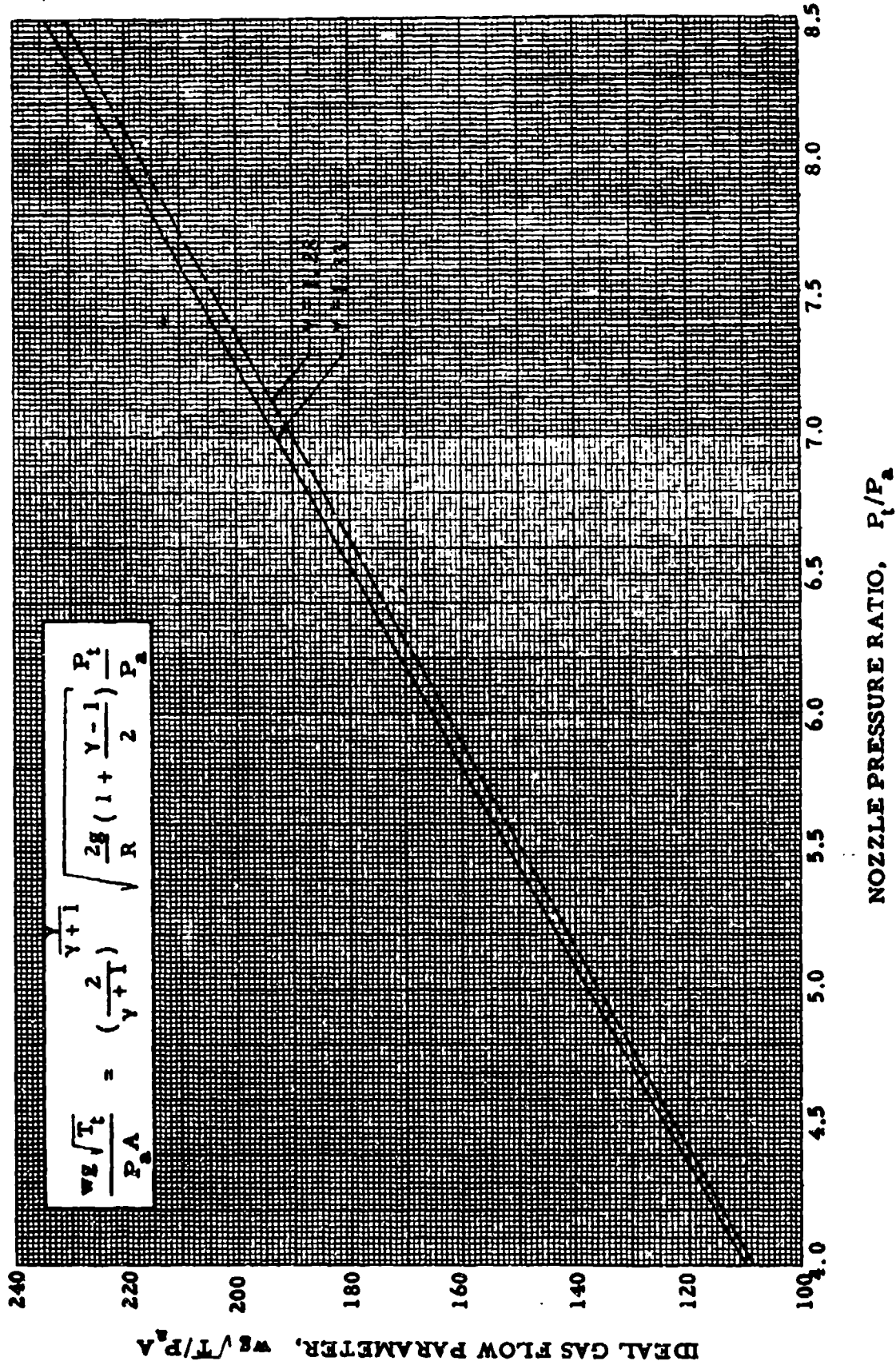


Chart 9.18 IDEALIZED GAS FLOW WITH SUPERCRITICAL OPERATION - CONVERGING NOZZLE



$$\frac{w_s \sqrt{T_1}}{P_1 A} = \left(\frac{2}{\gamma + 1} \right)^{\frac{\gamma + 1}{2}} \sqrt{\frac{2\gamma}{R} \left(1 + \frac{\gamma - 1}{2} \right) \frac{P_1}{P_2}}$$

Chart 9.18 IDEALIZED GAS FLOW WITH SUPERCRITICAL OPERATION - CONVERGING NOZZLE

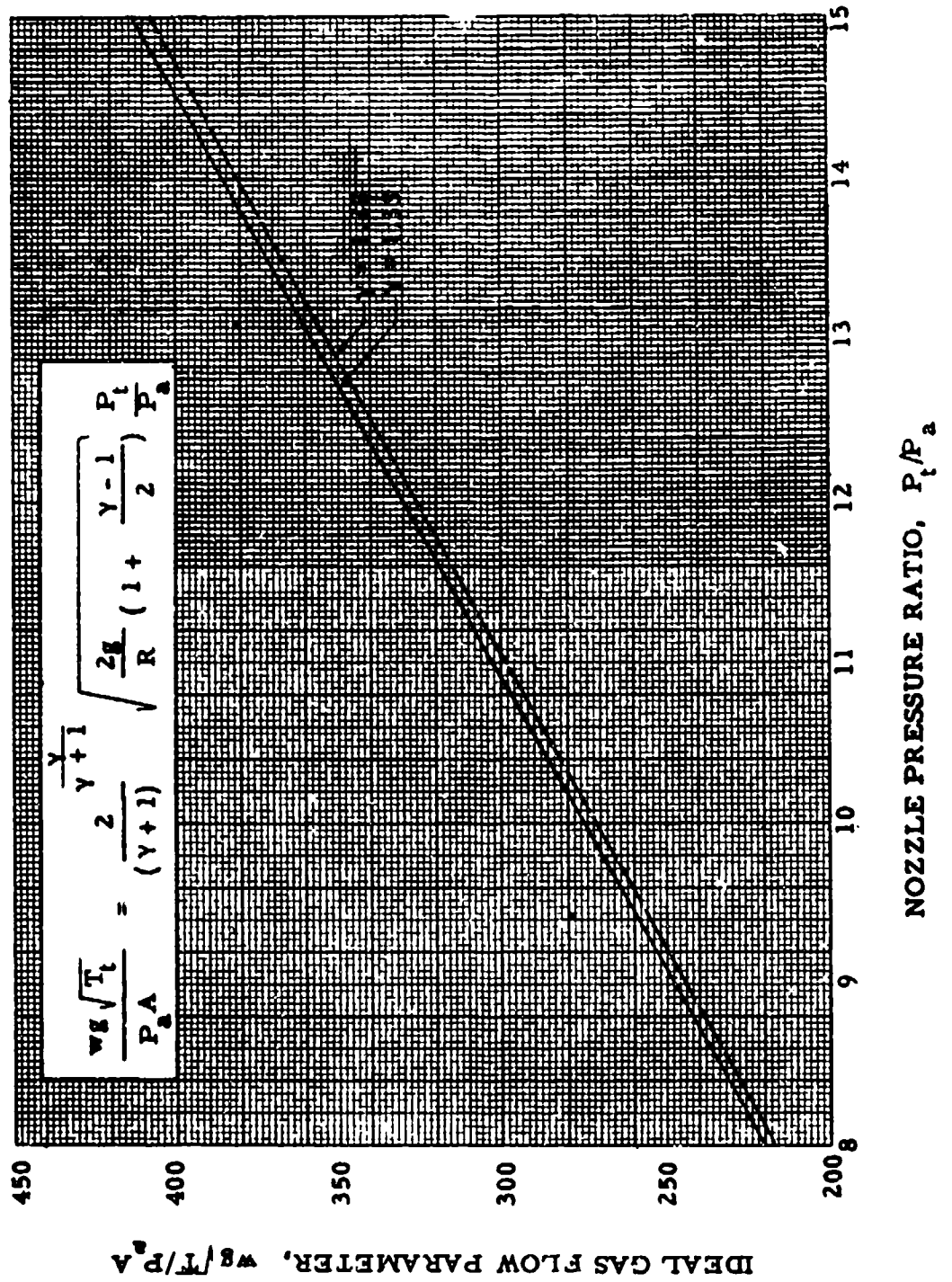


Chart 9.19 GROSS THRUST PARAMETER VERSUS NOZZLE PRESSURE RATIO WITH SUBCRITICAL OPERATION

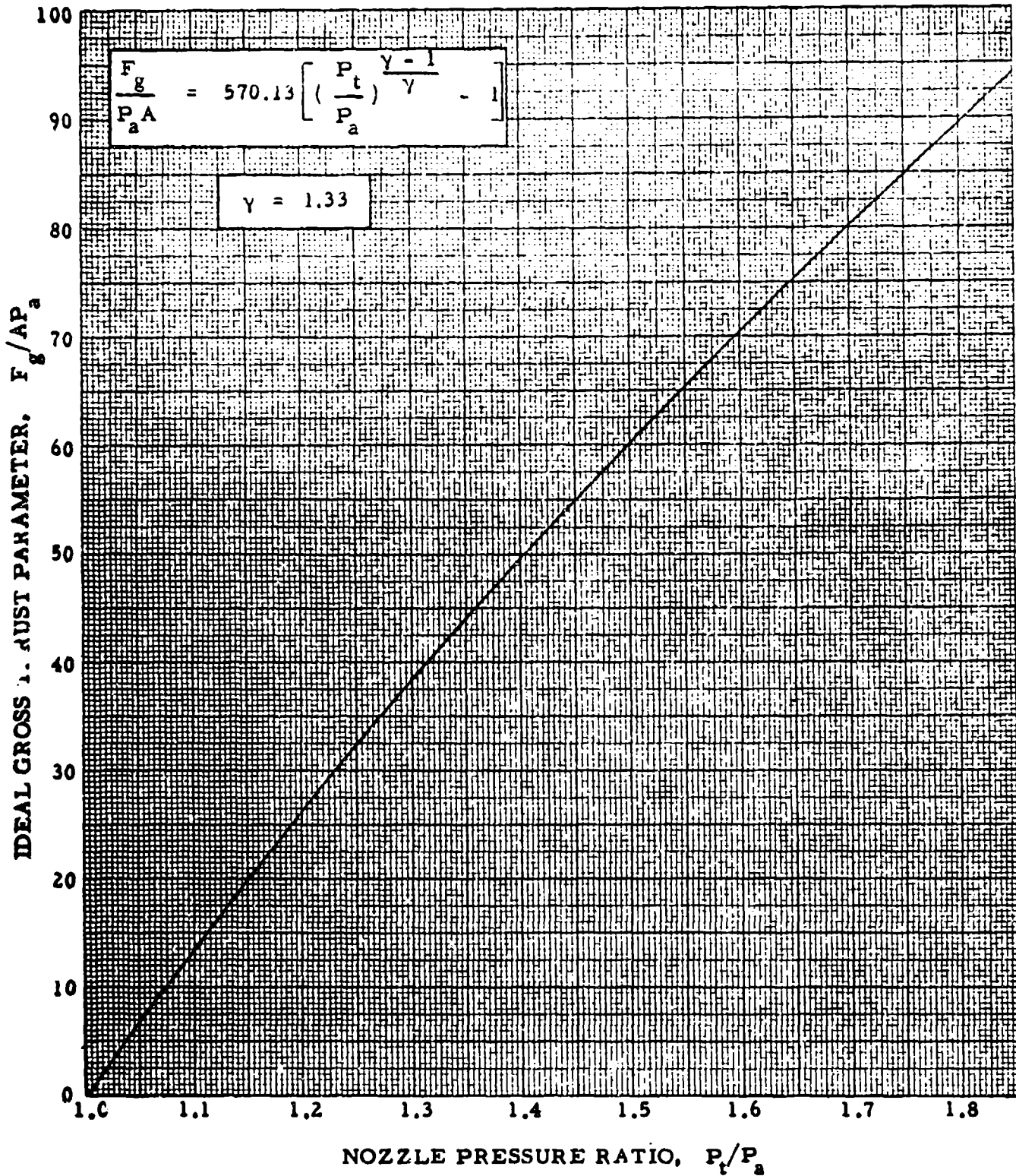


Chart 9.20 GROSS THRUST PARAMETER VERSUS NOZZLE PRESSURE RATIO WITH SUPERCRITICAL OPERATION - CONVERGING NOZZLE

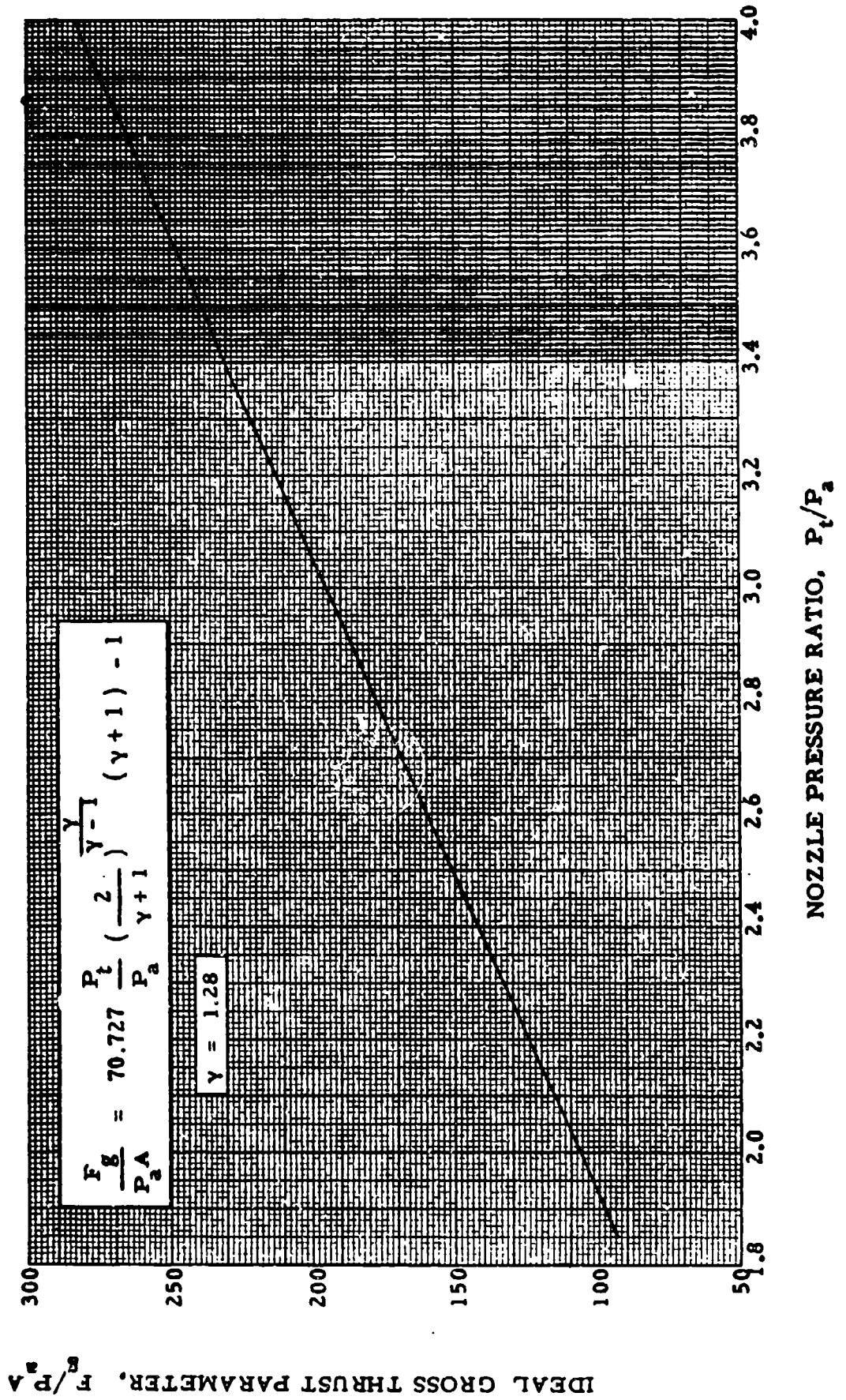


Chart 9.20 GROSS THRUST PARAMETER VERSUS NOZZLE PRESSURE RATIO WITH SUPERCRITICAL OPERATION - CONVERGING NOZZLE

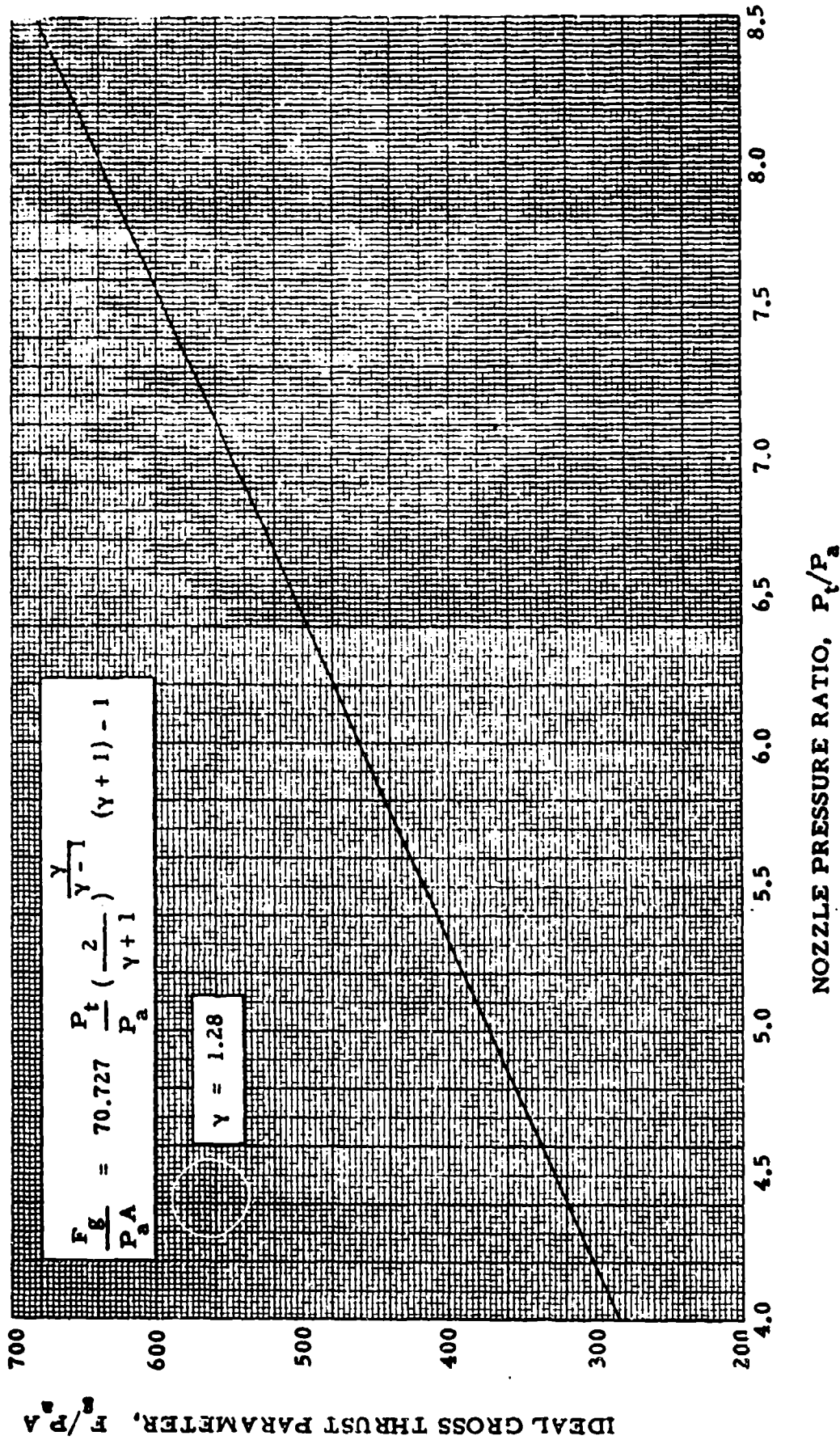


Chart 9.20 GROSS THRUST PARAMETER VERSUS NOZZLE PRESSURE RATIO WITH SUPERCRITICAL OPERATION - CONVERGING NOZZLE

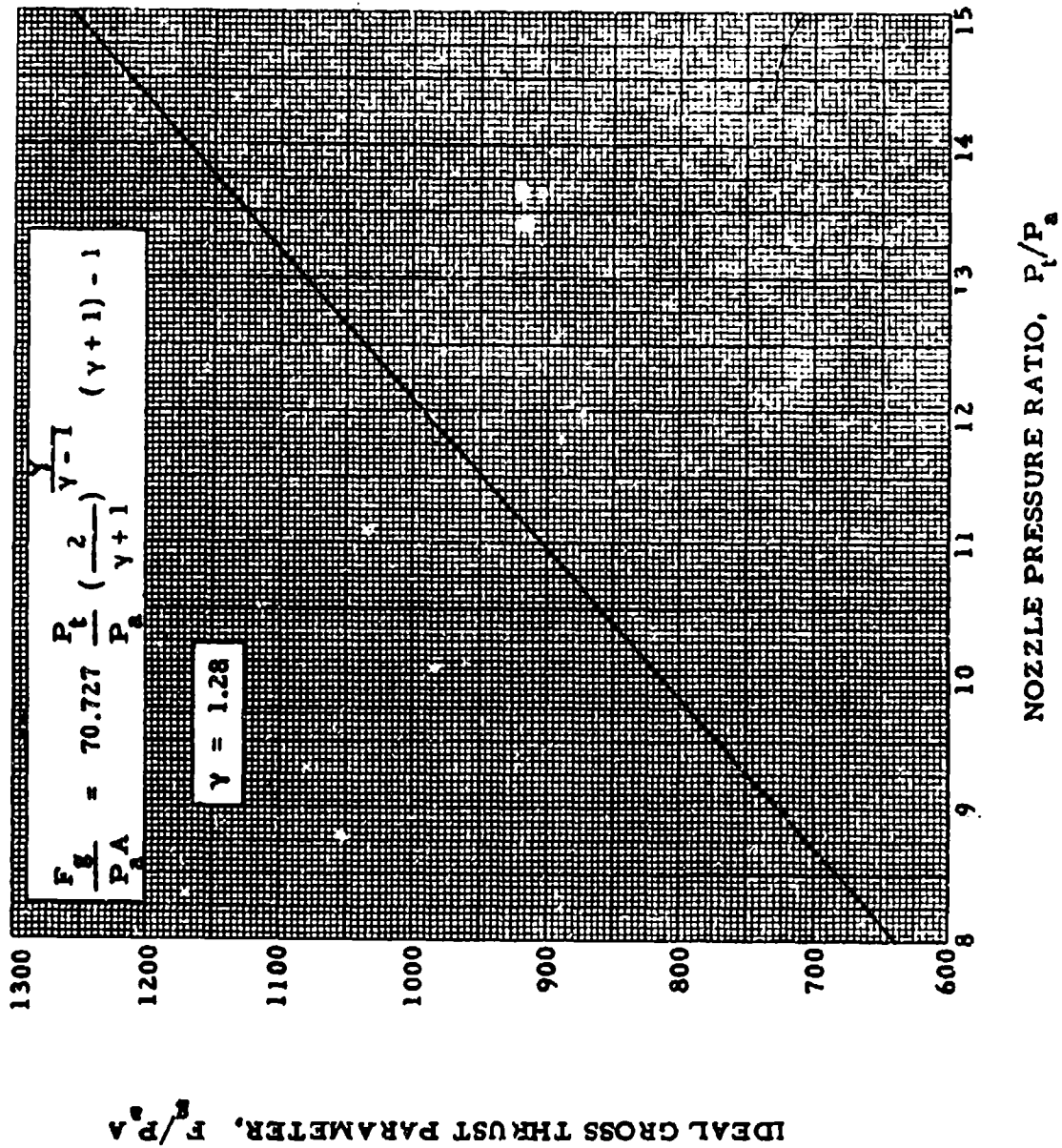


Chart 9.21 GROSS THRUST PARAMETER VERSUS NOZZLE PRESSURE RATIO WITH
 SUPERCRITICAL OPERATION - CONVERGING-DIVERGING NOZZLE

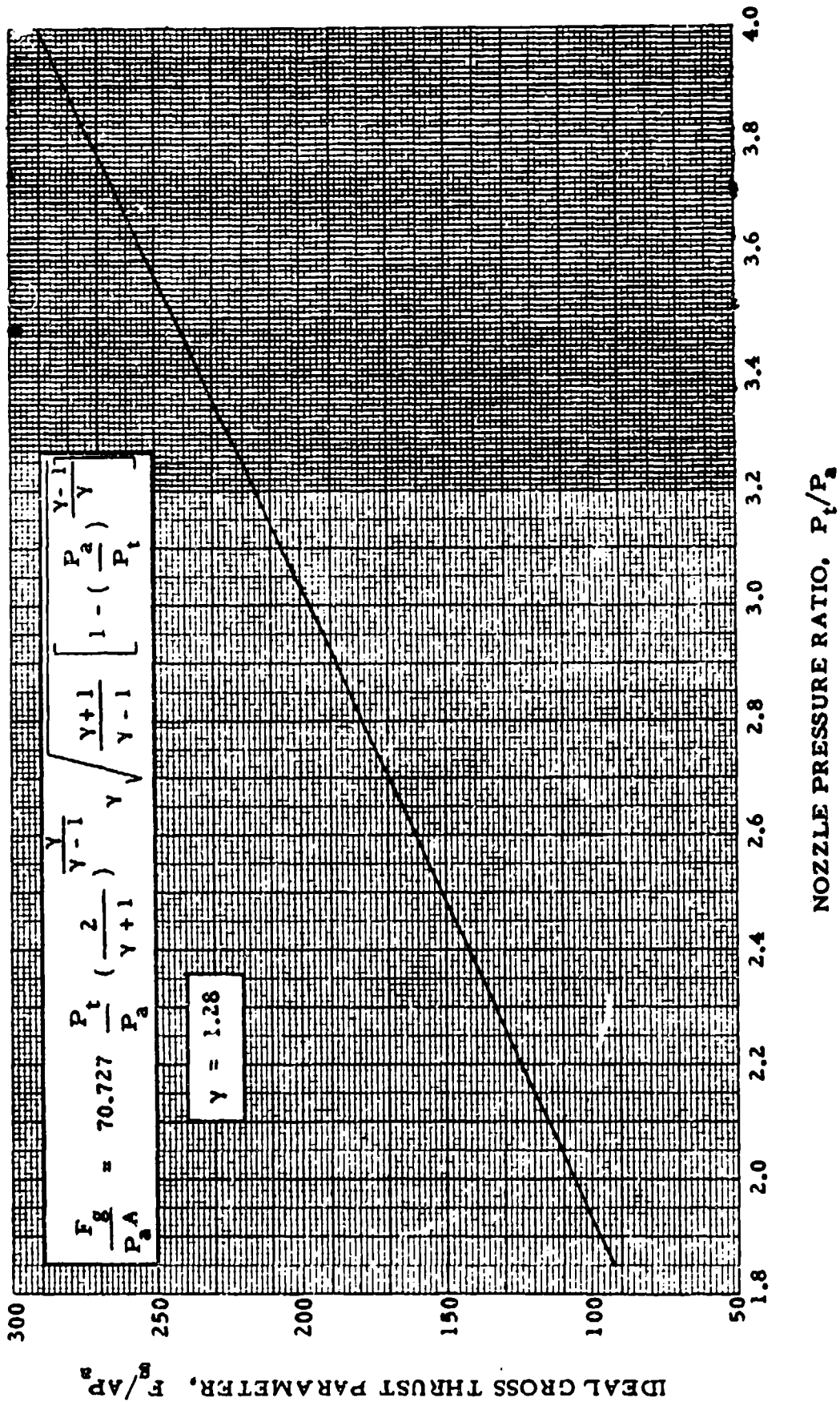


Chart 9.21 GROSS THRUST PARAMETER VERSUS NOZZLE PRESSURE RATIO WITH SUPERCRITICAL OPERATION - CONVERGING-DIVERGING NOZZLE

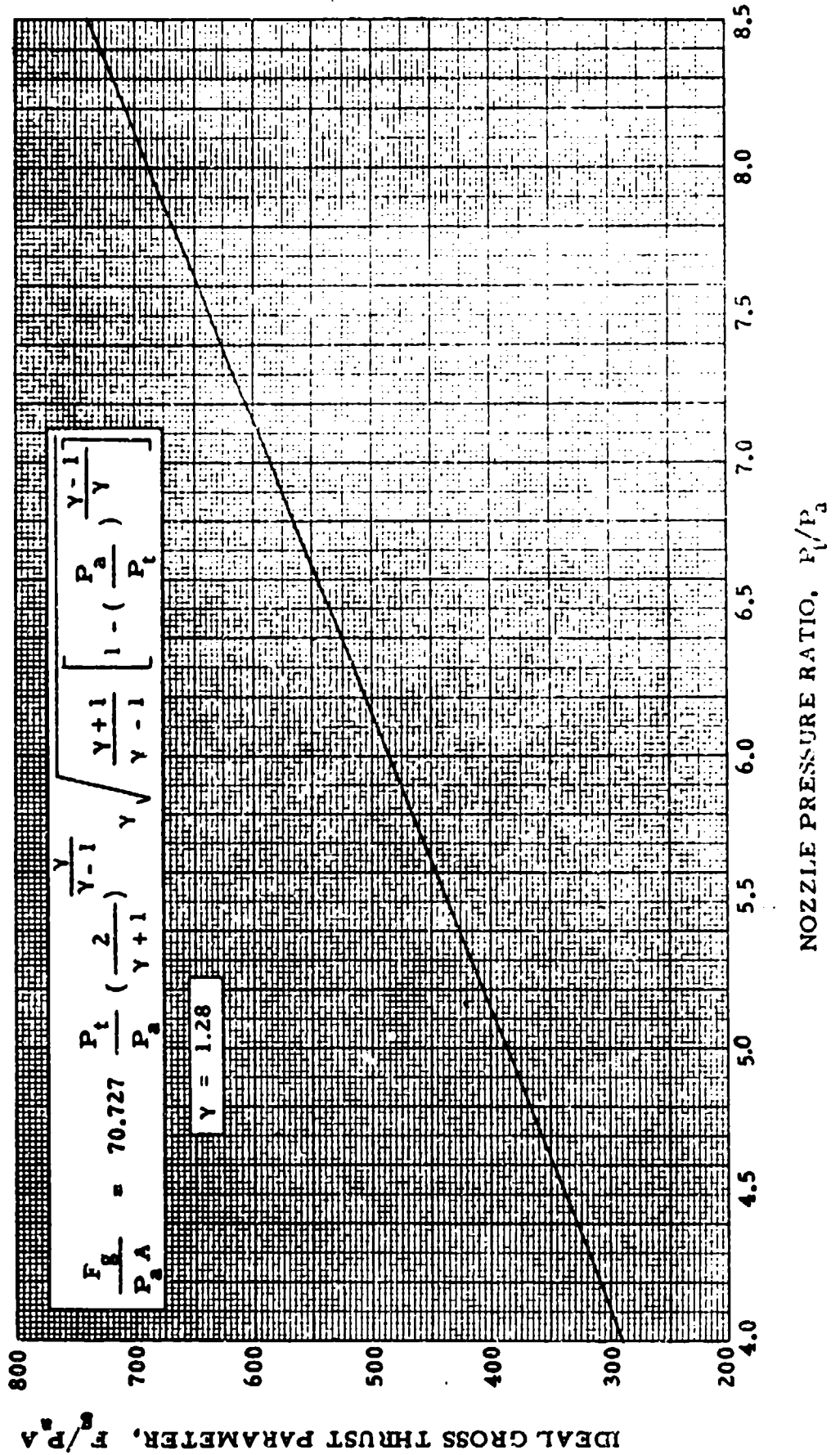


Chart 9.21 GROSS THRUST PARAMETER VERSUS NOZZLE PRESSURE RATIO WITH SUPERCRITICAL OPERATION - CONVERGING-DIVERGING NOZZLE

$$\frac{F_g}{P_a A} = 70.727 \frac{P_t}{P_a} \left(\frac{2}{\gamma + 1} \right)^{\frac{\gamma}{\gamma - 1}} \gamma \sqrt{\frac{\gamma + 1}{\gamma - 1} \left[1 - \left(\frac{P_a}{P_t} \right)^\gamma \right]}$$

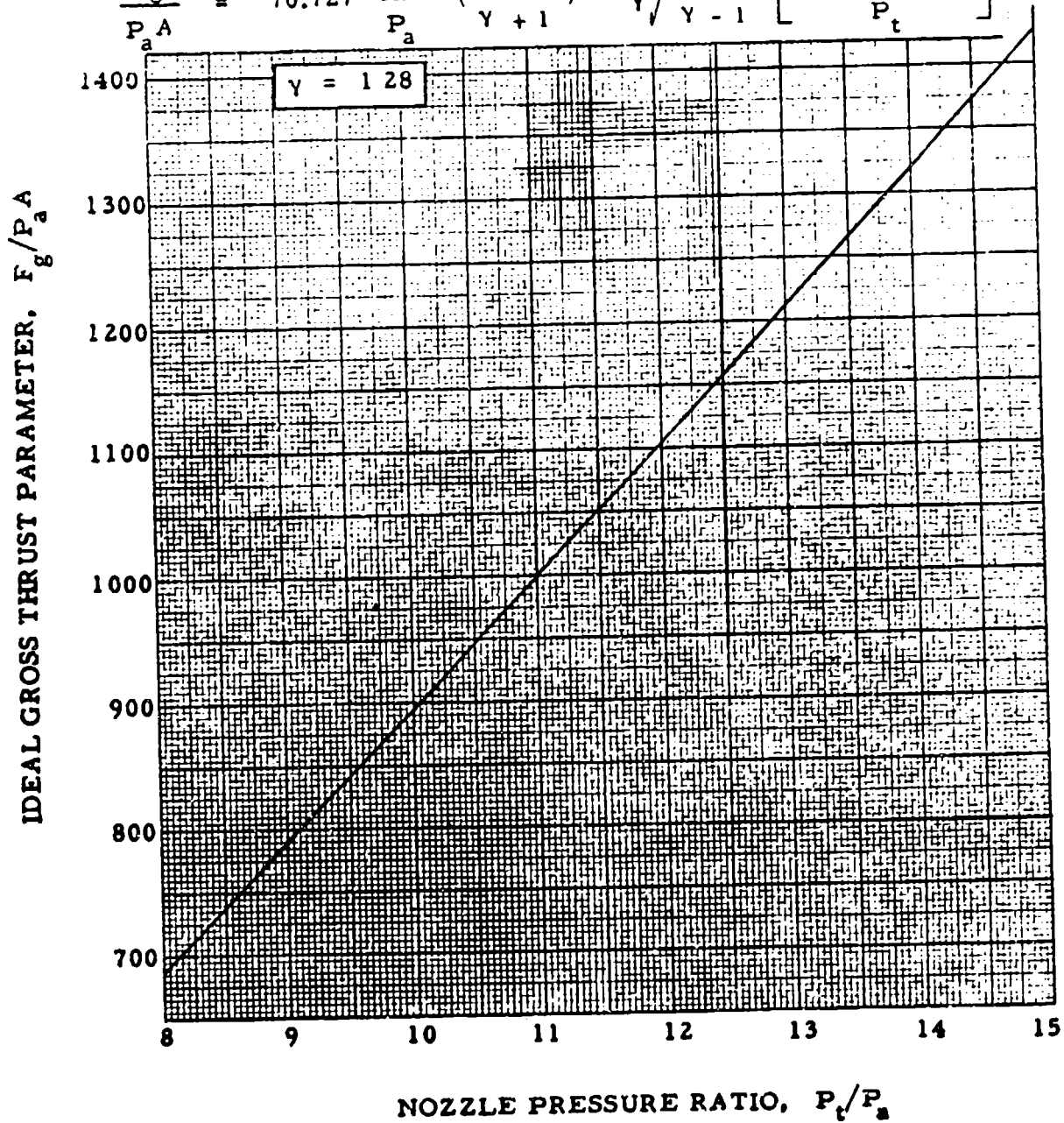


Chart 9.22 P_t'/P_s VERSUS MACH (RAYLEIGH SUPERSONIC PITOT FORMULA)

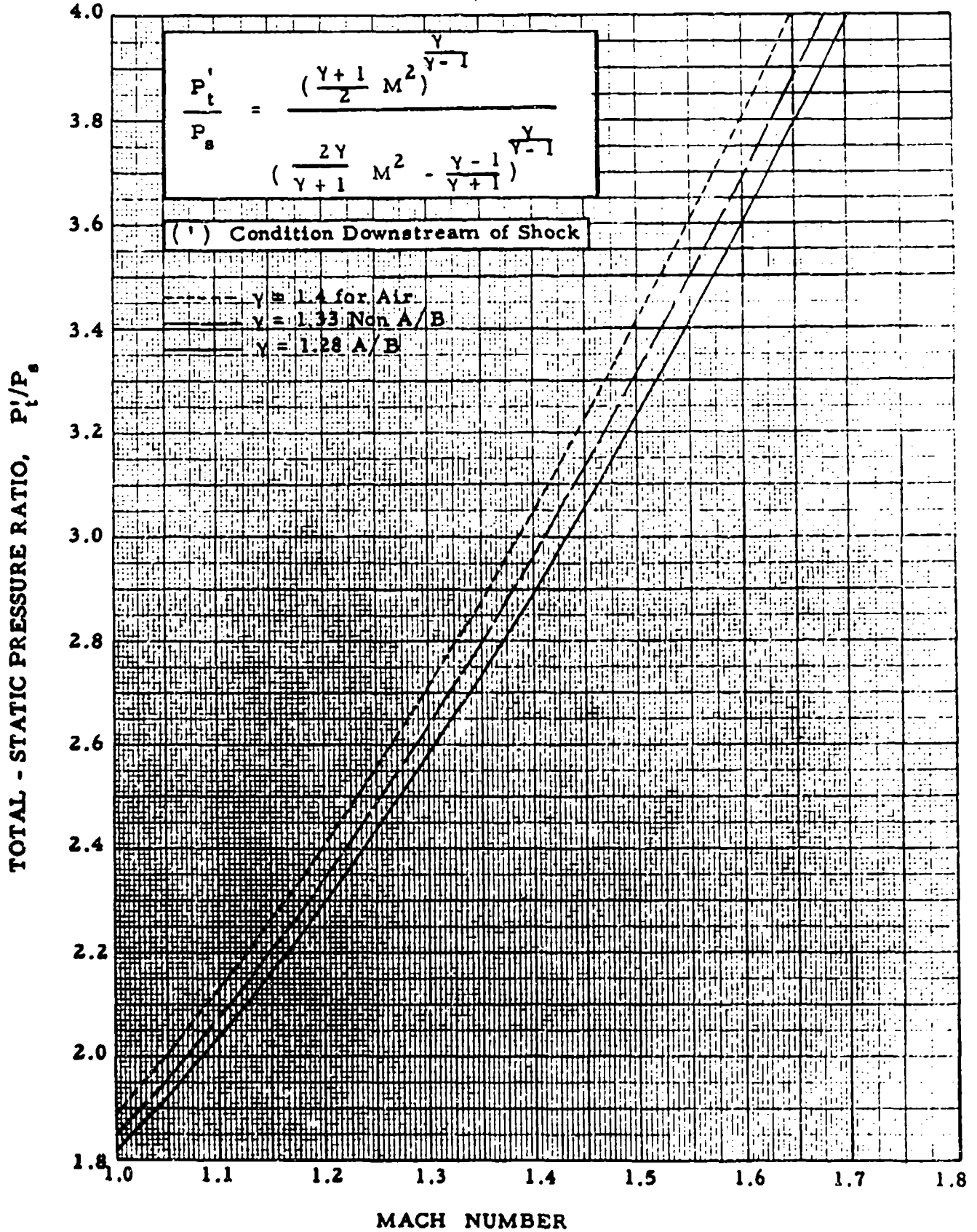


Chart 9.22 P_t'/P_s VERSUS MACH (RAYLEIGH SUPERSONIC
PITOT FORMULA)

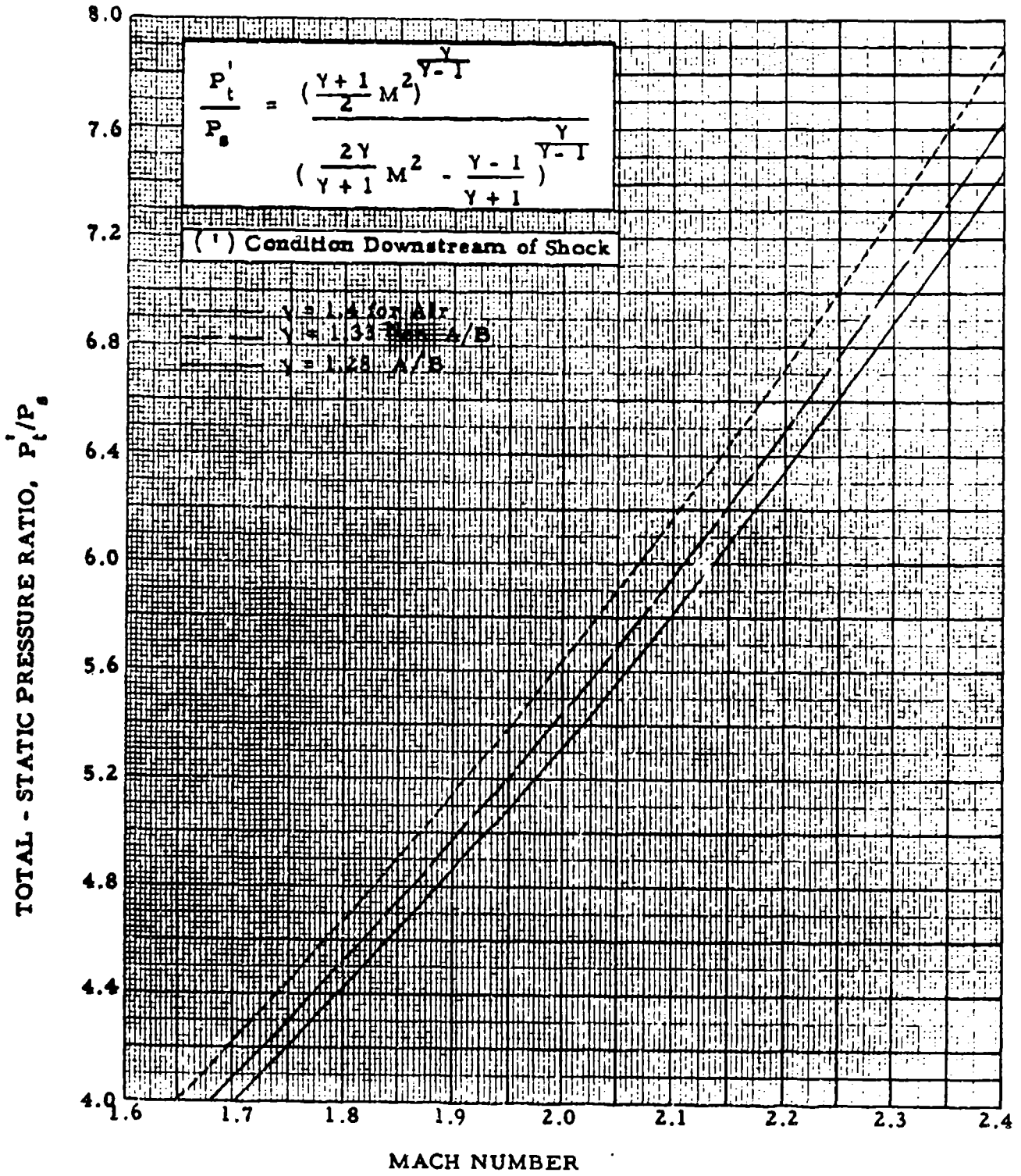
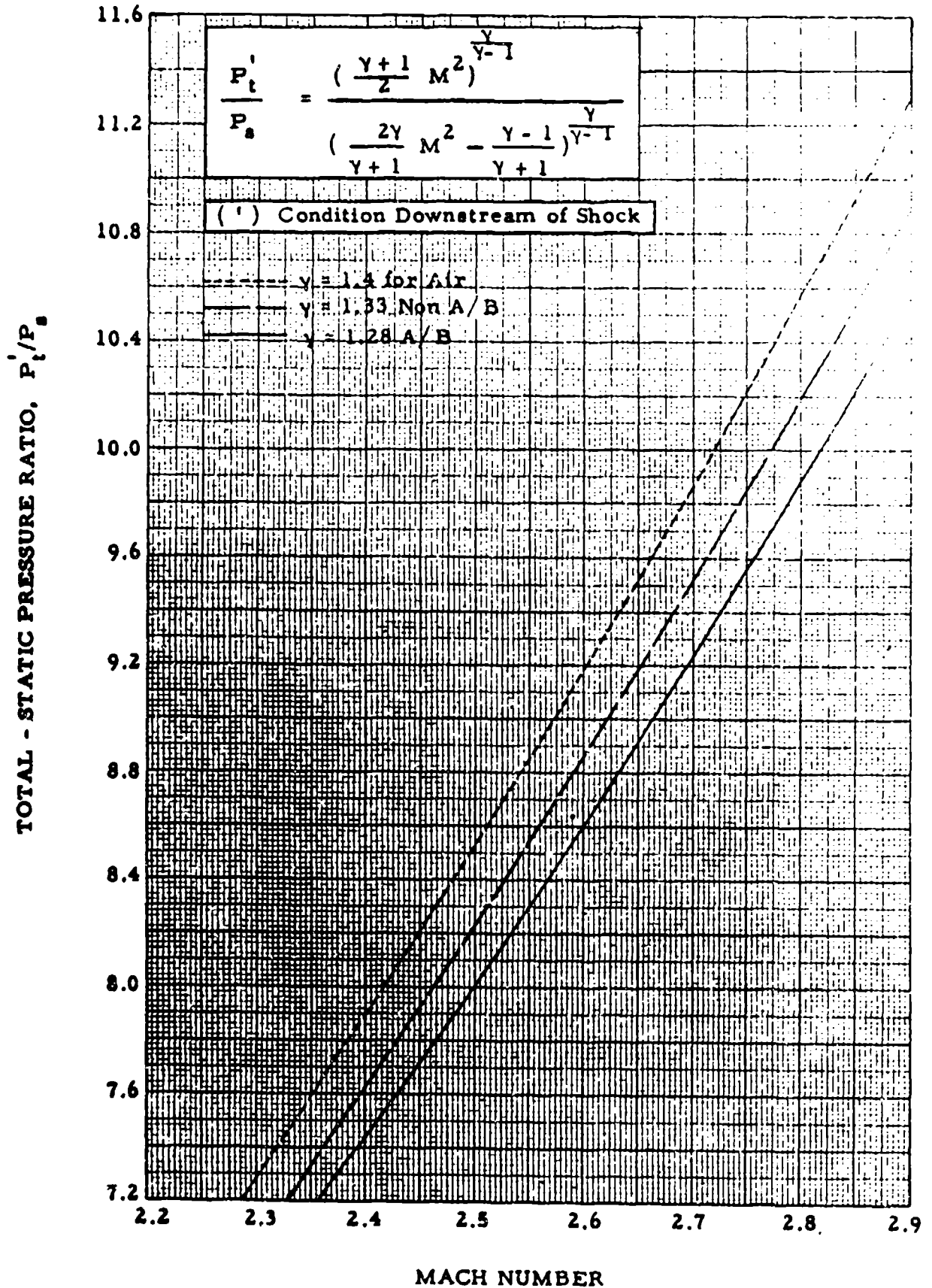


Chart 9.22 P_t'/P_s VERSUS MACH (RAYLEIGH SUPERSONIC
PITOT FORMULA)



CHAPTER FOUR

LEVEL FLIGHT PERFORMANCE

SECTION 4.1

Density Altitude and Pressure Altitude Flight Test Methods

Aircraft level flight performance analysis is the process of determining standard day level flight characteristics from data obtained during nonstandard conditions. Until the advent of high speed aircraft and the accompanying compressibility effects most flight test data were reduced by what is referred to as the "Density Altitude" method. With jet powered aircraft came the necessity of standardizing data for what might be called constant compressibility conditions, thus avoiding compressibility corrections. This latter type of data reduction is called the "Pressure Altitude" method.

The density altitude method of flight test data reduction has been used and, in many cases, is still used in the speed range where the assumption of constant drag for constant true speed and density altitude is valid. However, where effects of compressibility are not negligible this method will result in erroneous standard day data. The pressure altitude method is based on the concept of maintaining a constant pressure altitude and indicated air speed and correcting data only for temperature to obtain standard day performance. With these identical test and standard day indicated air speeds the test and standard day Mach numbers will be the same. This may be easily seen by examination of the Mach number equation (2.23) in terms of q_0 and P_a .

It is shown in aerodynamic theory that total drag is a function only of Mach number if weight and altitude are fixed. (Reynolds number effects are generally ignored in flight test work.) These facts are the basis for the simplicity and effectiveness of the pressure altitude method of flight data reduction. Using it, the performance engineer need make only temperature corrections to his test day data, and compressibility effects are automatically held constant.

As a general rule the pressure altitude method is applied to both reciprocating and jet engine aircraft. For, even in the low speed range, this method simplifies data reduction procedures in all departments of aircraft performance. In the case of reciprocating engine aircraft there is one exception to the pressure altitude method. In this exception a power parameter (PIW) is plotted against a speed parameter (VIW) to obtain a single, standard-day, weight corrected, sea-level, power-required polar for all level flight data. This PIW-VIW polar will not be valid in the compressibility speed range.

SECTION 4.2

Aerodynamic Forces and Their Relation to Engine Power and Propulsive Thrust

The aerodynamic forces acting on an airfoil are assumed to be functions of its size, angle of attack, speed, and atmospheric conditions (temperature, pressure, and viscosity of the air through which it is flying). The two primary forces acting on the unaccelerating aircraft are called the lift force and the drag force, and these may be defined by generalized nondimensional equations:

$$\text{Lift Force} = f(\text{angle of attack, size, speed, temperature, pressure, viscosity}) \quad (4.201)$$

$$\text{Drag Force} = f(\text{angle of attack, size, speed, temperature, pressure, viscosity}) \quad (4.202)$$

Letting the lift force equal the aircraft gross weight, the drag force may be redefined by use of the above equations.

$$\text{Drag Force} = f(\text{weight, size, speed, temperature, pressure, viscosity}) \quad (4.203)$$

By the methods of dimensional analysis equation 4.203 may be transformed to the form:

$$\frac{D}{P_a} = f\left(\frac{W}{P_a}, M, R_e\right) \quad (4.204)$$

(In this form the constant aircraft size factor is omitted)

where:

- D = total aircraft drag
- P_a = atmospheric pressure
- W = aircraft gross weight
- M = Mach number
- R_e = Reynolds number

In most flight test aircraft analysis the small variations of data with Reynolds number are neglected.

By lengthy analytical methods it is possible to develop a physical equation that will approximately define the drag force.

$$D = C_D S \quad (4.205)$$

The total drag coefficient, C_D , is further defined by analytical methods and equals the sum of the profile and induced drag coefficients.

$$C_D = C_{DP} + C_{Di} \quad (4.206)$$

With this equation 4.205 becomes

$$D = C_{DP}(qS) + C_{DI}(qS) \quad (4.207)$$

The induced drag coefficient, C_{DI} is further defined by analytical methods

$$C_{DI} = \frac{C_L^2}{\pi A e} \quad (4.208)$$

And the lift coefficient C_L is defined by analytical methods as:

$$C_L = \frac{W}{qS} \quad (4.209)$$

Substituting these last two equations in 4.207, a final analytical expression for the drag force is obtained.

$$D = C_{DP}(qS) + \frac{W^2}{\pi A e (qS)} \quad (4.210)$$

where:

$$\begin{aligned} q &= \frac{1}{2} \rho V^2 = 0.7 P_a M^2 \\ W &= \text{aircraft gross weight} \\ A &= \text{wing aspect ratio} \\ S &= \text{wing area} \\ e &= \text{wing efficiency factor} = \frac{C_L^2}{(C_D - C_{DP}) \pi A} \end{aligned}$$

Experimental wind-tunnel data show that C_{DP} is primarily a function of Mach number and lift coefficient, remaining constant until compressibility effects are evident at ($M \approx 0.5$). In this compressible range C_{DP} may also be appreciably affected by changes in C_L . It should be noted that the validity and usefulness of all aircraft performance parameters depend on the validity of the prevailing assumptions concerning C_{DP} .

Assuming C_{DP} to remain constant for the speed range of most reciprocating engine aircraft, several functional modifications of equation 4.210 may be derived in terms of speed, Mach number, thrust horsepower, gross weight, and atmospheric conditions.

$$THP = C_{DP} \sigma V^3 S k_1 + \frac{W^2 k_2}{\sigma V b^2 e} \quad (4.211)$$

In this form (THP) is a function of true velocity, density ratio and gross weight

$$THP \sqrt{\sigma} = k_1 C_{DP} (\sigma V^2)^{3/2} S + \frac{W^2 k_2}{\sqrt{\sigma V^2} b^2 e} \quad (4.212)$$

In this form $(\text{THP}\sqrt{\sigma})$ is a function of (σv^2) or v_e^2 and gross weight.

$$\frac{\text{THP}\sqrt{\sigma}}{W^{3/2}} = C_{DP} k_1 \left(\frac{\sigma v^2}{W}\right)^{3/2} S + \frac{k_2}{\left(\sqrt{\frac{\sigma v^2}{W}}\right) b^2 e} \quad (4.213)$$

In this form $(\text{THP}\sqrt{\sigma}/W^{3/2})$ is a function only of $(\sigma v^2/W)$

$$\frac{\text{THP}}{P_a \sqrt{T_a}} = C_{DP} M^3 S k_3 + \left(\frac{W}{P_a}\right)^2 \frac{k_4}{M b^2 e} \quad (4.214)$$

In this form $(\text{THP}/P_a \sqrt{T_a})$ is a function of Mach number and (W/P_a)

$$\frac{D}{P_a} = k_5 C_{DP} M^2 S + \left(\frac{W}{P_a}\right)^2 \frac{k_6}{M^2 b^2 e} \quad (4.215)$$

In this form (D/P_a) is a function of Mach number and (W/P_a) . These last two equations are both valid in the compressible speed range because M and (W/P_a) define C_{DP} . In the incompressible range C_{DP} is constant for all Mach numbers and (W/P_a) 's; in the compressible range C_{DP} as a function of M must be plotted for separate (W/P) parameters. It should be noted that at a constant Mach number an increasing value of (W/P_a) corresponds to an increase in C_L . It should also be noted that equation 4.204, derived by dimensional analysis, verifies 4.215.

The following notation applies to equations 4.211 through 4.215.

- THP = $(DxV)/326$, or BHPx η_p , = thrust horsepower
- η_p = Propeller efficiency
- σ = ρ/ρ_{SL} , = $9.625 P_a/T_a$, density ratio
- v = True speed, knots
- S = Wing area, ft^2
- W = lbs, gross weight
- b^2 = ft^2 , $R \times S$, wing span
- e = Airplane efficiency factor
- $v\sqrt{\sigma}$ = v_e = knots, equivalent speed
- P_a = inches Hg, atmospheric pressure
- T_a = °Kelvin, atmospheric temperature
- M = Mach number, $v/38.94 \sqrt{T_a}$, or $\sqrt{1/.7 P_a}$
- D = lbs, drag or propulsive thrust, F_n
- k_1 = 1.0414×10^{-5}
- k_2 = .28820
- k_3 = 5.9205
- k_4 = 7.6885×10^{-4}
- k_5 = 49.5089
- k_6 = 6.4293×10^{-4}

Graphically equations 4.210 through 4.215 all take the same general parabolic form as shown in Figure 4.21. Certain useful information concerning each type of plot is noted.

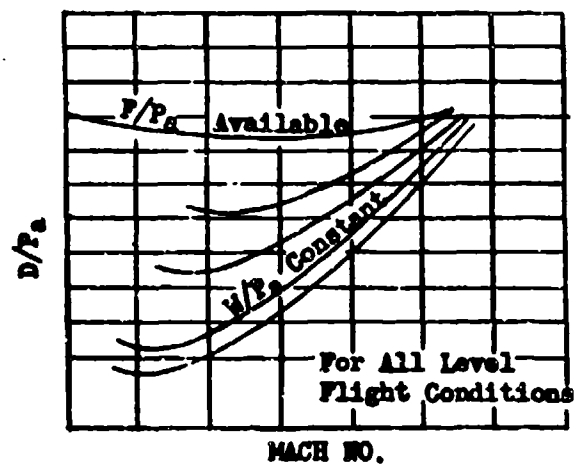
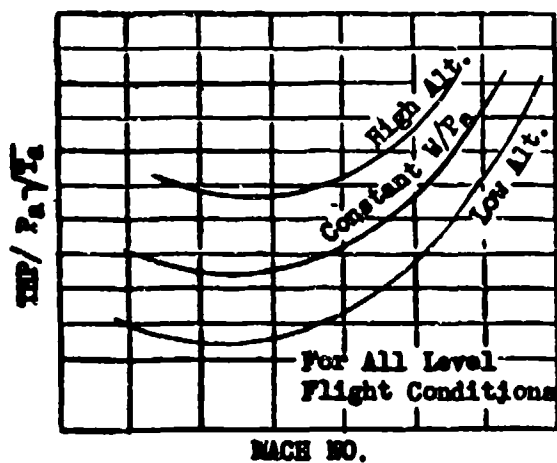
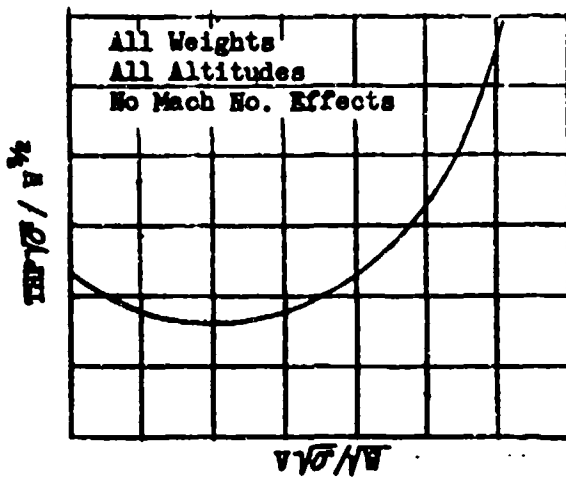
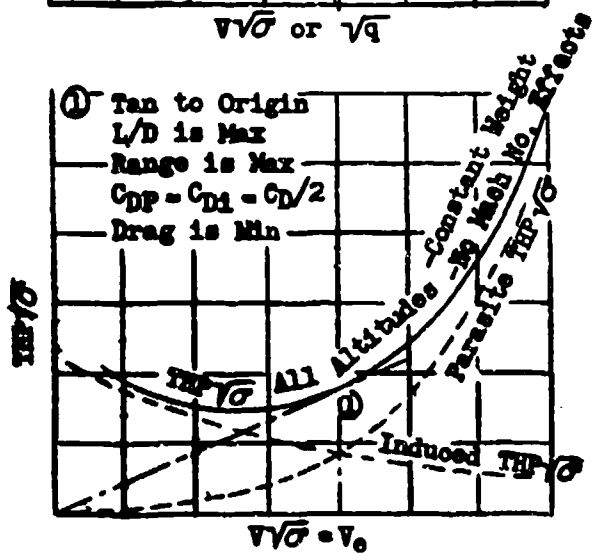
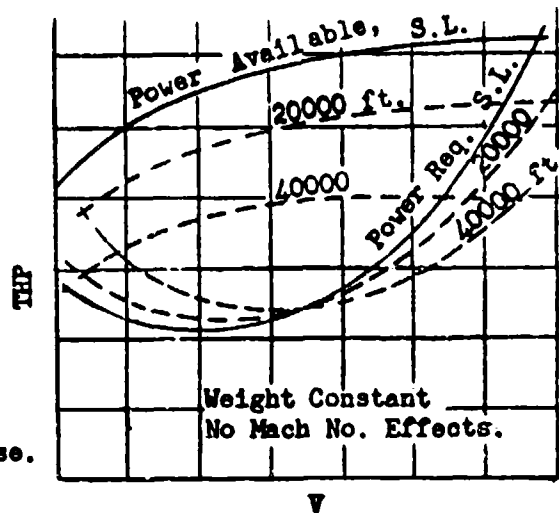
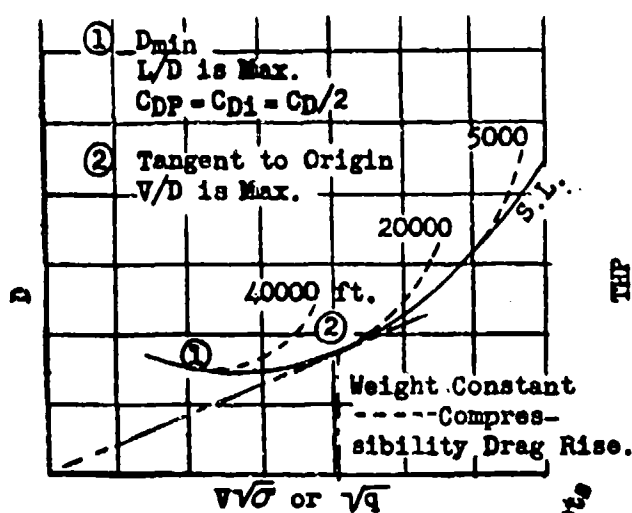


Figure 4.21
Polar Forms for Various Aircraft Performance Parameters.

SECTION 4.3

Speed Power Curves - Reciprocating Engine Aircraft

Equation 4.214 is the basis for the pressure altitude method of level flight data reduction. If a series of points is flown at a constant pressure altitude and weight, Mach number may be plotted against $THP/\sqrt{T_a}$.

$$\frac{THP}{\sqrt{T_a}} = f(M) \quad \begin{array}{l} \text{weight constant} \\ \text{pressure constant} \end{array} \quad (4.301)$$

Since engine brake horsepower is the desired power criteria, the difference between brake horsepower and thrust horsepower must be considered.

$$THP = \text{propeller efficiency } (\eta_p) \times BHP$$

The actual determination of the propeller efficiency is not generally required, because performance is to be measured in terms of engine shaft power. In order to insure that the performance parameters are valid on a standard day or a test day, it is necessary to consider the variation of propeller efficiency between two points flown at the same Mach number and pressure altitude but at different temperatures. Experience has shown that this variation in propeller efficiency is usually negligible, so equation 4.301 is valid in terms of brake horsepower for a constant weight and a constant pressure altitude.

$$\frac{BHP}{\sqrt{T_a}} = f(M) \quad (4.302)$$

For convenience in plotting the horsepower parameter is written, $BHP_t \sqrt{T_{as}/T_{at}}$, where T_{as} is the standard day temperature at the pressure altitude under consideration. This notation has a major value in that the radical, $\sqrt{T_{as}/T_{at}}$, equals unity on a standard day and the plot shows directly the standard day horsepower required to produce any given Mach number.

Another form of pressure altitude plot may be derived by considering Mach number as a function of calibrated speed (V_c) and pressure altitude (H_c) as defined in Chapter One.

$$BHP \sqrt{\frac{T_{as}}{T_{at}}} = f(V_c) \quad \begin{array}{l} \text{weight constant} \\ \text{atmospheric pressure constant} \end{array} \quad (4.303)$$

Typical plots of the horsepower parameter, $BHP \sqrt{T_{as}/T_{at}}$, vs M and V_c are shown in Figure 4.31.

From plots such as those in Figure 4.31 A & B the graphs of standard-day brake horsepower vs true speed may be drawn by simply converting V_c and H_c , or M and T_{as} for H_c , into standard-day true speed. In fact, this standard true speed may be computed and plotted vs $BHP \times \sqrt{T_{as}/T_{at}}$ as in Figure 4.31 without making the V_c or M plot shown. It should be remembered that the aircraft weight

has been assumed constant. Actually each level flight at a constant altitude will have to be at a different weight and will have to be corrected to a constant weight.

Cross plots of the BHP vs V_t plots and engine data at the various altitudes are made for report presentation to show standard-day true-speed altitude plots for normal rated power and for military power as shown in Figure 4.32.

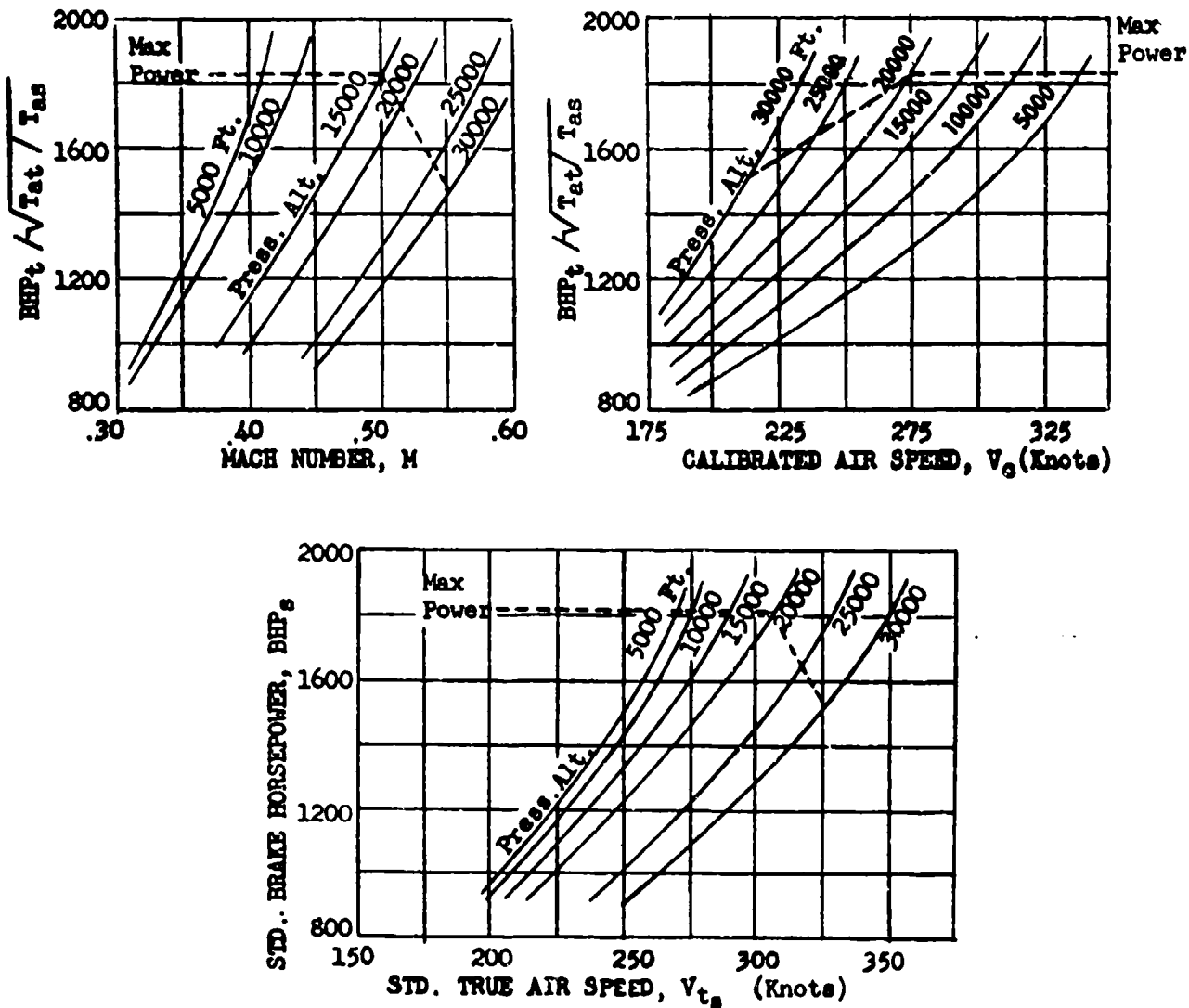


Figure 4.31
Typical Pressure Altitude Speed-Power
Plots for Level Flight

Level Flight Data

Intercooler Flaps 2° ● Approximately 10,000 Ft.
 Intercooler Flaps 5° ● Approximately 20,000 Ft.
 Intercooler Flaps 5° ● Approximately 30,000 Ft.
 --- Military Power 2700 RPM, 60 "Hg
 --- M R P 2550 RPM 50.5 "Hg

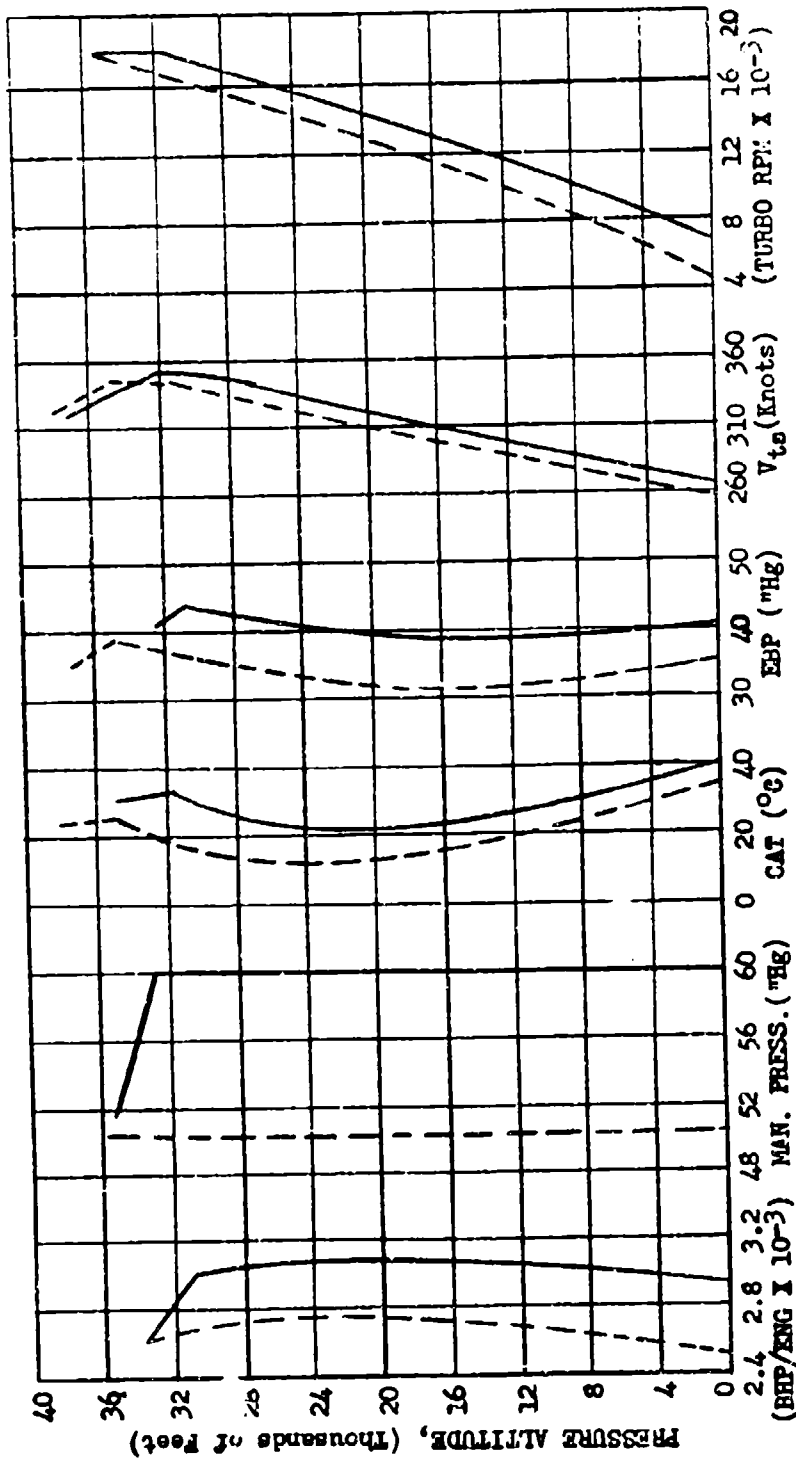


Figure 4.32
 Level Flight Power Data

SECTION 4.4

Weight Corrections for Speed Power Data
- Reciprocating Engine Aircraft

The speed power relationships would be completely defined if all tests could be run at desired weight at constant pressure altitude; however, varied test conditions and fuel consumptions generally make this impossible. A weight correction is usually made to all data at a given pressure altitude to make it represent a fixed weight. The standard weight is usually defined as the weight the aircraft would have if it started at its normal take-off gross weight and climbed to the specified altitude at best climb power and speed settings. The correction is made by considering the isolated effect of a change of weight on $BHP_t \sqrt{T_{as}/T_{at}}$ at a constant Mach number or V_0 and pressure altitude.

Since the correction is to be made at a constant Mach number and will involve only small changes in angle of attack, C_{DP} will be assumed constant. Using equation 4.214 with C_{DP} held constant;

$$\Delta \left(\frac{TEP}{P_a \sqrt{T_a}} \right) = \Delta \left(\frac{W^2 k_p}{P_a^2 M b^2 e} \right) \quad (4.401)$$

Converting to brake horsepower and a constant pressure altitude, temperature, and Mach number

$$\Delta BHP \sqrt{\frac{T_{as}}{T_{at}}} = \frac{\Delta W^2 k_p \sqrt{T_{as}}}{\eta_p P_a M b^2 e} \quad (4.402)$$

where:

$$\begin{aligned} \Delta BHP &= BHP_s - BHP_t \\ \Delta W &= W_s - W_t \\ k_p &= 7.6885 \times 10^{-4} \\ \eta_p &= 0.83, \text{ average value} \\ e &= 0.77, \text{ average value} \end{aligned}$$

The values of propeller efficiency and airplane efficiency within normal flying speeds of propeller driven aircraft are approximately constant. At speeds less than 30% greater than stall speed, differences between test weight and standard weight should be maintained less than 20% unless detailed information regarding " η_p " and "e" is available. For general work a propeller efficiency of .83 and an airplane efficiency of .77 are assumed. From equation 4.402, CHART 4.41 at the end of this chapter has been made giving $\Delta BHP \sqrt{T_{as}/T_{at}}$ from standard weight, change in weight, wing span, test Mach number, and pressure altitude. Notice should be taken that the $\Delta BHP \sqrt{T_{as}/T_{at}}$ is the total change, while speed-power graphs usually present horsepower/engine.

DATA REDUCTION OUTLINE (4.41)

For Determining Weight-Corrected
Standard BHP vs V_t and H_c

(1)	V_1	knots	Indicated air speed
(2)	ΔV_{10}	knots	Air-speed instrument correction
(3)	W_t	lbs	Gross weight test, take-off weight less lbs. fuel consumed
(4)	ΔV_{po}	knots	Air-speed position correction corres- ponding to (1) and (3) and calibration data
(5)	V_c	knots	Calibrated air speed (1) + (2) + (4)
(6)	H_1	feet	Indicated pressure altitude
(7)	ΔH_{1c}	feet	Altimeter instrument correction
(8)	ΔH_{po}	feet	Altimeter position correction corres- ponding to (1) and (3) and (6) and calibration data
(9)	H_o	feet	True pressure altitude, (6) + (7) + (8)
(10)	M		Mach number, from (5) and (9) and CHART 8.5
(11)	t_1	$^{\circ}C$	Indicated air temperature
(12)	Δt_{1c}	$^{\circ}C$	Temperature instrument correction
(13)	t_{1c}	$^{\circ}C$	Indicated instrument corrected air temperature (11) + (12)
(14)	t_{at}	$^{\circ}C$	Test free air temperature from (10) and (13) and CHART 8.2
(15)	t_{as}	$^{\circ}C$	Standard temperature for (9)
(16)	$\sqrt{T_{as}/T_{at}}$		$\sqrt{(15) + 273} / \sqrt{(14) + 273}$
(17)	BHP_t		Test brake horsepower per engine from torquemeter or power chart
(18)	$BHP_t \sqrt{T_{as}/T_{at}}$		(16) x (17), per engine
(19)	W_s	lbs	Standard gross weight selected
(20)	ΔW	lbs	($W_s - W_t$)
(21)	$\Delta BHP_t \sqrt{T_{as}/T_{at}}$		Horsepower weight correction at W_t , ΔW , b^2 , M and altitude, using CHARTS 4.41 thru 4.46
(22)	$BHP_{tw} \sqrt{T_{as}/T_{at}}$		Weight corrected standard BHP, (21) + (18)
(23)	V_{ts}	knots	Standard day true speed (10) x $[\frac{(15) + 273}{38.944}]$ or CHART 8.5 and (5) and (9)
(24)	Plot (22) vs (23) or (5) or (10), and (9) as shown in Figure 4.31.		

NOTE: The standard-day, weight-corrected BHP (22) requires corrections to carburetor air temperature, manifold pressure, turbo rpm, and exhaust back pressure. If the particular speed-power point is at full throttle the standard power (22) may not be obtainable and a speed correction will be in order. These engine condition corrections are determined by the methods of Chapter Two.

SECTION 4.5

Configuration Change Corrections for Speed Power Data

The preceding sections developed a method for determining speed vs power at specified weights, altitudes, and fixed configurations. From this data generalizations must be made to allow computations of performance at all possible weights, altitudes, and configurations. For reciprocating engine power aircraft these computations are all made on the basis of incompressible flow theory.

The first requirement is for information regarding the changes in power required for a given speed change caused by minor changes in configuration such as opening or closing cowl flaps, oil coolers, intercoolers, etc. To present this information from minimum flight test work, the assumption is made that, at a given speed, a minor change in configuration will not change the coefficient of induced drag (C_{Di}).

$$\text{Profile Drag} = C_{DP} \frac{\rho}{2} V_t^2 S$$

then

$$\Delta \text{Profile Drag} = \Delta \text{Thrust}$$

and

$$\Delta \text{THP} = k S \Delta C_{DP} \sigma V_t^3 \quad (4.501)$$

or

$$\Delta \text{THP} \sqrt{\sigma} = k S \Delta C_{DP} (V_t \sqrt{\sigma})^3 \quad (4.502)$$

where:

ΔTHP = increment of THP required to balance the effects of an increment of ΔC_{DP}

$$k = 1.0414 \times 10^{-3}$$

ΔC_{DP} = increment of C_{DP} caused by configuration change

V_t = true air speed, knots

If $V_t \sqrt{\sigma}$ and C_{Di} are held constant, any change in $\text{THP} \sqrt{\sigma}$ will be a function of the change in C_{DP} . Within a small range of $V \sqrt{\sigma}$ Propeller Efficiency, η_p , remains constant and ($\sqrt{\sigma} \text{THP} = \sqrt{\sigma} \text{BHP} \eta_p$). Since C_{DP} is a function of size and shape, it will change with the configuration change. Therefore, by running power calibrations at one altitude and weight while changing configuration, the effects of configuration on BHP, V_t , or V_e may be determined. A typical calibration of cowl flap position effects is shown in Figure 4.51.

The values of $\Delta \text{BHP} \sqrt{\sigma}$ are applicable at any altitude and can be applied to any power calibration to determine the power required for the specified configuration. Notice should be taken that these changes apply to power required only. Range and top speed can, in some cases, be increased in spite of an increased cooling drag, because engine operating limits are raised under lower temperature conditions.

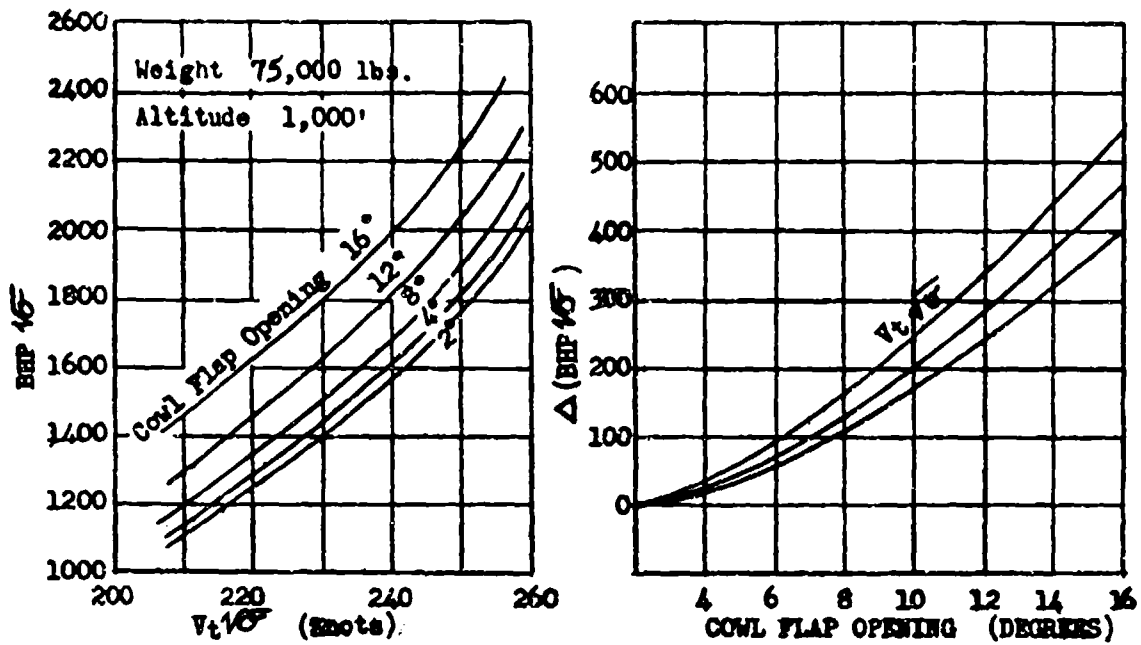


Figure 4.51
Cowl Flap Effects on Power

SECTION 4.6

The Generalized Power Parameter (PIW) and Speed
Parameter (VIW) - Reciprocating Engine Aircraft

The problem of generalizing data for all weights and altitudes is accomplished by the speed-power polar, PIW vs VIW plot. This plot presents all speed power information with a minimum amount of data. The parameters for this plot are determined from equation 4.213. By inserting some constant gross weight in this equation, two easily calculated terms are defined which completely resolve to a single curve all flight conditions for a given configuration.

$$\frac{THP\sqrt{\sigma}}{(W_t/W_g)^{3/2}} = k_1 C_{DP} S \left(\frac{\sigma v_t^2}{(W_t/W_g)} \right)^{3/2} + \left(\frac{k_2 W_g^2}{(W_t/W_g)^{1/2} b^2 \sigma} \right) \quad (4.601)$$

where:

$$\begin{aligned} k_1 &= 1.0414 \times 10^{-5} \\ k_2 &= .28820 \\ THP &= \eta_p BHP \\ \eta_p &= \text{propeller efficiency} \end{aligned}$$

Assuming the propeller efficiency to be virtually constant for given ranges of σv^2 , equation 4.601 may be written:

$$BHP \sqrt{\sigma} \frac{W_g}{W_t}^{3/2} = f \left[v_t \left(\sigma \frac{W_g}{W_t} \right)^{1/2} \right] \quad (4.602)$$

The left side is called "PIW." The right side is called "VIW." A typical PIW-VIW plot is illustrated in Figure 4.61. Generally the standard take-off gross weight is used as W_g .

The validity of the PIW-VIW plot can be demonstrated by dimensional analysis methods. By this means it can be shown that for a given configuration and propeller the parameters,

$$\frac{BHP \sqrt{\rho}}{W^{3/2}}, \quad \frac{N \sqrt{\rho}}{W^{1/2}}, \quad \frac{v_t \sqrt{\rho}}{W^{1/2}}$$

where: N is the engine rpm

will define speed power performance at any altitude and weight as shown in Figure 4.62. Since the three parameters can be presented on one graph the plot is most useful for estimating general performance and determining design criteria. In practice the parameters are divided by the appropriate constant standard weight to give PIW, VIW, and NIW.

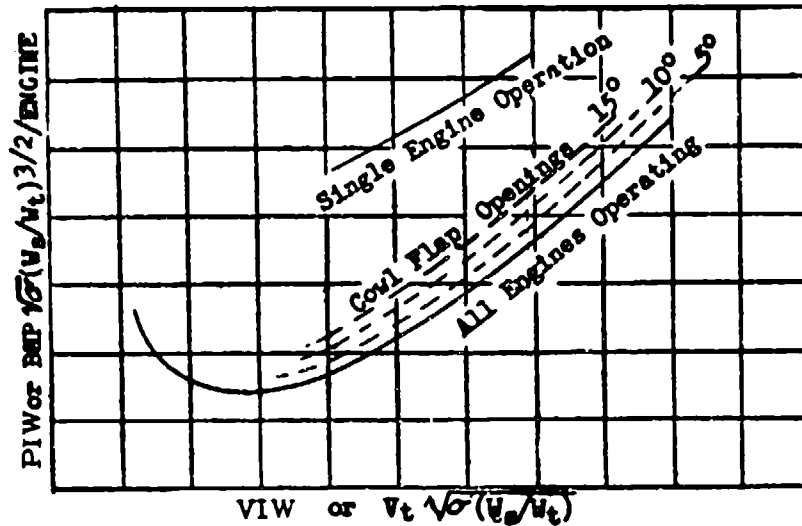


Figure 4.61
Typical PIW-VIW Plot

In practical applications the value of propeller efficiency will be approximately constant over most of the VIW range. In that case only the parameters PIW and VIW will be present, and the plot is very valuable for presentation and standardization of test data as discussed previously. Since the PIW-VIW plot is the aircraft polar reduced to sea-level, standard-weight conditions, only a change in propeller efficiency could produce more than one parameter for a given consideration. At very low or high flight speeds changes in propeller efficiency may be noticeable.

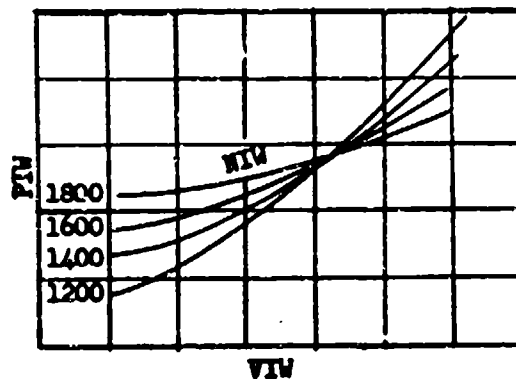


Figure 4.62
PIW-VIW Plot With rpm Parameters

DATA REDUCTION OUTLINE (4.61)

For PIW-VIW Plot

(1)	V_i	knots	Indicated air speed
(2)	ΔV_{i0}	knots	Air-speed instrument correction
(3)	W_t	lbs	Test gross weight
(4)	ΔV_{pc}	knots	Air-speed position error corresponding to (1) and (3) and calibration data
(5)	V_o	knots	Calibrated air speed (1) + (2) + (4)
(6)	H_i	feet	Indicated pressure altitude
(7)	ΔH_{i0}	feet	Altimeter instrument correction
(8)	ΔH_{pc}	feet	Altimeter position correction corresponding to (1) and (3) and (6) and calibration data
(9)	H_o	feet	True pressure altitude, (6) + (7) + (8)
(10)	P_a	"Hg	Atmospheric pressure corresponding to (9)
(11)	M		Mach number from (5) and (9) and CHART 8.5
(12)	t_{i0}	°C	Indicated temperature
(13)	Δt_{i0}	°C	Temperature instrument correction
(14)	t_{i0}	°C	Indicated instrument corrected temperature (12) + (13)
(15)	t_{at}	°C	Test free air temperature from (11) and (14) and CHART 8.2
(16)	\sqrt{W}		$\sqrt{9.625 (10) / \sqrt{(15) + 273}}$
(17)	W_s	lbs	Standard gross weight
(18)	$(W_t/W_s)^{1/2}$		$[(3) + (17)]^{1/2}$
(19)	$(W_t/W_s)^{3/2}$		$[(3) + (17)]^{3/2}$
(20)	V_{tt}	knots	Test true speed $38.944 (11) \times \sqrt{(15) + 273}$ or (11) and (15) and CHART 8.4
(21)	VIW	knots	(20) x (16) + (18)
(22)	BHP _t		Test brake horsepower from torque meter or power chart
(23)	PIW		(22) x (16) + (19)
(24)	Plot (23) vs (21) for each configuration.		

SECTION 4.7
Fuel Consumption - Range and Endurance
- Reciprocating Engine Aircraft

FUEL CONSUMPTION AND BSFC

Data relative to fuel consumption is obtained in flight whenever possible, rather than by use of the engine manufacturer's data. Flight fuel flow data is most accurately obtained by use of timed fuel totalizer readings or directly by use of rate of flow meters. In either case volume flow must be converted to weight flow. Generally, gasoline is considered to have an average sea level standard weight of 6.0 lbs/gal. If more accurate measurements are desired, where large quantities of fuel are involved at very low temperatures, the specific gravity should be determined before the flight and be used with a temperature correction factor to approximate in-flight specific gravity. This is only necessary where long-time high-altitude flights are involved and test gross weight may be appreciably affected. In most test work use of the before-flight specific gravity is sufficient.

$$W_f = \frac{\text{Gals}}{\text{hr}} \times 8.339 \times \text{Sp g} \quad (4.701)$$

where:

$$W_f = \text{lbs/hr, fuel}$$

$$\text{Sp g} = \text{fuel specific gravity}$$

In report presentation of fuel consumption or range data the test results should be corrected to a 6.0 lbs per gallon standard for gasoline.

The brake specific fuel consumption (BSFC) is determined from flow data taken during the normal power calibrations at various engine settings.

$$\text{BSFC} = \frac{W_f}{\text{BHP}} \quad (4.702)$$

This data is usually plotted vs BHP, alongside the speed-power curves as shown in Figure 4.71.

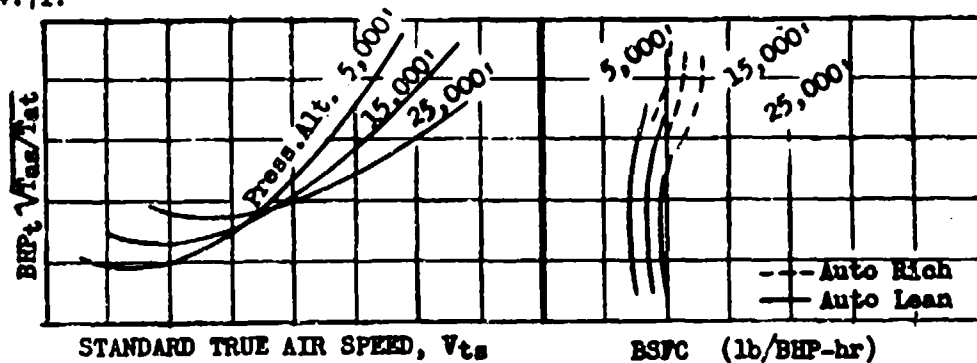


Figure 4.71
 Method of Presenting BSFC Data

SPECIFIC RANGE

Because the range charts are used for obtaining both flight distance and determining flying technique, the range data is sometimes plotted vs both true and calibrated or indicated speed. Range is not plotted as such except for sample mission studies. The usual presentation is specific range (SRg) vs true, calibrated or indicated speed.

$$SRg = \frac{V_t}{W_f} = \text{nautical air miles/lb} \quad (4.703)$$

A typical plot is shown in Figure 4.72.

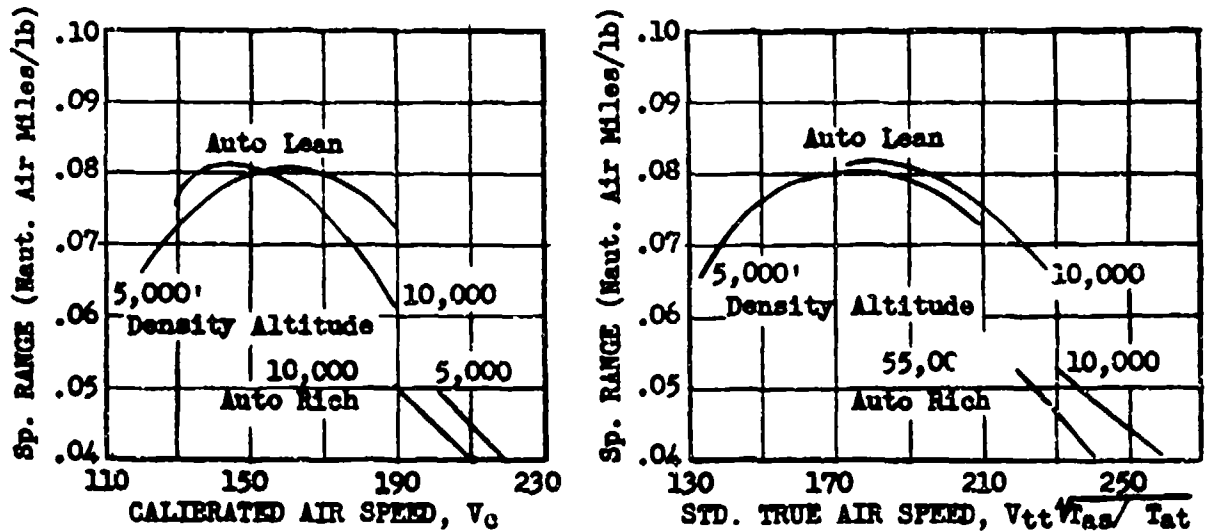


Figure 4.72
Specific Range Data - Constant Gross Weight

Notice should be taken that the altitudes shown on the brake specific fuel consumption graph are the various density altitudes at which the points were flown. The altitudes on the speed-power graphs are pressure altitudes. Experience has shown that, considering the small differences between test pressure altitude and test density altitude, fuel flow accuracy will not be measurably effected by assuming the fuel flow and speed-power graphs to agree at the same pressure altitude. In many cases specific fuel flow is completely independent of altitudes, but usually BSFC will increase with altitude for at least part of the altitude range.

Specific range data can be corrected for weight variations, but, because the BSFC may vary with altitude, the weight correction should not be applied across large altitude increments. Given the same density altitude, and mixture setting,

$$SRg_2 = SRg_1 \frac{(W_1)}{(W_2)} \quad (4.704)$$

When SR changes due to a weight change, V_t must change;

$$V_{t2} = V_{t1} \sqrt{\frac{W_2}{W_1}} \quad (4.705)$$

SPECIFIC ENDURANCE

Maximum specific endurance (SE_{max}) can be obtained from a fuel consumption plot made alongside the BHP_g vs V_t or V_o graphs as in Figure 4.73. Specific endurance is defined as the reciprocal of the fuel flow, W_f .

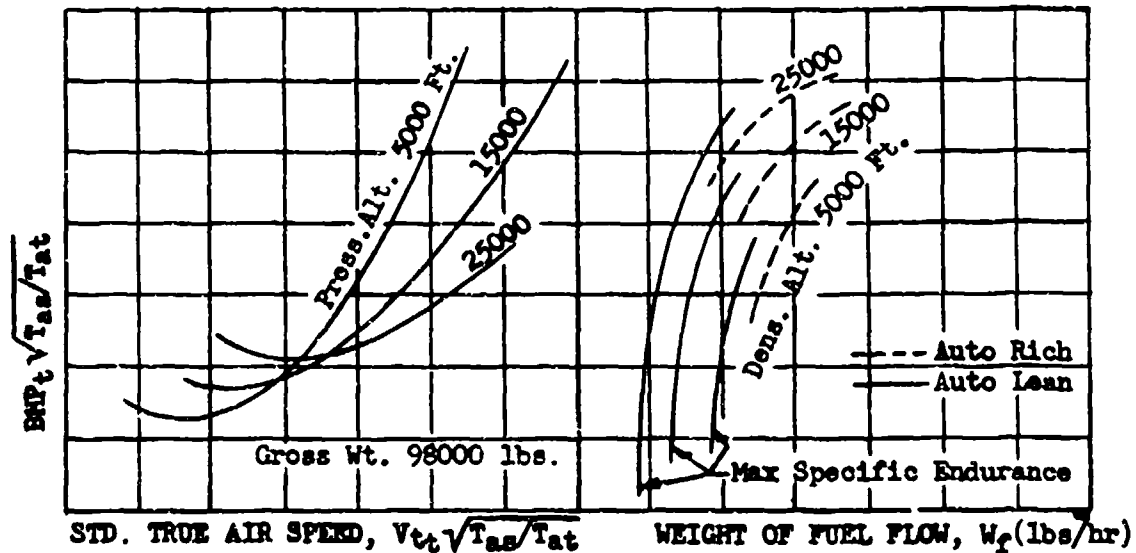


Figure 4.73
Method of Presenting Fuel Consumption Data

Specific endurance data may be corrected for weight variation, but, because the BSFC may vary slightly with density altitude the correction should not be applied across large altitude increments. At the same density altitude and mixture setting,

$$SE_2 = SE_1 \left(\frac{W_1}{W_2} \right)^{3/2} \quad (4.706)$$

When SE changes due to a weight change V_t must change,

$$V_{t2} = V_{t1} \sqrt{\frac{W_2}{W_1}} \quad (4.707)$$

ACTUAL RANGE AND ENDURANCE

From plots of specific range (nautical air miles per pound of fuel) vs true speed and altitude for each weight condition it will be possible to obtain the range for any desired cruising condition along with the corresponding BHP, rpm, manifold pressures and indicated speeds. For some aircraft performance reports it may be required that a test tactical mission be flown to compare expected and actual results, perhaps for a radius of action problem.

Actual range is best determined from a plot of the specific range parameter defined by equations 4.704 and 4.705 for a constant density altitude.

$$\frac{V_t W}{W_f} = r \left(\frac{V_t}{\sqrt{W}} \right) \quad (4.708)$$

where:

$$\frac{V_t W}{W_f} = \text{specific range parameter}$$

$$\frac{V_t}{\sqrt{W}} = \text{speed parameter}$$

Equation 4.708 is valid for both test and standard day conditions. For a constant value of the speed parameter the range is,

$$R_g = \frac{V_t W}{W_f} \int_{W_1}^{W_2} \frac{1}{W} dW \quad (4.709)$$

where:

$$dW = \text{fuel weight differential (negative)}$$

Integrating, the range becomes,

$$R_g = \left(\frac{V_t W}{W_f} \right) \ln \left(\frac{W_1}{W_2} \right) \quad (4.710)$$

Values of $\ln (W_1/W_2)$ may be determined from CHART 4.71 at the end of this chapter.

Actual endurance is best determined from a plot of the specific endurance parameter defined by equation 4.706 and 4.707 for a constant density altitude.

$$\frac{W^{3/2}}{W_f} = r \left(\frac{V_t}{\sqrt{W}} \right) \quad (4.711)$$

where:

$$\frac{W^{3/2}}{W_f} = \text{specific endurance parameter}$$

For a constant value of the speed parameter the endurance is,

$$E = \left(\frac{V}{W_f} \right)^{3/2} \int_{W_1}^{W_2} \frac{1}{W^{3/2}} dW \quad (4.712)$$

Integrating, the endurance becomes,

$$E = \left(\frac{V}{W_f} \right)^{3/2} \left(\frac{2}{\sqrt{W_2}} - \frac{2}{\sqrt{W_1}} \right) \quad (4.713)$$

Values of $2/\sqrt{W}$ may be determined from CHART 4.72 at the end of this chapter.

DATA REDUCTION OUTLINE (4.71)
For BSFC and Range Data - Reciprocating

(To be used with BHP Data Reduction Outline in Section 4.4)

(25)	W_{ft}	gals/hr	Test volumetric fuel flow
(26)	W_{ft}	lbs/hr	Test fuel weight-flow (25) x (conversion factor determined by fuel and temp)
(27)	BSFC	lbs/BHP-Hr	Brake specific fuel consumption (26) ÷ (17)
(28)	Plot (27) vs (23)		
(29)	SRG	nautical air miles per pound	Specific range, [(23) ÷ (16)] ÷ (26)
(30)	Plot (29) vs (23) or (5), at each altitude		

SECTION 4.8

Speed-Power Curves - Turbojet Aircraft

The aircraft drag parameter is a function of Mach number and the weight-pressure parameter as shown in equation 4.125.

$$D/P_a = f(M, W/P_a) \quad (4.801)$$

In jet-powered aircraft in stabilized level flight the propulsive or net jet thrust equals the aircraft's drag. For flight performance data engine rpm is a more convenient engine criterion than thrust horsepower or drag. As previously shown in Chapter Three,

$$F_n/P_a = f(M, N/\sqrt{T_a}) \quad (4.802)$$

By equating equations 4.801 and 4.802,

$$N/\sqrt{T_a} = f(M, W/P_a) \quad (4.803)$$

For convenience equation 4.803 is written,

$$N/\sqrt{\theta_a} = f(M, W/\delta_a) \quad (4.804)$$

where

$$\theta_a = T_a/288$$

$$\delta_a = P_a/29.92$$

$$M = f(V_c \text{ and } P_a)$$

$$N = \text{rpm}$$

If the value of the W/δ_a parameter is fixed, $N/\sqrt{\theta_a}$ versus M curves will define the speed power relationship.

Speed-power tests in turbojet aircraft are flown by setting an rpm and holding the aircraft at a specified pressure altitude until the speed is stabilized. This is done for each test point. However, at low speeds near the stall condition, jet airplanes will not stabilize well. This is because the thrust decreases as the speed decreases so that a condition may be reached where at a constant rpm the speed will slowly fall until the aircraft stalls. The aircraft can never be successfully operated in this range, but flight tests sometimes require drag evaluation at low speeds. In order to include this low speed range in the power required curves, a system has been devised to gather the necessary data from a test in which the aircraft is allowed to descend slightly to maintain its speed.

From climb data reduction (Chapter Five),

$$R/C = \frac{101.3 V_t (F_n - D)}{W}$$

or

$$R/D = \frac{101.3 V_t (D - F_n)}{W}$$

where:

R/D = rate of descent, ft/min

W = weight - lbs

V_t = true speed - knots

F_n = net thrust - lbs

D = drag - lbs. Assumed constant for the descent and level flight condition at the same V_t.

If the aircraft is stabilized on a Mach number while making a small descent at a measured rate, the value of (D - F_n) can be computed. This value will be the difference between the thrust required for level flight at the same Mach number and the thrust being delivered. By the use of net thrust computations or engine manufacturer's curves this additional thrust required can be converted to a required rpm increase giving equivalent level flight performance. This method is used at whatever speeds the pilot finds he cannot stabilize the airplane in level flight. But rates of descent of more than 200 ft/min will not produce satisfactory results. Once a level flight speed and rpm are obtained by this method, all other level flight corrections are applied in the normal manner.

In turbojet powered aircraft compressibility phenomena, Mach number effects, are significant at all altitudes. For this reason, no generalized speed-power curve, such as the PIW-VI_W curve, is applicable. Separate level flight data results must be presented as a function of rpm and speed or Mach number for each value of W/P_a flown, as in equation 4.803. The data is actually presented for each altitude, P_a, at a constant weight for that altitude. One level flight performance presentation is standard day rpm vs V_c for constant pressure altitudes, H_c. A typical plot of this type is shown in Figure 4.81. Standard day rpm is defined as:

$$\text{rpm std} = \frac{N}{\sqrt{T_{at}}} \times \sqrt{T_{as}}$$

This same plot is used also to show calibrated speed reduction (drag increases) resulting from configuration changes as in Figure 4.82.

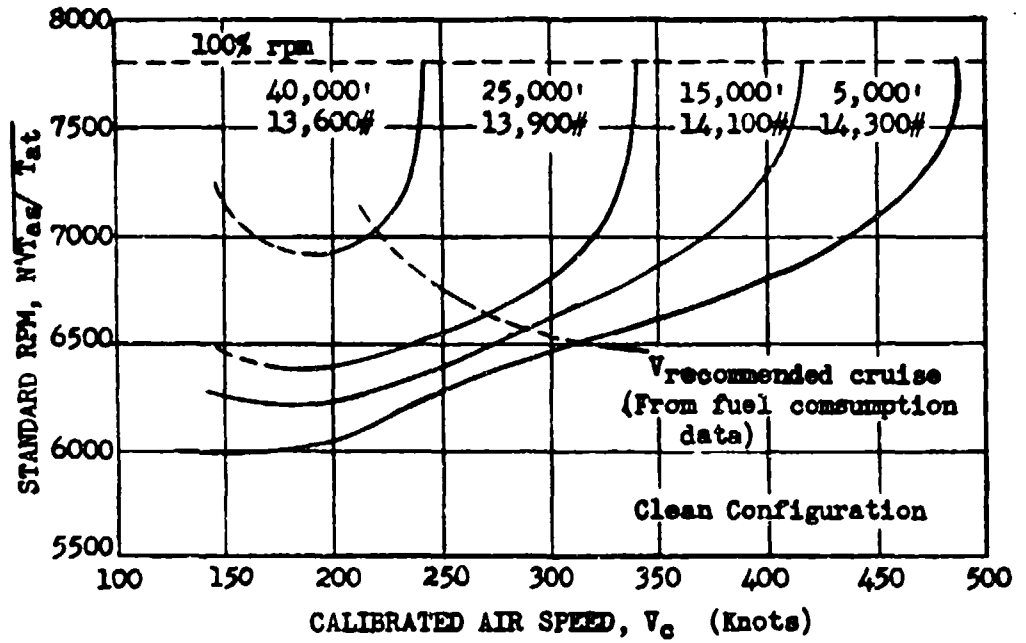


Figure 4.81
Turbojet Rpm- V_c Presentation

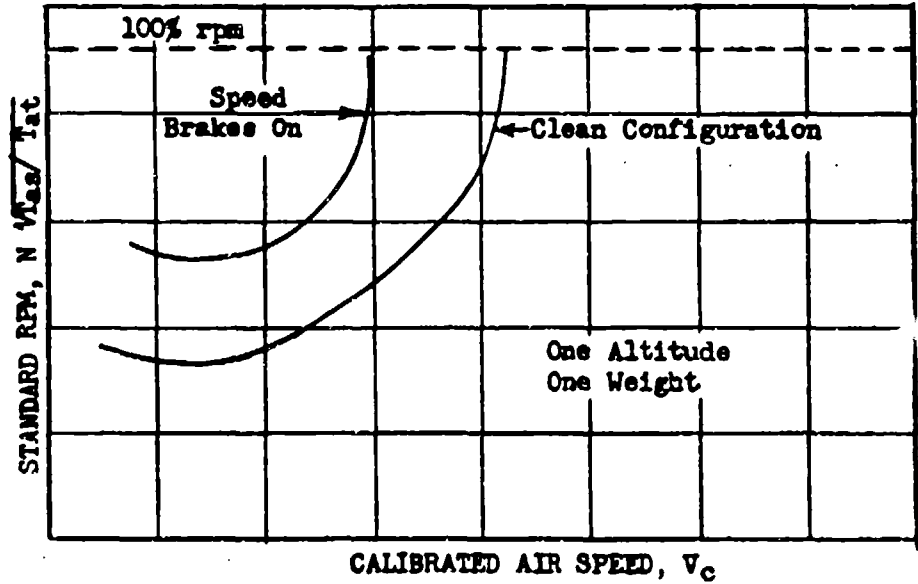


Figure 4.82
Effect of Configuration Change on
Turbojet Speed and Rpm

Using equation 4.804 it is possible to correct and plot all the level flight data for standard day sea level condition. This is done by plotting $N/\sqrt{\delta_a}$ vs Mach number for constant values of W/δ_a obtained at various altitudes. This plot, Figure 4.83, shows immediately the sea level weight limitations at maximum rpm at various Mach numbers. By interpolation the plot can be used to find speed power conditions for any weight and altitude. Figure 4.83 is presented in the final performance report to show the obvious Mach number-compressibility effects on engine performance requirements. It also must be used to obtain weight corrected data for plotting as shown in Figures 4.81 and 4.82. When external drag items such as rockets or bombs are added to the aircraft it is often necessary to present both the effects on indicated speed and the compressibility effects. Speed effects are shown on a graph similar to that of Figure 4.82. Mach number-compressibility effects on the power required for external drag items can be shown as illustrated in Figure 4.84.

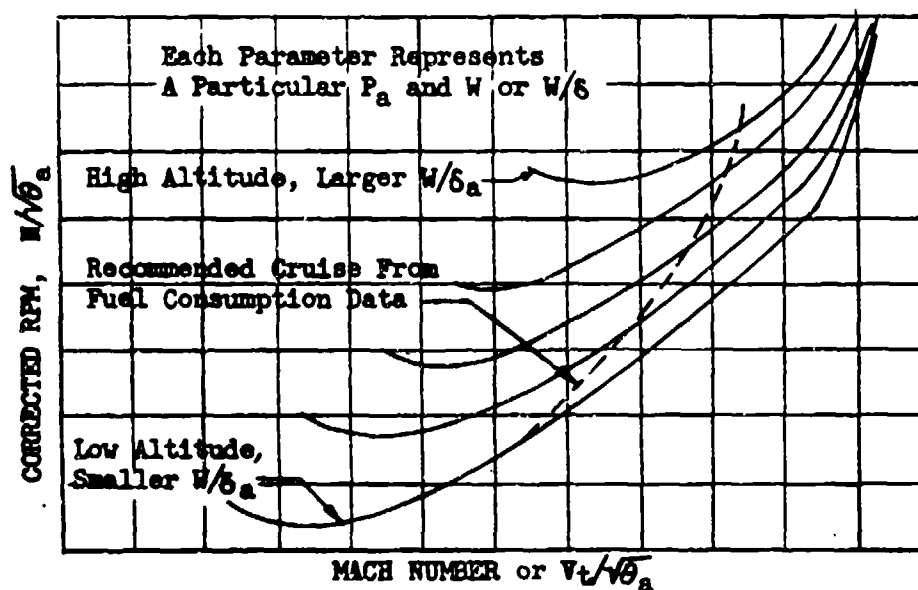


Figure 4.83
Typical Sea Level Turbojet Performance Data

The type of plot used to sum up the level flight performance for a turbojet aircraft is illustrated in Figure 4.85. This graph presents the standard day true speed vs altitude data for various actual engine rpm's. Also shown are a reference max. Mach number and a recommended max. range cruise condition. This speed vs altitude plot is generally presented for each major aircraft configuration, such as with wing tip tanks installed and without. The speed or altitude curves are most easily obtained by cross plotting weight corrected test data from Figures 4.81 or 4.83.

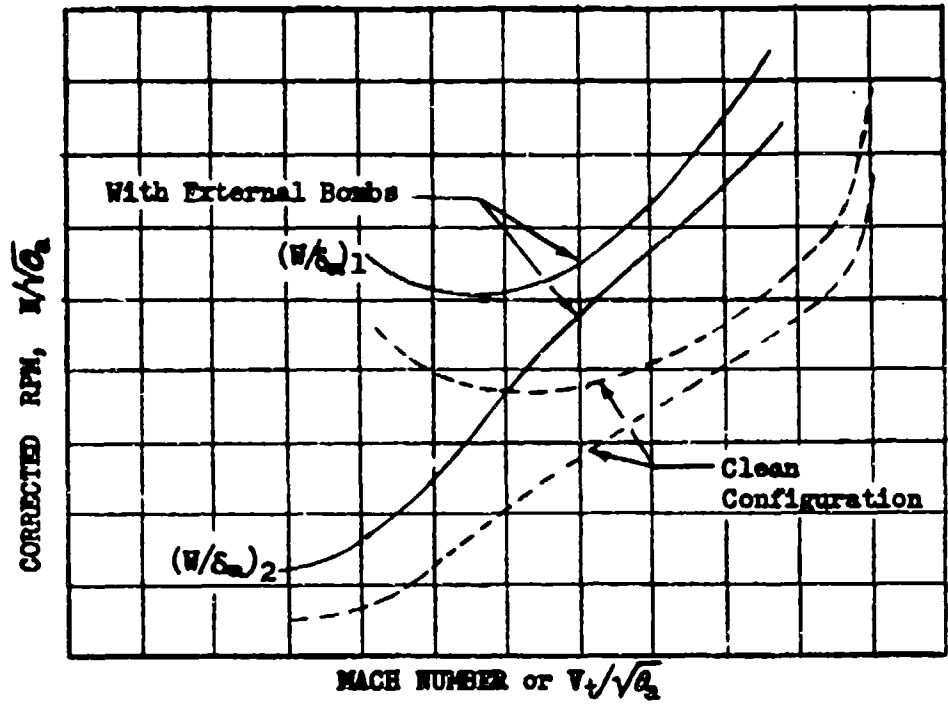


Figure 4.84
 Typical Configuration Effect on Sea
 Level Turbojet Performance Data

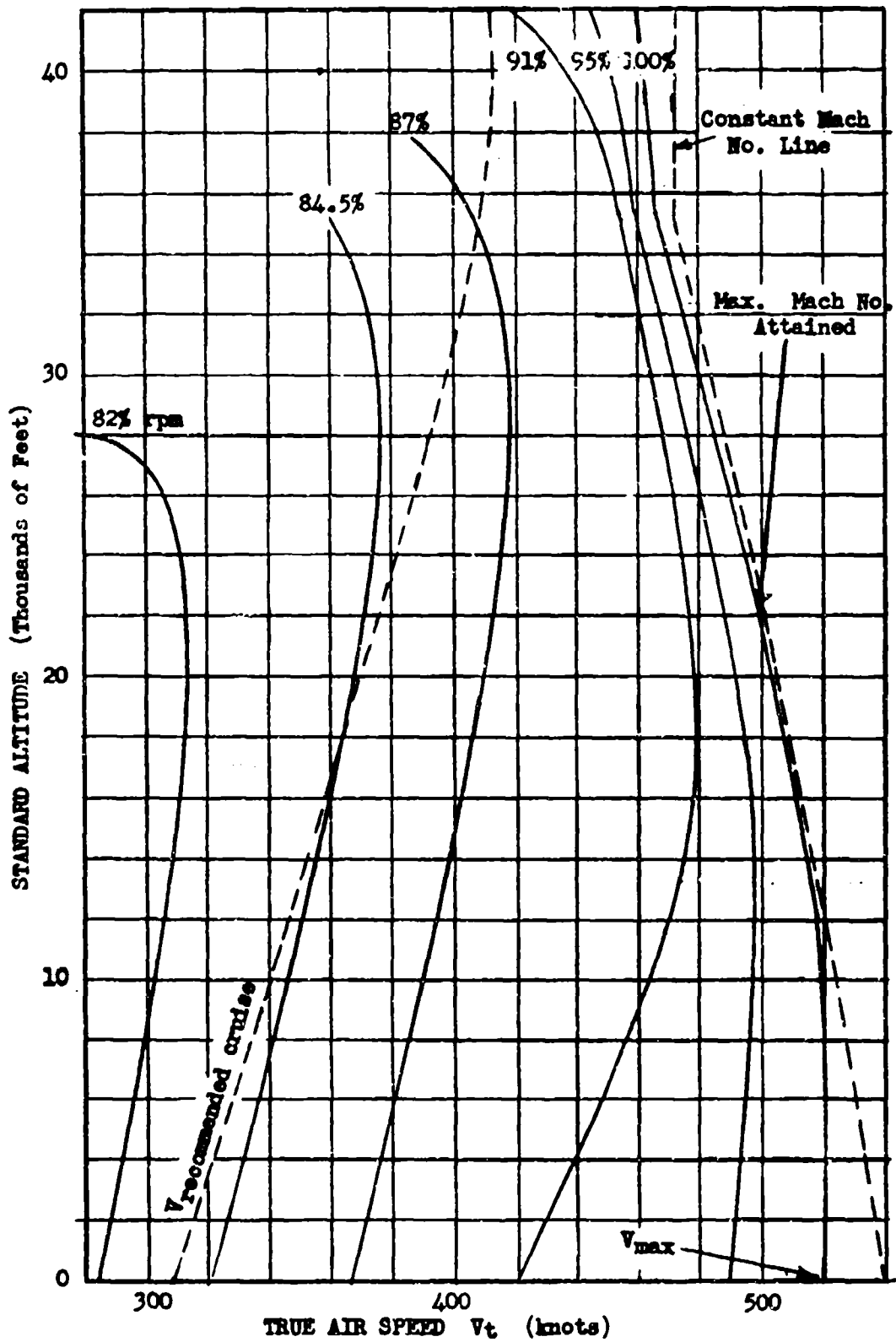


Figure 4.85
 Presentation of True Speed, Altitude and rpm Data

DATA REDUCTION OUTLINE (4.81)

For Level Flight Jet Aircraft Power Calibration

(1)	Test Point Number	
(2)	H_1	Indicated pressure altitude
(3)	ΔH_{1c}	Altimeter instrument correction
(4)	ΔH_{pc}	Altimeter position error correction
(5)	H_c	True pressure altitude, (2) + (3) + (4)
(6)	$\delta_a = (P_a/P_{SL})$	From (5) and standard altitude tables
(7)	V_1	Indicated air speed
(8)	ΔV_{1c}	Air-speed instrument correction
(9)	ΔV_{pc}	Air-speed position error correction
(10)	V_c	Calibrated air speed (7) + (8) + (9)
(11)	M	Mach number from (10) and (5) and CHART 8.5
(12)	V_{ts}	Standard-day, true speed, from (10) and (5) and CHART 8.5
(13)	t_1	Indicated air temperature
(14)	Δt_{1c}	Temperature instrument correction
(15)	t_{1c}	Instrument corrected indicated air temperature
(16)	T_{at}	True test air temperature - °Kelvin, from (15) and (11) and CHART 8.2
(17)	$\sqrt{\theta_{as}} = \sqrt{T_{as}/T_{SL}}$	From (5) and standard altitude tables
(18)	$\sqrt{\theta_{at}} = \sqrt{T_{at}/T_{SL}}$	$\sqrt{(16)/288^\circ K}$
(19)	Gallons fuel remaining - from fuel counter	
(20)	Gallons fuel start	
(21)	Gallons fuel used, (20) - (19)	
(22)	Fuel weight used, (21) x lbs/gallon	
(23)	Starting gross weight	
(24)	W_t	Test weight, (23) - (22)
(25)	W_t/δ_a	Test weight-pressure parameter (24) + (6)
(26)	W_s/δ_a	Standard weight-pressure parameter, W_s + (6)
(27)	$\Delta(W/\delta_a)$	Weight pressure parameter correction (26) - (25)
(28)	N_1	Indicated rpm
(29)	ΔN_{1c}	Rpm instrument correction
(30)	N	Test rpm, average of all engines
(31)	$N/\sqrt{\theta_{at}}$	Test rpm parameter (30) + (18)
(32)	$\Delta(N/\sqrt{\theta_{at}})_w$	Rpm parameter increment for $\Delta(W/\delta_a)$ from weight correction graphs similar to Figures 4.91 or 4.94
(33)	$(N_w/\sqrt{\theta_{at}})$	Weight pressure ratio corrected rpm parameter, (31) + (32)
(34)	$N_w \sqrt{\frac{T_{as}}{T_{at}}}$	Standard-day rpm at standard weight, (33) x (17)
(35)	Plot (33) vs (11) for constant W/δ_a	
(36)	Plot (34) vs (10) for constant W and P_a	
(37)	Plot (34) vs (12) and cross plot to get altitude vs V_{ts} for constant standard-day rpm's or percent rpm's	

SECTION 4.9

Weight Change Corrections for Speed Power Data - Turbojet Aircraft

Equation 4.210 presents the analytical expression for drag force in terms of W , q , and C_{DP} . If C_{DP} is constant, the equation reverts to a form in which increments of D for increments of W may be calculated. This is not the case for high-speed aircraft under the effects of compressibility. Since equation 4.210 assumes incompressible air flow conditions, it cannot be used as a means of drag-weight-speed correction at high Mach numbers. Essentially, C_{DP} is an unpredictable function of W/P_a and Mach number under these flight conditions, which means weight corrections to speed or drag must be accomplished empirically. The weight correction must be made on the basis of test data obtained from the given airplane and engine combination. Because this must be done in the high speed range the same procedure is used in the low speed range.

The basis for the two weight-correction methods described here is the fact that the parameter W/S_a can be changed either by changing W or P_a . If a series of test runs are made at different altitudes and at the same Mach number at each altitude, a range of $N/\sqrt{\theta_a}$ and W/S_a would be covered. By making a plot of $N/\sqrt{\theta_a}$ vs W/S_a , as in Figure 4.91, with each line representing a Mach number, the change in $N/\sqrt{\theta_a}$ with respect to change in W/S_a can be found. Or, more directly, the correct $N/\sqrt{\theta_a}$ for any W/S_a and M is immediately apparent.

If W/S_a values are $\pm 1\%$ of a given value, weight corrections are not required. This can be accomplished by good stabilization resulting from closely estimated speeds and rpm's required for a given W/S_a . A pitot connected rate of climb indicator can be used to show small amounts of acceleration in level flight and reduce time required to stabilize.

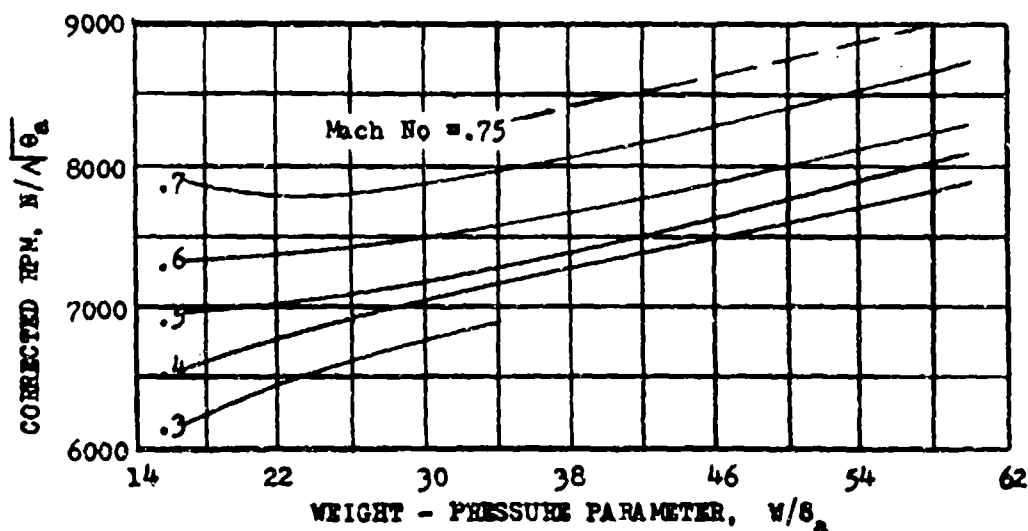


Figure 4.91
Turbojet Aircraft Performance with
Mach number Parameters

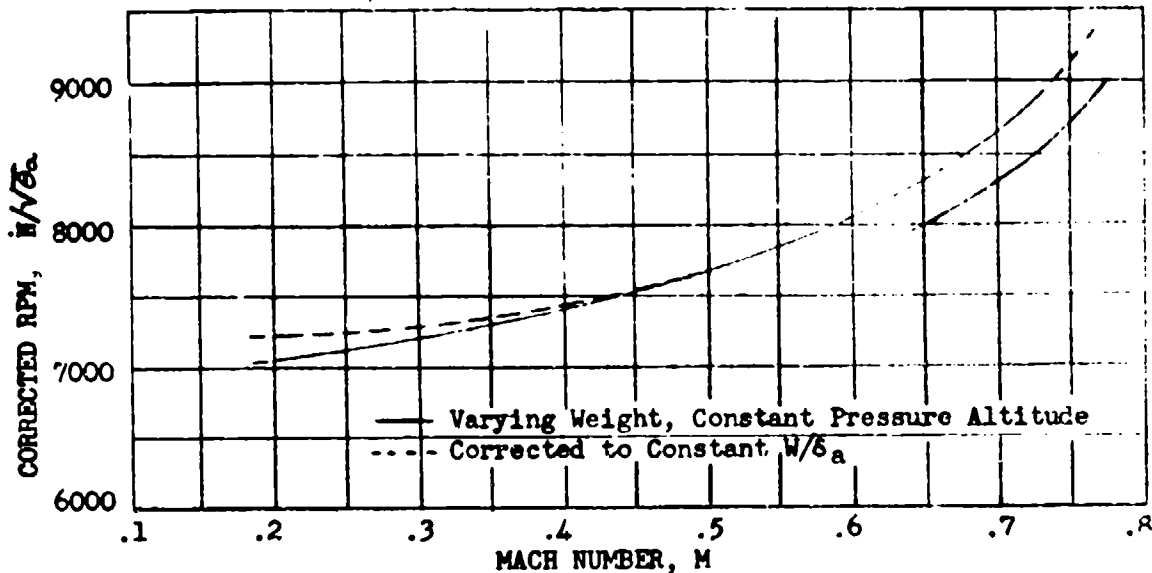


Figure 4.92
Corrected Turbojet Performance Data

In actual flight testing establishing stabilized flight on a specific Mach number is difficult, so level flight test data are plotted in the form of $N/\sqrt{\delta_a}$ vs M . If the test points are flown at successively lower Mach numbers at a constant pressure altitude, the W/δ_a value diminishes for each point. This effect is shown in Figure 4.92.

INCREMENT RATIO METHOD OF WEIGHT CORRECTION

To make necessary weight corrections an approximate method, using plots of $\Delta(N/\sqrt{\delta_a})/\Delta(W/\delta_a)$, has been devised. Normal power calibrations are flown by setting rpm and allowing speed to stabilize. A plot, Figure 4.93, is then made of $N/\sqrt{\delta_a}$ vs Mach number at each altitude, disregarding the fact that the W/δ_a for each point is different. Data at each altitude are accumulated in the same manner by starting the power calibration at high Mach numbers. Next, at each altitude the values of the W/δ_a 's of each point are averaged, and the entire calibration is assumed to have been flown at the average W/δ_a . Lines of constant Mach number are drawn on the graph as in Figure 4.93. They will intersect the power calibrations at various $N/\sqrt{\delta_a}$ values.

From these $N/\sqrt{\delta_a}$ values a plot of $N/\sqrt{\delta_a}$ vs W/δ_a at constant Mach numbers can be made and the slopes, $d(N/\sqrt{\delta_a})/d(W/\delta_a)$, determined, or $(\Delta N/\sqrt{\delta_a})/(\Delta W/\delta_a)$ can be determined directly by taking increments between power calibrations at two altitudes.

$$\text{Increment ratio} = \frac{(N/\sqrt{\delta_a})_2 - (N/\sqrt{\delta_a})_1}{(W/\delta_a)_2 - (W/\delta_a)_1} \quad (4.901)$$

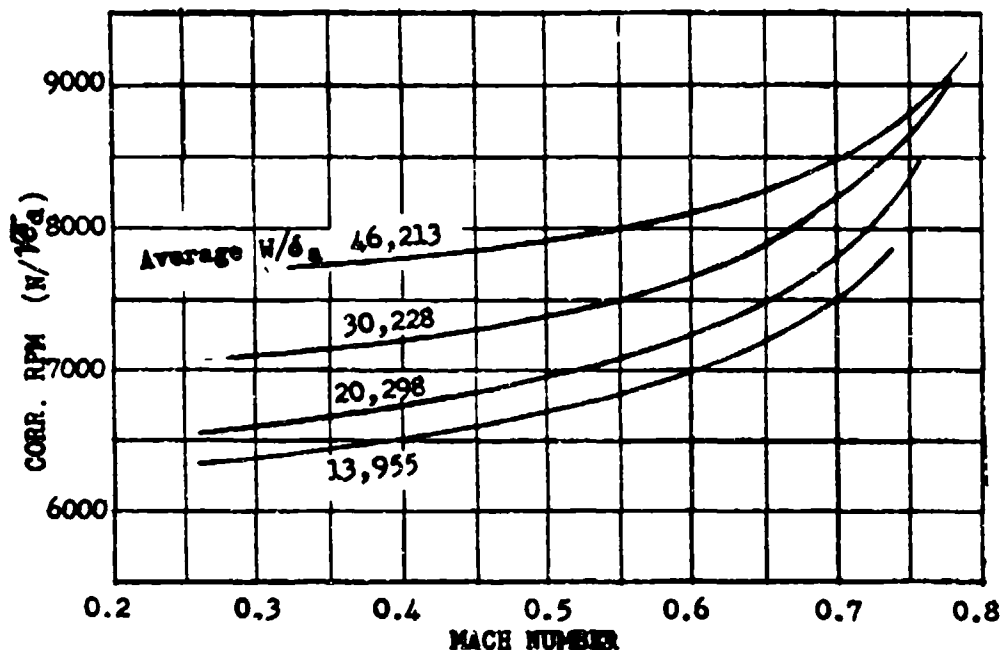


Figure 4.93
Actual Flight Data Plot

Since the assumption has already been made that each altitude calibration was flown at an average W/δ_a , or weight, accuracy will not be impaired by assuming that the W/δ_a midway between two W/δ_a 's represents the point where the increment ratio should be applied. The increment ratio is plotted against this average W/δ_a altitude as in Figure 4.94.

From Figure 4.94 all test points can be corrected to a desired value of W/δ_a which will correspond to some altitude when a weight is specified. With reciprocating engine aircraft weight correction was made at each altitude so that the concept was established that a weight correction brought data to the flown altitude at a standard weight; however, when the W/δ_a correction is made both weight and altitude can be changed. By selecting a standard weight, but not requiring the standard pressure altitude to be the flown altitude, a $(W/\delta_a)_{std}$ can be found that will minimize $\Delta W/\delta_a$ and consequently increase accuracy. For example: a series of points is flown at 20,000 ft. with weight varying from 14,000 to 12,000 lbs. giving an average W/δ_a of 28,000. The points are to be corrected to a weight of 14,000 lbs. If an altitude of 18,100 ft. is selected $(W/\delta_a)_{std}$ will equal the average W/δ_a flown. This should require a minimum point by point correction to the standard W/δ_a . Unless a special reason was required for the 20,000 ft. calibration, the 18,100 ft. calibration gives information of equal value.

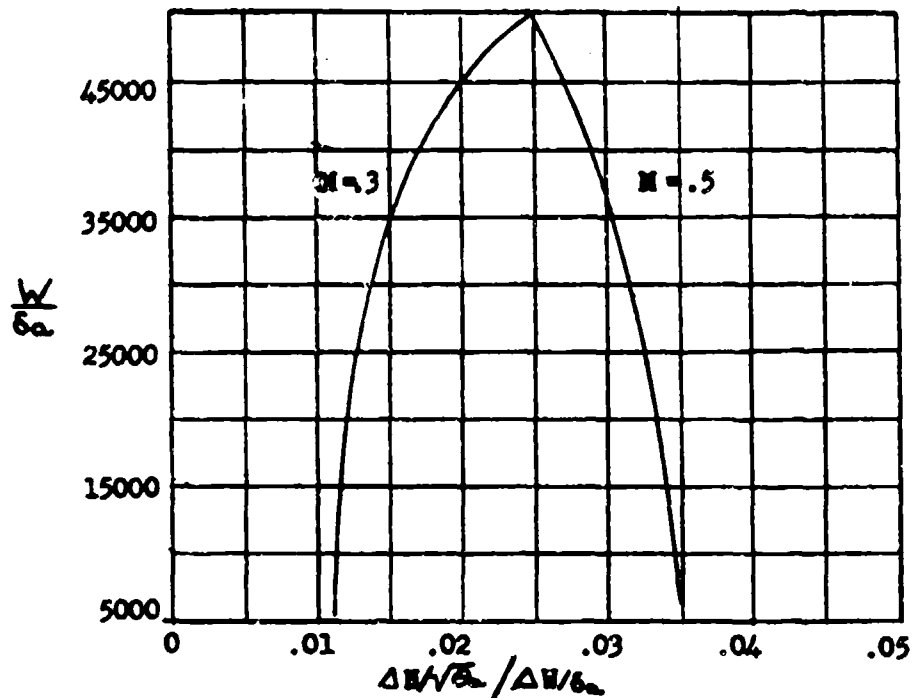


Figure 4.94
RPN-Weight Increment Ratio Plot for Making
Turbojet Level Flight Weight Corrections

CROSS PLOTTING AND IN-FLIGHT WEIGHT CORRECTION METHODS

Another weight correction method for jet aircraft is designed to obtain a very accurate plot of $N/\sqrt{\delta_a}$ vs W/δ_a for constant Mach number parameters as illustrated in Figure 4.91. This type weight correction employs four basic steps:

- (1) Test points are flown consecutively from high Mach number to low at a constant pressure altitude. Points should be flown at small and approximately equal time intervals.
- (2) Plot $N/\sqrt{\delta_a}$ vs M for each altitude flown.
- (3) Plot W/δ_a vs M for each altitude flown.
- (4) Cross plot, from (2) and (3) above, $N/\sqrt{\delta_a}$ vs W/δ_a for constant Mach number parameters as illustrated in Figure 4.91. This final cross plot can be used to obtain $N/\sqrt{\delta_a}$ for any M , W , and H_0 desired. In addition $N/\sqrt{\delta_a}$ values for max. rpm and various standard altitudes can be included to define the max. speed points.

To obviate the need for a weight correction the level flight tests for both conventional and jet powered aircraft can be flown at a constant value of W/δ_a . The value selected for this W/δ_a depends on the take-off gross weight, fuel used in climb, and rate of fuel used during level flight at a particular altitude.

If these factors are carefully analyzed, it is possible to make flight guides enabling the test pilot to record data at desired constant values of W/δ_a . A typical W/δ_a guide is shown in Figure 4.95.

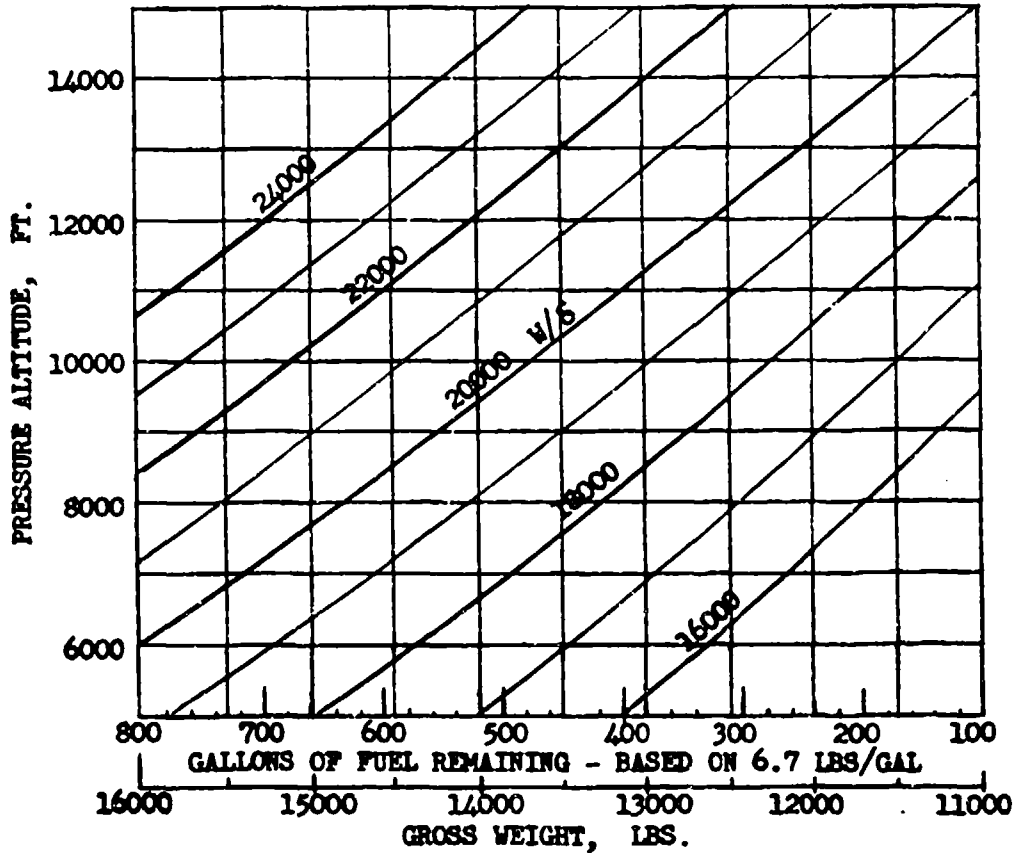


Figure 4.95
Guide Card for Flying at Constant W/δ_a

Using this guide the pilot needs only to keep a slight lead on his fuel flow counter at a particular altitude. When the fuel remaining counter value for the aircraft agrees with the fuel remaining value required by the guide card the pilot records the necessary data. The efficiency of this method for holding a constant W/P_a depends on the skill of the pilot and may require some training on his part to prevent long lapses between test points. A radio technique can also be applied this method. The ground end of the radio link doing the necessary calculations then informing the pilot of the fuel counter readings and altitudes at which to record data.

SECTION 4.10

Fuel Consumption Endurance and Range - Turbojet Aircraft

Data relative to fuel consumption for jet aircraft are obtained in flight whenever possible, rather than by use of the engine manufacturer's data. Flight fuel flow data is most accurately obtained by use of timed fuel totalizer readings or directly by use of rate of flow meters. In either case volume flow must be converted to weight flow. Generally, jet engine fuel is of two types:

AN-F-38 (JP-1) = 6.7 lbs/gal standard weight for sea level standard conditions

AN-F-58 (JP-3) = 6.42 lbs/gal standard weight for sea level standard conditions

If more accurate measurements are desired, where large quantities of fuel are involved at very low temperatures, the specific gravity should be determined before the flight and be used with a temperature correction factor to approximate the in-flight specific gravity. This procedure is only necessary where long-time high altitude flights are involved and the test gross weight is appreciably affected. In most test work use of the before flight specific gravity is sufficient.

$$W_f = \text{gals/hr} \times 8.334 \times \text{Sp g} \quad (4.701)$$

where:

$$W_f = \text{lbs/hr}$$

$$\text{Sp g} = \text{Specific gravity}$$

In report presentation of fuel consumption or range data the test results are corrected to average sea level standard pounds per gallon values for the fuel being used.

For turbojet aircraft fuel consumption is handled in the form of the fuel flow parameter developed in Chapter Three.

$$\text{Turbojet fuel flow parameter for compressor inlet conditions} = \frac{W_f}{P_{t2} \sqrt{T_{t2}}} \quad \text{or} \quad \frac{W_f}{\delta_{t2} \sqrt{\theta_{t2}}}$$

$$\text{Turbojet fuel flow parameter for ambient conditions} = \frac{W_f}{P_a \sqrt{T_a}} \quad \text{or} \quad \frac{W_f}{\delta_a \sqrt{\theta_a}}$$

where:

$$W_f = \text{fuel flow lbs/hr or gals/hr}$$

$$P_{t2} = \text{engine inlet, total pressure}$$

$$T_{t2} = \text{engine inlet total temperature}$$

$$\delta_2 = P_{t2}/\text{S.L. std pressure}$$

$$\theta_2 = T_{t2}/\text{S.L. std temperature}$$

As shown in Chapter Three, the fuel flow parameter is a function of $N/\sqrt{V_{t2}}$ and engine inlet Mach number. On the engine manufacturer's "expected performance curves" it can be seen that through most of the in-flight $N/\sqrt{V_{t2}}$ range the fuel flow parameter is a single curve at all Mach numbers. When actual flight data is plotted, $N/\sqrt{V_{t2}}$ vs $W_f/\delta_{t2} \sqrt{V_{t2}}$, the results form a family of curves which for all practical purposes is a single curve. Figure 4.10.1 illustrates this plot. It will be noted that at the lower corrected rpm values for each altitude the curves tend to diverge. This is a result of both decreased Mach number at the higher altitudes for the same corrected rpm values and decreased combustion efficiency at the higher altitudes.

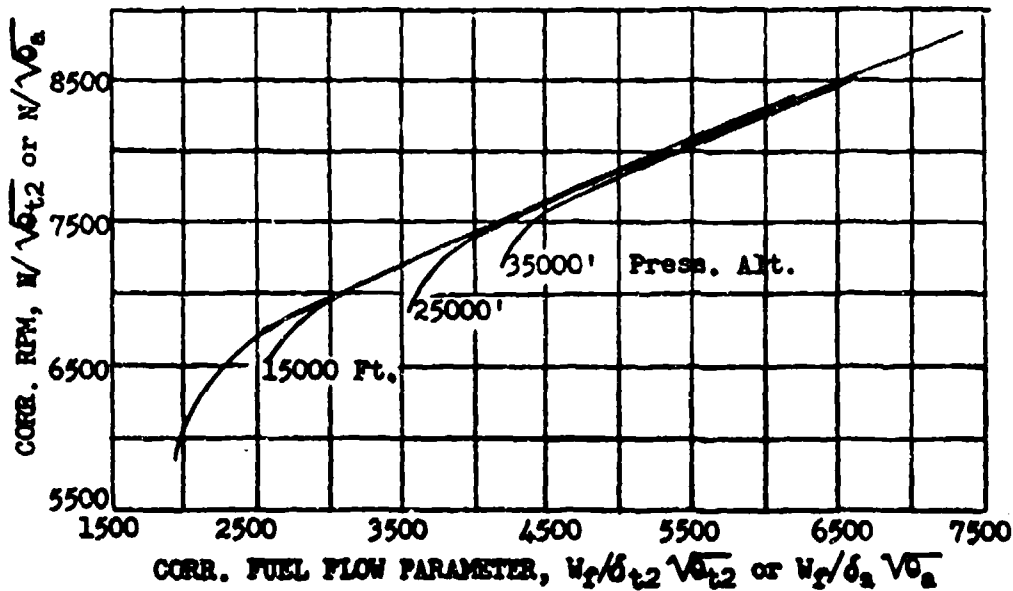


Figure 4.10.1
Turbojet Fuel Flow Presentation

It should be noted that ambient conditions may be used in the fuel flow parameter since the affects of Mach number are negligible unless large W/δ_a variations at low rpm are possible. A plot of $N/\sqrt{V_{t2}}$ vs $W_f/\delta_{t2} \sqrt{V_{t2}}$ appears nearly identical to Figure 4.10.1 and is as accurate for determining fuel consumption for most rpm, atmospheric conditions, and Mach numbers. Using engine inlet conditions the fuel flow parameter is applicable in both climb and level flight. With ambient conditions in the parameter it is only theoretically applicable to level flight data because of differences in the inlet pressure term resulting from differences in Mach number for the climb and level flight condition. Actually the ambient fuel flow parameter is usually applicable to climb data as the error from Mach number effects in the climb rpm range is negligible.

ENDURANCE

It can be seen from Figure 4.10.1 that maximum specific endurance, $1/W_f$, for jet aircraft will be at the lowest rpm that will maintain level flight above the stall condition. It is also seen that specific endurance increases with altitude. Endurance is best evaluated with the specific endurance parameter.

The engine fuel flow function is,

$$\frac{W_f}{P_a \sqrt{T_a}} = f \left(\frac{N}{\sqrt{T_a}}, \frac{V_t}{\sqrt{T_a}} \right) \quad (4.10.01)$$

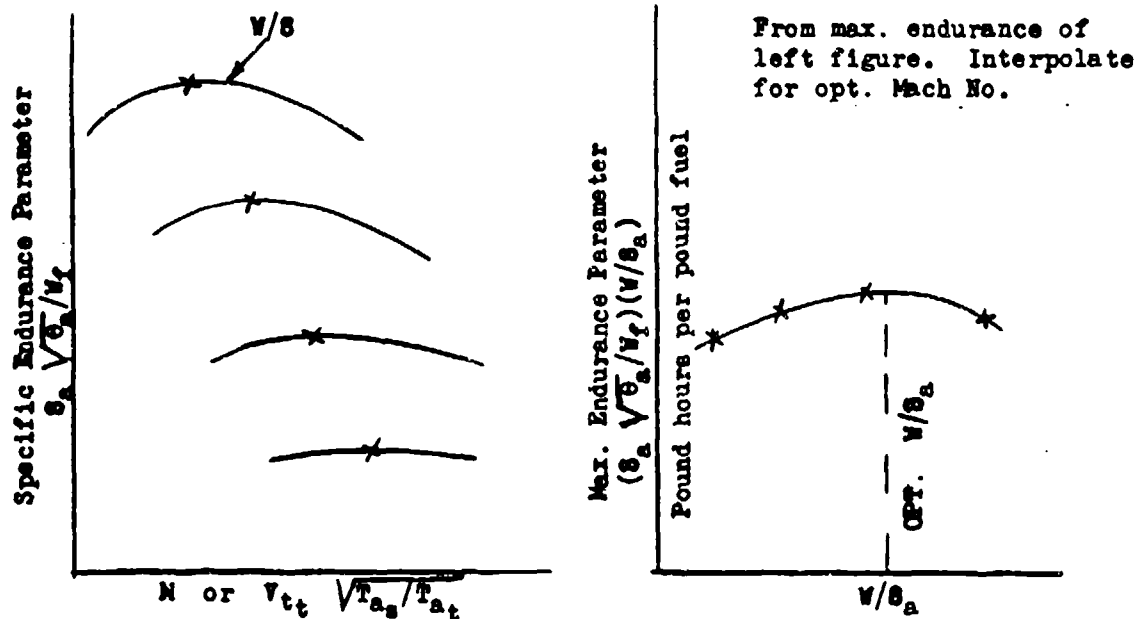
For the aircraft the rpm function is,

$$\frac{N}{\sqrt{T_a}} = f \left(\frac{V_t}{\sqrt{T_a}}, \frac{W}{P_a} \right) \quad (4.10.02)$$

Functionally combining the above two equations in terms of S , θ and M ,

$$\frac{S_a \sqrt{\theta_a}}{W_f} = f \left(M, \frac{W}{S_a} \right) \quad (4.10.03)$$

A plot of equation 4.10.03, as in Figure 4.10.2 should be made throughout the complete speed range of the aircraft, so that max. endurance and endurance at any speed can be computed.



4.10.2

Turbo-Jet Endurance and Max. Endurance Plots

Data for this plot should be obtained at constant W/S_a 's, but negligible errors are introduced if W/S_a changes are small during power calibrations at one altitude.

Best endurance is obtained by maintaining a constant W/S_a . This necessitates a slight rate of climb (20-50 ft/min) to decrease S_a as W decreases. By plotting as in Figure 4.10.2 a W/S_a for max. endurance can be found. Actual endurance at a constant W/S_a is found by integration.

$$E = \left(\frac{S_a \sqrt{\theta_a}}{W_f} \right) \int_{W_1}^{W_2} \frac{dW}{S_a \sqrt{\theta_a}} \quad (4.10.04)$$

where: $\frac{W_1}{S_{a1}} = \frac{W_2}{S_{a2}} = \frac{dW}{dS_a} = \text{constant}$, $\sqrt{\theta_a} = S_a^{0.095}$ (below 36089 ft)
 $dW = \text{fuel weight differential (-)}$

Substituting dS_a for dW , changing limits, integrating and simplifying

$$E = 10.512 \left(\frac{S_a \sqrt{\theta_a}}{W_f} \right) \left(\frac{W}{S_a} \right) \frac{1}{\sqrt{\theta_{a1}}} \left[\left(\frac{W_1}{W_2} \right)^{.095} - 1 \right] \quad (4.10.05A)$$

and

$$E = 1.15 \left(\frac{S_a \sqrt{\theta_a}}{W_f} \right) \frac{W}{S_a} \ln \left(\frac{W_1}{W_2} \right) \quad (4.10.05B)$$

Equation 4.10.05A assumes standard temperature lapse rate and may be used below the isothermal altitude. 4.10.05B assumes constant air temperature (-55°C) and is used above the isothermal altitude.

Values of $\ln(W_1/W_2)$ may be found in CHART 4.71 at the end of this chapter.

RANGE

The actual range of turbojet aircraft is best evaluated by using the specific range parameter derived from equation 4.10.03. By the rules of dimensional analysis this equation can be put in the form,

$$\frac{V_t S_a}{W_f} = f \left(M, \frac{W}{S_a} \right) \quad (4.10.06)$$

where:

$$\frac{V_t S_a}{W_f} = \text{SRg } S_a, \text{ specific range parameter, nautical miles/lb}$$

Data for plotting this equation should be obtained at constant values of W/S_a in level flight. However, if data are obtained at a constant altitude and small percent changes in weight are involved, the error introduced will be negligible. The data for equation 4.10.06 are plotted as in Figure 4.10.3. This figure may be cross plotted to present the data for constant Mach number parameters and to determine optimum W/S_a for maximum range.

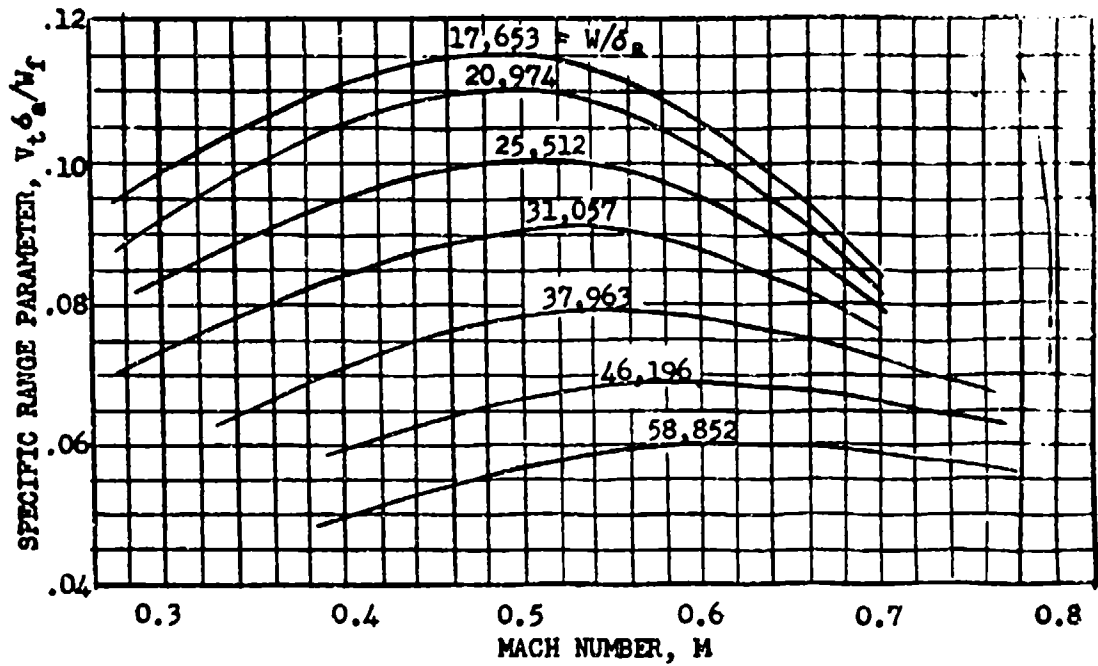


Figure 4.10.3
 Turbojet Specific Range Parameter Plot,
 Constant W/δ Values

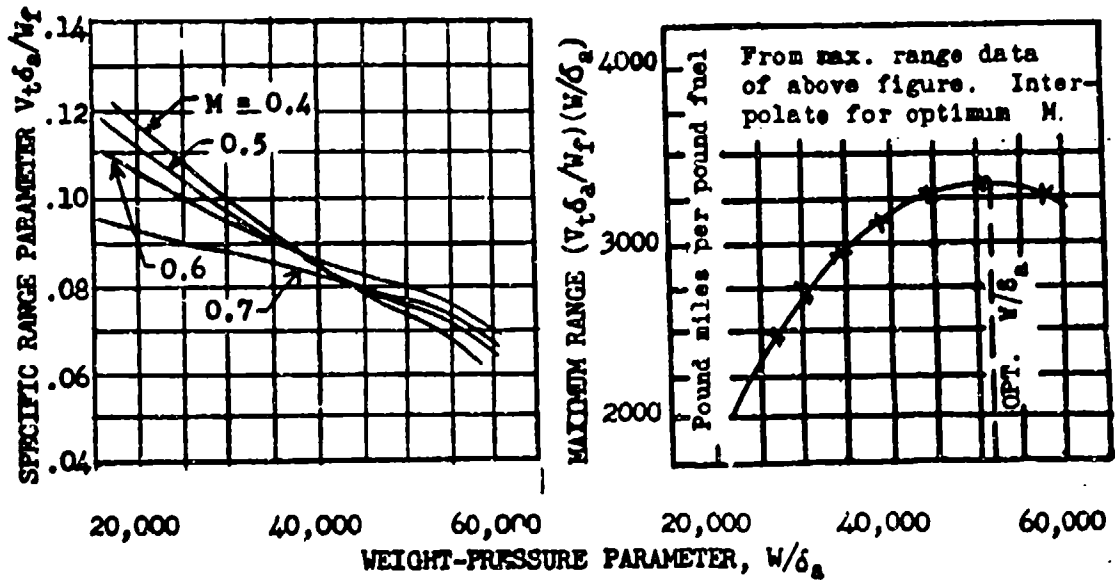


Figure 4.10.4
 Turbojet Specific Range Parameter
 and Maximum Range Plots, Constant Mach No. Values

From the two specific range parameter plots it is possible to determine the effects of any of the variables on the actual range. Also, if very high values of W/δ_a can be obtained, it is possible to determine from Figure 4.10.4 a value of W/δ_a and Mach number that gives max range independent of altitude.

It is apparent, from these figures and equation 4.10.06, that the best cruise condition for a given Mach number is at constant W/δ_a value. The higher the altitude the greater is the range until the W/δ_a for max range is reached. The cruise at constant W/δ_a requires a slight continuous climb (about 20-50 ft/min) to decrease atmospheric pressure as the weight decreases. Actual range at constant W/δ_a may be determined by integration.

$$\text{Range} = \left(\frac{v_t \delta_a}{W_f} \right) \int_{W_1}^{W_2} \frac{dW}{\delta_a} \quad (4.10.07)$$

where:

$$\frac{W_1}{\delta_1} = \frac{W_2}{\delta_2} = \frac{dW}{d\delta_a} = \text{constant}$$

dW = fuel weight differential (negative)

Substituting $d\delta_a$ for dW , changing limits and integrating

$$R_g = \left(\frac{v_t \delta_a}{W_f} \right) \frac{W}{\delta_a} \ln \left(\frac{W_1}{W_2} \right) \quad (4.10.08)$$

Values of $\ln(W_1/W_2)$ may be found in CHART 4.71 at the end of this chapter.

To determine the range at a constant altitude and Mach number, the plot in Figure 4.10.4 may be used and the integration accomplished in steps for intervals where the slope of the Mach number parameters is nearly constant. In this case,

$$\Delta R_g = \frac{(SRg \delta_a)_1 + (SRg \delta_a)_2}{2 \delta_a} (W_1 - W_2) \quad (4.10.09)$$

PERFORMANCE REPORT PRESENTATION

Ordinarily, the specific range and endurance parameters, equations 4.10.03 and 4.10.06 are not included in the aircraft performance report unless actual range and endurance data are to be included. In most cases only the specific range is presented as a function of calibrated or standard day true speed at specified altitudes and weights.

Since Mach number can be defined as a function of pressure altitude and calibrated (indicated) speed, equation 4.10.06 may be expressed at a constant altitude as,

$$\frac{V_t}{W_f} = f(V_c, W) \quad (4.10.10)$$

$$\frac{V_t}{W_f} = f(V_{ts}, W) \quad (4.10.11)$$

where:

V_{ts} = standard day true speed for V_c and given altitude

These equations are plotted in the final report as in Figures 4.10.5 and 4.10.6, for each major configuration. For reducing data, it should be noted that at a given Mach number, weight, and altitude the test and standard day specific range are equal. The plots of V_t/W_f vs V_c are used as an aid to pilot technique since it is simpler to fly at a constant V_c than at a constant V_t . It should be noted that in jet powered aircraft the specific range increases with altitude; however, if high enough altitudes or heavy enough weights are flown, a value of W/δ_a will be found that gives a max specific range.

The effects of weight variations on specific range are of much less magnitude for turbojet aircraft than for conventional aircraft of equal size. This is because the best range conditions are at about 0.5 Mach number or above, and the induced drag in this speed range is a very small percent of the total drag. Nevertheless, weight variation can have a considerable percentage effect on turbojet range because of their inherent short range characteristics for a given size. Typical weight effects on range can be seen graphically in Figure 4.10.3 where the specific range parameter is plotted vs M for constant values of W/δ_a . In this plot the sea level standard weight effects can be seen directly, and the effects of weight variation on specific ranges at any altitude can be readily computed.

Actual range can be computed with data from plots such as Figures 4.10.5 and 4.10.6 by assuming the Mach number be held constant and the weight pressure ratio to be held constant by a slow climb. The range in this case is,

$$Rg = \left(\frac{V_t}{W_f} \right) W_1 \ln \left(\frac{W_1}{W_2} \right) \quad (4.10.12)$$

The necessary rate of climb to hold a constant weight-pressure ratio is,

$$\frac{dH_c}{dt} = \frac{1.6 W_f T_a}{W_1} \quad (4.10.13)$$

where:

$\frac{dH_c}{dt}$ = altimeter rate of climb, ft/min
 W_f = fuel flow, lbs/hr
 T_a = standard temperature ($^{\circ}K$) for pressure altitude)
 W_1 = weight at start of cruise

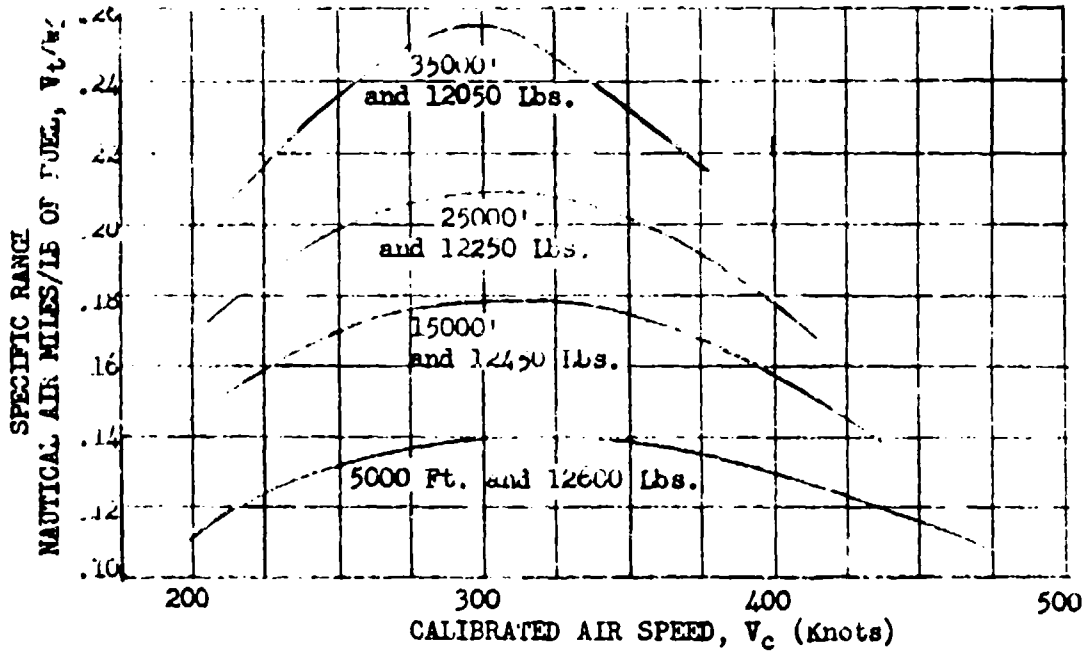


Figure 4.10.5
Usual Report Presentation of
Turbojet Specific Range Data

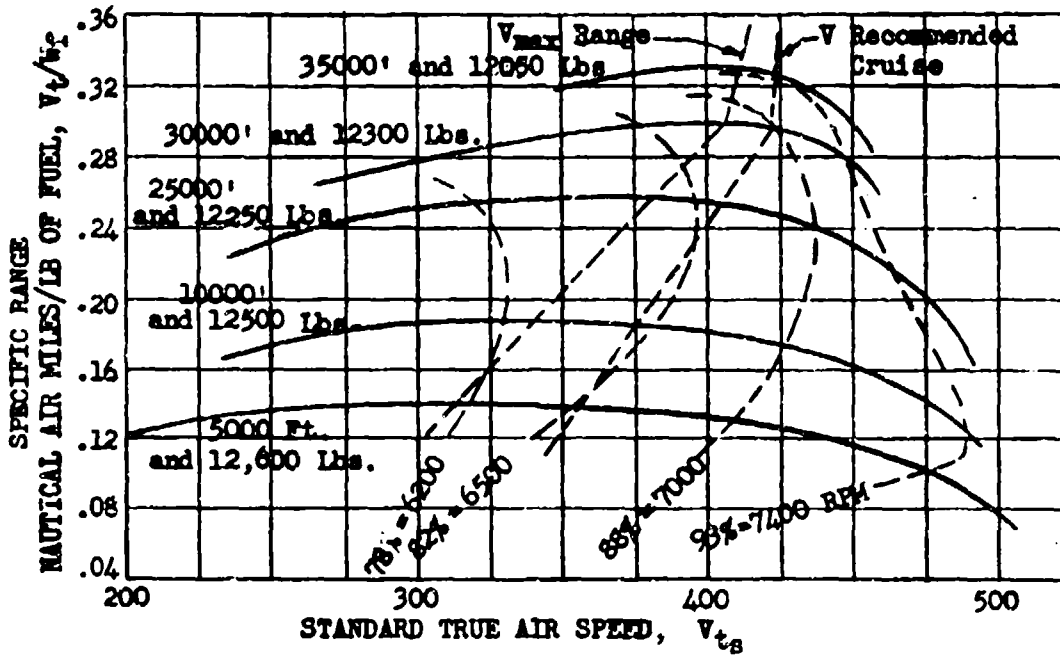


Figure 4.10.6
Usual Report Presentation of
Turbojet Specific Range Data

DATA REDUCTION OUTLINE (4.10.1)

For Fuel Flow Parameter and Specific Range
Calibrations, Turbojet Aircraft

NOTE: This data reduction is a sequel to the Level Flight Power Calibrations Data Reduction Outline 4.81.

(38) W_{ft} gals/hr Test volumetric fuel flow, from flow meter or timed increments at stabilized power conditions

(39) W_{ft} lbs/hr Test fuel weight-flow (38) x lb/gal

(40) $\frac{W_{ft}}{\delta_a \sqrt{\theta_{at}}}$ Fuel flow parameter, (39) + (6) and (18)

(41) Plot (40) vs (31) as in Figure 4.10.1

(42) $\left(\frac{W_{ft}}{\delta_a \sqrt{\theta_{at}}} \right)_w$ Fuel flow parameter at standard W/δ_a , from (41) and (33)

(43) $1/\delta_a \sqrt{\theta_{as}}$ From (5) and standard altitude tables

(44) SRg Nautical air miles per pound, (12) x (43) + (42)

NOTE: If fuel parameter weight correction is not used $SRg = [(12) \times (18)] + [(39) \times (17)]$

(45) Plot (44) vs (10) and (12)

SECTION 4.11

Flight Thrust Measurement Applications to Drag and Lift Coefficient and Aircraft Efficiency Determination

Whenever thrust measuring instrumentation is installed, actual thrust delivered may be computed by the methods of Chapter Three. In lieu of tail pipe instrumentation the engine manufacturer's expected performance curves may be used to approximate flight thrust. In this case values of $N/\sqrt{\theta_{t2}}$ and P_{t2}/P_a , ram pressure ratio, must be calculated. Since the engine net thrust equals the aircraft drag, it may be substituted wherever drag is used in plotting, or it may simply be called drag. Equations 4.210 and 4.215 define the two basic drag plots. In one plot drag is shown as a function of $V_t \sqrt{\sigma}$. This plot is valid only for the weight and altitudes at which it was flown. Figure 4.11.1 shows a typical F_n vs $V_t \sqrt{\sigma}$ plot.

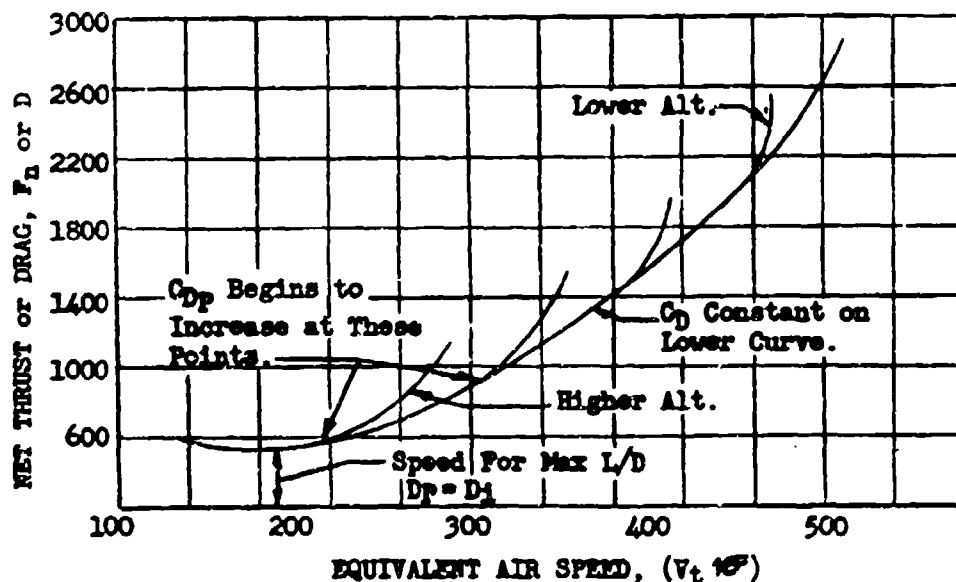


Figure 4.11.1
Typical Drag or Net Thrust vs
Equivalent Speed Plot

Two other forms of the drag plot are shown in Figure 4.11.2, in which the thrust parameter, F_n/P_a or F_n/θ_a , is plotted vs the weight pressure parameter, W/P_a or W/θ_a , and Mach number.

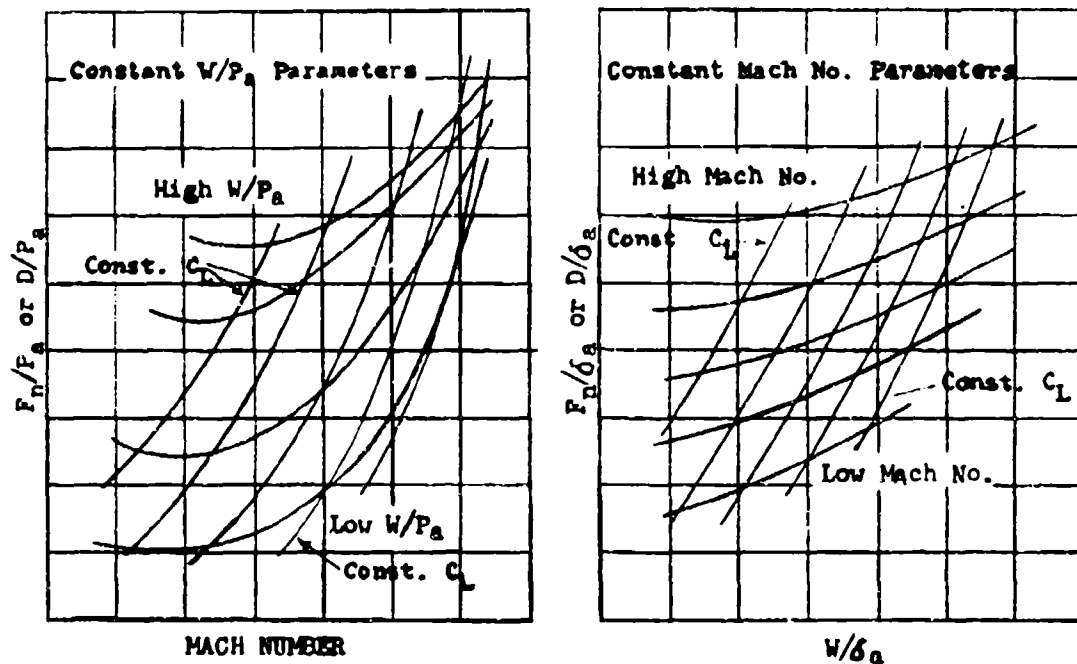


Figure 4.11.2
Two Forms of Plotting the Level Flight Drag Data

The F_n/δ_a vs W/δ_a plot with constant Mach number parameters may be derived by cross plotting as was done in Section 4.9 to obtain $N/\sqrt{\delta_a}$ vs W/δ_a for constant Mach number parameters. This plot is valuable in determining net thrust required for any altitude, weight, and speed.

When net thrust has been determined, C_D , C_{DP} , and "e" are determined from values of C_L , P_a , M and the aircraft dimensions. The following equalities and constants are useful in these computations.

$$F_n = D$$

$$C_D = \frac{295 F_n}{\sigma V_t^2 S} = \frac{0.0202 F_n}{P_a M^2 S} = \frac{0.000675}{M^2 S} \left(\frac{F_n}{S} \right)$$

$$C_L = \frac{295 W}{\sigma V_t^2 S} = \frac{0.0202 W}{P_a M^2 S} = \frac{0.000675}{M^2 S} \left(\frac{W}{S} \right)$$

$$e = \frac{C_L^2}{\pi AR (C_D - C_{DP})}$$

$$C_{D1} = \frac{C_L^2}{\pi AR}$$

NOTE: when C_L or $C_L^2 = 0$
then $C_{D1} = 0$
and $C_{DP} = C_D$

$$C_{DP} = C_D - C_{D1}$$

With the above equalities constant C_L parameters may be constructed as shown on Figure 4.11.2, from simple slide rule computations.

The intersections of C_L and W/δ_a parameters may be used to compute C_D values and a plot made as shown in Figure 4.11.5.

where:

F_{th} = lbs
 V_{gr} = knots
 S_{gr} = ft²
 ρ_a = "Hg

The C_L^2 vs C_D plot will be a straight line (Figure 4.11.3) as long as the incompressible theory is valid but will show breaks where the drag curves rise due to the effect of Mach number.

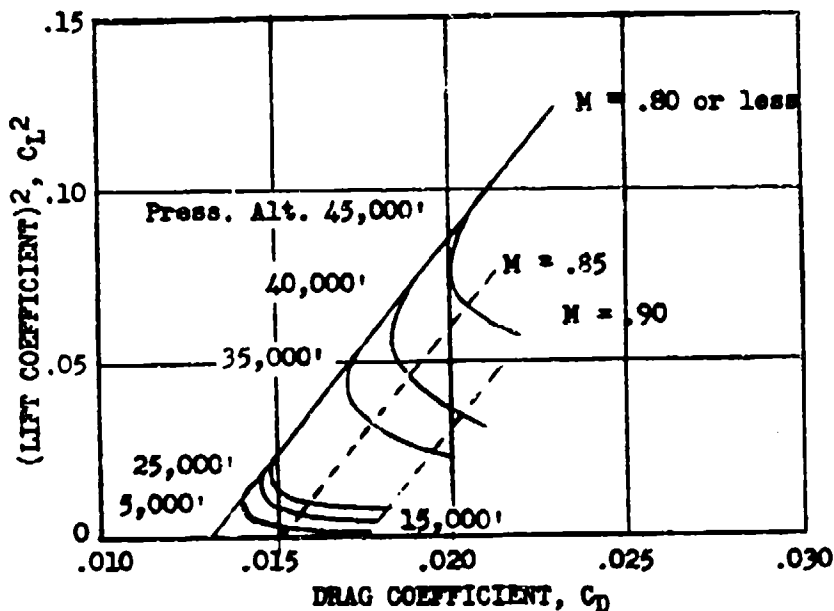


Figure 4.11.3
Method of Plotting Drag and Lift Coefficient
and Mach Number Data

Airplane efficiency is easily calculated by using the C_{DP} value defined by the point ($C_L^2 = 0$) on the C_L^2 vs C_D plot. This is accomplished by drawing a straight line through the incompressible points (low speed) on the C_L^2 vs C_D plot. The intersection of this line at ($C_L^2 = 0$) defines C_{DP} . In the incompressible range C_{DP} is constant but it increases rapidly as supersonic flow is developed over the wing; hence, a plot of C_{DP} vs Mach number as in Figure 4.11.4, will indicate the Mach numbers at which compressibility effects will be found. At higher altitudes (larger W/σ_a values) C_{DP} will show an increase from compressibility at lower Mach numbers than required at lower altitudes (smaller W/σ_a values). This illustrates the fact that C_{DP} in the compressible range increases with C_L or angle of attack at constant Mach numbers.

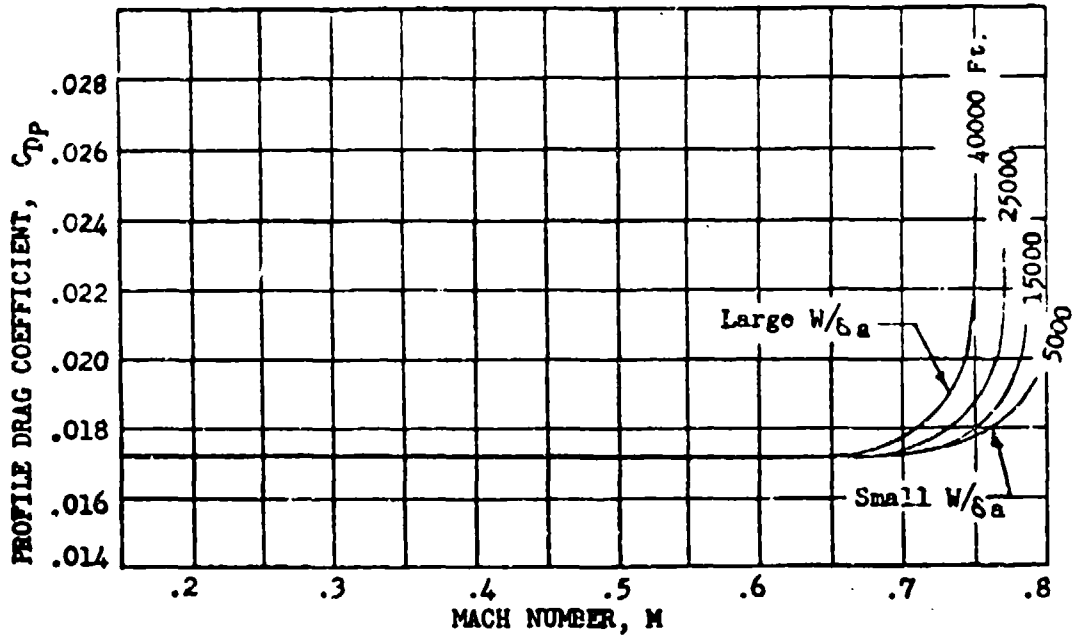


Figure 4.11.4
Plot Showing Effects of Mach Number and
 W/b_a on Profile Drag

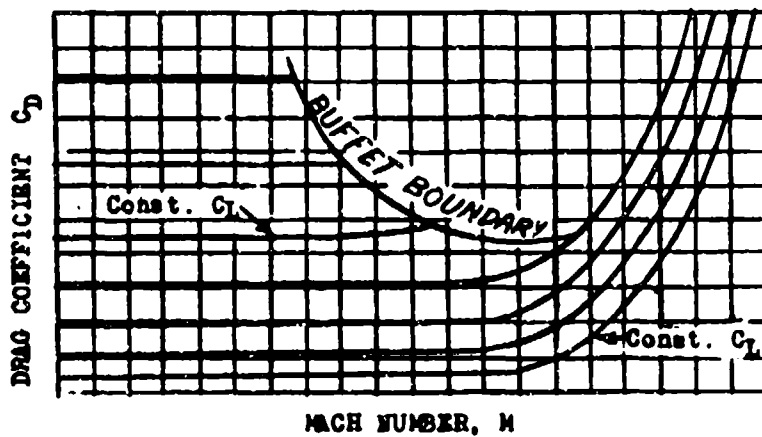


Figure 4.11.5
 C_D C_L Showing Critical Mach No. and Buffett Boundary

DATA REDUCTION OUTLINE (4.11.1)

For Determining Drag and Lift Coefficients and Aircraft Efficiency

NOTE: This data reduction is a sequel to the Level Flight and Range Data Reductions, 4.81 and 4.10.1

(46)	F_n	lbs	Net thrust
(47)	V_e	knots	Equivalent speed, from CHART 8.3 (5) and (11)
(48)	Plot (46) vs (47) as in Figure 4.11.1		
(49)	$F_n/6a$	lbg	Net thrust parameter, (46) ÷ (6)
(50)	S	ft ²	Wing area, from aircraft specs
(51)	A/S		Aspect ratio, from aircraft specs
(52)	M^2		From (11)
(53)	C_D		Total drag coefficient, $0.000675 \times (49) + [(50) \times (52)]$
(54)	C_L		Lift coefficient $0.000675 \times (25) + [(50) \times (52)]$ From (54)
(55)	C_L^2		From (54)
(56)	Plot (55) vs (53) as in Figure 4.11.3		
(57)	C_{DP}		Profile drag coefficient, from extrapolation to $C_L^2 = 0$ of incompressible portion of (56), Figure 4.11.3
(58)	C_{Di}		Induced drag coefficient, (53) - (57)
(59)	e		Aircraft efficiency factor (55) ÷ [(58) × (51) × π]
(60)	Plot (57) vs (11) as in Figure 4.11.4		

NOTE: "e" needs to be determined at only one point on the incompressible C_L^2 vs C_D plot.

SECTION 4.12

STANDARDIZATION OF JET LEVEL FLIGHT DATA FOR THRUST AUGMENTATION CONDITIONS OR PARTICULAR POWER LEVER SETTINGS ON AUTOMATICALLY CONTROLLED ENGINES

Data standardization in the high thrust range of automatically controlled engines, variable area nozzle engines, or for thrust augmentation conditions is not always amenable to the use of elementary engine operation parameters such as $N/\sqrt{\theta_a}$. In these cases various jet nozzle positions or particular throttle settings ("normal", "military", "maximum") will all give different flight speeds at a constant $N/\sqrt{\theta_a}$. For these conditions a plot such as Figure 4.83 would be meaningless.

Test requirements will usually demand standard speed, altitude, and weight data at a particular throttle position (detent), or rpm-jet temperature combination, or augmentation setting. Standardization under these conditions may be accomplished by use of $F_n/\theta_a - W/\theta_a - \text{Mach No.}$ plots as shown in Figure 4.11.2. The engine manufacturer's performance data will provide a means of obtaining incremental thrust correction for ambient (or inlet) temperature variations at the given power settings. Although the manufacturer's actual engine thrust data may be inaccurate the incremental values obtained from the slopes of his data will provide sufficiently accurate thrust corrections. If these net thrust corrections for ambient temperature variations (or any other non-standard engine condition) are available, the following steps will standardize the flight speeds and Mach No.'s. in conjunction with Figure 4.11.2. If possible, flight thrust measurement should be used to obtain this figure. The manufacturer's expected thrust data can be used for this plot without seriously impairing the accuracy of standard flight speed data obtained by this method.

- a. If test W/θ_a values are more than one (1) percent from average values, correct data to constant W/θ_a values as before.
- b. Select weight and altitude desired at average W/θ_a value. (This should not be more than ± 5000 ft. of test altitudes).
- c. Determine t_{a_s} for selected altitude and

$$\Delta t = t_{a_t} - t_{a_s}$$

- d. Calculate $\Delta F_n/\theta_a$ for Δt_a of (c) above and add to test value of F_n/θ_a for the given thrust setting.
- e. On Figure 4.11.2, using corrected F_n/θ_a , establish M for standard altitude on mean W/θ_a curve or, using $\Delta F_n/\theta_a$ values, move test point parallel to W/θ_a curve to standard F_n/θ_a and M.

The final standardised plot for a given weight will appear as in Figure 4.12.1.

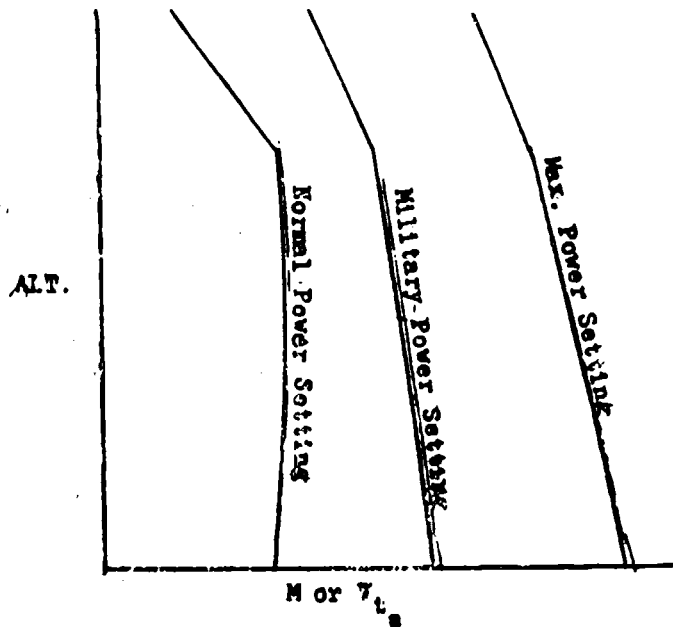


Figure 4.12.1

Effects of non-standard temperature may be computed as before and as shown in Figure 4.12.2.

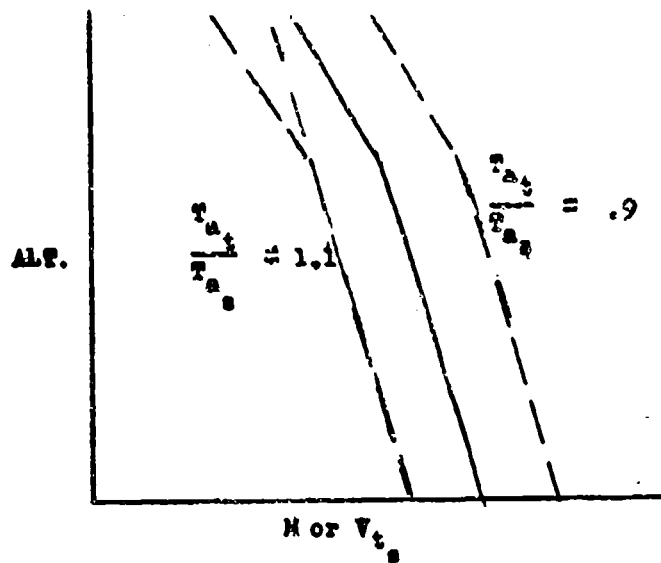
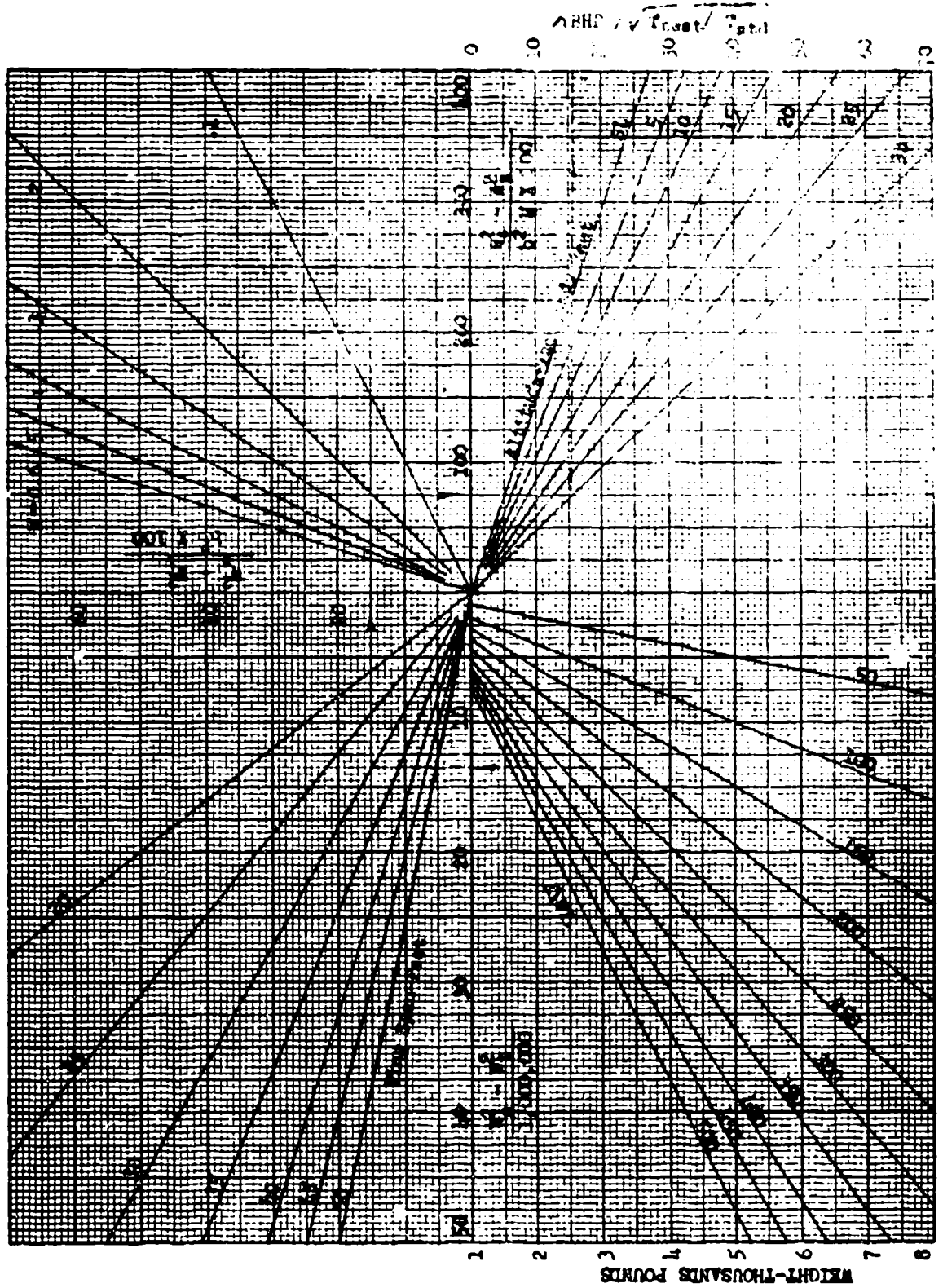


Figure 4.12.2

POWER CORRECTION FOR WEIGHT CHANGE

CHART 4.42

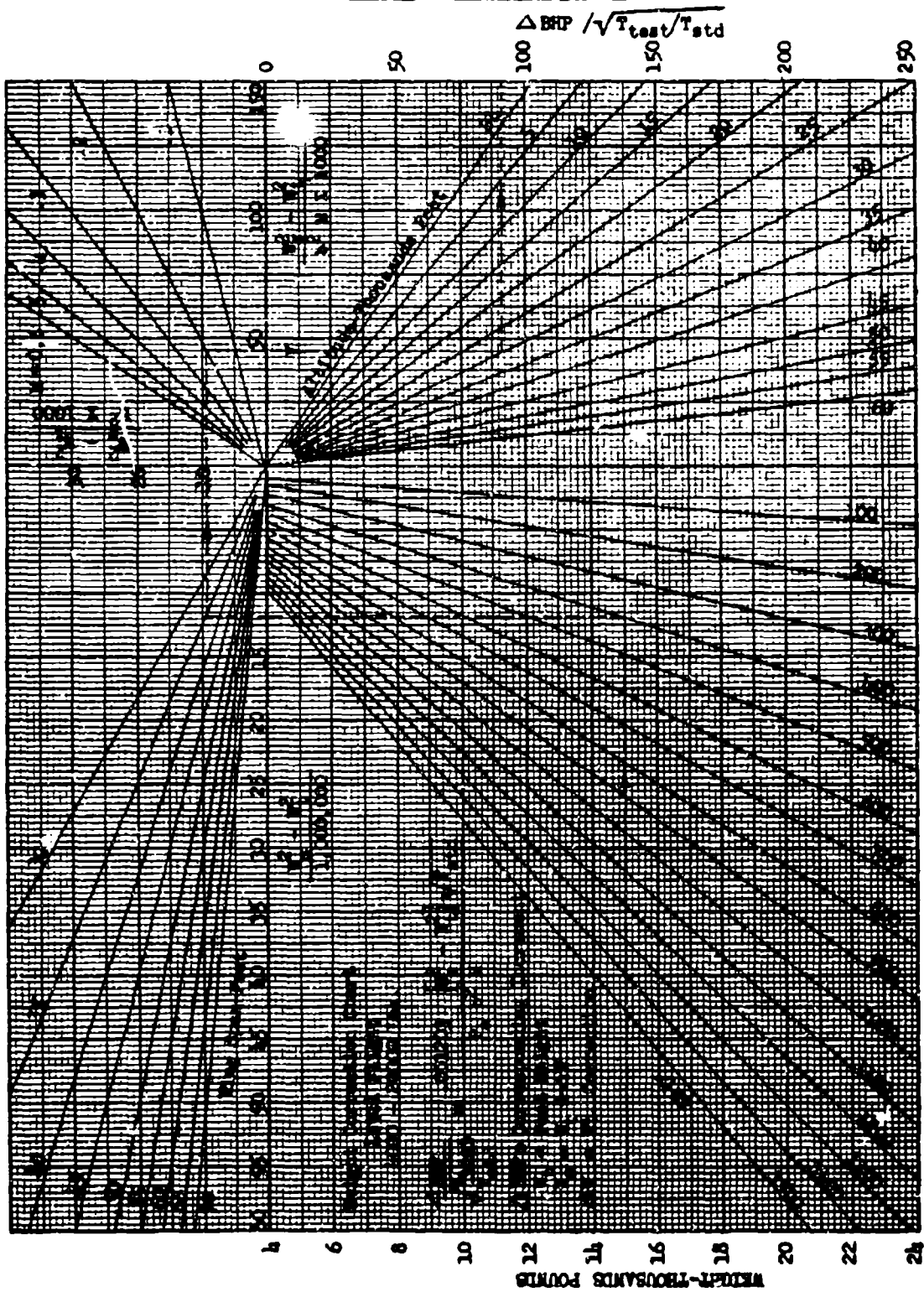


AFR 6273

CHART 4.41

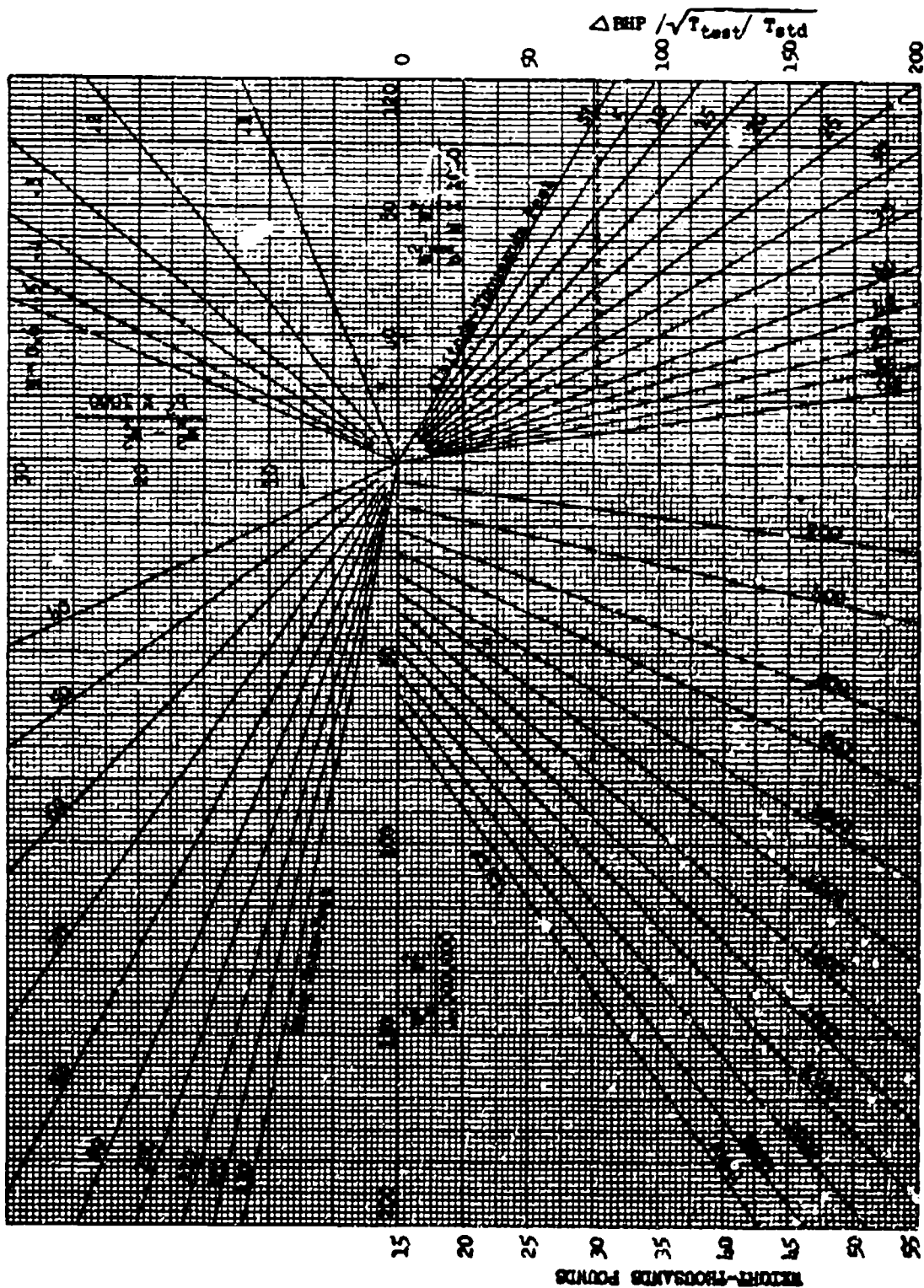
POWER CORRECTION FOR WEIGHT CHANGE

CHART 4.41



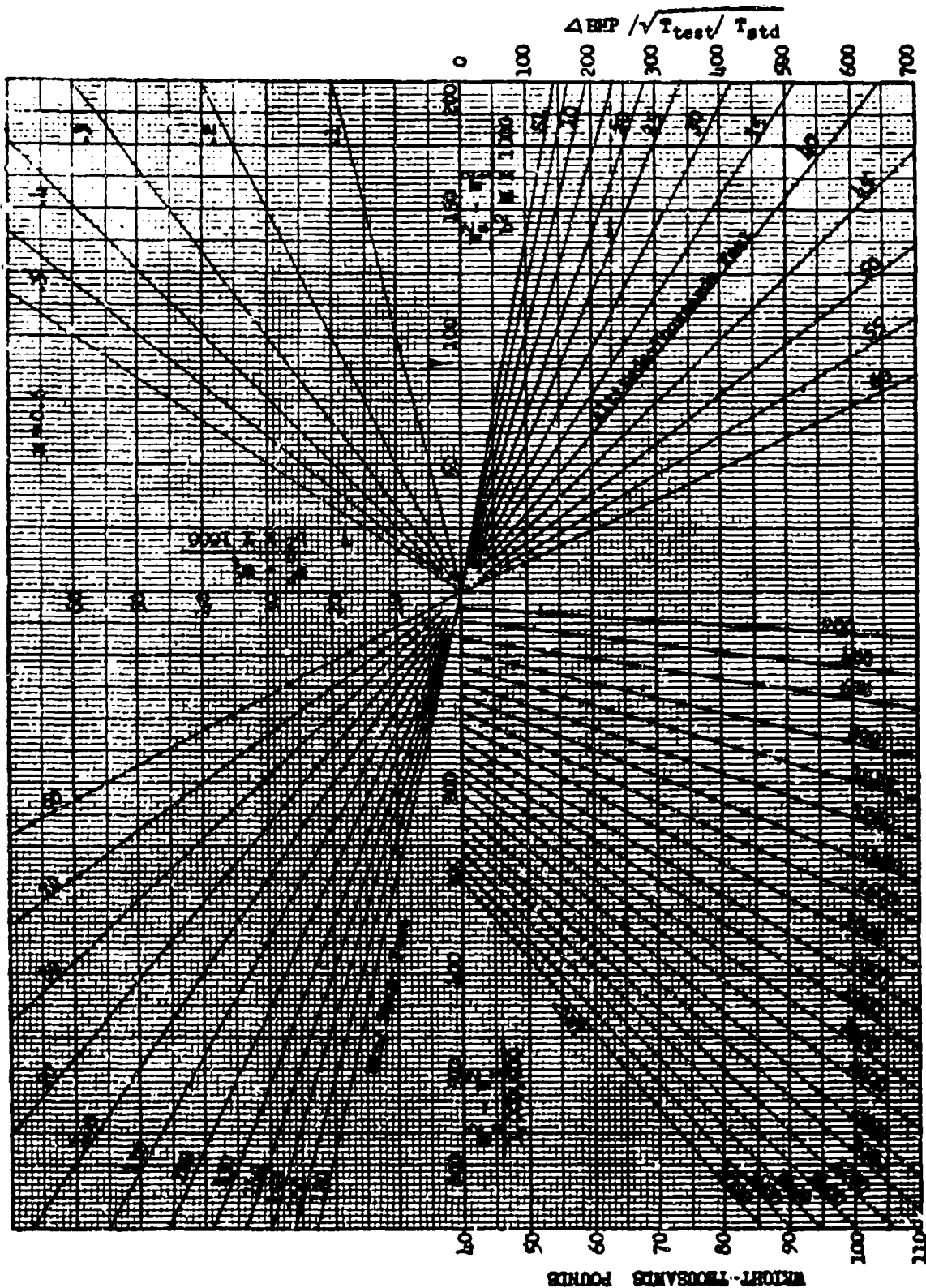
AFIP 6273

CHART 4.41



AFTR 6273

CHART 4.41

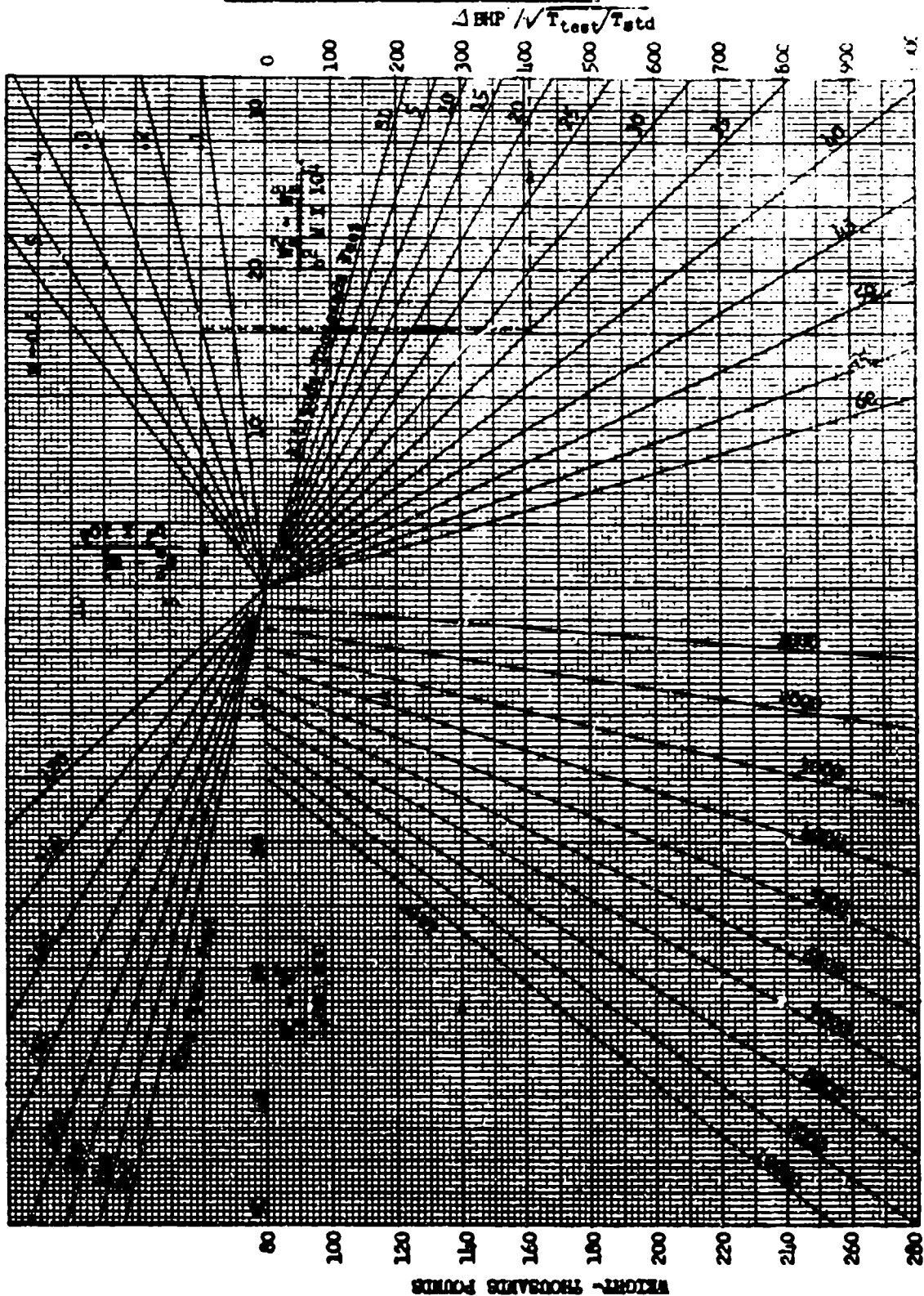


1949

CHART 4.41

POWER CORRECTION FOR WEIGHT CHANGE

CHART 4.11

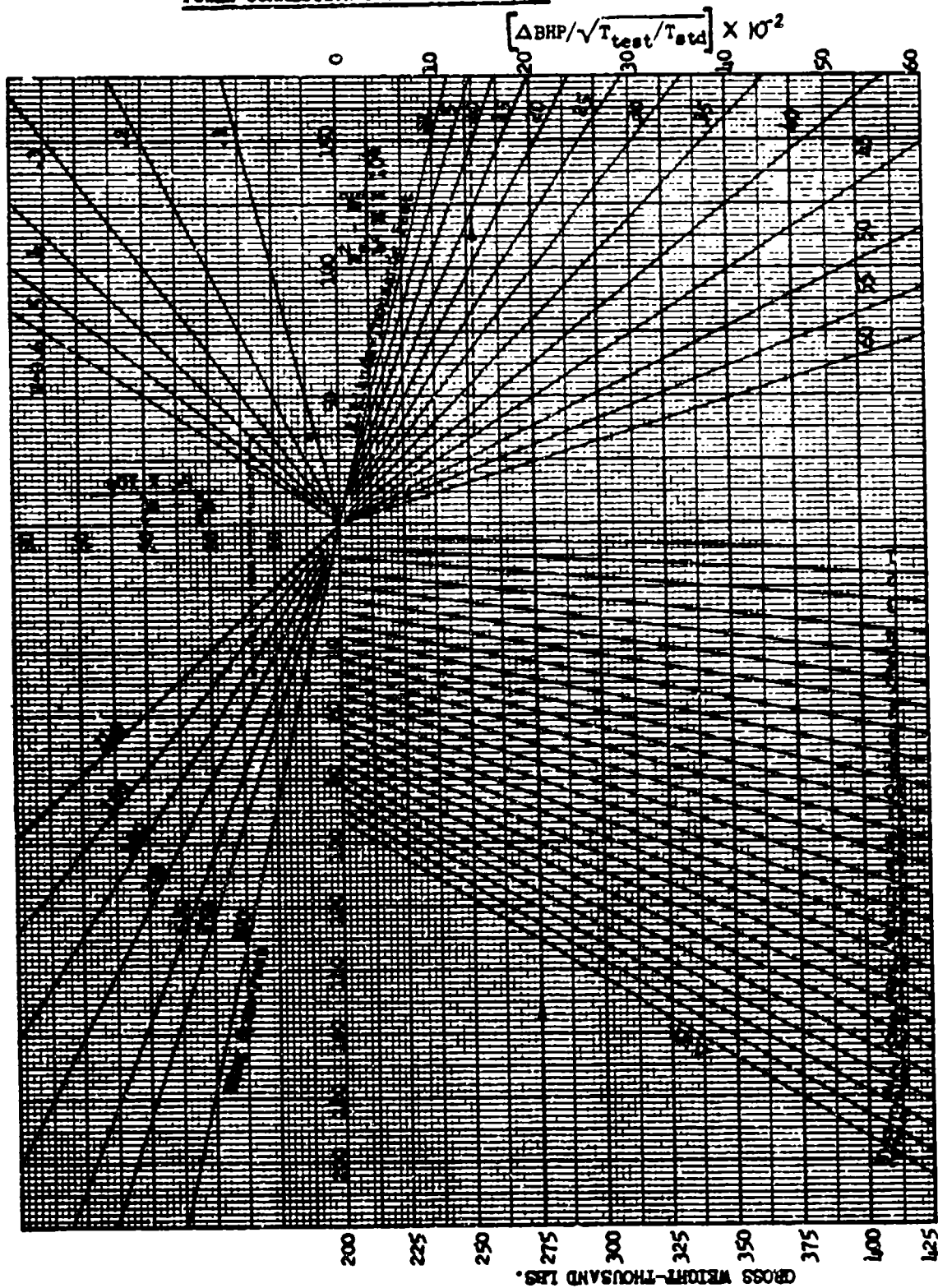


AFR 6273

CHART 4.11

POWER CORRECTION FOR WEIGHT CHANGE

CHART 4.41



AFTR 6273

CHART 4.41

NATURAL LOG OF INITIAL TO FINAL GROSS WEIGHT RATIO FOR CHART 4.71
RANGE AND ENDURANCE COMPUTATIONS

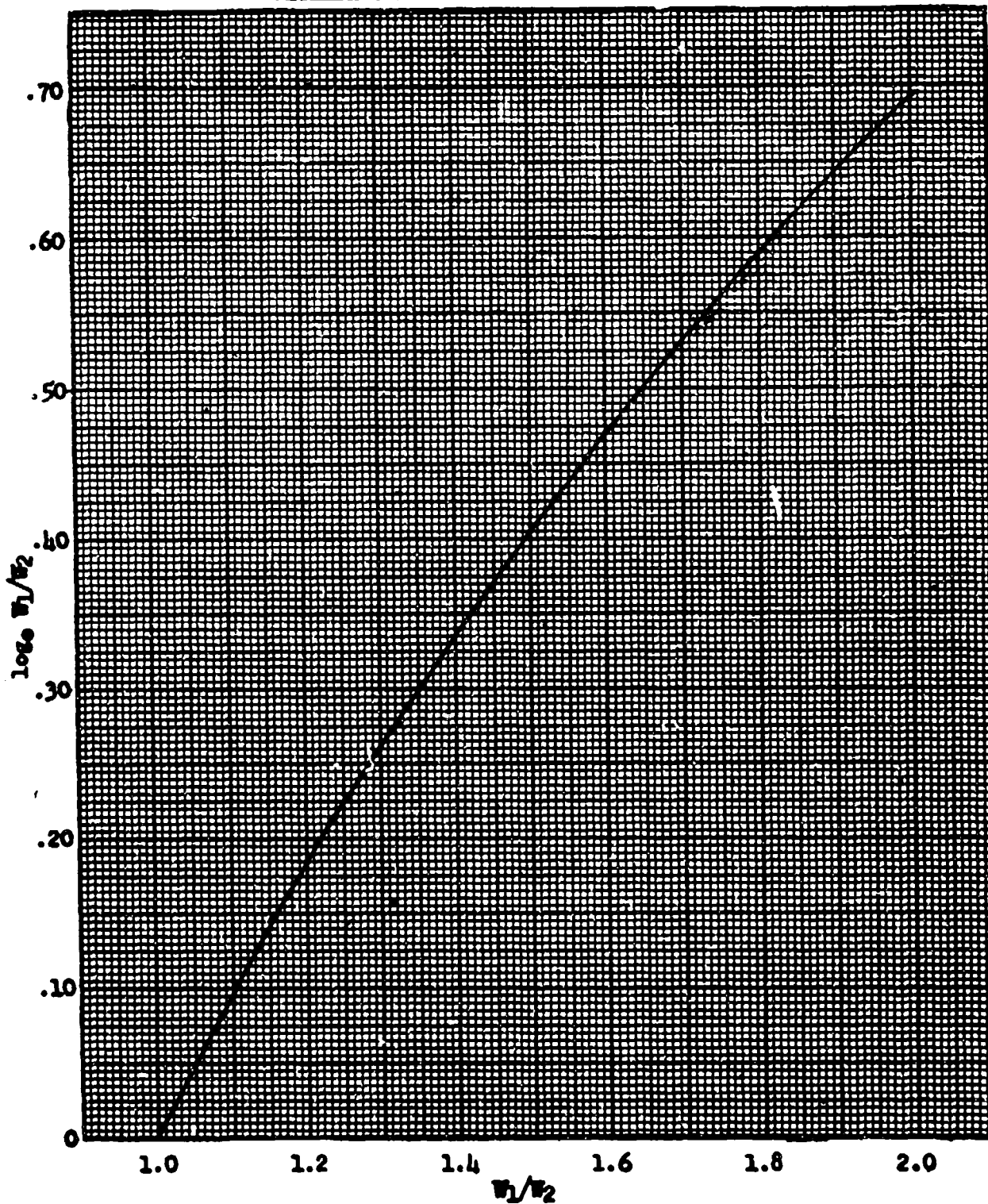


CHART 4.71

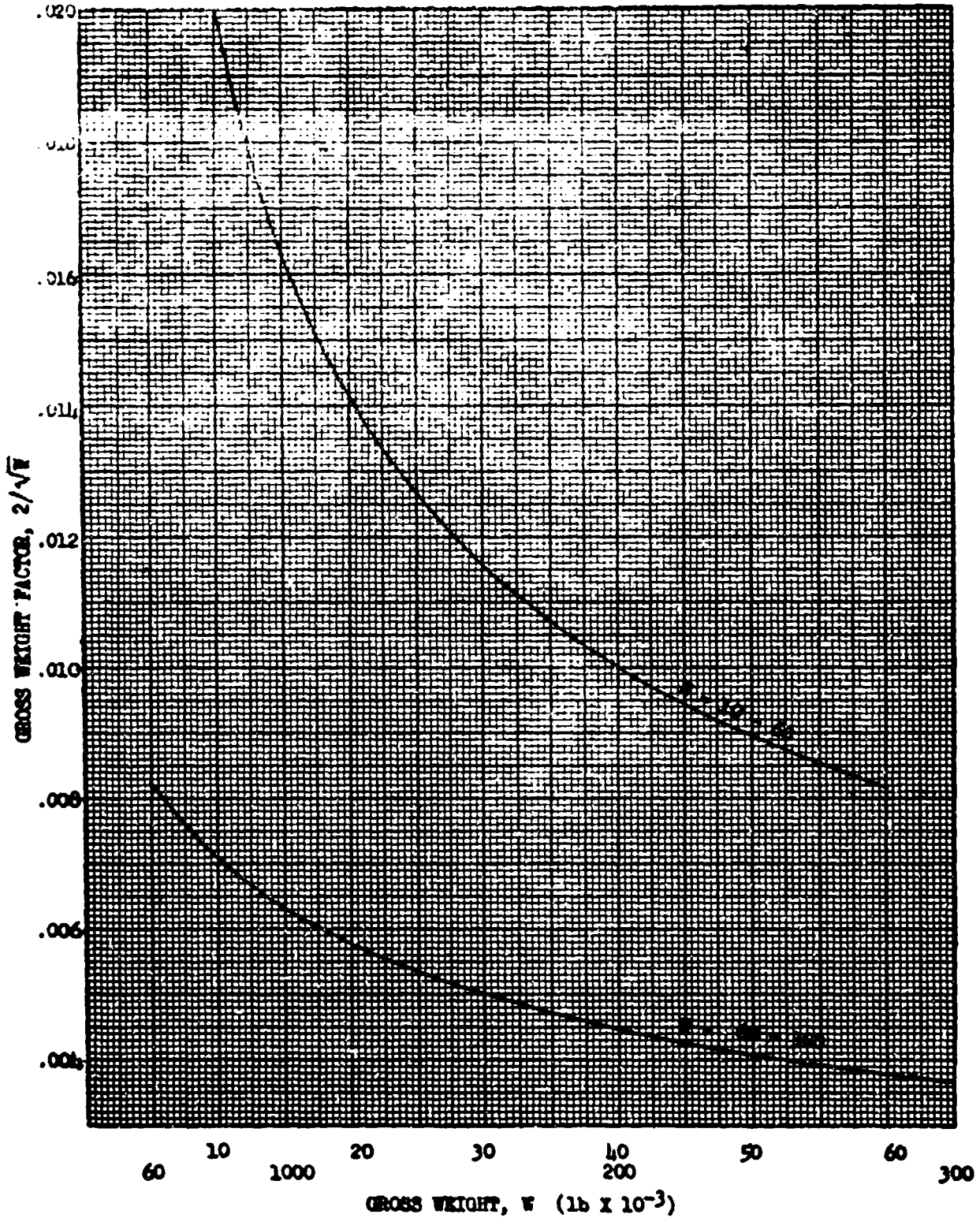


CHART 4.72

CHAPTER FIVE

CLIMB AND DESCENT PERFORMANCE

SECTION 5.1

Rate of Climb Parameters - Derivation

An aircraft climbs because the power being developed is greater than the power that would be required to maintain level unaccelerated flight under the same atmospheric and velocity conditions. This conversion of excess power into rate of climb may be shown graphically and analytically. Consider the forces acting on the aircraft as shown in Figure 5.11.

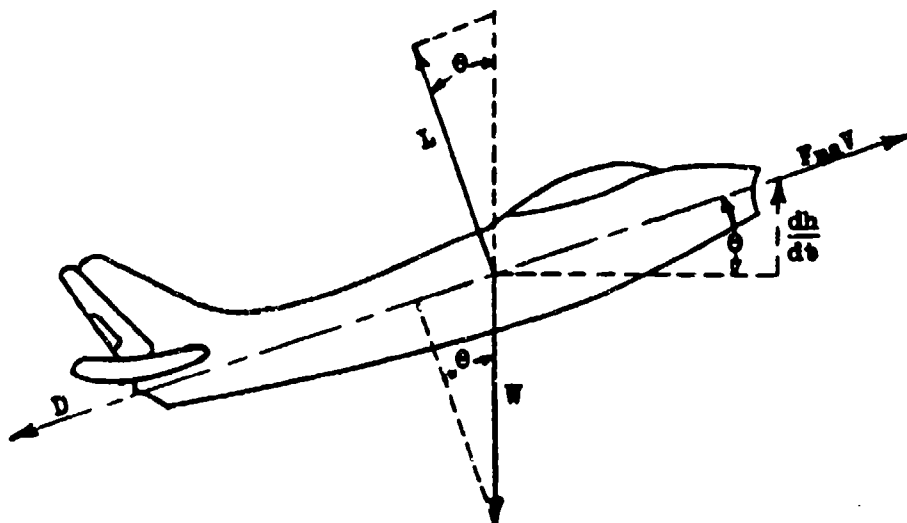


Figure 5.11
Vector Presentation for Climbing Aircraft

From this figure,

$$\begin{aligned}
 L &= W \cos \theta \\
 F_{na} &= D + W \sin \theta \\
 F_{na}V &= DV + WV \sin \theta \\
 V \sin \theta &= \frac{dh}{dt} = \frac{F_{na}V - DV}{W}
 \end{aligned}
 \tag{5.101}$$

$$\frac{dh}{dt} = 33,000 \frac{(THP_a - THP_r)}{W}
 \tag{5.102}$$

where:

- L = lift force (lbs)
- W = aircraft gross weight (lbs)
- θ = climb angle
- F_{na} = net thrust available (lbs)
- D = F_{nr} = drag force = level flight drag (lbs) = net thrust required
- V = aircraft velocity on climb path (ft/min)
- dh/dt = tape line rate of climb (ft/min)
- $THP_a = \frac{F_{na}V}{33,000}$ = available thrust horsepower
- $THP_r = \frac{DV}{33,000}$ = required thrust horsepower to maintain unaccelerated level flight

NOTE: Equations 5.101 and 5.102 are based on the assumption that for small values of θ , $0^\circ - 20^\circ$, the lift force is equal to the gross weight. The case of the large climb angle will be discussed later.

Figure 5.12 displays graphically the typical variation of $(THP_a - THP_r)$ with climbing velocity.

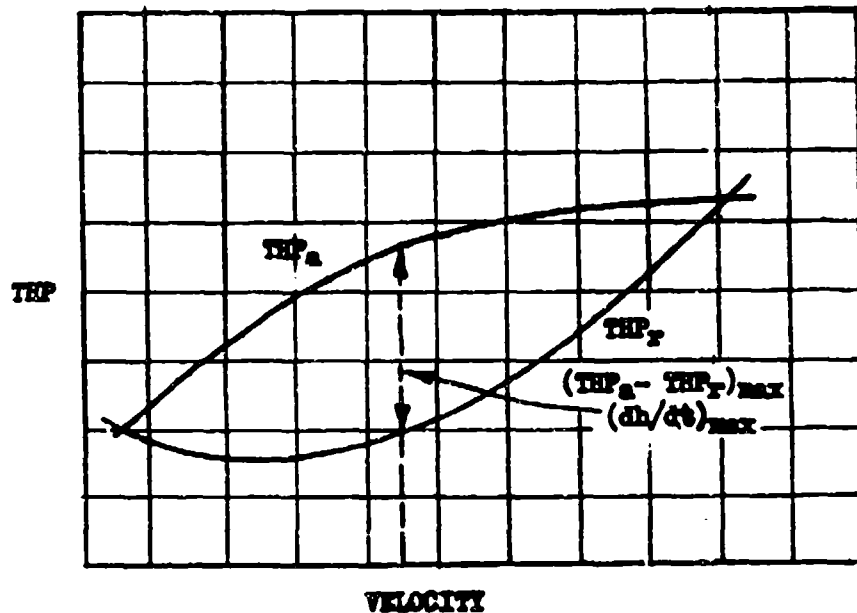


Figure 5.12
Typical Power Available and Power Required Curves

Certain aerodynamic considerations, assuming parabolic variation of C_D and C_L , are used in developing the rate of climb, induced power, and parasite power relationships.

$$D = C_{Dp}qS + C_{Di}qS \quad (5.103)$$

$$D = C_{Dp}qS + \left(\frac{W}{qS}\right)^2 \frac{qS}{\pi R e}$$

where: $L = W$

$$D = C_{Dp}qS + \left(\frac{W \cos \theta}{qS}\right)^2 \frac{qS}{\pi R e}$$

where: $L = W \cos \theta$

Substituting $0.7 P_a M^2$ for q ,

$$D = C_{Dp}k_1 P_a M^2 + \frac{W^2}{P_a M^2 k_2} \quad (5.104)$$

where: $L = W$

$$D = C_{Dp}k_1 P_a M^2 + \frac{W^2 \cos^2 \theta}{P_a M^2 k_2} \quad (5.105)$$

where: $L = W \cos \theta$

Dividing by P_a , the ambient pressure, in equation 5.104,

$$\frac{D}{P_a} = C_{Dp}k_1 M^2 + \frac{W^2}{P_a^2 M^2 k_2} \quad (5.106)$$

where:

- M = Flight Mach number
- C_{Dp} = $f(M \text{ and } W/P_a)$
- P_a = atmospheric pressure (lbs/ft²)
- k_1 = $0.7S$ (ft²)
- k_2 = $2.2b^2 e$ (ft²)
- b = wing span (ft)
- e = airplane efficiency factor
- R = b^2/S

It has been shown that,

$$THP_r = \frac{DV}{33,000} = \frac{F_{NR}V}{33,000}$$

where F_{NR} = thrust required to overcome Drag

or

$$\frac{\text{THP}_a}{P_a} = \frac{F_{DR} V}{33,000}$$

Dividing by $P_a \sqrt{T_a}$,

$$\frac{\text{THP}_r}{P_a \sqrt{T_a}} = \frac{D V}{33,000 P_a \sqrt{T_a}} = \frac{F_{DR} V}{33,000 P_a \sqrt{T_a}} \quad (5.107)$$

$$\frac{\text{THP}_a}{P_a \sqrt{T_a}} = \frac{F_{DR} V}{33,000 P_a \sqrt{T_a}} \quad (5.108)$$

As shown in Chapter One,

$$\frac{V}{\sqrt{T_a}} = M \times \text{constant}$$

Using this relationship, equations 5.107 and 5.108 may be written in the form,

$$\frac{\text{THP}_r}{P_a \sqrt{T_a}} = \frac{D}{P_a} \text{ KM} = \frac{F_{DR}}{P_a} \text{ KM} \quad (5.109)$$

$$\frac{\text{THP}_a}{P_a \sqrt{T_a}} = \frac{F_{DR}}{P_a} \text{ KM} \quad (5.110)$$

Substituting equation 5.109 in 5.106,

$$\frac{\text{THP}_r}{P_a \sqrt{T_a}} = C_{Dp} k_1 \text{ KM}^3 + \frac{W^2 k}{P_a^2 M k_2} \quad (5.111)$$

Therefore,

$$\frac{\text{THP}_r}{P_a \sqrt{T_a}} = f \left(M, \frac{W}{P_a} \right) \text{ level unaccelerated flight} \quad (5.112)$$

From engine performance analysis,

$$\frac{\text{THP}_a}{P_a \sqrt{T_a}} = \frac{\text{BHP}_a}{P_a \sqrt{T_a}} (\eta_p)$$

where: η_p = propeller efficiency

$$\frac{\text{THP}_a}{P_a \sqrt{T_a}} = \frac{F_{DR}}{P_a} \text{ KM} = f \left(\frac{W}{\sqrt{T_a}}, M \right) \quad \begin{array}{l} \text{turbojet} \\ \text{aircraft} \end{array} \quad (5.113)$$

Equation 5.112 applies to both propeller driven aircraft and turbojet aircraft, while equation 5.113 applies to turbojet aircraft only.

From the functional power and drag equations the rate of climb functional parameters are derived.

From the rate of climb equation,

$$\frac{dh}{dt} = 33,000 \frac{(THP_a - THP_r)}{W} \quad (5.102)$$

This may be divided by $\frac{P_a}{P_a}$ and $\sqrt{T_a}$, then,

$$\frac{\frac{dh}{dt}}{\sqrt{T_a}} = 33,000 \frac{P_a}{W} \left(\frac{THP_a}{P_a \sqrt{T_a}} - \frac{THP_r}{P_a \sqrt{T_a}} \right) \quad (5.114)$$

From equations 5.112, 5.113 and 5.114,

$$\frac{\frac{dh}{dt}}{\sqrt{T_a}} = f \left(\frac{THP_a}{P_a \sqrt{T_a}}, M, \frac{W}{P_a} \right) \quad \text{propeller driven} \quad (5.115)$$

$$\frac{\frac{dh}{dt}}{\sqrt{T_a}} = f \left(\frac{W}{\sqrt{T_a}}, M, \frac{W}{P_a} \right) \quad \text{turbojet} \quad (5.116)$$

$$\frac{\frac{dh}{dt}}{\sqrt{T_a}} = f \left(\frac{F_{D0}}{P_a}, M, \frac{W}{P_a} \right) \quad \text{turbojet} \quad (5.117)$$

SECTION 5.2

Temperature Variation Correction to Rate of Climb Data

As test day and standard day flights are assumed to be at the same pressure altitude, it is only necessary to make atmospheric performance corrections for temperature differences. The corrected pressure altitude at which the aircraft flies is denoted by the symbol, H_0 , and the tapeline altitude by the symbol, h . The relationship between tapeline and pressure altitude increments is given by

$$\frac{dh}{dH_0} = \frac{\rho_s}{\rho_t} = \frac{T_{at}}{T_{as}} \text{ for } (P_{as} = P_{at}) \quad (5.201)$$

where:

- ρ_s = Density for which instrument is calibrated - standard density at the pressure altitude
- ρ_t = Density at test pressure altitude
- T_{as} = Standard temperature at the pressure altitude
- T_{at} = Test temperature at the pressure altitude

Then,

$$\frac{dh}{dt} = \left(\frac{dH_0}{dt} \right) \left(\frac{T_{at}}{T_{as}} \right) = \text{tapeline rate of climb at test true speed} \quad (5.202)$$

In the parameters of equations containing T_a ; T_{at} may be substituted.

Then,

$$\frac{dh/dt}{\sqrt{T_{at}}} \sqrt{T_{as}} = R/C = \text{tapeline rate of climb at standard day true speed.}$$

And, from equation 5.202,

$$\frac{dh}{dt} \sqrt{\frac{T_{as}}{T_{at}}} = \frac{dH_0}{dt} \sqrt{\frac{T_{at}}{T_{as}}} = R/C = \text{tapeline rate of climb at standard day true speed} \quad (5.203)$$

In equations 5.115, 5.116 and 5.117 it is seen that, for a constant M and W/P_a , the rate of climb parameter varies with the power parameters,

$$\frac{THP_a}{P_a \sqrt{T_a}} \text{ or } \frac{H}{\sqrt{T_a}} \text{ or } \frac{P_{D2}}{P_a}$$

As climbs are flown at constant rpm in turbojets and at constant rpm-manifold pressure schedules in propeller driven aircraft, temperature variations from test conditions will cause changes in the value of the rate of climb parameter. This rate of climb increment for temperature effects on power is called $\Delta R/C_1$.

$$\Delta R/C_1 = \Delta \left(\frac{dh}{dt} \sqrt{T_{as}} \right) \sqrt{T_{at}} \quad (5.204)$$

From equation 5.101,

$$\Delta \left(\frac{dh}{dt} \sqrt{T_{as}} \right) = \Delta \left[\frac{101.3 v_{tt} (F_{na} - D)}{W_t \sqrt{T_{at}}} \right] \sqrt{T_{as}} = \Delta F_{na} \left(\frac{101.3 v_{tt} \sqrt{T_{as}}}{W_t \sqrt{T_{at}}} \right) \quad (5.205)$$

where:

$$\begin{aligned} v_{tt} &= \text{test aircraft climb true speed (knots)} \\ \Delta F_{na} &= \Delta(F_{na} - D), D \text{ assumed constant} \\ W_t &= \text{test weight} \end{aligned}$$

In terms of Mach number and (F_{na}/δ_a) ,

$$\frac{\Delta R/C_1}{\Delta(F_{na}/\delta_a)} = \frac{351.9 M P_a \sqrt{T_{as}}}{W_t} \quad (\text{turbojet aircraft}) \quad (5.206)$$

or

$$\frac{\Delta R/C_1}{M \Delta(F_{na}/\delta_a)} = \frac{3946 \sqrt{T_{as}}}{W_t/\delta_a} \quad (5.207)$$

$$\text{where: } \delta_a = P_a \text{ (inches Hg)/29.92}$$

From equation 5.102,

$$\Delta R/C_1 = \frac{33,000}{W_t} \left(\text{THP}_{as} - \text{THP}_{at} \sqrt{\frac{T_{as}}{T_{at}}} \right) \quad (\text{reciprocating engine aircraft}) \quad (5.208)$$

From reciprocating engine power theory the effects of temperature on power available are an effect on the carburetor temperature and the effect on manifold pressure.

From Chapter Two,

$$\text{BHP}_{as} \cong \text{BHP}_{at} \sqrt{\frac{T_{at}}{T_{as}}} \quad (2.201)$$

Substituting equation 2.201 in equation 5.208,

$$\Delta R/C_1 = \frac{33,000 \text{ BHP}_{as}}{W_t} \left(1 - \frac{T_{as}}{T_{at}} \right) \eta_p \quad (5.209)$$

or, in terms of test brake horsepower

$$\Delta R/C_1 = \frac{33,000 \text{ BHP}_{at}}{W_t} \left[\sqrt{\frac{T_{at}}{T_{as}}} - \sqrt{\frac{T_{as}}{T_{at}}} \right] \eta_p \quad (5.210)$$

And above critical altitude equation 5.208 becomes

$$\Delta R/C_1 = \frac{33,000 \text{ BHP}_{at}}{W_t} \left[\sqrt{\frac{T_{at}}{T_{as}}} + \frac{MP_s}{MP_t} - 1 - \sqrt{\frac{T_{as}}{T_{at}}} \right] \eta_p \quad (5.211)$$

where:

- MP_s = standard day manifold pressure
- MP_t = test day manifold pressure
- $\frac{MP_s}{MP_t} = f \left(\frac{T_{as}}{T_{at}} \text{ and } \frac{MP_t}{P_a} \right)$
- η_p = propeller efficiency, average value, 0.83

Equation 5.211 is plotted in CHART 5.21 for use in determining $\Delta R/C_1$ for reciprocating engine aircraft, from values of BHP_{at} , T_{as}/T_{at} , and MP_t/P_a . The manifold pressure correction for air only is applied in the chart without introducing any error of magnitude in cases of mixture blowers. Values of BHP_{at} , the power developed during the climb, may be determined from torque-meter readings or from engine power charts.

Equations 5.206 and 5.207, plotted in CHARTS 5.22 and 5.23, are used to determine $\Delta R/C_1$ for jet aircraft. Values of (F_N/δ_a) corresponding to increments of $N/\sqrt{\sigma_a}$ are found for jet aircraft from a plot of F_N/δ_a vs $N/\sqrt{\sigma_a}$ as described in Chapter Three and illustrated in Figure 5.21 below.

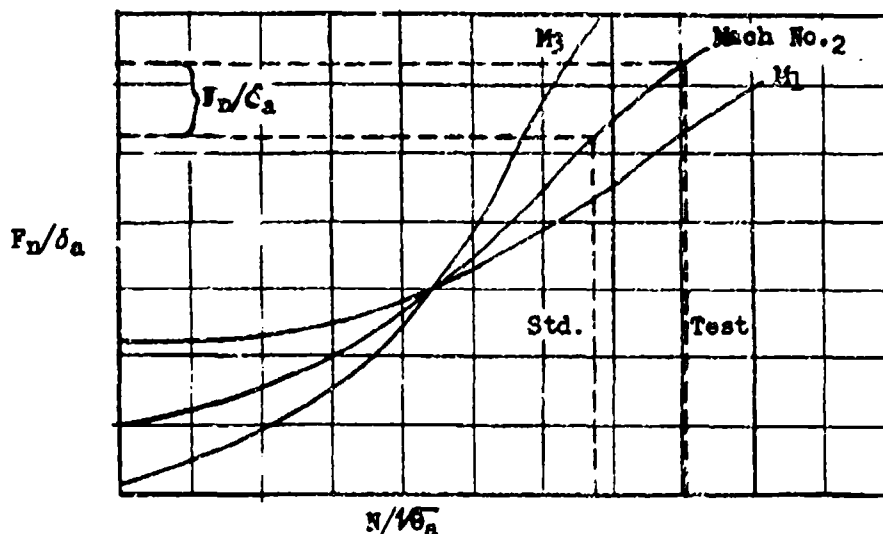


Figure 5.21
Typical Corrected Net Thrust-Rpm Plot for
Rate of Climb Corrections

SECTION 5.3

Weight Variation Correction to Rate of Climb Data

An aircraft rate of climb at some given gross weight may be corrected mathematically to give the rate of climb at some other gross weight. This mathematical rate of climb correction for weight variation assumes that all atmospheric, velocity, and power conditions are the same for both gross weights. For this reason, weight corrections are applied to standard day climb data. This method further implies that the effects of weight changes on the compressibility drag are negligible. This latter assumption is not generally valid for flight Mach numbers above 0.6. From equation 5.101,

$$F_{na} = \left(\frac{dh}{dt} \right) \left(\frac{W}{V} \right) + D \quad (5.301)$$

In terms of the drag or thrust required, equation 5.104,

$$F_{na} = \left(\frac{dh}{dt} \right) \left(\frac{W}{V} \right) + C_{Dp} k_1 P_a M^2 + \frac{W^2}{P_a M^2 k_2} \quad (5.302)$$

Differentiating, with W and dh/dt the only variables,

$$d \left(\frac{dh}{dt} \right) = - \left[\left(\frac{dh}{dt} \right) \frac{dW}{W} + \frac{2V dW}{P_a M^2 k_2} \right] \quad (5.303)$$

where:

$$\frac{dh}{dt} = R/C + \Delta R/C_1 = \left[\left(\frac{dH_c}{dt} \sqrt{\frac{T_{at}}{T_{as}}} \right) + \Delta R/C_1 \right], \text{ ft/min}$$

$$dW = (W_g - W_t) = \Delta W, \text{ lbs}$$

$$V = \text{flight velocity, ft/min}$$

$$P_a = \text{atmospheric pressure, "Hg}$$

$$k_2 = 155.6 \text{ b}^2 \text{ o (ft}^2)$$

Then,

$$\frac{\Delta R/C_2}{\Delta W} = - \frac{(dh/dt)}{W} \quad (5.304)$$

$$\frac{\Delta R/C_3}{\Delta W} = - \frac{50.65 \sqrt{T_{as}}}{P_a M \text{ b}^2 \text{ o}} \quad (5.305)$$

Values of $(\Delta R/C_2)/\Delta W$ are easily computed from W_t and dh/dt . Values of $(\Delta R/C_3)/\Delta W$ may be found from CHART 5.31 as a function of pressure altitude, Mach number and wing span. The total weight correction to rate of climb is,

$$\Delta R/C_2 + \Delta R/C_3 = - \left(\frac{\Delta R/C_2}{\Delta W} + \frac{\Delta R/C_3}{\Delta W} \right) \Delta W \quad (5.306)$$

Where the angle of climb is not negligible, $\theta > 20^\circ$, an error in $\Delta R/C_3$ of ten percent or larger will be introduced since the normal load factor departs significantly from 1g. In that case the induced drag may be set equal to

$$\frac{(nW)^2}{\pi R e(qS)}$$

and the following equation derived:

$$\Delta R/C_3 = \frac{25.36 \sqrt{T_{as}}}{P_{as} b^2 e M} \left[\frac{n_t^2 W_t^2 \frac{\delta_{as}}{\delta_{at}} - n_s^2 W_s^2}{W_s} \right] \quad 5.307$$

SECTION 5.4

Vertical Wind Gradient Correction to Rate of Climb

An aircraft climbing through a vertical wind-velocity gradient will experience a horizontal acceleration if the relative wind direction is negative and a horizontal deceleration if the relative wind is positive.

$$a_w = \frac{d V_w}{dt} - \left(\frac{d V_w}{dh} \right) \left(\frac{dh}{dt} \right)_a \quad (5.401)$$

where:

a_w = horizontal acceleration

$\frac{d V_w}{dh}$ = vertical wind-velocity gradient, (+) headwind, (-) tailwind

$\left(\frac{dh}{dt} \right)_a$ = accelerated rate of climb

The mass of the aircraft and this acceleration force is converted into a rate of climb increment if the climb path speed is considered constant.

Assuming small climb angles, the wind gradient results in a changing climb path speed relative to the earth. This results in a kinetic energy increment for the aircraft which must be balanced by a potential energy increment if the climb path speed relative to the air is maintained constant.

$$\left(\frac{V}{g} \right) \left(\frac{d V_w}{dt} \right) + W \left(\frac{dh}{dt} \right)_w = 0$$

From this equation,

$$\frac{V}{g} \frac{d V_w}{dh} \left(\frac{dh}{dt} \right)_a = - \frac{W}{V} \Delta \left(\frac{dh}{dt} \right)$$

$$\Delta \left(\frac{dh}{dt} \right) = - \frac{V}{g} \frac{d V_w}{dh} \left(\frac{dh}{dt} \right)_a \quad (5.402)$$

Then the unaccelerated rate of climb is,

$$\frac{dh}{dt} = \left(\frac{dh}{dt} \right)_a - \frac{V}{g} \frac{d V_w}{dh} \left(\frac{dh}{dt} \right)_a$$

$$\frac{dh}{dt} = \left(\frac{dh}{dt} \right)_a \left(1 - \frac{V}{g} \frac{d V_w}{dh} \right) \quad (5.403)$$

Values of the correction factor

$$\left(1 - .000089 V \frac{d V_w}{dh} \right)$$

where:

$$\frac{d V_w}{dh} = \frac{\text{knots}}{1000 \text{ ft}}$$

are plotted in CHART 5.41 at the end of this chapter for values of V_0 , $d V_w/dh$, and pressure altitude.

SECTION 5.5

Climb Path Acceleration Correction to Rate of Climb Data

An aircraft climbing on a standard day at a fixed calibrated air speed must accelerate because of atmospheric density change with altitude. This acceleration of the aircraft mass absorbs some of the thrust available, and the rate of climb during these conditions is less than the unaccelerated rate of climb.

The force absorbed is,

$$F_a = \frac{W}{g} \frac{dV}{dt} = \frac{W}{g} \frac{dV}{dh} \left(\frac{dh}{dt} \right)_a$$

and, from equation (5.101),

$$\Delta \left(\frac{dh}{dt} \right) = \frac{V F_a}{W} = \frac{V}{g} \frac{dV}{dh} \left(\frac{dh}{dt} \right)_a$$

Then,

$$\frac{dh}{dt} = \left(\frac{dh}{dt} \right)_a + \frac{V}{g} \frac{dV}{dh} \left(\frac{dh}{dt} \right)_a$$

or

$$\frac{dh}{dt} = \left(\frac{dh}{dt} \right)_a \left(1 + \frac{V}{g} \frac{dV}{dh} \right) \quad (5.501)$$

where:

F_a = the force absorbed in accelerating

$\frac{dh}{dt}$ = the unaccelerated climb

$\left(\frac{dh}{dt} \right)_a$ = the accelerated climb

V = the true climb path velocity

$\Delta \left(\frac{dh}{dt} \right)$ = rate of climb absorbed in accelerating

In terms of Mach number the correction factor in equation 5.501 becomes,

$$1 + \frac{V}{g} \frac{dV}{dh} = \frac{M^2 \gamma R}{2} \frac{dT}{dh} + M \gamma RT \left(\frac{dM}{dh} \right) + 1 \quad (5.502)$$

For a constant true climb speed the above factor has a value of one. For a constant Mach number climb (deceleration) the factor has a value of $(1 - 0.133 M^2)$ up to the isothermal altitude above which the factor is equal to one. For an accelerating climb condition the factor takes the form,

$$1 + \frac{V}{g} \frac{dV}{dh} = \frac{(1 + .2M^2)^{3.5} - 1}{(1 + .2M^2)^{2.5}} - 0.133 M^2 + \frac{V_c}{60} \left(\frac{1 + .2 M^2_{SL}}{1 + .2 M^2} \right)^{2.5} \frac{dV_c}{dh} + 1 \quad (5.503)$$

Equation 5.503 is plotted in CHARTS 5.51, 5.52, 5.53 and 5.54 in terms of V_c , P_a , M , V_t , dV_t/dh , and dV_c/dh . Chart 5.51 contains the first two right hand terms and is used for constant V_c climbs. Chart 5.52 contains the extreme right hand term and is an additive factor for a changing V_c . Chart 5.53 presents the first two right hand terms as a function of M . Chart 5.54 presents the function in terms of V_t and dV_t/dh .

During a climb to altitude (check climb) in jet type aircraft, the indicated climb speed is decreased with increasing altitude. This means that dV_c/dh in equation 5.503 is negative and, if large enough, may balance the other terms in the equation. In reciprocating engine aircraft the indicated speed is held constant, until the critical altitude for the engine is reached, and then is decreased. Charts 5.51 and 5.52 may be used to determine the bleed-off rate required for a constant climb true speed (zero acceleration factor). During sawtooth climbs in jet or conventional aircraft the calibrated speed is held constant over an increment of altitude. In these cases it may be desirable to determine the unaccelerated rate of climb that would be obtained under the same conditions at a constant true climbing speed as might be the case in a check climb. This may be accomplished using CHART 5.51 or 5.53 for the climb V_c and H_c or M , ($dV_c/dh = 0$). The factor is used as in equation 5.501.

Since equation 5.503 is plotted for standard day conditions it should be applied to the tapeline rate of climb at standard day true speed. This tapeline rate of climb has been defined as,

$$R/C = \frac{dH_c}{dt} \sqrt{\frac{T_{at}}{T_{as}}}$$

For an accelerating climbing aircraft requiring a power or thrust correction for temperature variation, the usual power correction is not all available to correct the R/C defined above since changing R/C changes the acceleration thrust required as shown on the preceding page.

$$(\Delta R/C)_a = \frac{\Delta R/C_1}{\left(1 + \frac{V}{g} \frac{dV}{dh}\right)}$$

where:

$$(\Delta R/C)_a = \text{rate of climb increment for temperature-power correction to the accelerated rate of climb, } \left(\frac{dH_c}{dt} \sqrt{\frac{T_{at}}{T_{as}}} \right)_a$$

Similarly, for an accelerating climbing aircraft requiring an induced drag weight correction to rate of climb at a constant air speed and thrust or power, an increased weight (induced drag) not only absorbs more of the excess thrust and reduces rate of climb, but it also results in less thrust being required for acceleration (reduced dH/dt) and some increase in rate of climb. In this case the total effect of climb acceleration on the induced drag weight correction is,

$$(\Delta R/C_3)_a = \frac{\Delta R/C_3}{\left(1 + \frac{V}{g} \frac{dV}{dh}\right)} \quad (5.505)$$

For jet powered aircraft, the best rate of climb is at approximately a constant true speed. For reciprocating engine aircraft, the best rate of climb is usually found in an accelerating climb condition.

APPLICATIONS OF THE ACCELERATION FACTOR TO SAW-TOOTH AND CHECK CLIMBS

The acceleration factor is applied to a saw-tooth rate-of-climb ($V_c = \text{const.}$) to simulate check climb data under identical conditions of standard thrust, altitude, weight, and standard speed. During check climbs at best climbing speeds some acceleration (\ddot{h}) may be evident; in these cases, the acceleration factor is applied only to the thrust and induced drag corrections. These two applications of the acceleration factor in climbing will be clarified by the equation below.

Basically, for the saw-tooth climb,

$$Rc_t = Rc_{ta} \times A_f \quad (5.506)$$

where

Rc_t = test tapeline rate-of-climb at standard day speed, no acceleration along flight path.

$Rc_{ta} = \frac{dH_c}{dt} \sqrt{\frac{T_{at}}{T_{a_s}}} =$ test tapeline rate-of-climb at standard day speed, with acceleration along climb path.

$A_f =$ standard atmosphere climb accelerations factor at standard day speed $\left(1 + \frac{V}{g} \frac{dV}{dh}\right)$

During a saw-tooth climb at constant V_c , the aircraft is accelerating and

$$Rc_s = \left[Rc_{ta} + \Delta Rc_{1a} + \frac{\Delta W}{W} (Rc_{ta} + \Delta Rc_{1a}) + \Delta Rc_{3a} \right] A_f \quad (5.507)$$

where:

$Rc_s =$ tapeline rate-of-climb at standard day speed thrust, and weight, no acceleration along flight path.

$\Delta Rc_{1a} = \frac{\Delta Rc_1}{A_f} =$ thrust correction to rate-of-climb during flight path acceleration of standard day speed.

$\Delta Rc_{3a} = \frac{\Delta Rc_3}{A_f} =$ induced drag rate-of-climb correction for weight variation during flight path acceleration at standard day speed.

With equation 5.506 and these definitions, equation 5.507 can be put in another form,

$$Rc_s = Rc_t + \Delta Rc_1 + \frac{\Delta V}{V} (Rc_t + \Delta Rc_1) + \Delta Rc_3 \quad (5.508)$$

A plot of Rc_s vs Vt_s defines check climb, rate-of-climb values for standard conditions except that the speeds for maximum rate-of-climb may result in some acceleration with increasing altitude. This will be immediately apparent from the plot mentioned above. From this same plot, the acceleration factor data (dVt_s/dh and Vt_s) for the check climb condition may be determined in the neighborhood of maximum rate-of-climb. The best climb points may then be readjusted to more exactly simulate actual check climb data. This is done by equation 5.509.

$$Rc_s \text{ check climb} = Rc_s / A_f \text{ check climb} \quad (5.509)$$

Standardizing on actual check climb requires a slightly different use of the acceleration factor, because any acceleration existing is common to both the test and standard day climbs. For this condition, equations 5.507 and 5.509 are combined.

$$\text{check climb } Rc_s = Rc_{ta} + \Delta Rc_{1a} + \frac{\Delta V}{V} (Rc_{ta} + \Delta Rc_{1a}) + \Delta Rc_{3a} \quad (5.510)$$

For climbs at constant V_c the acceleration factor is determined from charts 5.51 or 5.53. For plotted, zero acceleration, saw-tooth data, and for check climb data, the acceleration factor is best determined from the change of standard true speed with altitude and chart 5.54. Chart 5.52 is intended to be used only to determine the necessary decay of V_c with altitude to establish a zero acceleration. It should be noted that chart 5.51 is plotted for standard altitude data. This means that a temperature lapse rate of -2° C per thousand feet is assumed below the isothermal altitude. Generally, under test conditions up to altitudes of 30,000 ft., this standard lapse rate is realized approximately. The effect on A_f of temperature lapse rate can be seen on chart 5.53. The engineer should check all saw-tooth data for temperature inversions which greatly alter the standard lapse rate, but he should be especially alert on saw-tooth data obtained above 30,000 ft. The two curves on chart 5.53 may be used to interpolate for test temperature lapse rates between -2° and zero to be applied to equations 5.506 and 5.507 in place of A_f as defined.

SECTION 5.6

Temperature Effects on Fuel Consumption and Weight During Climb

In making a check climb from take-off to ceiling altitude, it is necessary to give consideration to fuel consumption variation between test day and standard day. This temperature variation may result in an appreciable and increasing difference in test and standard day gross weights as the climb progresses necessitating a conversion to a rate of climb increment by the methods previously described. If the temperature difference is not more than 10° C, this fuel-weight rate of climb correction is negligible. In this correction, the assumption is made that the fuel consumption rate is constant at a particular time and power setting irrespective of the rate of climb variation resulting from atmospheric temperature variation from standard. This assumption is also a valid approximation for climbs conducted at power settings varying as much as five per cent.

One method of determining the difference in fuel weight used because of temperature effects is by plotting and correcting for temperature the fuel rate of consumption.

- a. Plot fuel used vs time.
- b. Plot fuel rate vs altitude
- c. Correct fuel rate vs altitude plot to standard day fuel rate at standard day power conditions by use of engine manufacturer's performance data.
- d. Integrate power corrected rate of climb data and plot tentative standard day time vs altitude.
- e. Plot corrected fuel rate vs corrected time to climb to altitude.
- f. Integrate plot "e" and obtain corrected fuel used vs time.
- g. Determine fuel weight increment at each altitude from plots "a" and "f".
- h. Make $\Delta R/C_2$ and $\Delta R/C_3$ corrections for weight difference to $(R/C + \Delta R/C_1)$. This is the final corrected rate of climb.

A.-Fuel Used vs Time
(Test Temp.)

B.-Altitude vs Time to Climb
(Test Temp.)

C.-Altitude vs Time to Climb
(Standard Temp.)

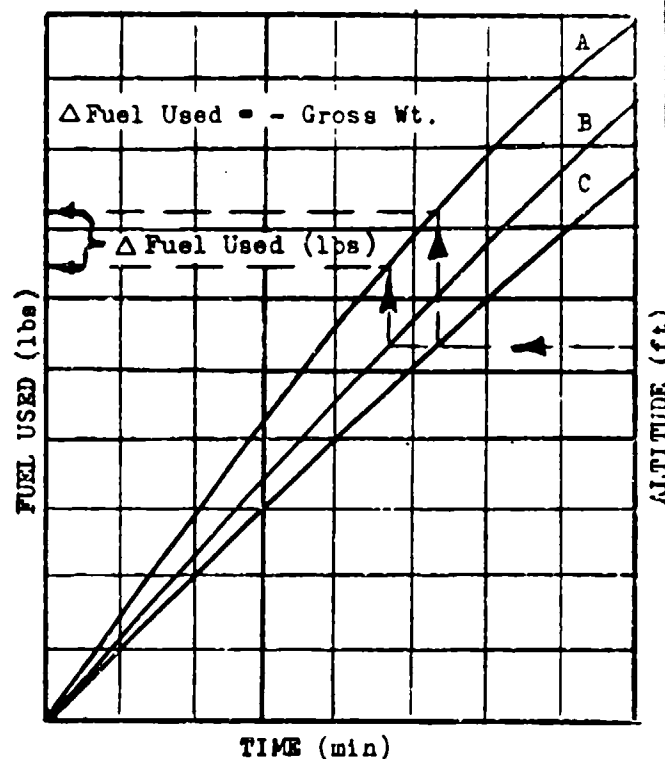


Figure 5.61
Method of Approximating a Rate of Climb
Weight Correction for Variation in
Fuel Used on Test and Standard Days

This same correction may be approximated by plotting the data as shown in Figure 5.61 and by making the assumption (based on actual climb data) that the fuel used vs time plot for the test temperature and power is very nearly identical to that for the standard temperature and power.

SECTION 5.7

Determination of Best Rate of Climb and Best Climbing Speed

SAWTOOTH METHOD

One method of obtaining climb data is the sawtooth climb. This name is derived from the barograph trace resulting from a series of short time climbs through the same pressure altitude. These climbs are made at different indicated climbing speeds from a point a little below the test altitude to a point a little above it. By plotting the resulting rates of climb for the various altitudes and air speeds, as shown in Figure 5.71, the best rate of climb and best climbing velocity will be apparent for all altitudes.

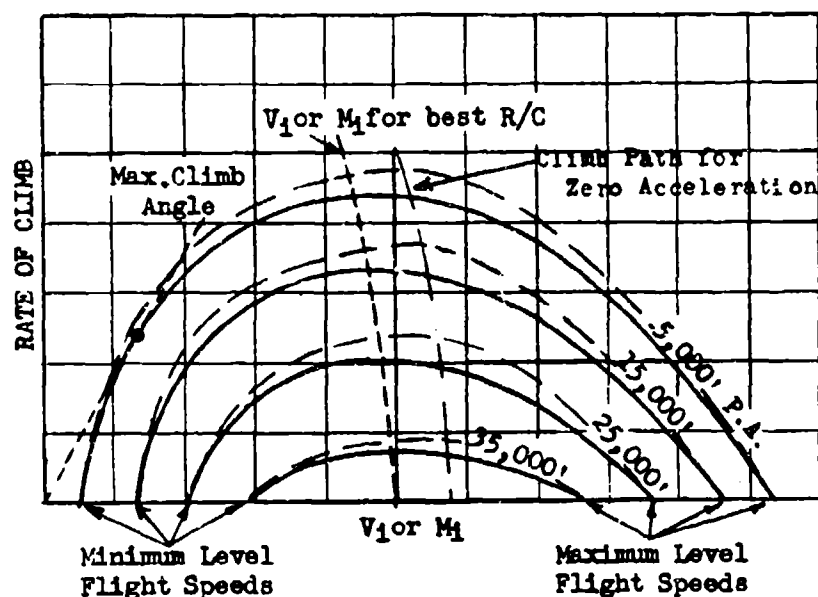


Figure 5.71

Typical Sawtooth Climb Plot

Sawtooth climbs are made at the same power settings and aircraft configurations that will be used in the continuous or check climbs. The sawtooth procedure is to climb through the altitude increment for a period of about one minute at each of the various speeds or Mach numbers selected to bracket the best rate of climb. In addition, the stalling point and high speed point for level unaccelerated flight at the climb altitude are plotted to complete the curves. Each sawtooth climb point is corrected to the gross weight that would be obtained by climbing at climb power setting from a standard gross weight take-off to the test altitude. Sawtooth climbs are corrected for temperature and weight variations by the methods indicated previously. For jet aircraft the data should be corrected to zero acceleration to simulate check climb data.

ACCELERATION METHOD FOR RATE OF CLIMB AND OPTIMUM CLIMB PATH EVALUATION

For aircraft having very large rates of climb and fuel consumption and a limited fuel supply, the sawtooth method may be difficult to fly accurately and may be excessively time consuming for complete results. In these cases the level flight acceleration method may be applied to the determination of climb data. In addition, vertical wind gradients do not affect R/C data from level accelerations.

Consider the accelerating aircraft in level flight. The total energy of the aircraft is,

$$E = Wh + \frac{WV^2}{2g} \quad (5.701)$$

$$\frac{E}{W} = h + \frac{V^2}{2g} \quad (5.702)$$

where:

E = total energy (ft-lbs)	V = true velocity (ft/sec)
W = gross weight (lbs)	g = acceleration of gravity
h = tapeline altitude (ft)	32.174 (ft/sec ²)

Differentiating equation 5.702, (including h to allow for altimeter position error)

$$\frac{dE}{W} = \frac{V dV}{g} + dh \quad (5.703)$$

Dividing by dt ,

$$\frac{dE}{dt} \frac{1}{W} = \frac{V}{g} \frac{dV}{dt} + \frac{dh}{dt} \quad (5.704)$$

The force available to accelerate the aircraft is,

$$(F_{n_a} - D) = F_{n_a} - F_{n_T} = F_{n_o} = \text{Excess net thrust}$$

Then,

$$F_{n_o} = \frac{W}{g} \frac{dV}{dt} + \frac{W}{V} \frac{dh}{dt} \quad (5.705)$$

From equation 5.101,

$$R/C = \frac{V F_{n_o}}{W} \quad (5.706)$$

Combining equations 5.706, 5.704, and 5.705,

$$R/C = \frac{dE}{dt} \frac{1}{W} = \frac{V}{g} \frac{dV}{dt} + \frac{dh}{dt} \quad (5.707)$$

where:

R/C = ft/sec
dt = seconds

By plotting the variable, V^2 in equation 5.702 against time, the rate of change of the total energy may be obtained. From equation 5.706 it is seen that the point of maximum slope of this curve is at the value of V^2 corresponding to V for maximum rate of climb. W has been assumed constant. In knots, equation 5.702 becomes,

$$\frac{V^2}{2g} = 0.0443 V_t^2 \text{ knots} \quad (5.708)$$

From a plot of $0.0443 V^2$ knots vs time in minutes and V_{1c} and M_{1c} vs time in minutes, the indicated speed and Mach number and best rate of climb may be obtained by inspection as shown in Figure 5.72. This acceleration method of obtaining climb data is more difficult to apply than may appear from the analysis, the primary source of error being the lag in the conventional type of air-speed indicating system. This may be overcome by calibrating the system for lag, by using a no-lag system which has its instrument very near the air-speed probe, or by use of electronic pressure measuring devices to determine indicated air speed. Another approach is to determine the time, distance, velocity and acceleration by radar tracking.

A plot of V^2 vs time as in Figure 5.72 is fairly adequate for determination of best climb speeds, but tests have shown it to be usually unsatisfactory for determining accurate R/C values. A better analysis of R/C and best climb speeds can be made by computation of dE/dt from level acceleration values of dV , dt , and dh . Because $dV \div dt$ is required, the accuracy with which these increments are determined sets the accuracy and data scatter of the results. Minimum increment values should be ten (10) knots dV or 15 seconds dt . Equation 5.709 is suitable for machine computation of dE/dt . Values of M should also be computed.

$$\left(\frac{dE}{dt}\right)_a = W_2 \left[\frac{19362 \theta_{a_a} (M_2^2 - M_1^2) + (E_{c2} - E_{c1})}{t_2 - t_1} \right] \sqrt{\frac{T_{at}}{T_{as}}} \quad (5.709)$$

Two level accelerations should be made at each altitude reciprocal headings. R/C is determined from dE/dt and desired weight; $\Delta R/C_1$ and $\Delta R/C_3$ corrections can also be applied. The dE/dt plot appears as in Figure 5.73.

Since dE/dt is a function of both h and $V^2/2g$ a maximizing function of dE/dt involves both and takes the form,

$$\frac{dE}{dt} = \text{max. when } \frac{\partial(dE/dt)}{\partial(V^2/2g)} - \frac{\partial(dE/dt)}{\partial h} = 0 \quad (5.710)$$

or when,

$$\frac{\Delta(dE/dt)}{\Delta V} = \frac{V}{g} \frac{\Delta(dE/dt)}{\Delta h} \quad (5.711)$$

This optimum dE/dt can be determined graphically and shown as on Figure 5.73. This climb schedule will then involve zooming or diving to obtain a given speed and altitude in minimum time as shown in Figure 5.74.

RATE OF CHANGE OF TOTAL PRESSURE FOR DEFINING $d(E/W)/dt$. Total pressure rate of change will approximately define $d(E/W)/dt$, and can be demonstrated by use of equations 2.21, 4.9, 4.10, and the equation of state. The resulting equation is applicable to a differential pressure gage.

$$\frac{dP_t}{\left(\sqrt{t} P_t\right) = \text{const.}} \left[\frac{T_a (1 + .2M^2)}{2} \right] = \frac{d(E/W)}{dt} - \frac{dT_a}{dt} \frac{(\gamma R M^2)}{2} - \frac{dh}{dt} (2 + .2M^2) \quad (5.712)$$

T_a is the instrument temperature and is essentially constant for a given altitude. Use of rate of climb instrument for this purpose has been suggested by Lt. Col. J.L. Ridley, USAF. The lag constant used must provide measurable differential pressures and not result in excessive lag in dP_t indications.

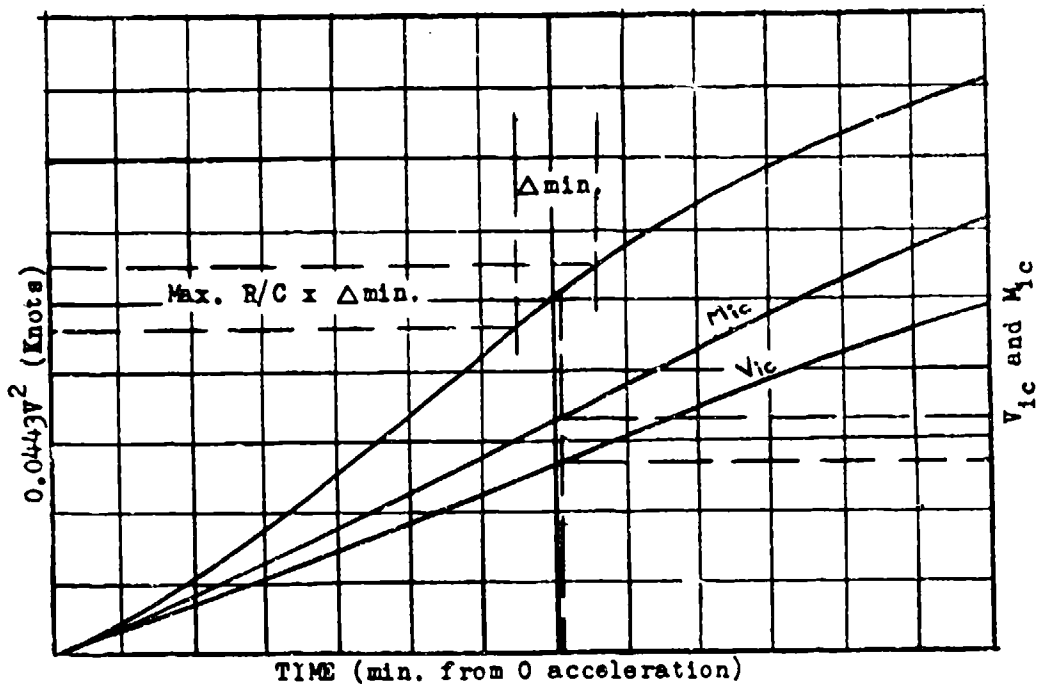


Figure 5.72
 Typical Plot of Level Flight Acceleration Data

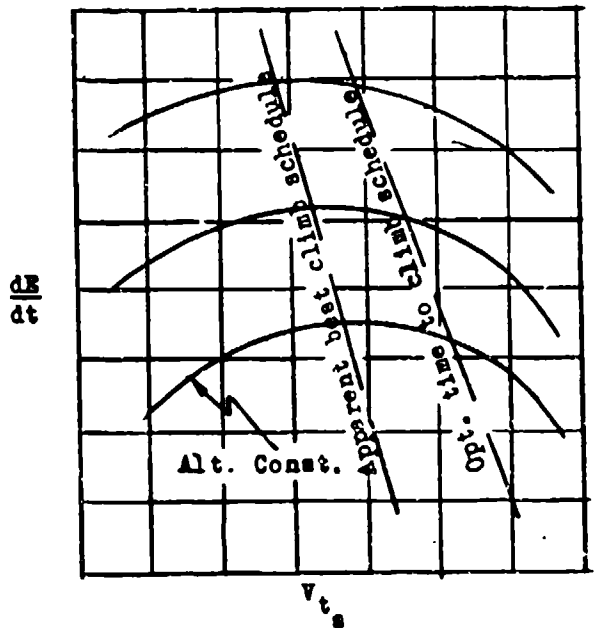


Figure 5.73
 Rate of Change of Total Energy Plot

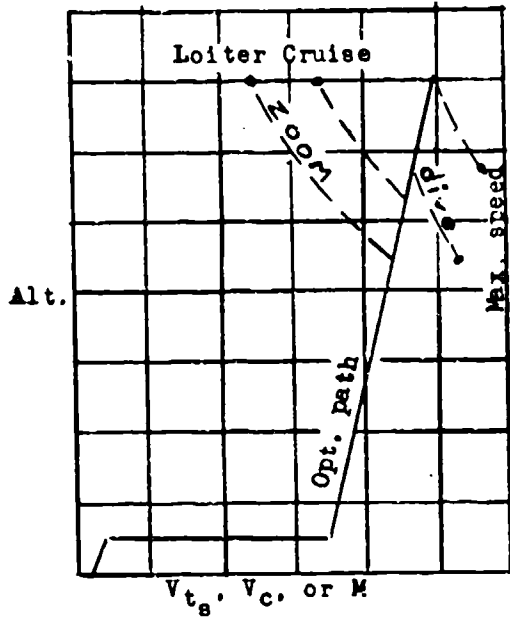


Figure 5.74
 Minimum-Time Climb Schedule Plot

SECTION 5.8

Dimensionless Rate of Climb Plotting

In equations 5.115, 5.116 and 5.117 it may be seen that the parameters

$$\frac{\left(\frac{dh}{dt}\right)}{\sqrt{T_a}}, \text{ and } M$$

are dimensionless in terms of the physical system of dimensions. The remaining parameters,

$$\frac{THP}{P_a \sqrt{T_a}}, \quad \frac{H}{\sqrt{T_a}}, \quad \frac{F_n}{P_a}, \quad \text{and} \quad \frac{W}{P_a},$$

may be made dimensionless by the insertion in each of a characteristic length raised to some power. As this characteristic length for a particular aircraft remains constant, these latter parameters may be considered functionally dimensionless. All the above parameters will result from a dimensional analysis of the variables effecting rate of climb.

For propeller driven aircraft, BHP from torque meter readings may be substituted for THP in equation 5.115. Then the parameters for dimensionless plotting are,

$$\frac{\left(\frac{dh}{dt}\right)}{\sqrt{T_a}}, \quad \frac{BHP}{P_a \sqrt{T_a}}, \quad M, \quad \frac{W}{P_a}$$

For turbojet powered aircraft equation 5.116 is applicable and the parameters are,

$$\frac{\left(\frac{dh}{dt}\right)}{\sqrt{T_a}}, \quad \frac{H}{\sqrt{T_a}}, \quad M, \quad \frac{W}{P_a}, \quad \text{or} \quad \frac{F_n}{P_a} \quad \text{in place of} \quad \frac{H}{\sqrt{T_a}}$$

Generally in this type of a plot the terms e_a and δ_a replace T_a and P_a

where:

$$e_a = \frac{T_a \cdot K}{288}$$

$$\delta_a = \frac{P_a \cdot Hg}{29.92}$$

As there are four variables involved, it is necessary to hold one of them constant during a particular climb. It can be seen that Mach number is the only term that could reasonably be held constant during a climb. By making check climbs at constant Mach number and two or three different constant rpm's it is possible to plot climb data without making weight or power corrections and to use the plotted data to determine standard day standard weight rate of climb even in the region where compressibility effects are large. Figure 5.81 illustrates a dimensionless rate of climb plot for a constant Mach number, data being obtained at three different power settings.

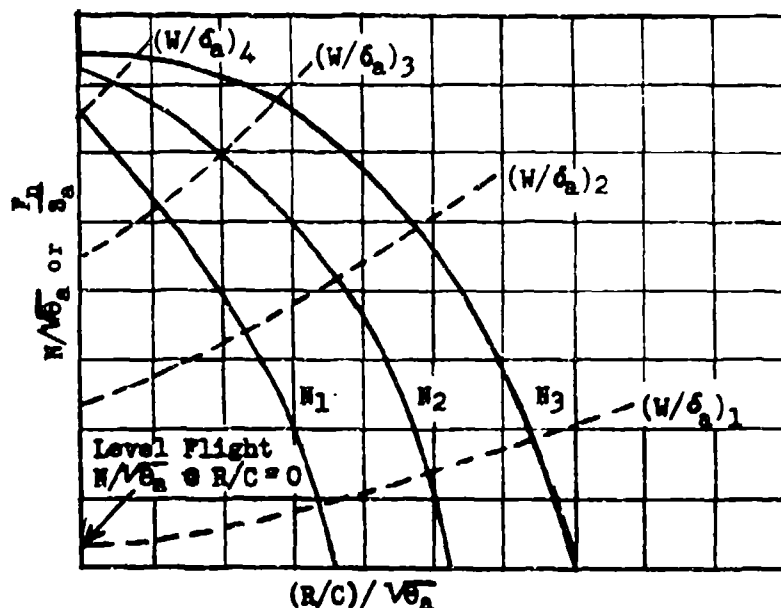


Figure 5.81
Typical Dimensionless Climb Data at Constant
Mach Number and Various W/δ_a Parameters

The methods used for Figure 5.81 can also be used for standardizing rate of climb data. For fighter type turbojet aircraft the best rate of climb will be at speeds that maintain approximately a constant Mach number for certain altitude ranges. Two climbing Mach numbers determined by sawtooth climbs may be enough to approximate all the climbing speeds and allow some interpolation. Such a plot would appear as in Figure 5.82 and may be used to correct climb data for all aircraft of the same model with same type of engine.

Figures 5.81 and 5.82 are easily plotted for constant values of W/δ_a at the different constant rpm's by first plotting $N/\sqrt{\delta_a}$ vs W/δ_a and $(R/C)/\sqrt{\delta_a}$ as shown in Figure 5.83.

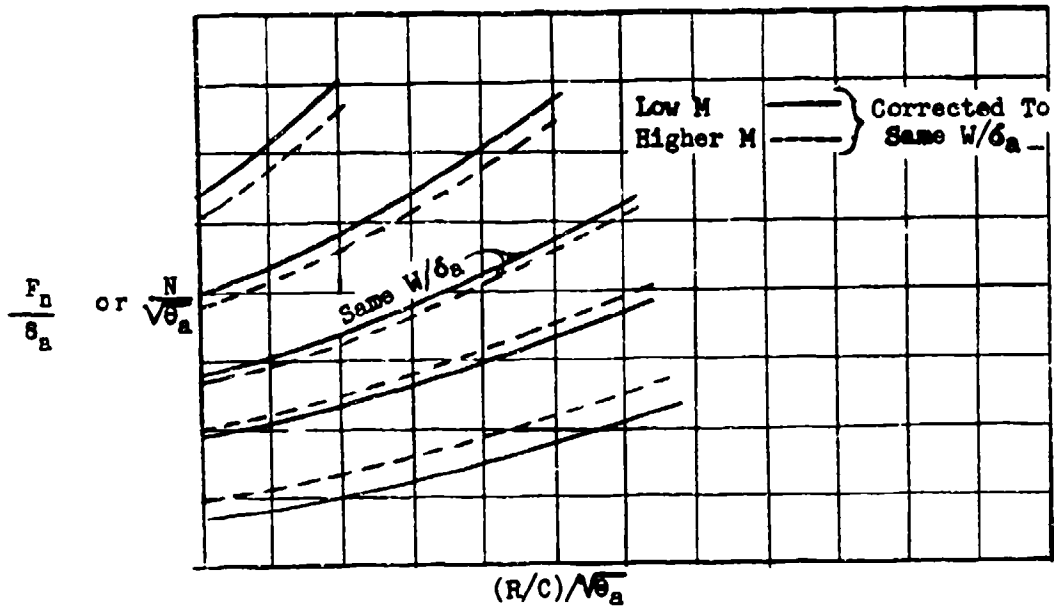


Figure 5.82
 Typical Dimensionless Climb Data Plot
 for Two Mach Numbers

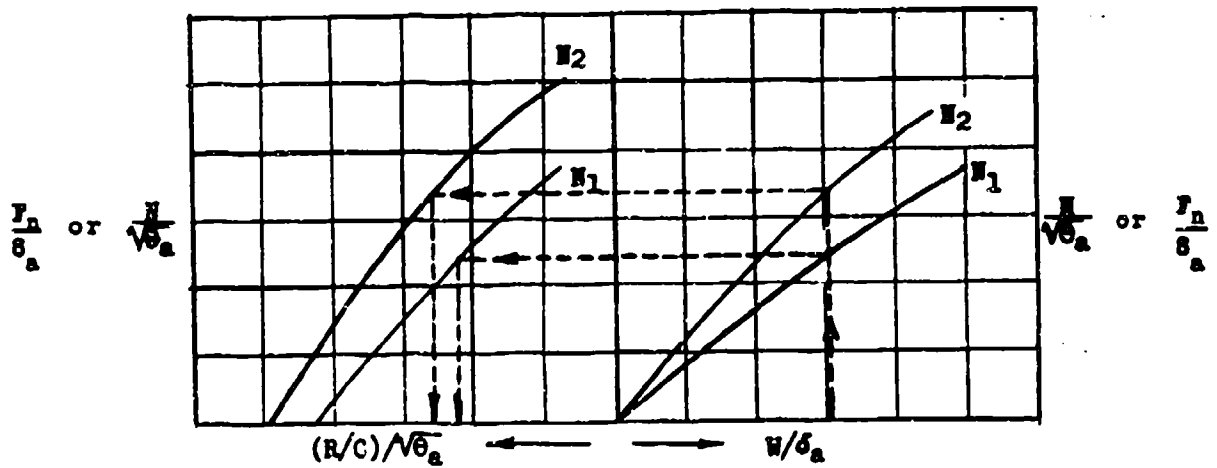


Figure 5.83
 Method of Correcting Climb Data to Constant W/δ_a

If the level flight data are included, two constant rpm climbs will provide enough points to determine the $N/\sqrt{V_{0a}} - (R/C)/\sqrt{V_{0a}}$ curve for constant W/δ_a .

In the speed range for best climb the change in F_N/δ_a with $N/\sqrt{V_{0a}}$ is approximately linear. This fact may be utilized to determine rate of climb data for any condition from a few constant Mach number climbs. This is especially useful for very large aircraft having large weight variations which affect the best climb speed. Figure 5.84 illustrates a dimensionless rate of climb plot that would be derived from three constant Mach number climbs and level flight data. A linear F_N/δ_a increase with $N/\sqrt{V_{0a}}$ is assumed for each of the constant W/δ_a parameters. These climbs would be made in a light weight condition so as to obtain maximum altitudes and $N/\sqrt{V_{0a}}$ values.

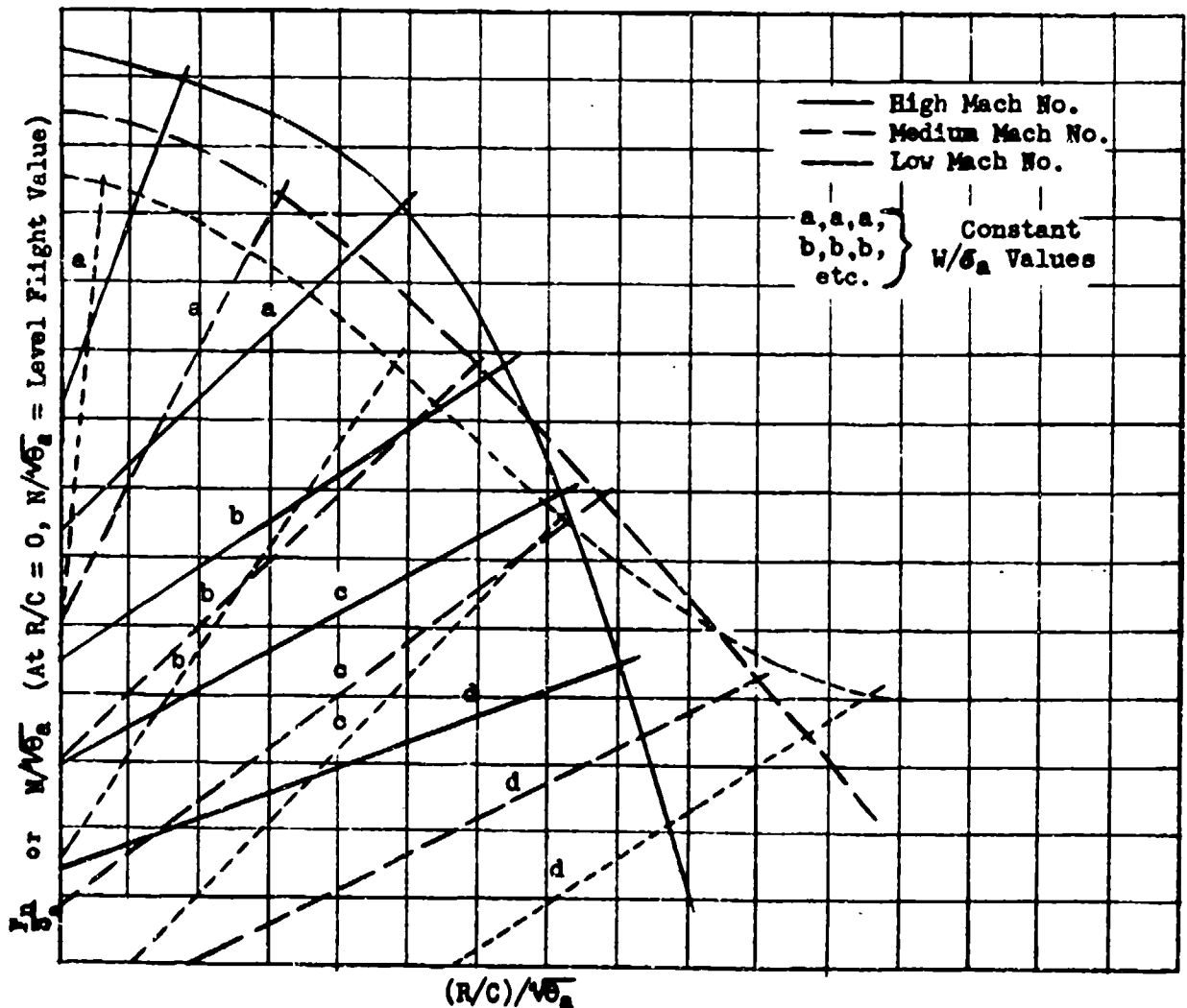


Figure 5.84
 Typical Dimensionless Rate of Climb Plot Showing Best
 Climb Mach Number for all Values of W/δ_a and $N/\sqrt{V_{0a}}$
 or F_N/δ_a

The method of dimensionless plotting described above may be especially applicable to aircraft having very large rates of climb where sawtooths are impractical. Also, when afterburner and rocket power are used to boost the rate of climb, this method may prove valuable because of the difficulty of making power corrections in this type of installation.

These same types of non-dimensional rate-of-climb presentations may be obtained from level acceleration data made at constant W/S_a values.

SECTION 5.9

General Climb Test Information

The absolute ceiling for an aircraft is defined as the altitude where the rate of climb is zero. The service ceiling is defined as the altitude at which the rate of climb is 100 feet per minute.

For propeller driven aircraft it will be necessary to make rate of climb corrections for variation in cooler flap position. This is accomplished by making several short climbs at a constant indicated speed and various cooler flap positions. Both the rate-of-climb increment and the engine temperature increment should be plotted vs flap position.

In the aircraft performance report it is desirable to show rate of climb and time to climb for two power settings. This is required for tactical use when a large number of aircraft are to take off during a period of time and meet in formation at a specified altitude. To accomplish this the first aircraft to take off must climb slower than those taking off at a later time.

It is usually required in performance reports that some data relative to rate of climb on a reduced number of engines be included. This is usually done by making a short climb of about 10,000 feet at a mean altitude between sea level and service ceiling. The top of this reduced-number-of engines climb should be close to the apparent service ceiling for that condition.

In heavy aircraft, bombers and transports, two climbs at normal rated power or maximum jet engine rpm should be conducted for the extreme gross weight conditions, light and heavy, when data are plotted in the conventional manner. In this way the rate of climb variation with weight can be seen graphically and a linear extrapolation used to make weight corrections or to compare the analytical weight corrections. Typical climb performance presentations are shown in Figure 5.91 for propeller driven aircraft and in Figure 5.92 for jet powered aircraft.

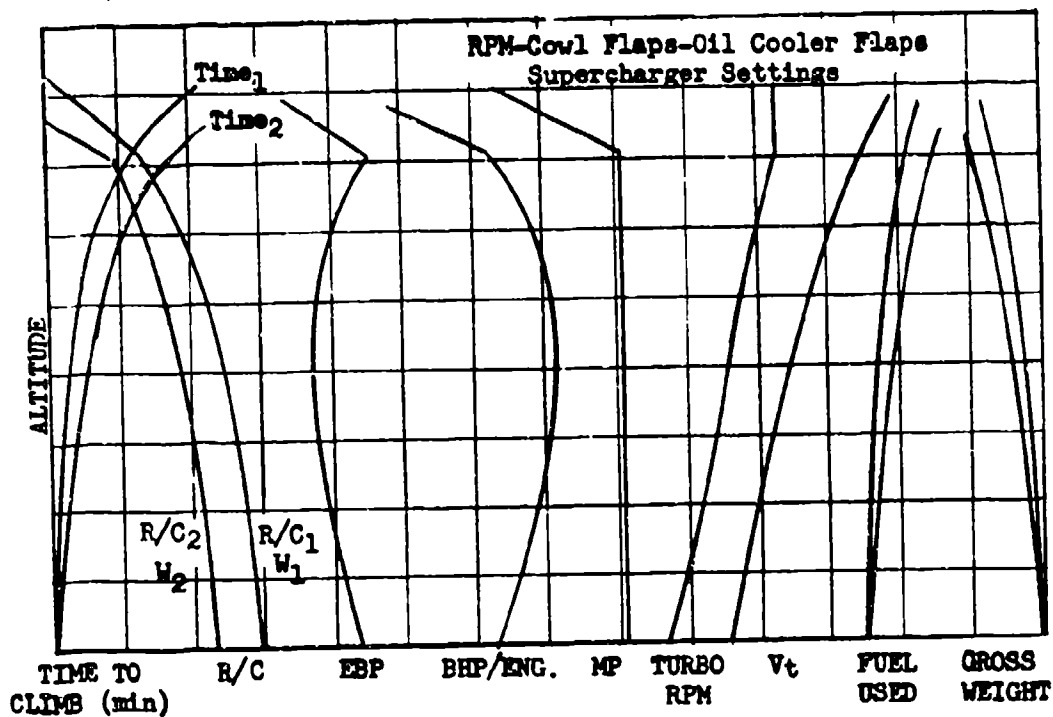


Figure 5.91
Standard Climb Data Presentation,
Reciprocating Engine Aircraft

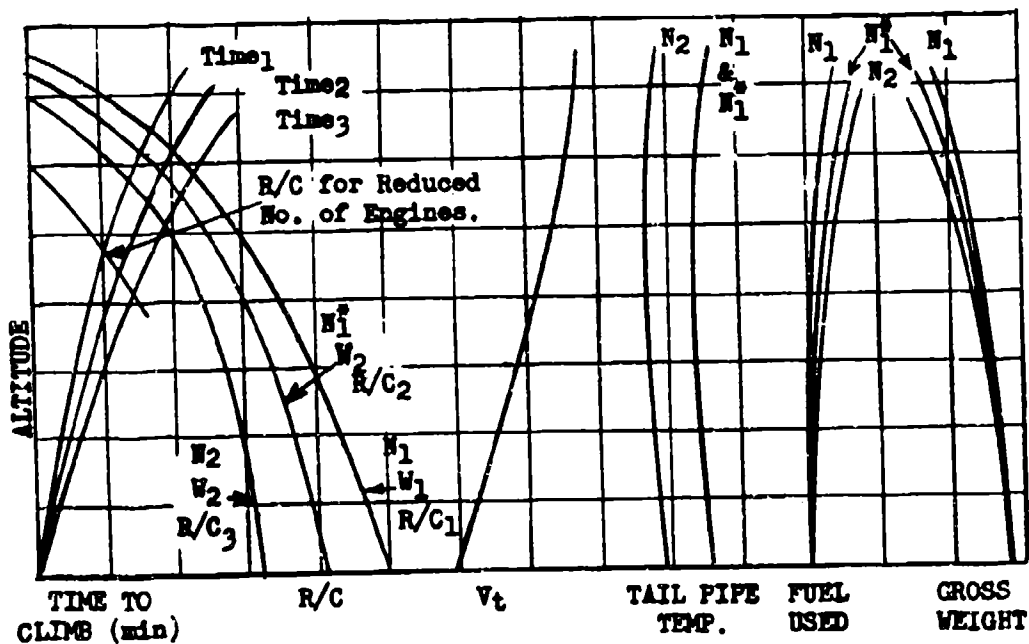


Figure 5.92
Standard Climb Data Presentation, Jet Engine Aircraft

DATA REDUCTION OUTLINE (5.91)

For Reciprocating Engine Aircraft
Sawtooth and Check Climbs

(1)	Test Point Number		
(2)	H_1	ft	Pressure altitude
(3)	ΔH_{ic}	ft	Altimeter instrument correction
(4)	ΔH_{pc}	ft	Altimeter position error correction
(5)	H_c	ft	True pressure altitude, (2) + (3) + (4)
(6)	V_1	knots	Indicated air speed
(7)	ΔV_{ic}	knots	Air-speed instrument correction
(8)	ΔV_{pc}	knots	Air-speed position error correction
(9)	V_c	knots	Calibrated air speed, (6) + (7) + (8)
(10)	V_{ts}	knots	Standard day true speed, from CHART 8.5 and (9) and (5)
(11)	M		Mach number, from CHART 8.5 and (9) and (5)
(12)	t_1	°C	Indicated air temperature
(13)	Δt_{ic}	°C	Temperature instrument correction
(14)	t_{ic}	°C	Instrument corrected indicated air temperature, (12) + (13)
(15)	T_{at}	°K	Absolute test air temperature from CHART 8.2 (14) and (11)
(16)	$\sqrt{\theta_{at}}, \sqrt{T_{at}/T_{SL}}$		$\sqrt{(15) / 288}$
(17)	$\sqrt{\theta_{as}}, \sqrt{T_{as}/T_{SL}}$		From standard altitude tables and (5)
(18)	P_a	"Hg	Atmospheric pressure, from standard altitude tables and (5)
(19)	$\sqrt{T_{at}/T_{as}}$		(16) + (17)
(20)	Fuel remaining,	gals	
(21)	Fuel at take off,	gals	
(22)	Fuel used,	gals	(21) - (20)
(23)	ΔW_f	lbs	Fuel weight used in climbing, (22) x lbs/gal
(24)	W_t	lbs	Test weight, take-off gross weight - (23)
(25)	W_s	lbs	Standard weight at altitude, from check climb or weight at initial sawtooth point
(26)	ΔW	lbs	Climb weight correction, (25) - (24)
(27)	ΔW per engine	lbs	(26) + number of engines
(28)	W_t per engine	lbs	(24) + number of engines
(29)	t_o	Decimal Minutes	Elapsed time to climb to altitude
(30)	t_s	Decimal Minutes	Time at start of climb
(31)	Δt	Decimal Minutes	Time to climb to test altitude, (29) - (30)
(32)	Plot (5) vs (31)		Time to climb curve
(33)	(dH_c/dt)	ft/min	Altimeter rate of climb from slopes of (32)

(34)	(dh/dt)	ft/min	Tapeline rate of climb at standard day true speed, test weight, and test power, (33) x (19)
(35)	Wind Gradient Factor		CHART 5.41, (when required)
(36)	dh/dt Corrected for Wind Gradient		(34) x (35) when required
(37)	Acceleration Factor		CHART 5.51 and (5) and (9) for sawtooth climb at constant V_c . CHARTS 5.51 and 5.52 and (5) and (9) for check climb not flown at constant V_c .
(38)	Throttle setting		
(39)	Mixture setting		
(40)	Tachometer Reading		
(41)	Tachometer Instrument Correction		
(42)	Engine rpm		(40) + (41)
(43)	MP _i	"Hg	Indicated manifold pressure
(44)	ΔMP_{ic}	"Hg	Manifold pressure instrument correction
(45)	MP _t	"Hg	Test manifold pressure, (43) + (44)
(46)	BHP _t		Test BHP, from power charts or torque meters
(47)	BHP _t per engine		(46) + number of engines
(48)	(MP_t/P_a)		Manifold pressure - ambient pressure ratio, (45) + (18)
(49)	Manifold pressure ratio factor		From CHART 5.21 and (19) and (48)
(50)	$\frac{\Delta R/C_1}{BHP_t \text{ per engine}}$		Rate of climb correction for power at unaccelerated climb conditions, from CHART 5.21 and (19) and (48) and (28)
(51)	$(\Delta R/C_1)_a$	ft/min	Rate of climb correction for power, accelerated climb conditions, (50) x (47) + (37)
(52)	$(R/C)_a + (\Delta R/C_1)_a$	ft/min	Standard day rate of climb at standard power and test weight for the accelerating aircraft, (34) or (36) + (51)
(53)	$\frac{MP_s}{MP_t}$		$\{[(49) - \text{one}] \times (19)\} + \text{two}$
(54)	MP _s	"Hg	Standard day manifold pressure, (53) x (45)
(55)	$\Delta R/C_2$	ft/min	Rate of climb weight correction, accelerated conditions, (-26) x (52) + (24)
(56)	$\frac{\Delta R/C_3}{\Delta W}$		Rate of climb induced drag correction, unaccelerated conditions, from CHART 5.31 and (5) and (11) and wing span
(57)	$(\Delta R/C_3)_a$	ft/min	Rate of climb induced drag correction for accelerated climb conditions, (56) x (26) + (37)
(58)	Standard weight corrected rate of climb, accelerated conditions		(52) + (55) + (57)
(59)	Plot (58) vs (5) and graphically integrate to get time to climb vs (5)		

NOTE: For turbo superchargers the corrections described in Chapter Two should be applied, and equation 5.208 used to find $\Delta R/C_1$.

DATA REDUCTION OUTLINE (5.92)

For Jet Aircraft Sawtooth and Check Climbs

(1)	Test Point Number		
(2)	H_1	ft	Pressure altitude
(3)	ΔH_{1c}	ft	Altimeter instrument correction
(4)	ΔH_{pc}	ft	Altimeter position error correction
(5)	H_c	ft	True pressure altitude, (2) + (3) + (4)
(6)	V_1	knots	Indicated air speed
(7)	ΔV_{1c}	knots	Air-speed instrument correction
(8)	ΔV_{pc}	knots	Air-speed position correction
(9)	V_c	knots	Calibrated air speed, (6) + (7) + (8)
(10)	M		Mach number, from CHART 8.5 and (9) and (5)
(11)	V_{ts}	knots	Standard day true speed, from CHART 8.5 and (9) and (5)
(12)	t_1	°C	Indicated air temperature
(13)	Δt_{1c}	°C	Temperature instrument correction
(14)	t_{1c}	°C	Instrument corrected indicated air temperature
(15)	T_{at}	°K	Absolute test air temperature from CHART 8.2 and (14) and (10)
(16)	$\sqrt{\theta_{at}}, \sqrt{T_{at}/T_{SL}}$		$\sqrt{(15)/288}$
(17)	$\sqrt{\theta_{as}}, \sqrt{T_{as}/T_{SL}}$		From standard altitude tables and (5)
(18)	$\sqrt{T_{at}/T_{as}}$		(16) + (17)
(19)	Fuel Remaining	gals	
(20)	Fuel at take off	gals	
(21)	Fuel used	gals	(20) - (19)
(22)	ΔW_f	lbs	Fuel weight used for climbing, (21) x lbs/gal
(23)	W_t	lbs	Test weight, take-off gross weight - (22)
(24)	W_s	lbs	Standard weight at altitude from check climb, or weight at initial sawtooth point
(25)	ΔW	lbs	Climb weight correction, (24) - (23)
(26)	ΔW per engine	lbs	(25) + number of engines
(27)	W_t per engine	lbs	(23) + number of engines
(28)	t_e	Decimal Minutes	Elapsed time to climb altitude
(29)	t_s	Decimal Minutes	Time at start of climb
(30)	Δt	Decimal Minutes	Time to climb to test altitude, (29) - (28)
(31)	Plot (5) vs (30)		Time to climb curve
(32)	dH_c/dt	ft/min	Altimeter rate of climb, from slopes of (31)
(33)	dh/dt	ft/min	Tapeline rate of climb at standard day true speed, test weight and test thrust, (32) x (18)
(34)	Wind Gradient Factor		CHART 5.41, (when required)

- (35) dh/dt
Corrected for Wind Gradient
- (36) Acceleration Factor
- (37) N_1
- (38) ΔN_{10}
- (39) N_t
- (40) $N/\sqrt{\theta_{at}}$
- (41) $N/\sqrt{\theta_{as}}$
- (42) $\Delta F_n/\delta_a$
- (43) $\frac{\Delta R/C_1}{\Delta F_n/\delta_a}$
- (44) $(\Delta R/C_1)_a$ ft/min
- (45) $(R/C)_a + (\Delta R/C_1)_a$ ft/min
- (46) $\Delta R/C_2$ ft/min
- (47) $\frac{\Delta R/C_3}{\Delta W}$
- (48) $(\Delta R/C_3)_a$ ft/min
- (49) Standard weight corrected rate of climb, accelerated conditions
- (50) Plot (49) vs (5) and graphically integrate to get time to climb vs (5)
- (33) x (34), when required
- CHART 5.51 and (5) and (9) for climb at constant V_c . CHARTS 5.51 and 5.52 and (5) and (9) for climb not flown at constant V_c
- Indicated rpm
- Rpm instrument correction
- Test rpm, (37) + (38), average of all engines
- Test rpm parameter, (39) + (16)
- Standard rpm parameter, (39) + (17)
- Net thrust correction from (40) and (41) and (10) and a graph similar to Figure 5.21
- Rate of climb thrust correction, unaccelerated conditions, from CHART 5.22 and (5) and (10) and (27)
- Rate of climb thrust correction for accelerated climb speed, (43) x (42) + (36). If no acceleration, (44) = $\Delta R/C_1$
- Standard day rate of climb at standard power and test weight for the accelerating aircraft, (33) or (35) + (44)
- Rate of climb weight correction, accelerated conditions, (-25) x (45) + (23)
- Rate of climb induced drag correction, unaccelerated climb speed, from CHART 5.31 and (5) and (10) and wing span
- Rate of climb induced drag correction for accelerated climb speed, (47) x (25) + (36). If no acceleration, (47) = $\Delta R/C_3$
- (45) + (46) + (48)

NOTE: If unaccelerated climb data is desired, correct (33) or (35) to unaccelerated conditions and make other corrections assuming no acceleration.

SECTION 5.10

Rate of Descent Data

Descent data are usually presented in the performance report only for jet powered aircraft. This is because the range of jet aircraft increases considerably more with altitude than does the range of reciprocating engine aircraft. Best range in jet aircraft is obtained by flying at a very high altitude until a minimum amount of fuel remains. This is followed by a high speed descent at minimum engine fuel pressure and resulting low fuel flow rate.

It is also important for tactical considerations to evaluate control forces, buffeting and other undesirable dive characteristics. The effects of dive brakes, tip tanks and external armament on high speed descents is extremely important in fighter and ground support aircraft.

Rate of descent data reduction is identical to rate of climb data reduction, except that no thrust correction is made for temperature variation from standard. This is because the descents are made at constant fuel pressure and the effects of temperature on thrust are very small relative to the high rates of descent. The tapeline rate of descent at standard day true speed is defined by,

$$-\frac{dh}{dt} = R/D = -\frac{dH_c}{dt} \sqrt{\frac{T_{st}}{T_{as}}} \quad (5.10.01)$$

The weight corrections are,

$$\frac{\Delta R/D_2}{\Delta W} = -\frac{R/D}{W_t} \quad (5.10.02)$$

$$\frac{\Delta R/D_3}{\Delta W} = \frac{50.65 \sqrt{T_{as}}}{P_a M b^2 e} \quad (5.10.03)$$

where:

$$\Delta W = W_g - W_t$$

Equation 5.10.03 is solved by CHART 5.31, but the sign of the parameter $(\Delta R/C)_3/\Delta W$ must be changed when the chart is applied to determine $(\Delta R/D)_3/\Delta W$. Since the aircraft accelerates during the descent at constant Mach number, $(\Delta R/D)_3$ from the chart should be corrected to the accelerated condition. This may be done by (5.10.04). Fuel consumption weight corrections are not required.

$$(\Delta R/D_3)_a = \frac{(\Delta R/D_3)_{\text{chart}}}{(1 + 0.133 M^2)} \quad (5.10.04)$$

In the aircraft performance report, rate of descent data is presented as in Figure 5.10.1 to show rate of descent, time to descend, Mach number, true speed, distance traveled, fuel pressure, and fuel used.

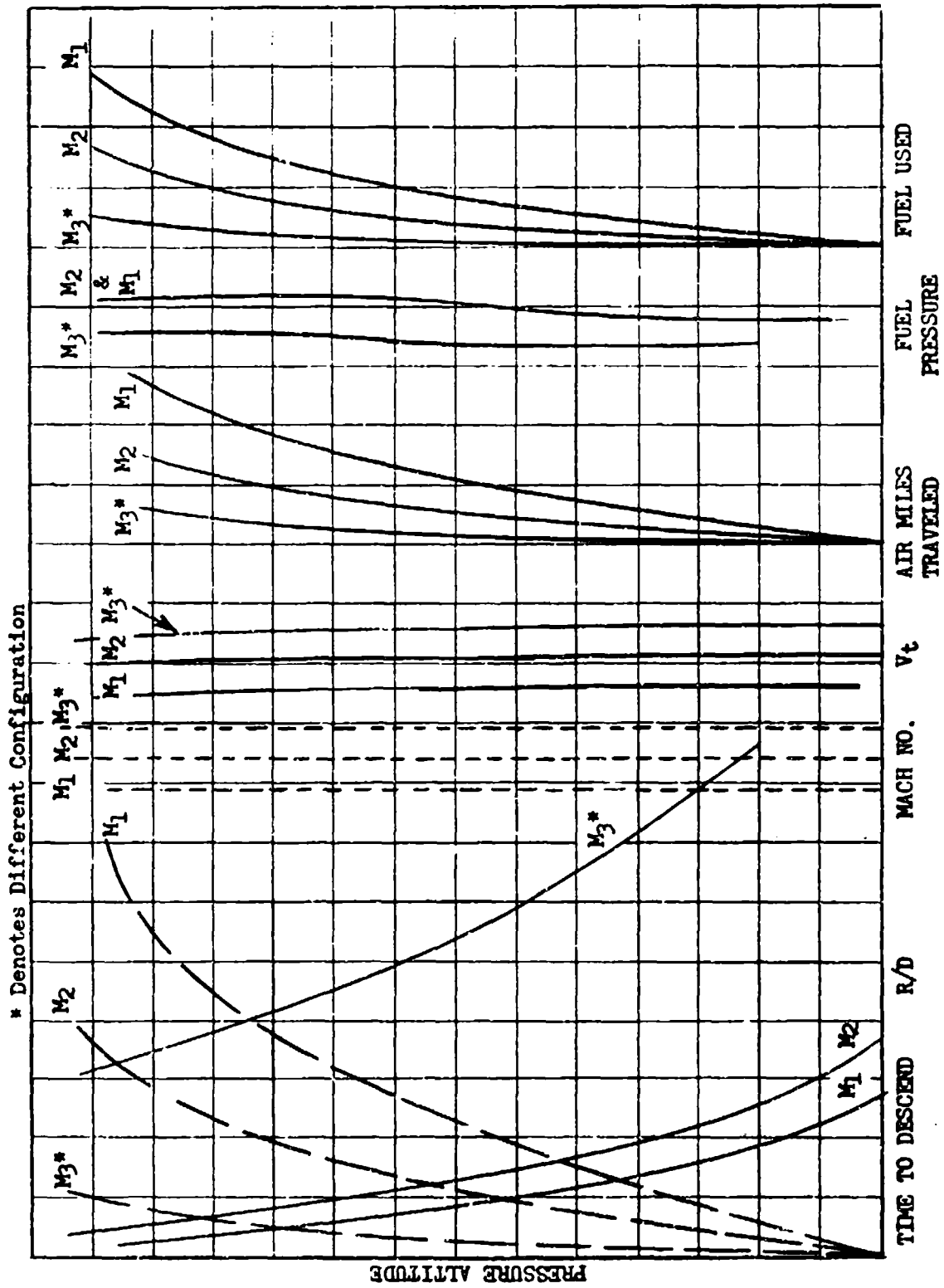
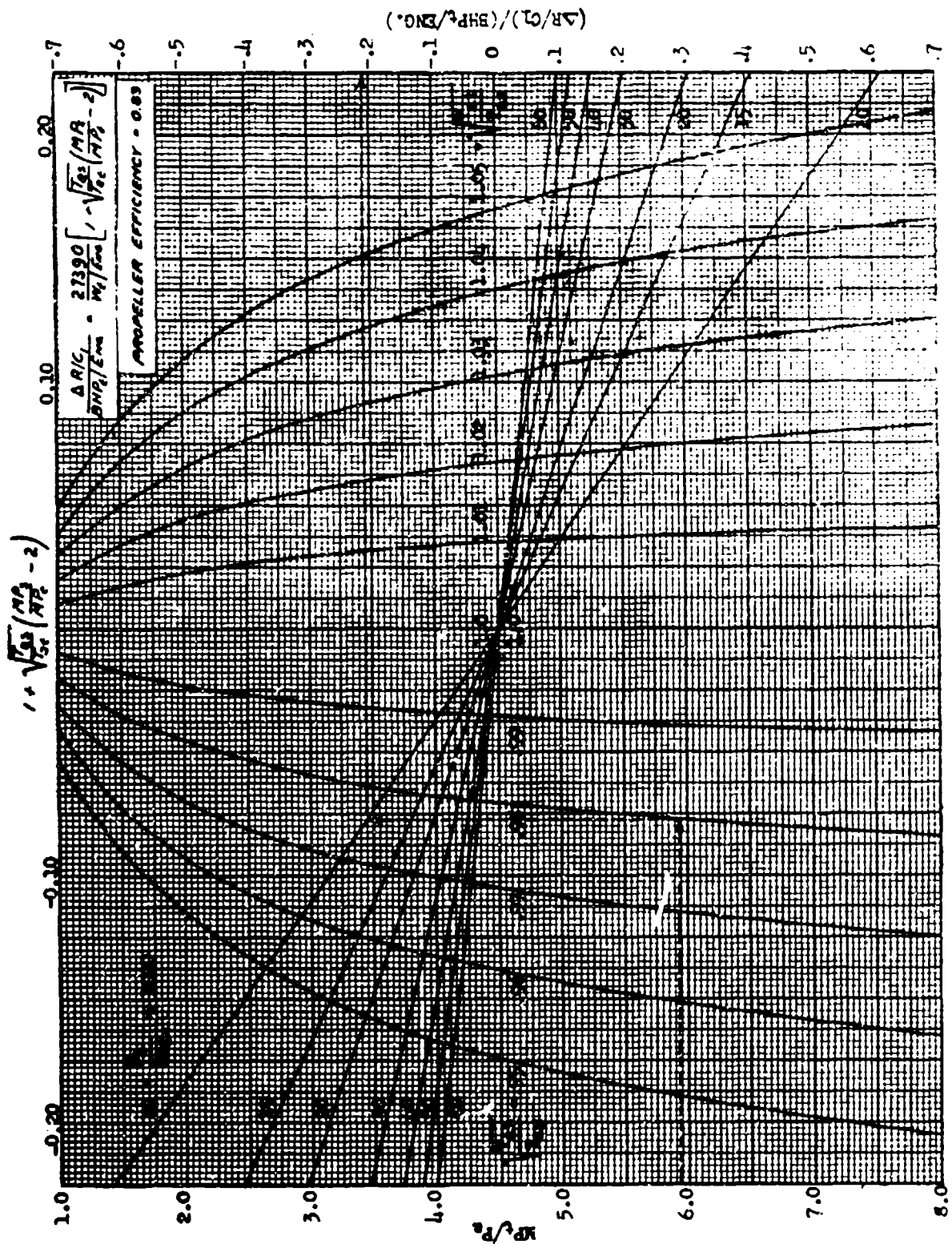


Figure 5.10.1 Report Presentation of Descent Data

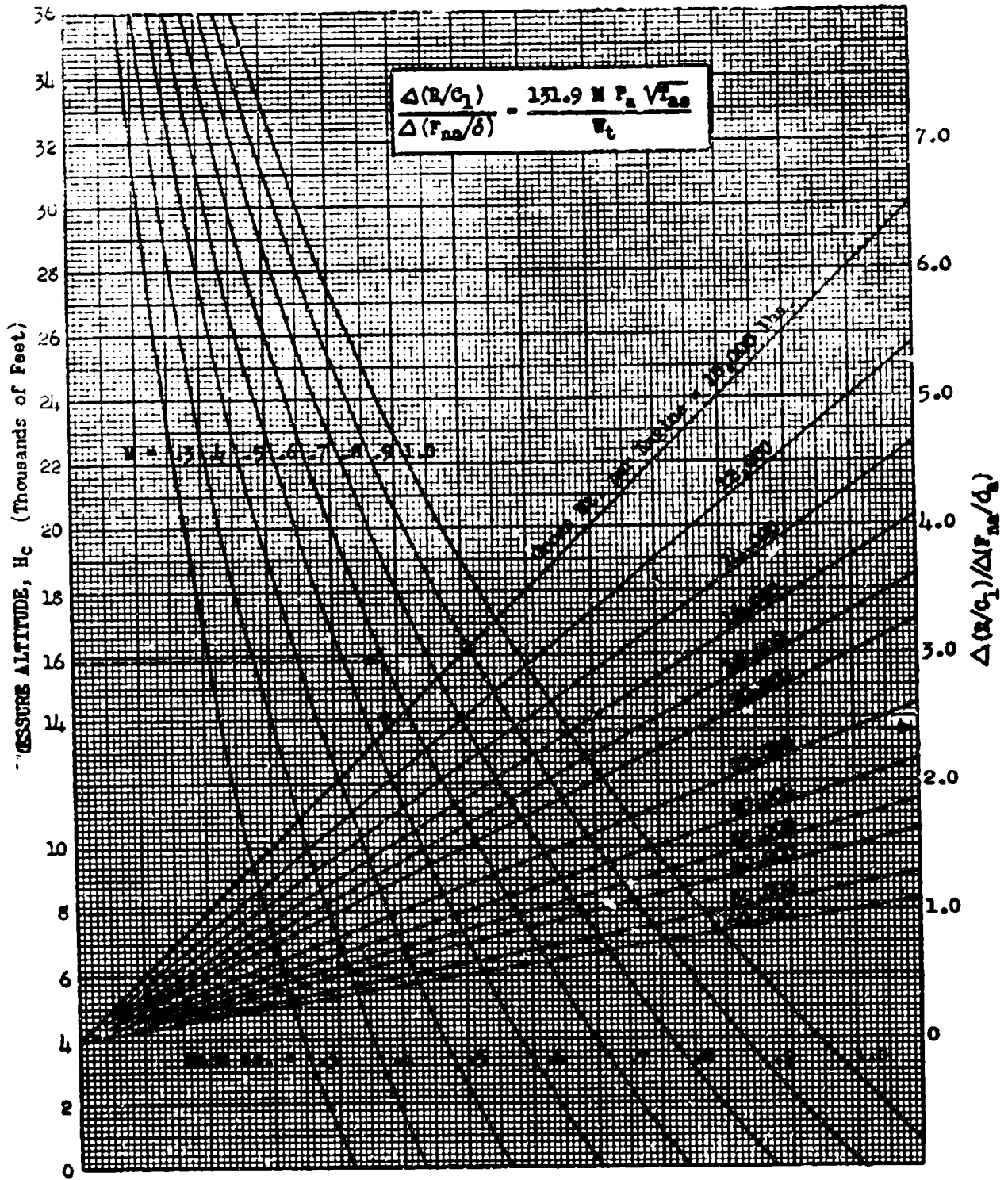
RATE OF CLIMB POWER CORRECTION FOR TEMPERATURE VARIATION

CHART 5.21



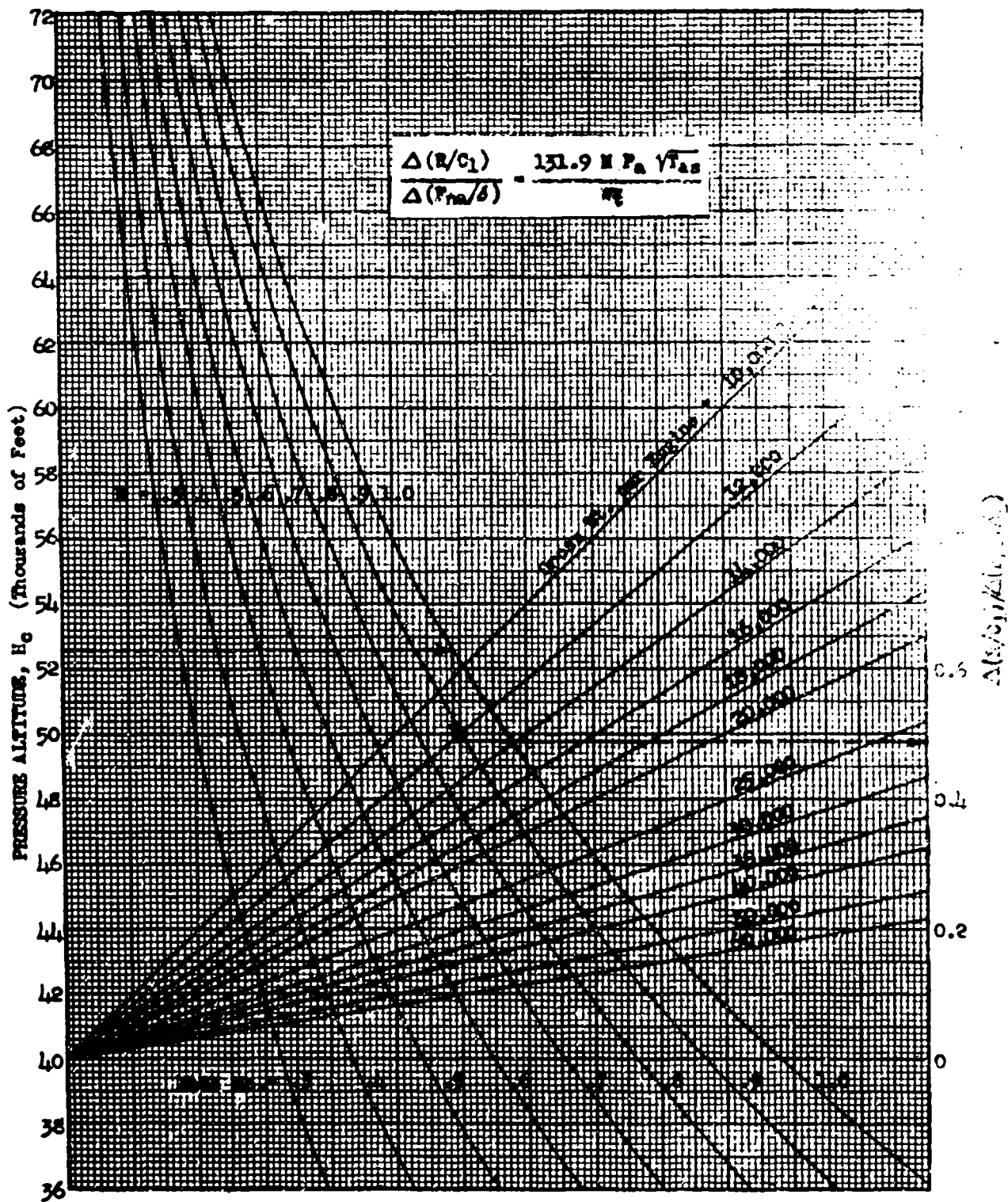
AFTR 6273

CHART 5.21



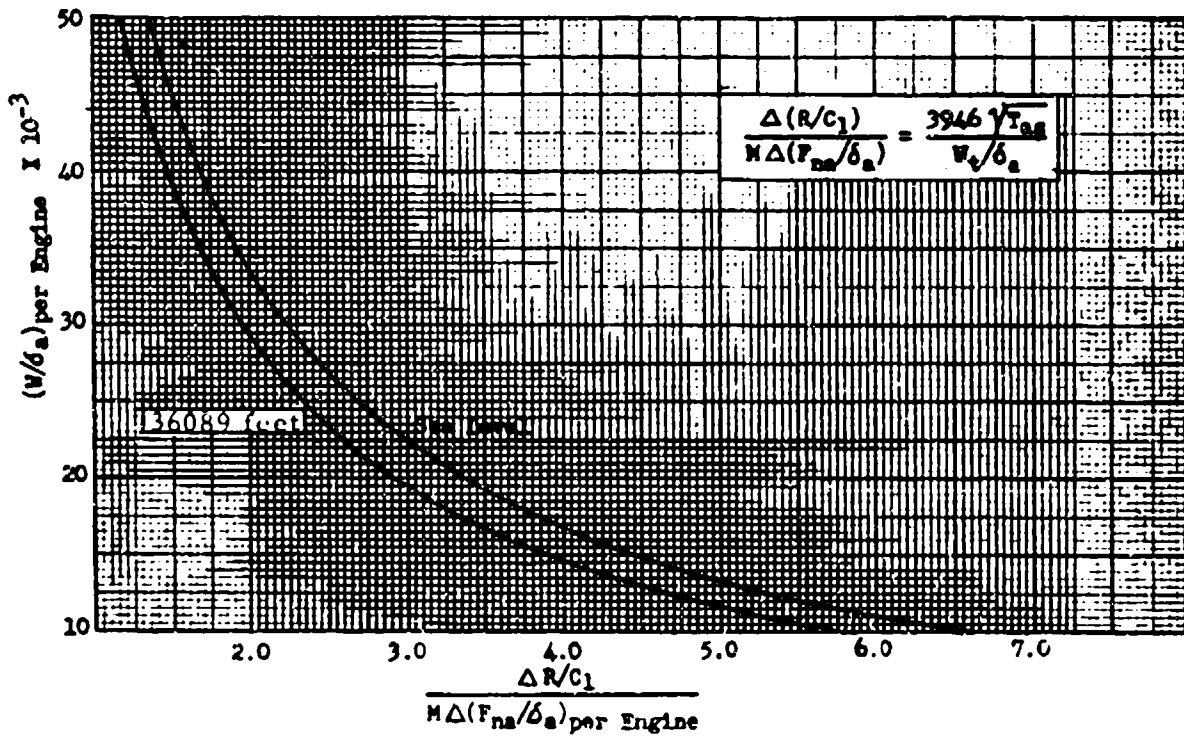
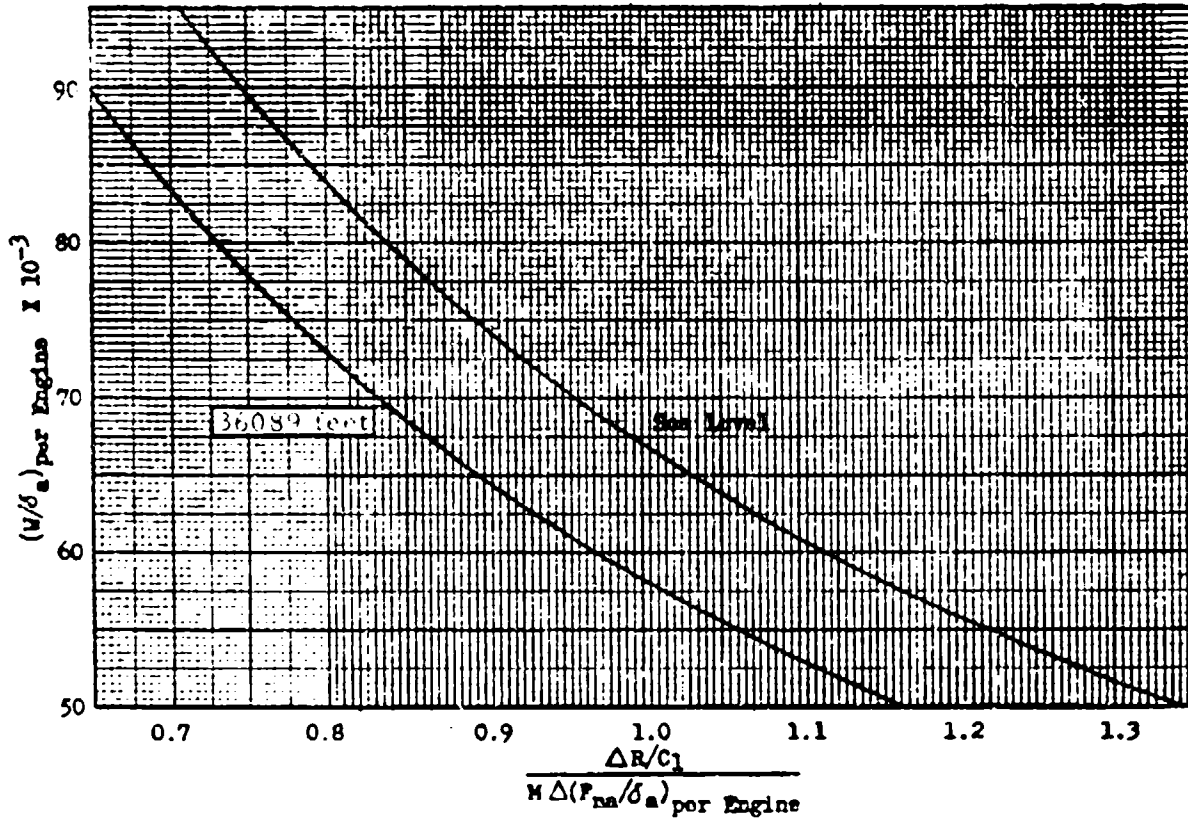
AFTR-6273

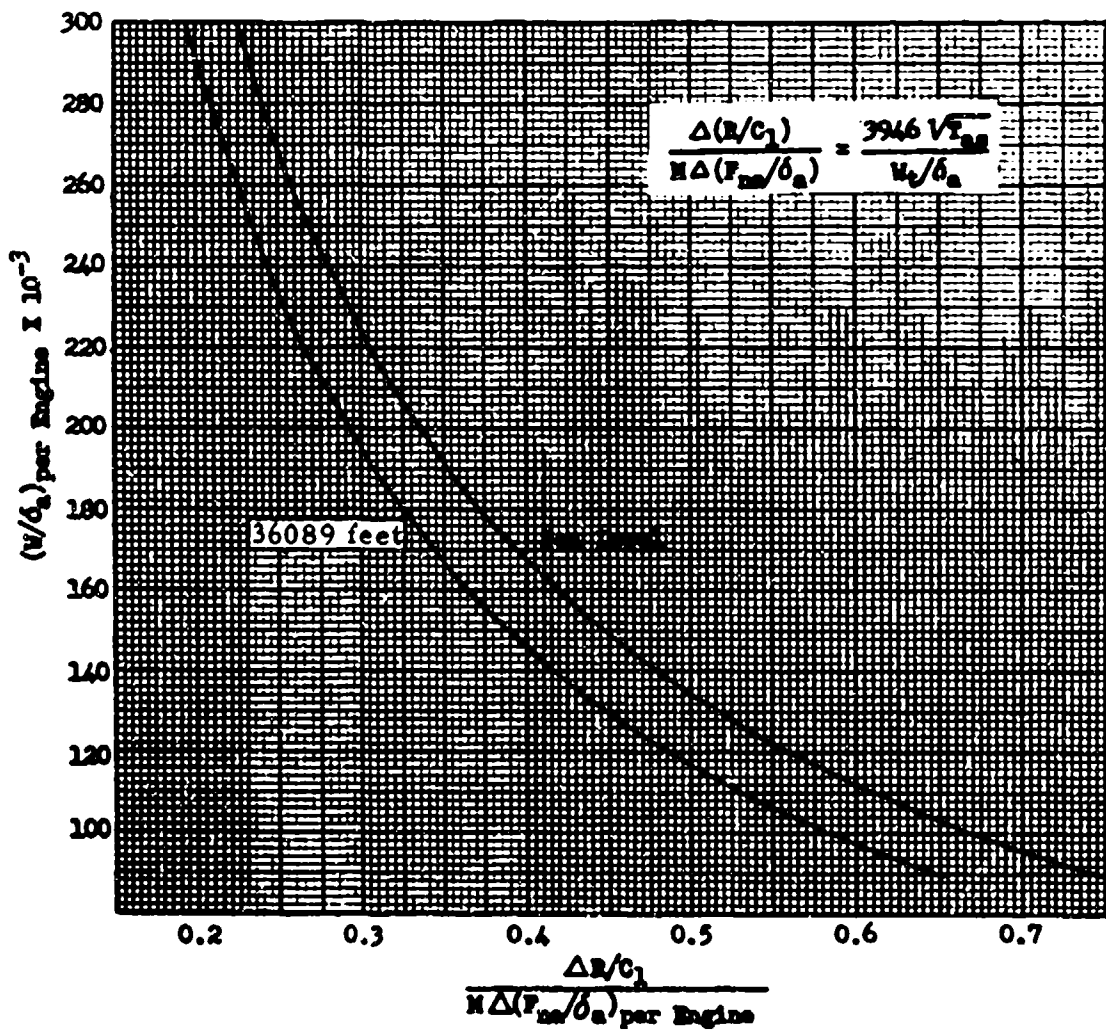
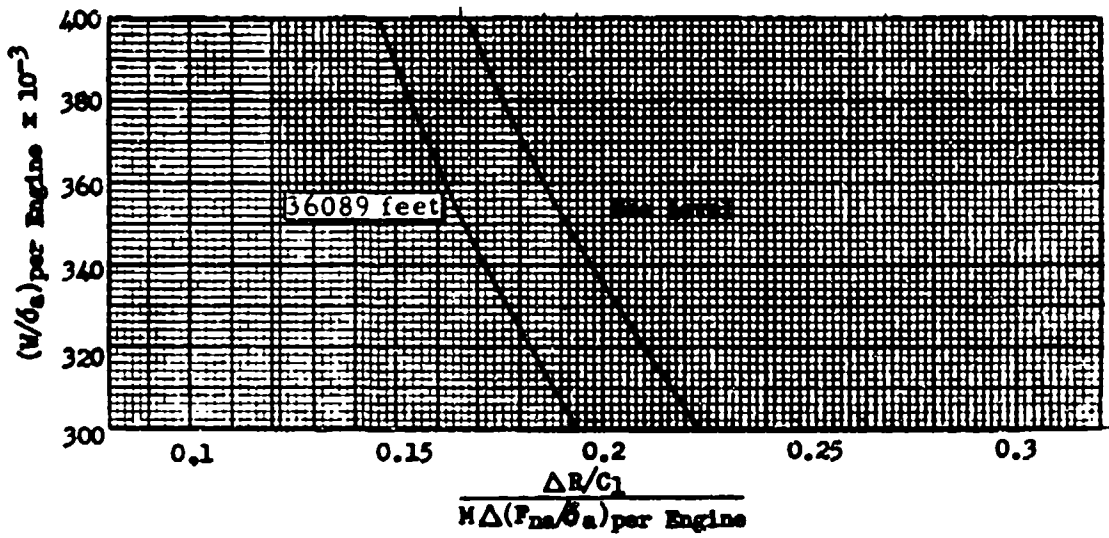
CHART 5.22

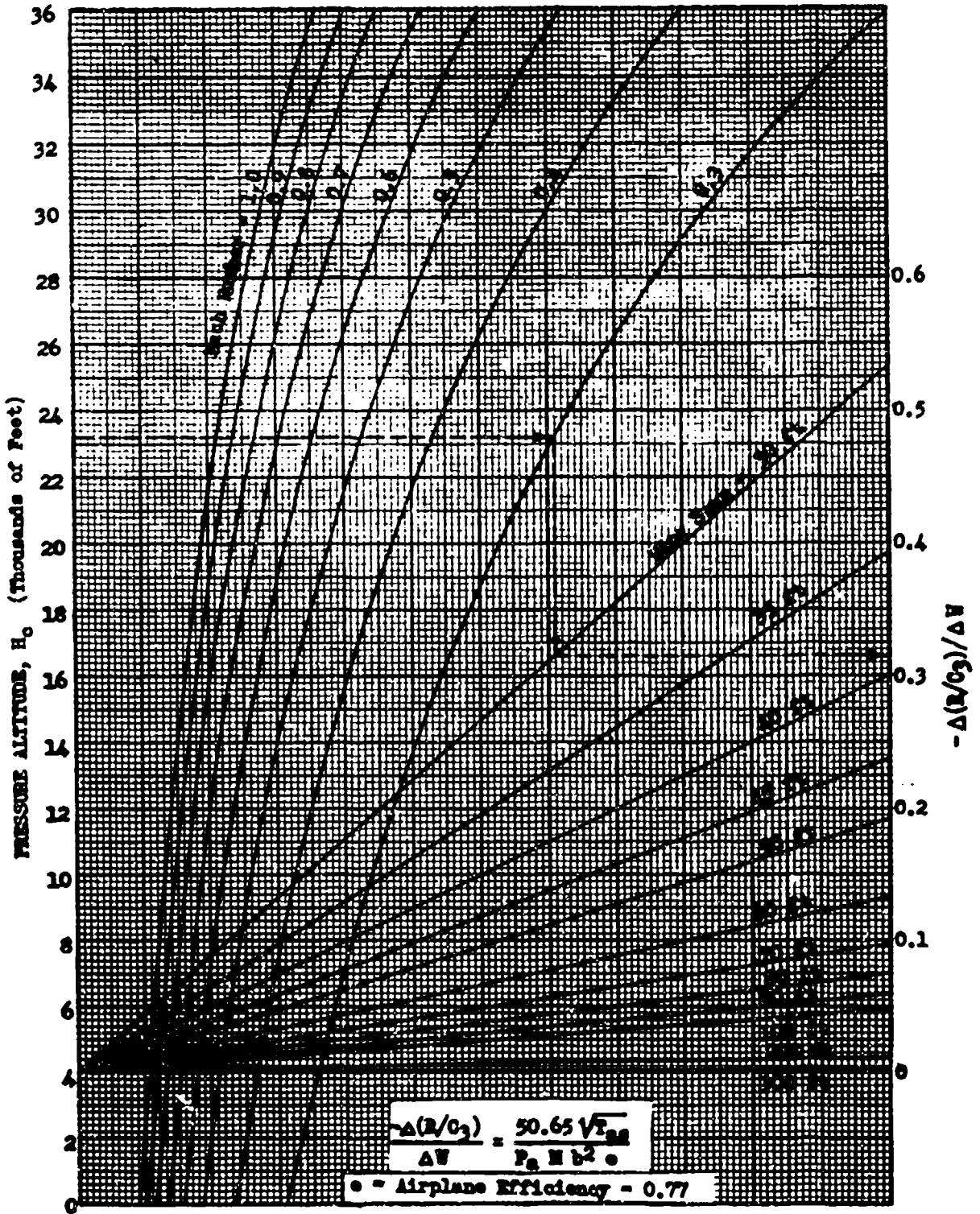


AFTR-6273

CHART 5.22





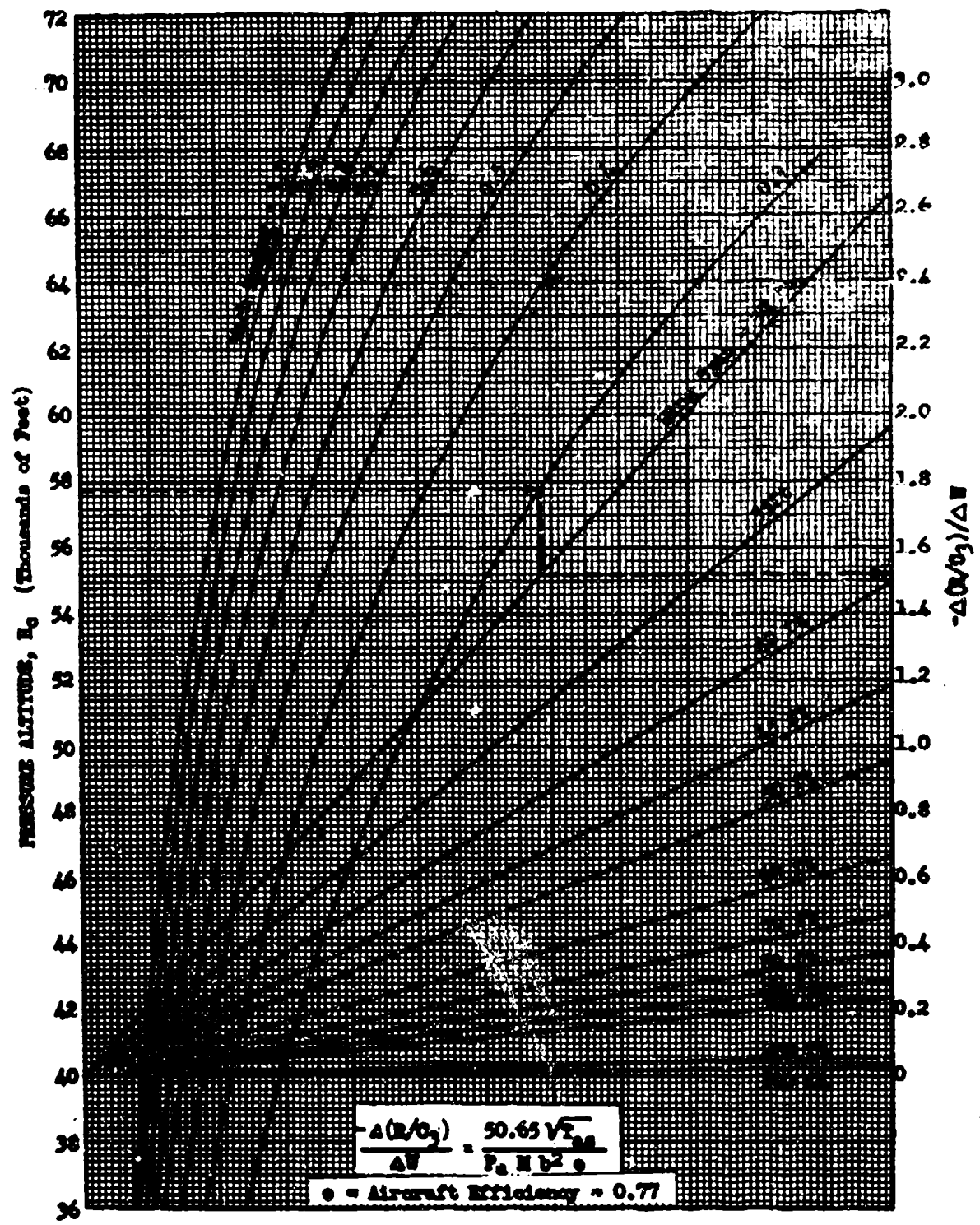


AFTR 6273

CHART 5.31

RATE OF CLIMB INDUCED DRAG CORRECTION FACTOR

CHART 5.31

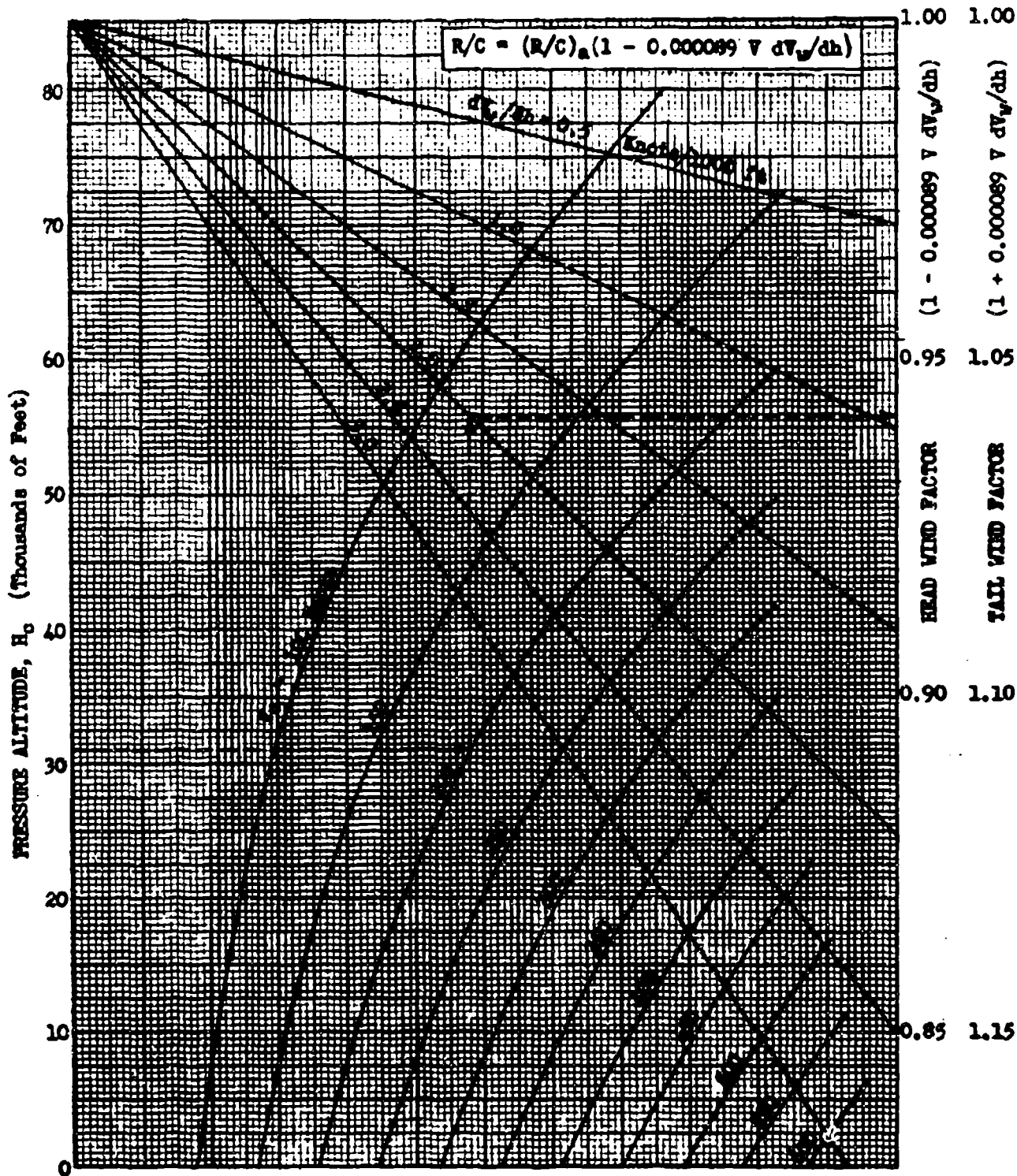


AFR 6273

CHART 5.31

RATE OF CLIMB VERTICAL WIND GRADIENT CORRECTION FACTOR

CHART 5.41

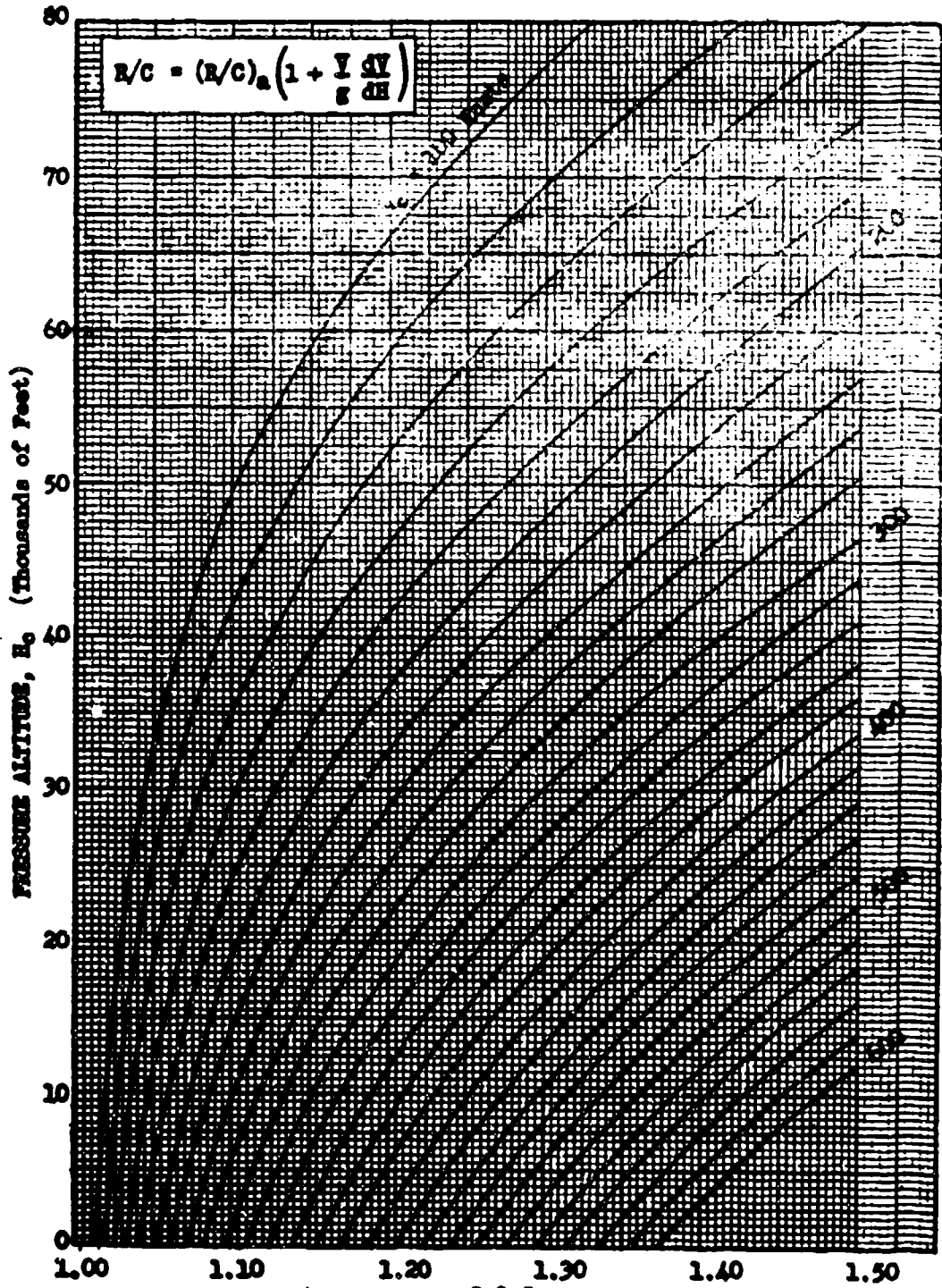


AFTR 6273

CHART 5.41

RATE OF CLIMB ACCELERATION CORRECTION FACTOR

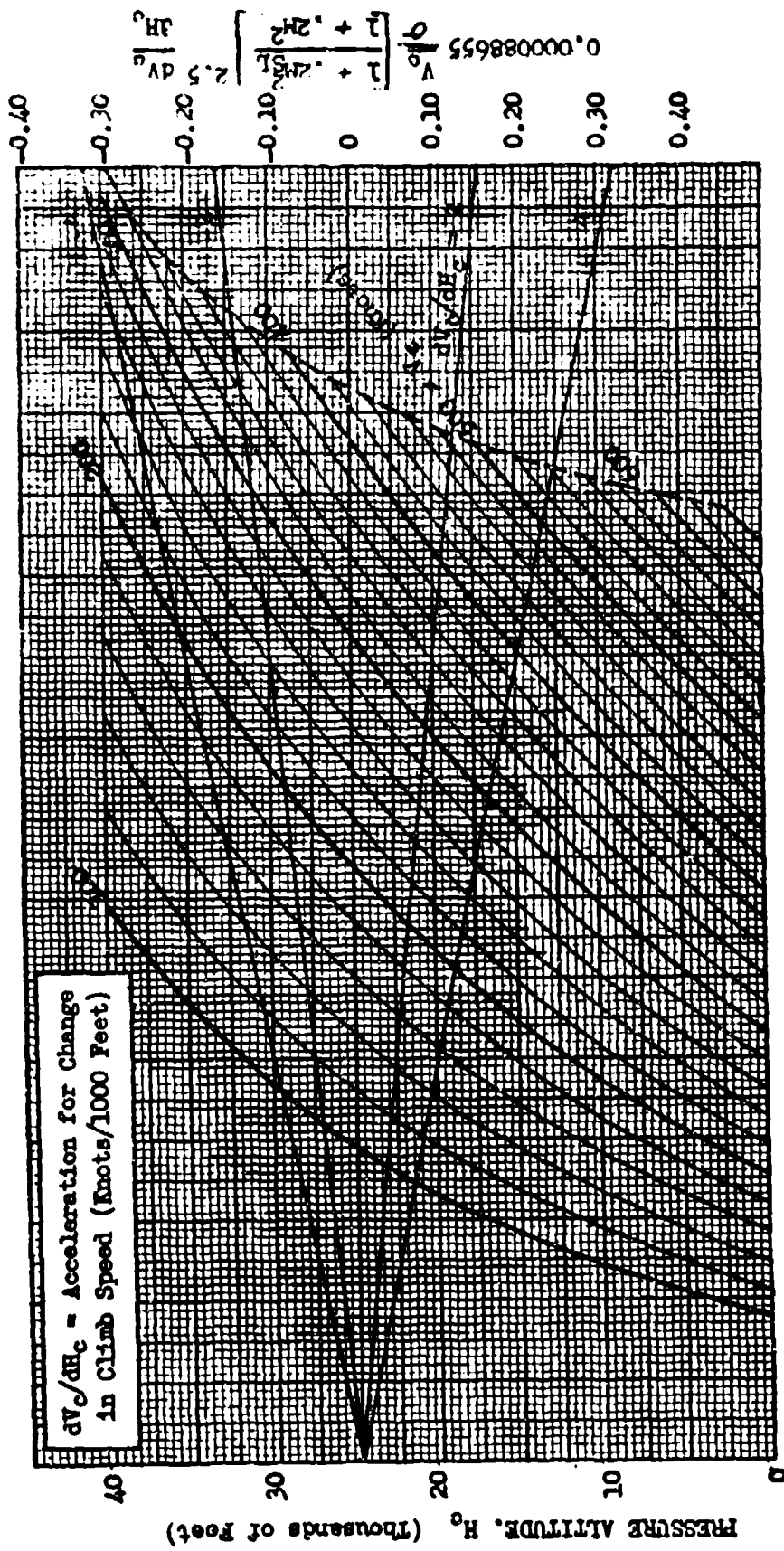
CHART 5.51



$$\left(1 + \frac{Y}{g} \frac{dY}{dH}\right) = \frac{(1 + .2M^2)^{3.5} - 1}{(1 + .2M^2)^{2.5}} = 0.133M^2 + 1$$

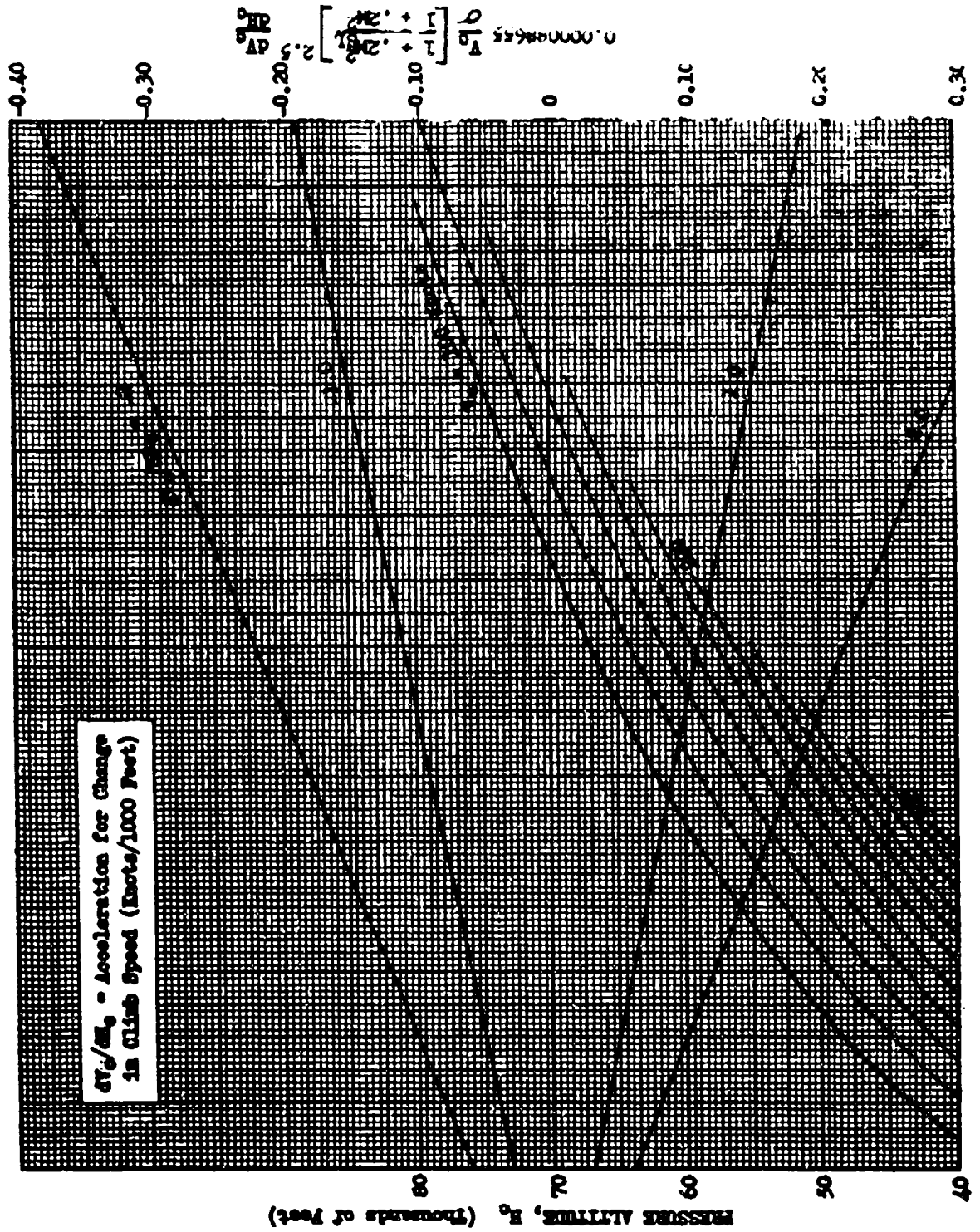
AFTER 6273

CHART 5.51



RATE OF CLIMB ACCELERATION CORRECTION FACTOR

CHART 5.52



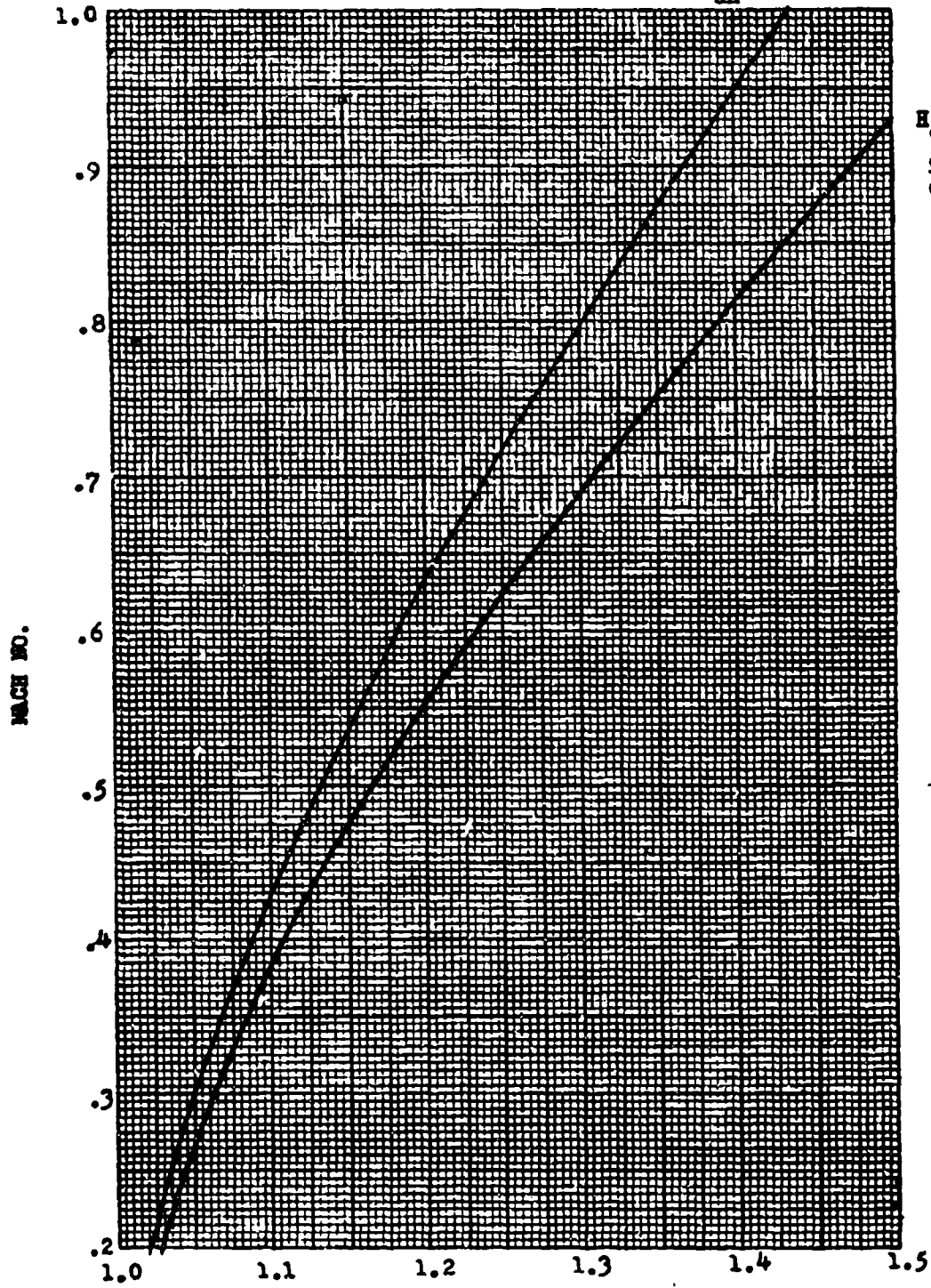
AFR 6273

CHART 5.52

Rate of Climb Acceleration Correction Factor CHART 5-53

$H_c < 36089$ feet

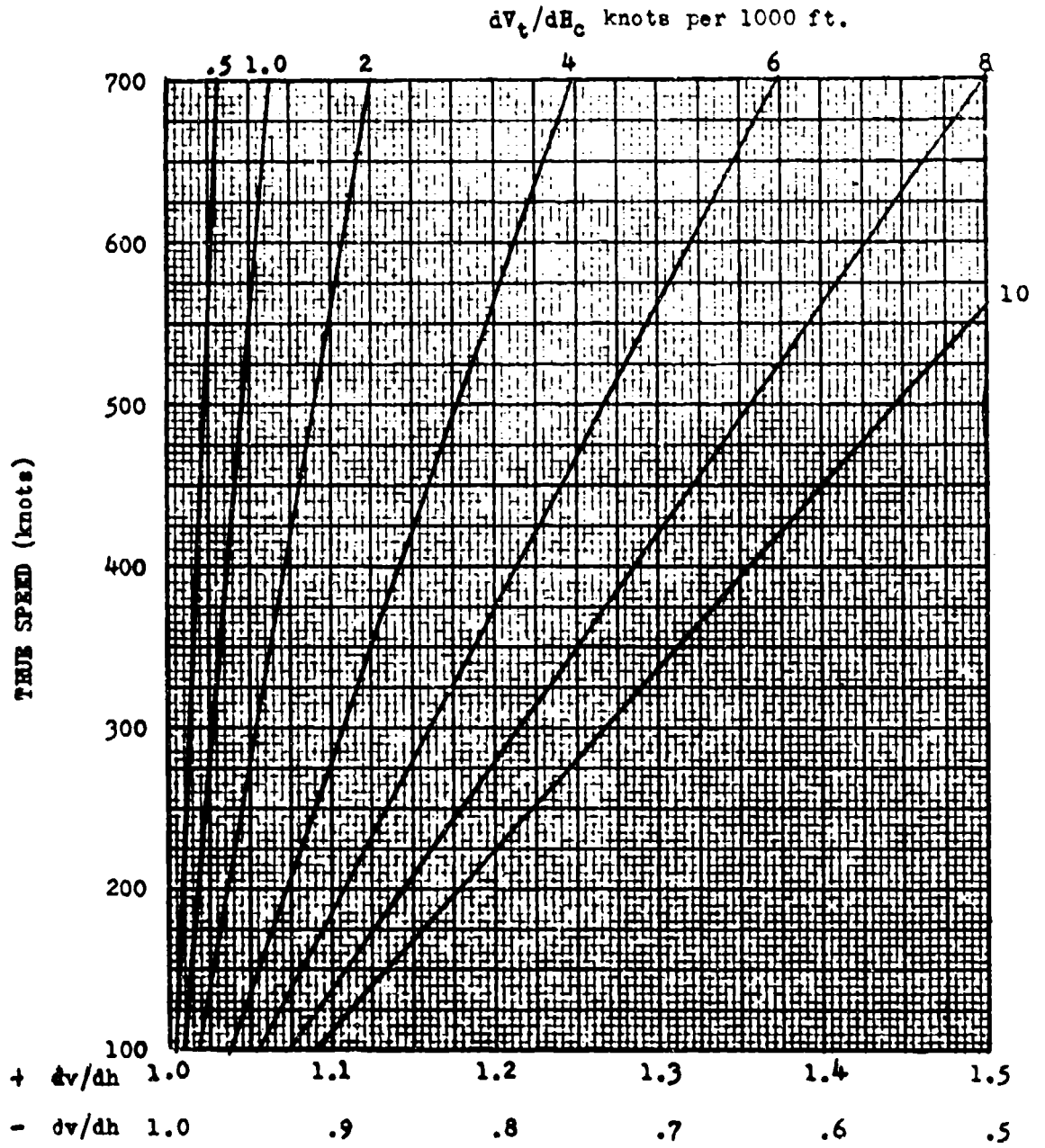
$\frac{dT_a}{dh} = -2^\circ \text{ C per } 1000 \text{ ft.}$



$H_c > 36089$ feet

$\frac{dT_a}{dh} = 0$

ACCELERATION FACTOR, $(1 + \frac{V}{g} \frac{dV}{dh})$, V_c Constant



ACCELERATION FACTOR $(1 + \frac{V}{g} \frac{dV}{dh})$

CHAPTER SIX

TAKE-OFF AND LANDING PERFORMANCE

SECTION 6.1

Techniques and Configurations for Take-Off Tests - JAIO Operation

Take-off tests consist of a series of take-offs to determine the ground distance from the start of the run to the point where the aircraft leaves the ground, and the air distance from this point to the place where the aircraft is 50 feet above the runway. During the tests, the airplane should be operated in a manner considered to give the best take-off performance within the operational limits of the airplane and engine. Unless otherwise specified, the gross weight for take-off tests includes the maximum load likely to be used in service. All tests are run as close as possible to the desired gross weight to keep all weight corrections to a minimum. As local wind conditions affect the take-off distance and techniques used, tests should not be conducted when the wind velocities exceed 10% of the take-off speed of the aircraft.

For airplanes with wing flaps that are used for take-off, several flap positions are used to determine the optimum flap position. Cowl flaps are open for take-off, the airplane is held with brakes and maximum allowable power is attained prior to brake release. Maximum power is obtained as soon as practicable during the take-off run. As an example, the F-51 aircraft is limited to 40 inches manifold pressure without anchoring the tail, but 61 inches is used for take-off power. Therefore, the maximum allowable power prior to brake release is 40 inches and the maximum power is 61 inches.

When jet assist take-offs are made and it is desired to obtain the most advantage from a short duration rocket, the rocket should be ignited at such a point during the take-off run that it will be expended as the airplane passes over the 50 foot obstacle. This point of ignition is normally obtained by estimating the number of seconds after brake release that the rocket should be ignited, and then bracketing this point by making one or two take-offs. In most cases this information should be given to the pilot in the form of a number of seconds after brake release; however, it may sometimes be advantageous to ignite the rockets at an indicated air speed. For long burning rockets, the shortest take-off will be made by igniting the rockets at brake release.

SECTION 6.2

Distance and Height Measurements and Equipment

Measurements should be taken to determine the distance from the take-off starting point to the place where the aircraft leaves the ground and to the point where the airplane reaches the altitude of 50 feet. These measurements may be made in various ways. A few of the methods of general use follow:

When camera equipment is not available either of the following systems may be used. The first consists of several theodolites (sighting bars) spaced along the runway so as to cover the distance from take-off point to the simulated 50 foot obstacle. The distance and time from take-off point to each sighting station will give an approximation of the aircraft speed and take-off distance. This method is shown schematically in Figure 6.21.

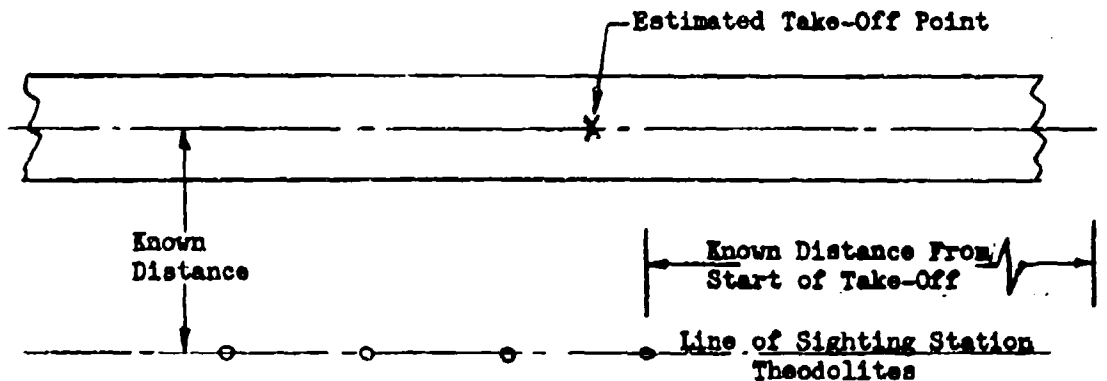


Figure 6.21
Basic Method for Obtaining Take-Off
and Landing Time and Distance Data

It is good practice to station two or three observers at the edge of the runway in the vicinity of the take-off point to mark the exact point of take-off. The data obtained by such observers are always a good check on ground roll distance regardless of the method used for obtaining data. Using this method the height of the aircraft above the runway may be obtained by a formula determined from Figure 6.22.

$$H = \frac{Dh}{d} + \Delta H \quad (6.201)$$

where:

- H = height of aircraft above the theodolite, ft.
- D = distance from runway centerline to theodolite eye piece, ft.
- h = height read on theodolite as aircraft passes, ft.
- d = length of theodolite, ft.
- ΔH = height of theodolite above runway, ft.

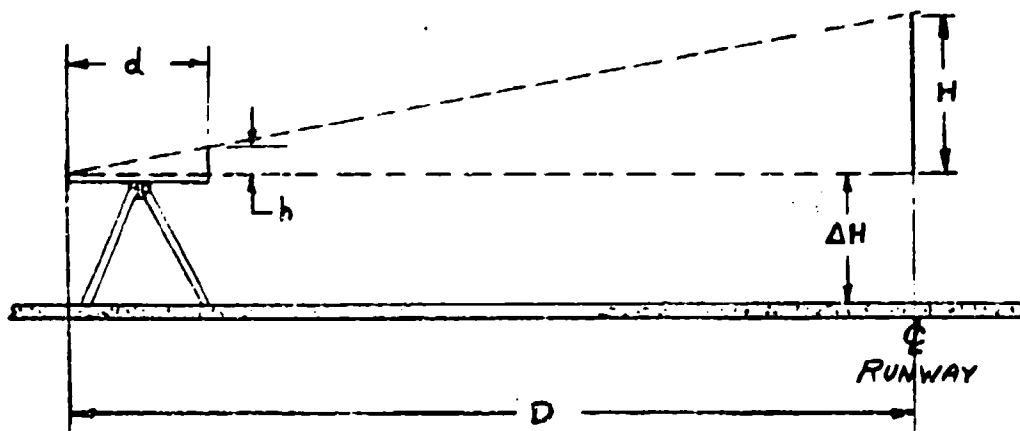


Figure 6.22
Theodolite Geometry

A more accurate field method of obtaining take-off data consists of a theodolite pivoted so it may track the aircraft during the take-off run, Figure 6.23. The theodolite is constructed in such a way that, by keeping cross-hairs on the aircraft, a pencil trace of the aircraft position is placed on a chart fastened rigidly to the theodolite supports. The swiveling theodolite is set up at a known distance from the runway and so aligned as to encompass only as much of the runway as will be necessary for the tests of the particular aircraft under consideration. This is done to obtain the greatest accuracy from the instrument.

Various standard distances from the runway may be arbitrarily determined and charts prepared in advance for use on this theodolite. A timing mechanism built into the sighting bar marks every second on the chart. Ground observers are used to mark the exact point of take off, and this information may be placed on the chart at the end of each test. A typical chart and take-off graph is illustrated in Figure 6.24.

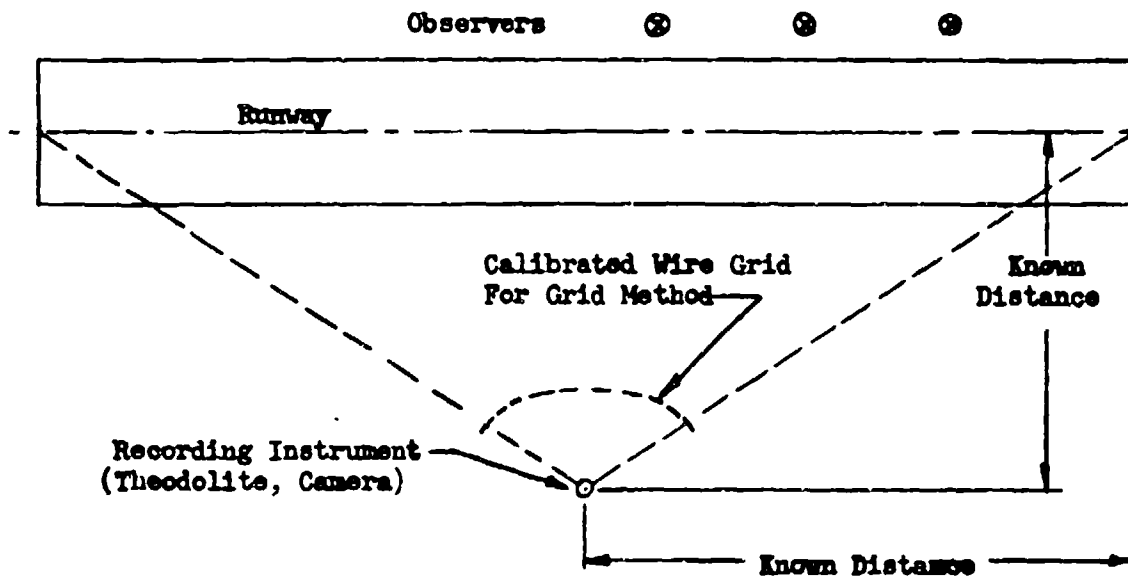


Figure 6.23
Take-off Data Installation for Swiveling
Camera or Recording Theodolite

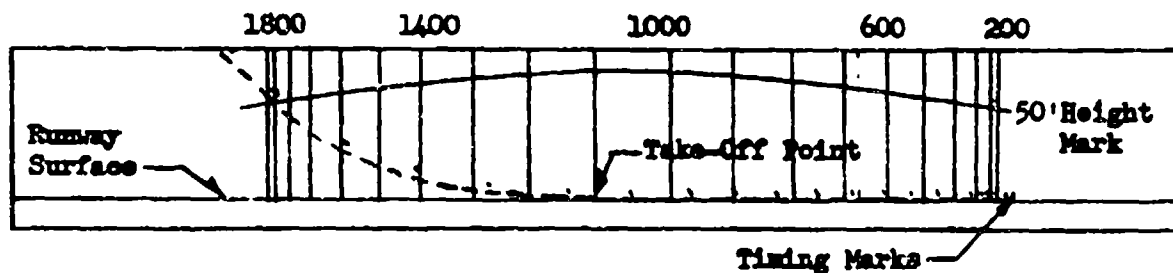


Figure 6.24
Recording Theodolite Chart

The most accurate means of recording take-off data is with a moving picture camera which will photograph the aircraft under test, a timing device, and either a grid or azimuth scale. A portable 16 mm. camera has been devised which photographs the runway, a stop watch and the position of the airplane with respect to an azimuth scale. Knowing the azimuth and the distance of the camera from the

runway along a normal to the runway, the position of the aircraft may be determined at any time during the test. A typical frame from a test camera would appear as in Figure 6.25.

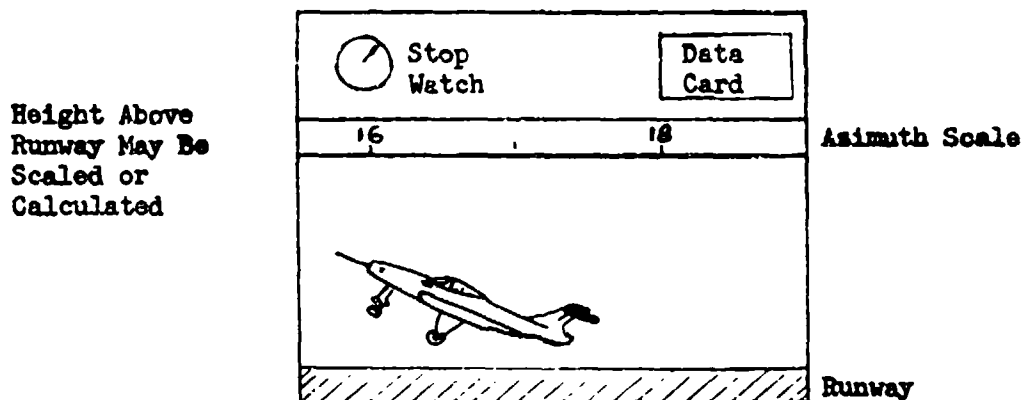


Figure 6.25
Typical Frame from Take-off Camera Film

A fixed grid may also be used to photographically record the tests. In this method a grid consisting of a network of calibrated wires is placed in front of a normal camera in the manner shown in Figure 6.25 and at such a distance that it will remain in focus along with the airplane being tested. A timing device may be mounted on either the grid or camera to give a time history of the take off or landing. A typical frame taken through this type of grid is shown in Figure 6.26.

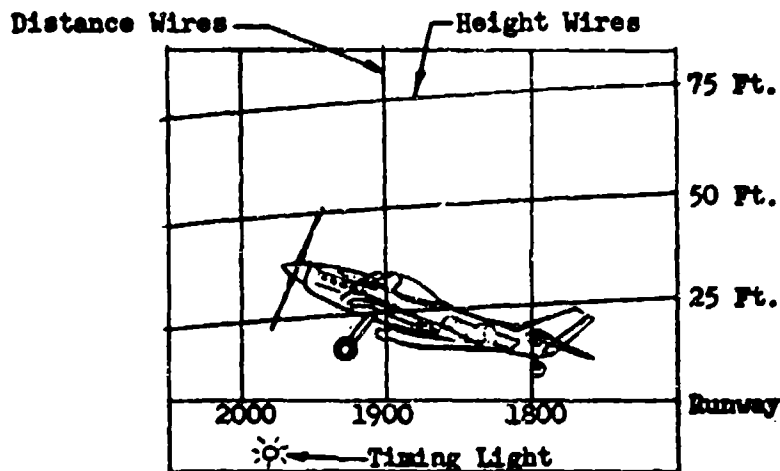


Figure 6.26
Typical Frame from Camera-Grid Film

SECTION 6.3

Take-Off Data Corrections for Wind, Weight, and Density

From information obtained by any of the above methods in the previous section, the observed data may be plotted as in Figure 6.31. This figure is usually included in the final report as is the corrected take-off data.

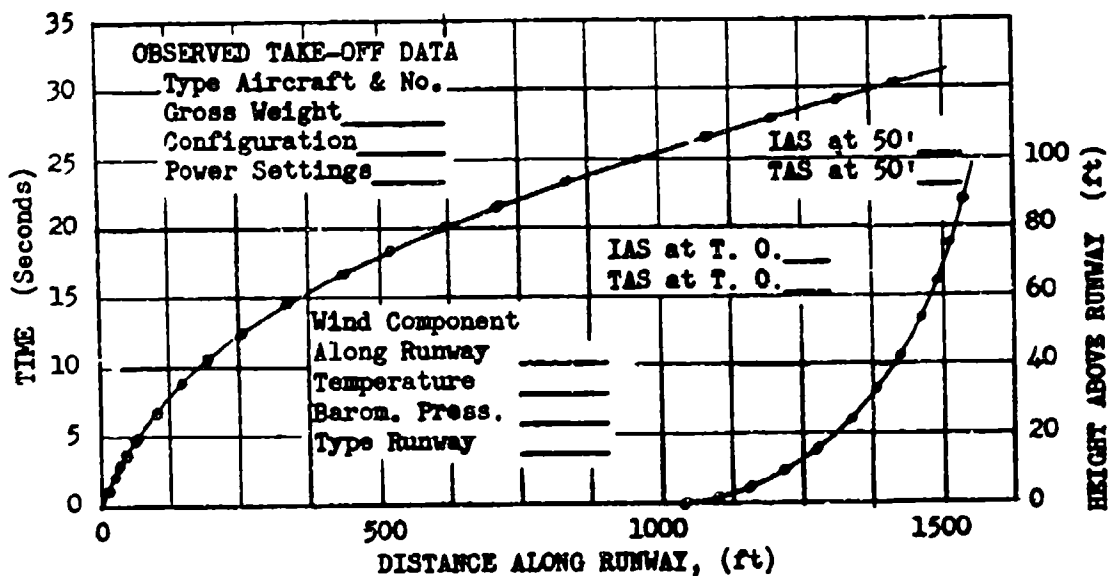


Figure 6.31
 Presentation of Actual Take-off Time
 and Distance Data

The indicated air speed at take-off and 50 feet as well as the true air speed should be shown, as the pilot is primarily concerned with the air speed that is read on the instrument panel, and this value is independent of pressure and temperature.

All take-off performance data are corrected to sea level standard conditions and zero wind unless otherwise specified. The average of the best two of at least four take-offs is reported as performance data. Corrected data are usually presented in the following chart form:

A - CONFIGURATION - WEIGHT - POWER SETTING

(1) Ground Roll (ft)	(2) Total Distance over 50' height	(3) Indicated Speed		(4) True Speed	
		At Take-Off	At 50' Height	At Take-Off	At 50' Height

B - CONFIGURATION - WEIGHT - POWER SETTING

--	--	--	--

C - CONFIGURATION - WEIGHT - POWER SETTING

TAKE-OFF DATA CORRECTION

The take-off performance of any aircraft is highly dependent on pilot technique. Even with experienced well-qualified pilots it is difficult to make the aircraft take off at the same value of lift coefficient each time. As this is the rule rather than the exception, a rigorous mathematical treatment of reducing observed take-off data to standard conditions is not warranted; therefore, no mathematically exact solutions will be given for reducing data.

The correction of ground roll for the effect of wind may be empirically expressed as,

$$S_t = S_{tw} \left(\frac{V_{to} + V_w}{V_{to}} \right)^{1.85} \quad (6.301)$$

where:

- S_{tw} = observed ground roll, ft, with wind component
- S_t = ground roll corrected for wind, ft
- V_{to} = ground velocity at take off
- V_w = component of wind along the runway
headwind (+); tailwind (-).

This relationship has been verified by extensive flight tests. Neglecting wind, the ground roll during take off is,

$$S = \int_0^{V_{to}} \frac{V}{a} dV \quad (6.302)$$

where:

- V_{to} = true speed at take-off point
- a = acceleration

Assuming "a" to have an effective constant value at a mean value of V^2 the above expression becomes,

$$s = \frac{1}{2} \frac{V_{to}^2}{a \odot (.7 V_{to})} \quad (6.303)$$

The effective thrust acting throughout the take-off is defined as the difference between propulsive net thrust at $.7 V_{to}$ and the aircraft resistance to forward motion at the same point. This take-off thrust equation may be written as,

$$F_{eff} = \frac{W}{g} a = \frac{W V_{to}^2}{2gS} \quad (6.304)$$

The basic take-off distance equation then becomes,

$$s = \frac{W V_{to}^2}{2g F_{eff}} = \frac{W V_{to}^2}{2g [F_n - \mu (W - L) - D] \odot .7 V_{to}} \quad (6.305)$$

One method of evaluating the effect of small changes in the variables of equation 6.305 is by use of logarithmic differentiation. With this mathematical process and with the assumption of constant C_L at take-off for all conditions of the variables,

$$\frac{dD}{D} = \frac{dL}{L} = \frac{dW}{W}$$

where,

D = aircraft drag, L = aerodynamic lift

then

$$\frac{dS}{S} = \frac{dW}{W} - \frac{d\sigma}{\sigma} + \frac{F_n}{F_{eff}} \left(\frac{dW}{W} - \frac{dF_n}{F_n} \right) + \frac{d\mu}{\mu} \left(\frac{F_n - D}{F_{eff}} - 1 \right) \quad (6.306)$$

or in another form

$$\frac{S_2}{S_1} = 1 + \frac{W_2}{W_1} - \frac{\sigma_2}{\sigma_1} + \frac{F_n}{F_{eff}} \left(\frac{W_2}{W_1} - \frac{F_{n2}}{F_{n1}} \right) + \left(\frac{\mu_2}{\mu_1} - 1 \right) \left(\frac{F_n - D}{F_{eff}} - 1 \right) \quad (6.307)$$

where $F_n = F_n \odot .7 V_{to}$

μ = coefficient of rolling resistance

Empirical values of μ are

$\mu = .02$ for hard surface runway

$\mu = .04$ for firm turf

$\mu = .10$ for soft turf

These equations should be used only where the ratios of the variables lie between 0.9 and 1.1.

If there is a weight variation the indicated speeds must be adjusted for a constant C_L assumption.

$$\frac{V_{c1}}{V_{c2}} = \sqrt{\frac{W_1}{W_2}}$$

An exact relationship between take-off distances for large changes in the variables of equation 6.305 can be found by making μ constant and defining S_2 in terms of S_1 , V_{to2} in terms of V_{to1} , and F_{eff2} in terms of F_{eff1} , at constant C_L . This expression is,

$$\frac{S_2}{S_1} = \frac{W_2}{W_1} \frac{\sigma_1}{\sigma_2} \left/ \left[\frac{F_{D1}}{F_{eff1}} \left(\frac{W_1}{W_2} \frac{F_{D2}}{F_{D1}} - 1 \right) + 1 \right] \right. \quad (6.308)$$

Equations 6.306, 6.307, and 6.308 as shown are directly applicable to turbo-jet aircraft where net thrust is quite easily determined for take-off conditions.

Correction for Runway Slope and C_L Variation

It is sometimes necessary to correct take-off data for runway slope. This is a simple geometric consideration. The effective thrust is,

$$F_{eff_{level}} = F_{eff_{slope}} + W \sin \theta$$

dividing by $F_{eff_{slope}}$ and substituting equation 6.304,

$$S_{level} = \frac{S_{slope}}{1 + \frac{2g S_{slope} \sin \theta}{V_{to_{slope}}^2}} \quad (6.309)$$

To correct data to constant C_L a relationship is found by multiplying equation 6.304 by $(W/W) = 1$.

Then,

$$S = \frac{V^2}{2g\sigma} \frac{V_{to}^2}{W}$$

and

$$S_2 = S_1 \frac{(V_{to}^2/W)_2}{(V_{to}^2/W)_1} \quad \begin{matrix} \text{(constant } \sigma) \\ \text{(for jet aircraft only)} \end{matrix} \quad (6.310)$$

The slope and C_L corrections along with the wind corrections should be applied to test data prior to density weight and thrust corrections.

AIR DISTANCE DATA CORRECTION

To determine the corrected horizontal air distance from lift-off point to clear a fifty foot obstacle the correction to zero wind is expressed as the product of wind velocity and time,

$$S'_a = S'_{a_v} + V_w t \quad (6.311)$$

where:

S'_a = wind corrected test air distance

S'_{a_v} = observed air distance in wind

V_w = wind component along runway

t = time from lift-off to 50 ft. point

Neglecting wind the following expressions may be written for the air distance and the aircraft energy change through it.

$$V = \frac{S_a}{t} \quad \text{and} \quad \frac{dE}{dt} = \frac{(50 + h_v) W}{t}$$

where:

V = mean true airspeed between take-off and 50 ft. height.

E = $(50 + V^2/2g)W$, total energy of the aircraft.

W = gross weight

$h_v = (V^2_{50} - V_{to}^2)/2g$

$\frac{dE}{dt} = V(F - D)$

F = net thrust

D = total air drag

Combining these expressions and substituting $V(F - D)$ for dE/dt a general expression for the air distance is derived.

$$S_a = \frac{W(50 + h_v)}{(F - D)_{\text{eff}}} \quad (6.312)$$

Logarithmic differentiation may be applied to equation 6.312 to determine the effect on air distance of small changes in the variables. This process gives for a constant C_L at V_{to} and V_{50} .

$$\frac{dS_a}{S_a} = \left(\frac{dW}{W} - \frac{d\sigma}{\sigma} \right) \frac{h_v}{50 + h_v} + \left(\frac{dW}{W} - \frac{dF_n}{F_n} \right) \frac{F_n S_a}{W (50 + h_v)} \quad (6.313)$$

or in another form

$$\frac{S_{a2}}{S_{a1}} = 1 + \left(\frac{W_2}{W_1} - \frac{\sigma_2}{\sigma_1} \right) \frac{h_v}{50 + h_v} + \left(\frac{W_2}{W_1} - \frac{F_{n2}}{F_{n1}} \right) \frac{F_{n1} S_{a1}}{W_1 (50 + h_v)} \quad (6.314)$$

where F_n = net thrust at a mean speed between V_{to}^2 and V_{50}^2 .

These equations should be used only where the ratios of the variables lie between 0.9 and 1.1.

An exact relationship between air distances for large changes in the variables of equation 6.312 can be found by defining S_{a2} in terms of S_{a1} , V_{to2} and V_{502} in terms of V_{to1} and V_{501} and $(F - D)_2$ in terms of $(F - D)_1$ at constant C_{Lto} and C_{L50} . This expression is,

$$\frac{S_{a2}}{S_{a1}} = \frac{\frac{W_2}{W_1} \frac{\sigma_1}{\sigma_2} h_{v1} + 50}{h_{v1} + 50 + S_{a1} \left(\frac{F_{n2}}{W_2} - \frac{F_{n1}}{W_1} \right)} \quad (6.315)$$

Equations 6.313, 6.314, and 6.315 as shown are directly applicable to turbo-jet aircraft where net thrust is quite easily determined for take-off conditions.

EMPIRICAL FORMULAS FOR CORRECTION OF GROUND ROLL AND AIR DISTANCE DATA OF BOTH JET AND PROPELLER POWERED AIRCRAFT

The following expressions for the effects of changes in the independent variables involved in equations 6.305 and 6.312 were developed and checked against experimental data by Mr. K.J. Lush of the Flight Research Branch, Air Force Flight Test Center. The complete study and analysis may be found in, "Standardization of Take-Off Performance Measurements for Airplanes", Technical Note B-12, Air Force Flight Test Center, Edwards Air Force Base, Edwards, California.

These formulas were developed by application logarithmic differentiation to equations 6.305, and 6.312, and to applicable propeller relationships. The constants were determined primarily by graphical analysis of a large amount of take-off data from typical aircraft. Corrections obtained by these formulas will give sufficiently accurate data for changes in the variables up to $\pm 20\%$.

The General Case: For propeller driven and jet airplanes, the general equations (6.316) and (6.317) will be used.

$$\frac{\Delta S}{S_{a_t}} = \frac{\Delta W}{W_t} \left\{ 2 + \frac{D}{F-D} \right\} - \frac{\Delta \sigma}{\sigma_t} - \frac{\Delta F}{F_t} \left\{ 1 + \frac{D}{F-D} \right\} \quad (6.316)$$

$$\begin{aligned} \frac{\Delta S_a}{S_{a_t}} &= \frac{\Delta W}{W_t} \left\{ 1 + \frac{D}{F-D} + \frac{h_v}{h_v + 50} \right\} - \frac{\Delta F}{F_t} \left\{ 1 + \frac{D}{F-D} \right\} \\ &- \frac{\Delta \sigma}{\sigma_t} \left\{ \frac{h_v}{h_v + 50} \right\} \end{aligned} \quad (6.317)$$

With the proposed constants

$$\frac{\Delta S}{S_{a_t}} = 2.3 \frac{\Delta W}{W_t} - \frac{\Delta \sigma}{\sigma_t} - 1.3 \frac{\Delta F}{F_t} \quad (6.318)$$

or alternatively
$$\frac{S_{a_s}}{S_{a_t}} = \left(\frac{W_s}{W_t} \right)^{2.3} \left(\frac{\sigma_s}{\sigma_t} \right) \left(\frac{F_s}{F_t} \right)^{-1.3} \quad (6.319)$$

and
$$\frac{\Delta S_a}{S_{a_t}} = 2.3 \frac{\Delta W}{W_t} - 0.7 \frac{\Delta \sigma}{\sigma_t} - 1.6 \frac{\Delta F}{F_t} \quad (6.320)$$

or alternatively
$$\frac{S_{a_s}}{S_{a_t}} = \left(\frac{W_s}{W_t} \right)^{2.3} \left(\frac{\sigma_s}{\sigma_t} \right)^{-0.7} \left(\frac{F_s}{F_t} \right)^{-1.6} \quad (6.321)$$

for light airplanes

$$\frac{\Delta S_a}{S_{a_t}} = 2.0 \frac{\Delta W}{W_t} - 0.4 \frac{\Delta \sigma}{\sigma_t} - 1.6 \frac{\Delta F}{F_t} \quad (6.322)$$

For moderate corrections either type of equation is satisfactory, but if the corrections are large (for example, $|\Delta S/S| < 0.2$) the exponential forms will be appreciably more accurate.

Propeller Thrust Corrections:

For fixed pitch propellers,

$$\frac{\Delta F}{F_t} = 1.1 \frac{\Delta \sigma}{\sigma_t} - 0.1 \frac{\Delta W}{W_t} \quad (6.323)$$

at constant engine speed

$$\frac{\Delta P}{P_t} = 1.1 \frac{\Delta \sigma}{\sigma_t} + 0.4 \frac{\Delta T_a}{T_{a_t}} - 0.1 \frac{\Delta V}{V_t} \quad (6.324)$$

at full throttle

While for constant speed propellers

$$\frac{\Delta P}{P_t} = 0.7 \frac{\Delta P}{P_t} + 0.5 \frac{\Delta \sigma}{\sigma_t} - 0.5 \frac{\Delta H}{H_t} - 0.2 \frac{\Delta V}{V_t} \quad (6.325)$$

Take-Off and Air Distance Corrections for Fixed Pitch Propellers: Corrections may be required at constant engine speed or at full throttle.

At constant engine speed

$$\frac{\Delta S_E}{S_{E_t}} = 2.4 \frac{\Delta V}{V_t} - 2.4 \frac{\Delta \sigma}{\sigma_t} \quad (6.326)$$

and

$$\frac{\Delta S_a}{S_{a_t}} = 2.2 \frac{\Delta V}{V_t} - 2.2 \frac{\Delta \sigma}{\sigma_t} \quad (6.327)$$

If $\Delta S/S$ is numerically large, it is again preferable to use the exponential forms

$$\frac{S_{E_a}}{S_{E_t}} = \left(\frac{V_a}{V_t} \right)^{2.4} \left(\frac{\sigma_a}{\sigma_t} \right)^{-2.4} \quad (6.328)$$

and

$$\frac{S_{a_a}}{S_{a_t}} = \left(\frac{V_a}{V_t} \right)^{2.2} \left(\frac{\sigma_a}{\sigma_t} \right)^{-2.2} \quad (6.329)$$

At full throttle there will be a correction to engine speed

$$\frac{\Delta S_E}{S_{E_t}} = 2.4 \frac{\Delta V}{V_t} - 2.4 \frac{\Delta \sigma}{\sigma_t} + 0.5 \frac{\Delta T_a}{T_{a_t}} \quad (6.330)$$

and

$$\frac{\Delta S_g}{S_{gt}} = 2.2 \frac{\Delta V}{V_t} - 2.2 \frac{\Delta \sigma}{\sigma_t} + 0.6 \frac{\Delta T_a}{T_{at}} \quad (6.331)$$

with the corresponding exponential forms

$$\frac{S_{gs}}{S_{gt}} = \left(\frac{V_g}{V_t} \right)^{2.4} \left(\frac{\sigma_g}{\sigma_t} \right)^{-2.4} \left(\frac{T_{ag}}{T_{at}} \right)^{0.5} \quad (6.332)$$

$$\frac{S_{as}}{S_{at}} = \left(\frac{V_g}{V_t} \right)^{2.2} \left(\frac{\sigma_g}{\sigma_t} \right)^{-2.2} \left(\frac{T_{ag}}{T_{at}} \right)^{0.6} \quad (6.333)$$

Constant Speed Propellers: This section applies to airplanes which are entirely, or almost entirely, propeller driven at take-off. For the ground roll,

$$\frac{\Delta S_g}{S_{gt}} = 2.6 \frac{\Delta V}{V_t} - 1.7 \frac{\Delta \sigma}{\sigma_t} - 0.7 \frac{\Delta H}{H_t} - 0.9 \frac{\Delta P}{P_t} \quad (6.334)$$

and the alternative form

$$\frac{S_{gs}}{S_{gt}} = \left(\frac{V_g}{V_t} \right)^{2.6} \left(\frac{\sigma_g}{\sigma_t} \right)^{-1.7} \left(\frac{H_g}{H_t} \right)^{-0.7} \left(\frac{P_g}{P_t} \right)^{-0.9} \quad (6.335)$$

For the air phase, distinguish between light and heavy airplanes. For light airplanes use,

$$\frac{\Delta S_a}{S_{at}} = 2.3 \frac{\Delta V}{V_t} - 1.2 \frac{\Delta \sigma}{\sigma_t} - 0.8 \frac{\Delta H}{H_t} - 1.1 \frac{\Delta P}{P_t} \quad (6.336)$$

or alternatively

$$\frac{S_{as}}{S_{at}} = \left(\frac{V_g}{V_t} \right)^{2.3} \left(\frac{\sigma_g}{\sigma_t} \right)^{-1.2} \left(\frac{H_g}{H_t} \right)^{-0.8} \left(\frac{P_g}{P_t} \right)^{-1.1} \quad (6.337)$$

For heavy airplanes in the air phase, use,

$$\frac{\Delta S_a}{S_{at}} = 2.6 \frac{\Delta W}{W_t} - 1.5 \frac{\Delta \sigma}{\sigma_t} - 0.8 \frac{\Delta N}{N_t} - 1.1 \frac{\Delta \text{BHP}}{\text{BHP}_t} \quad (6.338)$$

or alternatively

$$\frac{S_{as}}{S_{at}} = \left(\frac{W_s}{W_t} \right)^{2.6} \left(\frac{\sigma_s}{\sigma_t} \right)^{-1.5} \left(\frac{N_s}{N_t} \right)^{-0.8} \left(\frac{\text{BHP}_s}{\text{BHP}_t} \right)^{-1.1} \quad (6.339)$$

Thrust Corrections for Turbo Propellers: The general case equations 6.318 or 6.320 or their alternates, may be used for turbo propeller airplanes.

The thrust correction is given by

$$\frac{\Delta F}{F_t} = \frac{\Delta F_j}{F_t} + \left(1 - \frac{F_j}{F_t} \right) \frac{\Delta F_p}{F_{Pt}} \quad (6.340)$$

where: $F_t = F_{jt} + F_{Pt}$

and estimate $\Delta F_p/F_{Pt}$ by equation 6.325.

$$\frac{\Delta F_p}{F_{Pt}} = 0.7 \frac{\Delta \text{BHP}}{\text{BHP}_t} + 0.5 \frac{\Delta \sigma}{\sigma_t} + 0.5 \frac{\Delta N}{N_t} - 0.2 \frac{\Delta W}{W_t} \quad (6.325)$$

Generally for turbo propeller aircraft $\frac{\Delta F_j}{F_t}$ is negligible and may be ignored. Then $\frac{\Delta F}{F_t} = \frac{\Delta F_p}{F_{Pt}}$

Part-Time Assistance: Again, equations 6.318 and 6.320 are used basically, but with an effective mean thrust. The consideration here is primarily JATO, but the method can be applied to other forms of thrust boost operated over a limited period.

The test effective, mean thrust boost F_{R_e} in either the ground roll or air phase given by equation 6.341.

$$F_{R_e} = \frac{S_R}{S} F_R \quad (6.341)$$

where

$$F_R = \text{JATO thrust}$$

S_R = distance covered in phase with JATO operating

S = total length of phase

The standard effective mean thrust in the air phase is either zero (ATO to cease at take-off) or equal to the actual ATO thrust (ATO to last to 50 ft.). The standard effective mean thrust in the ground roll, however, depends on the time, t_{a_s} , during which the ATO is to operate in the air phase under standard conditions.

$$t_{R_{a_s}} = 0 \quad \text{ATO ceasing at take-off}$$

$$t_{R_{a_s}} = 2S_{a_s} / (V_{s_{to}} + V_{s_{50}}) \quad \text{for ATO ceasing at 50 ft.} \quad (6.342)$$

Hence, if t_{at} was the test duration of the ATO in the air phase, the ATO duration in the ground roll must be corrected by

$$\Delta t_{R_G} = t_{R_{at}} - t_{R_{a_s}} \quad (6.343)$$

The correction to the air phase is then given by equation 6.320 using the total mean effective thrust. For the ground roll, however, use equation 6.344

$$\frac{\Delta S_R}{S_{Gt}} = \left[2.3 - \frac{2.3}{\frac{F_{tt}}{F_{R_0}} - 1.3} \right] \frac{\Delta V}{V_t} - \left[1 + \frac{0.7}{\frac{F_{tt}}{F_{R_0}} - 1.3} \right] \frac{\Delta \sigma}{\sigma_t} - \frac{1.3}{\frac{F_{tt}}{F_{R_0}} - 1.3} \frac{\Delta t_{R_G}}{t_{R_{Gt}}} - \left[1.3 + \frac{1.7}{\frac{F_{tt}}{F_{R_0}} - 1.3} \right] \frac{\Delta F_b}{F_{tt}} \quad (6.344)$$

where:

F_{tt} = test total thrust

F_b = basic engine thrust

The thrust terms in all the above equations are the thrusts obtained at mean take-off or air distance speeds unless otherwise defined.

SECTION 6.4

Landing Performance Tests and Corrections

Landing tests consist of a series of landings to determine the total distance required to pass over a 50 foot obstacle, touch down, and come to a complete stop. The aircraft should be operated in such a manner as to give the best landing performance within the operational limits of the airplane.

The gross weight for landing tests is usually the maximum load used in service; for heavily loaded aircraft it may be less one-half the fuel and less any dropable load. All tests will be run as close as possible to the desired gross weight, as weight corrections for landing roll have not been proved consistent. The aircraft landing configuration is normally with wing flaps full down, engine at idling rpm, and cowl flaps, when installed, full closed. Any special configuration for landing will be so stated. After the aircraft has touched down maximum braking power is applied without skidding.

The measurement of air and ground distance for landing is accomplished in the same manner as described for take-off tests. The observed landing time and distance data are plotted similarly to the observed take-off data. All landing performance data are corrected to standard conditions unless otherwise specified. The average of the best two of at least four landings is reported. As in take-offs, pilot technique is a large factor in determining landing performance. Approach technique and the use of brakes are extremely important in order to produce consistent results.

LANDING DATA CORRECTIONS

In converting the observed data to standard, sea level conditions, the wind corrections as used for take-off are again used. These are:

$$\text{ground roll corrected for wind} = \text{obs. ground roll} \left(\frac{V_{td} + V_w}{V_{td}} \right)^{1.85}$$

$$\text{air distance corrected for wind} = \text{obs. air distance} + V_w t$$

During the approach from the 50 foot obstacle to touch down, the aircraft has both potential and kinetic energy which must be dissipated prior to touch down. This may be expressed as,

$$\frac{W}{g} \left(\frac{V_{50}^2}{2} - \frac{V_{td}^2}{2} \right) + 50 W = FS' \quad (6.401)$$

where:

- F = retarding force acting over the air distance S'
- V₅₀ = true speed at 50 foot height
- V_{td} = true speed at touch down

Solving for air distance,

$$S' = \frac{W}{F} \left(\frac{V_{50}^2 - V_{td}^2}{2g} + 50 \right) \quad (6.402)$$

The term W/F is actually an average ratio of lift to drag during the descent. Due to ground effect and transition from glide to flare out, the value of L/D is difficult to obtain, and it must be assumed to be constant for all weight and density conditions. The difference in the velocities V_{50} and V_{td} may be said to be negligible between test and standard conditions. Therefore, it is seen that the test air distance equals the standard air distance, except for the effects of wind, and the final expression for correcting air distance during landing is given as,

$$S'_{lt} = S'_{ltw} + V_w t \quad (6.403)$$

where:

- S'_{lt} = landing air distance from a 50 foot obstacle, zero wind, ft.
- S'_{ltw} = test landing air distance from a 50 foot obstacle, with wind component, ft.
- V_w = wind component, ft/sec
- t = time, sec

For the landing ground roll, the ground distance may be given as:

$$S = \int_{V_{td}}^0 \frac{V}{a} dV \quad (6.404)$$

Using an average deceleration during ground roll, this expression may be simplified by integration to the following form:

$$S = \frac{V_{td}^2}{-2a} \quad (6.405)$$

where:

$-a$ = deceleration

Assuming for constant test and standard day touch down true speeds that the change in C_L at standard and observed conditions is negligible, equation 6.405 may be standardized in the same manner as the take-off equation. The final expression for landing ground roll is,

$$S_{ls} = S_{ltw} \left(\frac{V_{td} + V_w}{V_{td}} \right)^{1.85} \left(\frac{W_s}{W_t} \right)^2 \left(\frac{\sigma_t}{\sigma_s} \right) \quad (6.406)$$

where:

- S_{ls} = standard landing ground distance
- S_{ltw} = test landing ground distance with wind component

and the total landing distance is then,

$$\text{Total } S'_{ls} = (S'_{ltw} + V_w t) + S_{ltw} \left(\frac{V_{td} + V_w}{V_{td}} \right)^{1.85} \left(\frac{W_s}{W_t} \right)^2 \left(\frac{\sigma_t}{\sigma_s} \right) \quad (6.407)$$

From observation of data obtained during many landings, it has been found that the weight correction as shown in equation 6.407 is not reliable, and, in the event of a departure from standard weight during landings, no weight corrections have been found usable because of the many factors involved in landing technique; these factors are: approach speeds, flare-out pattern, application of brakes, etc. As a result, every effort is made to keep the test weight as close to the standard weight as possible, and the final usable equation for landing roll is,

$$\text{Total } S_{ls} = (S'_{ltw} + V_w t) + S_{ltw} \left(\frac{V_{td} + V_w}{V_{td}} \right)^{1.85} \left(\frac{\sigma_t}{\sigma_s} \right) \quad (6.408)$$

DATA REDUCTION OUTLINE (6.41)

For Landing Test Data

(1)	S'_{ltw}	ft	Observed ground roll, with wind component
(2)	V_{td}	ft/sec	Ground velocity at touch down, from slope of time-distance curve
(3)	V_w	ft/sec	Wind component along runway, from observed data; headwind (+), tailwind (-)
(4)	S_{lt}	ft	Test ground roll corrected for wind, (1) x $\left[\frac{(2) + (3)}{(2)} \right]^{1.85}$
(5)	P_a	"Hg	Test barometric pressure, from observed data
(6)	t_{at}	°C	Test ambient temperature, from observed data
(7)	σ_t		Test density ratio, $9.625 \times (5) + [273 + (6)]$
(8)	σ_s		Standard density ratio, from standard altitude tables and field elevation
(9)	σ_t/σ_s		(7) ÷ (8)
(10)	S_{ls}	ft	Standard ground roll for zero wind (4) x (9)
(11)	S'_{ltw}	ft	Observed air distance from 50 foot height, with wind component
(12)	t	sec	Time from 50 foot height to touch down
(13)	S'_{ls}	ft	Standard landing air distance from 50 foot height, for zero wind (11) + [(3) x (12)]
(14)	Total S_{ls}	ft	Total standard landing distance from 50 foot height for zero wind, (10) + (13)

SECTION 6.5

Dimensionless Parameters for Take-Off and Landing Performance Data

Application of dimensional analysis to take-off performance may sometimes assist the engineer by reducing the apparent number of independent variables and, more vitally, by associating variables such as air density which are out of his control in "non-dimensional" groups with controllable variables such as airplane gross weight and engine power or thrust.

The practical value of such an approach has not yet been assessed. It seems however, to be potentially valuable in certain cases. In particular, if the test values of the non-dimensional groups derived can be accurately controlled at the values corresponding to standard conditions the standardization process can thereby be almost eliminated. Otherwise, the main attraction of the approach would be to enable more efficient use of test data obtained under a wide range of test conditions, particularly when it is desired to predict from such tests the take-off performance under a wide range of standard conditions.

Many non-dimensional groups can usually be made up in any one problem. Those given below are useful, but may be modified if circumstances so demand.

RECIPROCATING ENGINE AIRCRAFT

The functional relations between the ground roll and the independent variables for an airplane in a given configuration may be written in the following form, among others:

$$S_g = f_1(\text{BEP}, N, \rho, W, V_{t_1}, \mu, g) \quad (6.501)$$

where:

S_g = ground roll

A = some fixed area of the airplane

W = gross weight

N = engine speed

V_{t_1} = true speed at unstick

μ = coefficient of friction (with ground)

Similarly we can write for the total distance to reach a height "h".

$$S_t = f_2(\text{BEP}, N, \rho, W, V_{t_1}, V_{t_2}, \mu, g, h) \quad (6.502)$$

where V_{t_2} is the true speed at the height "h".

By application of dimensional analysis to the above functional relations we may deduce that

$$\frac{s_g}{\sqrt{A}} = \phi_1 \left(\frac{BHP \sqrt{A} \rho}{W \sqrt{W}}, \frac{NA^{\frac{1}{2}}}{\sqrt{g}}, v_{t1} \sqrt{\frac{\rho A}{W}}, \frac{g \rho}{W} \sqrt{A}, \mu \right) \quad (6.503)$$

$$\frac{s_t}{\sqrt{A}} = \phi_2 \left(\frac{BHP \sqrt{A} \rho}{W \sqrt{W}}, \frac{NA^{\frac{1}{2}}}{\sqrt{g}}, v_{t1} \sqrt{\frac{\rho A}{W}}, v_{t2} \sqrt{\frac{\rho A}{W}}, \frac{g \rho}{W}, \sqrt{A}, \mu, \frac{h}{\sqrt{A}} \right) \quad (6.504)$$

In any particular case we may omit "A" and also, for a given system of units, "g". We may also substitute σ for ρ and, for normal runway surfaces, omit μ . We then have for the ground roll,

$$s_g = \gamma_1 \left(\frac{BHP \sqrt{\sigma}}{W \sqrt{W}}, N, \frac{v_{t1} \sqrt{\sigma}}{\sqrt{W}}, \frac{\sigma}{W} \right) \quad (6.505)$$

and hence

$$s_g = \gamma_1 \left(\frac{BHP}{W}, N, \frac{v_{t1} \sqrt{\sigma}}{\sqrt{W}}, \frac{\sigma}{W} \right) \quad (6.506)$$

since $\frac{BHP \sqrt{\sigma}}{W \sqrt{W}}$ is proportional to $\frac{BHP}{W}$ at given σ/W

The term in v_{t1} is proportional to $C_L^{-\frac{1}{2}}$ and will therefore be approximately constant for a given level of piloting skill or of risk. (Changes in available C_L due to change of slipstream intensity may be ignored for moderate ranges of W). If its test range is not large the v_{t1} product may be omitted and its effects treated as scatter. Otherwise, it may be necessary to attempt to cross plot in terms of it.

From inspection of equation (6.506) it will be readily appreciated that if the tests can be made at the values of σ/W , N and BHP/W which correspond to standard conditions the ground roll will be equal to the standard ground roll for the same value of the take-off lift coefficient. No standardization of the observed ground roll is required. Alternatively, test ground rolls for a range of BHP/W and σ/W might be plotted against these variables and the ground roll at any desired combinations of power, density and gross weight deduced.

A similar consideration of the total distance to height "h" shows that for the particular case of the distance to 50 ft. we may write,

$$s_t = \gamma_2 \left(\frac{BHP}{W}, N, \frac{v_{t1} \sqrt{\sigma}}{\sqrt{W}}, \frac{v_{t2} \sqrt{\sigma}}{\sqrt{W}}, \frac{\sigma}{W} \right) \quad (6.507)$$

In this case the variable $\frac{V_{t1}\sqrt{\sigma}}{\sqrt{W}}$ will usually be relatively unimportant and may be omitted. The expression $V_{t2}\sqrt{\frac{\sigma}{W}}$ is a function only of the lift coefficient at 50 ft, and will be assumed constant between test and standard conditions for a given level of skill and risk. As with the ground roll, the expression would be ignored unless its variation from test to test was so large as to make cross plotting desirable.

AIRCRAFT WITH TURBO-JET OR MIXED SYSTEMS

A similar approach may be adopted for airplanes with turbo-jet engines or any propulsive system which operates throughout the take-off. If, instead of defining the performance of the propulsive system by the variables BHP, N and ρ , we write in only the net thrust F_N we may deduce the more general relations,

$$S_g = \psi_3 \left(\frac{F_N}{W}, \frac{V_{t1}\sqrt{\sigma}}{\sqrt{W}}, \frac{\sigma}{W} \right) \quad (6.508)$$

$$\text{and } S_t = \psi_4 \left(\frac{F_N}{W}, \frac{V_{t1}\sqrt{\sigma}}{\sqrt{W}}, \frac{V_{t2}\sqrt{\sigma}}{\sqrt{W}}, \frac{\sigma}{W} \right) \quad (6.509)$$

As with the reciprocating engined airplane the expressions containing V_{t1} and V_{t2} will usually be ignored and their effects treated as scatter. If, then, the tests can be made at the values of F_N/W and σ/W which correspond to standard conditions no further standardization is necessary. Alternatively, a plot of take-off distance against these groups would yield the take-off distances for any desired combination of F_N , W and σ within the experimental range of F_N/W and σ/W . For example, take-off distances at moderate weight and high altitude may be deduced from tests made at a high gross weight at low altitude (high density) with a suitable thrust.

Alternative relations which may sometimes be more convenient may be obtained by including ambient air pressure and temperature as independent variables instead of air density only. This would normally increase the resultant number of non-dimensional groups, but in this case it can be shown that one group is negligible. If we start with the relations,

$$S_g = f_5(F_N, W, P_a, T_a, V_{t1}, \mu, \epsilon, \Delta) \quad (6.510)$$

$$\text{and } S_t = f_6(F_N, W, P_a, T_a, V_{t1}, V_{t2}, \mu, \epsilon, \Delta, h) \quad (6.511)$$

it can be deduced from dimensional analysis that

$$\frac{S_g}{T_a} = \phi_5 \left(\frac{F_N}{AP_a}, \frac{W}{AP_a}, V_{t1} \sqrt{\frac{AP_a}{WT_a}}, \mu, \frac{\Delta}{T_a^2} \right) \quad (6.512)$$

and

$$\frac{S_t}{T_a} = \psi_6 \left(\frac{F_N}{AP_a}, \frac{W}{AP_a}, v_{t1} \sqrt{\frac{AP_a}{WT_a}}, v_{t2} \sqrt{\frac{AP_a}{WT_a}}, \mu, \frac{Aa^2}{T_a}, \frac{gh}{T_a} \right) \quad (6.513)$$

As before, we may now omit ϵ , A and μ , so deducing the relations

$$\frac{S_k}{T_a} = \psi_5 \left(\frac{F_N}{P_a}, \frac{W}{P_a}, v_{t1} \sqrt{\frac{\sigma}{W}}, T_a \right) \quad (6.514)$$

$$\frac{S_t}{T_a} = \psi_6 \left(\frac{F_N}{P_a}, \frac{W}{P_a}, v_{t1} \sqrt{\frac{\sigma}{W}}, v_{t2} \sqrt{\frac{\sigma}{W}}, T_a, \frac{h}{T_a} \right) \quad (6.515)$$

We thus have the very inconvenient variable T_a left uncombined with any controllable variable. If a dynamical analysis is made at this point, however, it can be shown with the above choice of variables T_a may be omitted. (This happens because P_a and T_a do not in fact affect take-off entirely independently but only through their ratio P_a/T_a — i.e., the density. They were introduced as independent variables only to produce the groups F_N/P_a and W/P_a). We thus have,

$$\frac{S_k}{T_a} = \psi_7 \left(\frac{F_N}{P_a}, \frac{W}{P_a}, v_{t1} \sqrt{\frac{\sigma}{W}} \right) \quad (6.516)$$

$$\text{and } \frac{S_t}{T_a} = \psi_8 \left(\frac{F_N}{P_a}, \frac{W}{P_a}, v_{t1} \sqrt{\frac{\sigma}{W}}, v_{t2} \sqrt{\frac{\sigma}{W}} \right) \quad (6.517)$$

where S_t is the distance required to reach a height equal to the value of h/T_a under standard conditions, is a height $h \times T_{a_s}/T_{a_t}$ where suffices s and t indicate standard and test conditions respectively. These equations are sometimes more convenient as F_N/P_a is usually independent of air temperature and W/P_a is more readily controlled than σ/W .

CHAPTER SEVEN

HELICOPTER FLIGHT TEST PERFORMANCE AND ANALYSIS

SECTION 7.1

Introduction

The flight testing techniques and performance data analysis methods for helicopter aircraft are still in the research and development stage. The many peculiarities of helicopter design and flight performance characteristics present difficult analytical problems in both performance standardization and instrumentation requirements. The problems of performance weight correction and accurate low, or zero, speed determination have not been solved in any simplified manner. Although the unstable flying characteristics of the helicopter may be corrected by future development, at present they present a very difficult flying task to the test pilot who seeks to obtain high quality test data.

The ability of the helicopter to move in any direction relative to its three axes presents a major control problem when stabilized flight in a certain direction is required. Although the helicopter can hover motionless at any altitude below the hovering ceiling, the determination of the true hovering condition is not possible without elaborate and ingenious devices for determining zero air speed. It might appear that, because this type aircraft is capable of maintaining stabilized flight between zero and maximum air speed, there would be no problems of stalling as are encountered in conventional aircraft. Actually, because the individual rotor blades are airfoils, a stall condition can occur on the blades individually or as a group, and this stall can be effective in limiting performance at any speed from zero to maximum. Blade stall is an important performance criterion, as it is accompanied by excessive power requirements and weight limitations at both high and low forward speeds. In addition, at high forward speeds the blade stall is more pronounced in the retreating portion of the rotor disk area. This may result in vibration and excessive control instability in addition to the increased power demands.

The basic aerodynamic analysis for the helicopter is essentially that of the conventional propeller or airscrew. In the helicopter, suitable mechanical devices allow part of the rotor thrust to act as a horizontal component which balances the fuselage drag and propels the aircraft. The remaining rotor thrust sustains the helicopter or provides enough thrust for vertical motion upwards. Part of the total power output of the engine is also used to overcome blade drag and gear losses and to provide directional control. Figure 7.11 illustrates the rotor thrust components.

The many aerodynamic factors involved in the performance of a helicopter rotor or system of rotors have conflicting effects on optimum performance; that which serves best for the hovering condition may detract from the high forward speed performance. A particular aircraft may be the result of many aerodynamic compromises that were made to obtain optimum overall performance. Generally these compromises are made, not in the variable factors that are of interest in flight performance analysis, but in some of the aerodynamic constants such as

the rotor configuration, the rotor area, the rotor solidity factor (blade area/ rotor area), and the blade twist or shape. Flight tests may be required to evaluate various configurations of these items, but they are not flight variables in themselves. As with conventional aircraft, the helicopter performance presentation should include the standard speed-power, rate of climb and descent, range, hovering performance and rotor efficiency for various gross weights and configurations of the particular design being tested.

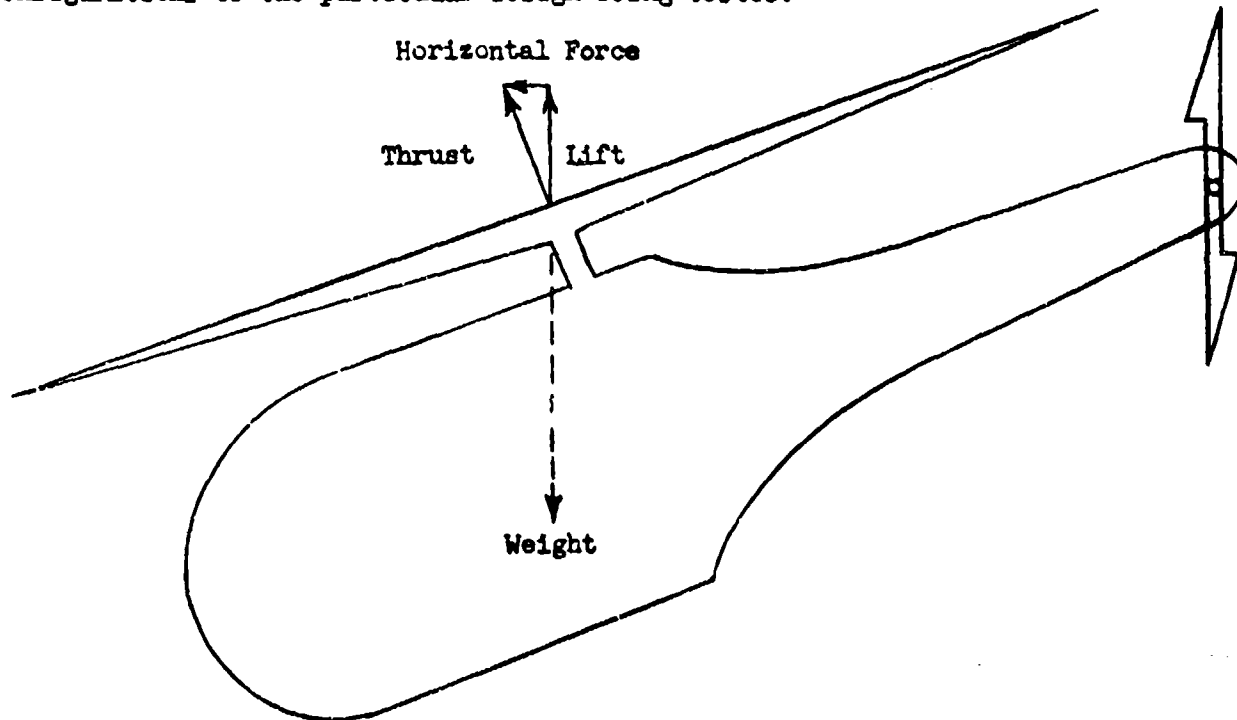


Figure 7.11
Simplified Sketch of Helicopter Thrust
and Lift Components

It should be noted here that theoretical studies and flight tests indicate that the most efficient level flight and hovering performance will be obtained by varying rotor rpm or tip speed. The most efficient rpm at high flight speed is greater than the most efficient rpm at low flight speed and hovering. Actually, it appears that future helicopters may have two rotor gear ratios, one giving a high rotor rpm for high-speed forward flight and one giving a lower rotor rpm at maximum engine power for hovering and low-speed forward flight. This factor will not complicate data reduction or presentation, because for most efficient operation, each of the two rotor rpm may be restricted to separate forward speed ranges and data may be plotted for a constant rotor rpm in each of these ranges.

SECTION 7.2

Level Flight Performance

The helicopter performance parameters are restricted herein to the density altitude method of data reduction and presentation. This is a result of the requirement for a rotor speed variable. If atmospheric pressure and temperature are separated, as is done in the pressure altitude approach, the level flight performance must be represented by four parameters and cannot easily be dealt with graphically.

Extensive analytical methods using the vortex theory and the blade element theory as applied to propellers can be used to determine the many design characteristics for helicopter rotors. The necessary flight performance parameters are more simply derived by the use of dimensional analysis. For the density altitude system the nondimensional functional equation is,

$$\text{BHP} = f(W, V_t, V_b, \rho, A) \quad (7.201)$$

where:

BHP = rotor shaft brake horsepower
 W = gross weight
 V_t = true horizontal speed
 V_b = rotor tip speed or rpm
 ρ = air density
 A = rotor disk area

From equation 7.201 two basic sets of parameters are derived by dimensional analysis.

$$\frac{\text{BHP}}{A \rho V_b^3} = f \left[\frac{W}{A \rho V_b^2}, \frac{V_t}{V_b} \right] \quad (7.202)$$

$$\frac{\text{BHP} (A \rho)^{\frac{1}{2}}}{(W)^{3/2}} = f \left[V_t \left(\frac{\rho A}{W} \right)^{\frac{1}{2}}, V_b \left(\frac{\rho A}{W} \right)^{\frac{1}{2}} \right] \quad (7.203)$$

These parameters are referred to as:

$$\frac{\text{BHP}}{A \rho V_b^3} = C_p, \text{ power coefficient}$$

$$\frac{W}{A \rho V_b^2} = C_T, \text{ thrust coefficient (a function of the average } C_L \text{ for the individual rotor blades)}$$

$$\frac{\text{BHP} (A \rho)^{\frac{1}{2}}}{W^{3/2}} = \text{power efficiency parameter}$$

$$\frac{V_t}{V_b} = \mu, \text{ tip speed ratio}$$

$$v_t \left(\frac{\rho A}{W} \right)^{\frac{1}{2}} = \text{speed parameter}$$

$$v_b \left(\frac{\rho A}{W} \right)^{\frac{1}{2}} = \frac{1}{C_T^{\frac{1}{2}}} = \text{rotor tip speed parameter}$$

Although BHP is defined as the horsepower delivered to the rotor, the engine BHP is used for performance work since power extraction for directional control does not vary much for given values of the various parameters.

Coefficient Type Performance Data

A typical plot of equation 7.202 is shown in Figure 7.21. It can be seen in this plot that as the values of C_T increase (increasing blade C_L) more power is required for a constant rotor tip speed. At a constant C_T the power required first decreases with forward speed and then increases at the higher forward speeds. This results from a slightly increasing rotor blade drag power with speed, a large reduction in power required to pull air through the rotor (induced power), and a large increase in fuselage drag power required with increasing forward speed. At high forward speeds the retreating rotor blades decrease their relative speed causing the blade C_L to increase momentarily; this can cause blade tip stall and result in rapidly increasing power requirements at high forward speeds. During hovering and low forward speeds, decreasing rotor tip speeds can mean a reduction in power required at increased values of C_p and C_T ; however, the extent of rotor tip speed reduction is limited by blade stall and reduction-gear power requirements.

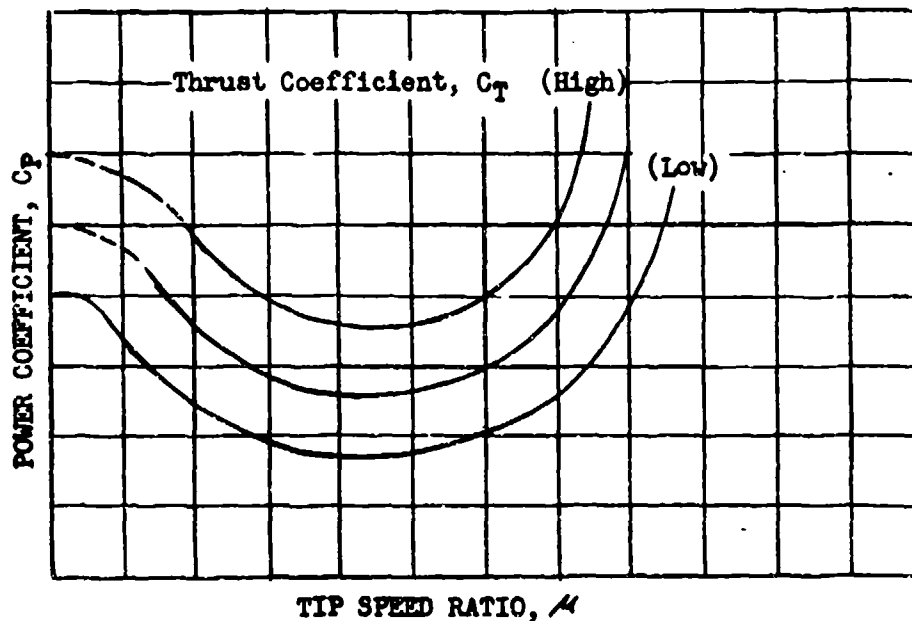


Figure 7.21
Typical Plot of the Coefficient Method of
Presenting Helicopter Level Flight Performance

One of the parameters in equation 7.202 must be held constant if data reduction is to be simplified. At constant rotor speeds, constant C_T values can be maintained during level flight power calibrations. This is done by using a chart of weight or fuel load vs density altitude for constant C_T values. This can also be done by flying at a constant value of W/δ_a as described in Section 4.9. Within an ambient temperature range of $\pm 3^\circ\text{C}$ the error introduced in C_T at constant W/δ_a will be only ± 1.0 percent.

For simplified reduction and presentation of data at a constant rotor rpm, equation 7.202 may be put in a dimensional form.

$$\frac{\text{BHP}}{\sigma} = f \left[\frac{W}{\sigma}, V_t \right] \quad (7.204)$$

A typical set of curves is shown in Figure 7.22. This plot gives sea level standard performance at a glance, and a complete set of faired curves can be easily converted to C_p , C_T , and μ values by use of the necessary sets of constants for the particular aircraft and values of BHP/σ , W/σ , and V_t from the faired curves.

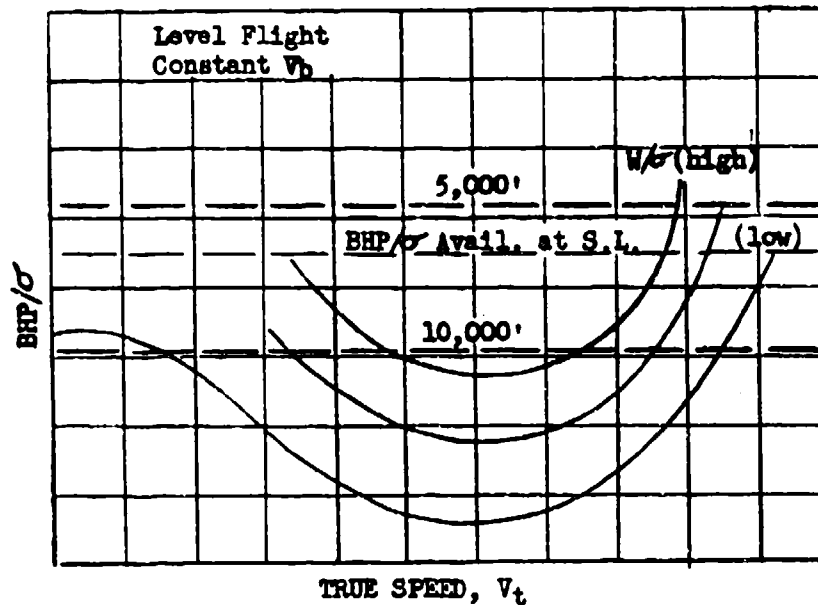


Figure 7.22
Typical Dimensional Presentation of Coefficient
Data at Constant Rotor Speed, Level Flight

If desired the term W/σ may be used in the form $\sigma W_g/W_t$. This allows power data for a constant rotor rpm to be directly interpreted in terms of density at standard weight, or weight ratio at sea level density. Paired data in this form can also be converted to C_T values by use of constants for the particular aircraft.

The dimensional plot of Figure 7.22 for a particular rotor rpm may be converted to that obtainable at another rotor rpm by these equalities:

$$\left(\frac{\text{BHP}}{\sigma}\right)_2 = \left(\frac{\text{BHP}}{\sigma}\right)_1 \left(\frac{v_{b2}}{v_{b1}}\right)^3$$

$$\left(\frac{W}{\sigma}\right)_2 = \left(\frac{W}{\sigma}\right)_1 \left(\frac{v_{b2}}{v_{b1}}\right)^2$$

$$v_{t2} = v_{t1} \left(\frac{v_{b2}}{v_{b1}}\right)$$

The important factor in these rotor rpm conversions is whether the reduced rotor rpm is also reduced engine rpm or if normal engine rpm and power may be maintained. Any rotor rpm extrapolations should be spot checked by actual flight tests.

The determination of test brake horsepower is easily accomplished if a torquemeter is installed on the engine. Usually this device is not available on helicopters and the engine manufacturer's power chart must be used. In many cases the power charts give very inaccurate results at altitude. If this appears to be the case, manifold pressure may be substituted for brake horsepower in data presentation like that of Figure 7.22. The ordinates would then be MP/σ and V_t . Obviously, manifold pressure should not be substituted in the power coefficient term.

POWER, FORWARD SPEED, AND ROTOR SPEED PARAMETER METHOD

For a particular helicopter, equation 7.203 may be put in a dimensional form:

$$\text{BHP } (\sigma)^{\frac{1}{2}} \left(\frac{W_g}{W_t}\right)^{3/2} = r \left[v_t (\sigma)^{\frac{1}{2}} \left(\frac{W_g}{W_t}\right)^{\frac{1}{2}}, v_b (\sigma)^{\frac{1}{2}} \left(\frac{W_g}{W_t}\right)^{\frac{1}{2}} \right] \quad (7.205)$$

where:

$W_g =$ some standard gross weight

The left side term in this equation is the effective power efficiency corresponding to the inverse of the figure of merit, M , the rotor efficiency. A typical plot of equation 7.205 as in Figure 7.23 shows the relative rotor efficiencies throughout the level flight range. Minimum values of the power

term correspond to maximum values of the figure of merit. The effect of reduced rotor rpm is also apparent on this plot; however, as mentioned before, the value of actual reduction of rotor rpm depends on its effect on the power output of the engine.

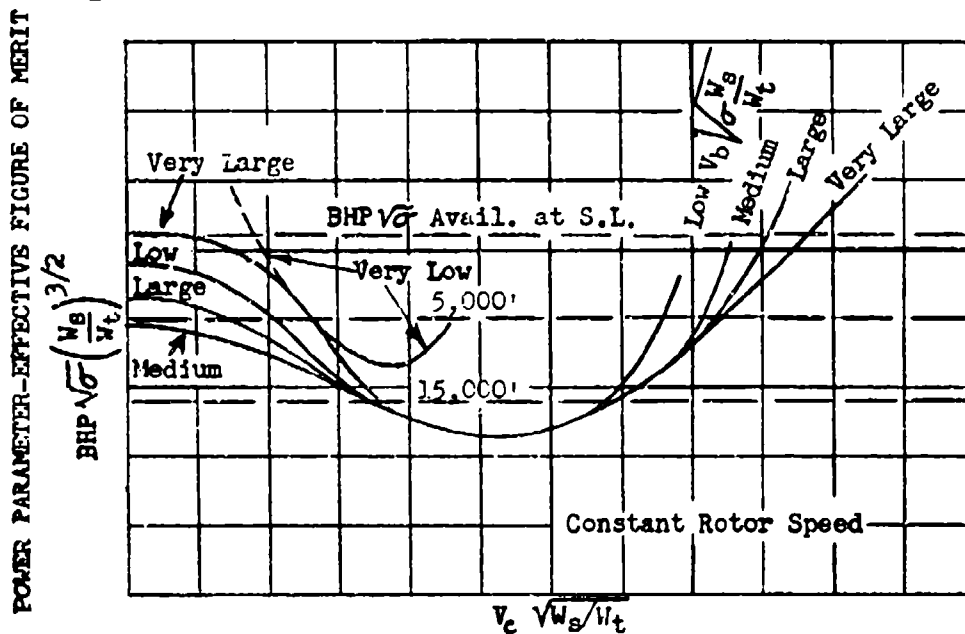


Figure 7.23
Typical Presentation of Level Flight Power,
Forward Speed, and Rotor Speed Data

For V_t equal to zero (hovering), equation 7.205 resolves into two parameters which are effectively the rotor efficiency, M , and $(C_T)^{1/2}$. It can be seen from the above plot that M is a function of C_T . The derivation of the figure of merit is discussed in the next section.

For flight at constant rotor rpm equation 7.205 may be plotted as in Figure 7.24. Here the parameter $(\sigma W_g/W_t)^{1/2}$ may be interpreted as $(W_g/W_t)^{1/2}$ for σ equal to 1.0, or as $(\sigma)^{1/2}$ for the standard weight, or as the percent of rated rotor rpm for standard sea level and weight conditions. If data are obtained at one rotor rpm it may be replotted for some other rotor rpm by using the equality:

$$\left(\sigma \frac{W_g}{W_t}\right)_2^{1/2} = \left(\sigma \frac{W_g}{W_t}\right)_1^{1/2} \left(\frac{v_{b1}}{v_{b2}}\right)$$

For the true speed and altitude ranges encountered by most helicopters, calibrated speed, V_c , may be substituted for the term $V_t \sqrt{\sigma}$. With the parameters of equation 7.205 a constant σ/W must be held during power calibrations. This is accomplished by the use of a density altitude-weight- C_T chart or a weight-pressure altitude- W/P_a chart as described previously.

POWER PARAMETER EFFECTIVE FIGURE OF MERIT

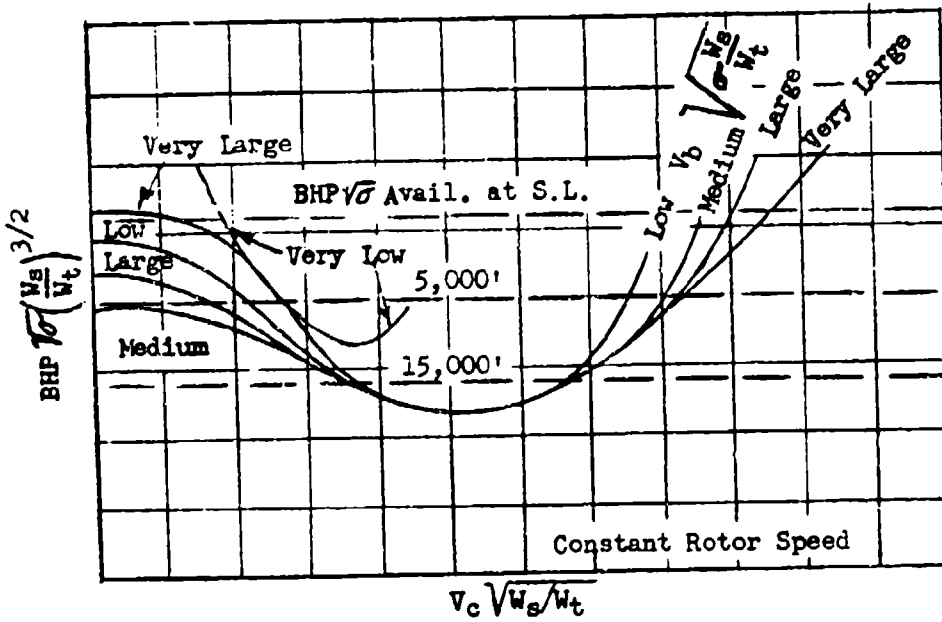


Figure 7.24
 Typical Presentation of Level Flight Power,
 Calibrated Speed, and Density Data

DATA REDUCTION OUTLINE (7.21)

Speed-Power or Speed-Manifold Pressure Plots for
Flight Test Data Obtained at Constant
 W/σ (C_T) and Constant Rotor Rpm

(1)	Test Point Number		
(2)	H_i	ft	Indicated pressure altitude
(3)	ΔH_{ic}	ft	Altimeter instrument correction
(4)	V_i	knots	Indicated air speed
(5)	ΔV_{ic}	knots	Air-speed instrument correction
(6)	ΔV_{pc}	knots	Air-speed position correction
(7)	V_c	knots	Calibrated air speed, (4)+(5)+(6)
(8)	ΔH_{pc}	ft	Altimeter position error correction
(9)	H_o	ft	True pressure altitude, (2)+(3)+(8)
(10)	t_i	$^{\circ}C$	Indicated ambient temperature
(11)	Δt_{ic}	$^{\circ}C$	Temperature instrument correction
(12)	t_{at}	$^{\circ}C$	Test ambient temperature, (10) + (11)
(13)	$1/\sqrt{\sigma}$		From (9) and (12) and CHART I-1
(14)	V_{tt}	knots	Test true speed, (7) x (13)
(15)	t_{ot}	$^{\circ}C$	Test carburetor temperature
(16)	t_{as}	$^{\circ}C$	Standard ambient temperature, from (9) and Table 9.2
(17)	$\sqrt{T_{as}/T_{ot}}$		$\sqrt{[(16) + 273] + [(15) + 273]}$
(18)	Engine rpm		
(19)	MP_t	"Hg	Test manifold pressure
(20)	BHP_o		Chart brake horsepower, from (9) and (18) and (19)
(21)	BHP_t		Test brake horsepower, (20) x (17)
(22)	W_t	lbs	Test aircraft weight
(23)	W_t/b	lbs	(22) x (13) ²
(24)	Plot (21) vs (14)		
(25)	t_{os}	$^{\circ}C$	Standard carburetor air temperature, (16) - (12) + (15)
(26)	$\sqrt{T_{ot}/T_{os}}$		$\sqrt{[(15) + 273] + [(25) + 273]}$
(27)	BHP_s		Standard brake horsepower, (21)x (26)
(28)	V_{ts}		Standard day true speed, from (27) and (24)
(29)	Plot (27) vs (28); this is the standard day speed power curve		

NOTE: If the manifold pressure-ambient pressure ratio exceeds 1.5, a correction to power and manifold pressure should be made.

If the chart power data is not reliable, plot (19) vs (14).

DATA REDUCTION OUTLINE (7.22)

For BHP/σ , V_t , W/σ Plot; Constant W/σ (C_T)
and Rotor Rpm Test Data

(This is a continuation of Data Reduction Outline 7.21)

- (24) BHP/σ (21) x (13)²
(25) Plot (24) vs (14)

Note: If the chart power data is not reliable, plot MP_t/σ vs V_{tt}

DATA REDUCTION OUTLINE (7.23)

For $BHP \sqrt{\sigma} (W_s/W_t)^{3/2}$, $V_c \sqrt{W_s/W_t}$, $\sqrt{\sigma W_s/W_t}$ Plot;
Constant W/σ (C_T) and Rotor Rpm Test Data

(This is a continuation of Data Reduction Outline 7.21)

- (24) W_s lbs Selected standard weight
(25) W_s/W_t Weight ratio, (24) ÷ (22)
(26) $\sqrt{W_s/W_t}$ $\sqrt{(25)}$
(27) $(W_s/W_t)^{3/2}$ (25) x (26)
(28) $BHP \sqrt{\sigma} (W_s/W_t)^{3/2}$ (21) x (27) ÷ (13)
(29) $V_c \sqrt{W_s/W_t}$ (7) x (26)
(30) Plot (28) vs (29)

Note: If the chart power data is not reliable, MP_t may be substituted for BHP_t .

DATA REDUCTION OUTLINE (7.24)

For C_p , C_T , M Plot; Constant W/σ (C_T) Flight Test Data

(This is a continuation of Data Reduction Outline 7.21)

- (24) D ft Rotor disk diameter
(25) A ft² Rotor area
(26) Rotor rpm
(27) V_b ft/sec Rotor tip speed, $0.0524 \times (24) \times (26)$
(28) $(V_b)^2$ (27)²
(29) $(V_b)^3$ (27)³
(30) $1/\sigma$ (13)²
(31) C_p Power coefficient, $[(21) \times (30) \times 231,300]$
 $+ [(25) \times (29)]$
(32) C_T Thrust coefficient, $[(23) \times 421] \div [(25) \times (28)]$
(33) M Tip speed ratio, $[(14) \times 1.69] \div (27)$
(34) Plot (31) vs (33) for constant C_T values.

SECTION 7.3

Rotor Thrust, Power, and Efficiency in Hovering Flight

The rotor air flow analysis is similar to that for the conventional propeller. The power required to hover is,

$$P = T V_r \quad (7.301)$$

where:

- P = power to the rotor
- T = thrust of the rotor
- V_r = air velocity through the rotor (induced velocity)

The thrust of the rotor is,

$$T = \rho A V_r V_d \quad (7.302)$$

where:

- A = rotor area
- V_d = downstream velocity given the air by the rotor

By using the actuator disk theory in which $V_r = \frac{1}{2} V_d$, the thrust of the rotor may be expressed also as,

$$T = 1/2 \rho A V_d^2 \quad (7.303)$$

From 7.302 and 7.303,

$$V_r = \left(\frac{T}{2 \rho A} \right)^{1/2} \quad (7.304)$$

From 7.304 and 7.301,

$$P = \frac{T^{3/2}}{(2 \rho A)^{1/2}} \quad (7.305)$$

The above equation assumes ideal inflow through the rotor disk and no power losses for control or other purposes.

Equation 7.305 is used to define the rotor efficiency, (M), or "figure of merit" as it is usually called.

$$M = \frac{.707 T^{3/2}}{550 \text{ BHP } (\rho A)^{1/2}} \quad (7.306)$$

where:

- .707 = $1/\sqrt{2}$, to make M_{max} equal unity
- BHP = brake horsepower to the rotor
- T = rotor thrust in hovering flight

Or, in terms of density ratio and weight, where the thrust equals the weight supported,

$$M = \frac{.0264 W^{3/2}}{\text{BHP} (\sigma A)^{1/2}} \quad (7.307)$$

The figure of merit is also defined by the rotor thrust coefficient, C_T , and the rotor power coefficient, C_p .

$$M = .707 \frac{C_T^{3/2}}{C_p} \quad (7.308)$$

where:

$$C_T = \frac{W}{A \rho v_b^2}$$

$$C_p = \frac{550 \text{ BHP}}{A \rho v_b^3}$$

v_b = rotor tip speed or rpm

As was shown in the previous section, the figure of merit is a function of the thrust coefficient and should be plotted as shown in Figure 7.31.

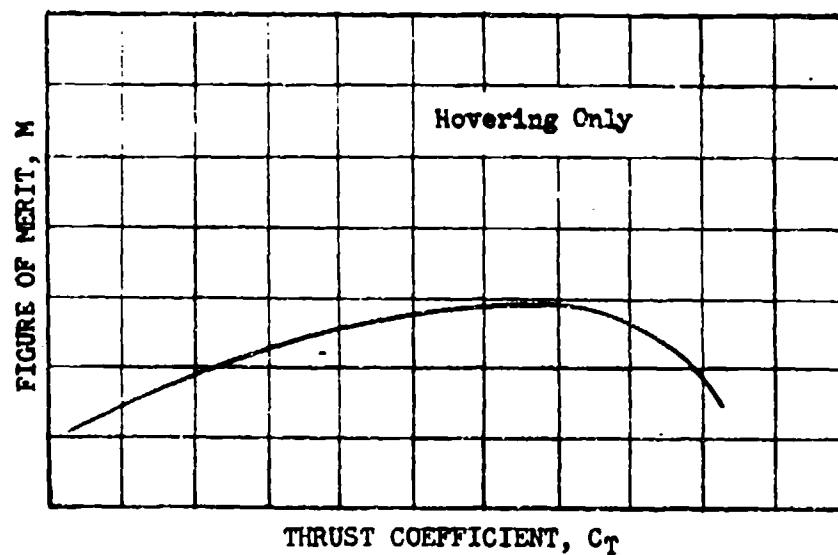


Figure 7.31
Typical Figure of Merit - Thrust Coefficient Plot

Equation 7.308 may be used to show graphically the figure of merit as in Figure 7.32.

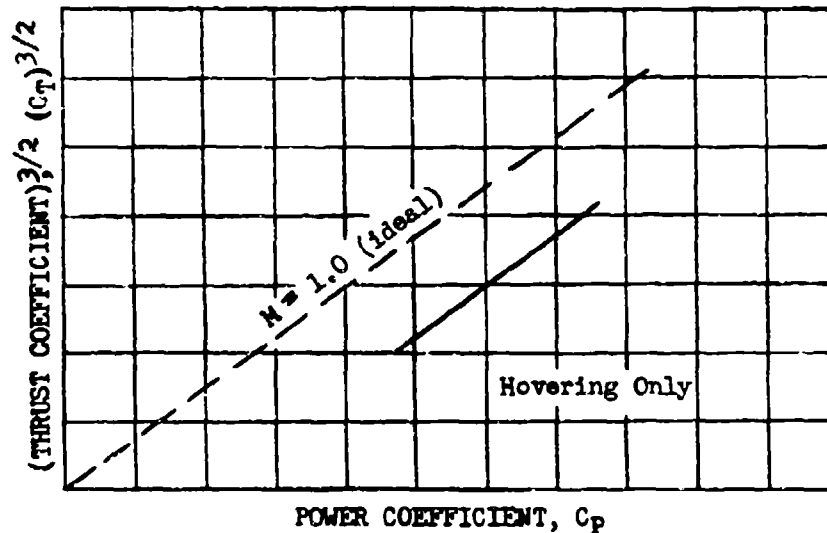


Figure 7.32
Typical Figure of Merit Comparison in Terms
of Thrust and Power Coefficients

This plot presumes a constant slope of M with C_T . This will be the case if the C_T range is limited. The same plot is shown in dimensional form for a particular helicopter and a constant rotor rpm in Figure 7.33. Data in this plot may be extrapolated to other rotor rpm by the equalities derived from equation 7.202,

$$\left(\frac{\text{BHP}}{\sigma}\right)_2 = \left(\frac{\text{BHP}}{\sigma}\right)_1 \left(\frac{v_{b2}}{v_{b1}}\right)^3, \quad \left(\frac{W_t/W_g}{\sigma}\right)_2^{3/2} = \left(\frac{W_t/W_g}{\sigma}\right)_1^{3/2} \left(\frac{v_{b2}}{v_{b1}}\right)^3$$

In Figure 7.34 is shown a method of plotting an effective figure of merit vs an effective rotor speed.

From Figure 7.34 the most efficient combinations of rotor speed and weight for a given $\text{BHP}\sqrt{\sigma}$ available can be determined. In this manner the hovering ceiling can also be determined for a particular set of conditions. Without gear shifting arrangements, a reduced rotor tip speed results in a reduced power. This must be included if data are extrapolated to lower rotor tip speeds. For single gear ratio helicopters an increased hovering performance (increased maximum payload) for decreased rotor speed is found to exist only at very low altitudes; and the hovering ceiling will be decreased materially at reduced rotor rpm.

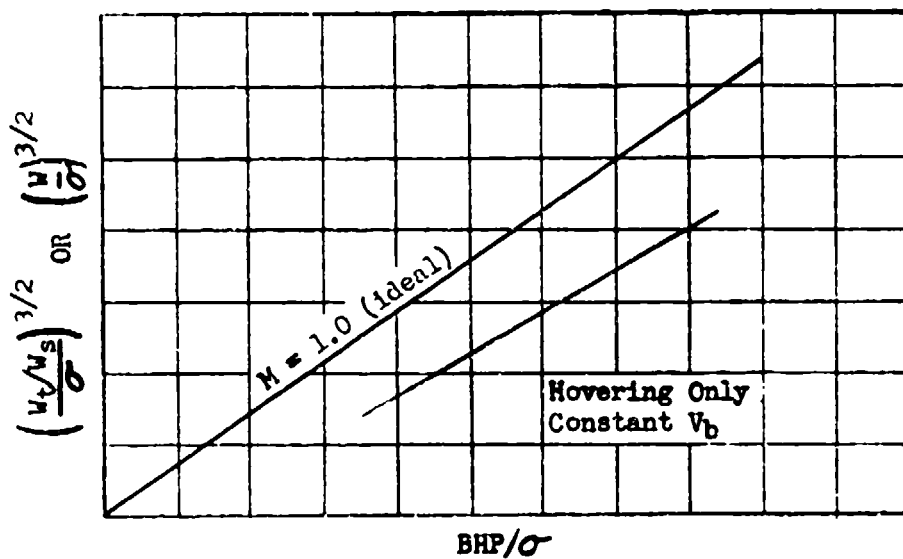


Figure 7.33
 Typical Effective Figure of Merit Comparison in
 Terms of Power, Weight, and Density

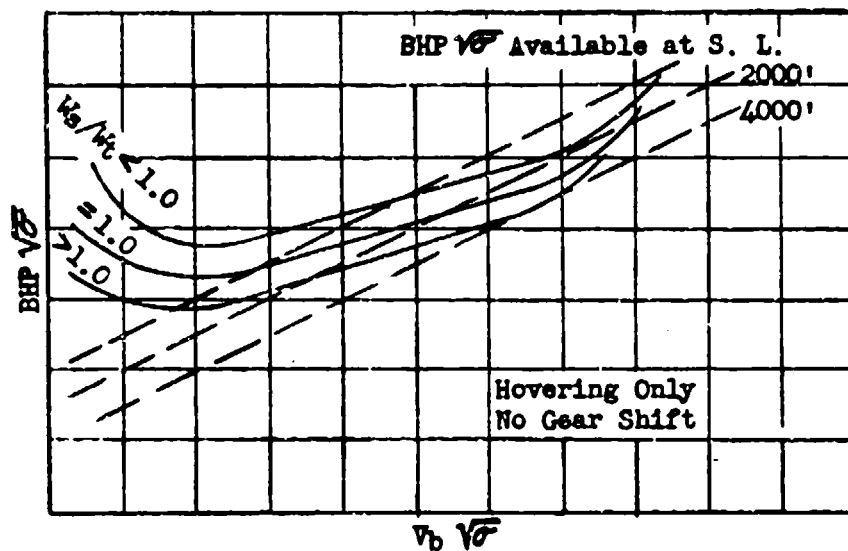


Figure 7.34
 Typical Effective Figure of Merit Plot in Terms
 of Power, Rotor Speed, and Density and Weight

Where maximum power is available in hovering, even when rotor speed is reduced by gearing, the weight limitations for any altitude and the hovering ceiling may be determined by plotting the effective figure of merit vs the effective weight ratio as in Figure 7.35. In this plot the dotted lines show the original data reduced to constant weights and density altitudes.

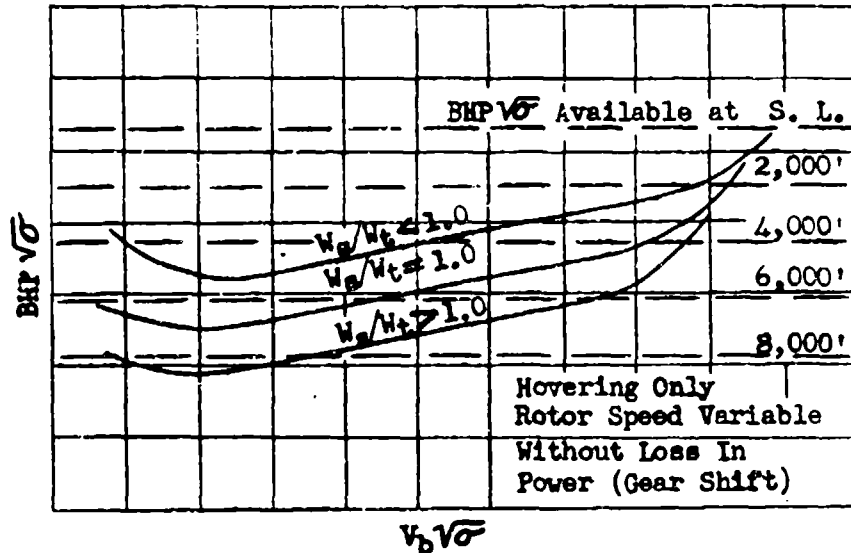


Figure 7.35
Typical Effective Figure of Merit Plot. in Terms
of Power, Rotor Speed, Density and Weight

When the helicopter is hovering above the ground at a height equivalent to about one rotor diameter a positive thrust increment is developed by the pressure field between the ground and the rotor. This so called "ground effect" has a noticeable influence on the take-off performance and acts as a cushion during landings. The ground effect actually increases the rotor efficiency relative to the rotor efficiency obtained when the aircraft is out of the ground effect. This relative efficiency increase can be shown by either of the plots illustrated in Figure 7.36.

If the slope of the rotor efficiency curve is nearly zero with respect to thrust coefficient or effective rotor speed, the ground effect hovering may be plotted as in Figure 7.37(a); if the slope is other than nearly zero a plot such as 7.27(b) must be used.

Determination of the true hovering condition is not easily done by use of present air-speed indicators. Near the ground a good reference for the pilot is the ground itself, but the tests must be conducted during low or zero wind conditions. At altitude or in appreciable winds the hovering condition can be determined by use of a long weighted cord attached to the fuselage. When the weighted cord hangs straight down from the helicopter, the aircraft is stationary with respect to the air mass in which it is flying. The weighted cord may be indexed to indicate the true hovering height during low altitude tests.

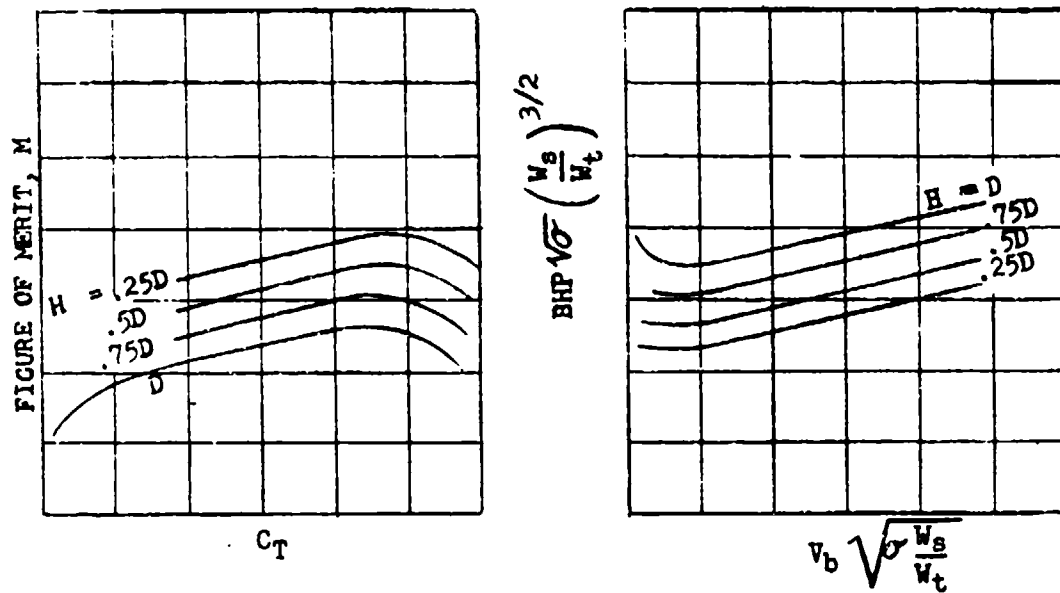


Figure 7.36
Method of Showing Ground Effect on Hovering Performance

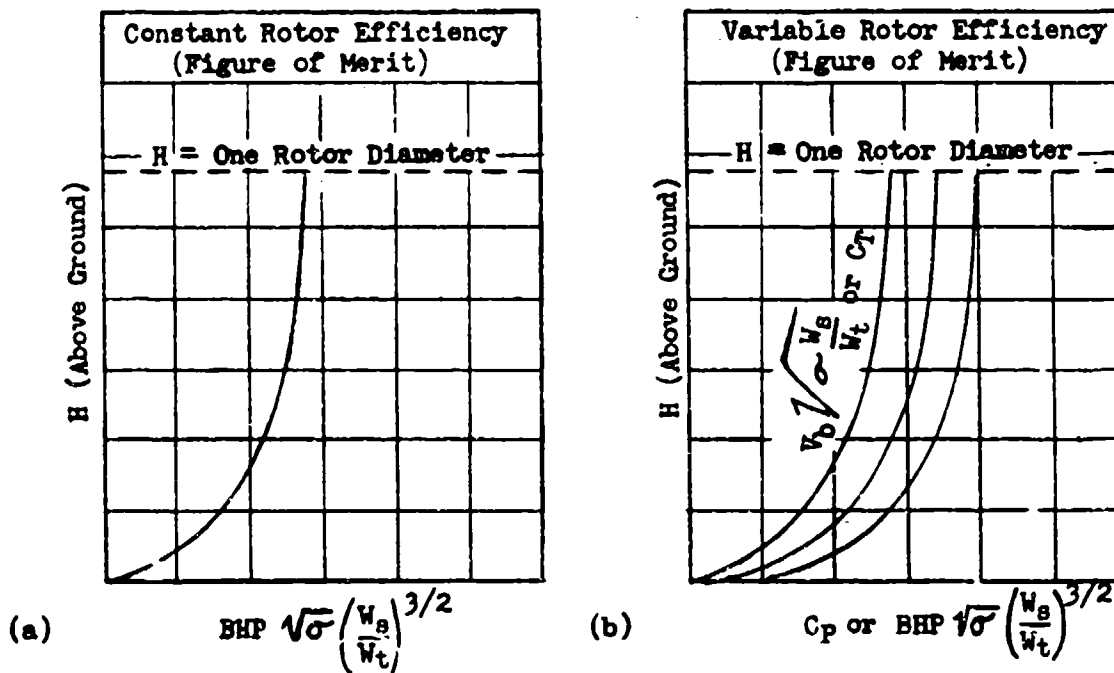


Figure 7.37
Method of Showing Ground Effect on Hovering Performance

DATA REDUCTION OUTLINE (7.31)

For $BHP \sqrt{\sigma} (W_s/W_t)^{3/2}$ vs $V_b \sqrt{\sigma} W_s/W_t$ Plot, and M vs C_T Plot; Constant or Variable Rotor Rpm Test Data

(1)	Test Point Number		
(2)	H_i	ft	Indicated pressure altitude
(3)	ΔH_{1c}	ft	Altimeter instrument correction
(4)	ΔH_{pc}	ft	Altimeter position error
(5)	H_o	ft	True pressure altitude, (2) + (3) + (4)
NOTE: If a tapeline is used to record height above the ground for low level work it may be used with the ground pressure altitude to obtain true pressure altitude.			
(6)	t_i	°C	Indicated ambient temperature
(7)	Δt_{1c}	°C	Temperature instrument correction
(8)	t_{at}	°C	Test ambient temperature, (6) + (7)
(9)	$1/\sqrt{\sigma}$		From (8) and (5) and CHART I-1
(10)	σ		From (8) and (5) and CHART I-1
(11)	t_{ct}	°C	Test carburetor temperature
(12)	t_{as}	°C	Standard ambient temperature, from (5) and Table 9.2
(13)	$\sqrt{T_{as}/T_{ot}}$		$\sqrt{[(12) + 273]} \div [(11) + 273]$
(14)	Engine rpm		
(15)	MP_t	"Hg	Test manifold pressure
(16)	BHP_o		Chart brake horsepower, from (5) and (14) and (15)
(17)	BHP_t		Test brake horsepower, (16) x (13)
(18)	W_t	lbs	Test aircraft weight
(19)	$(W_t)^{3/2}$		$(18)^{3/2}$
(20)	W	lbs	Standard aircraft weight
(21)	W_s/W_t		$(20) \div (18)$
(22)	$\sqrt{W_s/W_t}$		$\sqrt{21}$
(23)	$(W_s/W_t)^{3/2}$		$(21)^{3/2}$
(24)	Rotor rpm		
(25)	D	ft	Rotor disk diameter
(26)	A	ft ²	Rotor disk area
(27)	V_b	ft/sec	Rotor tip speed, $0.0524 \times (24) \times (25)$
(28)	V_b^2		$(27)^2$
(29)	$BHP_t \sqrt{\sigma} (W_s/W_t)^{3/2}$		$(17) \times (23) \div (9)$
(30)	$V_b \sqrt{\sigma} W_s/W_t$		$[(27) \text{ or } (24)] \times (22) \div (9)$
(31)	Plot (29) vs (30)		
(32)	M		Figure of merit, $[0.0298 \times (9) \times (19)] \div [(17) \times (25)]$
(33)	C_T		Thrust coefficient, $[421 \times (18)] \div [(10) \times (26) \times (28)]$

(34) Plot (32) vs (33)

NOTE: If the manifold pressure-ambient pressure ratio exceeds 1.4, a correction to power and manifold pressure should be made.

If the chart power data is not reliable, substitute MP_t for BEP_t in (29) and do not calculate M and C_T .

SECTION 7.4

Climbs and Descents (Autorotation)

Two types of climbs must be evaluated in helicopter performance; the vertical climb and the climb at the forward speed for best climb. Only one type of descent is usually evaluated. That is the autorotational or power-off descent.

The speed for best rate of climb and minimum rate of descent may be determined by the sawtooth climb procedures used for conventional aircraft. In making climb tests at the low rates of climb and forward speeds associated with helicopters, special care must be taken to obtain data during the best atmospheric conditions; that is, negligible wind and turbulence and no temperature inversions. Since weight corrections to climb and descent data cannot be accurately determined by mathematical derivations, it is best to take the first sawtooth points at the desired weight and at the best climbing speed from the manufacturer's data. Sawtooth climb and descent data are reduced to standard conditions by the procedures used for conventional aircraft and are presented as shown in Figure 7.41.

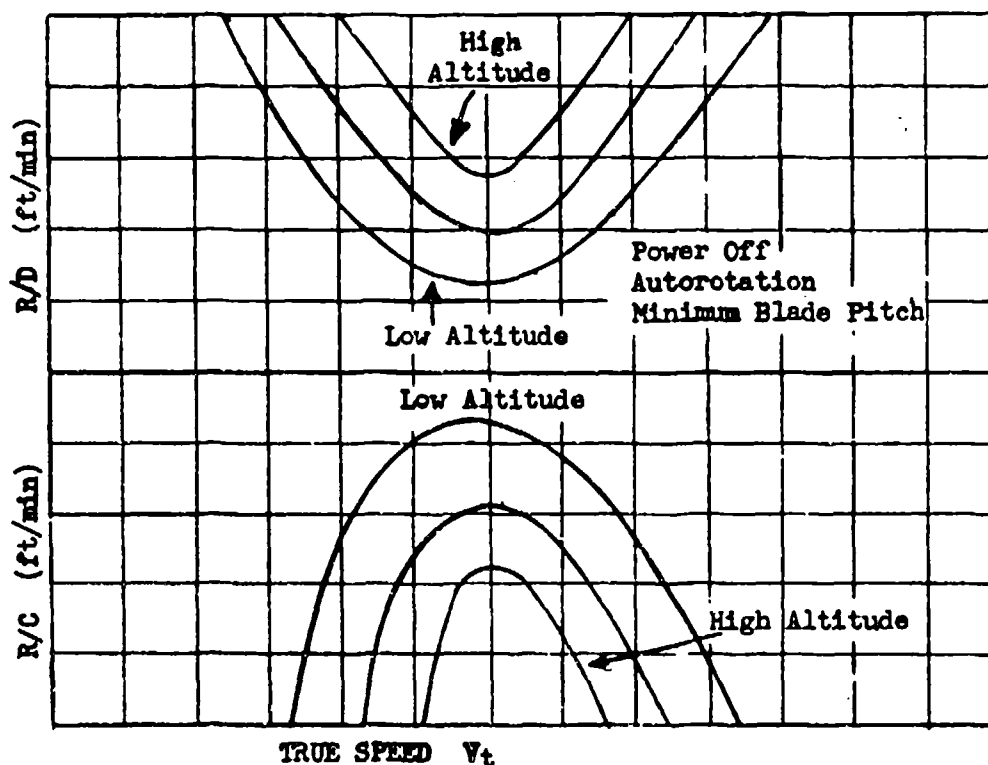


Figure 7.41
Typical Sawtooth Climb and Descent (Autorotation) Data

RATE OF CLIMB EVALUATION

For helicopters the power available in level flight is constant at a particular altitude. For this reason it is not necessary to conduct sawtooth climbs. At the level flight speed for minimum power required the maximum excess power for climb is available. This speed, corresponding to minimum C_D and BEP $(\sigma (W_S/W_T)^{3/2}$ in Figures 7.32 and 7.34 respectively, may be determined from the level flight speed-power performance for any values of C_T , (W/σ) , $V_b \sqrt{\sigma W_T/W_S}$, or $\sqrt{\sigma W_S/W_T}$ as shown in these figures.

To equation 7.301 may be added another variable, the vertical velocity (V_v). Using the new equation and dimensional analysis, the following equations may be obtained:

$$\frac{\text{BHP}}{A \rho V_b^3} = f \left[\frac{W}{A \rho V_b^2}, \frac{V_t}{V_b}, \frac{V_v}{V_b} \right] \quad (7.401)$$

$$\frac{\text{BHP}(A \rho)^{\frac{1}{2}}}{(W)^{\frac{3}{2}}} = f \left[V_t \left(\frac{\rho A}{W} \right)^{\frac{1}{2}}, V_b \left(\frac{\rho A}{W} \right)^{\frac{1}{2}}, V_v \left(\frac{\rho A}{W} \right)^{\frac{1}{2}} \right] \quad (7.402)$$

The value of the forward-speed parameter for best rate of climb in both of these equations may be determined by inspection of the level flight speed-power data. If it is assumed that, for a particular set of conditions, the rate of climb varies nearly linearly with the power available, then the above equations may be evaluated graphically for all climb conditions by using the data from two check climbs at best climb speed. Equation 7.402 is the easier of the two to work with in this respect and will be used in this discussion.

In a dimensional form for a particular aircraft the speed parameter is:

$$V_t \sqrt{\sigma \frac{W_S}{W_T}} = V_C \sqrt{\frac{W_S}{W_T}}$$

During a check climb to the actual altitude the take-off value of W_S/W_T will not change appreciably and the best V_C -altitude schedule from the speed-power data may be computed at a constant W_S/W_T . Two check climbs at best forward speed are now required. These climbs may be accomplished at two power settings for constant W_S/W_T or at two extreme values of W_S/W_T for a constant power setting. Data from these check climbs are not reduced to standard conditions. Instead the calibration-corrected data are plotted as in Figure 7.42.

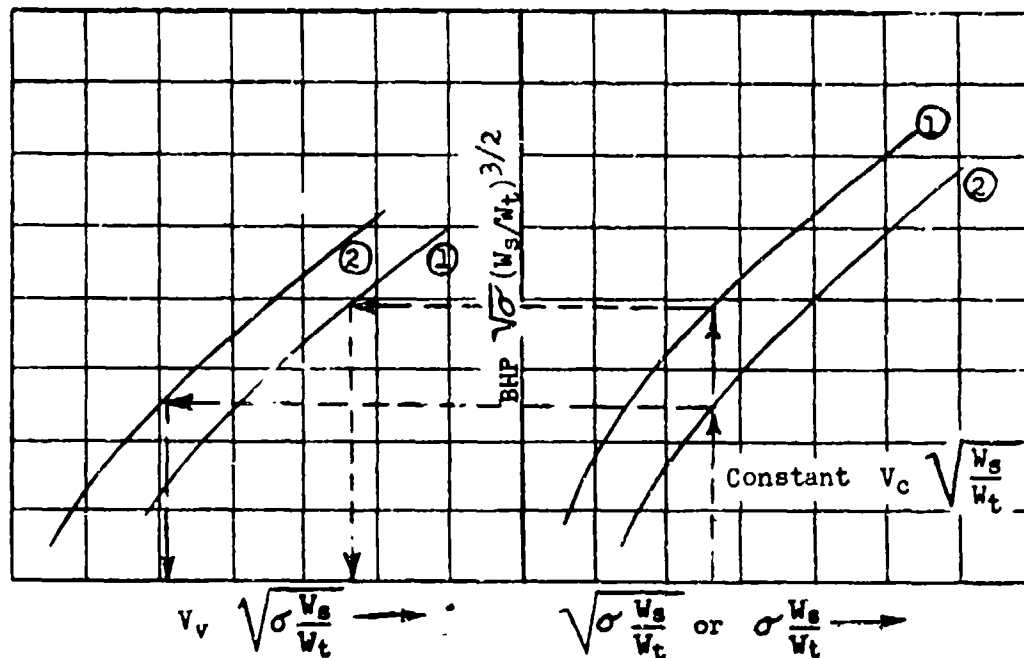


Figure 7.42
 Method of Determining Two Climb and Power Parameter
 Values for a Constant Effective Weight Ratio

This plot establishes two power-parameter values and two rate of climb parameter values for any value of the rotor rpm or effective weight ratio parameters. This data are then crossplotted as in Figure 7.43 to show the variation of the power and rate of climb parameters at constant rotor rpm or effective weight ratio parameters. From this plot the rate of climb can be determined for any weight, altitude, or power conditions.

The vertical climb case is identical to that described for the climb at best speed. Here the forward speed is zero, but the technique of determining rate of climb for all conditions is accomplished as described above. In vertical climbs the primary source of error is in determining and maintaining zero velocity relative to the air mass. This problem is partially solved by the use of a long weighted cord having short ribbons attached to it. Keeping the cord straight and the ribbons hanging down assists in approximating zero forward speed.

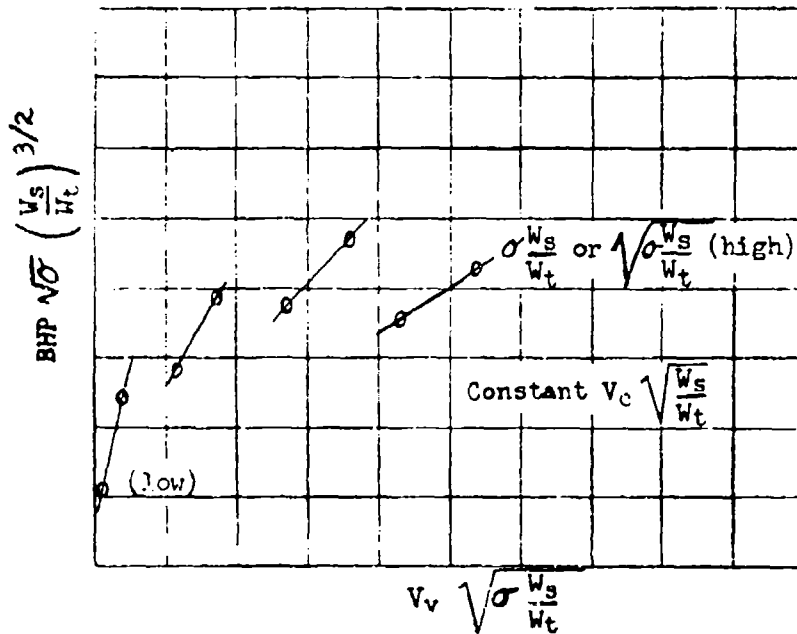


Figure 7.43
Method of Plotting Rate of Climb Data for All Values
of Power, Altitude, and Weight at Best Climb Speed

AUTOROTATIONAL DESCENT EVALUATION

Rotor operation without engine power is referred to as autorotation. Under certain conditions the helicopter may descend and land safely without engine power. Since, during autorotation, the air flow through the rotor is opposite to the flow during level flight power-on conditions, there is some instability and loss of altitude during the transition to autorotation and a minimum rate of descent. The helicopter performance investigation should determine altitudes and speeds at which autorotation can be assumed to result in a safe landing. The forward speed for minimum rate of descent and the effects of weight and altitude on autorotation should also be determined.

Equation 7.402 applies to the autorotative descent. In this case the power parameter is zero and the value of V_v is negative. The dimensional parameters are:

$$V_v \left(\sigma \frac{W_s}{W_t} \right)^{\frac{1}{2}} = r \left[v_t \left(\sigma \frac{W_s}{W_t} \right)^{\frac{1}{2}}, v_b \left(\sigma \frac{W_s}{W_t} \right)^{\frac{1}{2}} \right] \quad (7.403)$$

The maximum rotor efficiency in level flight is represented by the minimum value of C_p or $BHP \sqrt{\sigma} \left(\frac{W_s}{W_t} \right)^{3/2}$ for level flight. This condition represents the least power required relative to weight, forward velocity, fuselage drag, and rotor blade drag. In autorotation the total power absorbed by the helicopter is:

$$\begin{aligned}
 P_{\text{absorbed}} &= -V_v W \\
 W V_v &= P_{\text{induced}} + P_{\text{rotor drag}} + P_{\text{fuselage drag}} \\
 P_{\text{absorbed}} &= \text{minimum at } -V_v = \text{minimum}
 \end{aligned}$$

In autorotation the blade pitch angle is small and the angle of attack is large relative to level flight conditions. It may be assumed from drag and lift coefficient vs angle of attack data that P_i , P_{rd} , and P_{fd} are nearly proportional to level flight values at the same forward speeds, rotor speeds, and weight. Thus the forward speed for least power required in level flight is the speed for least power absorbed and minimum rate of descent in autorotation. In fact by using the standard rate of climb equation and assuming the same rotor efficiency:

$$\begin{aligned}
 W V_v &= P_{\text{avail}} - P_{\text{req level flight}} \\
 \text{if } P_{\text{avail}} &= 0 \\
 -V_v \text{ ft/min} &= \frac{550 (60) \text{ BHP}_{\text{level flight}}}{W} \quad (7.404)
 \end{aligned}$$

Equation 7.404 will give a close approximation of autorotation rate of descent at any forward speed.

An autorotative descent at best forward speed determined from the level flight speed power performance will establish the minimum rate of descent for all conditions of weight, rotor speed, and altitude. Since the weight during descent does not change, the best descent speed will be at a nearly constant V_c for an initial weight, and will increase slightly if the descent is started at the helicopter ceiling.

$$V_c \sqrt{\frac{W_B}{W_t}} = V_o \sqrt{\frac{W_B}{W_t}}$$

A descent should be conducted at a V_c higher and lower than the assumed best V_o to establish the magnitude of variation of rate of descent with small variation of V_c . Figure 7.44 shows a typical plot of data for equation 7.403.

POWER-OFF LANDINGS

With power on, a safe landing may usually be executed vertically. In autorotation a minimum rate of descent is in the middle speed range of the aircraft and the safest landings involve some ground roll if the terrain is suitable. The power-off descent is made at minimum blade pitch to provide minimum blade drag and maximum rotor speed. Within a rotor diameter of the ground this pitch angle may be rapidly increased and the rate of descent lowered considerably for a short interval. This reduces the forward speed considerably and upon touch-down a minimum ground roll will result.

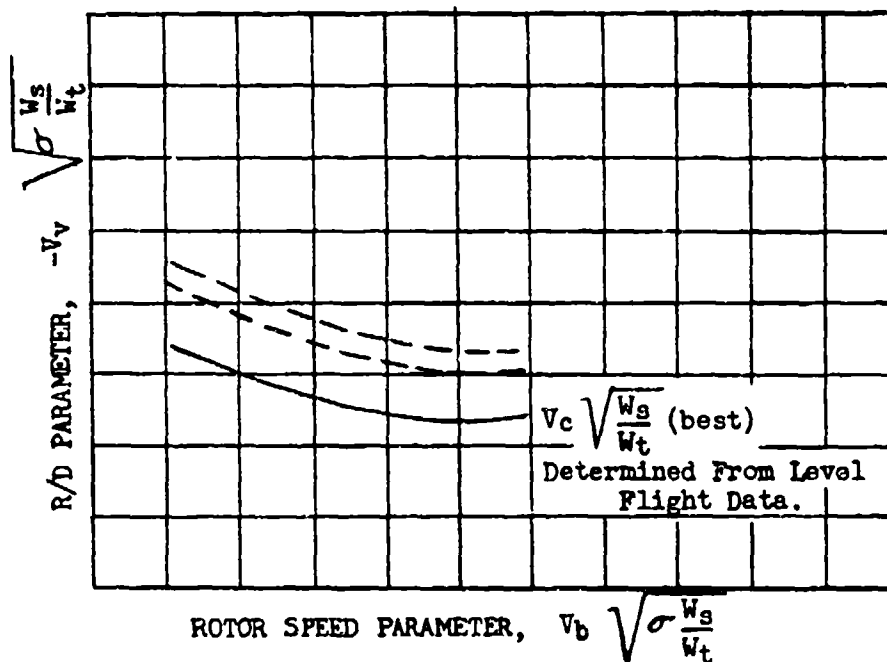


Figure 7.44
Method of Plotting Autorotation Descent Data

A safe altitude for entering into autorotation may be defined as the height above the ground at which entry into autorotation will result in a minimum rate of descent at a height of one rotor diameter above the ground. This safe altitude may be plotted as a function of the forward speed at which entry into autorotation is started as in Figure 7.45. Data should be obtained as near the ground as possible without actually making a landing; a 2000 ft altitude will give desirable results if continuous engine operation is assured.

Autorotative landings over a simulated 50 ft. obstacle should be conducted at the speed for minimum rate of descent. This data will establish the approximate air distance and ground distance required for safe power-off landings. These landing data are plotted as in Figure 7.46. Since the technique of making this type of landing is not always consistent and the distances are so short, it is not feasible to apply any standardization corrections.

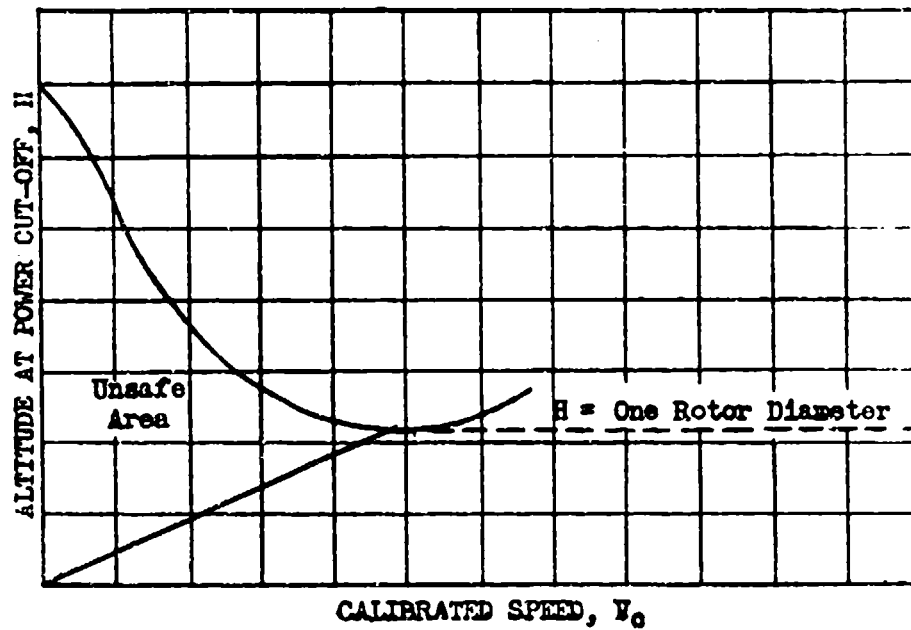


Figure 7.45
Method of Showing Safe Height for Entry into Autorotation

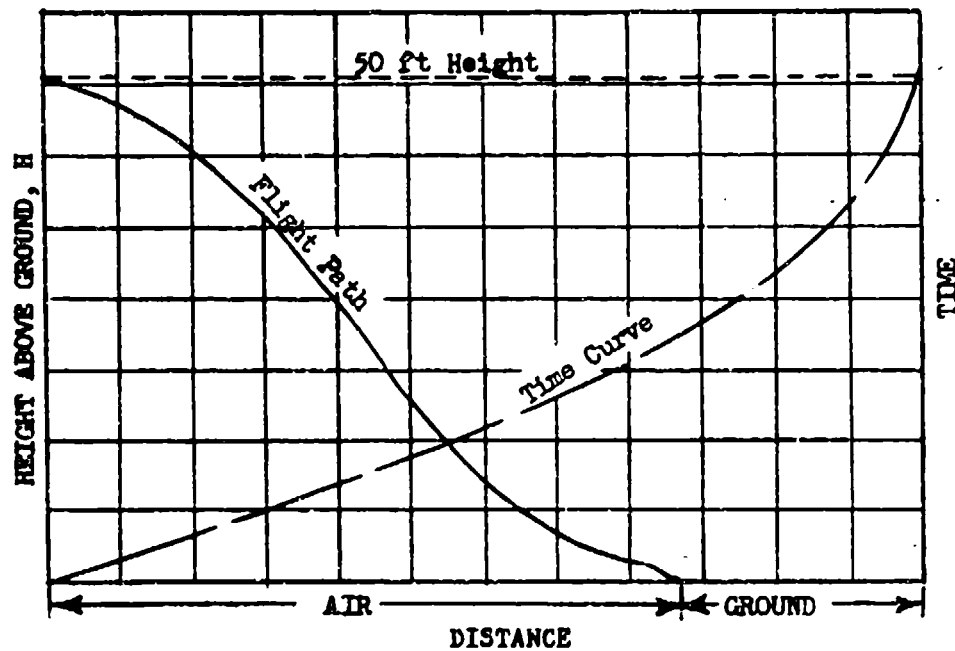


Figure 7.46
Method of Showing Autorotative Landing Time
and Distance Data

SECTION 7.5

Fuel Consumption, Endurance and Range

Fuel consumption, range, and endurance data for helicopters powered by reciprocating engines are handled in about the same manner as for conventional aircraft. One exception to the theory and technique of Chapter Four is the inclusion of the rotor tip speed parameter in the endurance and range equations. These equations are derived from equation 7.301, substituting specific endurance, SE, for BHP, in one case and specific range, SRg, for BHP, in the other case. The two dimensional equations that result are:

$$SE \sqrt{\sigma} \left(\frac{W_t}{W_s} \right)^{3/2} = \frac{(\sigma)^{1/2}}{W_f} \left(\frac{W_t}{W_s} \right)^{3/2} = r \left[v_t \left(\sigma \frac{W_s}{W_t} \right)^{1/2}, v_b \left(\sigma \frac{W_s}{W_t} \right)^{1/2} \right] \quad (7.501)$$

$$SRg \left(\frac{W_t}{W_s} \right) = \frac{v_t}{W_f} \frac{W_t}{W_s} = r \left[v_t \left(\sigma \frac{W_s}{W_t} \right)^{1/2}, v_b \left(\sigma \frac{W_s}{W_t} \right)^{1/2} \right] \quad (7.502)$$

where:

$$\begin{aligned} W_f &= \text{fuel flow (lbs/hr)} \\ v_t \sqrt{\sigma} &= v_c \end{aligned}$$

For each speed-power calibration a plot should be made of fuel flow versus brake horsepower. This plot is valid for both test and standard conditions at the approximate density altitude of the flight. Some altitude effects are usually noticeable as shown in Figure 7.51. It is essential to determine fuel consumption, range and endurance data at typical flight altitudes, since the exact effects of altitude on these variables cannot be determined by extrapolation except in a narrow range near the altitude flown.

ENDURANCE

The forward speed for maximum endurance is found from the speed-power calibrations at the point where C_p or BHP $\sqrt{\sigma} (W_s/W_t)^{3/2}$ is a minimum. This speed corresponds to minimum power required for the rotor parameter conditions existing. The effects of weight, altitude, rotor speed, and engine speed on SE may be evaluated at the best forward speed as illustrated in Figure 7.52. At a middle altitude the specific endurance parameter is determined at about four values of the rotor speed parameter at two engine rpm's (if reduced rotor rpm indicates reduced power required on speed-power plots). At a high and a low altitude the specific endurance parameter is found for only two extreme values of the rotor speed parameter and a curve is faired between them corresponding to that found for the complete survey at the middle altitude.

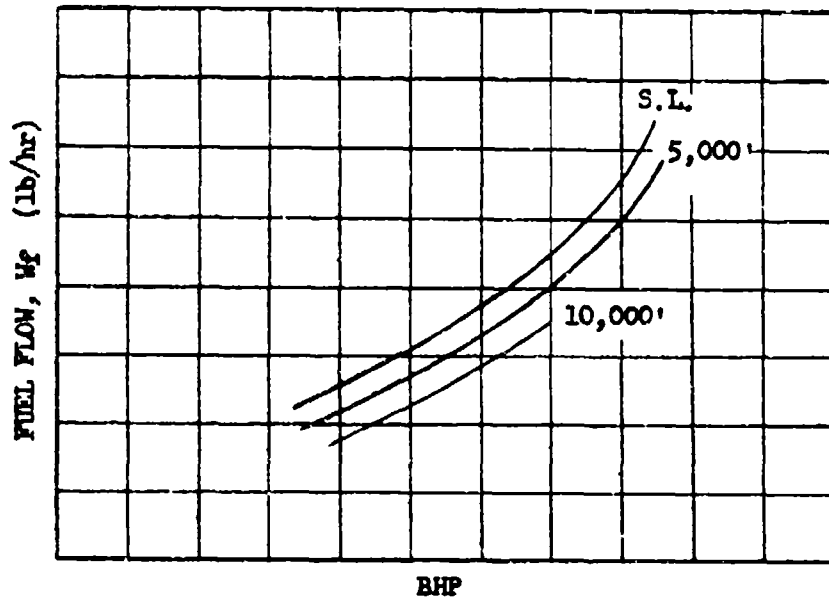


Figure 7.51
Typical Fuel Flow-Power Presentation

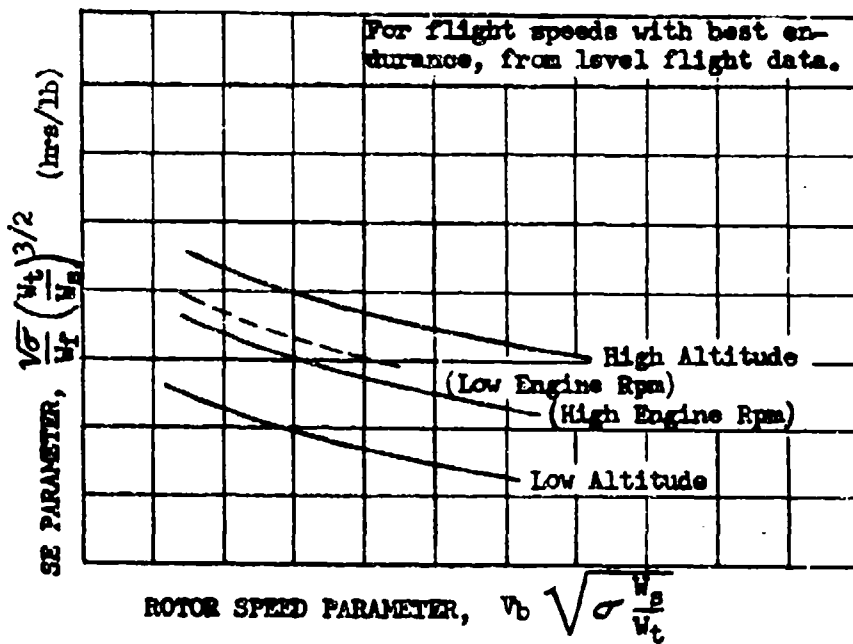


Figure 7.52
Typical Plot of Maximum Endurance Data

Although endurance data, as such, is not usually presented in the aircraft performance report, the requirement may arise for presentation of endurance at all forward speeds as well as at the speed for maximum endurance. This may be accomplished by showing the endurance parameters at three typical altitudes for high and low values of the rotor speed parameters as in Figure 7.53. Endurance during the hovering condition should be separately evaluated if such data is required.

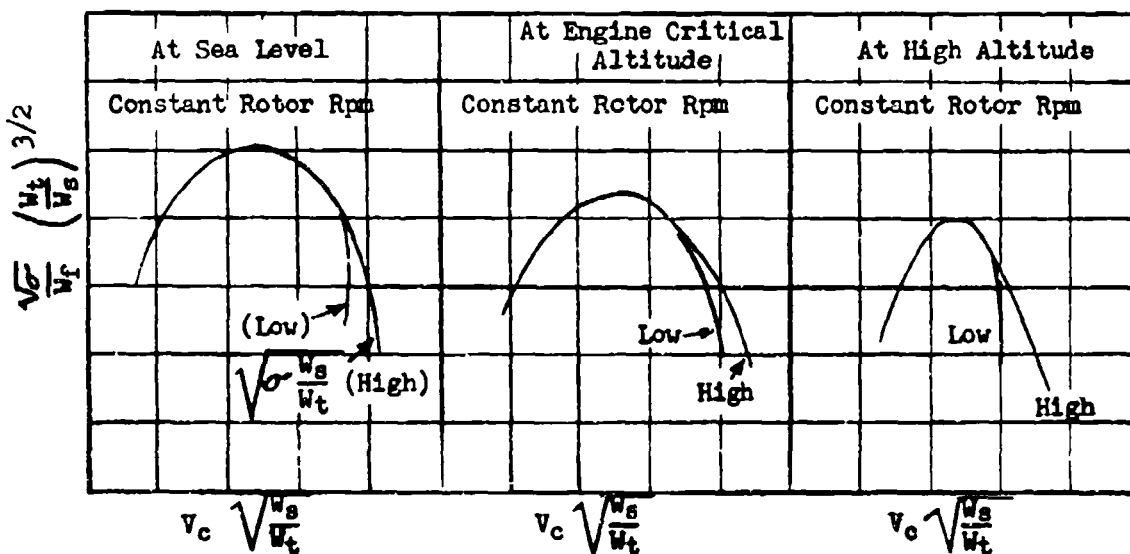


Figure 7.53
Typical Endurance Parameter Data for all Forward Speeds

RANGE

The maximum range for helicopters is found at relatively high forward speeds for the C_T or rotor speed parameter involved. In most cases some altitude effects are apparent in the fuel flow vs BHP plot and equation 7.502 does not strictly apply. If the fuel flow-BHP plots are identical at all altitudes, equation 7.502 may be plotted as indicated in Figure 7.54. One of the rotor speed parameters should be flown at a reduced engine rpm to establish any relative improvement in specific range for this condition. In general, for a given gross weight, a reduced engine speed resulting in a reduced power and forward speed does not result in any appreciable increase in range.

Altitude is usually an important factor in the specific range equations. Data should be obtained at about three representative altitudes and plotted for constant rotor rpm as in Figure 7.55.

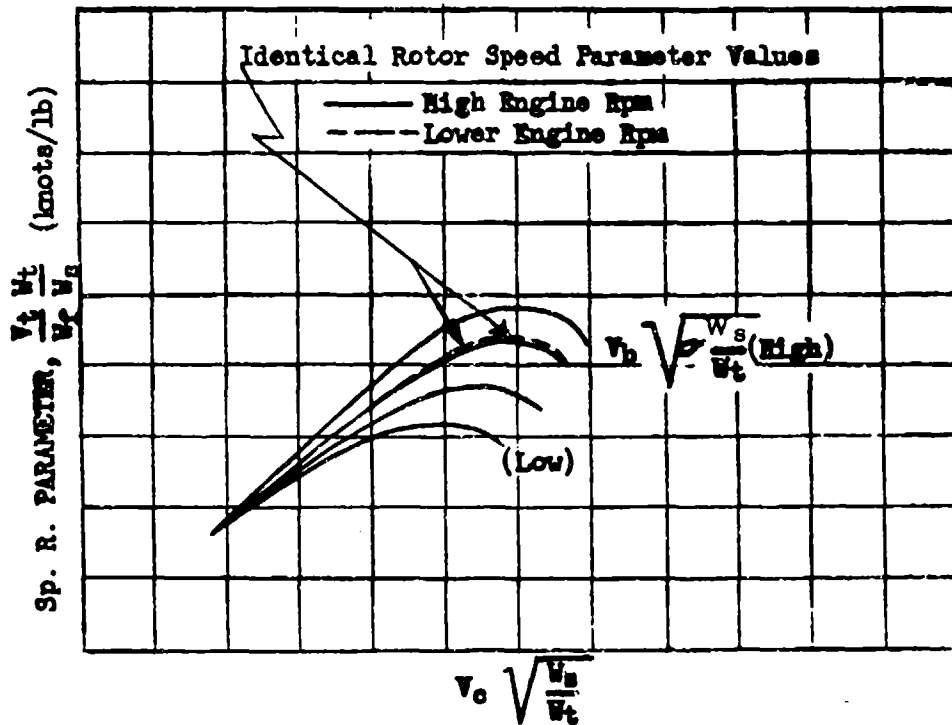


Figure 7.54
Typical Range Parameter Data for All Forward Speeds
(Fuel Flow - BHP Plots Identical at All Altitudes)

Two possible extremes of the rotor speeds parameter are obtained at each of the altitudes to permit extrapolation for this condition. If desired a range comparison for reduced engine speed may be added to Figure 7.55 as was done in Figure 7.54. When a complete range evaluation in parameter form is not considered necessary, data may be simply presented as specific range vs true speed as shown in Figure 7.56. Data for this plot, as for other types of range plots, should be obtained at various flight altitudes.

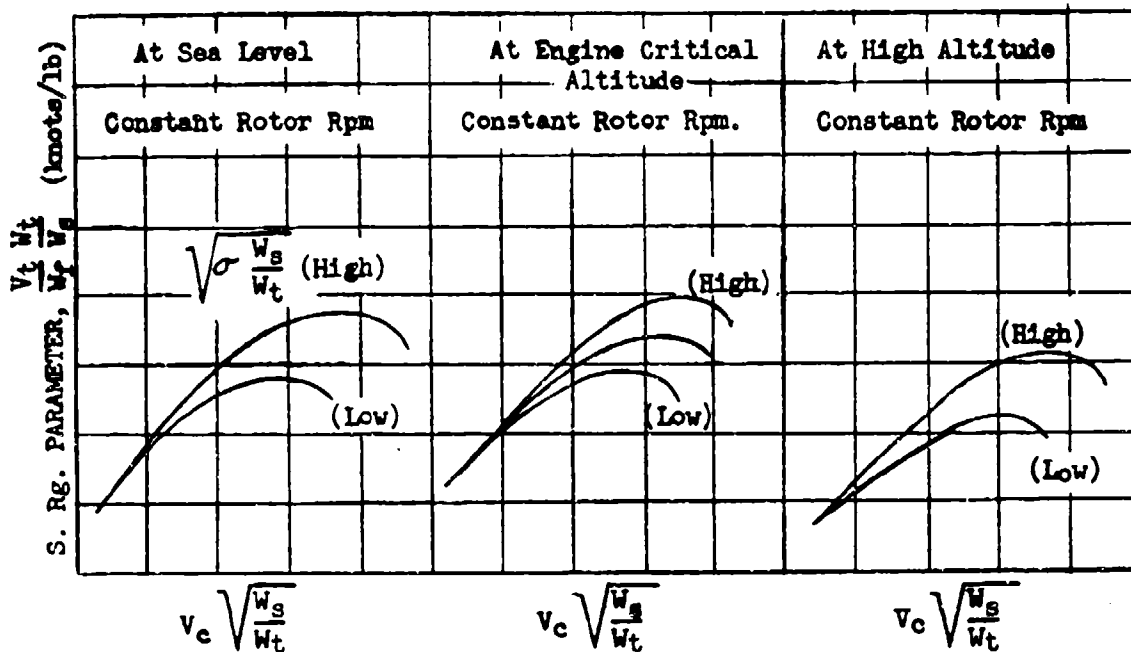


Figure 7.55
Typical Range Parameter Data for All Forward Speeds

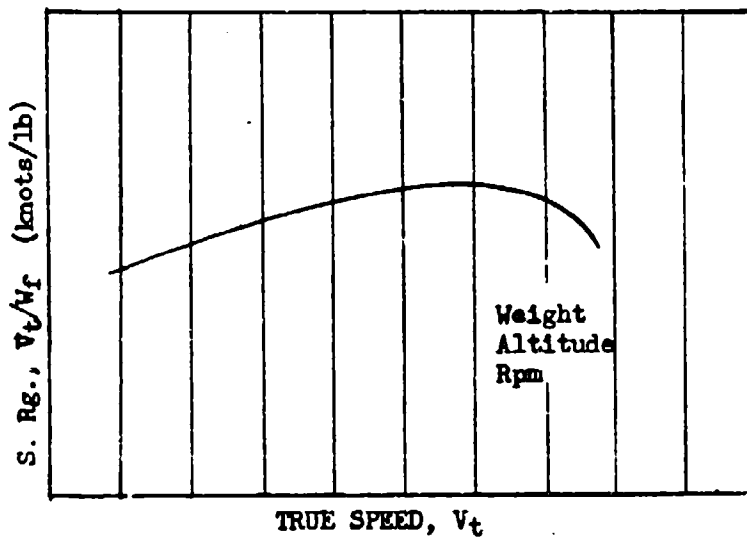


Figure 7.56
Typical Specific Range-True Speed Plot,
One Altitude, Weight, and Rotor Rpm

SECTION 7.6

Air Speed, Altimeter, and Temperature System Calibrations

Separate air-speed indicator and altimeter calibrations should be made with helicopters, because of possible errors in the total pressure at the air-speed probe. No conversion of dV to dH should be attempted at large forward speeds. At low speeds the total effects of air-speed error ($dV_0 = \pm 15$ knots) if converted to altimeter error would be negligible. A pacer aircraft may be used to determine altimeter and air-speed position errors at high speeds. At low speeds a take-off time and distance recording camera can be used. These calibration tests should always be flown out of ground effect. Data are reduced as described in Chapter One. The method of plotting the air-speed position error is illustrated in Figure 7.61. Altimeter position error is plotted in the customary manner, and data are usually obtained out of ground effect.

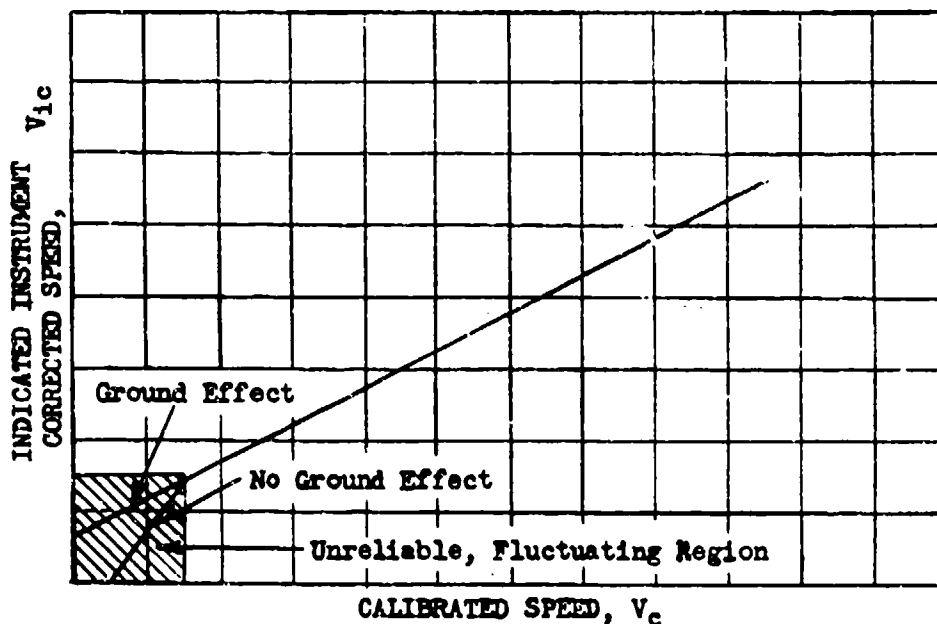


Figure 7.61
Typical Helicopter Air-speed Position Correction Plot

Because of the low true speeds of helicopters, adiabatic temperature rise is negligible. The temperature probe should be carefully shielded from engine exhaust heat and solar radiation.

REFERENCES

GENERAL

1. Anonymous, "Ground School Notes - Book B - Performance", The Empire Test Pilots' School, Farnborough, Ministry of Aviation, United Kingdom.
2. King, J. J. et al, "Aerodynamics Handbook for Performance Flight Testing - Volume I", USAF Experimental Flight Test Pilot School, AFFTC-TN-60-28, July 1960
3. Perkins, C. D. and Dommasch, D. O., eds. "Flight Test Manual- Volume I - Performance", Advisory Group for Aeronautical Research and Development, 1959.
4. Polve, J. H. "Performance Flight Testing", USAF Experimental Flight Test Pilot School FTC-TR-53-5, August 1953
5. Spillers, L. H. et al, "Pilots Handbook for Performance Flight Testing", USAF Experimental Flight Test Pilot School, FTC-TN-59-46, September 1960

STANDARD ATMOSPHERE

6. Anonymous, "Standard Atmosphere - Tables and Data for Altitudes to 65,800 Feet", International Civil Aviation Organization and Langley Aeronautical Laboratory NACA Report 1235, 1955
7. Minzner, R. A. et al, "U.S. Extension to the ICAO Standard Atmosphere - Tables and Data to 300 Standard Geopotential Kilometers", United States Committee on Extension to the Standard Atmosphere, U.S. Government Printing Office, 1958
8. Minzner, R. A. et al, "The ARDC Model Atmosphere 1959", Air Force Cambridge Research Center TR-59-267, ASTIA Document 229482, August 1959

RECIPROCATING ENGINE AIRCRAFT PERFORMANCE

9. Bikle, P. F., "A Simplified Manifold Pressure Correction", Army Air Forces, Hq. Air Technical Services Command, Wright Field, Dayton, Ohio, Flight Section Memorandum Report Serial No. TSCEP5E-1919, 29 June 1945
10. Bikle, P. F., "Performance Flight Testing Methods in Use by the Flight Section", USAF Air Materiel Command, Wright-Patterson AFB, Ohio, Army Air Forces Technical Report No. 5069, 15 January 1944

TURBOJET ENGINE AIRCRAFT PERFORMANCE

11. Shoernacher, P. E. and Schonewald, R. L., "Reduction and Presentation of Flight Test Data for the F-86 Airplane having Automatic Engine Control and a Continuously Variable Jet Nozzle Area", AFFTC Technical Note R-8, July 1952
12. O'Neal, R. L., "Performance Standardization for a Turbojet Engine Equipped with a Variable Area Nozzle Controlled by Engine Speed", AFFTC Technical Memorandum 56-7, March 1956

POWER PLANTS

13. Chapel, C. E. et al, "Aircraft Power Plants", Northrup Aeronautical Institute Series of Aviation Texts, McGraw-Hill, New York, 1955
14. Anonymous, "The Aircraft Engine and Its Operation", Pratt and Whitney Aircraft Operating Instruction 100, February 1955
15. Gagg, R. F. and Farrar, E. V., "Altitude Performance of Aircraft Engines Equipped with Gear-Driven Superchargers", S. A. E. Journal 34:217-225, June 1934
16. Pierce, E. F., "Altitude and the Aircraft Engine", SAE Journal 47:421-431, October 1940
17. Anonymous, "Performance Correction Procedures for Turbojet and Turbofan Commercial Engines", Pratt and Whitney Aircraft Operating Instruction 204, May 1961
18. Anonymous, "General Operating Instructions, Axial Compressor Nonafterburning Turbojet and Turbofan Engines", Pratt and Whitney Aircraft Operating Instruction 190, April 1963
19. Anonymous, "General Operating Instructions, Axial Compressor Afterburning Turbojet and Turbofan Engines", Pratt and Whitney Aircraft Operating Instruction 191, November 1963
20. Anonymous, "Aircraft Performance Engineer's Manual for B-36 Aircraft Engine Operation", Strategic Air Command Manual No. 50-35, 1952

LAG CORRECTION

21. Irwin, K. S., "Lag in Aircraft Altitude Measuring Systems", Air Force Flight Test Center FTC-TDR-63-26, 1963

CLIMB PERFORMANCE

22. Grosso, V. A., "Analytical Investigation of the Effects of Vertical Wind Gradients on High Performance Aircraft", AFFTC Technical Report 61-11, March 1961
23. Shoemaker, P. E., "Use of Corrected Non-Dimensional Parameters for Standardizing Jet Aircraft Rate-of-Climb Data", AFFTC Technical Report 52-13, May 1953
24. Grosso, V. A., "Investigation to Determine Effects of Several Parameters on Optimum Zoom Climb Performance", AFFTC Technical Note 59-32, October 1959
25. Grosso, V. A., "F-106A Zoom Climb Study", AFFTC Technical Information Memorandum 58-1047, October 1958

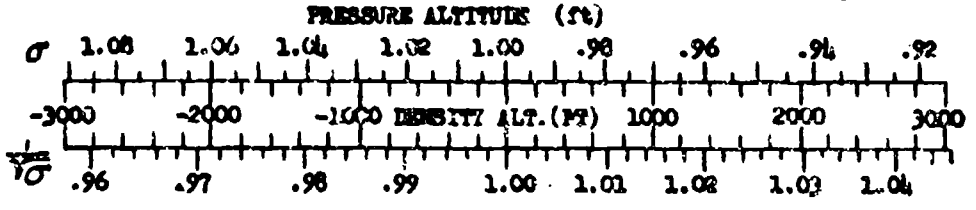
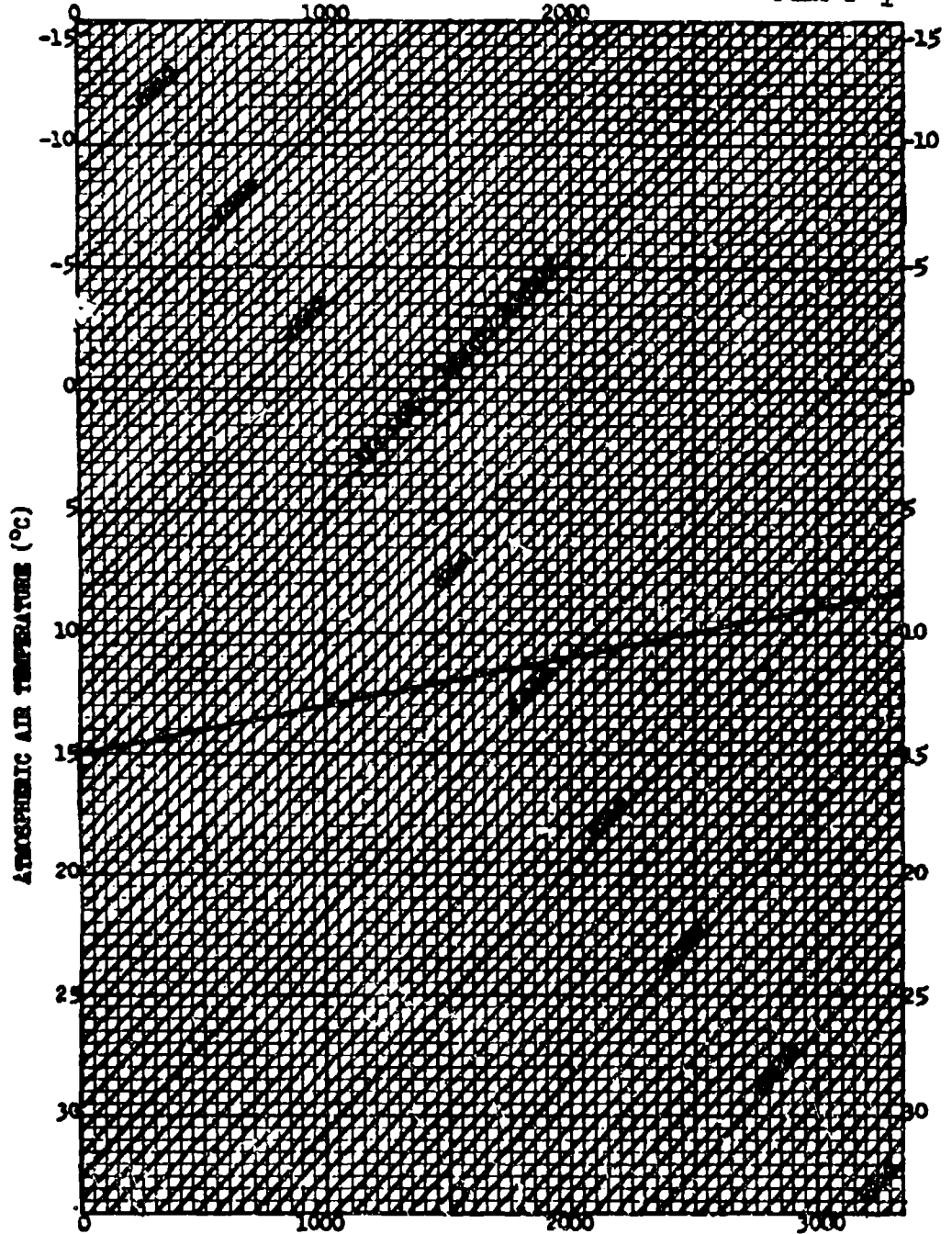
TAKE-OFF PERFORMANCE

26. Lush, K. J., "Standardization of Take-Off Performance Measurements for Airplanes", AFFTC FTC-TN-R12
27. Dunlap, E. W., "Corrections to Take-Off Data", AFFTC Technical Information Memorandum 59-1078, February 1959

HELICOPTER PERFORMANCE

28. Anonymous, "A Review of Current Helicopter Technology", Vertol Division of Boeing Co., Morton, Penna., Lectures to Graduating Class of Naval Test Pilot School, Patuxent Naval Air Station, February 1963
29. Swope, W. A., "Lectures on Rotary Wing Performance", U. S. Army Transportation Materiel Command, Aviation Test Office, Edwards AF Base, California, Lectures to USAF Experimental Test Pilot School, Spring 1960.
30. Wheelock, R. H., "An Introduction to the Helicopter", Bell Helicopter Co., Fort Worth, Texas, 1962

CHART I -1



AIR-6273

CHART I -1

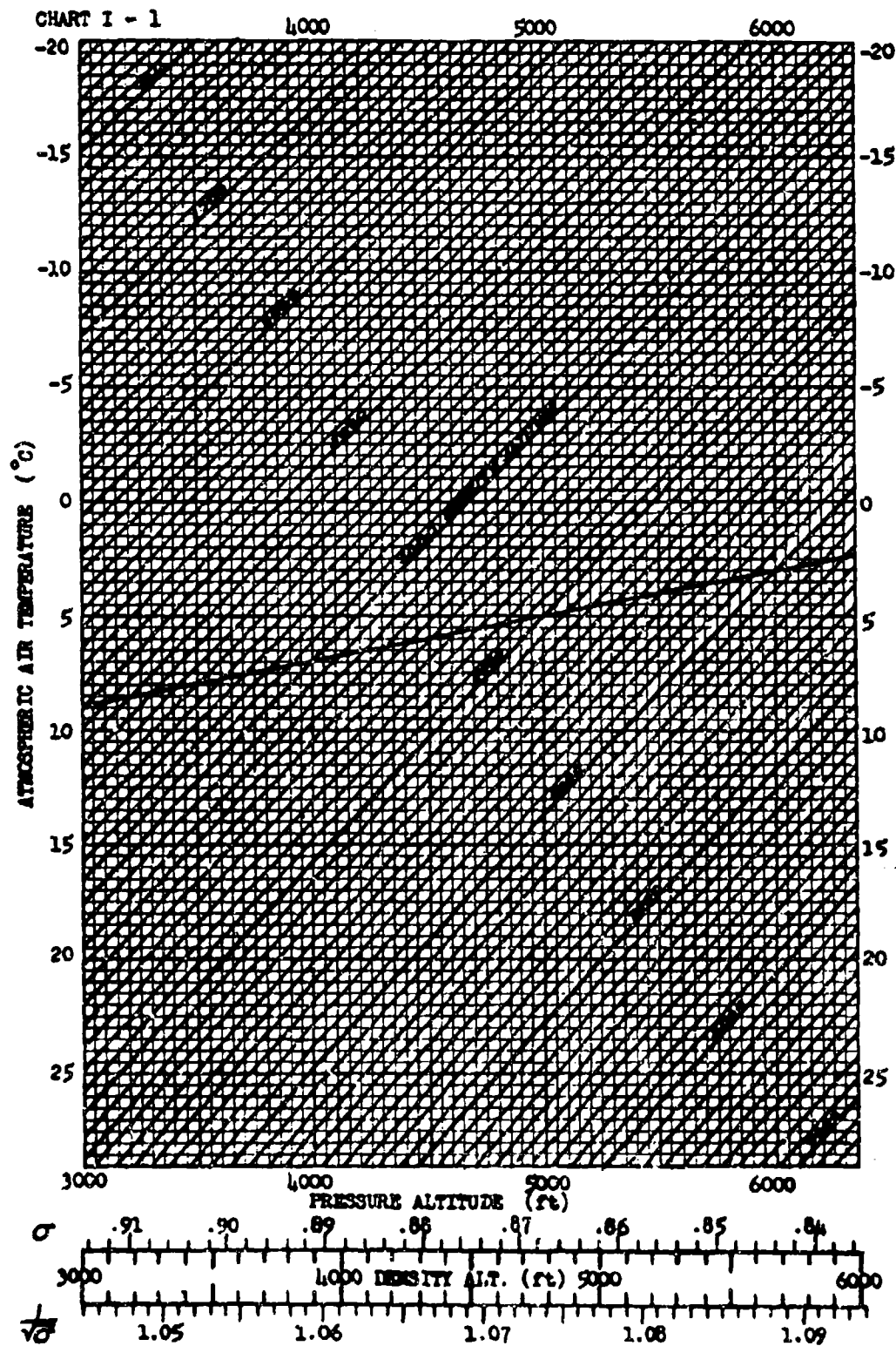
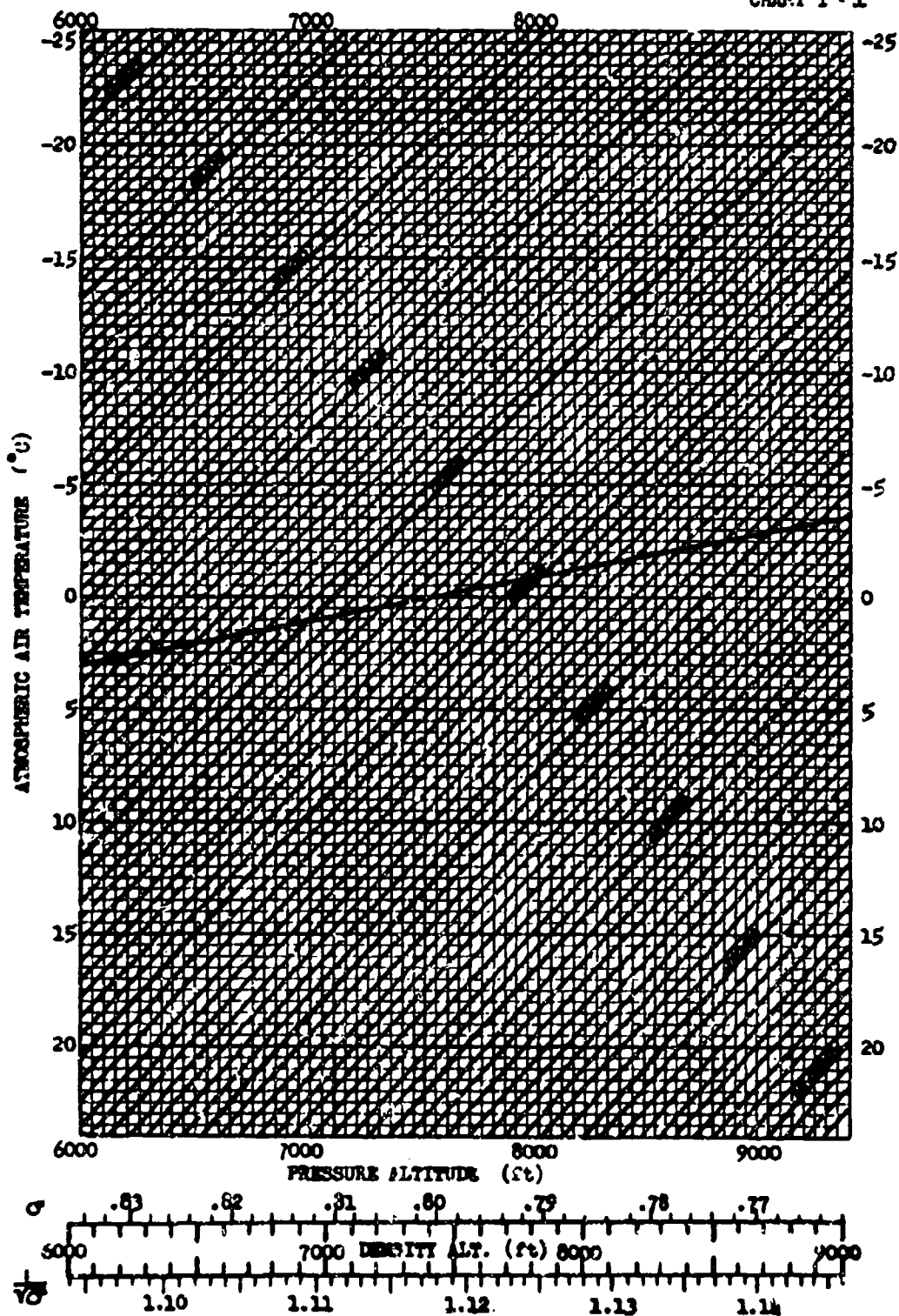


CHART I - 1

AFTI-6273

CHART I - 1



AFTR-6273

CHART I - 1

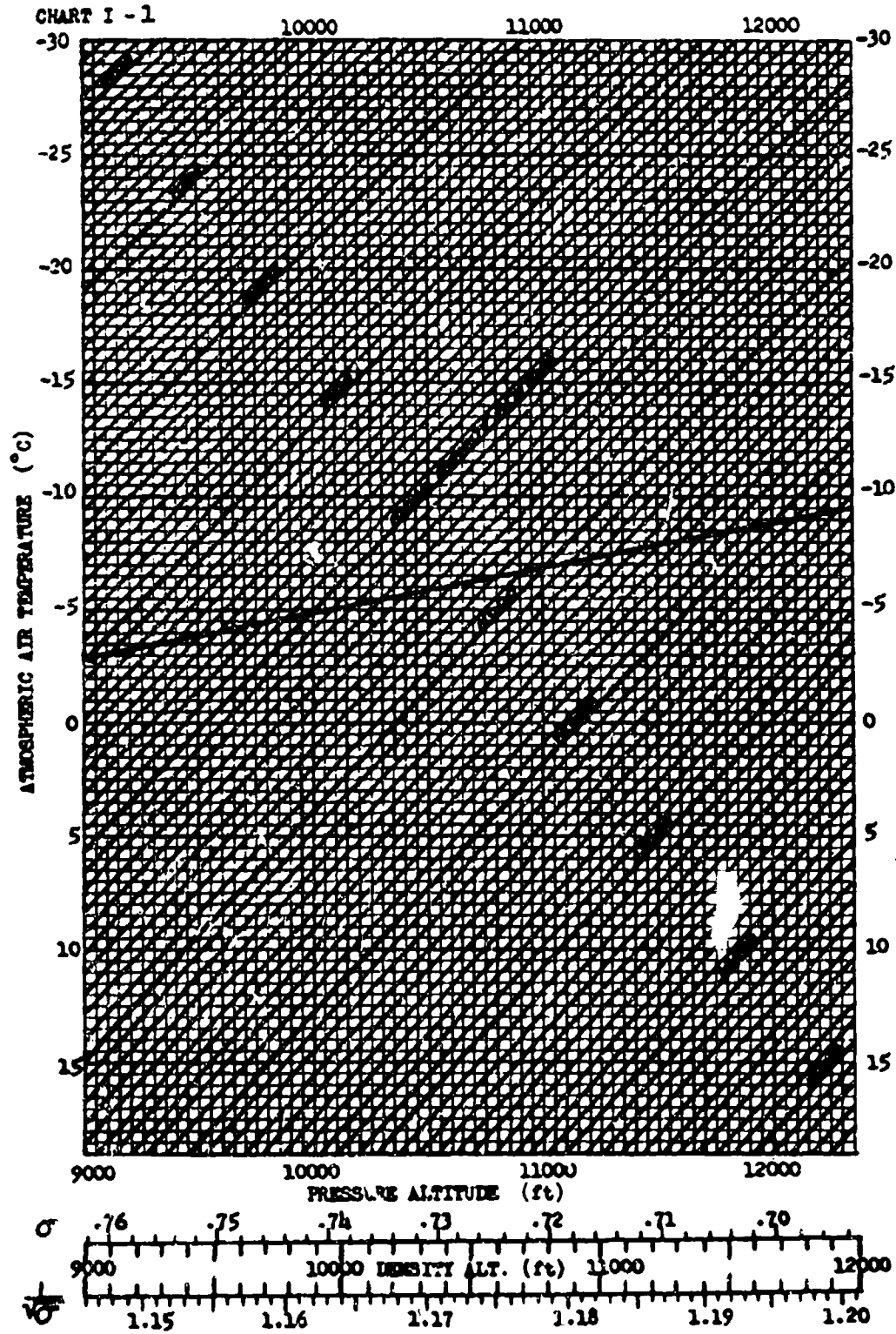
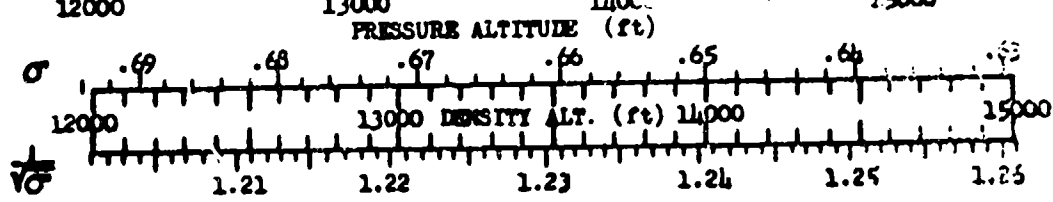
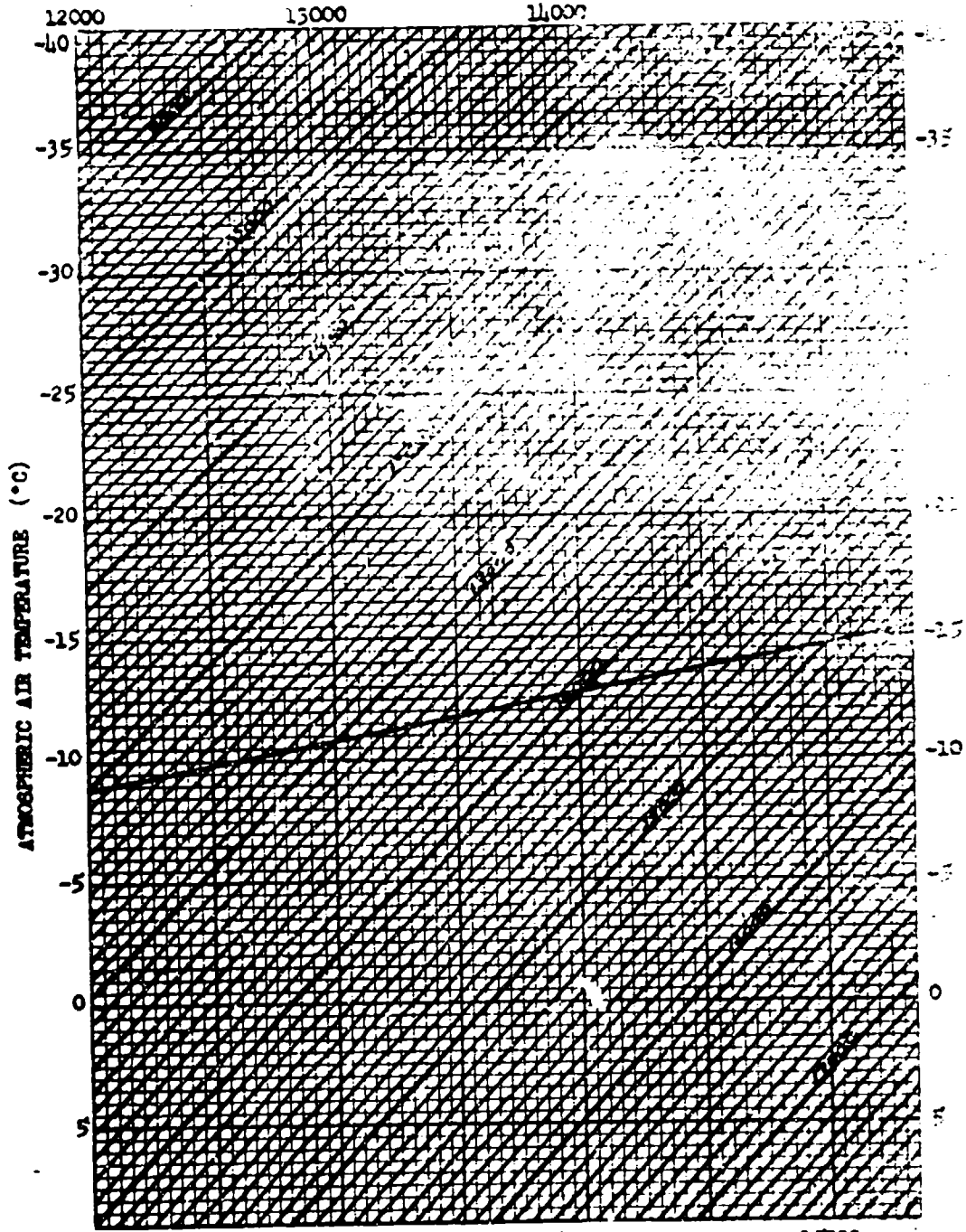


CHART I - 1

AFT-6273



AFTR-6273

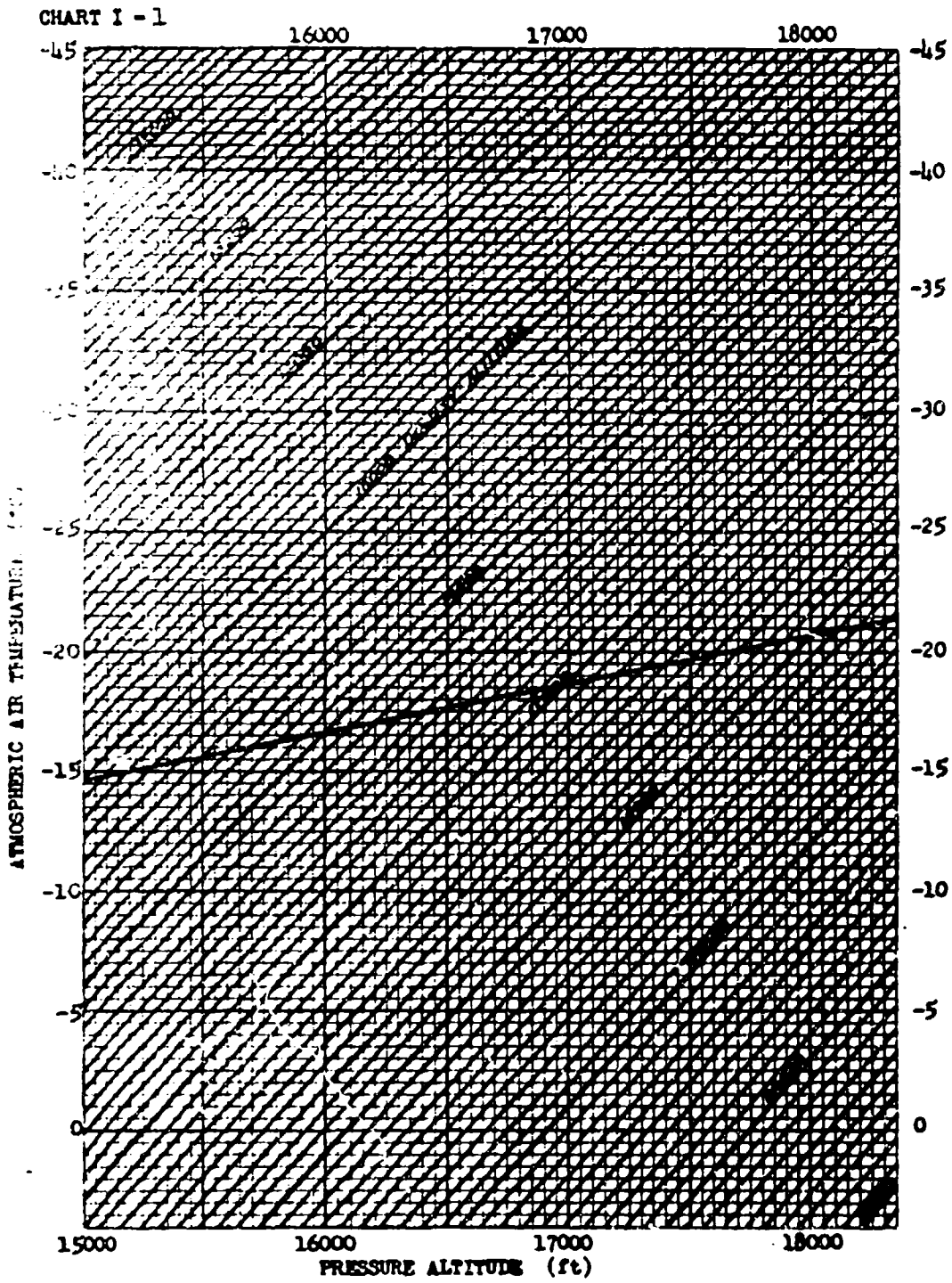
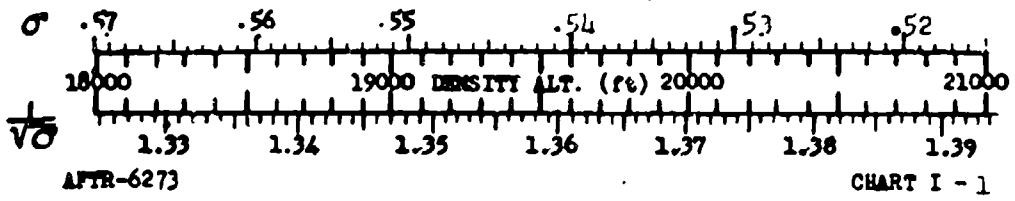
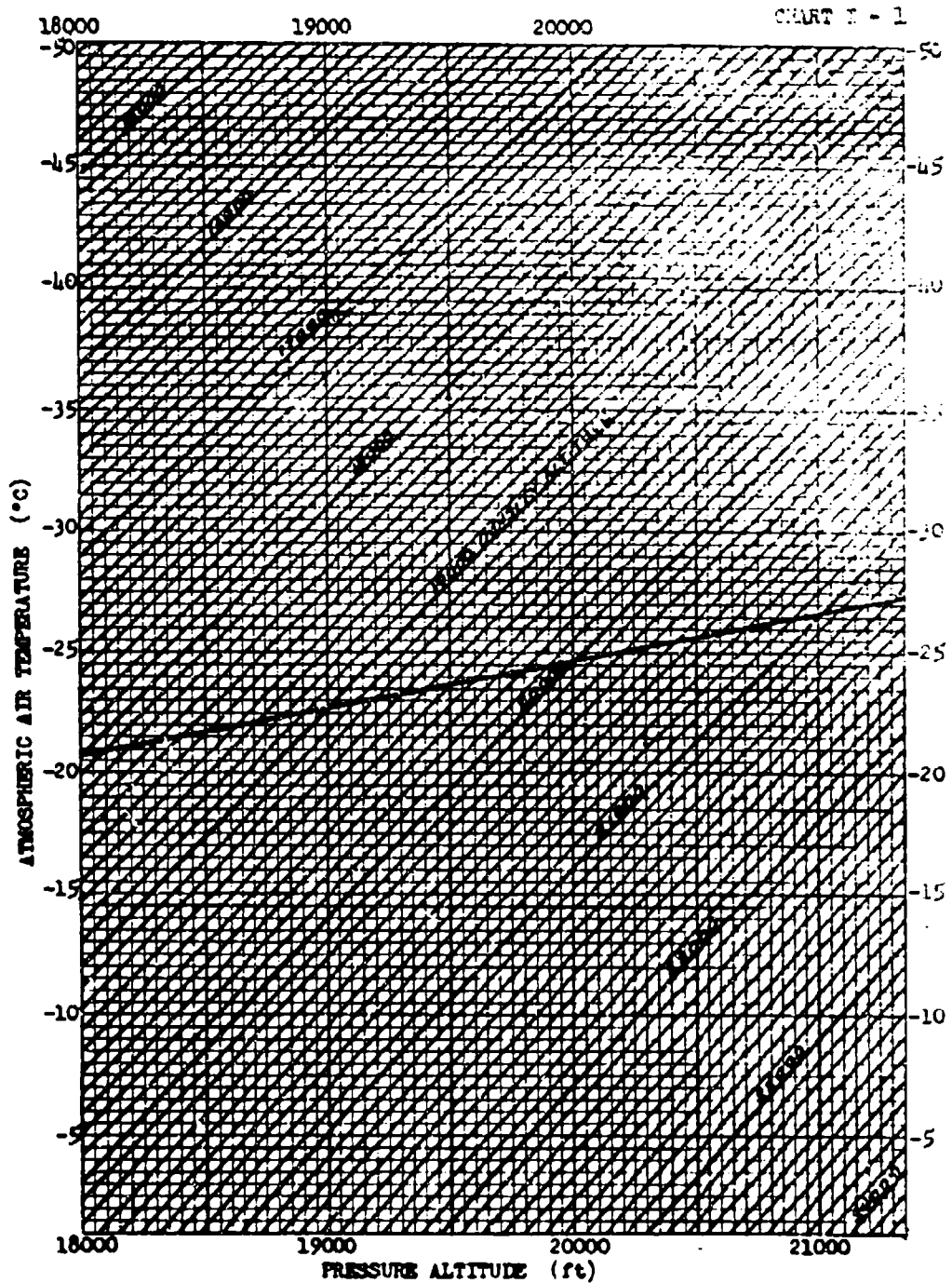


CHART I - 1

AFTR-6273



AFTR-6273

CHART I - 1

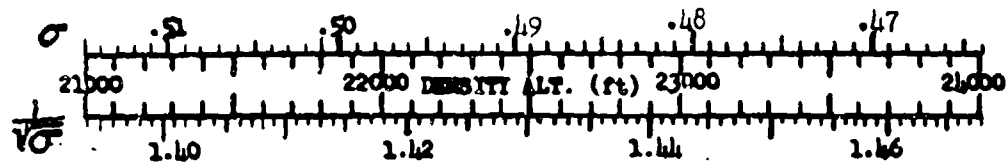
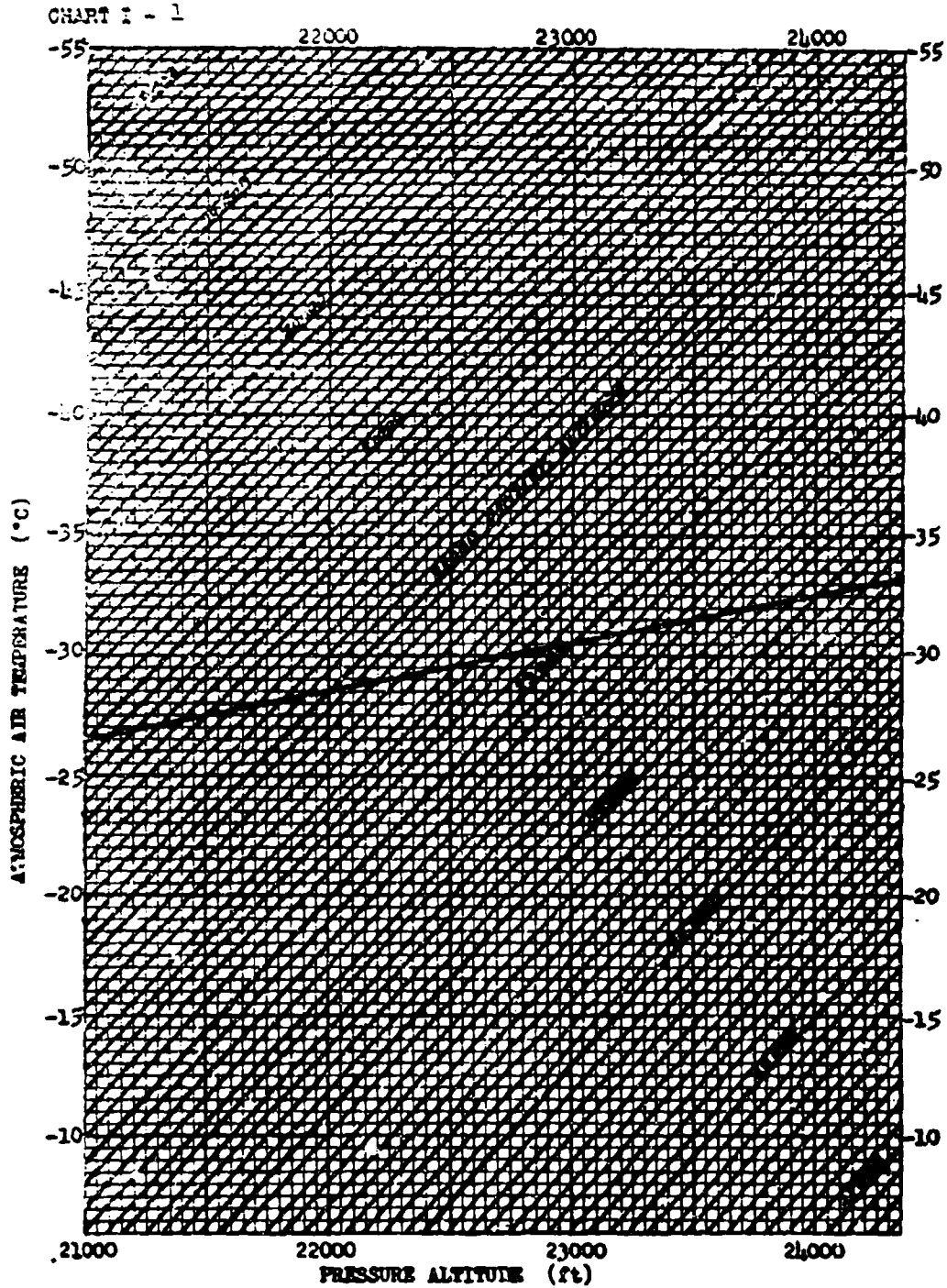
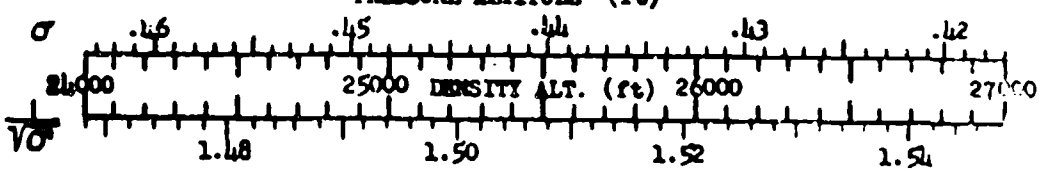
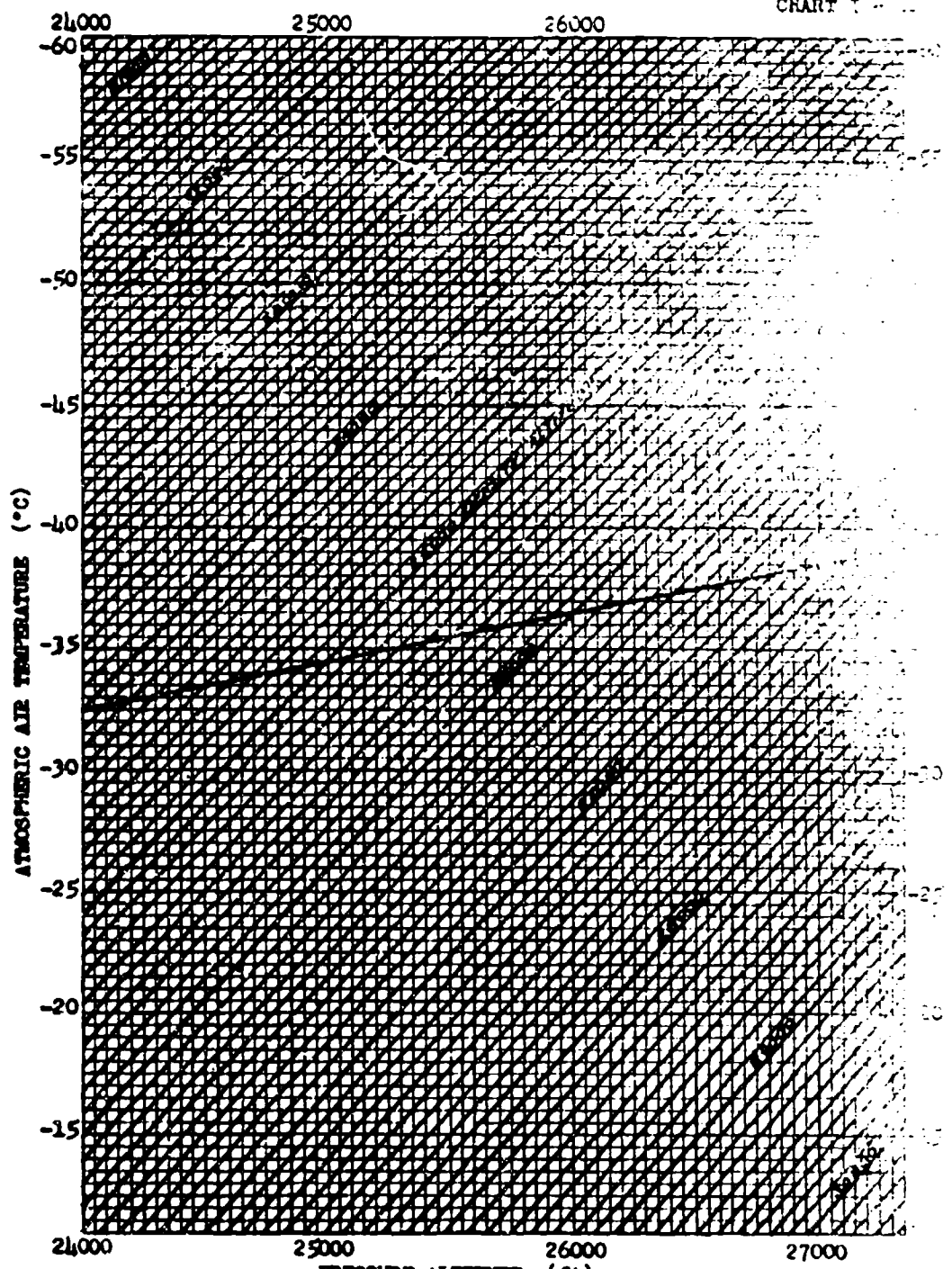


CHART I - 1

AFTR-6273



AFTN-6273

CHART I - 1

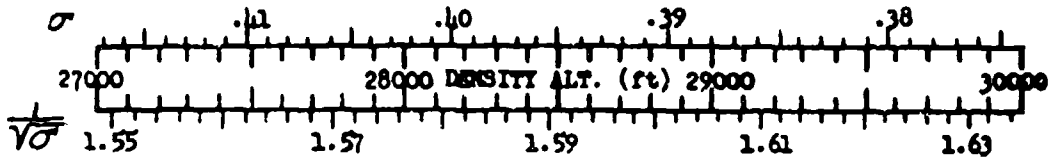
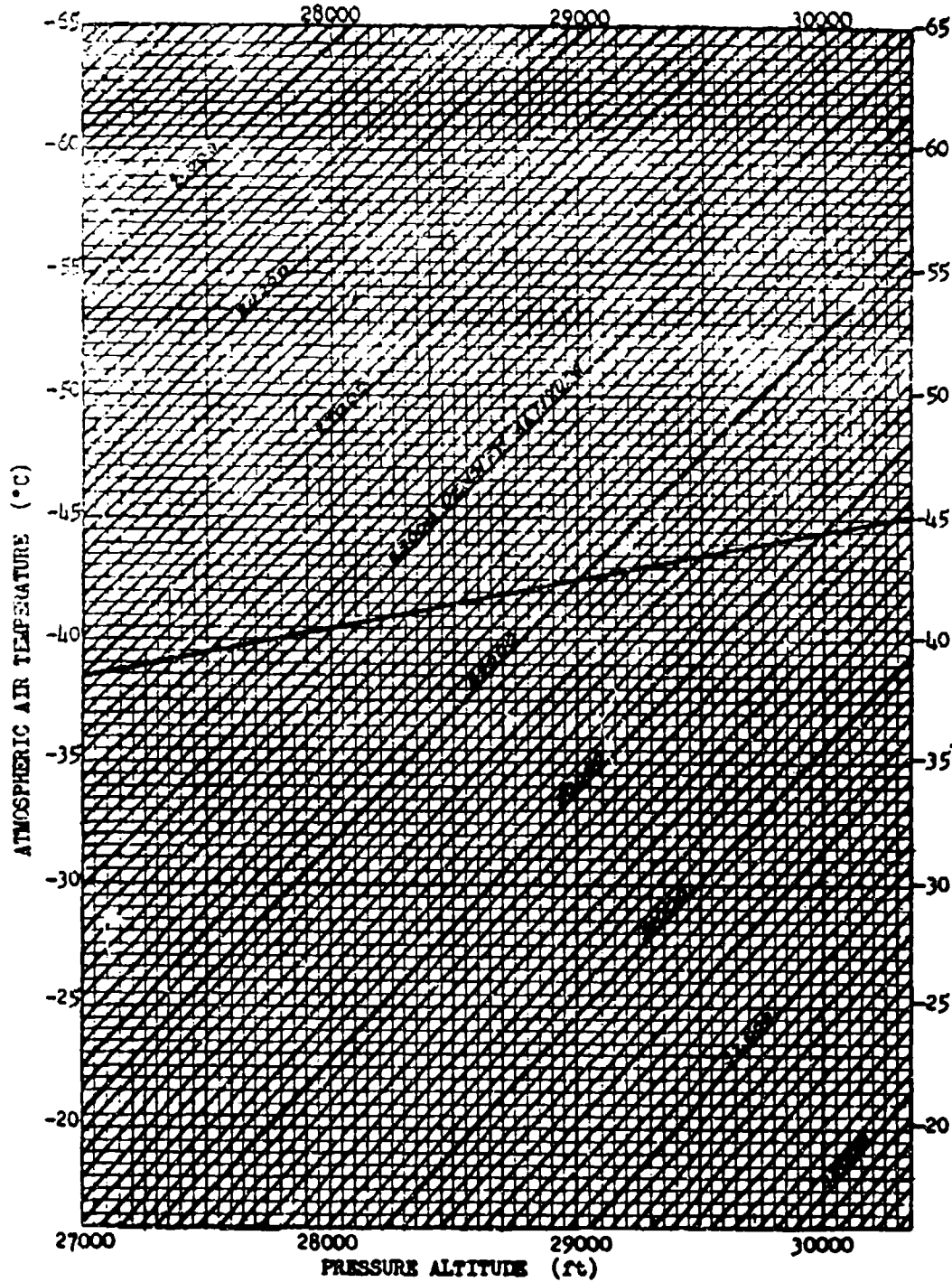
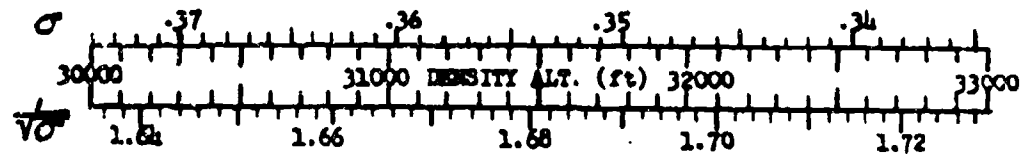
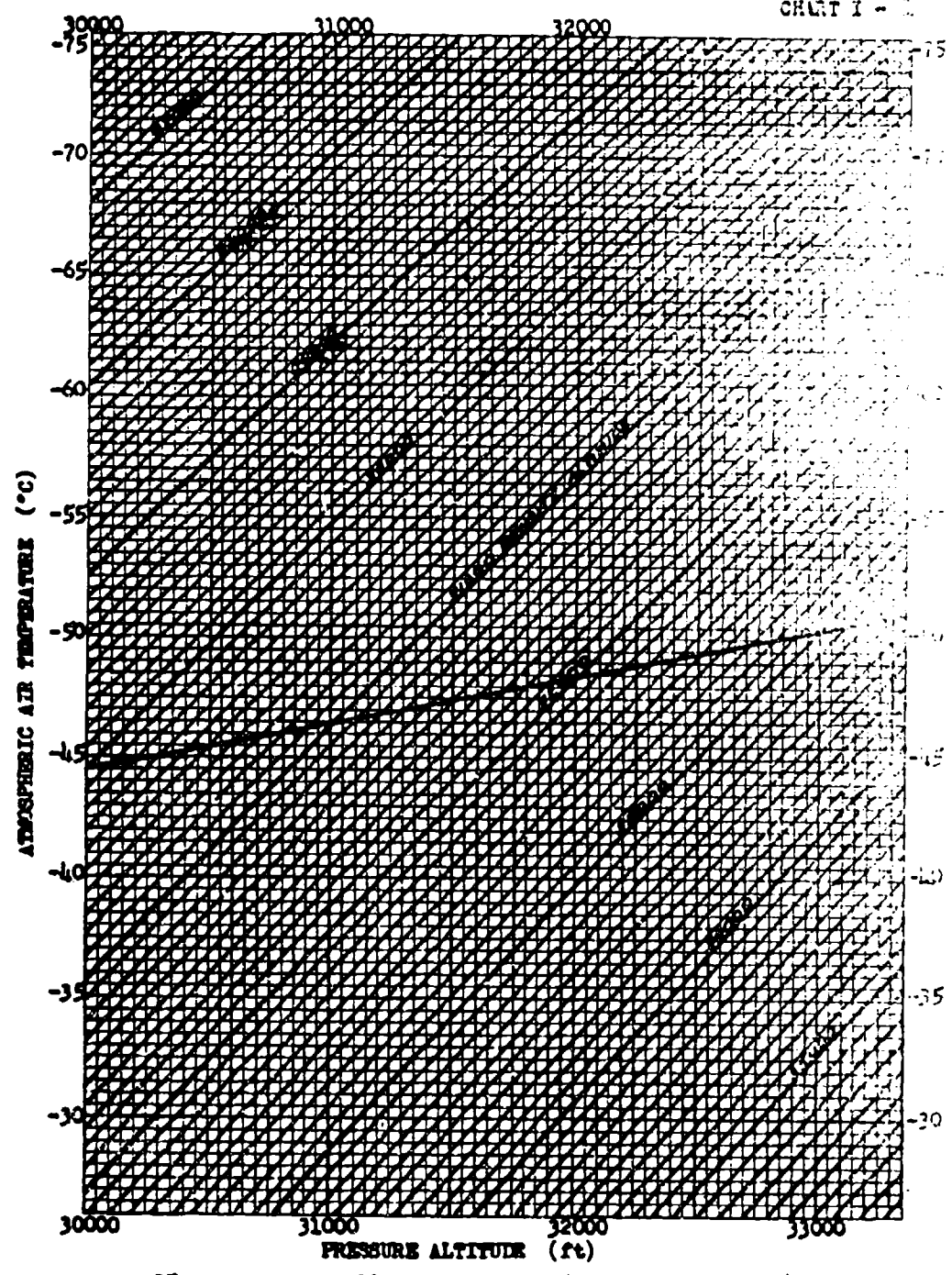


CHART I - 1

AFTR-6273



AFTR-6273

CHART I - 1

CHART I - 1

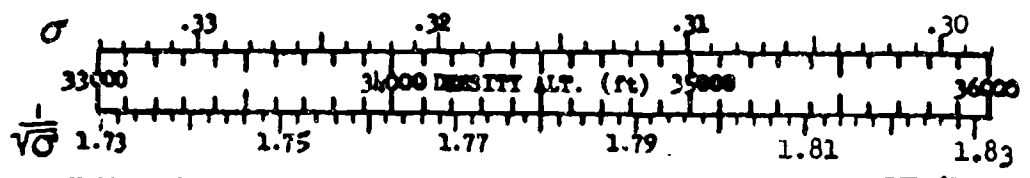
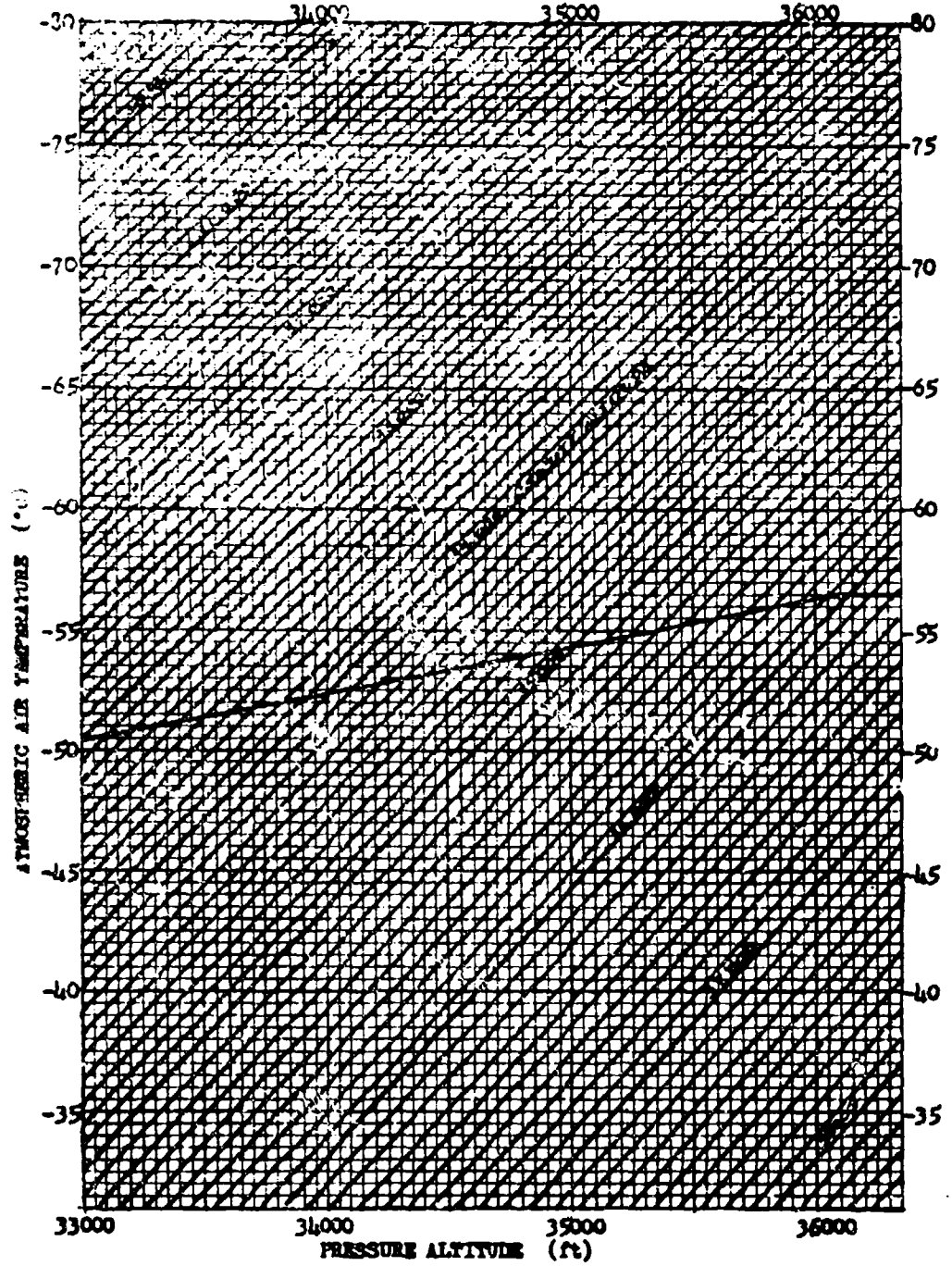
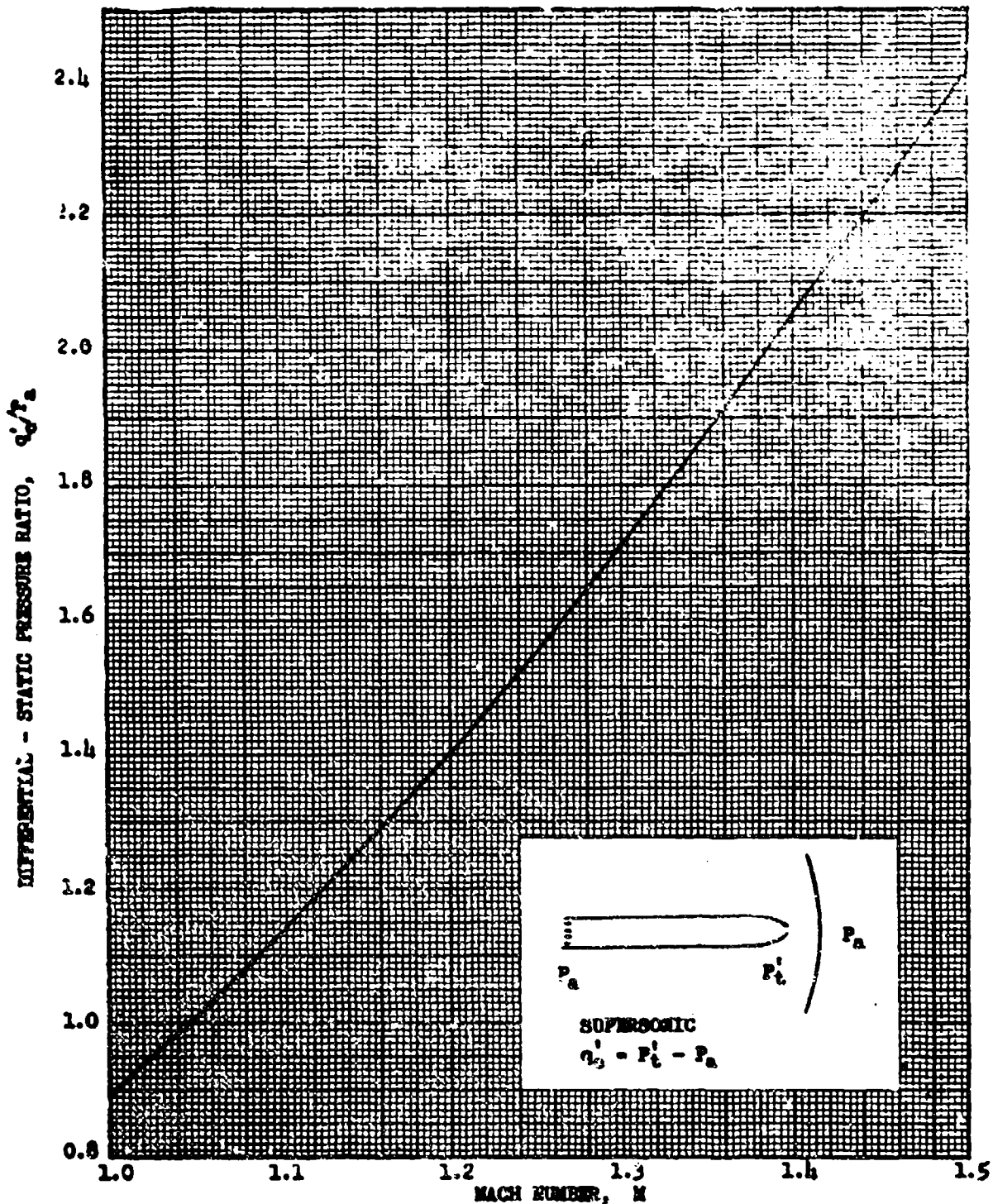


CHART I - 1

AFTR-6273

DIFFERENTIAL - STATIC PRESSURE RATIO vs MACH NUMBER
 (SUPERSONIC - NORMAL SHOCK CONDITIONS)

CHART I - 1



AFR 6273

CHART I - 2

CHART I - 3

REYNOLDS NO. - MACH NO. RATIO vs PRESSURE ALTITUDE

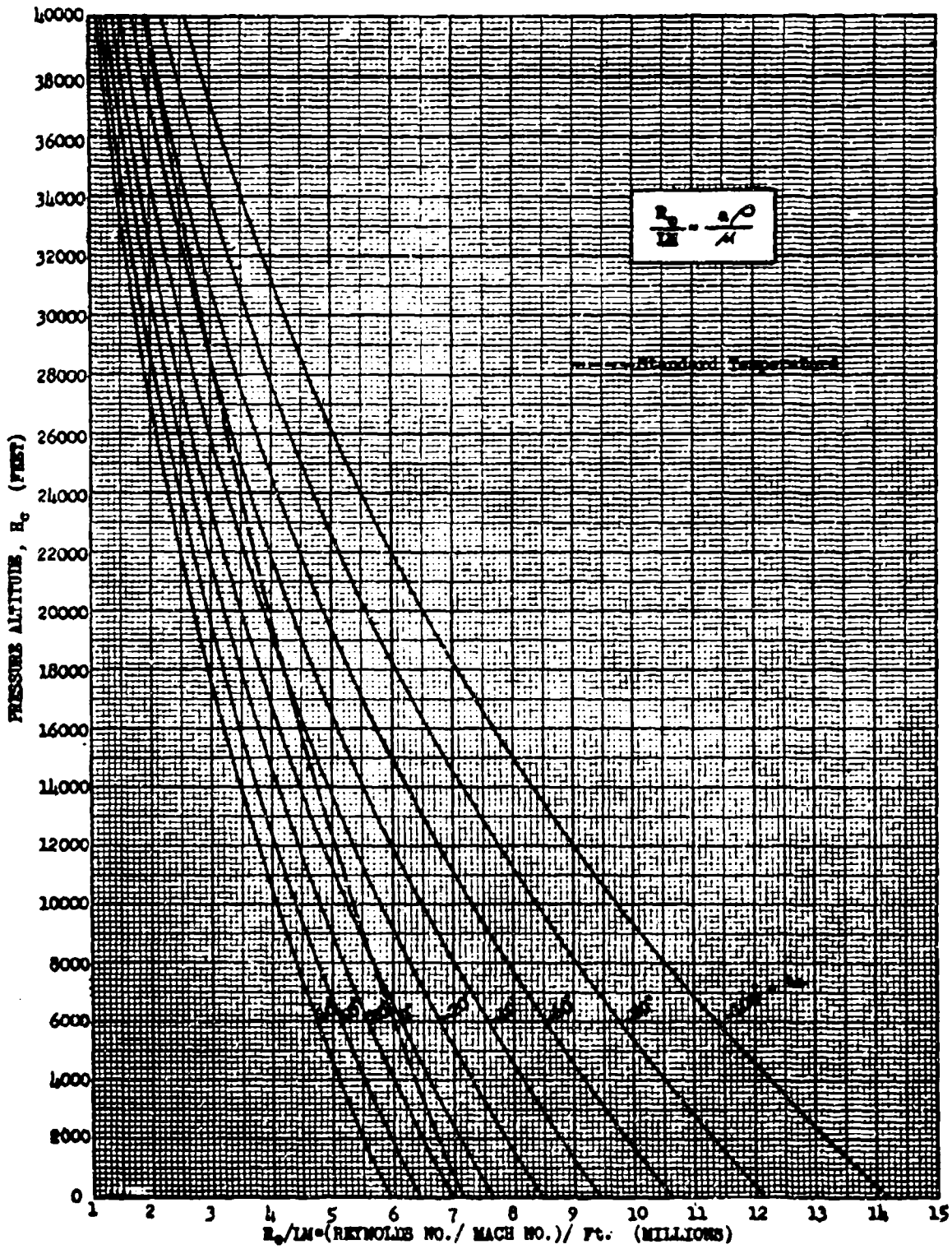
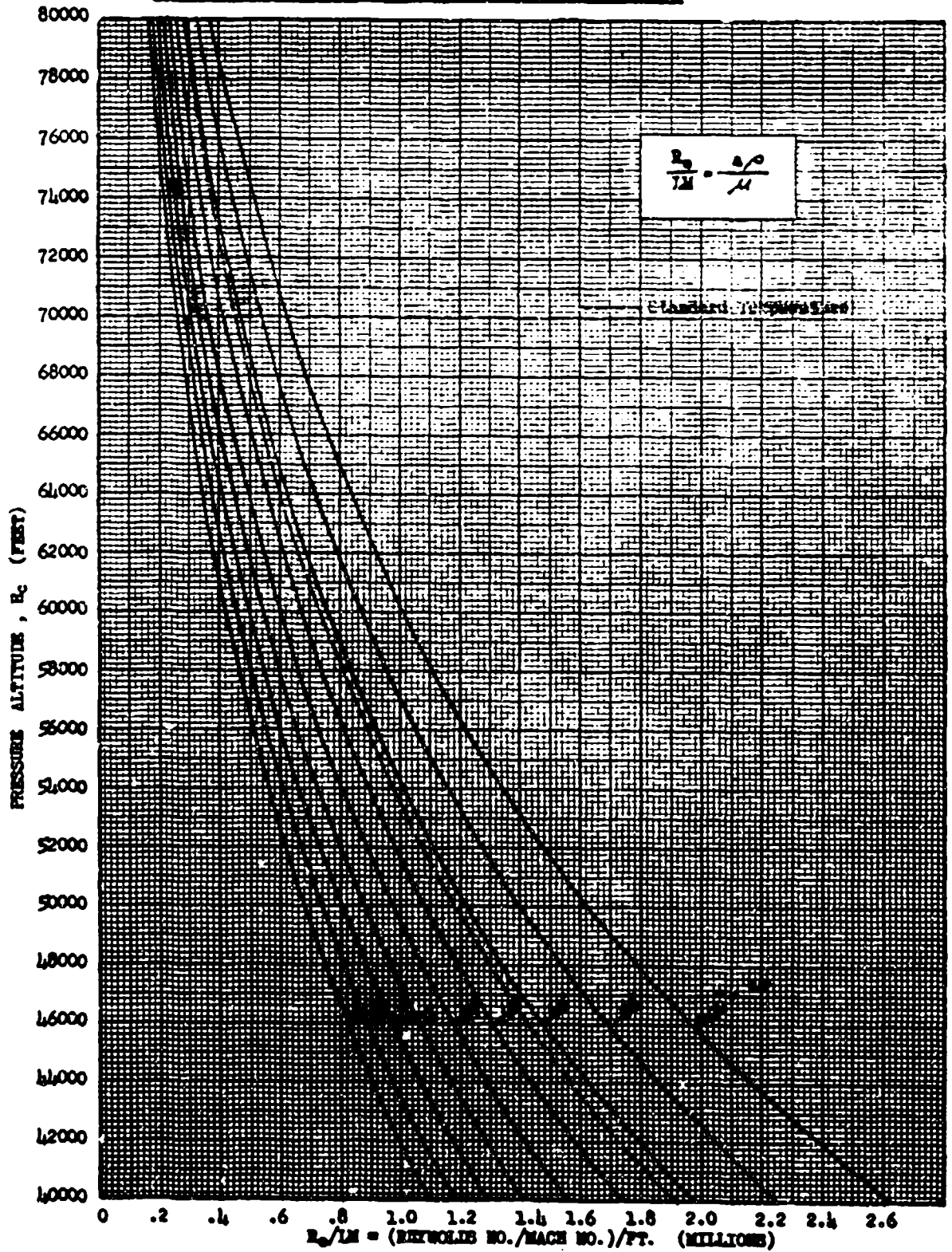


CHART I - 3

AFT 6273

REYNOLDS NO. - MACH NO. RATIO vs PRESSURE ALTITUDE

CHART I - 3



AFTER 6273

CHART I - 3

CHART I - 4

M vs P_t / P_a - ISENTROPIC FLOW

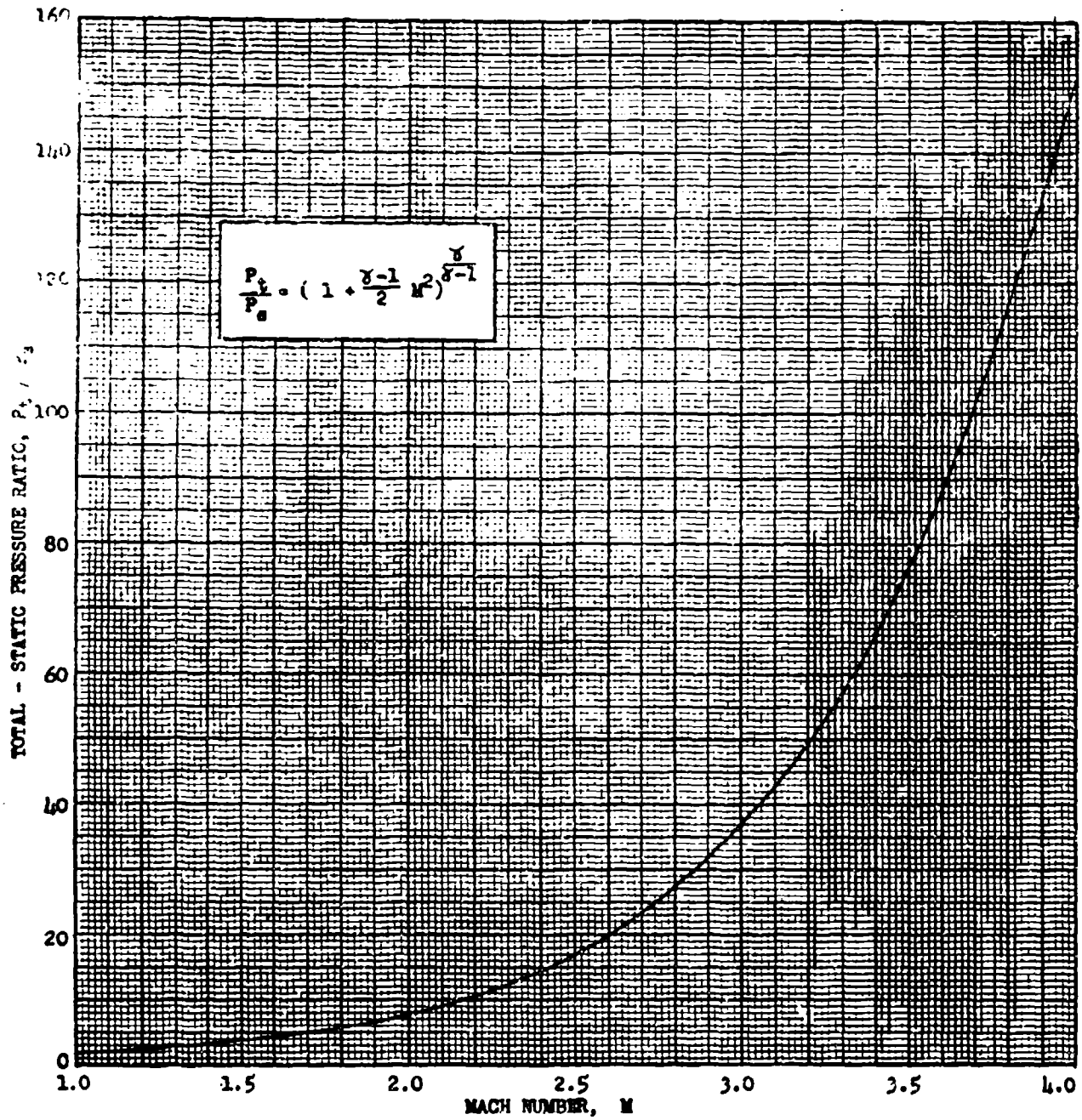


CHART I - 4

AFTR 6273

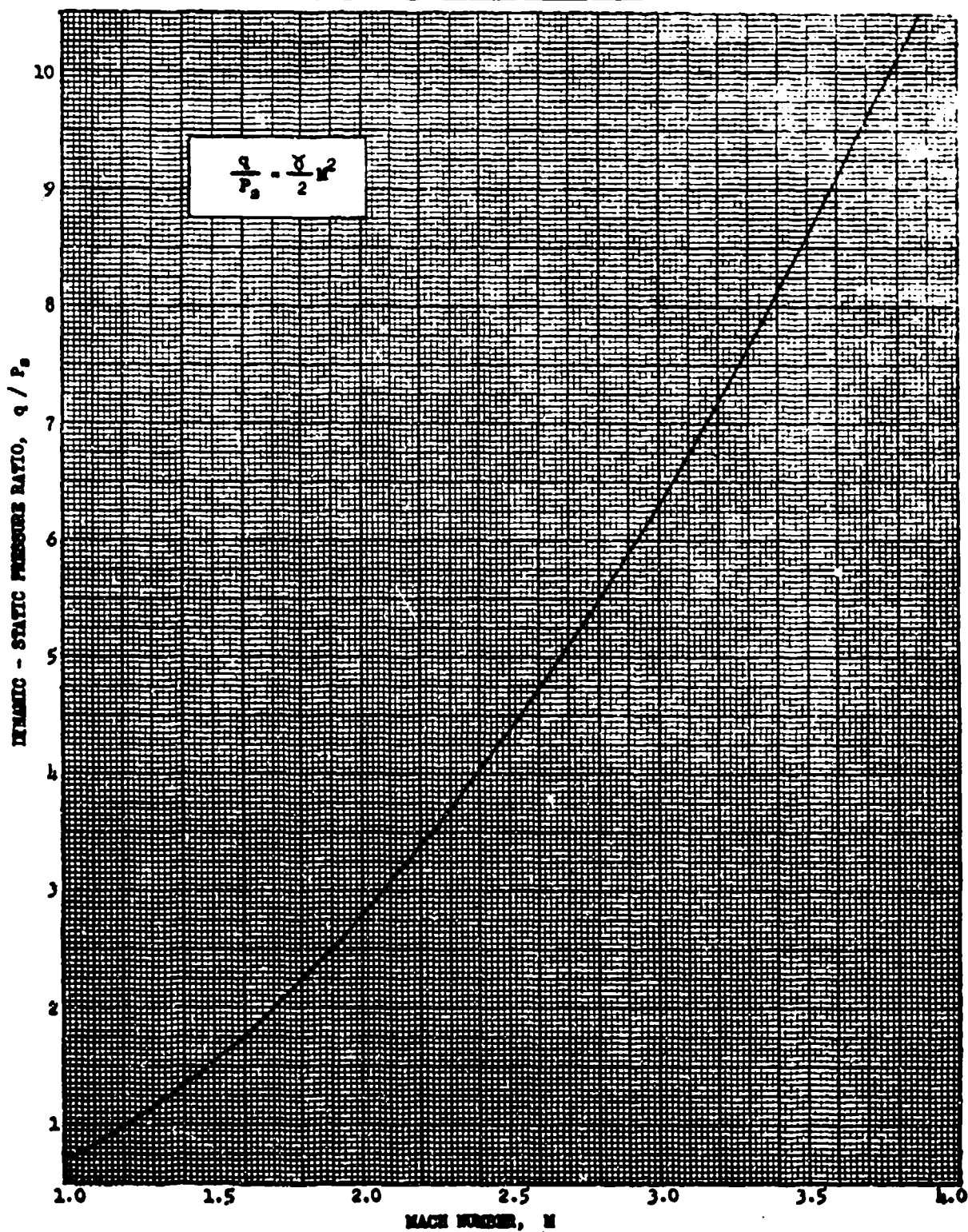


CHART I - 4

M vs q / P_t - ISENTROPIC FLOW

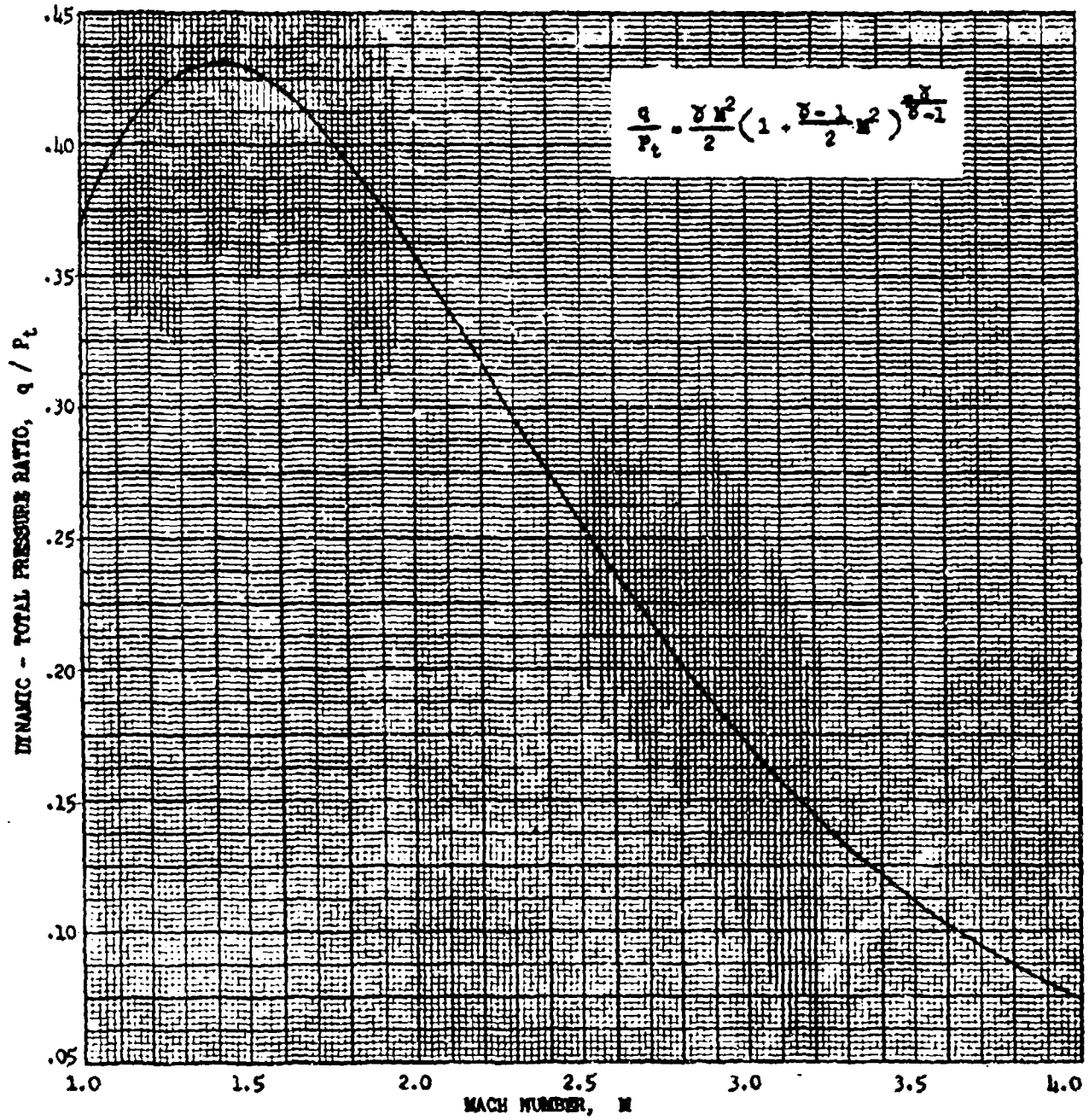


CHART I - 4

AFTI 6273

M vs ρ_t / ρ_s - ISENTROPIC FLOW

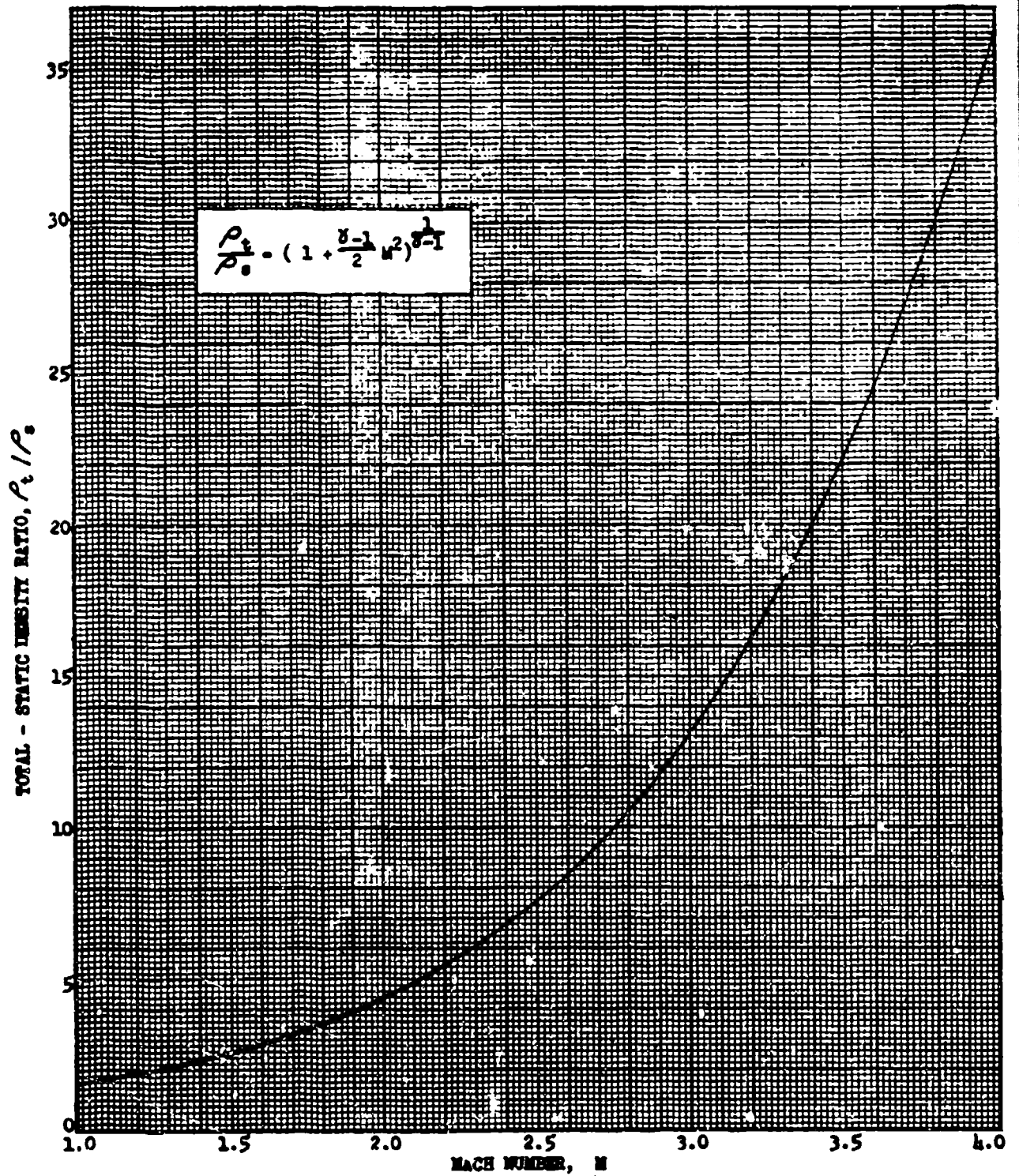


CHART I - 1

M vs T_t / T_s - ISENTROPIC FLOW

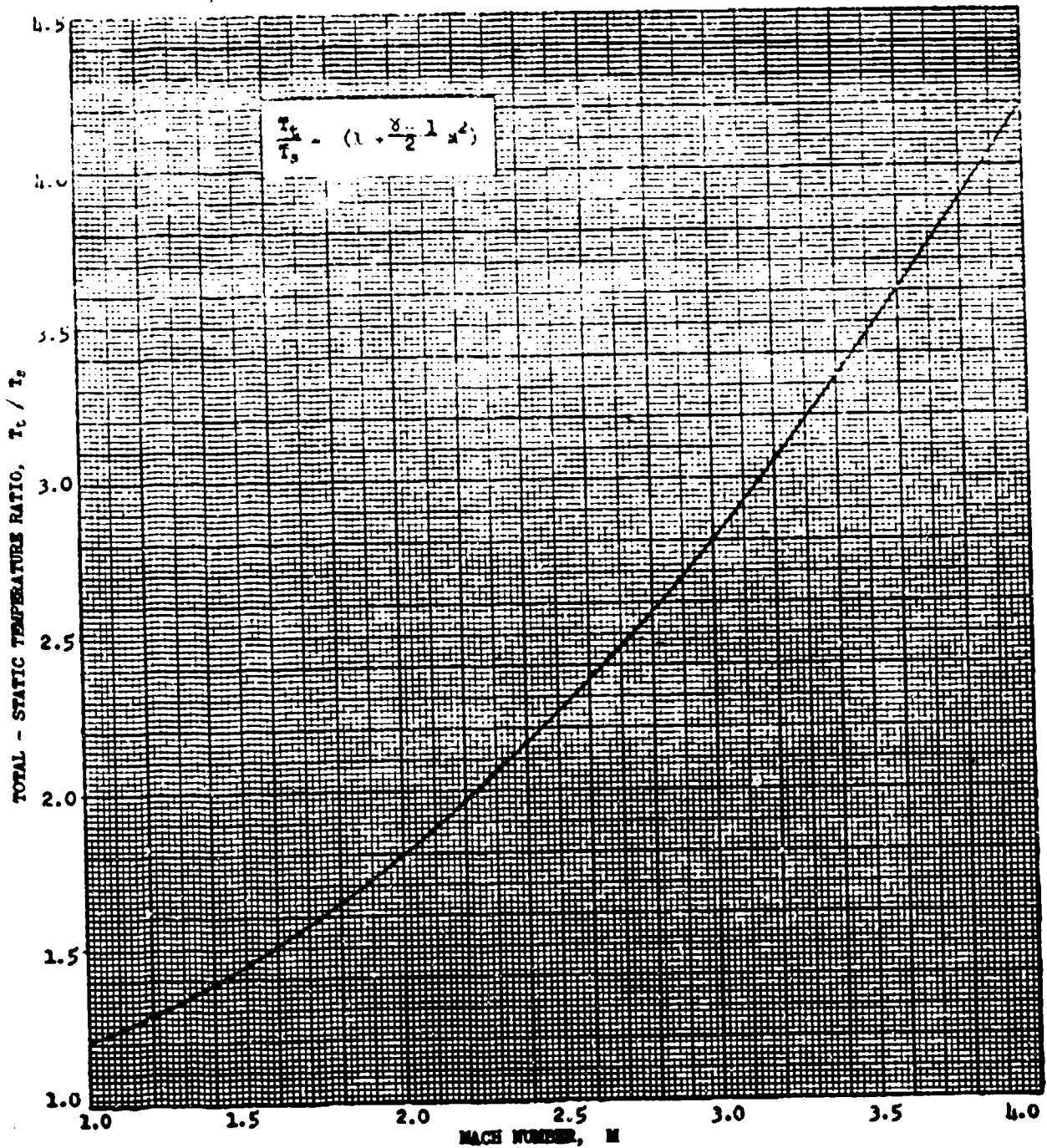
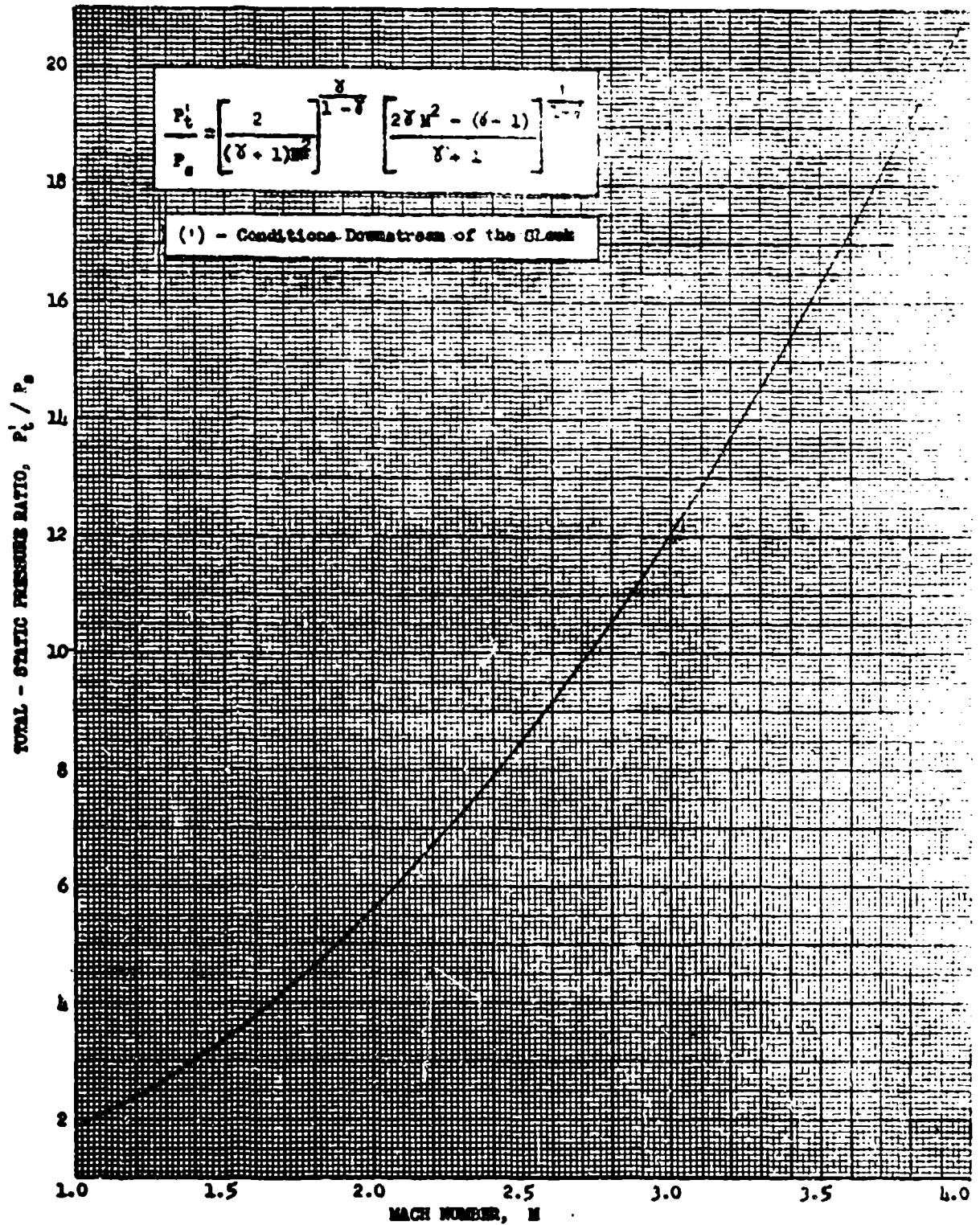


CHART I- 4

AFPR 6273



$$\frac{P_t^i}{P_o} = \left[\frac{2}{(\gamma + 1)M^2} \right]^{\frac{\gamma}{\gamma - 1}} \left[\frac{2\gamma M^2 - (\gamma - 1)}{\gamma + 1} \right]^{\frac{1}{\gamma - 1}}$$

(ⁱ) - Conditions Downstream of the Shock

CHART I - 5

M vs P_2' / P_2 - NORMAL SHOCK CONDITIONS - $\gamma=1.4$

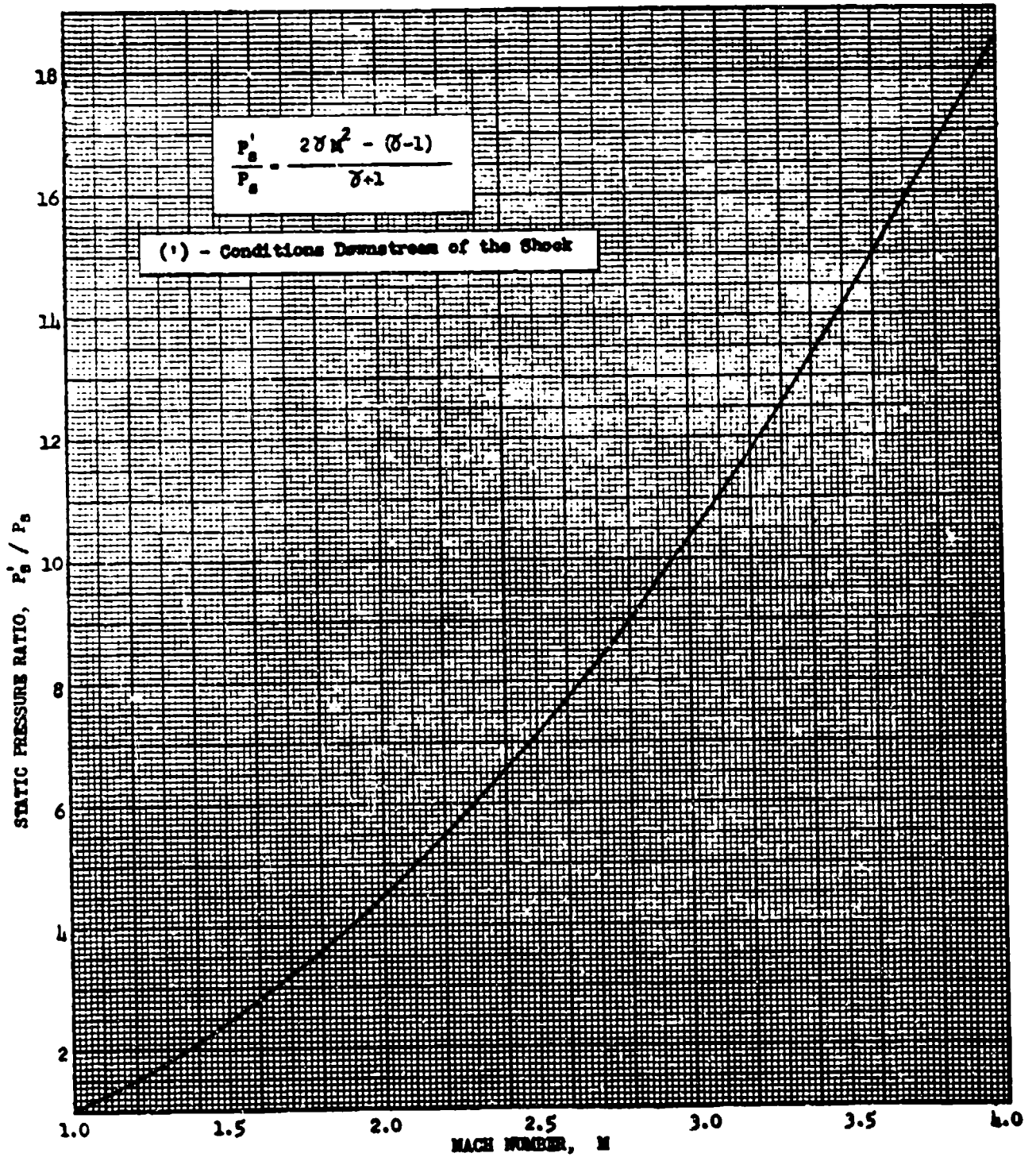


CHART I - 5

AFTR 6273

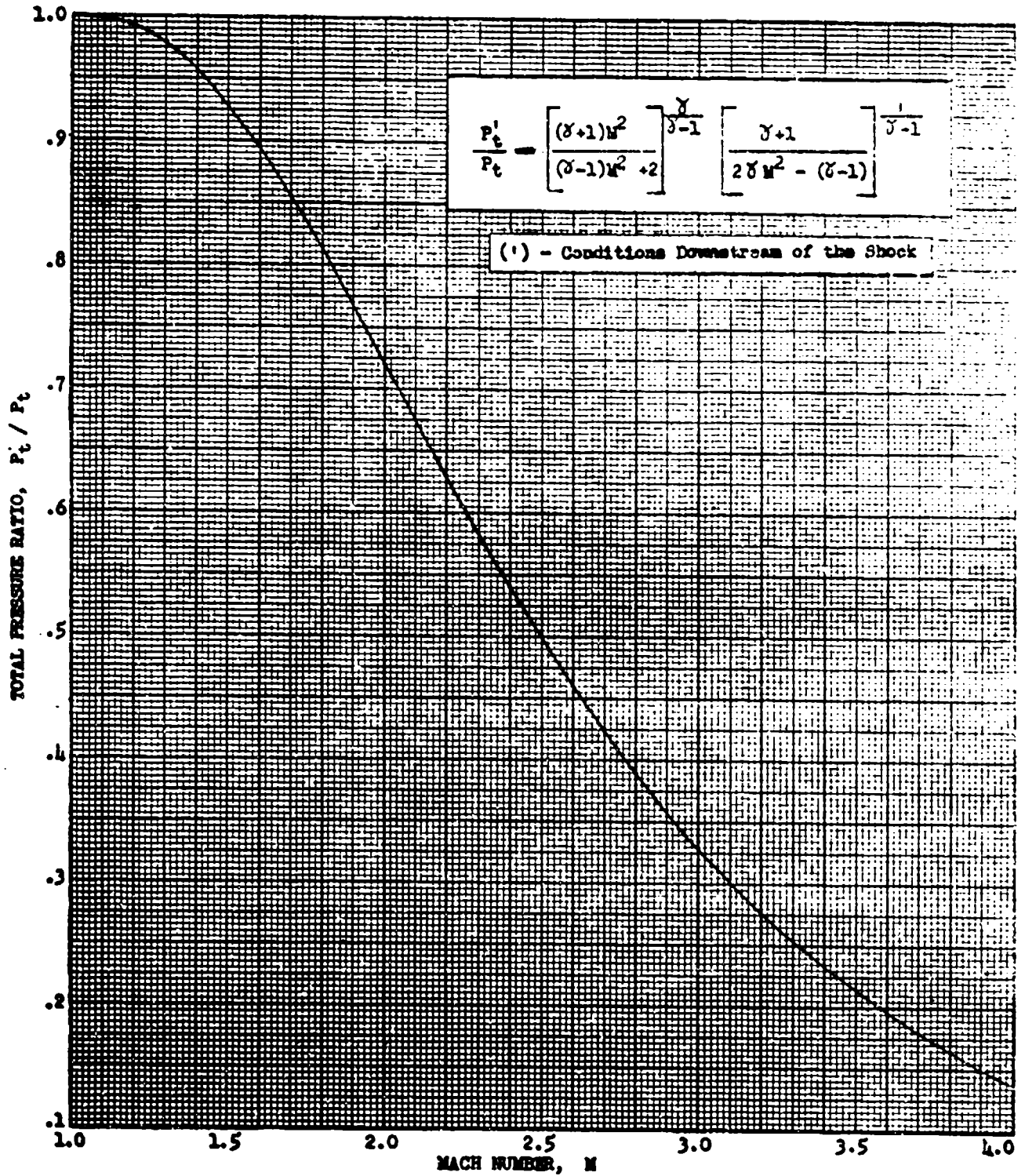


CHART I - 5

M vs ρ'_2/ρ_2 - NORMAL SHOCK CONDITIONS - $\gamma=1.4$

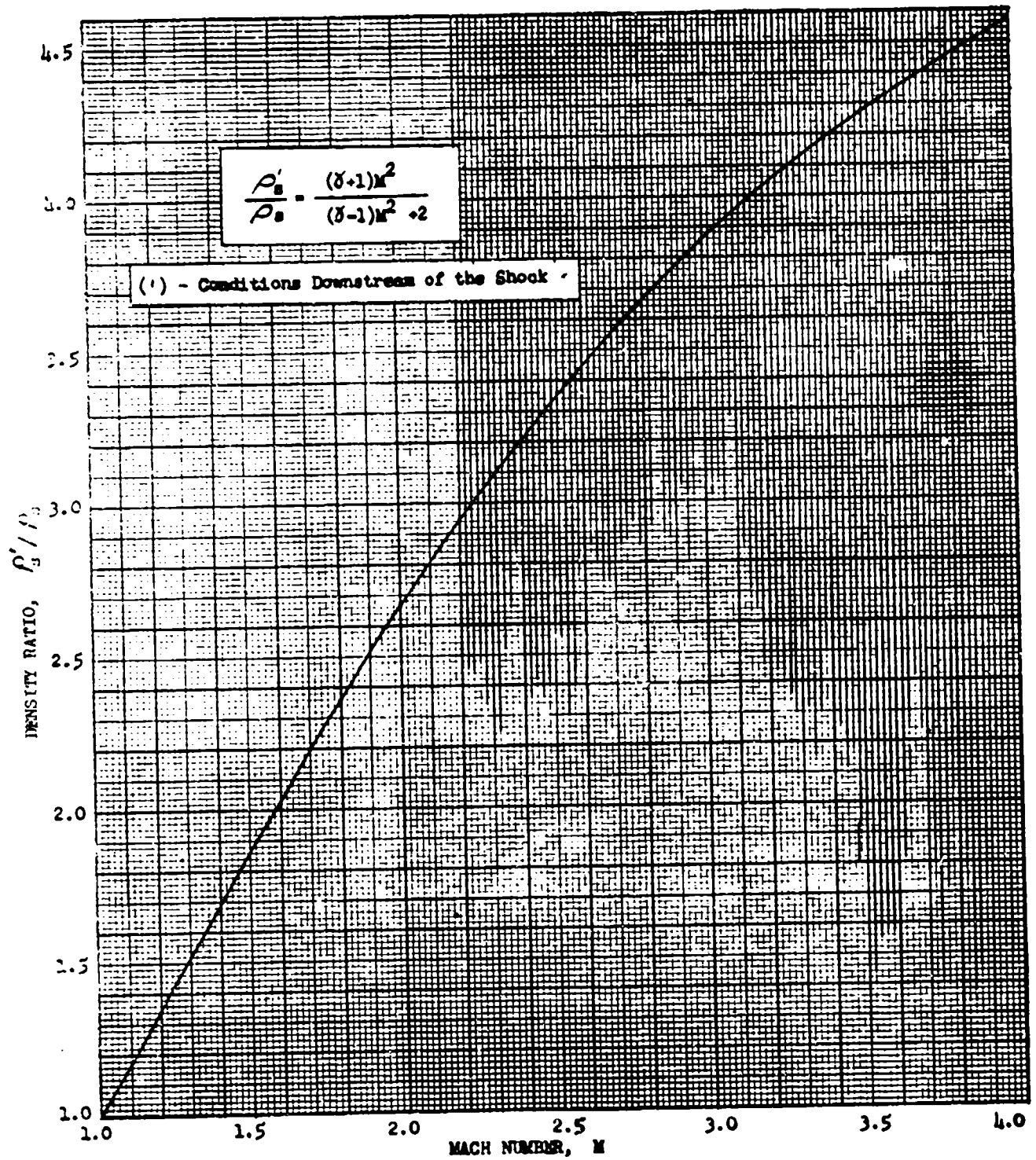
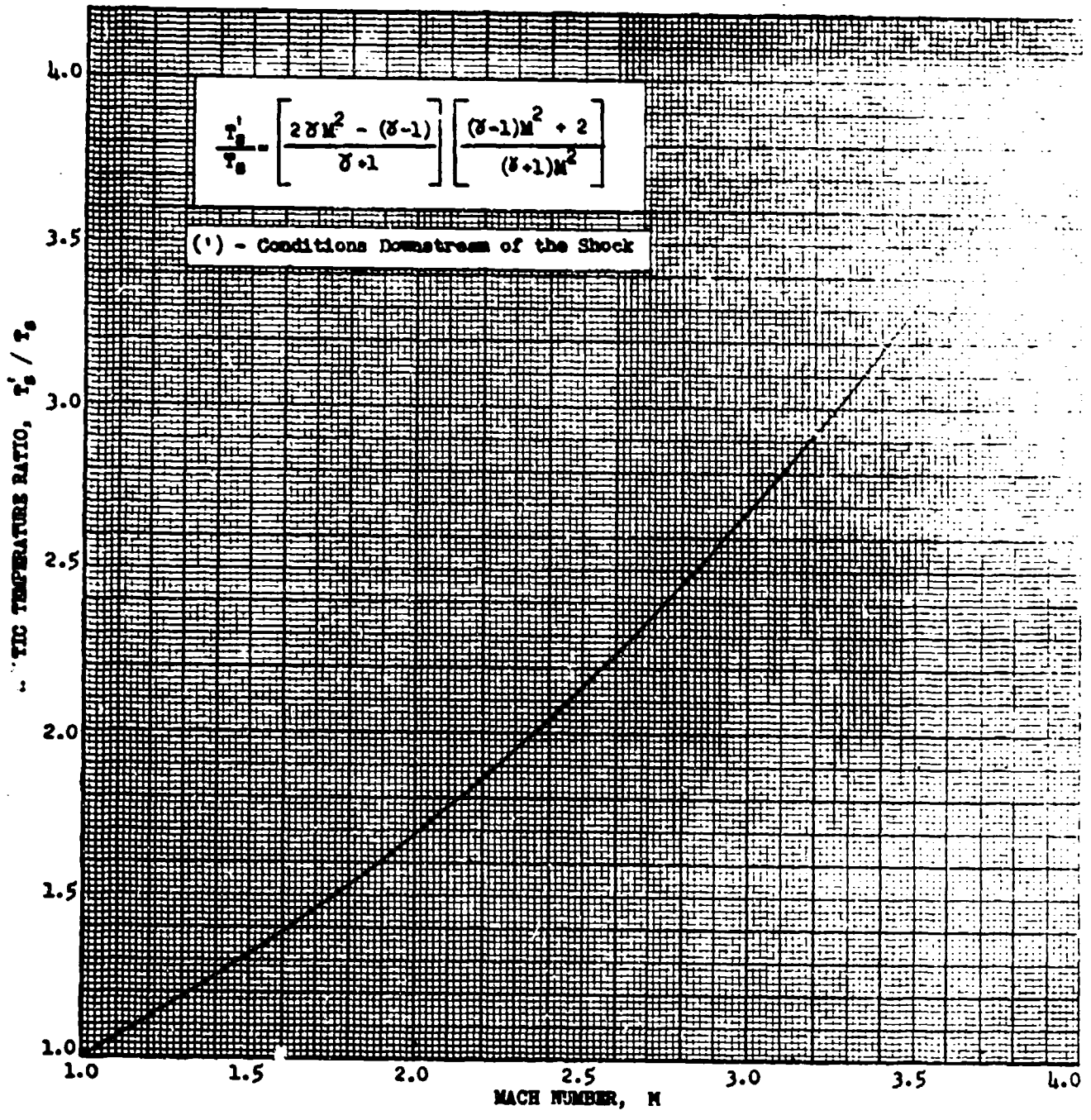


CHART I - 5

AFT 6273



AFT 6273

CHART I - 5

M vs M' - NORMAL SHOCK CONDITIONS - $\gamma=1.4$

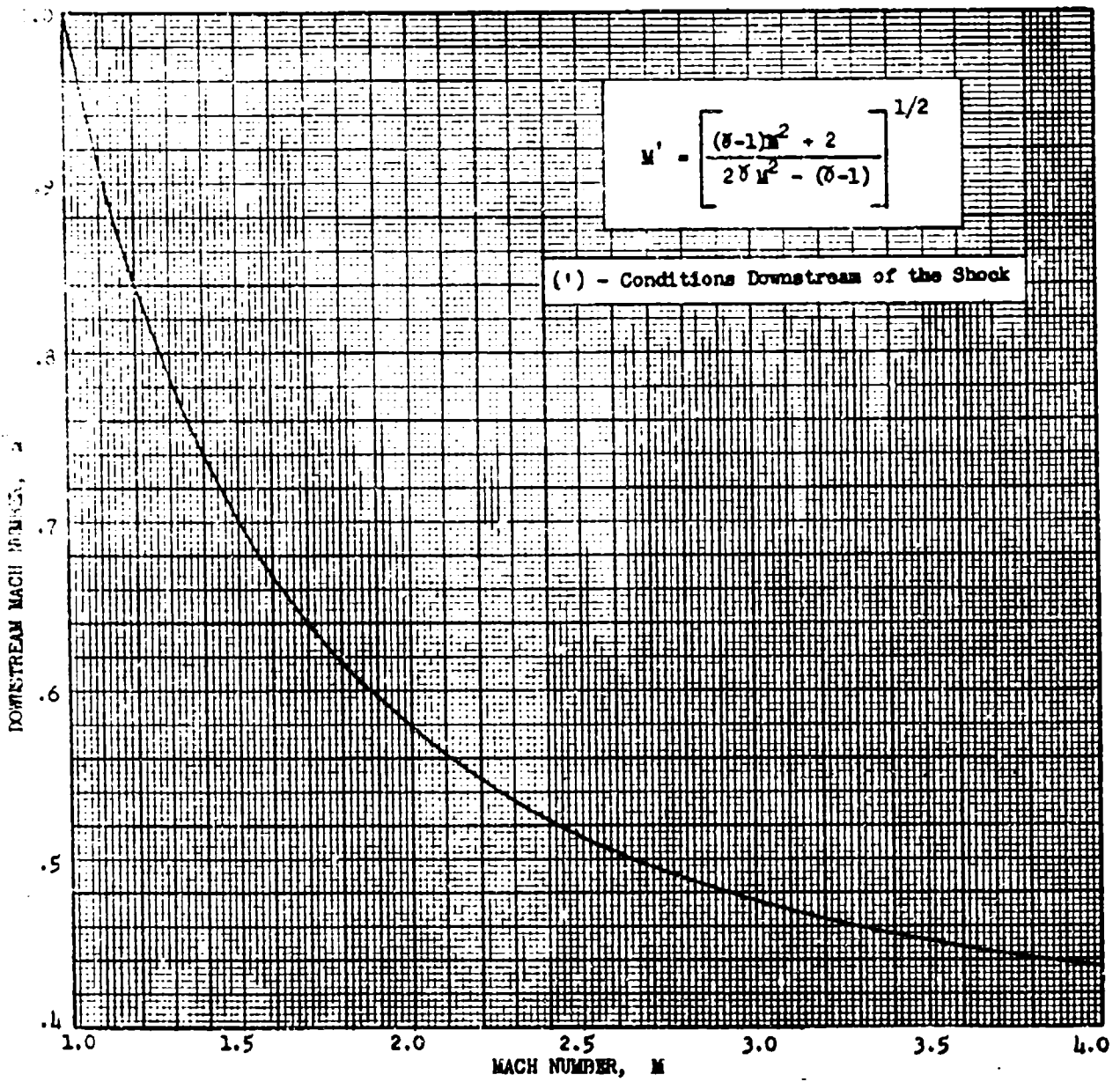
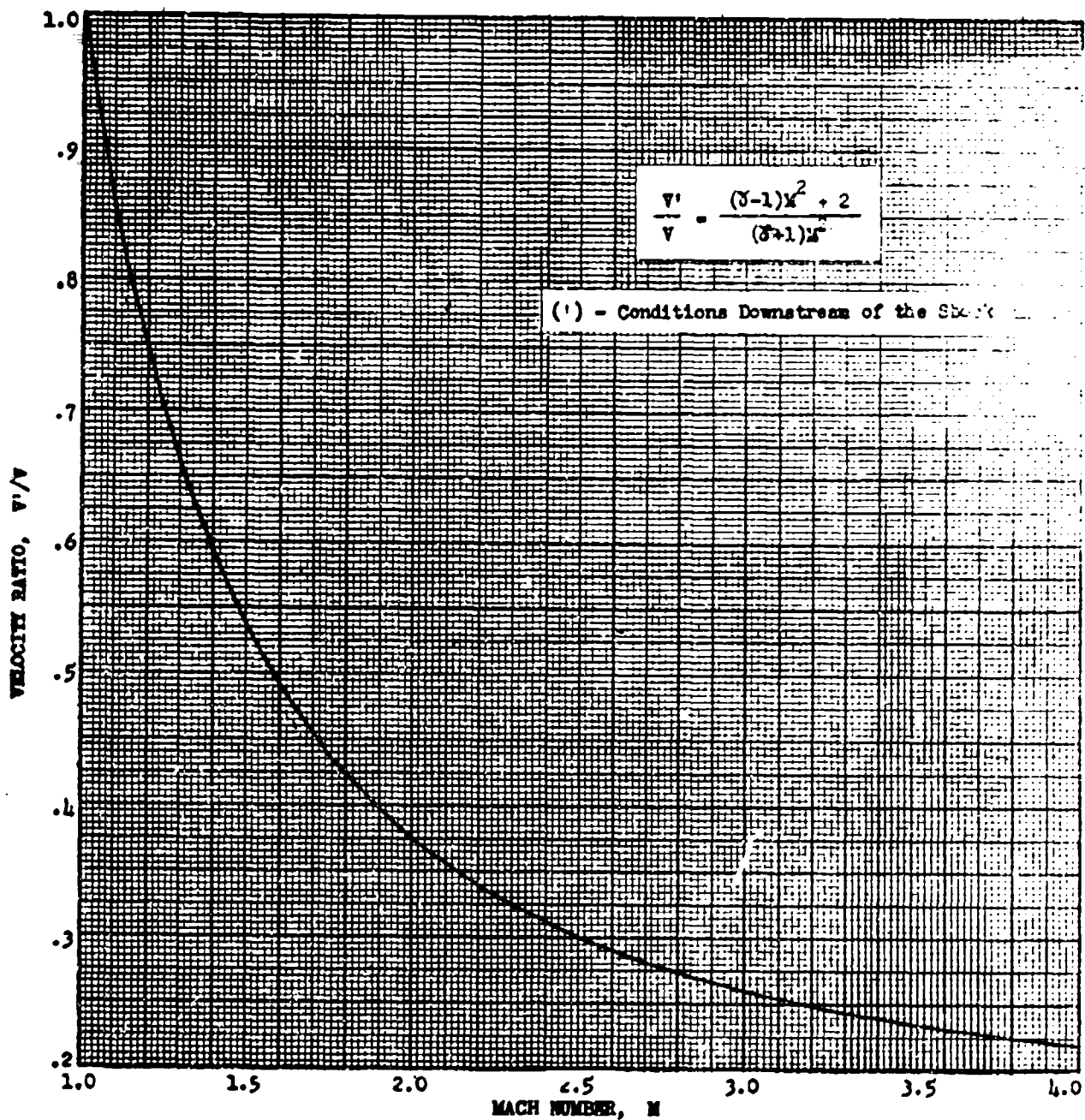
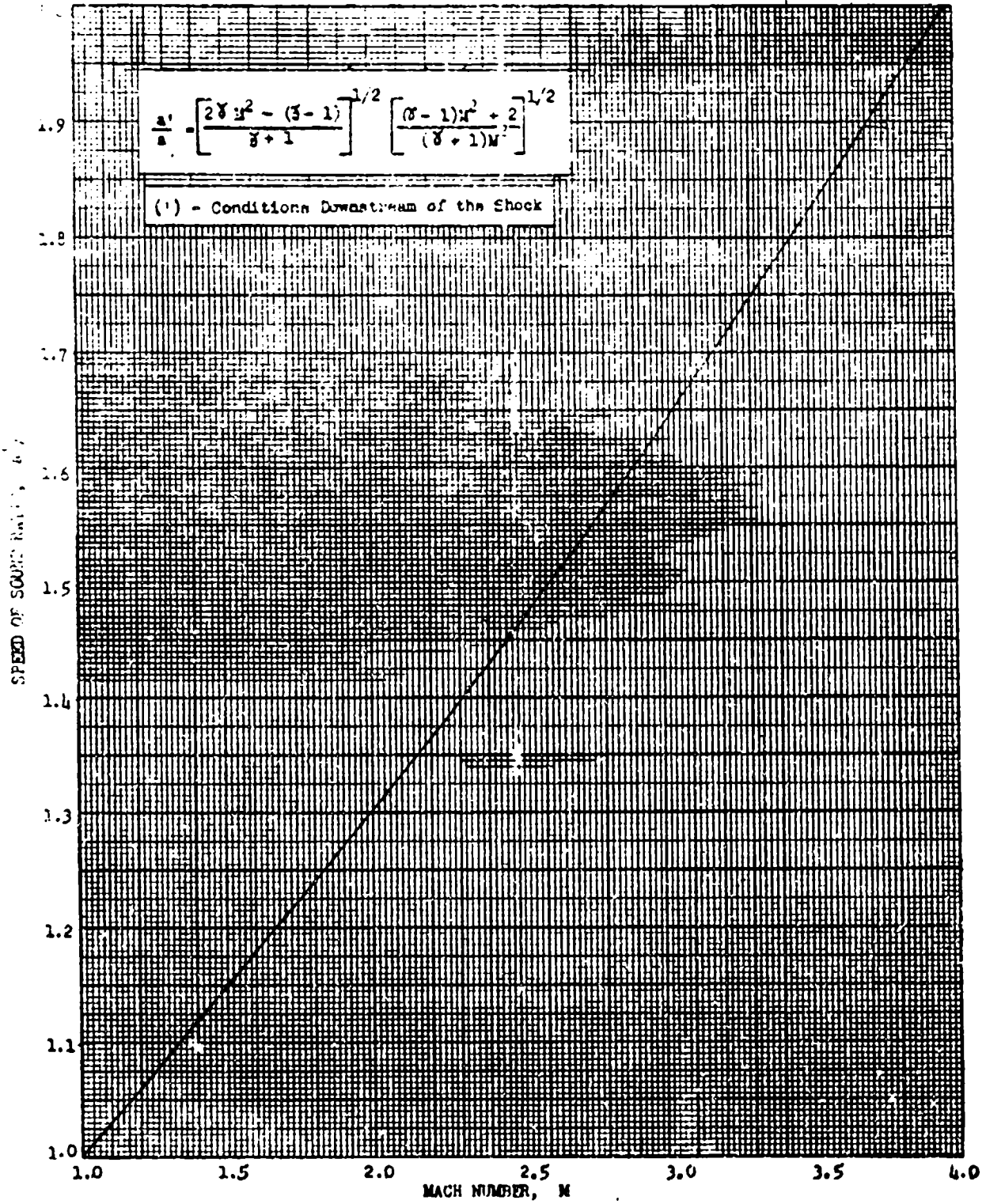


CHART I - 5

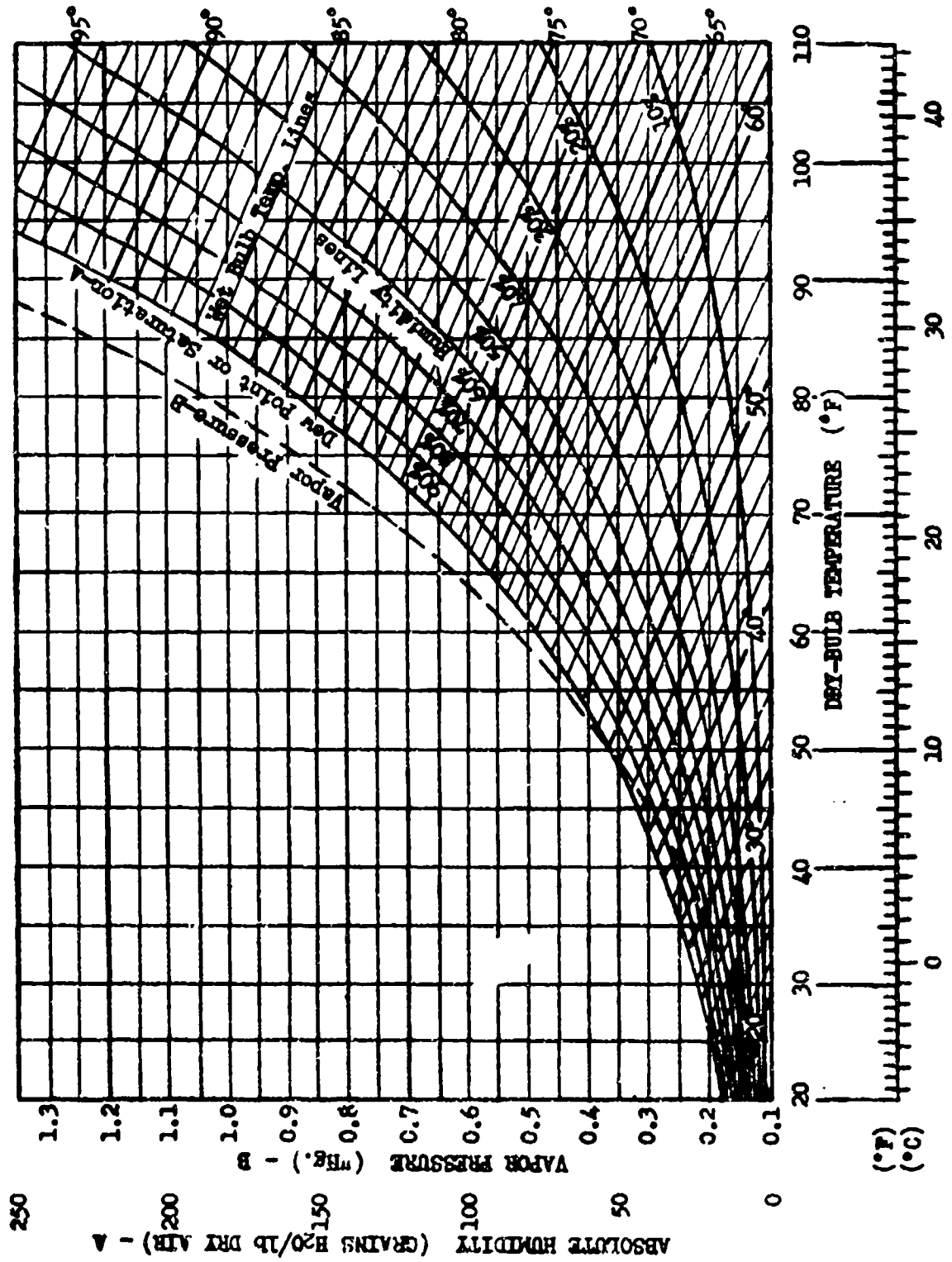
AFTR 6273





PSYCHROMETRIC CHART

CHART I - 6



AFIP-6273

8-33

CHART I - 6

APPENDIX II

NOMENCLATURE

CHART II-1

A	Area	ft ²
A _g	Jet Nozzle Area	ft ²
R	Aspect Ratio, b^2/S , b/c	
a	Velocity of Sound, $\sqrt{\gamma gRT}$	38.944 $\sqrt{^\circ K}$ Knots
a ₀	Velocity of Sound (Sea Level Standard)	761.06 mph 660.9 knots 1116 ft/sec
BHP	Brake Horsepower	550 ft-lbs/sec
BHP _{as}	Brake Horsepower (Available Standard)	550 ft-lbs/sec
BHP _{at}	Brake Horsepower (Available Test)	550 ft-lbs/sec
BHP _c	Brake Horsepower (Chart)	550 ft-lbs/sec
BHP _s	Brake Horsepower (Standard)	550 ft-lbs/sec
BHP _t	Brake Horsepower (Test)	550 ft-lbs/sec
BHP _{tos}	Brake Horsepower (Test at Standard Day Carburetor Temperature)	550 ft-lbs/sec
BSFC	Brake Specific Fuel Consumption	lbs/bhp-hr
c	Wing Chord	ft
°C	Degrees Centigrade	
C _D	Drag Coefficient, $C_D = \frac{2D}{\rho v^2 S} = \frac{D}{.7 P_a M^2 S} = \frac{D}{qS} = \frac{294.6D}{V_0^2 (\text{knots})^2 S}$	
C _{Di}	Induced Drag Coefficient, $\frac{C_L^2}{\pi Re}$	
C _{Df}	Profile Drag Coefficient, $C_D - C_{Di}$	
C _L	Lift Coefficient, $C_L = \frac{2W}{\rho v^2 S} = \frac{W}{.7 P_a M^2 S} = \frac{W}{qS} = \frac{294.6W}{V_0^2 (\text{knots})^2 S}$	
CAT	Carburetor Air Temperature	°C or °F

AFIP 6273

CHART II-1

CHART II-1

NOMENCLATURE

D	Aerodynamic Drag	lbs
dH_p	Altimeter Position Error, $H_{1c} - H_0$	ft
dH_{pc}	Altimeter Position Error Correction, $H_c - H_{1c}$	ft
dM_p	Mach Meter Position Error, $M_{1c} - M$	
dM_{pc}	Mach Meter Position Error Correction, $M - M_{1c}$	
dP_p	Static Pressure Position Error, $P_s - P_a$	"Hg
dP_{pc}	Static Pressure Position Correction, $P_a - P_s$	"Hg
dV_p	Air-speed Meter Position Error, $V_{1c} - V_c$	knots
dV_{pc}	Air-speed Meter Position Error Correction, $V_c - V_{1c}$	knots
dH	Pressure Altitude Increment	ft
dh	Tapeline Altitude Increment	ft
(dH_0/dt)	Rate of Climb (Altimeter)	ft/min
(dH/dV)	Altimeter-Air-speed Position Error Correction Ratio	ft/knot
(dM/dH)	Mach Number-Altimeter Position Error Correction Ratio	1/ft
(dM/dV)	Mach Number-Air-speed Position Error Correction Ratio	1/knot
(dV/dh)	Vertical Wind Gradient	knots/1000 ft
(dV_0/dH_0)	Air-speed-Altitude Change Ratio During Climb	knots/1000 ft
(dh/dt)	Rate of Climb (Tapeline)	ft/min
$(dh/dt)_a$	Rate of Climb (Tapeline, Accelerating Climb Speed)	ft/min
(dq_c/dV_0)	Impact Pressure-Calibrated Speed Change Ratio	"Hg/knot
E	Total Energy	foot-lbs
KBP	Exhaust Back Pressure	"Hg
KBP ₁	Exhaust Back Pressure (Indicated)	"Hg

CHART II-1

AFTR-6275

NOMENCLATURE

CHART II-1

EBP _s	Exhaust Back Pressure (Standard)	"Hg
EBP _t	Exhaust Back Pressure (Test)	"Hg
e	Partial Pressure of Water Vapor	"Hg
e	Airplane Efficiency Factor, $\frac{C_L^2}{C_{Di} \pi R^2}$	
F	Force or Thrust	lbs
°F	Degrees Fahrenheit	
F _o	Entrance Momentum per Second	lbs
F _{eff}	Thrust (Effective)	lbs
F _{effs}	Thrust (Effective Standard)	lbs
F _{efft}	Thrust (Effective Test)	lbs
F _g	Thrust (Gross)	lbs
F _n	Thrust (Net)	lbs
F _{na}	Thrust (Net Available)	lbs
F _{ne}	Thrust (Net Excess)	lbs
F _{nr}	Thrust (Net Required)	lbs
F _p	Thrust (Pressure)	lbs
F _v	Thrust (Velocity)	lbs
g	Acceleration of Gravity	32.174 ft/sec ²
H _o	Pressure Altitude (True), H _{1o} + ΔH _{po}	ft
H ₁	Pressure Altitude (Indicated)	ft
H _{1c}	Pressure Altitude (Indicated Instrument Corrected), H ₁ + ΔH _{1c}	ft
ΔH _{1c}	Altimeter Instrument Correction for H ₁	ft
ΔH ₁	Lag Correction to Altimeter	ft

AFIP 6273

CHART II-1

CHART II-1

NOMENCLATURE

ΔH_{po}	Position Error Correction to Altimeter	ft
"H ₂ O	Inches of Water	
"Hg	Inches of Mercury	
h	Tapeline Altitude	ft
IAS	Indicated Air Speed	knots or mph
in	Inches	
K	Total Temperature Recovery Factor	
°K	Degrees Kelvin	
K _g	Jet Nozzle Gas Flow Calibration Factor	
	$K_g = \frac{W_g \text{ actual}}{W_g \text{ theor.}}$	
Kmh	Kilometers per hour	
K _t	Jet Nozzle Gross Thrust Calibration Factor	
	$K_t = \frac{F_g \text{ actual}}{F_g \text{ theor.}}$	
k	Any Constant	
L	Lift Force	lbs
L	Length	ft
lb	Pound	
M	Mach Number (Free Stream), V/a	
M	Meter	
M _{alt}	Mach Number at Altitude for Same V_o , Relative to Mach Number at Sea Level for Same V_o	
M _i	Mach Number (Indicated)	
M _{ic}	Mach Number (Indicated Instrument Corrected, $M_i + \Delta M_{ic}$, or Mach Number Computed from V_{ic} and H_{ic})	

NOTATION

CHART II-1

ΔM_{10}	Mach Meter Instrument Correction for M_1	
ΔM_{p0}	Mach Meter Position Error Correction, $M - M_{10}$	
M_{SL}	Mach Number at Sea Level for Same V_0	
M.A.C.	Mean Aerodynamic Chord	
Min	Minutes	
MP	Manifold Pressure	"Hg
MP Δt	Temperature Corrected Manifold Pressure	"Hg
ΔMP_a	Manifold Pressure Correction for Air Only Stage	"Hg
ΔMP_f	Manifold Pressure Correction for Fuel-Air Mixture Stage	"Hg
MP _s	Manifold Pressure (Standard)	"Hg
MP _t	Manifold Pressure (Test)	"Hg
N	Engine RPM	rpm
N_{10}	Engine RPM Corrected for Instrument Error	rpm
N_r	Engine RPM Required	rpm
N_{IV}	$N \sqrt{\sigma} / (W_t/W_e)^{1/2}$	rpm
N_w	Weight Corrected RPM	rpm
P	Power	ft-lbs/time
P_a	Atmospheric Pressure at Pressure Altitude	"Hg
ΔP_p	Static Pressure Source Position Error	"Hg
P_d	Test Carburetor Deck Pressure	"Hg
ΔP_{10}	Pressure Instrument Correction	"Hg
P_s	Static Pressure (At a Point in a System)	"Hg
P_{s1}	Static Pressure (At a Point in a System Following Normal Shock Wave, or Under Lag Conditions)	"Hg
P_{s1}	Static Pressure (Indicated)	"Hg

AFR-6275

CHART II-1

CHART II-1

NOMENCLATURE

P_{SL}	Atmospheric Pressure (Sea Level Standard)	29.9212 "Hg
P_t	Total Flow Pressure	"Hg
P'_t	Total Flow Pressure	"Hg
P_{t2}	Total Flow Pressure (Jet Engine Compressor Inlet)	"Hg
P_{t1}	Total Flow Pressure (Indicated)	"Hg
P_{tj} or P_{t8}	Total Flow Pressure (Jet Nozzle)	"Hg
P_i	P_a/P_{SL}	
$(P_2/P_1)_a$	Carburetor Deck-Ambient Pressure Ratio	
$(P_2/P_1)_f$	Manifold Pressure-Carburetor Deck Pressure Ratio (For Fuel-Air Mixture)	
psf	Pounds per Square Foot	
psi	Pounds per Square Inch	
FTW	$BEP \sqrt{\sigma} / (W_t/W_a)^{3/2}$	ft-lbs/time
q	Dynamic Pressure, $q = \frac{\rho V^2}{2} = .7 P_a M^2$	lb/ft ²
q_o	Impact or Differential Pressure, $P_t - P_a$	"Hg
q'_o	Differential Pressure	"Hg
q_{ic}	Differential Pressure Corresponding to V_{i0} , $P_t - P_a$	"Hg
R	Gas Constant	96.04 ft/°K 53.355 ft/°R
R	Viscous Damping, $32 \mu L/D^2 A$	lbs-sec/ft ⁵
°R	Degrees Rankine	
Rg	Range	nautical air miles or statute air miles
R_e	Reynolds Number, VL/ν	
R/C	Rate of Climb (Standard Day Speed, Test Power and Weight), $(dH_o/dt) \sqrt{T_{at}/T_{as}}$	ft/min

NOMENCLATURE

CHART II-1

$(R/C)_s$	Rate of Climb (Standard), $R/C + \Delta R/C_2 + \Delta R/C_3 + \Delta R/C_1$	ft/min
$(R/C)_t$	Rate of Climb (Test), $(dH_0/dt) (T_{at}/T_{as})$	ft/min
(R/D)	Rate of Descent	ft/min
S	Wing Area	ft ²
S	Take-off Ground Roll Distance	ft
S'	Take-off Air Distance to 50' Obstacle	ft
S_L	Landing Ground Roll Distance	ft
S'_L	Landing Air Distance from 50' Obstacle	ft
S_{Ls}	Landing Ground Roll Distance (Standard, Zero Wind)	ft
S'_{Ls}	Landing Air Distance from 50' Obstacle (Standard, Zero Wind)	ft
S_{Lt}	Landing Ground Roll Distance (Test, Zero Wind)	ft
S'_{Lt}	Landing Air Distance from 50' Obstacle (Test, Zero Wind)	ft
S_{Ltw}	Landing Ground Roll Distance (Test, with Wind Component)	ft
S'_{Ltw}	Landing Air Distance from 50' Obstacle (Test, with Wind Component)	ft
S_s	Take-off Ground Roll Distance (Standard, Zero Wind)	ft
S'_s	Take-off Air Distance to 50' Obstacle (Standard, Zero Wind)	ft
S_t	Take-off Ground Roll Distance (Test, Zero Wind)	ft
S'_t	Take-off Air Distance to 50' Obstacle (Test, Zero Wind)	ft
S_{tw}	Take-off Ground Roll Distance (Test, with Wind Component)	ft
S'_{tw}	Take-off Air Distance to 50' Obstacle (Test, with Wind Component)	ft
SE	Specific Endurance	hrs/lb

CHART II-1

NOMENCLATURE

Sec	Seconds	
Sp g	Specific Gravity	
SRg	Specific Range	nautical air miles/lb or statute air miles/lb
T	Temperature	°K or °R
T _a	Atmospheric Temperature	°K or °R
T _{as}	Atmospheric Temperature (Standard)	°K or °R
T _{at}	Atmospheric Temperature (Test)	°K or °R
T _{cc}	Chart Carburetor Air Temperature for Pressure Altitude	°K or °R
T _{cs}	Standard Day Carburetor Air Temperature, $T_{as} - T_{at} + T_{ct}$	°K or °R
T _{ct}	Test Day Carburetor Air Temperature	°K or °R
T _i	Temperature (Indicated)	°K or °R
T _{ic}	Temperature (Indicated Instrument Corrected)	°K or °R
T _{ij} or T _{i8}	Temperature (Indicated Jet Nozzle)	°K or °R
T _s	Temperature (Static)	°K or °R
T' _s	Temperature (Static, Following Normal Shock Wave)	°K or °R
T _{SL}	Temperature (Standard Sea Level)	15°C 288°K 59°F 518.4°R
T _t	Temperature (Total Flow)	°K or °R
T _{t2}	Temperature (Total Flow at Compressor Inlet)	°K or °R
T _{t5}	Temperature (Total Exhaust Gas Temperature at Turbine Outlet)	°K or °R
T _θ	T_a/T_{SL}	
TAS	True Air Speed	knots or mph

CHART II-1

AFIR-6273

CHART II-1

NOMENCLATURE

ΔV_{pc}	Air-speed Position Error Correction	knots or mph
V_{td}	Landing Velocity	knots or mph
V_{SL}	Sea Level Standard V_t for Some V_c	knots or mph
V_t	Air Speed (True)	knots or mph
V'_t	Flow True Speed Following Normal Shock Wave	knots or mph
V_{to}	Take-off Velocity	knots or mph
V_{tos}	Take-off Velocity (Standard)	knots or mph
V_{tot}	Take-off Velocity (Test)	knots or mph
V_{ts}	True Speed (Standard)	knots or mph
V_{tt}	True Speed (Test)	knots or mph
V_w	Wind Component Along Runway, Headwind (+), Tailwind (-)	knots or mph
VIW	Speed Parameter, $V\sqrt{\sigma} / (W_t/W_s)^{\frac{1}{2}}$	knots or mph
W	Gross Weight	lbs
ΔW	Weight Increment, $W_s - W_t$	lbs
W_a	Air Flow	lbs/sec
W_f	Fuel Flow	lbs/hr
W_g	Gas Flow	lbs/sec
W_{SL}	Specific Weight of Air (Sea Level Standard)	0.0765 lbs/ft ³
W_s	Gross Weight (Standard)	lbs
W_t	Gross Weight (Test)	lbs
X	$\left[\left(\frac{P_t}{P_a} \right)^{.2481} - 1 \right]$	
γ	Ratio of Specific Heat ($\gamma = 1.4$ for Air)	
δ_a	P_a/P_{SL}	
δ_2	P_{t2}/P_{SL}	

NOMENCLATURE

CHART II-1

TEP	Thrust Horsepower, BHP x η_p	550 ft-lbs/sec
(TEP) _s	Thrust Horsepower (Standard)	550 ft-lbs/sec
(TEP) _t	Thrust Horsepower (Test)	550 ft-lbs/sec
(TEP) _{as}	Thrust Horsepower (Available Standard)	550 ft-lbs/sec
(TEP) _{at}	Thrust Horsepower (Available Test)	550 ft-lbs/sec
t	Time	
t	Temperature	°C or °F
t _a	Atmospheric Temperature	°C or °F
t _{as}	Atmospheric Temperature (Standard)	°C or °F
t _{at}	Atmospheric Temperature (Test)	°C or °F
t _e	Time Elapsed	
t _i	Temperature (Indicated)	°C or °F
t _{ic}	Temperature (Indicated Instrument Corrected)	°C or °F
Δt_{ic}	Temperature (Instrument Correction)	°C or °F
Δt	Compression Temperature Rise	°C or °F
t _s	Temperature (Static)	°C or °F
t _s	Time of Start	
t _t	Temperature (Total Flow)	°C or °F
V	Velocity	usually ft/sec
V _c	Air Speed (Calibrated), $V_{ic} + \Delta V_{pc}$	knots or mph
V _e	Air Speed (Equivalent)	knots or mph
V _i	Air Speed (Indicated)	knots or mph
V _{ic}	Air Speed (Indicated Instrument Corrected), $V_i + \Delta V_{ic}$	knots or mph
ΔV_{ic}	Instrument Correction for V _i	knots or mph
$\Delta V_{ic\ell}$	Indicated Air-speed Correction for Lag Condition	knots or mph

AFIR-6273

CHART II-1

NOMENCLATURE

CHART II-1

η_R	Ram Efficiency	
η_{RT}	Duct Ram Efficiency (Total, Through Normal Shock Wave and Duct)	
η_P	Propeller Efficiency	
θ	Aircraft Climb Angle	
θ_a	T_a/T_{SL}	
λ	Lag Constant	sec
λ_h	Lag Constant (Altimeter)	sec
λ_{hSL}	Lag Constant (Altimeter, Sea Level)	sec
λ_t	Lag Constant (Total Pressure)	sec
λ_{tSL}	Lag Constant (Total Pressure, Sea Level)	sec
μ	Coefficiency of Viscosity	lb-sec/ft ²
μ_o or μ_{SL}	Coefficient of Viscosity (Standard Sea Level)	3.725×10^{-7} lb-sec/ft ²
ν	Kinematic Viscosity, μ/ρ	ft ² /sec
ν_o or ν_{SL}	Kinematic Viscosity (Sea Level Standard)	1.5665×10^{-4} ft ² /sec
π	π	3.1416
ρ	Air Density	slugs/ft ³
ρ_o or ρ_{SL}	Air Density (Sea Level Standard)	0.002378 slugs/ft ³
σ	Air Density Ratio, ρ/ρ_{SL}	
η_{no}	Duct Ram Efficiency	

CHART II-2

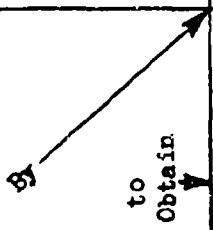
SYSTEMS OF UNITS

Name of Unit	ABSOLUTE UNITS		GRAVITATIONAL UNITS		Physical MLT System
	British FPS System	Metric CGS System	British	Metric	
Length	1 ft.	1 cm	1 ft.	1 M	L
Time	1 sec	1 sec	1 sec	1 sec	T
Force	1 poundal	1 dyne	1 lb	1 Kg	MLT^{-2}
Area	1 ft ²	1 cm ²	1 ft ²	1 M ²	L ²
Volume	1 ft ³	1 cm ³	1 ft ³	1 M ³	L ³
Velocity	1 ft/sec	1 cm/sec	1 ft/sec	1 M/sec	LT^{-1}
Acceleration	1 ft/sec ²	1 cm/sec ²	1 ft/sec ²	1 M/sec ²	LT^{-2}
Work or Energy	1 ft-pdl.	1 erg	1 ft-lb	1 Kg-M	ML^2T^{-2}
Pressure	1 pdl/ft ²	1 dyne/cm ²	1 lb/ft ²	1 Kg/M ²	$ML^{-1}T^{-2}$
Momentum	1 pdl-sec	1 dyne-sec	1 lb-sec	1 Kg-sec	MLT^{-1}
Power	1 ft-pdl per sec.	1 erg/sec	1 ft-lb per sec	1 Kg-M per sec	ML^2T^{-3}
Mass	1 lb	1 Gm	1 slug	1 slug	M
Temperature	1 °R	1 °K	1 °R	1 °K	L^2T^{-2}

	Cubic inches	Cubic feet	Liters	Gallons (U.S.)	Gallons (Br.)	Kilogram	Pound (avoird)
to Obtain	1	1728	61.024	230.98	267.40		
	5.787×10^{-4}	1	3.5316×10^{-2}	0.1337	0.1605		
by	1.6387×10^{-2}	28.317	1	3.7853	4.5460		
	4.3290×10^{-5}	7.4805	0.2642	1	1.2009		
	3.5971×10^{-5}	6.229	0.2200	0.8327	1		
						1	0.4536
						2.2046	1

Force* (MLT⁻²)
 Pressure or Force per Unit Area (ML⁻¹T⁻²)

Multiply Number of	Atmospheres	Centimeters of Mercury at 0°C	Inches of Mercury at 0°C	Inches of Mercury at 15°C	Pounds per Square Inch	Pounds per Square Foot	Dynes	Kilograms	Pounds	Poundals
1	1	1.3158 x 10 ⁻²	3.3421 x 10 ⁻²	2.4561 x 10 ⁻³	6.8046 x 10 ⁻²	4.7254 x 10 ⁻⁴				
86.180	1	2.5400	0.1867	5.1714	3.5913 x 10 ⁻²					
33.929	0.3937	1	7.3490 x 10 ⁻²	2.0360	1.4129 x 10 ⁻²					
407.15	5.3572	15.6074	1	27.7047	0.1924					
14.696	27.8357	0.4912	5.1977	1	6.9444 x 10 ⁻³					
2116.23	0.1934	0.7266	3.6095 x 10 ⁻²	144	1					
							1	9.807 x 10 ⁵	4.448 x 10 ⁵	1.383 x 10 ⁴
							1.020 x 10 ⁻⁶	1	0.4536	1.410 x 10 ⁻²
							2.248 x 10 ⁻⁶	2.205	1	3.108 x 10 ⁻²
							7.233 x 10 ⁻⁵	70.93	32.174	1



*Conversion factors between absolute and gravitational units apply only under standard acceleration due to gravity conditions.

Multiply Number of	to Obtain	Feet per second	Feet per second) ²	Feet per minute	Miles per minute	Miles per hour	(Miles per Hour) ²	Knots	(Knots) ²	Centimeters per second	Kilometers per hour
		1	---	1.6667 x 10 ⁻²	88	1.4667	---	1.6889	---	3.281 x 10 ⁻²	0.9113
		---	1	---	---	---	2.1511	---	2.8924	---	---
		60	---	1	2880	88	---	101.34	---	1.969	54.56
		1.136 x 10 ⁻²	---	1.894 x 10 ⁻⁴	1	.01667	---	1.9193 x 10 ⁻²	---	3.728 x 10 ⁻⁴	1.036 x 10 ⁻²
		0.6818	---	1.136 x 10 ⁻²	60	1	---	1.15155	---	2.237 x 10 ⁻²	0.6214
		---	0.4649	---	---	---	1	---	1.3621	---	---
		0.5921	---	9.868 x 10 ⁻³	32.10	0.8684	---	1	---	1.943 x 10 ⁻²	0.5396
		---	0.35058	---	---	---	00.7341	---	1	---	---
		30.48	---	0.5080	2682	44.704	---	51.48	---	1	27.78
		1.0973	---	1.829 x 10 ⁻²	96.34	1.6095	---	1.8532	---	.036	1

CHART II-3

Linear Acceleration (LT⁻²)

Multiply Number of	Centimeters per second per second	Feet per second per second	Kilometers per hour per second	Miles per hour per second	Knots per second
to Obtain	1	30.480	27.778	44.704	51.479
Centimeters per second per second	3.2808 x 10 ⁻²	1	0.9113	1.4667	1.6890
Feet per second per second	0.036	1.0973	1	1.6093	1.8532
Kilometers per hour per second	2.2369 x 10 ⁻²	0.6818	0.6214	1	1.15155
Miles per hour per second	1.9425	0.5921	0.5396	0.8684	1
Knots per second					

CHART II-3

AFTR 6273

CHART II-3

Angular Velocity (T^{-1}) and Angular Acceleration (T^{-2})

	Degrees per Second	Radians per Second	Revolutions per Second	Revolutions per Minute	Radians per Second	Revolutions per Second	Revolutions per Minute	Radians per Second	Revolutions per Second	Revolutions per Minute	Revolutions per Minute per Minute
Multiply Number of \rightarrow to Obtain \downarrow	Degrees per Second	1	57.30	360	6						
	Radians per Second	1.745×10^{-2}	1	6.2834	0.1047						
	Revolutions per Second	2.778×10^{-3}	0.1592	1	1.6667×10^{-2}						
	Revolutions per Minute	0.1667	9.549	60	1						
Radians per Second								1	6.283	0.1047	1.745×10^{-3}
Revolutions per Second								0.1592	1	1.6667×10^{-2}	2.778×10^{-4}
Revolutions per Minute								9.549	60	1	1.6667×10^{-4}
								573.0	3600	60	1

CHART II-3

Energy, Work and Heat (ML²T⁻²)

	Kilogram-Calorie	g	BTU (mean)	Foot-Pound	Kilogram-Meters	H-P Hours	Foot-Pounds	EH	
Multiply Number of ↓ to Obtain	Kilogram - Calories	2.3889 x 10 ⁻¹¹	0.2520	3.2389 x 10 ⁻⁴	2.3427 x 10 ⁻³	641.30	10.067	860.01	
	Ergs or centimeter-dynes.	4.186 x 10 ¹⁰	1.0548 x 10 ¹⁰	1.3558 x 10 ⁷	9.8067 x 10 ⁷	2.6843 x 10 ¹³	4.2140 x 10 ⁵	3.6000 x 10 ¹³	
	BTU (mean)	3.9683	1	1.2854 x 10 ⁻³	9.2972 x 10 ⁻³	2545.0	3.9952 x 10 ⁻³	3413.0	
	Foot-Pound	3087.4	7.7796 x 10 ⁻⁸	777.97	7.2330	1.9800 x 10 ⁶	3.1081 x 10 ⁻²	2.6532 x 10 ⁶	
	Kilogram-Meters	426.85	1.0197 x 10 ⁻⁸	107.56	0.1383	2.1374 x 10 ⁵	4.2972 x 10 ⁻³	3.6710 x 10 ⁵	
	Horsepower Hour	1.5593 x 10 ⁻³	3.7251 x 10 ⁻¹⁴	3.9292 x 10 ⁻⁴	5.0503 x 10 ⁻⁷	3.6539 x 10 ⁻⁶	1	1.3697 x 10 ⁻⁸	1.3410
	Foot-Pounds	993.34	2.3759 x 10 ⁻⁶	2.5030 x 10 ⁴	32.174	232.71	6.3706 x 10 ⁷	1	8.4709 x 10 ⁷
	Kilowatt Hours	1.1628 x 10 ⁻³	2.7777 x 10 ⁻¹³	2.930 x 10 ⁻⁴	3.7662 x 10 ⁻⁷	2.7232 x 10 ⁻⁶	0.7437	1.1803 x 10 ⁻⁸	1

CHART II-3

AFTR 6273

	Foot Pounds per Second	Gram Centimeter per Second	BTU per hour	Horsepower	Kilowatts
to Obtain	1	7.2330×10^{-5}	0.2161	550	737.56
Multiply Number of	1.3825×10^4	1	2.9869×10^3	7.5988×10^6	1.0127×10^7
	4.6274×10^{-4}	3.3471×10^{-4}	1	2545.1×10^{-3}	3413.76
	1.8182×10^{-3}	1.3151×10^{-7}	3.9261×10^{-4}	1	1.3410
	1.3558×10^{-5}	9.8066×10^{-8}	2.9292×10^{-4}	0.7452	1